DIVISION DE EDUCACION CONTINUA
FACULTAD DE INGENIERIA U.N.A.M.

INGENIERIA CIVIL EN EL PROYECTO DE

PLANTAS HIDROELECTRICAS

C F E

MECANICA DE ROCAS

Ing. Jorge E. Castilla Camacho

Abril 1981

INTRODUCCION

TABLE 14 — ROCK ANALYSIS IN-SITU TESTS

LEGEND

Test requirement	Mode of test work
a — analytical s — semi-empirical n — not necessary ( ) — alternative	F — Foundation (B) — Detailed design DC — During construction AC — After completion

IN SITU MECHANICAL TESTS	TYPE OF WORK: FOUNDATIONS — Dam/Weir Dams	FOUNDATIONS — Arch Dams	FOUNDATIONS — Large Structures	NATURAL AND ARTIFICIAL ROCK SLOPES — Retaining Barriers	NATURAL AND ARTIFICIAL ROCK SLOPES — Retaining other works	UNDERGROUND WORKS — Large Underground Works	UNDERGROUND WORKS — Tunnels, Shafts Underground Mines	ROCK EXCAVATION — Open Cut Mining, Quarries, Large Surface Excavations	HARBOURS AND OTHER SUBMARINE WORKS
1. Deformability Tests	nDD	nF; nDD; nAC	nDD			nDC			nF
1.1 *Static Method*									
1.1.1 Plate bearing (hydraulic jack; flat jack; cable jacking)		(n)DD; (n)AC				(n)DD	nDC		
1.1.2 Pressure tunnel (tunnel loading; radial jacks)		(n)DD; (n)AC				(n)DD			
1.1.3 Pressure borehole (dilatometer)	nF	(n)DD; (n)AC	nF			nF; (n)DD	nDC		nF
1.2 *Dynamic Method*	nDD	nF; nDD; nAC	nF			nF; nDC	nDC		
1.2.1 Measurement of longitudinal wave velocity (geophones)	nDD	nF; (n)AC				nF	nDC		
1.2.2 Measurement of the velocity of longitudinal and transverse waves Love's waves Rayleigh's (seismograph)		nDD; (n)AC				nDD			
1.2.3 Measurement of direct longitudinal waves velocity in boreholes (seismo-scoring)		nDD; (n)AC				nDC	nDC		
1.2.4 Detailed stratigraphic surveys									
2. Natural rock mass stresses tests						nF; nDD			
2.1 *Rock Surface Test:*									
2.1.1 Measurement of deformation after overcoring or load removal (by strain rosette)						(n)F			
2.1.2 Measurement of pressure to balance natural stresses (by flat jack)						nF			
2.2 *Test Inside Borehole*	nDD	nDD	nDD	nF		nDD			
2.2.1 Measurement of core deformation after overcoring						nDD			
2.2.2 Measurement of borehole wall deformation after overcoring						nDD			
3. Strength tests									nDD
3.1 Compression		nDD				nDD			
3.1.1 Triaxial tests	nDD	nDD	nDD	nDD	nDD	nDD	nDD	nDD	
3.2 Shear									
3.2.1 Rock block test along discontinuity surface	nDD	nDD	nDD	nDD	nDD	nDD	nDD	nDD	
3.2.2 Concrete block test along interface	nDD	nDD	nDD					nF	
4. Permeability						nF			
4.1. *Inside Borehole (Lugeon)*	nF; nAC	nF; nAC	nF	nF					
4.2 *In a test pumping well*	nF; nAC	nF; nAC					nF	nF	nF
4.3 *Piezometric levels and ground water flow*				nAC			nDD	nDD	nDC
5. Rock Anchor tests				nF; nDC; nAC	nF; nDC; nAC	nF; nDC; nAC			
6. Rock movement monitoring									
6.1 *Long base extensometer*	nAC	nAC		nAC	nAC	nAC			
6.2 *Inverted pendulum*	nAC	nAC	nAC	nIAC					nAC
6.3 *Slope inclinometer*				nAC					
6.4 *Shear and groundwater monitoring*	nDD	nDD		nDC	nDC	nF; nDC	nF; nDC		nDC
6.5 *Rock noise monitoring*				nAC				nAC	nAC

The interlooking of the Engineering Geology with the design itself begins with the initial feasibility studies and continues through the construction stage and even after the work completion.

As a guide for rock mechanics studies planning a table shaped tests recommendations is presented, establishing in general terms the degree of necessity of each rock mechanics test.

7.5 *RECOMMENDATIONS CHART*

Tables 7.1 and 7.2 give some suggestions regarding applications of the techniques described in this chapter, during the different stages of engineering investigations of various types. It must be understood that these tables are extremely generalized and should be used only as broad guides.

TABLE 7.2 — ROCK MECHANICS LABORATORY TESTS

LEGEND

Test importance	Stage of the work
a — necessary s — advisable si — of interest ( ) — alternative	P — Feasibility DD — Detailed design DC — During construction AC — After completion

LABORATORY MECHANICAL TESTS \ TYPE OF WORK	FOUNDATIONS			NATURAL AND ARTIFICIAL ROCK SLOPES		UNDERGROUND WORK		ROCK EXCAVATION	HARBOUR AND OTHER SUBMARINE WORKS
	Gravity Dams	Arch Dams	Large Structures	Involving Reservoirs	Involving other works	Large Underground Works	Tunnels, Shafts, Underground Mining	Open Air Mining, Quarries, Large Surface Excavations	
1. Uniaxial test		aF				aDD			
2. Biaxial triaxial test		aDD	aDD	aDD	aDD	aF; aDD			
3. Poisson's Ratio		aDD				aDD			
4. Sound velocity — Pulse and resonance		aF		aF		aP		aF	aF
5. Direct shear	aP				aDD	aDD		aDD	
6. Tensile (Brazilian) test				aDD	aDD	aDD			
7. Hardness (Rockwell identation, shore sclerocope, Schmidt Rebound Hammer)								aDD	
8. Triaxial chamber for determining body forces due to interstitial pressure								aDD	
9. Density		aDD	aDD	aF	aF			aDD	
10. Water content			aDD	aF	aF			aDD	
11. Porosity			aDD	aF	aF			aDD	
12. Absorption			aDD	aP	aF			aDD	
13. Permeability				aF	aF				aF

PROPIEDADES MECANICAS DE LAS ROCAS

CAPITULO 2. PROPIEDADES MECANICAS DE LAS ROCAS

2.1 INTRODUCCION

2.1.1 Distinción de roca intacta y macizo rocoso

2.1.2 Clasificación ingenieril de la roca intacta

(Capítulo 1. Consideraciones geológicas de D.U.Deere del libro "Mecánica de rocas en la ingeniería práctica" de Stagg y Zienkiewicz, Ed.Blume, 1968, pp.15-25) 11 págs.

2.2 PROPIEDADES FISICAS Y MECANICAS DE LA ROCA INTACTA

2.2.1 Estructura y propiedades índice

2.2.2 Resistencia y deformabilidad

2.2.3 Criterios de falla

(Capítulo III Propiedades mecánicas de las rocas de J. Alberro del libro "Presas de tierra y enrocamiento" de Marsal y Reséndiz, Ed. Limusa, 1975, pp. 269-281) 13 págs.

2.3 PROPIEDADES MECANICAS DE LOS MACIZOS ROCOSOS

2.3.1 Conceptos fundamentales

2.3.2 Su influencia en la estabilidad de las obras subterráneas y a cielo abierto

2.3.3 Su obtención en el sitio de las obras

(Apuntes sobre "Pruebas de campo en mecánica de rocas" de R. Cuéllar Borja)

(Apuntes sobre "Pruebas de permeabilidad in situ" de J. Alberro A.)

(Apuntes sobre "Instrumentación de mecánica de rocas de R. Cuéllar Borja).

2.3.4 Clasificación ingenieril de la masa rocosa

(Ejemplo elaborado por C. Castilla y R. Cuéllar B.)

(Z.T. Bieniawski "Geomechanics classification of rock masses and its application in tunneling". Memoria del tercer congreso de la ISRM, Denver, 1974).

Capítulo 1

Consideraciones geológicas *

D. U. Deere

1:1 Introducción

> La mecánica de Rocas es la ciencia teórica y aplicada que trata del comportamiento mecánico de las rocas; es la rama de la Mecánica que estudia la reacción de las rocas a los campos de fuerza de su entorno físico †.

Esta definición, dada recientemente por un grupo de investigadores en Mecánica de Rocas, puede parecer a primera vista que realza el papel de la mecánica, ignorando el de la geología. En realidad esta definición es de miras muy amplias. La frase «reacción de las rocas a los campos de fuerza de su entorno físico» es suficientemente general para que sea aplicable a problemas a cualquier escala. Por ejemplo, comprende los estudios del mecanismo de deformación de los cristales minerales sometidos a elevadas presiones y temperaturas, el comportamiento triaxial de una muestra de roca ensayada en laboratorio, la estabilidad del revestimiento de un túnel e incluso el mecanismo de los movimientos de la corteza terrestre.

El papel de la geología es evidente; todos los materiales estudiados son masas rocosas situadas en un entorno geológico o extraídas de él. Los materiales poseen ciertas características físicas que son función de su origen y de los procesos geológicos posteriores que han actuado sobre ellos. El conjunto de estos fenómenos en la historia geológica de una cierta zona conduce a una *litología* particular, a una determinada serie de *estructuras geológicas* y a un *estado tensional in situ* característico. Regionalmente se producen variaciones de estas condiciones y pueden también producirse localmente, aún con mayor importancia, dentro del emplazamiento de una obra determinada. Al realizar programas de reconocimiento, y al extrapolar los resultados de ensayo en un punto a las zonas adyacentes, es totalmente necesario considerar la distribución en el lugar de los diferentes elementos geológicos. La experiencia ha demostrado que quien mejor puede realizar este trabajo es un *ingeniero geólogo* que no sólo tenga base suficiente en ciencias geológicas para apreciar los detalles de la geología del lugar, sino que también esté bien enterado de los métodos modernos de reconocimiento de las rocas y esté familiarizado con las exigencias de los técnicos en Mecánica de Rocas.

* De una próxima edición, aún en dos volúmenes original de Donald U. Deere, Introducción y Fundamentos. *Engineering Geology* (Geología aplicada a la Ingeniería) y *Rock Mechanics* (Mecánica de las rocas). Esta reproducida con la autorización de Prentice-Hall, Inc., englewood Cliffs, New Jersey, EE. UU.

† Del Informe del Simposio de Mecánica de Rocas de la Academia Nacional de Ciencias en relación con sus problemas nacionales. *Nat. Acad. Sci.-Nat. Res. Council*, Washington, D. C., 1966.

En la Mecánica de Rocas aplicada, en especial en los campos de ingeniería civil y minería, el método de proyecto supone la selección de un anteproyecto y la predicción del comportamiento esperado. Se emplean para ello ecuaciones de la mecánica teórica y aplicada. Sin embargo, en la mayoría de los casos, deben introducirse en las ecuaciones algunas propiedades mecánicas de la roca. La validez de la solución obtenida no es mayor que la validez de la propiedad mecánica empleada. Las propiedades mecánicas de una muestra inalterada ensayada en laboratorio pueden ser muy diferentes de las propiedades del macizo rocoso del que se ha extraído la muestra. El reconocimiento de este hecho ha motivado en estos últimos años una gran atención hacia los ensayos *in situ*.

El comportamiento de un macizo rocoso sometido a una variación de tensiones viene determinado por las propiedades mecánicas del material rocoso y por el número y naturaleza de las discontinuidades geológicas existentes en el mismo. La importancia relativa de cada uno de estos factores sobre el comportamiento de la roca depende principalmente de la relación entre las dimensiones de la obra de ingeniería a realizar y la separación entre las discontinuidades. Cuando la variación introducida en el estado tensional afecta a una roca grande respecto a la distancia entre diaclasas *, por ejemplo, como es el caso de la cimentación de presas o grandes excavaciones subterráneas, la influencia de las diaclasas puede ser muy pronunciada. Sin embargo, en aquellos casos en que la separación entre las mismas es muy grande respecto a las dimensiones de la obra, como en la perforación de un barreno o la construcción de un túnel a través de una roca masiva con una perforación mecánica, el comportamiento de la roca depende más de las propiedades inherentes al material rocoso.

En muchos problemas de Mecánica de Rocas aplicada también se requiere conocer el estado tensional a una cierta profundidad en la zona estudiada. Como se señala en una sección posterior de este capítulo, el estado tensional es consecuencia directa de la historia geológica pasada de la zona. Sin embargo, el conocimiento de la historia geológica no basta por sí mismo para permitir una estimación razonable del estado de tensiones.

1.2 Importancia de la litología o tipo de roca

La litología de una roca hace referencia a su mineralogía, textura y fábrica, junto con un nombre o término descriptivo de algún sistema de clasificación reconocido, por ejemplo, caliza oolítica, pizarra bituminosa, granito, clorita-biotita, esquistos, etc. Los nombres y la clasificación son geológicos. Los técnicos en Mecánica de Rocas han reconocido frecuentemente lo inadecuado de un sistema de clasificación de este tipo, advirtiendo al menos que rocas de la misma litología pueden presentar una gama extraordinariamente amplia de propiedades mecánicas. Se ha propuesto incluso abandonar tales nombres geológicos y adoptar un nuevo sistema de clasificación basado únicamente en [illegible]

[illegible] necesario, [illegible] razones para [illegible] geológicos. En primer lugar [illegible] como mínimo una

* Par[illegible] por [illegible] y [illegible]

gama de valores para cualquier tipo de roca donde queda comprendido el valor de una cierta propiedad mecánica. Para algunas propiedades mecánicas y para algunos tipos de rocas este intervalo de variación puede ser desalentadoramente grande; para otras bastante más pequeño. Por ejemplo, la resistencia a compresión simple de una caliza puede variar de 350 a 2.500 kg/cm²; sin embargo, para la sal gema la variación es solamente de 200 a 350 kg/cm², aproximadamente. La dureza de una cuarcita será elevada y prácticamente constante, mientras que la de una arenisca será muy baja o muy alta según el tipo y grado de cementación.

Otra razón importante para el empleo del nombre litológico es la relación entre la textura, fábrica y anisotropía estructural de las rocas de un determinado origen. Por ejemplo, la mayoría de las rocas ígneas tienen una estructura densa, bien encajada, con muy pequeñas diferencias de dirección en las propiedades mecánicas (con la excepción, por supuesto, de muchas rocas volcánicas superficiales, rocas intrusivas subsuperficiales, y algunas intrusivas profundas, como los granitos gnéisicos, que presentan una estructura riolítica en la periferia de la intrusión). Las rocas sedimentarias, como las pizarras arcillosas, las areniscas y algunas calizas, están estratificadas y por tanto muestran una anisotropía considerable en las propiedades mecánicas. Otras rocas sedimentarias, como la sal gema, el yeso y muchas calizas y dolomías, han recristalizado en una textura compacta, presentando únicamente una ligera anisotropía. Las rocas metamórficas son quizá las más sorprendentes respecto a la anisotropía. La clorita, el talco y el micasquisto tienen superficies de exfoliación bien desarrolladas y se componen de minerales de estructura hojosa que dan lugar a grandes diferencias en la resistencia y el módulo de deformación según la dirección de ensayo. Los gneis * muestran alguna anisotropía pero en menor grado. La pizarra es también muy anisotropa debido a su pronunciada estratificación. Otras rocas metamórficas, como el mármol y la cuarcita, han recristalizado en una textura compacta, siendo bastante homogéneas.

Otra razón para conservar el nombre geológico es la asociación que puede hacerse entre ciertos tipos de rocas y otras características *in situ* que pueden presentarse. Por ejemplo, la presencia en el terreno de caliza, yeso y sal gema puede inclinar al investigador a la búsqueda de fenómenos de disolución como cavidades, torcas y fisuras agrandadas por la disolución. En otro caso, la presencia de una colada de lava basáltica puede indicar la posible presencia de un diaclasado columnar y llamar la atención sobre los problemas con él relacionados. Análogamente, algunos tipos de rocas presentan un comportamiento característico o problemas específicos. La existencia de sal gema u otras evaporitas puede dar lugar a problemas con deformaciones de fluencia. Debido a su contenido de arcilla, las pizarras arcillosas presentan frecuentemente hinchamiento y disgregación al aire por variaciones de presión y humedad. Resulta evidente que se da una información mucho más valiosa sobre las propiedades y el comportamiento de una roca cuando se indica su nombre geológico. Sin embargo, a efectos ingenieriles, el nombre geológico es insuficiente por sí solo y debe acompañarse de una clasificación de tipo mecánico según se indica en la sección siguiente.

* Aunque últimamente se tiende a escribir *neis* hemos preferido conservar la grafía tradicional. *(N. del T.)*

1.3 Clasificación de las rocas en ingeniería

Se entiende por roca «intacta» aquella de la cual pueden tomarse muestras para su ensayo en laboratorio, no presentando características estructurales de gran escala, como diaclasas, planos de estratificación, fracturas y zonas milonitizadas. Coates[1] ha empleado el término *sustancia rocosa*. Coates[1], Coates y Parsons[1] y Miller,[2] han realizado un trabajo acerca de la clasificación de la roca intacta a partir de las propiedades mecánicas determinadas en laboratorio. Deere y Miller[4] han dado una versión modificada del primer trabajo de Miller, siendo esta clasificación la que se describe a continuación.

La clasificación se basa en dos propiedades importantes de la roca: la resistencia a compresión simple y el módulo de elasticidad. El módulo empleado es el módulo tangente correspondiente a un nivel tensional igual a la mitad de la resistencia de la roca. La resistencia a compresión simple se determina con muestras de relación longitud/diámetro igual o superior a 2. La roca se clasifica en una de las cinco categorías de resistencia indicadas en la tabla 1.1.

Tabla 1.1 Clasificación de la roca intacta *

I. Basada en la resistencia (σ_c)

Clase	Descripción	Resistencia a compresión simple (kg/cm²)
A	Resistencia muy alta	> 2.250
B	Resistencia alta	1.120-2.250
C	Resistencia media	560-1.120
D	Resistencia baja	280-560
E	Resistencia muy baja	< 280

Se advierte que las categorías de resistencia siguen una progresión geométrica. La línea divisoria entre las categorías A y B se ha fijado en 2.250 kg/cm² ya que éste constituye el límite superior de resistencia de las rocas más comunes.

Tabla 1.2 Clasificación* de la roca intacta †

II. Basada en el módulo relativo (E_t/σ_c)

Clase	Descripción	Módulo relativo **
H	Elevado módulo relativo	> 500
M	Módulo relativo medio	200-500
L	Módulo relativo bajo	< 200

* Las rocas se clasifican según su resistencia y módulo relativo en AM, BL, BH, CM, etc.

** Módulo relativo = E_t/σ_c,

siendo E_t = módulo tangente para el 50 % de la carga de rotura,
σ_c = resistencia a compresión simple.

Unicamente unos pocos tipos de rocas entran en la categoría A, la cuarcita, la diabasa y los basaltos densos, entre ellas. La categoría B, 1.120-2.250 kg cm², comprende la mayoría de las rocas ígneas, las rocas metamórficas más duras y las areniscas bien cementadas, las pizarras arcillosas duras y la mayoría de las calizas y dolomías. En la categoría C, rocas de resistencia media en el intervalo 560-1.120 kg/cm², se encuentran muchas pizarras arcillosas, areniscas y

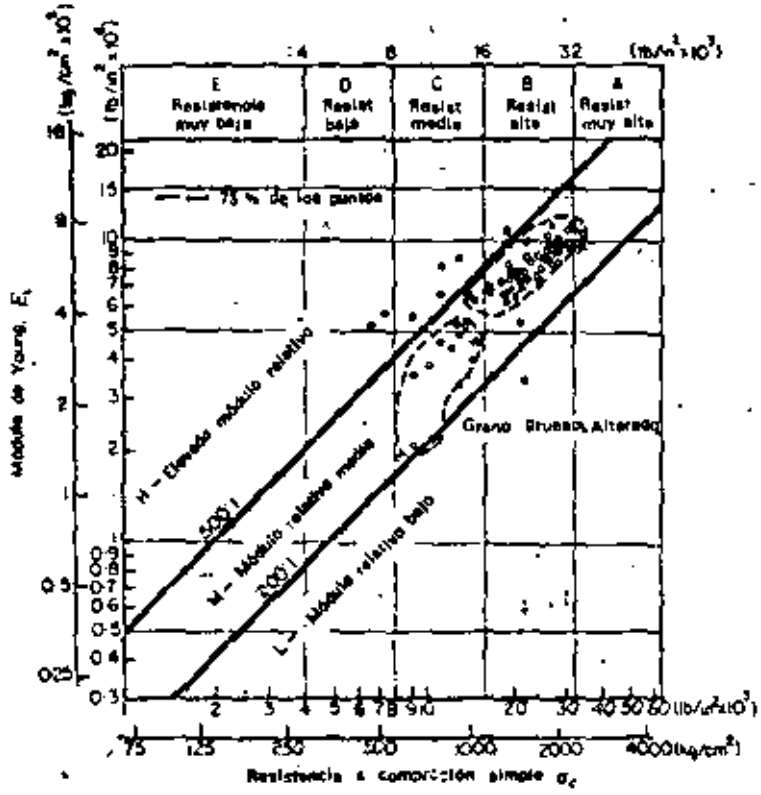

Figura 1.1 Clasificación de rocas intactas de la familia del granito (80 muestras, 16 emplazamientos, varios investigadores)[4]

E_t = módulo tangente para el 50 % de la carga de rotura.
La roca se clasifica como AM, BH, BL, etc.

calizas porosas, las variedades más esquistosas de las rocas metamórficas (por ejemplo la clorita, y los mica y talcoesquistos). Las categorías D y E, de resistencia baja a muy baja, comprenden rocas porosas o de baja densidad como la arenisca friable, la toba porosa, las pizarras muy arcillosas, la sal gema y las rocas meteorizadas o alteradas químicamente de cualquier litología.

El segundo elemento del sistema de clasificación es el módulo de elasticidad (E_t). Sin embargo, en lugar de emplear el módulo propiamente dicho,

se utiliza la relación entre este módulo y la resistencia a compresión simple, el *módulo relativo* *, según se indica en la tabla 1.2.

Puede emplearse un diagrama de clasificación como el de la figura 1.1. Los valores de la resistencia a compresión y del módulo de elasticidad se han representado en escala logarítmica para abarcar una amplia gama de valores. Las categorías de resistencia se indican en la parte superior de la figura. El mó-

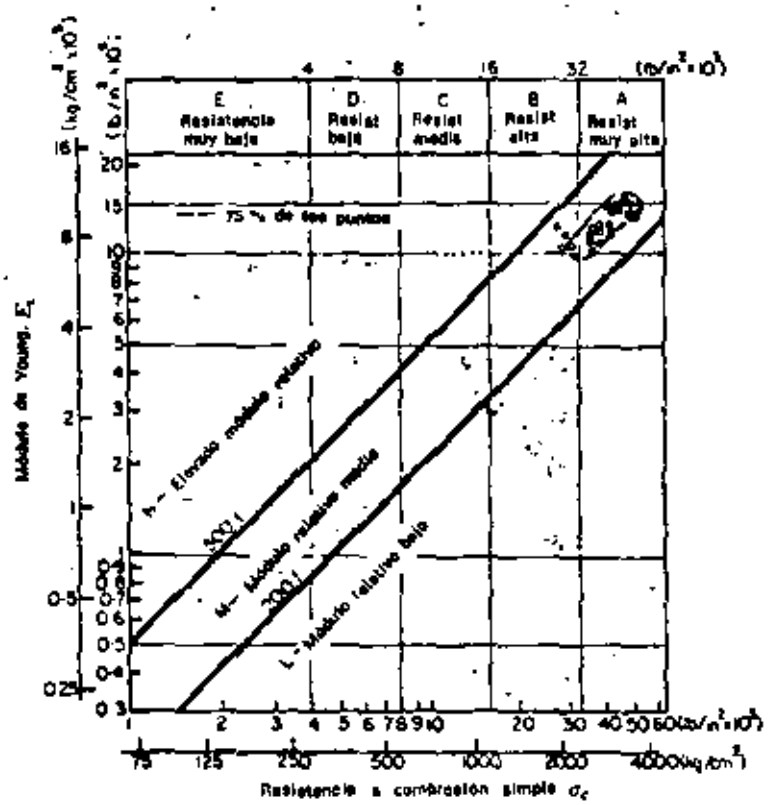

Figura 1.2 Clasificación de rocas intactas-Diabasas (26 muestras, 8 emplazamientos, varios investigadores) *

E_t = módulo tangente para el 50 % de la carga de rotura.
La roca se clasifica como AM, BH, BL, etc.

dulo relativo se deduce de la posición respecto a las diagonales. La zona central viene limitada por una línea superior con un módulo relativo de 500:1 y una línea inferior correspondiente a un módulo de 200:1. Esta zona se designa con la letra M, o zona de módulo relativo *medio*. Las rocas que poseen una estructura compacta y poca o ninguna anisotropía suelen entrar dentro de esta categoría. En ella están comprendidas la mayoría de las rocas ígneas. Los puntos marcados en la figura 1.1 representan 80 muestras de granito corres-

* Traducción arbitraria que proponemos para la *modulus ratio* del texto original *(N. del T.)*.

pondientes a 16 localidades. La figura 1.2 muestra los resultados de 26 probetas de diabasa, roca ígnea densa y uniforme de grano fino a medio. Se advierte que los resultados son más uniformes y que la roca entra principalmente en la clasificación AM, roca de muy alta resistencia con un módulo relativo medio. En la figura 1,3 aparecen los resultados de 70 muestras de basalto y otras rocas volcánicas de grano fino. Como era de esperar, los resultados abarcan una

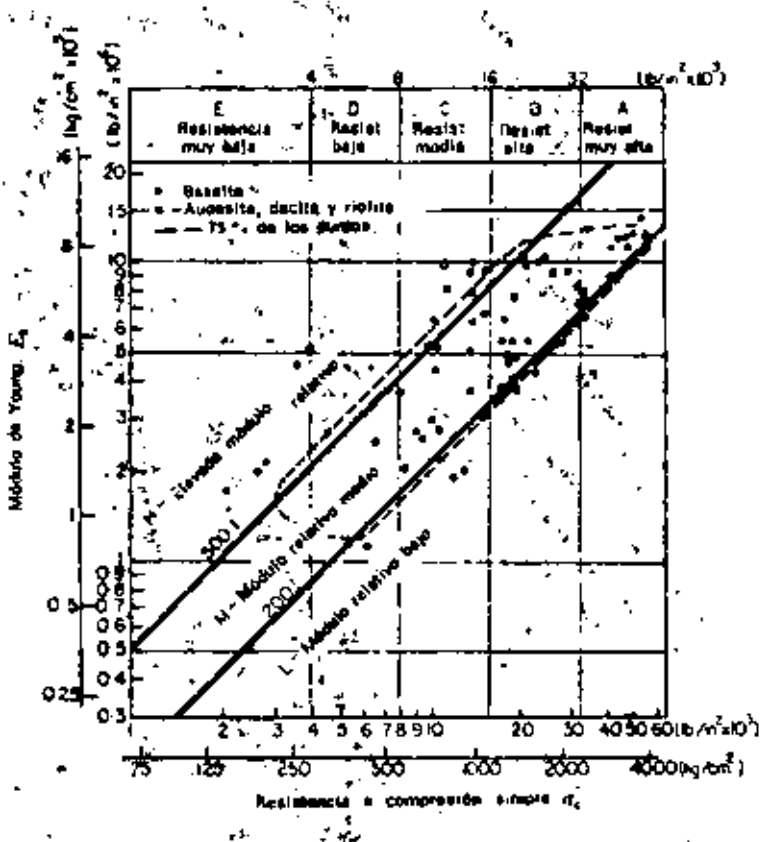

Figura 1.3 Clasificación de rocas intactas-Basalto y otras rocas volcánicas (70 muestras, 20 emplazamientos, varios investigadores)*

E_t = módulo tangente para el 50 % de la carga de rotura.
La roca se clasifica como AM, BH, BL, etc.

amplia gama de valores debido a la variación en la mineralogía, porosidad, tamaño del grano y estructura de cristalización. El diagrama resumen de las rocas ígneas se indica en la figura 1.4.

En la figura 1.5 aparece el diagrama resumen de las rocas sedimentarias. Se advierte que las calizas y dolomías entran principalmente en las categorías de resistencia B y C aunque algunas muestras son del tipo A, de muy elevada resistencia, o D, rocas muy débiles. Los detalles de estas calizas y dolomías se indican en la figura 1.6. Puede verse que muchos de los puntos caen próximos a la línea superior (módulo relativo 500:1) o por encima de ella. Esta situación

parece deberse a su particular estructura (compacta) y mineralogía (calcita y dolomía). Los diagramas correspondientes a la arenisca y pizarra arcillosa, en la figura 1.5 aparecen abiertos por su extremo inferior debido a que diversas probetas se rompieron con presiones inferiores a 75 kg/cm². Se aprecia que tanto la envolvente de las areniscas como la de las pizarras entran en la zona de módulo relativo bajo. Esta situación es el resultado de la anisotropía creada

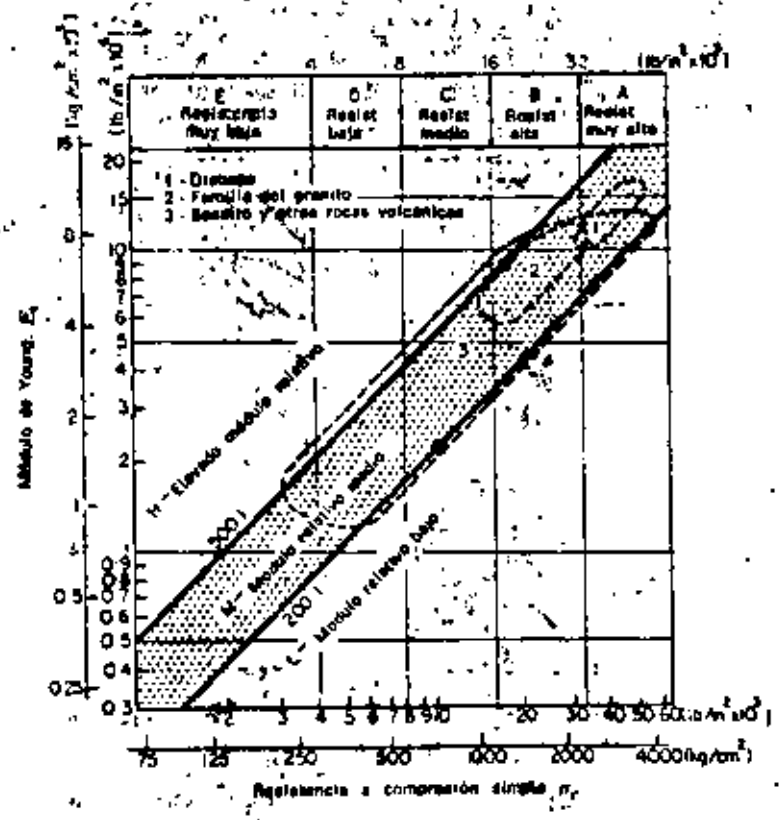

Figura 1.4 Clasificación de rocas intactas-Resumen de rocas ígneas (176 muestras, 75 % de los puntos)*

*E_t = módulo tangente para el 50 % de la carga de rotura.
La roca se clasifica como AM, BH, BL, etc.

por la estratificación o esquistosidad. Los módulos relativos son bajos ya que casi todas las muestras se ensayaron con el eje de carga normal al plano de estratificación. Esta orientación no modifica la resistencia pero da lugar a módulos bajos por efecto de la deformación originada por el cierre de los planos de estratificación incipientes y la alineación de los minerales, la mayoría de los cuales son aplanados, especialmente en las pizarras.

El diagrama resumen de las rocas metamórficas aparece en la figura 1.7. La dispersión de los resultados es superior a la de los otros tipos de rocas por la gran variación de mineralogía y grado de anisotropía. La mayoría de las

rocas cuarcíticas aparecen clasificadas como AM, en la misma posición que otros tipos de rocas densas, de granos iguales y estructura compacta, como la diabasa y los basaltos densos. Los gneis vienen representados de forma semejante a los granitos pero con una resistencia media algo menor y una mayor dispersión en el módulo relativo. La dispersión adicional proviene de la mayor variación de mineralogía respecto al granito y a la anisotropía por efecto de

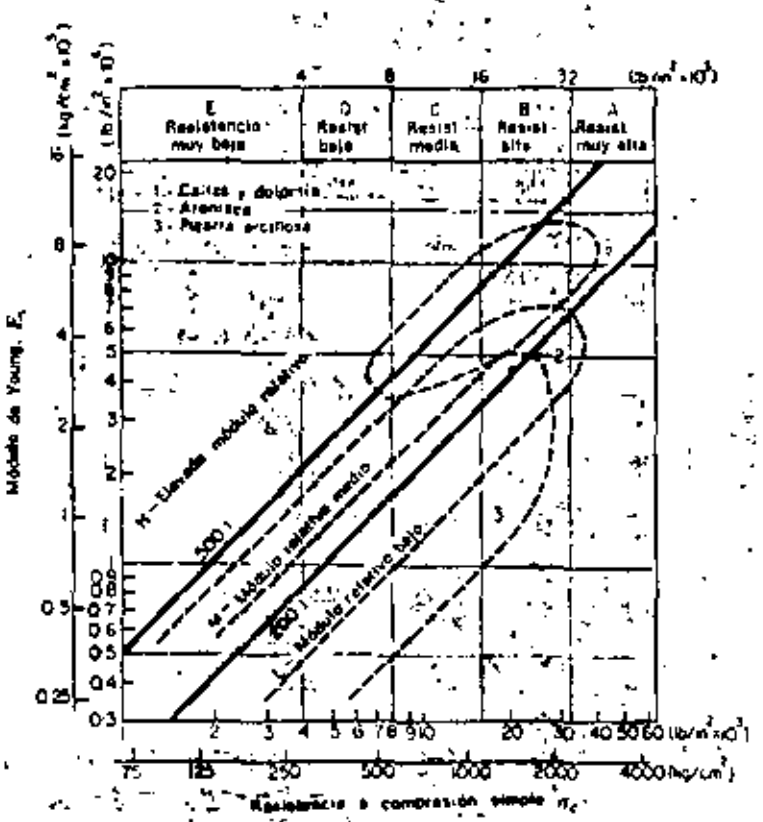

Figura 1.5 Clasificación de rocas intactas-Resumen de rocas sedimentarias (193 muestras, 75 % de los puntos)*
E_t = módulo tangente para el 50 % de la carga de rotura.
La roca se clasifica como AM, BH, BL, etc.

la esquistosidad. Muchos de los puntos que caen en la zona de elevado módulo relativo representan roturas según bandas esquistosas de muestras con una fuerte foliación.

Quizá el diagrama más interesante es el de los esquistos. La envolvente 4a, (fig. 1.7) corresponde a muestras con una esquistosidad orientada hacia la vertical, es decir con un ángulo elevado (45° o superior) entre el plano de esquistosidad y la horizontal (testigos ensayados con el eje en posición vertical). El elevado módulo relativo de la mayoría de las muestras no corresponde tanto a un valor inherentemente alto sino más bien a un caso de baja resis-

tencia por efecto de roturas prematuras según los planos de esquistosidad con fuerte buzamiento. Por otro lado, la envolvente de las muestras con un pequeño ángulo de esquistosidad (45° o menos respecto a la horizontal) cae en la zona de módulos relativos bajos. En este caso, la resistencia no resulta muy afectada por la esquistosidad pero el módulo de elasticidad es bajo por efecto del cierre de las microfisuras paralelas a los planos de esquistosidad. La envolvente del

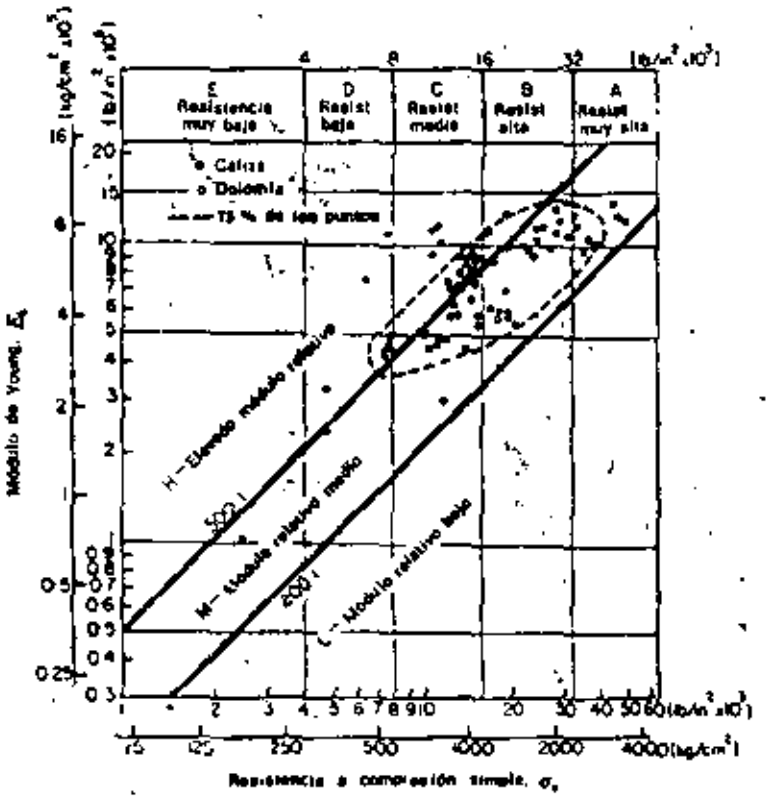

Figura 1.6 Clasificación de rocas intactas-Caliza y dolomía (77 muestras, 22 emplazamientos, varios investigadores)[4]

E_t = módulo tangente para el 50 % de la carga de rotura.
La roca se clasifica como AM, BH, BL, etc.

mármol (fig. 1.7) corresponde a un pequeño número de muestras y, aunque 15 de las 22 muestras ensayadas quedaron comprendidas en esa envolvente, se necesitan más resultados para poder generalizar. De hecho parece que el elevado módulo relativo se corresponde con la tendencia de las calizas y dolomías que contienen los mismos minerales.

En el diagrama resumen de las rocas metamórficas es significativo que la envolvente de los gneis se superponga con la de las cuarcitas y con las dos envolventes de los esquistos. Esta posición de transición indica una complejidad creciente de mineralogía y estructura, pasando de las cuarcitas a los gneis y

de éstos a los esquistos. Los diagramas resumen de las rocas ígneas y de las rocas sedimentarias muestran características semejantes en cuanto a las diferencias de mineralogía y estructura.

La clasificación propuesta se considera útil y manejable. Está basada en la resistencia a compresión simple y en el módulo de elasticidad —dos propiedades físicas importantes de la roca que intervienen en la mayoría de los

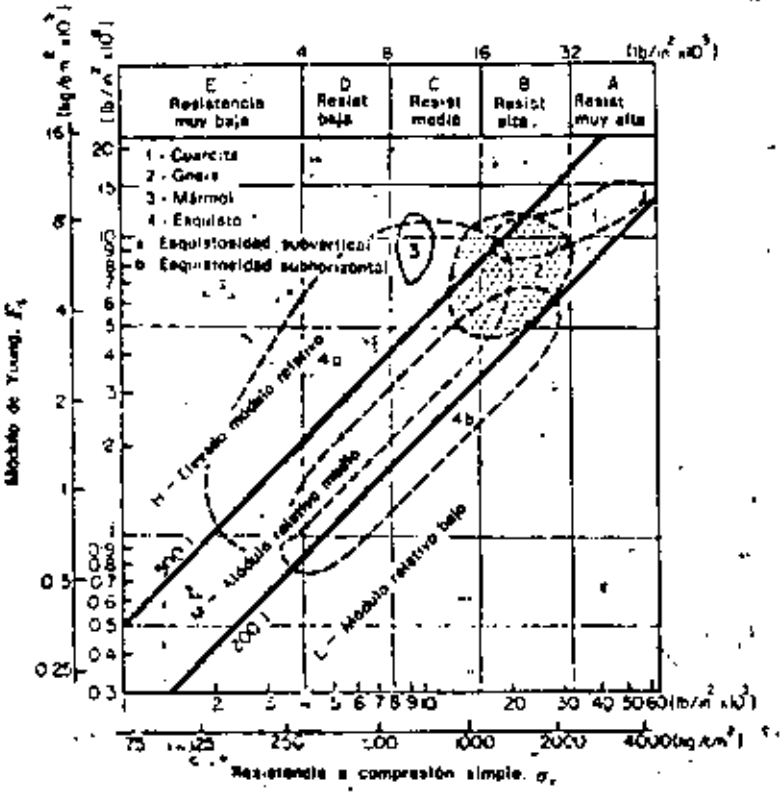

Figura 1.7 Clasificación de rocas intactas-Resumen de rocas metamórficas (167 muestras, 75 % de los puntos)[4]

E_t = módulo tangente para el 50 % de la carga de rotura.
La roca se clasifica como AM, BH, BL, etc.

problemas de ingeniería. La clasificación también considera la mineralogía, textura, estructura y dirección de anisotropía de la roca, de forma que tipos específicos de roca caen dentro de áreas determinadas del diagrama de clasificación. La clasificación completa debería incluir también la descripción litológica, por ejemplo, Caliza: *alta resistencia, elevado módulo relativo* (BH): grano fino, densa, uniforme.

CAPITULO 11

Propiedades mecánicas de las rocas

INTRODUCCION

El comportamiento de una presa de tierra y enrocamiento depende, en muchos aspectos, de las propiedades mecánicas de su roca de cimentación. En efecto, la inestabilidad o permeabilidad de las formaciones geológicas del sitio pueden ocasionar problemas serios durante la vida de la obra y aun reducir su utilidad en conjunto. Además, aunque en casos especiales la compresibilidad y capacidad de carga de las masas rocosas no son motivo de preocupación al proyectar la cimentación de una cortina de tierra y enrocamiento, revisten importancia al analizar la estabilidad de las obras auxiliares. El estudio de las propiedades mecánicas de las rocas es, por tanto, fundamental.

La característica principal de una masa rocosa es su fisuración, su carácter discontinuo. Ciertas discontinuidades de la masa son visibles directamente (diaclasas, fisuras, fallas), dando al macizo rocoso la apariencia de un amontonamiento de bloques más o menos regulares y de aspecto monolítico (fig 11.1). Un análisis más detallado muestra que los propios bloques están afectados por discontinuidades matriciales. De hecho, la existencia de fisuras de este tipo queda demostrada mediante la observación directa en láminas delgadas, con inyección de resinas. La generación de ruidos internos en una probeta sometida a una prueba de carga es, además, una manifestación cualitativa del crecimiento de dichas fisuras.

Son numerosas las propiedades mecánicas de las rocas que pueden ser interpretadas con base en la existencia de discontinuidades microscópicas o macroscópicas. En el laboratorio, la anisotropía, la influencia del agua en la resistencia, la compresibilidad, la variación de la permeabilidad hidráulica al aire y de la velocidad de trasmisión de ondas, en función del estado de esfuerzos aplicados, son ejemplos de la afirmación anterior. En el campo basta con mencionar la compresibilidad, permeabilidad y anisotropía de los macizos rocosos, esencialmente regidas por las juntas de estratificación, fracturas o fallas, para percatarse de la importancia de estas superficies de discontinuidad. Por tanto, no resulta excesivo afirmar que la propiedad fundamental de las rocas es su carácter discontinuo.

11.1 MUESTRAS DE ROCA

Una roca está formada por un conjunto de minerales surcado por discontinuidades. Se estudiará primero la estructura de la matriz rocosa, con objeto de definir las propiedades índice de las muestras de roca.

11.1.1 Estructura y propiedades índice de las rocas. **Porosidad.** Las rocas son materiales porosos. Ciertas rocas sedimentarias o ígneas extrusivas alcanzan valores de la porosidad de 20 por ciento, mientras que en las rocas ígneas intrusivas resultan del orden de 0.1 por ciento. La porosidad de la mayoría de las rocas queda comprendida entre esos límites.

La forma de las discontinuidades de la matriz rocosa es variable. Las rocas muy porosas tienen oquedades equidimensionales, aproximadamente esféricas, que provienen de desprendimientos de gases durante el enfriamiento de la roca ígnea extrusiva o de disoluciones por agua meteórica. Opuestamente, las rocas de porosidad reducida están surcadas por discontinuidades alargadas, en forma de grietas, producto de los esfuerzos internos generados en la matriz rocosa por efecto de la dilatación térmica diferencial de los minerales y, también, por efecto de los esfuerzos tectónicos. Los granitos, por ejemplo, formados por minerales de cuarzo y feldespato de coeficientes de dilatación volumétrica y de compresibilidad muy diferentes entre sí, son particularmente sensibles a los cambios de temperatura o del esfuerzo aplicado. Por tanto, no es sorprendente que tratando con granitos se haya podido

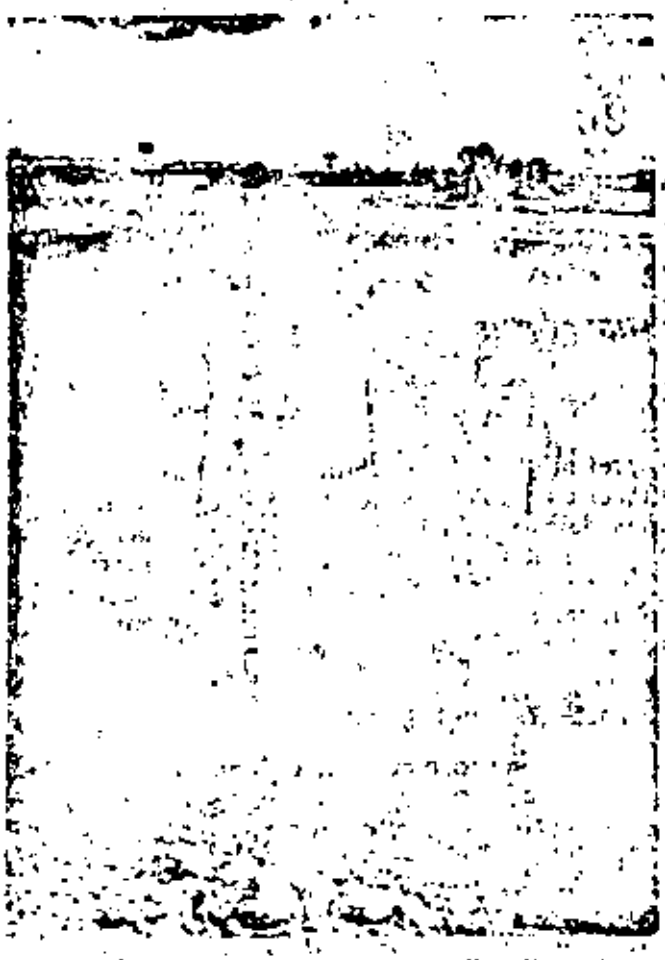

Fig 11.1 Los macizos rocosos son medios discontinuos

demostrar (Isnard y Leymarie, 1963) que las direcciones de fisuramiento de los minerales de cuarzo coinciden con las direcciones de las fracturas macroscópicas de la masa rocosa estudiada. En consecuencia, existe la posibilidad de que se puedan determinar las direcciones preferentes de las discontinuidades macroscópicas de un macizo rocoso (diaclasas, fallas, fracturas) a partir del estudio de las discontinuidades matriciales de la roca, lo que ha promovido el estudio detallado de la estructura matricial de las rocas en el laboratorio.

Con base en la distinción entre la porosidad ocasionada por las inclusiones y la debida a la presencia de grietas, se han definido la porosidad absoluta y la de fisuración. La primera se determina a partir de la medición del peso volumétrico de la muestra y de la densidad de sólidos. Este procedimiento, cuya precisión es del orden de 10 por ciento, arroja resultados variables, de acuerdo con el grado de conminución logrado en la roca. Para determinar la porosidad de fisuración se utiliza un porosímetro (Farran y Thenoz, 1965) que permite medir el volumen de aire que llena las grietas matriciales interconectadas. En forma indirecta, Walsh (1965) ha evaluado la porosidad de fisuración η_0 mediante la obten-

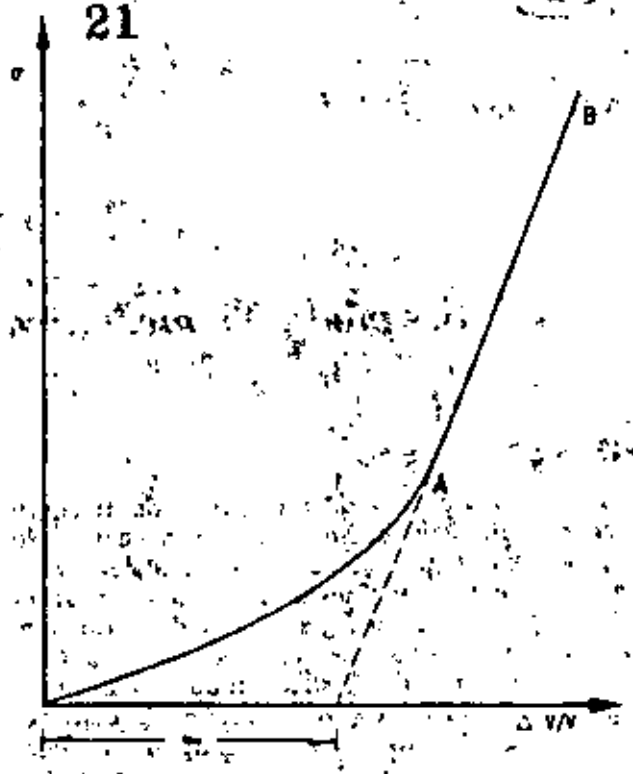

Fig 11.2 Variación del volumen de la muestra en función de la presión hidrostática aplicada

ción del módulo de compresibilidad volumétrica de una muestra de roca sometida a presión hi-

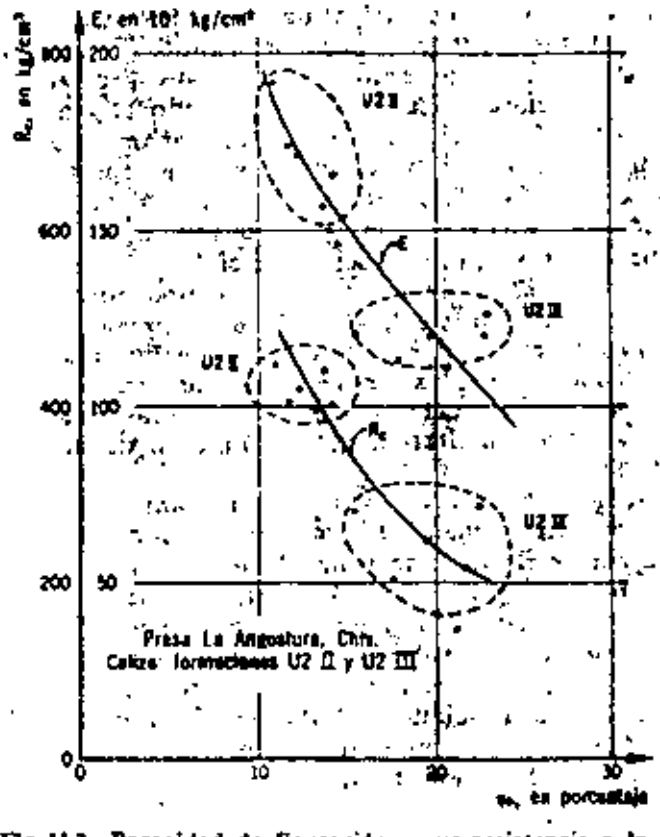

Fig 11.3 Porosidad de fisuración η_0 *vs* resistencia a la compresión, R_c, y módulo de deformabilidad, E

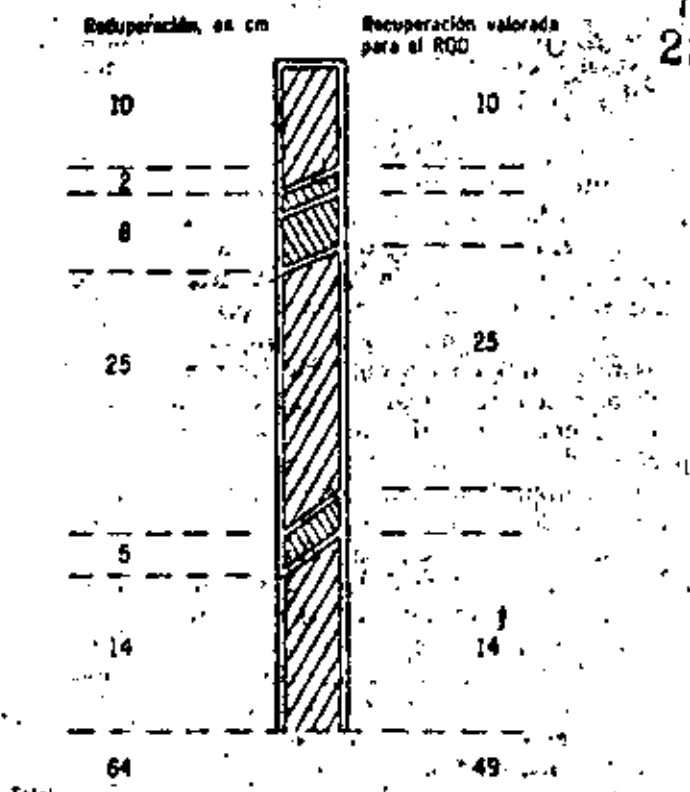

Fig 11.4 Recuperación total e índice de calidad de la roca

drostática. En la fig 11.2 se presenta un diagrama de variación del volumen de la muestra en función de la presión aplicada σ. Para niveles reducidos de σ, las fisuras se cierran progresivamente hasta alcanzar el punto A. La recta AB representa el comportamiento de la matriz no fisurada. En la misma gráfica se presenta la forma de valuar η_0.

La porosidad de fisuración está directamente ligada con la resistencia a la compresión simple de la roca y al módulo de deformabilidad inicial tangente (fig 11.3). También se ha establecido una correlación experimental entre la velocidad de las ondas longitudinales y transversales y la porosidad de fisuración (Morlier, 1969).

En ingeniería se ha definido (Deere, 1963) un índice de calidad de la roca, *RQD*, basado indirectamente en el número de fracturas observadas en los corazones provenientes de un muestreo. En lugar de determinar el número de fracturas de las muestras, se procede a valorar el cociente de la longitud que resulta de sumar únicamente los trozos de roca mayores de 10 cm (fig 11.4) y la longitud de avance del sondeo. La roca se clasifica de acuerdo con los valores del *RQD* (tabla 11.1).

Este índice se utiliza para establecer comparaciones entre muestras provenientes de diversos sondeos o zonas de un sitio estudiado.

Tabla 11.1 Descripción de la calidad de la roca

RQD, en porcentaje	*Calidad*
0- 25	Muy pobre
25- 50	Pobre
50- 75	Aceptable
75- 90	Buena
90-100	Excelente

Contenido de agua. Al aumentar el contenido de agua de una muestra de roca, disminuye su resistencia a la compresión simple. Dicha reducción de resistencia puede ser notoria, ya sea por la disminución de los esfuerzos efectivos o por efecto de cambios estructurales, particularmente en aquellos materiales ligeramente cementados y que no han estado sometidos previamente a saturación. En ciertas tobas muestreadas en el sitio de la presa Santa Rosa, Jal., la saturación produjo una disminución de la resistencia a la compresión simple de 210 a 30 kg/cm² en condiciones no drenadas (Instituto de Ingeniería, 1965). Más notorio es el caso mencionado por Colback y Wiid (1965). Al variar el contenido de agua de una cuarcita de 0.005 a 0.09 por ciento, pasando del estado seco al saturado, la resistencia a la compresión simple varió de 1 900 a 900 kg/cm² (fig 11.5).

La presencia de agua en las fisuras de las rocas provoca la reducción de la energía superficial de sus minerales, o sea, la cohesión de la

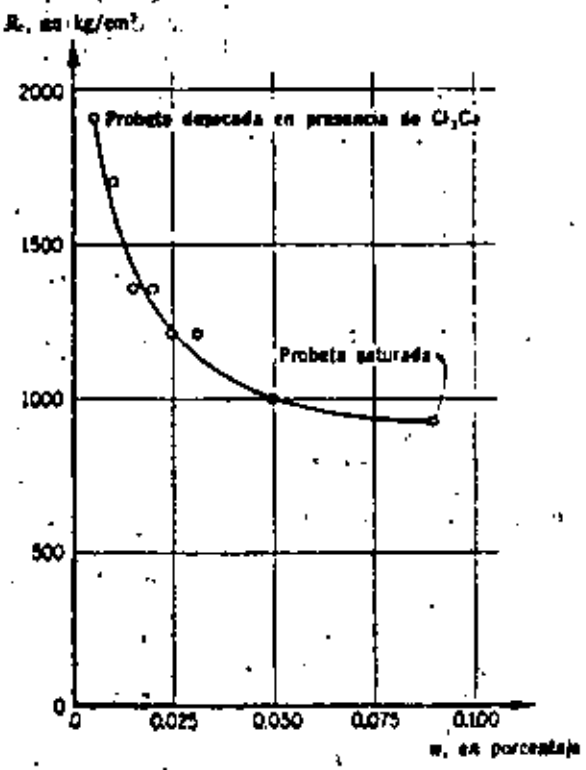

Fig 11.5 Relación entre la resistencia a la compresión simple, R_c, y el contenido de agua, w, de una cuarcita (Colback y Wiid, 1965)

roca disminuye por la simple presencia de agua en los poros; en consecuencia, al saturarse la muestra, su deformabilidad aumenta y su resistencia a la compresión simple disminuye (Boozer *et al*, 1962). Asimismo, las laderas del embalse y una presa, al saturarse, pueden sufrir una reducción drástica de su resistencia al cortante, por lo que pueden generarse movimientos notables de la masa rocosa y aun fallas de talud.

Alteración y alterabilidad. Las rocas, al ser sometidas a la acción agresiva del ambiente, sufren modificaciones en su estructura y composición mineralógica o, en otros términos, se alteran. En relación con este fenómeno, se estudian dos características de la roca: su alteración y su alterabilidad. El grado de alteración de una roca es un parámetro con el que se trata de definir el estado presente de la roca; la alterabilidad es la capacidad de una roca para alterarse en el futuro, bajo las condiciones ambientales reinantes en el sitio.

Cuando se altera una roca aumenta su porosidad. Las clasificaciones de las muestras provenientes de una formación rocosa dada, adoptando como criterios el grado de alteración o la porosidad serán, por tanto, idénticas. Sin embargo, resulta delicado determinar en forma precisa la porosidad de una roca. Por esta razón, tomando en cuenta la existencia de una relación entre esta magnitud y el peso de agua absorbida por la muestra previamente secada, al sumergirla (Krynine y Judd, 1957) se ha optado (Hamrol, 1962) por definir el grado de alteración como

$$i \text{ por ciento} = \frac{P_2 - P_1}{P_1} \times 100 \quad (11.1)$$

donde:

P_2 peso de la muestra al finalizar la prueba de absorción
P_1 peso de la muestra secada en horno a 105°C

La prueba de absorción se realiza manteniendo la muestra sumergida en agua durante un lapso constante de hora y media.

El grado de alteración se relaciona con la resistencia y deformabilidad de la roca: a mayor grado de alteración, menor resistencia y mayor deformabilidad del material. También el efecto de escala (inciso 11.1.2) disminuye al crecer el grado de alteración. Esto implica que la alteración, al aumentar, opaca el carácter discontinuo de la matriz rocosa y que, para valores grandes del índice de alteración, el comportamiento de la roca tiende al de un suelo en que el efecto de escala es reducido.

Al estudiar la alterabilidad de una roca es necesario subrayar nuevamente la importancia de su microfisuración. De hecho, las discontinuidades de la matriz rocosa juegan un papel fundamental en el proceso de alteración; las fisuras abiertas permiten el acceso del agua hacia la matriz rocosa, agua que actúa entonces sobre áreas importantes de los minerales. Sin fisuras, la alteración de la masa rocosa sería prácticamente nula; sin embargo, resulta difícil valorar la influencia de la fisuración sobre la alterabilidad de una roca, pues su importancia está condicionada por otro factor: la alterabilidad específica de los minerales en las condiciones ambientales del sitio, o sea que la alterabilidad de una roca es consecuencia de la fisuración y la alterabilidad específica de sus minerales.

Se ha comprobado experimentalmente que la circulación de agua en las rocas compactas es posible solo a partir de un valor de la permeabilidad al aire igual a 10^{-7} cm/seg, aproximadamente (Farran y Thenoz, 1965). De acuerdo con este criterio, que refleja la influencia de la fisuración de la roca en su alterabilidad, se pueden distinguir dos grandes familias de rocas. La primera queda integrada por las muy compactas, en las que el agua no circula y, por tanto, son inalterables sea cual fuere la alterabilidad específica de sus minerales. Las rocas de la segunda familia son permeables al agua y por tanto alterables, en caso de que sus minerales sean de elevada alterabilidad específica. Con objeto de valorar la alterabilidad específica de los minerales de una roca, se procede a una prueba de percolación con agua del sitio investigado a través de una muestra de la roca (Farran y Thenoz, 1965). La disminución o aumento del coeficiente de permeabilidad de la roca en función del tiempo indica la existencia de una reacción química entre el agua y los minerales constitutivos, o sea una alterabilidad específica diferente de cero. También es significativa la comparación entre la composición química del agua inyectada y la filtrada.

Al tratar de aplicar en la obra los resultados obtenidos en el laboratorio, es necesario tener en cuenta los daños ocasionados a la roca por los métodos de ataque, principalmente los explosivos. Una roca que es inalterable *in situ* por ser su permeabilidad al aire inferior a 10^{-7} cm/seg, puede tornarse alterable si los procedimientos de excavación utilizados aumentan en forma notable su fisuración.

En conclusión, la alterabilidad de una roca depende de su grado de fisuración, inherente o provocado, y de la alterabilidad específica de sus minerales.

Sensitividad. El concepto de sensitividad de una muestra de roca se establece analizando la variación de su permeabilidad al agua, en función del estado de esfuerzos aplicado (Bernaix, 1967).

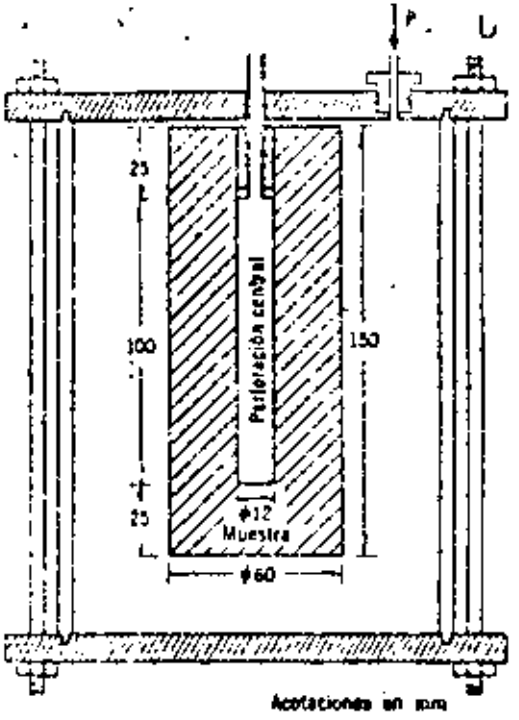

Fig 11.6 Prueba de permeabilidad. Flujo radial convergente

La muestra probada (fig 11.6) está formada por un corazón de 60 mm de diámetro y 150 mm de longitud, perforado en la parte central. En el extremo superior del conducto central, de 12 mm de diámetro y 100 mm de largo, se adapta un tubo metálico pegado a la roca con araldita. Las pruebas de permeabilidad se efectúan provocando un flujo radial de agua a través de la muestra, flujo que puede ser convergente o divergente. En el primer caso (fig 11.6), la muestra se introduce en un recipiente hermético alimentado con agua a presión, p. El conducto central, que comunica con el exterior del recipiente, colecta el agua de filtración. En el segundo caso el agua a presión se inyecta en el conducto central de la muestra y se mide el gasto de filtración que fluye a través de la superficie lateral de la muestra.

Las redes de flujo, en las muestras probadas con flujo convergente o divergente, son idénticas. En consecuencia, la magnitud de las fuerzas de volumen debidas al gradiente hidráulico son iguales en ambas pruebas, pero ocasionan esfuerzos efectivos de compresión en el caso de flujo convergente y de tensión en el de flujo divergente. Si las rocas son fisuradas, las permeabilidades medidas con flujo divergente o convergente resultan diferentes, debido a la apertura o cierre de las fisuras por efecto de los esfuerzos de tensión o de compresión inducidos en las respectivas pruebas. Se denomina sensitividad de la roca a la magnitud

$$S = \frac{k_{-1}}{k_{+1}} \qquad (11.2)$$

cociente de las permeabilidades medidas en condiciones de flujo radial divergente a presión de 1 kg/cm² y flujo radial convergente a una presión de 50 kg/cm².

En numerosos casos de roca de diversas características se ha podido establecer una correlación entre el valor de la sensitividad S y la intensidad de su fisuración (Habib y Bernaix, 1970). La sensitividad de las rocas porosas no fisuradas es igual a 1 y alcanza valores de 10 000 para las muy fisuradas, como por ejemplo el gneis de Malpasset en Francia.

La variación de la permeabilidad en función del estado de esfuerzos aplicado, que constituye la base del concepto de sensitividad, no solo permite valorar la intensidad de la fisuración de una muestra de roca, sino interpretar los resultados de las pruebas de permeabilidad Lugeon efectuadas en el campo (Sabarly, 1968). El gasto Q de inyección de agua con presión p en una masa de roca fisurada que se comporta elásticamente, sigue la ley

$$Q = A\,p^{n} \qquad (11.3)$$

siendo A una constante.

En otros términos, la permeabilidad de la masa rocosa depende de la magnitud de la presión aplicada, pues provoca la apertura de las fisuras preexistentes en el medio. Esta ley se ha verificado en ciertos casos (fig 11.7), como los presentados por Sabarly (1968).

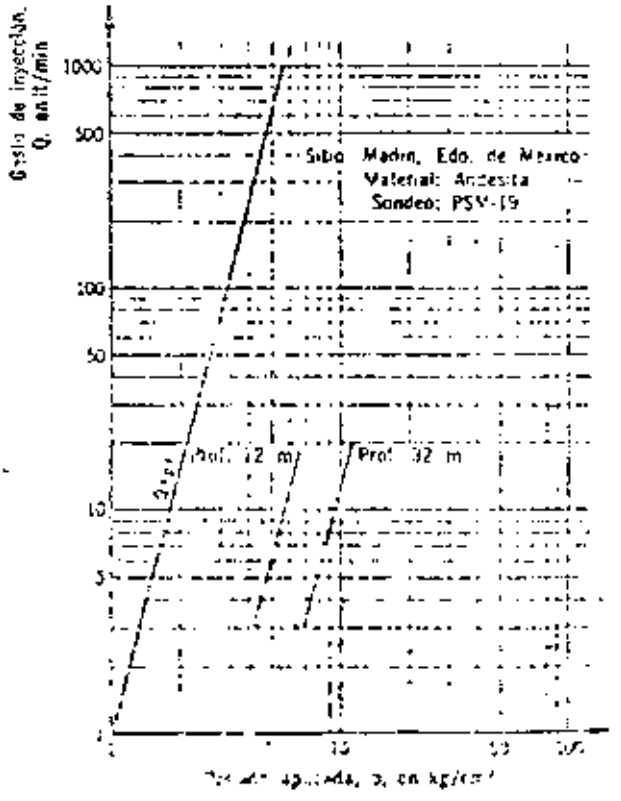

Fig 11.7 Resultados de las pruebas Lugeon

En conclusión, la permeabilidad de la roca, a pequeña o gran escala, es variable en función del estado de esfuerzos aplicados por su efecto en el ancho de las fisuras tanto microscópicas como macroscópicas. La falla de la presa Malpasset en Francia, así como la variación del gasto de filtración en la cimentación en función del nivel de agua en el embalse, son manifestaciones a gran escala de este fenómeno (Sabarly, 1968); asimismo, en la presa Santa Rosa, Jal. (fig 11.8*a*) se observaron filtraciones en la galería de drenaje del arco de concreto que aumentan conforme al nivel del embalse de acuerdo con la ley presentada en la fig 11.8*b*, según la cual

$$\frac{Q}{Q_1} = \left(\frac{Z - Z_0}{Z_1 - Z_0}\right)^{10} \qquad (11.4)$$

donde Q y Q_1 son los gastos de filtración correspondientes a los niveles Z y Z_1 del embalse. Esta ley de variación corresponde a la siguiente idealización del fenómeno de apertura y cierre de las fisuras: puede suponerse que el gasto de filtración en la cimentación de la presa es proporcional al cubo del ancho e de las fisuras y a la carga de agua H. A su vez, el ancho de las fisuras varía con el estado de esfuerzos en la cimentación de la presa, que se modifica de acuerdo con el nivel H del agua en el embalse. Suponiendo que el ancho e de las fisuras en la cimentación aguas arriba de la presa varía proporcionalmente al momento de empotramiento del arco en su base, resulta que

$$e \sim H^3$$

por lo cual

$$q \sim He^3 \sim H^{10}$$

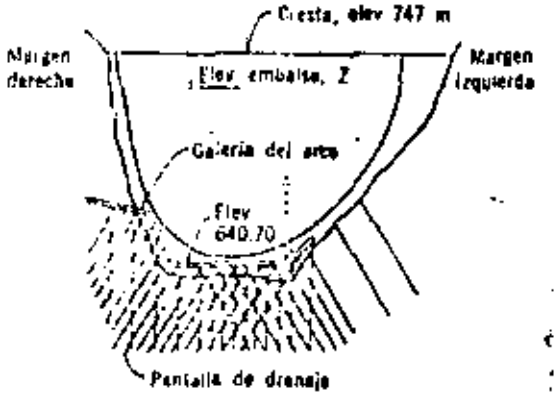

Fig 11.8*a* Presa Sta. Rosa, Jal. Vista desde aguas abajo

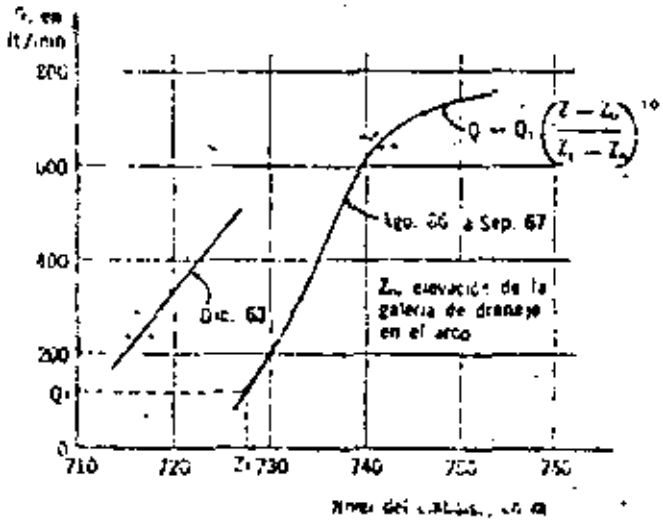

Fig 11.8*b* Variación de los gastos de filtración en la galería del arco vs elevación del agua en el embalse

11.1.2 Resistencia y deformabilidad. La resistencia y la deformabilidad de la matriz rocosa, ocasionalmente pueden ser de utilidad directa para el diseño de las obras (pilares de excavaciones subterráneas, por ejemplo). Sin embargo, en la mayoría de los problemas planteados en una obra, la resistencia y deformabilidad de la matriz rocosa es de poco interés; en efecto, tratando con masas rocosas, la resistencia de las discontinuidades macroscópicas, como fallas o juntas, es la que rige el problema. Por tanto, los estudios de laboratorio se han utilizado fundamentalmente para ahondar en el comportamiento básico de las rocas, consideradas como medios discontinuos, utilizando un enfoque estadístico. Se ha logrado determinar en el laboratorio la influencia de la forma y dimensiones de las probetas, velocidad de carga y presión del fluido intersticial. La dispersión de los resultados obtenidos con muestras probadas en iguales condiciones, es también un parámetro fundamental.

Efecto de escala. Los resultados numéricos de las pruebas de resistencia realizadas con muestras cilíndricas de igual relación de esbeltez, varían con el volumen de las probetas ensayadas. Esta propiedad es característica de los medios fracturados o discontinuos.

La interpretación teórica de la disminución de resistencia en compresión simple al aumentar el volumen se basa en conceptos probabilísticos expuestos por Weibull (Jaeger y Cook, 1969), como el del *eslabón más débil* de una cadena. Según este concepto, la resistencia de un material surcado por discontinuidades queda condicionada por la resistencia del elemento de volumen que contiene la zona más débil, o sea la más fisurada. Si para una densidad de fisuración dada el volumen de la probeta crece, el número total de discontinuidades aumenta, así como la probabilidad de incidir una fisura grande en la muestra.

Suponiendo una función de densidad probabilística de la resistencia, se puede establecer una

relación entre el volumen de la muestra y su resistencia. De acuerdo con la función exponencial para la densidad probabilística de la resistencia, propuesta por Weibull, la relación entre la resistencia media en compresión simple, $\bar{R}_c$, de una probeta y su volumen, V, esta dada por

$$\bar{R}_c = (\alpha V)^{-1/m} \left\{ \frac{1}{m} \Gamma\left(\frac{1}{m}\right) \right\} \qquad (11.5)$$

en que α y m son constantes características del material y Γ es la función gamma. También se puede establecer que la variancia de la resistencia es igual, en esas condiciones, a

$$\sigma^2 = (\alpha V)^{-2/m} \left\{ \frac{2}{m} \Gamma\left(\frac{2}{m}\right) - \frac{1}{m^2} \Gamma^2\left(\frac{1}{m}\right) \right\} \qquad (11.6)$$

Con base en las relaciones anteriores se obtiene que el coeficiente de variación de la resistencia a la compresión simple de un lote de muestras de una misma roca es

$$\frac{\sigma}{\bar{R}_c} = \sqrt{\frac{2/m!}{(1/m!)^2} - 1} \qquad (11.7)$$

Este resultado es interesante, pues indica que el coeficiente de variación de la resistencia a la compresión simple de un lote de muestras es, de acuerdo con la teoría de Weibull, independiente del volumen de la probeta. La experiencia muestra que, por lo menos en ciertos casos (Bernaix, 1957), este coeficiente de variación es efectivamente independiente del volumen de los especímenes probados y, por tanto, constituye un parámetro característico de la roca ensayada en el sentido de que depende únicamente de m, que es una constante para cada material.

Tomando entonces como valor índice del efecto de escala el cociente de las resistencias a la compresión simple de probetas de relación de esbeltez 2 y diámetros 1 cm y 6 cm, resulta, de acuerdo con la ec 11.5:

$$\frac{\bar{R}_c \phi_{10}}{\bar{R}_c \phi_{60}} = (216)^{1/m} \qquad (11.8)$$

$$\frac{\sigma}{\bar{R}_c} = \sqrt{\frac{2/m!}{(1/m!)^2} - 1} \qquad (11.9)$$

Ambas ecuaciones dependen únicamente del parámetro m y, en consecuencia, no son independientes. En la fig 11.9 se presentan las variaciones de los parámetros $\bar{R}_c \phi_{10}/\bar{R}_c \phi_{60}$ y $\sigma/\bar{R}_c$ en función de m.

De acuerdo con la ley de Weibull (fig 11.9), a mayor valor de m menor efecto de escala y menor coeficiente de variación de los resultados.

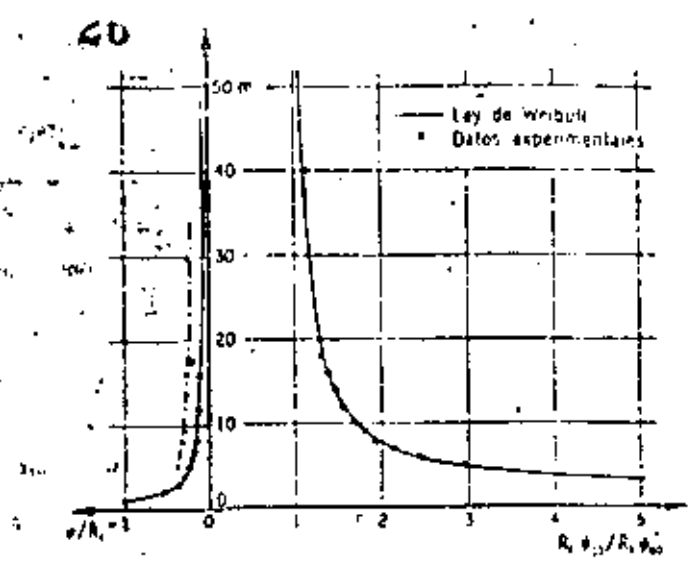

Fig 11.9 Efecto de escala y dispersión de los resultados de resistencia a la compresión simple

En otros términos, a mayor grado de fisuración de la roca, mayor efecto de escala y mayor dispersión.

La tendencia mostrada por los resultados experimentales es la misma (fig 11.9). Con estos mismos datos reportados por Bernaix (1967) y Jaeger y Cook (1969), que se obtuvieron ensayando un número grande de probetas, se formó la tabla 11.2.

Aunque la aplicación de la ley de Weibull al caso de las rocas sea conceptualmente discutible (Bernaix, 1967; Hudson, 1968), los resultados obtenidos en pruebas de compresión simple verifican satisfactoriamente esta ley.

El efecto de escala es un factor fundamental para el diseño de los pilares de excavaciones subterráneas. La resistencia a la compresión simple de un pilar de una mina puede ser notablemente inferior a la de corazones de tamaño reducido si la roca se encuentra muy fisurada. La dispersión de los resultados experimentales de pruebas de compresión simple permite orientar la elección del parámetro m que rige la magnitud del factor de escala.

El factor de escala disminuye al aumentar la presión confinante que actúa sobre la muestra, pues induce el cierre de las fisuras preexistentes y, por tanto, pierde importancia el carácter discontinuo de la roca (Habib y Vouille, 1966). Correlativamente, cuando aumenta la presión de confinamiento, disminuye el coeficiente de variación de la resistencia al corte.

La comparación de las resistencias al esfuerzo cortante determinadas en el laboratorio con probetas de dimensiones reducidas, *in situ* en áreas grandes, muestra también que el efecto de escala es tanto más pronunciado cuanto más acentuado es el carácter discontinuo de la roca. Por

Roca	Fisuración	m	$\frac{\sigma}{\bar{R}_c}$	$\frac{\bar{R}_c \phi_{10}}{\bar{R}_c \phi_\infty}$	Referencia
Gneis de Malpasset, margen derecha	Microfisuración y macrofisuración muy intensas	5	0.37	2.9	Bernaix (1967)
Gneis de Malpasset, margen izquierda	Microfisuración y macrofisuración intensas	8	0.30	1.9	Bernaix (1967)
Carbón de Duffryn	Surcado de fisuras y debilidades visibles	9.4	0.29	1.8	Jaeger y Cook (1969)
Caliza fisurada	Microfisuración débil. Macrofisuración intensa	16	0.25	1.4	Bernaix (1967)
Gneis con biotita y muscovita	Microfisuración media	30	0.22	1.2	Bernaix (1967)
Carbón de Barnsley Hards	Macrofisuración nula	17.5	0.19	1.35	Jaeger y Cook (1969)
Caliza de Saint Vaast	Fisuras inexistentes	∞	0.05	1.00	Bernaix (1967)

ejemplo, Rocha (1964) muestra que al aumentar el grado de alteración de un granito, o sea, al disminuir su carácter de material fisurado, el efecto de escala disminuye (fig 11.10).

En conclusión, y de acuerdo con lo expresado en el inciso 11.1.1, la sensitividad de una roca, así como el factor de escala o la dispersión de su resistencia a la compresión simple, son manifestaciones de una misma realidad: su fisuramiento. En consecuencia, no es raro que estos parámetros no sean independientes. De hecho, se ha establecido (Bernaix, 1967; Habib y Bernaix, 1970), una correlación entre la sensitividad S, el coeficiente de variación $\sigma/\bar{R}_c$ y el factor de escala $\bar{R}_c \phi_{10}/\bar{R}_c \phi_\infty$: a mayor sensitividad, mayor dispersión de la resistencia a compresión simple y mayor factor de escala.

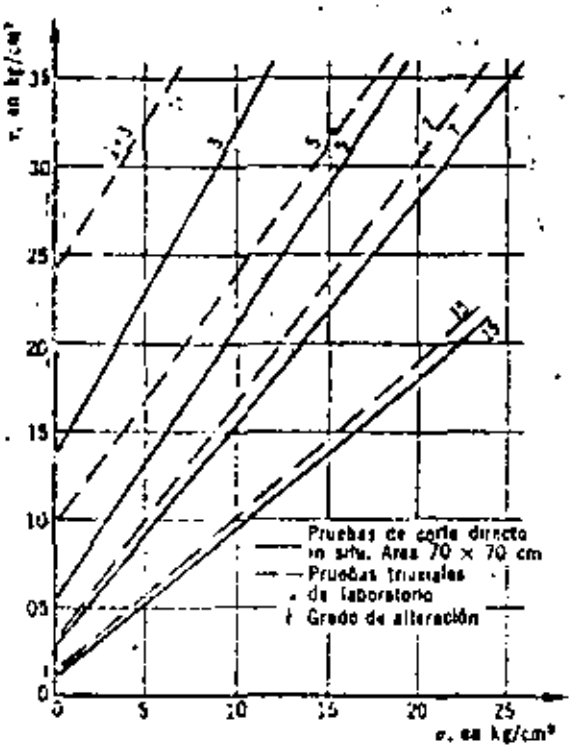

Fig 11.10 Disminución del efecto de escala con el aumento del grado de alteración, i (véase 11.1.1)

Efecto de la forma. Son numerosos los estudios relativos a la influencia de la forma de las probetas sobre la resistencia a la compresión simple, así como las fórmulas propuestas para representar la reducción de resistencia observada al aumentar la relación de esbeltez de los especímenes. Parece ilusoria, en realidad, la búsqueda de una fórmula general aplicable cualesquiera que sean los materiales probados, la forma de las muestras y los procedimientos de ensaye utilizados; sin embargo, los estudios efectuados por Berthier y Tourenq (1966) y Grosvenor (1963) han establecido que la resistencia disminuye apreciablemente al aumentar la relación de esbeltez hasta 2. Para valores superiores a 2, la variación de resistencia es reducida. En la fig 11.11 se presenta la variación de la resistencia a la compresión simple de muestras de andesita alterada en función de su relación de esbeltez.

En consecuencia, la práctica común consiste en efectuar las pruebas de resistencia con especímenes que tienen relación de esbeltez igual a 2.

Anisotropía. Las rocas metamórficas presentan a menudo textura foliada en la cual los minerales laminares, como mica y clorita, están alineados paralelamente unos con otros (gneis, pizarras, esquistos, por ejemplo). Se supone que en estos casos el comportamiento de las rocas es anisotrópico. En efecto, el módulo de deformabilidad en el sentido normal a la foliación es inferior al medido paralelamente a la foliación hasta en 40 por ciento para los esquistos (Dayre y Sirieys, 1965), 25 por ciento para las pizarras y las filitas, y 10 por ciento para las cuarcitas (Brace, 1970). Para estas últimas, en el plano

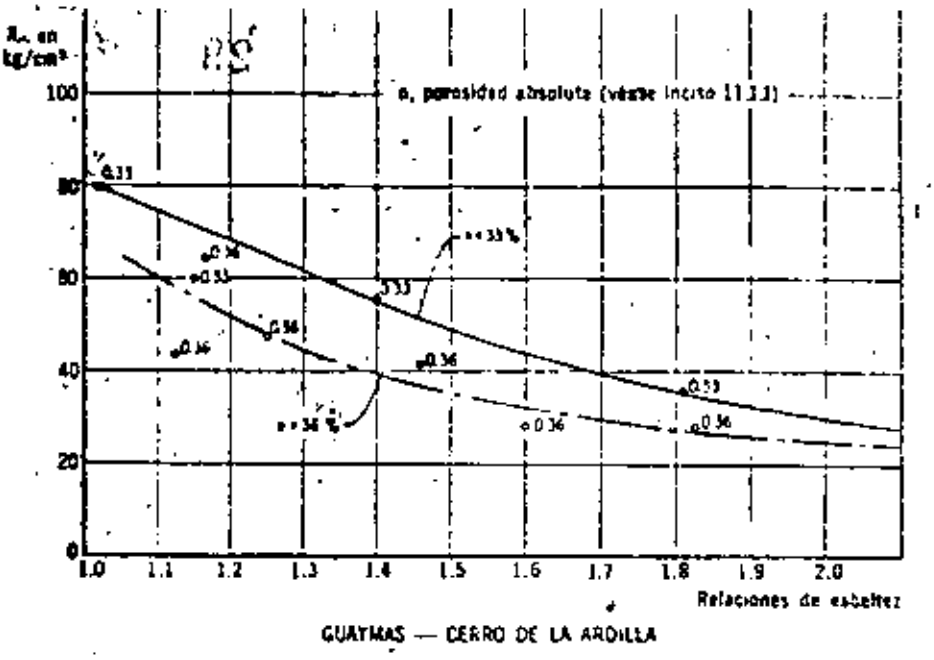

Fig 11.11 Variación de la resistencia a la compresión simple con la relación de esbeltez en la muestra de toba andesítica intemperizada

de la foliación, en cualquier dirección los módulos son aproximadamente iguales, o sea que se trata de materiales ortotrópicos. Su resistencia a la compresión simple varía con la magnitud del ángulo α, formado por la normal al plano de esquistosidad y la dirección del esfuerzo aplicado, y su valor mínimo se alcanza para α comprendido entre 50° y 80° (Dayre y Sirieys, 1965) (fig 11.12). A este tipo de anisotropía se denomina comúnmente anisotropía intrínseca.

La anisotropía en el comportamiento puede deberse a otra causa: una fisuración según direcciones privilegiadas, preexistente o inducida durante la prueba por los esfuerzos aplicados. A este respecto, Walsh (1965) mostró que el módulo de deformabilidad, en sentido normal a una fisura abierta, disminuye en función del cubo de la longitud de esta. En consecuencia, el estado de esfuerzos aplicado, sea por efecto del tectonismo, sea durante una prueba de laboratorio, y la consecuente fisuración inducida ocasiona una anisotropía cuya magnitud depende de la longitud de las fisuras así creadas.

La utilización de esos datos en la práctica resulta delicada, pues son numerosos los casos de problemas estructurales en los cuales es desconocida la dirección de los esfuerzos principales actuantes en cada punto de la masa. En esas condiciones, no queda otra solución que realizar el diseño utilizando los valores mínimos de los parámetros de resistencia de las rocas involucradas.

Efecto de las presiones de poro. Las pruebas triaxiales efectuadas con muestras de roca indican, sin lugar a dudas, que el principio de esfuerzos efectivos se aplica al comportamiento de las rocas. La resistencia a la falla de una muestra de roca sometida a una prueba triaxial es función del esfuerzo confinante efectivo, o sea del esfuerzo confinante total aplicado menos la presión de poro desarrollada (Bäron *et al*, 1963; Handin *et al*, 1963).

Es importante señalar que, en los experimentos diseñados con el fin de determinar la resistencia de una roca en términos de esfuerzos efectivos, resulta fundamental la consideración de la velocidad de carga o de deformación aplicada. En efecto, la permeabilidad de las probetas de rocas compactas es muy pequeña (del orden de 10^{-9} o 10^{-11} cm/seg), y en consecuencia el lapso de la presión de poro de la muestra es grande. Si el intervalo de tiempo a la falla impuesto no es mayor que el lapso de uniformación de la presión de poro, la medición de esta en la base de la probeta carece de sentido, pues no

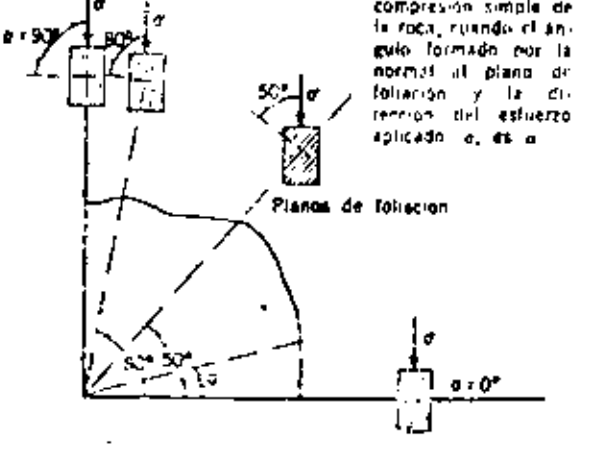

Fig 11.12 Diagrama polar de la resistencia a la compresión simple de una roca foliada

es representativa de la presión de poro media actuante en la muestra. Por tanto, la resistencia en términos de esfuerzos efectivos de un material dilatante y saturado, probado en forma rápida, resulta superior a la del mismo material en estado seco, porque las presiones de poro negativas que se desarrollan no son medidas correctamente en la base de la muestra (Brace, 1970).

La generación y disipación de estas presiones de poro negativas bajo el efecto de una carga rápida ocasiona, por tanto, un incremento transitorio de resistencia de la roca, en términos de esfuerzos totales. Este fenómeno puede explicar el retraso que se presenta en ciertas minas profundas entre la apertura del túnel y la falla violenta de las paredes (*popping*).

También en el caso de taludes se ha observado que el proceso de falla ocurre en forma discontinua, a saltos, y una de las causas de este mecanismo podría ser la mencionada antes.

Estas evidencias experimentales subrayan la importancia del factor tiempo en la resistencia y deformabilidad de las rocas, que además muestran a largo plazo un comportamiento viscoso.

Comportamiento viscoso. La reducción en el diámetro de lumbreras de las antiguas minas romanas en el norte del Adriático, del antiguo "Pozo de Abraham", cerca de Jerusalén, y de las lumbreras de acceso a túneles de riego de Irán, son ejemplos del comportamiento viscoso de las rocas a largo plazo (Westergaard, 1952).

En la fig 11.13 se presenta la variación con el tiempo de las deformaciones de muestras de una misma roca sometidas a esfuerzos desviadores σ crecientes. Cuando σ es menor que el esfuerzo s, llamado resistencia última, las deformaciones alcanzan un máximo siguiendo una ley asintótica. En cambio, si σ es mayor que s, el flujo viscoso de la roca presenta tres fases:

a) Transitoria (fase I), con velocidad decreciente de deformación.

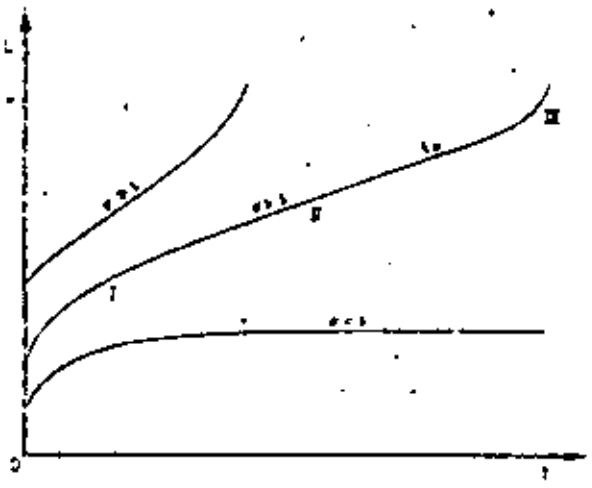

Fig 11.13 Variación de la deformación en función del tiempo

b) Estacionaria (fase II), con velocidad constante de deformación $\dot{\varepsilon}_m$.

c) De falla (fase III), en que la velocidad de deformación aumenta.

Las leyes experimentales utilizadas para describir cada una de estas fases son muy numerosas (Jaeger y Cook, 1969; Morlier, 1966).

Generalmente, la ley empírica utilizada para representar el comportamiento de flujo transitorio es la propuesta por Lomnitz (1956):

$$\varepsilon(t) = \varepsilon_e + A \ln(1 + \alpha t) \qquad (11.10)$$

donde ε_e es la deformación instantánea, y A y α son constantes del material que dependen de la temperatura y de la presión confinante aplicada.

La velocidad de deformación $\dot{\varepsilon}_m$, durante la etapa de flujo estacionario es, de acuerdo con Griggs

$$\dot{\varepsilon}_m = \dot{\varepsilon}_0 \operatorname{senh}\left(\frac{\sigma - s}{\sigma_0}\right) \qquad (11.11)$$

en que $\dot{\varepsilon}_0$ y σ_0 son constantes del material y s es su resistencia última.

Al comparar esta relación con la propuesta por Morlier (1966) para calcular el tiempo a la falla, t, de una muestra:

$$\dot{\varepsilon}_m t_r = cte \qquad (11.12)$$

resulta que

$$t \dot{\varepsilon}_0 \operatorname{senh}\left(\frac{\sigma - s}{\sigma_0}\right) = cte \qquad (11.13)$$

En otras palabras, el tiempo a la falla de una muestra sometida a un esfuerzo desviador σ es inversamente proporcional al seno hiperbólico de la diferencia $(\sigma - s)$. Este resultado es importante, pues coincide con numerosos datos experimentales (Morlier, 1966; Saito y Uesawa, 1961) y permite calcular el tiempo a la falla de una masa de roca a partir del momento en que su velocidad de deformación es constante.

Con base en su comportamiento reológico, las rocas pueden clasificarse en tres familias: densas-duras, porosas y plásticas-blandas. En la tabla 11.3 se presentan los valores de la resistencia última para distintas rocas sometidas a pruebas de *creep* bajo esfuerzo axial constante y esfuerzo confinante nulo, a la temperatura ambiente.

El comportamiento reológico de las rocas varía también en función del esfuerzo confinante y la temperatura; al aumentar el esfuerzo confinante aplicado o la temperatura ambiente, predomina el componente plástico. En consecuencia, aumen-

Tabla 11.3. Resistencia última de varias rocas

Familia	Roca	Resistencia última, en porcentaje de R_c	Referencia
I. Rocas densas-duras	Granito	80	Morlier (1966)
	Gneis	85	
	Caliza	80	
	Caliza	80	
II. Rocas porosas	Dolomita	50	Price (1966)
	Arenisca Wolstanton	60	
	Arenisca Darley	50	
	Caliza	35	
	Granodiorita	27	
	Alabastro	30	
	Arenisca Pennant	20	
III. Rocas plásticas blandas	Potasa	25	Morlier (1966)

R_c resistencia a la compresión simple

tan sus deformaciones diferidas y disminuye la relación de la resistencia última a la resistencia medida con velocidad de carga convencional.

Esos datos experimentales han sido integrados, mediante el uso de modelos reológicos tipo Kelvin o Burgers, en el análisis de las deformaciones a largo plazo medidas en pruebas de placa u observadas en excavaciones subterráneas.

Finalmente, es digno de mención el hecho de que al tratar de representar, mediante modelos, los fenómenos tectónicos que ocurren en la corteza terrestre, haya sido necesario elegir materiales tan viscosos como la parafina para representar el comportamiento de las rocas.

11.1.3 Criterios de falla. El comportamiento de las rocas sometidas a pruebas de compresión triaxial varía en función del tipo de roca y del nivel de esfuerzos confinantes aplicados.

Al probar una serie de muestras provenientes de un mismo macizo rocoso, a presiones confinantes σ_3 crecientes, se observa una variación en las relaciones esfuerzo-deformación (fig 11.14). En efecto, para presiones σ_3 reducidas, la muestra se comporta en forma elástica hasta niveles altos del esfuerzo desviador y falla repentinamente en forma frágil, produciéndose fisuras paralelas a la dirección del esfuerzo principal mayor σ_1. Cuando las presiones σ_3 aumentan, la curva esfuerzo-deformación presenta un máximo seguido de una disminución de resistencia y la muestra falla a lo largo de planos inclinados con respecto a la dirección del esfuerzo σ_1. Finalmente, para presiones σ_3 muy elevadas, el comportamiento de la muestra se asemeja al de un material elasto-plástico perfecto o con endurecimiento por deformación.

El valor del esfuerzo confinante σ_3 para el cual el material se torna plástico o dúctil a la temperatura del ambiente, depende del tipo de roca. Las rocas densas-duras (granitos inalterados, cuarcitas y calizas competentes) se tornan plásticas para valores del esfuerzo confinante superiores a 1 000 kg/cm² (Baron *et al*, 1963), que, evidentemente, no se presentan en ingeniería civil. Sin embargo, al tratar con problemas de vulcanología puede ser útil considerar esfuerzos confinantes de esta magnitud asociados a elevadas temperaturas (Mooser, 1969). Las rocas que se toman dúctiles a niveles de esfuerzos confinantes comunes en obras de ingeniería son las más blandas y porosas (calizas recientes, margas, silvinitas, etc). Puede decirse, sin embargo, que en general la mayoría de las rocas se comportan en forma frágil en los problemas de ingeniería civil.

En vista de la complejidad del comportamiento de una roca, es evidente que no se puede definir un criterio de falla único. Por tanto, en el intervalo de comportamiento frágil, el criterio comúnmente utilizado es el propuesto por Griffith (1925); para niveles intermedios de la presión confinante se emplea el criterio de falla de Mohr-Coulomb, y para valores elevados de la presión confinante se aplican los criterios clásicos de Tresca o de Von Mises.

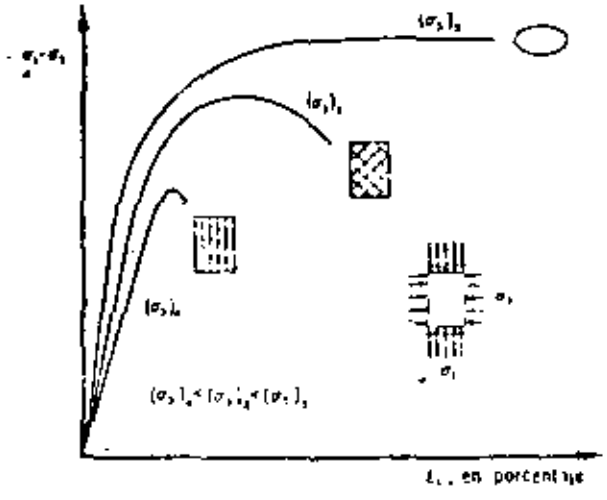

Fig 11.14 Variación del comportamiento de una roca en función del esfuerzo confinante aplicado

Criterio de falla frágil de Griffith. El esfuerzo T teóricamente necesario para fallar a tensión un material frágil y perfectamente homogéneo es:

$$T = \frac{E}{10} \qquad (11.14)$$

siendo E su módulo de elasticidad (Freudenthal, 1950). Sin embargo, este material ideal dista mucho de ser representativo de las rocas, que fallan a tensión bajo esfuerzos mucho menores. Por tanto, es preciso admitir que esta discrepancia se debe a las concentraciones de esfuerzos que se presentan en la cercanía de las fisuras que surcan la matriz rocosa. Griffith (1925) analizó estas concentraciones de esfuerzos y supuso que las discontinuidades de la matriz son de forma elíptica.

Consideremos el caso de una muestra de roca sometida a una prueba triaxial (fig 11.15). La discontinuidad supuesta se asemeja a una elipse de ejes Ox y Oy inclinados según el ángulo β con respecto a la dirección del esfuerzo principal mayor. En tales condiciones y suponiendo que el material es elástico, se demuestra que en la cercanía de la cúspide de la discontinuidad:

$$\sigma_s = \frac{2\,(\sigma_y\, m - \tau_{xy}\,\alpha)}{m^2 + \alpha^2} \qquad (11.15)$$

siendo m la excentricidad de la elipse, o sea el cociente de la longitud b de su eje menor y la de su eje mayor, a; α es el ángulo polar correspondiente al punto de intersección de la elipse con el plano normal a esta en que actúa σ_s (fig 11.15).

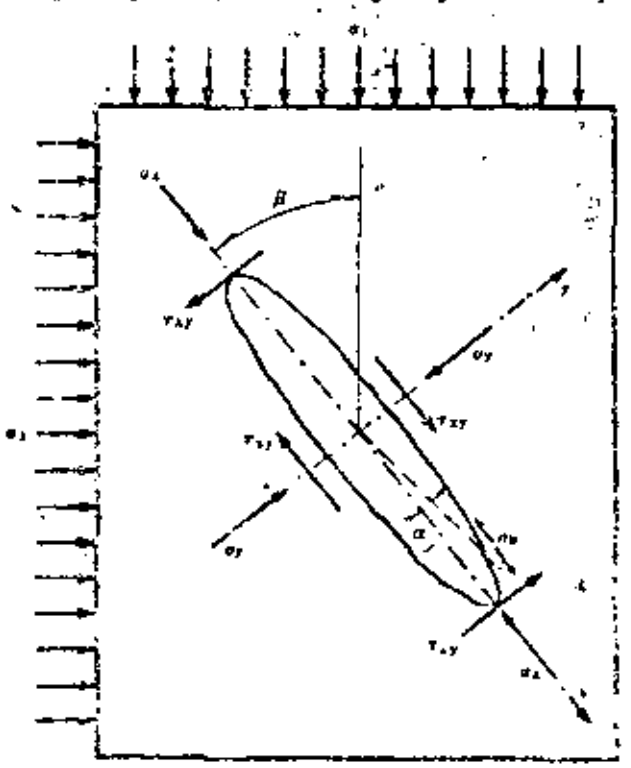

Fig 11.15 Criterio de Griffith. Nomenclatura

Para $\alpha = 0$, $\sigma_y = \sigma_1$ y $\tau_{xy} = 0$, la ec 11.15 se reduce a la propuesta por Griffith para la resistencia a tensión del material, σ_t

$$\sigma_t = \frac{2\,\sigma_1}{m} = 2\,\sigma_1 \sqrt{\frac{a}{r_m}} \qquad (11.16)$$

siendo r_m el radio de curvatura de la elipse, en su cúspide.

El máximo valor de σ_s se obtiene para

$$\alpha = -\frac{m\,\tau_{xy}}{\sigma_y - (\tau_{xy}^2 + \sigma_y^2)^{1/2}}$$

y vale

$$\sigma_s = \frac{1}{m}\left[\sigma_y - (\tau_{xy}^2 + \sigma_y^2)^{1/2}\right] \qquad (11.17)$$

Remplazando en esta última expresión la magnitud $m\,\sigma_s$ obtenida mediante la ec 11.16, resulta:

$$2\,\sigma_t = \left[\sigma_y - (\tau_{xy}^2 + \sigma_y^2)^{1/2}\right]$$

o sea

$$\tau_{xy}^2 = 4\,\sigma_t\,(\sigma_t - \sigma_y) \qquad (11.18)$$

La ecuación parabólica 11.18 representa la envolvente de Mohr correspondiente al criterio de Griffith.

Si en lugar de haber una sola discontinuidad en la masa la fisuración fuera isotrópica, la falla ocurriría a lo largo de las fisuras para las que el esfuerzo de tensión generado fuera máximo. Dichas fisuras están orientadas según el ángulo β, tal que

$$\cos 2\beta = \frac{\sigma_1 - \sigma_3}{2\,(\sigma_1 + \sigma_3)} \qquad (11.19)$$

En ese caso, los esfuerzos principales correspondientes a la falla se relacionan mediante la ecuación

$$(\sigma_1 - \sigma_3)^2 + 8\,\sigma_t\,(\sigma_1 + \sigma_3) = 0 \qquad (11.20)$$

La resistencia a la compresión simple resulta, por tanto, igual a ocho veces la resistencia a la tensión del material, lo cual coincide satisfactoriamente con los datos experimentales.

La teoría de Griffith aquí expuesta define las relaciones entre esfuerzos principales que determinan el inicio de la propagación de las fisuras,

pero no abarca su desarrollo subsecuente. Esta relación entre esfuerzos principales no siempre coincide con un criterio de falla. En efecto, si para una prueba de tensión es de esperarse que la propagación de la fisura normal al esfuerzo aplicado lleve de inmediato a la falla del espécimen, no ocurre lo mismo en una prueba de compresión triaxial. En este caso, la fisura se propaga siguiendo un camino curvo hasta que se torna paralela a la dirección del esfuerzo principal mayor de compresión; en ese momento la fisura deja de propagarse (Brace y Bombolakis, 1963). Este fenómeno se correlaciona con las observaciones de los microrruidos que se generan durante la prueba a partir de esfuerzos de 25 y 60 por ciento de la resistencia a compresión simple para granitos porosos y densos, respectivamente (Peraml y Thenoz, 1969).

En conclusión, el criterio de falla de Griffith representa adecuadamente el comportamiento de las muestras de roca sometidas a esfuerzos de tensión. En el caso de pruebas de compresión, la relación entre esfuerzos principales que resulta de la teoría de Griffith corresponde, más bien, al inicio de la fase de microfisuración de la roca; en cuanto a la falla, esta ocurre por generación de esfuerzos cortantes excesivos a lo largo de las discontinuidades así creadas (fig 11.16). En consecuencia, el criterio de falla comúnmente utilizado para el caso de compresiones triaxiales es el de Mohr-Coulomb.

Criterio de Mohr-Coulomb. Este criterio que matemáticamente puede expresarse

$$\tau = c + \mu \sigma \qquad (11.21)$$

implica la falla por cortante a lo largo de planos. La teoría de Griffith despreciaba el hecho de que las fisuras pueden cerrarse cuando los esfuerzos de compresión son suficientemente grandes. En tal caso, es de esperarse que se generen fuerzas de fricción entre las caras de la fisura, y para tomar en cuenta este efecto Mc Clintock y Walsh (1962) modificaron la teoría de Griffith. El resultado más importante de esta proposición es que para presiones normales elevadas, el criterio modificado de Griffith coincide estrictamente con el de Mohr-Coulomb. Por tanto, para fines prácticos y para presiones confinantes suficientemente grandes, puede considerarse válido el criterio de Mohr. Sin embargo, para presiones confinantes superiores a 1 000 kg/cm² y en el caso de rocas duras y densas, el material deja de comportarse como friccionante y se torna dúctil, siendo aplicables los criterios de falla de Tresca o Von Mises.

Criterios de Tresca y Von Mises. Se ha estudiado detenidamente el comportamiento dúctil de las rocas debido a sus implicaciones en problemas de geofísica y geología. En el campo de la mecánica de rocas su importancia es mucho menor, pues son pocas las circunstancias en que las temperaturas y presiones aplicadas a las rocas las tornan dúctiles.

Los criterios clásicos utilizados son los de Tresca y Von Mises, que suponen que la falla ocurre cuando el máximo esfuerzo cortante o la energía de distorsión, respectivamente, alcanzan un valor prefijado. Las expresiones correspondientes son, para el criterio de Tresca

$$\sigma_1 - \sigma_3 = cte \qquad (11.22)$$

y para el criterio de Von Mises

$$(\sigma_1 - \sigma_3)^2 + (\sigma_1 - \sigma_2)^2 + (\sigma_2 - \sigma_3)^2 = cte \quad (11.23)$$

siendo σ_1, σ_2 y σ_3 los esfuerzos principales.

11.2 MASAS ROCOSAS

El comportamiento mecánico e hidráulico de una masa de roca depende primordialmente de la configuración de sus discontinuidades. Estas se agrupan en familias de juntas, planos de estratificación, superficies de foliación y fallas. El primer paso al estudiar un sitio ha de ser, por tanto, la clasificación y levantamiento de las superficies de discontinuidad de la masa rocosa.

11.2.1 Clasificación y levantamiento de discontinuidades. La característica que permite diferenciar las fallas de las juntas es su corrimiento; las juntas son fracturas sin corrimiento y transversales a la estratificación o esquistosidad, mientras que las fallas constituyen superficies de discontinuidad con un corrimiento relativo entre ambos bloques de roca.

Las fallas se clasifican como normales, inversas, o transversas según las direcciones de los

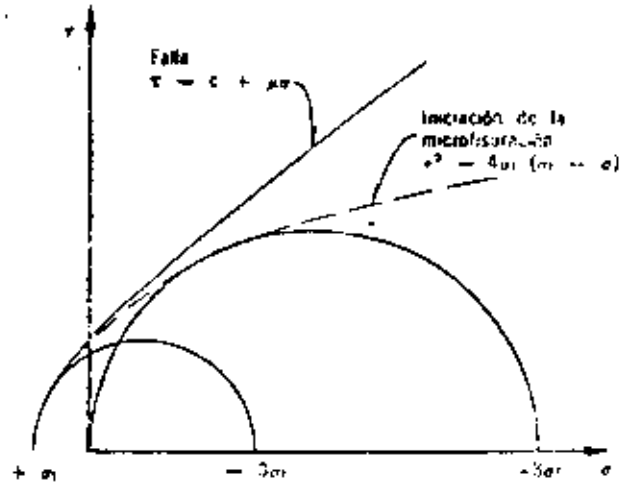

Fig 11.16 Envolvente de falla de las rocas

2.3 PROPIEDADES MECANICAS DE LOS MACIZOS ROCOSOS

2.3.1 Conceptos fundamentales

El comportamiento de los macizos rocosos queda determinado principalmente por las discontinuidades que lo afectan, tales como fallas, fracturas y planos de estratificación. La influencia de la masa rocosa o roca propiamente dicha en el comportamiento del macizo por ella integrada juega un papel secundario la mayoría de las veces.

El conocimiento de las características físicas de un macizo rocoso, es decir de las características de los accidentes que lo afectan, de su distribución, orientación y frecuencia, se logra con ayuda de la geología que nos aporta datos que ayudarán a calificar la calidad de un macizo rocoso más bien desde un punto de vista cualitativo que cuantitativo.

La cuantificación de las propiedades mecánicas e hidráulicas de los macizos en una de las actividades inherentes en el campo de la mecánica de rocas y dado que las propiedades de los macizos dependerán, como se anotó antes, de los accidentes geológicos que los afecten, la relación entre ambas disciplinas debe ser muy estrecha.

Las propiedades de los macizos que interesan al ingeniero civil para la adecuada planeación, diseño, construcción y operación de sus obras son la deformabilidad, resistencia y permeabilidad, así como el estado de esfuerzos que actúa en el macizo antes de ejecutar en él cualquier obra y las deformaciones o desplazamientos que lo estén afectando. Cada tipo de obra demandará el conocimiento de propiedades específicas.

La determinación de propiedades en los macizos obviamente se efectúa mediante ensayes "in situ" a gran escala, tanto como sea práctico y representativo.

La clasificación de los macizos rocosos desde el punto de vista ingenieril, puede efectuarse cualitativamente, con base en datos geológicos levantados o bien cuantitativamente con base en resultados de ensayes "in situ", zonificándolos de acuerdo a criterios establecidos que definan zonas

del macizo con características semejantes.

2.3.2. Su influencia en la estabilidad de las obras subterráneas y a cielo abierto.

Diferentes obras requieren del conocimiento de diferentes propiedades del macizo rocoso en el que se proyectarán. Las solicitaciones impuestas por las estructuras (presas, túneles, excavaciones, etc.) definen la necesidad de conocer la respuesta del macizo a ellas mismas. Asimismo, definen o condicionan el tipo de prueba más conveniente a llevar a cabo para determinación de la propiedad respectiva.

Como fue dicho, la cuantificación de las propiedades de un macizo puede considerarse como la expresión en términos ingenieriles de los efectos que causan los accidentes geológicos en el macizo, sin embargo, el conocimiento de la propiedad cuantitativamente no es suficiente para estimar el comportamiento de un macizo ante la presencia de una estructura en él. Hace falta siempre la descripción de accidentes en el macizo para conocer tamaño de bloques que pudieran formarse, relleno existente en fracturas, frecuencia de las mismas, etc. etc., en fin datos que ayuden a interpretar los resultados de los ensayes de campo con las características del macizo, y como ambos influenciarán el comportamiento de la estructura, para tomarlo en cuenta en el diseño de la misma.

La tabla siguiente, tomada del reporte de la Comisión para efectuar recomendaciones sobre las técnicas de investigación de sitios, de la Sociedad Internacional de Mecánica de Rocas, orienta sobre el tipo de prueba conveniente a efectuar en relación con la propiedad requerida y el tipo de obra.

2.3.3. Su obtención en el sitio de las obras

A continuación se incluyen notas en las que se describe la obtención de propiedades mecánicas e hidráulicas de

de macizos rocosos "in situ" y de técnicas para monitorizar macizos rocosos en su comportamiento antes y después de efectuar obras en ellos.

TABLE 7.1 — ROCK MECHANICS IN-SITU TESTS

LEGEND

Test importance	Stage of the work
n — necessary s — advisable o — of interest ( ) — alternative	P — Feasibility DD — Detailed design DC — During construction AC — After completion

IN SITU MECHANICAL TESTS \ TYPE OF WORK		FOUNDATIONS			NATURAL AND ARTIFICIAL ROCK SLOPES		UNDERGROUND WORK		ROCK EXCAVATION	HARBOURS AND OTHER SUBMARINE WORKS
		Gravity Dams	Arch Dams	Large Structures	Tunnelling Excavations	Involving other works	Large Underground Works	Tunnels, Shafts Underground Mining	Open Air Mining, Quarries, Large Surface Excavations	
1.	**Deformability Tests**									
1.1	*Static Method*	nDD	aF; nDD; nAC	aDD			nDC			oF
1.1.1	Plate bearing (hydraulic jack; flat jack; cable jacking)		(n)DD; (n)AC				(n)DD	nDC		
1.1.2	Pressure tunnel (water loading; radial jacks)		(n)DD, (n)AC				(n)DD			
1.1.3	Pressure borehole (dilatometer)	nF	(n)DD; (n)AC	oF			aF; (n)DD	oDC		
1.2	*Dynamic Method*	nDD	nF; nDD; nAC	oF			aF; aDC	hDC		aF
1.2.1	Measurement of longitudinal waves velocity (geophones)	nDD	nF; (n)AC				aF	nDC		
1.2.2	Measurement of the velocity of longitudinal and transversal waves Love's waves Rayleigh's (vibrograph)		nDD; (n)AC				nDD			
1.2.3	Measurement of direct longitudinal waves velocity in borehole (sonic-coring)		aDD; (n)AC				aDC			
1.2.4	Detailed stratigraphic surveys							nDC		
2.	**Natural rock mass stresses tests**									
2.1	*Rock Surface Tests*						aF; nDD			
2.1.1	Measurement of deformation after overcoring or bond removal (by strain									

	...ests)						(n)F			
2.1.2	Measurement of pressure to balance natural stresses (by flat jack)						s(P			
2.2	*Test fault: Partially*	oFDD	oDD	oDD	oiF		oDD			
2.2.1	Measurement of core deformation after overcoring						oDD			
2.2.2	Measurement of borehole wall deformation after overcoring						nDD			
3.	Strength tests									
3.1	*Compressive*		nDD							oiDD
3.1.1	Triaxial tests		oiDD				nDD			
3.2	*Shear*	nDD	nDD	nDD	nDD	nDD	nDD	nDD	nDD	
3.2.1	Rock block test along discontinuity surface	nDD	nDD	nDD	nDD	nDD	nDD	nDD	nDD	
3.2.2	Concrete block test along interface	nDD	nDD	nDD					oiF	
4.	Permeability									
4.1	*Inside Borehole (Lugeon)*	nF; nAC	nF; nAC	nF	nF		nF			
4.2	*In c joint sampling test*	nF; nAC	nF; nAC							
4.3	*Piezometric level and ground-water flow*				nAC		nF	nF	oiF	nF
5.	Rock Anchor tests				nF; nDC; oiAC	nF; nDC; oiAC	nDD	nDD	nDC	oiDC
6.	Rock movement monitoring									
6.1	*Long base extensometer*	nAC	nAC		nAC	nAC	nAC			
6.2	*Inverted pendulum*	nAC	nAC	nAC	oiAC					
6.3	*Slope indicator*				nAC				nAC	
6.4	*Bloor and ground-motion monitoring*	oiDD	oiDD		nDC	nDC	nF; nDC	nF; nDC		oiDC
6.5	*Rock noise monitoring*				nAC				oiAC	oiAC

PRUEBAS DE CAMPO EN MECANICA DE ROCAS

POR: RAUL CUELLAR BORJA

OFICINA DE MECANICA DE ROCAS

COMISION FEDERAL DE ELECTRICIDAD

C O N T E N I D O

1.- PROPIEDADES GEOMECANICAS

1.1.-Introducción

El conocimiento de las propiedades geomecánicas de las rocas tiene por objeto el comprendimiento del comportamiento estructural de los macizos rocosos durante la ejecución de obras de ingeniería tales como cimentaciones, excavaciones subterráneas o a cielo abierto, taludes artificiales o naturales.

Estas propiedades geomecánicas de las rocas se obtienen mediante ensayes de laboratorio y de campo, tanto estáticos como dinámicos.

A continuación se indican algunas de estas propiedades:

Porciento de recuperación de barrenación

Porciento de recuperación de barrenación modificado (R.Q.D. - Rock Quality Designation)

Permeabilidad de la masa de roca

Composición mineralógica

Textura

Estructura

Densidad

Peso volumétrico

Porosidad

Indice de alteración

Permeabilidad al aire o al agua

Resistencia en compresión simple

Resistencia en tensión simple

Resistencia en tensión bajo flexión(módulo de ruptura)

Resistencia en corte simple, doble y punzonado

Resistencia en corte directo

Resistencia al corte bajo compresión triaxial

Relación de Poisson

Módulo elástico en especímenes de laboratorio

Módulo de deformabilidad de campo

Módulo elástico dinámico

Velocidad sónica

Resistividad eléctrica

1.2.- Aplicaciones

En seguida mencionaremos algunas aplicaciones de las propiedades geomecánicas de las rocas:

a) Determinación de la capacidad de carga de la roca para efecton de diseño de cimentaciones. (Edificios, cortinas de concreto)

b) Diseño de excavaciones subterráneas y a cielo abierto

c) Diseño de sistemas de soporte (anclas, marcos, concreto lanzado, revestimiento de concreto, camisas metálicas,etc.)

d) Tratamiento de la roca para consolidación o impermeabilización, mediante la inyección de mezclas de cemento y productos químicos

e) Proyecto de sistemas de drenaje

f) Proyecto de sistemas de excavación

g) Diseño de voladuras

2. MEDICION DE ESFUERZOS Y DEFORMACIONES EN MACIZOS ROCOSOS

2.1. Introducción

El comportamiento estructural de los macizos rocosos bajo solicitaciones de carga estáticas o dinámicas depende tanto de sus propiedades geomecánicas como del estado natural de esfuerzos.

En este capítulo describiremos algunos de los métodos empleados en la medición del estado de esfuerzos internos de los macizos de roca.

2.2. Estado natural de esfuerzos

Se entiende por estado natural o virgen de esfuerzos a los esfuerzos existentes en la corteza terrestre previamente a la ejecución de cualquier obra de ingeniería.

A la actualidad no ha sido posible desarrollar técnicas para la medición del estado natural de esfuerzos, pues siempre este se encuentra alterado en la vecindad de las excavaciones.

En los esfuerzos naturales están incluidos los esfuerzos ocasionados por fuerzas gravitatorias debidas al peso de la cobertura de roca, así como esfuerzos por procesos de cristalización, metamorfismo, sedimentación, consolidación desecación y tectónicos.

El concepto de un estado de esfuerzos gravitacional en un macizo rocoso en el cual la roca se comporta como un material elástico con deformación lateral totalmente restringida, es el siguiente, para un punto situado a una profundidad Z.

Esfuerzo principal vertical:

$$\sigma_1 = \gamma Z \quad \text{(donde } \gamma = \text{peso por unidad de volumen)}$$

Esfuerzo principal lateral:

$$\sigma_2 = \sigma_3 = \frac{\gamma}{1-\gamma}\ \sigma_1 \qquad \gamma = \text{relación de Poisson}$$

Puede darse el caso en que la roca se comporte como un material plástico ideal, en el cual la relación $\frac{\gamma}{1-\gamma} = 1$, teniéndose entonces el caso de un estado de presión hidrostático, el cual se ha demostrado que existe a grandes profundidades (> 300 m).

2.2.1.- Distribución de esfuerzos en torno a excavaciones en roca.

A continuación vamos a analizar los esfuerzos que se generan en la vecindad de una excavación, los cuales en algunos casos pueden alcanzar una magnitud varias veces superior a los esfuerzos naturales.

La distribución y magnitud de los esfuerzos alrededor de una sola abertura en roca elástica masiva puede ser determinada apropiadamente por la teoría elástica, o utilizando modelos fotoelásticos, haciendo suposiciones respecto de las propiedades mecánicas de la roca, la forma de la abertura y los esfuerzos de campo o sea el estado natural de esfuerzos antes de la excavación.

En el desarrollo de este problema deberán tomarse en cuenta las siguientes suposiciones:

1.- Roca masiva, elástica linealmente, homogénea e isotrópica

2.- La abertura está en un medio infinito. (La distancia de la abertura a la frontera más cercana deberá estar por lo menos a 3 veces la dimensión de la abertura)

3.- La abertura es larga comparada con su sección transversal, y

el eje longitudinal de la abertura es horizontal.

4.- La sección transversal de la abertura puede ser representada por formas geométricas simples como un círculo, elipse, óvalo, o rectángulo con esquinas redondeadas

5.- Los ejes de la sección transversal de la abertura son horizontal y vertical

6.- La distribución de esfuerzos a lo largo de la longitud de la abertura es uniforme e independiente de su longitud. Para esta condición el problema de la distribución de esfuerzos alrededor de la abertura se reduce a un estado de deformación plana y puede ser resuelto considerando un agujero en una placa sujeta a un estado bidireccional de esfuerzos de campo en el plano de la placa.

7.- El esfuerzo vertical sobre una sección horizontal de la roca, es igual al peso de la roca por arriba de la sección.

Esto es:

$S_v = - \gamma Z$ en donde: S_v = Esfuerzo de compresión vertical

γ = Peso volumétrico de la roca

Z = Cobertura de roca

8.- El esfuerzo horizontal correspondiente es

$S_h = MS_v$, en donde: S_h = Esfuerzo de compresión horizontal

M = Constante dependiente del estado de esfuerzos de campo

Vamos a considerar tres diferentes estados de esfuerzos de campo:

Relación entre esfuerzos horizontales y verticales $Sh = \frac{\gamma}{1-\gamma} S_v$

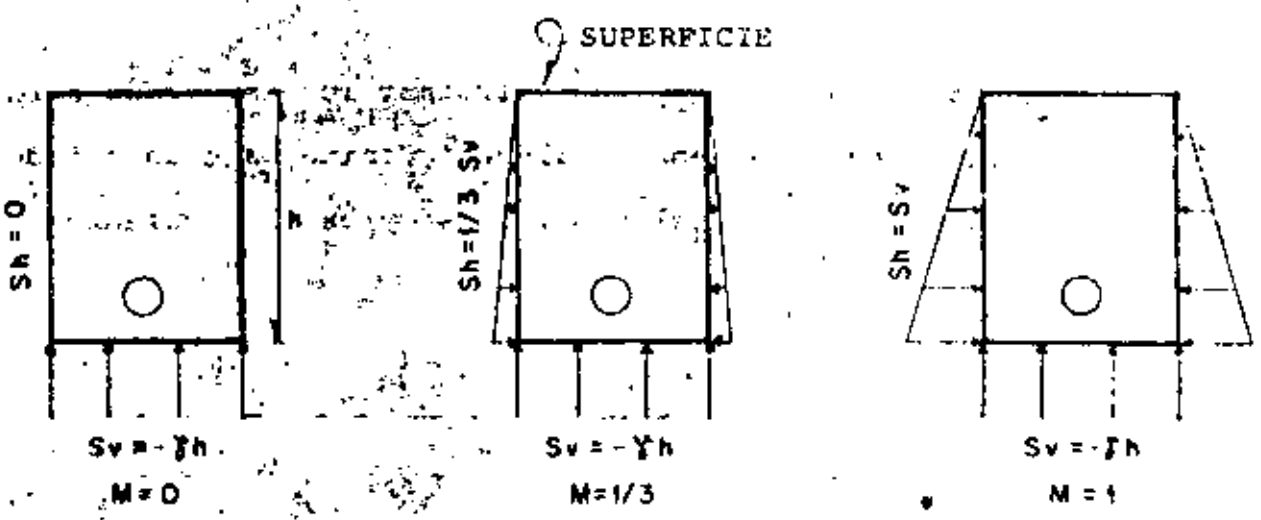

TIPOS SUPUESTOS DE ESFUERZOS DE CAMPO

El estado de esfuerzos representado por M = 0 puede ocurrir a bajas profundidades o cerca de superficies verticales libres.

El estado de esfuerzos representados por $M = \frac{1}{3}$ puede ocurrir para un amplio intervalo de profundidades. La relación entre esfuerzos horizontales y verticales para que no ocurra deformación lateral está dada por:

$$S_h = \frac{\gamma}{1-\gamma} S_v$$

en donde:

γ = relación de Poisson

Cuando $\gamma = 0.25$, la relación S_h a S_v es igual a $\frac{1}{3}$. Esto es, que el estado de esfuerzos corresponde a la condición de que no se presente deformación lateral en una roca con $\gamma = 0.25$.

El estado de esfuerzos representado por M = 1, puede ocurrir a gran profundidad o en rocas semiplásticas.

La solución exacta para determinar los esfuerzos alrededor de un agujero circular en una placa infinita bajo un estado biaxial de esfuerzos fue resuelto por Kirsh y es el siguiente:

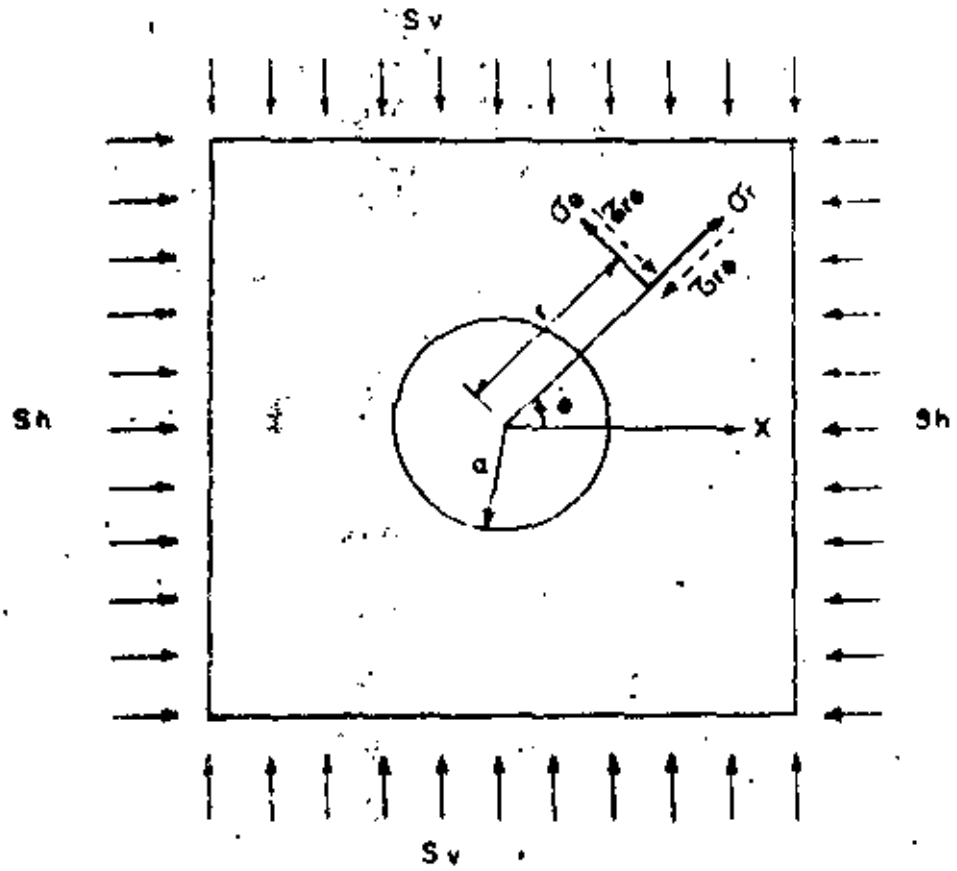

Esfuerzo radial: $\sigma_r = \frac{Sh+Sv}{2}\left(1-\frac{a^2}{r^2}\right)+\frac{Sh-Sv}{2}\left(1-\frac{4a^2}{r^2}+\frac{3a^4}{r^4}\right)\cos 2\theta$

Esfuerzo tangencial: $\sigma_\theta = \frac{Sh+Sv}{2}\left(1+\frac{a^2}{r^2}\right)-\frac{Sh-Sv}{2}\left(1+\frac{3a^4}{r^4}\right)\cos 2\theta$

Esfuerzo cortante: $\tau_{r\theta} = \frac{Sv-Sh}{2}\left(1+\frac{2a^2}{r^2}-\frac{3a^4}{r^4}\right)\operatorname{Sen} 2\theta$

En donde:

S_h = Esfuerzo horizontal aplicado

S_v = Esfuerzo vertical aplicado

σ_r = Esfuerzo radial

σ_θ = Esfuerzo tangencial

$\tau_{r\theta}$ = Esfuerzo cortante

a = radio del agujero

γ = distancia radial desde el centro del agujero

θ = ángulo con la horizontal

En este caso los esfuerzos dependen únicamente de S_v y S_h, no intervienen el módulo elástico E, ni la relación de Poisson γ, tampoco la dureza del material.

Análisis de esfuerzos en el túnel para una distribución de presiones de tipo hidrostático, o sea, $\sigma_h = \sigma_v$; este caso se presenta en túneles de gran cobertura, propuesto por el geólogo Heim en 1878. En este caso las expresiones para calcular los esfuerzos radiales y tangenciales corresponden a las fórmulas de Lamé para conductos de pared gruesa sujetos a una presión $\sigma_{h=\sigma v}$

Esfuerzo radial: $\sigma_r = \frac{S_h + S_v}{2} \left(1 - \frac{a^2}{r^2}\right)$

Esfuerzo tangencial: $\sigma_\theta = \frac{S_h + S_v}{2} \left(1 + \frac{a^2}{r^2}\right)$

Esfuerzo cortante: $\tau_{r\theta} = 0$

En este caso en toda la periferia del túnel el esfuerzo tangencial $\sigma_\theta = 2 S_v$

A continuación representaremos gráficamente las concentraciones de esfuerzos alrededor de un agujero circular para un estado biaxial de esfuerzos de campo.

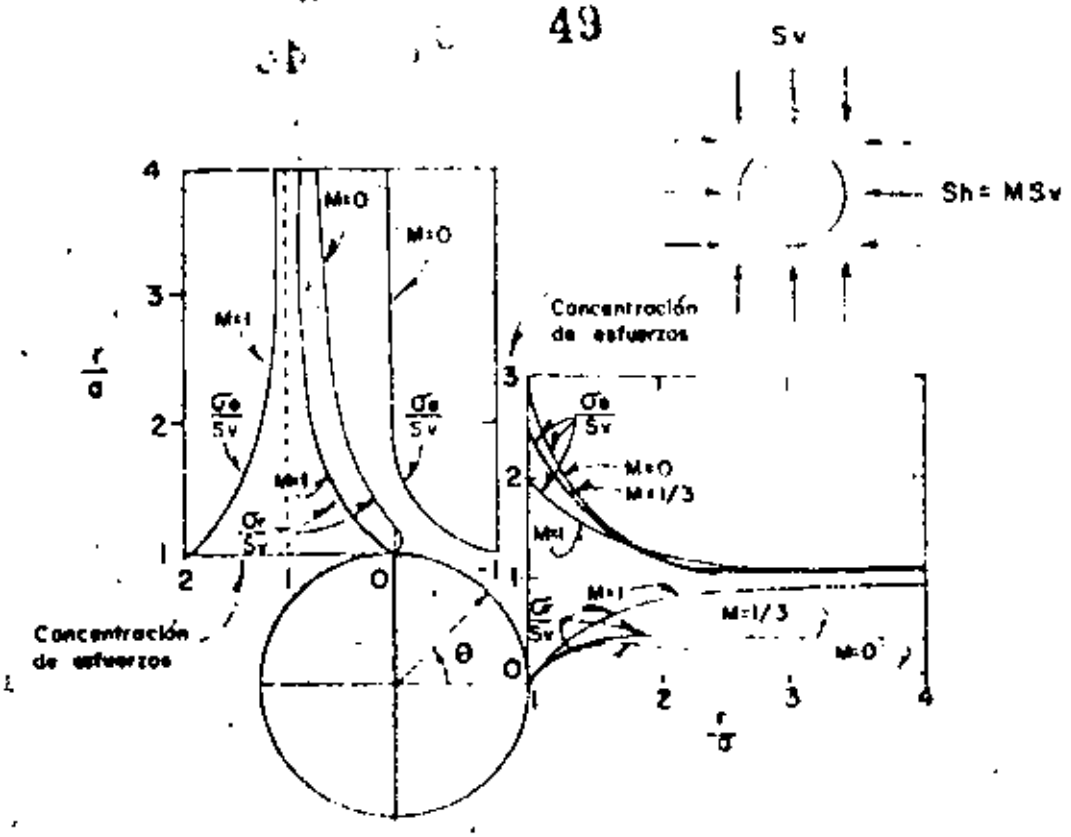

CONCENTRACION DE ESFUERZOS EN UN AGUJERO CIRCULAR PARA UN ESTADO BIAXIAL DE ESFUERZOS DE CAMPO

Una concentración de esfuerzos con signo positivo significa que los esfuerzos en un punto dado tienen el mismo signo que los esfuerzos exteriores aplicados.

Una concentración de esfuerzos con signo negativo significa que los esfuerzos en un punto dado tienen signo contrario a los esfuerzos exteriores aplicados.

2.3.- Principios de la medición de esfuerzos en roca

Existen dos tipos de mediciones:

a) Determinación del estado de esfuerzos absoluto

b) Determinación de esfuerzos relativos, es decir variaciones de esfuerzos.

Existe una amplia variedad de aparatos y métodos para ambos tipos de medidas.

En las rocas que muestran un comportamiento elástico, la medida de esfuerzos absolutos puede requerir la aplicación de un método de relajación de esfuerzos en el que el elemento rocoso donde se ha introducido el aparato de medida, se descarga de los esfuerzos ejercidos por la roca circundante. A continuación se mide la deformación a que ha dado lugar esta eliminación de esfuerzos y l conversión de la misma en esfuerzos se hace a partir de relaciones conocidas o supuestas de esfuerzo-deformación para la roca estudiada.

Los esfuerzos relativos pueden determinarse midiendo los esfuerzos absolutos al principio y al final de un intervalo de tiempo dado, pero esto no es siempre necesario y mientras sea posible no se utilizan para medir esfuerzos relativos las técnicas de relajación de esfuerzos que son lentas y costosas. En general los instrumentos empleados en ambos tipos de medidas son semejantes, algunos de ellos no pueden utilizarse para las dos determinaciones de esfuerzos.

2.3.1.- Método de relajación de esfuerzos

En este método el instrumento de medida debe adherirse a la superficie de la roca expuesta en la excavación. A continuación la zona de roca a la que se ha unido el instrumento se separa del entorno, cortando la roca con sierra haciendo ranuras que formen un cuadro o perforando una corona de barrenos secantes en torno a la misma. En otros casos la parte de roca y el instrumento asociado se recortan mediante una corona de perforación hueca de diámetro apropiado. A continuación se miden las deformaciones registradas en la roca independizada.

Entre los instrumentos empleados de esta forma se encuentran los extensómetros que miden la deformación superficial según tres direcciones, las rosetas de extensómetros y los medidores fotoelásticos biaxiales. Los resultados permiten identificar los esfuerzos principales, en un estado bidimensional, en el plano de la pared de la excavación. En este caso el tercer esfuerzo principal es nulo

La determinación del estado natural de esfuerzos requiere la realización de medidas más allá de la zona de influencia de la excavación. Esto puede conseguirse efectuando una perforación en el frente de la excavación y colocar el medidor dentro de la perforación. A continuación se realiza una sobrebarrenación y se miden las deformaciones ocasionadas al quedar libre la roca.

También en este caso los resultados proporcionan esfuerzos principales en el plano perpendicular al eje de la perforación. Hasta ahora prácticamente no se ha podido lograr medir los esfuerzos en tres dimensiones.

Se han empleado tres tipos de medidores de deformaciones en barrenos. Pueden clasificarse como "medidores de deformación transversal", "tensímetros de inclusión" y "celdas de deformación".

2.4.- Medidores de deformación transversal

(Borehole deformation meters)

Estos aparatos miden las variaciones en las dimensiones transversales de un taladro realizado en roca, cuando este se deforma como resultado de la variación de los esfuerzos. Los esfuerzos se calculan utilizando la teoría elástica que relaciona esfuerzos y deformaciones para un estado de deformación plana.

Entre estos medidores se encuentra el medidor del U.S.B.M. de Merril, que mide la deformación transversal del barreno en una sola dirección. Este aparato utilizado con éxito en los países de habla inglesa, se muestra en la figura 1, el elemento sensibl está constituido por una barra de cobre al berilio que trabaja en voladizo y está instrumentada con 4 celdas de deformación eléctrica (strain gages). Para efectuar la medición de esfuerzos mediante este aparato se requiere colocarlo en tres posiciones a 60° para lo que es necesario desplazarlo, lo cual limita la utilidad del aparato. Este aparato requiere una calibración previa a su uso.

En la Fig. 2 puede verse esquemáticamente el uso de este dispositivo.

Otro de estos medidores es el de Maihak, utilizado con éxito en Europa y Africa del Sur, el elemento sensible es de cuerda vibrante conectado a un vástago que se hace salir mediante un mecanismo de tornillo hasta que entra en contacto con las paredes del b[illegible]a

no. Como solo registra en una sola dirección diametral se requieren varias posiciones para obtener la solución del estado de esfuerzos.

El dispositivo de Cibek utilizado en Europa Central registra variaciones diametrales en dos direcciones ortogonales. En este aparato los vástagos de contacto actúan sobre una palanca mecánica haciendo variar la resistencia eléctrica de un potenciómetro. Como las medidas de los diámetros del barreno no se hacen en un mismo plano se han proyectado medidores múltiples en los Estados Unidos, por Grosvenor y Griswold y recientemente por Crouch y Fairhust. El de estos últimos los elementos sensibles están recogidos mientras el dispositivo se coloca en posición dentro del barreno, empujándolos contra las paredes del mismo mediante aire comprimido en el momento de realizar la medida. Los elementos sensibles son vástagos que apoyan sobre placas en voladizo instrumentadas con celdas de deformación eléctricas (strain gages).

2.4.1.- Medida de perfiles transversales

Susuki ha descrito un método para determinar los esfuerzos residuales en rocas, rectificando las paredes de un barreno mediante una piedra abrasiva y midiendo el perfil transversal antes y después de la sobrebarrenación. Las medidas se realizan con una celda cilíndrica y un micrómetro eléctrico o una celda presiométrica. Yorukan emplea también un presiómetro en un barreno acondicionado previamente revistiéndolo con una película de resina epoxy, vertida contra un molde para conseguir un perfil circular exacto.

2.5. Tensímetros de inclusión (borehole inclusión strenometer)

La diferencia entre un tensímetro de inclusión y un medidor de deformación transversal, es que aquellos pueden calibrarse directamente en esfuerzos. Los tensímetros son de hecho, inclusiones rígidas.

Las variaciones en los esfuerzos del macizo rocoso dan lugar a variaciones en el tensímetro que están poco influenciadas por variaciones en el módulo elástico de la roca. Es decir, no es necesario tener un conocimiento exacto del módulo de la roca. Cuanto más rígido sea el tensímetro, menor importancia tendrá el conocimiento del módulo del macizo rocoso.

Todos estos aparatos requieren de calibración previa, ya sea en una muestra de roca o en una placa de acero, por lo tanto no son medidores de esfuerzos en el sentido verdadero de la palabra.

La base teórica para los medidores de esfuerzos de inclusión fue dada por Sazawa y Nishamura basado en la distribución de esfuerzos en un tensímetro de inclusión circular en una placa sujeta a un estado biaxial de esfuerzos. En este caso la placa y el tensímetro se consideran linealmente elásticos, homogéneos e isotrópicos y con diferente módulo elástico. También debe existir una unión perfecta entre el tensímetro y las paredes del barreno.*

Estos medidores deben tener una precompresión inicial de manera que tengan posibilidad de medir esfuerzos de tensión. En ocasiones esto es una limitación pues al realizar la sobrebarrenación

*Coutinho derivó las relaciones entre los esfuerzos biaxiales aplicados a la placa y los esfuerzos desarrollados en el tensímetro de inclusión rígido que dió la base para el desarrollo de los tensímetros.

puede ocurrir que se rompa el cilindro de roca aislado por efecto de la presión inicial de precompresión de colocación del tensímetro.

Medidores que utilizan los principios indicados arriba son los de Hast, Wilson, Potts, May y Hawkes, requieren de una precompresión inicial previa a la sobrebarrenación. Estos medidores requieren de más de una utilización, en cambio los tensímetros fotoelásticos de Hiramtsu y Roberts son más sencillos y requieren una sola utilización para la determinación del estado de esfuerzos interno de la roca.

Tensímetro de Hast.- El elemento sensible de este dispositivo está constituido por un transformador diferencial lineal variable (LVDT).

Tensímetro de Potts. Este dispositivo tiene un sistema de presión hidráulica controlada por celdas de deformación eléctricas (strain gages) colocadas sobre un diafragma deformable. Ver Fig.3

Tensímetro de Wilson.- Es un dispositivo de bronce constituido por dos mitades con un hueco interior, una de las mitades está instrumentada con celdas de deformación eléctricas (strain gages) y es de forma cónica con diferencia angular de las paredes de 1°. Este dispositivo requiere preparar previamente en forma cónica el barreno o de lo contrario se usará resina epoxy para adherirlo a las paredes de la perforación. Ver Fig. 4.

Tensímetro de Hawkes.- El elemento sensible de este dispositivo es un disco de vidrio sometido a compresión por dos placas que se ponen en contacto con la pared del barreno mediante un mecanismo

de cuñas deslizantes accionadas por un tornillo. Una fuente luminosa de batería incorporada y una lámina polarizadora circular colocada detrás del disco de vidrio producen luz polarizada de forma que, bajo carga, el cilindro presenta birrefringencia. Se obtiene así una señal óptica cuando se observa el cilindro a través de un analizador telescópico. Ver Fig. 5.

En general, el empleo de estos aparatos plantea problemas especiales, tanto en el campo como en el laboratorio. Por tanto el uso de los tensímetros con precompresión inicial se ha limitado casi invariablemente a su diseñador y ninguno de ellos ha resultado de aceptación general. Existe un amplio campo de investigación para desarrollar un tensímetro de inclusión con módulo elevado que resulte aceptable universalmente.

2.6.- Tensímetros fotoelásticos

Aprovechando las propiedades birrefrintes del vidrio sometido a carga como indicador óptico de los esfuerzos producidos en una estructura sólida han sido utilizados por Hiramatsu y otros en Japón en 1957. Esta celda está constituida por un cilindro de vidrio, realizándose la observación mediante un polariscopio de reflexión. Ver. Figs. 6, 7 y 8. Existen otros tensímetros fotoelásticos desarrollados por Roberts y por la Post Graduate School of Mining de la Universidad de Sheffield que permiten lecturas a mayores profundidades que la diseñada por Hiramatsu.

El tensímetro fotoelástico más sencillo está constituido por un anillo de vidrio que se inserta en la pared del barreno y se introduce luego una fuente luminosa polarizada. La observación se

realiza con una pequeña lupa analizadora de mano, utilizando también un visor telescópico cuando se requiere una observación a distancia. Ver Fig. 9. Estos tipos de tensímetros también requieren calibración en laboratorio.

2.7.- Celdas de deformación eléctricas (Strain gages cells)

Otro sistema para la medición de esfuerzos por el método de sobrebarrenación es el de colocar en el fondo del barreno celdas de deformación eléctricas (straingages). Para ello se utilizan los siguientes dispositivos.

2.7.1.- El "Doorstopper" de Leeman

Este sistema de medición de esfuerzos tiene la dificultad de aislamiento de las celdas de deformación eléctrica, por el uso del agua durante la ejecución de la barrenación.

El dispositivo de Leeman tiene empotradas las celdas en una banda de hule con silicón protegidas por una película de araldita como se ve en la Fig. 10. Se utilizan tres celdas con direcciones a 90° y 45°. El elemento de inserción se presenta en la Fig. 11. Se emplea un inyector de aire caliente para secar el taladro.

Si las diferencias de lectura de las celdas en las direcciones vertical, a 45° y horizontal, antes y después de la sobrebarrenación son respectivamente ε_v, ε_{45} y ε_h, las deformaciones principales ε_1 y ε_2 de la roca en el extremo del taladro son:

$$\varepsilon_1 \text{ ó } \varepsilon_2 = \left\{ (\varepsilon_h + \varepsilon_v) \pm \sqrt{2\,\varepsilon_{45} - (\varepsilon_h + \varepsilon_v)^2 + (\varepsilon_h - \varepsilon_v)^2} \right\}$$

Las direcciones de ε_1 y ε_2 son θ_1 y θ_2, medidas en sentido contrario a las agujas del reloj respecto a la dirección de ε_h

$$\tan \theta_1 = \frac{2(\varepsilon_1 - \varepsilon_h)}{2\varepsilon_{45} - (\varepsilon_h + \varepsilon_v)}$$

$$\tan \theta_2 = \frac{2(\varepsilon_2 - \varepsilon_h)}{2\varepsilon_{45} - (\varepsilon_h + \varepsilon_v)}$$

Los esfuerzos principales en la roca en el fondo del barreno son:

$$\sigma_1 = \frac{E}{1-\nu^2}(\varepsilon_1 + \nu\varepsilon_2) \; ; \quad \sigma_2 = \frac{E}{1-\nu^2}(\varepsilon_2 + \nu\varepsilon_1)$$

2.7.2 Celda biaxial fotoelástica

Hawkes y Moxon han desarrollado la técnica del empleo de una celda fotoelástica biaxial, formada por un cilindro de resina epoxy de 44 mm de diámetro y 3 mm de espesor, con un agujero central. La base de la celda está pintada con una película reflectante que deja un reborde bien diferenciado en el cilindro. Este se adhiere a la roca mediante cemento de fraguado rápido. Se emplea un inyector de acetona para desplazar el agua del fondo del barreno.

La celda se observa con un polariscopio de reflexión, cuyas señales ópticas son semejantes a las descritas para el tensímetro de vidrio. En las Figs. 12, 13 puede verse este dispositivo, que requiere de calibración previa.

2.73.- Celda de deformación VNIMI

Este dispositivo diseñado en la unión soviética consiste de cuatro brazos en forma de cruz (No. 6) en cuyos extremos lleva fijas celdas de deformación eléctricas y se sujeta al fondo del ba-

rreno mediante un perno de expansión como se indica en la Fig. 14.

Todos estos aparatos que se colocan en el fondo del barreno dan errores por concentración de esfuerzos entre 30% y 60% por el hecho de considerar que el tercer esfuerzo principal, coincide con el eje del barreno.

2.7.4.- Celda múltiple de Leeman

Leeman desarrolló una celda múltiple para medir nueve deformaciones, tres de ellas en cada uno de los emplazamientos siguientes:

a) En la bóveda
b) En la pared lateral
c) En un punto intermedio que forma un ángulo de 7%/4 respecto al diámetro horizontal. Ver Fig. 15.

Las rosetas de celdas de deformación eléctricas están empotradas en sellos de hule y se comprimen contra las paredes del barreno mediante presión neumática, después de recubrir cada sello con un adhesivo. El dispositivo también lleva una celda compensadora pegada a un disco de roca.

2.8.- Determinación de esfuerzos mediante celdas de presión hidráulica

2.8.1. Técnica del gato plano

El empleo de gatos planos para la medida de esfuerzos en roca procede de Francia, habiéndose utilizado posteriormente en muchos paises, principalmente en Australia, Estados Unidos y Portugal. En la Fig. 16 se muestra una disposición típica de la

ranura de inserción y los puntos de medida. Algunos investigadores han intentado medir esfuerzos en un estado biaxial en dos ranuras perpendiculares.

La ejecución de la ranura produce una liberación local de esfuerzos midiéndose la deformación resultante durante un período de tres o cuatro días mediante un extensómetro colocado entre diversas combinaciones de puntos. A continuación se coloca el gato plano en la ranura, cementándolo con mortero, dejándolo 3 a 4 días para el endurecimiento del mortero. Pasado este tiempo se aplica una presión hidráulica el gato, aumentándola por escalones, y tomando medidas entre diversas combinaciones de puntos hasta que se alcanzan los valores originales anteriores a la apertura de la ranura. A continuación se realizan dos o cuatro ciclos de carga y descarga durante un período de varios días determinando la presión media de equilibrio. El ensaye completo dura de dos a tres sema

Alexander ha dado fórmulas basadas en la teoría elástica, suponiendo una ranura elíptica y un estado de esfuerzos plano, para el que se deduce (con una relación de Poisson = 0.2)

$$S = a P + bQ$$

donde S es el esfuerzo normal al gato producido por la roca, Q es el esfuerzo paralelo al gato, P es la presión media de equilibrio, y a y b son constantes que dependen de las dimensiones del gato y de la geometría de los puntos de medida respecto al mismo.

En el estudio teórico de Alexander, la presión de equilibrio depende de las dimensiones de la ranura y del gato, del campo de esfuerzos biaxial y de la relación de Poisson. Es independiente del módulo elástico de la roca.

En la práctica, aunque sea independiente de la linealidad de l relación esfuerzo-deformación, el éxito del método radica en la existencia de las mismas características de deformación en la descarga y en la carga hasta la presión de equilibrio. Esto puede no producirse siempre. Thayer y otros han encontrado diferencias apreciables entre distintos puntos de medida, siendo el resultado función de la distancia de los puntos al gato.

Las objeciones principales al método del gato plano son que las medidas deben hacerse en el borde de la excavación en una distribución de esfuerzos irregular y desconocida, y que puede estar descomprimida.

2.8.2.- Técnica del gato curvo

Jaeger y Cook han modificado el método del gato plano, para emplear gatos de sección curva colocados en barrenos de 10 cm de diámetro y de hasta 6 m de profundidad. El método se ilustra en la Fig. 17. Se supone que el esfuerzo principal σ_3 coincide con la dirección del barreno donde están colocados los gatos A y B, en la ranura anular hecha con una corona de diamante. Se aumenta la presión de estos gatos hasta que comienza a romperse la roca situada en los cuadrantes C y D exteriores al anillo. Se supone que estas roturas se producen en la dirección del esfuerzo principal σ_1, observándolas y registrando su dirección mediante sobrebarrenación y rotura de un testigo concéntrico mayor.

Los gatos A y B forman el elemento sensible y se les comunica presión registrando el descenso de presión al sobrebarrenar. A

continuación se colocan otros dos pares de gatos EF y GH en el anillo de roca sobrebarrenado aplicándoles presión para restrar los esfuerzos en A y B. Según el estudio teórico de Alexander, puede demostrarse que en función de los desplazamientos que se producen al perforar la ranura (2W):

$$E = \frac{cS - dQ}{W}$$

y para los desplazamientos producidos al aplicar presión a los gatos ($2W_1$):

$$E = \frac{fp}{W_1}$$

donde c, d y f son constantes que dependen de la geometría del ensayo.

2.8.3.- Celdas Menard y Gloetzl

La celda "Geogell" de Menard está formada esencialmente por dos cámaras coaxiales, conectadas a manómetros, en una celda cilíndrica de acero. Se utiliza para determinar el módulo elástico de las rocas.

La celda Gloetzl es un gato plano de 7 cm x 14 cm x 2 mm de espesor, que utiliza mercurio como fluido transmisor de la presión, lo cual se mide equilibrando presiones transmitidas a través de un diagrama como se indica en la Fig. 18. Se utiliza para medir esfuerzos en revestimientos de concreto p.ej. de concreto lanzado.

2.9.- Medida indirecta de esfuerzos en roca

2.9.1. Métodos geofísicos

Se han hecho varios intentos a través de los años para utilizar

la velocidad sónica con los esfuerzos, para la medida de esfuerzos en roca. Sin embargo, los resultados han sido en general desalentadores, al igual que en los métodos para encontrar una correlación práctica entre los esfuerzos y las resistividades "in situ". Un mayor éxito ha alcanzado el empleo de métodos acústico-microsísmicos para la observación de la velocidad de aumento de los esfuerros en minas susceptibles de desprendimientos, especialmente en Europa Central.

Por ejemplo, los ensayes de laboratorio con muestras de roca extraidas de la mina Pribam en Checoeslovaquia, muestran que aparecen impulsos microsísmicos cuando la presión aplicada alcanza el 80% de la resistencia de la roca a la ruptura, y con presiones mayores el número de impulsos presenta un notable aumento.

Como consecuencia, es posible seguir la formación de presiones en el interior de las rocas a partir de varias estaciones que registren los sonidos internos, pudiendo, a partir de la evidencia acumulada, establecer un código de seguridad para la entibación à colocar en las minas según los impulsos registrados por hora.

2.9.2.- Rotura hidráulica

El método de rotura hidráulica se emplea en la industria del petróleo para estimular la producción de un pozo agotado. Consiste en taponar una sección del pozo introduciendo un fluido a presión en el mismo y aumentando la presión hasta que las paredes del pozo se fractura.

En la rotura hidráulica se supone que las paredes del barreno se rompen cuando el esfuerzo máximo provocado en la zona puesta en

carga alcanza la resistencia a tensión en un punto cualquiera de la pared, es decir, cuando los esfuerzos de tensión provocados por el fluido a presión superan los esfuerzos de compresión creados en las paredes del barreno por la perforación del mismo en el campo regional de esfuerzos del macizo rocoso.

Al estudiar los conceptos teóricos relativos a la rotura hidráulica, Fairhurst ha señalado que si el campo regional de esfuerzos está definido por tres esfuerzos ortogonales principales, uno de los cuales se supone coincide con el eje del barreno, la rotura se producirá en una dirección normal al máximo esfuerzo de tensión inducido cuando se alcance la resistencia en tensión de la roca. La rotura se propagará en un plano perpendicular al esfuerzo principal menor y la presión del fluido necesaria para propagar la rotura, una vez iniciada, será igual a este esfuerzo. Ver Fig. 19. Este sistema puede proporcionar información acerca del estado de esfuerzos naturales en barrenos de exploración profundos sin conocimiento de las propiedades elásticas de la roca. Por otro lado, como se supone que uno de los esfuerzos principales tiene la dirección del barreno, puede ser un razonamiento aceptable para rocas sedimentarias receptoras de petróleo, pero no para rocas ígneas y metamórficas en la cual esta suposición es totalmente invalida.

2.10.- Medición de esfuerzos en la P.H. La Angostura, Chis.

Con objeto de preveer problemas de estabilidad durante la excavación de la caverna que aloja la casa de máquinas de la Planta Hidroeléctrica La Angostura, Chis., cuyas dimensiones aproximadas son de 20 m de ancho, 120 m de largo y 40 m de alto, la Comi-

el flanco sur y 65° en el flanco norte (lado de las montañas de San Cristobal de las Casas).

El macizo rocoso está constituido por calizas margosas estratificadas, del cretácico superior, existiendo capas de arcilla con espesores variables entre 5 cm y 80 cm, interestratificadas con los estratos de caliza.

Existen tres familias de fracturas subverticales cuya localización se presenta en la Fig. 21. La dirección del sinclinal es la misma que la dirección de las fracturas a sobre las que escurre el río en el sitio del cañón de La Angostura.

2.10.2.- Roseta de deformaciones

En las Figs. 22 y 23 se indican el procedimiento seguido en la ejecución de estas pruebas y la determinación de la dirección de esfuerzos principales utilizando el círculo de Mohr.

Los esfuerzos principales para un estado de deformación plana son:

$$N_1 = \frac{E}{1-\nu^2}(\varepsilon_1 + \nu\varepsilon_2)$$

$$N_2 = \frac{E}{1-\nu^2}(\varepsilon_2 + \nu\varepsilon_1)$$

En este caso los esfuerzos se determinaron utilizando la siguiente expresión de Lekhnitskii para un medio continuo con anisotropía transversa para un estado de esfuerzos plano:

$$\begin{Bmatrix} n_x \\ n_y \\ t_{xy} \end{Bmatrix} = \frac{E_y}{(1-n\nu^2)} \begin{bmatrix} n & n\nu & 0 \\ n\nu & 1 & 0 \\ 0 & 0 & m(1-\nu^2) \end{bmatrix} \begin{Bmatrix} e_x \\ e_y \\ \gamma_{xy} \end{Bmatrix} = [D] \begin{Bmatrix} e_x \\ e_y \\ \gamma_{xy} \end{Bmatrix}$$

en donde:

e_x = deformación longitudinal unitaria en dirección horizontal x.

e_y = deformación longitudinal unitaria en dirección vertical y.

γ_{xy} =deformación transversal unitaria en la dirección o y

n_x = esfuerzo normal horizontal

n_y = esfuerzo normal vertical

t_{xy}= esfuerzo cortante en un plano normal al eje del cilindro

n = relación de módulos = $\frac{E_y}{E_x}$.

E_y = módulo de Young en la dirección vertical

ν = relación de Poisson

m = relación $\frac{G_2}{E_2}$

Se utilizaron los siguientes valores:

E_y = 55 000 kg/cm^2. Obtenido de ensayes dinámicos, Fig. 24

ν = 0.25

n = 1.63

m = 0.4

Se tiene:

$$[D] = \begin{Bmatrix} 11 & 2.8 & 0 \\ 2.8 & 6.7 & 0 \\ 0 & 0 & 2 \end{Bmatrix} \times 10^4$$

Basados en esta relación, se calcularon para cada una de las pruebas los valores de N_x, N_y y t_{xy}. Los resultados se presentan en la tabla de la Fig. 25.

Esfuerzos debidos a peso propio

Al abrir un túnel en un medio semi-infinito sometido a la acción de peso propio, se producen concentraciones de esfuerzos en el

contorno del túnel como las indicadas en 2.2.1.

Para el caso de un medio anisotrópico sometido a esfuerzos de peso propio P y Q, obtenemos en los puntos localizados sobre el diámetro horizontal de la sección del túnel:

$$n_y = (1+\gamma_1)(1+\gamma_2)\left[\frac{P(3+\gamma_1+\gamma_2-\gamma_1\gamma_2)}{(1+\gamma_1)^2(1+\gamma_2)^2} + \frac{Q(\gamma_1+\gamma_2-\gamma_1\gamma_2-1)}{(1-\gamma_1)^2(1-\gamma_2)^2}\right]$$

(Expresión de Jaeger y Cook) Ver Fig. 26.

en donde

$$\alpha_1\alpha_2 = \frac{E_y}{E_x} = 0.6$$

$$\alpha_1+\alpha_2 = \frac{E_y}{G-2\delta} = 2$$

$$\gamma_1 = \frac{(\alpha_1^{1/2}-1)}{(\alpha_1^{1/2}+1)}$$

$$\gamma_2 = \frac{(\alpha_2^{1/2}-1)}{(\alpha_2^{1/2}+1)}$$

Aplicando estas relaciones al caso específico de la galería transversal No. 2 y suponiendo $Q = \frac{P}{3}$, resulta $n_y = 2.87P$. P es el esfuerzo vertical debido a peso propio. La galería está a 110 m de profundidad y el peso volumétrico de la roca es igual a 2.3 ton/m^3, por lo que, P = 25.3 kg/cm^2 y n_y = 72.6 kg/cm^2.

Comparando este valor de n_y, o sea del esfuerzo vertical en la zona central de la pared vertical del túnel, con el esfuerzo n_y promedio medido en las pruebas, se aprecia prácticamente que son iguales. En consecuencia el esfuerzo n_y medido en las pruebas corresponde al esfuerzo n_y teórico bajo el efecto del peso propio del material.

El esfuerzo n_x, horizontal, debido al efecto de peso propio es igual a γn_y, suponiendo que el estado de deformación es plano en un plano normal al eje de la galería. Por tanto el esfuerzo horizontal debido al efecto del peso propio de la galería es $n_x = 18.1$ kg/cm^2, mientras el esfuerzo horizontal medido es igual en promedio a 101.8 kg/cm^2. En este caso la diferencia es notoria y del orden de 80 kg/cm^2.

Finalmente el valor de t_{xy} debido al efecto de peso propio ha de ser nulo teóricamente, mientras el valor medido promedio es igual a 0.6 kg/cm^2. Se puede despreciar esta discrepancia.

Esfuerzos tectónicos

De acuerdo con lo indicado anteriormente, resulta que el sistema de esfuerzos tectónicos está dado por:

$$(n_x)_{tect.} = 80 \text{ kg/cm}^2 \qquad (n_y)_{tect.} = 0 \qquad (t_{xy})_{tect.} = 0$$

El resultado de las pruebas parece indicar, por tanto, la existencia de una compresión en sentido horizontal, paralela al río Grijalva de 80 kg/cm^2 de magnitud.

Con el fin de comprobar, por lo menos cualitativamente la existencia de este esfuerzo horizontal de compresión tectónico se pueden analizar la dirección de fracturas reportadas en la Fig. 21.

Puede verse que la familia de fracturas α, paralela al río, es bisectriz respecto a la dirección de las fracturas β y γ, lo cual confirma la dirección de un empuje paralelo al río que coincide

con la dirección del empuje que dió lugar al sinclinal.

Conclusiones

Analizando los resultados de las mediciones de esfuerzos mediante las pruebas de relajación de esfuerzos de roseta, realizadas en la galería 2, cercana a la casa de máquinas de la Planta Hidroeléctrica La Angostura, puede decirse que existe un esfuerzo tectónico de compresión horizontal y paralelo al río de aproximadamente 80kg/cm^2. Tal esfuerzo debe tener un papel importante en las condiciones de estabilidad de la caverna de la casa de máquinas.

2.10.3.- Pruebas de gato plano

En las Figs. 27, 28, 29, se indica el procedimiento utilizado en la ejecución de estas pruebas, un ejemplo de una prueba indicando la relación carga-desplazamiento hasta la obtención de la presión de cancelación y finalmente una comparación de los esfuerzos horizontales y verticales medidos con las pruebas de roseta y gato plano realizadas en las galerías 2 y 3 cercanas a la casa de máquinas de la Planta Hidroeléctrica La Angostura, en la que puede observarse una buena concordancia en los valores de los esfuerzos verticales y diferencias de hasta 20 kg/cm^2 en los esfuerzos horizontales paralelos al río.

Puede concluirse que los resultados obtenidos con este procedimiento para la medición de esfuerzos internos resulta confiable y sencillo, observándose que en las zonas de cizallamiento no hay transmisión de esfuerzos horizontales.

3.- ENSAYES "IN SITU" EN MACIZOS ROCOSOS

3.1.- Introducción

Para poder determinar la magnitud y distribución de esfuerzos en los macizos rocosos es necesario conocer las características carga-deformación de los materiales componentes de dichos macizos.

Los macizos rocosos son conjuntos heterogéneos y generalmente discontínuos, lo que da lugar a que la escala de un experimento determine en cierto grado los resultados del mismo. Como ejemplo puede citarse la obtención de la rigidez de la roca. Al comparar los resultados de ensayos "in situ" en macizos rocosos con los resultados de laboratorio sobre la misma roca se ve que los ensayes de laboratorio conducen invariablemente a una sobrestimación de la rigidez de la roca. Se han descrito comparaciones de este tipo en un gran número de sitios, apreciándose que es posible una sobreestimación de la rigidez del orden de 20 o más veces, siendo bastante habituales las diferencias de 5 a 15 veces.

La razón principal de esta discrepancia es la presencia discontinuidades en el macizo rocoso. Estas pueden adoptar una o varias formas, p.ej.:

a) fracturamiento y estratificación más o menos sistemáticos

b) microfisuras en roca aparentemente masiva

c) fallas

d) zonas localizadas de roca alterada

Por razones prácticas las muestras de laboratorio se suelen tomar casi invariablemente de la roca comprendida entre discontinuidades principales. La presencia de las discontinuidades, con su rigidez considerablemente baja, reduce la rigidez total del macizo

rocoso. 71

No existe un método exacto para predecir de antemano la rigidez total de un macizo rocoso a partir de los resultados de ensayes en laboratorio, por lo que son necesarios ensayos "in situ" a pesar de un mayor costo.

Otras propiedades importantes, además de la rigidez, son la resistencia y capacidad de carga, porosidad y permeabilidad. Estas propiedades están también sujetas a errores de escala y toma de muestras por lo que, para la mayoría de las finalidades prácticas, se suelen determinar a partir de ensayes "in situ".

3.1.- Ensayes de deformabilidad

Existen dos métodos básicos para determinar la deformabilidad de los macizos rocosos: los denominados métodos "estáticos" y "dinámicos".

En los primeros se aplican cargas estáticas relativamente grandes sobre superficies seleccionadas del macizo rocoso, midiéndose las deformaciones resultantes. En los ensayes dinámicos se mide la velocidad de transmisión de perturbaciones vibratorias.

Aunque, ciertamente la roca no es ni homogénea ni elástica, se acostumbra interpretar los resultados de ensaye a partir de la teoría elástica, asignando a la roca valores de constantes elásticas apropiadas como el módulo de Young (E) y la relación de Poisson (ν). La justificación de este procedimiento radica en el hecho de que, con cargas moderadas, las relaciones esfuerzo-deformación son aproximadamente lineales, resultando de importancia secundaria las características de fluencia.

3.2.1.- Ensayes de carga con placa

Este ensaye que consiste en la aplicación de presión a una superficie dada de roca, a través de placas rígidas o flexibles y midiendo las deformaciones de la roca ha tenido un amplio uso en la Mecánica de Rocas. Puede utilizarse dentro de galerías apoyándose el sistema de carga en las paredes del túnel (Fig. 30) o en la superficie utilizando cables de anclaje para estudio de cimentación de presas, Fig. 31.

El módulo elástico se calcula utilizando la solución de Boussinesq para el desplazamiento normal de la superficie de un semiespacio elástico bajo la acción de una carga puntual normal.

Placa rígida llena

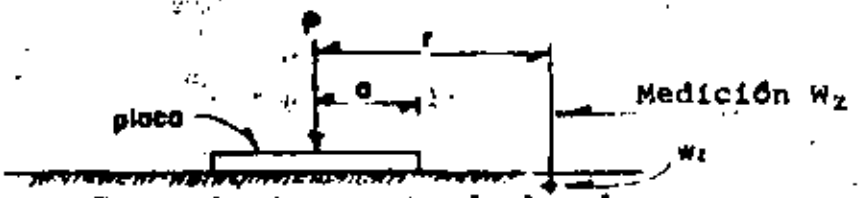

En cualquier punto de la placa, ya que las deformaciones son constantes, se tiene:

$$W_{z(0<r<a)} = \frac{P(1-\nu^2)}{2Ea}$$

Cuando la medición se hace fuera de la placa, se tiene:

$$W_z = \frac{P(1-\nu^2)}{\pi Ea} \quad \text{arco sen } \frac{a}{r}$$

Placa flexible llena

Para r = 0 $\qquad W_{z_{(r=0)}} = \frac{2(1-\nu^2)P}{\pi Ea}$

para r = a $\qquad W_{z_{(r=a)}} = \frac{4(1-\nu^2)P}{\pi Ea}$

Para un punto fuera de la placa:

$$W_z = \frac{4(1-\nu^2)}{\pi E a} p \left[\int_0^{\pi/2} \sqrt{1 - \frac{a^2}{r^2} \operatorname{sen}\theta}\, d\theta - \left(1 - \frac{a^2}{r^2}\right) \int_0^{\pi/2} \frac{d\theta}{\sqrt{1 - \frac{a^2}{r^2} \operatorname{sen}^2 \theta}} \right]$$

Se obtienen mediante las tablas de integrales elípticas

Placa flexible con agujero en el centro

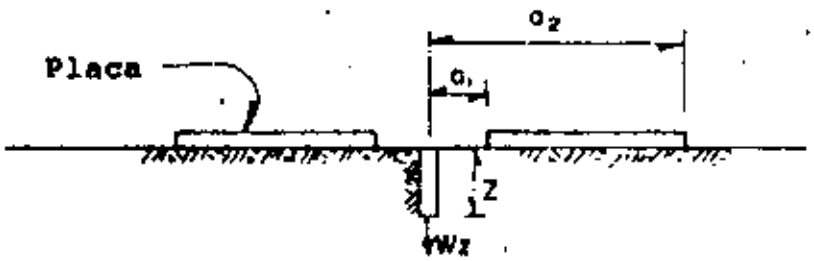

El módulo elástico se determina mediante la siguiente expresión:

$$E = \frac{p}{W_z} \left\{ \left[(1+\nu) Z^2 \right] \left[\frac{1}{(a_1^2 + Z^2)^{1/2}} - \frac{1}{(a_2^2 + Z^2)^{1/2}} \right] + 2(1-\nu^2) \left[(a_2^2 + Z^2)^{1/2} - (a_1^2 + Z^2)^{1/2} \right] \right\}$$

en donde: p = presión uniforme aplicada en la placa

$$p = \frac{P}{\pi a_2^2 - \pi a_1^2}$$

En estas pruebas el volumen de roca involucrado alcanza cuando mas 1 diámetro de la placa, pero a distancias grandes las deformaciones son prácticamente iguales y entonces aunque la placa sea chica estaremos involucrando un volumen mayor de roca.

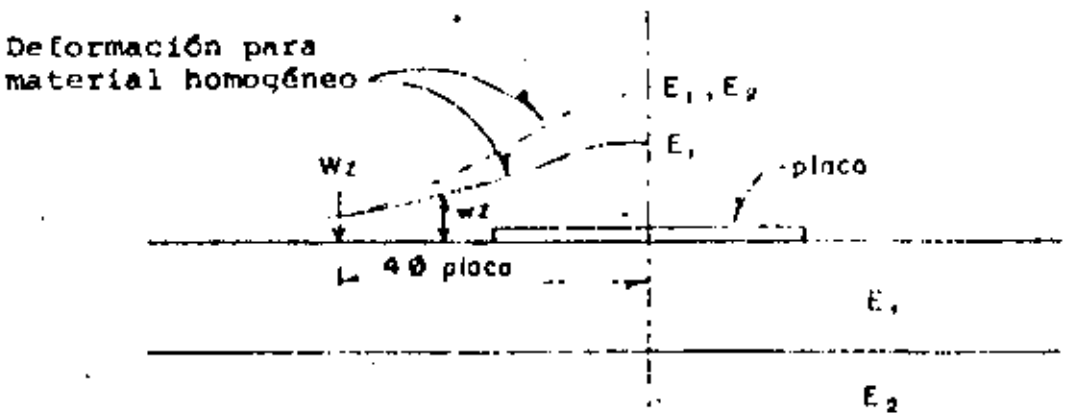

En la Fig. 32 se presenta una gráfica representativa de estas pruebas.

En la Fig. 33 se presenta la gráfica esfuerzo-deformación obtenida en ensaye con placa flexible con agujero al centro en pruebas realizadas en el sitio de la P.H. La Angostura, Chis.

3.2.2.- Ensayes de presión en túneles o galerías

Con objeto de involucrar en el ensaye un volumen mayor de roca se realizan ensayes de deformabilidad en túneles o galerías, principalmente en los lugares de construcción de centrales hidroeléctricas y tuberías a presión. Este ensaye en galerías es muy caro, dadas sus dimensiones, por otro lado se presenta el problema que estos túneles son excavados con el uso de explosivos y el módulo elástico corresponderá entonces a la zona de roca fracturada.

Una característica importante del ensaye de presión en galerías es que introduce esfuerzos de tensión anulares en la roca, los cuales pueden vencer cualquier compresión residual dando lugar a la abertura de grietas radiales. Esto puede reducir mucho la rigidez del macizo rocoso.

Los ensayes de carga convencionales tienen dos graves inconvenientes: el primero es la presencia del terreno perturbado (por las operaciones de excavación). El segundo es la necesidad de limitar la extensión de la superficie cargada y el número de puntos de ensayo por razones económicas, reduciendo por tanto la utilidad de los resultados.

Se pretende que el empleo de presiómetros o dilatómetros, tiende a superar estas objeciones, principalmente la segunda. Sus venta

jas son;

a) si se realiza la perforación con corona de diamante, la roca queda casi inalterada.

b) debido a su menor costo y tiempo de prueba, pueden realizarse un gran número de ensayes.

De esta forma es posible obtener datos de carácter estadístico sobre la distribución de la deformabilidad en el interior del macizo rocoso, incluida su anisotropía. Otras ventajas son la posibilidad de realizar ensayes bajo agua (cauces de ríos) y a considerables profundidades para el proyecto de túneles. Un inconveniente es el pequeño volumen de roca abarcado en cada ensaye, por lo cual los resultados no pueden ser verdaderamente representativos, especialmente en rocas fracturadas. Sin embargo, la posibilidad de realizar muchos ensayes en una cierta zona ofrece la oportunidad, en muchos casos, de obtener resultados útiles para un estudio estadístico de muchas medidas aisladas. Esto puede proporcionar con seguridad resultados comprendidos dentro del orden de precisión relativamente bajo, exigido por el ingeniero.

En la Fig. 34 se presenta esquemáticamente este tipo de ensaye:

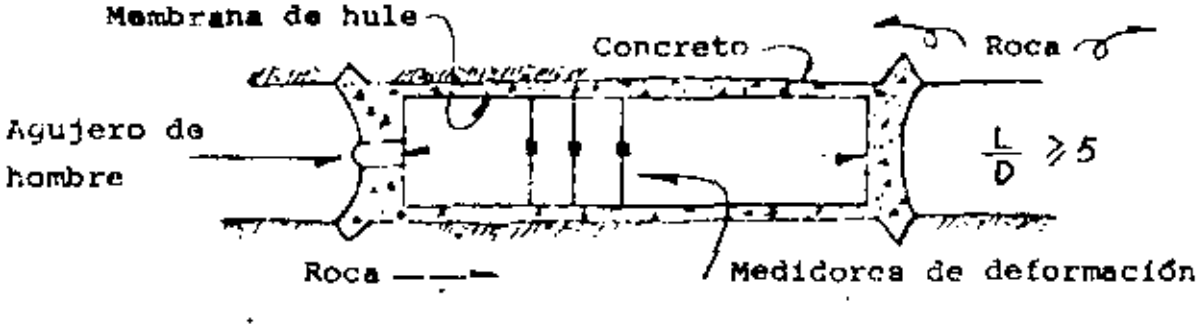

Fig. 34.- Ensaye de presión en galería

El módulo elástico se determina mediante la siguiente expresión:

$$E = \frac{P\,D}{\Delta D}\,(1 + \nu)$$

en donde:

P = presión del agua

D = diámetro interior

ν = relación de presión

ΔD = variación del diámetro

Esta expresión se utiliza si no se tiene revestimiento de concreto, en cuyo caso el agua puede causar presión intersticial importante en la roca.

Tomando en cuenta la deformación ocurrida en el concreto, se tiene:

$$E_{roca} = \frac{P\,D}{\Delta D} - \frac{2e}{D}\,E_{concreto}$$, siendo e = espesor del concreto

Si la prueba se realiza sin revestimiento de concreto y el material está fracturado se tiene:

$$E = \frac{P\,D^2}{4\,r\,\delta_r}\,(1 + \nu)$$

en donde:

r = distancia radial hasta el punto de medición dentro de la roca

δr = variación de la distancia radial de medición

Los portugueses han utilizado una corrección cuando se produce fisuramiento:

$$E = \frac{P\,D}{\Delta D}\,\underbrace{\left(\log_e \sqrt{\frac{P}{R_t}}\right)}_{\text{Factor de corrección}} + 1 + \nu)$$

en donde: R_t = resistencia a tensión de la roca

En Yugoslavia han realizado este sistema aplicando la presión radial mediante gatos hidráulicos curvos. Fig. 35.

3.2.3.- Ensayes con Gato Goodman

Goodman ha diseñado este dispositivo para determinar la deformabilidad de la roca dentro de barrenos ØNX; está constituido por dos placas rígidas de acero semicirculares que se desplazan diametralmente bajo el empuje de 12 pistones hidráulicos. Los desplazamientos diametrales se miden utilizando dos transducers de transformador diferencial lineal variable (LVDT).

El módulo elástico de la roca se obtiene a partir de la relación carga-deformación.

En las Figs. 36 y 37 se muestra el dispositivo y los resultados de una prueba realizada en la P.H. La Angostura, Chis.

3.2.4. Ensayes con dilatómetro LNEC, Portugal

Este presiómetro consta fundamentalmente de un cilindro de acero inoxidable de 54 cm de largo, con un diámetro de 6.6 cm y un espesor de pared de 1 cm, embutido de una membrana de neopreno de 0.4cm de grueso. Este aparato puede utilizarse dentro de perforaciones ØNX. El fluido (agua o aceite) que aplica la presión sobre las paredes del barreno se inyecta en el espacio que queda entre la superficie exterior del cilindro metálico y la membrana de neopreno. Uno de los extremos está cerrado por un tapón a través de los cuales pasa la válvula de retención del líquido que aplica la presión, los tubos y los cables eléctricos del elemento de medida se conectan por el otro extremo. El instrumento se introduce dentro

del barreno por medio de varillaje atornillado a este mismo extremo y se determinan la profundidad y orientación del mismo. La válvula de retención se controla a distancia mediante aire comprimido de forma que la presión se puede eliminar después de cada ensayo para trasladar el dispositivo dentro del barreno.

La medición de deformaciones se realiza mediante 4 transformadores diferenciales variables lineales (LVDT).

Cada transformador tiene su núcleo metálico y su bobina en contacto con la roca por medio de dos pequeñas varillas. Estas varillas se aplican contra la roca por medio de una muelle. Para introducir el dispositivo dentro del barreno, las dos varillas de cada transformador se recogen mediante succión con aire comprimido.

En la Fig. 38 puede verse este dispositivo.

3.2.5.- Ensayes con gatos planos gigantes

El Laboratorio Nacional de Ingeniería Civil de Portugal (LNEC) ha desarrollado unos gatos planos tipo Freysinet para la determinación de la deformabilidad de la roca. Los gatos se introducen dentro de ranuras de unos 7 mm de espesor, realizadas con sierra. Los gatos tienen aproximadamente 1 m^2 de sección y pueden utilizarse hasta tres a un mismo tiempo. Las deformaciones de la pared de roca se miden utilizando muelles instrumentadas con celdas de deformación eléctrica.

El volumen de roca involucrado en estos ensayes cuando se utilizan tres gatos alcanza aproximadamente 50 m^3, y la roca es poco perturbada por el corte realizado con sierra. Este equipo es muy promete

dor pues no es pesado y puede utilizarse en muchos sitios a relativo bajo costo.

En la Fig. 39 puede verse este dispositivo.

3.3.- Métodos dinámicos de ensaye "in situ"

En estos métodos, el módulo elástico se deduce de la velocidad de propagación de ondas de sonido, constituyendo por tanto una derivación del método sísmico de prospección geofísica.

Cuando se aplica un impulso dinámico a la superficie de un sólido semi indefinido, la energía se irradia desde la fuente emisora en forma de dos tipos diferentes de impulsos vibratorios elásticos. El más rápido solo origina desplazamientos de las partículas del material en la dirección de avance de la perturbación y se denomina onda longitudinal o de compresión. La velocidad de esta onda (α) en un medio elástico isótropo viene dada por:

$$\alpha^2 = \frac{E\,(1-\nu)}{\rho\,(1+\nu)\,(1-2\nu)}$$

La segunda onda es la transversal o de cortante queda lugar a un desplazamiento de las partículas normal a la dirección de avance. Esta velocidad (β) se determina como sigue:

$$\beta = \frac{E}{2\rho(1+\nu)}$$

En donde:

ν = relación de Poisson

ρ = densidad del medio de propagación

E = módulo elástico del medio

Este método tiene las extraordinarias ventajas de ser relativamente

barato y rápido de aplicar, abarcando grandes volúmenes de roca. Sin embargo, los resultados no suelen concordar con los ensayos táticos, siendo más próximos a los obtenidos en ensayes de laboratorio sobre muestras pequeñas. No se ha encontrado una correlación exacta entre los resultados sísmicos y estáticos, aunque Serafim ha advertido una semejanza entre los módulos sísmicos y los módulos tangentes al comienzo de la curva de descarga de los ensayes estáticos.

Esta discrepacia suele ser tan grande que los ensayes sísmicos no pueden sustituir directamente a los estáticos. Se han hecho varios intentos para obtener correlaciones generales con éxito muy diverso (en gran parte función del tipo de roca y de la fase de degradación)

Se han dado explicaciones de esta discrepancia, pero ninguna parece ser completamente adecuada. Las dos más probables son:

a) que la deformabilidad "estática" resulta afectada en gran extensión por la fisuración, pero debido a los pequeños desplazamientos producidos, las fisuras pequeñas no influyen grandemente en los resultados sísmicos, especialmente si estan rellenas de agua

b) que las velocidades sísmicas dependen solamente de las deformaciones elásticas y no están influenciadas por las deformaciones plásticas que reducen la rigidez encontrada en los ensayes estáticos.

En la Fig. 24 se presenta la relación entre los módulos "estáticos" y la frecuencia de la onda transversal encontrada por Schneider.

3.4.- Ensayes de corte directo "in situ"

Por la mismas razones de ejecución de los ensayes de deformabilidad, es esencial realizar alguna forma de ensayos de corte "in situ" en el macizo rocoso para intentar determinar su resistencia al esfuerzo cortante. El sistema utilizado se presenta en la Fig. 40.

3.4.1 Ensayes realizados en La Angostura y Chicoasén, Chis.

En las Figs. 41, 42, 43, 44 se presentan los resultados de pruebas realizadas por la Comisión Federal de Electricidad en los sitios de las Presas La Angostura y Chicoasén, Chis., cuyos datos se emplearon en análisis de estabilidad de taludes. Las probetas tenían dimensiones aproximadas de 60 cm x 60 cm x 40 cm. Usualmente las probetas tienen secciones $\geq$ 1 m^2.

En las pruebas realizadas en Angostura donde el plano de contacto fue prácticamente roca-roca el comportamiento observado es frágil en cambio en las realizadas en Chicoasén en las que en el plano de corte existía una capa de arcilla de unos 5 cm de espesor el comportamiento es plástico. En estos ensayes se supone que se puede aplicar la ley de Coulomb, es decir: $s = c + \sigma \tan \phi$.

4.- RECONOCIMIENTOS

El autor agradece la colaboración de los Ings. Carlos Bernal, Raúl Ramírez Aranda y Sergio Ochoa Ochoa quienes estuvieron a cargo de la ejecución de los ensayes de campo realizados por la Comisión Federal de Electricidad en las Presas de La Angostura y Chicoasén, Chis.

MEDIDOR DE DEFORMACIONES EN BARRENOS
(Borehole Gage) (Merrill, USBM)

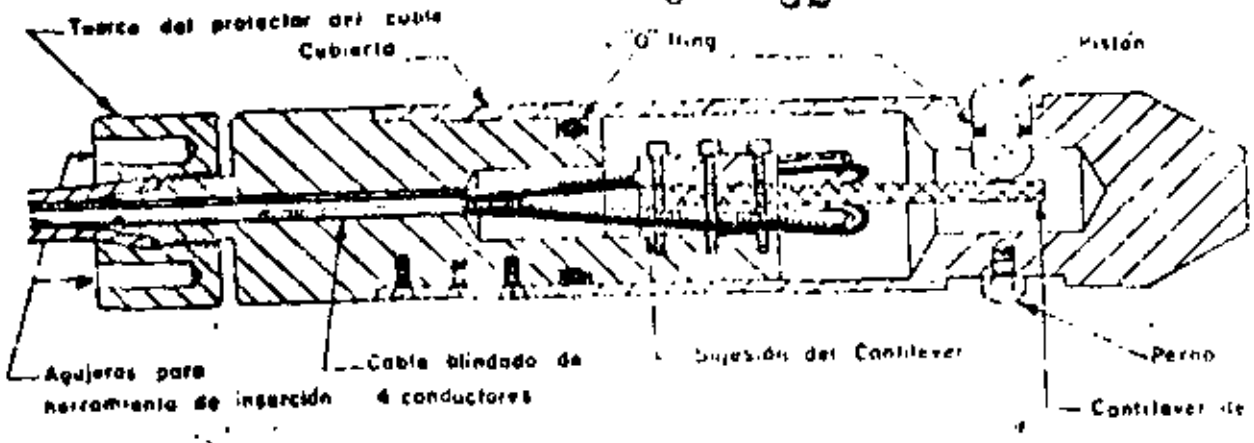

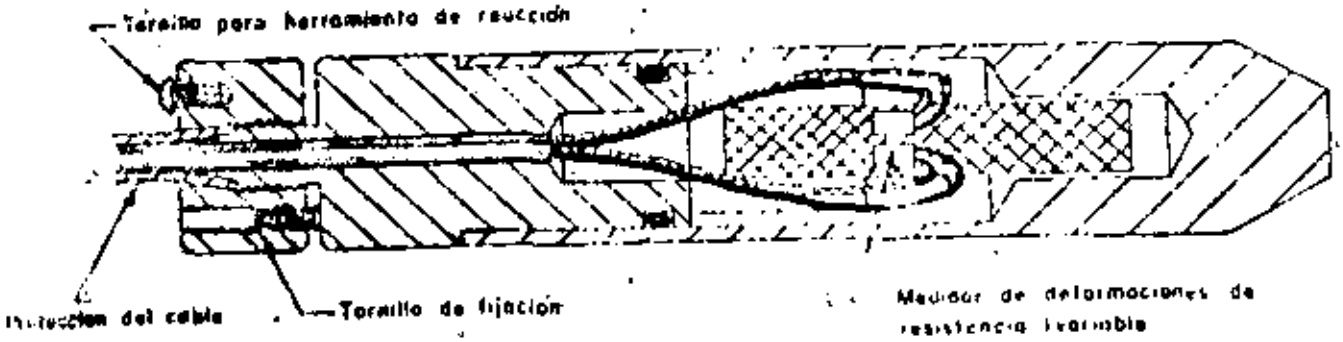

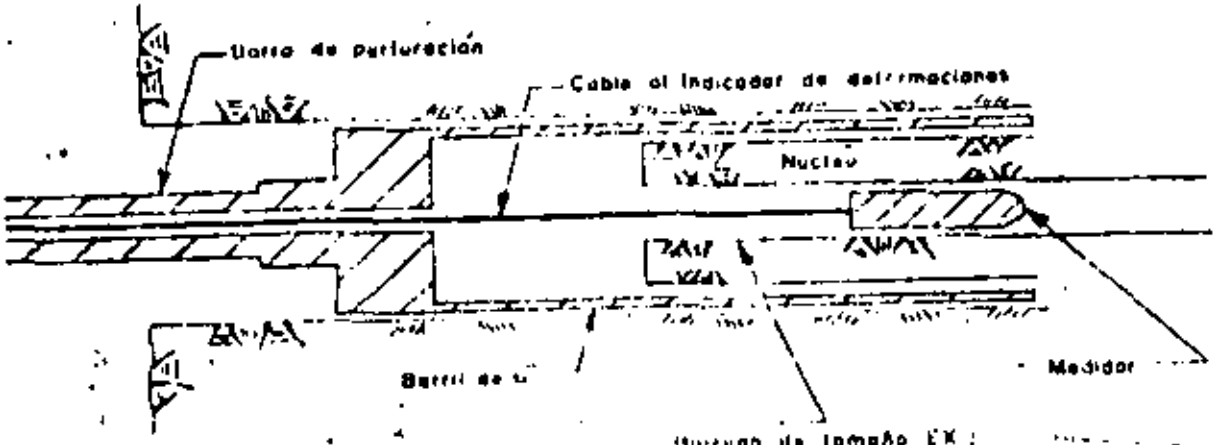

Fig. 1

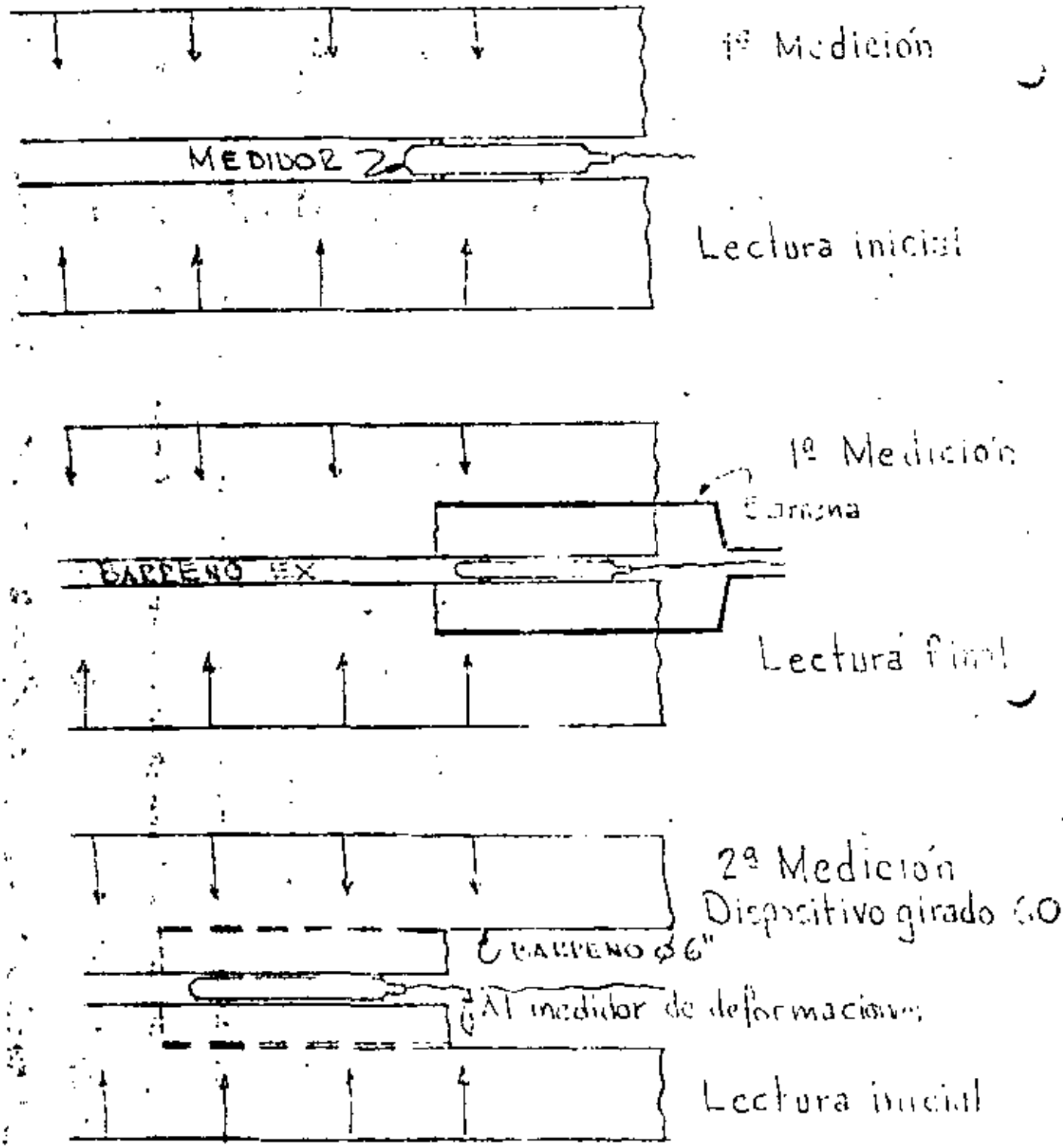

PRUEBA DE SOBREEXCAVACION

MEDICION DE DEFORMACION TRANSVERSAL

DISPOSITIVO DE MEDELL, UNAM

fig. 2

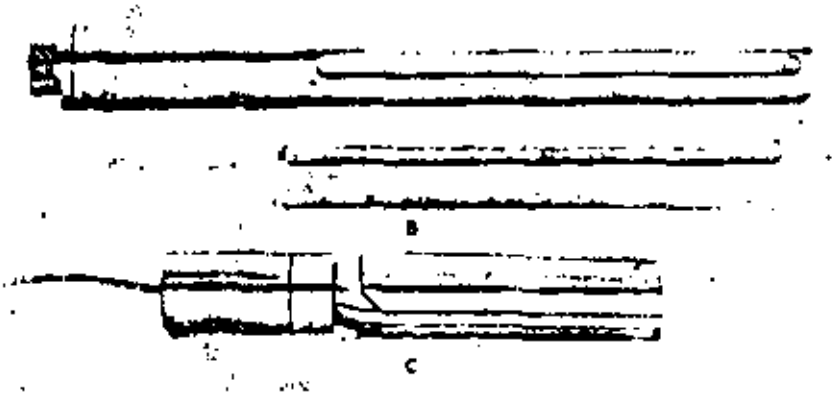

Fig. 3 : Rigid inclusion gage with tapered mounting sleeve. (After Potts and Tomlin,[11])

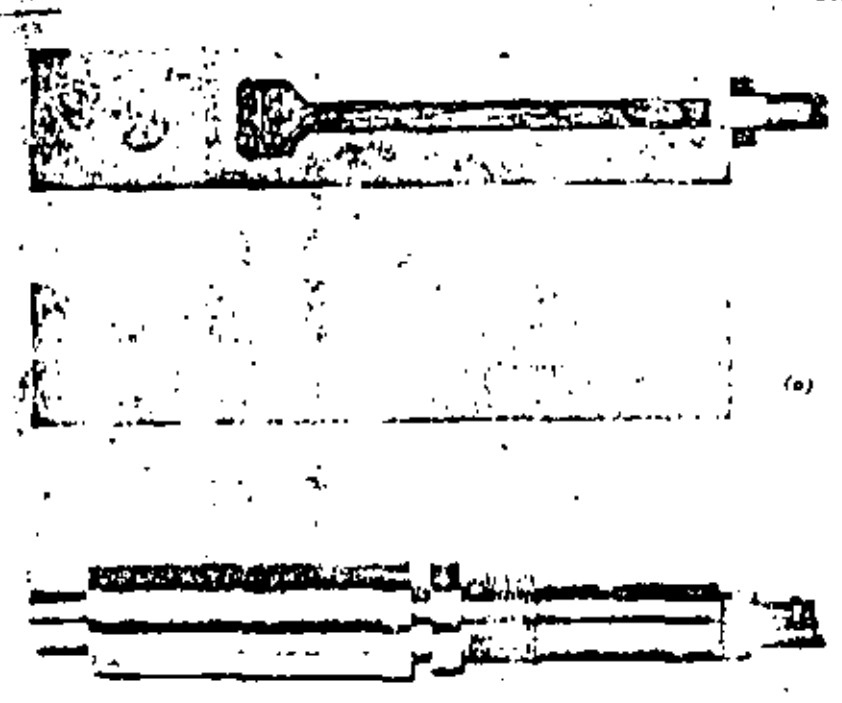

Fig. 4 : Rigid inclusion gage. (After Wilson.[12]) (a) Two halves ready for joining. (b) Assembled gage.

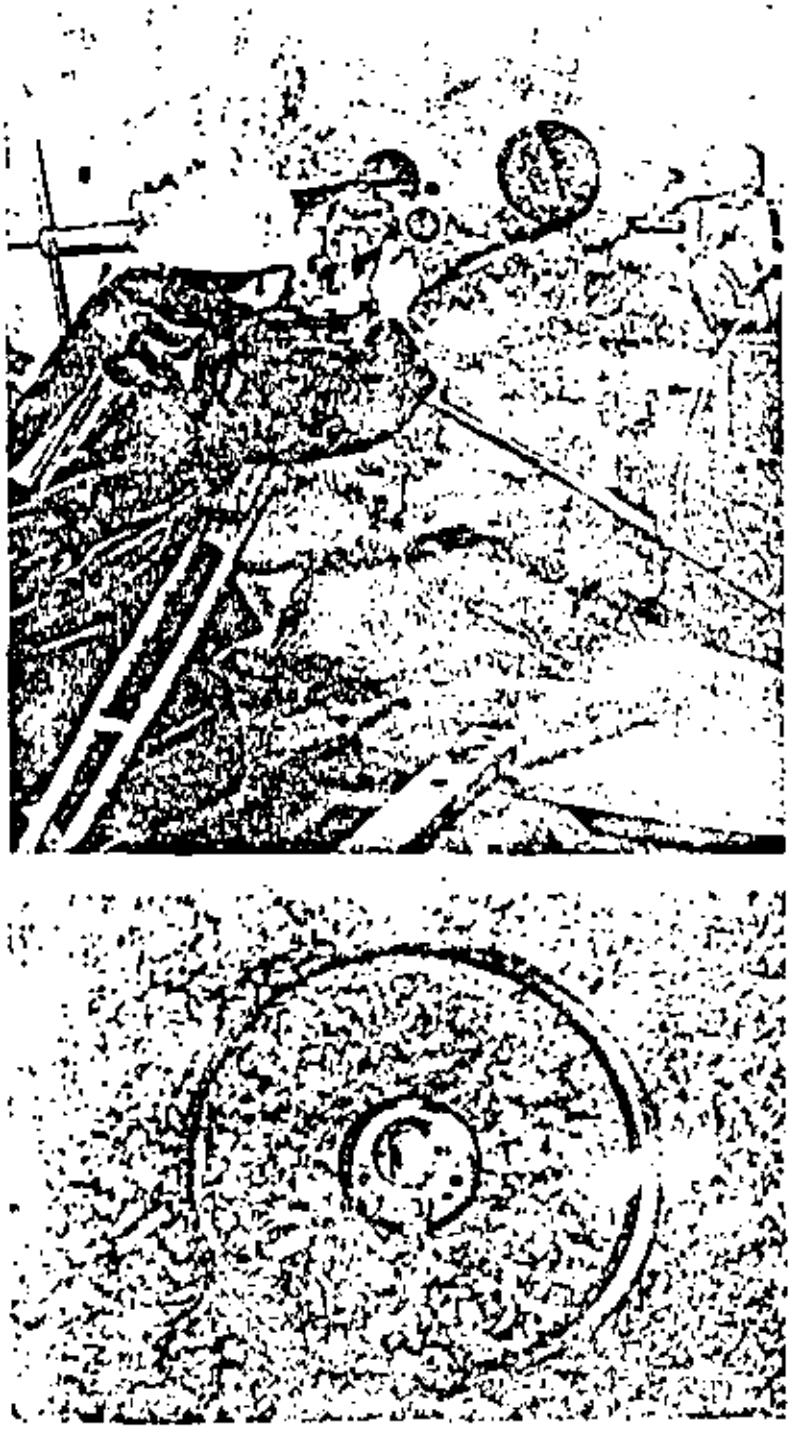

Figura 5 Tensiometro de Hawkes

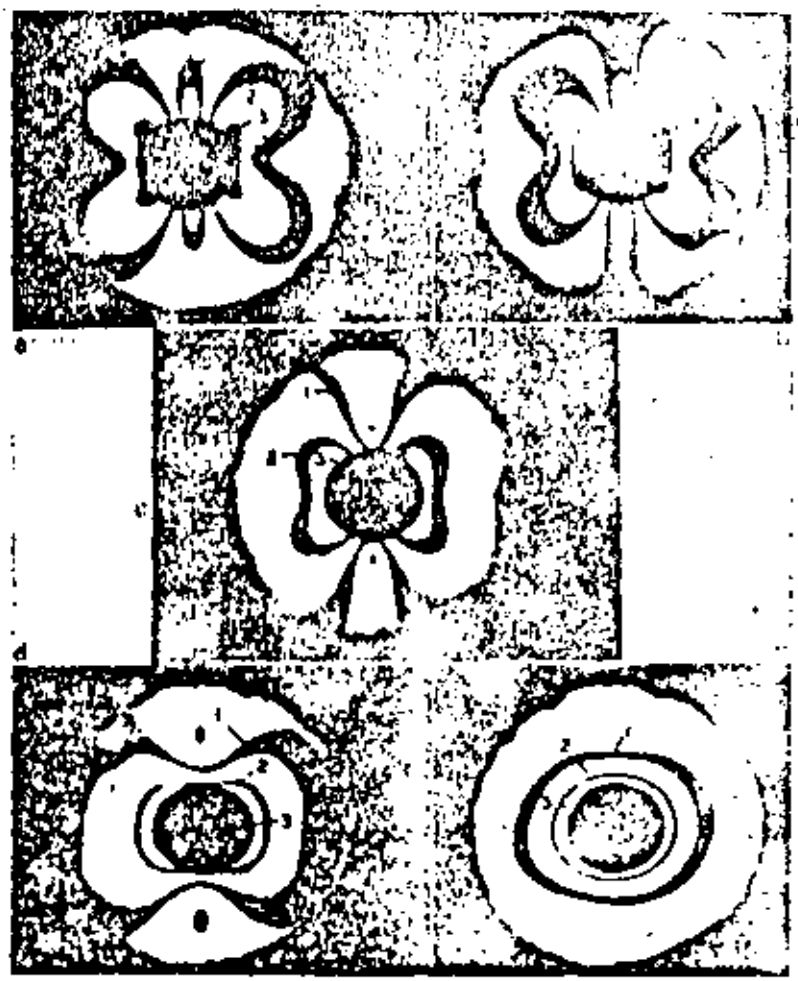

Figura 6: Señales presentadas por una célula ganglionar bipolar en diversos campos tridimensionales cuales con una franja de tercer orden.

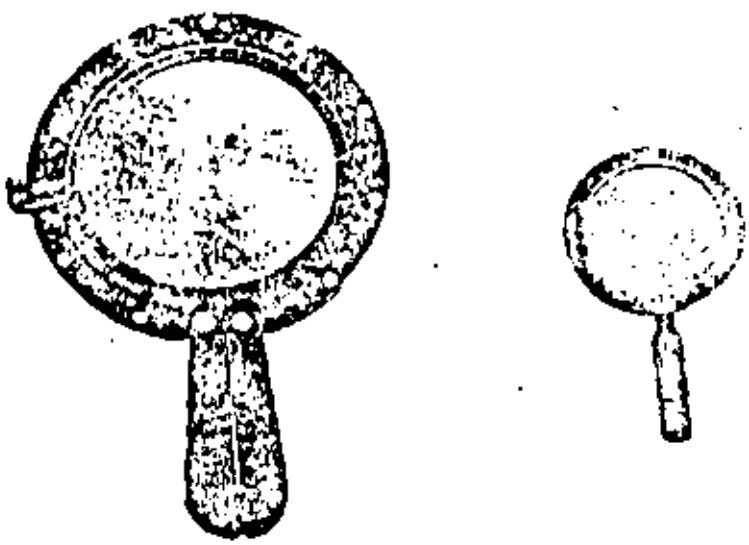

Figura 7 Lupas amplificadoras

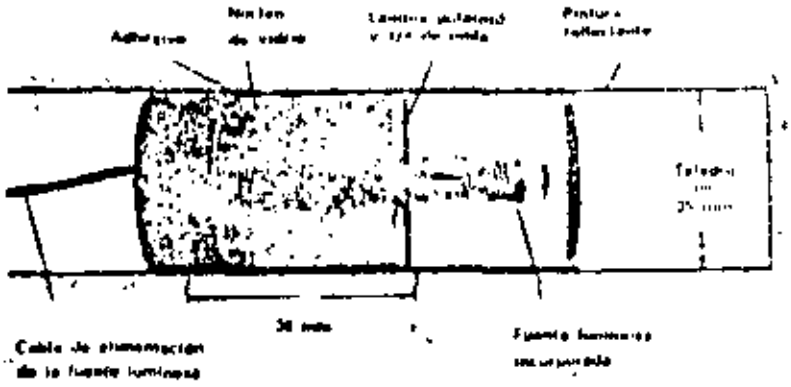

Extensómetro fotoelástico

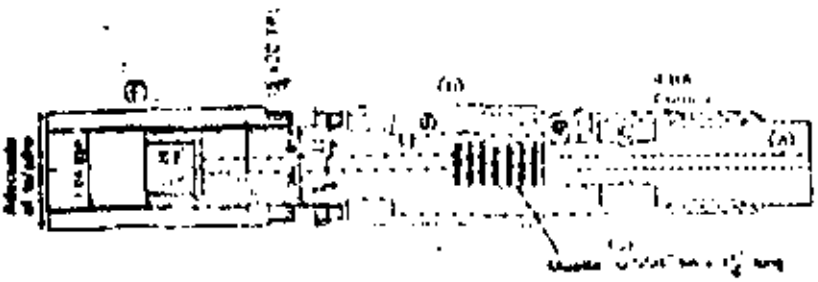

Figura 8 Dispositivo con molde de liberación automática para la colocación del extensómetro fotoelástico en taladros profundos

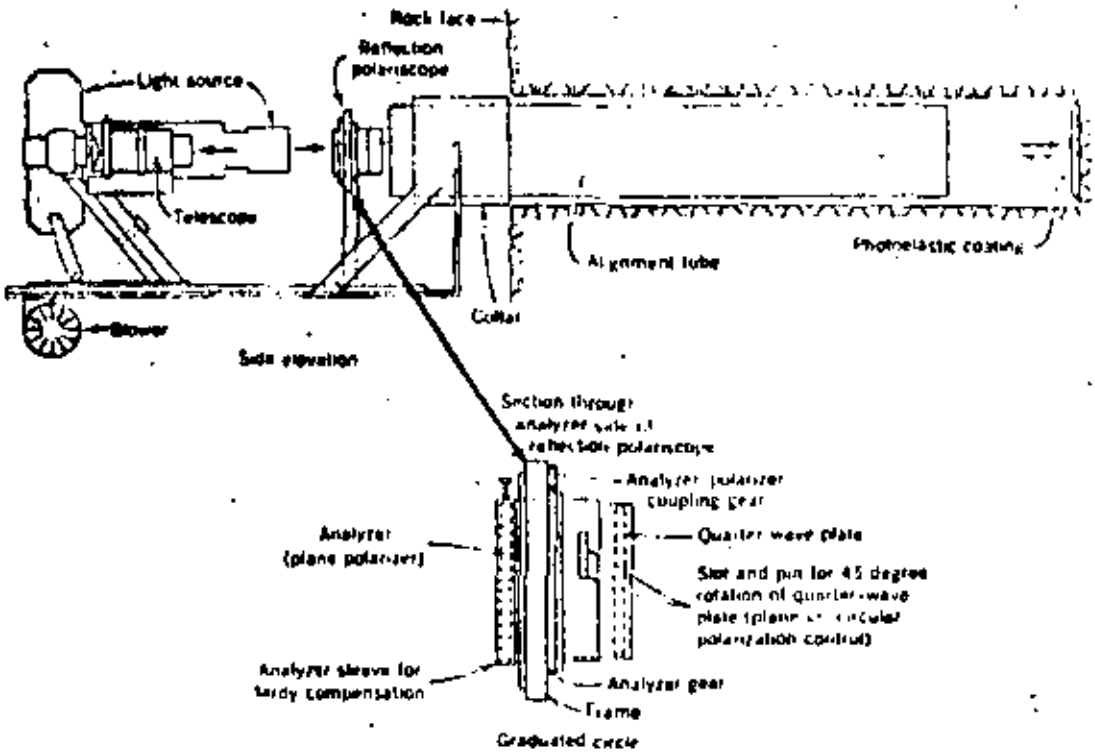

Fig. 9 Tarciole polariscope (private communication from Professor Pincus).

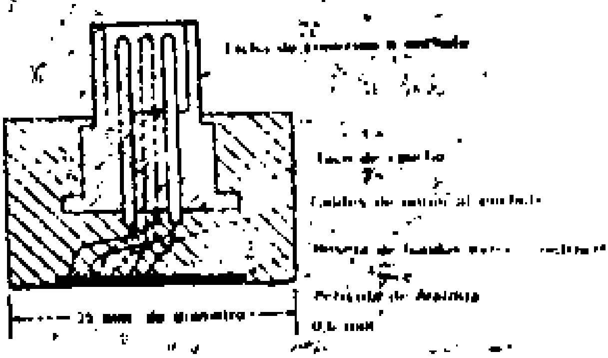

Figura 10 «Doorstopper» de Leeman

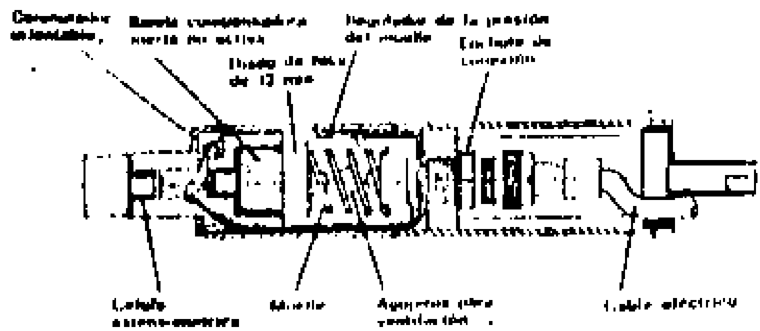

Figura 11 Elemento de inserción de la célula de Leeman

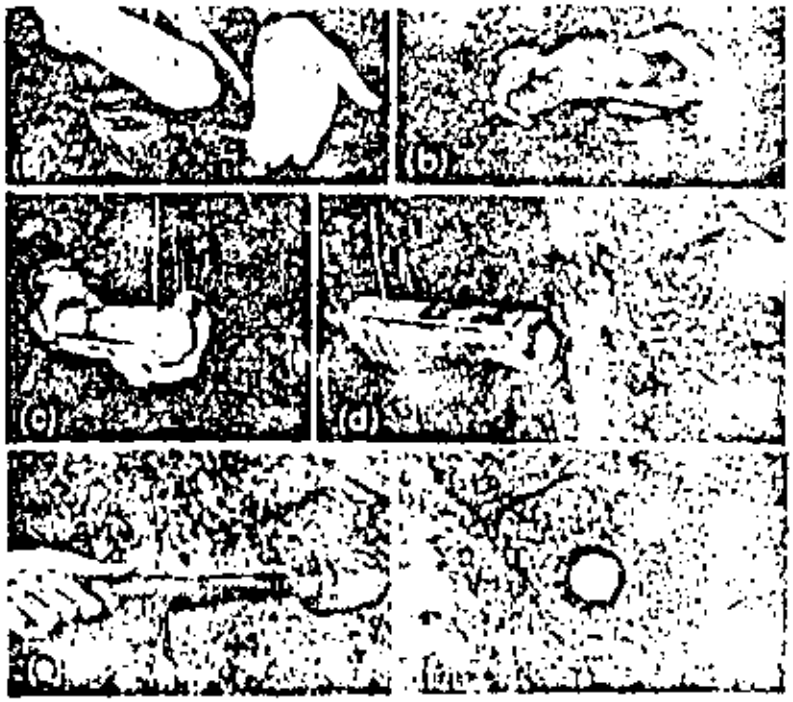

Figura 12. Colocación de la célula fotoelástica biaxial para su uso en ensayos en vera

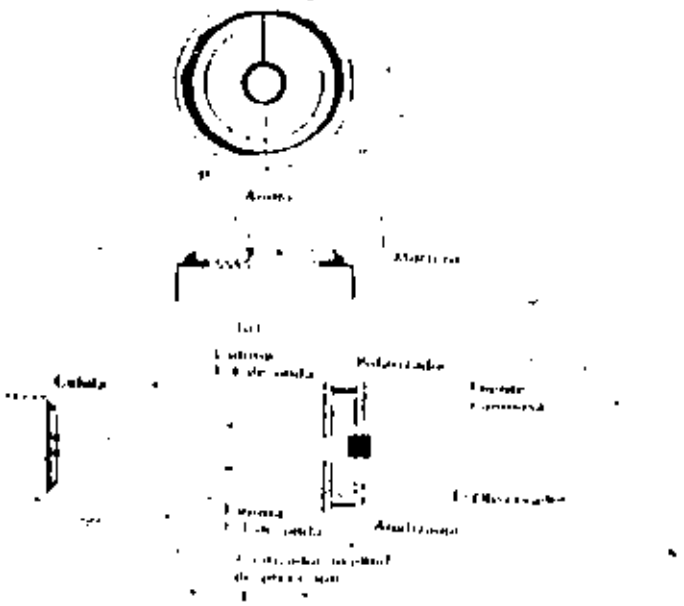

(a) Célula fotoelástica biaxial; (b) Sistema de observación

Figura 13. (a) Equipo de calibración de la célula fotoelástica biaxial

Figura 14 Célula de Skoda (ex-SIAD)

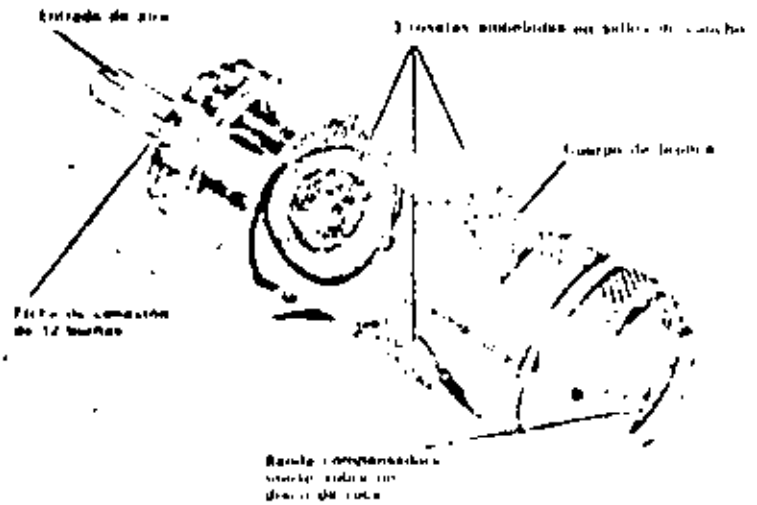

Figura 15 Célula multiple de Escher-Wyss

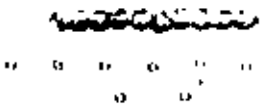

Figura 16 Disposición de la roseta en los puntos [illegible] para la determinación de tensiones [illegible]

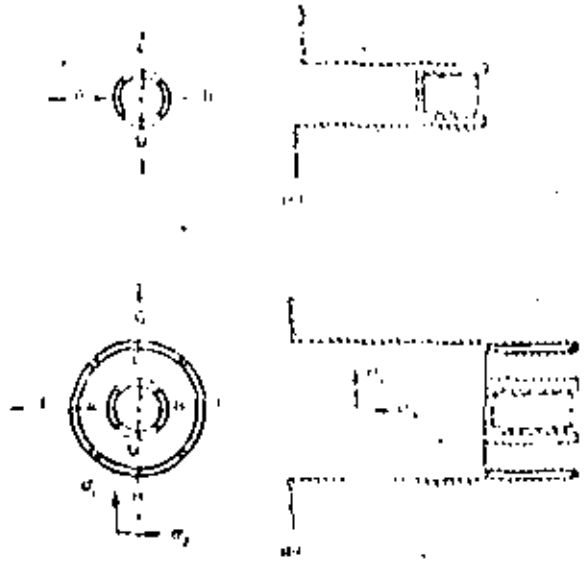

Figura 17 Determinación de tensiones absolutas mediante [illegible]

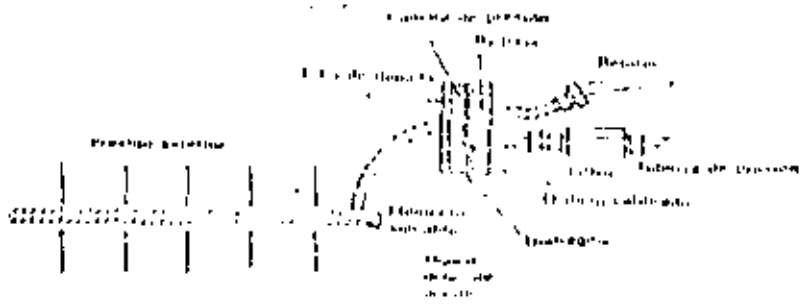

Figura 18 [illegible]

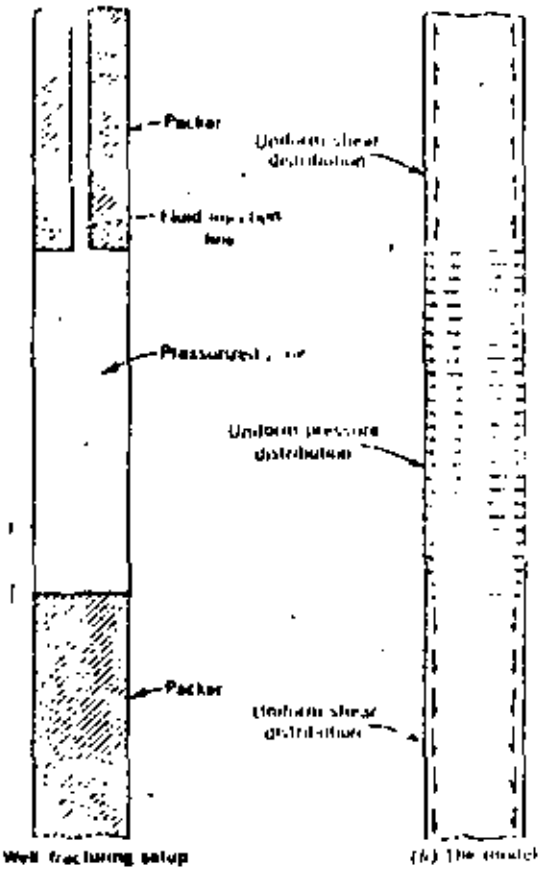

Fig. 19. Schematic diagram of the pressurized section and the accompanying stresses. (After Kettle.[4])

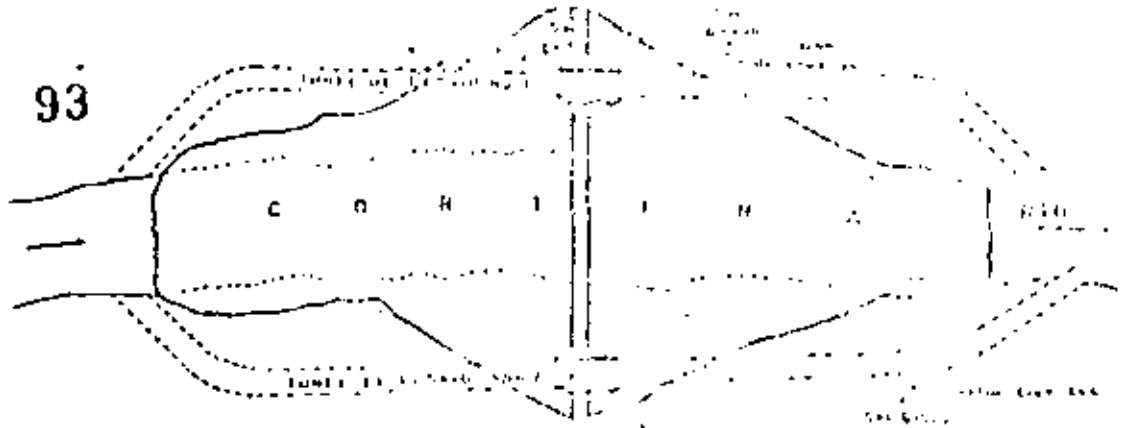
C O R T I N A

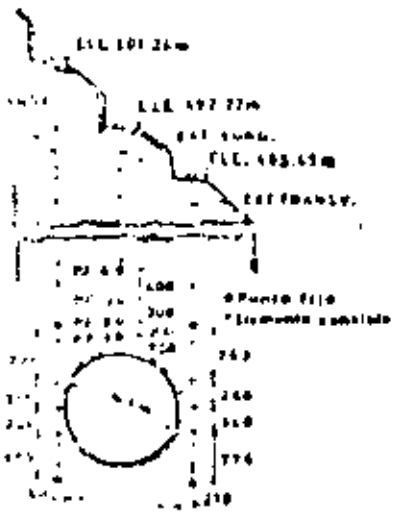

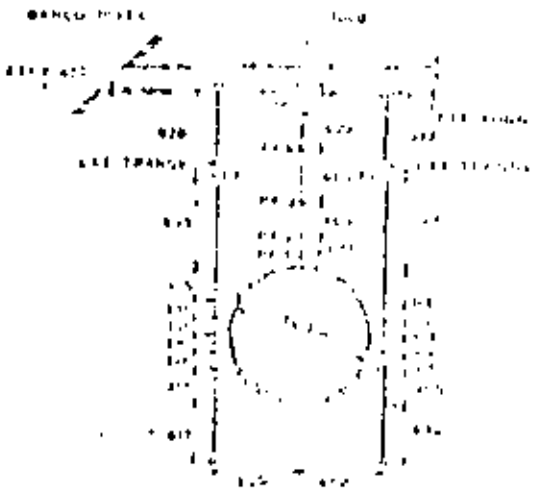

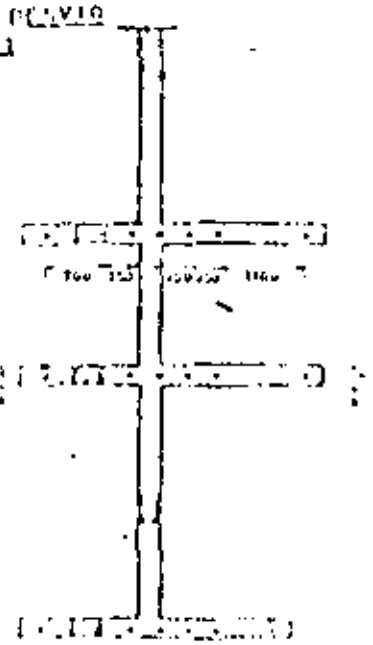

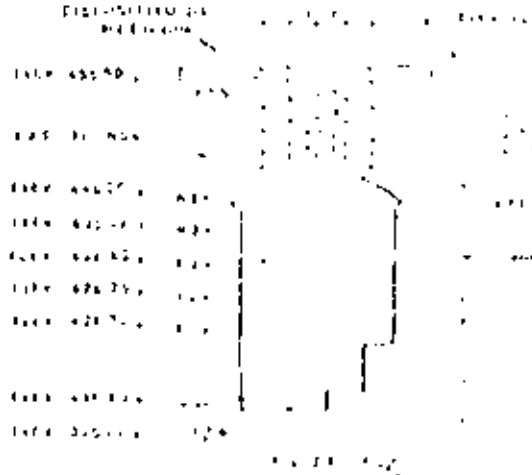

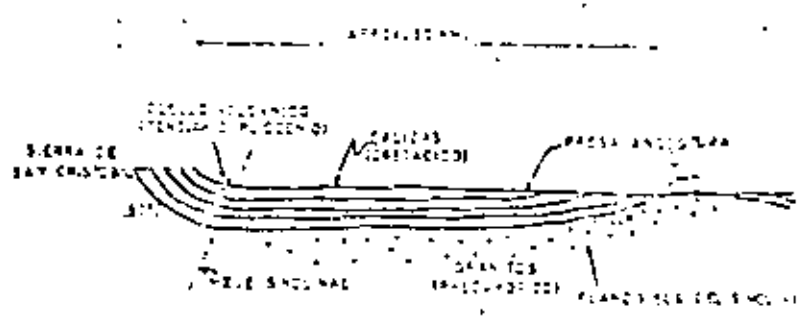

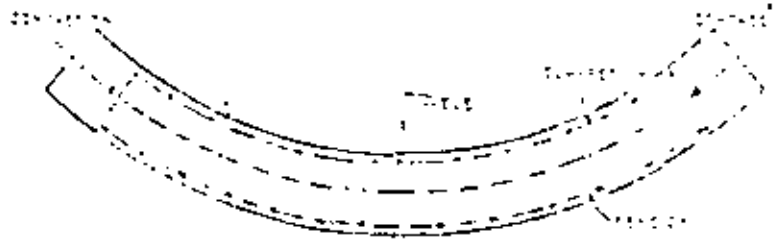

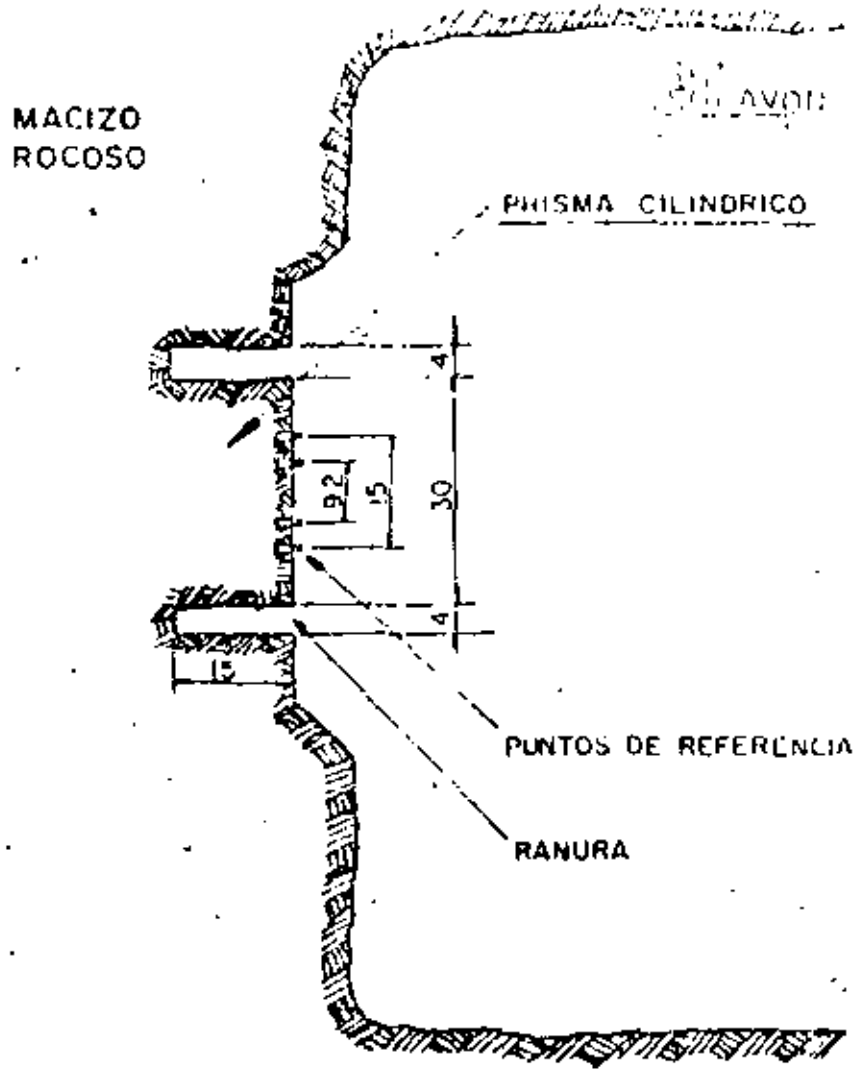

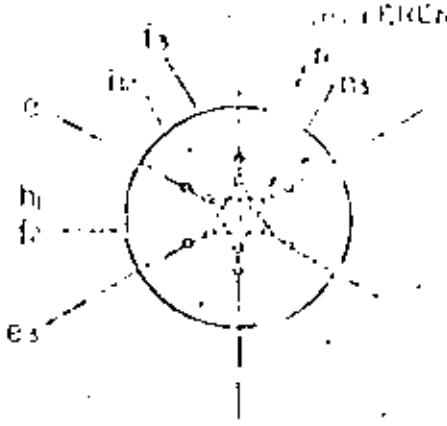

"PRUEBA DE ROSETA"

DIRECCION Y MAGNITUD DE ESFUERZOS INTERNOS

METODO DE LIBERACION DE ESFUERZOS

EJECUCION DE LA PRUEBA

1.- Pulido superficie de la roca.
2.- Colocación de puntos de referencia, fijandolos con epoxy.
3.- Medición inicial de la separación entre los puntos de referencia, con medidor mecánico tipo Whittemore, de carátula, con precisión de 0.001 mm.
4.- Barrenación de la ranura de forma circular de 30cm de diámetro, 15cm de profundidad y 4cm de ancho.
5.- Proceso de deformación de la roca inducida por rotura de la continuidad de la misma al efectuar la ranura (liberación de esfuerzos que produce deformaciones en el prisma cilindrico de roca).
6.- Medición de estas deformaciones en tres direcciones a 60°.
7.- Obtención de la dirección de deformaciones principales.

FIG. 22

_ DIRECCION DE ESFUERZOS PRINCIPALES _ "ROSETA DE DEFORMACIONES"

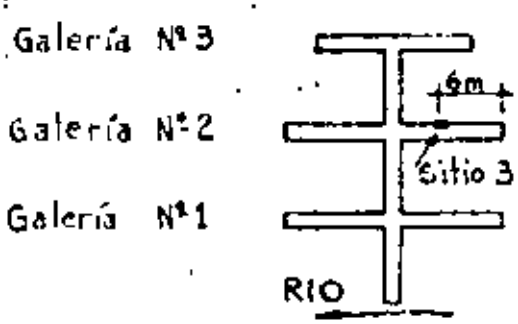

_ P.H. ANGOSTURA, CHIS. _
_ CASA DE MAQUINAS _

Fig. 23

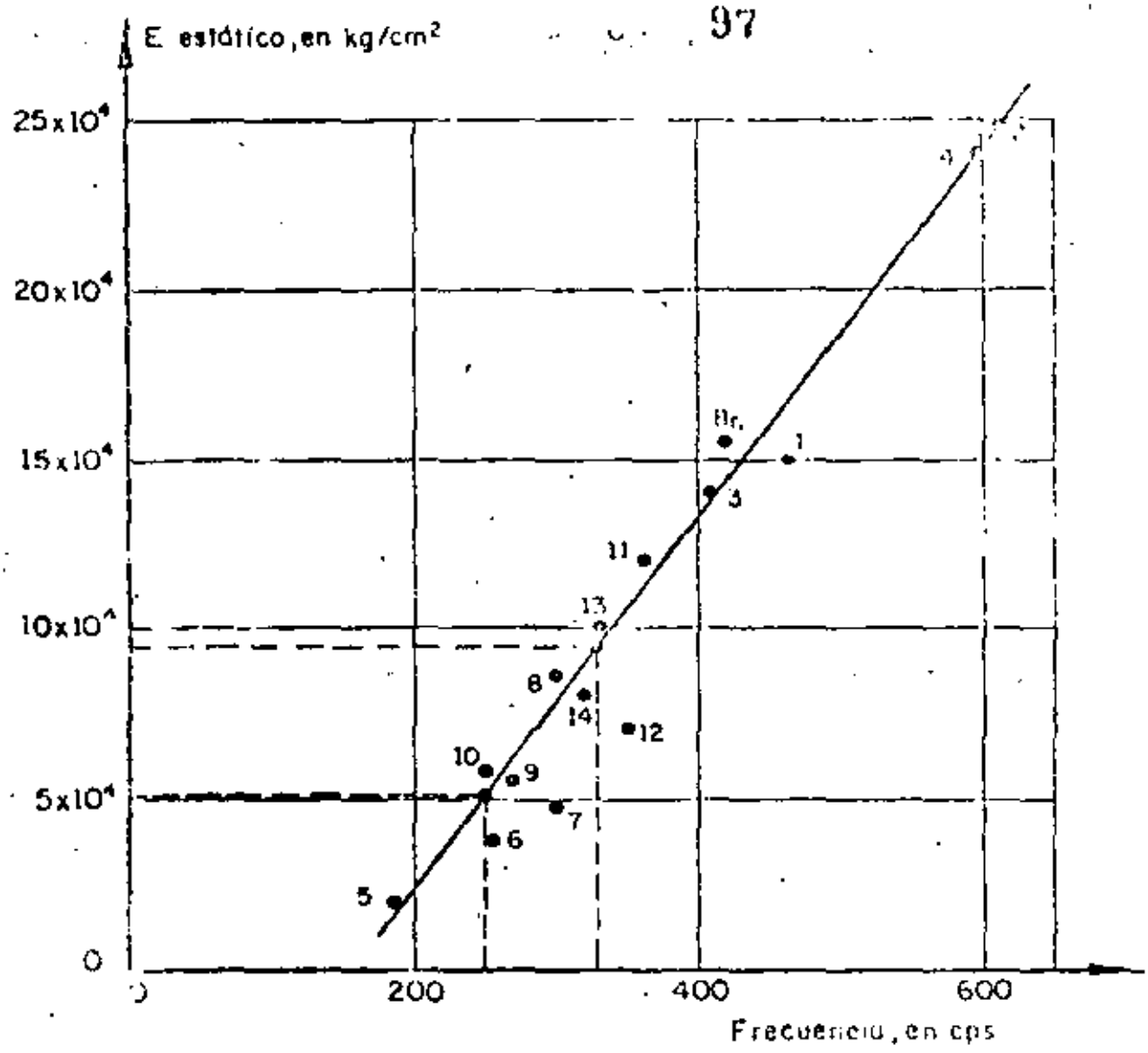

Fig 24 Relación experimental entre el módulo estático medido con placa y la frecuencia de la onda transversal

TABLA 1. PRUEBAS DE ALIVIO DE ESFUERZ

Sitio N°	$\varepsilon_x \times 10^4$ promedio	$\varepsilon_y \times 10^4$ promedio	$\frac{1}{2}\gamma_{xy} \times 10^4$ promedio	σ_x kg/cm²	σ_y kg/cm²	τ_{xy} kg/cm²	Observaciones
2	7	9.2	-3.5	102.8	81.2	-14	Diámetro del cilindro de prueba: 15 cm Profundidad de la ranura: 7.5 cm
2	5.5	6.7	-4.0	90.3	63.1	-15	Diámetro del cilindro de prueba: 15 cm Profundidad de la ranura: 15 cm
3	6.2	5.3	-1.9	84.8	52.2	- 7.8	Diámetro del cilindro de prueba: 21 cm Profundidad de la ranura: 21 cm
5	5.2	11.0	3.0	88.0	88.3	12.0	Diámetro del cilindro de prueba: 15 cm Profundidad de la ranura: 7.5 cm
5	3.5	12.3	3.1	74.0	92.4	12.4	Diámetro del cilindro de prueba: 15 cm Profundidad de la ranura: 15 cm
6	9.4	6.1	1	120.5	67.6	4.0	Diámetro del cilindro de prueba: 21 cm Profundidad de la ranura: 21 cm
9	10.0	4.9	0.4	123.7	60.8	1.5	Operador 1. Diámetro del cilindro de prueba: 30 cm Profundidad de la ranura: 15 cm
9	9.3	6.1	0.4	111.4	65.9	1.6	Operador 2. Diámetro del cilindro de prueba: 30 cm Profundidad de la ranura: 15 cm
9	9.5	5.8	0.3	120.7	66.3	1.2	Operador 3. Diámetro del cilindro de prueba: 30 cm Profundidad de la ranura: 15 cm

Valor promedio de todos los sitios σ_x = 101.3 kg/cm² σ_y = 71.0 kg/cm² τ_{xy} = 0.6 kg/cm²

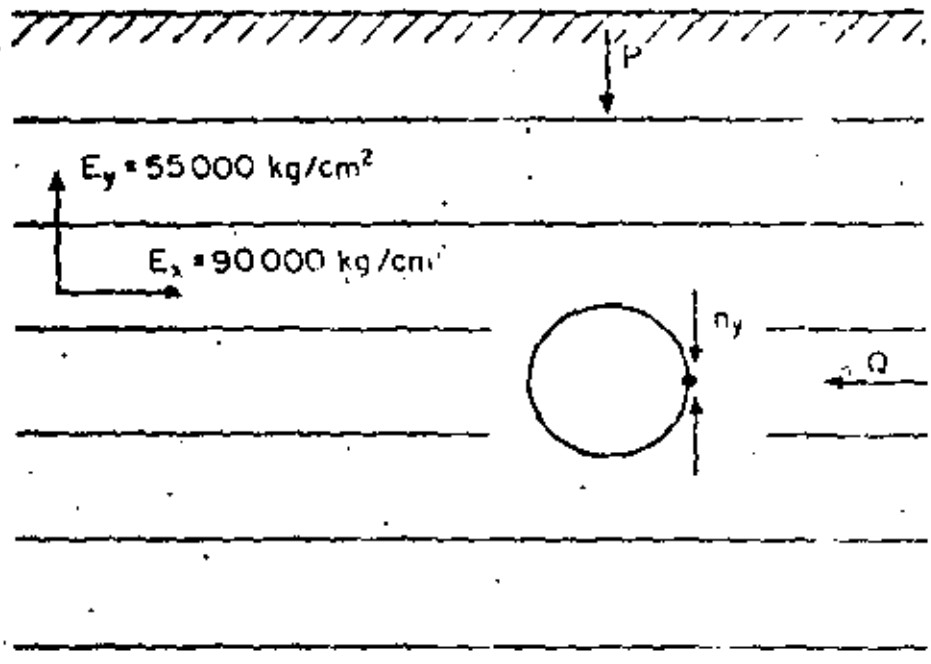

$$n_y = (1+\gamma_1)(1+\gamma_2)\left[\frac{P(3+\gamma_1+\gamma_2-\gamma_1\gamma_2)}{(1+\gamma_1)^2(1+\gamma_2)^2} + \frac{Q(\gamma_1+\gamma_2-\gamma_1\gamma_2-1)}{(1-\gamma_1)^2(1-\gamma_2)^2}\right]$$

Fig.26 Túnel en un medio de anisotropía transversa

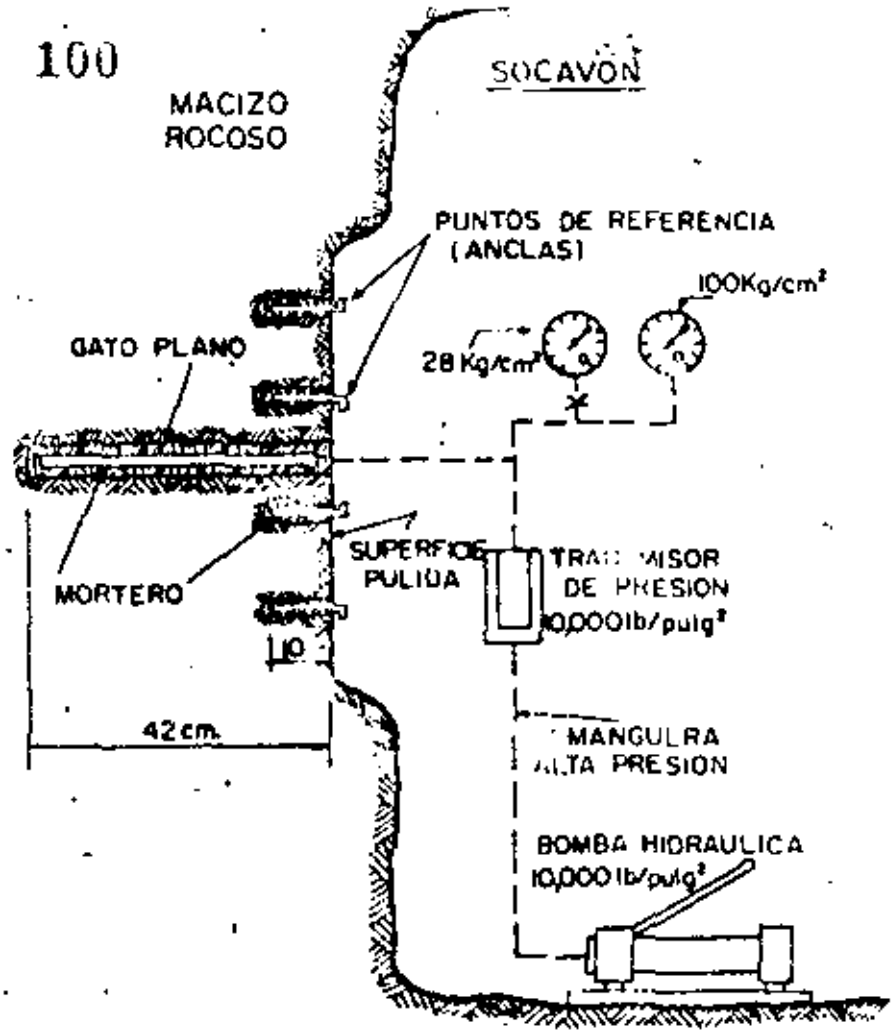

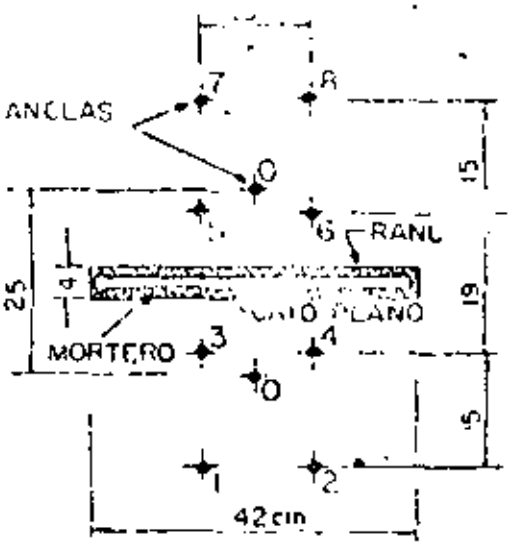

DISTRIBUCION DE ANCLAS

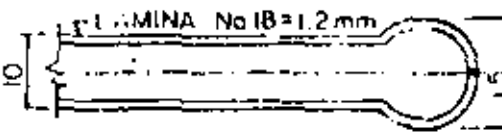

SECCION GATO PLANO

ESQUEMA, PRUEBA DE "GATO PLANO"

DETERMINACION DE ESFUERZOS INTERNOS EN ROCA

METODO DE LIBERACION DE ESFUERZOS

EJECUCION DE LA PRUEBA

1.- Pulido superficie de la roca.
2- Colocación de "puntos de referencia" (anclas), fijándolos a la roca usando mortero con aditivo estabilizador de volumen.
3- Medición inicial de la separación entre los puntos de referencia, con medidor mecánico tipo Whittemore, de carátula, con separación mínima de 0.0005
4- Barrenación de la ranura de 42 x 42 x 4 cm.
5- Proceso de deformación de la roca inducida por rotura de la continuidad de la misma al efectuar la ranura (liberación de esfuerzos que produce deformaciones perpendiculares al plano de la ranura).
6- Medición de estas deformaciones, tomando lecturas inmediatamente después de ranurar (que son del orden del 90% de la deformación total), y durante un período de tiempo entre 1 y 3 días después de haber hecho la ranura.
7 Inserción del "gato plano" cuadrado en la ranura, ahogándolo en mortero con aditivo estabilizador de volumen, con resistencia de 50 Kg/cm² a los 7 días.
8- Tiempo de fraguado del mortero 3 días.
9- Aplicación de presión hidráulica hasta que los "puntos de referencia" regresen a su posición inicial, obteniéndose la "presión de cancelación" que es el valor del esfuerzo interno de la roca en dirección perpendicular al plano de la ranura.

FIG. 2

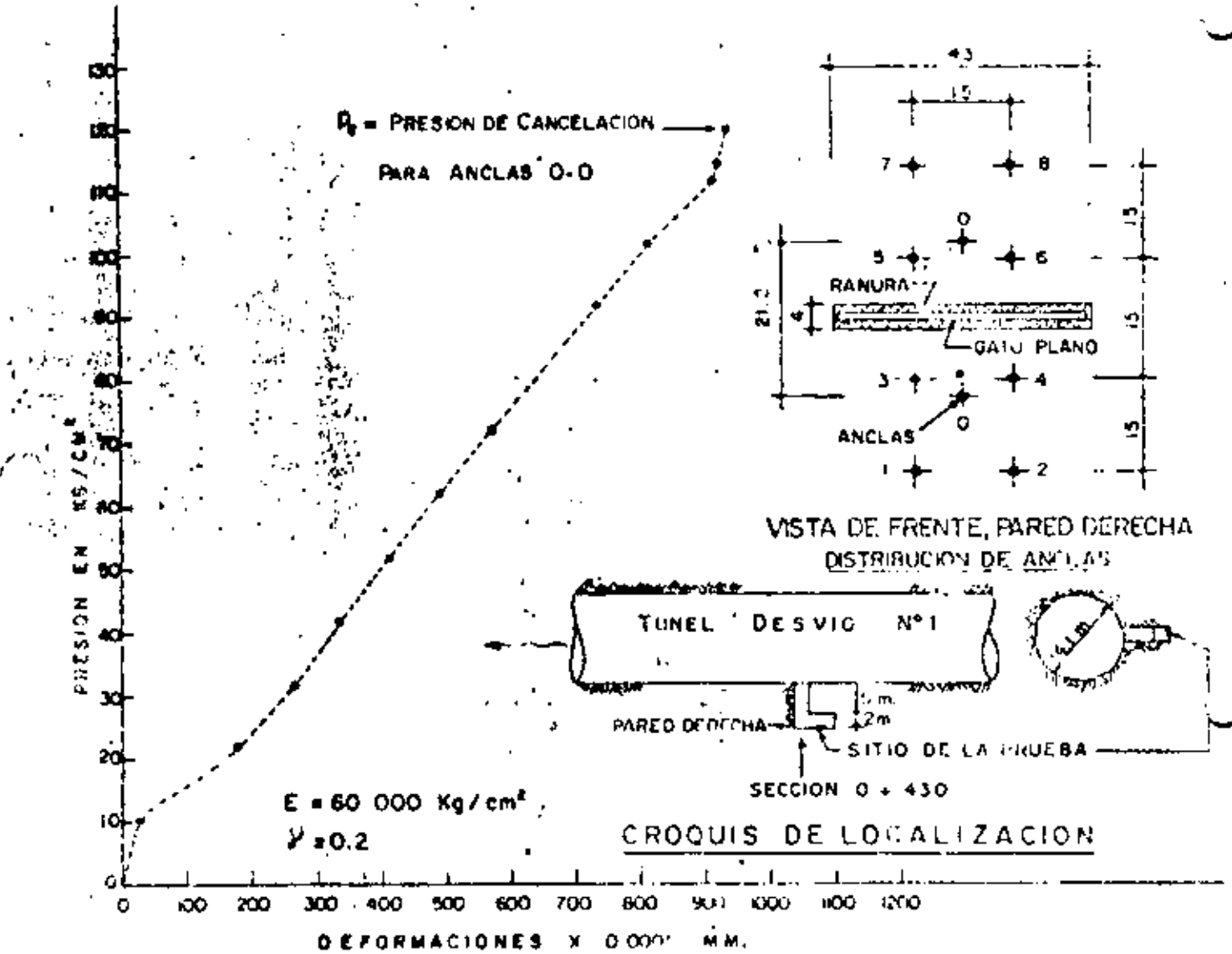

LECTURAS EN EL EXTENSOMETRO *

LINEA	ANTES DE RANURAR	DESPUES DE RANURAR	PARA 120 Kg/cm² DE PRESION
1-3	515	795	505
1-4	548	670	525
2-4	485	550	-----
2-3	410	535	420
3-5	1060	50	1015
3-6	1130	415	1138
4-6	1180	225	-----
4-5	930	225	925
5-7	370	570	400
5-8	510	670	300
6-8	288	505	300
6-7	578	760	655
0-0	1090	155	1090

* EXTENSOMETRO MECANICO, 2 UNIDADES/ MICRA

F.E., LAB. MEC. DE ROCAS
MAYO 16 DE 1970 OPERADOR: ING. J.H.O. Y E. G. G.

P.H. ANGOSTURA, CHIS.
TUNEL DE DESVIO N°1
SOCAVON DE PRUEBAS
SECCION 0+430

PRUEBA DE "GATO PLANO"

GATO EN POSICION HORIZONTAL
PRESION DE CANCEL... AL VERTICAL

$$\sigma_n = \frac{p_c(cj - a)}{c} = \frac{120(18.5 - \quad)}{21.5}$$

σ_n = 80.5 kg/cm²

FIG 28

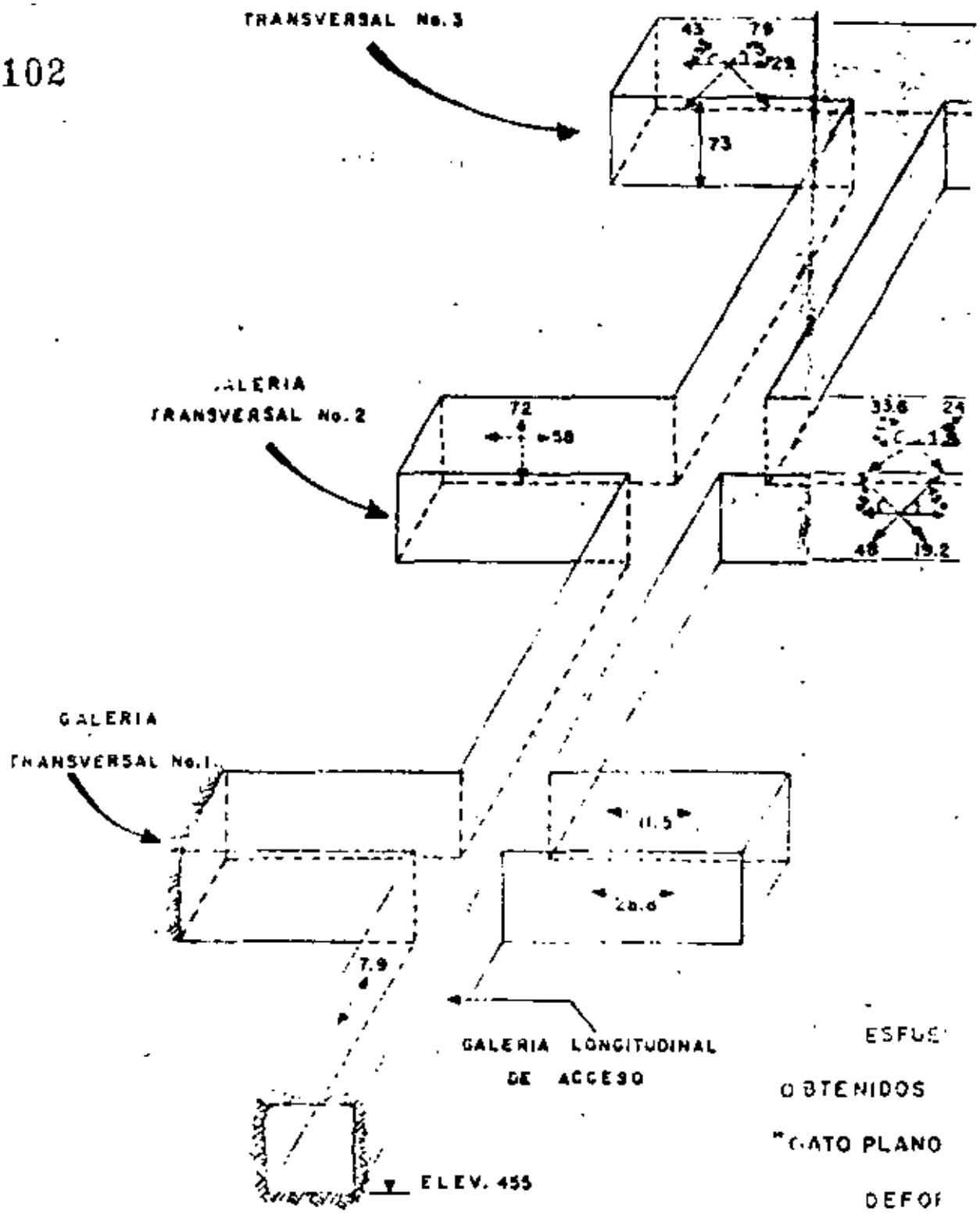

ESFUE
OBTENIDOS
"CATO PLANO
DEFOR

GALERIAS DE EXPLORACION GEOLOGI
E INSTRUMENTACION SOBRE LA CAS
DE MAQUINAS, MARGEN DERECHA.

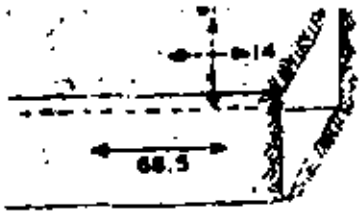

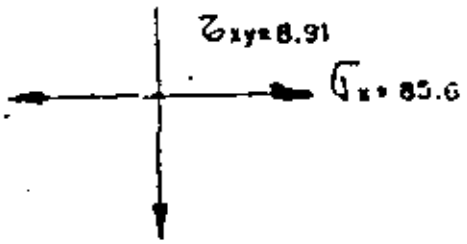

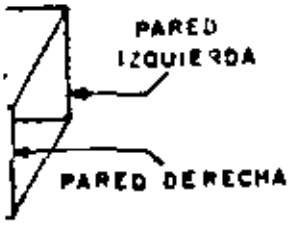

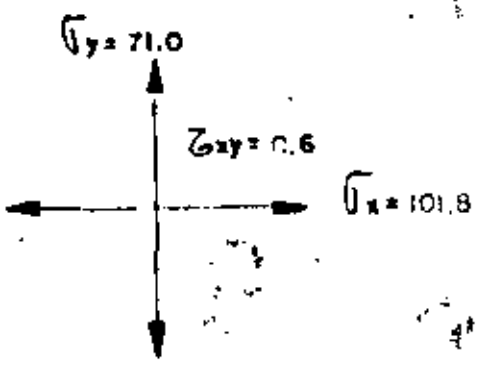

Valores de esfuerzos normales calculad
de ensayes de roseta de deformaciones

RZOS NORMALES

EN PRUEBAS DE

" y "ROSETA DE

MACIONES"

CA

A

FIG. 29

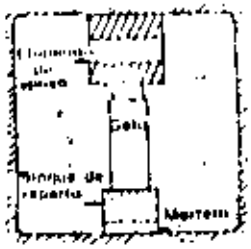

Figura 30 Ensaye de carga en un fondo

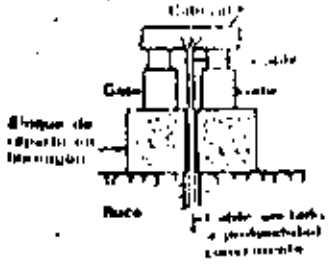

Figura 31 Ensaye con cable de anclaje

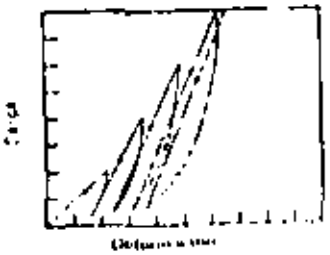

Figura 32 Típica curva carga-deformación

P. H. CHICOASEN, CHIS.
MARGEN DERECHA
SOCAVON No I
"PRUEBA DE PLACA"
POSICION VERTICAL
PISO
15 OCT 1974

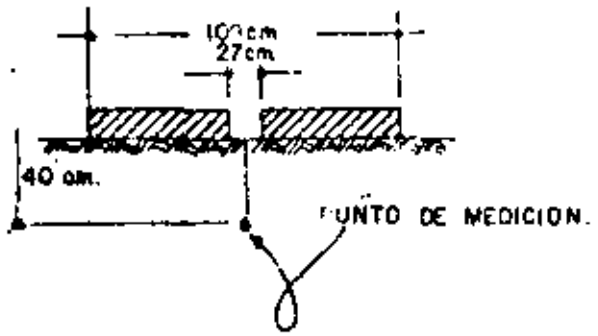

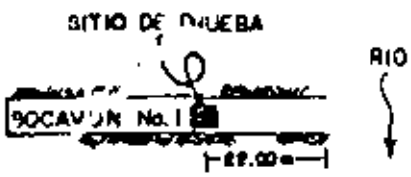

CROQUIS DE LOCALIZACION

$$E = \frac{\mu}{\delta}\left\{\left[(1-\gamma)z^2\right]\left[\frac{1}{(a_2^2+z^2)^{1/2}} - \frac{1}{(a_1^2+z^2)^{1/2}}\right] + (1-\gamma^2)\left[(a_2^2+z^2)^{1/2} - (a_1^2+z^2)^{1/2}\right]\right\}$$

$z = 40.0$ cm.
$a_2 = 54.5$ cm
$a_1 = 13.5$ cm.
$\gamma = 0.25$

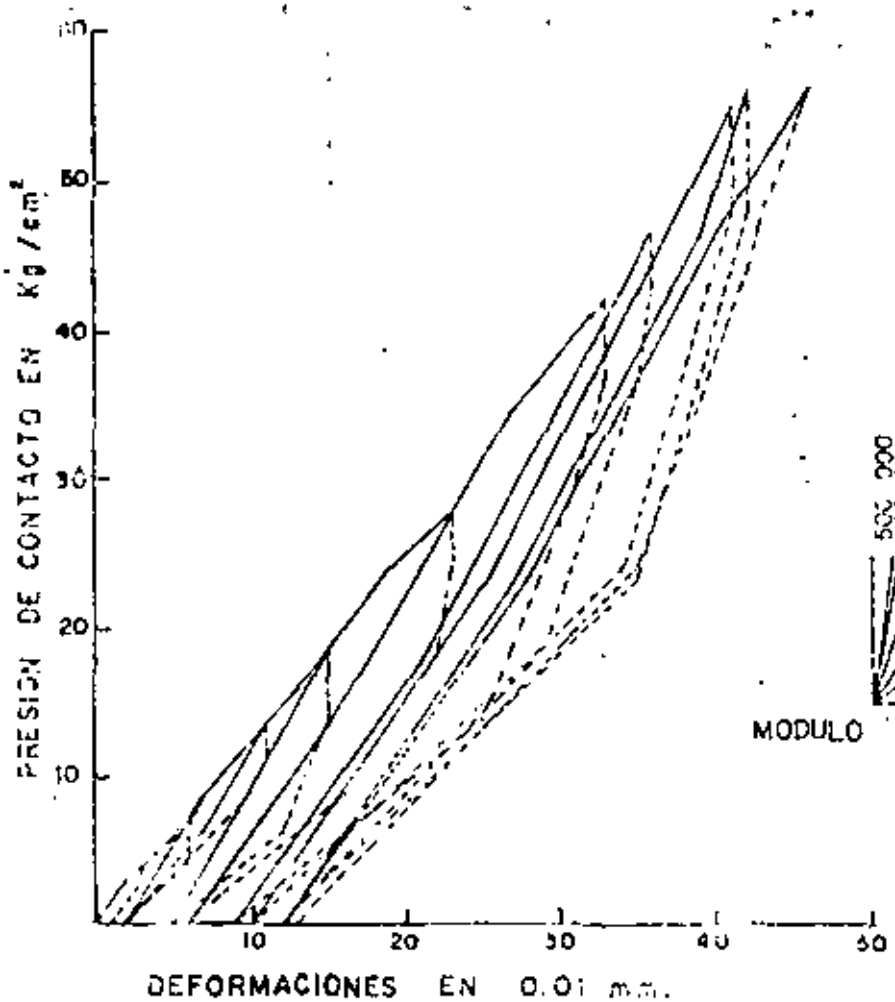

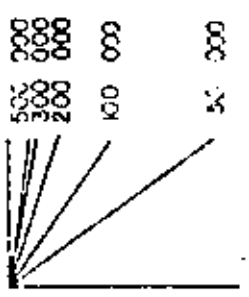

FIG. 33

Figura 34 Ensayo de presión en galería normalizada. (a) Galería en c...
(b) Sección A-A

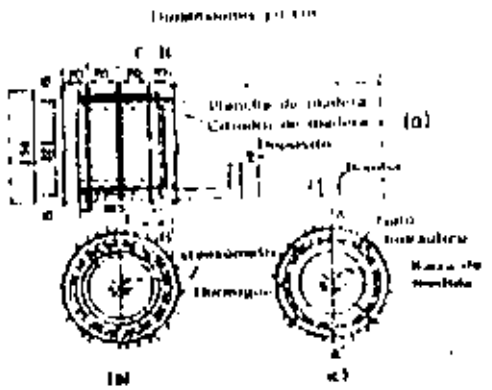

Figura 35 Gato radial. (a) Sección A-A'; (b) Sección B-B'; (c) Sección C-C'
(dimensiones en mm)

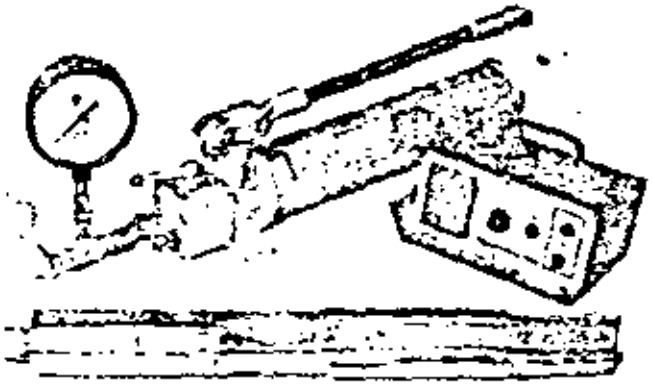

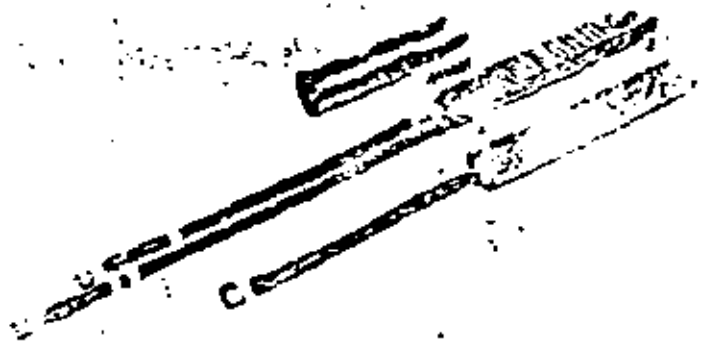

above: Goodman Jack System

above right: Model 52101

right: Model 52102

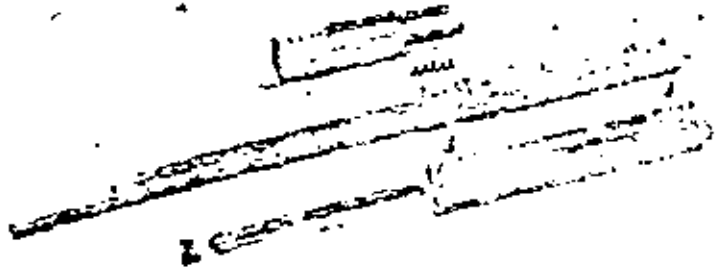

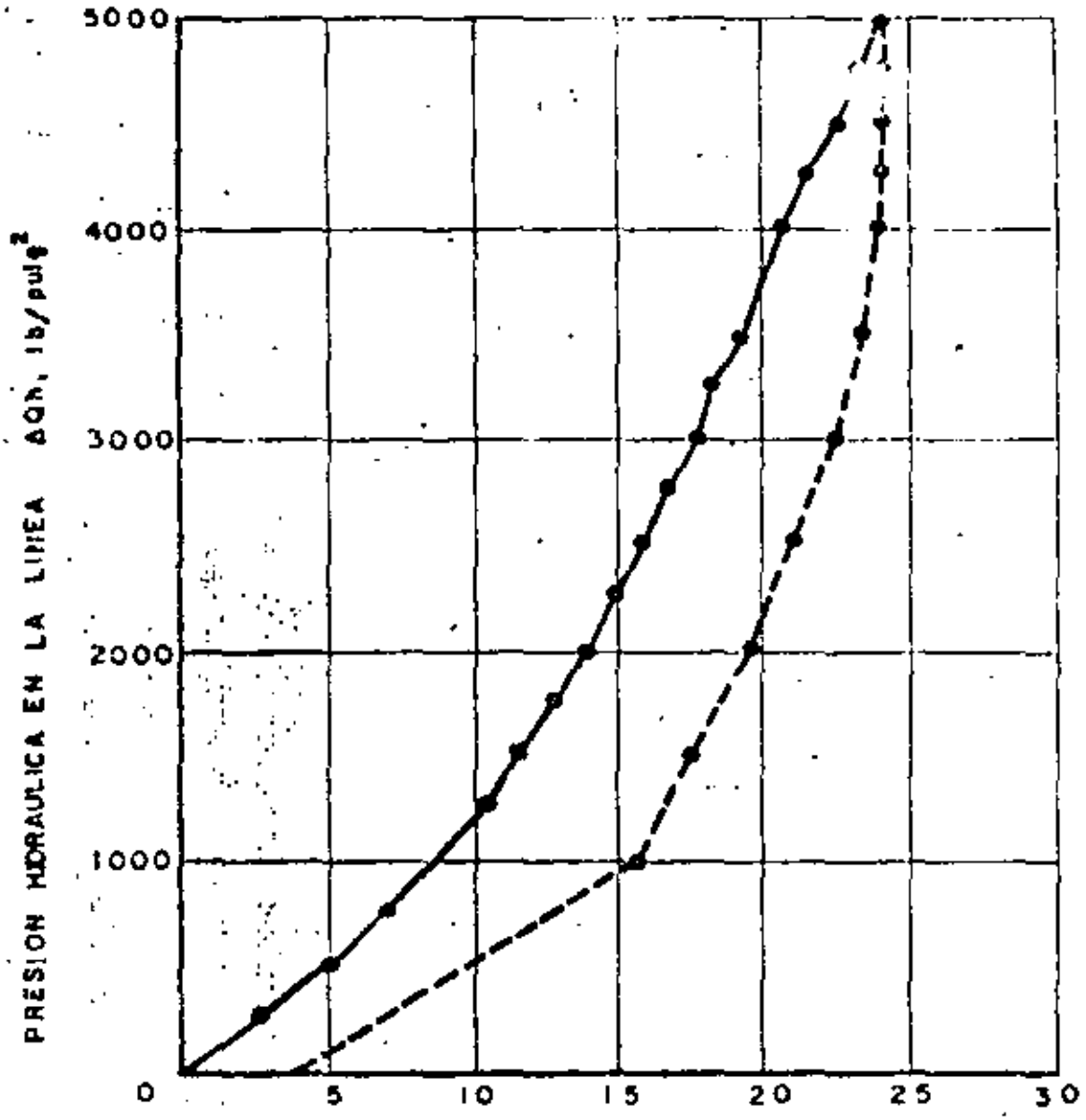

"MODULO DE ELASTICIDAD" $E = 3.05 \frac{\Delta Qh}{2\Delta u}$

INTERVALO DE PRESION (ΔQh) lb/pulg²	DESPLAZAMIENTO (2Δu)X 10⁻³ pulg	MODULO ELASTICO E lb/pulg²×10⁶	Kg/cm²×10³
CARGA 1000 — 5000	15.0	0.82	58
DESCARGA 5000 — 1000	8.5	1.49	105

P.H. LA ANGOSTURA, CHIS.

PRUEBA CON GATO GOODMAN

POSICION VERTICAL

Fig. 37

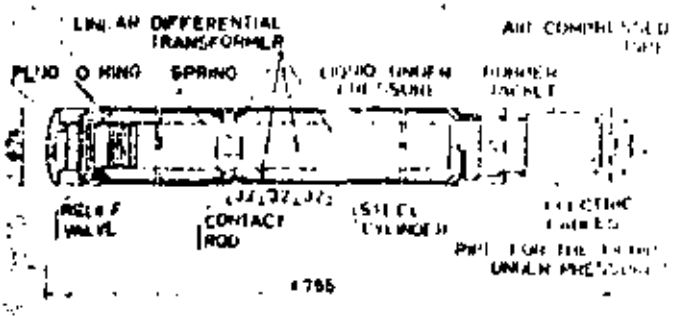

Fig. 10

Dilatometer — Dilatomètre — Dilatometer
Linear differential transformer — Transformateur différentiel linéaire — Differenzialtransformer
Plug — Bouchon — Stöpsel
Ring — Anneau d'étanchéité — Dichtring
Spring — Ressort — Feder
Liquid under pressure — Liquide sous pression — Unter Druck stehende Flüssigkeit
Rubber jacket — Chemise en caoutchouc — Gummimantel
Air compressed pipe — Tuyau de fuite comprimé — Preßluftrohr
Relief valve — Soupape d'échappement — Ablaufventil
Contact rod — Tige de contact — Kontaktstab
Steel cylinder — Cylindre en acier — Stahlzylinder
Electric cables — Câbles électriques — Elektrische Kabel
Pipe for the liquid under pressure — Tuyau contenant le liquide sous pression — Rohr mit der unter Druck stehenden Flüssigkeit

FIG.

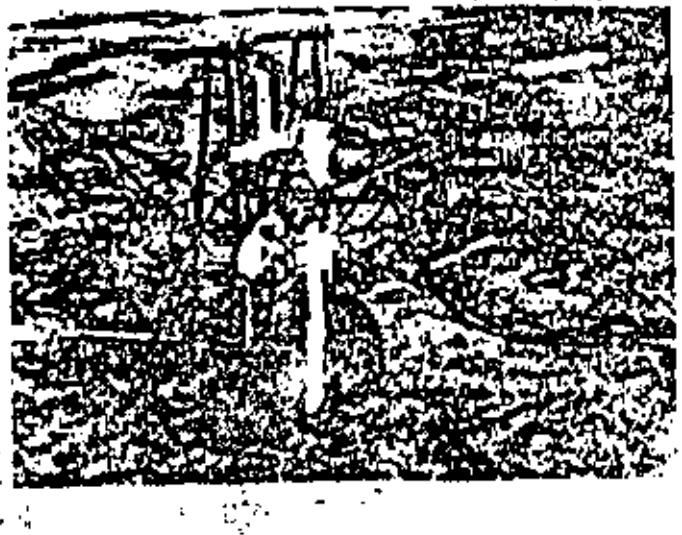

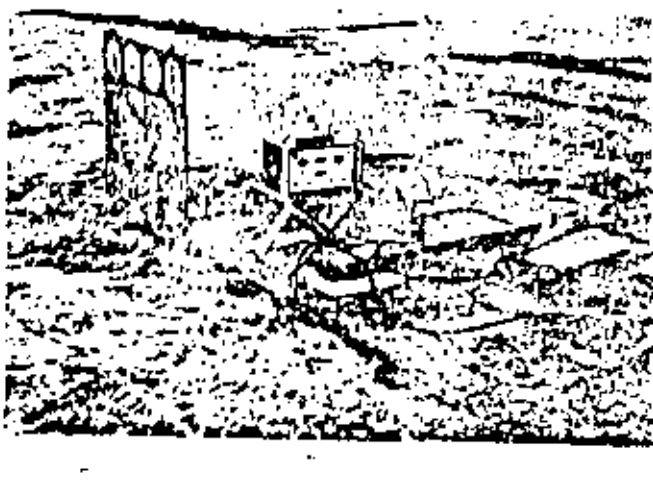

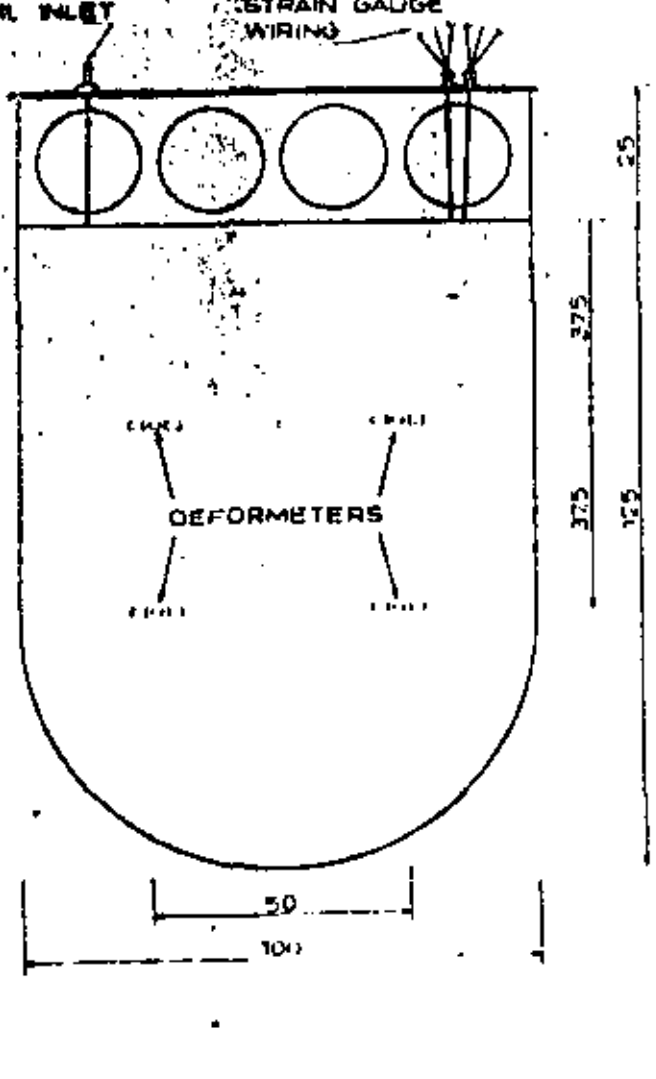
OIL INLET
STRAIN GAUGE WIRING
DEFORMETERS
25
375
375
125
50
100

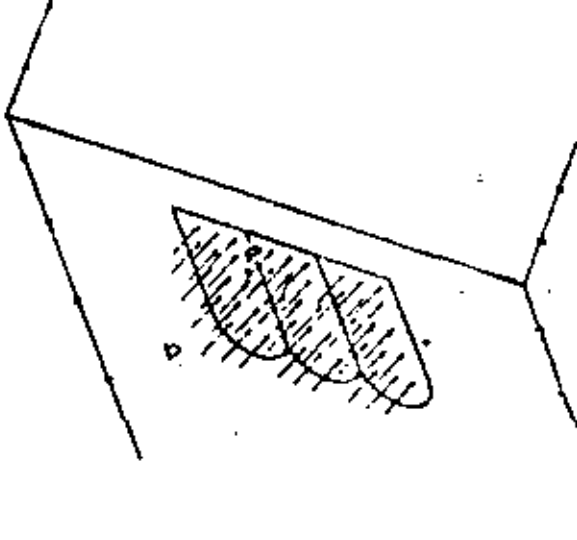

Fig. 39

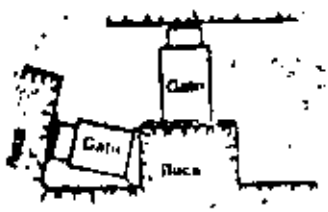

Ensayo de corte *in situ*

FIG. 4

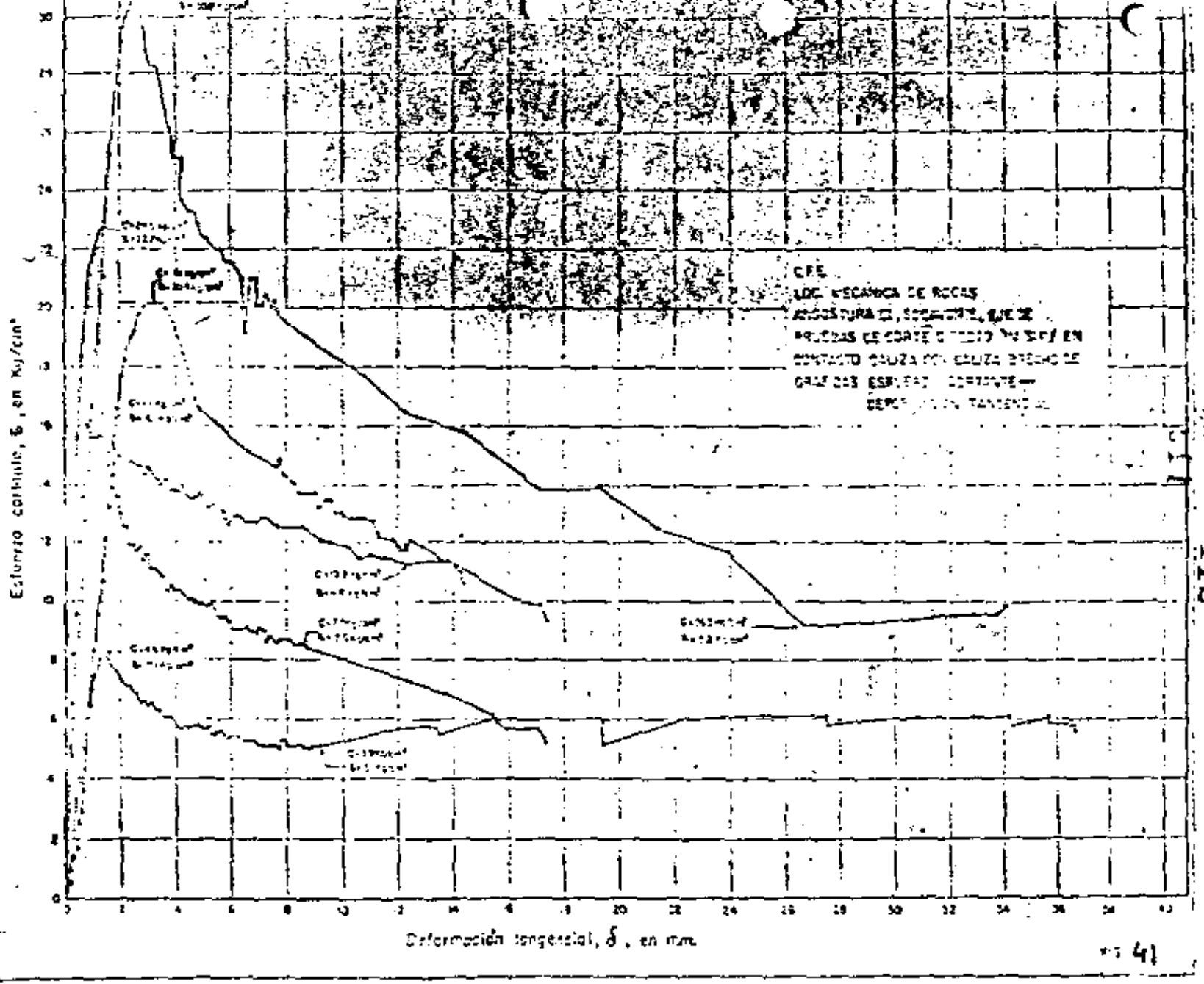
Esfuerzo cortante, τ, en Kg/cm²
Deformación tangencial, δ, en mm.
C.F.E.
LOC. MECANICA DE ROCAS

112

Fig. 41

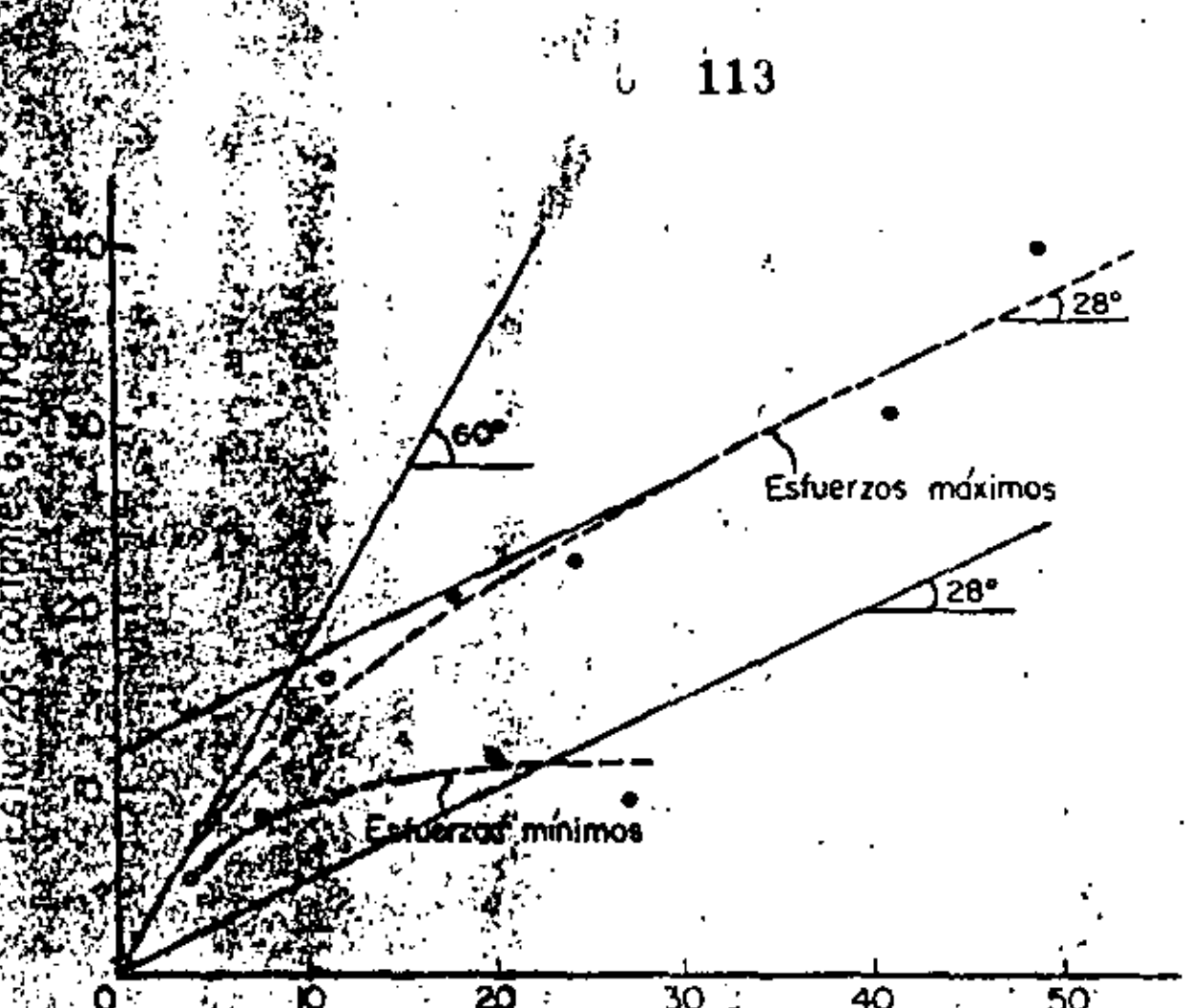

ENVOLVENTE DE MOHR

C. F. E.
O.E.E. MECANICA DE ROCAS
ANGOSTURA III SOCAVON 1, EJE V

PRUEBAS DE CORTE DIRECTO "IN SITU" EN CONTACTO CALIZA CON CALIZA BRECHOIDE EN PROBETAS PRISMATICAS DE 65x65x40 CM

ENERO 1969

FIG. 42

GRAFICA	ESFUERZOS NORMALES	
	PEAK	RESIDUAL
▲——▲	2.00	2.00
●——●	5.00	4.70
■——■	11.00	10.20
△——△	2.00	1.90
○——○	5.00	4.30
□——□	9.70	9.65
×——×	2.00	1.90

P.H. CHICOASEN, CHIS.
MARGEN IZQUIERDA
SOCAVON No. 7
PRUEBA DE CORTE DIRECTO "IN SITU" EN ARCILLAS
Dimensiones del especimen de roca: 60x60x30cm.
Espesor de la arcilla: 3-7cm.

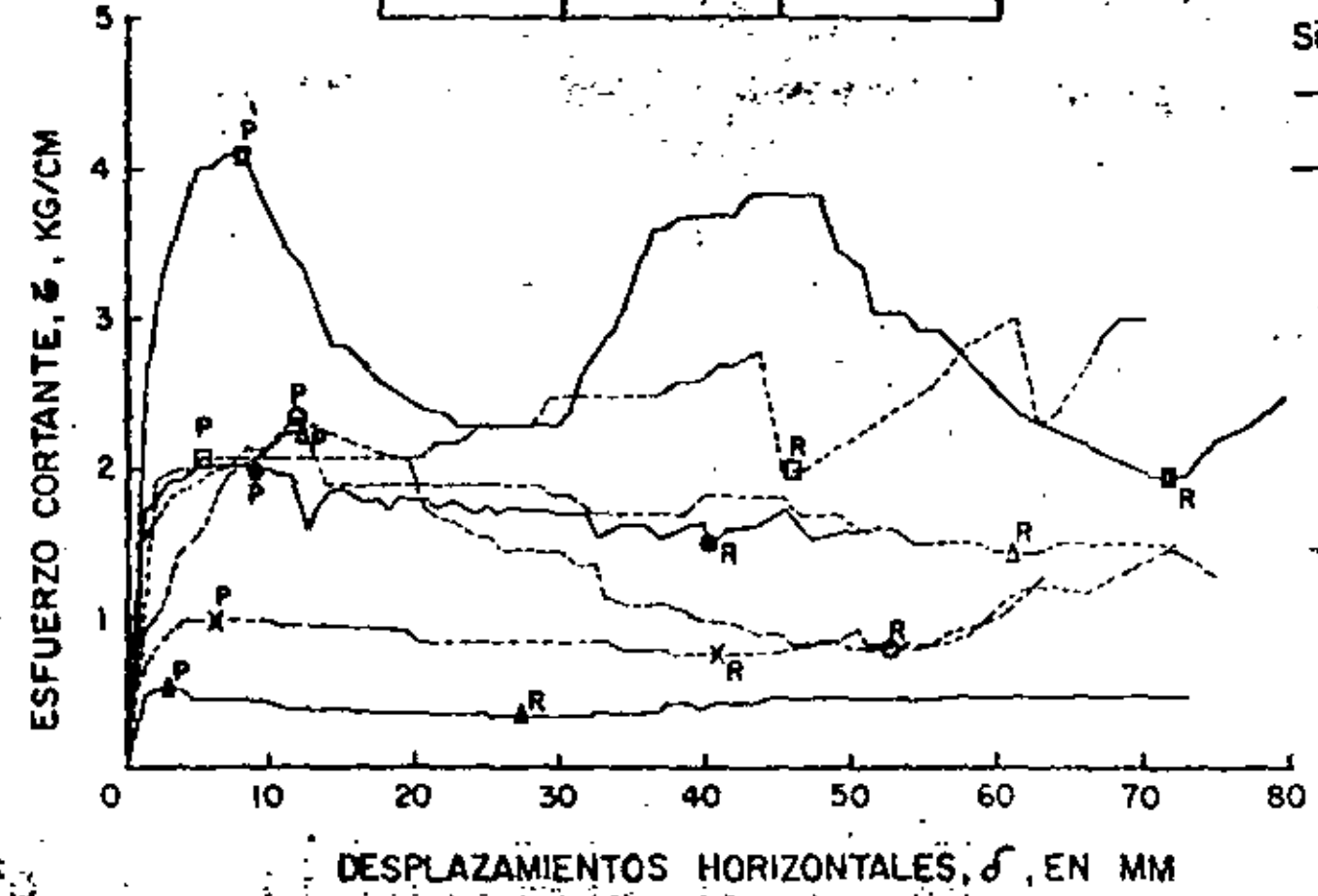

Simbología

——— Con contenido de agua natural

– – – – Saturada (no se sabe cuantitativamente el grado de saturación)

P – Peak
R – Residual

P.H. CHICOASEN, CHIS.
MARGEN IZQUIERDA
SOCAVON No. 7.
PRUEBAS DE CORTE DIRECTO EN ARCILLAS SATURADAS
Dimensiones del especimen de roca: 60x60x30 cm.
Espesor de la arcilla: 3-7 cm.

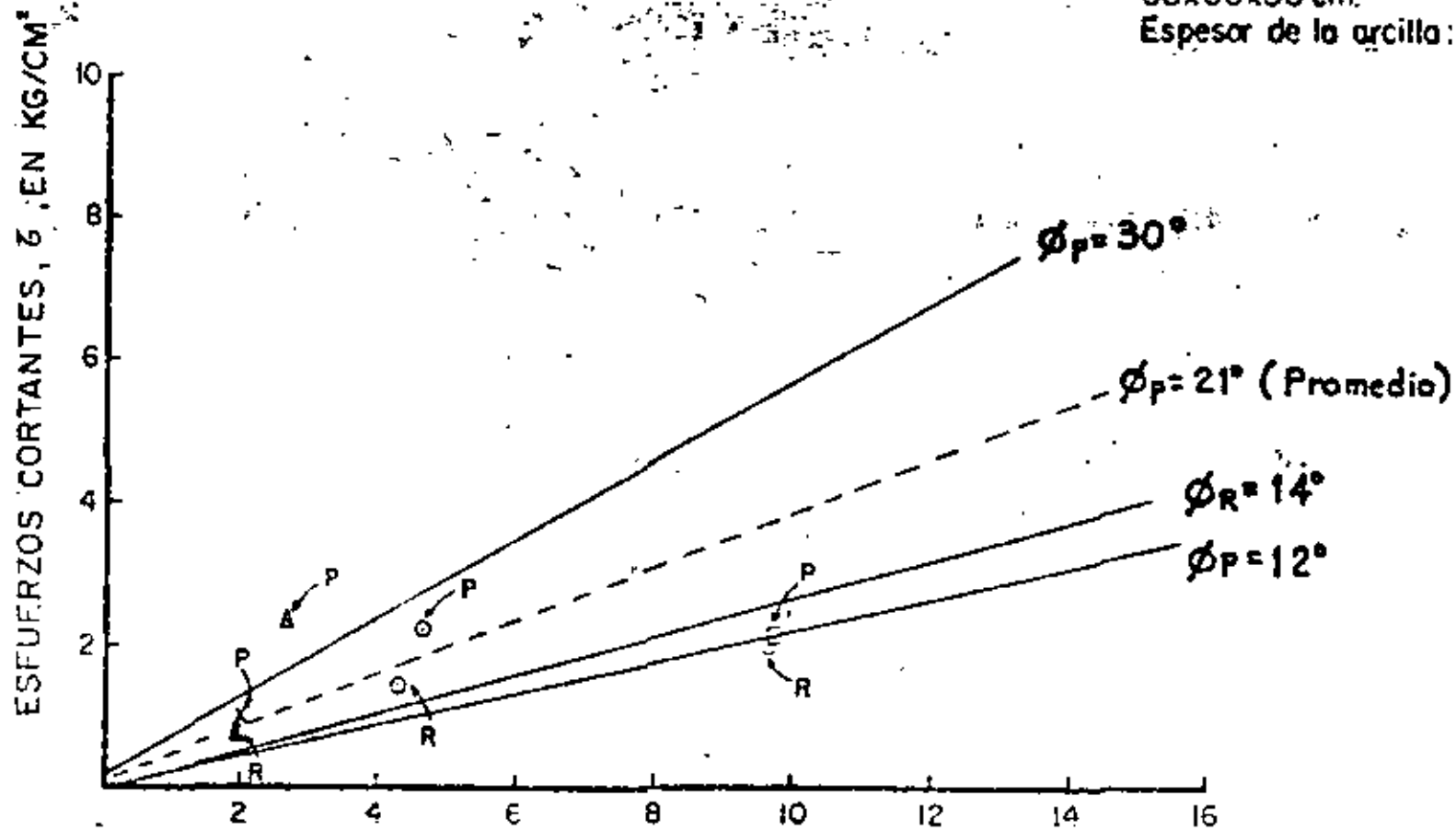

dad. Con esta tabla, se pretende únicamente orientar la selección del tipo de prueba por efectuar.

TABLA I

APLICABILIDAD DE LAS PRUEBAS DE PERMEABILIDAD

Material	Localización del nivel freático	Descripción del material		Prueba Lugeon	Prueba Lefranc	Bombeo con medición del cono de abat.	Bombeo con medición de piezómetros	Matsuo Nawayi	Trazadores radiactivos	Misceláneas
Roca	Por encima del nivel freático	Homogéneo	Muy fracturada					X		
			Poco fracturada							
		Heterogéneo	Muy fracturada					X		X
			Poco fracturada							
	Por debajo del nivel freático	Homogéneo	Muy fracturada		X					
			Poco fracturada	X						
		Heterogéneo	Muy fracturada		X				X	X
			Poco fracturada	X						
Aluvión	Por encima del nivel freático	Homogéneo						X		
		Heterogéneo						X		
	Por debajo del nivel freático	Homogéneo			X	X				
		Heterogéneo			X		X		X	X

Cada tipo de prueba se analiza con métodos de cálculo más o menos elaborados; sin embargo, los resultados obtenidos de los diversos métodos de interpretación propios de cada prueba, son muy semejantes; la atención debe enfocarse por tanto en la forma en que se llevó a cabo la prueba, ya que dependiendo de los procedimientos utilizados, los resultados pueden ser muy diferentes.

2. PRUEBAS LUGEON

2.1 Descripción e hipótesis

Es una prueba de inyección de agua a presión en tramos de perforación, que tiene por objeto formarse una idea aproximada de la permeabilidad en grande, o sea, la debida a las fisuras de la roca. Se varía la longitud de los tramos probados, así como, la presión de inyectado del agua. La llamada unidad Lugeon corresponde a una absorción de 1 litro de agua por minuto, por metro de sondeo y con una presión de inyección de 10 kg/cm^2.

Ahondando en esta descripción escueta, señalaremos la influencia de los diversos factores que intervienen en esta prueba:

- longitud de los tramos
- presiones de inyección
- tiempo de estabilización

2.1.1 Longitud de los tramos

Se acostumbra realizar la prueba en tramos de 5 m; sin embargo, la longitud del tramo de prueba no debe fijarse rígidamente, sino que, por lo contrario, ha de adaptarse a la naturaleza del terreno. En un material interestratificado con estratos de permeabilidad muy variable y de espesor menor a 5 m, resulta preciso reducir la longitud del tramo de prueba con objeto de obtener resultados referentes a un sólo estrato. En tal caso, evidentemente, el procedimiento que consiste en fijar los tramos de prueba posteriormente a la perforación y clasificación de las muestras extraidas, es preferi-

ble, de no ser que las paredes de la perforación sean inestables. En numerosos casos, resulta muy adecuado el empleo de tramos de prueba de longitud reducida (1 m o aun menos) con objeto de analizar detalladamente zonas de características excepcionales; por ejemplo, es saludable la práctica que consiste en aislar con empaques una zona en donde se notó pérdida del agua de perforación y probarla.

Por lo contrario, en caso que la masa de roca por estudiar sea homogénea, se podrá prefijar la longitud del tramo de prueba, a priori, por ejemplo en 5 m y llevar a cabo la serie de pruebas simultáneamente con el avance de la perforación. Sin embargo, si se mantiene constante la longitud del tramo de prueba, resulta imposible formarse una idea precisa de la fisuración de la roca. En efecto, si un tramo de cinco metros de longitud, absorbe 50 litros por minuto bajo una presión de 10 kg/cm^2, esto puede deberse a la presencia de una sola fisura grande, ó a 10 fisuras de dimensiones reducidas, ó a 100 fisuras muy finas. Para tener un conocimiento más detallado de la fisuración de la roca es necesario, en este tramo de 5 m, efectuar las pruebas metro por metro. En caso que exista una fisura única en el tramo de 5 m, en 4 de las pruebas efectuadas con longitud de 1 m la absorción será nula, mientras la 5a. lo absorberá todo. En el caso de una distribución homogénea de las fisuras a lo largo de los 5 m del tramo, las absorciones medidas en las 5 pruebas serán idénticas.

Las anteriores consideraciones explican la falta de correla-

ción existente entre los resultados de las pruebas Lugeon y la penetrabilidad de lechadas de agua cemento, para inyecciones. En efecto, la abertura y número de las fisuras existentes en dos masas de roca pueden ser muy variables, aun cuando las pruebas Lugeon dan resultados idénticos para las dos formaciones.

2.1.2 Presiones de inyección

Con objeto de obtener la curva de gastos de absorción en función de la presión de inyección, se varía en un mismo tramo dicha presión. La secuencia de presiones de inyección aplicadas es, por ejemplo: 1, 2, 4, 6, 8, 10, 8, 6, 4, 2, 1 kg/m^2.

La presión que se toma en cuenta en los cálculos, es la leída en el manómetro corregida por pérdidas de carga en la tubería y altura del nivel freático con respecto al tramo probado, como lo veremos con detalle al hablar de la interpretación de las pruebas.

Las formas de las curvas de gastos de absorción en función de la presión de inyección son muy variables, y se discutirán en el inciso 2.4.

2.1.3 Tiempo de estabilización

Los gastos de absorción útiles para la interpretación de los datos son los obtenidos cuando el flujo de agua que penetra en el terreno está estabilizado. Por tanto, es preciso mantener durante un tiempo mínimo (5 a 10 minutos) la presión y, verificar que en ese lapso de tiempo el gasto es constante.

2.2 Equipo necesario

Los elementos necesarios para llevar a cabo una prueba Lugeon son:

a) Un obturador o empaque de las diferentes formas conocidas con su correspondiente tubo de inyección
b) Una bomba
c) Un medidor de gastos de agua
d) Un cronómetro, o en su defecto, un reloj con segundero
e) Uno o varios manómetros
f) Agua
g) Herramienta diversa

A continuación señalaremos los problemas planteados por cada uno de estos elementos.

2.2.1 Obturadores

Para esta prueba es preciso aislar el tramo por probar. No existe un obturador ideal, de colocación fácil y rápida cuya impermeabilidad sea perfecta y adecuada para cualquier tipo de terreno. Son numerosos los tipos de obturadores, y se pueden clasificar en distintas categorías:

- obturadores mecánicos; se comprime una serie de rondanas de hule por medio de una doble columna de tubos (Fig. 1). Así comprimidas, las rondanas se expanden y sellan el tramo por probar, presionando sobre las paredes de la perforación. Este tipo de obturador funciona satisfactoriamente, pero su colocación es lenta y conviene únicamente para perforaciones de diámetro mayor que 90 mm .

- obturador de copa de cuero (Fig. 2). Bajo el efecto de la

presión de inyección, una serie de copas de cuero se acuña contra las paredes de la perforación. Para que este dispositivo dé resultados satisfactorios, es preciso que las copas de cuero estén prácticamente en contacto con las paredes antes de la aplicación de la presión. Este tipo de obturador necesita que las perforaciones sean muy regulares y perfectamente cilíndricas. Además, sufren mucho durante la etapa de recuperación, debido al giro que se les impone.

- obturadores neumáticos (Fig. 3). Constan de cubiertas cilíndricas de hule que se inyectan con aire comprimido. Estos obturadores son muy eficientes, pero su colocación es delicada por necesitan una tubería de alimentación de aire comprimido, y pueden acuñarse en las fisuras que se cierran al eliminar la presión, atrapándose en ellas la cubierta de hule.

La longitud del obturador debe ser por lo menos de 30 cm y ~~preferentemente~~ preferentemente mayor de 1 m.

2.2.2 Bomba

La bomba necesaria para inyectar agua a presión, debe ser tal que no produzca variaciones rápidas de la presión. Por tanto, debe usarse una bomba de varios pistones, o de gusano y preferentemente una bomba centrífuga de alta presión.

2.2.3 Medidor de gastos de agua

La medida del gasto inyectado es muy delicada. Se puede utilizar un contador, pero además de los inconvenientes de estos aparatos que mencionaremos a continuación, este contador debería poder funcionar bajo presiones variables, lo cual no es cierto.

La medida del gasto con contador presenta varios inconvenientes: estos aparatos, rara vez, dan una precisión superior al 10% y esta precisión puede variar muchísimo según su estado de mantenimiento. El rango de valores del gasto, para el cual la precisión es aceptable, es muy reducido. También introducen en el sistema pérdidas de carga que es preciso tomar en cuenta, a menos que el manómetro se coloque después de dicho medidor. Estos contadores necesitan una frecuente calibración, y miden volúmenes en vez de gastos, por tanto, se debe asociar una medida de tiempo a la lectura en ellos registrada.

Por tanto, resulta mucho más indicado el empleo de medidores del tipo Venturi, que constan de un tubo en el cual se coloca un diafragma que disminuye localmente la sección. La medición de la presión diferencial entre las zonas aguas arriba y aguas abajo del diafragma, permite determinar el gasto con errores del orden de 1%.

La Fig. 4 representa un tubo Venturi en el que se consideran dos secciones, cuyas velocidades medias V, áreas A, presiones p y alturas Z sobre un plano de referencia están caracterizados por los índices 1 y 2.

Si γ representa el peso específico, se tiene, según el teorema de Bernoulli:

$$\frac{p_1}{\gamma} + z_1 + \frac{V_1^2}{2g} = \frac{p_2}{\gamma} + z_2 + \frac{V_2^2}{2g}$$

$$V_1 A_1 = V_2 A_2 \Rightarrow \frac{V_1}{V_2} = \frac{A_2}{A_1}$$

$$\frac{V_1^2}{V_2^2} = \frac{A_2^2}{A_1^2}$$

$$\frac{V_1^2 - V_2^2}{V_2^2} = \frac{A_2^2 - A_1^2}{A_1^2}$$

$$V_1^2 - V_2^2 = \frac{V_2^2}{A_1^2}\left(A_2^2 - A_1^2\right) = -2g\,\frac{P_1 - P_2}{\gamma}$$

$$\frac{V_2^2}{A_1^2}\left(A_1^2 - A_2^2\right) = 2g\,\frac{P_1 - P_2}{\gamma}$$

$$V_2^2 = \frac{A_1^2}{A_1^2 - A_2^2}\left[2g\,\frac{P_1 - P_2}{\gamma}\right]$$

$$V_2 = \sqrt{\frac{A_1^2}{A_1^2 - A_2^2}}\sqrt{2g\,\frac{P_1 - P_2}{\gamma}}$$

$$\boxed{Q = \sqrt{\frac{A_1^2 A_2^2}{A_1^2 - A_2^2}}\sqrt{2g\,\frac{P_1 - P_2}{\gamma}}}$$

2.2.5 Uno o varios manómetros

La medida de las presiones parece sencilla; sin embargo, basta con haber visto en algunas obras un manómetro abollado, sin vidrio, cuya aguja, en caso de que aun exista, marca alternativamente 5 y 15 kg/cm^2, para entender que, no siempre la situación real es saludable.

Resulta preciso, pues, además de corregir los defectos obvios de un manómetro, calibrarlo por medio de un manómetro calibrador que no se deje tirado en la obra antes de utilizarlo.

Por lo demás, será preciso no colocar el manómetro directamente en la manguera o tubería de desfogue de la bomba, ya que en tal caso sufriría el golpeteo debido a un funcionamiento más o menos regular de los pistones de la bomba. Sometido a semejante tratamiento, ningún manómetro se mantiene en buenas condiciones de trabajo.

2.2.6 Agua

El agua de inyección debe ser agua limpia que no contenga materiales en suspensión en cantidad excesiva, De no ser así, se arriesga taponamientos en el medidor de gastos de agua así como, en las fisuras del terreno por probar, induciendo en esa forma, errores que pueden ser de consideración.

El esquema general de montaje del equipo necesario para llevar a cabo una prueba Lugeon aparece en la Fig. 5.

2.3 Formas de llevar a cabo la prueba

La colocación de los empaques en la perforación, con objeto de sellar el tramo por probar puede resultar muy delicada.

Se debe asegurar que obtura perfectamente dicho tramo. Para comprobar lo anterior, se hace pasar agua y se observa si sube por la perforación.

Si sube, esto puede deberse a dos causas:

1) La perforación no es regular y el empaque no ajusta.

2) El terreno está muy fisurado y entonces se forma un corto circuito alrededor del empaque, pasando el agua por el terreno y volviendo a salir a la perforación al nivel del suelo.

En el primer caso es necesario desplazar el empaque algunos centímetros, o aún algunos metros, hasta poderlo ajustar perfectamente. Cuanto mayor sea la longitud del obturador utilizado, mayor será la probabilidad de obtener un buen sello de las extremidades del tramo por probar. Por este motivo, se recomienda una longitud del obturador no menor de 1 m. En caso de utilizar un obturador de copas de cuero, es necesario tener un buen contrapeso en la máquina, o sobrecargarla para evitar que suba la tubería bajo el efecto de las presiones utilizadas durante las pruebas.

En caso que el terreno esté muy fisurado y entonces se forme un corto circuito alrededor del empaque, resulta difícil la realización correcta de la prueba. Desde luego, una solución sería la de cementar el pozo, pero en tal caso, los costos y tiempo necesarios para llevar a cabo la prueba aumentan considerablemente, por lo cual, se recomienda realizar, si el terreno está saturado, pruebas Lefranc, y si no, pruebas Mateuo o Nasberg.

presión. Veamos, pues, cómo se produce la absorción por una fisura.

Consideremos una fisura plana de espesor "e" cortada normalmente por una perforación de radio "r", en la que se inyecta agua a una presión "P" (Fig. 10). Si a una distancia "R", la presión en la fisura es nula, y se considera el ancho de la fisura como constante, se establece la relación:

$$q = \frac{\pi}{6 \gamma \operatorname{Log} \frac{R}{r}} p e^3$$

siendo "q" el gasto absorbido y "γ" la viscosidad del agua. Pero la fisura por la cual escurre el agua, no es en realidad indeformable. Consideremos una superficie circular de radio R sobre la cual se ejerce una presión p; con base en las fórmulas de Boussinesq, el desplazamiento elástico en el centro del círculo es:

$$W(o) = \frac{2(1-\sigma^2)}{E} R\, p$$

y en el borde del círculo

$$W(R) = \frac{4(1-\sigma^2)}{\pi E} R\, p$$

siendo E el módulo de elasticidad de la roca y σ su relación de Poisson. La abertura de la fisura, debida al aumento de presión, será igual con el doble de este desplazamiento ya que el mismo fenómeno ocurre sobre la cara superior; por tanto

$$\Delta e = \alpha P/\epsilon \quad \text{y}$$
$$e_o + \Delta e = e_o + \alpha \frac{p}{E}$$

y por tanto:

$$q = \frac{\pi}{6 \eta \log \frac{R}{r}} p \left(e_o + \alpha \frac{p}{E}\right)^3$$

Si e_o es pequeño se puede despreciar y obtendremos:

$$q = A\, p^4$$

siendo A una constante independiente de la presión aplicada.

Este resultado explica que se observe a menudo una pseudo-discontinuidad en las curvas gasto-presión, a partir de la cual los gastos aumentan muy rápidamente. En realidad, esta pseudo-discontinuidad, por lo general asemeja a un fracturamiento inducido en la roca al aumentar la presión, se debe a la variación del gasto con la cuarta potencia de la presión

En las Figs. 11 y 12, presentamos dos ejemplos típicos de esta situación. Es bastante sorprendente comprobar que estos cálculos someros y simplistas, encuentran una justificación experimental notable.

Para calcular el valor de la absorción, en unidades Lugeon, basta con trazar una recta que represente la ley de la permeabilidad y anotar el gasto correspondiente a una presión de 10 kg/cm^2. Si se divide este gasto (expresado en lts/min) entre la longitud de la zona probada se obtendrá el número de U L que corresponda a la prueba en estudio. Si se desea tener una noción aproximada de lo que representa una unidad Lugeon, se puede establecer que, si se tuviera un medio poroso y homogéneo, en lugar de roca fisurada, sometido a una

dedor de la cavidad de inyección y colmatar sus paredes.

3.2 Equipo necesario

El equipo necesario para llevar a cabo una prueba Lefranc, aunque sencillo, no debe descuidarse. Consta de varios elementos que permiten la medición del gasto permanente de agua inyectada y del nivel de agua dentro de la perforación.

3.2.1 Medición del gasto

Para obtener un gasto constante, se utiliza por lo general, un depósito de nivel constante que alimenta la perforación por medio de un orificio regulable. El tipo más sencillo de depósito de nivel constante es el formado por un depósito alimentado con una bomba que proporciona un gasto superior al gasto de inyección (Fig. 14). El rebosadero asegura un nivel constante. Para no influenciar la prueba, el agua vertida debe canalizarse hasta cierta distancia del punto de medición, o establecer un circuito cerrado con el agua bombeada.

La medición del gasto inyectado es más delicada. Se puede utilizar un contador de agua, pero en vista de las deficiencias ya señaladas de este aparato, es preferible medir el gasto en la forma señalada en la Fig. 14a. Al terminar la prueba se conecta por medio de una válvula de 3 vías, la alimentación en agua del pozo con un recipiente de volumen conocido, y se mide el tiempo necesario para su llenado.

Es preciso asegurarse de la no variación de las condiciones hidráulicas al interrumpir la prueba para medir el gasto inyectado. Para subrayar este punto, en la Fig. 14, se han pre

sentado dos soluciones muy semejantes en su concepción, pero que difieren sin embargo, pues una de ellas es correcta mientras la otra es incorrecta. En la Fig. 14a el gasto depende sólo de H, para una posición dada de la válvula de aguja. En efecto, al cerrar con la válvula de 3 vías la alimentación del pozo, y abrir el conducto hacia el recipiente de medición del gasto, no se varía en absoluto las condiciones hidráulicas del flujo y la medición de dicho gasto es, por tanto, confiable. Por lo contrario en el sistema presentado en la Fig. 14b, el gasto durante la inyección queda gobernado por la altura H_1, mientras durante la etapa de medición de dicho gasto influye la altura H_2. No siendo comparables las condiciones hidráulicas durante éstas dos etapas, la medición del gasto no es confiable.

3.2.2 Medición del nivel de agua en la perforación

En lo referente a medición de los niveles de agua, se utilizan sondas eléctricas que constan de dos alambres de cobre aislados en toda su longitud, salvo en sus extremidades. Dichas extremidades, al estar en contacto con el agua, permiten el paso de la corriente, que se registra en el brocal del pozo, por medio de un amperímetro.

El principio de esta medición es sencillo; sin embargo, plantea unas cuantas dificultades prácticas:

- los electrodos pueden crear un corto circuito al entrar en contacto con el ademe de la perforación, o bien debido a la presencia de gotas de agua en su parte no aislada, etc.

- la tensión de alimentación debe ser lo suficientemente al-

ta como para evitar fenómenos de polarización espontánea

- el aparato de detección del paso de la corriente debe ser lo suficientemente sensible para indicar el paso de la corriente, aún cuando el agua en que se sumergen los electrodos es muy pura

- cuando la sonda sale del agua, no deben permanecer gotas de agua entre los electrodos

- la medición precisa de la longitud del cable plantea problemas.

En resumen, el equipo necesario para llevar a cabo una prueba Lefranc-Mandel, consta de los siguientes elementos:

- una bomba
- un recipiente elevado con rebosadero
- una válvula de aguja
- un cono al que se le adapta una válvula de tres pasos
- tubería
- un recipiente de volumen conocido
- un cronómetro, o en su defecto un reloj con segundero
- una sonda eléctrica con sus aditamentos: batería de alimentación e instrumento de medición de longitudes
- un amperímetro
- herramientas diversas.

3.3 Formas de llevar a cabo la prueba

La prueba Lefranc-Mandel se lleva a cabo en los aluviones y rocas muy fracturadas, localizados bajo el nivel freático. El problema esencial que plantea la ejecución de esta prueba

es el asegurar la estabilidad de las paredes de la perforación, en la cavidad que se hará de crear en el terreno para inyectar agua.

Esta estabilización se efectúa mediante el uso de un ademe durante la perforación (desde luego, queda en este caso descartado el uso de lodos bentoníticos para estabilizar las paredes del pozo). La parte interna del ademe, al llegar a la profundidad deseada, se rellena con grava limpia de muy alta permeabilidad (por ejemplo grava uniforme de 1") sobre una longitud igual a la deseada para la prueba, por lo general igual con 1 m. A continuación se levanta el ademe 1 m, quedando la perforación lista para realizar la prueba.

La prueba se realiza en la siguiente forma, de acuerdo con el esquema presentado en la Fig. 14:

1. Se mide el nivel freático en la perforación
2. Se echa a andar la bomba que alimenta el recipiente elevado con rebosadero
3. Al derramar agua dicho recipiente, se abre la válvula 1, con la válvula 2 conectada a la perforación
4. Se mide la variación del nivel de agua en el pozo h_1 con respecto al tiempo
5. Cuando el nivel del agua queda estable durante 10 min, se anota el nivel estabilizado H_1
6. La válvula 2 se conecta con el recipiente de volumen conocido y se mide y anota el tiempo T necesario para llenarlo.

En un mismo punto se realiza la prueba variando los gastos

inyectados, y midiendo los respectivos niveles estabilizados de agua en la perforación.

3.4 Registro e interpretación de los datos

Los datos que se necesitan registrar son:

- nivel freático
- niveles estabilizados del agua en la perforación
- gastos inyectados
- diámetro del difusor
- longitud probada.

Es preciso señalar que el nivel freático no debe confundirse con el nivel del agua dentro de la perforación, al terminar de perforar un tramo. Basta con ver algunos resultados en los que en un mismo pozo los llamados niveles freáticos se localizan entre 4 y 40 m según el avance de la perforación, hecha con agua como fluido de perforación, a priori obvia. Para asegurarse de que se está midiendo realmente el nivel freático es preciso tomar lecturas a distintos tiempos y comprobar que los resultados de estas mediciones son idénticos. En caso contrario, resulta necesario esperar, antes de empezar la prueba, la estabilización del nivel del agua dentro de la perforación.

En la Fig. 15, se presenta una forma de registro de la prueba Lefranc. La interpretación de los datos se hace con base en la fórmula:

$$Q = C\,K\,\Delta H$$

En el caso más común en que la prueba se realiza con un tra-

mo perforado de longitud L y radio r, el coeficiente C es igual con:

$$C = \frac{4\pi}{\frac{2}{L} \operatorname{Log} \frac{L}{\beta r} - \frac{1}{2H}}$$

siendo H la profundidad del tramo probado con respecto al nivel freático.

Aplicando las anteriores fórmulas se obtiene el coeficiente de permeabilidad K de Darcy del material probado.

4. PRUEBAS DE BOMBEO

4.1 Descripción e hipótesis

Los cálculos de permeabilidad de un terreno por medio de pozos de bombeo, se analizan basándose en las fórmulas de Dupuit-Thiem o de Theis-Lukin. Estas teorías se basan en diversas hipótesis que son respectivamente para Dupuit-Thiem:

- el material es homogéneo
- el nivel freático es estático
- lejos del pozo, el gradiente hidráulico es constante con la profundidad a lo largo de la superficie exterior de un cilindro cuyo eje de revolución coincide con el eje del pozo
- el pozo abarca la totalidad del manto permeable
- suponiendo que se verifican tales hipótesis, el gradiente a lo largo de un cilindro de revolución de radio r es igual con el valor de la pendiente de la superficie libre del escurrimiento en el punto de intersección de dicha superficie con el cilindro de radio r (Fig. 16).

La fórmula de Theis-Lukin presupone que:

1) La formación permeable es homogénea o isótropa
2) Su extensión es infinita
3) El pozo de bombeo atraviesa todo el espesor del acuífero
4) El coeficiente de permeabilidad k es constante en todo punto
5) El radio del pozo de bombeo es muy pequeño
6) El agua fluye inmediatamente fuera de la zona abatida.

Los errores debidos a la no observación de las hipótesis 3 a 5 son por lo general despreciables.

Las pruebas de bombeo se llevan a cabo perforando un pozo central de bombeo, cuya profundidad, de acuerdo con las hipótesis anteriores, debe ser igual al espesor total del manto permeable. Sin embargo, en numerosos casos el estrato de material permeable es muy potente y en tal caso resultaría anti-económico, realizar una perforación tan profunda. Por tanto, en estos casos se efectúa una perforación que no abarca la totalidad del manto permeable, lo cual redunda en un error de pequeña magnitud al interpretar los datos así obtenidos. Los ensayos de Ph. Forchheimer dieron por resultado que el nivel freático sólo en los alrededores inmediatos del pozo está influido por la posición del fondo del mismo en relación con la situación de la capa impermeable, pero que a cierta distancia la forma del embudo figurado por la superficie libre del agua alrededor del pozo de bombeo es, independiente de su profundidad.

Alrededor del pozo de bombeo, en forma concéntrica, se colo-

can, en perforaciones, sea ademes ranurados para observar directamente la superficie libre del cono de abatimiento creado por el bombeo, sea piezómetros, con objeto de conocer en toda la zona afectada las presiones en el agua (Fig. 16). El segundo método es más eficiente. En efecto, en caso de suponer que las hipótesis 1 y 2 de las teorías de Dupuit o de Theis-Lukin se verificarán, la red de flujo correspondiente sería la representada en la Fig. 17. En esta red puede verse que en tal caso, teóricamente, tiene importancia para la determinación de la permeabilidad la posición de los pozos de observación, pues dependiendo de sus distancias respectivas al pozo central se verificará o no la hipótesis 5 de la teoría de Dupuit. Los pozos de observación no permiten juzgar de la aplicabilidad de la hipótesis 5, por lo contrario, los piezómetros localizados a distintas profundidades y distancias del pozo central proporcionan la forma de las equipotenciales, lo cual permite comparar los resultados obtenidos con las hipótesis de cálculo.

El método de interpretación de Dupuit se basa en la forma de la superficie libre del escurrimiento en régimen permanente, mientras la teoría de Theis-Lukin estudia el mismo caso analizando los resultados del régimen transitorio. Un bombeo iniciado en un manto de agua tarda por lo general mucho tiempo en estabilizarse. El escurrimiento provocado por dicho bombeo alcanza el régimen permanente sólo después de un intervalo de tiempo considerable cuando se consigue movilizar las fuentes de alimentación del manto. En el caso de pruebas de bombeo, aún al cabo de varios días, es poco común

el alcanzar el régimen permanente, y por tanto, lo que se observa es un régimen transitorio. De ahí surge el interés del estudio del régimen transitorio, pero además semejante estudio proporciona datos sobre el manto de agua y el terreno que la interpretación basada en la teoría de Dupuit, no proporciona como lo veremos en el inciso 4.4.

4.2 Equipo necesario

El equipo necesario para llevar a cabo una prueba de bombeo es el siguiente:

- un ademe ranurado para el pozo de bombeo
- una bomba de pozo profundo
- un tanque amortiguador en la descarga de la bomba, que constará de una pantalla de malla de acero relleno con grava para disipar la energía del agua, así como de un medidor de gastos (del tipo vertedor triangular delgado y escala de gancho, o Venturi)
- canal para alejar de la zona bajo estudio el gasto de agua bombeada
- tubería ranurada con ranuras cuatrapeadas (de 1/8" de espesor y 4" de longitud en un total de 20 ranuras por metro por ejemplo), para los pozos de observación o los piezómetros
- sonda (de tipo eléctrico por ejemplo) para medición de los niveles en los pozos de observación o los piezómetros
- un reloj
- herramientas diversas.

En las fotografías 1 a 6 se presentan los elementos utilizados para una prueba de bombeo en el sitio de la presa de las

Tórtolas, Dgo. En ellas pueden apreciarse los siguientes elementos:

- bomba de pozo profundo
- tanque amortiguador con pantalla de malla de acero
- vertedor triangular delgado y escala de gancho
- canal de conducción del agua bombeada.

En este caso, se midieron los niveles "h" de la superficie libre de la lámina vertedora en el vertedor triangular delgado con lo cual aplicando la fórmula

$$Q = 1.34\ h^{5/2}$$

se obtuvo el gasto en m^3/seg, conociendo el nivel "h" expresado en metros.

4.3 Forma de llevar a cabo las pruebas

Habiendo instalado en la zona de interés el conjunto de elementos necesarios para la realización de la prueba, se empieza a bombear con un valor del gasto prefijado después de haber anotado los niveles iniciales del agua en los pozos testigo. Durante los primeros momentos del bombeo, es necesario tomar en forma continua lecturas de los piezómetros de observación con objeto de tener muchos datos durante la etapa de flujo transitorio. Posteriormente, puede aumentarse el intervalo de tiempo entre mediciones. En caso de querer interpretar los datos con base en la teoría de Dupuit, es necesario esperar, manteniendo el gasto de bombeo constante, que el flujo de agua se torne permanente, lo cual significa que los niveles de la superficie de escurrimiento alrededor del pozo

Lefranc-Mandel no se cumplen. También mencionaremos rápidamente las pruebas de inyección y bombeo con agua marcada por trazadores radioactivos, pruebas que en caso de una estratificación muy fina proporcionan resultados cualitativos de gran interés.

5.1 Pruebas en materiales no saturados

5.1.1 Nasberg ha estudiado en forma teórica el escurrimiento en un suelo seco, a partir de una fuente situada en la masa. Terlertskata, con base en este estudio y en resultados experimentales, ha obtenido una fórmula que relaciona el gasto de absorción "Q" en un pozo, bajo un tirante de agua constante h, con el coeficiente de permeabilidad del terreno

$$K = \frac{0.423}{h^2} Q \log_e \frac{4h}{d}$$

siendo d el diámetro de la perforación, bajo la condición $25 < \frac{h}{d} < 100$ (Fig. 23).

5.1.2 Pruebas Matsuo-Akai

Matsuo y Akai han descrito en una comunicación al Tercer Congreso Internacional de Mecánica de Suelos (Zürich 1958) un método de medición de la permeabilidad de un suelo seco.

En una zanja (Fig. 24) de longitud infinita y de ancho B, y en la cual se mantuviera un tirante de agua H, se obtendrían las siguientes fórmulas para el escurrimiento plano provocado, con gasto Q por unidad de longitud:

$B = \frac{Q}{K} - 2H$ en caso de que el estrato impermeable fuera muy profundo

$B = \frac{Q}{K} + 2B$ en caso de que el estrato impermeable quedara cerca del fondo de la zanja

La prueba consiste en realizar una zanja rectangular y medir el gasto de agua de inyección necesario para mantener el nivel del agua constante. Posteriormente la zanja se alcanza de cierta cantidad y de nuevo se mide dicho gasto Q . La diferencia entre estos gastos es el gasto de absorción del terreno para la longitud complementaria de zanja. En tal forma se elimina el efecto de las extremidades. Las fórmulas anteriores permiten determinar el valor de K.

5.2 Trazadores radioactivos y micromolinete

Con objeto de poder determinar en los materiales finamente interestratificados la presencia de capas permeables, se han ideado pruebas de inyección y bombeo con agua marcada por trazadores radioactivos. En este caso, después de haber inyectado el agua marcada, se inicia el bombeo y por medio de un cortador Geiger se mide el número de golpes registrados a distintas profundidades durante el bombeo. Evidentemente al nivel de una capa muy permeable el número de golpes registrado a distintas profundidades durante el bombeo. Evidentemente, al nivel de una capa muy permeable el número de golpes registrado es elevado, mientras es reducido al nivel de una capa poco permeable. Se puede en esa forma, diferenciar cualitativamente con gran resolución la permeabilidad de los diversos estratos existentes.

En forma semejante, por medio de la medición de las velocidades de flujo horizontal con un micromolinete, en una perfora

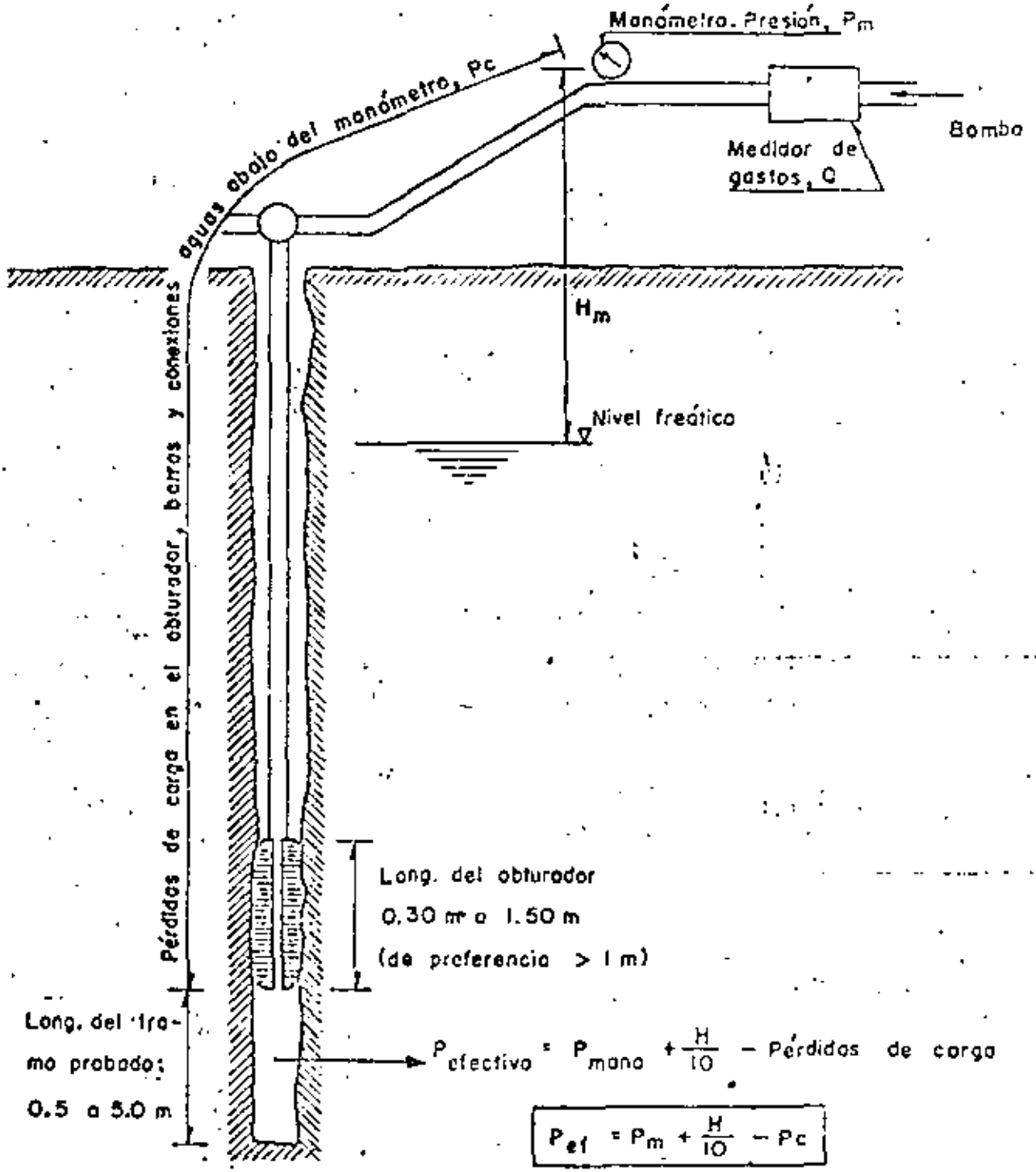

1 Lugeon = 1 litro por metro y por minuto bajo 10 kg/cm^2 de presión efectiva

1 Lugeon # 10^{-7} m/seg

Fig 11.35. Prueba Lugeon

FIG. 6. PERDIDAS DE CARGA EN TUBOS LIMPIOS

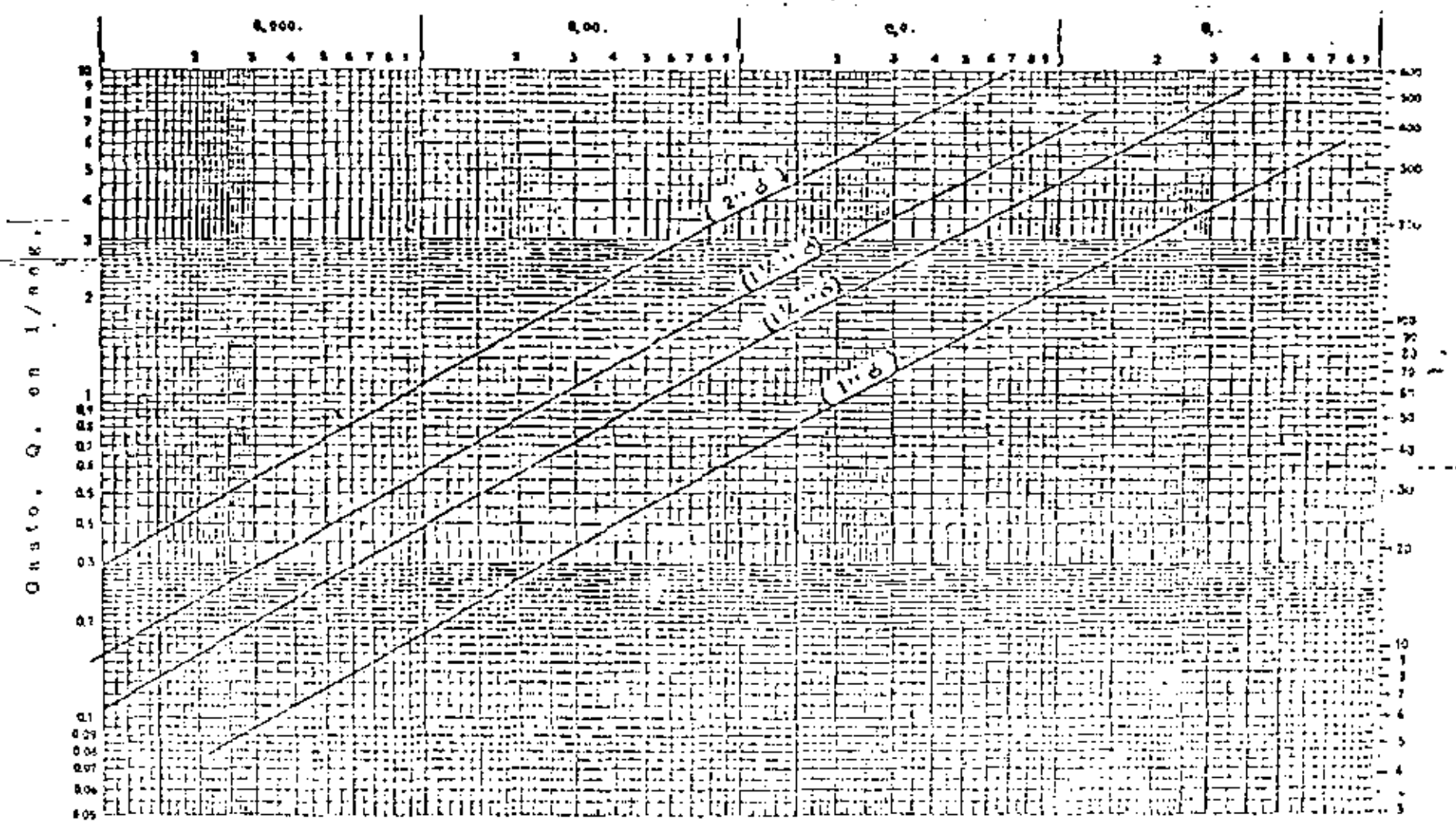

FIG. - 7. - PERDIDAS DE CARGA EN MANGUERAS LIMPIAS

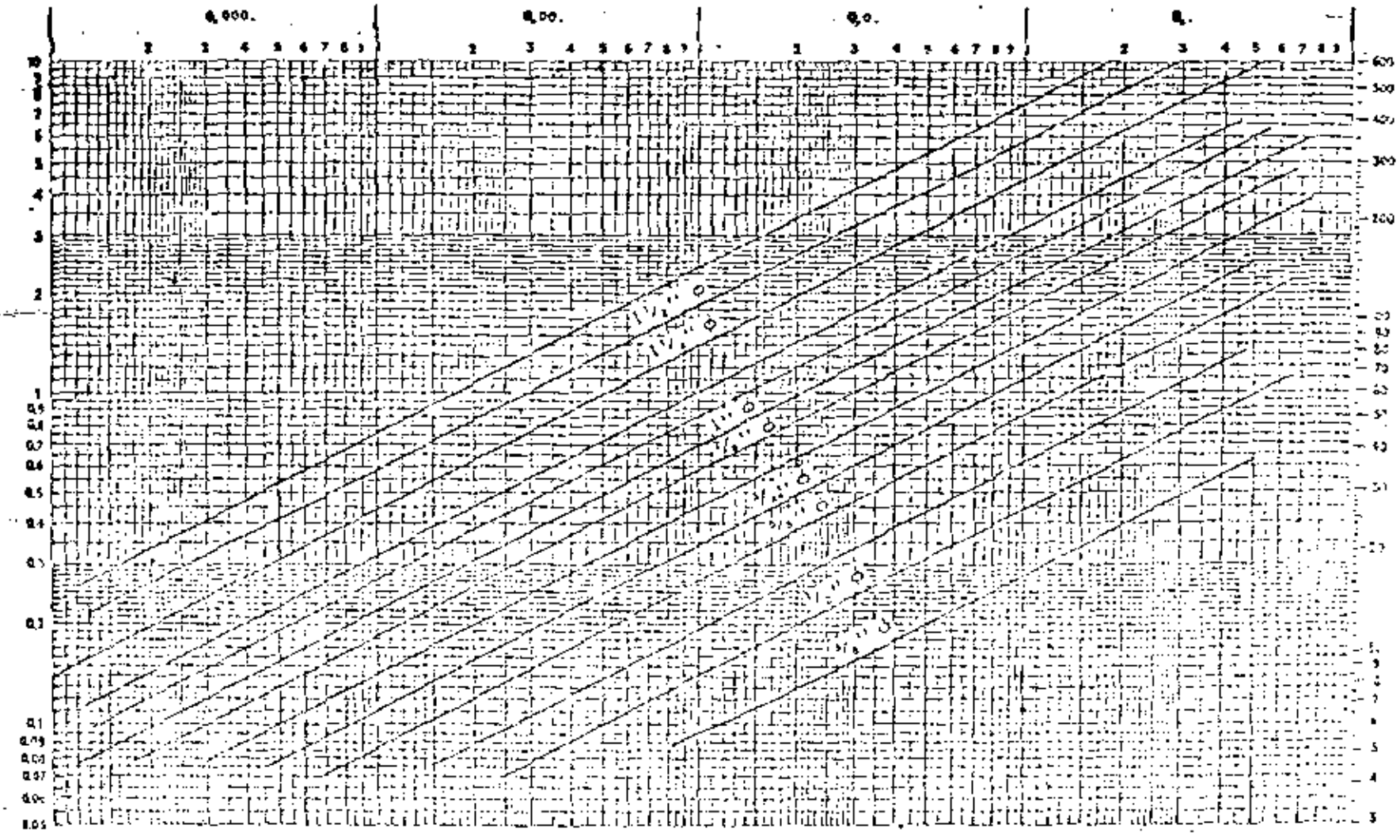

REGISTRO DE PRUEBAS LUGEON

Obra. _____

Operador _____

Fecha _____

Pozo _____

Prueba Nº _____

Inclinación _____

Profundidad del nivel freático _____

Altura del manómetro con respecto al nivel del terreno _____

TUBERIA DE INYECCION

Diámetro interior _____

Nº de coples _____

OBTURADOR

Tipo _____

Longitud _____

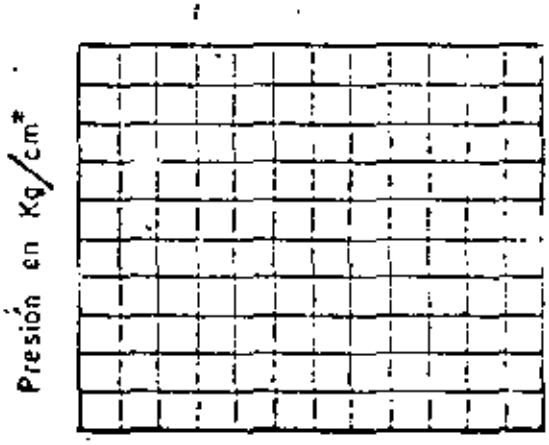

Presión en Kg/cm² leída en el manómetro	Gasto (Venturi) lit/min	Duración lit/min	Observaciones	Presión corregida Kg/cm²	Gasto lit/min

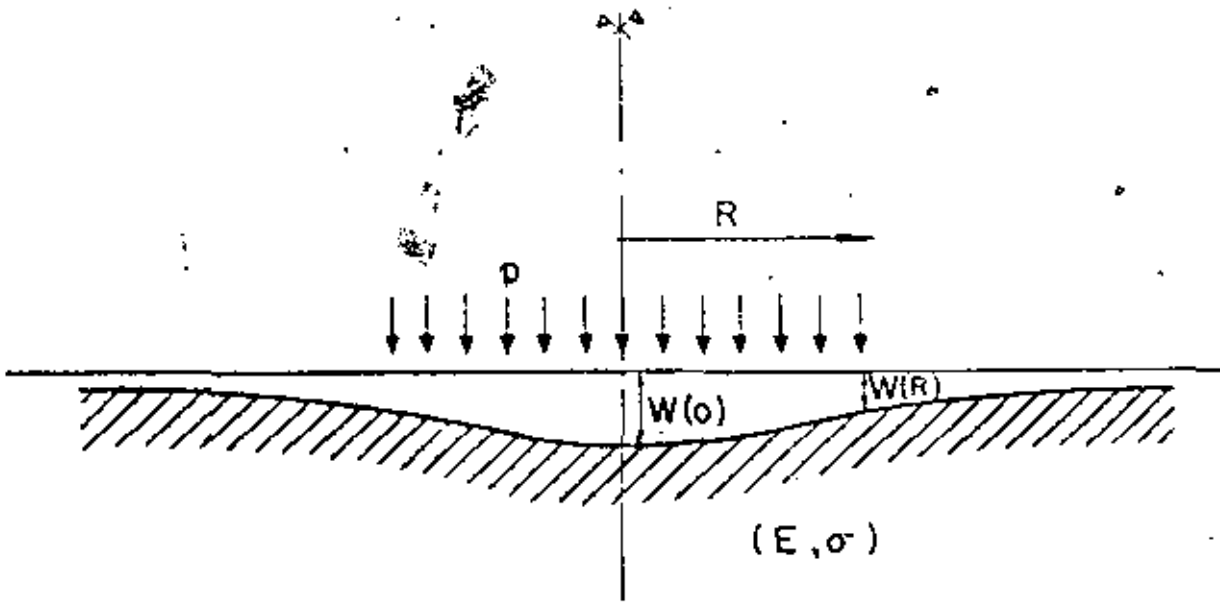

$$W(o) = \frac{2(1-\sigma^2)}{E} Rp \qquad W(R) = \frac{4(1-\sigma^2)}{\pi E} Rp$$

Fig 10a

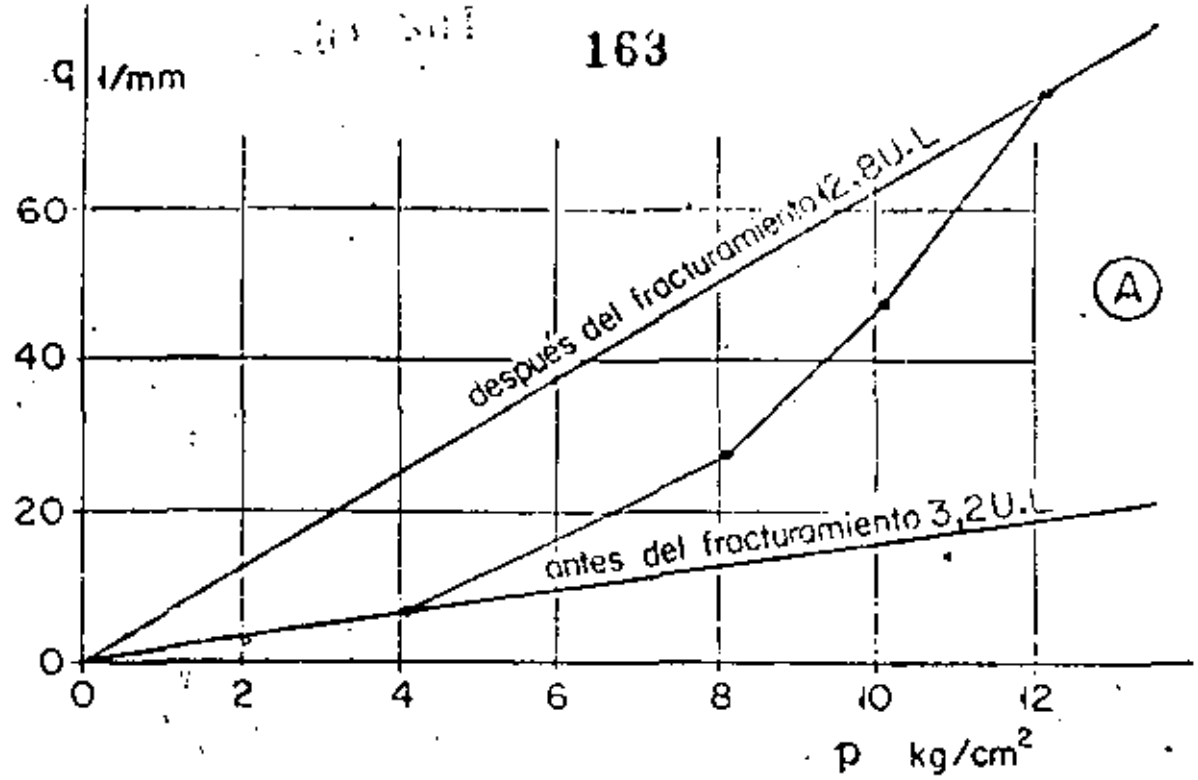
q l/mm
60
40
20
0
0
2
4
6
8
10
12
p kg/cm²
después del fracturamiento 12,8U.L
antes del fracturamiento 3,2U.L
A

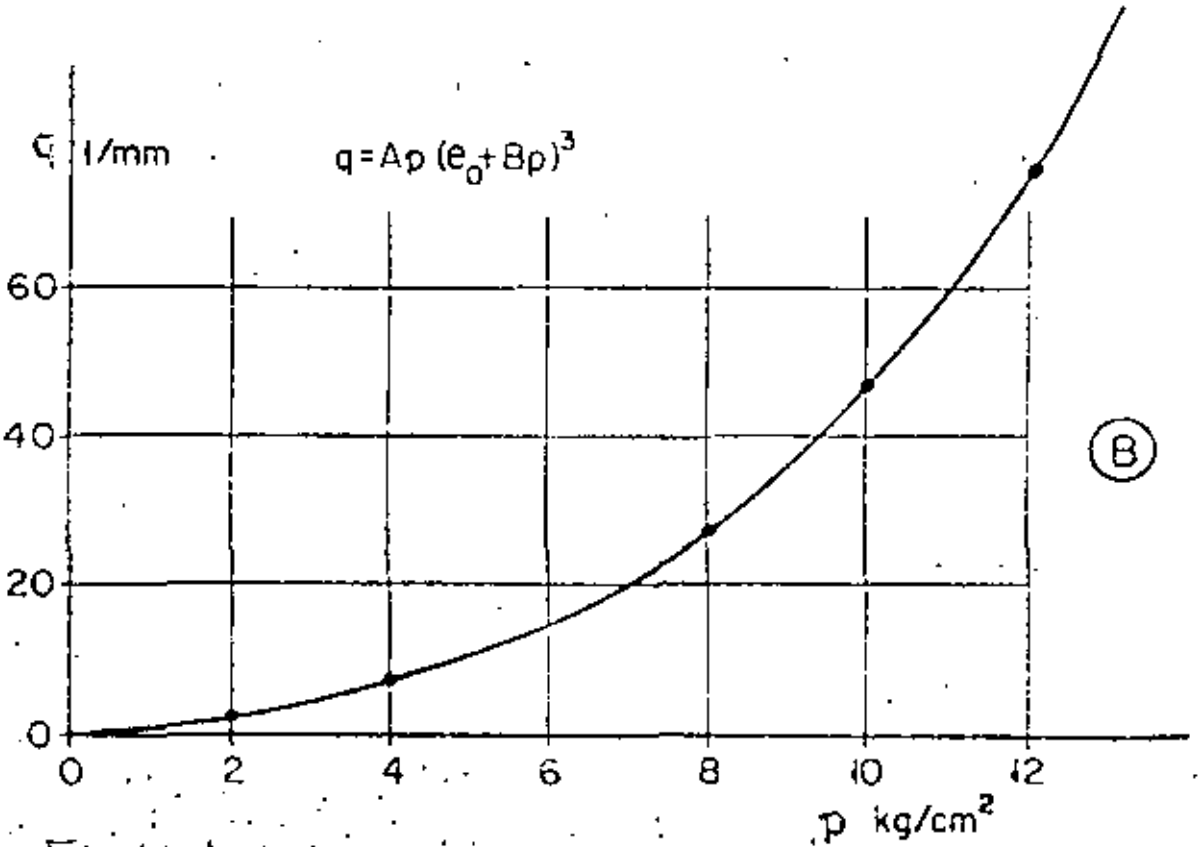
q l/mm
q = Ap (e0 + Bp)³
60
40
20
0
0
2
4
6
8
10
12
p kg/cm²
B

Fig 10 b

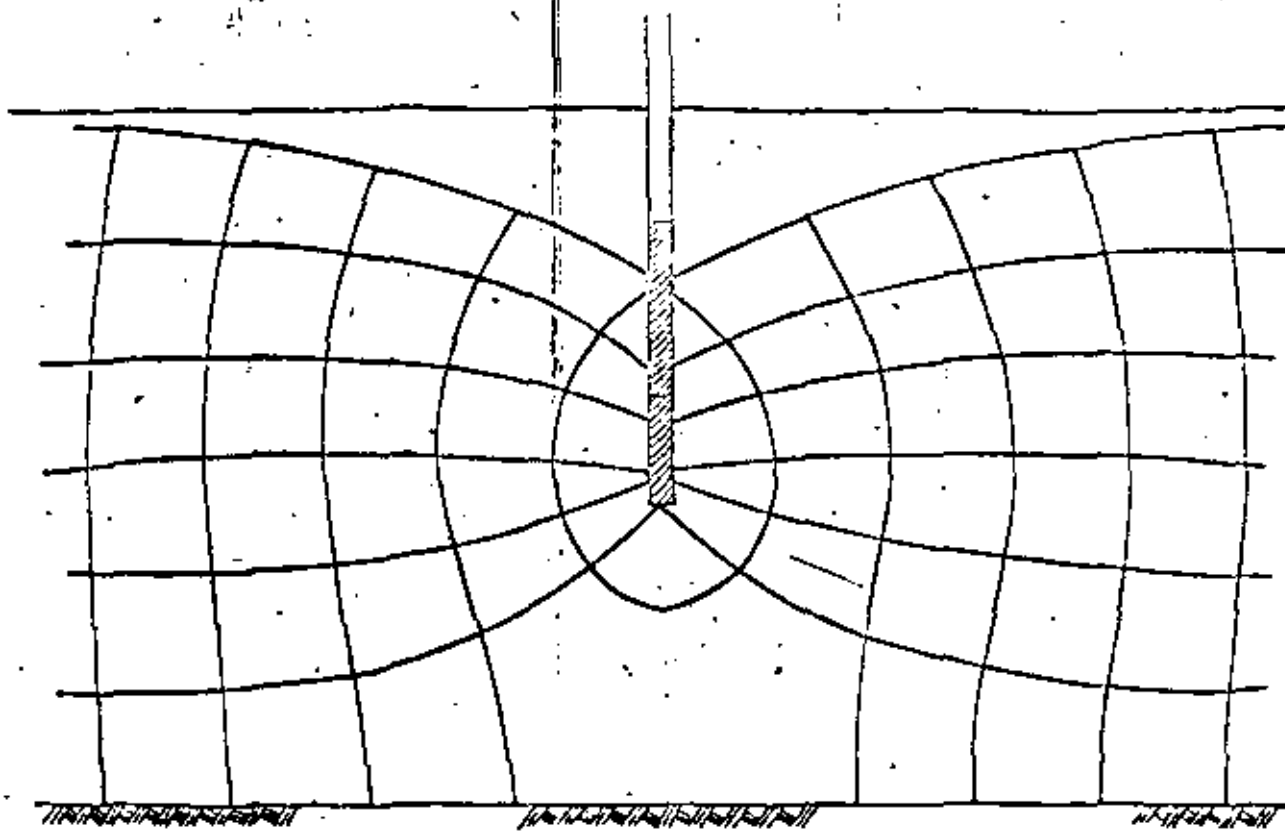

Red de flujo para un suelo homogeneo y un pozo que no atraviesa la totalidad del manto permeable

REGISTRO DE NIVELES EN POZOS TESTIGO

Obra _____

Fecha _____

Operador _____

Bombeo iniciado, a las _____ hr. _____ min.

Medidas tomadas de las _____ hr. _____ min a las _____ hr. _____ min.

Altura del agua en el vertedor triangular _____ cm.

CAMPO			CALCULO					
Pozo Nº	Nivel del agua en el pozo	Hora de lectura	K Tiempo en min. desde el inicio del bombeo	Abatimiento del nivel freático en m	R Distancia al pozo de bombeo	R^2	$\frac{1}{R^2}$	t Tiempo en min. desde la suspensión del bombeo

FIG. 18

REGISTRO DE NIVELES PIEZOMETRICOS

Obra _____

Fecha _____

Operador _____

Medidas tomadas de las _____ hr _____ min a las _____ hr _____ min

Altura del agua en el vertedor triangular _____ cm

Nº	Nivel del agua en el piezómetro

FIG.

PRUEBAS DE BOMBEO

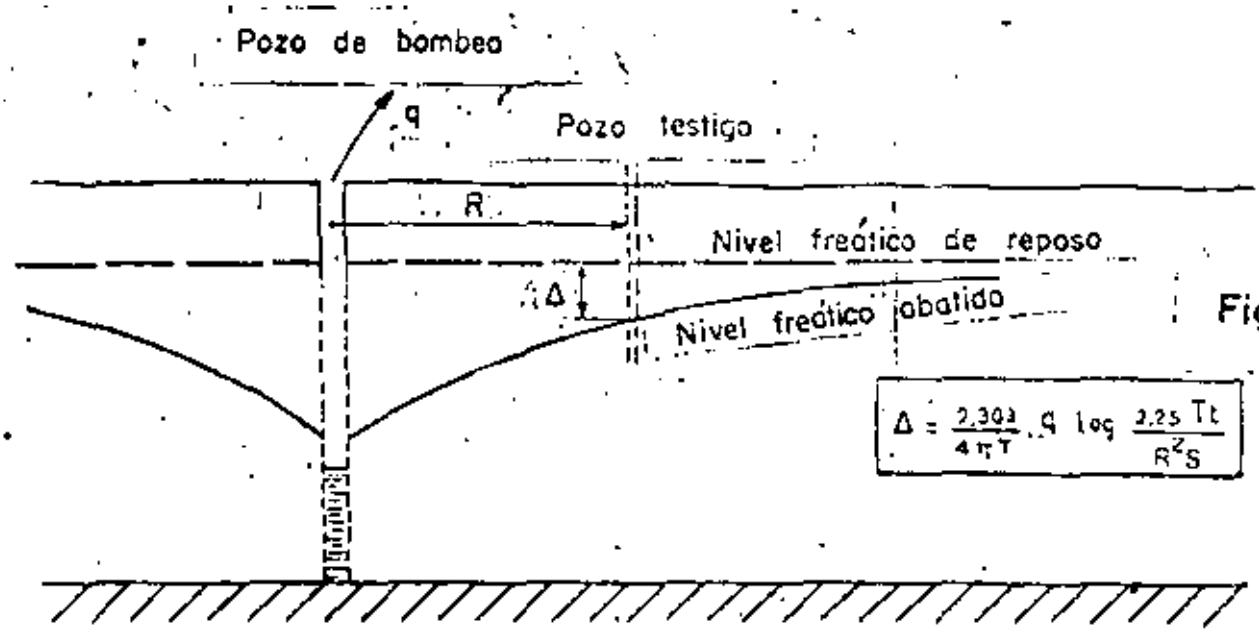

Fig. 20

FLUJO TRANSITORIO (Forma I)

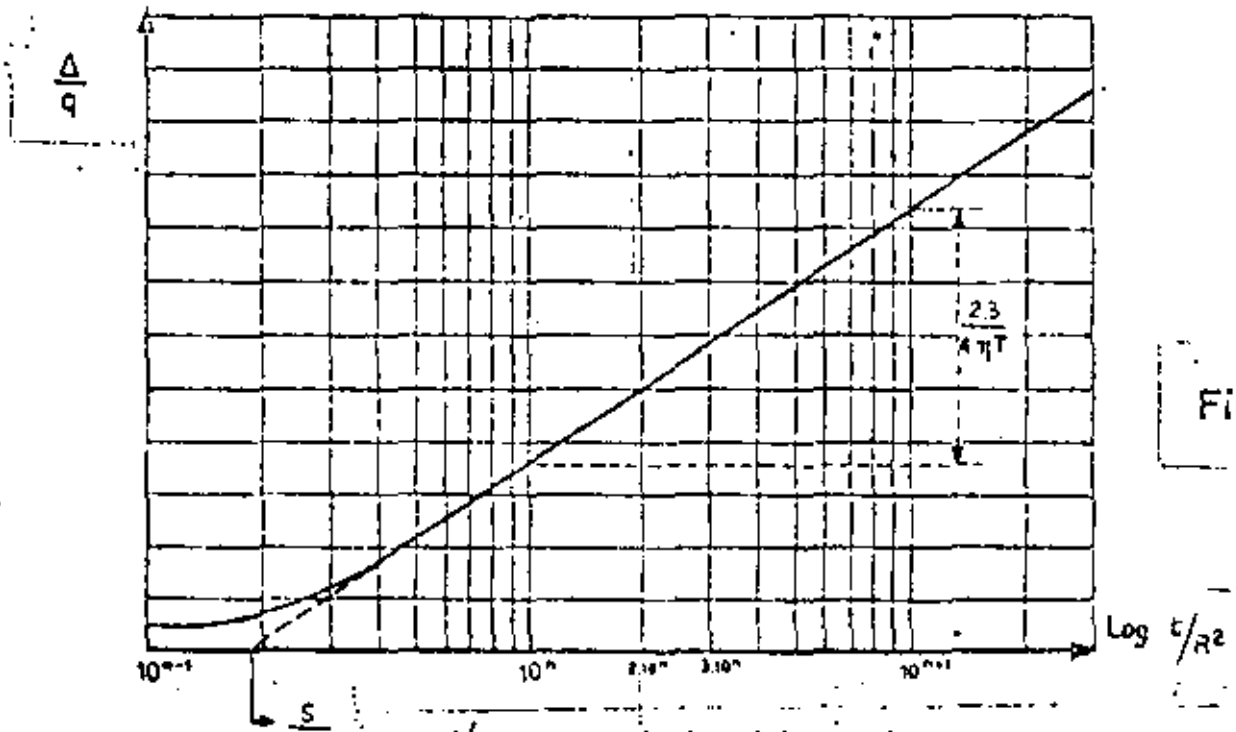

Fig. 21

Evolución de conjunto del manto de agua para un bombeo con gasto constante

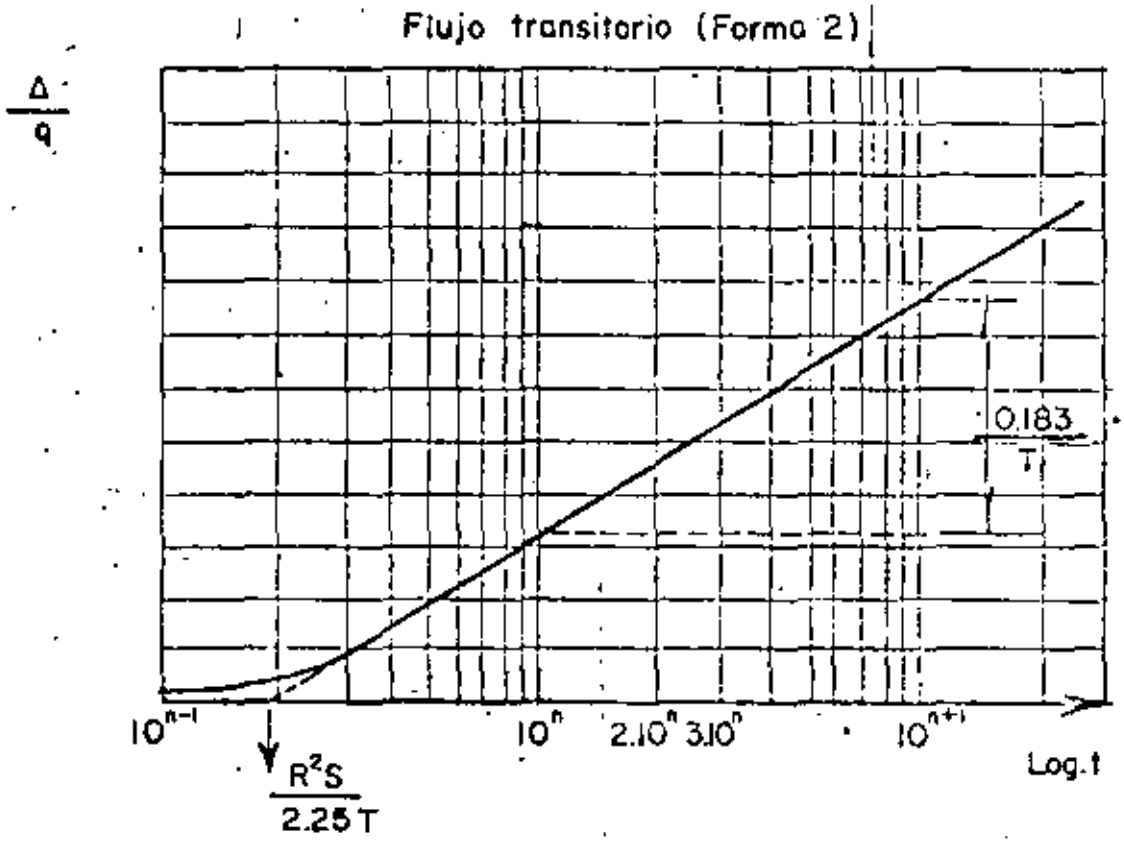

EVOLUCION DE LOS ABATIMIENTOS EN UN POZO TESTIGO PARA BOMBEO CON GASTO CONSTANTE

Fig. 22

Solum geotecnia

CROQUIS DE LOCALIZACION

México, D.F. de 19 Fig. 1

PRUEBAS NASSERC

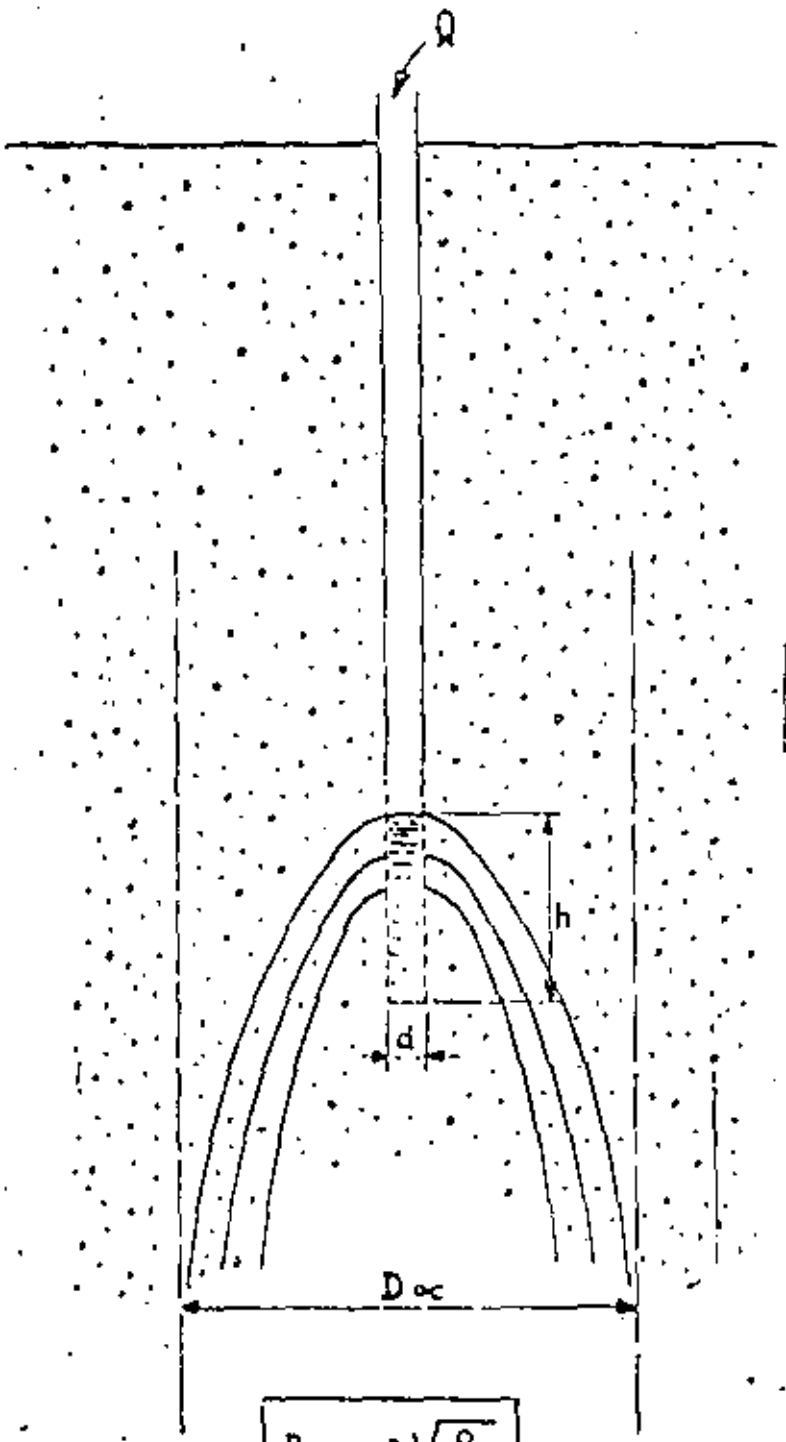

$$K = \frac{0,423}{n^2} Q \log_{10} \frac{4h}{d}$$

con $25 < \frac{h}{d} < 100$

$$D_\infty = 2\sqrt{\frac{Q}{\pi h}}$$

Fig. 23

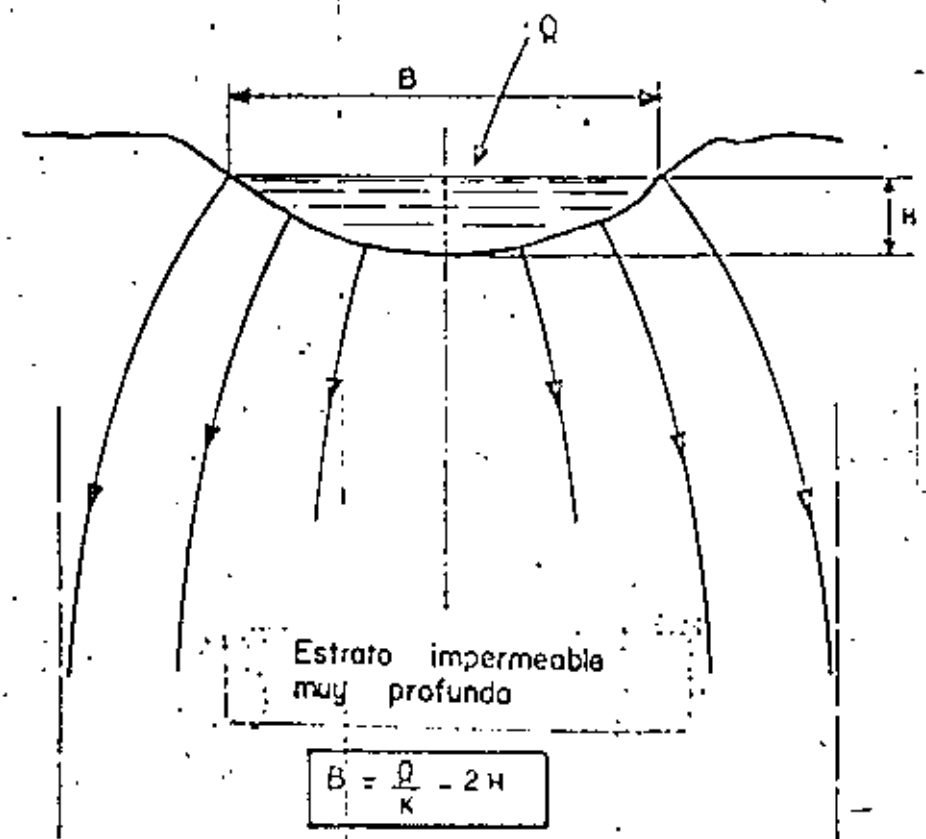

$$B = \frac{Q}{K} - 2H$$

Fig. 23a
24

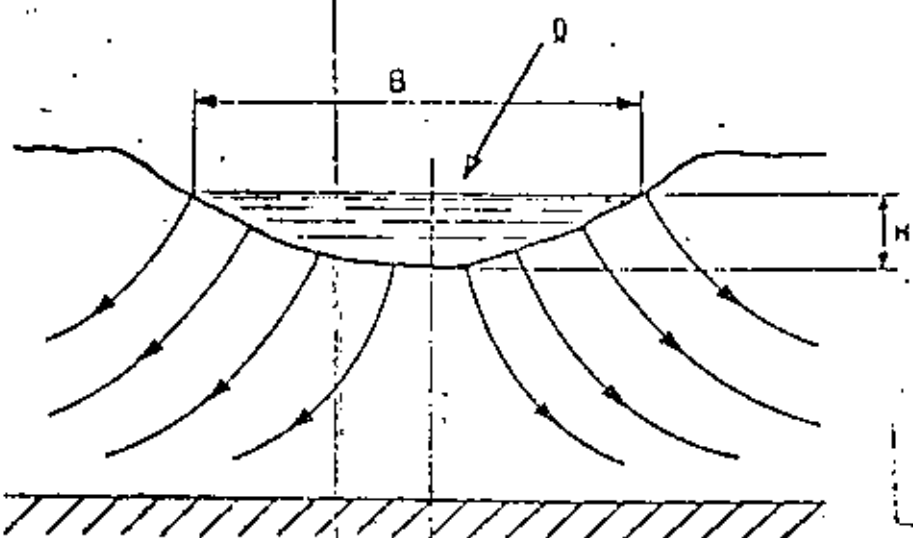

$$B = \frac{Q}{K} + 2H$$

Fig. 23b
24

Fig. 23
24

ESTABILIDAD DE TALUDES

Chapter 2 : Basic mechanics of slope failure

Continuum mechanics approach to slope stability

A question which frequently arises in discussions on slope stability is how high and how steep can a rock slope be cut. One approach to this problem, which has been adopted by a number of investigators[11-15], is to assume that the rock mass behaves as an elastic continuum. The success which has been achieved by the application of techniques such as photoelastic stress analysis or finite element methods in the design of underground excavations has tempted many research workers to apply the same techniques to slopes. Indeed, from the research point of view, the results have been very interesting but in terms of practical rock slope engineering, these methods have limited usefulness. These limitations arise because our knowledge of the mechanical properties of rock masses is so inadequate that the choice of material properties for use in the analysis becomes a matter of pure guesswork. For example, if one attempts to calculate the limiting vertical height of a slope in a very soft limestone on the basis of its intact strength, a value in excess of 3500 feet is obtained[16]. Clearly, this height bears very little relation to reality and one would have to reduce the strength properties by a factor of at least 10 in order to arrive at a reasonable slope height.

It is appropriate to quote from a paper by Terzaghi[17] where, in discussing the problem of foundation and slope stability, he said ".....natural conditions may preclude the possibility of securing all the data required for predicting the performance of a real foundation material by analytical or any other methods. If a stability computation is required under these conditions, it is necessarily based on assumptions which have little in common with reality. Such computations do more harm than good because they divert the designer's attention from the inevitable but important gaps in his knowledge....".

Muller[18] and his co-workers in Europe have, for many years, emphasised the fact that a rock mass is not a continuum and that its behaviour is dominated by discontinuities such as faults, joints and bedding planes. Most practical rock slope designs are currently based upon this discontinuum approach and this will be the approach adopted in all the techniques presented in this book. However, before leaving the question of the continuum mechanics approach, the author wishes to emphasise that he is not opposed in principle to its application and indeed, when one is concerned with overall displacement or groundwater flow patterns, the results obtained from a numerical method such as the finite element technique can be very useful. Developments in numerical methods such as those reported by Goodman et al[19] and Cundall[20] show that the gap between the idealised elastic continuum and the real discontinuum is gradually being bridged and the author is optimistic that the techniques which are currently interesting research methods will eventually become useful engineering design tools.

Maximum slope height - slope angle relationship for excavated slopes

situations where the orientation and inclination of these discontinuities is such that simple sliding of slabs, blocks or wedges is not possible. Failure in these slopes will involve a combination of movement on discontinuities and failure of intact rock material and one would anticipate that, in such cases, higher and steeper slopes than average could be excavated. What practical evidence is there that this is a reasonable assumption?

A very important collection of data on excavated slopes was compiled by Kley and Lutton[21] and this collection has recently been added to by Ross-Brown[22]. The information refers to slopes in opencast mines, quarries, dam foundation excavations and highway cuts. The slope heights and corresponding slope angles for the slopes in materials classified as hard rock have been plotted in Figure 7 which includes both stable and unstable slopes. Ignoring, for the moment, the unstable slopes, this plot shows that the highest and steepest slopes which have been successfully excavated, as far as is known from this collection of data, fall along a fairly clear line* shown dashed in the figure. (One additional point at 42° and a height of 2200 feet from an opencast mine in Austria falls on the curve but has been omitted from the figure). This line gives a useful practical guide to the highest and steepest slopes which can be contemplated for normal open pit mine planning. In some exceptional circumstances, higher or steeper slopes may be feasible but these could only be justified if a very comprehensive stability study had shown that there was no risk of inducing a massive slope failure

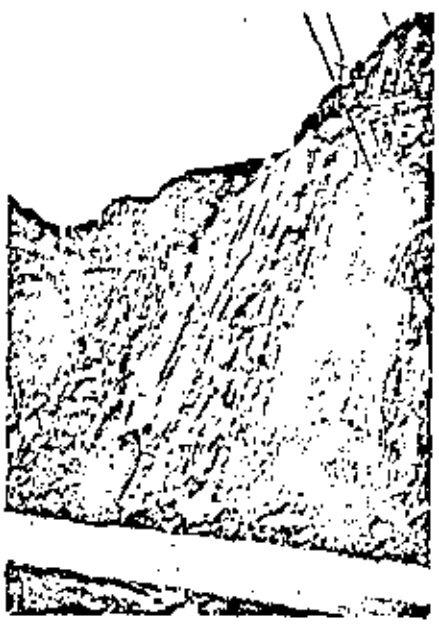

A planar discontinuity surface in an open pit bench.

Role of discontinuities in slope failure

Figure 7 shows that, while many slopes are stable at steep angles and at heights of several hundreds of feet, many flat slopes fail at heights of only tens of feet. This difference in stability results from the difference in inclination of the discontinuity surfaces upon which sliding can take place. This is strikingly illustrated in the simple example given in Figure 8 in which the critical height of a vertical slope containing an inclined weakness plane is given** for both dry and saturated slopes[16]. This critical height decreases from more than 200 feet for a slope with discontinuities which are nearly horizontal and vertical to approximately 70 feet for slopes containing

*The dashed curve corresponds to circular failure in a material with a friction angle ϕ=30° and a cohesive strength c = 6400 lb/ft^2. Methods of analysing this type of failure are discussed later in this book.

**The critical height of this vertical slope is given by

$$H = \frac{2c}{\gamma \cos\psi (\sin\psi - \cos\psi \tan\phi + \gamma_w/\gamma . \tan\phi \tan\phi)}$$

where c, the cohesive strength of the surface = 2000 lb/ft^2
ϕ, the friction angle of this surface = 20°
γ, the rock density = 160 lb/ft^3
and γ_w, the density of water = 62.5 lb/ft^3.
γ_w/γ=0 for dry slopes.
For discontinuity angles between 0 and 30° and 80 and 90°,

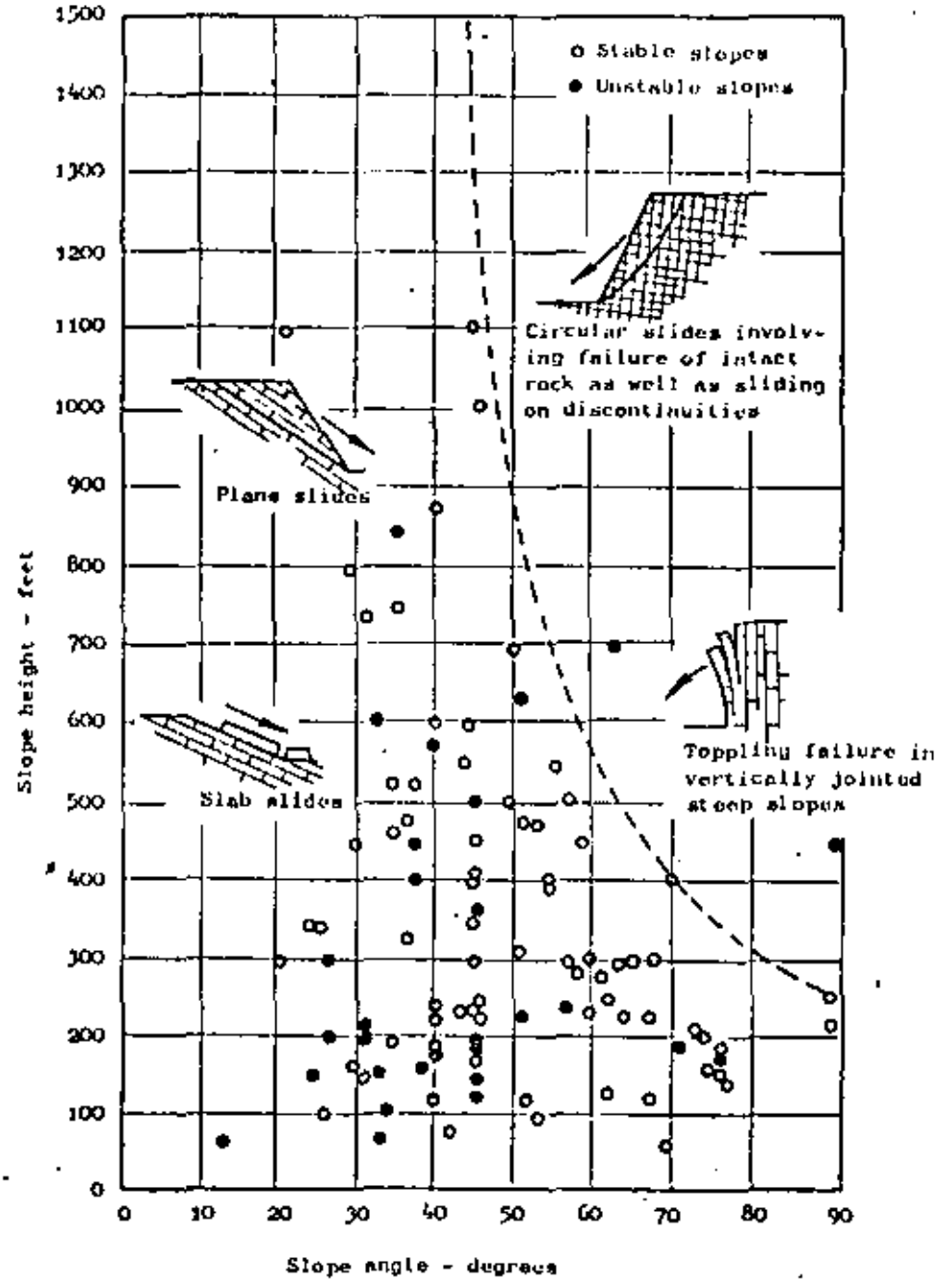

Figure 7 : Slope height versus slope angle relationships for hard rock slopes including data collected by Kley and Lutton[21] and by Hoek-Brown[22].

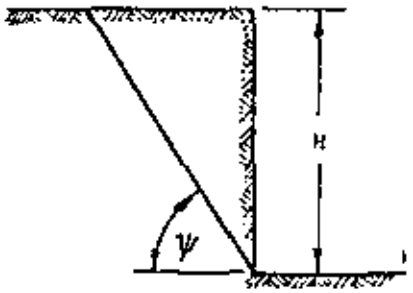
H
ψ

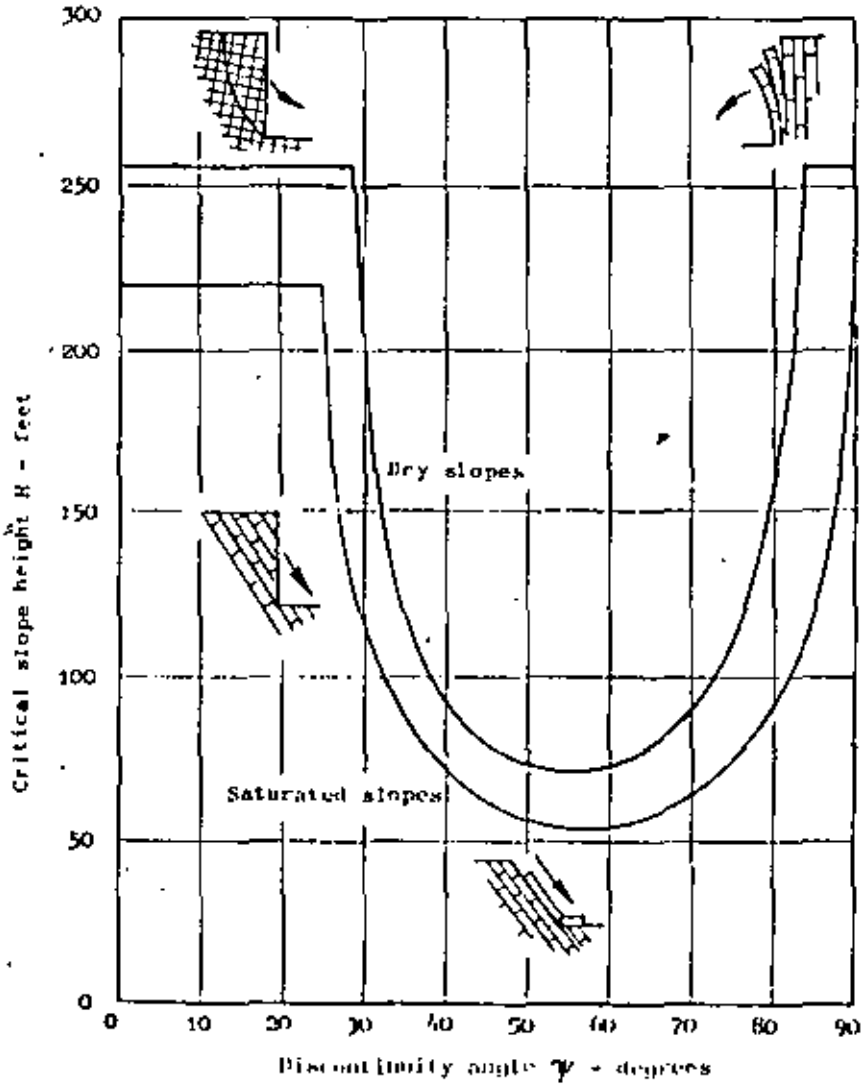
300
250
200
150
100
50
0
Critical slope height H - feet
Dry slopes
Saturated slopes
0
10
20
30
40
50
60
70
80
90
Discontinuity angle ψ - degrees

discontinuities inclined at 40 to 70°. Clearly the presence, or absence, of such discontinuities will have a very important influence upon the stability of rock slopes and the detection of these geological features is one of the most critical parts of a stability investigation. Techniques for dealing with this problem are discussed in the next chapter of this book.

Friction, cohesion and density

The material properties which are most relevant to the discussion on slope stability presented in this book are the angle of friction, the cohesive strength and the density of rock and soil masses.

Friction and cohesion are best defined in terms of the plot of shear stress versus normal stress given in Figure 9. This plot is a simplified version of the results which would be obtained if a rock specimen containing a geological discontinuity such as a joint is subjected to a loading system which causes sliding along the discontinuity. The shear stress τ required to cause sliding increases with increasing normal stress σ. The slope of the line relating shear to normal stress defines the angle of friction ϕ. If the discontinuity surface is initially cemented or of it is rough, a finite value of shear stress τ will be required to cause sliding when the normal stress level is zero. This initial value of shear strength defines the cohesive strength c of the surface.

The relationship between shear and normal stresses for a typical rock surface or for a soil sample can be expressed as:

$$\tau = c + \sigma \operatorname{Tan} \phi \qquad (1)$$

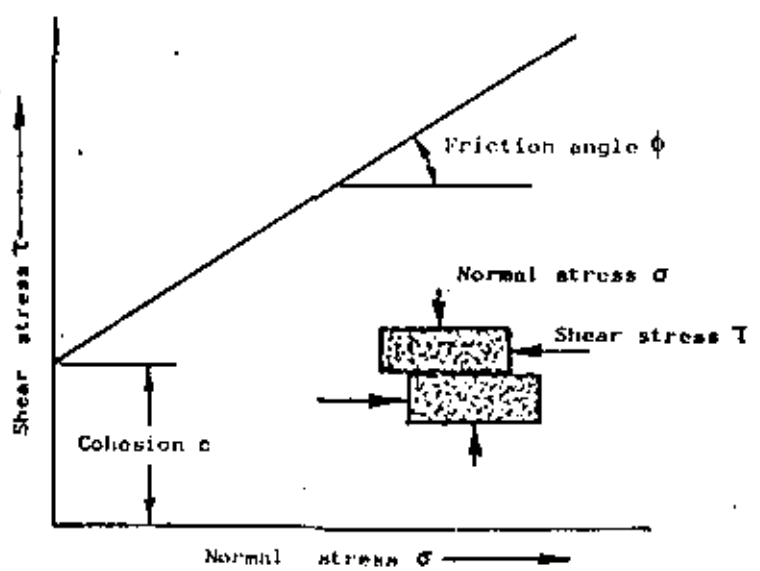

Figure 9 : Relationship between the shear stress τ required to cause sliding along a discontinuity to the normal stress σ acting across it .

TABLE 1 - TYPICAL ROCK AND SOIL PROPERTIES

Type		Material	Density γ Kg/m³	Density γ Lb/ft³	Friction angle φ Material	Friction angle φ Degs.	Material	Cohesion c Kg/m²	Cohesion c Lb/ft²
COHESIONLESS	Sand	Dry coarse sand	1440	90	Compacted, well graded, uniform	40-45			
		Dry fine sand	1600	100					
		Wet sand	1840	115	Uniform, coarse, medium fine or silty sand	35-40			
		Very wet sand	1920	120					
					Loose, well graded sand	35-40			
					Fine dry sand	30-35			
	Gravel	Common mixed	1760	110	Common mixed	35-45			
		River gravel	2240	140	Shingle	40			
		Loose Shingle	1840	115	Sandy, compact	40-45			
		Sandy gravel	1920	120	Sandy loose	35-40			
	Waste rock	Granite	1600-2000	100-125	Crushed or broken rock	35-45			
		Basalt and dolerite	1760-2240	110-140	Broken chalk	35-45			
		Limestone and sandstone.	1280-1920	80-120	Broken shale	30-35			
		Chalk	1000-1280	62-80					
		Shale	1600-2000	100-125					
COHESIVE	Clay	Dry clay	1760	110	Dry boulder clay	30	Very stiff boulder clay	17600	3600
		Damp, drained clay	1840	115	Damp, drained boulder clay	40	Hard shaley clay	14600	3000
		Wet clay	1920	120	Stiff clay	10-20	Stiff clay	9800	2000
		Sandy loam	1600	100	Soft clay	5-7	Firm clay	4900	1000
		Marl	1760	110	Clay gouge	10-20	Soft clay	2400	500
		Gravelly clay	2000	125	Calcite shear zone material	20-27			
					Shale fault material	14-22			
	Overburden	Top soil	1360	85					
		Dry soil	1440	90	Overburden soil	30-35	Overburden soil	490-4900	100-1000
		Moist soil	1600	100					
		Wet soil	1680	105					
	Rock mass	Granite	2614	164	Granite	30-50	Hard rock mass (granite, porphyry etc)	9800-30000	2000-6400
		Quartzite	2614	164	Quartzite	30-45			
		Sandstone	1950	122	Sandstone	30-45	Sandstone or limestone mass	4900-14600	1000-3000
		Limestone	3169	180	Limestone	30-50			
		Porphyry	2580	160	Porphyry	30-40	Shale or soft rock mass	2400-9800	500-2000
		Shale	2400	150	Shale	27-45			
		Chalk	1760	110	Chalk	30-40			

Typical values for the angle of friction and cohesion which are found in shear tests on a range of rocks and soils are listed in Table 1 together with densities for these materials. The values quoted in this table are intended to give the reader some idea of the magnitudes which can be expected and they should only be used for obtaining preliminary estimates of the stability of a slope.

There are many factors which cause the shear strength of a rock or soil to deviate from the simple linear dependence upon normal stress illustrated in Figure 9. These variations, together with methods of shear testing, are discussed in a later chapter.

Sliding due to gravitational loading

Consider a block of weight W resting on a plane surface which is inclined at an angle ψ to the horizontal. The block is acted upon by gravity only and hence the weight W acts vertically downwards as shown in Figure 10. The resolved part of W which acts down the plane and which tends to cause the block to slide is W Sin ψ. The component of W which acts across the plane and which tends to stabilise the slope is W Cos ψ.

The normal stress σ which acts across the potential sliding surface is given by

$$\sigma = (W \cos \psi)/A \qquad (2)$$

where A is the base area of the block.

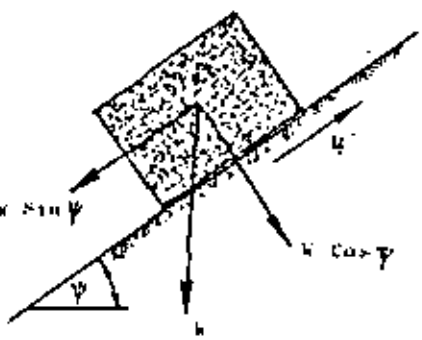

Assuming that the shear strength of this surface is defined by equation (1) and substituting for the normal stress from equation (2)

$$\tau = c + \frac{W \cos \psi}{A} \cdot \tan \phi$$

or $$R = cA + W \cos \psi \cdot \tan \phi \qquad (3)$$

where $R = \tau A$ is the shear *force* which resists sliding down the plane.

The block will be just on the point of sliding or in a condition of *limiting equilibrium* when the disturbing force acting down the plane is exactly equal to the resisting force:

$$W \sin \psi = cA + W \cos \psi \cdot \tan \phi \qquad (4)$$

If the cohesion $c = 0$, the condition of limiting equilibrium defined by equation (4) simplifies to

$$\phi = \psi \qquad (5)$$

Influence of water pressure shear strength

The influence of water pressure upon the shear strength of two surfaces in contact can most effectively be demonstrated by the beer can experiment.

An opened beer can rests on an inclined piece of wood as shown in Figure 11a. (Drink the beer and refill the can

to a minimum). The forces which act in this case are precisely the same as those acting on the block of rock in Figure 10 but, for simplicity, the cohesion between the beer can base and the wood is assumed to be zero. According to equation (5), the can with its contents of water will slide down the plank when $\psi_1 = \phi$.

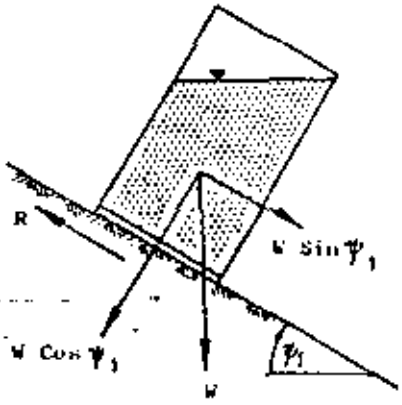

The base of the can is now punctured so that water can enter the gap between the base and the plank, giving rise to a water pressure u or to an uplift force U = uA, where A is the base area of the can.

The normal force W Cos ψ_2 is now reduced by this uplift force U and the resistance to sliding is now

$$R = (W \cos \psi_2 - U) \tan \phi \qquad (6)$$

If the weight per unit volume of the can plus water is defined as γ_t while the weight per unit volume of the water is γ_w, then $W = \gamma_t . h.A$ and $U = \gamma_w . h_w . A$, where h and h_w are the heights defined in the sketch opposite. From this sketch it will be seen that $h_w = h.\cos\psi_2$ and hence

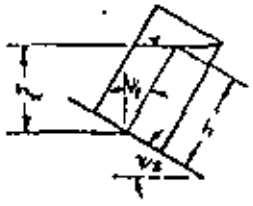

$$U = \frac{\gamma_w}{\gamma_t} . W \cos \psi_2 \qquad (7)$$

Substituting in (6)

$$R = W.\cos \psi_2 (1 - \gamma_w/\gamma_t) \tan \phi \qquad (8)$$

and the condition for limiting equilibrium defined in equation (4) becomes

$$\tan \psi_2 = (1 - \gamma_w/\gamma_t) \tan \phi \qquad (9)$$

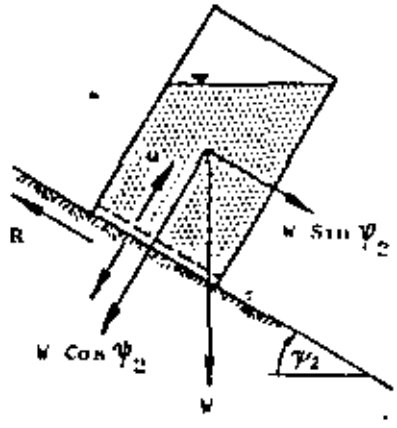

Assuming the friction angle of the can/wood interface is 30°, the unpunctured can will slide when the plane is inclined at $\psi_1 = 30°$ (from equation (5)). On the other hand, the punctured can will slide at a much smaller inclination because the uplift force U has reduced the normal force and hence reduced the frictional resistance to sliding. The total weight of the can plus water is only slightly greater than the weight of the water only. Assuming $\gamma_w/\gamma_t = 0.9$ and $\phi = 30°$, equation (9) shows that the punctured can will slide when the plane is inclined at $\psi_2 = 3° 18'$.

The effective stress law

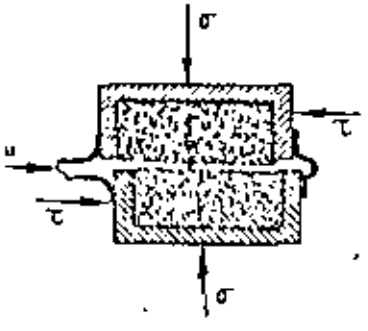

The effect of water pressure on the base of the punctured beer can is the same as the influence of water pressure acting on the surfaces of a shear specimen as illustrated in the sketch opposite. The normal stress σ acting across the failure surface is reduced to the *effective stress* $(\sigma - u)$ by the water pressure u. The relationship between shear strength and normal strength defined by equation (1) now becomes

$$\tau = c + (\sigma - u) \tan \phi \qquad (10)$$

In most hard rocks and in many sandy soils and gravels, the cohesive and frictional properties (c and ϕ) of the materials are not significantly altered by the presence of

materials is due, almost entirely to the reduction of normal stress across failure surfaces. Consequently, it is *water pressure* rather than *moisture content* which is important in defining the strength characteristics of hard rocks, sands and gravels. In terms of the stability of slopes in these materials, the presence of a small volume of water at high pressure, trapped within the rock mass, is more important than a large volume of water discharging from a free draining aquifer.

In the case of soft rocks such as mudstones and shales and also in the case of clays, both cohesion and friction can change markedly with changes in moisture content and it is necessary, when testing these materials, to ensure that the moisture content of the material during test is as close as possible to that which operates in the field. Note that the effective stress law defined in equation (10) still applies to these materials but that, in addition, c and ϕ change.

The effect of water pressure in a tension crack

Consider the case of the block resting on the inclined plane but, in this instance, assume that the block is split by a tension crack which is filled with water. The water pressure in the tension crack increases linearly with depth and a total force V, due to this water pressure acting on the rear face of the block, acts down the inclined plane. Assuming that the water pressure is transmitted across the intersection of the tension crack and the base of the block, the water pressure distribution illustrated in the sketch opposite occurs along the base of the block. This water pressure distribution results in an uplift force U which reduces the normal force acting across this surface.

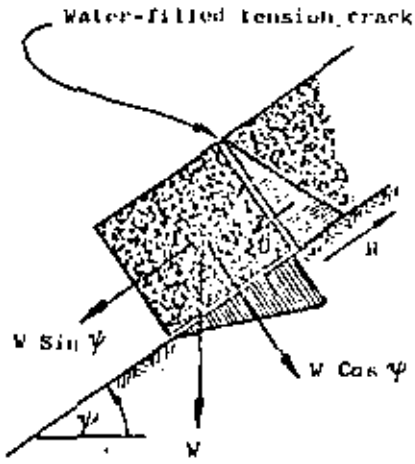

The condition of limiting equilibrium for this case of a block acted upon by water forces V and U in addition to its own weight W is defined by

$$W \sin\psi + V = cA + (W \cos\psi - U) \tan\phi \qquad (11)$$

From this equation it will be seen that the disturbing force tending to induce sliding down the plane is increased and the frictional force resisting sliding is decreased and hence, both V and U result in decreases in stability. Although the water *pressures* involved are relatively small, these pressures act over large areas and hence the water *forces* can be very large. In many of the practical examples considered in later chapters, the presence of water in the slope giving rise to uplift forces and water forces in tension cracks is found to be critical in controlling the stability of slopes.

Reinforcement to prevent sliding.

One of the most effective means of stabilising blocks or slabs of rock which are likely to slide down inclined discontinuity surfaces is to install tensioned rockbolts or cables. Consider the block resting on the inclined plane and acted upon by the uplift force U and the force V due to water pressure in the tension crack. A rockbolt,

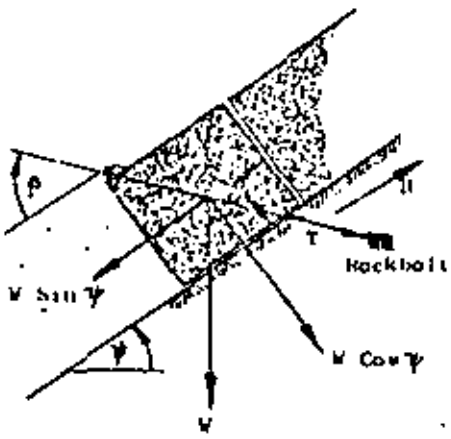

T acting parallel to the plane is T Cosβ while the component acting across the surface upon which the block rests is T sin β. The condition of limiting equilibrium for this case is defined by

$$W \sin\psi + V - T\cos\beta = cA + (W\cos\psi - U + T\sin\beta)\tan\phi \qquad (12)$$

This equation shows that the bolt tension reduces the disturbing force acting down the plane and increases the normal force and hence the frictional resistance between the base of the block and the plane.

The minimum bolt tension required to stabilise the block is obtained by differentiation of equation (12) with respect to the angle β and this shows that the optimum bolt inclination is given by

$$\beta = \phi \qquad (13)$$

Factor of safety of a slope

All the equations defining the stability of a block on an inclined plane have been presented for the condition of *limiting equilibrium*, i.e. the condition at which the forces tending to induce sliding are exactly balanced by those resisting sliding. In order to compare the stability of slopes under conditions other than those of limiting equilibrium, some form of index is required and the most commonly used index is the *Factor of Safety*. This can be defined as the ratio of the total force available to resist sliding to the total force tending to induce sliding. Considering the case of the block acted upon by water forces and stabilised by a tensioned rockbolt (equation 12), the factor of safety is given by

$$F = \frac{cA + (W\cos\psi - U + T\sin\beta)\tan\phi}{W\sin\psi + V - T\cos\beta} \qquad (14)$$

Note that the condition of limiting equilibrium is represented by a factor of safety F = 1. Stable slopes must obviously have a factor of safety in excess of unity and a vital question for the slope engineer is - what value for the factor of safety should be used for design purposes?

This is one of the most controversial questions in rock engineering and many eminent engineers have argued that, because of the uncertainty associated with the input data for a factor of safety calculation, the value obtained is too unreliable to have relevance in engineering design.

Some authors have suggested that a *probabilistic* approach is more meaningful in that the safety of a slope can be assessed in terms of the variation of each of the factors which control its stability [23,24,25]. Although this approach has many attractive features, it has two drawbacks which have inhibited its development as a design tool. The first of these is the difficulty of obtaining adequate input data for a meaningful statistical analysis of all the parameters involved. The second drawback is associated with the average engineer's lack of understanding of statistical concepts and of the mathematical jargon which is so freely used in discussions on this subject. How does one relate the adequacy of a design to a probability of failure of 1 in 100,000? Indeed, to some clients, the

admission, by a consulting engineer, that there is a possibility of failure, however small, is totally unacceptable.

The author does not consider these drawbacks to be so serious that they will not be overcome in time and it is more than likely that the use of a factor of safety will eventually be replaced by some design index which has been determined by probabilistic methods. However, in the absence of acceptable statistical methods, the design engineer of today is still faced with the problem of how to compare a number of alternative slope designs or to assess the stability of an existing slope.

The most satisfactory solution to this problem is to carry out *a sensitivity analysis* of the influence of each variable upon the stability of the slope and to use the results of this analysis as a basis for engineering decisions. There are several ways in which such an analysis can be done and a simple example is given in Figure 2 on page 9 which shows the variation in factor of safety of a particular slope with changes in slope angle and groundwater conditions. Other types of sensitivity analysis will be illustrated in later chapters of this book in which detailed analyses of practical slope problems are presented.

The merit of such a sensitivity analysis is that it does not place too much emphasis upon the *absolute* value of the factor of safety or of any other index which is used to measure the stability of a slope. The *relative* values of the index, for a range of different conditions, can usually be determined with reasonable accuracy and these relative values, together with sound engineering common sense, will usually provide an adequate basis for a practical slope design.

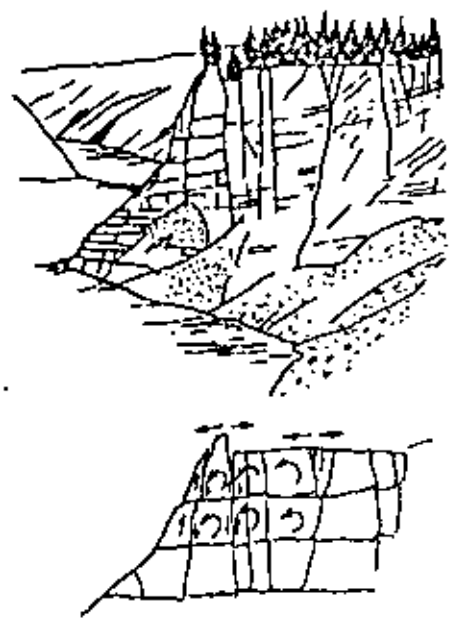

Suggested toppling failure mechanism of north face of Vajont slide. After Ilamanti[26] and Muller[27].

Slope failure due to toppling

One of the limitations of the factor of safety computed from equation (14) is that it is based upon sliding of the block and does not allow for rotational or toppling failure. The simplest conditions under which toppling can occur can be deduced by returning to the model of a block resting on an inclined plane. In this case, the shape of the block as well as its weight is important. This shape is defined by the height h and width b as illustrated in Figure 10a.

The condition for toppling is defined by the position of the weight vector in relation to the base of the block. If the weight vector, which passes through the centre of gravity of the block, falls outside the base of the block, toppling will occur.

In Figure 10b, the conditions for toppling and sliding are plotted. The criterion for sliding is based upon friction only (equation (5)) and a friction angle $\phi = 35^{\circ}$ has been assumed. From this figure it will be seen that the danger of toppling increases with increasing discontinuity angle and steep slopes in vertically jointed rocks frequently exhibit signs of toppling failure[26,27,28].

Potential toppling condition

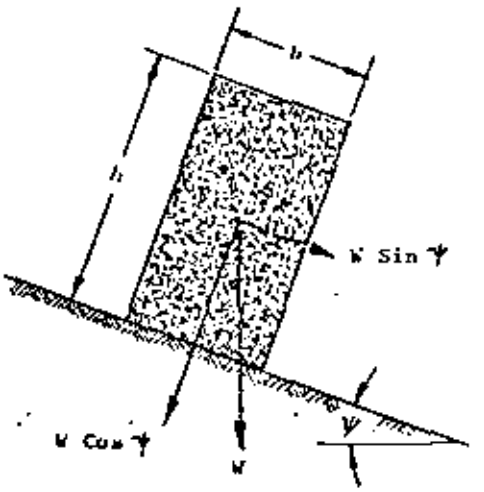

Figure 10a : Geometry of block on inclined plane

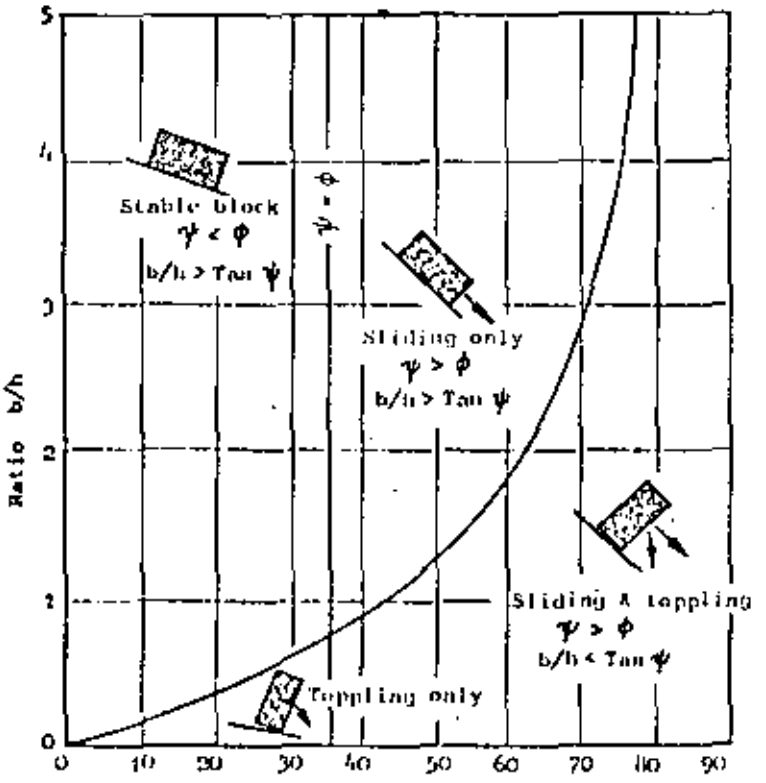

Figure 10b : Conditions for sliding and toppling of a block on an inclined plane .

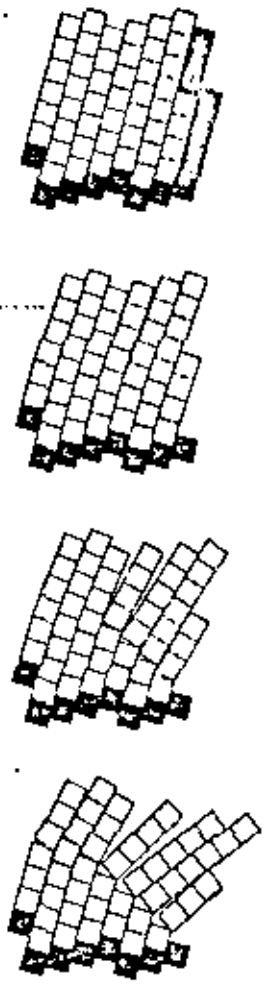

Computer produced drawings of toppling failure. After Cundall[30].
(Dark blocks are fixed)

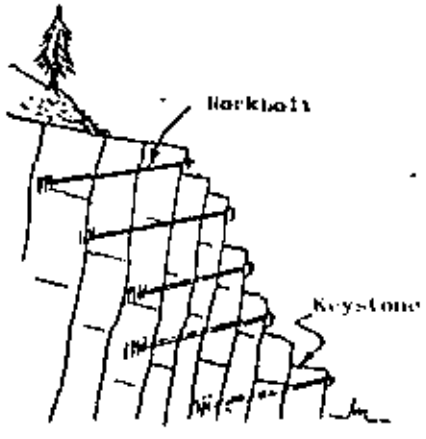

Rock reinforcement to prevent

In an actual rock slope consisting of a large number of blocks of irregular shape, simple toppling such as that illustrated in Figure 10 will seldom occur. Failure will involve complex movement, both sliding and toppling, of blocks which will be in contact with surrounding blocks and will, therefore, be restricted in their movements. No satisfactory analytical techniques for dealing with this complex situation are currently available although a promising start on the development of such techniques has been made by Cundall[20].

A useful qualitative technique for studying the possibility of toppling failure in a rock slope with steeply inclined discontinuities is illustrated in Figure 11. This method employs the base friction principle proposed by Goodman[29] and depends upon the simulation of gravitational loading by the frictional forces exerted on the base of a model when the paper on which it rests is pulled from under the model. The model can be constructed from any suitable material which happens to be available; the plastic blocks which make up childrens toys such as "Lego" being ideal for simple models. In the example illustrated in Figure 11 a sheet of cork, such as that used for making gaskets for motor car engines, has been used as the model material. The geometry of the slope under consideration is traced onto the cork and the discontinuities are then cut by means of a modelling knife. A drawing board with a parallel movement system makes an ideal base for the model and the frictional load exerted on the base of the model as it is pushed over the surface of the board provides a remarkably accurate simulation of gravity loading[30].

Although the results obtained from such a model are qualitative, they do provide the engineer or geologist with an understanding of the possible failure modes which are likely to occur in a particular slope and thereby enable him to arrive at a rational decision on how the problem should be tackled.

Reinforcement to prevent toppling

The conditions for toppling defined in Figure 10 show that the danger of this type of failure occurring is greatest when tall slender rock columns are present in a slope. The principal aim of reinforcement, in the forms of rockbolts or cables, installed to prevent toppling should be to tie these columns together to form wider blocks. It is particularly important that the "keystone" which prevents the front face of the slope from moving should be identified and securely anchored since loss of the restraining action of this block will initiate a progressive failure process in the slope.

It is unlikely that attempts to stabilise a rock slope, in which toppling is the dominant failure mechanism, by drainage would be successful since the structure of the rock mass is disturbed to a much greater extent than in the case of failure by sliding and the slope is therefore self-draining.

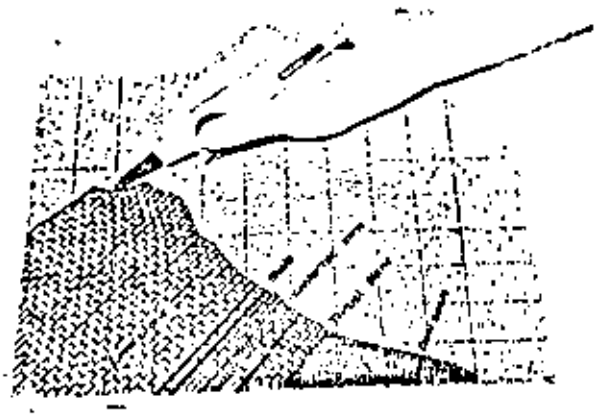

Figure 11a : Model is cut out from a sheet of cork with a modelling knife. The model in this case is of the Frank slide in Alberta, Canada which occurred in 1903 and which is discussed by Coates[32] and Terzaghi 33.

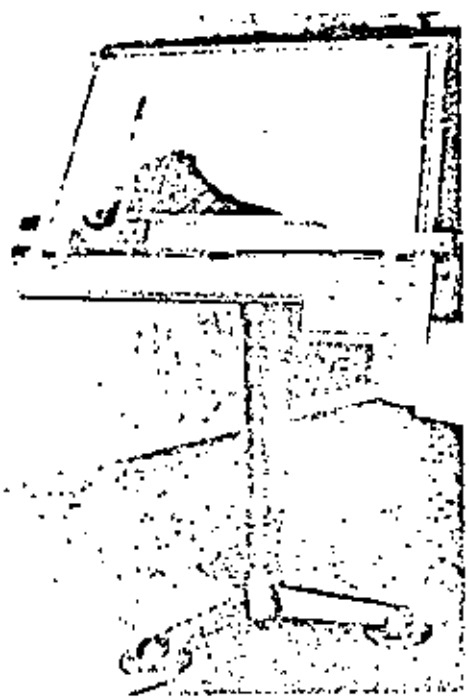

Figure 11b : Model resting on a drawing board. Upward displacement of the parallel movement of the board results in the base of the model being subjected to frictional forces which simulate gravitational loading.

Figure 11c : The Frank slide as it is today. The slide involved approximately 30 million tons of rock and mining of a coal seam at the base of the mountain may have been partially responsible for this failure.

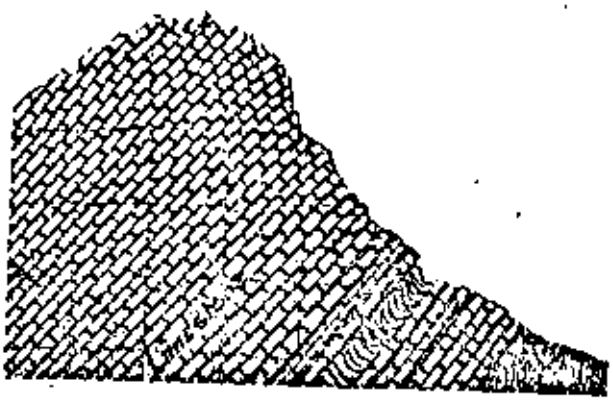

Figure 11d : Original profile of Turtle mountain on which the Frank slide occurred.

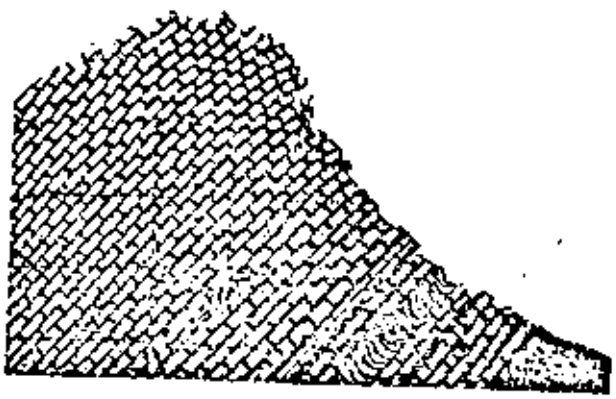

Figure 11e : Bending of strata on mountain top and start of block movement.

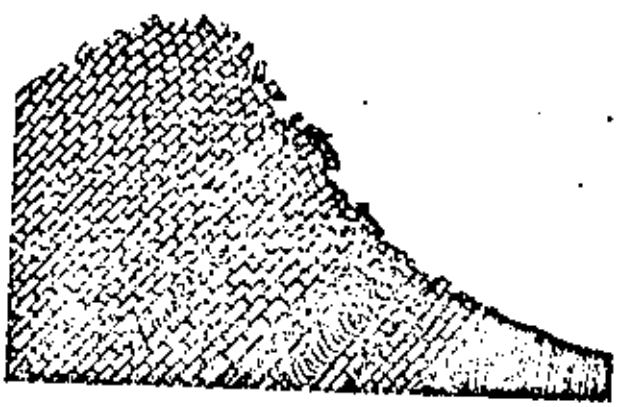

Figure 11f : Toppling and rolling of rock blocks

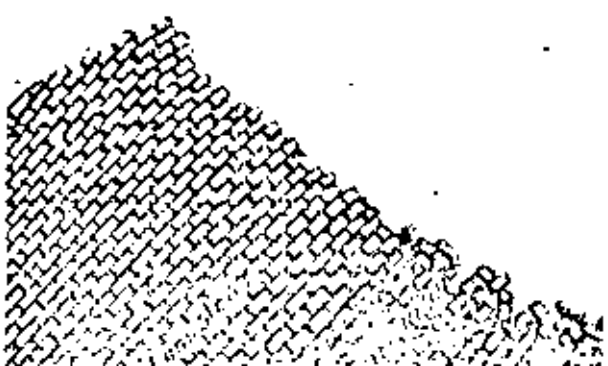

Figure 11g : Stable slope remaining after slide.

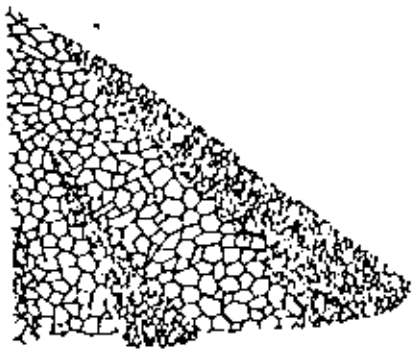

Waste rock dump

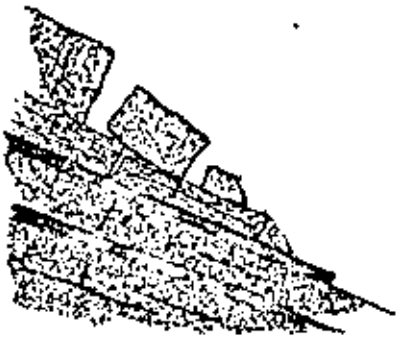

Stratified rock mass

Slope in weathered surface material.

Angle of repose of waste dumps

A question which frequently arises in discussions on open cast mine slope design is whether the slope angle can be chosen on the basis of the angle of repose of waste dumps. The answer is a most emphatic *no* because the geometery of the rock mass is entirely different from that of the packing pattern in the waste rock. Although the rock mass may be heavily fractured, this fracturing generally follows systematic patterns and failure, when it occurs, usually follows a continuous feature such as a joint or a bedding plane. This is not the case in a waste rock pile in which no regular discontinuity pattern exists and in which failure involves a complex movement path for each individual piece of rock. The groundwater conditions in the rock slope and in the waste pile are also significantly different because of the differences in the drainage characteristics of the two systems.

Table I shows that the effective friction angle for waste rock generally lies between 35 and 45° and the angle of repose of waste rock dumps is frequently found to be approximately 38°. Failures in waste rock dumps can and do occur due to a variety of causes, most of which are associated with sliding on the surface upon which the dump has been placed or breakage of particles within the dump. These factors will be examined in more detail in a later chapter.

An interesting corollary to this difference between the behaviour of a waste rock dump and a rock mass is the proposal which is sometimes put forward to stabilise a slide by breaking up the plane on which sliding occurs by means of carefully placed blasts. This proposition is discussed by Zaruba and Mencl[28] and they conclude that the technique is unreliable and that the risk of inducing a major slide by blasting probably outweighs the advantage of a slight increase in stability which may be achieved if the blast can be successfully carried out. The author is in complete agreement with this assessment and would not recommend this method of slope stabilisation except under very unusual conditions and subject to the control of a blasting specialist.

Slope failure induced by weathering

Engineers are sometimes so concerned with the mechanics of slope failure that they forget that rock does not have the same predictable behaviour characteristics as man-made engineering materials such as steel and concrete. Weathering, which results in a progressive deterioration of the properties of the rock with time, is a factor which is sometimes not assigned sufficient importance by engineers.

A complete discussion on weathering exceeds the scope of this handbook and the interested reader is referred to the extensive literature on the subject, recently reviewed by Saunders and Fookes[31]. One example will serve to warn the reader of the type of problem which may arise in rock slopes as a result of weathering.

The de Beer's diamond mine at Kimberley in South Africa is currently being reopened, having ceased operations in 1908

As shown in the sketch opposite, the vertically jointed dolerite which occurs on the surface rests on a thick bed of shale. This shale, which is a good medium/hard rock in its unweathered state, gradually weathers on exposure to a residual soil. This weathered material has a cohesive strength of zero and a friction angle of approximately 32° and progressive failure of the originally steep slopes in the shale has induced failure in the overlying dolerites as illustrated in the photograph reproduced below.

In the case of the de Beer's mine, weathering has taken tens of years to produce the slope conditions illustrated. There are many other situations in which weathering of mudstones, siltstones and soft shales can occur in a matter of months and can give rise to severe slope problems unless their presence has been recognised and provided for in the design.

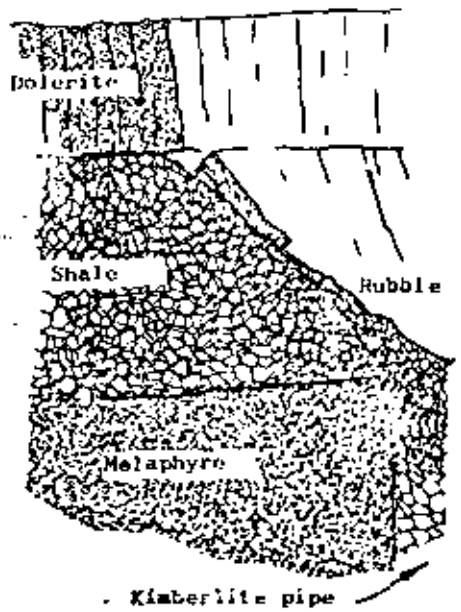

Approximate section through the de Beer's diamond mine.

Upper slopes on the de Beer's diamond mine at Kimberley in South Africa. Failure of the vertically jointed dolerite is induced by progressive weathering of the underlying shales.

Chapter 2 references

Selected reference on slope behaviour.

11. BLAKE, W. Stresses and displacements surrounding an open pit in a gravity loaded rock. *U.S. Bureau of Mines Report of Investigations* 7002, Aug. 1967, 20p.

12. BLAKE, W. Finite element model is excellent pit tool. *Mining Engineering*, A.I.M.E., Vol. 21, No. 8, 1969, pp. 79-80.

13. YU, Y.S., GYENGE, M. and COATES, D.F. Comparison of stress and displacement in a gravity loaded slope by photoelasticity and finite element analysis. *Canadian Dept. Energy, Mines and Resources Report* MR 68-24 10, 1968.

14. WANG, F.D. and SUN, M.C. Slope stability analysis by finite element stress analysis and limiting equilibrium method. *U.S. Bureau of Mines Report of Investigations* 7341, January 1970, 16p.

15. STACEY, T.R. The stresses surrounding open-pit mine slopes. *Planning open pit mines*, Johannesburg Symposium 1970. Published by A.A. Balkema, Amsterdam, 1971. pp.199-207.

16. HOEK, E. The influence of structure upon the stability of rock slopes. *Proc. 1st Symposium on Stability in Open Pit Mining, Vancouver 1970.* A.I.M.E., New York, 1971, p49-60.

17. TERZAGHI, K. Stability of steep slopes on hard unweathered rock. *Geotechnique*, Vol. 12, 1962, pp.251-270.

18. MULLER, L. The European approach to slope stability problems in open-pit mines. Proc. Third Symposium on Rock Mechanics. *Colorado School of Mines Quarterly*. Vol. 54, No. 3, 1959, pp.116-133.

19. GOODMAN, R.E., TAYLOR, R.L. and BREKKE, T.L. A model for the mechanics of jointed rock. *J. Soil Mech. Foundation Div.* Vol. 94, No. SM6, 1968, p.637.

20. CUNDALL, P.A. A computer model for simulating progressive large-scale movements in blocky rock systems. *Proc. Symposium on Rock Fracture*, Nancy, France. October 1971. Section 2-8.

21. KLEY, R.J. and LUTTON, R.J. Engineering properties of nuclear craters; a study of selected rock excavations as related to large nuclear craters. *Report U.S. Army Engineers*, No. PNE 5010 1967, 159p.

22. ROSS-BROWN, D.R. Slope design in opencast mines. *Ph.D. Thesis*, London University, in preparation.

23. MCMAHON, B.K. A statistical method for the design of rock slopes. *Proc. 1st Australia-New Zealand Conference on Geomechanics, Melbourne, August 1971.*

198

24. SHUE, T. Optimisation of slopes designed in rock. *Proc. 2nd Congress Intnl. Society of Rock Mechanics, Belgrade*, 1970, Vol. 2, Section 7-2.

25. LANGLIAN, A. Some aspects of safety factors in soil mechanics considered as a problem of probability. *Proc. 6th Intnl. Conference on Soil Mech. and Foundation Engineering*, Montreal 1965, Vol. 2, pp.500-502.

26. HOFMANN, H. The deformation process of regularly jointed discontinuum during the excavation of a cut (in German). *Proc. 2nd Congress Intnl. Society of Rock Mechanics, Belgrade* 1970, Vol. 2, Section 7-1.

27. MÜLLER, L. The rock slide in the Valont Valley. *Rock Mechanics and Engineering Geology*, Vol. II/3-4, 1964.

28. ZARUBA, Q. and MENCL, V. *Landslides and their control*. Academia press, Prague, 1969, 205 p. (available through Elsevier, London, New York and Amsterdam).

29. GOODMAN, R.E. Geological investigations to evaluate stability. *Proc. 2nd Symposium on stability for Open Pit Mining*, Vancouver, November 1971. Publishers A.I.M.E., New York - in press.

30. ASHBY, J.P. Sliding and toppling modes of failure in models and jointed rock slopes. *M.Sc. Thesis*, Univ. of London (Imperial College), 1971, 40 p.

31. SAUNDERS, M.K. and FOOKES, P.G. A review of the relationship of rock weathering and climate and its significance to foundation engineering. *Engineering Geology*, Vol. 4, 1970, pp.289-325.

32. COATES, D.F. *Rock Mechanics Principles*. Canadian Department of Energy, Mines and Resources, Mines Branch Monograph 874, 1965, 300 p.

33. TERZAGHI, K. Mechanism of Landslides in *Application of Geology to Engineering Practice* (Berkey Volume). Geological Society of America, 1950, p 83-123.

Chapter 5 : Shear strength determination

Introduction

In considering the stability of slopes in rock, the most important factor is the *geometry* of the rock mass. The next most important factor is the *shear strength* of the planes or the discontinuity patterns upon which or through which failure is likely to occur. This chapter is concerned with methods for the determination of shear strength.

Two basic methods are available:

a. Triaxial testing
b. Shear testing

The various conditions under which these methods are used are outlined in Figure 24 which shows that, where clearly defined structural discontinuities are present, shear testing should be used. In soils, waste rock or in very heavily fractured rock, triaxial testing is more appropriate.

In addition to the direct testing methods outlined in Figure 24, a number of indirect index tests, have been used to obtain estimates of strength and these methods will also be examined.

Before discussing the actual testing techniques, it is necessary briefly to consider methods for the collection and preparation of samples for these tests.

Sample collection and preparation

Some, but by no means all, of the samples used for strength testing are obtained from borehole core. The special drilling techniques required to recover these samples have been discussed in the previous chapter but no mention was made of the preservation of the core for testing.

When clean joints in hard rock specimens have been collected for shear testing, it is probably satisfactory to transport these to the laboratory or testing station in a normal core box. If it is considered that excessive movement may damage the surfaces, the two pieces of core can be taped or wired together.

When very heavily fractured rock is collected for triaxial testing as described by Jaeger[77], the core can be transported inside the inner core-barrel which is only split when the core is ready to be transferred into the triaxial cell. In his tests on heavily fractured andesite cores from Bougainville, Jaeger transferred the core from one half of a split-barrel into a copper sheath by gently rotating the barrel with the copper wrapped around it. When the core was supported by the copper sheath, the barrel was removed and the sheath folded over and soldered to form a tight fitting container for the core.

When very friable cores or cores which are liable to very rapid deterioration upon exposure are to be transported, a technique used by Stimpson, Metcalfe and Walton[87] and illustrated in Figure 25 can be used. This method has been successfully used to transport cores containing seat earths and clay mylonites in coal measure rocks and also cores of kaolinised granite, all of which would not

200

TEST	CONDITIONS AND REMARKS
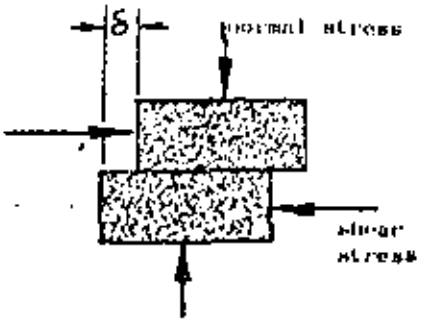	SHEAR TEST FOR DISCONTINUITIES . The shear stress required to cause displacement along a discontinuity is measured for a range of normal stresses . The shear displacement δ as well as the normal displacement (dilation) are measured during the test . The shear stress must be applied parallel to the discontinuity and the test is not suitable for testing intact rock specimens unless these contain weakly cemented discontinuity planes which must then be aligned parallel to the shear stress direction . Practical problems make it difficult to apply water pressure although the surface can be wet before and during the test . Loading rate is of secondary importance for most hard rock surfaces.
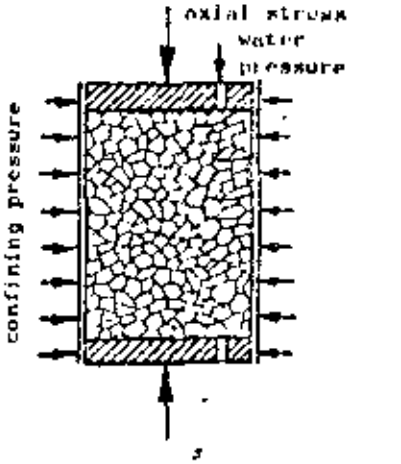	TRIAXIAL TEST FOR FRACTURED ROCK . For heavily fractured rock in which the discontinuities do not follow a clearly defined pattern, triaxial testing is most appropriate . This test is also used for waste rock, rock fill and gravel. The minimum dimension of the triaxial cell should be approximately ten times the average size of individual pieces of rock . A flexible rubber sleeve prevents confining pressure fluid from entering the specimen . Water pressure can be included in the test by means of a separate circuit with entry through the axial loading platens. Loading rate is not critical for hard rock but should be low enough to allow pore water pressures to stabilise.
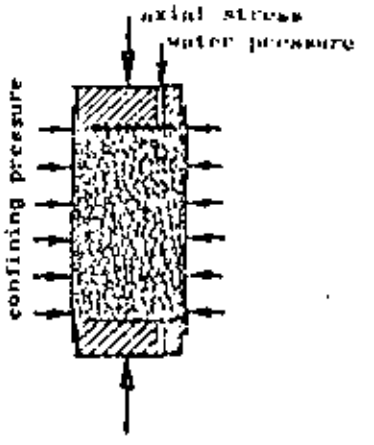	TRIAXIAL TEST FOR OVERBURDEN SOILS . For overburden soils and fine waste material , standard soil triaxial tests should be used . Experimental procedure set out in recognised texts [75,76] should be followed carefully as results are sensitive to test conditions such as loading rate and inaccuracies in load and pressure measurement . Control of pore water pressures is particularly important. Shear tests in machines with low load capacity can also be used on these materials .

Figure 56 : Test methods for the determination of the shear strength of materials which may be involved in slope failures .

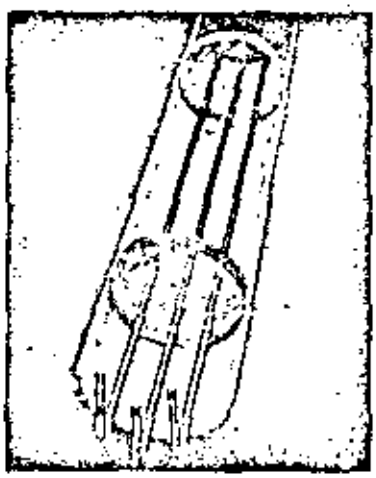

Step 1

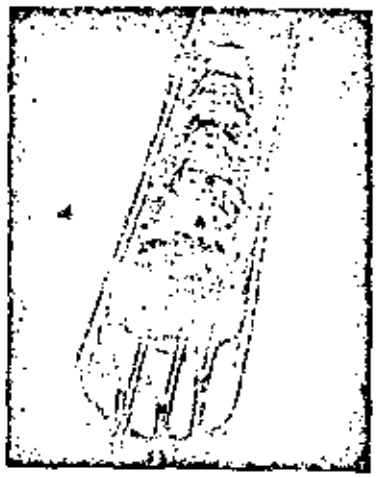

Step 2

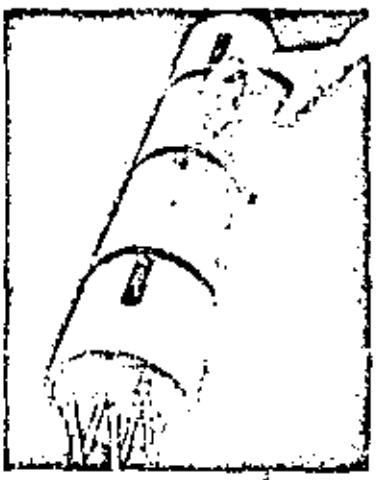

Step 3

Step 4

Step 5

Figure 25 : Preservation of fragile core (Ref.80)

Step 1 : Mould consisting of a plastic pipe split along its axis ready to receive core.

Step 2 : Core, wrapped in aluminium foil, placed on supporting rods and end stops adjusted to core length.

Step 3 : Upper half of mould fixed in place and polyurethane foam poured in through access slot. Suitable material is Bibthane BM14 manufactured by Bibby Chemicals Ltd., Liverpool, England.

Step 4 : Foam sets rigid in approximately 30 minutes and mould may then be split and supporting rods removed.

Step 5 : Core encased in rigid foam exhibits low moisture loss and withstands rough handling during transportation. Foam is easily cut with saw for removal of the core.

normally survive exposure or transport for more than a few hours.

Samples for shear testing are frequently collected by methods other than core drilling. The most obvious of such methods is to use a geologist's hammer to chip the required sample out of the rock mass. This will sometimes work but a great deal of time and energy can be expended in attempts to collect an "undisturbed" sample.

In soft materials such as coal measure rocks, Walton[83] of the National Coal Board in England has successfully used a logger's type chain saw fitted with a tungsten-carbide tipped chain to remove samples for shear testing. The field set-up is illustrated in Figure 26.

Londe[74] describes a variety of techniques used for collection of samples for shear testing. One of these involves drilling out a large diameter core by means of a thin-walled diamond core barrel. Another, illustrated in Figure 27, involves using a specially adapted wire saw of the type used in the stone-working industry. Londe's description of this technique is as follows:

"Four slightly converging 120 mm diameter holes are drilled 1 meter deep on either side and parallel to the joint plane. These form the edges of the long sides of the rectangular block to be extracted.

Two tubes with small pulleys lying in their diametric planes are fitted into two of the holes. Their position can be adjusted with screw jacks. The running steel cable passes between two pulleys and is looped over larger pulleys taking it to the drive and straining device. The abrasive, carborundum is thrown onto the cable with a water jet. As the tubes with their pulleys are forced into the holes, the cable cuts a slot forming one of the walls of the block. This operation is repeated for the sides and top.

To cut the remaining two faces, i.e. the back and base, the two tubes with their pulleys are introduced into the two lower holes and the cable is slid through the side and top slots already cut and passed over the back face of the block. The cable is tensioned quite strongly, and it cuts the back as it descends.

Once the near face is completely freed, the small pulleys are turned parallel to the joint plane and slowly withdrawn to cut the base of the block. As the cable is withdrawn, chocks are placed under the block to prevent it breaking under its own weight. Once this operation is completed, the block is free on all sides. It has at no time been subjected to shocks or strains liable to disturb the material".

Index testing of rock

Some rock engineers argue (with justification) that the time and expense involved in rock testing means that only a limited number of tests will be carried out and that the data provided will not be adequate for design purposes. It is therefore suggested that the gaps in this data should be filled by simple, inexpensive index tests which can be

Figure 26 : Use of power saw with tungsten carbide tipped chain for collection of shear test specimens in coal measure rocks (Ref. 83). The saw is a Stihl 090 power chain saw manufactured by Andreas Stihl Maschinenfabrik, Waiblingen,Germany .

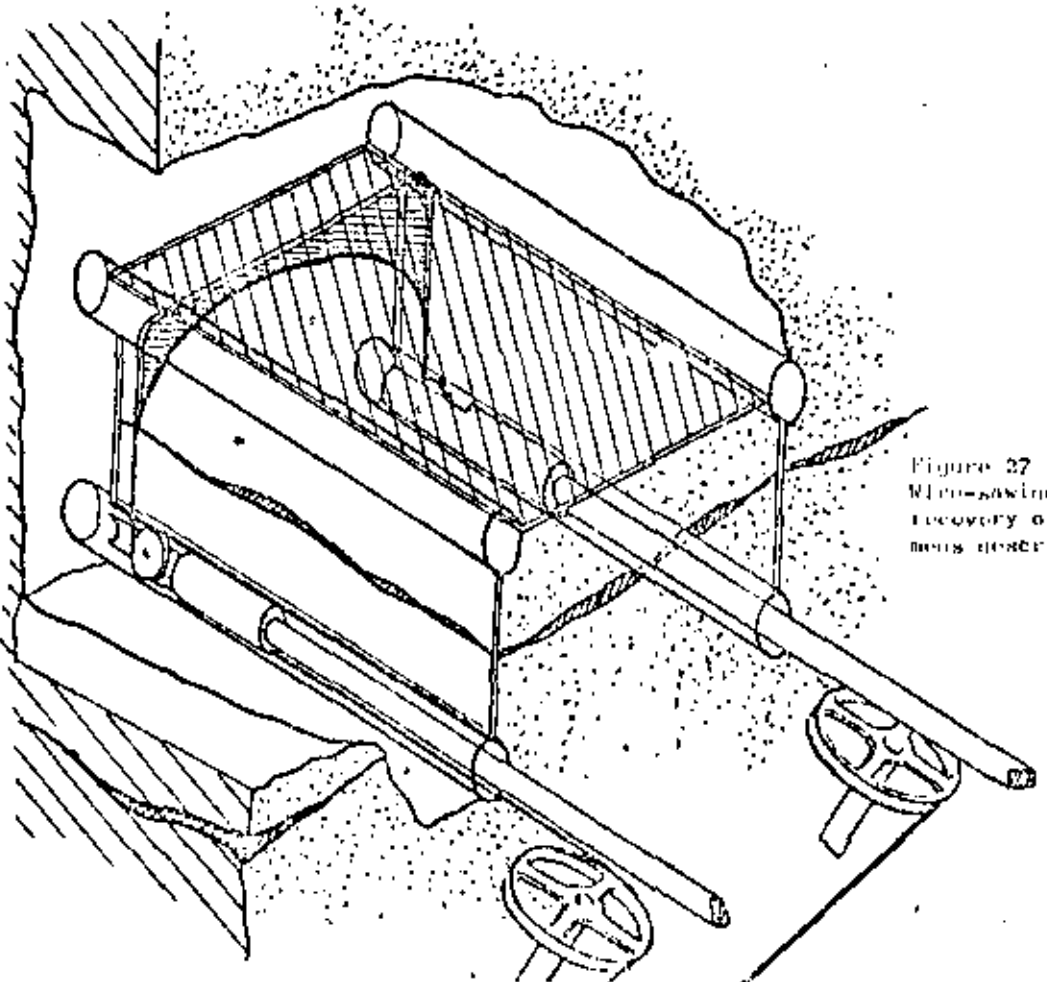

Figure 27 : Wire-sawing technique for the recovery of shear test specimens described by Jaeger [74].

carried out in the field.

Londe[74] discusses the use of seismic tests to estimate mechanical properties of rock masses. This approach is attractive because it does not involve disturbing the rock as is necessary in all other testing techniques. Although the author has no personal experience of seismic testing, the impression gained from studying the literature is that the interpretation of results is heavily dependent upon the skill and experience of the operator. In other words, if a company which uses seismic techniques regularly is hired to provide an assessment of rock properties, useful information will probably be obtained. A do-it-yourself operation will probably be a poor investment.

More directly interpretable results are likely to be obtained from the logging techniques suggested by Franklin, Broch and Walton[84], all of which are intended to add to the information obtained from normal core logging. These authors suggest that, as the core is removed from the barrel, spacing between discontinuities would be logged (those fractures judged to have been induced by drilling should be excluded). The fracture spacing index is simply the number of discontinuities per unit length of core, e.g. 5 fractures per foot.

An alternative system is used by Deere *et al*[85] who defined an index known as Rock Quality Designation (R.Q.D.) as the percentage of core in intact pieces over 4 inches (10 cm) in length. Hence the R.Q.D. of a 60 inch length of core in which 30 inches was in pieces of greater than 4 inches in length would be 50% (NX (2¼ inch diameter) is the smallest core size which should be used for R.Q.D. evaluation).

Practical experience shows that both fracture spacing and R.Q.D. can give a useful indication of the "quality" of a rock mass and of its probable response to loading and excavation. Care should, however, be taken to ensure that the numbers obtained are treated as qualitative guides and not as absolute values upon which decisions can be based.

Another index test suggested by Franklin *et al* is the Point Load Index which is the ratio of the load P required to fracture a core to the square of the diameter D, i.e. $I_s = P/D^2$. Two types of portable point load testing machine are illustrated in Figure 28 and the correlation between Point Load Index and uniaxial compressive strength is given in Figure 29 from results obtained by D'Andrea *et al*[86].

These index tests, and others suggested by these and other authors, add considerably to the value of the information obtained from normal core logging. While little of this information can be used in a precise quantitative manner, it does add to the overall picture and should assist the engineer or geologist in assessing the most likely behaviour of the rock mass.

Shear strength of rock discontinuities

Failure in a rock slope generally occurs as a result of movement along a discontinuity and shear strength tests in which the load and displacement conditions which occur in

Figure 28a : A portable point load tester being used for core logging in the field. This machine is manufactured by Engineering Laboratory Equipment Limited , Hemel Hempstead , Hertfordshire , England.

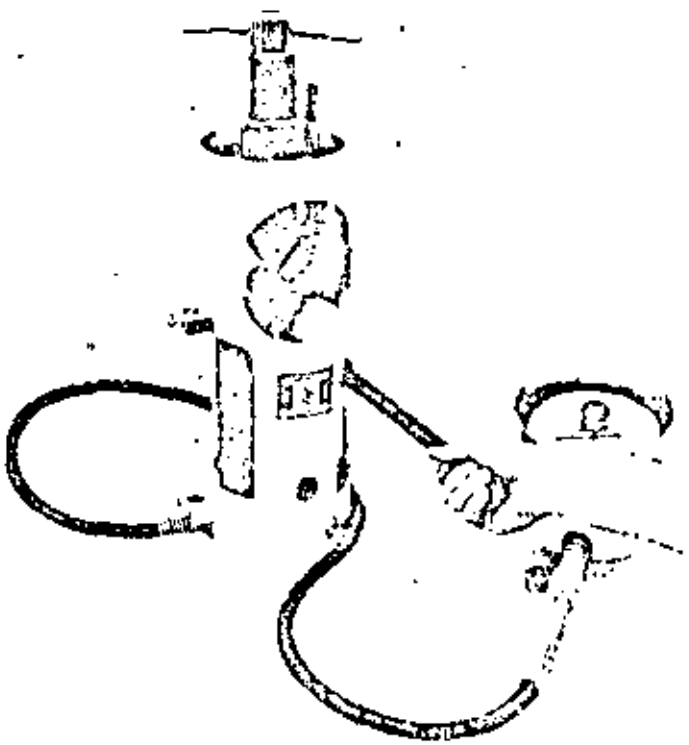

Figure 28b : An alternative machine for point load strength determination , manufactured by Robertson Research Mineral Technology Limited , Llandudno, Denbighshire, Wales .

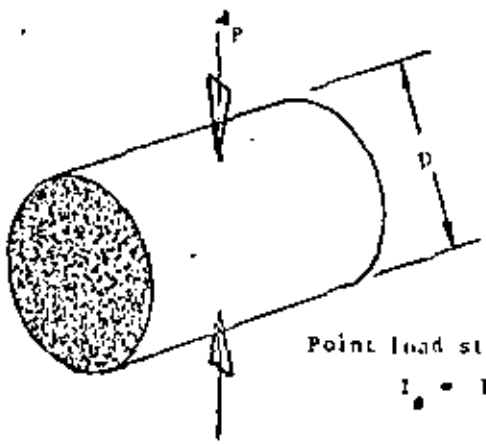

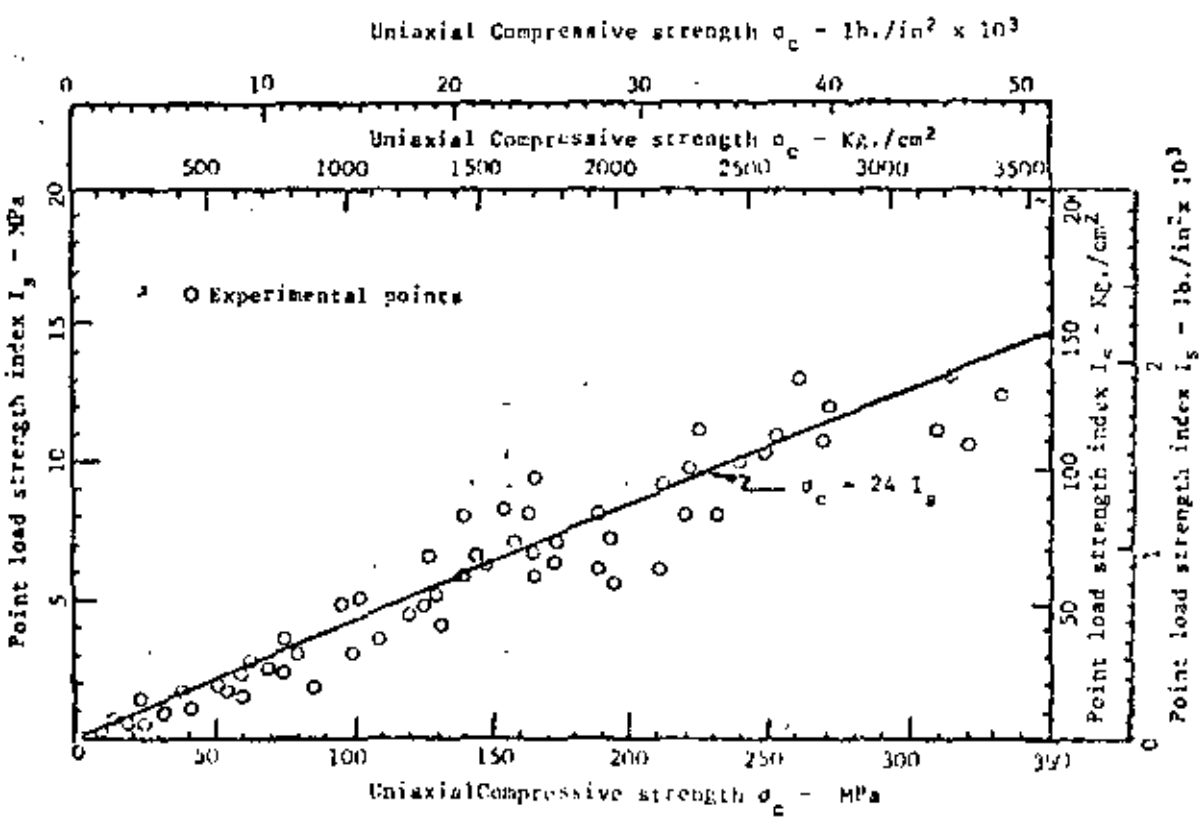

Figure 29 : Relationship between point load strength index and uniaxial compressive strength.

the slope are reproduced as closely as possible are therefore extensively used by engineers concerned with slope design. Laboratory shear testing machines have been extensively discussed in the literature[76,78,79,80,87,88] while other authors have advocated in-situ shear testing as the correct approach to this problem[89,90,91].

The uninitiated reader, embarking upon a study of this literature in the naive hope of finding shear strength values which he can use for a particular design, is likely to be driven to near despair by the lack of consistency in the reporting of results and in the variety of interpretations placed upon these results. As a result of this unsatisfactory situation, many rock engineers resort to guessing the strength values to be used for a slope design, arguing that these guesses are probably as accurate as some of the test results which could be obtained. The author does not accept this view since, even if they are difficult to find, there are rational laws which govern the shear behaviour of rock discontinuities and rock masses. If, having studied and understood these laws, the engineer is still convinced that a guess is adequate then at least this will be a logical and informed guess and not the irresponsible opinion of someone who has simply given up trying to understand the complexities of shear testing.

Consequently, before discussing actual shear testing techniques, the author will discuss some of the factors which influence the shear strength of rock. Only those questions of direct relevance in practical rock slope engineering are included in this simplified presentation and the reader who wishes to study this subject in greater detail is referred to the papers listed at the end of this chapter.

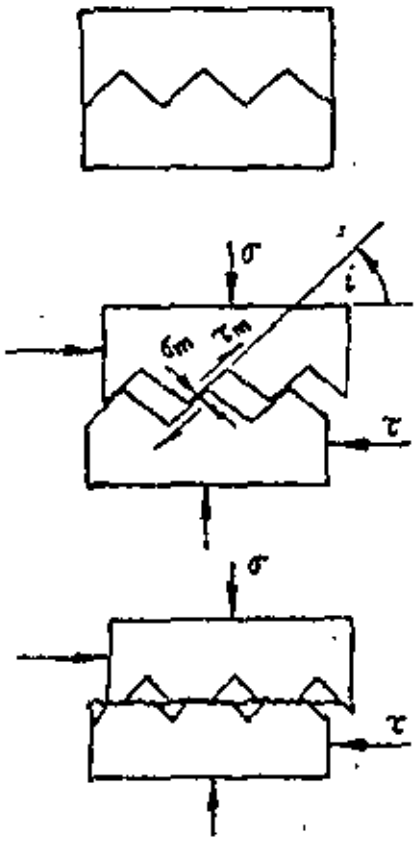

Influence of surface roughness on shear strength

Consider a rock sample containing a set of "teeth" as illustrated in the sketch opposite. If this specimen is subjected to shear and normal loads as in conventional shear testing (see Figure 9 on page 22 for details), shear movement can only take place if the projections ride over one another or if they are sheared through. In the case of the projections riding over one another, initial movement is no longer parallel to the shear stress τ but it takes place along a line inclined at an angle i to the direction of τ where i is the angle of incidence of the projections. Consequently, the shear and normal stresses acting along and perpendicular to the direction of movement must be considered.

Resolving along the line of initial movement, the shear stress τ_m is given by

$$\tau_m = \tau \cos i - \sigma \sin i \qquad (15)$$

Similarly, the normal stress σ_m is obtained by resolving at right angles to the line of initial movement

$$\sigma_m = \sigma \cos i + \tau \sin i \qquad (16)$$

If the relationship between the shear stress τ_m required to cause movement is related to the normal stress σ_m by

$$\tau_m = \sigma_m \tan \phi \qquad (17)$$

where ϕ is the basic friction angle of the material and it is assumed that the surfaces have no cohesive strength, then equations (15) and (16) can be substituted into equation (17) giving

$$\tau = \sigma \tan(\phi + i) \qquad (18)$$

This relationship was confirmed on models with regular surface projections by Patton[41] who must be credited with having emphasised the importance in rock slope stability analysis of the simple relationship presented in equation (18).

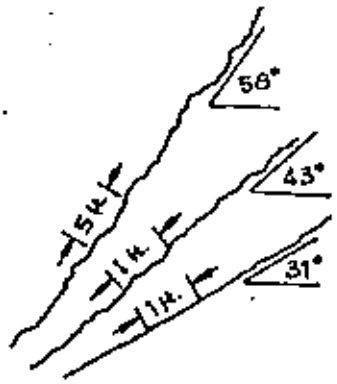

Figure 30 :
Bedding plane traces in unstable limestone slopes studied by Patton [41].

Patton convincingly demonstrated the practical significance of this relationship by measurements of the average value of the angle i from photographs of bedding plane traces in unstable limestone slopes. Three of these traces are reproduced opposite and it will be seen that the rougher the bedding plane trace, the steeper the angle of the slope. He found that equation (18) was reasonably satisfied if values for the average measured angle i and values of the friction angle ϕ from laboratory tests on smooth limestone surfaces were substituted into it.

The riding of surface irregularities over one another can only take place if the overall volume of the specimen increases or if *dilation* occurs. This dilation is inhibited as the normal stress across the discontinuity increases and, at very high normal stresses, movement along the discontinuity can only take place if the interlocking surface irregularities are sheared through. This shearing involves fracturing of the intact rock which forms the walls of the discontinuity and hence the surface will exhibit apparent cohesion c. Its failure behaviour can be defined by the equation

$$\tau = c + \sigma \tan \phi \qquad (19)$$

An idealised diagram showing both dilatant and shearing behaviour is given in Figure 32. The relationship between shear and normal strength for a specimen containing a discontinuity with smooth walls is included in this figure for comparison.

So far the discussion has been limited to an idealised model with regular projections of uniform shape. An actual rock surface is not regular but, as suggested in Figure 31, has a surface profile which may be divided into first and second order irregularities. For slopes of practical engineering interest the first order irregularities are considered to be of major importance although the second order irregularities also play a part in the failure process.

Shear strength of tension joints in hard unweathered rock

Barton[42] has examined this question in considerable detail and suggests that the relationship presented in equation (18) is too simple because it assumes that the average angle i remains constant throughout the range of normal stresses under which dilation can take place. He suggests that the effective value of i depends upon the magnitude of the normal stress σ. At very low normal stresses, smaller and steeper sided projections control movement. As the normal stress increases, these smaller projections are broken off and the gentler undulations of the first order irregularities control the behaviour. In a series of experiments on model material which had been fractured in

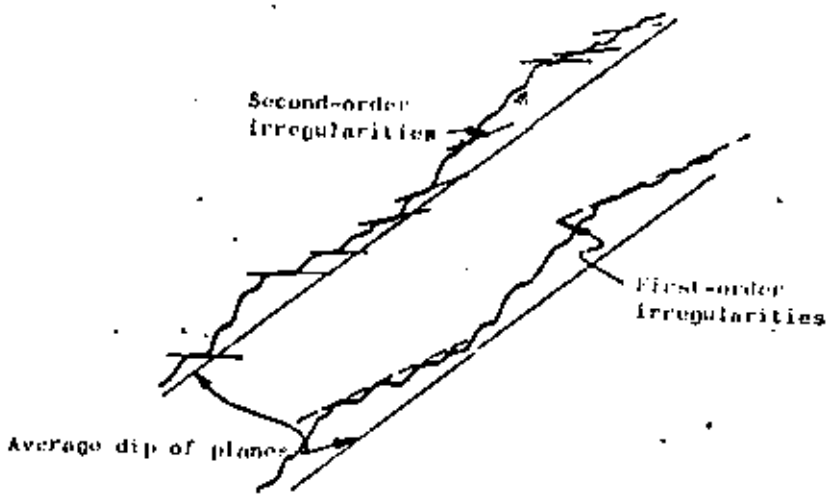

Figure 31 : Rough rock surface with first- and second-order irregularities.
(After Patton and Deere 93)

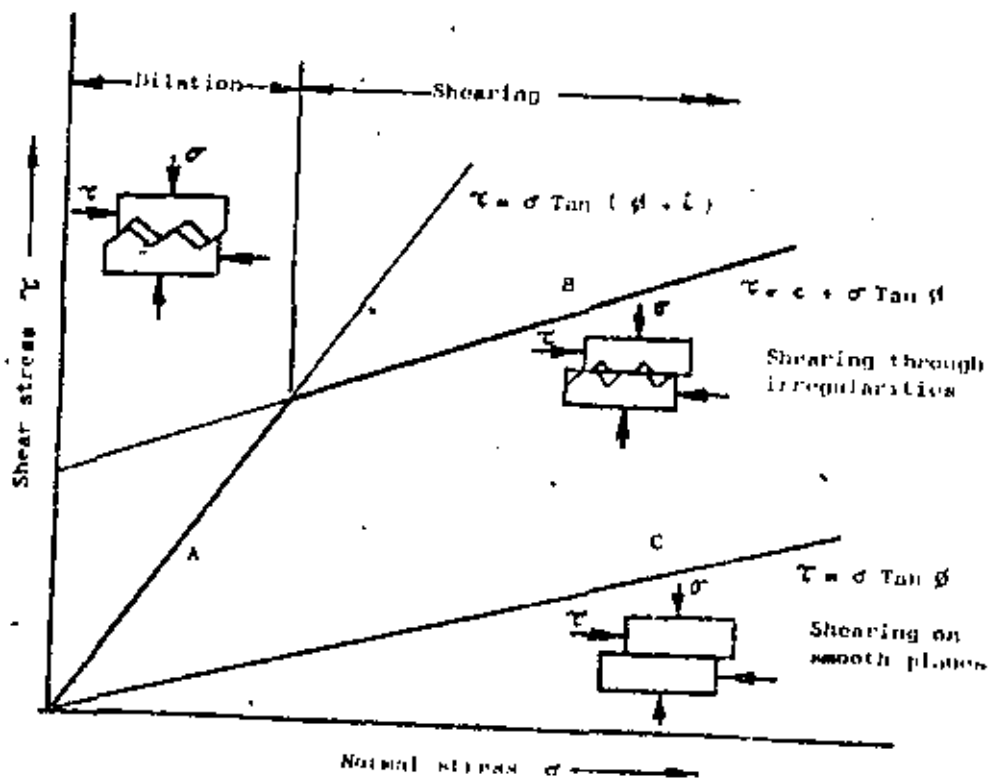

Figure 32 : Simplified relationships between shear strength and normal stress for rough surfaces .

these results and Barton's experimental relationship between roughness and normal stress. This similarity suggests that, as the normal stress increases, the wavelength of the surface roughness profiles which contribute to the shear strength of the surface also increases. In other words, small second order projections are broken off and the first order roughness profile (see Figure 31) become important.

Patton and Deere[93] also conclude, on the basis of field observations, that first order roughness profiles are important in controlling the behaviour of large slopes in which a history of tectonic loading and of weathering will have reduced the interlocking effect of the smaller second order irregularities.

Direct experimental evidence linking normal stress σ to the wavelength of roughness profiles S is very difficult to obtain except on a model scale as was attempted by Barton[92]. Consequently, any attempt to quantify this scale-effect must be treated with extreme caution. Never-the-less, such an attempt must be made and, on the basis of what little evidence there is, the author suggests that the approximate relationship plotted in Figure 33 may not be unreasonable.

Much of the literature dealing with this matter of surface roughness gives no indication of how surface roughness measurements such as those presented in Figure 22 should be used in practical slope design. Figure 33 is presented in an attempt to remedy this deficiency and it is suggested that it be used as follows:

1) Measure the effective roughness angle i for different measuring bases, as outlined in Figure 22, and plot the results on Figure 33.

2) The best straight line through these plotted points (passing through $\sigma/\sigma_c = 1$ and $i = 0$) will give an approximate relationship between σ/σ_c and i.

3) From an estimate of the uniaxial compressive strength of the rock, e.g. from a point load test, values of i corresponding to different normal stresses (σ) can be obtained.

4) Substitution of these values of i into equation (18) gives a relationship between shear strength τ and normal stress σ.

In figure 34, the average normal stress acting across an inclined discontinuity plane is plotted for various conditions. Taking a slope with a face angle $i = 60^\circ$ and a discontinuity angle $\beta = 30^\circ$, the value of $2\sigma/\gamma H = 0.5$. Substituting for the rock density γ a value of 160 lb/ft^3, the stress σ for a slope of 100 feet high is found to be 4000 lb/ft^2 (28 lb/in^2). For a rock with a uniaxial compressive strength $\sigma_c = 10{,}000$ lb/in^2, the value of σ/σ_c for this particular slope is 0.003 and, from Figure 33, the effective roughness angle for an "average" rough surface (line B) is approximately 25°. If the basic friction angle $\phi = 30^\circ$, then the value of $(\phi+i) = 55^\circ$.

For a slope height of $H = 1000$ feet, $\sigma/\sigma_c = 0.03$ and $i = 15^\circ$, therefore $(\phi+i) = 45^\circ$.

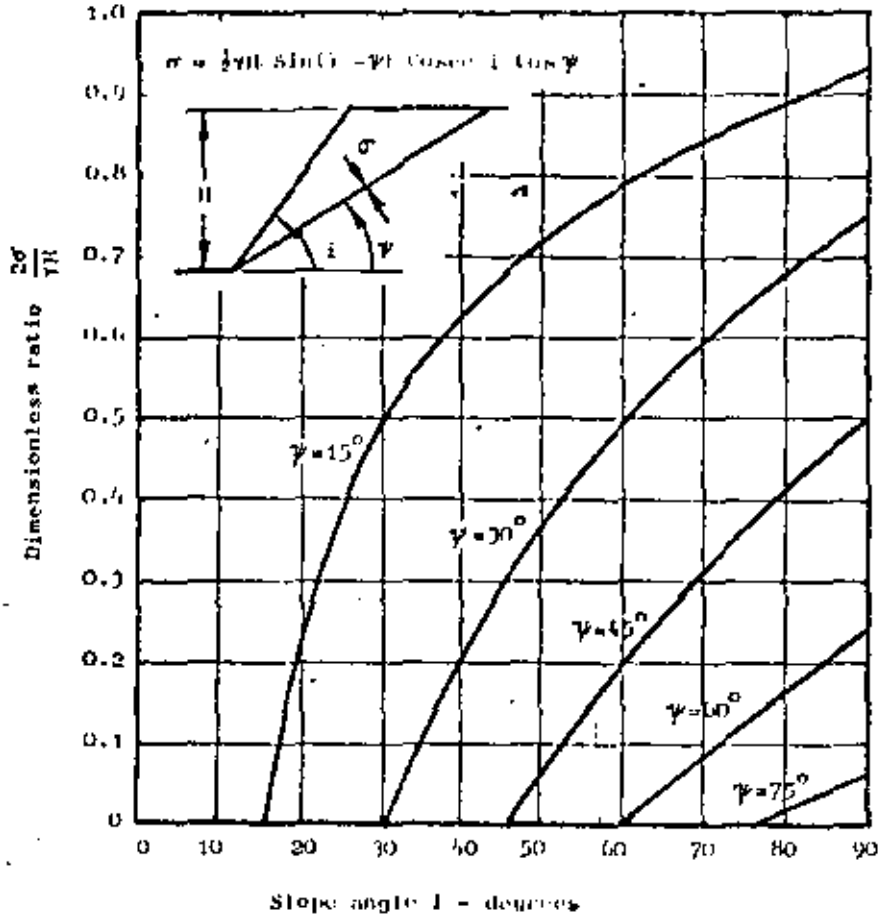

Figure 34 : Plot of normal stress acting across an inclined discontinuity plane in a slope .

Figure 35 : Imperial College 100 ton shear machine for testing specimens measuring up to 15 in. x 12 in. (38 cm. x 30 cm.)

Comparing these values with the bedding plane traces in limestone reproduced on page 83, it will be seen that the results are not unreasonable.

Methods for incorporating the non-linear relationship between shear strength τ and normal stress σ (Figure 32) into stability analyses will be discussed later.

Size of specimen in shear testing

Equation (18) provides a means for calculating the shear strength of a rough discontinuity from information on the basic friction angle ϕ of the rock and the effective roughness value i. From the discussion given above it will be clear that this calculation can never be very precise and hence, one is tempted to consider means for measuring the shear strength τ directly by carrying out a shear test which is large enough to include surface roughness effects. This reasoning has lead to the development of large (and very expensive) shear testing machines such as the illustrated in Figure 35 and to large scale *in-situ* shear tests. Estimates in 1970 suggested that an *in-situ* shear test on a specimen of 1m x 1 m would cost approximately £2000, while a test on a 5 m x 5 m specimen would cost in the region of £10,000. One must therefore examine the potential return on this magnitude of investment.

In order to give representative results, a specimen should contain several roughness waves - say at least 3. This means that, for a typical rock surface with first order irregularities of 10 to 100 cm wavelength, one should be thinking in terms of specimens of up to 3 m x 3 m. The practical difficulties involved in preparing these specimens, the very high loads required in order to generate even moderate normal and shear stresses and the difficulty of ensuring that these stresses are correctly applied accounts for the very high cost of these tests.

There is one major advantage to *in situ* shear testing which should not be overlooked and this is that the engineers and geologists responsible for carrying out the test are forced into long and intimate contact with the rock. There is no better classroom in which to learn practical rock engineering than the field and a few weeks spent carrying out *in situ* shear tests is worth a year spent in the laboratory. It should also be added that, if you can afford to have large scale *in situ* shear tests correctly done, the results can be very useful.

On balance, the author's opinion is that the best solution to this problem is to carry out a reasonable number of shear tests on small samples in order to determine the basic friction angle ϕ, to measure the surface roughness angle i and to calculate the shear strength τ from equation (18).

A source of high quality data which is frequently ignored is that provided by actual rock slope failure in the field. Patton's observations (page 83) demonstrated the usefulness of examining such failures and rock engineers would do well to devote more time and energy to the study of these free large scale shear tests. Even the small scale plane or wedge failures which can generally be found in open-pit mine benches can provide a useful source of strength

information if interpreted in accordance with the basic principles outlined in this book.

Before leaving the question of the influence of scale on shear strength, a further question which must be considered is whether the basic friction angle ϕ is size dependent.

Londe[74] describes a series of tests in which joints in limestone were tested in the laboratory and *in-situ*. The laboratory samples measured 8 cm x 30 cm while the *in-situ* test involved a joint surface measuring 2m x 2m. The specimen for the *in-situ* test was carefully excavated inside an underground chamber and the normal and shear loads were applied by means of a number of flat jacks packed between the specimen and the roof and wall of the chamber. In both laboratory and *in-situ* tests, the joint surfaces, which had some initial clay coating, were subjected to large shear displacements in order to reduce the shear strength to its lowest or residual value.

The results obtained from these tests are plotted in Figure 36 and it will be seen that the basic friction angle ϕ is essentially the same for the small scale laboratory test and the large *in-situ* test. As a result of these and other tests, it can be concluded that, for practical engineering purposes, the basic friction angle ϕ of a plane surface is independent of the size of the surface.

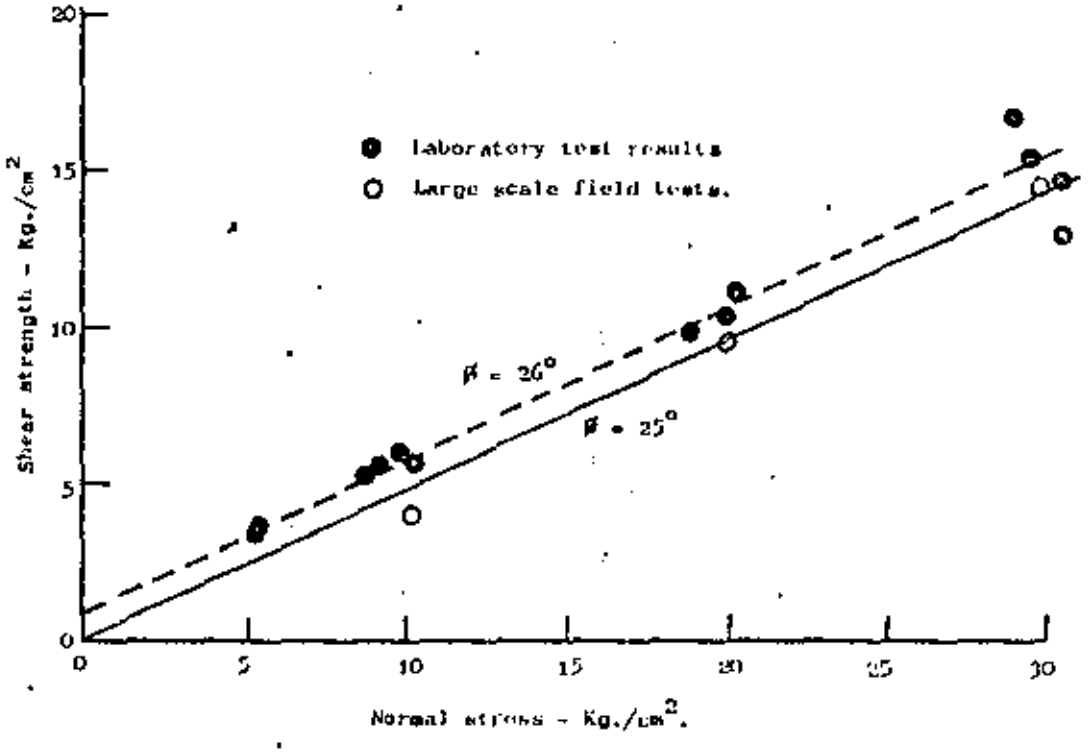

Figure 36 : Comparison between basic friction angle β measured in small scale laboratory tests and in a large scale field test on joints in limestone. After Londe [74].

c = 24

Cohesion and apparent cohesion

The cohesive strength c of an intact rock specimen is approximately equal to twice the uniaxial tensile strength σ_t of that material[94]. This tensile strength is due largely to the cement which binds the mineral grains together and, before relative movement such as shearing between these grains can take place, the cement bonds must be broken. Taking typical tensile strength values for hard rock, the cohesive strength would lie in the range of 2000 to 10,000 lb/in^2 (140 to 700 Kg/cm^2).

The shear stress τ which occurs in a slope is very low* and slope heights of the order of 10,000 feet (3000 m) have to be considered before the cohesive strength of intact rock is likely to be exceeded. Consequently, apart from local failure at points of high stress concentration, failure of intact rock can generally be ignored when considering the stability of slopes of interest to mining and civil engineers.

When pre-existing fractures occur due to tectonic forces or to blasting damage, the cohesive strength of these fractures or discontinuities is reduced to the level at which failure under average slope conditions becomes possible. In the extreme case, for example in the large scale field test results given in Figure 36, the cohesive strength falls to zero and the shear strength of the discontinuity is entirely dependent upon its frictional characteristics. Under these conditions, as shown by equation (5) on page 24, sliding will occur as soon as the dip ψ of the plane exceeds the friction angle ϕ.

Experience in rock slope engineering suggests that most rock masses exhibit some real or apparent cohesion and a question which must be examined is - can this cohesive strength be relied upon for slope design purposes? As will become apparent in the detailed discussions on stability analysis in later chapters, the factor of safety of a slope is extremely sensitive to changes in cohesion and, if cohesion is to be taken into account in a slope design, it is essential that the factors which can influence cohesive strength should be fully understood.

a. *Cohesive strength of gouge-filled discontinuities*

In a discontinuity such as a fault where gouge has been created by shear movement resulting from geological forces, the cohesive strength of the discontinuity is equal to the cohesive strength of this gouge material. In some cases, this cohesion may be appreciable and it can have a significant influence upon the factor of safety of the slope. However, it should only be included in a slope design if its value has been reliably established, either by carefully controlled shear tests or by analysis of existing failures on the same planes as those which exist in the proposed

*The shear stress τ acting along a plane dipping at an angle ψ in a slope can be obtained from Figure 34 by utilising the relationship $\tau = \sigma \tan \phi$. Hence, a plane inclined at $\psi = 45^\circ$ in a slope with $i = 70^\circ$ gives $2\sigma/\gamma H = 0.3$ or $\tau = 0.15\ \gamma H \tan \psi$. For $\gamma = 160$ lb/ft^3 and $H = 1000$ feet, $\tau = 24{,}000$ lb/ft^2 (167 lb/in^2 or 12 Kg/cm^2)

slope.

Terzaghi[31] has emphasised the fact that the cohesive strength of materials such as fault gouge and clay tends to decrease with time. In the sketch opposite, the percentage reduction in the cohesive strength of stiff, fissured London clay with time has been plotted from results obtained by Skempton[95] from the analysis of slope failure records. This curve shows that even if the cohesive strength of a gouge-filled discontinuity has been determined, great care should be exercised in designing a slope which includes such a discontinuity. The author's personal preference in designing slopes in which continuous features such as faults are known to exist is to design on the basis of friction only ($c = 0$) for these places.

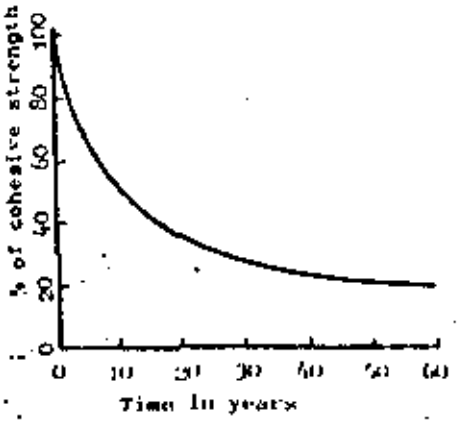

Percentage reduction of cohesive strength of stiff, fissured clay with time. Adapted from Skempton[95].

b. Cohesive strength of cemented discontinuities

Discontinuities such as faults which are continuous over tens or hundreds of feet are not present in every rock mass and it is therefore necessary to consider the cohesive strength of discontinuities such as joints which terminate within the rock mass in which a slope is to be excavated.

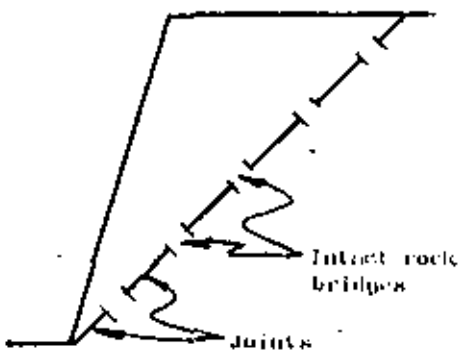

Model proposed by Jennings[37] for slope failure along a mean plane.

This matter has been considered in great detail by Jennings[37] who suggests that in a slope containing joints and similar features of limited extent, failure occurs as a result of sliding on the joints and fracturing of the intact rock bridges between the ends of these joints. While not rejecting the theoretical concepts proposed by Jennings, the author has grave doubts on the practical application of this model in slope design. This doubt arises because of the uncertainty associated with the field measurement of joint continuity (see page 38). Because the cohesive strength of the intact rock is several orders of magnitude greater than that of the discontinuities, small errors in the estimates of the area of rock bridges can lead to gross errors in the calculated cohesive strength of the entire system. The fracture process involved in the failure of these rock bridges is extremely complex and the model proposed by Jennings may be too simple[96].

If joint continuity has been measured and it is decided to include the cohesive strength of the rock bridges in the stability calculation, the author would urge extreme caution in choosing the values to be used. Even small over-estimates of this cohesive strength can lead to grossly optimistic factors of safety.

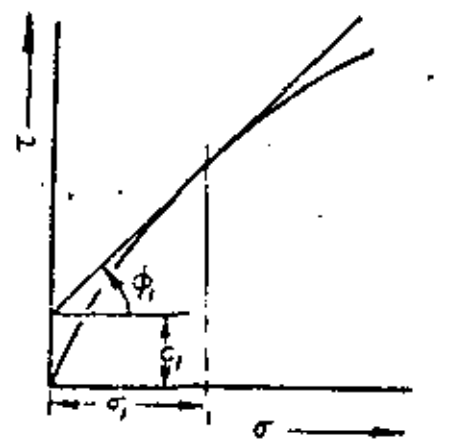

Apparent cohesion defined by the tangent to a non-linear failure curve.

c. Apparent cohesion due to surface roughness

In the discussions presented on pages 82 to 85, it was shown that the relationship between shear strength and normal stress for a rough rock surface is generally non-linear. Barton[79] has shown that it is possible to include non-linear failure criteria into slope stability calculations but the author prefers a simpler approach which involves the use of *apparent cohesion*. As shown in the sketch opposite, a tangent to a non-linear failure curve at a specific normal stress σ_i defines a cohesion intercept c_i and a friction angle ϕ_i.

These values can be used in factor of safety calculations (equation (14) on page 27) provided that it is realised that the factor of safety obtained is only valid for the specified normal stress σ_1. Figure 34 can be used for determination of the normal stress acting across a discontinuity for a particular slope geometry and slope height.

This analysis can be extended to a range of slope heights by taking successive tangents as illustrated in Figure 37a and calculating corresponding factors of safety. As shown in Figure 37b, the design curve in this particular example is the envelope of the curves determined for different normal stress levels. Further examples of this type of analysis are included in later chapters of this book.

d. Influence of water on cohesive strength

On page 26 it was stated that *water pressure*, which reduces the normal stress σ acting across the discontinuity, is extremely important in slope stability calculations but, in addition, certain materials suffer changes as a result of changes in *moisture content*.

Figure 38 gives the relationship between shear strength and normal stress for a quartzitic shale tested by Colback and Wild[97] under wet and dry conditions. It will be noted that a significant reduction in the cohesive strength occurs under these conditions and, although this may represent an extreme example, it does suggest that the influence of water on strength cannot be ignored.

The author recommends that, if cohesive strength is to be included in stability calculations for a slope design, its value should be determined from tests in which the rock surfaces are kept wet. Care must be exercised in such tests to ensure that the loading rate is kept low enough so that pore water pressures on the failure surface have time to dissipate, otherwise misleading results will be obtained.

Influence of gouge thickness on the shear strength of a discontinuity

Figure 39 illustrates the influence of the gouge thickness on the shear strength of a rough rock surface. When no infilling is present, the surfaces behave in the manner described on pages 82 to 85. When the thickness of the gouge infilling exceeds the height of projections on the rock surface - say 10 cm - the shear strength of the discontinuity is controlled by the shear strength of the gouge material.

The intermediate situation in which a relatively thin layer of gouge infilling - say 5 cm - is present is the most complex.

The failure curve given for this case in Figure 39 suggests that this discontinuity starts off behaving as though its strength was controlled by the infilling. As the normal

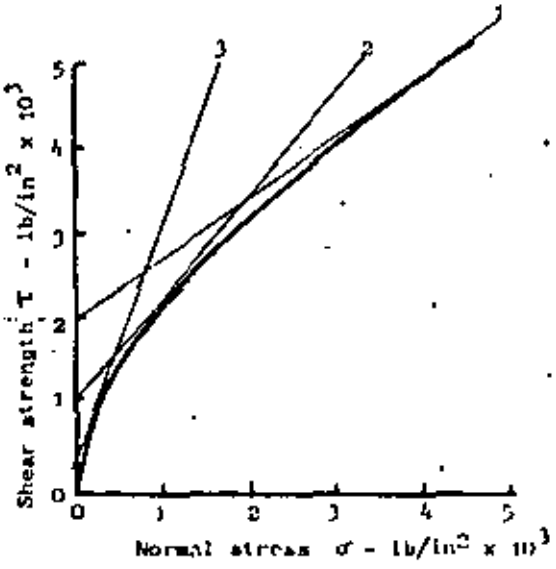

Figure 37a :

Non-linear relationship between shear strength and normal stress with tangents at various levels of normal stress.

Figure 37b :

Relationship between slope angle and slope height for a factor of safety of 1.5 in a slope with normal groundwater drawdown and on the assumption that failure occurs along a circular arc . The design curve is given by the envelope of the individual curves given by the values of cohesion and friction defined by the tangents in figure 37a.

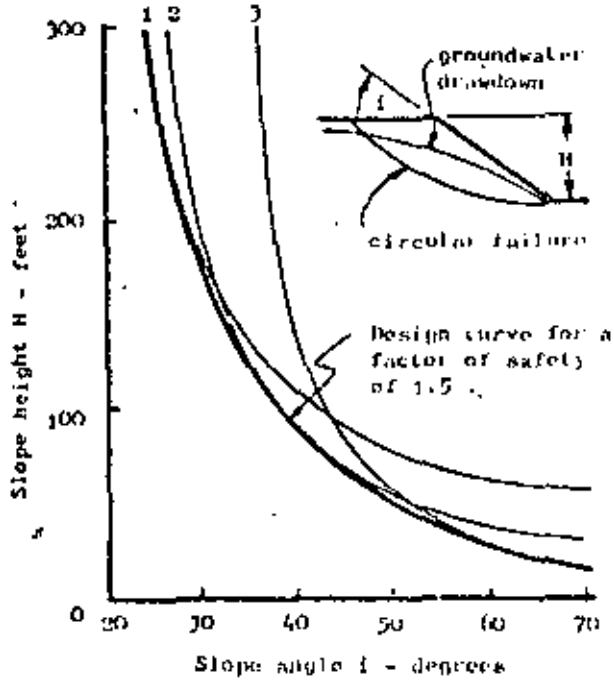

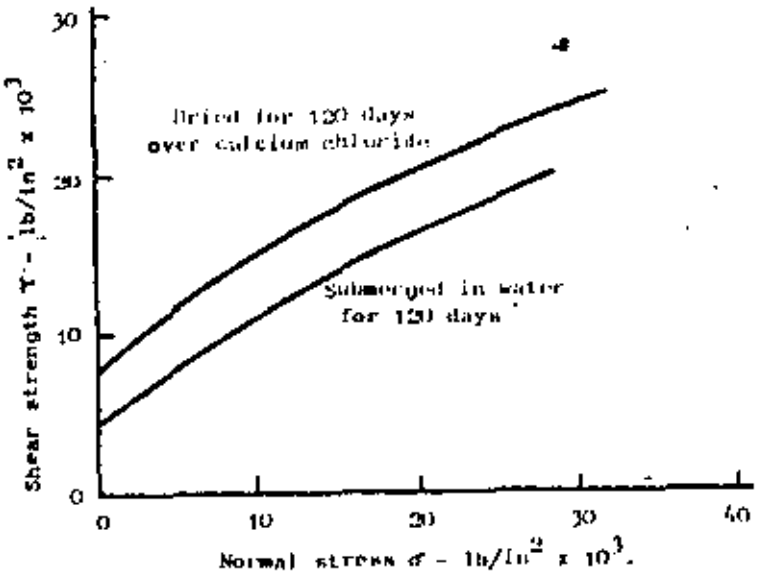

Figure 38 : Influence of water upon the shear strength of intact specimens of quartzitic shale tested by Colback and Wild [97]. A very low loading rate was used to minimise pore water pressure .

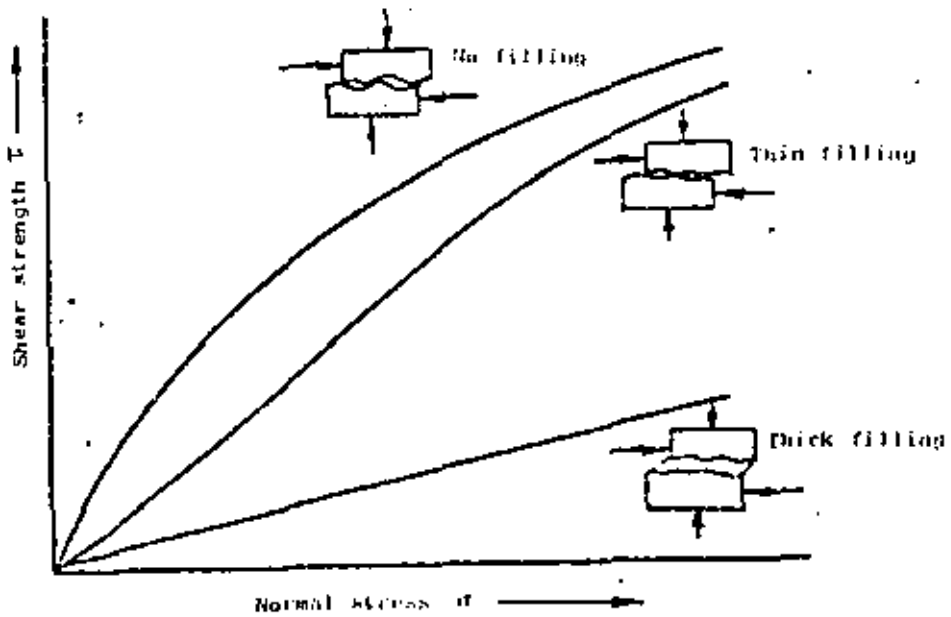

Figure 39 : Relationship between shear strength and normal stress for discontinuities with different thicknesses of gouge infilling .

stress level increases, the gouge layer is punctured by the projections on the rough surface and an increase in the slope of the failure curve takes place as these projections interlock. As the normal stress is increased further, these interlocking projections are sheared through and the discontinuity reverts to normal behaviour which is now largely controlled by the rock surface rather than by the infilling. Many variations of this picture can be visualised, depending upon the thickness of the gouge infilling and the roughness of the surface.

The properties of the gouge itself are also obviously important. Goodman[40] and Tulinov and Molokov[98] have investigated the influence of factors such as mineral composition, grain size and moisture content on the properties of filling material and they show that all these factors can have a significant influence.

From this discussion it will be seen that so many factors can influence the shear strength behaviour of a gouge filled discontinuity that it is very difficult to give general guidance on the cohesion and friction angle which should be used in dealing with these discontinuities. Some very approximate values are given in Table 1 on page 23 but it is preferable to carry out shear tests on the material itself.

Peak and residual strength

When a typical discontinuity such as a joint in a hard rock is subjected to shear and normal stresses, its response is generally similar to that illustrated in Figure 40. At a constant normal stress level, the shear stress required to cause displacement along the discontinuity increases very rapidly for the first ½ to 1 cm. of displacement. This initial stress increase occurs as a result of the projections on the rough surfaces of the joint locking together and deforming elastically. Note that these projections may only be second - or even third - order irregularities (see Figure 3) on page 84) and hence no marked deviation from linearity of the failure curve need occur.

At a certain level of shear stress, the shear strength of the surfaces is exceeded and further displacement will take place without any further increase in shear stress. This limiting value defines the *peak* shear strength at that particular normal stress. As the peak strength is exceeded, fracturing of interlocking projections on the surfaces occurs and the broken pieces are ground into detrital material as shear displacement continues. Eventually, after a displacement of about 5 cms in the example illustrated, the surfaces become slickensided and covered with gouge material and shear displacement takes place at a constant shear stress level. This shear stress is called the *residual* or ultimate shear strength of the discontinuity.

In Figure 41, the range of peak and residual strengths obtained from shear tests on clean joints in porphyry have been plotted. In considering these results, an obvious question which arises is - what values for

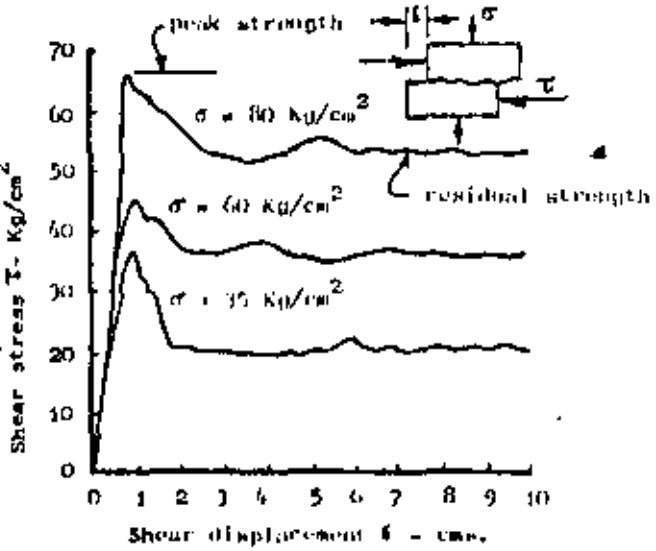

Figure 60:
Shear stress versus shear displacement results for tests on porphyry joints from Rio Tinto Espanola's Atalaya open pit mine.

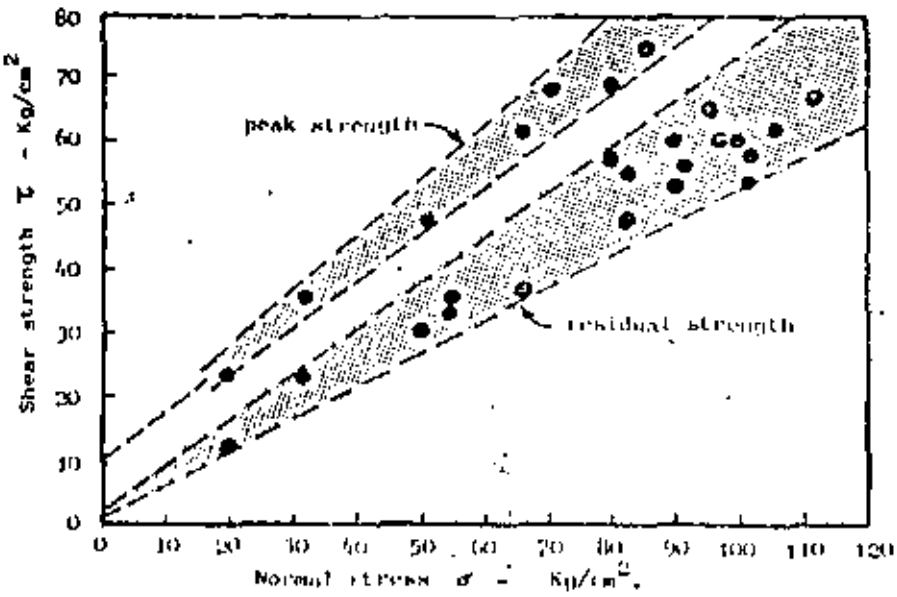

Figure 61 : Range of peak and residual strengths measured from stress-displacement results given in Figure 60 .

purposes?

Curves relating slope height H to the slope angle i at which failure could occur have been derived from these results[16] and are plotted in Figure 42. On the same Figure, nine slope failures in porphyry in mines near Rio Tinto Espanola's Atalaya open pit (there are no porphyry slope failures in Atalaya itself) have been plotted. From this figure it is clear that the peak shear strength values (curves A and B) give grossly optimistic slope angles, even if the lower bound curve of peak strength (Figure 41) is used in conjunction with assumed adverse groundwater conditions. Curves C and D, corresponding to the upper and lower bound curves for the residual strength, show a good correlation with the slope failure results.

In deriving the slope angle-slope height relationships presented in Figure 42, a linear relationship between shear strength and normal stress was assumed. A cohesive strength of approximately 10 Kg/cm^2 (142 lb/in^2) was assumed for the peak strength and the value assumed for the residual strength was approximately 2 Kg/cm^2 (28 lb/in^2). Since the friction angles for both peak and residual strength results are not significantly different, it can be concluded that the difference between the curves plotted in Figure 42 is due mainly to this difference in cohesive strengths.

The extreme sensitivity of slope stability calculations to the value of cohesive strength used is emphasised in this example. The clear warning which emerges from this discussion is - if a cohesive strength value for a slope design is to be determined from the intercept of a straight line drawn through shear test results, the residual strength and *not* the peak strength results should be used.

A more elaborate analysis of the nine failures plotted in Figure 42 has been published by Barton[100]. This analysis is based upon a non-linear shear strength versus normal stress relationship. Barton also found the analysis to be very sensitive to the shear strength at low normal stresses or, in terms of the analysis illustrated in Figure 27 the *apparent cohesion* given by a tangent at a low normal stress.

Summary of role of friction and cohesion in slope design

The engineer concerned with rock slope design is primarily interested in the question - how high and how steep can a particular slope be excavated? In the detailed discussions on shear strength determination in this chapter and in considering methods of slope design in later chapters, the general trends may not be too obvious. An attempt has therefore been made to summarise these trends diagrammatically in Figure 44.

This summary shows that:

a) A decrease in cohesion causes a reduction in the safe slope height of steep slopes. This trend suggests that the determination of cohesion or apparent cohesion is most important when considering the stability of open pit benches or steep overall slopes. Accurate determination of cohesion is not so critical when

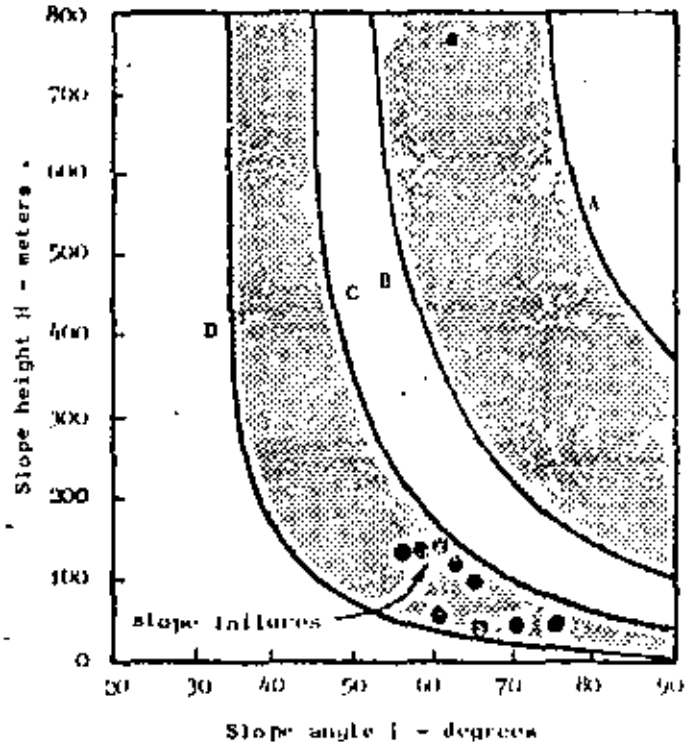

Figure 42 : Slope angle versus slope height relationships derived from test results presented in figure 41 and compared with 9 slope failures in the Rio Tinto area.
A - Maximum peak strength , dry slope.
B - Minimum peak strength , wet slope.
C - Maximum residual strength , dry slope.
D - Minimum residual strength , dry slope.

Figure 43 :
Rio Tinto Espanola's Atalaya open pit.

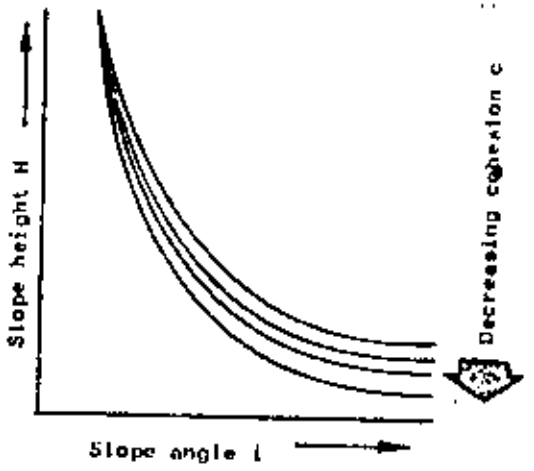

Figure 44a :
Decrease in cohesion c reduces safe height of steep slopes.

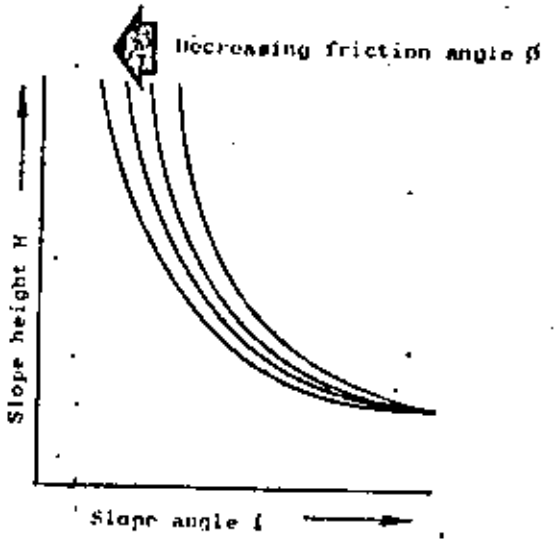

Figure 44b :
Decrease in friction angle β reduces safe angle for high slopes .

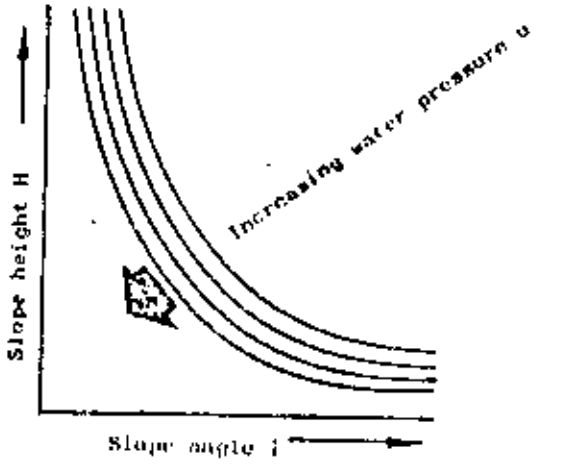

Figure 44c :
Increase in water pressure u reduces safe slope height and safe slope angle.

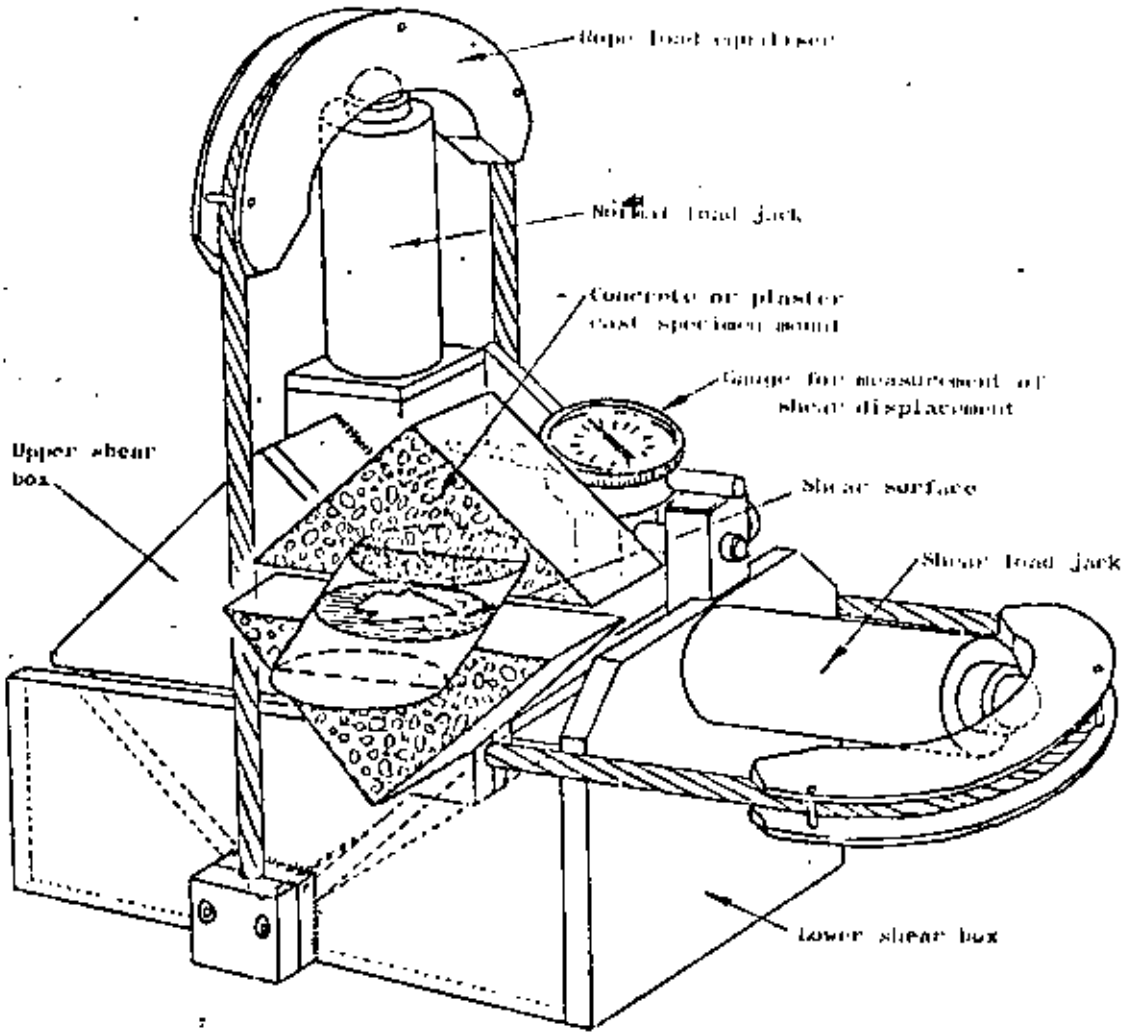

Figure 45 : Drawing of portable shear machine showing position of specimen and of shear surface . (Drawing adapted from one by Robertson Research Mineral Technology Limited . A typical machine is 20 in. (51 cm.) long , 10 in. (25 cm.) high and weighs 85 lb. (39 kg.)

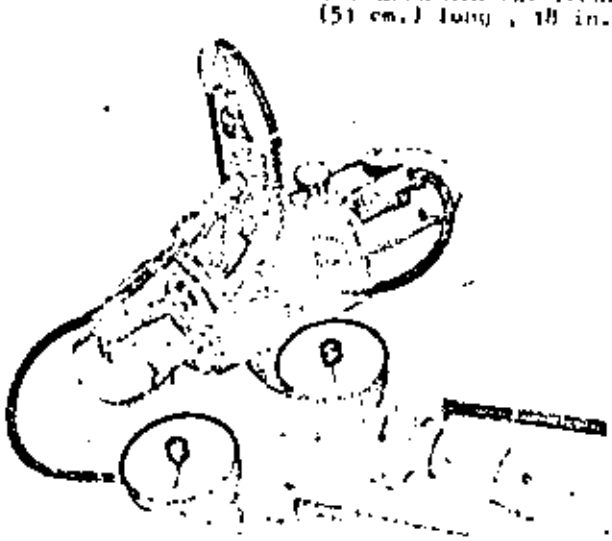

Figure 46 :
Portable shear testing machine manufactured by Robertson Research Mineral Technology Limited . The machine illustrated is fitted with a second shear load jack for reversing direction of shearing while maintaining the normal load constant - a feature which is useful for determining the residual shear strength of certain types of discontinuity.

provided that a wet mix is used for the concrete or plaster, the gravel can be left in place so that it becomes part of the casting.

b) Once the castings have set, the mould is stripped and the specimen transferred to the shear machine. The upper shear box is set in position and a small clamping load is applied to prevent movement of the specimen. The wires binding the specimen halves together are then cut and the shear load cable placed in position.

c) The specimen is now ready for testing and the normal load is increased to the value decided upon. This normal load is maintained constant while the shear load is increased. A note is kept of displacement during application of the shear load.

d) Once the peak shear strength has been exceeded, usually after approximately 1 cm. (0.4 in.) of movement, the displacement is continued. It will be found that a lower shear load is required to sustain movement.

e) The machine illustrated is limited to a displacement of approximately 1 in. (2.5 cm) and, in order to determine the residual shear strength, a displacement in excess of 2 in (5 cm) is usually necessary. In the machine with the single shear jack, this can only be achieved if the normal load is released and the upper half of the specimen moved back to its starting position. The machine illustrated in Figure 46 has two shear load jacks and the direction of shearing can be reversed without the need to release the normal load.

Which of these systems is more representative of the actual shearing process in a rock mass is uncertain since, in the one case, detrital material is disturbed while, in the other, the direction of rolling of particles is reversed. It is possible that different rock surfaces may behave differently under these conditions. It is suggested that both testing systems be tried out on a few specimens and that the one which gives the lowest value of residual shear strength be used for the remainder of the tests. If a reversible shear machine (Figure 46) is not available, a few specimens can be submitted for testing to a laboratory which has one and the results compared with those obtained from tests in which the normal load is released between successive runs.

f) In this, as in most shear testing machines, the *loads* applied to the specimen are measured and these have to be divided by the surface area of the discontinuity in order to obtain *stresses*. The initial area should be determined by direct measurement and the reduction in area with displacement should be calculated. A good record of both shear and normal loads versus displacement is essential if the test results are to be correctly interpreted.

g) The shear strength of rock is not generally sensitive to the rate of loading and no difficulty should arise if the loads are applied at a rate which

Figure 47a :
Sample , wired together to prevent premature movement along the discontinuity , is aligned in a mould and the lower half is cast in concrete , plaster or other suitable material. When lower half is set , upper half of mould is fitted , entire mould plus sample turned upside-down and the second half of the casting is poured .

Figure 47b :
Specimen , still wired together , is fitted into the lower shear box and the upper shear box is then fitted in place . Note that the cable supports swing out of the way to allow access.

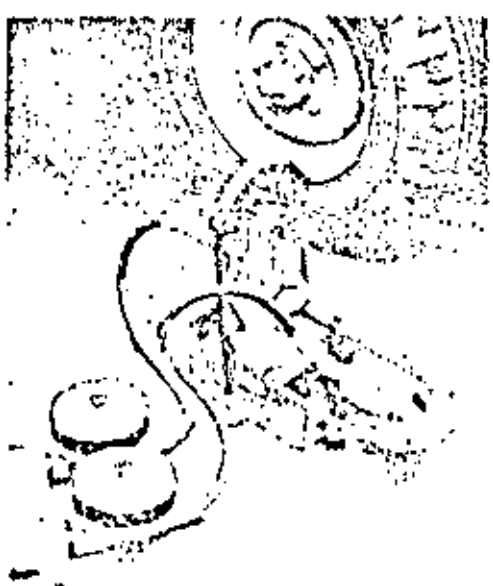

Figure 47c :
The wires binding the specimen halves together are cut and normal and shear loads are applied.

will permit measurement of these loads and the displacement to be made at regular intervals. A normal test would therefore occupy 15 to 30 minutes.

This discussion has been presented as a guide for the reader who wishes to carry out his own shear tests. With experience, he will soon find alternative methods which may be better suited to his own requirements. There are no "standard" methods of shear testing and the reader should feel free to experiment and to use his own ingenuity to achieve the results in which he has sufficient confidence to base a design. Remember that the object of the exercise is the design of rock slopes and that the shear strength of the discontinuities is only one of many factors which must be considered. An excessive amount of time and energy devoted to shear testing in an effort to achieve perfection will almost certainly mean that some of these other factors have been ignored.

Selected references on shear strength testing.

75. BISHOP, A.N. and HENKEL, D.J. *The measurement of soil properties in the triaxial test*. Arnold, London, 1962.

76. BRITISH STANDARDS INSTITUTION. Methods of testing soils for civil engineering purposes. *British Standard 1377*, 1967.

77. JAEGER, J.C. The behaviour of closely jointed rock. *Proc. 11th Symposium on Rock Mechanics*, Berkeley 1970, pp. 57-68.

78. KRSMANOVIĆ, D., Initial and residual shear strength of hard rocks. *Geotechnique*, Vol. 17, No.2, 1967, pp 145-160.

79. JAEGER, J.C. Friction of rocks and the stability of rock slopes. *Geotechnique*, Vol. 21, No. 2, 1971, pp. 97-134.

80. HOEK, E. Estimating the stability of excavated slopes in opencast mines. *Transactions Inst. Mining and Metallurgy*, Vol. 79, 1970, pp. A109-A132.

81. WALTON, C. Discussion on paper "Estimating the stability of excavated slopes in opencast mines" by E. Hoek. *Transactions Inst. Mining and Metallurgy*, Vol. 80, 1971, pp. A75-A76.

82. STIMPSON, B., METCALFE, R.G. and WALTON, C. A new technique for sealing and packing rock and soil samples. *Quarterly Journal of Engineering Geology*, Vol. 3, No.2 1970, pp. 127-133.

83. WALTON, C. Slope stability in coal measure rocks. *Ph.D. Thesis, Imperial College, London*, in preparation.

84. FRANKLIN, J.A., BROCH, E. and WALTON, C. Logging the mechanical character of rock. *Transactions Inst. Mining and Metallurgy*, Section A, Vol. 80, 1971, pp. A1-A9.

85. DEERE, D.U., HENDRON, A.J., PATTON, F.D. and CORDING, E.J. Design of surface and near surface construction in rock. *Proc. 8th Symposium on Rock Mechanics*, Univ. of Minnesota 1966, pp. 327-302.

86. D'ANDREA, D.V., FISCHER, R. L. and FOGELSON, D.E. Prediction of compressive strength from other rock properties. *U.S. Bureau of Mines Report of Investigations* 6702, 1965, 23p.

87. ROGERS, N. Influence of surface roughness on the friction properties of rock planes. *Proc. 2nd Congress of Intnl. Society of Rock Mechanics*, Belgrade 1970, paper 1-31.

88. MATHEWS, K.E. Excavation design in hard and fractured rock at Mount Isa Mine, Australia. *M.Sc. Thesis*, Univ. of Queensland, 1970.

89. ROCHA, M. Mechanics behaviour of rock foundations in concrete dams. *Transactions 8th Congress on Large Dams*,

Edinburgh 1964, pp. 785-831.

90. ROBERO, S.U. In situ direct shear tests on irregular surface joints filled with clayey material. *Proc. 2nd International Symposium on Rock Mechanics*, Madrid, 1968, Vol. 1, pp. 189-194.

91. WALLACE, G.B., SILBER, E.J. and ANDERSON, F.A. Foundation testing for Auburn dam. *Proc. 11th Symp. on Rock Mechanics*, Berkeley 1969, pp. 461-498.

92. BARTON, N. A relationship between joint roughness and joint shear strength. *Proc. Symposium on Rock Fracture*, Nancy, France 1971, paper I-8.

93. PATTON, F.D. and DEERE, D.U. Significant geological factors in rock slope stability. *Proc. Symposium on Planning Open Pit Mines*, Johannesburg 1970. Published by A.A. Balkema, Amsterdam, pp. 143-151.

94. HOEK, E. Brittle fracture of rock in *Rock Mechanics and Engineering Practice*. Edited by Stagg, K.G. and Zienciewicz, O.C., Wiley, London 1968, pp. 99-124.

95. SKEMPTON, A.W. The rate of softening of stiff, fissured clays. *Proc. 2nd International Conf. Soil Mech. Foundation Engineering*, Rotterdam 1948, Vol. II, pp. 50-53.

96. HOEK, E. and BIENIAWSKI, Z.T. Brittle fracture propagation in rock under compression. *International Journal of Fracture Mechanics*, Vol. 1, No.3, 1965, pp. 137-155.

97. COLBACK, P.S.B. and WILD, B.L. The influence of moisture content on the compressive strength of rock. *Proc. 3rd Canadian Symposium on Rock Mechanics*, Toronto, 1965.

98. TULINOV, R. and MOLOKOV, L. Role of joint filling material in shear strength of rocks. *Proc. Symposium on Rock Fracture*, Nancy, France 1971, paper II-24.

99. ZARUITSKII, N.I. Zones and planes of weakness in rocks and slope stability. Translation from Russian by *Consultants Bureau*, New York 1968, 108 p.

100. BARTON, N.R. Estimation of in-situ shear strength from back analysis of failed rock slopes. *Proc. Symposium on Rock Fracture*, Nancy, France 1971, paper 2-27.

101. BRAY, J.W. A study of jointed and fractured rock. *Rock. Mech. and Eng. Geology*, Vol. 5, 167, pp. 119-136 (part I), 197-216 (part II).

102. ROSENGREN, K.J. and JAEGER, J.C. The mechanical properties of an interlocking, low-porosity aggregate. *Geotechnique*, Vol. 18, No. 3, 1968, pp. 317-326.

103. BROWN, E.T. Strength of models of rock with intermittent joints. *Journal Soil Mech. Foundation div.*, ASCE, Vol. 96, No. SM6, 1970, pp. 1935 - 1949.

Introduction

The presence of groundwater in the rock mass surrounding an open pit has a deterimental effect upon the mining programme for the following reasons:

a) *Water pressure* reduces the stability of the slopes by reducing the shear strength of potential failure surfaces as described on pages 24 and 25. Water pressure in tension cracks or similar near vertical fissures reduces stability by increasing the forces tending to induce sliding (page 26).

b) High *moisture content* results in an increased unit weight of the rock and hence gives rise to increased transport costs. Changes in moisture content of some rocks, particularly shales, can cause accelerated weathering with a resulting decrease in stability (page 33).

c) *Freezing* of groundwater during winter can cause wedging in water-filled fissures due to temperature dependent volume changes in the ice. Freezing of surface water on slopes can block drainage paths resulting in a build-up of water pressure in the slope with a consequent decrease in stability.

d) *Erosion* of both surface soils and fissure infilling occurs as a result of the velocity of flow of groundwater. This erosion can give rise to a reduction in stability and also to silting up of drainage systems.

e) *Discharge* of groundwater into an open pit gives rise to increased operating costs because of the requirement to pump this water out and also because of the difficulties of operating heavy equipment on very wet ground.

f) *Liquefaction* of overburden soils or waste tips can occur when water pressure within the material rises to the point where the uplift forces exceed the weight of the soil. This can occur if drainage channels are blocked or if the soil structure undergoes a sudden volume change as can happen under earthquake conditions.

Liquefaction is critically important in the design of tailings dams and waste dumps and it is dealt with in the references numbered 104 to 108 listed at the end of this chapter. It will not be considered further in this book since it does not play a significant part in controlling the stability of rock slopes.

By far the most important effect of the presence of groundwater in a rock mass is the reduction in stability resulting from water pressures within the discontinuities in the rock. Methods for including these water pressures into stability calculations are dealt with in later chapters of this book. This chapter is concerned with methods for estimating or measuring these water pressures.

Groundwater flow in rock masses

There are two possible approaches to obtaining data on water pressure distributions within a rock mass:

a) Deduction of the overall groundwater flow pattern from consideration of the permeability of the rock mass and sources of groundwater.

b) Direct measurement of water levels in boreholes or wells or of water pressures by means of piezometers installed in boreholes.

As will be shown in this chapter, both methods abound with practical difficulties but, because of the very important influence of water pressure on slope stability, it is essential that the best possible estimates of these pressures should be available before a detailed stability analysis is attempted. Because of the large number of factors which control the groundwater flow pattern in a particular rock mass, it is only possible to highlight the general principles which may apply and to leave the reader to decide what combination of these principles is relevant to his specific problem.

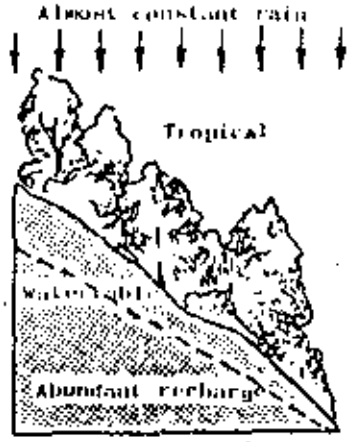

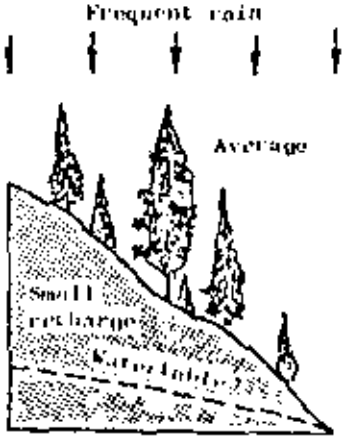

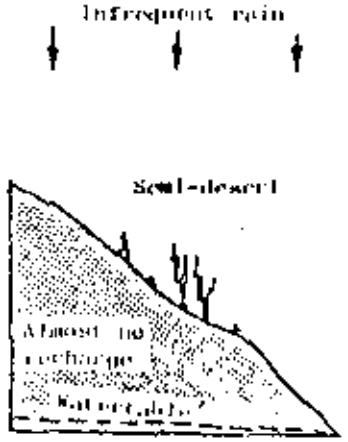

(After Davis and de Wiest [107])

The hydrologic cycle

A simplified hydrologic cycle is illustrated in Figure 48 to show some typical sources of groundwater in a rock mass. This figure is included to emphasise the fact that groundwater can and does travel considerable distances through a rock mass. Hence, just as it is important to consider the regional geology of an area when starting the design on an open pit mine, so it is important to consider the regional groundwater pattern when estimating probable groundwater distributions at a particular site.

Clearly, precipitation in the catchment area of the pit is an important source of groundwater, as suggested in the sketch opposite, but other sources cannot be ignored. Groundwater movement from adjacent river systems, reservoirs or lakes can be significant, particularly if the permeability of the rock mass is highly anisotropic as suggested in Figure 49. In extreme cases, the movement of groundwater may be concentrated in open fissures or channels in the rock mass and there may be no clearly identifiable water table. The photograph reproduced in Figure 50 shows a solution channel of about 1 inch in diameter in limestone. Obviously, the hydraulic conductivity of such a channel would be so high as compared with other parts of the rock mass that the conventional picture of a groundwater flow pattern would probably be incorrect in the case of a slope in which such features occur.

These examples emphasise the extreme importance of considering the geology of the site when estimating water table levels or when interpreting water pressure measurements.

Definition of permeability

Consider a cylindrical samples of soil or rock beneath the watertable in a slope as illustrated in Figure 51. The

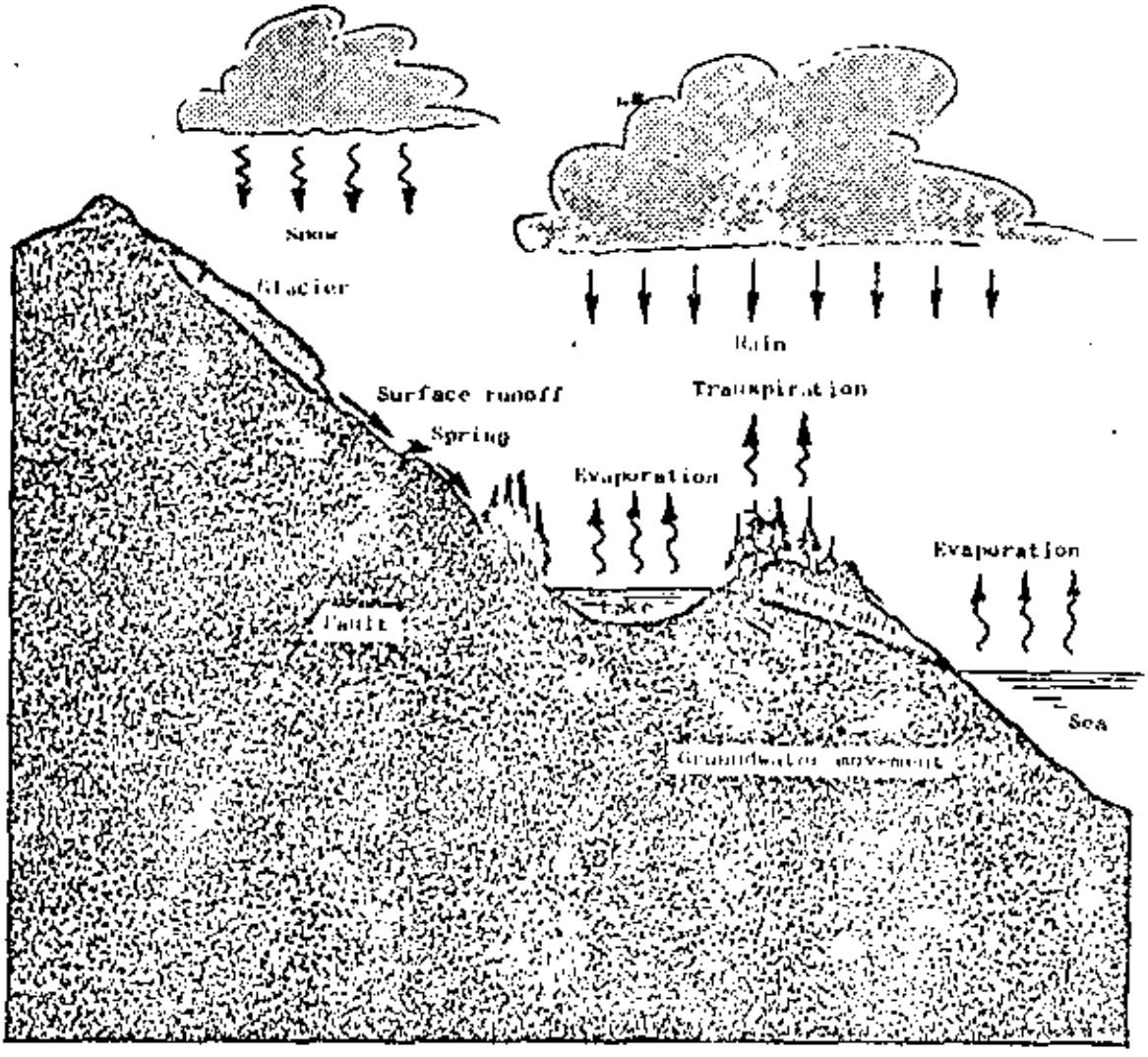

Figure 48 : Simplified representation of a hydrologic cycle showing some typical sources of groundwater .

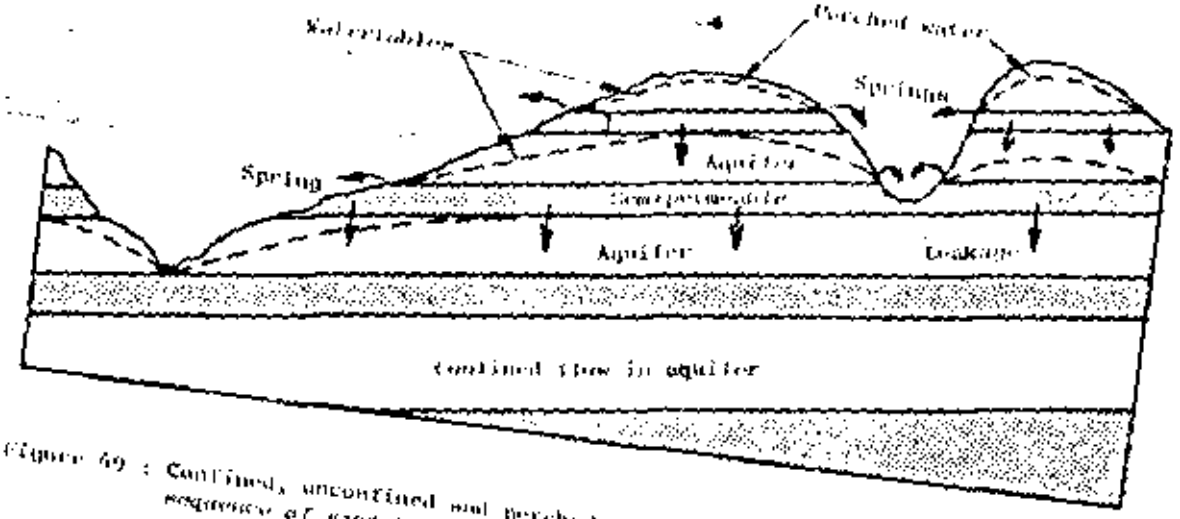

Figure 69 : Confined, unconfined and perched water in a simple stratigraphic sequence of sandstone and shale. After Davis and de Wiest [10].

Figure 70:
Solution channel in a limestone specimen. The hydraulic conductivity of such a channel would be very high as compared with the permeability of the intact rock or of rather discontinuities and it would have a major influence on the groundwater flow pattern in a rock mass.

sample has a cross-sectional area of A and a length l. Water levels in boreholes at either end of this sample are at heights h_1 and h_2 above a reference datum and the quantity of water flowing through the sample in a unit of time is Q. According to Darcy's law, the coefficient of permeability of this sample is defined as [110,111,112]:

$$k = \frac{Q.l}{A(h_1 - h_2)} = \frac{V.l}{(h_1 - h_2)} \qquad (21)$$

Where V is the discharge velocity. Substitution of dimensions for the terms in equation (21) shows that the permeability coefficient k has the same dimensions as the discharge velocity V, i.e. length per unit time. The dimension most commonly used in groundwater studies is centimetres per second and typical ranges of permeability coefficients for rock and soil are given in Table 11[113].

Figure 51 shows that the total *head* h can be expressed in terms of the pressure p at the end of the sample and the height Z above a reference datum. Hence

$$h = \frac{p}{\gamma_w} + Z \qquad (22)$$

where γ_w is the density of water. As shown in the figure, h is the height to which the water level rises in a borehole or standpipe.

Permeability conversion table.	
To convert cm/sec to :	Multiply by
metres/min	0.600
P/sec	10^{4}
ft/sec	0.0328
ft/min	1.968
ft/year	1.034×10^{6}
cm^2 *	1.031×10^{-5}
Darcy *	1.065×10^{3}

* for water at 20°C.

Permeability of jointed rock

Table 11 shows that the permeability of intact rock is very low and hence poor drainage and low discharge would normally be expected in such material. On the other hand, if the rock is discontinuous as a result of the presence of joints, fissures or other discontinuities, the permeability can be considerably higher because these discontinuities act as channels for the water flow.

The flow of water through fissures in rock has been studied in great detail by Bulit[114], Snow[115], Louis[116], Sharp[117], Maini[118] and others and the reader who wishes to pursue this complex subject is assured of many happy hours of reading. For the purposes of this discussion, the problem is simplified to that of the determination of the equivalent permeability of a planar array of parallel smooth cracks[116]. The permeability parallel to this array is given by:

$$k = \frac{gw^3}{12\nu.b} \qquad (23)$$

where g = gravitational acceleration (981 cm/sec^2)

w = opening of cracks or fissures

b = spacing between cracks and

ν is the coefficient of kinematic viscosity (0.0101 cm^2/sec for pure water at 20°C)

The equivalent permeability k of a parallel array of cracks with different openings is plotted in Figure 52 which shows that the permeability of a rock mass is very sensitive to the opening of discontinuities. Since this opening changes with stress, the permeability of a rock mass will therefore be sensitive to stress.

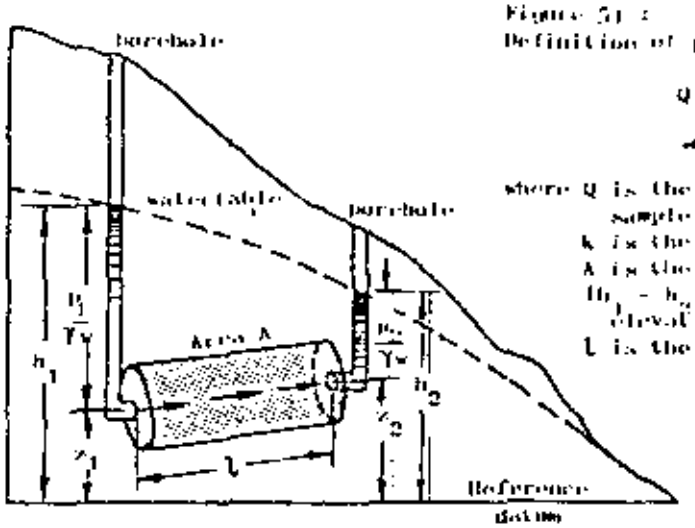

Figure 21 :
Definition of permeability in terms of Darcy's law.

$$Q = kA\frac{(h_1 - h_2)}{l}$$

where Q is the amount of water flowing through the sample in unit time,
k is the coefficient of permeability,
A is the cross-sectional area of the sample,
$(h_1 - h_2)$ is the difference in water table elevation between the ends of the sample and
l is the length of the sample .

TABLE II - PERMEABILITY COEFFICIENTS FOR TYPICAL ROCKS AND SOILS

	k - cm/sec	Intact rock	Fractured rock	Soil
practically impervious	10^{-10}	Slate		Homogeneous clay below zone of weathering
	10^{-9}	Dolomite		
	10^{-8}	Granite		
	10^{-7}			
low discharge poor drainage	10^{-6}	— Limestone —		Very fine sands, organic and inorganic silts, mixtures of sand and clay, glacial till , stratified clay deposits
	10^{-5}		Clay-filled joints	
	10^{-4}			
	10^{-3}	— Sandstone —		
High discharge free draining	10^{-2}		Jointed rock	Clean sand, clean sand and gravel mixtures
	10^{-1}			
	1.0		Open jointed rock	
	10^{1}			
	10^{2}		Heavily fractured rock	Clean gravel

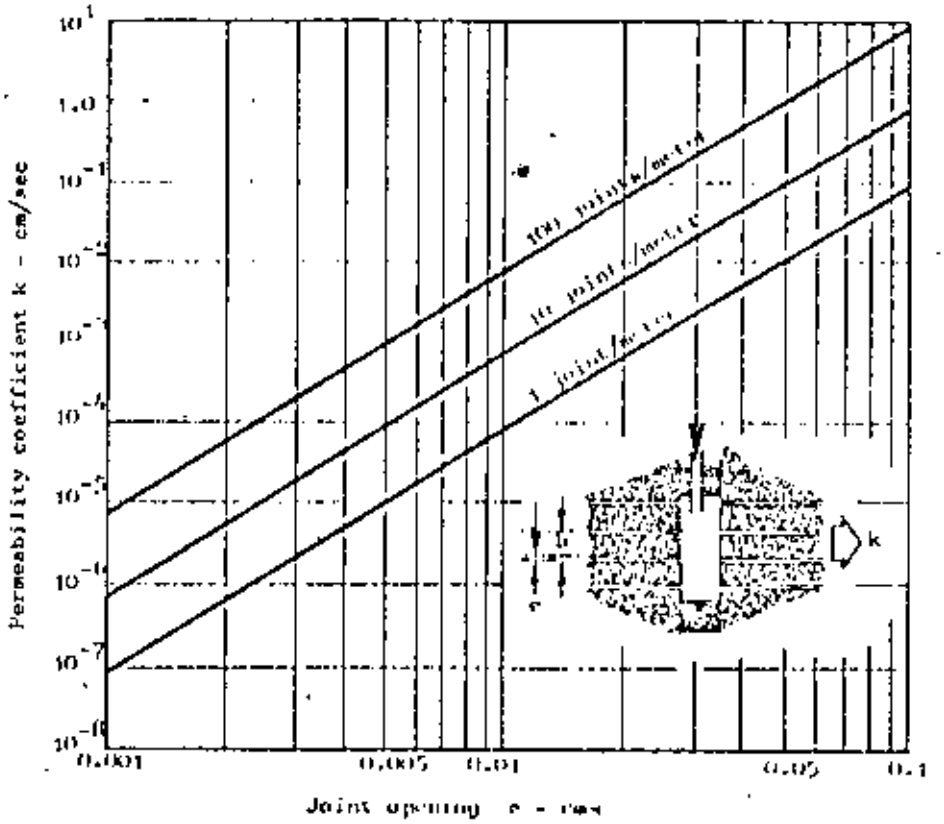

Figure 52 : Influence of joint opening e and joint spacing b on the permeability coefficient k in the direction of a set of smooth parallel joints in a rock mass.

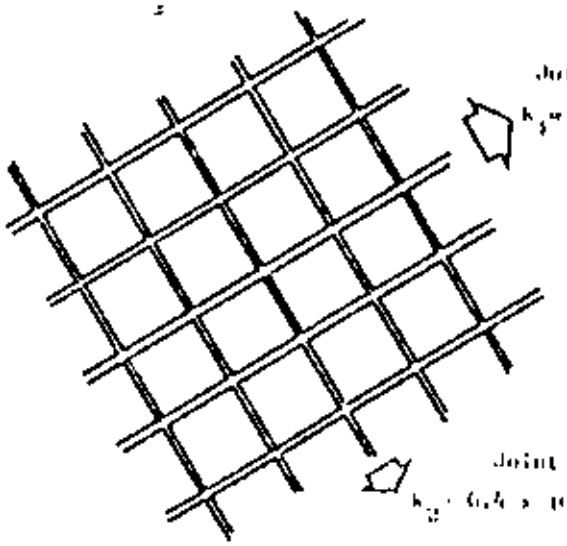

Figure 53 :
Idealized representation of two orthogonal joint systems in a rock mass . The spacing of both sets is 1 joint per meter. The joint opening e_1 of set 1 is 0.18cm and the to set 2 is $e_2 = 0.02$ cm. It is assumed that there is no cross-flow from one joint set to another.

Louis[11] points out that equation (23) only applies to laminar flow through planar parallel fissures and that it gives rise to significant errors if the flow velocity is high enough for turbulent flow to occur, if the fissure surfaces are rough or if the fissures are infilled. Louis lists no fewer than 8 equations to describe flow under various conditions. Equation (23) gives the highest equivalent permeability coefficient. The lowest equivalent permeability coefficient, for an infilled fissure system, is given by

$$k = \frac{n}{b} k_f + k_r \qquad (24)$$

where k_f is the permeability coefficient of the infilling material and

k_r is the permeability coefficient of the intact rock.

(Note that k_r has been ignored in equation (23) since it will be very small as compared with the permeability of open joints).

An example of the application of equation (23) to a rock mass with two orthogonal joint systems is given in Figure 53. This shows a major joint set in which the joint opening a_1 is 0.10 cm and the spacing between joints is b_1 = 1 meter. The equivalent permeability k_1 parallel to these joints is $k_1 = 8.1 \times 10^{-2}$ cm/sec. The minor joint set has a spacing b_2 = 1 joint per meter and an opening a_2 = 0.02 cm. The equivalent permeability of this set is $k_2 = 6.5 \times 10^{-4}$ cm/sec, i.e. more than two orders of magnitude smaller than the equivalent permeability of the major joint set.

Clearly the groundwater flow pattern and the drainage characteristics of a rock mass in which these two joint sets occur would be significantly influenced by the orientation of the joint sets.

Flow nets

The graphical representation of groundwater flow in a rock or soil mass is known as a flow net and a typical example is illustrated in Figure 54. Several features of this flow net are worthy of consideration.

Flow lines are paths followed by the water in flowing through the saturated rock or soil.

Equipotential lines are lines joining points at which the total head h is the same. As shown in Figure 54, the water level is the same in boreholes or standpipes which terminate at points A and B on the same equipotential line.

Water pressures at points A and B are not the same since, according to equation (22), the total head h is given by the sum of the pressure head p/w and the elevation z of the measuring point above the reference datum. The *water pressure* increases with depth along an equipotential line as shown in Figure 54.

A complete discussion on the construction or computation of flow nets exceeds the scope of this book and the interested reader is referred to the comprehensive texts by Cedergren[12]

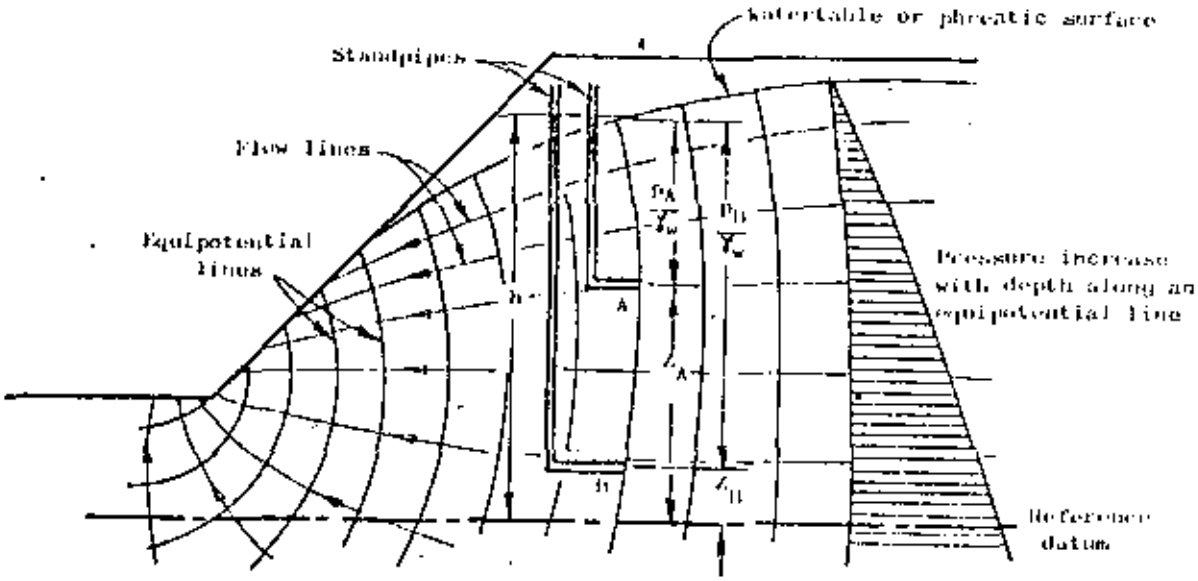

Figure 54: Two-dimensional flow net in a slope.

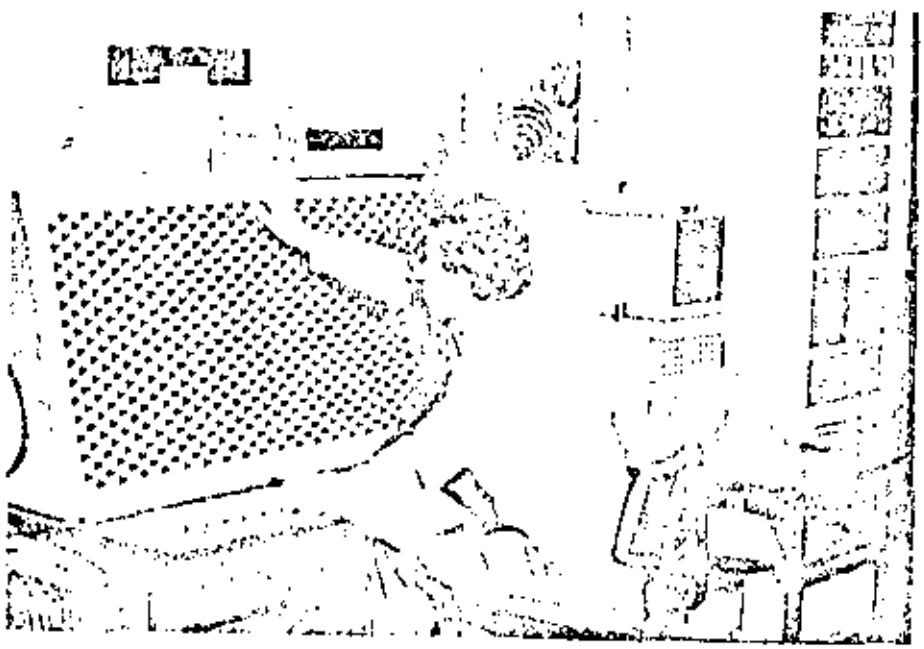

Figure 55 : Electrical analogue for the study of anisotropic groundwater flow and drainage problems [12].

and Baar[119] for further details. Traditional graphical methods for constructing flow nets[120] have now largely been superceded by analogue[121,122] and numerical methods[123].

An example of an electrical resistance analogue for the study of anisotropic seepage and drainage problems is illustrated in Figure 55. Some typical examples of equipotential distributions, determined with the aid of this analogue, are reproduced in Figure 56[124].

Field measurement of permeability

Determination of the permeability of a rock mass is necessary if estimates are required of groundwater discharge into an open pit or if an attempt is to be made to design a drainage system for the pit.

For evaluation of the stability of the pit slopes it is the *water pressure* rather than the volume of groundwater flow in the rock mass which is important. The water pressure at any point is independent of the permeability of the rock mass at that point but it does depend upon the path followed by the groundwater in arriving at that point (Figures 49 and 56). Hence, the anisotropy and the *distribution* of permeability in a rock mass is of interest in estimating the water pressure distribution in a slope.

In order to measure the permeability at a "point" in a rock mass, it is necessary to change the groundwater conditions at that point and to measure the time taken for the original conditions to be re-established or the quantity of water necessary to maintain the new conditions. These tests are most conveniently carried out in a borehole in which a section is isolated between the end of the casing and the bottom of the hole or between packers within the hole. The tests can be classified as follows:

a) Falling head tests in which water is poured into a vertical or near vertical borehole and the time taken for the water level to fall to its original level is determined.

b) Constant head tests in which the quantity of water which has to be poured into the borehole in order to maintain a specific water level is measured.

c) Pumping tests or lugeon tests in which water is pumped into or out of a borehole section between two packers and the changes induced by this pumping are measured.

The first two types of test are suitable for measurement of the permeability of reasonably uniform soils or rock. Anisotropic permeability coefficients cannot be measured directly in these tests but, as shown in the example given below, allowance can be made for this anisotropy in the calculation of permeability. Pumping tests, although more expensive, are more suitable for permeability testing in jointed rock.

Falling head and constant head tests

A very comprehensive discussion on falling head and constant head permeability testing is given by Hvorslev[125] and a few of the points which are directly relevant to the present

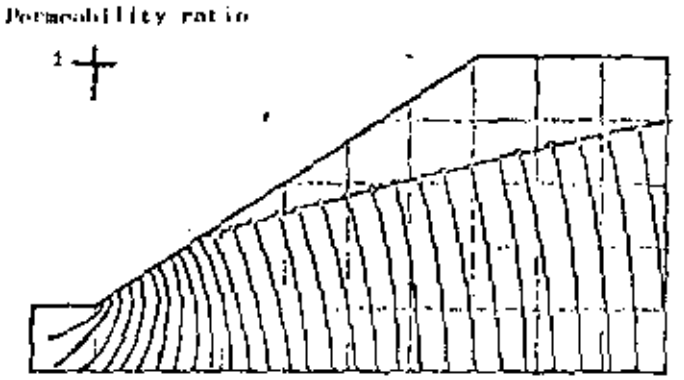

a) Isotropic rock slope.

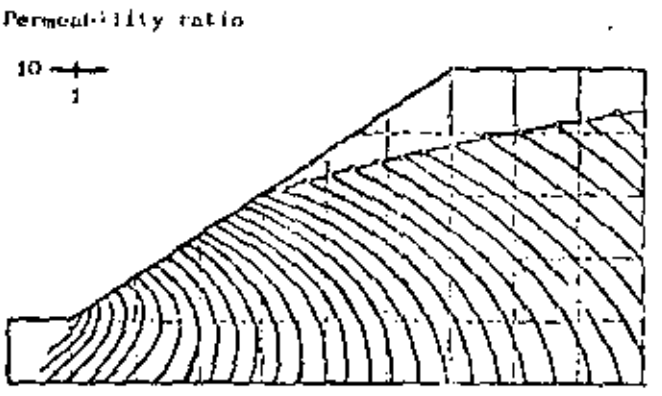

b) Anisotropic rock slope - horizontally bedded strata.

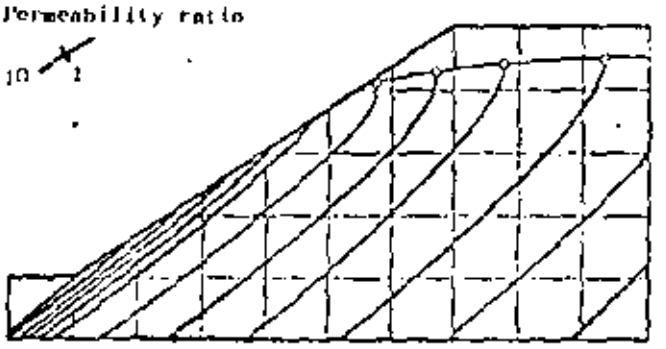

c) Anisotropic rock slope - strata dipping parallel to slope.

Figure 56 : Equipotential distributions in slopes with various permeability configurations.

discussion are summarised hereunder.

The coefficient of permeability k is calculated from falling-head and constant head tests in saturated ground (test section below water table) as follows.

$$\text{Falling head:} \quad k = \frac{A}{F(t_2 - t_1)} \cdot \log_e \frac{H_1}{H_2} \qquad (25)$$

$$\text{Constant head:} \quad k = \frac{q}{F H_c} \qquad (26)$$

where A is the cross section area of the water column. $A = \frac{1}{4}\pi d^2$ where d is the inside diameter of the casing in a *vertical* borehole. For an inclined hole, A must be corrected to account for the elliptical shape of the horizontal water surface in the casing.

F is a shape factor which depends upon the conditions at the bottom of the hole. Shape factors for typical situations are given in Figure 57.

H_1 and H_2 are water levels in the borehole, measured from the rest water level, at times t_1 and t_2 respectively.

q is the flow rate and

H_c is the water level, measured from the rest water level, maintained during a constant head test.

(Note that Naperian logarithms are used in these equations and that $\log_e = 2.3026 \log_{10}$)

Consider an example of a falling head test carried out in a borehole of 7.6 cm diameter with a casing of 6.0 cm diameter. The borehole is extended a distance of 100 cms beyond the end of the casing and the material in which the test is carried out is assumed to have a ratio of horizontal to vertical permeability $k_h/k_v = 5$.

The first step in this analysis is to calculate the shape factor F from the equation given for the 4th case in Figure 57. The value of $n = \sqrt{5} = 2.24$ and substituting D = 7.6 cm and L = 100 cm,

$$F = \frac{2\pi L}{\log_e (2n\,L/D)} = \frac{628}{\log_e 59.10} = 156$$

Measurement of water levels at different times for the falling head test gave the following values:

H_1 = 10 metres at t_1 = 30 seconds

H_2 = 5 metres at t_2 = 150 seconds

The cross-sectional area A of the water column is $A = \frac{1}{4}\pi(6)^2 = 28.3\ cm^2$.

Substituting in equation (25), the horizontal permeability k_h is given by

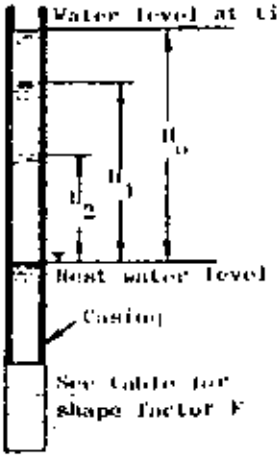

Falling head test

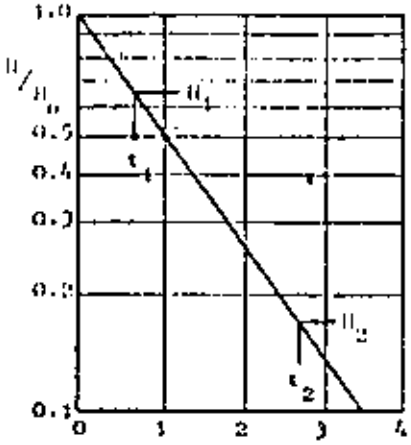

Time t - hours

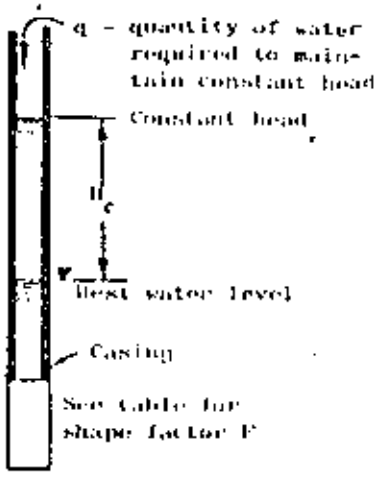

Constant head test

End conditions		Shape factor F
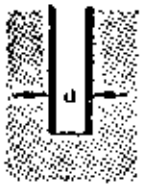	Casing flush with end of borehole in soil or rock of uniform permeability. Inside diameter of casing is d cms.	$F = 2.75d$
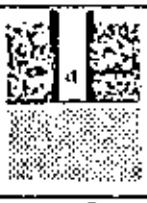	Casing flush with boundary between impermeable and permeable strata. Inside diameter of casing is d cms.	$F = 2.0\ d$
	Borehole extended a distance L beyond the end of the casing. D is borehole diameter.	$F = \dfrac{2\pi L}{\log_e (2L/D)}$ For $L > 4D$.
	Borehole extended a distance L beyond the end of the casing in a stratified soil or rock mass with horizontal and vertical permeabilities.	For determination of k_h: $F = \dfrac{2\pi L}{\log_e (2mL/D)}$ where $m = (k_h/k_v)^{\frac{1}{2}}$, $L > 4D$.
	Borehole extended a distance L beyond the end of the casing which is flush with an impermeable boundary	$F = \dfrac{2\pi L}{\log_e (4L/D)}$ For $L > 4D$.

Figure 57 : Details of falling head and constant head tests for permeability measurement in soil or rock masses with shape factors for borehole end conditions.

$$k_h = \frac{28{\cdot}3 \log_e 2}{154 \cdot (190-81)} = 1.06 \times 10^{-4} \text{ cm/sec.}$$

Since the ratio of horizontal to vertical permeability has been estimated, from examination of the core, as $k_h/k_v = 5$, $k_v = 2.12 \times 10^{-5}$ cm/sec.

Laboratory tests on core samples are useful in checking this *ratio* of horizontal to vertical permeability but, because of the disturbance to the sample, it is unlikely that the *absolute values* of permeability measured in the laboratory will be as reliable as those determined by the borehole tests described above. Laboratory methods for permeability testing are described in standard texts such as that by Lambe[1-6].

Pumping tests in boreholes

In a rock mass in which the groundwater flow is concentrated within regular joint sets, the permeability will be highly directional. If joint opening e could be measured in situ, the permeability in the direction of each joint set could be calculated directly from equation (23). Unfortunately, such measurements are not possible under field conditions and the permeability must therefore be determined by pumping tests.

A pumping test for the measurement of the permeability in the direction of a particular set of discontinuities such as joints involves drilling a borehole perpendicular to these discontinuities as shown in Figure 58. It is assumed that most of the flow is concentrated within this one joint set and that cross-flow through other joint sets, past the packers and through the intact rock surrounding the hole is negligible. A section of the borehole is isolated between packers or a single packer is used to isolate a length at the end of the hole and water is pumped into or out of this cavity.

A variety of borehole packers are available commercially[127] but the author considers that many of these packers are too short to eliminate leakage. Leakage past packers is one of the most serious sources of error in pumping tests and every effort should be made to ensure that an effective seal has been achieved before measurements are commenced. A simple, inexpensive and highly effective packer has been described by Harper and Moss-Brown[128] and the principal features are illustrated in Figure 59. This packer is manufactured from rubber hosing which is normally used in the building industry for forming voids in concrete*. It consists of inner and outer rubber tubes enclosing a diagonally braided cotton core and this arrangement allows an increase in diameter of approximately 20% when the hose is inflated. Because of its low cost and simplicity, long packers can be used and packer lengths of 10 feet (3 meters) have proved extremely effective in pumping tests in 3 inch (7.6 cm) diameter boreholes.

The permeability of the discontinuities perpendicular to the borehole is calculated as follows:

---

* Available in a wide range of diameters from Interdale Company Limited, Dunehill Road, Tonad, West Retford, Nottinghamshire, England.

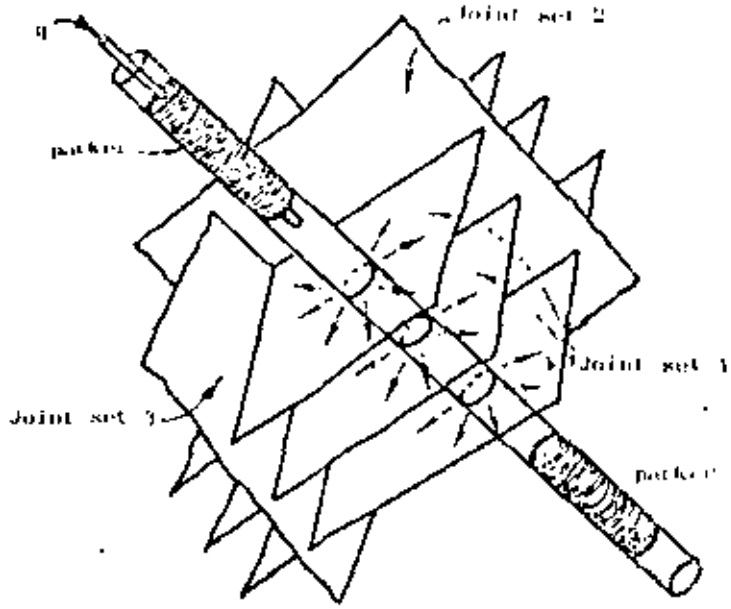

Figure 58 : Pumping test in regularly jointed rock. The borehole is drilled at right angles to the joint set in which the permeability is to be measured.

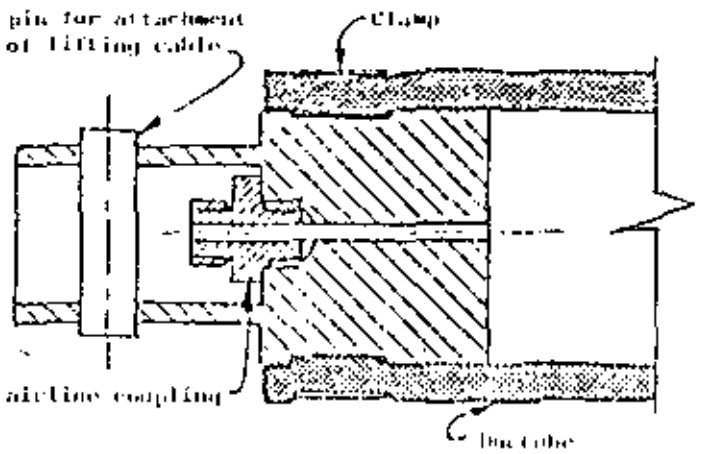

Figure 59 : Section through the end of a packer for sealing the bottom end of a pumping test cavity. The upper packer and has additional fittings for pressure inlet and piezometer tubes.

249

$$k = \frac{q \log_e (2R/D)}{2\pi L (H_1 - H_2)} \qquad (27)$$

where q is pumping rate required to maintain a constant pressure in the test cavity

L is the length of the test cavity

H_1 is the total head in the test cavity

D is the borehole diameter

H_2 is the (total) head measured at a distance R from the borehole

The most satisfactory means of obtaining the value of H_2 is to measure it in a borehole parallel to and at a distance R from the test hole. Where a pattern of boreholes is available, as is the case on many opencast mine sites, this does not present serious problems. Techniques for water pressure measurement are dealt with in the following section of this chapter.

When only one borehole is available, an approximate solution to equation (27) can be obtained by using the shape factor F for a stratified system (Figure 57). Substituting this value into equation (26) gives

$$k = \frac{q \log_e (2\pi L/D)}{2\pi L H_c} \qquad (28)$$

where, in this case, $m = (k/k_p)^{\frac{1}{2}}$,

k is the permeability at right angles to the borehole (the quantity required)

k_p is the permeability parallel to the borehole which, if cross flow is neglected, is equal to the permeability of the intact rock

H_c is the constant head above the original groundwater level in the borehole.

The value of the term $\log_e (2\pi L/D)$ in this equation does not have a major influence upon the value of k and hence a crude estimate of m is adequate. Consider the example where L = 4D; the values of $\log_e (2\pi L/D)$ are as follows:

k/k_p	1.0	10^2	10^4	10^6	10^8	10^{10}	10^{12}
m	1.0	10^1	10^2	10^3	10^4	10^5	10^6
$\log_e (2\pi L/D)$	2.1	4.6	6.7	9.0	11.3	11.6	15.9

A reasonable value of k for most practical applications is given by assuming $k/k_p = 10^6$, $m = 10^3$ which gives

$$k = \frac{1.4q}{L H_c} \qquad (29)$$

uities (say 100) and that the value of k represents a reasonable average permeability for the rock mass (in the direction at right angles to the borehole). When the discontinuity spacing varies along the length of the hole, water flow will be concentrated in zones of closely spaced discontinuities and the use of an average permeability value can give misleading results. Under these circumstances, it is preferable to express the permeability in terms of the permeability kj of individual discontinuities where

$$k_j = \frac{k}{n} \qquad (30)$$

n is the number of discontinuities which intersect the test cavity of length L.

The value of n can be estimated from the borehole core log and, assuming that the discontinuity opening (e in equation (23)) remains constant, the variation in permeability along the borehole can then be estimated.

Before leaving this question of permeability testing, it must be pointed out that the discussion which has been presented has been grossly simplified. This has been done deliberately since the literature dealing with this subject is copious, complex and confusing. A number of techniques, more sophisticated than those which have been described here, are available for the evaluation of permeability but the author believes that these are best left in the hands of experienced specialist consultants. The simple tests which have been described are generally adequate for open pit stability and drainage studies.

Measurement of water pressure

The importance of water pressure in relation to the stability of slopes has been emphasised in several of the previous chapters. If a reliable estimate of stability is to be obtained or if the stability of a slope is to be controlled by drainage, it is essential that water pressures within the slope should be measured. Such measurements are most conveniently carried out by *piezometers* installed in boreholes.

A variety of piezometer types are available and the choice of the type to be used for a particular installation depends upon a number of practical considerations. A detailed discussion on this matter has been given by Terzaghi and Peck[129] and only the most important considerations will be summarised here.

The most important factor to be considered in choosing a piezometer is the time lag of the complete installation. This is the time taken for the pressure in the system to reach equilibrium after a pressure change and it depends upon the permeability of the ground and the volume change associated with the pressure change. Open holes can be used for pressure measurement when the permeability is greater than 10^{-4} cm/sec but, for less permeable ground, the time lag is too long. In order to overcome this problem, a pressure measuring device or piezometer is installed in a sealed section of the borehole. The volume change within this sealed section, caused by the operation of the piezometer

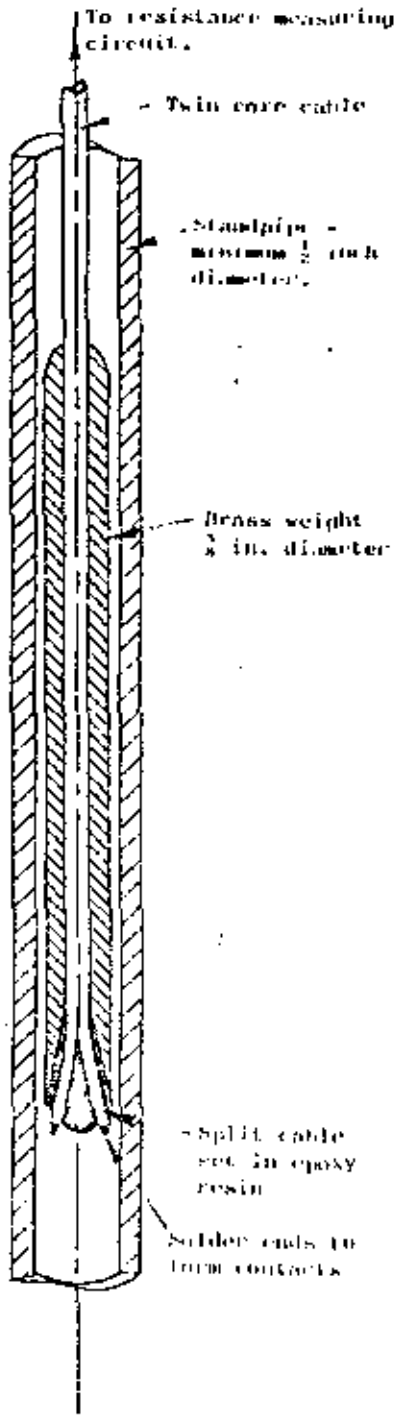

A simple probe for water level detection.

should be very small in order that the response of the complete installation to pressure changes in the surrounding rock should be rapid. If a device which requires a large volume change for its operation is used, the change in pressure induced by this change in volume may give rise to significant errors in measurement.

Some of the common types of piezometer are briefly discussed hereunder.

a) Open piezometers or observation wells

As discussed above, open ended cased holes can be used to measure water pressure in rock or soil in which the permeability is greater than about 10^{-5} cm/sec. All that is required for these measurements is a device for measuring water level in the borehole. A very simple probe consisting of a pair of electrical contacts housed in a brass weight is illustrated in the sketch opposite. When the contacts touch the water, the resistance of the electrical circuit drops and this can be measured on a standard "Avometer" or similar instrument. The depth of water below the collar of the hole is measured by the length of cable and it is convenient to mark the cable off in feet or meters for this purpose. Portable water level indicators, consisting of a probe, a marked cable and a small resistance measuring instrument, are available from Soil Instruments Ltd., Townsend Land, London N.W.9 or from Soiltest Inc., 2205 Lee Street, Evanston, Illinois 60202, U.S.A.

b) Standpipe piezometers

When the permeability of the ground in which water pressure is to be measured is less than 10^{-5} cm/sec, the time lag involved in using an open hole will be unacceptable and a standpipe piezometer such as that illustrated in Figure 60 should be used. This device consists of a perforated tip which is sealed into a section of borehole as shown. A small diameter standpipe passing through the seals allows the water level to be measured by means of the same type of water level indicator as described above under open hole piezometers. Because the volume of water within the standpipe is small, the response time of this piezometer installation will be adequate for most applications likely to be encountered on an open pit mine site.

An advantage of the standpipe piezometer is that, because of the small diameter of the standpipe, a number can be installed in the same hole. Hence different sections can be sealed off along the length of the borehole and the water pressure within each section monitored. This type of installation is important when it is suspected that water flow is confined to certain layers within a rock mass.

c) Closed hydraulic piezometers

When the permeability of the ground falls below about 10^{-6} cm/sec, the time lag of open ended boreholes or standpipe piezometers becomes unacceptable. For example, approximately 5 days would be required for a typical standpipe piezometer to reach an acceptable state of equilibrium after a change in water pressure in a rock or soil mass having a permeability of 10^{-7} cm/sec.

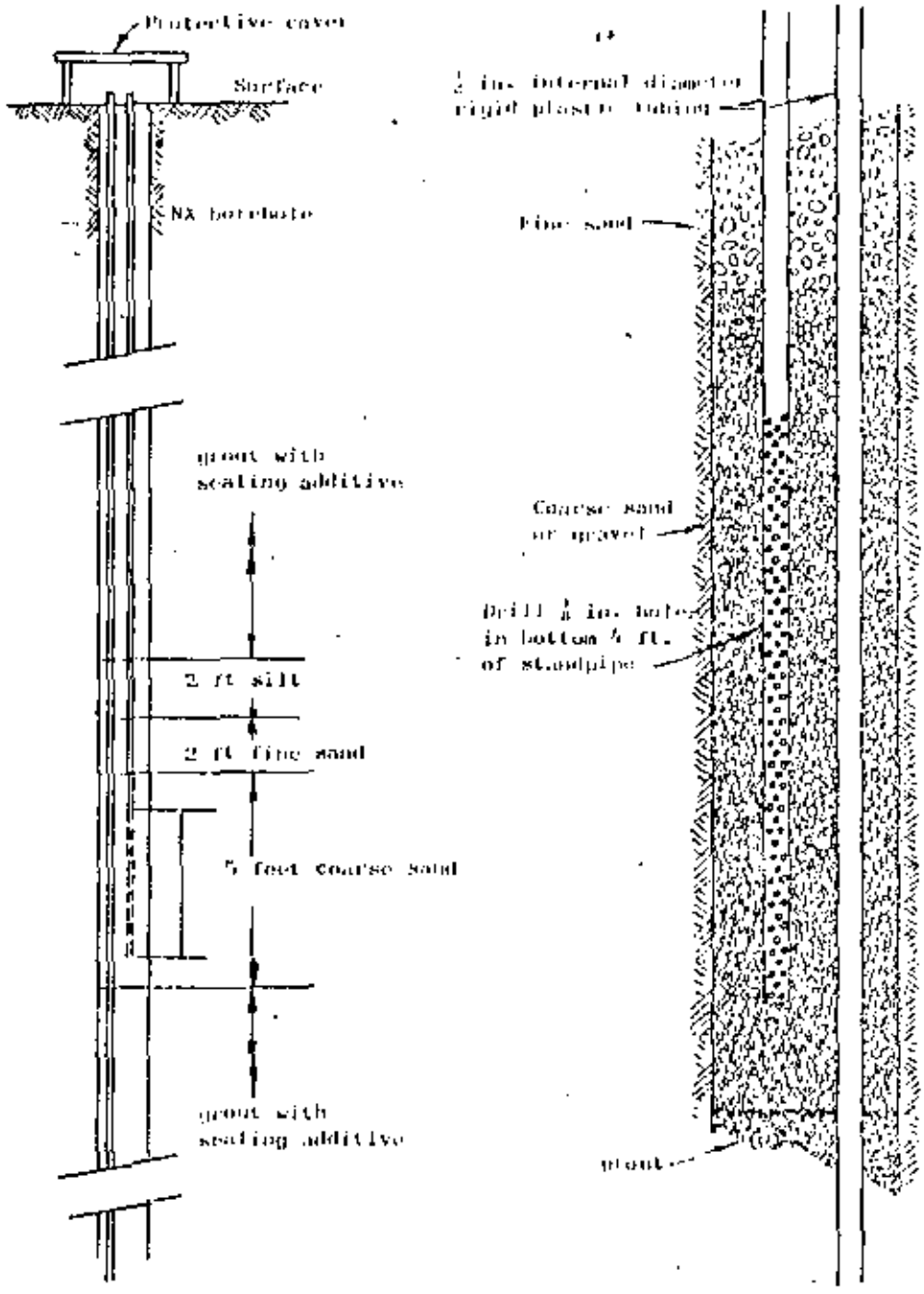

Figure 80 : Typical standpipe piezometer installation . Variations should be made to suit local conditions and to utilize local materials.

An improved time lag can be obtained by using a closed hydraulic piezometer such as that described by Bishop et al[130]. This type of piezometer is completely filled with de-aired water and is suitable for measurement of small water pressures. Such piezometers are generally used for pore pressure measurement during construction of embankments or dams where they can be installed during construction and left in place.[4]

d) Air Actuated Piezometers

A very rapid response time can be achieved by use of air actuated piezometers in which the water pressure is measured by a balancing air pressure acting against a diaphragm. As shown in Figure 61, an air valve allows air to escape when the air and water pressures on either side of the diaphragm are equal[131]. A commercially available air piezometer, manufactured by Soil Instruments Ltd., Townsend Lane, London N.W.9, England, is illustrated in Figure 62. Similar types of instrument are available from other suppliers and the author believes that these devices will play an increasingly important role in slope stability studies.

e) Electrically indicating piezometers

An almost instantaneous response time is obtained from piezometers in which the deflection of a diaphragm as a result of water pressure is measured electrically by means of some form of strain gauge attached to the diaphragm. A wide variety of such devices are available commercially and they are ideal for measuring the water pressure within the test cavity during a pumping test[116]. Because of their relatively high cost and because of the possibility of electrical faults, these piezometers are less satisfactory for permanent installation in boreholes.

General comments

A frequent mistake made by engineers or geologists in examining rock or soil slopes is to assume that groundwater is not present if no seepage appears on the slope face. In many cases, the seepage rate may be lower than the evaporation rate and hence the slope surface may appear completely dry and yet there may be water at significant pressure within the rock mass. Remember that it is water pressure and not rate of flow which is responsible for instability in slopes and it is essential that measurement or calculation of this water pressure should form part of the site investigation for stability studies. Drainage, which is discussed in a later chapter, is one of the most effective and most economical means available for improving the stability of open pit mine slopes. Rational design of drainage systems is only possible if the water flow pattern within the rock mass is understood and measurement of permeability and water pressure provides the key to this understanding.

, Y.N. In situ parameters in jointed rock - measurement and interpretation. *M.Sc. Thesis, University of London* (Imperial College)

, W.E. *Groundwater and Seepage*, McGraw Hill Co. New York, 1967.

, D.W. *Fundamentals of Soil Mechanics*. Wiley & Sons, New York, 1948.

, W.J. *Analog Simulation. Solution of Problems*. McGraw Hill Co., New York, 1968.

, R.L. and BORGNSTEDT, H.R. The approximate solution of seepage problems by a simple electrical analogue method. *Civil Engineers and Public Works Rev.* Vol. 63, 1968, pp.65-70.

, O.C., HAYER, P. and CHEUNG, Y.K. Solution of anisotropic seepage by finite elements. *Journal Eng. Mech. Div.*, ASCE, Vol. 92, EM1, 1966, pp.111-120.

, J.C., NAINI, Y.N. and HARPER, T.P. Influence of groundwater on the stability of rock masses. *Trans. Institute Mining and Metallurgy*, London. Vol. 81, Bulletin No. 782, 1972, pp.A13-A20.

, H.S. Time lag and soil permeability in groundwater measurements. *U.S. Corps of Engrs Waterways Experiment Station, Bulletin No. 60*, 1951, 50p.

, T.W. *Soil testing for engineers*. John Wiley and Sons, New York, 1951.

, A.H. In-situ testing for the Channel Tunnel. *Proc. Conference on in-situ investigations in soils and rocks*, London 1969. Published by Institution of Civil Engineers, London, 1969. pp.79-86.

, T.R. and ROSS-BROWN, D.N. An inexpensive portable borehole packer. *Imperial College Rock Mechanics Research Report No. 024*, 1972, 5p.

, K. and PECK, R. *Soil Mechanics in Engineering Practice*. John Wiley and Sons Inc., New York, 1967. 729p.

, A.W., KENNARD, M.F. and PENMAN, A.D.M. Pore-pressure observations at Selset dam. *Proc. Conf. on Pore Pressure and Suction in Soils*, Butterworth, London, 1960, pp.91-102.

, A.A. and THOMAS, E.W. Measurement of hydrostatic uplift pressure on Spillway weir with air piezometers. *Instruments and apparatus for soil and rock mechanics*. American Society for Testing and Materials Special Technical Publication No. 392, 1965, pp.143-151.

A typical open pit mine slope face containing several sets of discontinuities which could be involved in failure. The different types of failure which could occur in such a slope will be analysed on the following

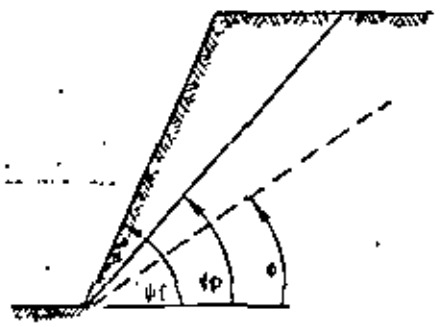

For sliding

$\psi_f > \psi_p > \phi$

Introduction

A plane failure is a comparatively rare sight in rock slopes because it is only occasionally that all the geometrical conditions required to produce such a failure occur in an actual slope. The wedge type of failure, considered in Chapter 8, is a much more general case and many rock slope engineers treat the plane failure as a special case of the more general wedge failure analysis.

While this is probably the correct approach for the experienced slope designer who has a wide range of design tools at his disposal, it would not be right to ignore the two-dimensional case in this general discussion on slope failure. There are many valuable lessons to be learned from a consideration of the mechanics of this simple failure mode and it is particularly useful for demonstrating the sensitivity of the slope to changes in shear strength and groundwater conditions - changes which are less obvious when dealing with the more complex mechanics of a three-dimensional slope failure.

Geometrical conditions for plane failure

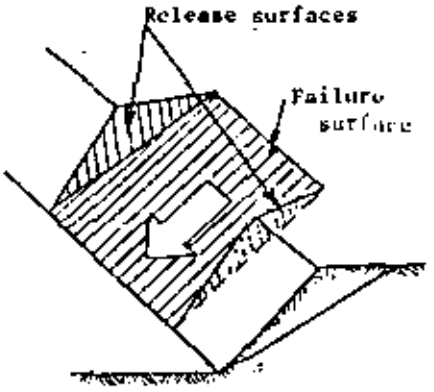

In order that sliding should occur on a *single plane*, the following geometrical conditions must be satisfied:

a. The plane on which sliding occurs must strike parallel or nearly parallel (within approximately ±20°) to the slope face.

b. The failure plane must "daylight" in the slope face. This means that its dip must be *smaller* than the dip of the slope face, i.e. $\psi_f > \psi_p$.

c. The dip of the failure plane must be *greater* than the angle of friction on this plane, i.e. $\psi_p > \phi$.

d. Release surfaces which provide negligible resistance to sliding must be present in the rock mass to define the lateral boundaries of the slide. Alternatively, failure can occur on a failure plane passing through the convex "nose" of a slope.

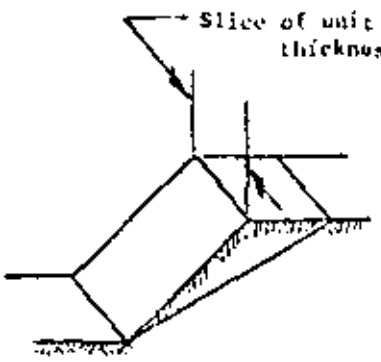

In analysing two-dimensional slope problems, it is usual to consider a slice of unit thickness taken at right angles to the slope face. This means that the area of the sliding surface can be represented by the length of the surface visible on a vertical section through the slope and the volume of the sliding block is represented by the area of the figure representing this block on the vertical section.

Plane failure analysis

The geometry of the slope considered in this analysis is defined in figure 61. Note that two cases must be considered:

a. A slope having a tension crack in its upper surface.

b. A slope with a tension crack in its face.

The transition from one case to another occurs when the tension crack coincides with the slope crest, i.e. when

259

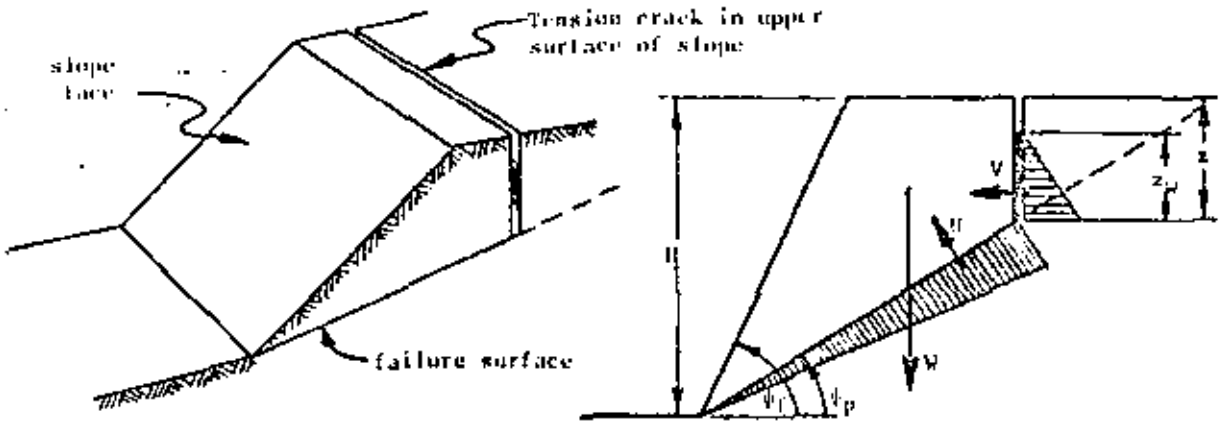

Figure 61a : Geometry of slope with tension crack in upper slope surface

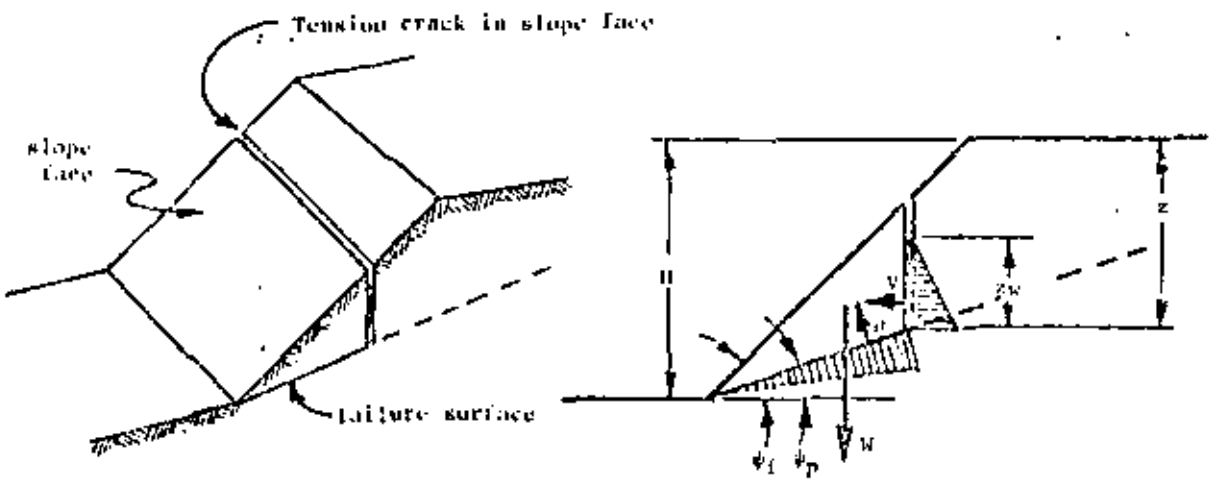

Figure 61b: Geometry of slope with tension crack in slope face

The following assumptions are made in this analysis:

a. Both sliding surface and tension crack strike parallel to the slope face.

b. The tension crack is vertical and is filled with water to a depth z_w.

c. Water enters the sliding surface along the base of the tension crack and seeps along the sliding surface, escaping at atmospheric pressure where the sliding surface daylights in the slope face. The pressure distribution induced by the presence of water in the tension crack and along the sliding surface is illustrated in figure 63.

d. The forces W (the weight of the sliding block), U (uplift force due to water pressure on the sliding surface) and V (force due to water pressure in the tension crack) all act through the centroid of the sliding mass. In other words, it is assumed that there are no moments which would tend to cause rotation of the block and hence failure is by sliding only. While this assumption may not be strictly true for most actual slopes, the errors introduced by ignoring moments are small enough to neglect. However, in steep slopes with steeply dipping discontinuities, the possibility that toppling failure (discussed on page 29) may occur should be kept in mind.

e. The shear strength of the sliding surface is defined by cohesion c and a friction angle ϕ which are related by the equation $\tau = c + \sigma \tan\phi$ as discussed on page 22.

f. A slice of unit thickness is considered and it is assumed that release surfaces are present so that there is no resistance to sliding at the lateral boundaries of the failure.

The factor of safety of this slope is calculated in precisely that same way as that for the block on an inclined plane considered on pages 26 and 27. In this case the factor of safety, given by the total force resisting sliding to the total force tending to induce sliding, is

$$F = \frac{cA + (W.\cos\psi_p - U - V.\sin\psi_p)\tan\phi}{W.\sin\psi_p + V.\cos\psi_p} \qquad (32)$$

where, from figure 63 :

$$A = (H - z).\mathrm{Cosec}\psi_p \qquad (33)$$

$$U = \tfrac{1}{2}\gamma_w.z_w(H - z).\mathrm{Cosec}\psi_p \qquad (34)$$

$$V = \tfrac{1}{2}\gamma_w.z_w^2 \qquad (35)$$

For the tension crack in the upper slope surface (figure 63a)

$$W = \tfrac{1}{2}\gamma H^2\left[(1 - (z/H)^2)\cot\psi_p - \cot\phi_f\right] \qquad (36)$$

and, for the tension crack in the slope face (figure 63b)

When the geometry of the slope and the depth of water in the tension crack are known, the calculation of a factor of safety is a simple enough matter. However, it is sometimes necessary to compare a range of slope geometries, water depths and the influence of different shear strengths. In such cases, the solution of equations 32 to 37 can become rather tedious. In order to simplify the calculations, equation 32 can be rearranged in the following dimensionless form :

$$F = \frac{(2c/\gamma H).P + \left\{ Q.\cot\phi_p - k(P + S)\right\}\tan\phi}{Q + R.S.\cot\phi_p} \qquad (38)$$

where

$$P = (1 - z/H).\operatorname{Cosec}\phi_p \qquad (39)$$

When the tension crack is in the upper slope surface :

$$Q = \left\{(1 - (z/H)^2)\cot\psi_p - \cot\phi_f\right\}\sin\phi_p \qquad (40)$$

When the tension crack is in the slope face :

$$Q = \left\{(1 - z/H)^2\cos\phi_p(\cot\phi_p.\tan\phi_f - 1)\right\} \qquad (41)$$

$$R = \frac{\gamma_w}{\gamma}.\frac{z_w}{z}.\frac{z}{H} \qquad (42)$$

$$S = \frac{z_w}{z}.\frac{z}{H}.\sin\phi_p \qquad (43)$$

The ratios P, Q, R and S are all dimensionless which means that they depend upon the geometry but not upon the size of the slopes. Hence, in cases where the cohesion $c = 0$, the factor of safety is independent of the size of the slope. The important principle of dimensionless grouping, illustrated in these equations, is a useful tool in rock engineering and extensive use will be made of this principle in the study of wedge and circular failures.

In order to facilitate the application of these equations to practical problems, values for the ratios P, Q and S, for a range of slope geometries, are presented in graphical form in figure 64. Note that both tension crack positions are included in the graphs for the ratio Q and hence the values of ψ may be determined for any slope configuration without having first to check on the tension crack position. One point to keep in mind when using these graphs is that the depth of the tension crack is always measured from the top of the slope as illustrated in figure 63b.

Consider an example in which a 100 foot high slope with a face angle $\phi_f = 60^0$ is found to have a bedding plane running through it at a dip $\psi_p = 30^0$. A tension crack occurs 20 feet behind the crest of the slope and, from an accurately drawn cross-section of the slope, the tension crack is found to have a depth of 50 feet. The rock density $\gamma = 160$ lb/ft^3, that of water is $\gamma_w = 62.5$ lb/ft^3. Assuming that the cohesive strength of the bedding plane $c = 1000$ lb/ft^2 and the friction angle $\phi = 30^0$, find the influence of water depth z_w upon the factor of safety of the slope.

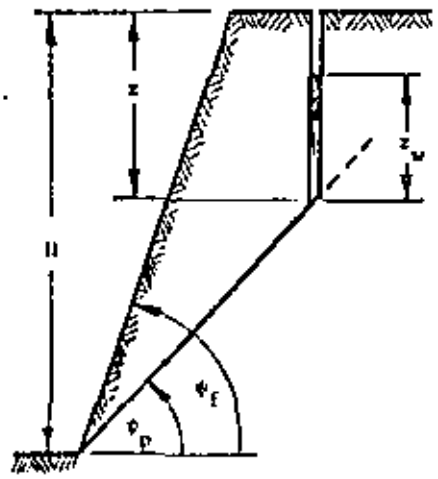

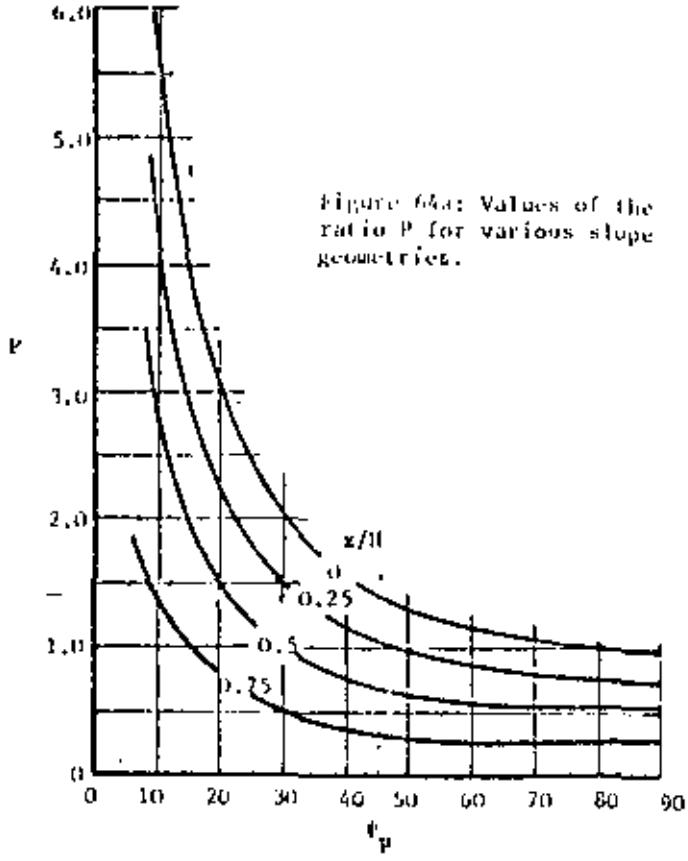

Figure 64a: Values of the ratio P for various slope geometries.

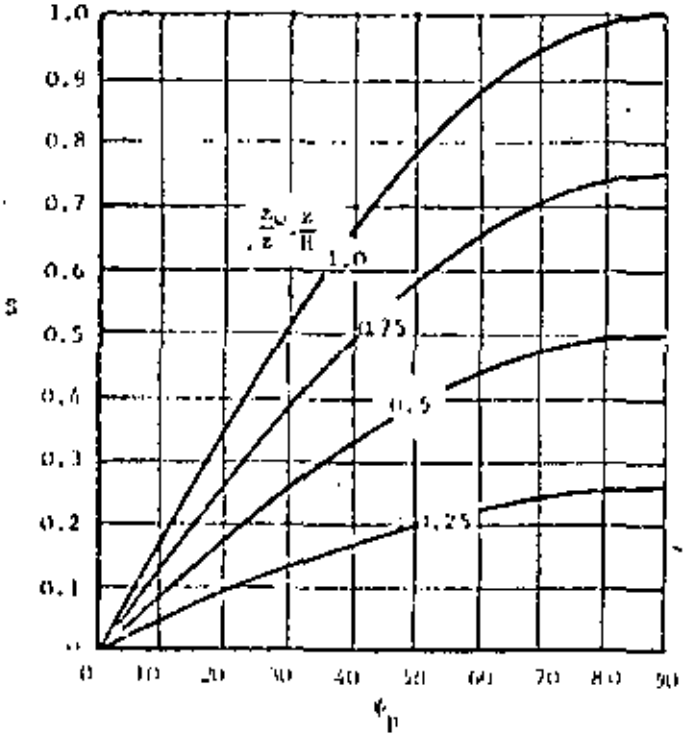

Figure 64b: Values of the ratio S for various geometries.

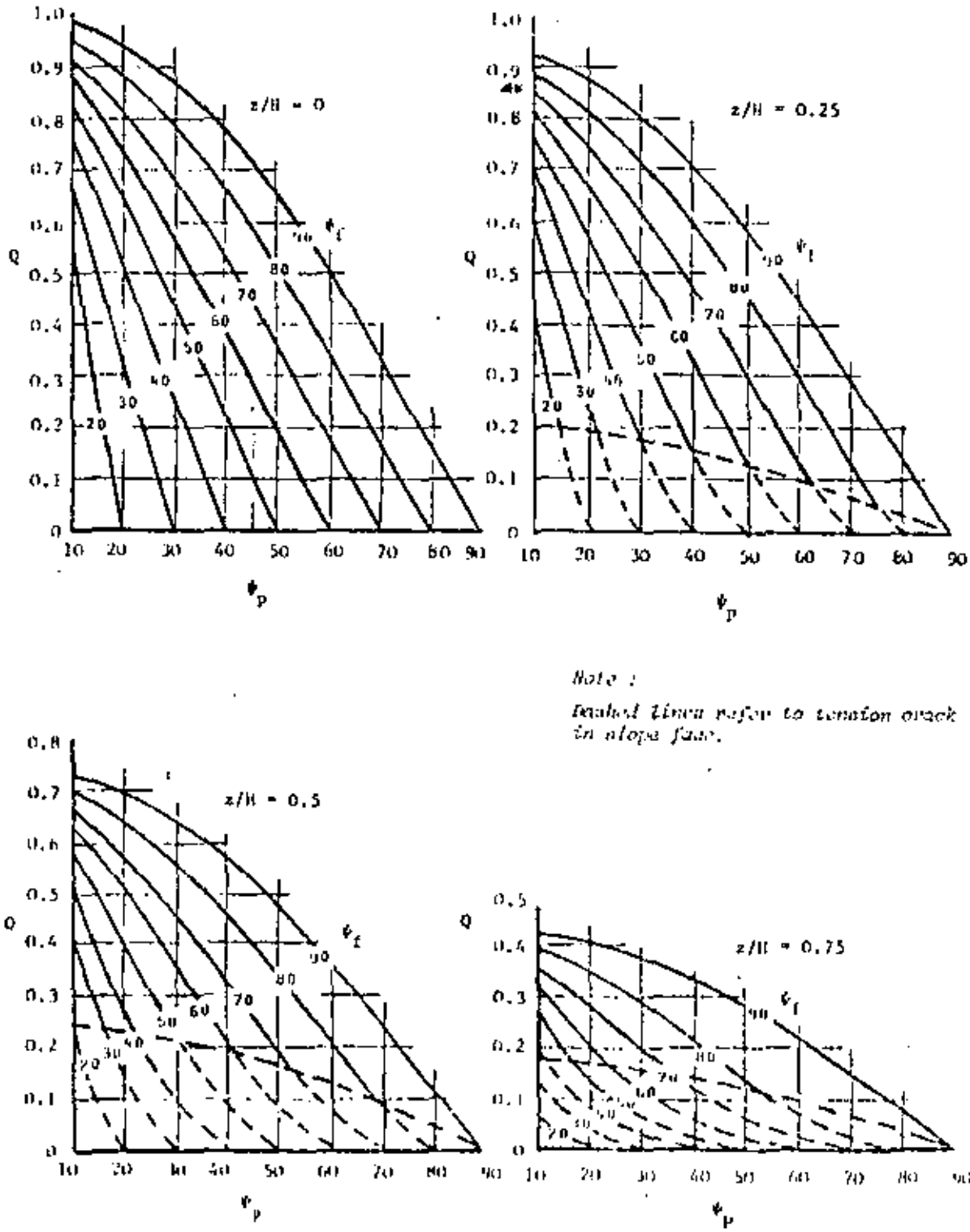

Note :

Dashed lines refer to tension crack in slope face.

Figure 6.6 : Values of the ratio Q for various slope geometries.

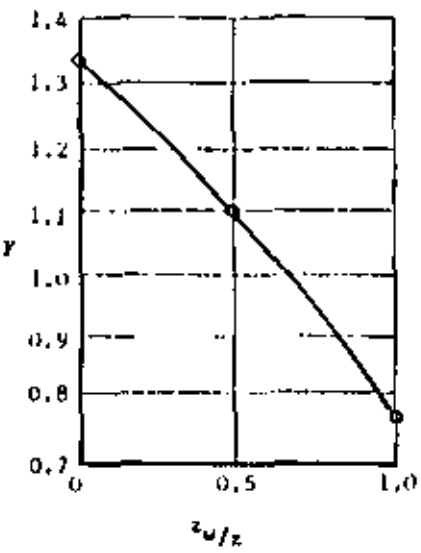

The values of P and Q are found from figure 64, for $z/H = 0.5$ to be :

$$P = 1.0 \text{ and } Q = 0.36$$

The values of R (from equation 42) and S (from figure 64b), for a range of values of z_w/z, are :

z_w/z	1.0	0.5	0
R	0.195	0.098	0
S	0.26	0.13	0

The value of $2c/\gamma H = 0.125$.

Hence, the factor of safety for different depths of water in the tension crack, from equation 38, varies as follows:

z_w/z	1.0	0.5	0
F	0.77	1.10	1.34

These values are plotted in the graph in the margin and the sensitivity of the slope to water in the tension crack is obvious. Simple analyses of this sort, varying one parameter at a time, can be carried out in a few minutes and are useful aids to decision making. In the example considered, it would obviously be worth taking steps to prevent water from entering the top of the tension crack. In other cases, it may be found that the presence of water in the tension crack does not have a significant influence upon stability and that other factors are more important.

Graphical analysis of stability

As an alternative to the analytical method presented above, some readers may prefer the following graphical method :

a. From an accurately drawn cross-section of the slope, scale the lengths B, X, D, A, z and z_w shown in figure 65a.

b. Calculate the forces W, V and U from these dimensions by means of the equations given in figure 65a. Also calculate the magnitude of the cohesive force A.c.

c. Construct the force diagram illustrated in figure 65b as follows :

i) Draw a vertical line to represent the weight W of the sliding wedge. The scale should be chosen to suit the size of the drawing board used.

ii) At right angles to the line representing W, draw a line to represent the force V due to water pressure in the tension crack.

iii) Measure the angle ψ_a as shown in figure 65b and draw a line to represent the uplift force U due to water pressure on the sliding surface.

iv) Project the line representing U (shown dashed in figure 65b) and, from the upper extremity of the line representing W, construct a perpendicular to the projection of the U line.

v) From the upper extremity of the U line, draw a line at an angle ϕ to intersect the line from W to the projection of the U line.

vi) The length I on figure 65b represents the frictional force which resists sliding along

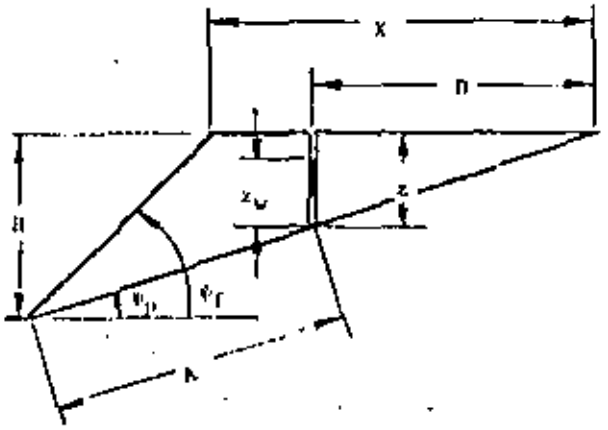

Weight of sliding wedge:

$W = \frac{1}{2}\gamma(HX - Dz)$

Horizontal water force : $V = \frac{1}{2}\gamma_w \cdot z_w^2$

Uplift water force : $U = \frac{1}{2}\gamma_w \cdot z_w \cdot A$

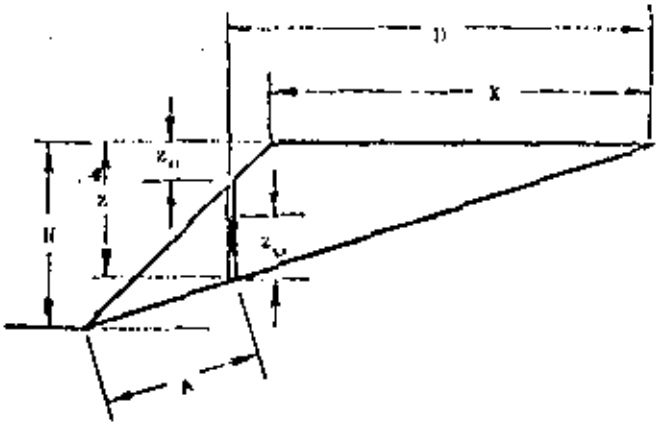

Weight of sliding wedge:

$W = \frac{1}{2}\gamma\left(HX - Dz + z_o(D - X)\right)$

Figure 65a: Slope geometry and equations for calculating forces acting on slope.

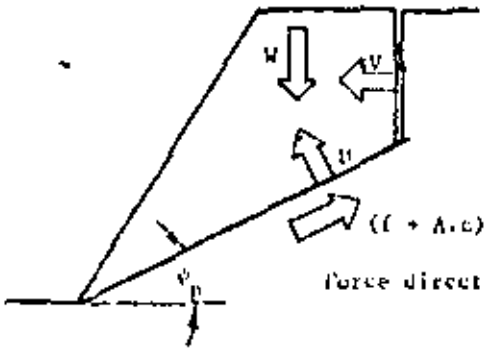

Force directions

Factor of safety $F = \frac{f + A.c}{S}$

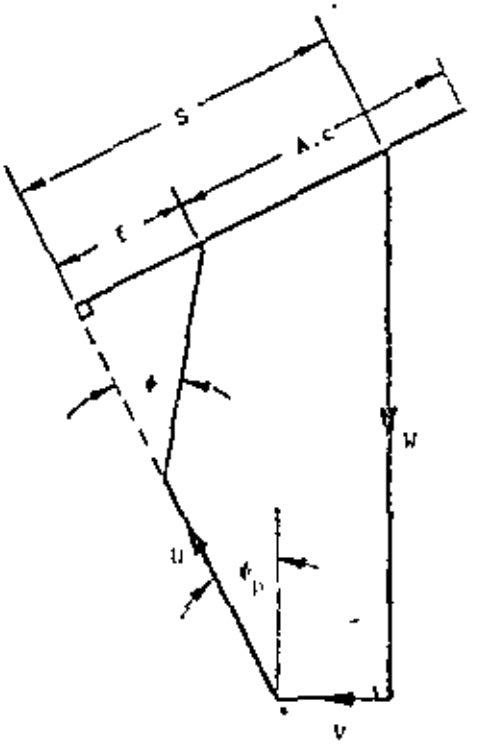

Figure 65b: Force diagram for two-dimensional slope stability analysis.

the failure plane.

vii) The cohesive resisting force A.c can be drawn parallel to I. Although this step is not essential, drawing A.c on the force diagrams ensures that there is no error in converting to and from the various scales which may have been used in this analysis since it provides a visual check of the magnitude of A.c.

viii) The length of the line marked S on the force diagram represents the total force tending to induce sliding down the plane.

ix) The factor of safety F of the slope is given by the ratio of the lengths (I + A.c) to S.

An example of the application of this graphical technique will be given later in this chapter.

Influence of groundwater on stability

In the preceding discussion it has been assumed that it is only the water present in the tension crack and that along the failure surface which influences the stability of the slope. This is equivalent to assuming that the rest of the rock mass is impermeable, an assumption which is certainly not always justified. Consideration must, therefore, be given to water pressure distributions other than that upon which the analysis so far presented is based.

The current state of knowledge in rock engineering does not permit a precise definition of the groundwater flow patterns in a rock mass. Consequently, the only possibility open to the slope designer is to consider a number of realistic extremes in an attempt to bracket the range of possible factors of safety and to assess the sensitivity of the slope to variations in groundwater conditions.

a. Dry slope

The simplest case which can be considered is that in which the slope is assumed to be completely drained. In practical terms, this means that there is no water pressure in the tension crack or along the sliding surface. Note that there may be moisture in the slope but, as long as no *pressure* is generated, it will not influence the stability of the slope.

Under these conditions, the forces V and U are both zero and equation 32 reduces to :

$$F = \frac{c.A}{W.\sin\psi_p} + \cot\psi_p.\tan\phi \qquad (44)$$

Alternatively, equation 38 reduces to

$$F = \frac{2c}{\gamma H}\cdot\frac{P}{Q} + \cot\psi_p.\tan\phi \qquad (45)$$

b. Water in tension crack only

A heavy rain storm after a long dry spell can result in the rapid build-up of water pressure in the tension crack which will offer little resistance to the entry of surface

flood water unless effective surface drainage has been provided. Assuming that the remainder of the rock mass is relatively impermeable, the only water pressure which will be generated during and immediately after the rain will be that due to water in the tension crack. In other words, the uplift force U = 0.

The uplift force U could also be reduced to zero or nearly zero if the failure surface was impermeable as a result of clay filling. In either case, the factor of safety of the slope is given by

$$F = \frac{c.A + (W.\mathrm{Cos}\psi_p - V.\mathrm{Sin}\psi_p)\mathrm{Tan}\phi}{W.\mathrm{Sin}\psi_p + V.\mathrm{Cos}\psi_p} \qquad (46)$$

or, alternatively

$$F = \frac{2c/\gamma H.P + (Q.\mathrm{Cot}\psi_p - RS)\mathrm{Tan}\phi}{Q + RS.\mathrm{Cot}\psi_p} \qquad (47)$$

c. Water in tension crack and on sliding surface

These are the conditions which were assumed in deriving the general solution presented on the preceding pages. The pressure distribution along the sliding surface has been assumed to decrease linearly from the base of the tension crack to the intersection of the failure surface and the slope face. This water pressure distribution is probably very much simpler than that which occurs in an actual slope but, since the actual pressure distribution is unknown, this assumed distribution is as reasonable as any other which could be made.

It is possible that a more dangerous water pressure distribution could exist if the face of the slope became frozen in winter so that, instead of the zero pressure condition which has been assumed at the face, the water pressure at the face would be that due to the full head of water in the slope. Such extreme water pressure conditions may occur from time to time and the slope designer should keep this possibility in mind. However, for general slope design, the use of this water pressure distribution would result in an excessively conservative slope and hence the triangular pressure distribution used in the general analysis is presented as the basis for normal slope design.

d. Saturated slope with heavy recharge

If the rock mass is heavily fractured so that it becomes relatively permeable, a groundwater flow pattern similar to that which would develop in a porous system would occur (see Figure 56 on page 119). The most dangerous condition which would develop in this case would be those given by prolonged heavy rain.

Flow nets for saturated slopes with heavy surface recharge have been constructed [16] and the water pressure distributions obtained from these flow nets have been used to calculate the factors of safety of a variety of slopes.

[illegible] to include in this

chapter but the results can be summarised in a general form. It has been found that the factor of safety for a permeable slope, saturated by heavy rain and subjected to surface recharge by continued rain, can be approximated by equation 32 (or 38), assuming that the tension crack is water-filled, i.e. $z_w = z$.

In view of the uncertainties associated with the actual water pressure distributions which could occur in rock slopes subjected to these conditions, there seems little point in attempting to refine this analysis any further.

Critical tension crack depth

In the analysis which has been presented, it has been assumed that the position of the tension crack is known from its visible trace on the upper surface or on the face of the slope and that its depth can be established by constructing an accurate cross-section of the slope. When the tension crack position is unknown, due, for example, to the presence of a waste dump on the top of the slope, it becomes necessary to consider the most probable position of a tension crack.

The influence of tension crack depth and of the depth of water in the tension crack upon the factor of safety of a typical slope is illustrated in figure 66 (based on the example considered on page 136).

When the slope is dry or nearly dry, the factor of safety reaches a minimum value which, in the case of the example considered, corresponds to a tension crack depth of 0.42H. This critical tension crack depth for a dry slope can be found by partial differentiation of equation 44 with respect to z/H. Equating this partial differential to zero gives the critical tension crack depth as

$$z_c/H = 1 - \sqrt{\cot\phi_f . \tan\psi_p} \qquad (48)$$

From the geometry of the slope, the corresponding position of the tension crack is:

$$b_c/H = \sqrt{\cot\psi_f . \cot\psi_p} - \cot\psi_f \qquad (49)$$

Critical tension crack depths and locations for a range of dry slopes are plotted in figure 67.

Figure 66 shows that, once the water level z_w exceeds about one quarter of the tension crack depth, the factor of safety of the slope does not reach a minimum until the tension crack is water-filled. In this case, the minimum factor of safety is given by a water-filled tension crack which is coincident with the crest of the slope ($b = 0$).

It is most important, when considering the influence of water in a tension crack, to consider the sequence of tension crack formation and water filling. Field observations suggest that tension cracks usually occur behind the crest of a slope and, from figure 66, it must be concluded that these tension cracks occur as a result of movement in a dry or nearly dry slope. If this tension crack becomes water-filled as a result of a subsequent rain storm, the influence of the water pressure will be in accordance with the rules laid down earlier in this chapter. The depth

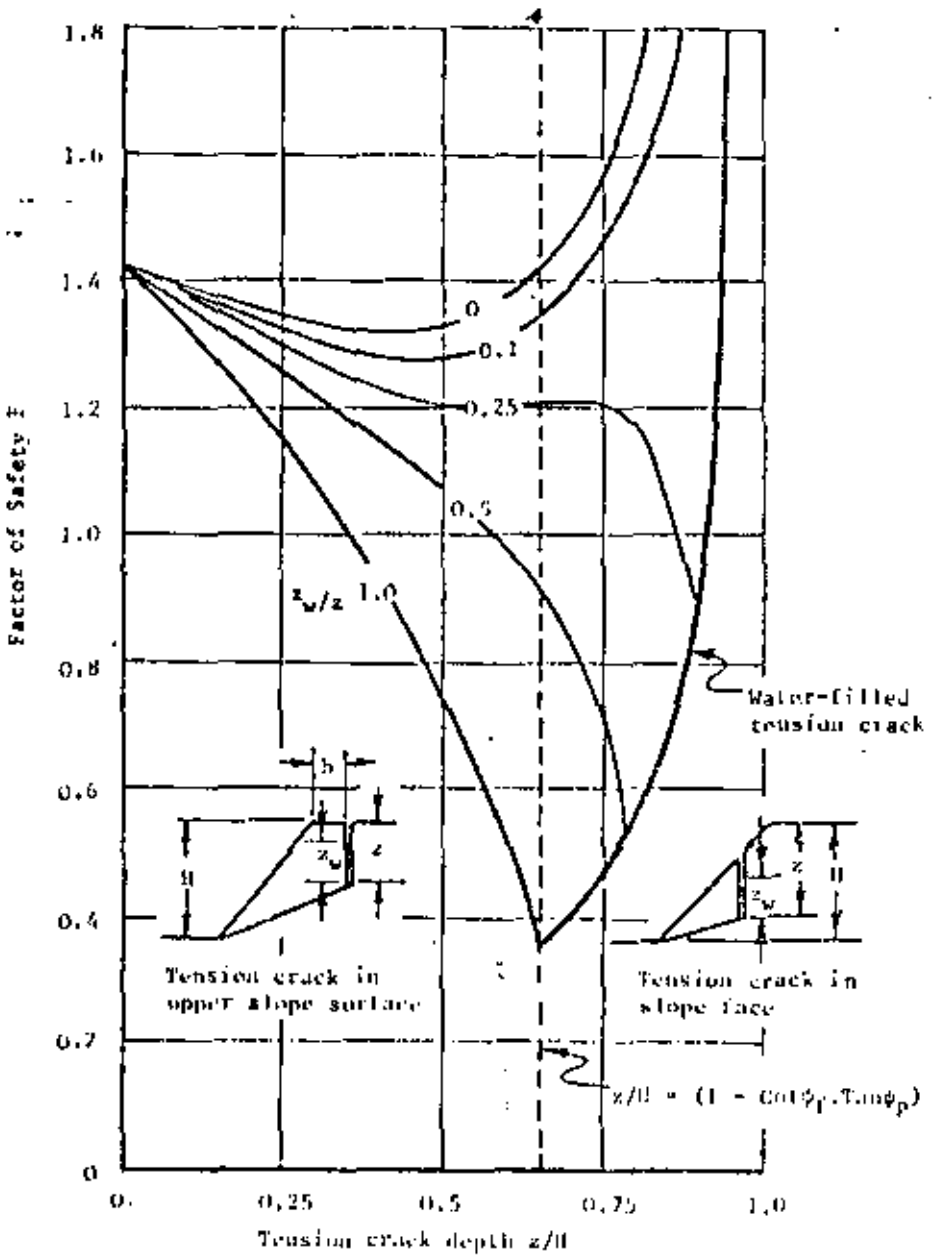

Figure 66: Influence of tension crack depth and of depth of water in the tension crack upon the factor of safety of a slope. (Slope geometry and material properties as for example on page 186).

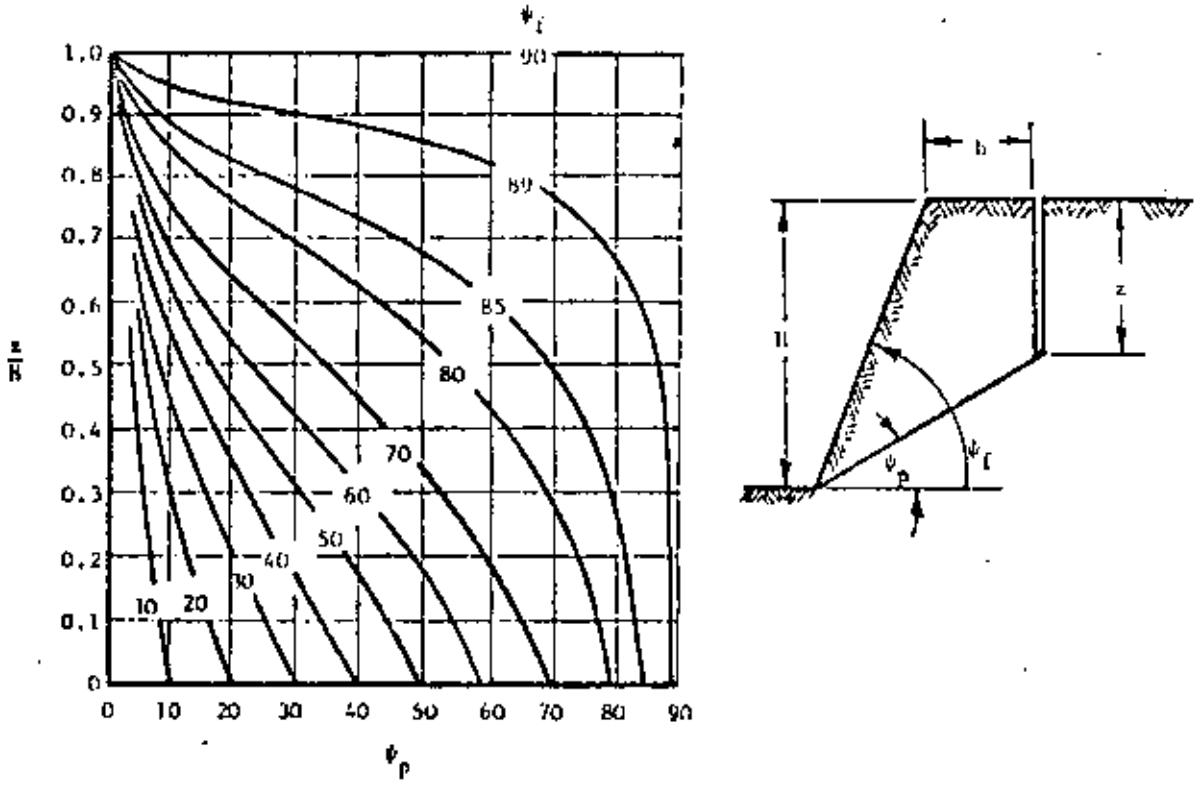

Figure 67a: Critical tension crack depth for a dry slope .

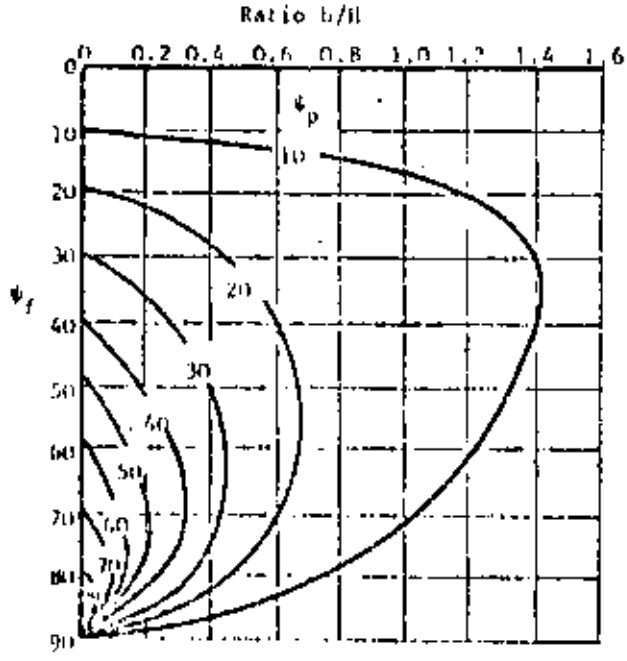

Figure 67b : Critical tension crack location for a dry slope.

and location of the tension crack are, however, independent of the groundwater conditions and are defined by equations 48 and 49.

If the tension crack forms *during* heavy rain or if it is located on a pre-existing geological feature such as a vertical joint, equations 48 and 49 no longer apply. In these circumstances, when the tension crack position and depth are unknown, the only reasonable procedure is to assume that the tension crack is coincident with the slope crest and that it is water-filled.

The tension crack as an indicator of instability

Anyone who has examined excavated rock slopes cannot have failed to notice the frequent occurrence of tension cracks in the upper surfaces of these slopes. Some of these cracks have been visible for tens of years and, in many cases, do not appear to have had any adverse influence upon the stability of the slope. It is, therefore, interesting to consider how such cracks are formed and whether they can give any indication of slope instability.

In a series of very detailed model studies on the failure of slopes in jointed rocks, Barton [133] found that the tension crack was generated as a result of small shear movements within the rock mass. Although these individual movements were very small, their cumulative effect was a significant displacement of the slope surface - sufficient to cause separation of vertical joints behind the slope crest and to form "tension" cracks. The fact that the tension crack is caused by shear movements in the slope is important because it suggests that, when a tension crack becomes visible in the surface of a slope, it must be assumed that shear failure has initiated within the rock mass.

It is impossible to quantify the seriousness of this failure since it is only the start of a very complex progressive failure process about which very little is known. It is quite probable that, in some cases, the improved drainage resulting from the opening up of the rock structure and the interlocking of individual blocks within the rock mass could give rise to an *increase* in stability. In other cases, the initiation of failure could be followed by a very rapid decrease in stability with a consequent failure of the slope.

In summary, the authors recommend that the presence of a tension crack should be taken as an indication of potential instability and that, in the case of an important slope, this should signal the need for detailed investigation into the stability of that particular slope.

Critical failure plane inclination

When a through-going discontinuity such as a bedding plane exists in a slope and the inclination of this discontinuity is such that it satisfies the conditions for plane failure defined on page 131, the failure of the slope will be controlled by this feature. However, when no such feature exists and when a failure surface, if it were to occur, would follow minor geological features and, in some places, would cross the intact material, how could the inclination

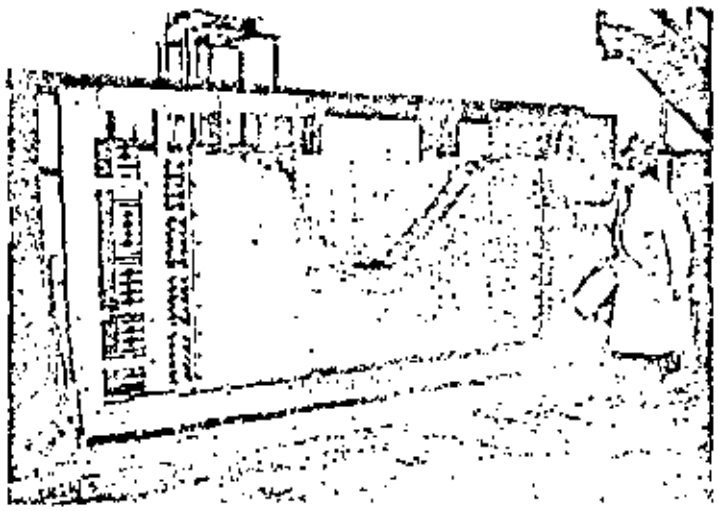

Figure 68: Two-dimensional model used by Barton[133] for the study of slope failure in jointed rock masses.

cion of such a failure path be determined ?

The first assumption which must be made concerns the shape of the failure surface. In a soft rock slope or a soil slope with a relatively flat slope face ($\psi_f < 45^o$), the failure surface would have a circular shape. The analysis of such failure surfaces will be dealt with in chapter 9.

In steep rock slopes, the failure surface is almost planar and the inclination of such a plane can be found by partial differentiation of equation 32 with respect to ψ_p and by equating the resulting differential to zero. For dry slopes this gives the critical failure plane inclination ψ_{pc} as

$$\psi_{pc} = \frac{1}{2}(\psi_f + \phi) \qquad (50)$$

The presence of water in the tension crack will cause the failure plane inclination to be reduced by up to 10% and, in view of the uncertainties associated with this failure surface, the added complication of including the influence of groundwater is not considered justified. Consequently, equation 50 can be used to obtain an estimate of the critical failure plane inclination in steep slopes which do not contain throughgoing discontinuity surfaces. An example of the application of this equation in the case of a chalk cliff failure will be given later in this chapter.

Influence of under-cutting the toe of a slope

It is not unusual for the toe of a slope to be under-cut, either intentionally by mining or by natural agencies such

the weathering of underlying strata or, in the case of sea cliffs, by the action of waves. The influence of such under-cutting on the stability of the slope is important in many practical situations and an analysis of this stability is presented here.

In order to provide as general a solution as possible, it is assumed that the geometry of the slope is as illustrated in the sketch opposite. A previous failure is assumed to have left a face inclined at ψ_f and a vertical tension crack of depth z_1. As a result of an under-cut of ΔH, inclined at an angle ψ_o, a new failure occurs on a plane inclined at ϕ_p and involves the formation of a new tension crack of depth z_2.

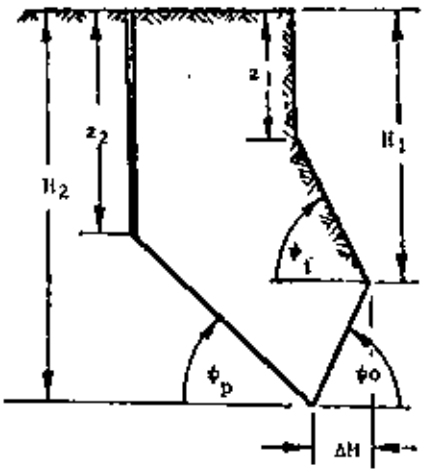

Geometry of under-cut slope

The factor of safety of this slope is given by equation 32 but it is necessary to modify the expression for the weight term as follows :

$$W = \tfrac{1}{2}\gamma\left[(H_2^2 - z_2^2)\mathrm{Cot}\phi_p - (H_1^2 - z_1^2)\mathrm{Cot}\psi_f + (H_1 + H_2)\Delta H\right] \quad (51)$$

Note that, for $\psi_o > 0$,

$$\Delta H = (H_2 - H_1)\mathrm{Cot}\psi_o \quad (52)$$

The critical tension crack depth, for a dry under-cut slope, is given by

$$z_2 = \frac{c.\ \mathrm{Cos}\phi}{\gamma\ \mathrm{Cos}\psi_p.\ \mathrm{Sin}(\phi_p - \phi)} \quad (53)$$

The critical failure plane inclination is

$$\phi_p = \tfrac{1}{2}\left(\phi + \mathrm{Arctan}\ \frac{H_2^2 - z_2^2}{(H_1^2 - z_1^2)\mathrm{Cot}\psi_f - (H_1 + H_2)\Delta H}\right) \quad (54)$$

The application of this analysis to an actual slope problem is presented at the end of this chapter.

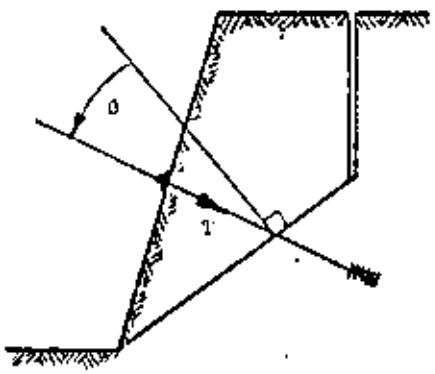

Reinforcement of a slope

Reinforcement of a slope

When it has been established that a particular slope is unstable, it becomes necessary to consider whether it is possible to stabilise the slope by drainage or by the application of external loads. Such external loads may be applied by the installation of rock bolts or cables anchored into the rock mass behind the failure surface or by the construction of a waste rock berm to support the toe of the slope.

The factor of safety of a slope with external loading of magnitude T, inclined at an angle θ to the failure plane as shown in the sketch opposite, is given by

$$F = \frac{cA + (W.\mathrm{Cos}\psi_p - U - V.\mathrm{Sin}\psi_p + T.\mathrm{Cos}\theta)\mathrm{Tan}\phi}{W.\mathrm{Sin}\phi_p + V.\mathrm{Cos}\psi_p - T.\mathrm{Sin}\theta} \quad (55)$$

This equation gives an indication of the influence of reinforcing upon the factor of safety of a slope. The decision on whether such reinforcing is either practical or economically feasible will depend upon other considerations which are best illustrated by practical examples such as

Back analysis of failed slopes

From the discussion on shear strength testing in chapter 5, the reader will have been left in little doubt about the difficulties of determining shear strength values, particularly the cohesive strength, from small scale laboratory type tests. As a result of these difficulties, many slope engineers prefer to base their designs on shear strength values determined by back analysis of full scale slope failures in the field. The method used for carrying out such a back analysis, for slopes in which two-dimensional plane failures have occurred, is described below.

When a failure has taken place, the implication is that the factor of safety of that particular slope has fallen to a value of unity. Putting F = 1 and rearranging equations 32 and 38 gives the following relationships between the cohesion c and the friction angle ϕ which are mobilised at failure.

$$c = \frac{W.\mathrm{Sin}(\phi_p - \phi) + V.\mathrm{Cos}(\phi_p - \phi) + U.\mathrm{Sin}\phi}{A.\mathrm{Cos}\phi} \qquad (56)$$

alternatively

$$c = \frac{\gamma H}{2P}\left(q(1 - \mathrm{Cot}\psi_p.\mathrm{Tan}\phi) + RS(\mathrm{Cot}\phi_p + \mathrm{Tan}\phi) + RP.\mathrm{Tan}\phi\right) \qquad (57)$$

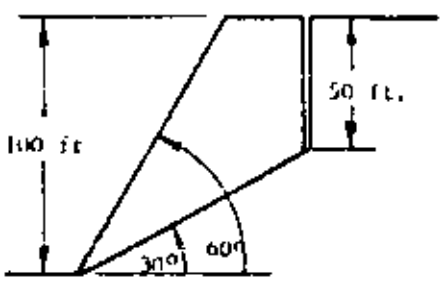

Slope geometry for example of back analysis.

In order to demonstrate the application of these equations, consider the hypothetical example illustrated in the sketch opposite. The values of cohesion c and friction angle ϕ mobilised at failure are determined, using equation 57 and figure 64, for the following conditions :

A - Dry slope with no tension crack (R = S = z/H = 0)
B - Dry slope with tension crack (R = S = 0)
C - Slope with water in tension crack only (R,P = 0)
D - Slope with water-filled tension crack and water pressure on sliding surface ($z_w = z$)

The results of this analysis are plotted in figure 69 which shows the range of friction angles and cohesive strengths which satisfy the conditions of limiting equilibrium for the slope geometry considered.

In an actual slope problem, examination of the failed slope would reveal whether a tension crack had been present and an enquiry into the rainfall conditions before the failure would enable the engineer to decide which of the conditions examined could be regarded as representative of the condition of the slope at the time of failure. A few simple shear tests * would give an indication of the angle of friction of the discontinuity surface upon which sliding had taken place and, considering all these facts, the cohesion mobilised at failure could be established.

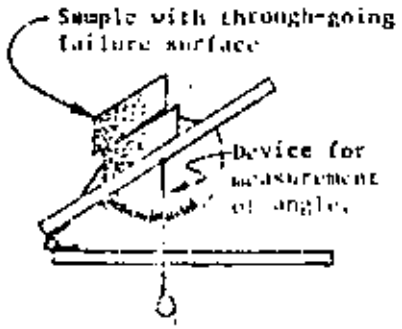

Simple test for estimating friction angle of sliding surface.

* When a clearly defined failure surface exists, a reasonable estimate of its angle of friction can be obtained by a simple tilt test in which the inclination required to cause sliding of one half of a specimen upon the other is measured as illustrated in the sketch opposite [9].

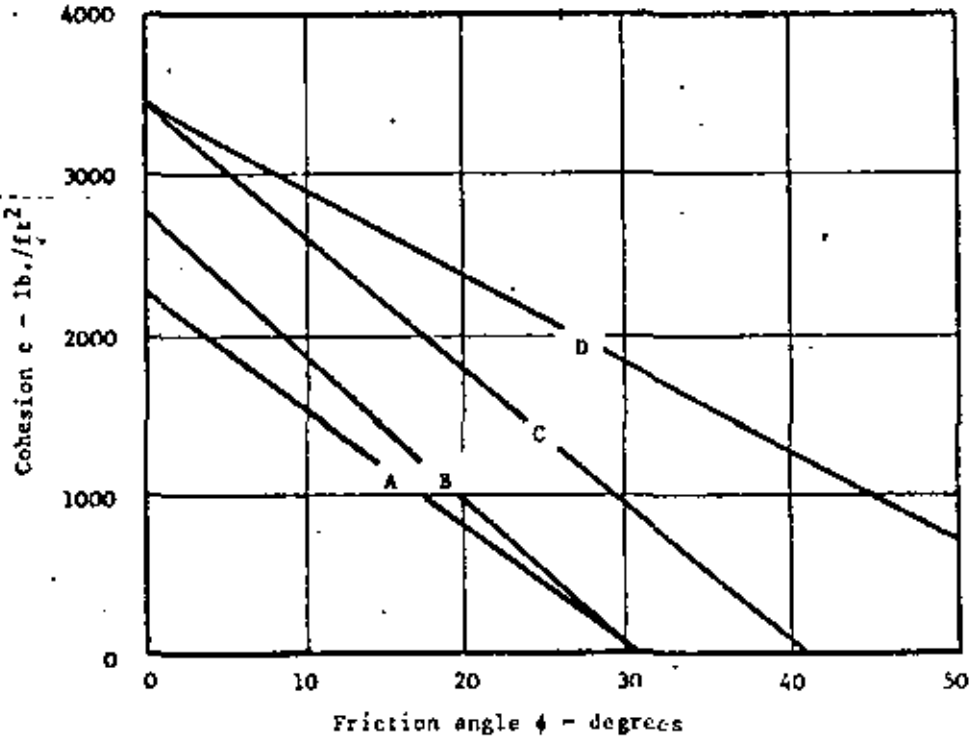

Figure 69: Friction angle and related cohesion mobilised at failure for various conditions considered in hypothetical example discussed on page 149.

The example considered in deriving the values plotted on figure 69 is one in which two-dimensional plane failure has been assumed. The same approach can obviously be used to analyse the shear strength mobilised at failure in the case of wedge or circular slope failures (discussed in chapters 8 and 9 respectively). Many such back analyses have been carried out and a fair number of them have been adequately written-up for publication. These published case histories provide an invaluable source of data on real shear strength data and the authors recommend that every slope engineer should make a point of collecting such data whenever he comes across it in the literature. A good collection of this data provides a valuable check on the reasonableness of shear strength values which the slope engineer proposes to use in his own designs. It is particularly important in times of crisis when it is not possible to carry out tests and when shear strength values have to be estimated.

One of the authors (E.H.) has collected shear strength data from back analyses for several years and a selection of this data is presented in figure 70. The numbered points on this plot are identified in table III which also lists

the sources of the data.

Also included above and to the right of this plot are a set of notes which provide a rough engineering classification of the various areas of the graph. The authors have found this classification to be useful but they accept that a classification is something upon which no two engineers are likely to agree and, consequently, suggest that the reader may prefer to add his own notes to his own collection of shear strength data.

TABLE III - SOURCES OF SHEAR STRENGTH DATA PLOTTED IN FIGURE 70

Point number	Material	Location	Analysed by	Reference
1	Disturbed slates and quartzites.	Knob Lake, Canada	Coates, Cyenge and Stubbins	134
2	Soil	-	Whitman and Bailey	135
3	Jointed porphyry	Rio Tinto, Spain	Hoek	80
4	Ore body hanging wall	Grangesborg, Sweden	Hock*	136
5	Maximum height and angle of excavated slopes - see figure 7 on page 20			
6	Bedding planes in limestone	Somerset, England	Roberts and Hock	138
7	London clay	England	Skempton and Hutchinson	139
8	Gravelly alluvium	Pima, Arizona	Hamel	140
9	Faulted rhyolite	Ruth, Nevada	Hamel	141
10	Sedimentary series	Pittsburgh, Pennsylvania	Hamel	142
11	Kaolinised granite (China clay)	Cornwall, England	Ley	143
12	Clay shale	Fort Peck Dam, Montana	Middlebrooks	144
13	Clay shale	Gardiner Dam, Canada	Fleming *et al*	145
14	Chalk	Chalk cliffs, England	Hutchinson	146
15	Bentonite/clay	Oahe Dam, South Dakota	Fleming *et al*	145
16	Clay	Garrison Dam, North Dakota.	Fleming *et al*	145

* This point represents the shear strength mobilised in the failure of the hanging wall of an ore body, induced by caving of the ore at Grangesborg in Sweden. The values were obtained by Hock as a result of a re-analysis of data published by Hall and Bolt [137]. Note that this magnitude of cohesion should not be used for slope design purposes unless detailed geological investigations had shown that no unfavourable structural discontinuities were present in the rock mass.

277

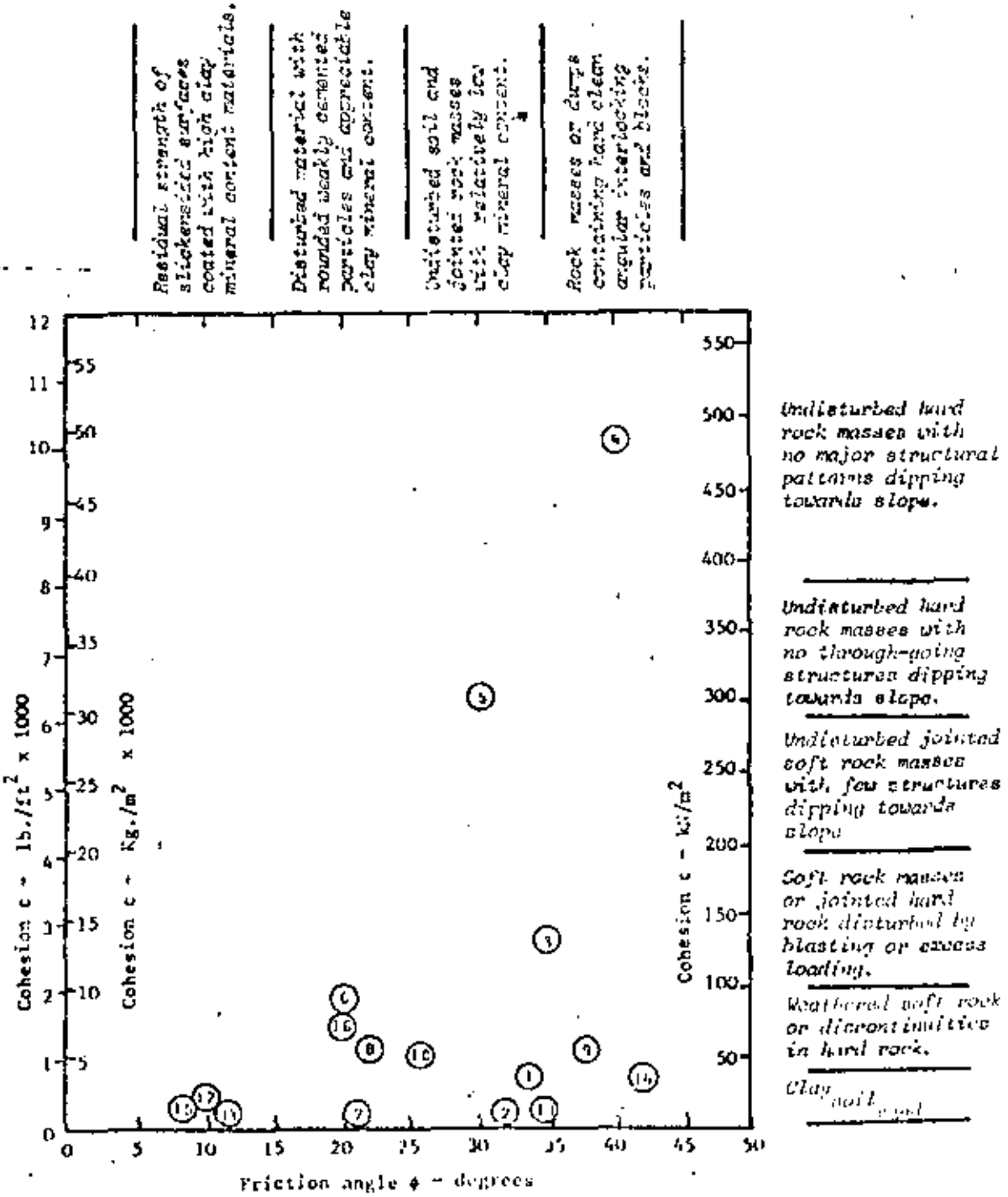

Figure 70: Relationship between friction angle and cohesion mobilised at failure for slope failures listed in table III.

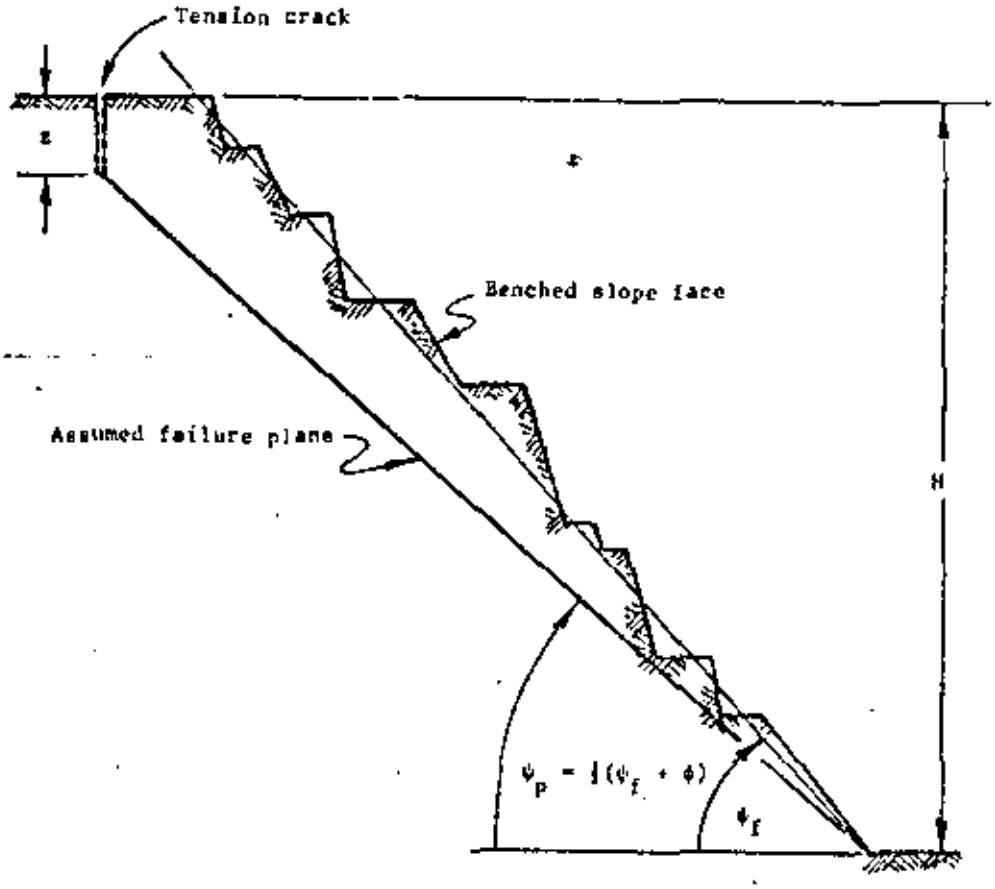

Figure 70 : Section through a typical porphyry slope in the Atalaya open pit at Rio Tinto in Spain.

It was assumed that these tension cracks would occur in all slopes, including those with factors of safety in excess of unity, and the typical failure geometry is illustrated in figure 70 above.

The factor of safety for a dry slope is defined by equation 45 on page 141 which, for the purposes of this analysis, can be rearranged in the following form :

$$H = \frac{2c.P}{\gamma Q(F - Cot\psi_p.Tan\phi)} \qquad (58)$$

Solving equations 50,48,39 and 40 for a range of slope angles gives the following :

ψ_f	ψ_p	z/H	P	Q	H
85	60.0	0.610	0.450	0.238	0.90c/F - 0.484
80	57.5	0.474	0.624	0.268	1.25c/F - 0.446
70	52.5	0.311	0.868	0.261	1.76c/F - 0.537
60	47.5	0.206	1.077	0.221	2.15c/F - 0.641
50	42.5	0.123	1.300	0.159	2.60c/F - 0.764
40	37.5	0.064	1.572	0.097	3.14c/F - 0.915

279

Practical example number 1

Stability of porphyry slopes in a Spanish open pit mine

In order to assist the mine planning engineers in designing an extension to the Atalaya open pit operated by Rio Tinto Española in Southern Spain, an analysis was carried out on the stability of the porphyry slopes forming the northern side of the pit (the left hand side of the pit in the photograph reproduced in figure 43 on page 99). A summary of this analysis is presented in this example.

At the time of this design study (1969), the Atalaya pit was 260 meters deep and the porphyry slopes, inclined at an overall angle of approximately 45° as shown in figure 70, appeared to be stable. The proposed mine plan called for deepening the pit to an excess of 300 meters and required that, if at all possible, the porphyry slopes should be left untouched. The problem, therefore, was to decide whether these slopes would remain stable at the proposed mining depth.

Since no slope failures had taken place in the porphyry slopes of the Atalaya pit, deciding upon the factor of safety of the existing slopes posed a difficult problem. Geological mapping and shear testing of discontinuities in the porphyry (figures 40 and 41 on page 97) provided a useful guide to the possible failure modes and the range of shear strengths which could be expected but this range was too wide to permit the factor of safety to be determined with a reasonable degree of confidence.

Consequently, it was decided to use a technique similar to that employed by Salamon and Munro [147] for the analysis of coal pillar failures in South Africa. This method involved collecting data on slope heights and slope angles for both stable and unstable slopes in porphyry in order to establish a pattern of slope behaviour based upon full scale slopes. The data on unstable slopes had to be collected from other open pit mines in the Rio Tinto area in which failures had occurred in porphyrys judged to be similar to those in the Atalaya pit. The collected slope height versus slope angle data are plotted in figure 71.

In order to establish the theoretical relationship between slope height and slope angle, the following assumptions were made :

a. Because the geological mapping had failed to reveal any dominant through-going structures which could control the stability of the slopes in question but had revealed the presence of a number of intersecting joint sets, it was assumed that failure, if it were to occur, would be on a composite planar surface inclined at $\psi_p = \frac{1}{2}(\psi_f + \phi)$ as defined by equation 50 on page 147.

b. From the shear strength data, figure 41 on page 97, the friction angle was chosen as $\phi = 35°$.

c. Because of the presence of underground workings, the porphyry slopes were assumed to be fully drained and it was assumed that tension cracks would occur in accordance with the critical conditions defined by equation 58 on page 161.

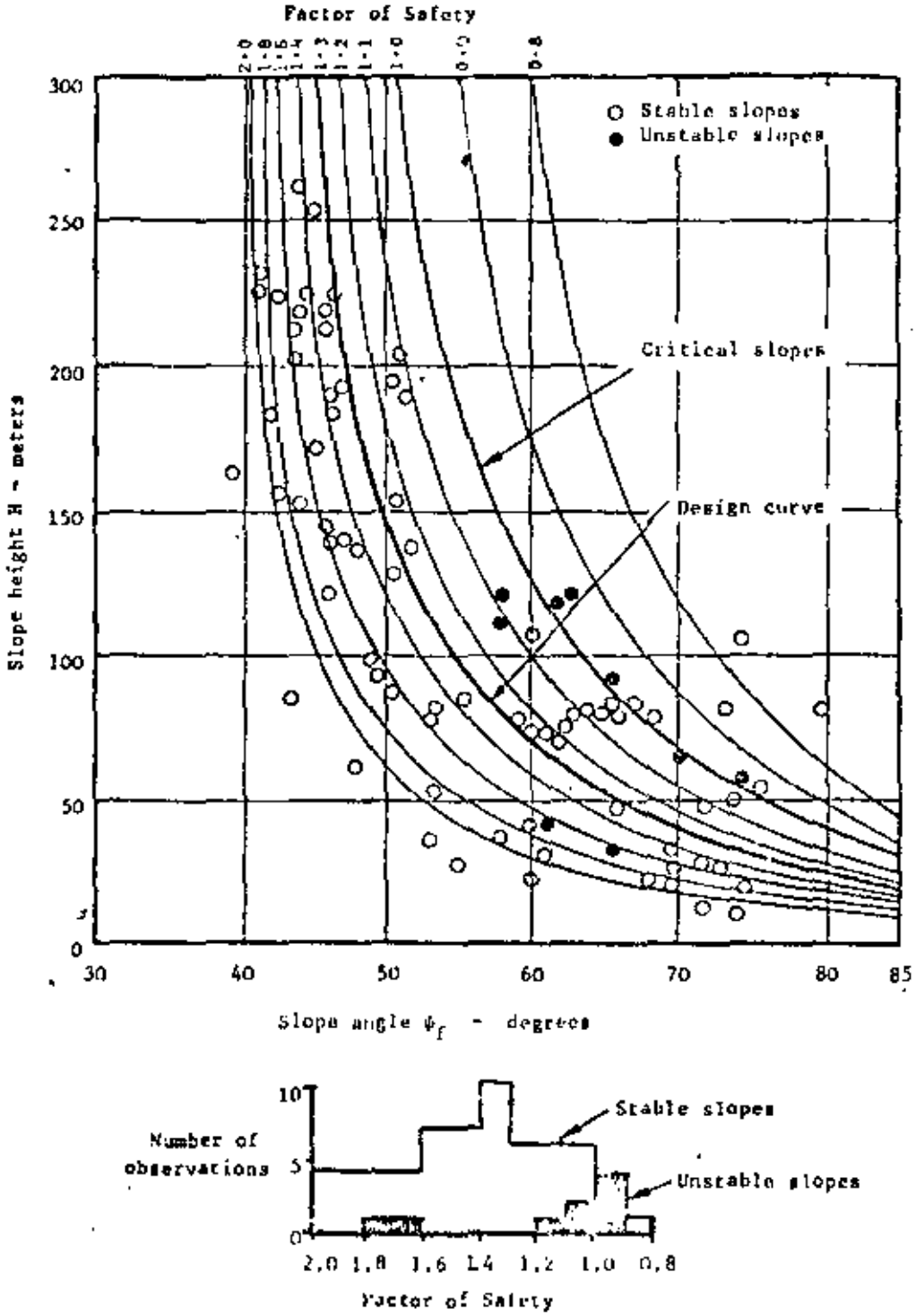

Figure 71 : Relationship between slope heights and slope angles for porphyry slopes in the Rio Tinto area, Spain.

281

The problem now is to find a value for the cohesion c which gives the best fit for a limiting curve (F = 1) passing through the slope height/slope angle points for unstable slopes. The two points at ψ_f = 61° and 66° and H = 40m and 35m respectively are ignored in this curve fitting since they were identified as individual bench failures on through-going discontinuities and they would not, therefore, belong to the same family as the other slopes.

A number of trial calculations showed that the best fit for the F = 1 curve to the seven failure point shown in figure 71 is given by a cohesive strength c = 14000 Kg/m^2 (1.4 Kg/cm^2 or 20 lb/in^2 for engineers who are used to working in smaller units)*.

Substitution of this value of c into the relationships for H listed in the table on page 154 (for different factors of safety) gives the curves which have been plotted in figure 71. By counting the number of points falling between factor of safety increments, it is possible to construct the histogram reproduced in the lower part of figure 71. This histogram confirms that the seven unstable slopes are tightly clustered around a factor of safety F = 1 while the stable slopes show a peak between 1.3 and 1.4.

From a general consideration of the anticipated working life of the slope and of the possible consequences of slope failure during the mining operations, it was concluded that a factor of safety of 1.3 would be acceptable for the porphyry slopes in the Atalaya pit and, hence, the design curve presented to the mine planning engineers is that shown as a heavy line in figure 71. This curve shows that, for the slope heights in excess of 250m under consideration, the factor of safety changes very little for a change in slope angle. It was therefore concluded that the proposed deepening of the pit would not decrease the overall stability of the porphyry slopes, provided that no major changes in rock mass properties or drainage conditions were encountered in this deepening process.

Before leaving this example it is important to point out that this analysis deals with the stability of the *overall* pit slope and not with possible failures of *individual benches*. In a large pit such as the Atalaya pit, it would be totally uneconomic to attempt to analyse the stability of each bench and, in any case, small bench failures are not particularly important in large pits provided that they do not influence haul roads. On the other hand, a failure of the wedge illustrated in figure 70, involving approximately 20000 tonnes/ meter of face (from equation 36 assuming γ = 2.95 tonnes/m^3) would obviously represent a very serious problem which has to be avoided. On the basis of the analysis presented in this example, the authors have every confidence that no major failures of the overall slopes will occur.

---

* In an earlier analysis of this problem, published by Hoek [80], a cohesive strength of [illegible] was found by using a set of approximate design charts. These charts have since been discarded in favour of the more accurate methods of analysis presented in the chapter but the conclusions reached in the original [illegible]

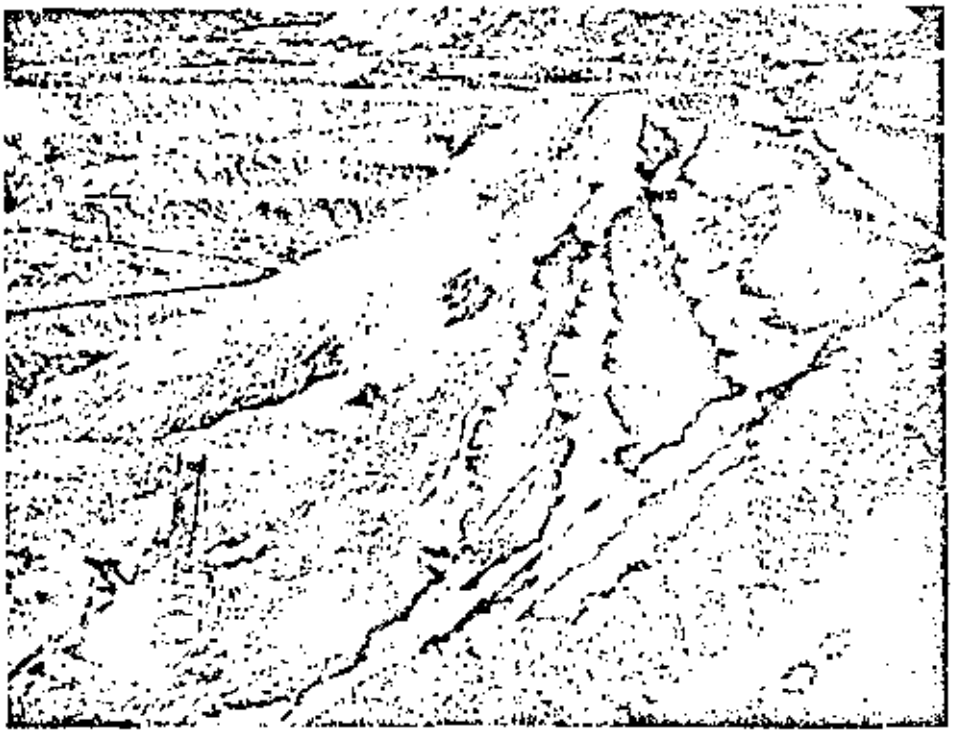

Figure 72 : Small failures of individual benches are not usually significant in open pit mining unless they cause disruption of haul roads.

Figure 73 : The open pit designer is primarily concerned with minimising the risk of overall slope failure ;

283 :

Practical example number 7

Investigation of the stability of a limestone quarry face

Figure 74 shows a hillside limestone quarry in the Mendip hills in England, owned and operated by the Amalgamated Roadstone Corporation *. This photograph was taken in 1968 after a slope failure had occurred during a period of exceptionally heavy rain.

In 1970, it was decided to expand the quarry facilities and this involved the installation of new plant on the floor of the quarry. In view of the large horizontal movement of material which had occurred in the 1968 slope failure (as shown in figure 74), it was considered that an investigation of the stability of the remainder of the slope was necessary. This example gives a summary of the most important aspects of this stability study , full details of which have been published by Roberts and Rock[138].

The 1968 failure occurred after a week or more of steady soaking rain had saturated the area. This was followed by an exceptionally heavy downpour which flooded the upper quarry floor, filling an existing tension crack in the slope crest. The geometry of the failure is illustrated in figure 75. As seen in figure 74, the failure is basically two-dimensional , the sliding surface being a bedding plane striking parallel to the slope crest and dipping into the excavation at 20°. A vertical tension crack existed 41 feet behind the slope crest at the time of failure.

In order to provide shear strength data for the analysis of the stability of the slope under which the new plant was to be installed, it was decided to analyse the 1968 failure by means of the graphical method described in figure 65 on page 140.

Assuming a rock density of 0.08 tons/ft^3 (160 lb/ft^3)
and a water density of 0.031 tons/ft^3 (62.4 lb/ft^3);

Weight of sliding mass $W = \frac{1}{2}\gamma(XH - Dz) = 404.8$ tons/ft.

Horizontal water force $V = \frac{1}{2}\gamma_w.z_w^2 = 85.5$ tons/ft.

Uplift water force $U = \frac{1}{2}\gamma_w.z_w.A = 110.8$ tons/ft.

From the force diagram , figure 76a, the shear strength mobilised in the 1968 failure can be determined and this is plotted in figure 76b.

From an examination of the surface upon which failure had taken place in 1968, it was concluded that the friction angle was probably 20° ± 5° . This range of friction angles and the associated cohesive strengths, shown in figure 76b, are used to determine the stability of the overall slopes in this illustrative example **.

---

* Now Amey Roadstone Corporation.

** In the original analysis, a more severe water pressure distribution was assumed and this resulted in a higher cohesive strength than that found in this analysis. Since the same water pressure distribution was assumed for the

284

Figure 74 : Air photograph of Amalgamated Roadstone Corporation's Batts Combe limestone quarry in Somerset, England showing details of the 1962 slope failure (Roberts and Hoek [136]).

285

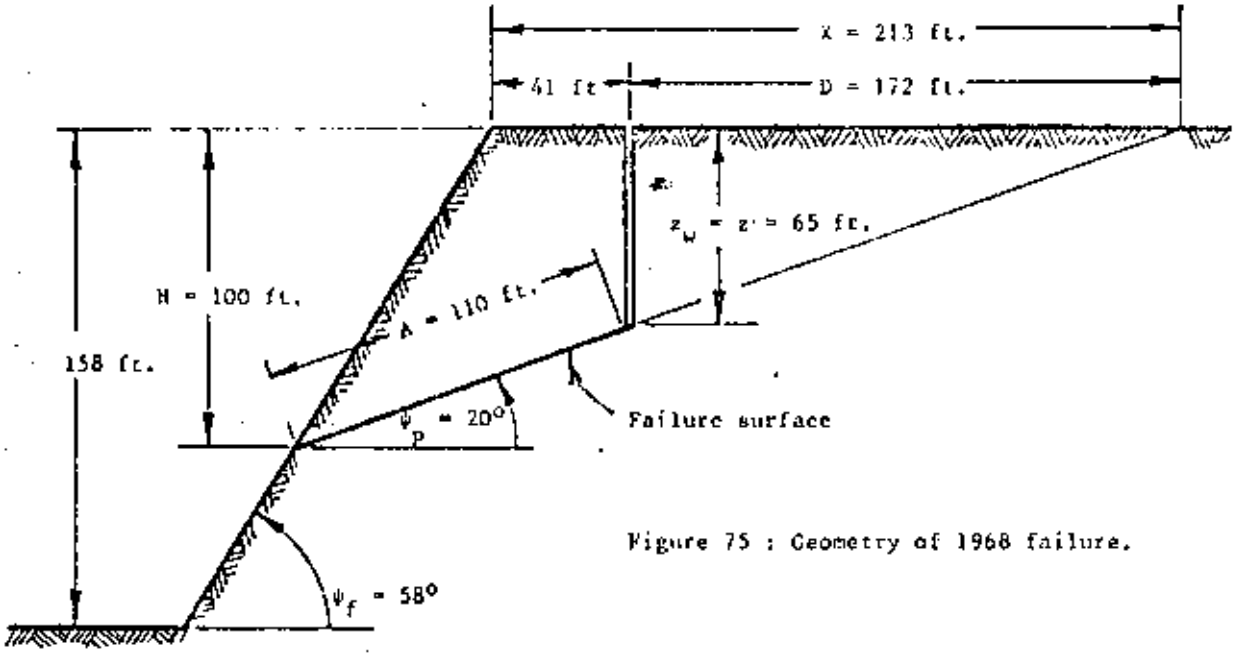

Figure 75 : Geometry of 1968 failure.

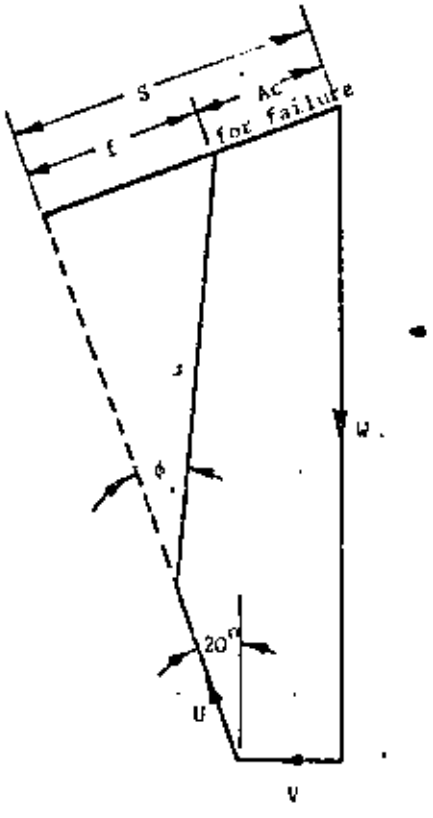

a. Force diagram

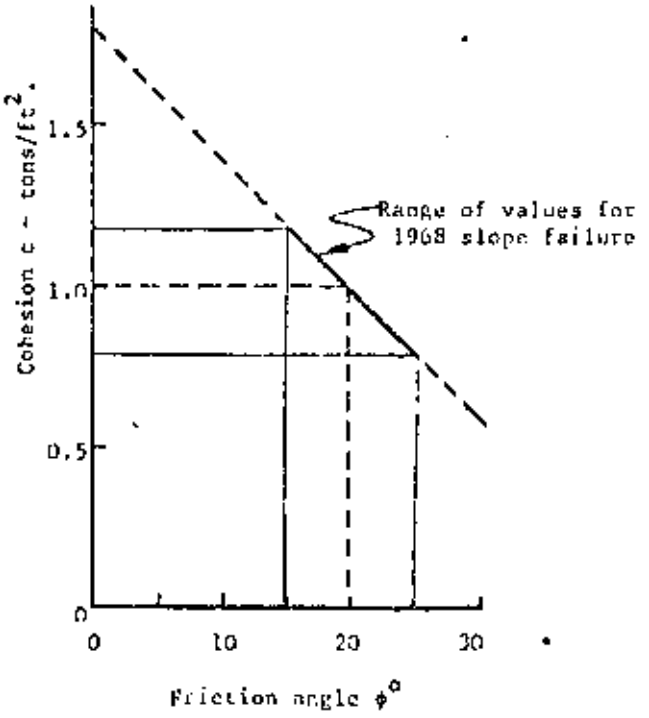

b. Shear strength mobilised

Figure 76 : Determination of shear strength mobilised in 1968 failure.

286

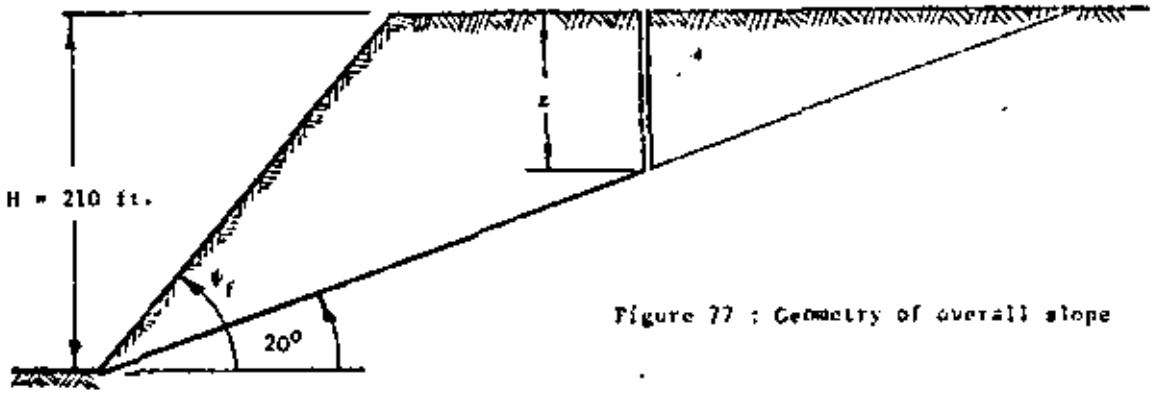

Figure 77 : Geometry of overall slope

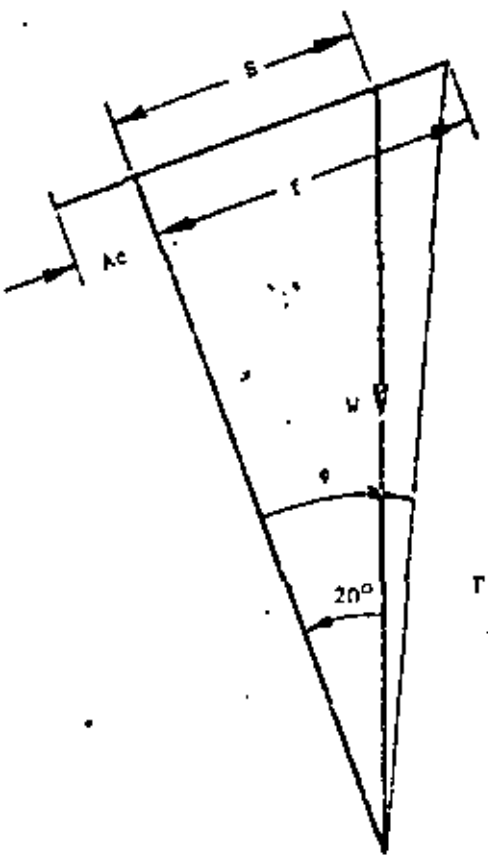

Factor of Safety

$$F = \frac{(Ac + t)}{S}$$

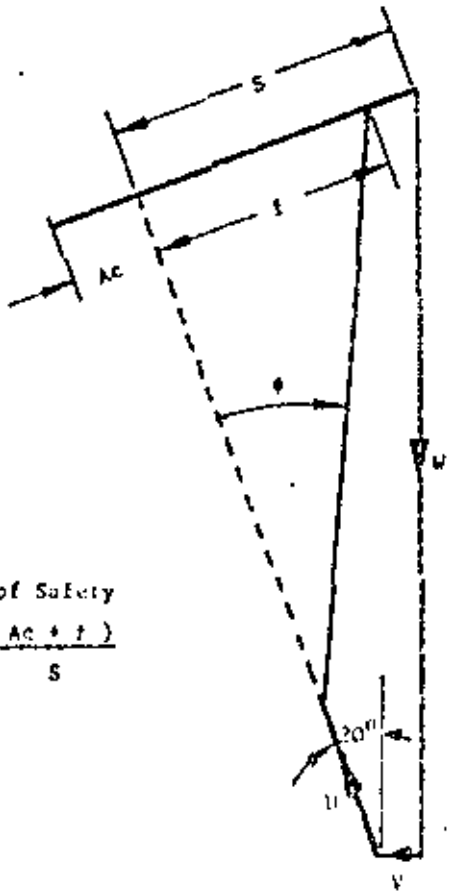

a. Dry slope

b. Saturated slope

Figure 78 : Force diagrams for design of overall quarry slopes .

287

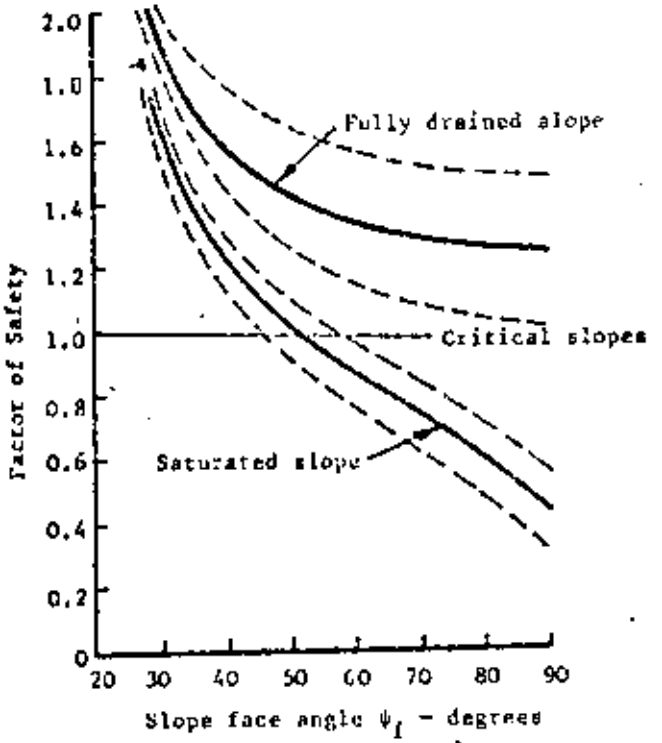

Figure 79 : Factor of safety for dry and saturated slopes with different face angles.

Having established the range of shear strengths mobilised in the 1968 failure, these values were now used to check the stability of the 210 ft. high slopes under which the new plant was to be installed. The geometry of the slope analysed is illustrated in figure 77 which shows that , in order to provide for the worst possible combination of circumstances, it was assumed that the bedding plane on which the 1968 slide had occurred daylights in the toe of the slope.

Figure 78 shows typical force diagrams for dry and saturated slopes, assuming a slope face angle $\psi_f = 50^\circ$ and a friction angle $\phi = 25^\circ$. A range of such force diagrams were constructed and the factors of safety determined from these constructions are plotted in figure 79 above. In this figure the full lines are for a friction angle $\phi = 20^\circ$, considered the most probable value, while the dashed lines define the influence of a 5° variation on either side of this angle.

It is clear from figure 79 that 50° slopes are unstable under the heavy rainfall conditions which caused the slopes to become saturated in 1968. Drainage of the slope, particularly the control of surface water which could enter the top of an open tension crack, is very beneficial but, since it cannot be guaranteed that such drainage could be fully effective, it was recommended that the slope should also be

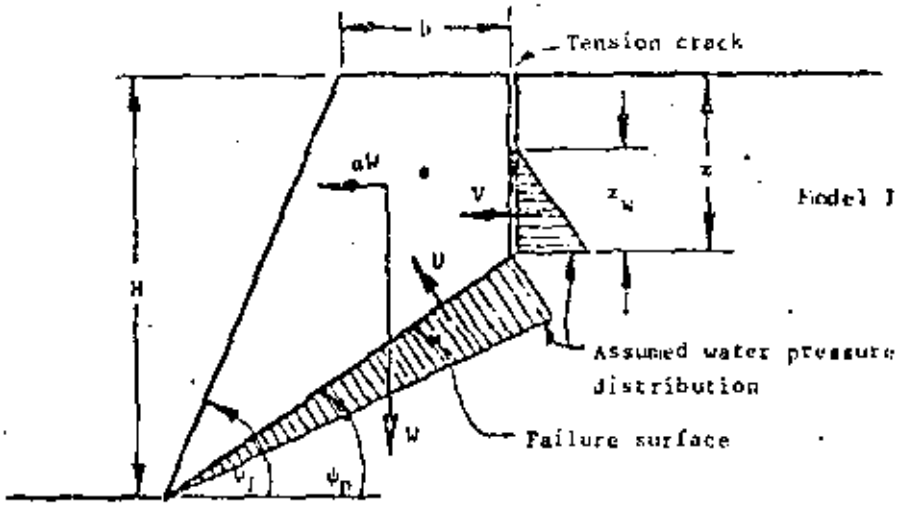

$$F = \frac{cA + \{W(\cos\psi_p - a\sin\psi_p) - U - V\sin\phi_p\}\tan\phi}{W(\sin\psi_p + a\cos\psi_p) + V\cos\phi_p} \quad (59)$$

Where

$$z = H(1 - \sqrt{\cot\psi_f \cdot \tan\phi_p}) \quad (48)$$

$$A = (H - z)\,\mathrm{Cosec}\phi_p \quad (33)$$

$$W = \tfrac{1}{2}\gamma H^2\{(1 - (z/H)^2)\cot\phi_p - \cot\phi_f\} \quad (36)$$

$$U = \tfrac{1}{2}\gamma_w \cdot z_w \cdot A \quad (34)$$

$$V = \tfrac{1}{2}\gamma_w \cdot z_w^2 \quad (35)$$

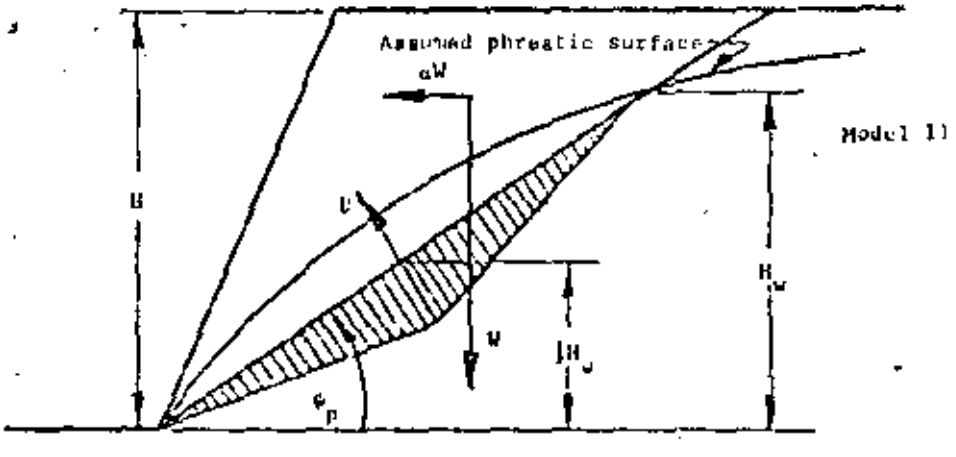

$$F = \frac{cA + \{W(\cos\psi_p - a\sin\psi_p) - U\}\tan\phi}{W(\sin\psi_p + a\cos\psi_p)} \quad (60)$$

Where

$$U = \tfrac{1}{2}\gamma_w H_w^2\,\mathrm{Cosec}\psi_p \quad (61)$$

Figure 81 : Theoretical models for example number 3.

293

of the slope to the different conditions to which it is likely to be subjected.

Summarising the available input data :

Slope height	H = 60m
Overall slope angle	ϕ_f = 50°
Bench face angle	ϕ_f = 70°
Bench height	H = 20m
Failure plane angle	ϕ_p = 35°
Rock density	γ = 2.6 tonnes/m^3
Water density	γ_w = 1.0 tonnes/m^3
Earthquake acceleration	a = 0.08g

Substituting in equations 59 and 60 :

Overall slopes Model I

$$F = \frac{80.2c + (1850 - 40.1z_w - 0.287z_w^2)\tan\phi}{1529 + 0.410z_w^2} \qquad (62)$$

Overall slopes Model II (Note z = 0)

$$F = \frac{104.6c + (2132 - 0.436H_w^2)\tan\phi}{1762} \qquad (63)$$

Individual benches Model I

$$F = \frac{17.6c + (287.1 - 8.8z_w - 0.287z_w^2)\tan\phi}{237.3 + 0.410z_w^2} \qquad (64)$$

Individual benches Model II

$$F = \frac{34.9c + (428.0 - 0.436H_w^2)\tan\phi}{353.7} \qquad (65)$$

One of the most useful studies which can be carried out with the aid of equations 62 to 65 is to find the shear strength which would have to be mobilised for failure of the overall slope or for the individual benches. Figure 84 gives the results of such a study and the numbered lines on this plot represent the following conditions :

1 - Overall slope, Model I , dry , z_w = 0.
2 - Overall slope, Model I , saturated, z_w = z = 14m.
3 - Overall slope, Model II, dry, H_w = 0.
4 - Overall slope, Model II, saturated, H_w = H = 60m.
5 - Individual bench, Model I, dry, z_w = 0.
6 - Individual bench, Model I, saturated, z_w = z = 9.9m.
7 - Individual bench, Model II, dry, H_w = 0.
8 - Individual bench, Model II, saturated, H_w = H = 20m.

The reader may feel that a consideration of all these possibilities is unnecessary but it is only coincidental that, because of the geometry of this particular slope, the shear strength values found happen to fall reasonably close together. In other cases, one of the conditions may be very much more critical than the others and it would take a very experienced slope engineer to detect this condition without going through the calculations required to produce figure 84. In any case, these calculations should only take about one hour with the aid of a calculating machine and this is a very reasonable investment of time when lives and property may be in danger.

296

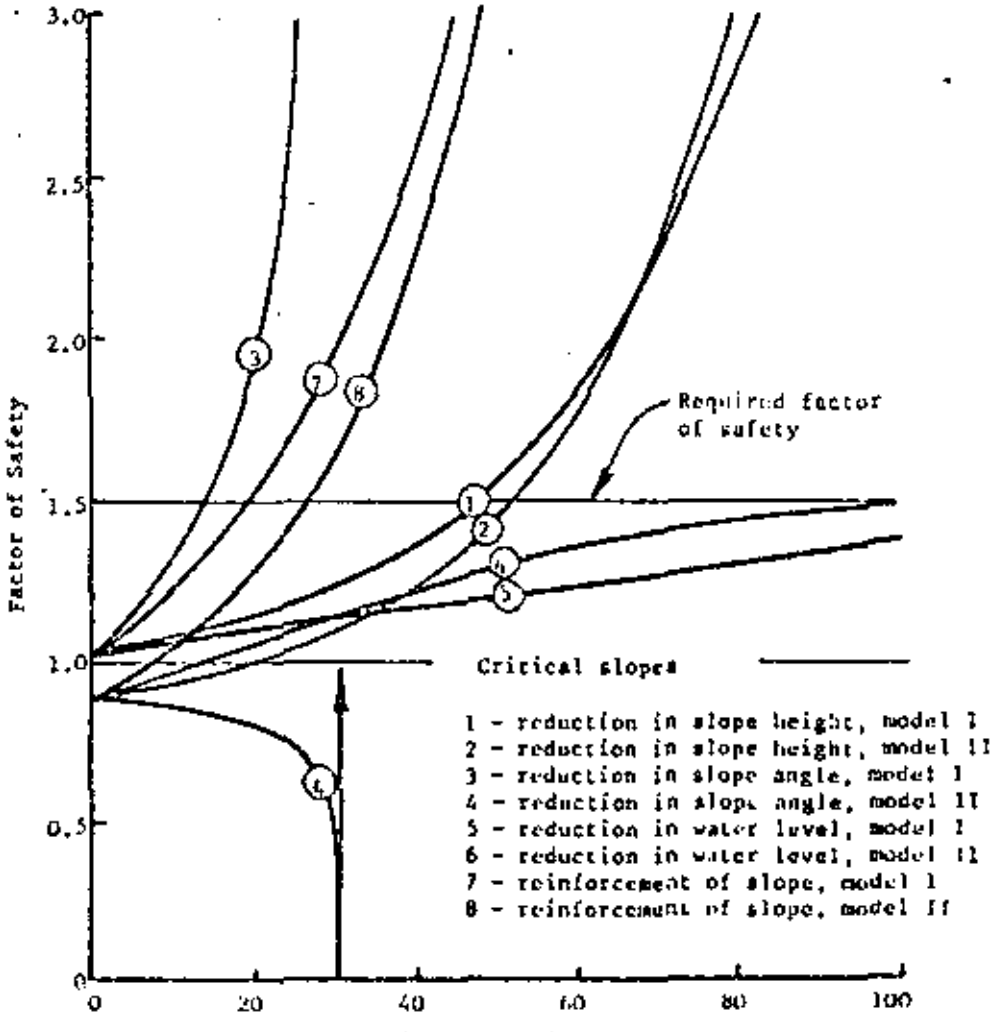

Figure 85 : Comparison between alternative methods of increasing stability of overall slope considered in example 3 .

the term $Cot\psi_f$ and hence both z and W are decreased as the slope face angle ψ_f is reduced. A reduction in tension crack depth reduces both water forces U and V and the final result is a dramatic increase in factor of safety for a decrease in slope face inclination. Note that, if the tension crack occurs *before* the slope is flattened, the tension crack depth z will remain unaltered at 14m and the water forces U and V will remain at their maximum values. Under these conditions, the factor of safety will still be increased for a reduction in slope face inclination but not to the same extent as shown by line J in figure 85.

In the case of model II in figure 83, it is only the weight term which is altered by the reduction in slope angle and, because the uplift force term U $\tan\phi$ is greater than the cohesive force cA, the factor of safety actually *reduces* as the slope face is flattened. As the slope face angle approaces the failure plane angle, the thin sliver of material resting on the failure plane will be floated off by the excess water force U. Although many practical arguments could be put forward to show that this extreme behaviour would be very unlikely, the example does illustrate the danger of indiscriminate alteration of the slope geometry without having first considered the possible consequences. The practical conclusion to be drawn from this discussion is that, if model II in figure 83 is representative of the conditions which exist in an actual slope, partial flattening of the slope would achieve no useful purpose. The wedge of rock resting on the failure plane would have to be *removed entirely* if it was decided that flattening the slope was the only means to be used for increasing the stability.

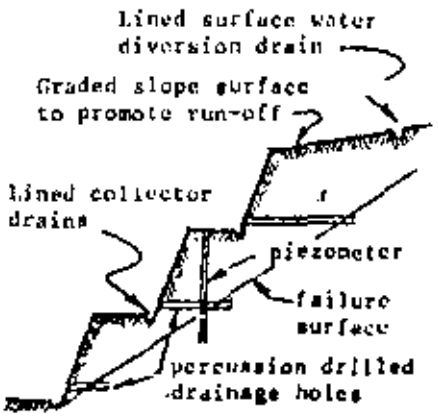

Possible drainage measures

Drainage of the slope is probably the cheapest remedial measure which can be employed and, as shown in figure 85, complete drainage, if this could be achieved, would increase the factor of safety to very nearly the required value. Unfortunately, complete drainage can never be achieved and hence, in this particular slope, drainage would have be supplemented by some other remedial measure such as bolting in order to produce an acceptable level of safety. In any event, nothing would be lost by the provision of some drainage and the authors would recommend careful consideration of surface water control and also the drilling of horizontal drain holes to intersect the potential failure surface.

Reinforcing the slope by means of bolts or cables may create a useful illusion of safety but, unless the job is done properly, the result would be little more than an illusion. In order to achieve a factor of safety of 1.5, assuming the bolts or cables to be installed in a horizontal plane, the total force required amounts to about 500 tonnes per meter of slope length. In other words, the complete reinforcement of a 100 meter face would require the installation of 500 one hundred tonne capacity cables. Simultaneous drainage of the slope, even if only partially successful, would reduce this number by about one half but reinforcing a slope of this size would obviously be a very costly process.

Considering all the facts now available, the authors would

298

offer the following suggestions to the engineer responsible for the hypothetical slope which has been under discussion in this example :

a. Immediate steps should be taken to have a series of standpipe piezometers (see page 127) installed in vertical drillholes from the upper slope surface or from one of the benches. The importance of groundwater has been clearly demonstrated in the calculations which have been presented and it is essential that further information on possible groundwater flow patterns should be obtained.

b. If diamond drilling equipment of reasonable quality is readily available, the vertical holes for the piezometers should be cored. A geologist should be present during this drilling programme and should log the core immediately upon removal from the core barrel. Particular attention should be given to establishing the exact position of the sheet joint or joints so that an accurate cross-section of the slope can be constructed. If adequate diamond drilling equipment is not available, the piezometer holes may be percussion drilled.

c. As soon as the piezometers are in position and it has been demonstrated that groundwater is present in the slope, horizontal drainholes should be percussion drilled into the bench faces to intersect the sheet joints. These holes can be drilled at an initial spacing of about 10 meters and their effectiveness checked by means of the piezometers. The hole spacing can be increased or decreased according to the water level changes observed in the piezometers.

d. During this groundwater control programme, a careful examination of the upper surface of the slope should be carried out to determine whether open tension cracks are present and whether any recent movements have taken place in the slope. Such movements would be detected by cracks in concrete or plaster or by displacements of vertical markers such as telephone poles. If the upper surface of the slope is covered by overburden soil, it may be very difficult to detect cracks and it may be necessary to rely upon the reports of persons resident on or close to the top of the slope.

e. Depending upon the findings of this examination of the upper slope surface, a decision could then be made on what surface drainage measures should be taken. If open tension cracks are found, these should be filled with gravel and capped with an impermeable material such as clay. The existence of such cracks should be taken as evidence of severe danger and serious consideration should be given to remedial measures in addition to drainage.

f. Further geological mapping to confirm the geological structure of the slope, together with the evidence on groundwater and tension cracks, would provide information for a review of the situation to decide upon the best means of permanent stabilisation, in addition to the drainage measures which have already been implemented.

299

Practical example number 4

Chalk cliff failure induced by undercutting

Hutchinson [146] has described the details of a chalk cliff failure at Joss Bay on the Isle of Thanet in England. This failure, induced by the undercutting action of the sea, provides an interesting illustration of the analysis of undercutting discussed on page 148 and Hutchinson's data is reanalysed on the following pages.

The failure is illustrated in the photograph reproduced in figure 86 and a cross-section, reconstructed from the paper by Hutchinson, is given in figure 87. Apart from a thin capping of overburden and the presence of a few flint bands, the chalk is reasonably uniform. Bedding is within one degree of horizontal and two major joint sets, both almost vertical, are present. The cliff face is parallel to one of these joint sets.

Measurement of water levels in wells near the coast together with the lack of face seepage caused Hutchinson to conclude that the chalk mass in which the failure occurred could be taken as fully drained. Since the failure does not appear to have been associated with a period of exceptionally heavy rain, as was the case of the quarry failure discussed in example number 2, the possibility of a water-filled tension crack is considered to be remote and will not be included in this analysis. The interested reader is left to check the influence of various water pressure distributions upon the behaviour of this slope.

Laboratory tests on samples taken from the cliff face gave a density of 1.9 tonnes/m^3 and a friction angle of about 42° for the peak strength and 30° for the residual strength. The cohesive strength ranged from 13.3 tonnes/m^2 for the peak strength to zero for the residual strength. Since this failure can be classed as a fall in which relatively little movement may have taken place before failure, as opposed to a slide in which the shear strength on the failure plane is reduced to its residual value by movements before the actual failure, there is some justification for regarding the peak strength of the chalk as relevant for this analysis. The purpose of this analysis is to determine the shear strength mobilised in the actual failure and to compare this with the laboratory values.

Summarising the available input data :

H = slope height ($H_1 = H_2$)	15.4m
z_1= original tension crack depth	6.8m
z_2= new tension crack depth	7.8m
ΔM= depth of undercut	0.5m
ψ_o= inclination of undercut	0°
ψ_f= slope face angle	80°
ϕ_p= failure plane angle	67°

The effective friction angle of the chalk mass can be determined by rearranging equation 54 on page 148 :

$$\phi = 2\phi_p - \text{Arctan}\ \frac{H_2^2 - z_2^2}{(H_1^2 - z_1^2)\text{Cot}\psi_f - (H_1 + H_2)\Delta M} \qquad (68)$$

Substitution gives $\phi = 49.9°$.

300

Figure 86 : Chalk cliff failure at Joss Bay, Isle of Thanet, England. (Photograph reproduced with permission of Dr.J.N.Hutchinson, Imperial College, London)

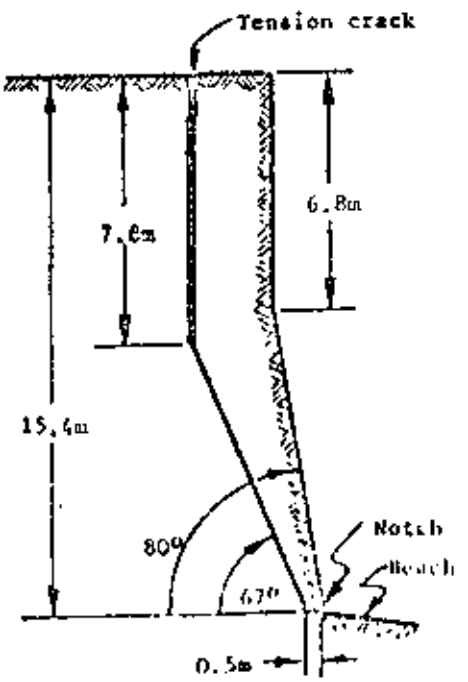

Figure 87 : Cross section of chalk cliff failure in Joss Bay.

301

This value is significantly higher than the friction angle of 42° measured on laboratory specimens but the influence of the roughness of the actual failure surface must be taken into account in comparing the results. The photograph reproduced in Figure 86 shows that this surface is very rough indeed and it is not surprising that a roughness angle i of almost 8° is indicated by this analysis (see discussion on page 83).

The cohesion mobilised at failure can be estimated by rearranging equation 53 on page 148:

$$c = \frac{\gamma z_2 \cos \psi_p \sin (\psi_p - \phi)}{\cos \phi} \qquad (69)$$

Substituting $z_2 = 7.8$ m, $\psi_p = 67°$ and $\phi = 49.9°$ gives $c = 2.64$ tonnes/m^2. As would be expected, this value is considerably lower than the value of $c = 13.3$ tonnes/m^2 determined by laboratory shear tests on intact chalk.

Hutchinson's paper (Figure 9) contains further data on the shear strength mobilised in chalk cliff failures at Wellington Gardens and Paragon Baths and this data is reproduced in Figure 88. The dashed curve, drawn on the basis of the relationship suggested by Figure 32 on page 86, suggests a strongly dilatant behaviour at low normal stresses and it will be seen that the line defined by $\tau = 2.64 + \sigma \tan 49.9°$ is a good tangent to the dashed curve. The evidence presented in Figure 88 suggests that the values of cohesion and friction angle determined from the failure geometry illustrated in Figure 87 are reasonable.

Before leaving this example, it is instructive to consider what will happen to the Joss Bay cliff as the sea continues to undercut its toe. The input data for the next step in the failure process is now as follows:

H	= slope height ($H_1 = H_2$)	15.4m
z_1	= original tension crack depth	7.8m
ψ_f	= slope face angle	67°
c	= cohesive strength of chalk mass	2.65 tonnes/m
ϕ	= friction angle of chalk mass	49.9°

The unknowns in this analysis are

z_2 = new tension crack depth

ψ_p = failure plane angle

Δx = depth of undercut

Since there are three unknowns and only two equations (53 and 54 on page 148), the solution to this problem is obtained in the following manner:

a. From equation 53, the depth of the tension crack z_2 is calculated for a range of possible failure plane angles (ψ_p). The results of this calculation are plotted in Figure 89. Since z_2 must lie between z_1 and H, Figure 89a shows that the angle of the failure plane ψ_p must lie between 67° and 56°.

302

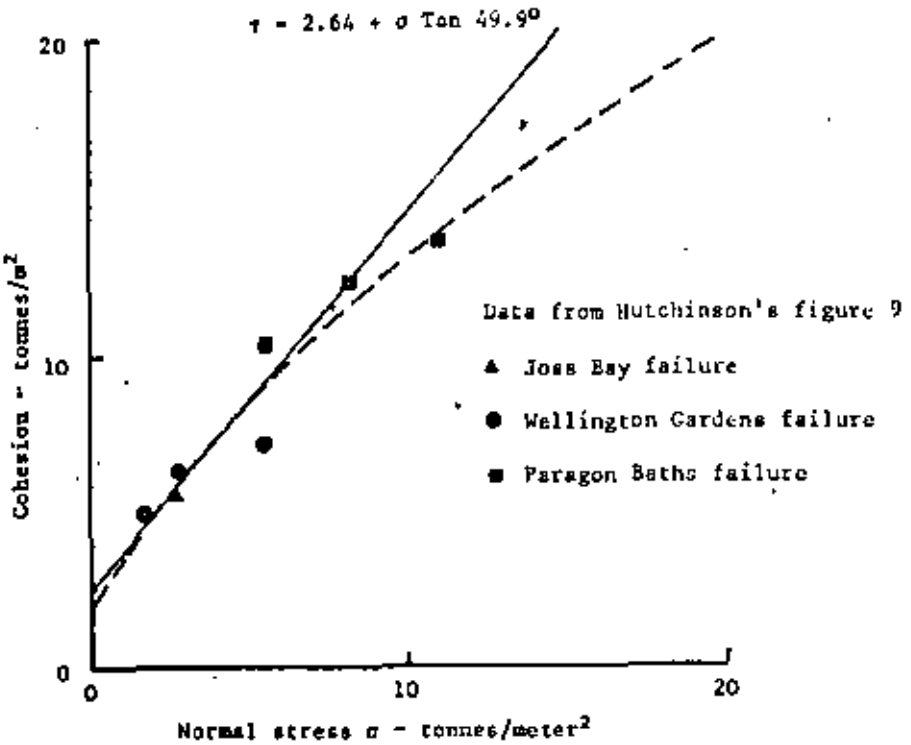

Figure 88 : Relationship between shear and normal stress for chalk cliff failures analysed by Hutchinson [146].

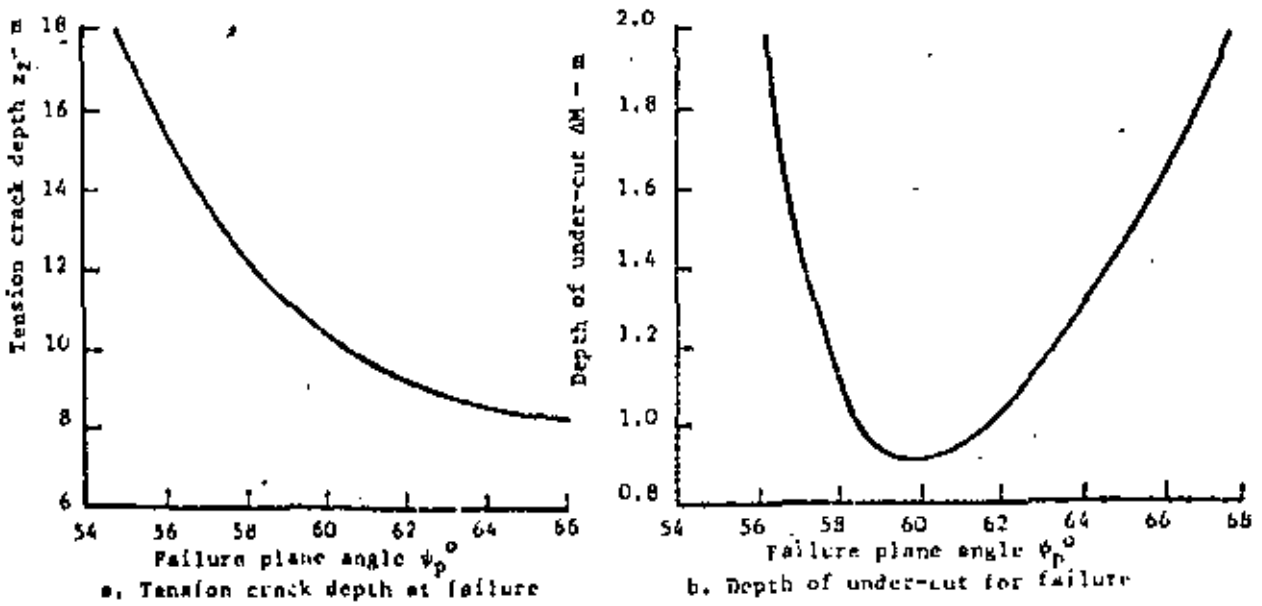

a. Tension crack depth at failure

b. Depth of under-cut for failure

Figure 89 : Tension crack depths and under-cut depths required for failure for different failure plane inclinations.

303

b. Rearranging equation 54 gives:

$$\Delta M = \frac{(H^2 - z_1^2)\text{Cot } \phi_f}{2H} - \frac{H^2 - z_2^2}{2H \text{ Tan } (2\phi_p - \phi)} \qquad (70)$$

Solving for a range of corresponding values of ϕ_p and z_2 gives the depth of undercut shown in Figure 89b.

It is clear, from this figure, that a further cliff failure will occur when the undercut reaches a depth of approximately 0.9m and that the corresponding failure plane angle will be $\phi_p = 60^0$ and the new tension crack depth will be $z_2 = 10.2$m. This new failure geometry is illustrated in Figure 90.

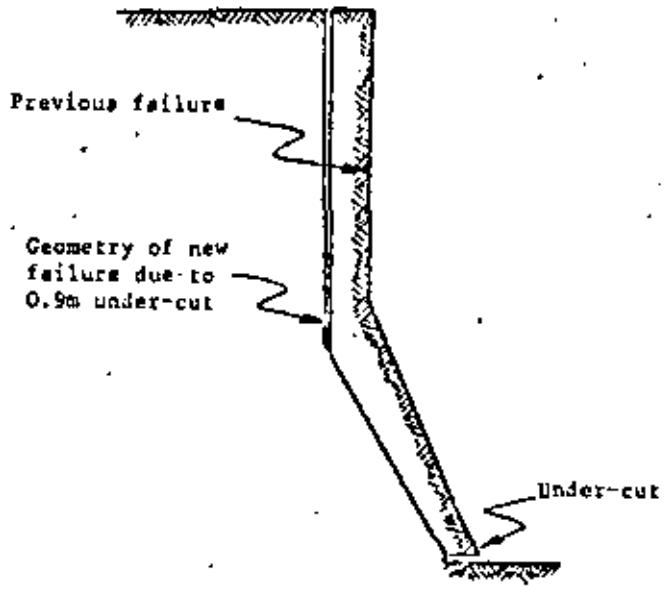

Figure 90 : Predicted geometry of next cliff failure due to under-cutting.

306

146. HUTCHINSON, J.N. Field and Laboratory studies of a fall in upper chalk cliffs at Joss Bay, Isle of Thanet. *Proc. Roscoe Memorial Symposium, Cambridge* 1970.

147. SALAMON, M.D.G. and MUNRO, A.H. A study of the strength of coal pillars. *J. S. African Inst. Min. Metall.* Vol 68. 1967. p 55-67.

148. BROADBENT, C.D. and ARMSTRONG, C.W. Design and application of microseismic devices. *Proc. 5th Canadian Symposium on Rock Mech.* 1968.

149. SEED, H.B. Slope stability during earthquakes. *J. Soil Mech. Found. Div. ASCE*, Vol 93. No SM 4. 1967. p 299-323.

150. IDRISS, I.M. and SEED, H.B. The response of earth banks during earthquakes. *Report Soil Mech. and Bituminous Matls. Lab. University of California. Berkeley.* April 1966.

151. FINN, W.D.L. Static and dynamic stresses in slopes. *Proc. 1st Congress, Intnl. Soc. Rock Mechanics, Lisbon.* 1966. Vol 2. p 167.

Chapter Four

GRAPHICAL SLOPE STABILITY ANALYSIS BY USE OF STEREONETS

4.1 Properties of Spherical Projections

4.1.1 General

The orientation (strike and dip) of planes or lines in space can be represented by the intersection of the plane or line with the surface of a reference sphere through whose center the plane or line passes. As can be seen in Figure 4.1, the intersection of a plane with the sphere is a great circle, while a line which parallels the plane will plot as two points, 180 degrees apart, on the great circle. A plane can also be represented by the intersection of its normal with the sphere (the pole of the plane), which will plot as a point located 90 degrees from the great circle, in both the upper and lower hemispheres of the sphere.

To communicate this information, a two-dimensional representation of the spherical projection is necessary. Several types of projection can be used to transfer great circles and points from the spherical surface to the equatorial plane of the sphere.

The equal angle projection (termed a Wulff net or stereonet) is the method used in this report because of the simplicity in plotting the projections. Each great circle on the sphere plots as an arc of a circle on the equatorial plane of the sphere.

Another type of projection, the equal area projection, is used for compiling statistical information on the frequency and orientation of lines or planes. It therefore should be used to plot and evaluate the

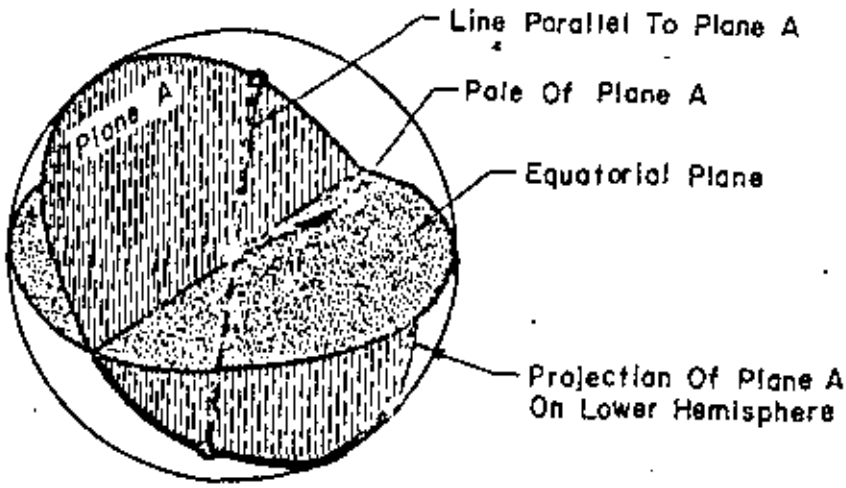

FIG. 4.1 PROJECTION OF PLANE AND LINES ON A SPHERE

raw data from field and borehole mapping of joints and other geologic discontinuities. The equal area projection of great circles from the sphere to the equatorial plane results in a distortion from the circular arc, and therefore is not quite as simple to use for stability analyses as the equal angle projection.

4.1.2 Equal Angle Projections

Figures 4.2 and 4.3 show the lower hemisphere, equal angle method for projecting a point from the surface of the sphere to equatorial plane.

A line is drawn from point P on the sphere to the upper pole, U, of the equatorial plane (dashed line in Fig. 4.2 and 4.3). The intersection of this line with the equatorial plane (P') is the desired projection of point P. In Figure 4.2, the projection of plane A and point P from the lower hemisphere to the equatorial plane is shown; the projection of plane A plots as an arc of a circle (or line of meridian) on the equatorial plane.

The projection of a vertical plane will project as a straight line through the origin of the equatorial plane. A horizontal plane will project as a line of meridian having a radius equal to the radius of the sphere, with the same origin. All points projected from the lower hemisphere will plot within this circle on the equatorial plane. Points from the upper hemisphere projected on the equatorial plane will plot outside the radius of the sphere, as can be seen for the projection, Q', of point Q in Figure 4.3.

A diagram of the stereonet obtained from an equal angle, lower hemisphere projection is shown in Fig. 4.4. The lines of meridian

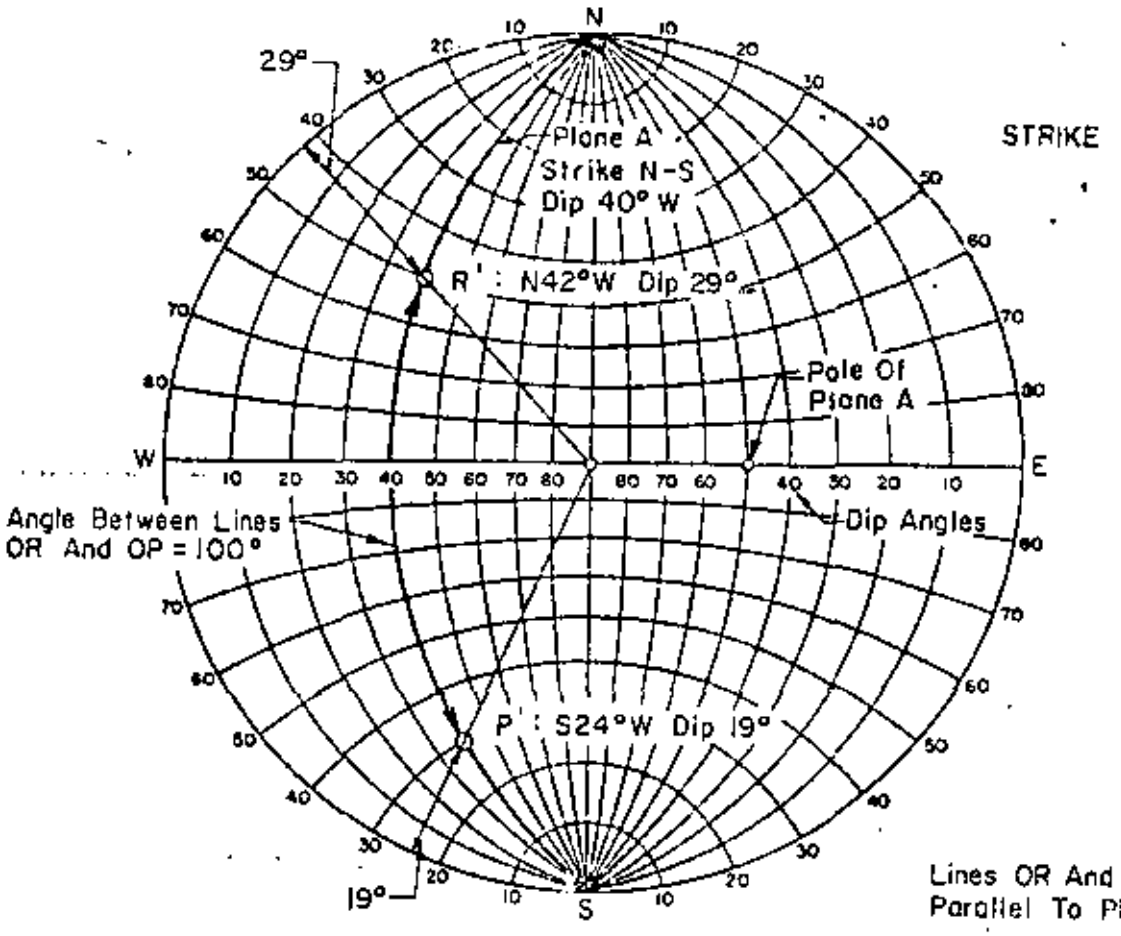

FIG. 4.4 STEREONET (WULFF NET) (EQUAL ANGLE PROJECTION)

the N and S poles of this diagram represent great circles resulting
ne intersection of N-S- striking planes with the reference sphere.
gles for these planes are shown on the E-W axis of the stereonet.
idians for steeply dipping planes will approach straight lines
s plot, while the meridians for flat-lying planes will plot as
circles having radii approaching the radius of the reference
. Each of the meridians is divided into 180 degrees by E-W lines
tude, which plot as arcs of circles on the equal angle stereonet.
esent a plane which strikes other than N-S, the stereonet of
must be rotated so that its N-S axis is aligned in the direction
trike of the given plane. The meridian can then be traced from
eonet so that it is oriented in its proper strike direction.
the true dip of a plane or line should be determined by orient-
E-W axis of the stereonet so that it is in the direction of the
line or plane.

nets similar to that shown in Fig. 4.4 are available from
suppliers. It is suggested that such a stereonet be used for
problems of this report by overlaying clear vellum on the
rotating the stereonet about its center, beneath the sheet
plot planes and lines of various strikes and dips.

4.4 the great circle projection of Plane A (dipping 40°
N-S) plots as a line of meridian. The pole (or normal)
ated 90° from the plane. Lines parallel to plane A
this line of meridian. The angle between two such
is 100° and is found by counting the lines of latitude
between points R' and P'.

Figure 4.5 shows the projection of two planes on the stereonet, one striking N-S, the other N 42° E. The orientation of the line of intersection of the two planes is determined from the point of intersection of the two meridians. In this case the line of intersection dips at an angle 24° in a direction of S 32° W. All of this information can be determined by using the stereonet, rotating it as required to plot lines of meridian and read angles. The dip angle is read by rotating the stereonet until either the NS or EW axis coincides with the direction of dip. The dip angle is then read in degrees from the outer edge of the stereonet.

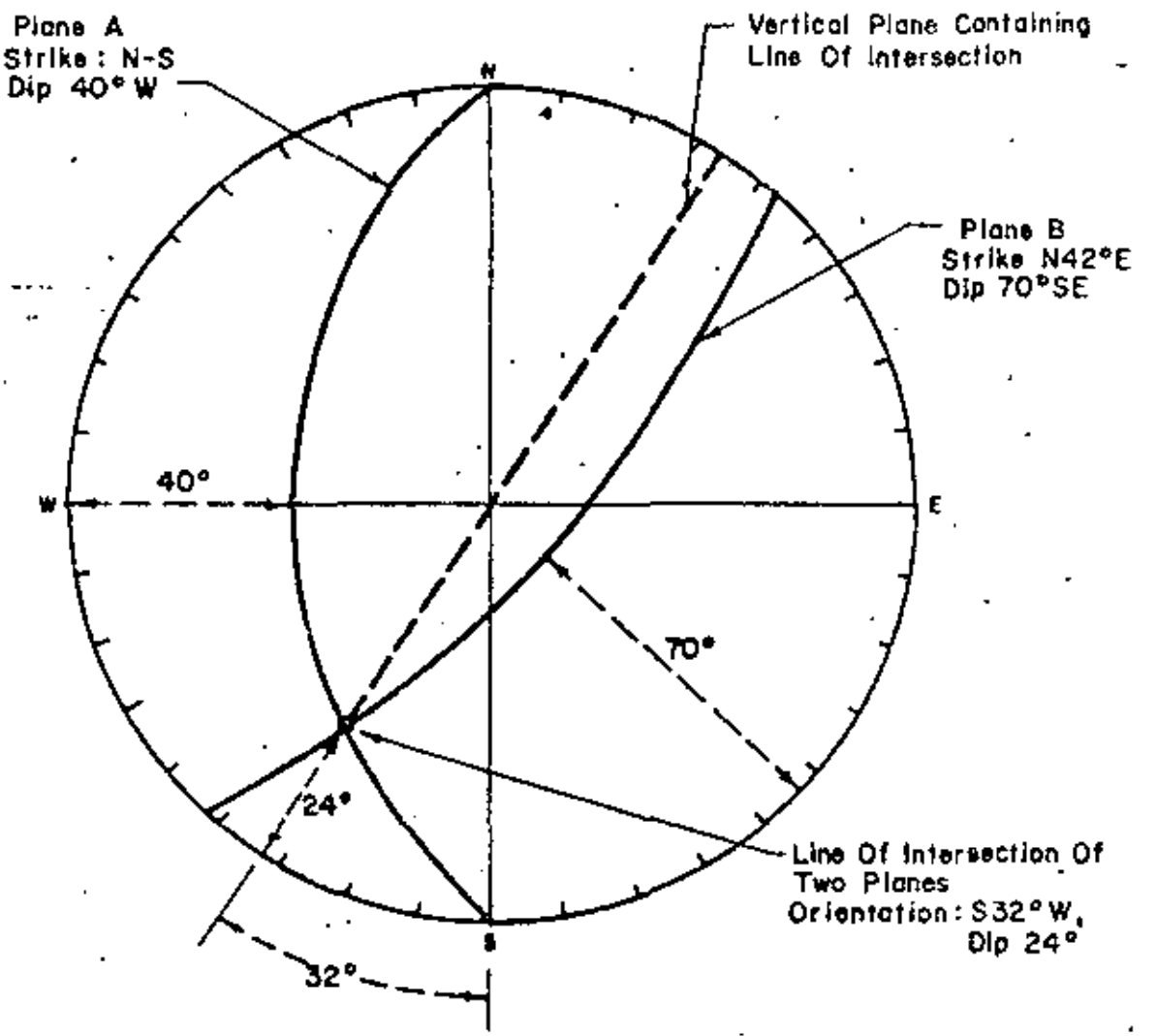

FIG. 4.5 DETERMINATION OF LINE OF INTERSECTION OF TWO PLANES

Chapter 8 : Wedge failure

316

Introduction

The previous chapter was concerned with slope failure resulting from sliding on a single planar surface dipping into the excavation and striking parallel or nearly parallel to the slope face. It was stated that the plane failure analysis is valid provided that the strike of the failure plane is within ±20° of the strike of the slope face. This chapter is concerned with the failure of slopes in which structural features upon which sliding can occur strike across the slope crest and where sliding takes place along the line of intersection of two such planes.

This problem has been extensively discussed in geotechnical literature and the authors have drawn heavily upon the work of Londe, John, Wittke, Goodman and others listed in references 152 to 162 at the end of this chapter. The reader who has examined this literature may have been confused by some of the mathematics which has been presented. It must, however, be appreciated that our understanding of the subject has grown rapidly over the past decade and that many of the simplifications which are now clear were not at all obvious when some of these papers were written. The basic mechanics of failure are very simple but, because of the large number of variables involved, the mathematical treatment of the mechanics can become very complex unless a very strict sequence is adhered to in the development of the equations.

In this chapter, the basic mechanics of failure involving the sliding of a wedge along the line of intersection of two planar discontinuities are presented in a form which the non-specialist reader should find easy to follow. Unfortunately, the very simple equations which are presented to illustrate the mechanics are of limited practical value because the variables used to define the wedge geometry cannot easily be measured in the field. Consequently, the second part of the chapter deals with the stability analysis in terms of the dips and dip directions of the planes and the slope face. In the transformation of the equations which is necessary in order to accommodate this information, the basic mechanics becomes obscure but it is hoped that the reader should be able to follow the logic involved in the development of these equations.

In the chapter itself, the discussion is limited to the case of the sliding of a simple wedge such as that illustrated in figure 91, acted upon by friction, cohesion and water pressure. The influence of a tension crack and of external forces due to bolts, cables or seismic accelerations results in a significant increase in the complexity of the equations and, since it would only be necessary to consider these influences on the fairly rare occasions when critical slopes are being examined, the complete solution to the problem has been presented in Appendix I at the end of the book. The analytical treatment of the problem presented in part III of the Appendix is particularly suitable for processing by computer and, once the reader has understood the basic mechanics of the problem, he should have no difficulty in having this general solution programmed for almost any type of computer, including the desk top machines which are now available.

317

Figure 91 : A typical wedge failure involving sliding along the line of intersection of two planar discontinuities.

Figure 92 : Sets of intersecting discontinuities can sometimes give rise to the formation of families of wedge failures.

318

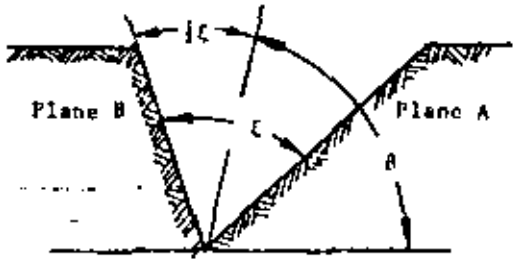

View along line of intersection

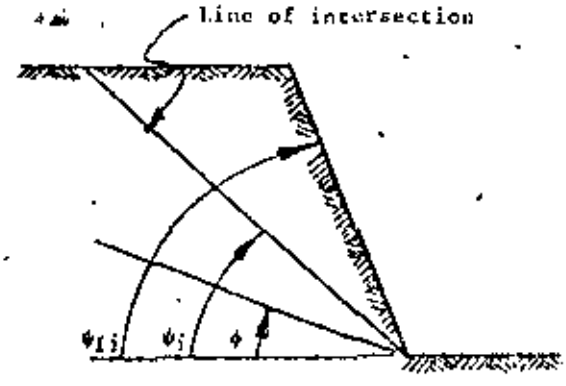

View at right angles to line of intersection

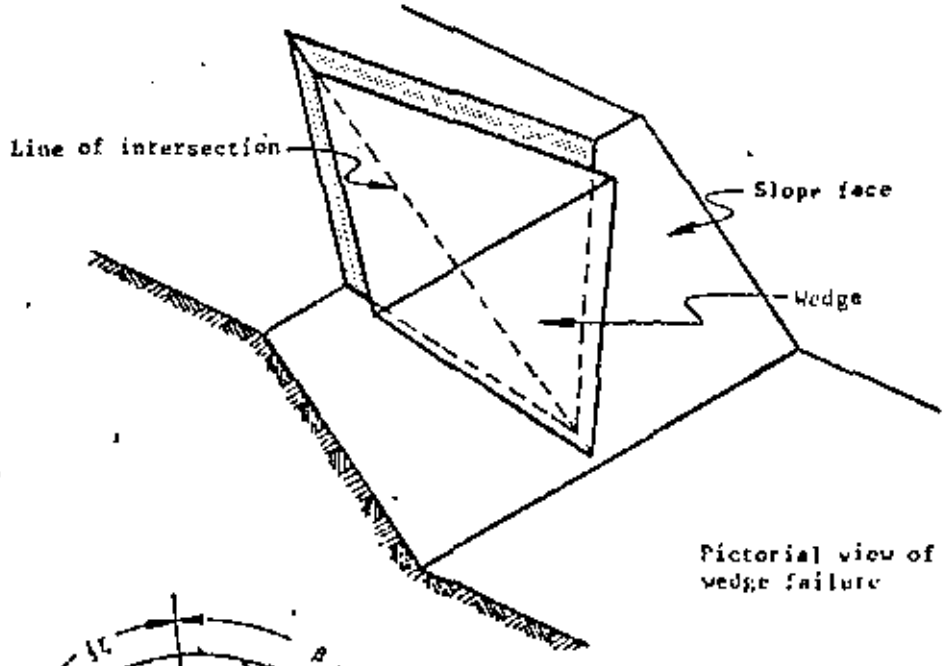

Pictorial view of wedge failure

Note : The convention adopted in this analysis is that the plane with the flatter of the two dips is always referred to as Plane A.

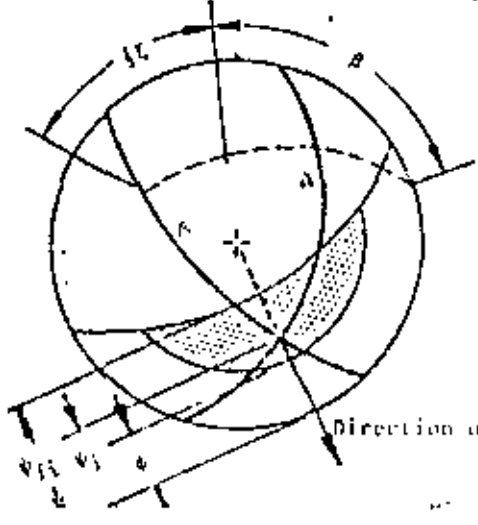

Stereoplot of wedge failure geometry

319

Definition of wedge geometry

Typical wedge failures are illustrated in figures 91 and 92 which show, in the one case, the through-going planar discontinuities which are normally assumed for the analytical treatment of this problem and, in the other case, the wedge formed by sets of closely spaced structural features. In the latter case, the analytical treatment would still be based upon the assumption of through-going planar features although it would have to be realised that the definition of the dips and dip directions and the locations of these planes may present practical difficulties. The failure illustrated in figure 92 would probably have involved the fairly gradual ravelling of small loose blocks of rock and it is unlikely that this failure was associated with any violence. On the other hand, the failure illustrated in figure 91 probably involved a fairly sudden fall of a single wedge which would only have broken up on impact and which would, therefore, constitute a threat to anyone working at the toe of the slope.

The geometry of the wedge, for the purpose of analysing the basic mechanics of sliding, is defined in figure 93. Note that, throughout this book, the *flatter* of the two planes is called Plane A while the *steeper* plane is called Plane B.

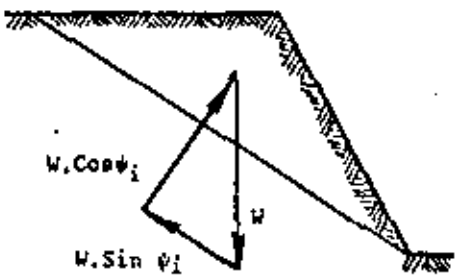

View at right angles to line of intersection

As in the case of plane failure, a condition for sliding is defined by $\psi_{fi} > \psi_i > \phi$, where ψ_{fi} is the inclination of the slope face, measured in the view at right angles to the line of intersection, and ψ_i is the dip of the line of intersection. Note the ψ_{fi} would only be the same as ψ_f, the true dip of the slope face, if the dip direction of the line of intersection was the same as the dip direction of the slope face.

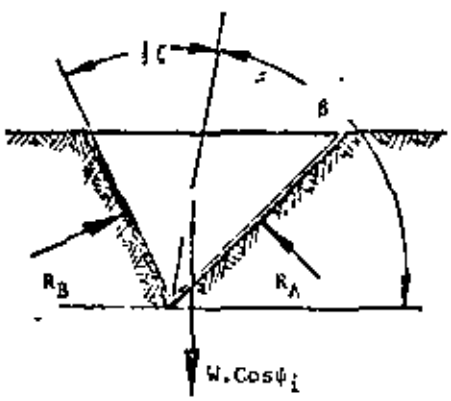

View along line of intersection

Analysis of wedge failure

The factor of safety of the wedge defined in figure 93, assuming that sliding is resisted by *friction only* and that the friction angle ϕ is the same for both planes, is given by

$$F = \frac{(R_A + R_B)\ \mathrm{Tan}\phi}{W.\mathrm{Sin}\psi_i} \qquad (71)$$

where R_A and R_B are the normal reactions provided by planes A and B as illustrated in the sketch opposite.

In order to find R_A and R_B, resolve horizontally and vertically in the view along the line of intersection :

$$R_A.\mathrm{Sin}(\beta - \tfrac{1}{2}\zeta) = R_B.\mathrm{Sin}(\beta + \tfrac{1}{2}\zeta) \qquad (72)$$

$$R_A.\mathrm{Cos}(\beta - \tfrac{1}{2}\zeta) - R_B.\mathrm{Cos}(\beta + \tfrac{1}{2}\zeta) = W.\mathrm{Cos}\psi_i \qquad (73)$$

Solving for R_A and R_B and adding :

$$R_A + R_B = \frac{W.\mathrm{Cos}\psi_i.\ \mathrm{Sin}\beta}{\mathrm{Sin}\tfrac{1}{2}\zeta} \qquad (74)$$

Hence $F = \dfrac{\mathrm{Sin}\beta\ \ \mathrm{Tan}\phi}{\qquad\qquad}$ (75)

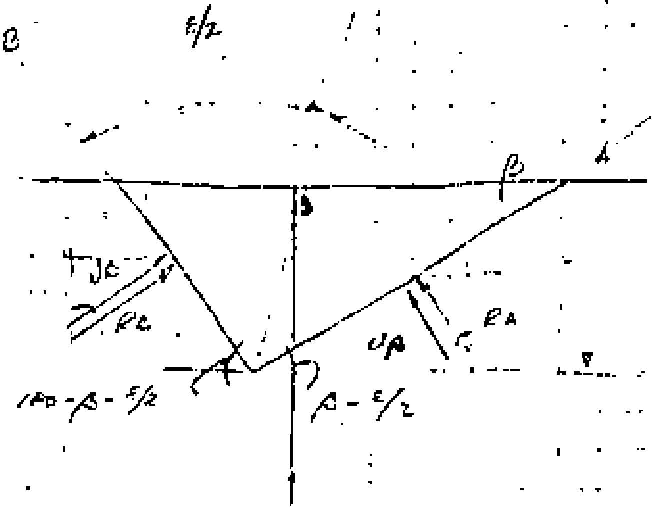

$W\cos i - W k \,\mathrm{sen}\, i$

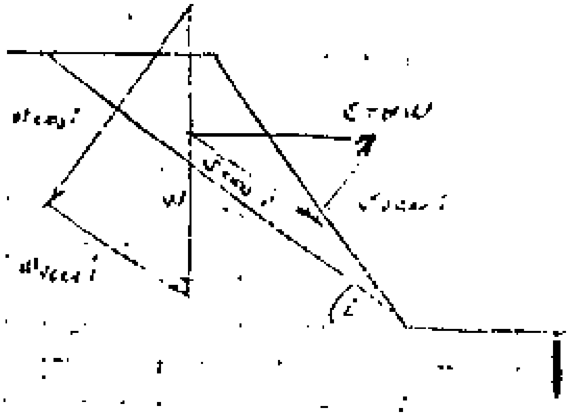

A es el plano con círculo colores

Para fuerzas horizontales:

$$P_B\,\mathrm{sen}(180-\beta-\epsilon/2) - P_A\,\mathrm{sen}(\beta-\epsilon/2) + U_B\,\mathrm{sen}(180-\beta-\epsilon/2) - U_A\,\mathrm{sen}(\beta-\epsilon/2) = 0$$

$$P_B\,\mathrm{sen}(\beta+\epsilon/2) - P_A\,\mathrm{sen}(\beta-\epsilon/2) = U_A\,\mathrm{sen}(\beta-\epsilon/2) - U_B\,\mathrm{sen}(\beta+\epsilon/2)$$

Para fuerzas verticales:

$$P_B\cos(180-\beta-\epsilon/2) + P_A\cos(\beta-\epsilon/2) + U_B\cos(180-\beta-\epsilon/2) + U_A\cos(\beta-\epsilon/2)$$
$$- W(\cos i - k\,\mathrm{sen}\, i) = 0$$

$$P_A\cos(\beta-\epsilon/2) - P_B\cos(\beta+\epsilon/2) = U_B\cos(\beta+\epsilon/2) - U_A\cos(\beta-\epsilon/2) +$$
$$+ W(\cos i - k\,\mathrm{sen}\, i)$$

Despejando P_A y P_B:

$$P_B = \frac{U_A\,\mathrm{sen}\,\beta^- - U_B\,\mathrm{sen}\,\beta^+ + P_A\,\mathrm{sen}\,\beta^-}{\mathrm{sen}\,\beta^+}$$

$$P_A\cos\beta^- - \frac{(U_A\,\mathrm{sen}\,\beta^- - U_B\,\mathrm{sen}\,\beta^+ + P_A\,\mathrm{sen}\,\beta^-)}{\mathrm{sen}\,\beta^+}\cos\beta^+ = U_B\cos\beta^+ -$$

$$- U_A\cos\beta^- + W(\cos i - k\,\mathrm{sen}\, i)$$

$$R_A \cos\beta^- \sin\beta^+ = -U_A \sin\beta^- \cos\beta^+ + U_B \sin\beta^+ \cos\beta^+ -$$

$$- R_B \sin\beta^- \cos\beta^+ = -U_A \cos\beta^+ \sin\beta^+ - U_B \cos\beta^- \sin\beta^+$$
$$+ W(\cos i - \nu \sin i) \sin\beta^+$$

$$R_A (\cos\beta^- \sin\beta^+ - \sin\beta^- \cos\beta^+) = -U_A (\cos\beta^+ \sin\beta^+ - \sin\beta^+ \cos\beta$$
$$- U_B (\cos\beta^- \sin\beta^+ - \sin\beta^- \cos\beta^+) + W(\cos i - \nu \sin i) \sin\beta$$

$$R_A = \frac{-U_A (\cos\beta^- \sin\beta^+ - \sin\beta^- \cos\beta^+) + W(\cos i - \nu \sin i) \cos\beta}{\cos\beta^- \sin\beta^+ - \sin\beta^- \cos\beta^+}$$

$$R_{AE} = \frac{-U_A \sin\varepsilon + W(\cos i - \nu \sin i) \sin\beta^+}{\sin\varepsilon}$$

$$R_B = \frac{U_A \sin\beta^- - U_B \sin\beta^+ + \frac{-U_A \sin\varepsilon + W(\cos i - \nu \sin i) \sin\beta^+}{\sin\varepsilon}}{\sin\beta^+}$$

$$R_B = \frac{U_A \sin\beta^- \sin\varepsilon - U_B \sin\beta^+ \sin\varepsilon - U_A \sin\varepsilon \sin\beta^- + W(\cos i - \nu \sin i)}{\sin\beta^+ \sin\varepsilon}$$

$$R_{BE} = \frac{-U_B \sin\beta^+ \sin\varepsilon + W(\cos i - \nu \sin i) \sin\beta^+ \sin\beta^-}{\sin\beta^+ \sin\varepsilon}$$

$$R_A = W(\cos i - \nu \sin i) \frac{\sin\beta^+}{\sin\varepsilon} - U_A$$

$$R_B = W(\cos i - \nu \sin i) \frac{\sin\beta^-}{\sin\varepsilon} - U_B$$

324

In other words :

$$F_w = K.F_p \qquad (76)$$

where F_w is the factor of safety of a wedge supported by friction only. F_p is the factor of safety of a plane failure in which the slope face is inclined at ψ_f and the failure plane is inclined at ψ_i.

K is a wedge factor which, as shown by equation 75, depends upon the included angle of the wedge and upon the angle of tilt of the wedge. Values for the wedge factor K, for a range of values of β and ζ, are plotted in figure 94.

As shown in the stereoplot given in figure 93, measurement of the angles β and ξ can be carried out on the great circle, the pole of which is the point representing the line of intersection of the two planes. Hence, a stereoplot of the features which define the slope and the wedge geometry can provide all the information required for the determination of the factor of safety. It should, however, be remembered that the case which has been dealt with is very simple and that, when different friction angles and the influence of cohesion and water pressure are allowed for, the equations become more complex. Rather than develop these equations in terms of the angles β and ξ, which cannot be measured directly in the field, the more complete analysis is presented in terms of directly measurable dips and dip directions.

Before leaving this simple analysis, the reader's attention is drawn to the important influence of the wedging action as the included angle of the wedge decreases below 90°. The increase by a factor of 2 or 3 on the factor of safety determined by plane failure analysis is of great practical importance. Some authors have suggested that a plane failure analysis is acceptable for *all* rock slopes because it provides a lower bound solution which has the merit of being conservative. Figure 94 shows that this solution is so conservative as to be totally uneconomic for most practical slope designs. It is therefore recommended that, where the structural features which are likely to control the stability of a rock slope do not strike parallel to the slope face, the stability analysis should be carried out by means of the three-dimensional methods presented in this book or published by the authors listed in references 152 to 162 at the end of this chapter.

Wedge analysis including cohesion and water pressure

Figure 95 shows the geometry of the wedge which will be considered in the following analysis. Note that the upper slope surface in this analysis can be obliquely inclined with respect to the slope face, thereby removing a restriction which has been present in all the stability analyses which have been discussed so far in this book. The total height of the slope, defined in figure 95b, is the total difference in vertical elevation between the upper and lower extremities of the line of intersection along which sliding is assumed to occur.

The water pressure distribution assumed for this analysis is based upon the hypothesis that the water itself is

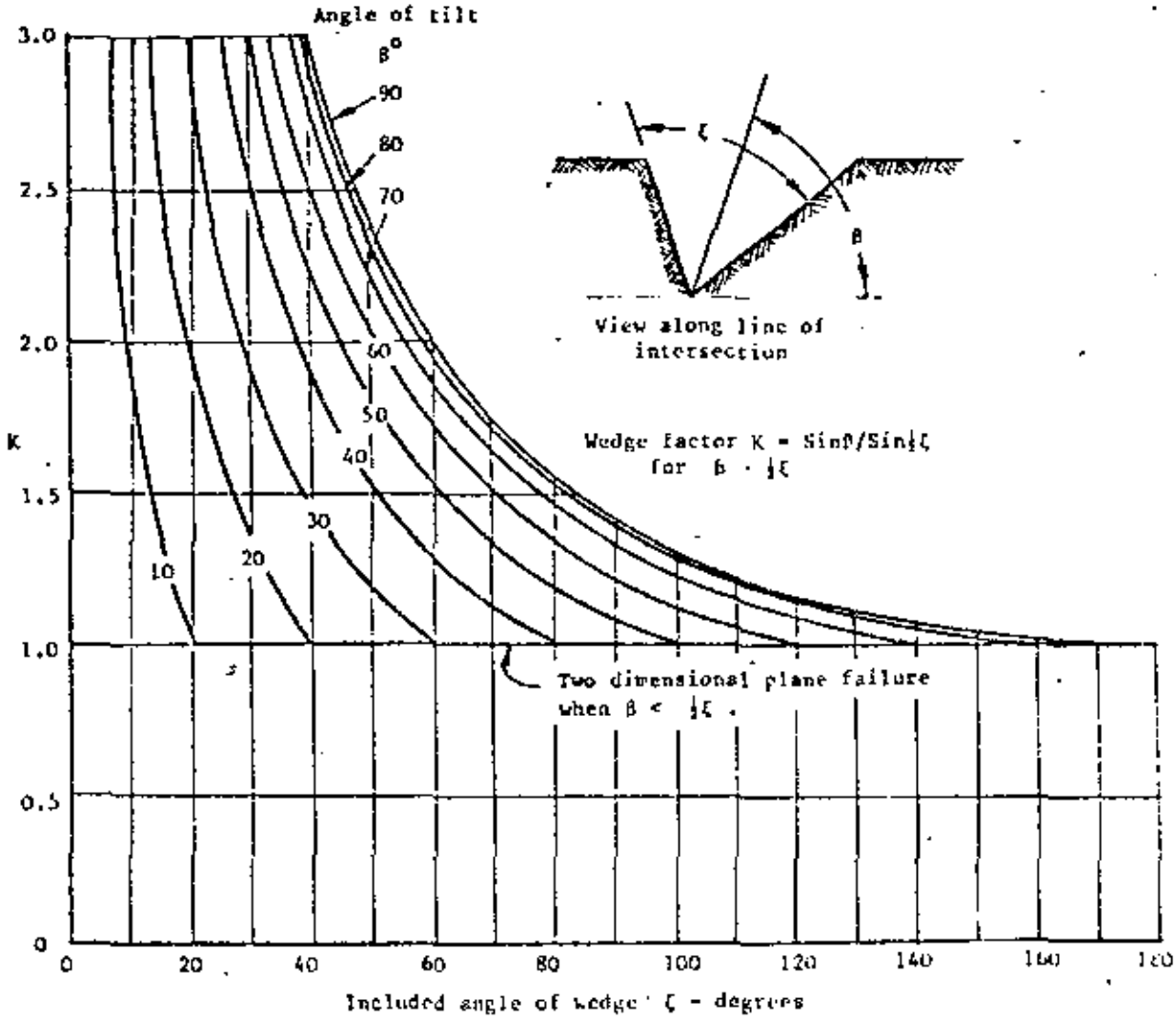

Figure 94 : Wedge factor K as a function of wedge geometry.

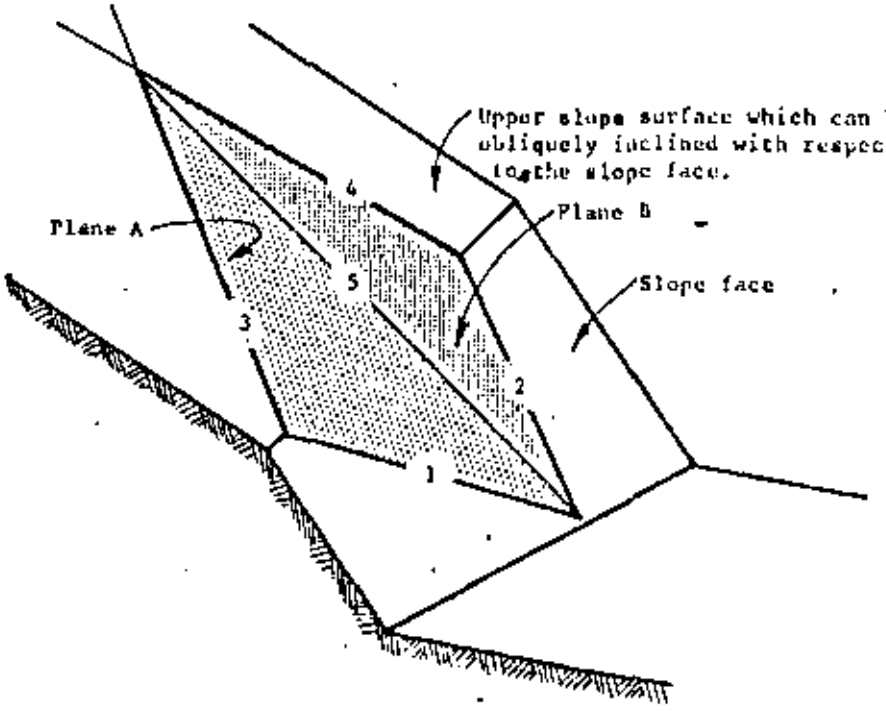

a. Pictorial view of wedge showing the numbering of intersection lines and planes.

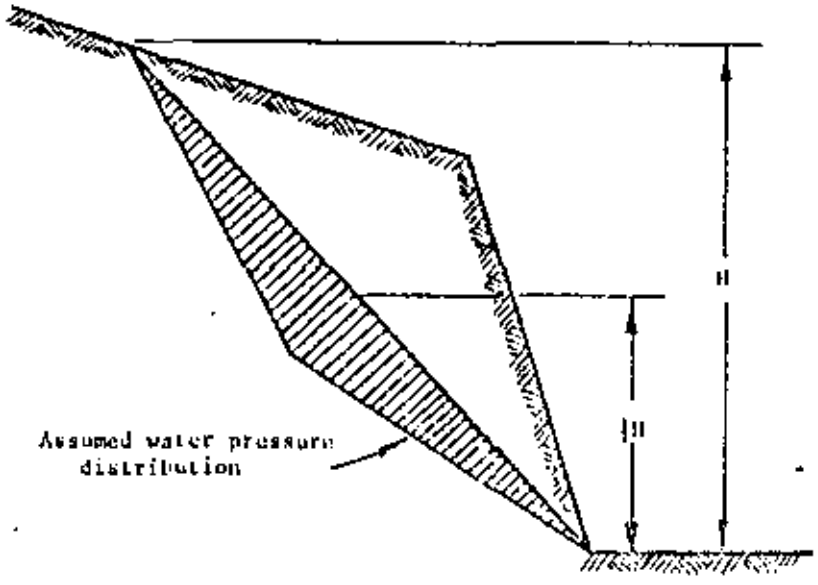

b. View normal to the line of intersection 5 showing the total wedge height and the water pressure distribution.

Figure 95 : Geometry of wedge used for stability analysis including the influence of cohesion and of water pressure on the failure surfaces.

impermeable and that water enters the top of the wedge along lines of intersection 3 and 4 and leaks from the slope face along lines of intersection 1 and 2. The resulting pressure distribution is shown in figure 95b - the maximum pressure occurring along the line of intersection 5 and the pressure being zero along lines 1,2,3 and 4. This water pressure distribution is believed to be representative of the extreme conditions which could occur during very heavy rain.

The numbering of the lines of intersection of the various planes involved in this problem is of extreme importance since total confusion can arise in the analysis if these number are mixed-up. The numbering used throughout this book is as follows :

1 - intersection of plane A with the slope face
2 - intersection of plane B with the slope face
3 - intersection of plane A with upper slope surface
4 - intersection of plane B with upper slope surface
5 - intersection of planes A and B .

It is assumed that sliding of the wedge always takes place along the line of intersection numbered 5.

The factor of safety of this slope is derived from the detailed analysis presented in part III of Appendix I at the end of this book and is :

$$F = \frac{3}{\gamma H}(c_A.X + c_B.Y) + (A - \frac{\gamma_w}{2\gamma}.X)\text{Tan}\phi_A + (B - \frac{\gamma_w}{2\gamma}.Y)\text{Tan}\phi_B \qquad (77)$$

Where

c_A and c_B are the cohesive strengths of planes A and B

ϕ_A and ϕ_B are the angles of friction on planes A and B

γ is the density of the rock

γ_w is the density of water

H is the total height of the wedge (see figure 95)

X,Y,A and B are dimensionless factors which depend upon the geometry of the wedge.

$$X = \frac{\text{Sin}\theta_{24}}{\text{Sin}\theta_{45}.\text{Cos}\theta_{2,na}} \qquad (78)$$

$$Y = \frac{\text{Sin}\theta_{13}}{\text{Sin}\theta_{35}.\text{Cos}\theta_{1,nb}} \qquad (79)$$

$$A = \frac{\text{Cos}\psi_a - \text{Cos}\psi_b.\text{Cos}\theta_{na,nb}}{\text{Sin}\psi_5.\text{Sin}^2\theta_{na,nb}} \qquad (80)$$

$$B = \frac{\text{Cos}\psi_b - \text{Cos}\psi_a.\text{Cos}\theta_{na,nb}}{\text{Sin}\psi_5.\text{Sin}^2\theta_{na,nb}} \qquad (81)$$

where ψ_a and ψ_b are the dips of planes A and B respectively and ψ_5 is the dip of the line of intersection 5.

The angles required for the solution of these equations can most conveniently be measured on a stereoplot of the

data which defines the geometry of the wedge and the slope.

Consider the following example :

Plane	dip°	dip direction°	Properties
A	45	105	$\phi_A=20^\circ$, $c_A=500 lb/ft^2$
B	70	235	$\phi_B=30^\circ$, $c_B=1000 lb/ft^2$
Slope face	65	185	$\gamma=160 lb/ft^3$
Upper surface	12	195	$\gamma_w=62.5 lb/ft^3$

The total height of the wedge H = 130 feet.

The stereoplot of the great circles representing the four planes involved in this problem is presented in figure 96 and all the angles required for the solution of equations 78 to 81 are marked in this figure.

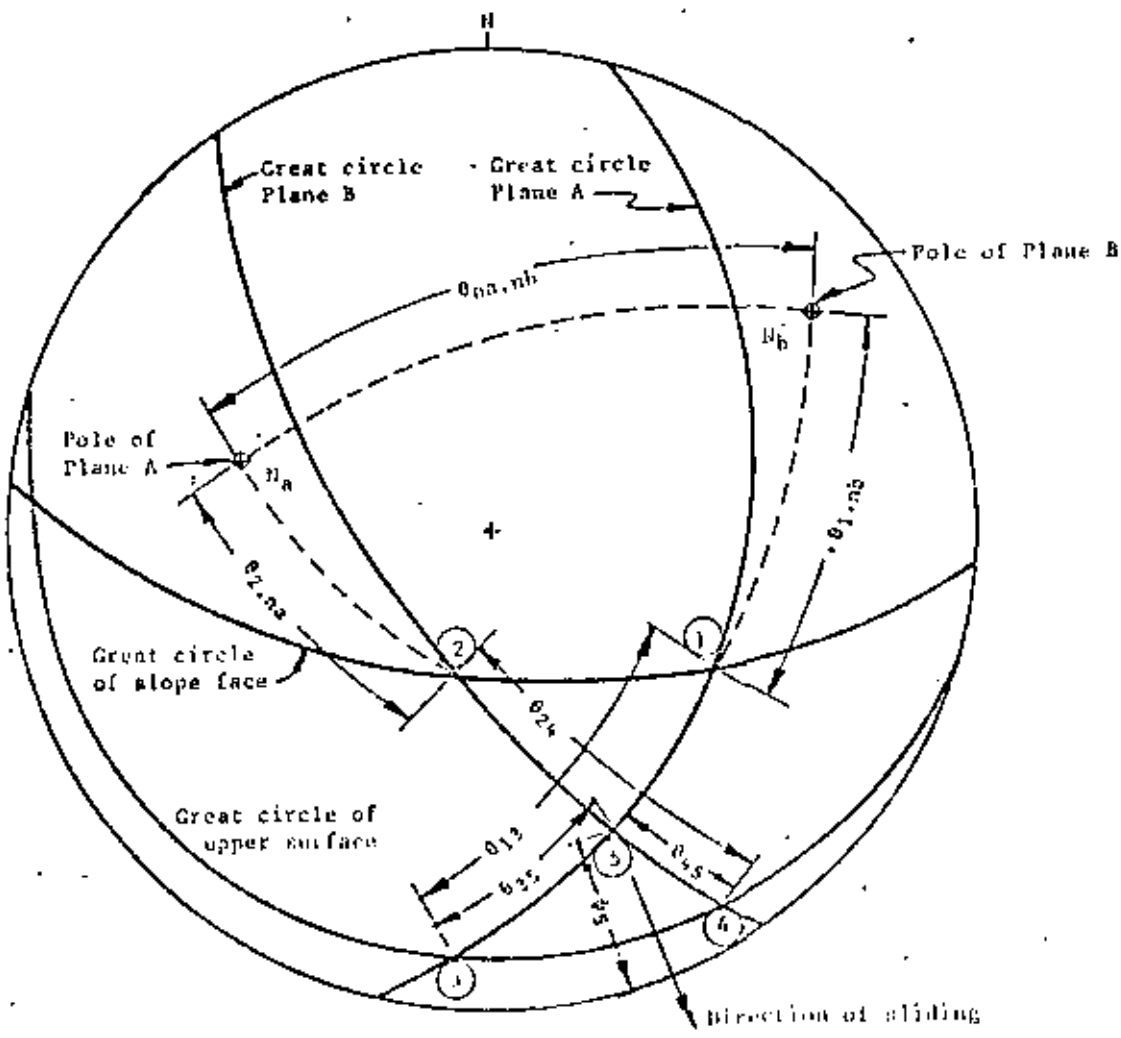

Figure 96 : Stereoplot of data required for wedge stability analysis.

WEDGE STABILITY CALCULATION SHEET

INPUT DATA	FUNCTION VALUE	CALCULATED ANSWER
$\psi_a = 45^\circ$ $\psi_b = 70^\circ$ $\psi_s = 31.2^\circ$ $\theta_{na,nb} = 101^\circ$	$\cos\psi_a = 0.7071$ $\cos\psi_b = 0.3420$ $\sin\psi_s = 0.5180$ $\cos\theta_{na,nb} = -0.191$ $\sin\theta_{na,nb} = 0.982$	$A = \dfrac{\cos\psi_a - \cos\psi_b.\cos\theta_{na,nb}}{\sin\psi_s.\sin^2\theta_{na,nb}} = \dfrac{0.7071 + 0.342 \times 0.191}{0.5180 \times 0.9636} = 1.6475$ $B = \dfrac{\cos\psi_b - \cos\psi_a.\cos\theta_{na,nb}}{\sin\psi_s.\sin^2\theta_{na,nb}} = \dfrac{0.3420 + 0.7071 \times 0.191}{0.5180 \times 0.9636} = 0.9557$
$\theta_{24} = 68^\circ$ $\theta_{45} = 58^\circ$ $\theta_{2,na} = 55^\circ$	$\sin\theta_{24} = 0.9063$ $\sin\theta_{45} = 0.4226$ $\cos\theta_{2,na} = 0.5428$	$X = \dfrac{\sin\theta_{24}}{\sin\theta_{45}.\cos\theta_{2,na}} = \dfrac{0.9063}{0.4226 \times 0.5428} = 3.3362$
$\theta_{13} = 82^\circ$ $\theta_{35} = 31^\circ$ $\theta_{1,nb} = 60^\circ$	$\sin\theta_{13} = 0.9829$ $\sin\theta_{35} = 0.5150$ $\cos\theta_{1,nb} = 0.5000$	$Y = \dfrac{\sin\theta_{13}}{\sin\theta_{35}.\cos\theta_{1,nb}} = \dfrac{0.9829}{0.5150 \times 0.500} = 3.8287$
$\phi_A = 30^\circ$ $\phi_B = 20^\circ$ $\gamma = 150$ lb/ft^3 $\gamma_w = 64.0$ lb/ft^3 $c_A = 800$ lb/ft^2 $c_B = 1500$ lb/ft^2 $H = 130$ ft	$\tan\phi_A = 0.5773$ $\tan\phi_B = 0.3640$ $\gamma_w/2\gamma = 0.2203$ $3c_A/\gamma H = 0.0721$ $3c_B/\gamma H = 0.1443$	$F = \dfrac{3c_A}{\gamma H}.X + \dfrac{3c_B}{\gamma H}.Y + (A - \dfrac{\gamma_w}{2\gamma}.X)\tan\phi_A + (B - \dfrac{\gamma_w}{2\gamma}.Y)\tan\phi_B$ $F = 0.2405 + 0.4944 + 0.6934 - 0.3762 + 0.3478 - 0.2427 = 1.3568$

Determination of the factor of safety is most conveniently carried out on a calculation sheet such as that presented on page 191. Setting the calculations out in this manner not only enables the user to check all the data but it also shows how each variable contributes to the overall factor of safety. Hence, if it is required to check the influence of the cohesion on both planes falling to zero, this can be done by setting the two groups containing the cohesion values c_A and c_B to zero, giving a factor of safety of 0.62. Alternatively, the effect of drainage can be checked by putting the two water pressure terms (i.e. those containing γ_w) to zero, giving F = 1.98.

As has been emphasised in previous chapters, this ability to check the sensitivity of the factor of safety to changes in material properties or in slope loading is probably as important as the ability to calculate the factor of safety itself. Hoek and Londe, in a general review of rock slope and foundation design methods [105], have concluded that the information which is most useful to the design engineer is that which indicates the response of the structure to changes in significant parameters. Hence, decisions on remedial measures such as drainage can be based upon the rate of change of factor of safety, even if the absolute value of the factor of safety cannot be relied upon. To quote from this general review : " The function of the design engineer is not to compute accurately but to judge soundly".

Wedge stability charts for friction only

If the cohesive strength of the planes A and B is zero and the slope is fully drained, equation 77 reduces to

$$F = A.\tan\phi_A + B.\tan\phi_B \qquad (82)$$

The dimensionless factors A and B are found to depend upon the dips and dip directions of the two planes and values of these two factors have been computed for a range of wedge geometries and the results are presented as a series of charts on the following pages.

In order to illustrate the use of these charts, consider the following example :

	dip°	dip direction°	friction angle°
Plane A	40	165	35
Plane B	70	285	20
Differences	30	120	

Hence, turning to the charts headed "Dip difference 30°" and reading off the values of A and B for a difference in dip direction of 120°, one finds that

$$A = 1.5 \quad \text{and} \quad B = 0.7$$

Substitution in equation 82 gives the factor of safety as F = 1.30. The values of A and B give a direct indication of the contribution which each of the planes makes to the total factor of safety.

Note that the factor of safety calculated from equation 82 is independent of the slope height, the angle of the slope face and the

331

rather surprising result arises because the weight of the wedge occurs in both the numerator and denominator of the factor of safety equation and, for the friction only case, this term cancells out, leaving a dimensionless ratio which defines the factor of safety (see equation 75 on page 184). This simplification is very useful in that it enables the user of these charts to carry out a very quick check on the stability of a slope on the basis of the dips and dip directions of the discontinuities in the rock mass into which the slope has been cut. An example of such an analysis is presented later in this chapter.

Many trial calculations have shown that a wedge having a factor of safety in excess of 2.0, as obtained from the friction only stability charts, is unlikely to fail under even the most severe combination of conditions to which the slope is likely to be subjected. Consider the example discussed on pages 190 to 192 in which the factor of safety for the worst conditions (zero cohesion and maximum water pressure) is 0.62. This is exactly 50% of the factor of safety of 1.24 for the friction only case. Hence, had the factor of safety for the friction only case been 2.0, the factor of safety for the worst conditions would have been 1.0, assuming that the ratio of the factors of safety for the two cases remains constant.

On the basis of such trial calculations, the authors suggest that the friction only stability charts can be used to define those slopes which are adequately stable and which can be ignored in subsequent analyses. Such slopes, having a factor of safety in excess of 2.0, pass into category 3 in the chart presented in figure 6 on page 14. Slopes with a factor of safety, based upon friction only, of less than 2.0 must be regarded as potentially unstable and pass into category 4 of figure 6, i.e. these slopes require further detailed examination.

In many practical problems involving the design of the overall slopes of an open pit mine or the cuttings for a highway, it will be found that these friction only stability charts provide all the information which is required. It is frequently possible, having identified a potentially dangerous slope, to eliminate the problem by a slight realignment of the pit benches or of the road cutting. Such a solution is clearly only feasible if the potential danger is recognised before excavation of the slope is started and the main use of the charts is during the site investigation and preliminary planning stage of a slope project.

Once a slope has been excavated, these charts will be of limited use since it will be fairly obvious if the slope is unstable. Under these conditions, a more detailed study of the slope will be required and use would then have to be made of the method described on pages 186 to 191 or of one of the methods described in Appendix I. In the authors' experience, relatively few slopes require this detailed analysis and the reader should beware of wasting time on such an analysis when the simpler methods presented in this chapter would be adequate. A full stability analysis may look very impressive in a report but, unless it has enabled the slope engineer to take positive remedial measures, it may not have served any useful purpose.

332

WEDGE STABILITY CHARTS FOR FRICTION ONLY

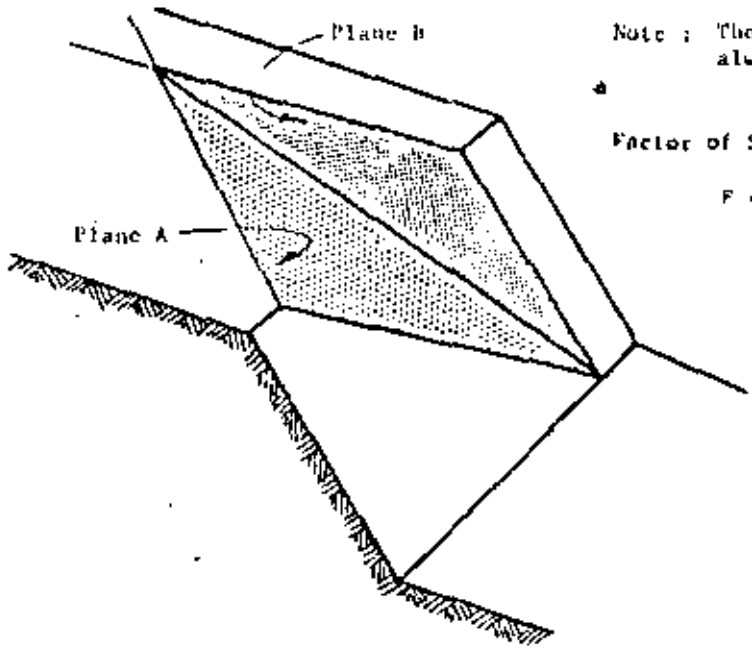

Note : The flatter of the two planes is always called Plane A .

Factor of Safety

$$F = A.\tan\phi_A + B.\tan\phi_B$$

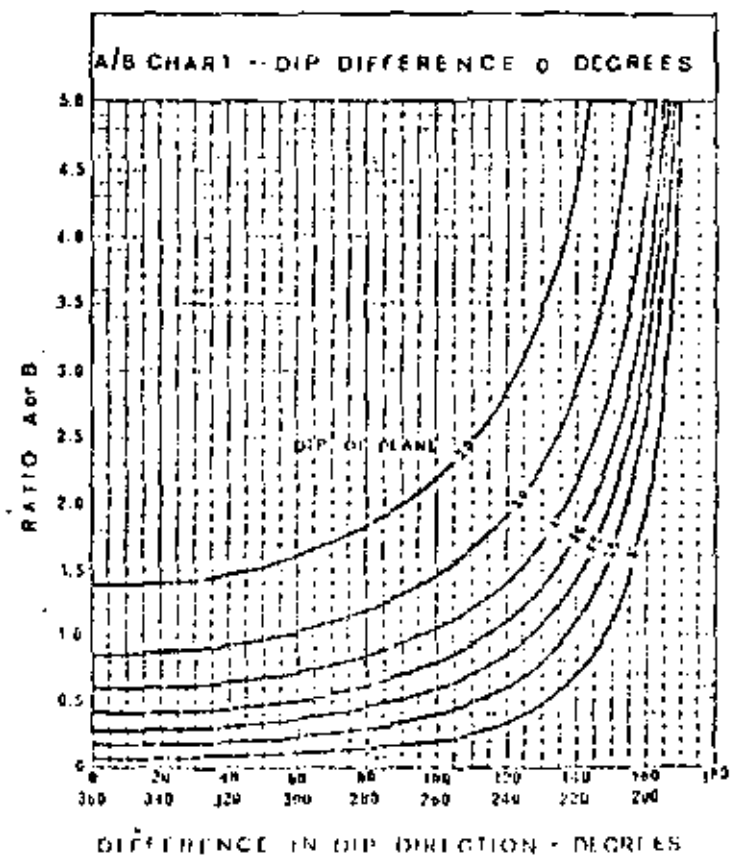

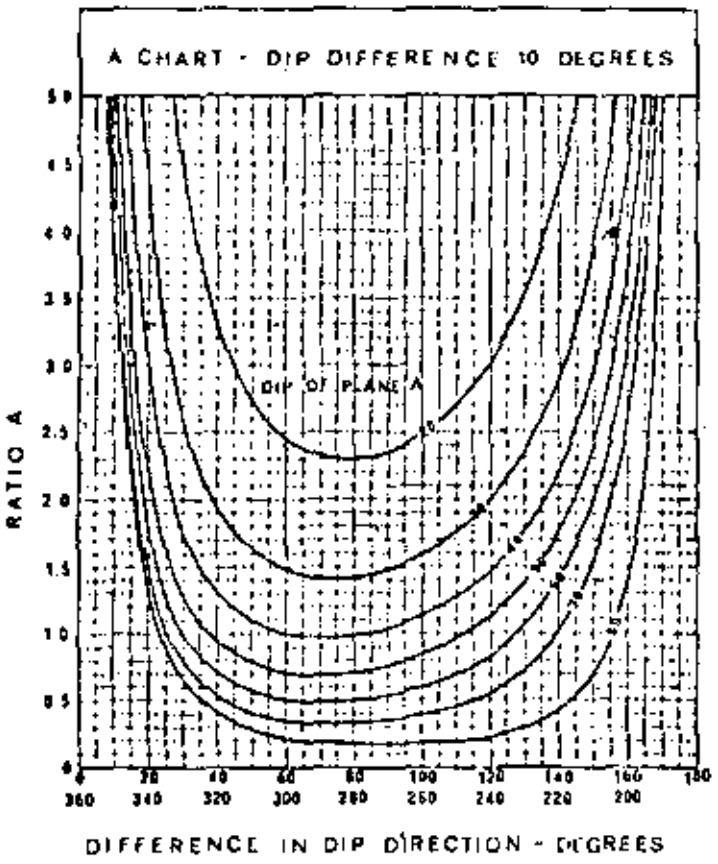
A CHART - DIP DIFFERENCE 10 DEGREES
RATIO A
DIP OF PLANE A
DIFFERENCE IN DIP DIRECTION - DEGREES

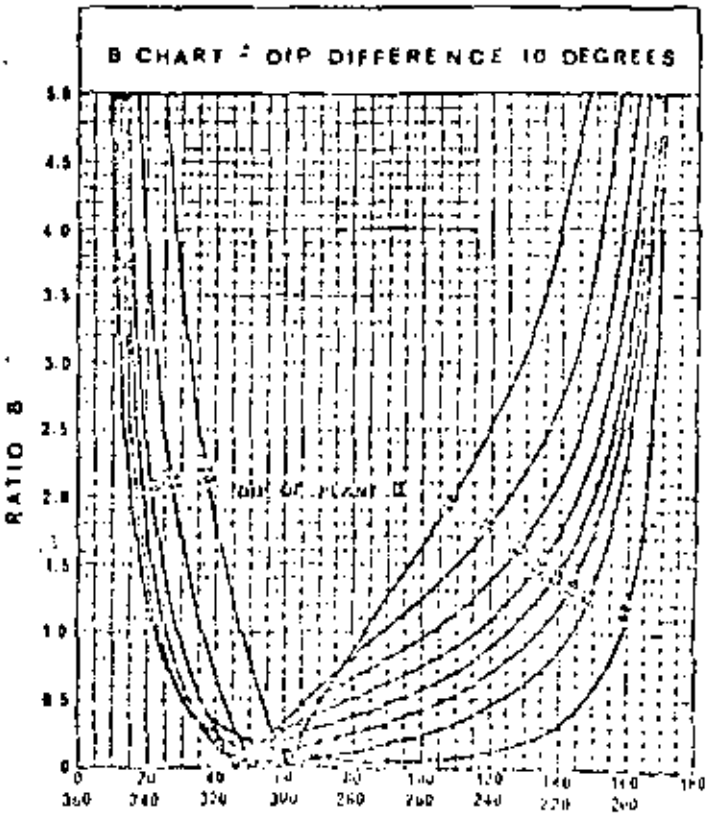
B CHART - DIP DIFFERENCE 10 DEGREES
RATIO B
DIFFERENCE IN DIP DIRECTION - DEGREES

338

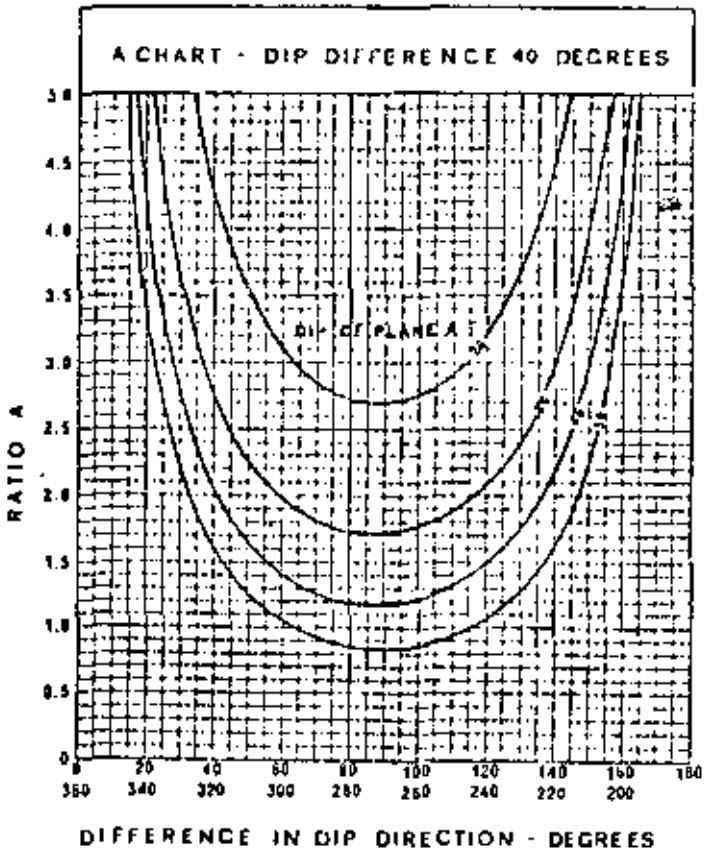
A CHART - DIP DIFFERENCE 40 DEGREES
RATIO A
DIP OF PLANE A
DIFFERENCE IN DIP DIRECTION - DEGREES

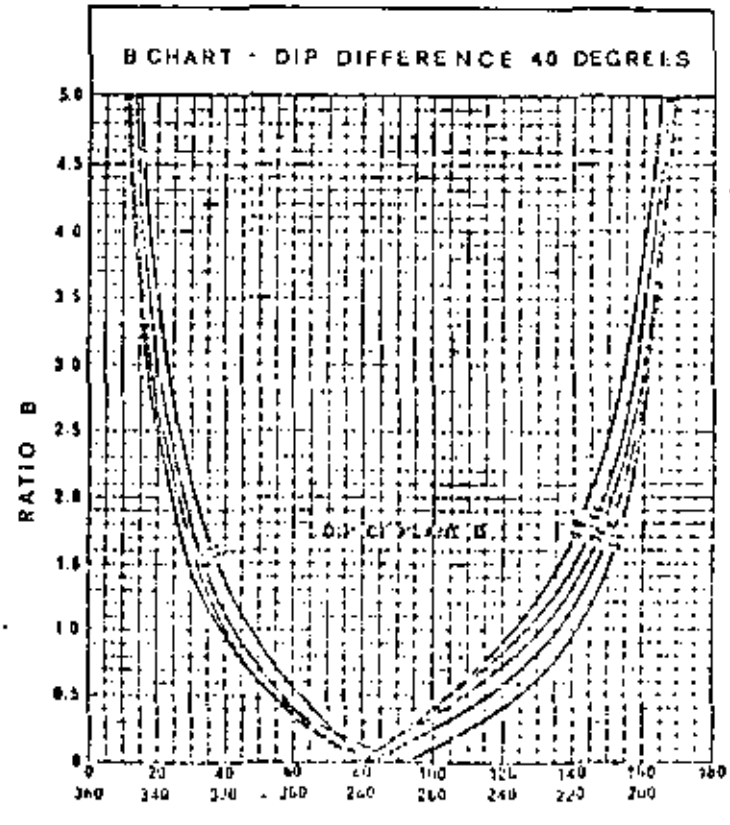
B CHART - DIP DIFFERENCE 40 DEGREES
RATIO B
DIP OF PLANE B
DIFFERENCE IN DIP DIRECTION - DEGREES

337

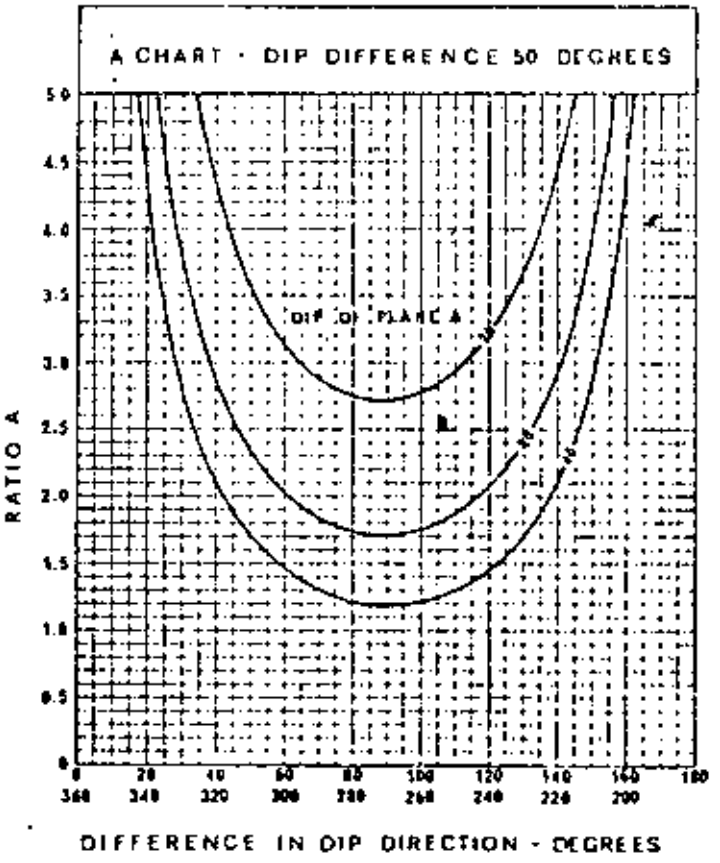
A CHART - DIP DIFFERENCE 50 DEGREES
RATIO A
DIP OF PLANE A
DIFFERENCE IN DIP DIRECTION - DEGREES

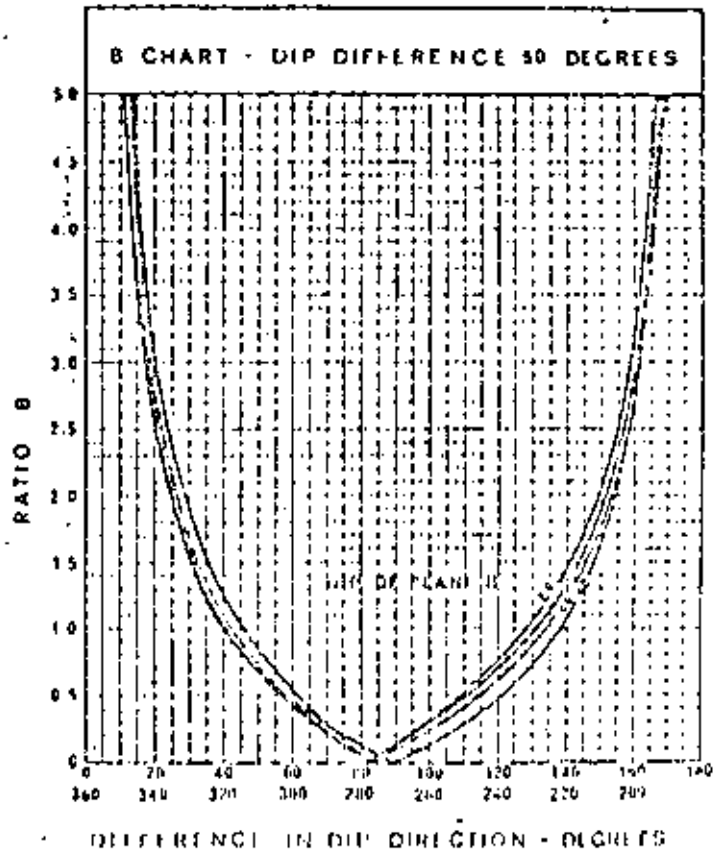
B CHART - DIP DIFFERENCE 50 DEGREES
RATIO B
DIFFERENCE IN DIP DIRECTION - DEGREES

340

Practical example of wedge analysis

During the feasibility study for a proposed open pit mine, the mine planning engineer responsible for the pit layout has requested guidance on the maximum safe angles which may be used for the design of the overall pit slopes. Extensive geological mapping of outcrops on the site together with a certain amount of core logging has established that there are five sets of geological discontinuities in the rock mass surrounding the ore body. The dips and dip directions of these discontinuities are as follows :

Discontinuity set	dip°	dip direction°
1	66 ± 2	298 ± 2
2	68 ± 6	320 ± 15
3	60 ± 16	360 ± 10
4	58 ± 6	76 ± 6
5	54 ± 4	118 ± 2

Note that, because this mapping covers the entire site which extends over several acres, the scatter in the dip and dip direction measurements is considerable and must be taken into account in the analysis. This scatter can be reduced by more detailed mapping in specific locations, e.g. figure 17 on page 54, but this may not be possible because of shortage of time or because suitable outcrops are not available.

Figure 97 shows the pole locations for these five sets of discontinuities. Also shown on this figure are the extent of the scatter in the pole measurements and the great circles corresponding to the most probable pole positions. The dashed figure surrounding the great circle intersections is obtained by rotating the stereoplot to find the extent to which the intersection point is influenced by the scatter around the pole points. The technique described on page 47 is used to define this dashed figure. The intersection of great circles 2 and 5 has been excluded from the dashed figure because it defines a line of intersection dipping at less than 20° and this is considered to be less than the angle of friction.

The factors of safety for each of the discontinuity intersections is determined from the wedge charts (some interpolation is necessary) and the values are given in the circles over the intersection points. Because all of the planes are relatively steep , some of the factors of safety are dangerously low (assuming a friction angle of 30°). Since it is unlikely that slopes with a factor of safety of less than 0.5 could be economically stabilised, the only practical solution is to cut the slopes in these regions to a flat enough overall angle to eliminate the problem.

The construction given in figure 98 is that which is used to find the maximum safe slope angle for different parts of the pit. This construction involves positioning the great circle representing the slope face for a particular dip direction in such a way that the unstable region (shaded) is avoided. The maximum safe slope angles are marked around the perimeter of this figure and their positions correspond to the position on the pit perimeter.

341

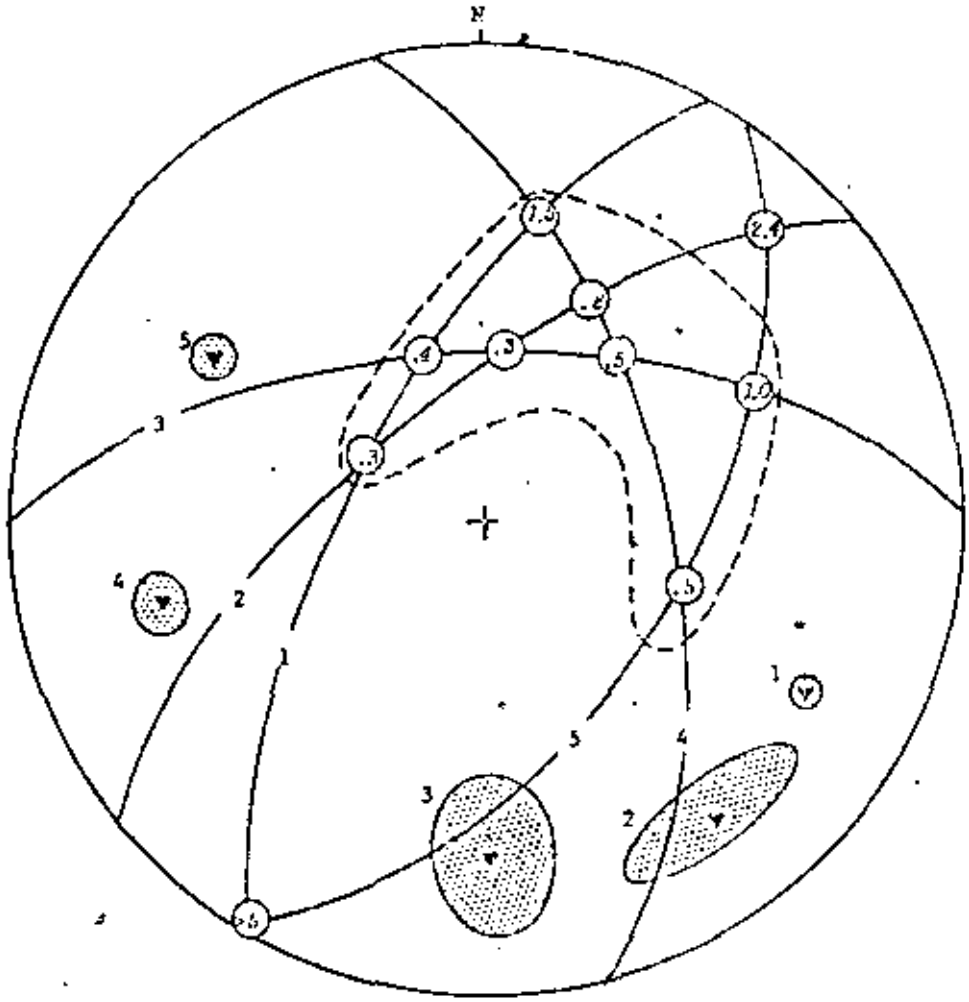

Notes :
a. Black triangles mark most likely position of poles of five sets of discontinuities present in rock mass.
b. Shaded area surrounding pole position defines extent of scatter in measurements.
c. Factors of safety for each combination of discontinuities is given in *italics* in circle over corresponding intersection.
d. Dashed line surrounds area of potential instability.

Figure 97 : Stereoplot of geological data for the preliminary design of an open pit

342

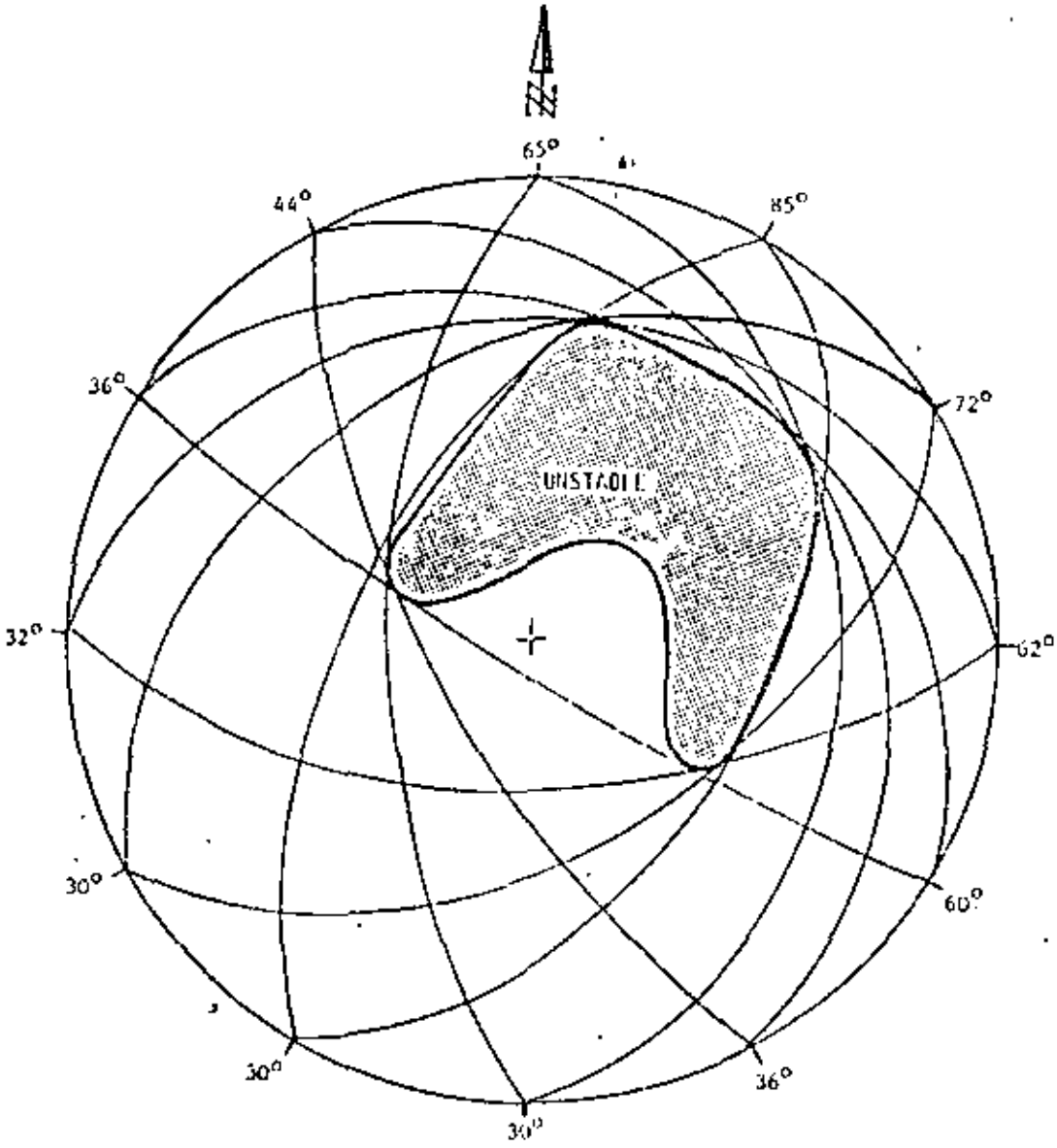

Note : Figures around the perimeter are the recommended stable slope angles for the corresponding position on the pit perimeter.

Figure 98 : Stereoplot of great circles representing stable slopes around an open pit in a rock mass containing the five sets of discontinuities defined in figure 97.

343

Figure 99 shows the suggested pit layout as presented to the mine planning engineer by the rock slope engineer. The pit floor shape and elevation is that originally specified by the mine planning engineer on the basis of the shape of the ore body. This layout is for the overall slopes only, no benches or haul road have been included. It must also be pointed out that the slopes on the north-eastern side of the pit have been specified at 70° instead of the 85° suggested by figure 98. This laying back results from a consideration of the maximum slope height - slope angle relationship presented in figure 7 on page 20.

On no account should the layout suggested in figure 99 be regarded as the final pit plan. The next stage in the feasibility study would obviously be to consider the implications of this suggested pit shape on the overall stripping ratio and hence the economics of the operation. This could easily result in a re-definition of the economic ore body shape and the need for a new pit layout.

Once the general pit shape has been decided upon, the next step is to consider the layout of both production and final benches and to make provision for a haul road or for an alternative transportation system.

Wedge failures in the benches forming the south-western part of this pit would be unavoidable since any faces cut steeper than 30° would allow the wedge intersections to daylight and, considering the factors of safety shown in figure 97, stabilisation of these benches would not be economically feasible. It could, of course, happen that the assumption of friction only is grossly conservative and that the factors of safety are much too low. It may, therefore, be worth carrying out further stability studies on the south-western side of the pit to determine whether any cohesive strength could be relied upon. Back analysis of local quarry slopes, if such quarries exist in the area, would provide the most reliable source of cohesive strength data. Alternatively, shear strength testing would have to be carried out.

If further studies showed that the benches in the south-western part of the pit would be reasonably stable, this side of the pit would provide a good haul road route since this would permit the stripping ratio to be kept to a minimum by retaining the steep overall slopes on the north-eastern side of the pit.

On the other hand, many open pit operators dislike steep slopes and it may be decided, without further stability studies, to sacrifice on the stripping ratio and to place the haul road on the north-eastern side of the pit. While this would result in a considerable flattening of this side of the pit, it would ensure trouble-free benches since, with the reduced height of benches, 80° bench faces could be tolerated and, according to figure 98, such benches would be safe. This solution would probably be the most satisfactory from an operational point of view - provided that the ore body grade was high enough to stand the high stripping ratio.

344

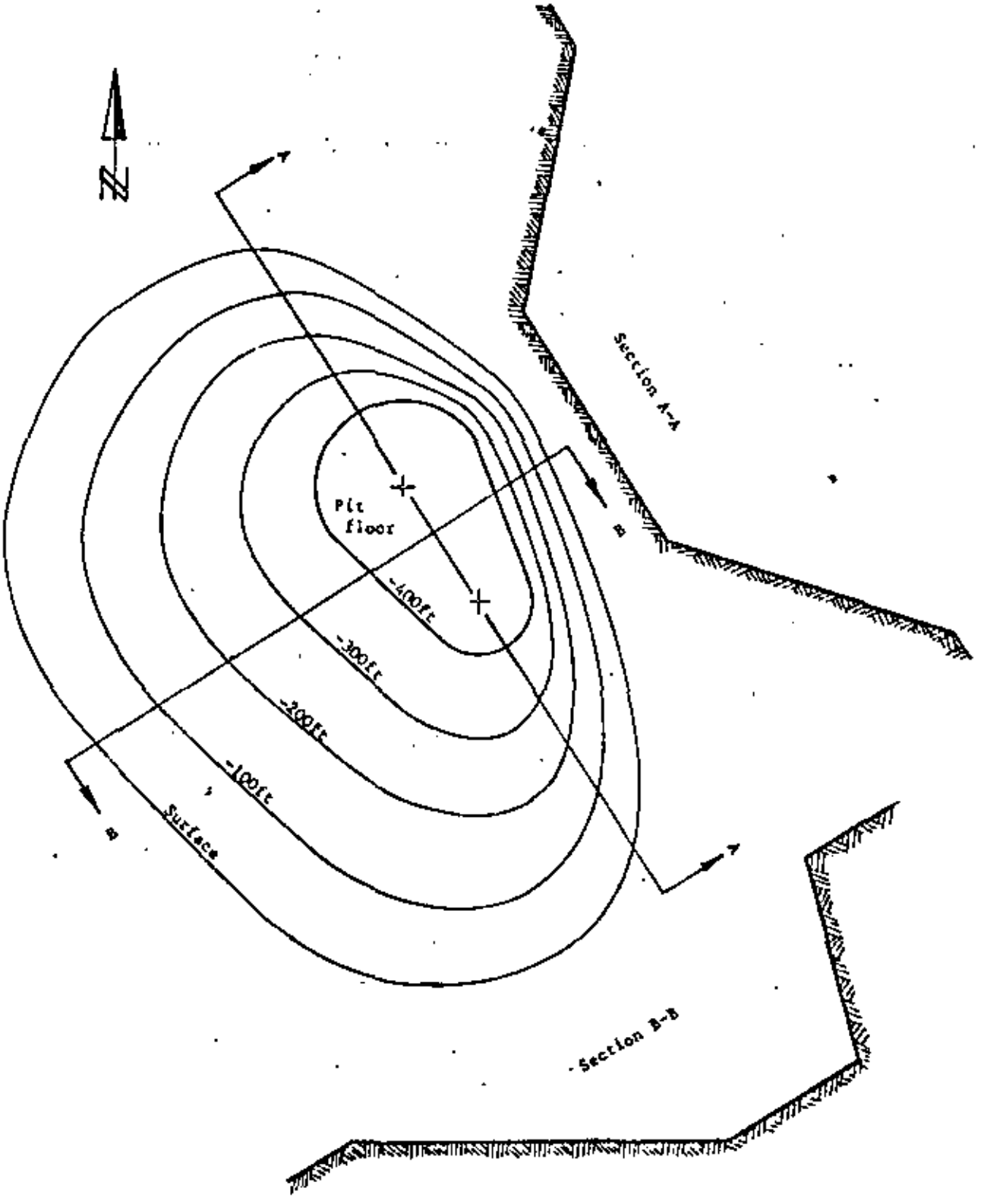

Figure 99 : Design of overall pit slopes according to safe angles defined in figure 98. Note that no benches or haul roads are included in this pit layout.

Chapter 8 references

152. LONDE, P. Une méthode d'analyse a trios dimensions de la stabilité d'une rive rocheuse. *Annales des Ponts et Chaussées*. Paris. 1965. p 37-60.

153. LONDE, P., VIGIER, G. and VORSERINGER, R. The stability of rock slopes, a three-dimensional study. *J. Soil Mech. and Foundation Div. ASCE*. Vol. 95, No. SM 1, 1969. p 235-262.

154. LONDE, P., VIGIER, G. and VORSERINGER, R. Stability of slopes - graphical methods. *J. Soil Mech. and Foundation Div. ASCE*. Vol. 96, No. SM 6, 1970, p 1411-1434.

155. JOHN, K.W. Engineering analysis of three-dimensional stability problems utilising the reference hemisphere. *Proc. 2nd Congress. Intnl. Soc. Rock Mech.* Belgrade. 1970. Vol. 2, p 314-321.

156. WITTKE, W.W. Method to analyse the stability of rock slopes with and without additional loading. (in German). *Felsmechanik und Ingenieurgeologie*. Supp. II. Vol. 30. 1965. p 52-79.

(English translation in Imperial College Rock Mechanics Research Report No. 6, July 1971)

157. GOODMAN, R.E. The resolution of stresses in rock using stereographic projection. *Intnl. J. Rock Mech. Mining Sci.* Vol. 1 , 1964. p 93-103.

158. GOODMAN, R.E. and TAYLOR, R.L. Methods of analysis of rock slopes and abutments : a review of recent developments. in *Failure and breakage of Rocks*. Edited by C.Fairhurst. AIME. 1967. p 303-320.

159. HEUZE, F.E. and GOODMAN, R.E. Three-dimensional approach for the design of cuts in jointed rock. *Proc. 13th Symp. Rock Mech.* Urbana, Illinois. 1971.

160. HENDRON, A.J., CORDING, E.J. and AIYER, A.K. Analytical and graphical methods for the analysis of slopes in rock masses. *U.S. Army Engineering Nuclear Cratering Group*. Tech. Rep. No. 30, 1971. 168p.

161. SRIVASTAVA, L.S. Stability of rock slopes and excavations. *J. Eng. Geology*. Indian Soc. Engineering Geology. Vol. 1/1, 1966. p 57-72.

162. SAVKOV, I.V. Considerations of fracture in the calculation of rock slope stabilities. *Soviet Mining Science* 1967. p 1 - 6.

163. HOEK, E., BRAY, J.W. and BOYD, J.M. The stability of a rock slope containing a wedge resting on two intersecting discontinuities. *Quarterly J. Engineering Geology*. Vol. 6, No. 1, 1973.

164. HOEK, E. Methods for the rapid assessment of the stability of three-dimensional rock slopes. *Quarterly J. Engineering Geology*. Vol.6, No. 3. 1973.

165. HOEK, E. and LONDE, P. General report on the design of rock slopes and foundations. *Proc. 3rd Congress*

346

166. TAYLOR, C.L. Geometric analysis of geological separation for slope stability investigations. *Bull. Aust. Engineering Geologists*, Vol. VII, Nos 1 & 2, 1970. p 67-85.

167. TAYLOR, C.L., Geometric analysis of rock slopes, *Proc. 21st Annual Highway Geology Symposium*. Univ. Kansas, April, 1970.

168. WILSON, S.D. The application of soil mechanics to the stability of open pit mines. *Colorado School of Mines Quarterly*. Vol. 54 No.3. 1959. p 95-113.

169. MULLER, L. The European approach to slope stability problems in open-pit mines. *Colorado School of Mines Quarterly*. Vol. 54, No. 3. 1959. p 117-133

170. MULLER, L and JOHN, K.W. Recent developments of stability studies of steep rock slopes in Europe. *Trans. Soc. Min. Engineers, AIME*. Vol. 226, No.3 1963. p 326-332.

171. MULLER, L. Application of rock mechanics in the design of rock slopes. *Intnl. Conf. State of Stress in the Earth's Crust*. Santa Monica, 1963. Elsevier, New York. 1964.

172. PETZNY, H. On the stability of rock slopes (in German) *Felsmechanik und Ingenieurgeologie*. Suppl. III. 1967.

Chapter 9: Circular failure

347

Introduction

Although this book is concerned primarily with the stability of rock slopes, the reader will occasionally be faced with a slope problem involving soft materials such as overburden soils or crushed waste. In such materials, failure occurs along a surface which approaches a circular shape and this chapter is devoted to a brief discussion on how stability problems involving these materials are dealt with.

In a recent review on the historical development of slope stability theories, Golder [173] has traced the subject back almost 300 years. During the past half century, a vast body of literature on this subject has accumulated and no attempt will be made to summarise this material in this chapter. Standard soil mechanics text books such as those by Taylor[120], Terzaghi [174] and Lambe and Whitman [175] all contain excellent chapters on the stability of soil slopes and it is suggested that at least one of these books should occupy a prominent place on the bookshelf of anyone who is concerned with slope stability. In addition to these books, a number of important papers dealing with specific aspects of soil slope stability have been published and a selected list of these is given under references 176 to 197, at the end of this chapter.

The approach adopted in this chapter is to present a series of slope stability charts for circular failure. These charts enable the user to carry out a very rapid check on the factor of safety of a slope or upon the sensitivity of the factor of safety to changes in groundwater conditions or slope profile. Although these charts do not cover all the conditions which can be dealt with in more sophisticated methods of analysis, they do provide a factor of safety which is adequate for most practical purposes. The authors suggest that the main role of these circular failure charts is similar to that of the wedge charts presented in chapter 8, namely that they enable the user to identify those slopes which are potentially unstable and which require further detailed investigation and those slopes which are safe and which require no further study.

Conditions for circular failure

In the previous chapters it has been assumed that the failure of rock slopes is controlled by geological features such as bedding planes and joints which divide the rock body up into a discontinuous mass. Under these conditions, the failure path is normally defined by one or more of the discontinuities. In the case of a soil, a strongly defined structural pattern no longer exists and the failure surface is free to find the line of least resistance through the slope. Observations of slope failures in soils suggests that this failure surface generally takes the form of a circle and most stability theories are based upon this observation.

The conditions under which circular failure will occur arise when the individual particles in a soil or rock mass are very small as compared with the size of the slope and when these particles are not interlocked as a result of their shape. Hence, crushed rock in a large waste dump

348

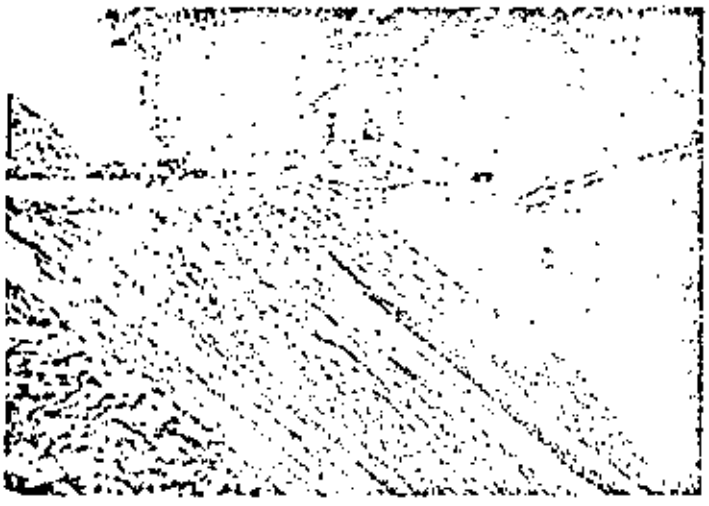

Figure 100 : Shallow surface failures in large waste dumps are generally of a circular type.

Figure 101 : Circular failure in the highly altered and weathered rock forming the upper benches of an open pit mine.

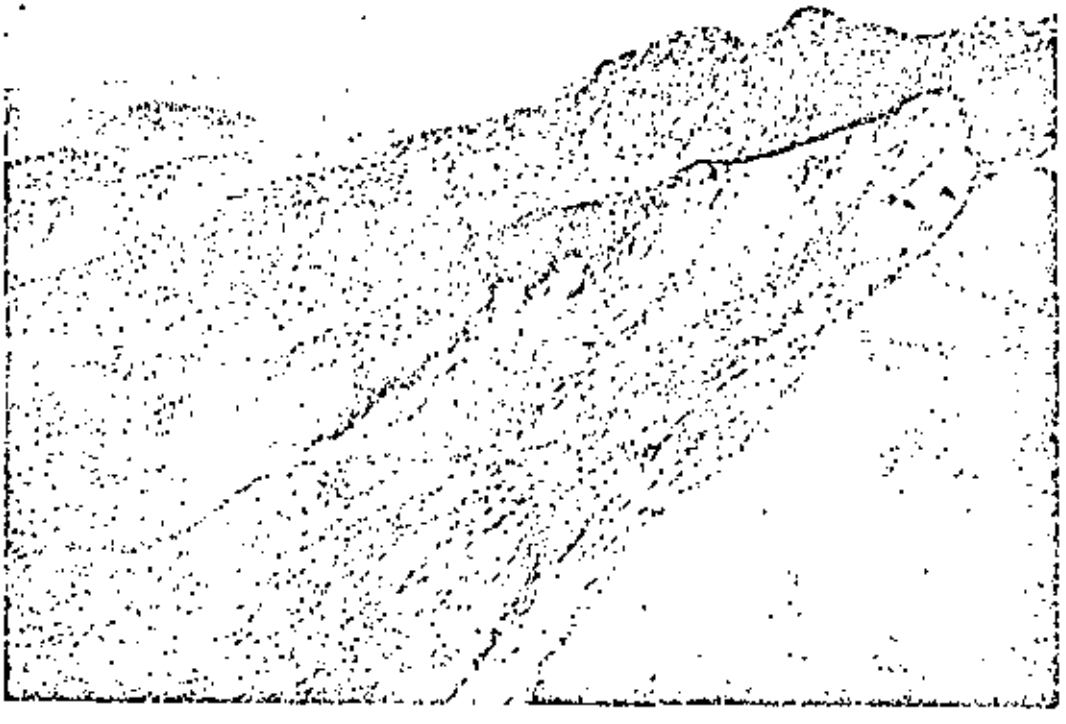

Figure 102 : A very large natural slope will sometimes fail on a surface which is similar in appearance to that observed in a shallow circular slip. This is because the stresses involved in the failure process are high enough to over-ride the control of small scale geological features in the rock mass. The photograph illustrates the Hope Mountain slide in British Columbia, Canada. This slide involved the movement of 130 million tons of material over a slide surface 10 000 feet long.

350

in a circular mode. Alternatively, the finely ground waste material which has to be disposed of after completion of a milling and metal recovery process will exhibit circular failure surfaces, even in slopes of only a few feet in height. Highly altered and weathered rocks will also tend to fail in this manner and it is appropriate to design the overburden slopes around an open pit mine on the assumption that failure would be by a circular failure process.

Derivation of circular failure charts

The following assumptions are made in deriving the stability charts presented in this chapter :

a. The material forming the slope is assumed to be homogeneous, i.e. its mechanical properties do not vary with direction of loading.

b. The shear strength of the material is characterised by a cohesion c and a friction angle ϕ which are related by the equation $\tau = c + \sigma.\tan\phi$ (see page 22).

c. Failure is assumed to occur on a circular failure surface which passes through the toe of the slope *.

d. A vertical tension crack is assumed to occur in the upper surface or in the face of the slope.

e. The locations of the tension crack and of the failure surface are such that the factor of safety of the slope is a minimum for the slope geometry and groundwater conditions considered.

f. A range of groundwater conditions, varying from a dry slope to a fully saturated slope under heavy recharge, are considered in the analysis. These conditions are defined later in this chapter.

Defining the factor of safety of the slope as

$$F = \frac{\text{Shear strength available to resist sliding}}{\text{Shear stress mobilised along failure surface}}$$

and rearranging this equation,

$$\tau_{mb} = \frac{c}{F} + \frac{\sigma.\tan\phi}{F} \qquad (83)$$

where τ_{mb} is the shear stress mobilised along the failure surface.

Since the shear strength available to resist sliding is dependent upon the distribution of the normal stress σ along this surface and, since this normal stress distribution is unknown, the problem is statically indeterminate. In order to obtain a solution it is necessary to assume a specific normal stress distribution and then to check whether this distribution gives meaningful practical results.

---

* Terzaghi [175], page 170, shows that the toe failure assumed for this analysis gives the lowest factor of safety provided that $\phi > 5^{0}$. The $\phi = 0$ analysis, involving failure below the toe of the slope through the base material has been discussed by Skempton [190] and by Bishop and Bjerrum [199] and is applicable to failures which occur during or after the rapid construction of a slope. Such conditions are

The influence of various normal stress distributions upon the factor of safety of soil slopes has been examined by Frohlich [179] who found that a *lower bound* for all factors of safety which satisfy statics is given by the assumption that the normal stress is concentrated at a single point on the failure surface. Similarly, the *upper bound* is obtained by assuming that the normal load is concentrated at the two end points of the failure arc.

The unreal nature of these stress distributions is of no consequence since the object of the exercise, up to this point, is simply to determine the extremes between which the actual factor of safety of the slope must lie. In an example considered by Lambe and Whitman [174], the upper and lower bounds for the factor of safety of a particular slope corresponded to 1,62 and 1,27 respectively. Analysis of the same problem by Bishop's simplified method of slices gives a factor of safety of 1.30 which suggests that the actual factor of safety may lie reasonably close to the lower bound solution.

Further evidence that the lower bound solution is also a meaningful practical solution is provided by an examination of the analysis which assumes that the failure surface has the form of a logarithmic spiral [191]. In this case, the factor of safety is independent of the normal stress distribution and the upper and lower bounds coincide. Taylor [120] compared the results from a number of logarithmic spiral analyses with the results of lower bound solutions * and found that the difference was negligible. On the basis of this comparison, Taylor concluded that the lower bound solution provides a value of the factor of safety which is sufficiently accurate for most practical problems involving simple circular failure of homogeneous slopes.

The authors have carried out similar checks to those carried out by Taylor and have reached the same conclusions. Hence, the charts presented in this chapter correspond to the lower bound solution for the factor of safety, obtained by assuming that the normal load is concentrated at a single point on the failure surface. These charts differ from those published by Taylor in 1948 in that they include the influence of a critical tension crack and of groundwater in the slope.

Groundwater flow assumptions

In order to calculate the uplift force due to water pressure acting on the failure surface and the force due to water in the tension crack, it is necessary to assume a set of groundwater flow patterns which coincide as closely as possible with those conditions which are believed to exist in the field.

In the analysis of rock slope failures, discussed in chapters 7 and 8, it was assumed that most of the water flow took place in discontinuities in the rock and that the rock itself was practically impermeable. In the case

---

* The lower bound solution discussed in this chapter is usually known as the *Friction Circle Method* and was used by Taylor [120] for the derivation of his stability charts.

of slopes in soil or in waste rock, the permeability of the mass of material is generally several orders of magnitude higher than that of intact rock and, hence, a general flow pattern will develop in the material behind the slope.

Figure 56a on page 119 shows that, within the soil mass, the equipotentials are approximately perpendicular to the phreatic surface. Consequently, the flow lines (figure 65 on page 117) will be approximately parallel to the phreatic surface for the condition of steady state drawdown. Figure 103a shows that this approximation has been used for the analysis of the water pressure distribution in a slope under conditions of normal drawdown. Note that the phreatic surface is assumed to coincide with the ground surface at a distance x, measured in multiples of the slope height, behind the toe of the slope. This may correspond to the position of a surface water source such as a river or dam or it may simply be the point where the phreatic surface is judged to intersect the ground surface.

The phreatic surface itself has been obtained, for the range of slope angles and values of x considered, by a computer solution of the equations proposed by L.Casagrande [200], discussed in the text book by Taylor [320].

For the case of a saturated slope subjected to heavy surface recharge, the equipotentials and the associated flow lines used in the stability analysis are based upon the work of Han [132] who used an electrical resistance analogue method for the study of groundwater flow patterns in isotropic slopes.

Production of circular failure charts

The circular failure charts presented in this chapter were produced by means of a Hewlett-Packard 9100 B calculator with graph plotting facilities. This machine was programmed to seek out the most critical combination of failure surface and tension crack for each of a range of slope geometries and groundwater conditions. Provision was made for the tension crack to be located in either the upper surface of the slope or in the face of the slope. Detailed checks were carried out in the region surrounding the toe of the slope where curvature of the equipotentials results in local flow which differs from that illustrated in figure 103a.

The charts are numbered 1 to 5 to correspond with the groundwater conditions defined in the table presented on page 217.

Use of the circular failure charts

In order to use the charts to determine the factor of safety of a particular slope, the steps outlined below and shown in figure 104 should be followed.

Step 1 : Decide upon the groundwater conditions which are believed to exist in the slope and choose the chart which is closest to these conditions , using the table presented on page 217.

Step 2 : Calculate the value of the dimensionless ratio

353

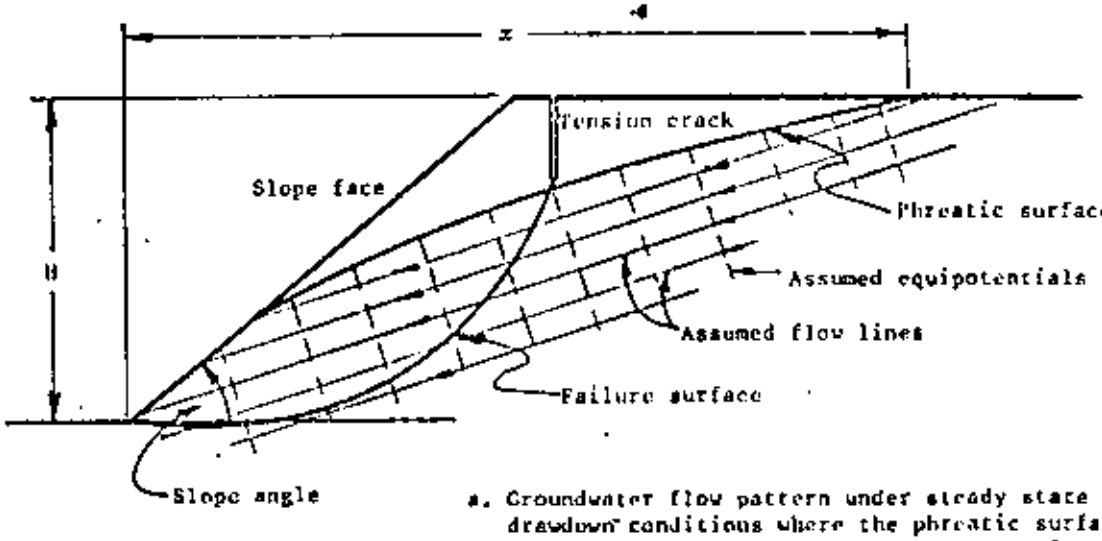

a. Groundwater flow pattern under steady state drawdown conditions where the phreatic surface coincides with the ground surface at a distance x behind the toe of the slope. The distance x is measured in multiples of the slope height H.

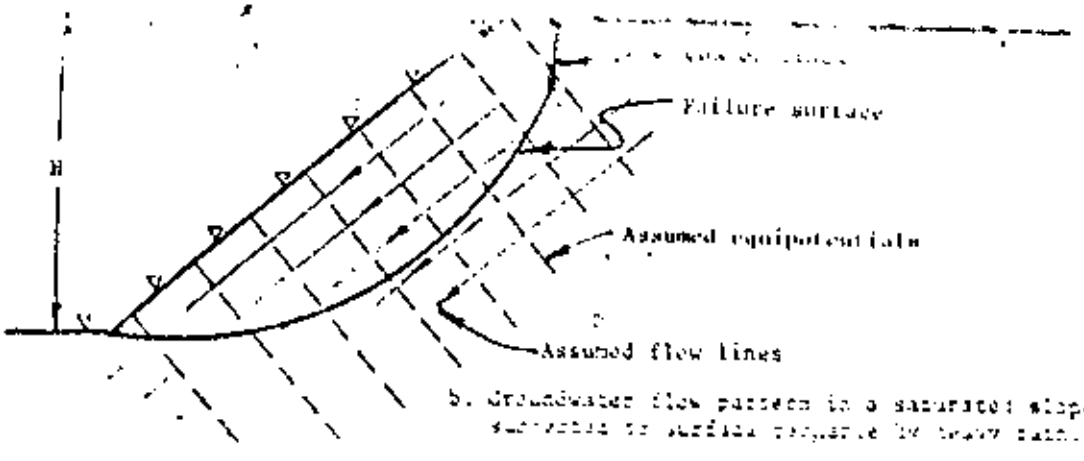

b. Groundwater flow pattern in a saturated slope [illegible]

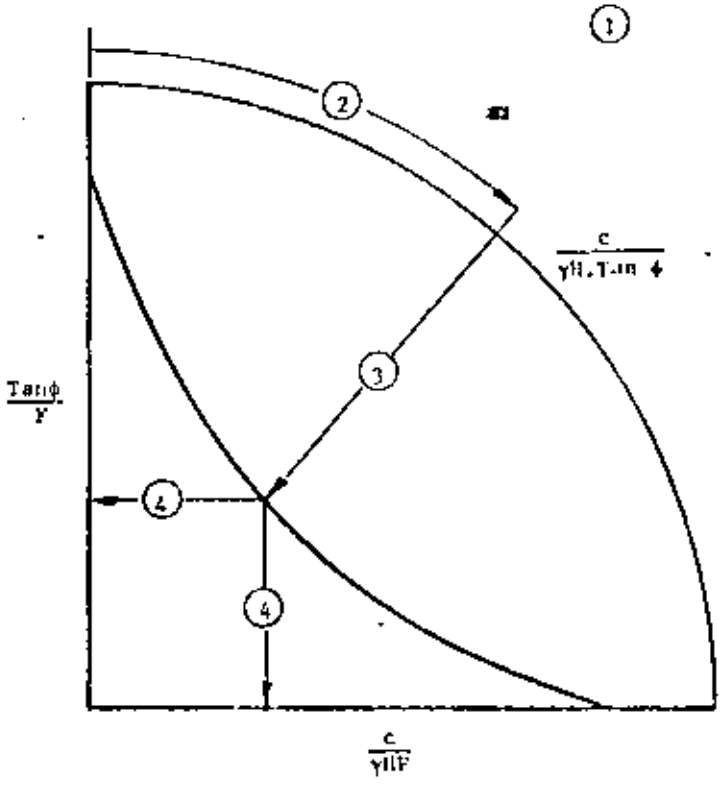

Figure 104 : Sequence of steps involved in using circular failure charts to find the factor of safety of a slope.

Find this value on the outer circular scale of the chart.

Step 3 : Follow the radial line from the value found in step 2 to its intersection with the curve which corresponds to the slope angle under consideration.

Step 4 : Find the corresponding value of $Tan\phi/F$ or $c/\gamma HF$, depending upon which is more convenient, and calculate the factor of safety.

Consider the following example:

A 50 foot high slope with a face angle of 40^0 is to be excavated in overburden soil with a density $\gamma = 100\ lb/ft^3$, a cohesive strength of $800 lb/ft^2$ and a friction angle of 30^0. Find the factor of safety of the slope, assuming that there is a surface water source 200 feet behind the toe of the slope.

The groundwater conditions indicate the use of chart number 3. The value of $c/\gamma H.Tan\phi = 0.28$ and the corresponding value of $Tan\phi/F$, for a 60^0 slope, is 0.32. Hence, the factor of safety of the slope is 1.80.

Because of the speed and simplicity of using these charts, they are ideal for checking the sensitivity of the factor of safety of a slope to a wide range of conditions and the

355

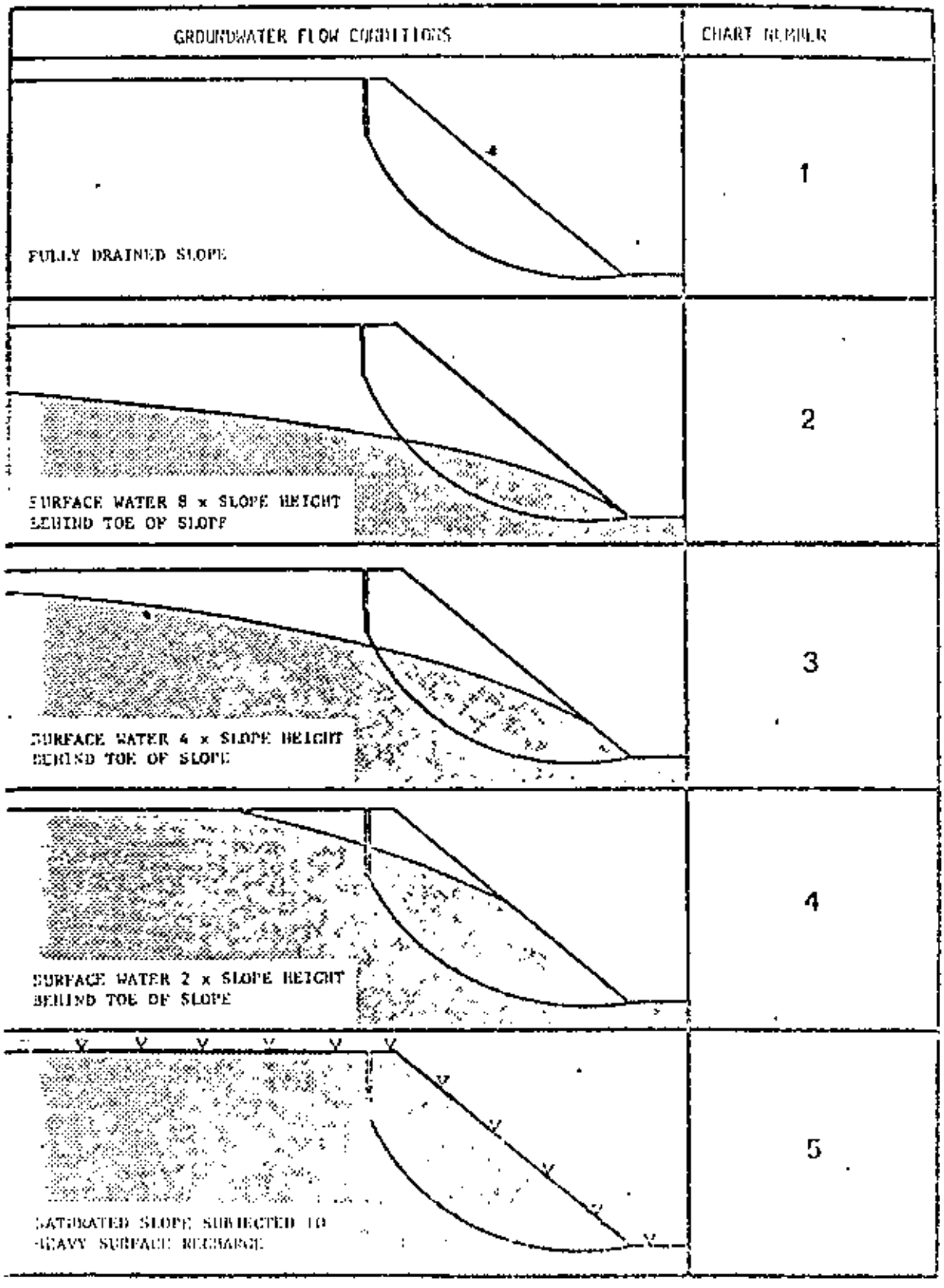
GROUNDWATER FLOW CONDITIONS
CHART NUMBER
1
FULLY DRAINED SLOPE
2
SURFACE WATER 8 x SLOPE HEIGHT
BEHIND TOE OF SLOPE
3
SURFACE WATER 4 x SLOPE HEIGHT
BEHIND TOE OF SLOPE
4
SURFACE WATER 2 x SLOPE HEIGHT
BEHIND TOE OF SLOPE
5
SATURATED SLOPE SUBJECTED TO
HEAVY SURFACE RECHARGE

356

CIRCULAR FAILURE CHART NUMBER 1

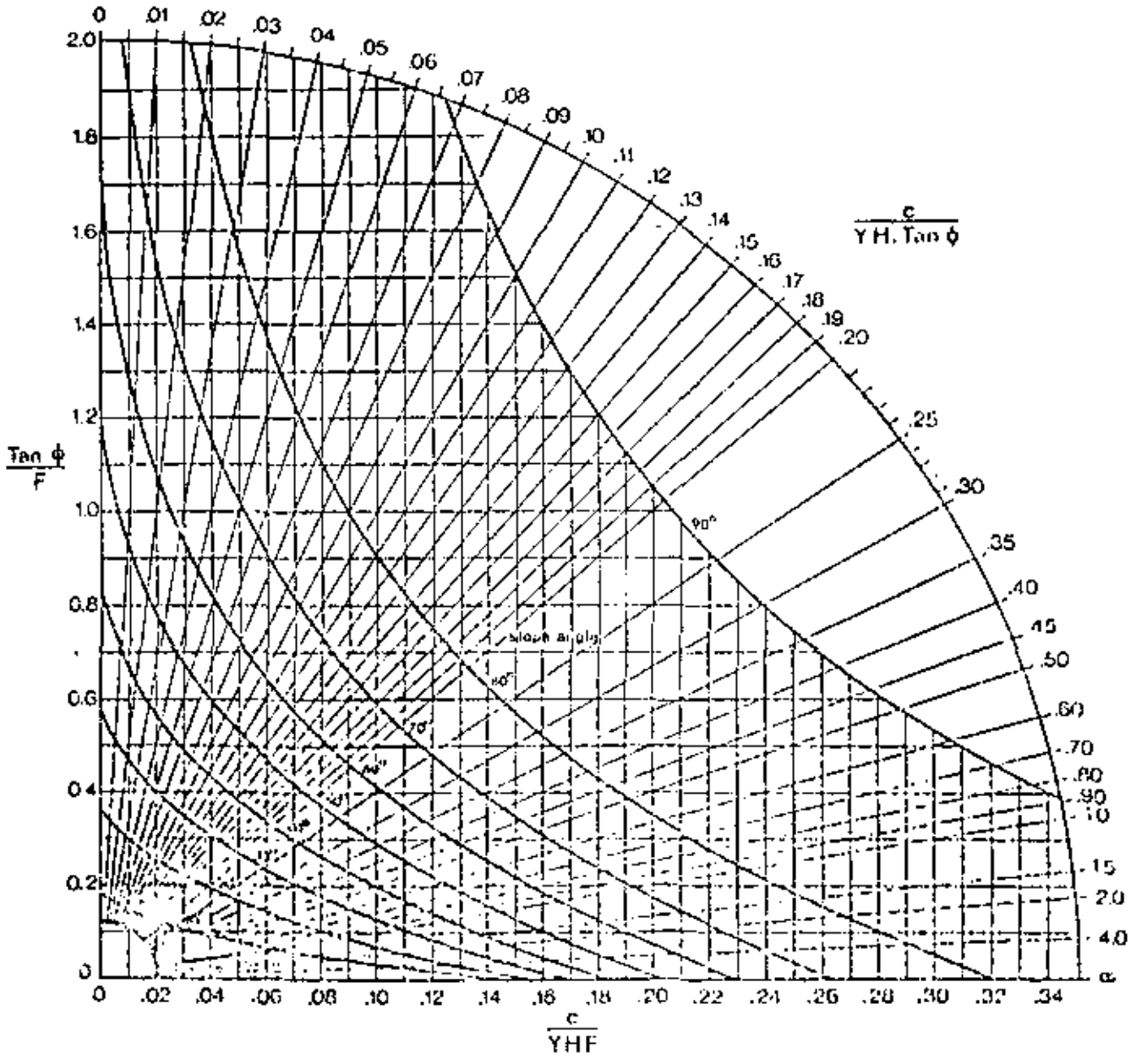

CIRCULAR FAILURE CHART NUMBER 2

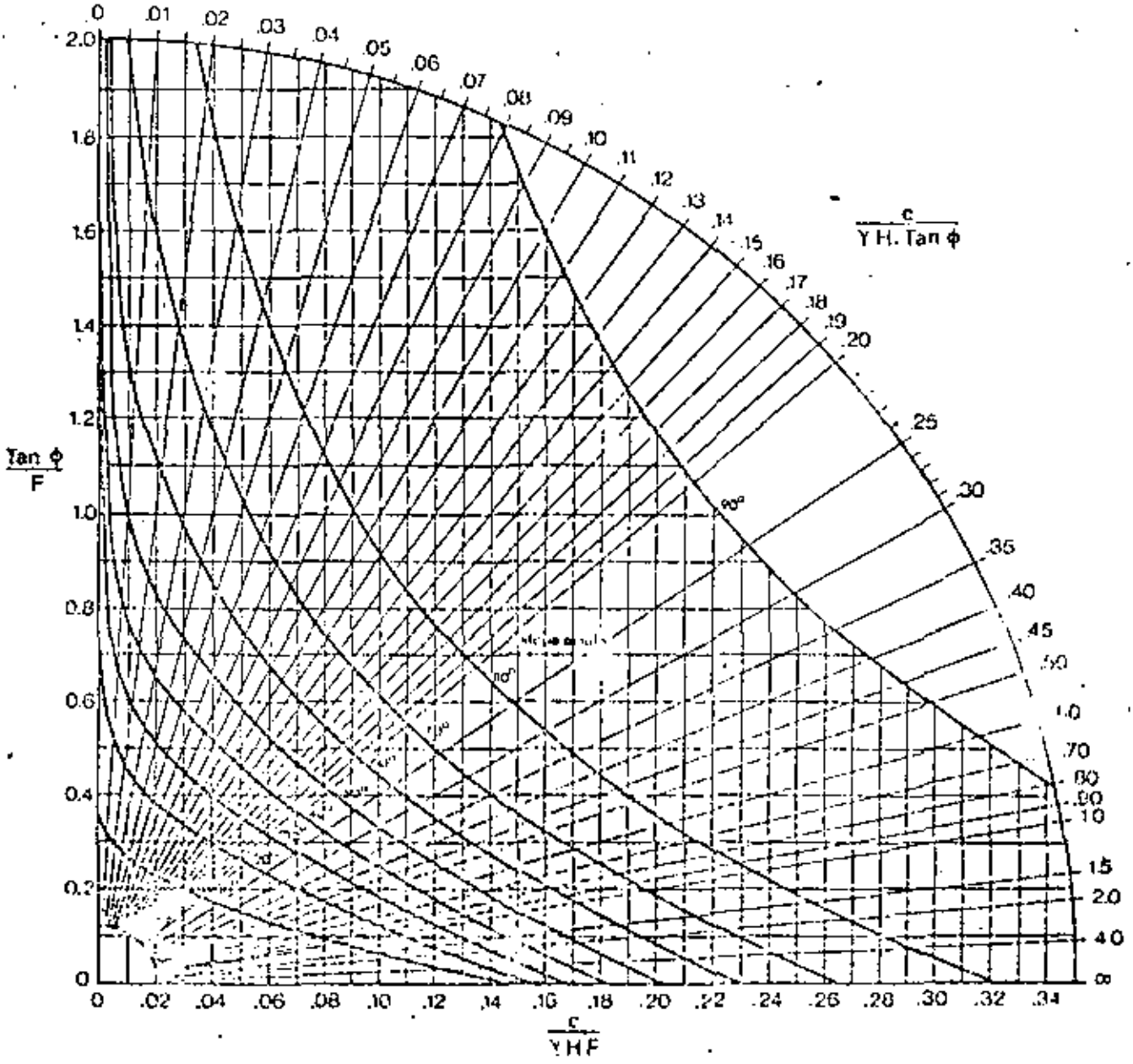

35b

CIRCULAR FAILURE CHART NUMBER 3

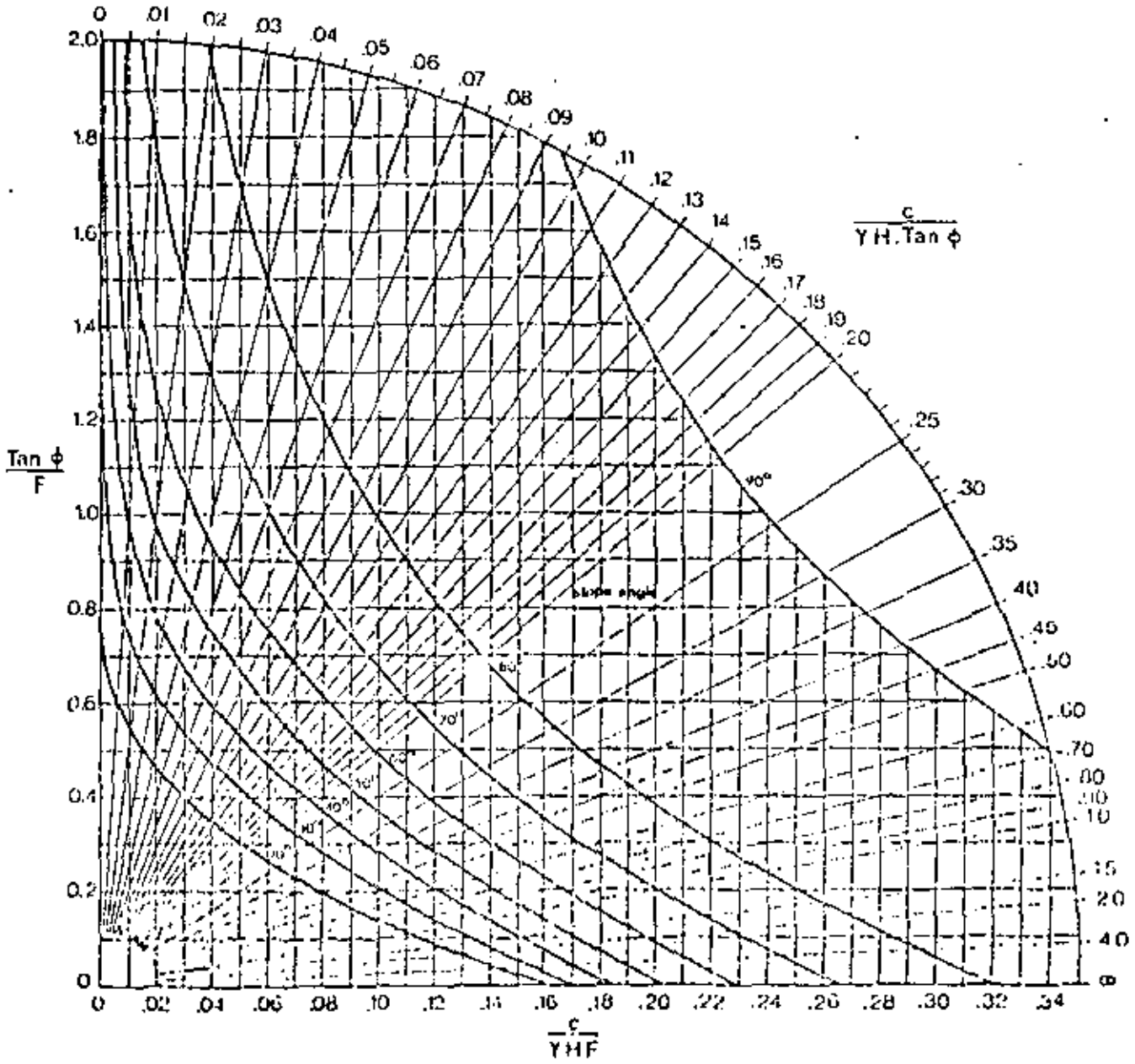

353

CIRCULAR FAILURE CHART NUMBER 4

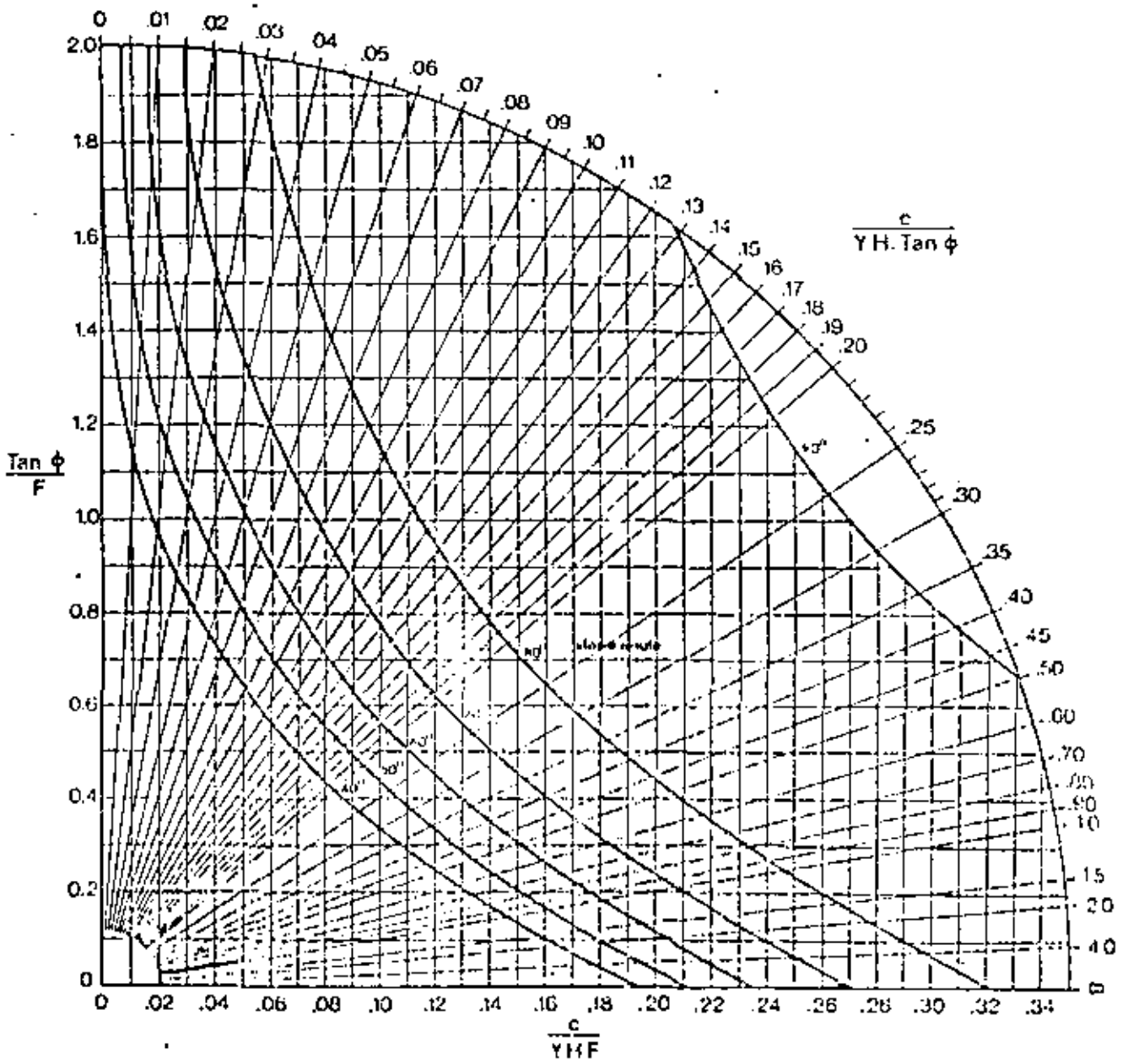

360

CIRCULAR FAILURE CHART NUMBER 5

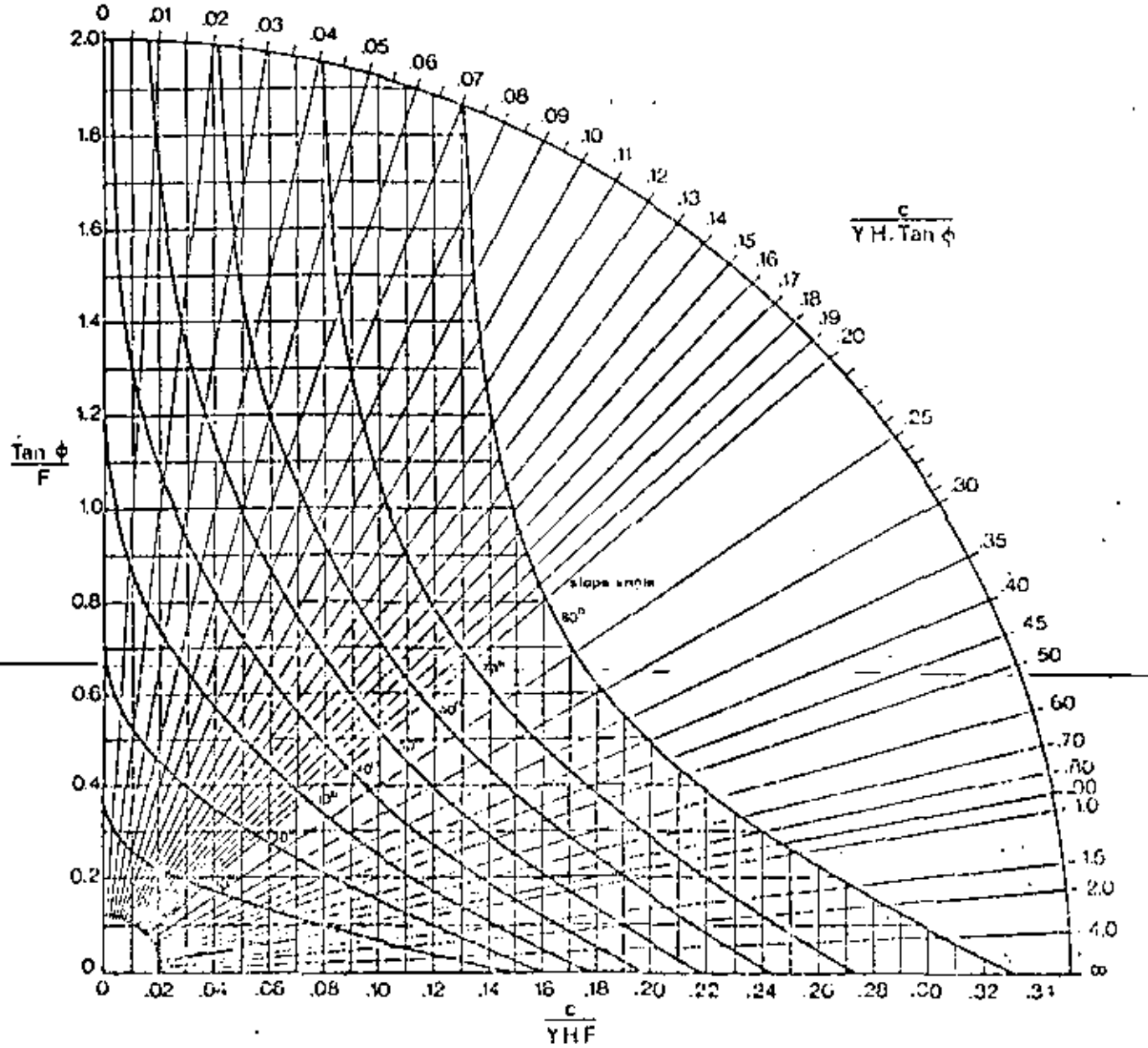

361

Practical example number 1

China clay pit slope

Ley [143] has investigated the stability of a China clay pit slope which was considered to be potentially unstable. The slope profile is illustrated in figure 105 below and the input data used for the analysis is included in this figure. The material, a heavily kaolinised granite, was carefully tested by Ley and the friction angle and cohesive strength are considered reliable for this particular slope.

Two piezometers in the slope and a known water source some distance behind the slope enabled Ley to postulate the phreatic surface shown in figure 105. The chart which corresponds most closely to these groundwater conditions is considered to be chart number 2.

From the information given in figure 105, the value of the ratio $c/\gamma H.Tan\phi = 0.0056$ and the corresponding value of $Tan\phi/F$, from chart number 2, is 0.76. Hence, The factor of safety of the slope is 1.01 .

Ley also carried out a number of trial calculations using Janbu's method [201] and, for the critical slip circle shown in figure 105, found a factor of safety of 1.03.

These factors of safety indicated that the stability of the slope was inadequate under the assumed conditions and steps were taken to deal with the problem.

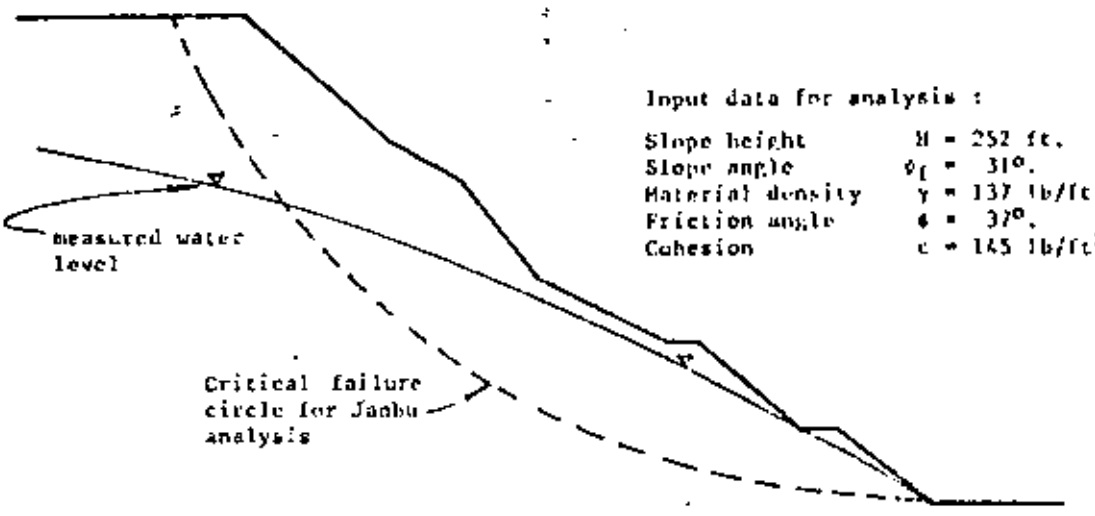

Figure 105 : Slope profile of China clay pit slope considered in example number 1 .

Practical example number 2

Projected open pit slope

An open pit mine plan calls for a slope on one side of the pit to have an angle of 42°. The total height of the slope will be 200 feet when completed and it is required to check whether the slope will be stable. A site visit enables the slope engineer to assess that the slope is in weathered and altered material and that failure, if it occurs, will be of a circular type. Insufficient time is available for groundwater levels to be accurately established or for shear tests to be carried out. The stability analysis is carried out as follows :

For the condition of limiting equilibrium , F = 1 and $Tan\phi/F = Tan\phi$. For a range of friction angles, the values of $Tan\phi$ are used to find the values of $c/\gamma H.Tan\phi$, for 42°, by reversing the procedure outlined in figure 104. The value of the cohesion c which is mobilised at failure, for a given friction angle, can then be calculated. This analysis is carried out for dry slopes, using chart number 1, and for saturated slopes, using chart number 5. The resulting range of friction angles and cohesive strengths which would be mobilised at failure are plotted in figure 106.

The shaded circle included in figure 106 indicates the range of shear strengths which are considered probable for the material under consideration, based upon the data presented in figure 70 on page 152. It is clear from this figure that the available shear strength may not be adequate to maintain stability in this slope, particularly when the slope is saturated. Consequently, the slope engineer would have to recommend that, either the slope should be flattened or, that investigations into the groundwater conditions and material properties should be undertaken in order to establish whether the analysis presented in figure 106 is too pessimistic.

The effect of flattening the slope can be checked very quickly by finding the value of $c/\gamma H.Tan\phi$ for a flatter slope, say 30°, in the same way as it was found for the 42° slope. The dashed line in figure 106 indicates the shear strength which would be mobilised in a dry slope with a face angle of 30°.

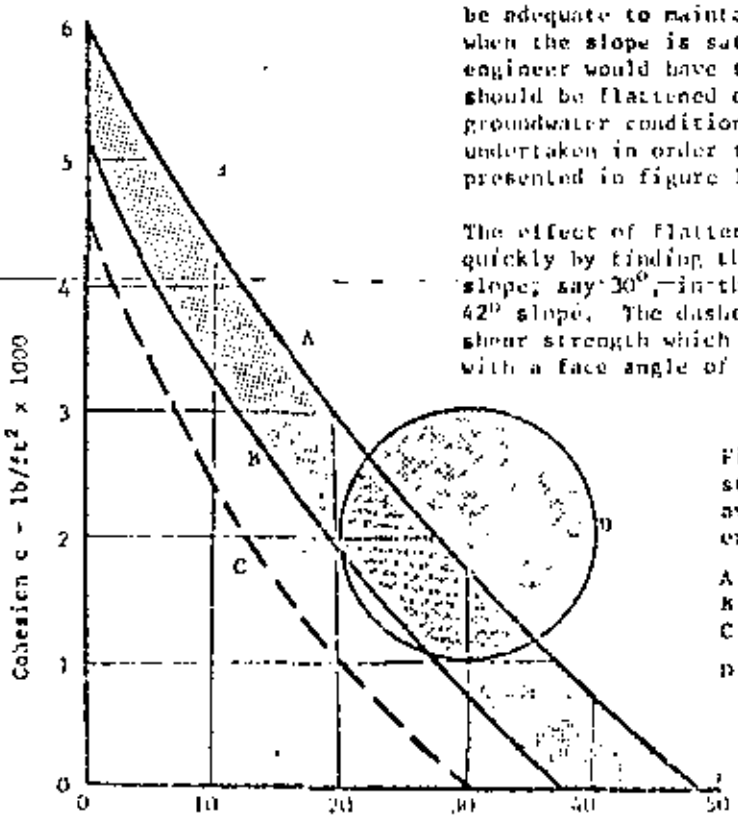

Figure 106 : Comparison between shear strength mobilised and shear strength available for slope considered in example number 2 .

A = saturated 42° slope.
B = dry 42° slope.
C = dry 30° slope .
D = probable shear strength range for material in which slope is cut.

363

Practical example number 3

Stability of waste dumps

As a result of the catastrophic slide in colliery waste material at Aberfan in Wales on October 22, 1966, attention was focussed on the potential danger associated with large dumps of waste material from mining operations [202]. Since 1966, a number of excellent papers and handbooks dealing with waste dump stability and with the disposal of finely ground waste have become available [203 - 206] and the authors do not feel that a detailed discussion on this subject would be justified in this book. The purpose of this example is to illustrate the application of the design charts for circular failure, presented earlier in this chapter, to waste dump stability problems.

McKechnie Thompson and Rodin [203] have shown that the relationship between shear strength and normal stress for colliery waste material is usually non-linear as shown in figure 107. In view of the discussion on shear strength presented in chapter 5, this finding is not particularly surprising and the authors suspect that most waste materials exhibit this non-linearity to a greater or lesser degree. Consequently, the methods used in this example, although applied specifically to colliery waste, are believed to be equally applicable to most rock waste dumps.

The method used in analysing the stability of a slope in material which exhibits non-linear shear strength behaviour was discussed on page 92 and illustrated in figure 37. This figure shows that a number of tangents are drawn to the failure curve, giving values for apparent cohesion and angle of friction for various normal stress levels. These values are then used for stability analyses in exactly the same way as the cohesion and friction values for a normal soil.

In the case of the failure curve for colliery waste, shown in figure 107, the apparent cohesion values and the friction angles given by the three tangents are as follows :

Tangent number	Apparent cohesion kN/m^2	Friction angle degrees.
1	0	38
2	20	26
3	40	22

The relationship between slope height and slope angle for the condition of limiting equilibrium, F = 1, will be investigated for a dry dump (using chart no. 1) and for a dump with some groundwater flow (using chart no.3).

Tangent number 1

Since the cohesion intercept is zero for this tangent, the value of the dimensionless ratio $c/\gamma H$, $\tan\phi = 0$ and hence, the slope angle at which the face would repose is given by the slope angle corresponding to the value of $\tan 38^{\circ} = 0.78$ on the $\tan\phi/F$ axis (noting that F = 1). From chart number 1, this intercept is 38° and for chart number 3 it is approximately 25°.

Note that, for zero cohesion, the dump face angle would be

364

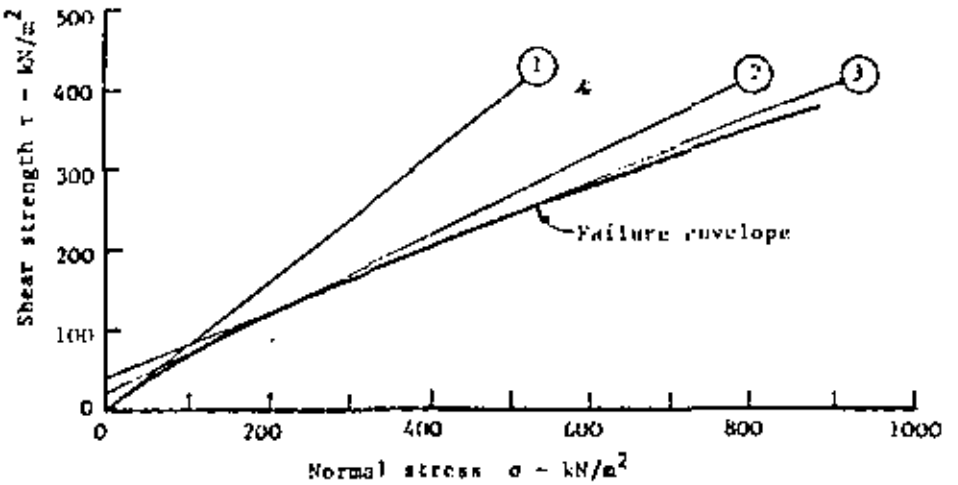

Figure 107 : Shear strength of typical colliery waste material.

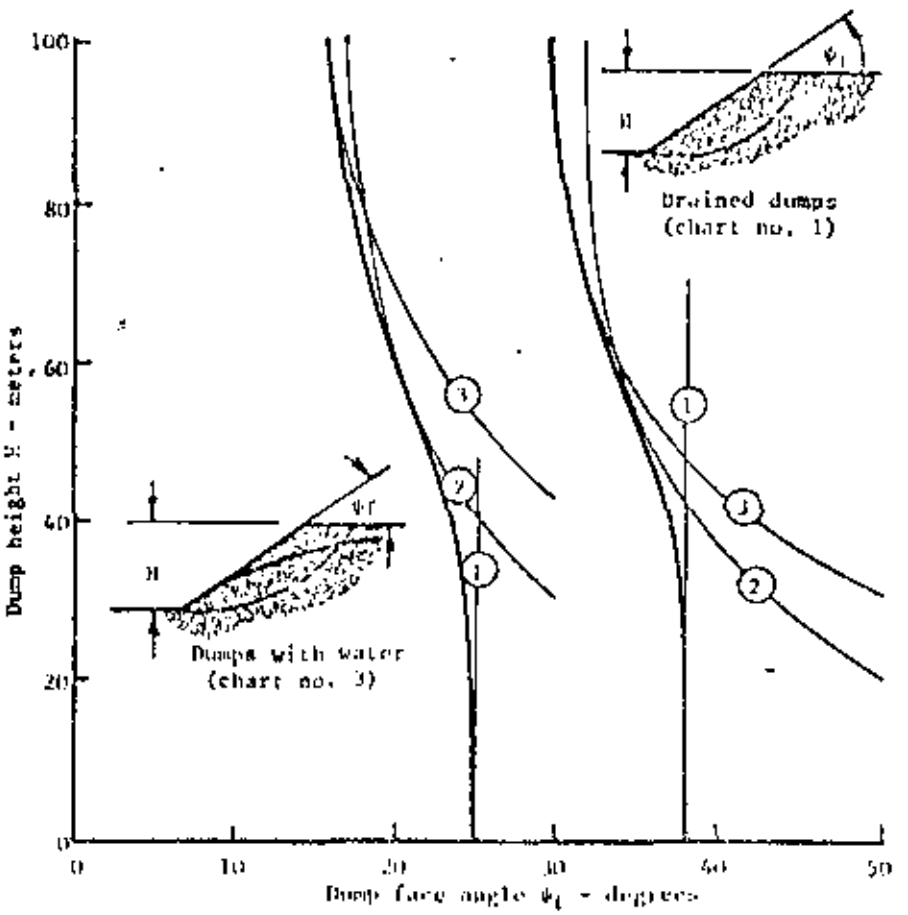

Figure 108 : Relationship between slope height and slope angle for a

independent of the slope height. It is normally assumed that the angle of repose of a waste dump is independent of the height of the dump and is equal to the angle of friction of the material. Figure 108 shows that this assumption is only correct for a dry slope of limited height. Any build-up of water pressure within the dump causes a serious reduction in the stable face angle and, once the normal stress across the potential failure surface becomes high enough for the next tangent to become operative, the high initial friction angle no longer applies and the dump face assumes a flatter angle.

Tangent number 2

For $c = 20\ kN/m^2$, $\gamma = 18\ kN/m^3$ and $\phi = 26^\circ$

$$\frac{c}{\gamma H.\ Tan\ \phi} = \frac{20}{18.Tan\ 26^\circ.H} = \frac{2.78}{H}$$

and $Tan\phi/F = Tan\ 26^\circ = 0.49$

Hence

H meters	$\frac{c}{\gamma H.Tan\ \phi}$	Slope angle° Chart 1	Chart 3
20	0.114	50	39
40	0.057	39	25
60	0.038	34	20
80	0.029	32	18
100	0.023	31	17

Plotting these values on figure 108 give the curves numbered 2 for the drained and the wet dumps.

Tangent number 3

$c = 40\ kN/m^2$, $\gamma = 18\ kN/m^3$ and $\phi = 22^\circ$, hence

$c/\gamma H.Tan\phi = 5.5/H$ and $Tan\ \phi/F = 0.4$

H meters	$\frac{c}{\gamma H.Tan\phi}$	Slope angle° Chart 1	Chart 3
20	0.275	61	56
40	0.138	43	31
60	0.092	34	22
80	0.069	31	18
100	0.055	30	16

The relationships between dump face angle and dump height, for both drained and wet dumps, are given by the envelopes to the curves derived from tangents 1, 2 and 3. These envelopes, shown in figure 108, illustrate the danger in continuing to increase the height of a dump on the assumption that it will remain stable at an angle of repose equal to the friction angle. The dangers associated with poor dump drainage are also evident in this figure.

The reader who attempts this type of analysis for himself, and it is strongly recommended that he should, will find that the slope height versus slope angle relationship is extremely sensitive to the shape of the shear failure curve. This emphasises the need for reliable in situ shear test methods such as those described by McKechnie Thompson and Kolin [201] and Schultze and Horn [207] to be further developed for application to waste dump problems.

Figure 111 : A hard rock slope face damaged by excessively heavy blasting during the excavation of a road cut.

Figure 112 : An 18 meter high rock face created by pre-split blasting. Note the clean fracture running between the parallel holes in the face, in spite of the variability of the rock through which the holes have been drilled. (Photograph reproduced with permission of Atlas Copco Ltd, Sweden)

It would exceed the scope of this book to enter into a full discussion on either the detailed techniques or the costs of controlled blasting applied to rock slope engineering. The purpose of this discussion is simply to draw the reader's attention to the benefits to be gained from the use of smooth blasting and pre-split blasting techniques in the creation of the final slopes of an open pit mine or a roadcut. More detailed information on these methods can be obtained from the excellent textbook by Langefors and Kihlström [217] or from papers such as that by Ouiard [218]. Much of the material upon which the following discussion is based has been drawn from an unpublished memorandum by Kihlström [219] which was made available to one of the authors (E.H.) by Nitro Nobel AB during a recent visit to Sweden.

Smooth blasting is a technique which is used for trimming the face of an excavation which has already been created. Figure 113 shows a smooth blasting operation in progress on the site of a large arch dam site in Tasmania. The purpose of this particular operation was to trim off loose and unstable surface rock from an existing natural slope in order to provide sound stable abutments for the dam. The method involves the drilling of small diameter parallel holes along the line of the desired slope profile. In the example illustrated, the holes were drilled with a normal hand held percussion drill to a depth of approximately ten feet for each blast. The holes are lightly charged and detonated simultaneously and, as can be seen from the photograph reproduced in figure 113, this results in a clean cut face in which the fractures have propagated along planes passing through the parallel holes. Two more examples of smooth blasting are illustrated in figures 114 and 115 which show, in the one case, an air-track machine being used to drill a pattern of holes and, in the other, a tunnel profile created by smooth blasting.

Pre-split blasting is similar to smooth blasting except that the line of lightly charged holes is detonated *before* the normal excavation blast and this results in a smooth fracture which protects the rock mass behind the face from the effects of the normal blast. An example of slopes in which pre-split blasting was used on a large scale is illustrated in figure 116.

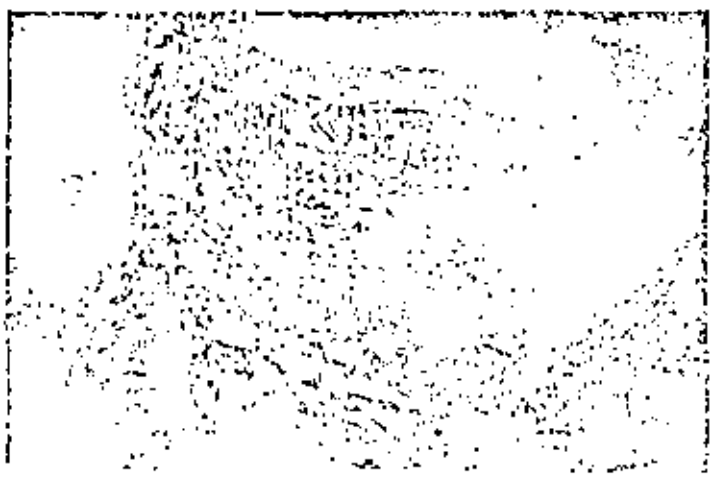

Figure 113 : Smooth blasting being used to trim loose and unstable rock from a natural slope face on the site of the Gordon arch dam in Tasmania.

374

Figure 114 : Drilling a pattern of holes for a smooth blasting operation to trim a rock slope. (Photograph reproduced with [illegible] Sweden)

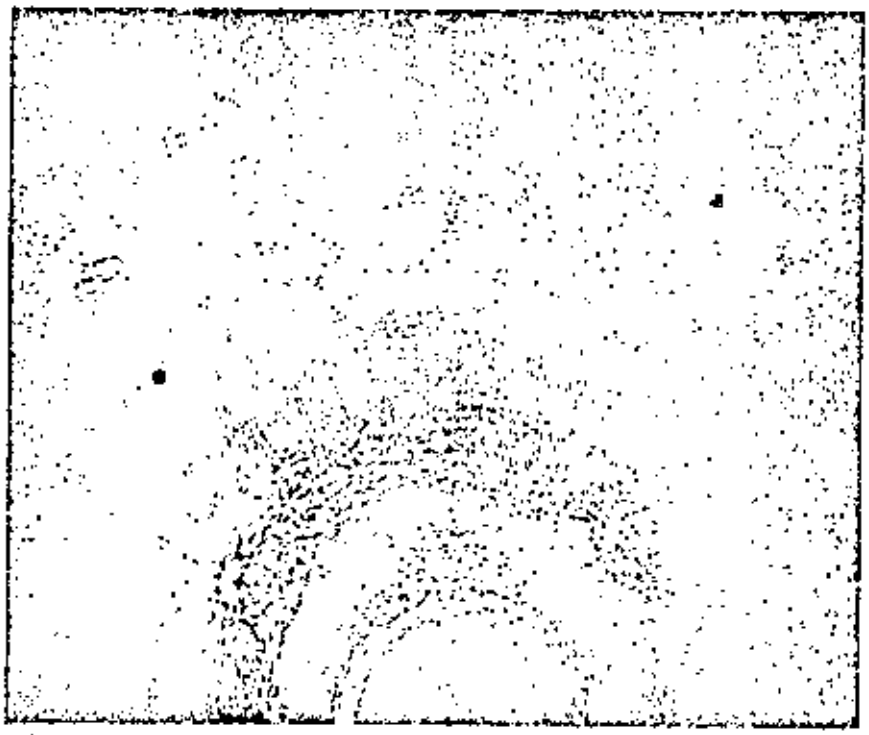

Figure 115 : Tunnel profile trimmed by smooth blasting. (Photograph reproduced with permission of Atlas Copco Ltd. and Nitro Nobel AB, Sweden).

Figure 116 : Slopes excavated after pre-splitting final faces on the site of a hydro-electric project in Austria. (Photograph reproduced with permission of Atlas Copco Ltd, Sweden).

376

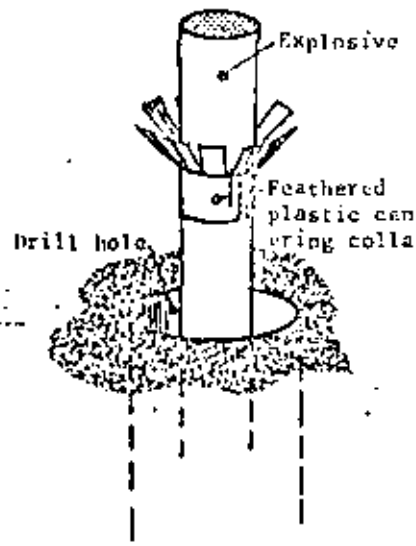

Typical arrangement of explosive charge in drill hole for smooth or pre-split blasting.

The factors which are important in a smooth blasting or a pre-split blasting operation are :

The specific charge (weight of explosive per unit length of hole),
Detonation sequence and delay,
Ratio of hole diameter to charge diameter,
Burden V (distance between free face and hole) and
Spacing E (distance between successive holes).

The table given below is taken from the memorandum by Kihlström[219] and lists recommended values for hole diameter, charge diameter, specific charge, burden and spacing for typical hard Swedish rock. This table can be regarded as a guide for both smooth blasting and pre-split blasting and may be varied to suit local rock conditions.

Note that no value for the burden is given for pre-split blasting because the charges in these holes are detonated before the normal blast and hence the burden is either infinite or very large as compared with the spacing between holes.

In both smooth blasting or pre-split blasting, all the charges in a line should be detonated as nearly simultaneously as possible. Best results are obtained using instantaneous detonators or a pentyl fuse but acceptable results can be obtained as long as the delay between detonators does not exceed ± 100 milliseconds. The purpose of the simultaneous detonation is to allow gas pressures to build up at the same time in all the holes, thereby encouraging the propagation of a planar fracture between successive holes [228].

Recommended dimension for smooth blasting and pre-split blasting

Drill hole diameter.		Charge diameter		Specific charge*.		Smooth blasting Spacing E		Burden V		Pre-split blasting Spacing E	
mm.	in.	mm.	in.	Kg/m.	Lb/ft	m.	ft.	m.	ft.	m.	ft.
30	1¼	11	½	0.07	0.05	0.5	1.6	0.7	2.3	0.25-0.3	0.8 -1.0
37	1½	17	¾	0.12	0.08	0.6	2.0	0.9	3.0	0.30-0.5	1.0 -1.6
44	1¾	17	¾	0.17	0.11	0.6	2.0	0.9	3.0	0.30-0.5	1.0 -1.6
51	2	22	¾	0.25	0.17	0.8	2.6	1.1	3.6	0.45-0.75	1.5 -2.5
62	2½	22	¾	0.35	0.23	1.0	3.3	1.3	4.2	0.55-0.8	1.8 -2.6
75	3	25	1	0.50	0.34	1.2	4.0	1.6	5.2	0.6 -0.9	2.0 -3.0
87	3½	25	1	0.70	0.50	1.4	4.6	1.9	6.2	0.7 -1.0	2.3 -3.1
100	4	29	1¼	0.90	0.60	1.6	5.2	2.1	6.9	0.8 -1.2	2.6 -4.0
125	5	40	1½	1.40	0.90	2.0	6.6	2.7	8.8	1.0 -1.5	3.3 -4.9
150	6	50	2	2.00	1.30	2.4	7.9	3.2	10.5	1.2 -1.8	4.0 -5.9
200	8	52	2	3.00	2.00	3.0	9.8	4.0	13.0	1.5 -2.2	4.9 -6.9

* based upon Nitro Nobel's Dynamex B

As with all other techniques described in this book, smooth blasting and pre-split blasting techniques should only be applied after due consideration of all the factors involved and after trials of limited extent in the rock mass being worked. Berger [221] reports that, in some preliminary experiments carried out by the Canadian Department of Energy, Mines and Resources, pre-splitting in heavily fractured ore resulted in more damage to the slopes than a normal blast because of the venting of the gasses from the closely spaced holes. On the other hand, the photographs reproduced on the previous pages should have served to convince the reader that, when correctly applied, these techniques can result in considerable improvements in the appearance and the stability of slope faces. Obviously, pre-splitting a slope face will not prevent a deep-seated slide if the slope is inherently unstable but the authors suggest that the slope face itself can probably be cut 10° or more steeper if controlled blasting methods are used. The main benefits which derive from the use of these methods are in the reduced maintainance and the reduced danger of rock falls from a face which has not been shattered by excessively heavy blasting.

Drainage of slopes

The very important influence of water pressure upon the stability of a slope has been emphasised time and time again in this book. Since water pressure reduces the stability of a slope, it follows that drainage will increase the stability of that slope. The following discussion is concerned with methods of slope drainage.

The three basic principles to be kept in mind when considering slope drainage are:

a. prevent surface water from entering the slope through open tension cracks and fissures,
b. reduce water pressure in the vicinity of the potential failure surface by selective sub-surface drainage and
c. position the drainage so that only the water in the immediate vicinity of the slope is drained - there is no point in draining the country-side for miles around the pit.

The most common methods of slope drainage are illustrated in the composite sketch presented in figure 117 and the following comments refer to the methods illustrated:

Surface drains are designed to collect run-off and to divert it before it reaches the area immediately behind the crest of the slope. This is the area in which the most dangerous tension cracks are likely to occur. Attempts to line these surface drains are usually unsuccessful because of movements in the slope and because of the damage which results from heavy traffic in the area. The authors suggest that the surface drain can be left unlined provided that it is steeply graded to promote rapid water movement and that it is regularly maintained and kept free of blockages. Some of the most effective surface drains are those which are cut by a narrow bladed bull-dozer and where the same machine is run along the drain at fairly regular intervals.

The slope surface, immediately behind the slope crest, is an area of considerable potential danger in that water which is allowed to collect in cracks in this area is likely

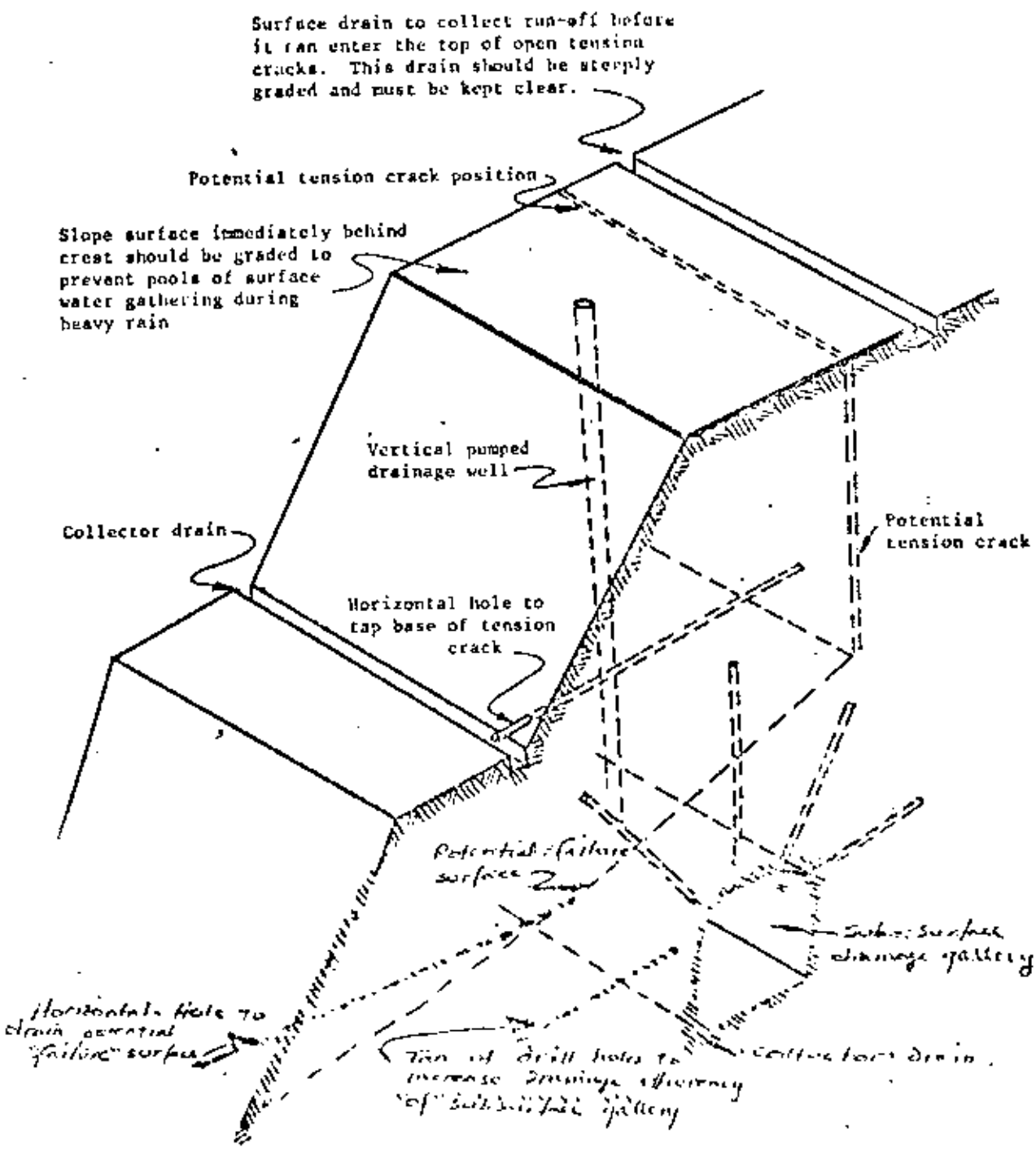

Figure 117 : Slope drainage methods .

and fissures. Grading of this surface and the removal of obstructions which could cause damming of surface water is probably adequate in most cases. Sometimes additional measures are considered necessary and the slope surface is sealed with a flexible layer such as lateritic soil. In one instance, old engine oil from the workshops was used to bind the soil into a surface sealing layer above a particularly important slope.

Open tension cracks are very dangerous in areas liable to high intensity rain storms since the water forces which are generated if these cracks become full of water are likely to induce violent slope failures (see practical example number 2 on page 158). In addition to diverting surface water away from such cracks, it is also advisable to take steps to prevent water entering the crack by sealing the top of the crack with a flexible material such as clay. When the crack is more than a few inches wide it should be filled with gravel or waste rock before the flexible cap is placed. This permeable filling will allow the free passage of sub-surface water while, at the same time, providing support for the surface seal. Under no circumstances should the tension crack be grouted or concrete filled since the creation of an impermeable barrier at this point in the slope could result in the build-up of dangerous water pressures within the rock mass.

Horizontal drain holes drilled into the slope face can be very effective in reducing water pressures near the base of a suspected tension crack or along a potential failure surface. The spacing and positioning of these holes depends upon the slope geometry and the structural discontinuities within the rock mass. In a hard rock slope, the water is generally transmitted along joints and the horizontal drain holes will only be effective if they penetrate such features. In the case of a soft rock or soil slope, the drain holes can be regularly spaced but a certain amount of trial and error is necessary in order to determine the optimum spacing. In either case, the installation of *piezometers before* the drilling of the horizontal holes is strongly recommended since, without an indication of the change in water level, the rock slope engineer will have no idea of the effectiveness of the drainage measures which he has implemented.

Collector drains to lead the water discharged from horizontal drains are important otherwise this water will simply find its way into the next bench down and the problem will have been transferred from one level to the next.

Vertical drainage wells drilled from the slope surface and fitted with down-hole pumps can be effective in slope drainage and they have the advantage that they can be in operation *before* the slope is excavated. The disadvantage of this method of drainage is the expense of keeping the pumps running and also the danger of power failure during the most critical period - a heavy rain storm. In some cases, vertical wells have been used during the early stages of a drainage programme and these will have later been connected to a sub-surface drainage scheme so that they become gravity drains.

Drainage galleries, with or without fans of radial holes,

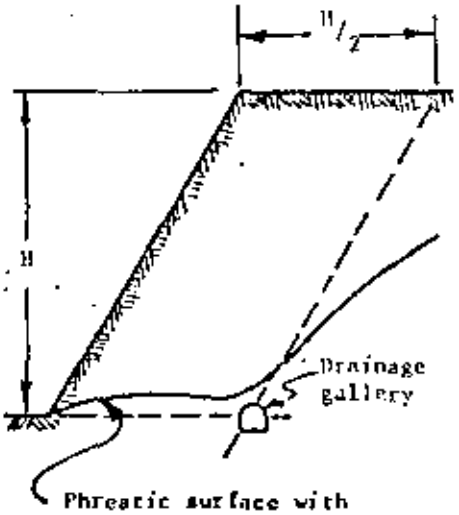

Phreatic surface with drainage

Sub-surface drainage gallery location in a slope.

but they are also the most expensive. In many open pit mining situations, such galleries already exist in the form of underground mine workings. In other cases, the excavation of suitable galleries can be justified as part of the ore body exploration programme. The excavation of a gallery for the sole purpose of drainage would only be justified in the case of a very important hard rock slope in which the groundwater flow pattern was known with a reasonable degree of certainty. The optimum location of drainage galleries has been investigated by Sharp [117] and has been discussed by Sharp, Beck and Brawner [222]. In very general terms, the optimum gallery position is at the corner of the parallelogram defined in the sketch opposite. A sub-surface drainage gallery will effectively drain about 200 feet of over-lying material and, hence, for very large slopes, two or more levels of drainage galleries may be required.

The effectiveness of any slope drainage scheme is very difficult to gauge. Piezometers installed in the slope before the drainage system is brought into operation can give very valuable information on the reduction in water pressure which is brought about by drainage. Knowledge of the overall groundwater flow pattern in the slope is also of considerable help in planning the most effective drainage measures and some of the concepts discussed in chapter 8 may be useful in building up this knowledge. One positive aspect of slope drainage is that it can never do any harm - some drainage, however inefficient, is better than no drainage. The drainage characteristics of most slopes can be improved with relatively little effort or expense and simple precautions such as the diversion of surface run-off should be an integral part of any slope design. More elaborate drainage measures designed to improve the stability of critical slopes are generally more expensive but they are sometimes the only means available for achieving the desired results.

Surface protection of slopes

Slopes in soft rock or soil are liable to serious erosion during heavy rain and some rock slopes are prone to severe weathering when exposed. The surface protection of such slopes can be a serious problem and the following comments offer some guidance on this subject although it must be emphasised that local conditions and the availability of suitable materials may be the dominant consideration in many cases.

Vegetation is almost certainly the best form of surface protection against the erosion of soil slopes. A grass mat covering the slope will not only bind the surface material together but will also tend to inhibit the entry of water into the slope. Establishing the grass or other vegetation is the most difficult problem since the rain which is needed to promote the growth of the young plants is also capable to removing these plants from the slope, particularly when the slope is relatively steep and when the rainfall intensity is high. Various schemes for stabilising the surface layer during the initial growing period of the vegetation have been tried but finding the best method for a particular slope is very much a question of trial and error.

One system which has proved successful in some applications is to mix grass seed and fertilizer into a liquid rubber or plastic which is then sprayed onto the slope surface and which serves to bind the seeds, soil and fertilizer together until growth has been established. Another system involves mechanically anchoring the top soil in place by means of trays anchored into the slope or suspended from the slope crest by means of wire ropes.

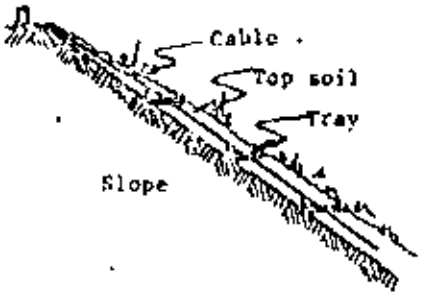

Mechanical anchoring of top soil layer on slope.

Choice of the correct grass type and deciding upon the best method of establishing growth depends so much upon the local conditions on the site that the authors feel that there is little value in discussing this topic further in this text. Instead, it is recommended that the slope engineer should consult the local agricultural officers who will have experience of local conditions and who would normally be very willing to help in a project which, to them, would be unusual and interesting.

In the case of rock slopes, surface protection is necessary when these slopes are prone to rapid weathering. Materials such as shales and, in some cases, granites have to be treated with care when they are exposed in a slope face and, since it is not normally possible to establish vegetation on such slopes, some form of protective layer must be used. Probably the most common form of surface layer is a cement-sand mortar which is sprayed onto the slope surface. This pneumatically applied mortar, known as "Gunnite" or "Shotcrete", depending upon the moisture content of the mix, is very successful if applied immediately after excavation of the face, before the weathering process has set in. The mortar is sometimes applied by hand, as in the case of the "Chunam" surface layers which are common in Hong Kong.

When a slope surface is to be protected by means of a surface layer, it is essential to remember that this layer may not only keep water out but it may also keep it in the rock mass behind the slope and the resulting water pressure can induce instability in the slope. Shallow drains or weep holes left at regular intervals in the layer will serve to dissipate these potentially dangerous water pressures and should be included in the specifications for the protective surface layer. It is also important that these layers should be inspected at regular intervals and that repairs should be carried out if the layer is damaged since failure to repair a hole in the layer can give rise to progressive damage to the whole layer.

More elaborate, and more expensive, methods of surface protection are sometimes used and figure 118 illustrates a scheme used to protect the surface of a large soil slope in Hong Kong. Interlocking precast concrete members form an open framework into which a layer of no-fines concrete is placed. This porous layer supports a layer of top soil which is then seeded to produce a grass-covered slope.

Another form of surface protection is to use various types of gabions which are wire baskets filled with waste rock. Figure 119 illustrates two typical applications of gabions for the surface protection of slopes. This form of protection is particularly effective when the slope is subjected to wave action or scour from rapidly flowing water.

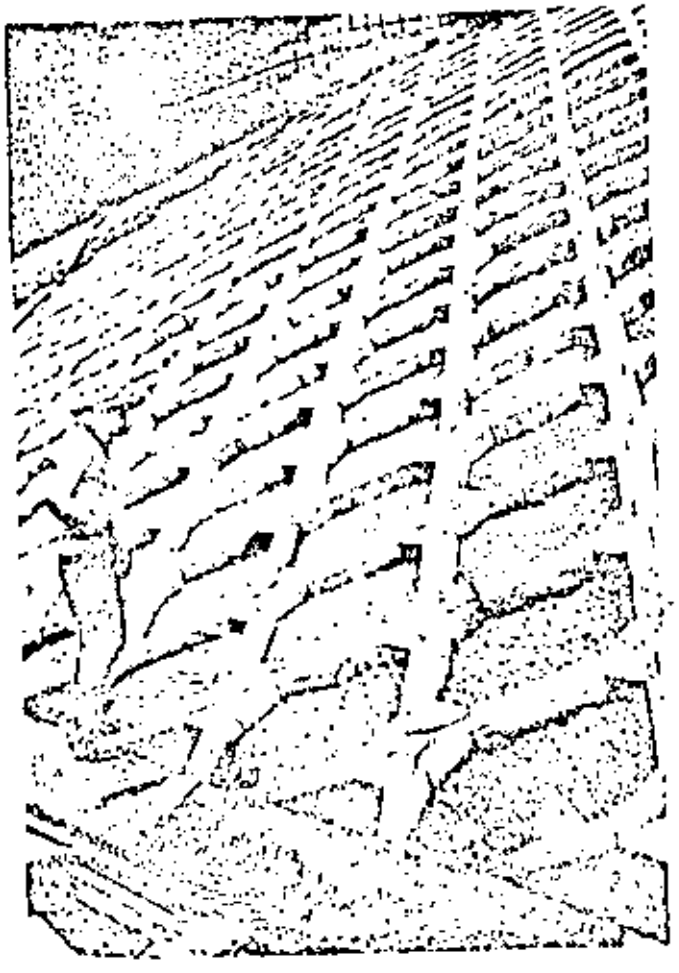

Figure 118 : Protection of the surface of a large soil slope in Hong Kong. Precast concrete members interlock to form a framework into which layers of no-fines concrete are placed. These layers support top soil which is seeded to produce a grass covered slope.

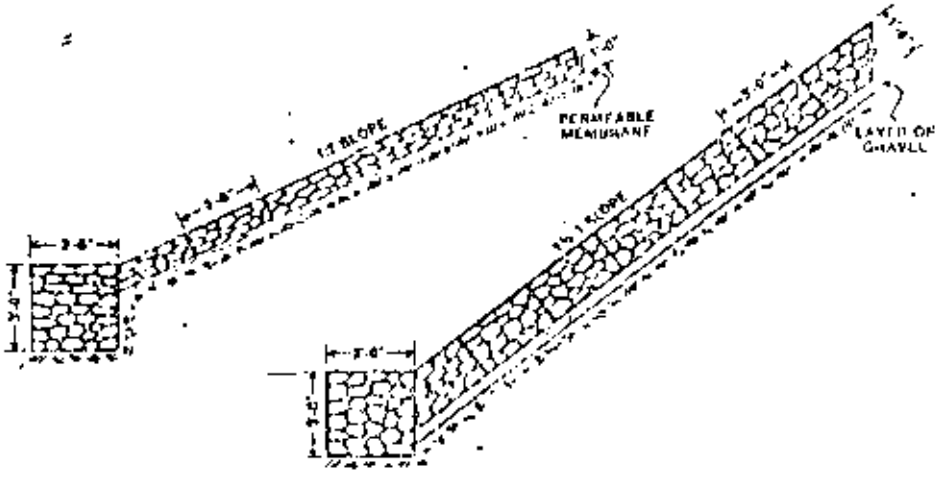

Figure 119 : The use of gabions for the stabilisation and surface protection of slopes. Technical literature on gabions is available from River and Sea Gabions (London) Ltd, Princes Street, London WIR 8PJ and from Terra Aqua Conservation Ltd., 4910 Energy Way, Reno, Nevada 89502.

Control of rockfalls

One of the dangers associated with rock slopes is that of falls of loose boulders from the top of the slope. Such boulders can fall, bounce or roll down the slope as shown in figure 120 and, unless steps are taken to dissipate the energy which has been acquired by the boulder, considerable damage can be caused. This danger is particularly acute in the case of highway slopes and a study carried out by Ritchie in 1963 [223] was aimed at minimising this hazard.

Figure 120, adapted from a drawing in Ritchie's paper, summarises the main recommendations for the control of rockfalls. A ditch at the foot of the slope will contain much of the energy of the fall and a chain link fence on the shoulder of this trench will prevent the rock from bouncing onto the roadway. Unfortunately, to be fully effective, the ditch should be as much as 25 feet wide and 6 feet deep for a 100 foot high slope. The authors suggest that it may be possible to reduce these dimensions by placing a thick layer of gravel in the base of the ditch since recent work has shown that such a layer of gravel is very effective in dissipating the energy of a runaway airplane or truck. However, in most open pit mining situations, the space required for such a ditch could not be made available and these suggestions could only be used for critical haul roads or public roads.

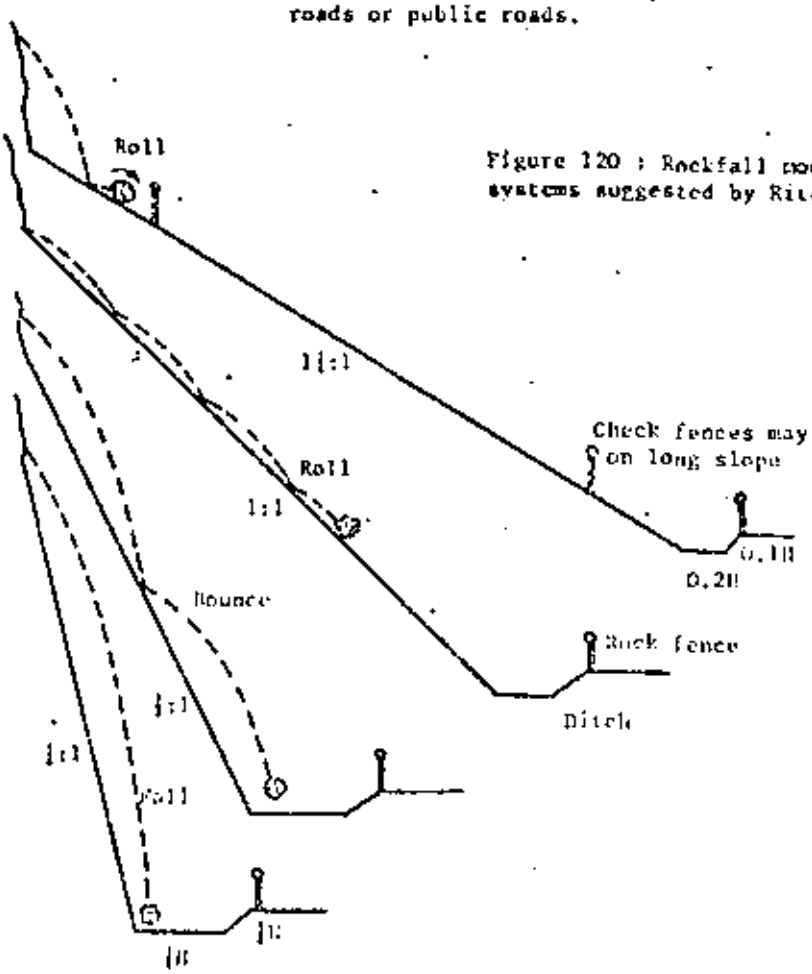

Figure 120 : Rockfall modes and protection systems suggested by Ritchie [223].

384

Monitoring and interpretation of slope displacements

When, in spite of all his efforts to design a stable slope or to improve the stability of a potentially dangerous slope, the engineer finally comes to accept that a major failure is inevitable, what steps, other than catching the next plane, can he take ? The answer lies in attempting to provide a reliable prediction of the slope behaviour up to and including the final failure so that appropriate action can be taken to minimise the danger to men and equipment.

The most spectacular set of predictions of this sort was associated with a major slope failure in the Chuquicamata mine in Chile [224,225], to be discussed in more detail later in this section. There have, however, been a number of other cases of slope failure prediction which, although less spectacular, have been just as important in preventing the serious consequences which invariably result from an unexpected failure. The lesson to be learned from these cases is that a large slope will almost always give warning of failure, provided that the slope engineer knows what to look for and takes heed of the warning.

Since shear movement on a failure surface within a soil or rock mass will be transmitted into the overlying mass of material, monitoring of the movements of the slope surface will give an indication of overall movements resulting from instability in the slope. Experience has shown that detailed knowledge of the precise movement pattern within the rock mass is not important and that measurement of surface displacement is usually adequate for the prediction of slope behaviour.

Measurement of these surface displacements is basically a survey problem of establishing adequate targets or bench-marks, a stable reference datum and using the correct instruments for the measurements themselves. These problems have been discussed by Kennedy and Niermeyer[225], Watt [226] and St John [227] and will not be dealt with in detail in this chapter. Most mine survey departments would have adequate equipment for the measurement of slope surface displacements but these departments would almost certainly require assistance in the interpretation of these measurements.

Obviously, the earlier a displacement measuring system is established around an open pit the better since the gradual change in the movement pattern would reveal any anomalous slope behaviour which would identify areas requiring detailed examination. Unfortunately, the cost and the time required to establish and to maintain such a system can seldom be justified, particularly when slope problems are not anticipated. Consequently, a displacement monitoring system is normally only installed when slope instability is evident or when local mining regulations require that a check must be kept on surface movements.

Since the serious instability of a slope is almost always accompanied by the development of one or more tension cracks behind the crest of the slope, one of the best and most reliable methods of displacement monitoring is to measure the opening of the tension crack at regular

An electro-optical distance measuring instrument set up to monitor displacements across a large quarry.

tape stretched between pegs on either side of the crack, have proved very effective and have provided sufficient information for sound decisions to be made in many mines and quarries. More sophisticated systems, using more precise measureing methods, have been used and one such system is illustrated in figure 121. Even more sophisticated systems, using electro-optical distance measuring devices have also been used in certain cases [227].

The authors do not wish to enter into a discussion on the merits of these different systems of measurement. The choice of the method to be used in a particular situation will depend upon the magnitudes of the anticipated movements, the local site conditions and the availability of staff and equipment. While it may be interesting to measure the displacements in thousandths of an inch, this is seldom necessary and the slope engineer should avoid demanding an unnecessarily high degree of accuracy. In the case of the Chuquicamata slide, movements of the order of 6 meters were recorded and it would certainly not require a micrometer to measure such displacements. It is preferable to get a simple measuring system functioning early than to argue about the required accuracy while the slope falls down.

In some cases, loose overburden on the upper surface of the slope may make it impossible to establish stable bench marks for displacement measurements. Under these conditions, a borehole method of displacement monitoring can be considered. Several systems for this type of measurement are available commercially and most of them depend upon the lowering of some form of borehole survey instrument down a borehole lined with a grooved plastic casing. The casing is left permanently in place and measurements are taken at the same depths at regular intervals. The relative movements with time of different points in the rock or soil mass will give an indication of instability in the slope.

The interpretation of the displacement versus time plot obtained from these measurements poses the most difficult problem for the rock slope engineer. There are no theories which define the movement patterns in slopes and the authors feel that it will be a long time before such theories are developed. Experience does suggest , however, that the rate of movement in an unstable slope will gradually accelerate until the point of failure is reached and that this rate of movement, rather than the magnitude of the movement itself, provides the most sensitive indication of slope behaviour. This is best illustrated by means of the Chuquicamata slide prediction which is discussed on the following pages *.

Figure 122 illustrates the eastern slopes of the Chuquicamata pit. The overall height of the slope in the failure region, in the centre of the photograph, was 248 meters and the overall slope angle approximately 40°. The main rock type in the slide area is unaltered porphyritic granodiorite.

---

*The Authors claim no credit for this example which has been taken from the papers by Kennedy et al [224,225].

386

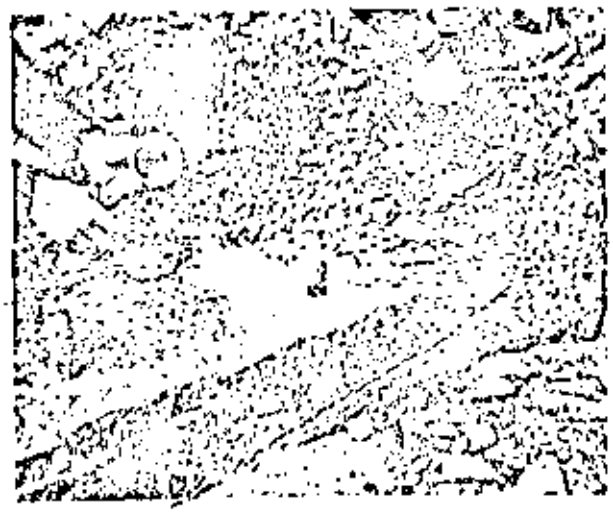

a. Four pegs are set into holes drilled into the rock on either side of the tension crack by means of epoxy resin. The measuring heads are protected by grease-filled caps screwed onto the peg. These caps should be left unpainted otherwise they are likely to attract vandals.

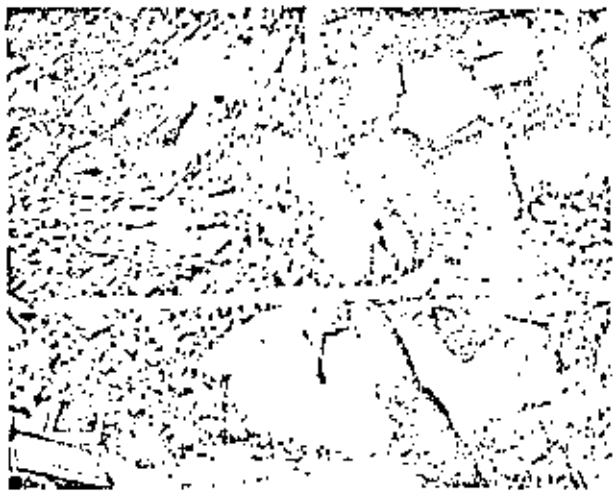

b. A large vernier caliper can be adapted to measure the displacements across a tension crack of up to 5 feet wide. The attachments on the caliper are cone seatings which are centred on balls on the top of the measuring pegs.

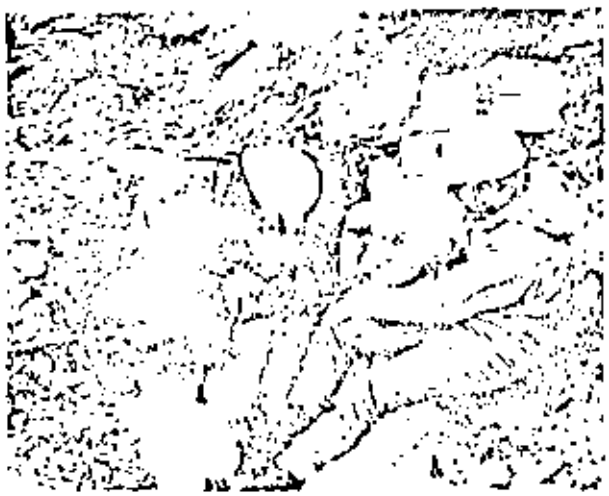

c. A precision level placed along the caliper bar can be used to determine the change in level of the pegs. Note that measurements are made across the diagonals as well as along the sides of the measuring square in order to detect any shear movement along the tension crack.

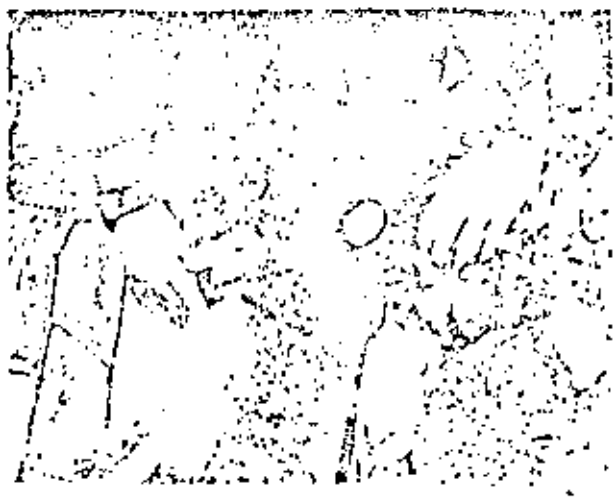

d. Precise measurement of movements across a narrow tension crack can be made by means of a mechanical extensometer. Measurements of this accuracy have proved useful for correlation with daily rainfall and blasting records for research purposes.

Figure 121 : Measurement of movements across a tension crack .

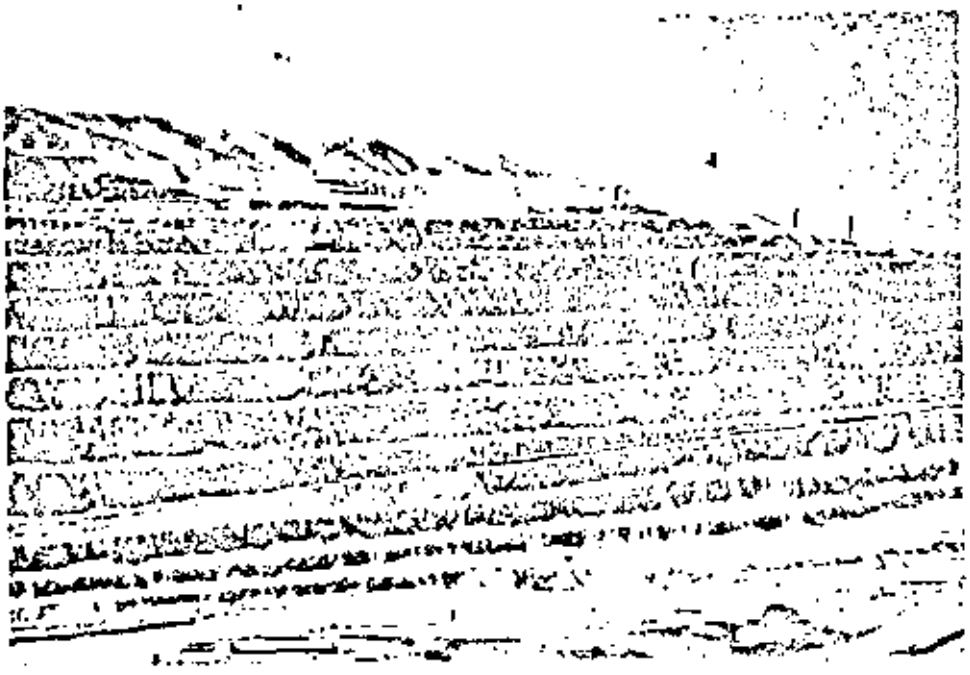

Figure 122 : Eastern slope of the Chuquicamata mine in Chile in late 1968. The area on the top of the slope to the left of the two smelter stacks is where 4½ million tons of material was removed in the unloading programme.

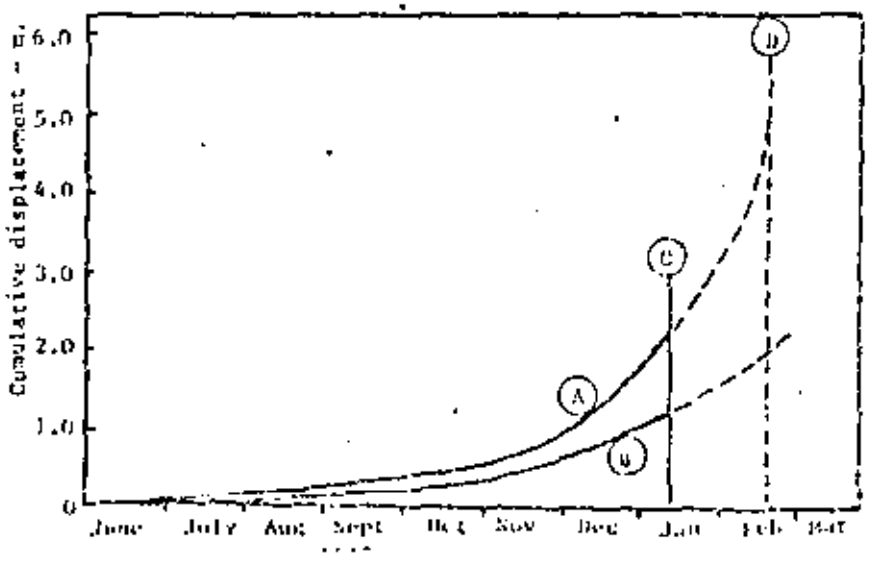

Figure 123 : Plot of slope displacement versus time used for prediction of the Chuquicamata mine slide.

A - Plot of fastest moving target on slope face.
B - Plot of slowest moving target on slope face.
C - Prediction of slope failure date made on the basis of existing data on January 13.
D - Predicted and actual failure date - February 18, 1969.

398

Tension cracks were first noticed in this slope in August 1966 and a simple monitoring system was established. Movements were found to be extremely small and eventually ceased so that monitoring was discontinued. An earthquake, on December 20, 1967 of magnitude 5 on the Richter scale, was apparently responsible for reactivating movement. Incidentally, Chuquicamata is in a desert area with extremely low annual rainfall and hence groundwater is not a factor in this slide.

Displacement monitoring commenced in June 1968 when it was evident that movements were taking place in the slope. The monitoring systems, described by Kennedy and Niermeyer[225], were basically very simple, consisting of tension crack measurements, survey measurements and some extensometer measurements. A three channel, short period siesmograph was also installed on the site and, although the results produced by this instrument were not used in the failure prediction, it is interesting to compare them with the displacement records[225].

In an effort to stabilise the slope, an unloading programme was started in August 1968 and a total of 4.5 million tons of material was eventually stripped from the top of the slope. This stripping is visible on the top of the slope, to the left of the water stocks, in the photograph reproduced in Figure 122. Although the amount of material finally deposited on the pit floor by the slide was probably reduced by this stripping programme, it is unlikely that the unloading of the slope had any significant influence on the slide. The analysis presented in Figure 85 on page 171 shows that a very large reduction in slope height is necessary before the factor of safety of a slope is significantly improved.

By late 1968 it was evident that a major slope failure was inevitable and steps were taken to reroute the haul road system and to stockpile material for the mill. On January 13, 1969, a projection of the displacement data, plotted in Figure 123, was made. The earliest predicted failure date, based upon the fastest moving target on the slope, was given as February 18, 1969.

The failure itself, illustrated in the photograph reproduced in Figure 124, occurred at 6.58 p.m. on February 18 and involved the movement of approximately 12 million tons of material. Figure 125 shows the slide, as seen from the air, and the relocated haul road can be seen in the lower right hand side of the photograph.

Full production resumed on February 19 after a shut-down of the pit of 65 hours. The mill continued working throughout this period on stockpiled material.

The spectacular accuracy of this prediction is not particularly relevant to this discussion since the overall result would have been the same had the prediction been a few days or even weeks out. The point of this example is that by knowing what to look for and by making full use of the available data, a set of sound engineering decisions could be made and the serious consequences which could have resulted from this failure were avoided.

389

Figure 124 : Failure of the Chuquicamata mine east slope at 6.58 p.m., February 18, 1969.

Figure 125 : The Chuquicamata slide seen from the air. Note the new haul road position in the bottom right hand side of the photograph.

The photographs reproduced in figures 122, 124 and 125 are prints of colour slides released to Imperial College by the Anaconda Company.

Chapter 10 references

Selected references

214. JENIKE, A and YEN, B. Slope stability in axial symmetry. *Proc. 4th Symp. Rock Mech.*, Univ. Minnesota 1962. Pergamon Press 1963, pp. 689-711.

215. PITEAU, D.R. and JENNINGS, J.E. The effects of plan geometry on the stability of natural slopes in rock in the Kimberley area of South Africa. *Proc. 2nd Congress Intnl. Soc. Rock Mechanics, Belgrade 1970.* Vol. 3, paper 7-4.

216. RANA, M.H. and BULLOCK, W.D. The design of open pit mine slopes. *Canadian Mining Journal*, August 1969, pp. 58-66.

217. LANGEFORS, U. and KIHLSTROM, B. *Rock Blasting.* Wiley & Sons, New York 1963, 404p.

218. ORIARD, L.L. Blasting effects and their control in open pit mining. *Geotechnical practice for stability in open pit mining.* Editors Brawner, C.O. and MILLIGAN, V., AIME, New York, 1972, pp. 197-222.

219. KILHSTROM, B. The technique of smooth blasting and presplitting with reference to completed projects. *Nitro Nobel AB Technical Memorandum No. B672, January, 1972.*

220. KUTTER, H.K. and FAIRHURST, C. On the fracture process in blasting. *Intnl. J. Rock Mechanics, Mining Sci.*, Vol. 8, No. 3, 1971, pp. 181-202.

221. HERGET, G. Recent research on rock slope stability by the Mining Research Centre (Ottawa). *Geotechnical practice for stability in open pit mining.* Editors Brawner, C.O. and Milligan, V., AIME, New York, 1972, pp. 47-66.

222. SHARP, J.C., HOEK, E. and BRAWNER, C.O. Influence of groundwater on the stability of rock masses - drainage systems for increasing the stability of slopes. *Trans. Inst. Min. Metall., London.* Sect. A, Vol. 81, No. 788, 1972, pp. 113-120.

223. RITCHIE, A.M. The evaluation of rockfall and its control. *Highway Research*, Vol. 17, 1963, pp. 13-28.

224. KENNEDY, B.A., NIERMEYER, K.E. and YAHN, B.A. Major slope failure at the Chuquicamata Mine. *Mining Engineering*, AIME, Vol. 21, No. 12, 1969, p.60.

225. KENNEDY, B.A. and NIERMEYER, K.E. Slope monitoring systems used in the prediction of a major slope failure at the Chuquicamata Mine, Chile. *Proc. Symp. Planning Open Pit Mines, Johannesburg,* September 1970, A.A. Balkema, Amsterdam, pp. 215-225.

226. WATT, J.H. Control for early warning of potential danger in open pits. *Proc. Symp. Planning Open Pit Mines, Johannesburg,* Sept. 1970, A.A. Balkema, Amsterdam, pp. 103-13.

391

227. ST. JOHN, C.M. A note on displacement measurement for open pit monitoring. *Proc. Symp. Planning Open Pit Mines, Johannesburg*, September 1970. A.A. Balkema, Amsterdam, pp. 328–330.

DIVISION DE EDUCACION CONTINUA
FACULTAD DE INGENIERIA U.N.A.M.

CURSOS DE INGENIERIA CIVIL EN EL PROYECTO
DE PLANTAS HIDROELECTRICAS

MECANICA DE ROCAS -

2a. parte

Ing. Jorge E. Castilla C.

junio 1981

AD

NCG TECHNICAL REPORT No. 36

ANALYTICAL AND GRAPHICAL METHODS FOR THE ANALYSIS OF SLOPES IN ROCK MASSES

A. J. HENDRON, JR.

E. J. CORDING

A. K. AIYER

SPONSORED BY:

U. S. ARMY ENGINEER NUCLEAR CRATERING GROUP
LIVERMORE, CALIFORNIA

PREPARED FOR:

U. S. ARMY ENGINEER WATERWAYS EXPERIMENT STATION
VICKSBURG, MISSISSIPPI

BY:

DEPARTMENT OF CIVIL ENGINEERING
UNIVERSITY OF ILLINOIS

JULY 1971

NCG TECHNICAL REPORT NO. 36

ANALYTICAL AND GRAPHICAL METHODS FOR THE ANALYSIS OF SLOPES IN ROCK MASSES

by
A. J. Hendron, Jr.
E. J. Cording
and
A. K. Aiyer

July 1971

Sponsored by:

U. S. Army Engineer Nuclear Cratering Group
Lawrence Livermore Laboratory
Livermore, California

Prepared for:

U. S. Army Engineer Waterways Experiment Station
Corps of Engineers
Vicksburg, Mississippi

By:

Department of Civil Engineering
University of Illinois

FOREWORD

This study was performed by the Department of Civil Engineering, University of Illinois, under contract to the U. S. Army Engineer Waterways Experiment Station, Vicksburg, Mississippi (WES) for the U. S. Army Engineer Nuclear Cratering Group, Lawrence Radiation Laboratory, Livermore, California (NCG). The study was performed under Contract No. DACW 39-67-C-0097, "Evaluation of Analytical Methods of Determining the Stability of Rock Slopes," and was funded by NCG IAD 2-63, "Engineering Properties of Nuclear Craters." The contract was negotiated on 16 June 1967.

This report was prepared by Messrs. Hendron, Cording and Aiyer; and, was reviewed by Don C. Banks, Chief, Rock Mechanics Section, Soils Division, WES and by Major Richard H. Gates, C.E., Chief, Engineering Geology Division, NCG.

The contract was monitored by Don C. Banks, WES. The Contracting Officer at the time of publication was COL Ernest D. Peixotto, CE, Direction of WES. Technical Director of WES was Mr. Fred R. Brown. The Director of NCG was LTC Robert L. LaFrenz, CE, and the Technical Director was Mr. Walter C. Day.

ABSTRACT

In this report the methods of analyzing the static stability of rock slopes cut by a three dimensional network of discontinuities are given. The general use of vector analysis to solve these problems analytically is described and a method utilizing stereonets to solve these problems graphically is also given. For both the graphical and analytical methods the general analysis of slopes cut by one, two, or three sets of discontinuities is presented which can take into account the porepressures acting on the discontinuities and external forces acting on the slope. Detailed examples are given to illustrate both the graphical and vector methods of analysis.

The dynamic stability of slopes is also treated in this report. It is shown that the dynamic resistance of a three-dimensional rock slope can be calculated by either the graphic-stereonet method or the analytic vector analysis method. The dynamic resistance can then be used to estimate the movement of the slope under dynamic loading using a procedure given by Newmark (1965). A criterion is then given for determining if the calculated movement of the rock slope is acceptable or harmful.

TABLE OF CONTENTS

TABLE OF CONTENTS (continued)

TABLE OF CONTENTS (continued)

TABLE OF CONTENTS (continued)

LIST OF FIGURES

LIST OF FIGURES

LIST OF FIGURES

Page

LIST OF TABLES

CHAPTER ONE

INTRODUCTION

1.1 General

The design and analysis of rock slopes is somewhat different than the design and analysis of slopes in soil because of the patterns of discontinuities in the rock mass. The spatial orientation of these discontinuities and the shearing resistance along them govern the stability of rock slopes. Thus the method of analysis used must take into account the three dimensional intersection of the joint sets with each other and intersection of these discontinuities with the face or surface of the rock slope. Limit equilibrium methods of analysis have recently been developed to analyze these problems in three dimensions which will be explained and illustrated in this report.

In all methods of limit equilibrium analysis the shape of the potential failure is assumed at the outset. In the limit equilibrium methods used for soil slopes, sections of log spirals or circles are normally chosen to represent the failure surface. Although displacements are ignored in limit equilibrium methods, it must be kinematically possible for the displacements to take place in the direction assumed along the failure surface chosen. Surfaces composed of sections of circles or log spirals pose no kinematic difficulties. In rock slopes the potential system of failure surfaces already exist in the mass but the kinematics of sliding must be checked to delineate the possible directions and surfaces on which it is physically possible for sliding to take place.

After the potential failure surface is assumed in either the rock or soil slope stability analysis, the next step in the limit equilibrium method is to calculate the shearing resistance required along the potential failure surface to keep the potential sliding mass in equilibrium. This portion of the analysis is basically an exercise in statics.

After the shearing resistance required for equilibrium has been found, it is compared with the available shearing resistance. This comparison is usually expressed in terms of a factor of safety, which must be defined very carefully. Finally the slip surface giving the lowest factor of safety is found. In soils this is usually an iterative process with failure surfaces of the same shape but with different sizes and orientations. But in rock slopes there may only be several potential failure wedges to consider, each having a different shape goverened by various intersections of the sets of discontinuities.

I.2 Scope

In this report the methods of analyzing the static stability of rock slopes in three dimensions are given and a method is suggested for assessing the dynamic stability of rock slopes. The methods of static analysis for three dimensional wedges are based primarily on the work of Wittke (1964, 1965a, 1965b, 1966), and Londe (1965). Since vector analysis is used in the analyses of Wittke and Londe, a review of vector operations commonly used in slope stability calculations is given in Chapter 2. The notation used for expressing strikes, dips, etc. in terms of vectors is also given in Chapter 2.

In Chapter 3 various combinations of the vector analyses of Wittke and Londe are presented for determining the static factor of safety

of rock slopes. The cases treated include slopes in rock masses containing one, two, or three sets of joints. Example calculations are given for determining the factor of safety of several typical problems by these methods. The concept of the dynamic resistance of rock slopes is also introduced in Chapter 3. The method given in Chapter 3 for computing the dynamic resistance of a rock slope in three dimensions is original with this report. The dynamic resistance can be used for predicting dynamic displacements due to earthquake motions in the method of dynamic analysis given by Newmark (1965).

In Chapter 4 procedures are given for performing graphical solutions of three dimensional rock slope stability problems by the use of stereonets. The principles of the equal angle and equal area projections are reviewed in this chapter and the equal angle projection is used in this report for the three dimensional analysis of rock slopes. The methods for analyzing rock wedges bounded by one, two, and three joint planes are similar to those given by John (1968) and example problems are illustrated. In cases where the static factor of safety is greater than unity a method is also shown for computing the magnitude and direction of the limiting dynamic resistance of a rock slope in three dimensions by the use of stereonets. In cases where the factor of safety is either less than unity or less than the desired value a method is also shown for determining the optimum direction and magnitude of rock anchor or rock bolting forces required to achieve the desired factor of safety.

In Chapter 5 procedures are given for estimating the dynamic displacement of rock slopes by utilizing the method proposed by

Newmark (1965). The minimum dynamic resistance for rock slopes as developed in Chapter 3 is used in these calculations. Guldelines are also given for determining if the dynamic displacement calculated is harmful to the stability of the slope.

In Chapter 6 a summary and conclusions are given.

CHAPTER TWO

FUNDAMENTALS OF VECTOR ANALYSIS

2.1 General

In this chapter the elements of vector analysis used in three dimensional slope stability analyses are reviewed to serve as a ready reference for the reader. Then the system used in this report for describing the three-dimensional orientation of joint planes, the line of intersection of different joint sets, and the resolution of forces, is introduced in terms of vector notation.

2.2 Fundamental Vector Operations

A vector is a quantity which possesses both a magnitude and a direction. Velocity, force, and momentum are examples of vector quantities. Vectors of unit length may also be used to describe certain reference directions such as a normal to a plane or the direction of any line with respect to a set of orthogonal axes. A vector $\bar{A}$ may be described by the set of its directional components (A_x, A_y, A_z) parallel to the rectangular Cartesian axes (x,y,z). Thus,

$$\bar{A} = (A_x, A_y, A_z) \tag{2.1}$$

A vector may alsc be expressed in terms of its components. For example,

$$\bar{A} = \bar{i}A_x + \bar{j}A_y + \bar{k}A_z \tag{2.2}$$

where $\bar{i}$, $\bar{j}$, and $\bar{k}$ are unit vectors directed along positive (x,y,z) axes respectively.

The magnitude of a vector $\bar{A}$ is given by its absolute value denoted by

$$A = (A_x^2 + A_y^2 + A_z^2)^{1/2} \tag{2.3}$$

Vectors may be added simply by summing the components in the x, y, and z directions. Thus if $\bar{C}(C_x,C_y,C_z)$ represents the sum of two vectors $\bar{A}(A_x,A_y,A_z)$ and $\bar{B}(B_x,B_y,B_z)$, then it follows that

$$\bar{C} = (\bar{i}A_x + \bar{j}A_y + \bar{k}A_z) + (\bar{i}B_x + \bar{j}B_y + \bar{k}B_z)$$

$$= \bar{i}(A_x + B_x) + \bar{j}(A_y + B_y) + \bar{k}(A_z + B_z)$$

$$= \bar{i}C_x + \bar{j}C_y + \bar{k}C_z \qquad (2.4)$$

Equating the components in the x, y, and z directions,

$$C_x = A_x + B_x,\ C_y = A_y + B_y,\ C_z = A_z + B_z \qquad (2.5)$$

The scalar product or the dot product of two vectors $\bar{A}$ and $\bar{B}$ is denoted in the form $\bar{A}\cdot\bar{B}$ and has a magnitude given by

$$\bar{A}\cdot\bar{B} = A_xB_x + A_yB_y + A_zB_z \qquad (2.6)$$

$$= AB\cos\theta \qquad (2.7)$$

where θ denotes the angle formed by the vectors A and B (Fig. 2.1). The scalar project is frequently used to obtain the component of a vector in a given direction. For example, if $\bar{i}$ is a unit vector in the x direction, $\bar{A}\cdot\bar{i}$ yields $A_x = A\cos\alpha'$ where α' is the direction angle between the vector $\bar{A}$ and the positive x axis. Similarly, $A_y = A\cos\beta'$, $A_z = \cos\gamma'$ where β', and γ' denote direction angles between the vector $\bar{A}$ and the positive y and z axes respectively. Substitution of these expressions into Eq. (2.3) yields

$$\cos^2\alpha' + \cos^2\beta' + \cos^2\gamma' = 1 \qquad (2.8)$$

Thus the cosines of the direction angles (direction cosines) of vector $\bar{A}$ are not independent; they must satisfy Eq. (2.8)

A vector product or cross product of two vectors $\bar{A}$ and $\bar{B}$ is defined

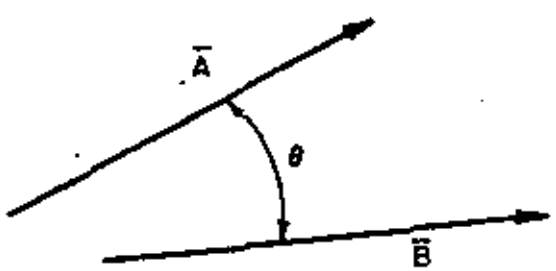

FIG. 2.1 SCALAR PRODUCT OF TWO VECTORS

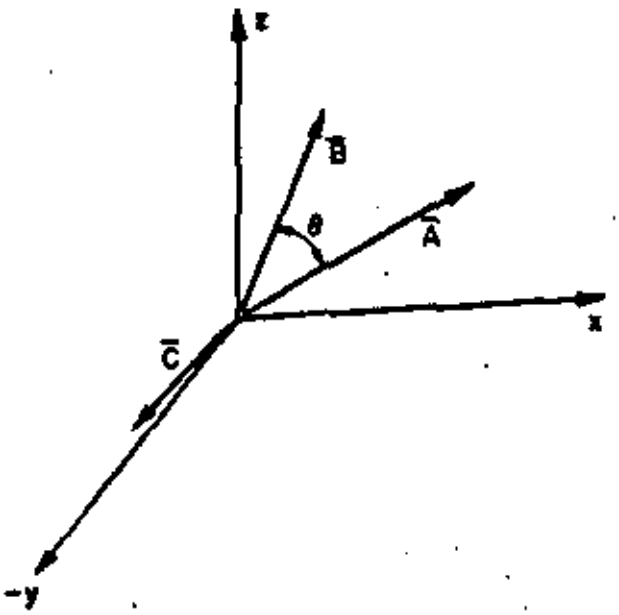

FIG. 2.2 CROSS PRODUCT OF TWO VECTORS

to be a third vector $\bar{C}$ whose magnitude is given by the relation

$$C = AB \sin \theta \tag{2.9}$$

where θ denotes the angle between vectors $\bar{A}$ and $\bar{B}$. The direction of $\bar{C}$ is perpendicular to the plane formed by vectors $\bar{A}$ and $\bar{B}$ as shown in Fig. 2.2. The vector product of $\bar{A}$ and $\bar{B}$ is denoted in the form

$$\bar{C} = \bar{A} \times \bar{B} \tag{2.10}$$

where X denotes vector product or cross product. The sense of $\bar{C}$ is such that it is in the direction a right hand threaded screw perpendicular to the plane formed by $\bar{A}$ and $\bar{B}$ would move if $\bar{A}$ were rotated into $\bar{B}$. In determinant notation the vector product is given as

$$\bar{C} = \bar{A} \times \bar{B} = \begin{vmatrix} \bar{i} & \bar{j} & \bar{k} \\ A_x & A_y & A_z \\ B_x & B_y & B_z \end{vmatrix} \tag{2.11}$$

It should be noted that

$$\bar{A} \times \bar{B} = -\bar{B} \times \bar{A} \tag{2.12}$$

2.3 Vector Operations Used in Three Dimensional Analysis of Slopes

2.3.1 Unit Vectors Defining the Orientation of Joint Planes and the Line of Intersection of Joint Sets

The orientation of joints and planes of weakness are normally reported by the field geologist in terms of strike and dip. In this report, the system given by Wittke (1964) will be used to describe the orientation of the discontinuities in relation to the slope face being investigated. According to this system, as shown in Fig. 2.3, the x axis is parallel to the strike of the slope surface, the positive z axis is upward and the positive y axis is directed toward the slope. The strike of a plane of weakness is given by the angle β measured in

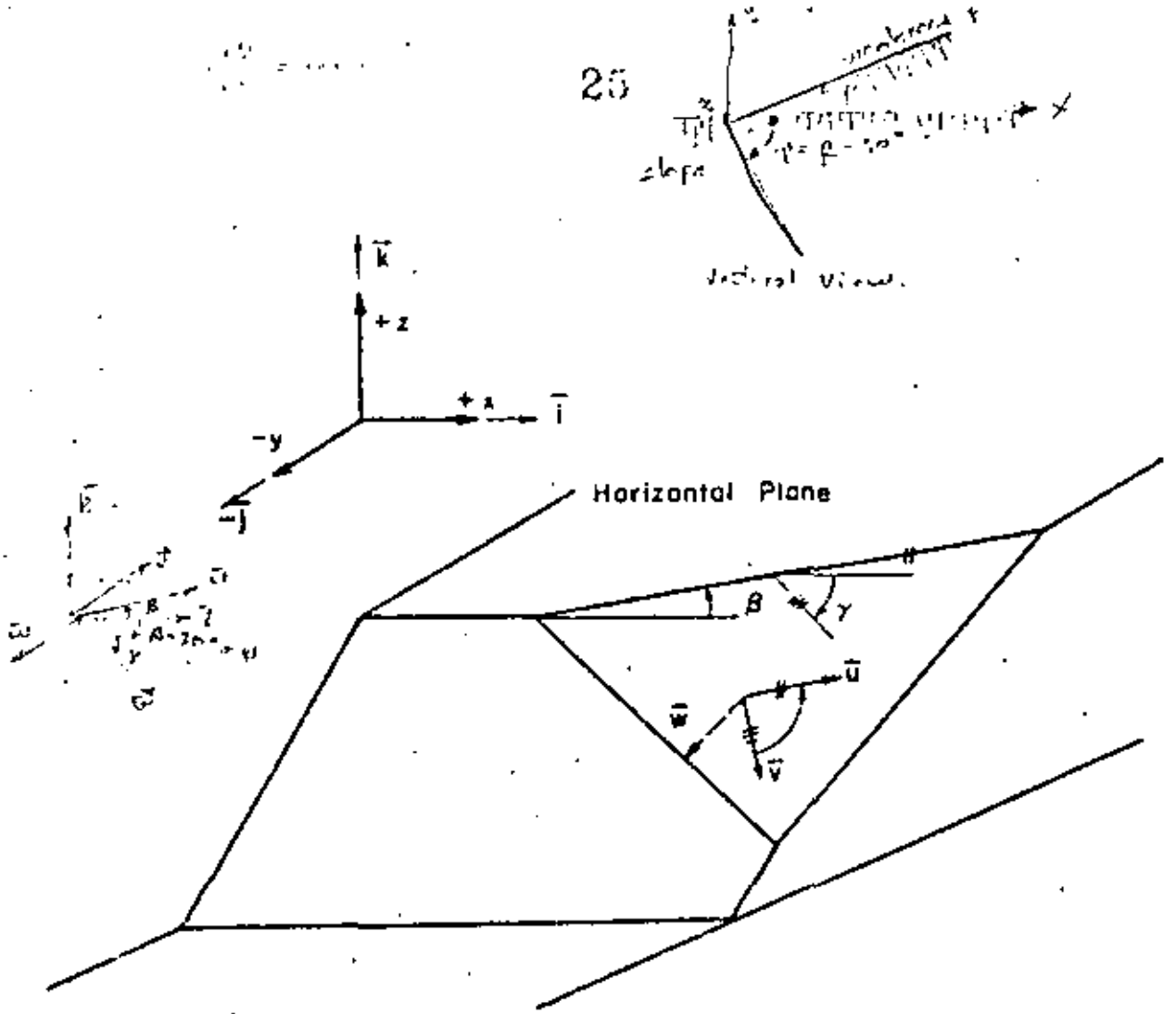

$$\vec{u} = \cos\beta\,\vec{i} + \sin\beta\,\vec{j}$$

$$\vec{v} = \cos\gamma\,\sin\beta\,\vec{i} - \cos\gamma\,\cos\beta\,\vec{j} - \sin\gamma\,\vec{k}$$

$$\vec{w} = \vec{u} \times \vec{v} = \begin{vmatrix} \vec{i} & \vec{j} & \vec{k} \\ u_x & u_y & u_z \\ v_x & v_y & v_z \end{vmatrix}$$

FIG. 2.3 ORIENTATION OF A PLANE IN VECTOR NOTATION

a horizontal plane in a counterclockwise direction from the positive x-axis as shown in Fig. 2.3. The value of β can range between 0 and 180 degrees. The dip of a plane with the horizontal is denoted by the angle γ in a direction at 90 degrees to the strike. The dip, γ, can range from 0 to 180 degrees and is measured downward from a horizontal line directed at an angle, α equal to $\beta - 90^{\circ}$ to the positive x axis. An example of the use of this notation to describe the orientation of two planes is shown in Fig. 2.4. The strike and dip are described by the unit vectors $\bar{u}$ and $\bar{v}$ respectively, and are written in terms of the angles β and γ as shown in Fig. 2.3, i.e.,

$$\bar{u} = \cos\beta\,\bar{i} + \sin\beta\,\bar{j}$$

and

$$\bar{v} = \cos\gamma\sin\beta\,\bar{i} - \cos\gamma\cos\beta\,\bar{j} - \sin\gamma\,\bar{k}$$

or

$$\bar{u} = (\cos\beta, \sin\beta, 0) \tag{2.13}$$

$$\bar{v} = (\cos\gamma\sin\beta, -\cos\gamma\cos\beta, -\sin\gamma) \tag{2.14}$$

Since the strike and dip are at 90 degrees, the scalar product $\bar{u}\cdot\bar{v}$ should be zero, $\bar{u}\cdot\bar{v} = +\cos\beta\cos\gamma\sin\beta - \sin\beta\cos\gamma\cos\beta = 0$. Thus Eqs. (2.13) and (2.14) satisfy the orthogonal relationship required for the unit vectors describing the strike and dip.

The cross product of $\bar{u}$ and $\bar{v}$ gives a unit vector $\bar{w}$ which is perpendicular to both $\bar{u}$ and $\bar{v}$ and thus directed normal to the plane described by $\bar{u}$ and $\bar{v}$. The vector $\bar{w}$ is obtained by expanding the determinant given in Eq. (2.15).

$$\bar{w} = \bar{u} \times \bar{v} = \begin{vmatrix} \bar{i} & \bar{j} & \bar{k} \\ u_x & u_y & u_z \\ v_x & v_y & v_z \end{vmatrix} \tag{2.15}$$

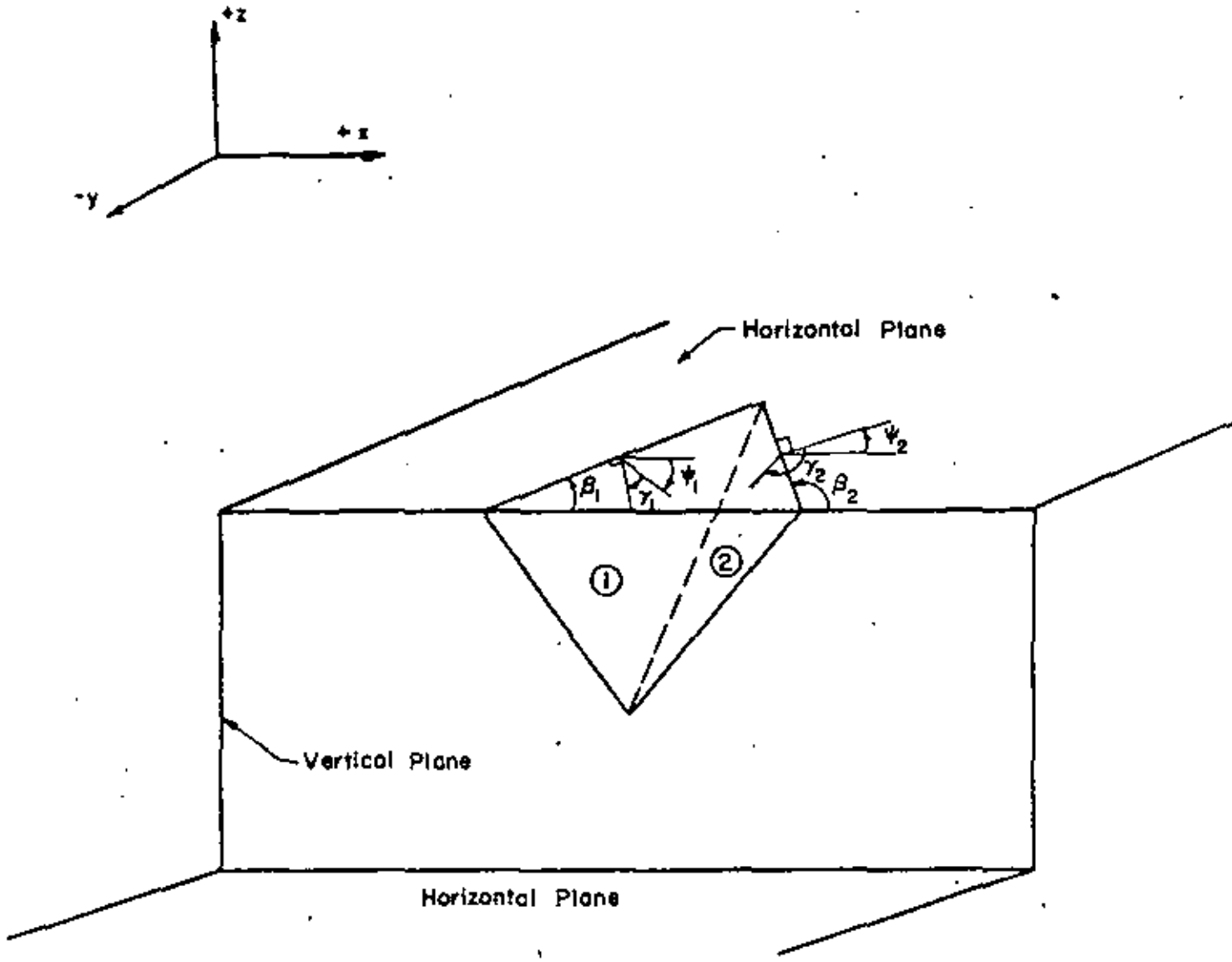

FIG. 2.4 CO-ORDINATE SYSTEM FOR DESCRIBING STRIKES AND DIPS

The direction of $\bar{w}$ is normal to the plane of $\bar{u}$ and $\bar{v}$ in the direction of advance of a right hand screw in turning from $\bar{u}$ to $\bar{v}$ through the smallest angle between these vectors ($< 180^{\circ}$). The magnitude of $\bar{w}$ is equal to the quantity uv sin θ which assumes the value of unity because $\theta = 90^{\circ}$ and $\bar{u}$ and $\bar{v}$ are unit vectors. The sense of $\bar{w}$ for the two planes shown in Fig. 2.4 is shown in Fig. 2.5. Note that for plane 1 the direction of $\bar{w}_1$ is normal to plane 1 and directed downward into the slope and $\bar{w}_2$ is normal to plane 2 directed upward out of the slope. The specification of the unit vector $\bar{w}$ normal to a plane is sufficient to completely describe the orientation of that plane.

The direction of the line of intersection of two joint planes (planes 1 and 2) is given by a vector $\bar{x}_{12}$ having the direction of the cross product of the normal unit vectors to the two planes. Thus for planes 1 and 2 shown in Fig. 2.5 a vector $\bar{x}_{12}$ along the line of intersection is given by

$$\bar{x}_{12} = \bar{w}_2 \times \bar{w}_1 \tag{2.16}$$

where $\bar{x}_{12}$ is directed downward along the line of intersection as shown in Fig. 2.5.

2.3.2 Resolution of Forces

The component of a force $\bar{R}$ in the direction given by a unit vector $\bar{n}$ is given by

$$\bar{R} \cdot \bar{n} = R \cos \theta \tag{2.17}$$

where θ is the angle between $\bar{R}$ and $\bar{n}$. Thus, for example, the component of a force $\bar{R}$ normal to a plane is given by $\bar{R} \cdot \bar{w}$ and is given by

$$R_N = \bar{R} \cdot \bar{w} = R_x w_x + R_y w_y + R_z w_z \tag{2.18}$$

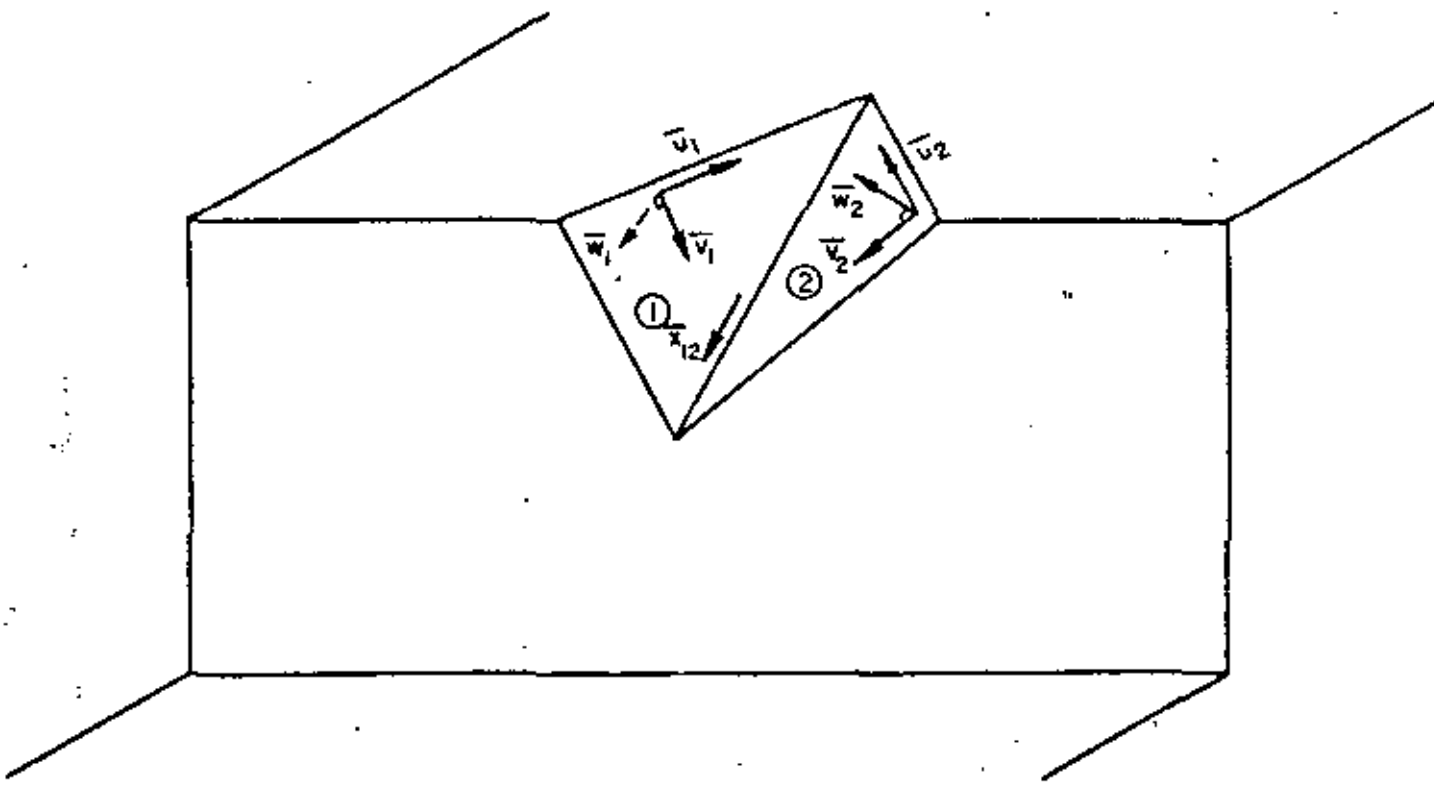

FIG. 2.5 VECTOR DESCRIPTION OF THE ORIENTATION OF TWO PLANES AND THEIR LINE OF INTERSECTION

Similarly the component of $\bar{R}$ in the direction of the line of intersection of two planes is $\bar{R}\cdot\frac{\bar{x}_{12}}{x_{12}}$.

The obliquity of a force $\bar{R}$ on a given plane is the angle ϕ', which the force $\bar{R}$ makes with the normal to the plane $\bar{w}$ as shown in Fig. 2.6.

$$\tan \phi' = R_T/R_N$$

where R_N and R_T are the components of R normal and tangential to the plane, respectively. Note that $R_N = \bar{R}\cdot\bar{w} = R_x w_x + R_y w_y + R_z w_z = R \cos \phi'$ and

$$R_T = |\bar{R} \times \bar{w}| = R \sin \phi'$$

$$= [(R_y w_z - R_z w_y)^2 + (R_z w_x - R_x w_z)^2 + (R_x w_y - R_y w_x)^2]^{1/2} \quad (2.19)$$

Therefore the obliquity of a force on a plane is given by

$$\tan \phi' = \frac{R_T}{R_N} = \frac{[(R_y w_z - R_z w_y)^2 + (R_z w_x - R_x w_z)^2 + (R_x w_y - R_y w_x)^2]^{1/2}}{(R_x w_x + R_y w_y + R_z w_z)} \quad (2.20)$$

The vector $\bar{R}_T$ may also be given by $\bar{R} - R_N\bar{w}$ which is given by

$$\bar{R}_T = (R_x - R_N w_x)\bar{i} + (R_y - R_N w_y)\bar{j} + (R_z - R_N w_z)\bar{k}$$

since $R_N\bar{w} = R_N w_x \bar{i} + R_N w_y \bar{j} + R_N w_z \bar{k}$. Thus the obliquity may also be given as

$$\tan \phi' = \frac{[(R_x - R_N w_x)^2 + (R_y - R_N w_y)^2 + (R_z - R_N w_z)^2]^{1/2}}{R_x w_x + R_y w_y + R_z w_z} \quad (2.21)$$

2.3.3 Line of Application of a Force and Point of Intersection of Two Forces

In order to analyze rotational stability, the point of application of a force and its direction must be known. If the vector $\overline{OS}$ from the selected origin of coordinates O to a point S on the line of action of the force $\bar{W}$ is known, the line of action of $\bar{W}$ may be expressed as the line joining the tips of the set of radius vectors given by

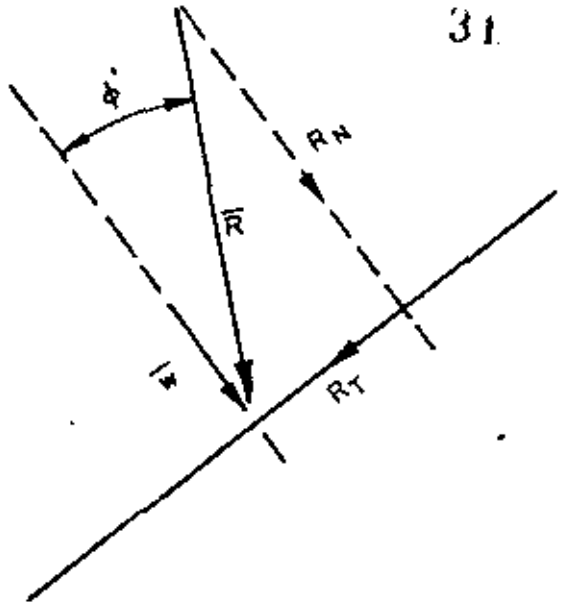

FIG. 2.6 RESOLUTION OF FORCES ON A PLANE INTO NORMAL AND TANGENTIAL COMPONENTS

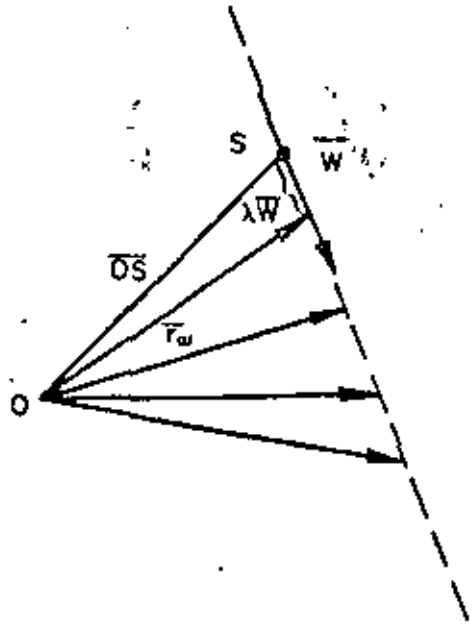

FIG. 2.7 EQUATION OF A LINE IN VECTOR NOTATION

$$\bar{r}_w = \overline{OS} + \lambda\bar{W} \tag{2.22}$$

and shown in Fig. 2.7.

In a three-dimensional problem the set of applied forces will not in general intersect, and the moment of each force about a particular axis of rotation may be considered separately, or the forces may be moved parallel to the axis of rotation about which moments are being summed until the forces intersect. For example, in analyzing the rotation of a wedge as shown in Fig. 2.8 around the axis defined by the unit vector $\bar{d}$, for the external force $\bar{P}$ applied at point N and the weight $\bar{W}$ applied through the center of gravity S, either of these forces may be shifted any distance K parallel to $\bar{d}$ without changing the moment about $\bar{d}$. Thus the forces may be moved in this manner until their lines of action intersect. If the line of action of $\bar{W}$ is defined by

$$\bar{r}_w = \overline{OS} + \lambda\overline{W} \qquad (\lambda = \text{constant}) \tag{2.23}$$

and the line of action of $\bar{P}$ is defined by

$$\bar{r}_p = \overline{ON} + \delta\overline{P} \qquad (\delta = \text{constant}) \tag{2.24}$$

the resultant $\bar{R}$ of $\bar{P}$ and $\bar{W}$ can be considered to act at a point of intersection I by setting

$$\bar{r}_w = \bar{r}_p + K\cdot\bar{d} \tag{2.25}$$

Substitution of Eqs. (2.23) and (2.24) in Eq. (2.25) yields

$$\overline{OS} + \overline{\lambda W} = \overline{ON} + \overline{\delta P} + \overline{Kd} \tag{2.26}$$

If three equations are written from Eq. (2.26) in terms of the x, y, and z components of $\bar{P}$ and $\bar{W}$ they can be solved simultaneously for

$$\lambda = \lambda_1,\ \delta = \delta_1 \text{ and } K = K_1$$

which locate the point of intersection I. The vector from the origin O,

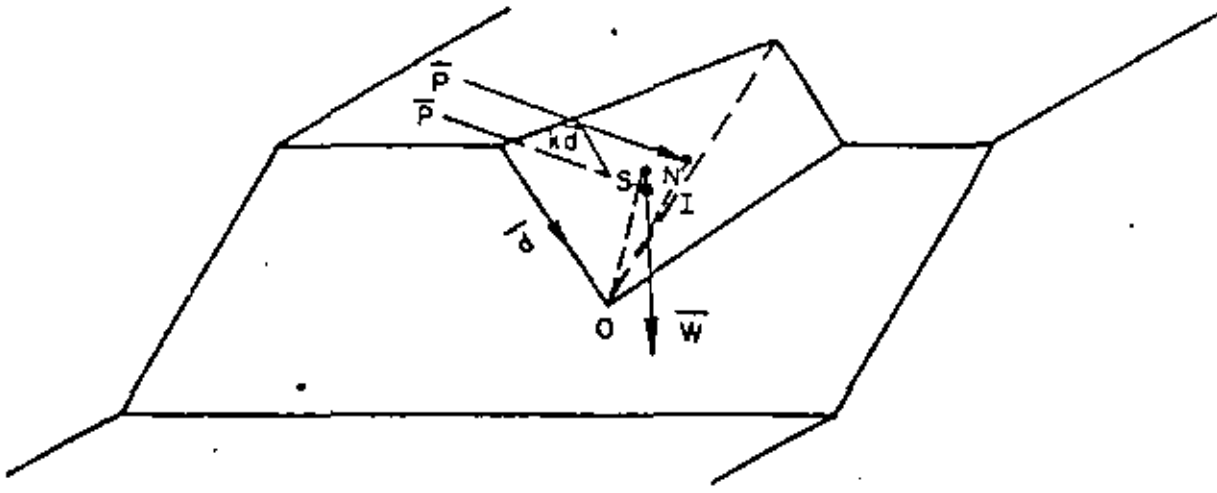

FIG. 2.8 MOMENT CAUSED BY TWO FORCES WITH DIFFERENT POINTS OF APPLICATION

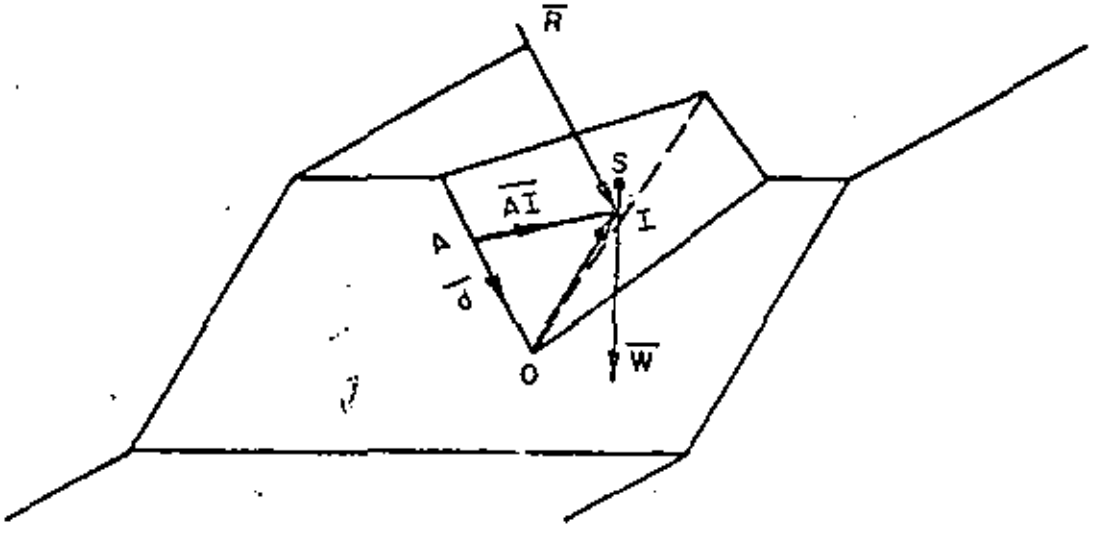

FIG. 2.9 MOMENT OF A FORCE ABOUT A GIVEN AXIS

to I, the point of application of $\bar{R}$, is thus

$$\overline{OI} = \overline{OS} + \lambda_1 \bar{W} \tag{2.27}$$

2.3.4 Moment about an Axis

The magnitude of the moment about axis $\bar{d}$ through point A as shown in Fig. 2.9 caused by the force $\bar{R}$ acting at point I is

$$M_d = (\overline{AI} \times \bar{R}) \cdot \bar{d} \tag{2.28}$$

where

$$\overline{AI} = \overline{AO} + \overline{OI}$$

2.3.5 Point of Intersection of a Force and a Joint Plane

The point of intersection of a force and a joint plane is found by equating the line of action of the force and the equation of a plane. The equation of a plane is given by

$$\bar{r}_p \cdot \bar{w} = \text{constant} \tag{2.29}$$

where $\bar{r}_p$ is a radius vector from the origin to a point in the plane, and $\bar{w}$ the unit vector normal to the plane. If the vector $\overline{OF}$ from the origin to any point F in the plane is known, then the constant is determined and the equation of the plane is:

$$\bar{r}_p \cdot \bar{w} = (\overline{OF} \cdot \bar{w})$$

The point where the force P intersects the plane is thus given by solving simultaneously the equation for the line of action of the force and the equation of the plane giving

$$(\overline{ON} + \overline{\delta P}) \cdot \bar{w} = (\overline{OF} \cdot \bar{w}) \tag{2.30}$$

The solution yields δ_Q, the value of δ defining the piercing point Q of the force $\bar{P}$ on the plane p as shown in Fig. 2.10.

2.3.6 Geometry of a Triangle

The area of the triangle OKL shown in Fig. 2.11 is given by

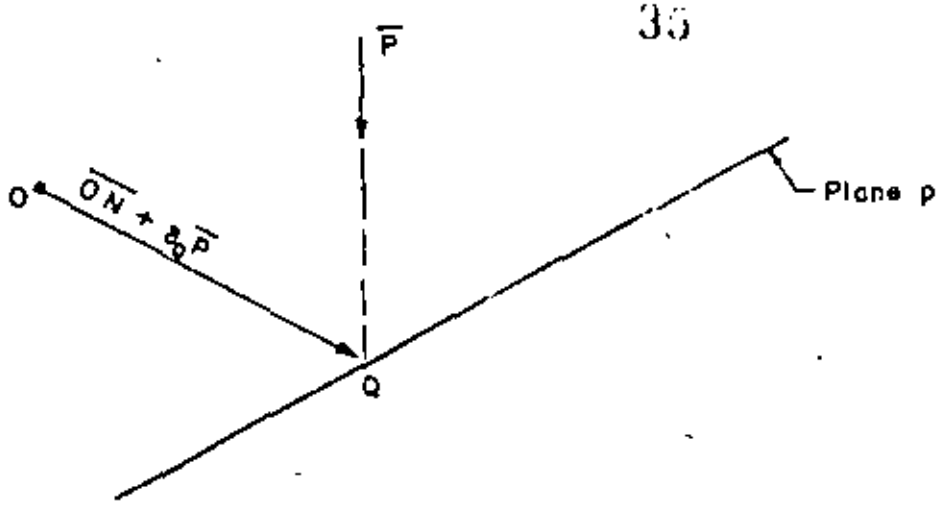

FIG. 2.10 INTERSECTION OF THE LINE OF ACTION OF A FORCE ON A PLANE

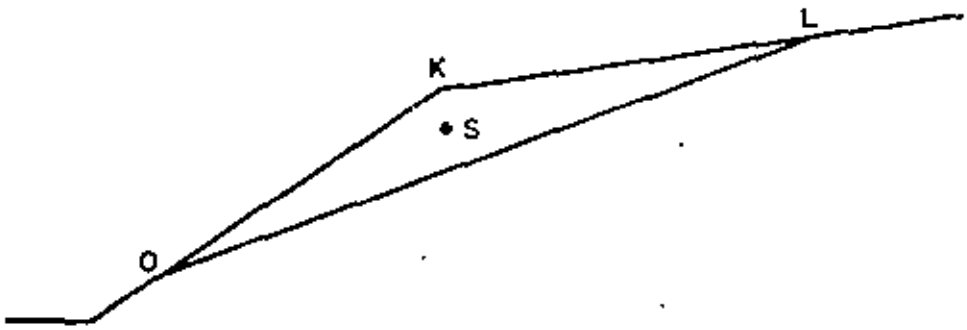

FIG. 2.11 GEOMETRY OF A TRIANGLE

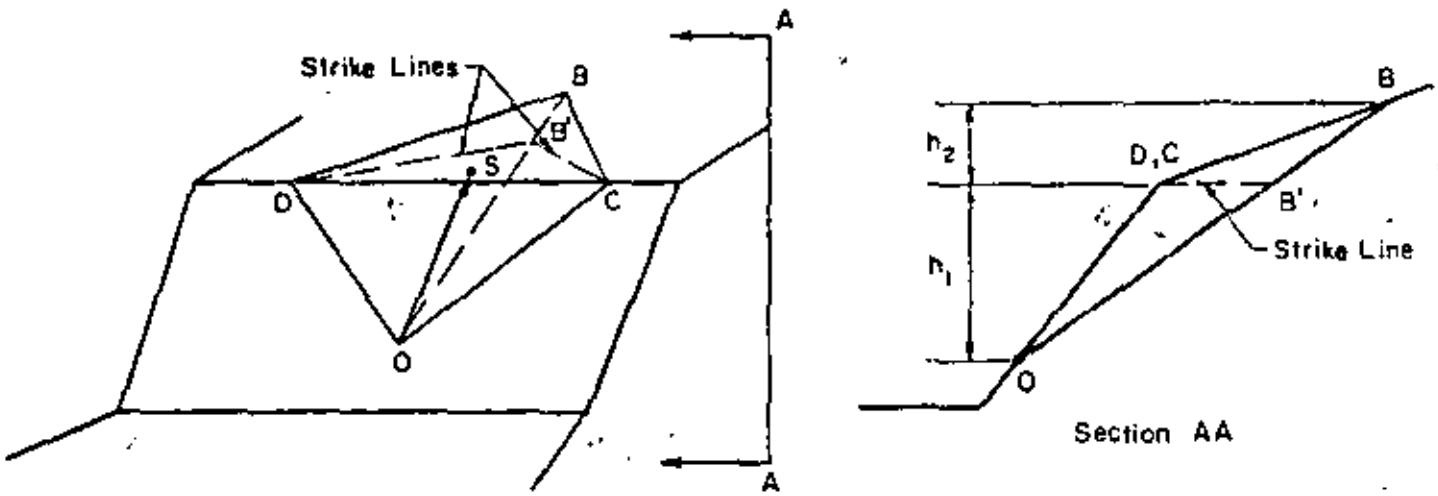

FIG. 2.12 GEOMETRY OF A TETRAHEDRON

$$A = 1/2 \quad |\overrightarrow{OK} \times \overrightarrow{OL}| \tag{2.31}$$

and the vector from O to the centroid, S, is given by

$$\overrightarrow{OS} = 1/3 \ (\overrightarrow{OK} + \overrightarrow{OL}) \tag{2.32}$$

2.3.7 Geometry of a Tetrahedron

The volume of a tetrahedron as shown in Fig. 2.12 is given by

$$V = 1/6 \quad |\overrightarrow{DB'} \times \overrightarrow{DC}| \ (h_1 + h_2) \tag{2.33}$$

The centroid at point S may be described by the vector from the origin, $\overrightarrow{OS}$, given by

$$\overrightarrow{OS} = 1/4 \ (\overrightarrow{OD} + \overrightarrow{OC} + \overrightarrow{OB}) \tag{2.34}$$

The components of $\overrightarrow{OS}$ are thus the coordinates of the centroid.

3.1 General

In this chapter analytical methods are presented for determining the static factor of safety of rock slopes. The cases covered include rock slopes cut by one, two, or three joint sets. Example problems are given where various combinations of the vector analyses of Wittke and Londe are utilized. A typical example problem is also worked by common engineering graphics. The notion of dynamic resistance is also introduced in this chapter for rock slopes and example calculations of the minimum dynamic resistance are illustrated. The methods given in this chapter for computing the dynamic resistance of a rock slope in three dimensions is original with this report and is intended to be used for predicting dynamic motions under earthquake loadings in conjunction with Newmark's method of analysis for the dynamic stability of slopes.

3.2 Stability Calculations by Vector Analysis for Sliding on One Plane

3.2.1 Calculation of Factor of Safety for Static Loads

The simplest special case of a rock slope stability problem is where the strike of one of the planes of weakness is parallel to the strike of the slope face as shown in Fig. 3.1. For the coordinate system adopted in Chapter 2, this condition can be expressed when the unit vector $\bar{u}$ in the direction of the strike has components of zero in the y and z directions i.e.,

$$\bar{u} = (u_x, u_y, u_z) = (1, 0, 0).$$

Then the unit vector $\bar{v}$ in the direction of the dip has its x component equal to zero, i.e.,

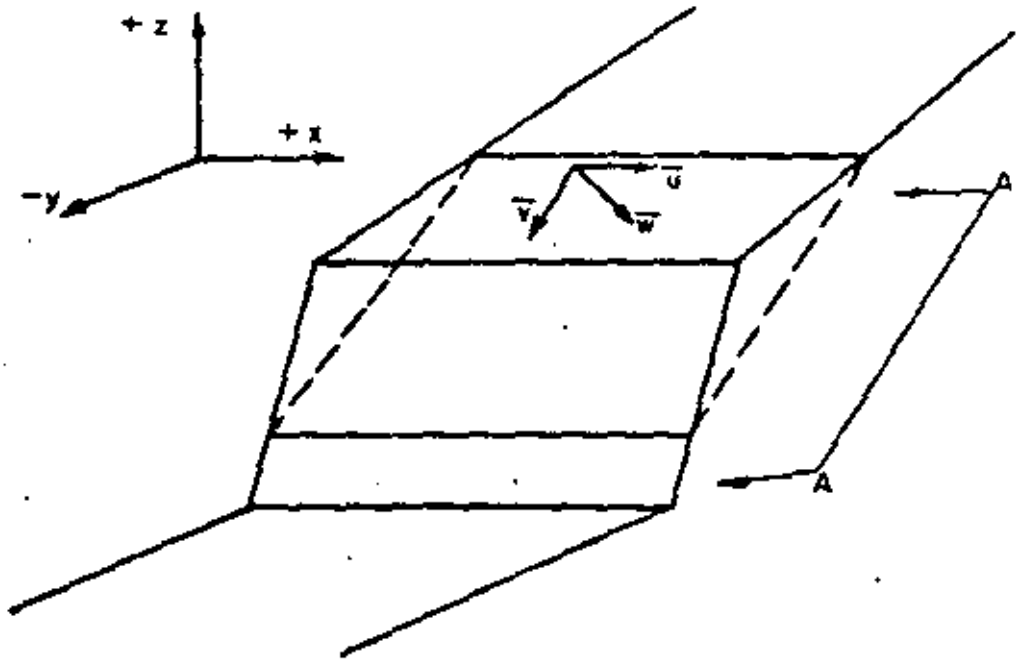

(a)

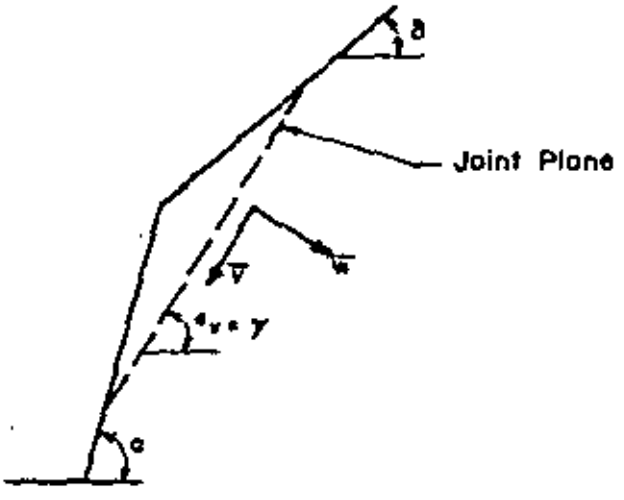

(b)
Section A–A

FIG. 3.1 SLIDING ON ONE PLANE — STRIKE OF PLANE PARALLEL TO STRIKE OF SLOPE FACE

$$\bar{v} = (v_x, v_y, v_z) = (0, v_y, v_z) \quad 3:)$$

The inclination of the line of fall of the plane , ϵ_v, will determine the kinematic possibility of sliding. The angle of fall ϵ_v is given by

$$\tan \epsilon_v = \frac{v_z}{v_y} = \tan(\gamma) \tag{3.1}$$

where γ is the angle of dip of the plane. In order for sliding to be kinematically possible, ϵ_v must be smaller than α if $0 < \alpha < \pi$ as shown in Fig. 3.1(b). If $\alpha = \pi$, then ϵ_v must be smaller than ζ for the sliding to be possible.

For a slope acted upon only by gravity and the plane of weakness striking parallel to the slope face, the sliding will occur parallel to the unit vector $\bar{v}$ in the direction of the dip. The magnitude of the component T of the weight $\bar{W}$ acting parallel to $\bar{v}$ may be obtained from

$$T = \bar{W} \cdot \bar{v} \tag{3.2}$$

where $\bar{W} = (0, 0, -W)$. The vector $\bar{T}$ is given by

$$\bar{T} = T\bar{v} \tag{3.3}$$

The magnitude of the component of $\bar{W}$ normal to the direction of sliding is

$$N = \bar{W} \cdot \bar{w}$$

where $\bar{w}$ is the unit vector normal to the plane of sliding as given by $\bar{u} \times \bar{v}$. The magnitude of the available resisting force is given by N tan ϕ where ϕ is the angle of shearing resistance between the joint surfaces in the direction of sliding. The factor of safety against sliding is the quotient of the resisting and the driving force in the direction of sliding and is given by

$$F.S. = \frac{N \tan \phi}{T} = \frac{(\bar{W} \cdot \bar{w}) \tan \phi}{(\bar{W} \cdot \bar{v})} \tag{3.4}$$

For the case shown in Fig. 3.1, the unit vector in the direction of the strike is given by $\bar{u} = \bar{i}\, u_x = \bar{i}$ and the dip is given by $\bar{v} = \bar{j}v_y + \bar{k}v_z$. The unit vector $\bar{w}$ normal to the plane of weakness is given by

$$\bar{w} = \bar{u} \times \bar{v} = \begin{vmatrix} \bar{i} & \bar{j} & \bar{k} \\ 1 & 0 & 0 \\ 0 & v_y & v_z \end{vmatrix} = -\bar{j}v_z + \bar{k}v_y$$

Thus the magnitude of the component of the weight in the direction of sliding is given by

$$T = \bar{W} \cdot \bar{v} = -Wv_z \tag{3.5}$$

and the component of the weight normal to the plane of weakness is

$$N = \bar{W} \cdot \bar{w} = -Wv_y \tag{3.6}$$

Thus the factor of safety according to Eq. (3.4) is:

$$F.S. = \frac{-Wv_y \tan \phi}{-Wv_z} = \frac{v_y}{v_z} \tan \phi = \frac{\tan \phi}{\tan \gamma} \tag{3.7}$$

which is a well known expression for the factor of safety of slopes potentially free to slide down the dip angle γ under gravity loading only.

If a slope is loaded by its own weight $\bar{W}$, and a pore water force $\bar{U}$ acting on the potential failure plane in the direction of the unit vector $-\bar{w}$, then the factor of safety is given by

$$F.S. = \frac{(\bar{W} \cdot \bar{w}) - U}{(\bar{W} \cdot \bar{v})} \tan \phi \tag{3.8}$$

When the magnitude of the porewater force U is given by KW, Eq. (3.8) reduces to

$$F.S. = \frac{(-Wv_y - KW)}{-Wv_z} \tan \phi$$

$$F.S. = \frac{\tan \phi}{\tan \gamma} + K \frac{\tan \phi}{v_z} = \frac{\tan \phi}{\tan \gamma} - K \frac{\tan \phi}{\sin \gamma} \quad (3.9)$$

where γ is the dip of the potential failure plane and $v_z = -\sin \gamma$.

The case may also be considered where sliding can take place on one joint or bedding plane as shown in Fig. 3.2(a) or 3.2(b). In the general case the potential sliding wedge can be acted on by its weight $\bar{W}$, the porewater force $\bar{U}$ acting on the plane of sliding, and an external force $\bar{Q}$ which may be applied by a structure, such as a dam. In many cases where we are concerned with large slopes, however, the weight $\bar{W}$ will be large compared with $\bar{Q}$. In the analysis of sliding on one plane with the forces $\bar{W}$, $\bar{U}$ and $\bar{Q}$ acting on the wedge, the forces are added vectorially into a resultant $\bar{R}$ which is given by

$$\bar{R} = \bar{W} + \bar{U} + \bar{Q} \quad (3.10)$$

The resisting reaction in plane a b c as shown in Fig. 3.3 is $\bar{R}'$ and is equal and opposite to $\bar{R}$. Thus the direction of sliding is in the direction of the projection of $\bar{R}$ on plane a b c and not necessarily in the direction of the dip. The angle of friction mobilized, ϕ', by the force $\bar{R}$ is given by Eq. 2.20 for sliding on one plane as

$$\tan \phi' = \frac{[(R_y w_z - R_z w_y)^2 + (R_z w_x - R_x w_z)^2 + (R_x w_y - R_y w_x)^2]^{1/2}}{R_x w_x + R_y w_y + R_z w_z} \quad (3.11)$$

Thus the factor of safety for this case is given by

$$F.S. = \frac{\tan \phi}{\tan \phi'} \quad (3.12)$$

3.2.2 Calculation of Dynamic Resistance

It should also be noted that Wittke[1] (1965) has treated an earthquake loading as an equivalent static load applied in a horizontal plane and parallel to the projection of the unit vector in a direction of the dip,

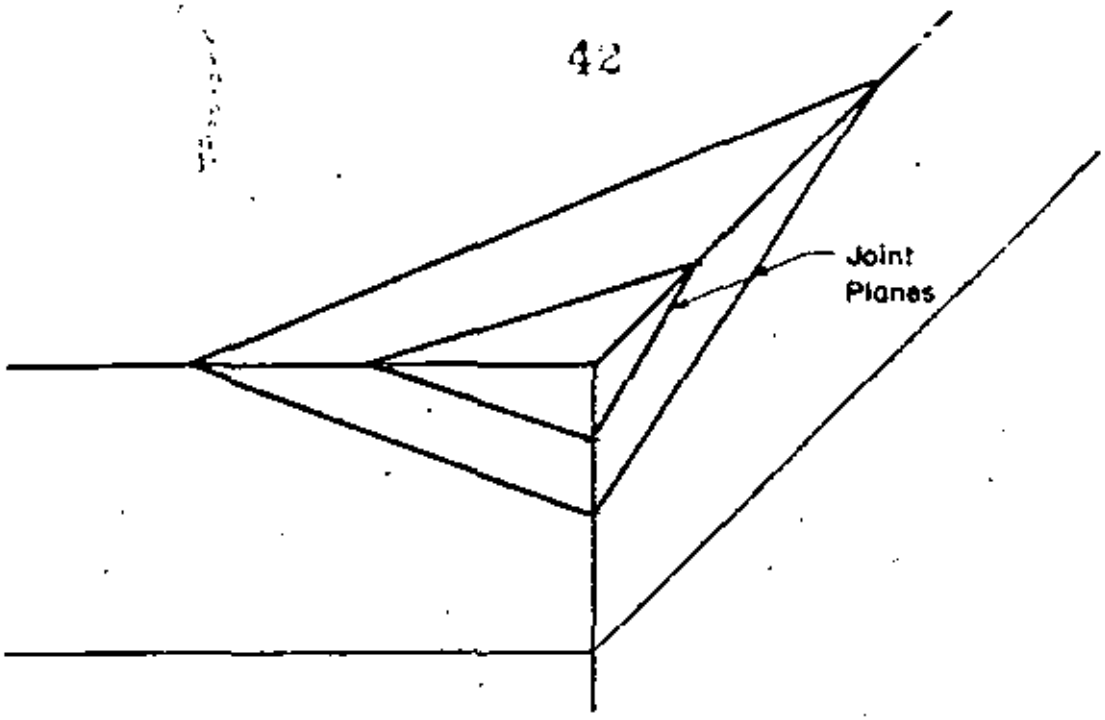

(a) Cutslope

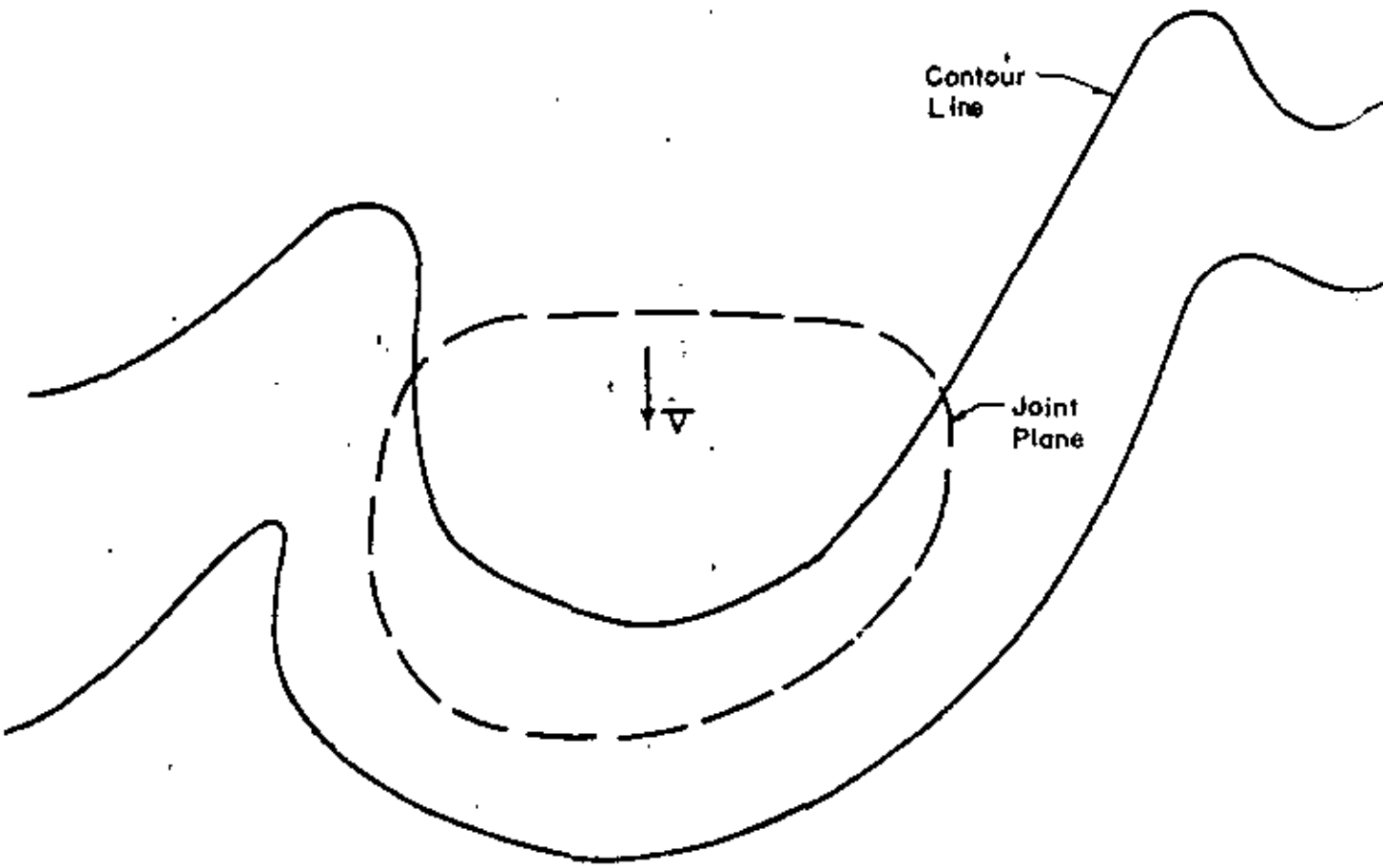

(b) Natural Slope — Bedding Planes Dipping Toward Valley — Sliding Block Isolated from Mass by Gully on Each Side

FIG. 3.2 SLIDING ON ONE PLANE — STRIKE OF PLANE NOT PARALLEL TO STRIKE OF SLOPE FACE

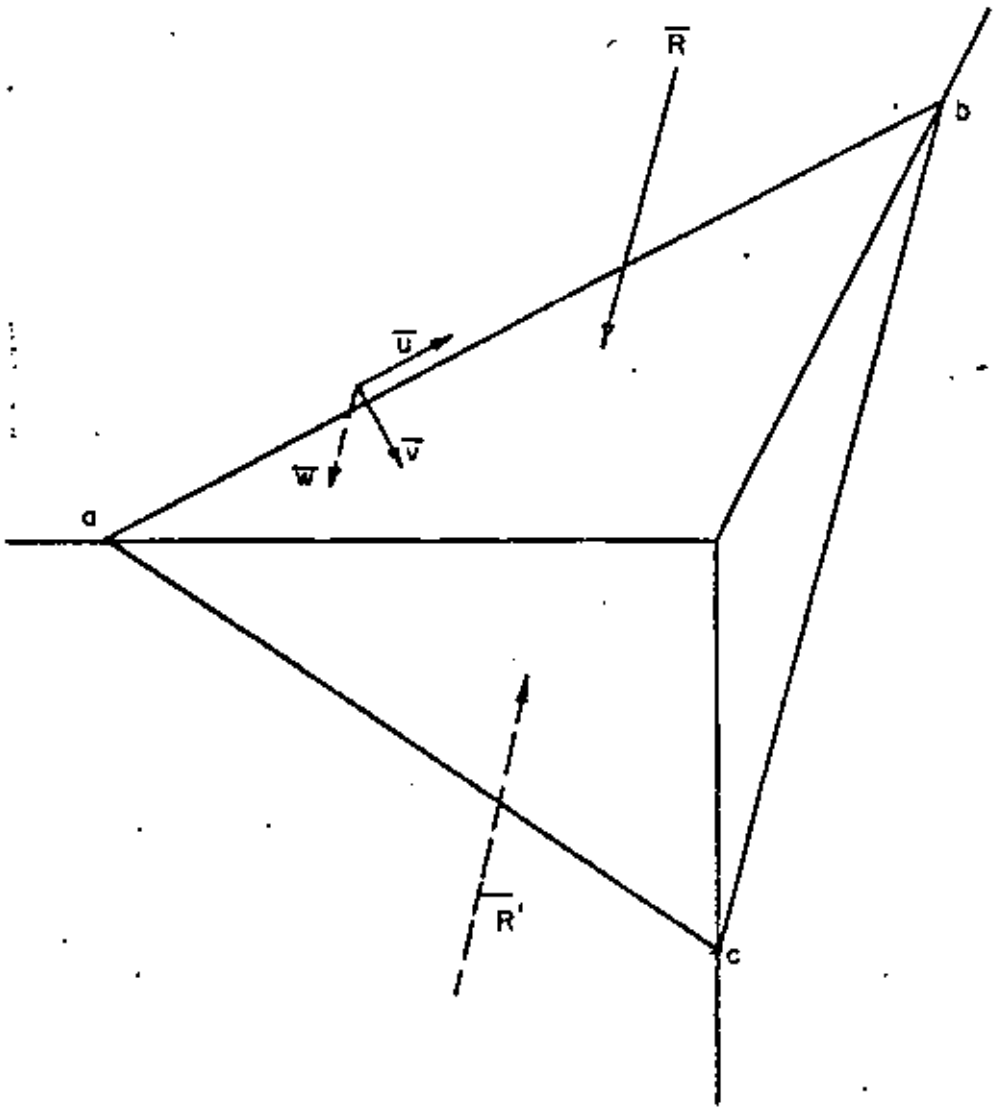

FIG. 3.3 SLIDING ON ONE PLANE

$\bar{v}$, in a horizontal plane. Thus, according to the analysis of Wittke (1965) for earthquake loading, the problem is simply analyzed as for the general case presented above where

$$\bar{R} = \bar{W} + \bar{U} + \bar{Q} + \bar{H}$$

where

$$\bar{H} = \bar{i} \frac{v_x}{(v_x^2 + v_y^2)^{\frac{1}{2}}} k_1 W + \bar{j} \frac{v_y}{(v_x^2 + v_y^2)^{\frac{1}{2}}} k_1 W$$

The seismic coefficient k_1 is taken between 0 and 0.2 depending on the intensity of the earthquake motion expected, and the force $\bar{H}$ is in a horizontal plane and parallel to the projection of the unit vector in a direction of the dip, $\bar{v}$, in a horizontal plane. The factor of safety is as given by Eq. 3.12. This approach, however, is not recommended by the authors since it is considered as being an unduly conservative approach to earthquake stability. The approach proposed in this report for assessing the dynamic stability of rock slopes will essentially follow the concepts proposed by Newmark (1965), which are presented in Chapter 5. In order to use the Newmark method of analysis, however, it is necessary to establish the resistance available to resist dyanmic loads. This dynamic resistance is the resistance which is available in addition to the resistance required for static stability. The dynamic resistance is denoted by $\overline{NW}$ where $\bar{W}$ is is the weight of the potential sliding block and N is a coefficient to be determined in the following manner. The force $\overline{NW}$ is that force applied to the potential sliding block which is necessary to just make the block slide (i.e. F.S. = 1). Depending on the direction in which $\overline{NW}$ is applied, its magnitude will vary. The magnitude of $\overline{NW}$ appropriate for design or analysis is the magnitude of $\overline{NW}$ applied in such a direction as to make $\overline{NW}$

a minimum. For a potential failure of a block sliding on one plane as shown in Fig. 3.4(a) $\overline{NW}$ should be applied in a direction γ to the horizontal which will give the minimum value of $\overline{NW}$ to just cause the block to slide. The direction and magnitude of the minimum value of $\overline{NW}$ can be determined as shown in Fig. 3.4(b). The direction and magnitude of the weight $\bar{W}$ is known and the direction of a resultant $\bar{R}$ is known and is inclined at ϕ to the normal of the plane of sliding when sliding begins to take place. Then the magnitude of the vector $\overline{NW}$ is minimum when it joins the tip of the weight vector $\bar{W}$ in a direction which makes an angle of 90^{o} with the resultant $\bar{R}$. Thus from geometry, the minimum magnitude of $\overline{NW}$ is given by

$$NW = W \sin (\phi - \gamma)$$

or

$$N = \sin (\phi - \gamma) \qquad (3.13)$$

where ϕ is the angle of shearing resistance and γ is the dip. Thus the minimum value of N occurs when $\overline{NW}$ is in the same direction of the horizontal projection of the dip but is inclined upward from the horizontal at an angle of $\theta = (\phi - \gamma)$ and N has a magnitude of $\sin (\phi - \gamma)$ for the case of sliding on one plane. Using this minimum value of $\overline{NW}$ as the dynamic resistance is a conservative estimate because it is assumed that the earthquake motions are in the most unfavorable orientation for the slope being investigated.

3.3 Example Problems of Sliding on One Plane by Vector Analysis

Slope stability calculations by vector analysis are performed in this section for several cases involving sliding on one plane. In some of these cases the same answer could be arrived at quickly by means of

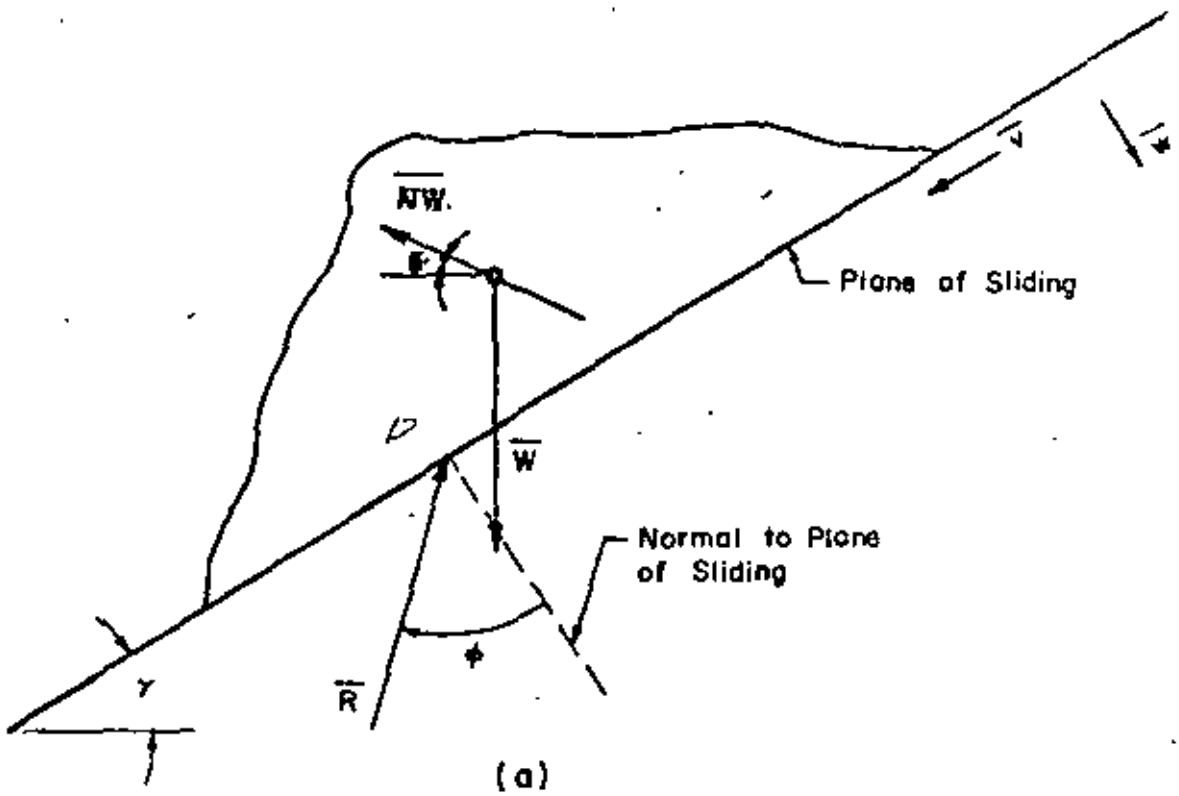

(a)

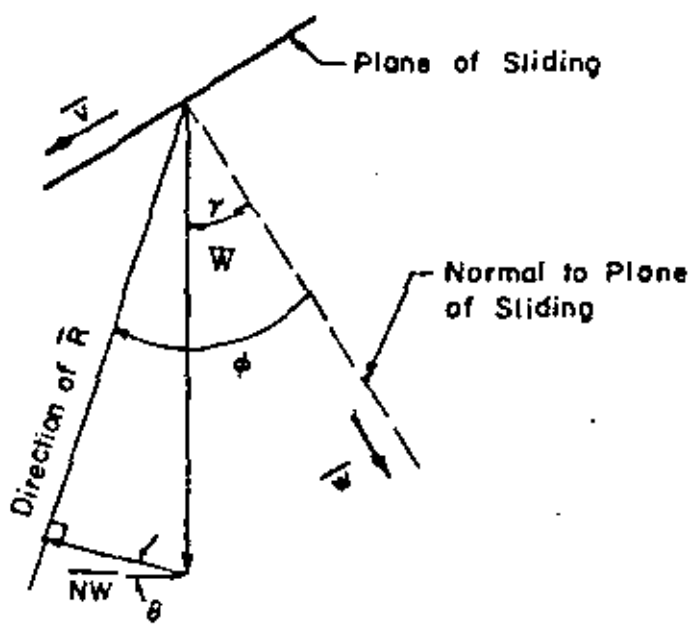

(b)

FIG. 3.4 FAILURE OF A BLOCK SLIDING ON ONE PLANE

conventional analysis, in others it would be more difficult to do by conventional means.

For example, consider a wedge of rock sliding on a plane which strikes East-West and dips 30° South and which has a friction angle of 40°. Consider the positive x direction to be East, the positive y direction to be North and the positive z direction to be upwards. The unit vector in the direction of the strike is given by

$$\bar{u} = (1, 0, 0)$$

The unit vector in the dip direction is given by

$$\bar{v} = (0, -0.866, -0.500)$$

and the unit vector normal to the plane is

$$\bar{w} = \bar{u} \times \bar{v} = (0, 0.500, -0.866)$$

and $\bar{w}$ is directed downward normal to the plane.

Case I

First consider the factor of safety of the block acted on by its own weight only. In this case the resultant force $\bar{R}$ acting on the block is equal to the weight $\bar{W}$ given by

$$\bar{R} = \bar{W} = (0, 0, -W)$$

The magnitude of the component of $\bar{R}$ normal to the plane is given by

$$N = \bar{R} \cdot \bar{w} = 0.866\ W$$

then $\bar{N} = 0.866\ W\bar{w} = (0, 0.433W, -0.750W)$

the tangential component of $\bar{R}$ on the plane of sliding is

$$\bar{T} = \bar{R} - \bar{N} = (0, -0.433W, -0.25W)$$

the magnitude of $\bar{T}$ is given by

$$T = W\ [(-0.433)^2 + (-0.25)^2]^{1/2} = 0.50W$$

then $F.S. = \frac{N \tan \phi}{T} = \frac{0.866W \tan 40^\circ}{0.50W} = 1.455$ ✓3

Check: By Eq. 3.7

$$F.S. = \frac{\tan 40^\circ}{\tan 30^\circ} = 1.455$$ ✓3

Case II

Consider now that a force $\bar{A}$ acts on the wedge in addition to the weight of the wedge $\bar{W}$. The force $\bar{A}$ acts parallel to the strike (East) and has a magnitude of 0.20W.

Thus $\bar{R} = \bar{A} + \bar{W} = (0.20W, 0, -W)$

and $N = \bar{R} \cdot \bar{w} = 0.866W$

and $\bar{N} = N\bar{w} = (0, 0.433W, -0.75W)$

The component of $\bar{R}$ tangential to the plane is

$\bar{T} = \bar{R} - \bar{N} = (0.200W, -0.433W, -0.250W)$ and $T = 0.540W$.

$\therefore F.S. = \frac{N \tan \phi}{T} = \frac{0.866W \tan 40^\circ}{0.54W} = 1.35$

Note that in this case sliding does not take place down the dip but in the direction of the vector $\bar{T}$.

Case III

Consider now that the wedge is acted on by its own weight and a force $\bar{A}$ having a magnitude of 0.20W and acting in a direction parallel to the unit vector in the direction of the dip. In this case the normal component is still given by $N = \bar{W} \cdot \bar{w} = 0.866W$ as given in Case I. The magnitude of the driving tangential force $\bar{T}$ is the sum of the magnitudes of $\bar{A}$ and the tangential component of the weight on the plane. The factor of safety is therefore given by

$$F.S. = \frac{0.866W \tan 40^\circ}{0.50W + 0.20W} = 1.05$$

Case IV

Now consider that the plane under the wedge of weight $\bar{W}$ as in Case I is acted upon by a porewater force, $\bar{U}$, which increases until the factor of safety decreases from 1.455 to 1.0. The porewater force does not change the driving force $\bar{T}$. Therefore, as in Case I,

$$T = 0.50W$$

The magnitude of the normal force N as given in Case I is reduced by the magnitude of the porewater force, U. That is

$$N = 0.866W - U$$

and $F.S. = 1.0 = \frac{0.866W - U}{0.50W} \tan 40^\circ$

and solving for U

$$U = 0.271W$$

Check: By Eq. 3.9

$$F.S. = 1.0 = \frac{\tan \phi}{\tan \gamma} - \frac{K \tan \phi}{\sin \gamma} = \frac{\tan 40^\circ}{\tan 30^\circ} - K \frac{\tan 40^\circ}{\sin 30^\circ}$$

Solving $K = 0.271$

$\therefore U = 0.271W$

Case V

Consider the same wedge to be acted on by its own weight $\bar{W}$, a porewater force $\bar{U}$ of magnitude $0.44W$ acting normal to and on the plane of sliding, and a force $\bar{A}$ having a magnitude $A = 0.60W$ and acting in a direction S 45°W at a dip of 10°. Then

$$\bar{W} = (0, 0, -W)$$

$$\bar{U} = 0.44W(-\bar{w}) = (0, -0.22W, 0.371W)$$

The unit vector, $\bar{a}$, in the direction of force $\bar{A}$ is given by Eq. 2.14 with $\gamma = 170^\circ$ and $\beta = 135^\circ$, thus,

$$\bar{a} = [-\cos 10^\circ \sin 45^\circ, -(-\cos 10^\circ)(-\cos 45^\circ), -\sin 10^\circ]$$

$$\bar{a} = (-0.696, -0.696, -0.174)$$

Thus

$$\bar{A} = A\bar{a} = (-0.418W, -0.418W, -0.105W)$$

and $$\bar{R} = \bar{W} + \bar{U} + \bar{A} = (-0.418W, -0.638W, -0.734W)$$

The magnitude of the component of R normal to the plane of sliding is given by

$$N = R \cdot w = 0.316W$$

$$\bar{N} = N\bar{w} = (0, 0.158W, -0.274W)$$

The component of $\bar{R}$ tangential to the plane of sliding is

$$\bar{T} = \bar{R} - \bar{N} = (-0.418W, -0.796W, -0.460W)$$

$$T = 1.009W$$

$$F.S. = \frac{N \tan 40^\circ}{T} = \frac{0.316W \tan 40^\circ}{1.009W}$$

$$= 0.262$$

Case VI

Consider the slope acted on by only its own weight as in Case I. It is desired to calculate the magnitude of the minimum dynamic resistance $\overline{NW}$. This is simply given by Eq. 3.13 as

$$NW = W \sin (\phi - \gamma) = W \sin 10^\circ$$

or $$N = \sin 10^\circ = 0.174$$

3.4 Stability Calculations by Vector Analysis for Slopes Containing Two Sets of Joint Planes.

3.4.1 Calculation of Factor of Safety for Static Loads

3.4.1.1 Description of Geometry and Loads

The general case of two systems of joint planes is as shown in Fig. 3.5 where planes 1 and 2 denote the joint planes, planes 3 and 4 denote the planes defining the faces of the slope, γ_1 and γ_2 denote the dip angles of planes 1 and 2, β_1 and β_2 denote the strike angles of planes 1 and 2 measured counterclockwise from the positive x direction and α and δ denote the inclination of planes 3 and 4 with the horizontal. The unit vectors in the direction of the strike planes 1 and 2 are given by Eq. 2.13:

$$\bar{u}_1 = (\cos \beta_1, \sin \beta_1, 0) \quad \bar{u}_2 = (\cos \beta_2, \sin \beta_2, 0)$$

and the unit vectors in the direction of the dip for planes 1 and 2 are given by Eq. 2.14:

$$\bar{v}_1 = (\cos \gamma_1 \sin \beta_1, -\cos \gamma_1 \cos \beta_1, -\sin \gamma_1)$$

$$\bar{v}_2 = (\cos \gamma_2 \sin \beta_2, -\cos \gamma_2 \cos \beta_2, -\sin \gamma_2)$$

The unit vectors normal to each plane are given by

$$\bar{w}_1 = \bar{u}_1 \times \bar{v}_1$$

and

$$\bar{w}_2 = \bar{u}_2 \times \bar{v}_2$$

Note on Fig. 3.5 that $\bar{w}_1$ is directed downward into plane 1 and $\bar{w}_2$ is directed outward from plane 2 when the normals are defined in this manner. Also note that the plane designated as plane 1 is the one with the lowest value of β. In the case where the strikes of two planes are the same the plane designated as plane 1 is the one with the smallest value of γ. This convention is necessary to maintain the proper sign convention for the following vector operations.

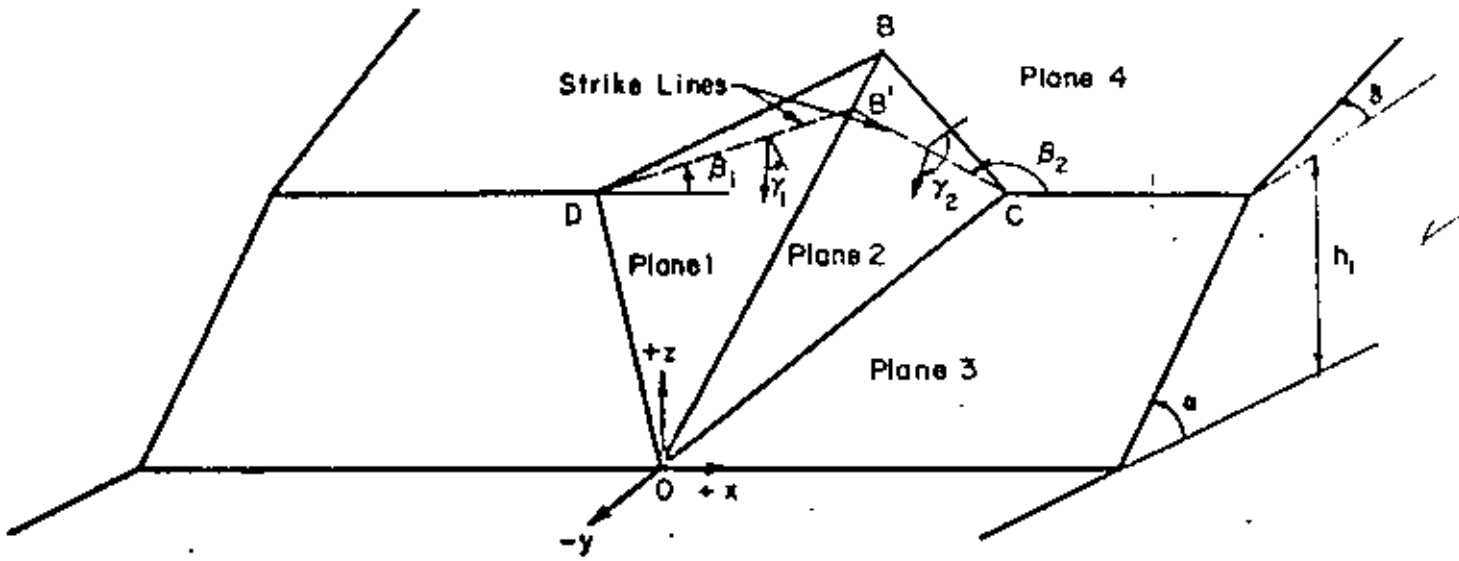

(a)

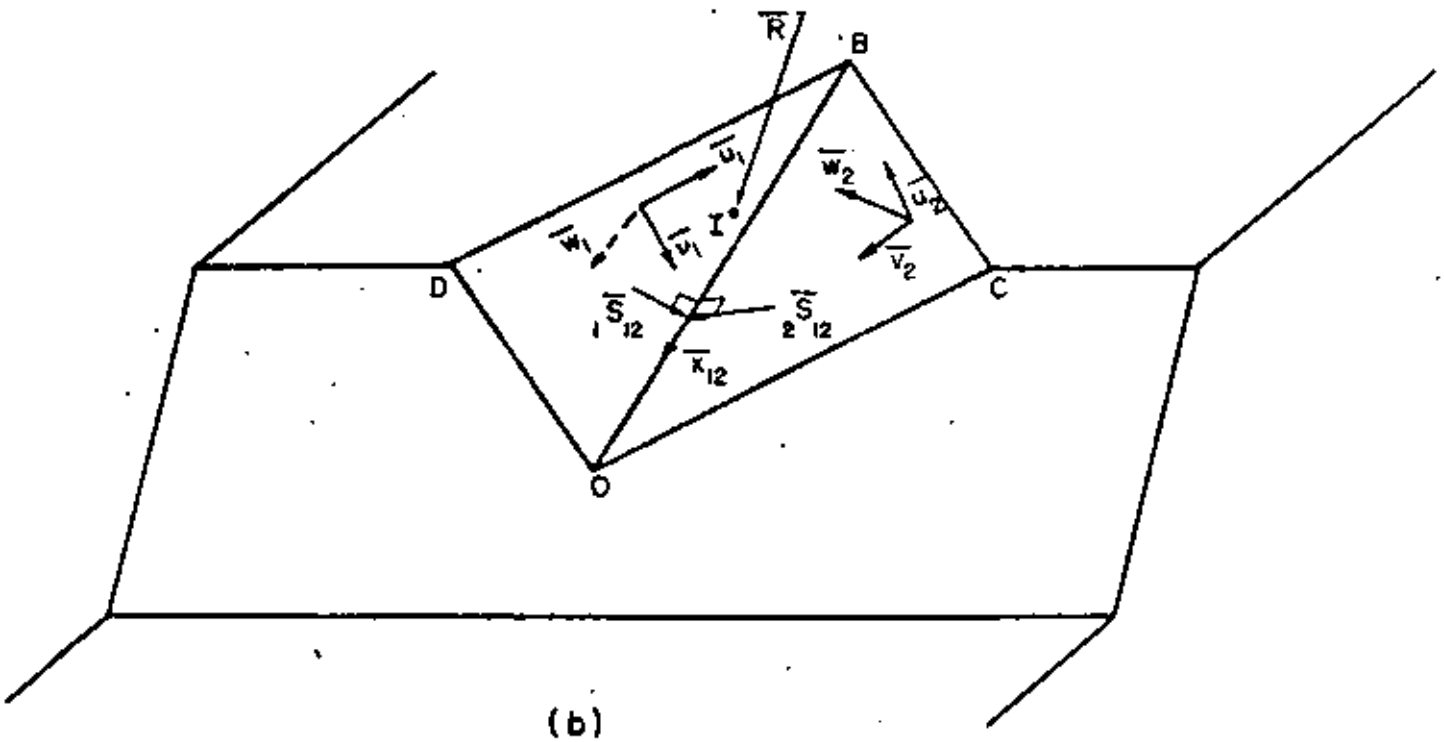

(b)

FIG. 3.5 STABILITY OF A WEDGE BOUNDED BY TWO JOINT PLANES

The loading of the slope consists of (1) dead load $\bar{W}$ acting at the center of gravity of the mass considered, (2) live load $\bar{Q}$ applied at any point, (3) porewater forces $\bar{U}_1$ and $\bar{U}_2$ acting on planes 1 and 2 respectively and (4) dynamic loads induced by ground motions from earthquakes or nuclear detonations. The resultant $\bar{R}$ of the loads in any given case can be determined, and let the point of application of the resultant be at point I.

3.4.1.2 Determination of the Mode of Sliding Failure

For the case of a tetrahedron bounded by two base planes which may be intersecting joint sets, failure may occur by sliding along the line of intersection of the two planes or by sliding on either one of the two planes.

The first step in determining the mode of failure is to check if the distrubing forces tend to lift the tetrahedron from either or both of the supporting planes. Thus considering the rock wedge OBCD (Fig. 3.5), the resultant force $\bar{R}$ tends to break the contact between the tetrahedron and planes 1 and 2 respectively if

$$\bar{R} \cdot \bar{w}_1 < 0 \qquad (3.14)$$

and $$\bar{R} \cdot \bar{w}_2 > 0$$

If Eqs. 3.14 show that the resultant force $\bar{R}$ tends to lift the tetrahedron off of both supports, then equilibrium is not possible unless the joints can take tension or rock bolts are added to take the computed tension. Normally this will not happen for large slopes acted on by their own weight and porepressures, but could occur for small tetrahedrons near the surface of steep or overhanging slopes. If Eqs. 3.14 show that lifting occurs off of one of the supporting planes then we can definitely say that sliding cannot occur on that plane.

If Eqs. 3.14 show that lifting off of the wedge from the supporting planes does not occur, i.e.

$$\bar{R} \cdot \bar{w}_1 > 0$$
$$\bar{R} \cdot \bar{w}_2 < 0 \tag{3.14a}$$

then we must make further kinematic tests to see whether sliding takes place on plane 1 only or plane 2 only or along the line of intersection of planes 1 and 2.

In order to evaluate the mode of sliding it is necessary to define two new vectors ${}_1\bar{S}_{12}$ and ${}_2\bar{S}_{12}$ which are given by

$${}_1\bar{S}_{12} = \bar{x}_{12} \times \bar{w}_1$$
$${}_2\bar{S}_{12} = \bar{x}_{12} \times \bar{w}_2 \tag{3.15}$$

and are as shown in Fig. 3.5(b). The vector ${}_1\bar{S}_{12}$ is in plane 1 perpendicular to the line of intersection $\bar{x}_{12}$ and the vector ${}_2\bar{S}_{12}$ is in plane 2 perpendicular to the line of intersection $\bar{x}_{12}$.

If sliding is to occur along the line of intersection $\bar{x}_{12}$, then Eqs. 3.16, 3.17 and 3.18 must be satisfied simultaneously.

$$\bar{R} \cdot {}_1\bar{S}_{12} > 0 \tag{3.16}$$

$$\bar{R} \cdot {}_2\bar{S}_{12} > 0 \tag{3.17}$$

$$\epsilon_x < \alpha \quad \text{if} \quad 0 < \alpha < \pi \text{ and } \epsilon_x < \delta \quad \text{if } \alpha = \pi \tag{3.18}$$

where

$$\epsilon_x = \tan^{-1}\left(\frac{x_{12z}}{x_{12y}}\right) \tag{3.19}$$

and x_{12y}, x_{12z} = y and z components of vector $\bar{x}_{12}$

The vector $\bar{x}_{12}$ along the line of intersection is defined in Chapter 2 and is given by Eq. 2.16 as

$$\bar{x}_{12} = \bar{w}_2 \times \bar{w}_1$$

If sliding is to occur on plane 1 only, then both the following equations must be satisfied:

$$\bar{R} \cdot \bar{w}_1 > 0 \tag{3.20}$$

and

$$\bar{R} \cdot {}_1\bar{S}_{12} < 0 \tag{3.21}$$

Similarly if sliding is to occur on plane 2 only, then Eqs. 3.22 and 3.23 must be satisfied.

$$\bar{R} \cdot \bar{w}_2 < 0 \tag{3.22}$$

$$\bar{R} \cdot {}_2\bar{S}_{12} < 0 \tag{3.23}$$

The physical interpretation of Eqs. 3.16 - 3.23 may be made as follows. Eq. 3.16 is satisfied only if the resultant force $\bar{R}$ has a component which tends to push the wedge on plane 1 toward the line of intersection $\bar{x}_{12}$. Similarly Eq. 3.17 is satisfied only if the resultant force $\bar{R}$ has a component pushing the wedge on plane 2 toward the line of intersection $\bar{x}_{12}$. Thus Eqs. 3.16 and 3.17 ensure that the resultant force $\bar{R}$ wedges the tetrahedron between the two plane so that sliding can only take place on both the planes along the line of intersection. In order for sliding along the line of intersection to be kinematically possible, it should also be ensured that the line of intersection does not plunge into the rock slope and this check is provided by Eq. 3.18. Thus when all the three kinematic conditions specified by Eqs. 3.16 through 3.18 are satisfied simultaneously sliding can occur along the line of intersection. The tendency to slide will be downhill if $\bar{R} \cdot \bar{x}_{12} > 0$ and uphill if $\bar{R} \cdot \bar{x}_{12} < 0$ (Fig. 3.5).

Eq. 3.21 indicates a component of $\bar{R}$ on plane 1 tending to move the block away from plane 2 by sliding on plane 1 and Eq. 3.20 establishes the condition for contact on plane 1. Thus Eqs. 3.20 and 3.21 are suf-

ficient and necessary conditions for sliding to occur on plane 1. Similarly Eqs. 3.22 and 3.23 specify the conditions for sliding on plane 2.

3.4.1.3 Calculation of the Factor of Safety for Sliding

If the kinematic tests discussed above show that sliding takes place on only plane 1 or on only plane 2, then the factor of safety can be computed from Eq. 3.4 for sliding on one plane. Thus for sliding on plane 1 the factor of safety may be computed as

$$F.S. = \frac{N_1 \tan \phi_1}{T_1} = \frac{(\bar{R} \cdot \bar{w}_1) \tan \phi_1}{T_1} \qquad (3.24)$$

where

$$\bar{T}_1 = \bar{R} - (\bar{R} \cdot \bar{w}_1)\bar{w}_1 = T_{1x}\bar{i} + T_{1y}\bar{j} + T_{1z}\bar{k}$$

Thus Eq. 3.24 becomes

$$F.S. = \frac{(\bar{R} \cdot \bar{w}_1) \tan \phi_1}{\left(T_{1x}^2 + T_{1y}^2 + T_{1z}^2\right)^{1/2}} \qquad (3.25)$$

which may be written as:

$$F.S. = \frac{\tan \phi_1 [R_x w_{1x} + R_y w_{1y} + R_z w_{1z}]}{[(R_y w_{1z} - R_z w_{1y})^2 + (R_z w_{1x} - R_x w_{1z})^2 + (R_x w_{1y} - R_y w_{1x})^2]^{1/2}} \qquad (3.26)$$

For sliding on plane 2 only, the factor of safety is given as

$$F.S. = \frac{N_2 \tan \phi_2}{T_2} = \frac{-(\bar{R} \cdot \bar{w}_2) \tan \phi_2}{T_2} \qquad (3.27)$$

The minus sign appearing in Eq. 3.27 is due to the direction of the unit normal $\bar{w}_2$ as shown in Fig. 3.5.

Eq. 3.27 can be expanded to yield

$$F.S. = \frac{\tan \phi_2 [(-R_x w_{2x} - R_y w_{2y} - R_z w_{2z})]}{[(R_y w_{2z} - R_z w_{2y})^2 + (R_z w_{2x} - R_x w_{2z})^2 + (R_x w_{2y} - R_y w_{2x})^2]^{1/2}} \qquad (3.28)$$

If the kinematic tests of Eqs. 3.16, 3.17 and 3.18 are satisfied and sliding takes place on both planes 1 and 2 along the line of intersection $\bar{x}_{12}$, then the factor of safety may be computed in the following manner.

The first step is to compute the magnitude of the driving force, T_{12}, shown in Fig. 3.6, in the direction of sliding. This is simply given by

$$T_{12} = \frac{\bar{R} \cdot \bar{x}_{12}}{x_{12}} \tag{3.29}$$

where x_{12} represents the magnitude of the vector $\bar{x}_{12}$. The vector $\bar{T}_{12}$ is in the same direction as $\bar{x}_{12}$ and is given by

$$\bar{T}_{12} = \frac{T_{12}\bar{x}_{12}}{x_{12}} \tag{3.30}$$

It is convenient to define the vector $\bar{N}_{12}$, normal to the line of intersection which is given by

$$\bar{N}_{12} = \bar{R} - \bar{T}_{12} \tag{3.31}$$

In order to evaluate the frictional resistances on planes 1 and 2, it is necessary to determine the components $\bar{N}_1$ and $\bar{N}_2$ of $\bar{N}_{12}$ acting normal to planes 1 and 2 respectively. The relationship of the vectors $\bar{R}$, $\bar{T}_{12}$, $\bar{N}_{12}$, $\bar{N}_1$ and $\bar{N}_2$ are shown in Sections AA and BB of Fig. 3.6. From Fig. 3.6 it is obvious that

$$N_1\bar{w}_1 + N_2(-\bar{w}_2) = \bar{N}_{12} \tag{3.32}$$

where N_1 and N_2 represent the magnitudes of the two component vectors $\bar{N}_1$ and $\bar{N}_2$ respectively.

Thus

$$N_1 w_{1x} - N_2 w_{2x} = N_{12x} \tag{3.33}$$

$$N_1 w_{1y} - N_2 w_{2y} = N_{12y} \tag{3.34}$$

$$N_1 w_{1z} - N_2 w_{2z} = N_{12z} \tag{3.35}$$

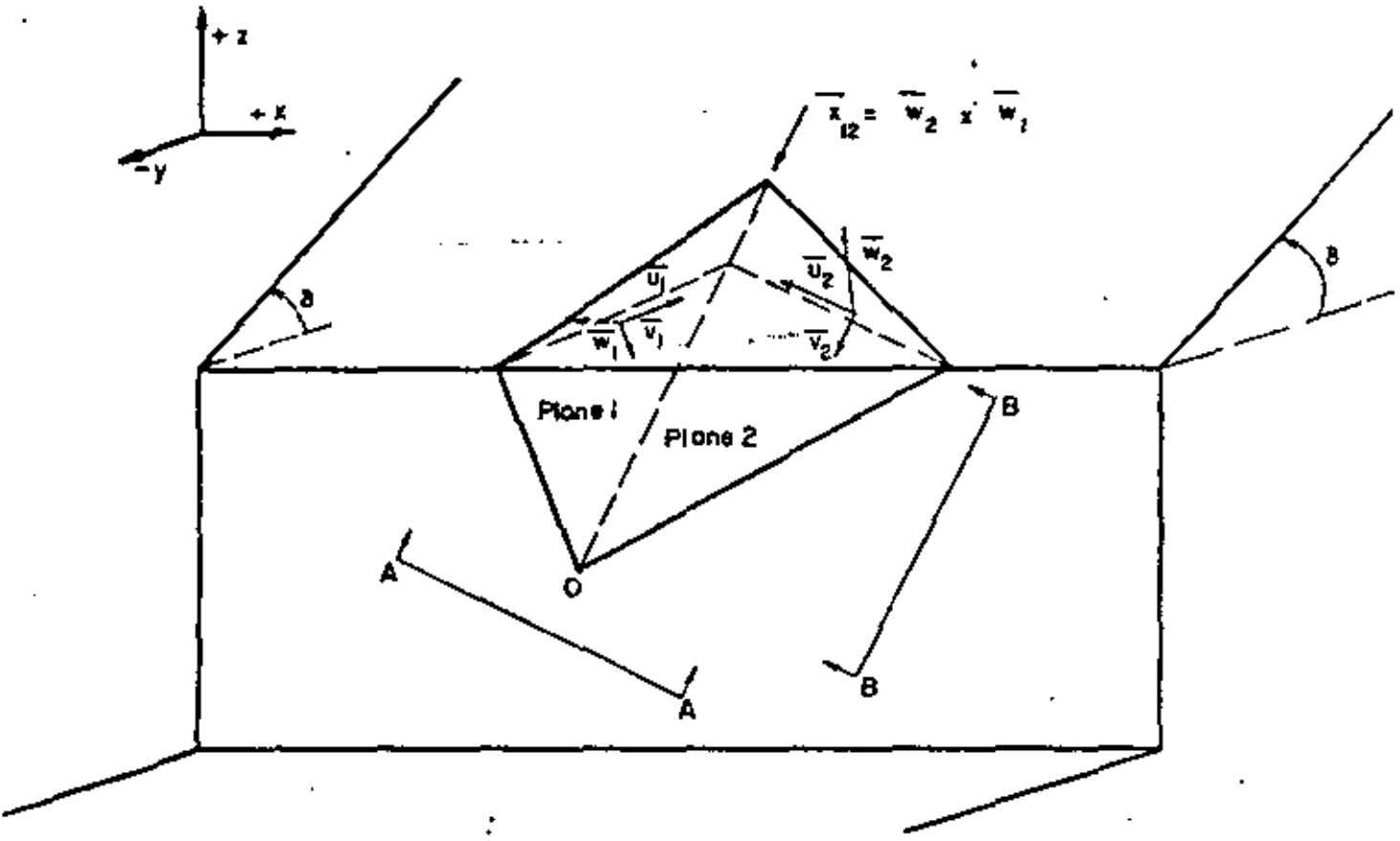

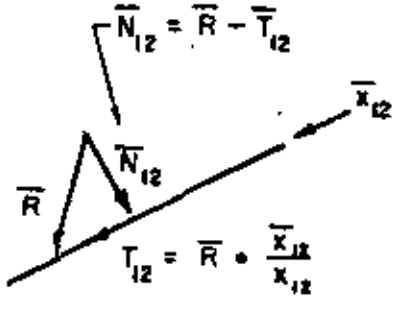

Section B-B

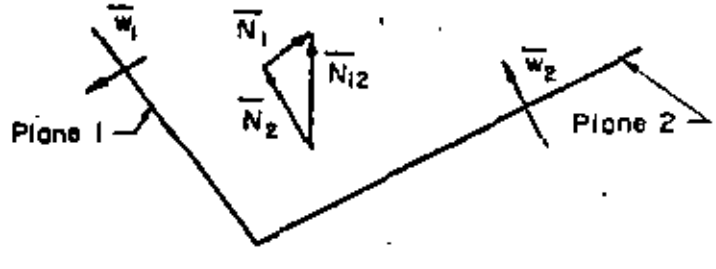

Section A-A

FIG. 3.6 SLIDING ON TWO PLANES

Any two of Eqs. 3.33, 3.34, and 3.35 can be used to determine N_1 and N_2 and the third equation can be used to check the numerical values of N_1 and N_2. After N_1 and N_2 are obtained the factor of safety for sliding on both planes may be determined from the equation

$$F.S. = \frac{N_1 \tan \phi_1 + N_2 \tan \phi_2}{\tau_{12}} \tag{3.36}$$

3.4.1.4 Calculation of Static Factor of Safety for Rotations

In addition to the previously investigated sliding movements which endanger stability, the rock wedge OBCD may rotate about the support edges, OC or OD, or about the axes at point O perpendicular to planes 1 and 2, when the resultant load exerts an overturning moment about these axes (Fig. 3.7). Even though all the above modes of failure by rotation are conceivable, under normal conditions the most probably axes of rotation are $\bar{d}_{10}$ and $\bar{d}_{20}$ (Fig. 3.7) and therefore consideration is given only to rotations about these two axes in this section. The treatment of rotation about $\overline{OC}$, $\overline{OD}$, $\bar{d}_{1B}$ or $\bar{d}_{2B}$ is similiar and is not developed in this report. The axes of rotation $\bar{d}_{10}$ and $\bar{d}_{20}$ pass through O and are perpendicular to planes 1 and 2 respectively. In a rotation, say about the $\bar{d}_{10}$ axis, all points of the wedge in the region of the area ODB move tangential to plane 1 while the surface OCB of the rock wedge separates from plane 2. The equations of the $\bar{d}_{10}$ and $\bar{d}_{20}$ axes are obtained as follows:

$$\bar{d}_{10} = -\bar{w}_1 \tag{3.37}$$

$$\bar{d}_{20} = -\bar{w}_2 \tag{3.38}$$

In the analysis for rotations, it is necessary to know the points of application of the various forces acting on the rock wedge OBCD so

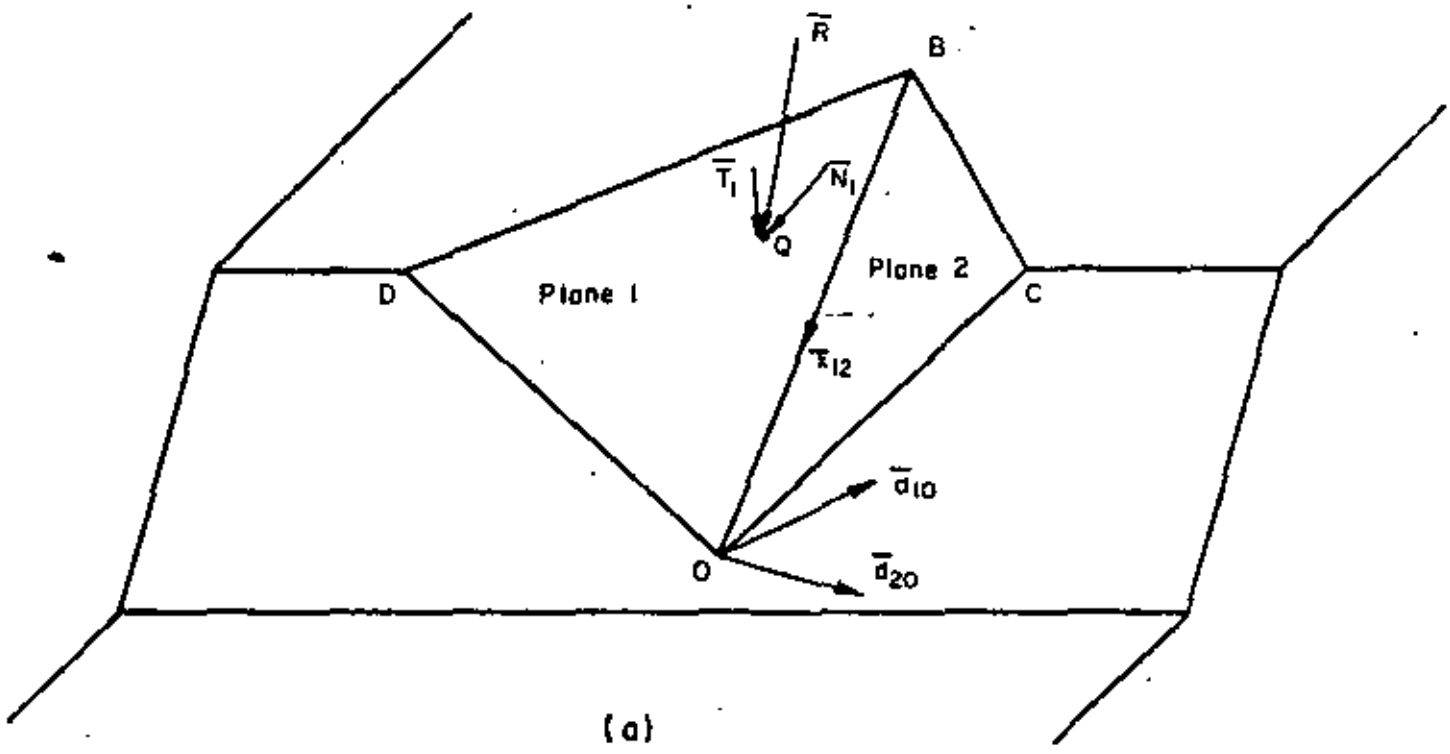

(a)

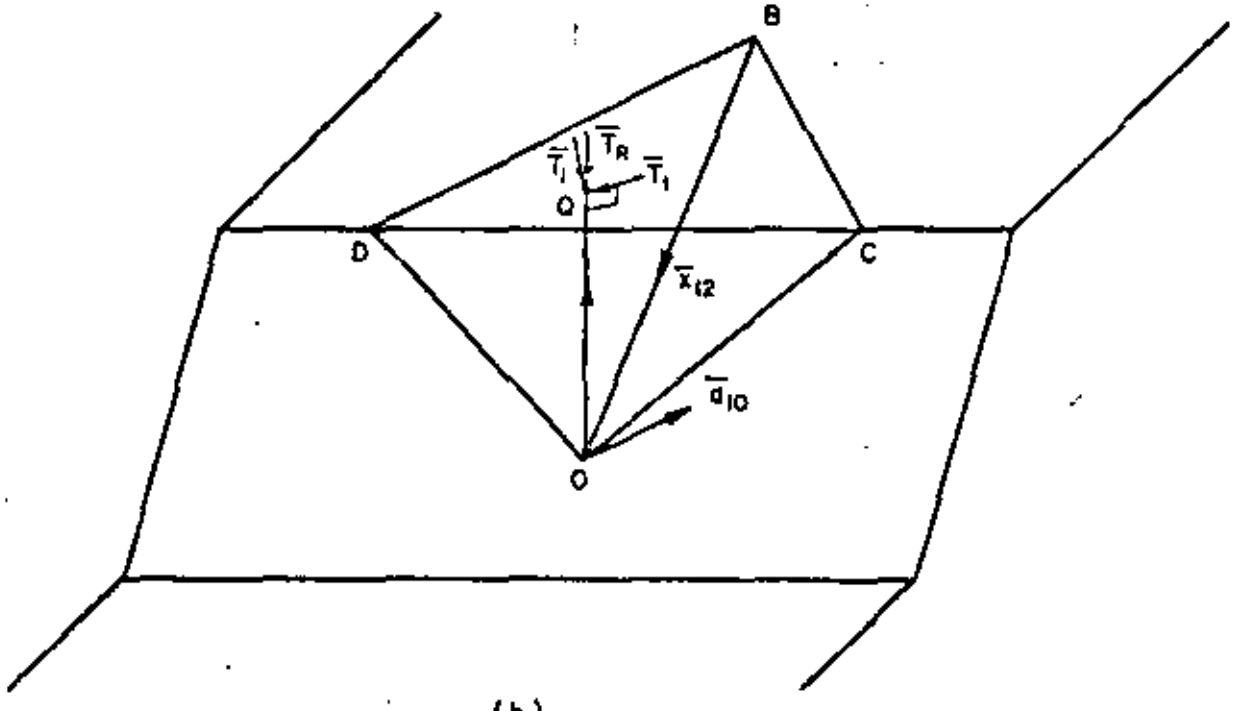

(b)

FIG. 3.7 ROTATIONAL STABILITY OF A WEDGE BOUNCED BY TWO JOINT PLANES

that the point of application I (Fig. 2.8) of the resultant force $\bar{R}$ can be determined. The weight $\bar{W}$ acts vertically downwards at the center of gravity S of the rock wedge as shown in Fig. 2.8. The vector $\overline{OS}$ as shown in Fig. 2.8 can be obtained from geometrical considerations as

$$\overline{OS} = 1/4(\overline{OD} + \overline{OC} + \overline{OB}) \tag{3.39}$$
(also Eq. 2.34)

where the vectors $\overline{OD}$, $\overline{OC}$ and $\overline{OB}$ are given by the following equations:

$$\overline{OD} = \left(\frac{h_1}{\tan\alpha \tan\beta_1} - \frac{h_1}{\tan\gamma_1 \sin\beta_1}, \frac{h_1}{\tan\alpha}, h_1\right) \tag{3.40}$$

$$\overline{OC} = \left(\frac{h_1}{\tan\alpha \tan\beta_2} - \frac{h_1}{\tan\gamma_2 \sin\beta_2}, \frac{h_1}{\tan\alpha}, h_1\right) \tag{3.41}$$

$$\overline{OB} = \frac{\bar{x}_{12}}{x_{12z}} (h_1 + h_2) \tag{3.42}$$

$$h_2 = \frac{\tan\alpha - \tan\epsilon_x}{\tan\epsilon_x - \tan\delta} \cdot \frac{\tan\delta}{\tan\alpha} \cdot h_1 \tag{3.43}$$

where h_1, h_2, α, δ, γ_1, β_1, γ_2, and β_2 are defined in Fig. 3.9.

The weight of the rock wedge can be determined from its volume V which is given by:

$$V = \frac{1}{6} |DB' \times DC| (h_1 + h_2) \tag{3.44}$$
(also Eq. 2.33)

where

$$\overline{DC} = \overline{OC} - \overline{OD} \tag{3.45}$$

$$\overline{DB'} = \overline{OB'} - \overline{OD} \tag{3.46}$$

$$\overline{OB'} = \frac{\bar{x}_{12}}{x_{12z}} h_1 \tag{3.47}$$

The point of application, I, of the resultant force $\bar{R}$ is determined from the known magnitudes and lines of action of the component forces by using Eq. (2.27) and the principles of vector analysis as explained in Chapter 2.

For a rotation to be possible about the $\bar{d}_{10}$ axis, the resultant force $\bar{R}$ must have a positive scalar component of moment about the $\bar{x}_{12}$ and $\bar{d}_{10}$ axes as evaluated by Eq. (2.28); i.e.,

$$M_x = \text{moment of } \bar{R} \text{ about } \bar{x}_{12} = \bar{x}_{12} \cdot (\overline{OI} \times \bar{R}) > 0 \qquad (3.48)$$

and

$$M_{d10} = \text{moment of } \bar{R} \text{ about } \bar{d}_{10} = \bar{d}_{10} \cdot (\overline{OI} \times \bar{R}) > 0 \qquad (3.49)$$

Similarly the moments of $\bar{R}$ about the $\bar{x}_{12}$ and $\bar{d}_{20}$ axes have to satisfy Eqs. (3.50) and (3.51) if a rotation is to occur about the $\bar{d}_{20}$ axis.

$$M_x = \bar{x}_{12} \cdot (\overline{OI} \times \bar{R}) < 0 \qquad (3.50)$$

and

$$M_{d20} = \bar{d}_{20} \cdot (\overline{OI} \times \bar{R}) > 0 \qquad (3.51)$$

In addition a few kinematic tests must also be satisfied and these tests are dependent on the magnitude of the angles η, k_{10} and k_{20} which are defined as follows:

η = wedge angle between planes 1 and 2

$$= \cos^{-1} (\bar{w}_1 \cdot \bar{w}_2) \qquad 0 < \eta < \pi \qquad (3.52)$$

$$k_{10} = \text{DOB} = \cos^{-1} \frac{\overline{OD} \cdot \overline{OB}}{(\overline{OD})(\overline{OB})} \qquad 0 < k_{10} < \pi \qquad (3.53)$$

$$k_{20} = \text{COB} = \cos^{-1} \frac{\overline{OC} \cdot \overline{OB}}{(\overline{OC})(\overline{OB})} \qquad 0 < k_{20} < \pi \qquad (3.54)$$

The range of angles η, k_{10} and k_{20} for which a rotation about the $\bar{d}_{10}$ and $\bar{d}_{20}$ axes is kinematically impossible, is given in Table 3.1.

The analyses for determining the static factor of safety for rotations about $\bar{d}_{10}$ and $\bar{d}_{20}$ axes are similar in principle and therefore the details of the analysis will be given only for the case of rotation about the $\bar{d}_{10}$ axis.

The resultant $\bar{R}$ is first resolved into components $\bar{N}_1$ and $\bar{T}_1$ at its point of intersection, Q, with plane 1, as shown in Fig. 3.7(a). Thus

Axis of Rotation: $\hat{d}_{10}$

η	k_{10}	k_{20}	Supplementary Condition
$0<\eta<\pi$	$>\pi/2$	$>\pi/2$	-
$0<\eta<\pi$	$<\pi/2$	$>\pi/2$	-
$<\pi/2$	$>\pi/2$	$<\pi/2$	$\frac{\tan k_{20}}{\tan(\pi-k_{10})} > \sec(\pi-\eta)$

Axis of Rotation: $\hat{d}_{20}$

η	k_{10}	k_{20}	Supplementary Condition
$0<\eta<\pi$	$>\pi/2$	$>\pi/2$	
$0<\eta<\pi$	$>\pi/2$	$<\pi/2$	
$<\pi/2$	$<\pi/2$	$>\pi/2$	$\frac{\tan k_{10}}{\tan(\pi-k_{20})} > \sec(\pi-\eta)$

Table 3.1 Range of Angles for which a rotation is kinematically impossible.

$$\bar{N}_1 = (\bar{R}\cdot\bar{w}_1)\bar{w}_1 \tag{3.55}$$

and

$$\bar{T}_1 = \bar{R} - \bar{N}_1 \tag{3.56}$$

The component $\bar{T}_1$ tangential to plane 1 is now resolved into components $\bar{T}_r$ and $\bar{T}_t$ (Fig. 3.7(b)). The force $\bar{T}_r$ has the direction of the vector $\overline{QO}$ and the force $\bar{T}_t$ has the direction of the tangent to the rotation which Q executes in the case of a rotation about $\bar{d}_{10}$. The force $\bar{T}_t$ is thus the only component of the loading which exerts an overturning moment about the $\bar{d}_{10}$ axis. The resolution of force $\bar{T}_1$ into its components $\bar{T}_t$ is done as follows:

$$\bar{T}_1 = \bar{T}_r + \bar{T}_t = c_1(-\overline{OQ}) + c_2(\overline{OQ} \times \bar{w}_1) \tag{3.57}$$

In Eq. 3.57, $-\overline{OQ}$ and $\overline{OQ} \times \bar{w}_1$ are vectors in the direction of $\bar{T}_r$ and $\bar{T}_t$. By equating the x, y and z components of $\bar{T}_1$ as given by Eqs. 3.56 and 3.57, the values of the two coefficients c_1 and c_2 may be determined. Eqs. 3.56 and 3.57 give three equations for the two unknowns c_1 and c_2 and therefore one of these equations can be used to check the calculations for c_1 and c_2. With c_1 and c_2 known, $\bar{T}_r$ and $\bar{T}_t$ are obtained as follows:

$$\bar{T}_r = -c_1\,\overline{OQ} \tag{3.58}$$

$$\bar{T}_t = c_2(\overline{OQ} \times \bar{w}_1) \tag{3.59}$$

The magnitude of the overturning moment M_{d10} can be obtained by the relation:

$$M_{d10} = T_t\,OQ \tag{3.60}$$

The magnitude of the restoring moment of the frictional force on plane 1 due to the normal component $\bar{N}_1$ is obtained as

$$M_{rd10} = N_1 \tan\phi_1\,OQ \tag{3.61}$$

The factor of safety against rotation can now be obtained as the ratio of the restoring moment to the overturning moment

$$F.S.(\text{against rotation}) = \frac{N_1 \tan \phi_1 \ OQ}{T_t \ OQ} = N_1 \tan\phi_1 / T_t \qquad (3.62)$$

The factor of safety against rotation about the $\bar{d}_{20}$ axis can also be determined in a similar manner. Moments M_{d10} and M_{d20} are very often negative and in these cases only the sliding stability need be analyzed.

3.4.2 Calculation of Dynamic Resistance Against Sliding on Two Planes

The direction and magnitude of the minimum dynamic resistance $\overline{NW}$ which is necessary to just make the potential block slide on the two base planes may be found by the following procedure.

A unit vector $\bar{r}_1$ is first defined in the direction of the resultant reaction $\bar{R}_1$ on plane 1 (Fig. 3.8). In the limiting state of equilibrium $\bar{R}_1$ is inclined at an angle ϕ_1 to the upward normal $-\bar{w}_1$ to plane 1 and tends to oppose the downward movement along the line of intersection $\bar{x}_{12}$. Therefore,

$$\bar{r}_1 = -\bar{w}_1 \cos \phi_1 - \bar{x}_{12} \sin \phi_1 / x_{12} \qquad (3.63)$$

Similarly a unit vector $\bar{r}_2$ is defined in the direction of the resultant reaction $\bar{R}_2$ on plane 2. From Fig. 3.8 it can be seen that

$$\bar{r}_2 = \bar{w}_2 \cos \phi_2 - \bar{x}_{12} \sin \phi_2 / x_{12} \qquad (3.64)$$

where ϕ_2 is the angle of friction on plane 2.

The magnitude of the dynamic resistance vector $\overline{NW}$ will be a minimum when the vector $\overline{NW}$ is normal to the plane containing $\bar{R}_1$ and $\bar{R}_2$. Therefore a unit vector $\bar{n}$ in the direction of $\overline{NW}$ may be obtained by the equation:

$$\bar{n} = (\bar{r}_1 \times \bar{r}_2) / |\bar{r}_1 \times \bar{r}_2| \qquad (3.65)$$

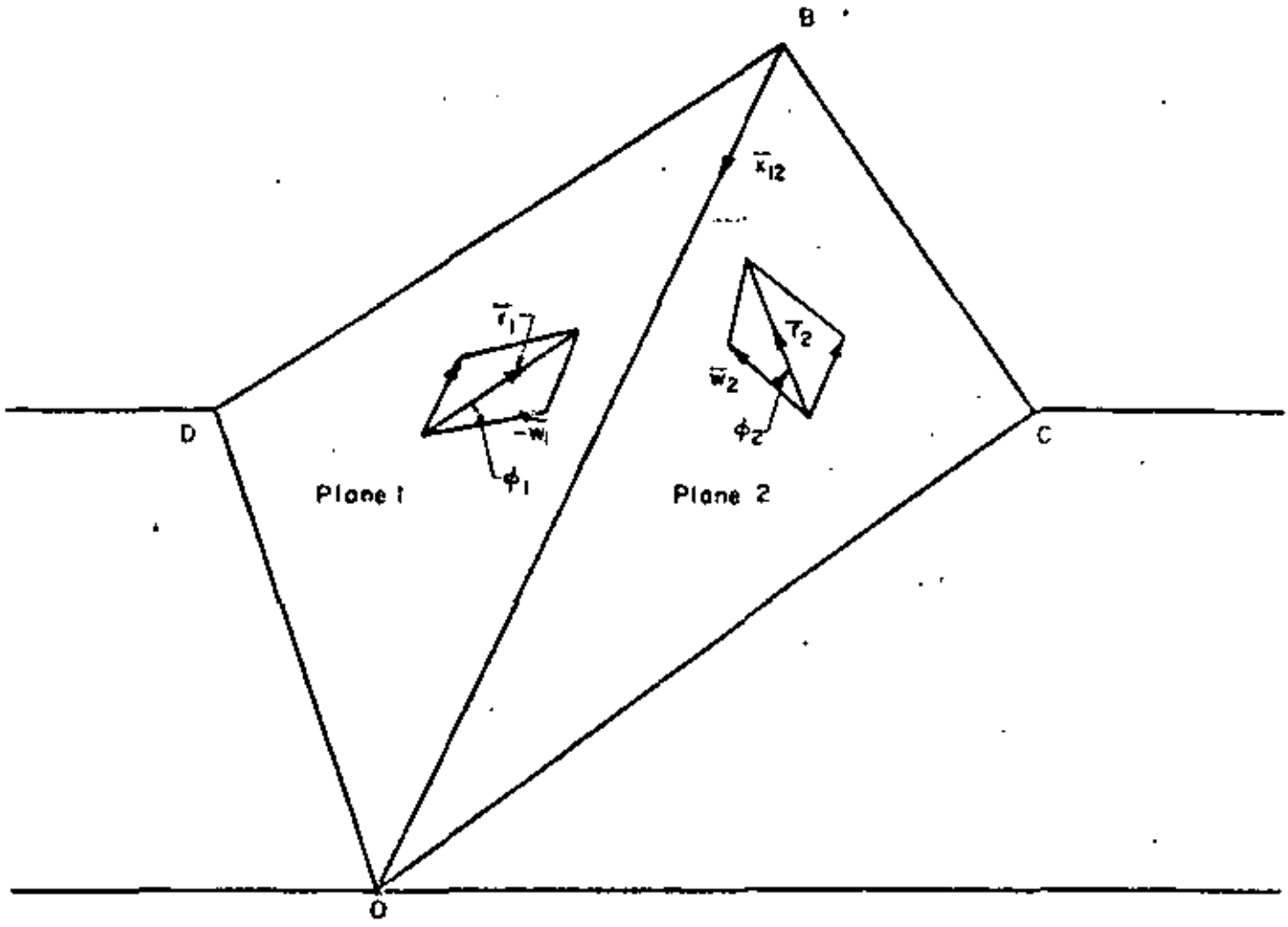

$|\bar{r}_1| = 1$

$|\bar{r}_2| = 1$

$$\bar{r}_1 = -\bar{w}_1 \cdot \cos\phi_1 - \frac{\bar{x}_{12}}{|\bar{x}_{12}|} \sin\phi_1$$

$$\bar{r}_2 = \bar{w}_2 \cdot \cos\phi_2 - \frac{\bar{x}_{12}}{|\bar{x}_{12}|} \sin\phi_2$$

FIG. 3.8 STABILITY OF A WEDGE BOUNDED BY TWO JOINT PLANES

where $|\bar{r}_1 \times \bar{r}_2|$ represents the magnitude of the vector $(\bar{r}_1 \times \bar{r}_2)$.

The magnitude of the minimum dynamic resistance, NW, may now be determined by the equation

$$NW = \bar{R} \cdot \bar{n} \tag{3.66}$$

where $\bar{R}$ is the resultant of all static loads acting on the sliding rock wedge. From Eq. 3.66 it follows that

$$N = \frac{\bar{R} \cdot \bar{n}}{W} \tag{3.67}$$

3.4.3 Example Problems for Slopes with Two Intersecting Planes of Discontinuity Worked by Vector Analysis.

Problem 1

Determine the factor of safety of the rock wedge OBCD shown in Fig. 3.9. Also estimate the direction and magnitude of the minimum dynamic resistance $\overline{NW}$ which is necessary to just make the potential block OBCD slide.

Plane 1	Plane 2
$\beta_1 = 36^\circ$	$\beta_2 = 94^\circ$
$\gamma_1 = 62^\circ$	$\gamma_2 = 121^\circ$
$\phi_1 = 20^\circ$	$\phi_2 = 40^\circ$

$\alpha = 70^\circ$ $\quad$ $\delta = 20^\circ$

Solution

Static Factor of safety against sliding

According to Eqs. 2.13, 2.14 and 2.15, for plane 1,

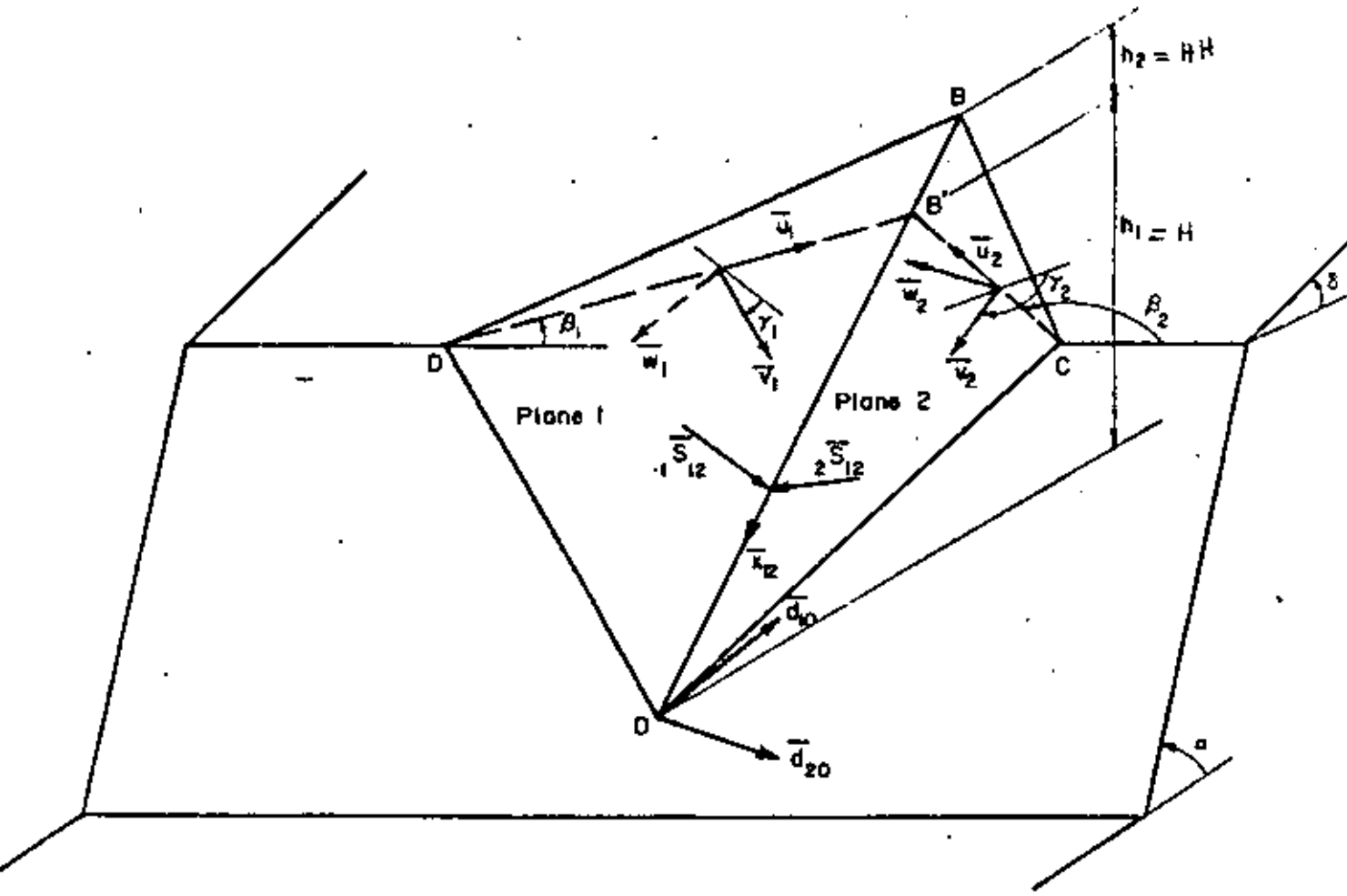

FIG. 3.9 STABILITY OF A ROCK WEDGE BOUNDED BY TWO JOINT PLANES

$$\bar{u}_1 = (0.809,\ 0.588,\ 0.000) \tag{2.13}$$

$$\bar{v}_1 = (0.276,\ -0.380,\ -0.883) \tag{2.14}$$

$$\bar{w}_1 = (-0.519,\ 0.714,\ -0.469) \tag{2.15}$$

and for plane 2,

$$\bar{u}_2 = (-0.070,\ 0.998,\ 0.000) \tag{2.13}$$

$$\bar{v}_2 = (-0.514,\ -0.036,\ -0.857) \tag{2.14}$$

$$\bar{w}_2 = (-0.855,\ -0.060,\ 0.515) \tag{2.15}$$

The only load that enters the calculation in this problem is the weight W of the rock wedge OBCD acting vertically downwards in the -z direction. Therefore the resultant load $\bar{R}$ may be expressed as

$$\bar{R} = (0,\ 0,\ -W)$$

$$\bar{R} \cdot \bar{w}_1 = 0.469W > 0$$

and

$$\bar{R} \cdot \bar{w}_2 = -0.515W < 0 \tag{3.14a}$$

Therefore lifting off of the rock wedge from the support planes does not occur.

$$\bar{x}_{12} = \bar{w}_2 \times \bar{w}_1$$

$$= (-0.340,\ -0.669,\ -0.642) \tag{2.16}$$

and

$$x_{12} = 0.987$$

$$_1\bar{S}_{12} = \bar{x}_{12} \times \bar{w}_1 \tag{3.15}$$

$$= (0.722,\ 0.172,\ -0.590)$$

and

$$_2\bar{S}_{12} = \bar{x}_{12} \times \bar{w}_2 \tag{3.15}$$

$$= (-0.383,\ 0.725,\ -0.551)$$

$$\bar{R} \cdot {}_1\bar{S}_{12} = 0.590W > 0 \tag{3.16}$$

$$\bar{R} \cdot {}_2\bar{S}_{12} = 0.551W > 0 \tag{3.17}$$

$$\epsilon_x = \tan^{-1}\left(\frac{x_{12z}}{x_{12y}}\right)$$

$$= \tan^{-1}\left(\frac{-0.642}{-0.669}\right) = 43.8^\circ \qquad (3.19)$$

$$\therefore \delta < \epsilon_x < \alpha \qquad (3.18)$$

Thus according to Eqs. 3.16, 3.17, and 3.18, sliding is kinematically possible only along the line of intersection $\bar{x}_{12}$. Since $\bar{R}\cdot\bar{x}_{12} = 0.642W > 0$ sliding tends to occur down the line of intersection.

$$T_{12} = \bar{R} \cdot \bar{x}_{12}/x_{12} = 0.642W/0.987 \qquad (3.29)$$

$$= 0.650W$$

and

$$\bar{T}_{12} = 0.650W\,\frac{\bar{x}_{12}}{x_{12}} = (-0.223W,\ -0.440W,\ -0.420W) \qquad (3.30)$$

$$\bar{N}_{12} = \bar{R} - \bar{T}_{12} = (0.223W,\ 0.440W,\ -0.580W) \qquad (3.31)$$

$$= N_1\bar{w}_1 + N_2(-\bar{w}_2) \qquad (3.32)$$

$$= N_1(-0.519\ ,\ 0.714,\ -0.469) +$$

$$N_2(0.855,\ 0.060,\ -0.515)$$

Solving

$$N_1 = 0.565W, \quad N_2 = 0.605W$$

$$F.S. = \frac{N_1 \tan\phi_1 + N_2 \tan\phi_2}{T_{12}} \qquad (3.36)$$

$$= \frac{0.565W \tan 20^\circ + 0.605W \tan 40^\circ}{0.650W}$$

$$= 1.10$$

Stability against rotation,

According to Eqs. 3.39 through 3.43 :

$$\overline{OD} = (-0.404h_1,\ 0.346h_1,\ h_1) \qquad (3.40)$$

$$OD = 1.138h_1$$

$$\overline{OC} = (0.602h_1,\ 0.364h_1,\ h_1) \qquad (3.41)$$

$$OC = 1.220h_1$$

$$\overline{OB} = (0.741h_1,\ 1.460h_1,\ 1.398h_1) \qquad (3.42)$$

$$OB = 2.155h_1$$

$$\overline{OS} = (0.235h_1,\ 0.547h_1,\ 0.850h_1) \qquad (3.39)$$

In order to apply the kinematic tests for rotation, it is necessary to establish the values of the angles k_{10}, k_{20} and η.

$$k_{10} = \cos^{-1}\frac{\overline{OD}\cdot\overline{OB}}{(OD)(OB)} = 48.1^\circ < \pi/2 \qquad (3.53)$$

$$k_{20} = \cos^{-1}\frac{\overline{OC}\cdot\overline{OB}}{(OC)(OB)} = 25.3^\circ < \pi/2. \qquad (3.54)$$

$$\eta = \cos^{-1}(\bar{w}_1 \cdot \bar{w}_2) = 80.9^\circ < \pi/2 \qquad (3.52)$$

$$M_x = \bar{x}_{12} \cdot (\overline{OI}\times\bar{R}) \qquad (3.48)$$

$$= \bar{x}_{12} \cdot (\overline{OS} \times \bar{R}) = 0.03Wh_1 > 0$$

For these values of η, k_{10}, k_{20} and M_x, a rotation about axis $\bar{d}_{10}$ is kinematically possible. However the rotation can occur only if $M_{d10} > 0$.

$$\bar{d}_{10} = -\bar{w}_1 = (0.519,\ -0.714,\ 0.469) \qquad (3.37)$$

$$\overline{OI} = \overline{OS} = (0.235h_1,\ 0.547h_1,\ 0.850h_1)$$

$$M_{d10} = \bar{d}_{10} \cdot (\overline{OI} \times \bar{R}) \qquad (3.49)$$

$$= -0.452Wh_1 < 0$$

Therefore rotation about $\bar{d}_{10}$ axis does not occur.

Minimum Dynamic Resistance

The unit vector $\bar{r}_1$ in the direction of the resultant reaction on plane 1 is given by Eq. 3.63 as

$$\bar{r}_1 = (0.607,\ -0.439,\ 0.663) \qquad (3.63)$$

The unit vector $\bar{r}_2$ in the direction of the resultant reaction on plane 2 can be obtained in a similar manner from Eq. 3.64

$$\bar{r}_2 = (-0.434,\ 0.388,\ 0.810) \tag{3.64}$$

The unit vector in the direction of the minimum dynamic resistance vector $\overline{NW}$ is then given by

$$\bar{n} = \frac{\bar{r}_1 \times \bar{r}_2}{|\bar{r}_1 \times \bar{r}_2|} = (-0.616,\ -0.785,\ 0.046) \tag{3.65}$$

The magnitude of the minimum dynamic resistance is now obtained as

$$NW = |\bar{R} \cdot \bar{n}| = 0.046W \tag{3.66}$$

or

$$N = 0.046 \tag{3.67}$$

Problem 2

Determine the factor of safety of the rock wedge OBCD shown in Fig. 3.10 when (a) P = 0 and (b) P = 10 tons in the positive y direction.

Plane 1	Plane 2
$\phi_1 = 30^\circ$	$\phi_2 = 30^\circ$
$\beta_1 = 17^\circ$	$\beta_2 = 63^\circ$
$\gamma_1 = 60^\circ$	$\gamma_2 = 80^\circ$

$\alpha = 90^\circ$ $\quad \delta = 0^\circ$

Point of application of P is S such that $\overline{OS} = (-6.1,\ 2.0,\ 9.0)$. The dimensions are in feet units.

Solution

Case (a) P = 0

Static Factor of Safety against sliding

For plane 1,

$$\bar{u}_1 = (0.955,\ 0.292,\ 0.000) \tag{3.13}$$

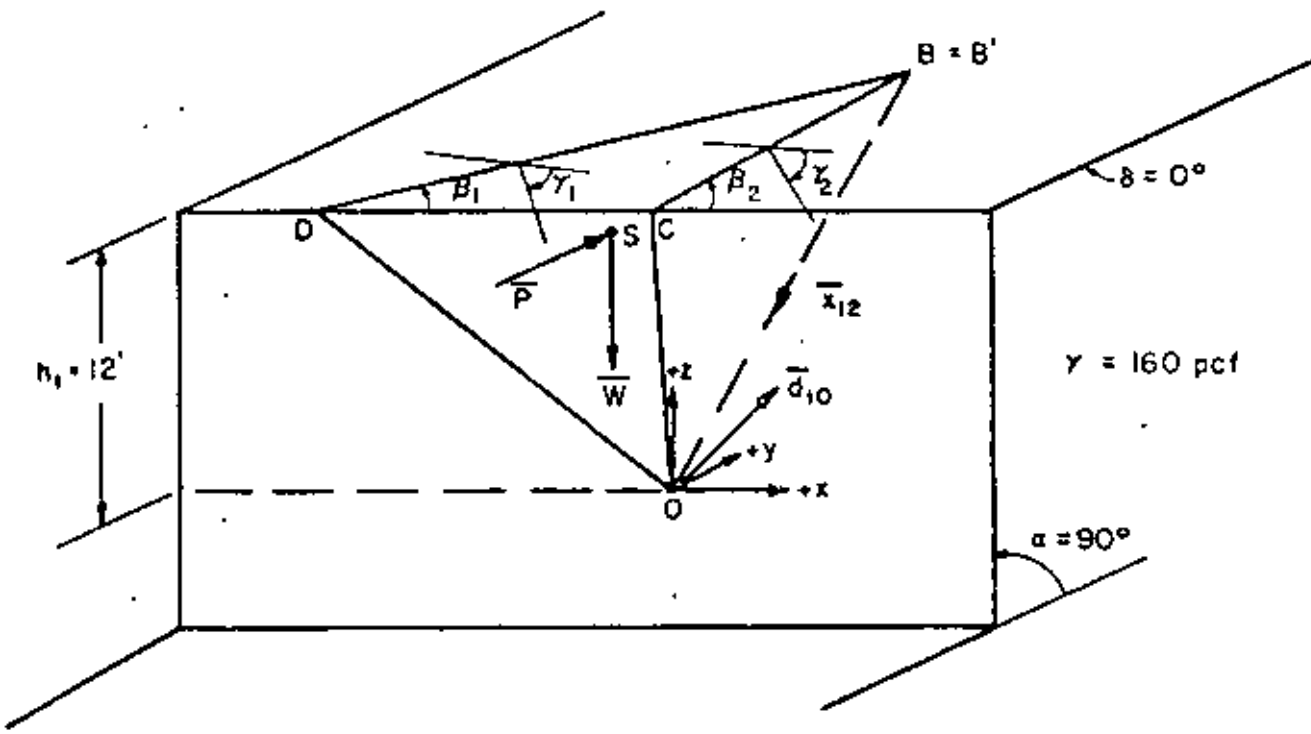

FIG. 3.10 STABILITY OF A ROCK WEDGE BOUNDED BY TWO JOINT PLANES

$$\bar{v}_1 = (0.146, -0.478, -0.866) \quad (2.14)$$

$$\bar{w}_1 = (-0.253, 0.827, -0.499) \quad (2.15)$$

For plane 2,

$$\bar{u}_2 = (0.454, 0.890, 0.000) \quad (2.13)$$

$$\bar{v}_2 = (0.155, -0.079, -0.985) \quad (2.14)$$

$$\bar{w}_2 = (-0.877, 0.447, -0.174) \quad (2.15)$$

When $\bar{P} = 0$

$$\bar{R} = (0, 0, -W)$$

where W = weight of the rock wedge OBCD

$$\bar{x}_{12} = \bar{w}_2 \times \bar{w}_1 \quad (2.16)$$

$$= (-0.079, -0.394, -0.594)$$

$$x_{12} = 0.717$$

$$_1\bar{S}_{12} = \bar{x}_{12} \times \bar{w}_1 \quad (3.15)$$

$$= (0.688, 0.110, -0.165)$$

$$_2\bar{S}_{12} = \bar{x}_{12} \times \bar{w}_2 \quad (3.15)$$

$$= (0.334, 0.507, -0.381)$$

$$\bar{R} \cdot {}_1\bar{S}_{12} = 0.165W > 0 \text{ and} \quad (3.16)$$

$$\bar{R} \cdot {}_2\bar{S}_{12} = 0.381W > 0 \quad (3.17)$$

$$\epsilon_x = \tan^{-1}\left(\frac{x_{12z}}{x_{12y}}\right) = \tan^{-1}\left(\frac{-0.594}{-0.394}\right) \quad (3.19)$$

$$= 56.4^\circ$$

$$\therefore \delta < \epsilon_x < \alpha \quad (3.18)$$

Thus according to Eqs. 3.16, 3.17 and 3.18, sliding is kinematically possible only along the line of intersection $\bar{x}_{12}$.

Since $\bar{R}\cdot\bar{x}_{12} = 0.594W > 0$, sliding tends to occur down the line of intersection.

$$T_{12} = \bar{R} \cdot \bar{x}_{12}/x_{12} = 0.549W/0.717 \tag{3.29}$$

$$= 0.828W$$

$$\bar{T}_{12} = 0.828W \frac{\bar{x}_{12}}{x_{12}}$$

$$= (-0.091W, -0.455W, -0.696W) \tag{3.30}$$

$$\bar{N}_{12} = \bar{R} - \bar{T}_{12}$$

$$= (0.091W, 0.455W, -0.314W) \tag{3.31}$$

$$= N_1\bar{w}_1 + N_2(-\bar{w}_2)$$

$$= N_1(-0.253, 0.827, -0.499) +$$

$$N_2(0.877, -0.477, 0.174)$$

Solving $N_1 = 0.733W, \quad N_2 = 0.314W$

$$F.S. = \frac{0.733 \tan 30^\circ + 0.314W \tan 30^\circ}{0.828W}$$

$$= 0.73 < 1$$

Stability against Rotation.

$$\overline{OD} = (-23.70, 0, 12.00) \tag{3.40}$$

$$OD = 26.60$$

$$\overline{OC} = (-2.40, 0, 12.00) \tag{3.41}$$

$$OC = 12.25$$

$$\overline{OB} = \frac{12}{-0.594} (-0.079, -0.394, -0.594) \tag{3.42}$$

$$= (1.60, 8.00, 12.00)$$

$$\overline{OB} = 14.50$$

$$\overline{OS} = \frac{1}{4}(\overline{OB} + \overline{OC} + \overline{OD}) \qquad (3.39)$$

$$= (-6.10,\ 2.00,\ 9.00)$$

$$k_{10} = \cos^{-1}\left(\frac{\overline{OD}\cdot\overline{OB}}{OD\cdot OB}\right) = 74^{o} < \pi/2 \qquad (3.53)$$

$$k_{20} = \cos^{-1}\left(\frac{\overline{OC}\cdot\overline{OB}}{OC\cdot OB}\right) = 38^{o} < \pi/2 \qquad (3.54)$$

$$\eta = \cos^{-1}(\bar{w}_1 \cdot \bar{w}_2) = 47.4^{o} < \pi/2 \qquad (3.52)$$

$$M_x = \bar{x}_{12} \cdot (\overline{OS} \times \bar{R}) \qquad (3.48)$$

$= \underline{2.561W} > 0$ indicating thereby that the resultant $\bar{R}$ intersects plane 1. For these values of η, k_{10}, k_{20}, and M_x a rotation about axis $\bar{d}_{10}$ is kinematically possible.

$$\bar{d}_{10} = -\bar{w}_1 = (0.253,\ -0.827,\ 0.499) \qquad (3.37)$$

$$M_{d10} = \bar{d}_{10} \cdot (\overline{OS} \times \bar{R}) \qquad (3.49)$$

$$= 4.539W > 0$$

Therefore a rotation can occur about the $\bar{d}_{10}$ axis and the factor of safety against rotation can be determined as follows:

$$N_1 = \bar{R} \cdot \bar{w}_1 = 0.499W$$

$$\bar{N}_1 = (\bar{R} \cdot \bar{w}_1)\bar{w}_1 = (-0.126W,\ 0.413W,\ -0.250W) \qquad (3.55)$$

$$\bar{T}_1 = \bar{R} - \bar{N}_1 = (0.126W,\ -0.413W,\ -0.750W) \qquad (3.56)$$

$$= c_1(-\overline{OQ}) + c_2(\overline{OQ} \times \bar{w}_1) \qquad (3.57)$$

$$\overline{OQ} = \overline{OI} + \psi\bar{R} = \overline{OS} + \psi\bar{R}$$

$$= [-6.1,\ 2.0,\ (9.0 - \psi W)]$$

Since $\overline{OQ}$ and $\bar{w}_1$ are mutually perpendicular, $\overline{OQ} \cdot \bar{w}_1 = 0$

$$\therefore \quad (6.1 \times 0.253) + (2.0 \times 0.827) - 0.499\,(9.0 - \tfrac{1}{3}W) = 0$$

$$\therefore \quad (9.0 - \tfrac{1}{3}W) = 6.40$$

$$\therefore \quad \overline{OQ} = (-6.10,\ 2.00,\ 6.40)$$

$$\overline{OQ} \times \bar{w}_1 = (-6.29,\ -4.67,\ -4.54)$$

$$\therefore \quad \bar{T}_1 = (0.126W,\ -0.413W,\ -0.750W)$$

$$= c_1(6.10,\ -2.00,\ -6.40) + c_2(-6.29,\ -4.67,\ -4.54)$$

Solving $c_1 = 0.078W$; $c_2 = 0.055W$

$$\bar{T}_t = c_2(\overline{OQ} \times \bar{w}_1) \qquad (3.59)$$

$$= (-0.346W,\ -0.257W,\ -0.250W)$$

$$T_t = 0.498W$$

$$F.S. = \frac{N_1 \tan \phi_1}{T_t} = \frac{0.499W \times \tan 30^\circ}{0.498W} = 0.58 \qquad (3.62)$$

Note: It may be noted that all the lengths in the above case are expressed in feet-units.

Case (b) $\bar{P} = (0,\ 10,\ 0)$

In Case (a) the only force in the system is the weight $\bar{W}$ of the rock wedge and it is not necessary to know the magnitude of $\bar{W}$ for estimating the factor of safety of the rock wedge. But in Case (b) there is an additional external force $\bar{P}$ of magnitude 10 tons acting in the positive y-direction through the center of gravity, S, of the rock wedge and therefore it becomes necessary, in the present case, to compute the magnitude of $\bar{W}$.

Como $\delta = 0°$ → $h_2 = 0$ (3.43)

$$\overline{DC} = \overline{OC} - \overline{OD} \quad (3.45)$$

$$= (21.30,\ 0,\ 0)$$

$$\overline{OB'} = \frac{\bar{x}_{12}}{x_{12z}} h_1 \quad (3.47)$$

$$= (1.60,\ 7.96,\ 12.00)$$

$$\overline{DB'} = \overline{OB'} - \overline{OD} \quad (3.46)$$

$$= (25.30,\ 7.96,\ 0) \quad (3.46)$$

$\overline{DB'} \times \overline{DC} = 0, 0, -169.548$

$|\overline{DB'} \times \overline{DC}| = 169.549$

$$V = \frac{1}{6}\left|\overline{DB'} \times \overline{DC}\right|(h_1^{12} + h_2^{0})$$

$$= 339.1\ ft^3 \quad (3.44)$$

$$W = \frac{339.1 \times 160}{2000} = 27.13 \text{ tons}$$

24.58 ton

1 Ton = 2207.5 lb

$$\bar{W} = (0,\ 0,\ -27.13)$$

$$\bar{P} = (0,\ 10,\ 0)$$

$$\bar{R} = \bar{W} + \bar{P} = (0,\ 10,\ -27.13)$$

$$\bar{R} \cdot {}_1\bar{S}_{12} = 5.58 > 0 \quad (3.16)$$

$$\bar{R} \cdot {}_2\bar{S}_{12} = 15.41 > 0 \quad (3.17)$$

$$6 < \epsilon_x < \alpha$$

The above values show that sliding is kinematically possibly only along the line of intersection of planes 1 and 2. Since $\bar{R} \cdot \bar{x}_{12} = 12.48 > 0$, sliding tends to occur down the line of intersection.

$$T_{12} = \bar{R} \cdot \bar{x}_{12}/x_{12} = 12.48/0.717 = 17.41 \qquad (3.29)$$

$$\bar{T}_{12} = 17.41\ \bar{x}_{12}/x_{12} = (-1.918, -9.567, -14.423) \qquad (3.30)$$

$$\bar{N}_{12} = \bar{R} - \bar{T}_{12} = (1.918, 19.567, -12.707) \qquad (3.31)$$

$$= N_1(-0.253, 0.827, -0.499) +$$

$$N_2(0.877, -0.447, 0.174)$$

Solving $N_1 = 29.4$ tons $N_2 = 10.7$ tons

$$F.S. = \frac{29.4 \tan 30^\circ + 10.7 \tan 30^\circ}{17.41}$$

$$= 1.33$$

Stability against Rotation.

$$M_x = \bar{x}_{12} \cdot (\overrightarrow{OS} \times \bar{R})$$

$$= 112.84 > 0$$

∴ The resultant $\bar{R}$ intersects plane 1 as in Case (a).

$$n = 47.4^\circ < \pi/2$$

$$k_{10} = 74^\circ < \pi/2$$

$$k_{20} = 38^\circ < \pi/2$$

For these values of n, k_{10}, k_{20}, and M_x, a rotation about d_{10} is kinematically possible.

$$d_{10} = -\bar{w}_1 = (0.253, -0.827, 0.499) \qquad (3.37)$$

$$M_{d10} = \bar{d}_{10} \cdot (\overrightarrow{OS} \times \bar{R})$$

$$= 70.0 > 0$$

Therefore a rotation tends to occur about the $\bar{d}_{10}$ axis. The factor of safety aginst rotation can be determined as follows.

$$N_1 = \bar{R} \cdot \bar{w}_1 = 21.83$$

$$\bar{N}_1 = N_1 \bar{w}_1 = (-5.523,\ 18.053,\ -10.893) \tag{3.55}$$

$$\bar{T}_1 = \bar{R} - \bar{N}_1 = (5.523,\ -8.053,\ -16.237) \tag{3.56}$$

$$= c_1(-\overline{OQ}) + c_2(\overline{OQ} \times \bar{w}_1) \tag{3.57}$$

$$\overline{OQ} = \overline{OI} + \Psi \bar{R} = \overline{OS} + \Psi \bar{R}$$

$$= [-6.1,\ (2.0 + 10\Psi),\ (9.0 - 27.13\Psi)]$$

$\overline{OQ}$ and $\bar{w}_1$ are mutually perpendicular

$$\therefore\ \overline{OQ} \cdot \bar{w}_1 = 0$$

$$\therefore\ (6.1 \times 0.253) + (2.0 + 10\Psi)\ 0.827 - 0.499(9.0 - 27.13\Psi) = 0$$

Solving $\Psi = 0.0593$

$$\therefore\ \overline{OQ} = (-6.10,\ 2.59,\ 7.39)$$

$$\overline{OQ} \times \bar{w}_1 = (-7.41,\ -4.91,\ -4.39)$$

$$\bar{T}_1 = (5.523,\ -8.053,\ -16.237)$$

$$= c_1(6.10,\ -2.59,\ -7.39) +$$

$$c_2(-7.41,\ -4.91,\ -4.39)$$

Solving $c_1 = 1.77$ $c_2 = 0.71$

$$\bar{T}_t = c_2(\overline{OQ} \times \bar{w}_1) \tag{3.59}$$

$$= 0.71(-7.41,\ -4.91,\ -4.39)$$

$$= (-5.261,\ -3.496,\ -3.117)$$

$$T_t = 7.04 \text{ tons}$$

$$F.S. = \frac{N_1 \tan \phi_1}{T_t} = \frac{21.83 \tan 30^\circ}{7.04}$$

$$= 1.79$$

Thus the provision of the lateral force P increases the stability of the wedge OBCD against both sliding and rotation.

Note: In case (b) all the forces are in ton-units and all the lengths are in feet-units.

3.5 Analysis for Sliding on Two Planes by Engineering Graphics

The factor of safety of a rock wedge sliding on the two base planes can also be determined graphically by using the principles of engineering descriptive geometry. To illustrate the procedure, Problem 1 of section 3.4.3 will be solved using this method. The details of this graphical solution are shown in Fig. 3.11.

The lines DB' and CB' represent the strikes of planes 1 and 2 inclined at angles β_1 and β_2 with the front of the slope, I-I. An edge view of each plane is drawn as an auxiliary elevation to locate the position of a point O common to both the planes situated at any depth, d, below the horizontal plane DCB'. Since B' is also a point common to both the planes, B'O represents the line of intersection of planes 1 and 2. A side elevation parallel to B'O gives the true dip of the line of intersection B'O. The weight vector $\bar{W}$ is then resolved into components $\bar{N}_{12}$ and $\bar{T}_{12}$, respectively normal and parallel to the line of intersection B'O as shown in Fig. 3.11. An auxiliary elevation of the two planes looking in the direction OB' is obtained and the components $\bar{N}_1$ and $\bar{N}_2$ of $\bar{N}_{12}$ normal to planes 1 and 2 respectively are then determined. Once the magnitudes of $\bar{N}_1$ and $\bar{N}_2$ are known, the factor of safety is computed using the relationship

$$F.S. = \frac{N_1 \tan \phi_1 + N_2 \tan \phi_2}{T_{12}} \qquad (3.36)$$

3.6 Method of Stability Analysis for Rock Slopes with Three Intersecting Joint Sets.

In this section, the stability against sliding of a tetrahedral volume of rock, ABCD bounded by three planes 1, 2 and 3 and an exterior surface ABD, is investigated by using Londe's method of analysis (Fig. 3.12).

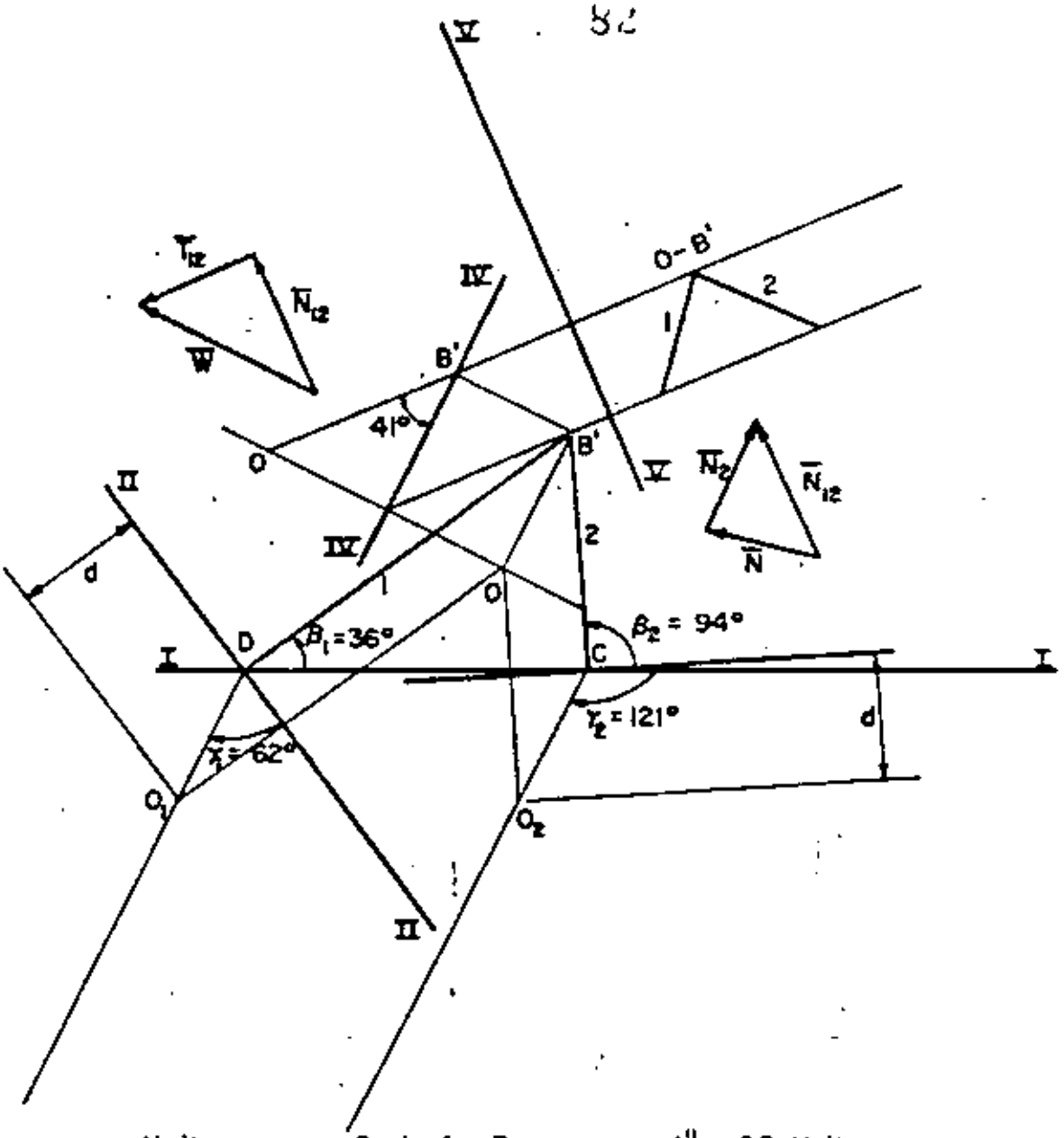

Units	Scale for Forces	1" = 60 Units
W = 66		
T_{12} = 42		
N_1 = 38	tan 20° = .364	38 x .364 = 13.8
N_2 = 40	tan 40° = .840	40 x .840 = 33.6
		47.4

$$F.S. = \frac{47.4}{42.0} = 1.12$$

FIG. 3.11 GRAPHICAL SOLUTION OF SLIDING STABILITY OF A ROCK WEDGE BOUNDED BY TWO JOINT PLANES

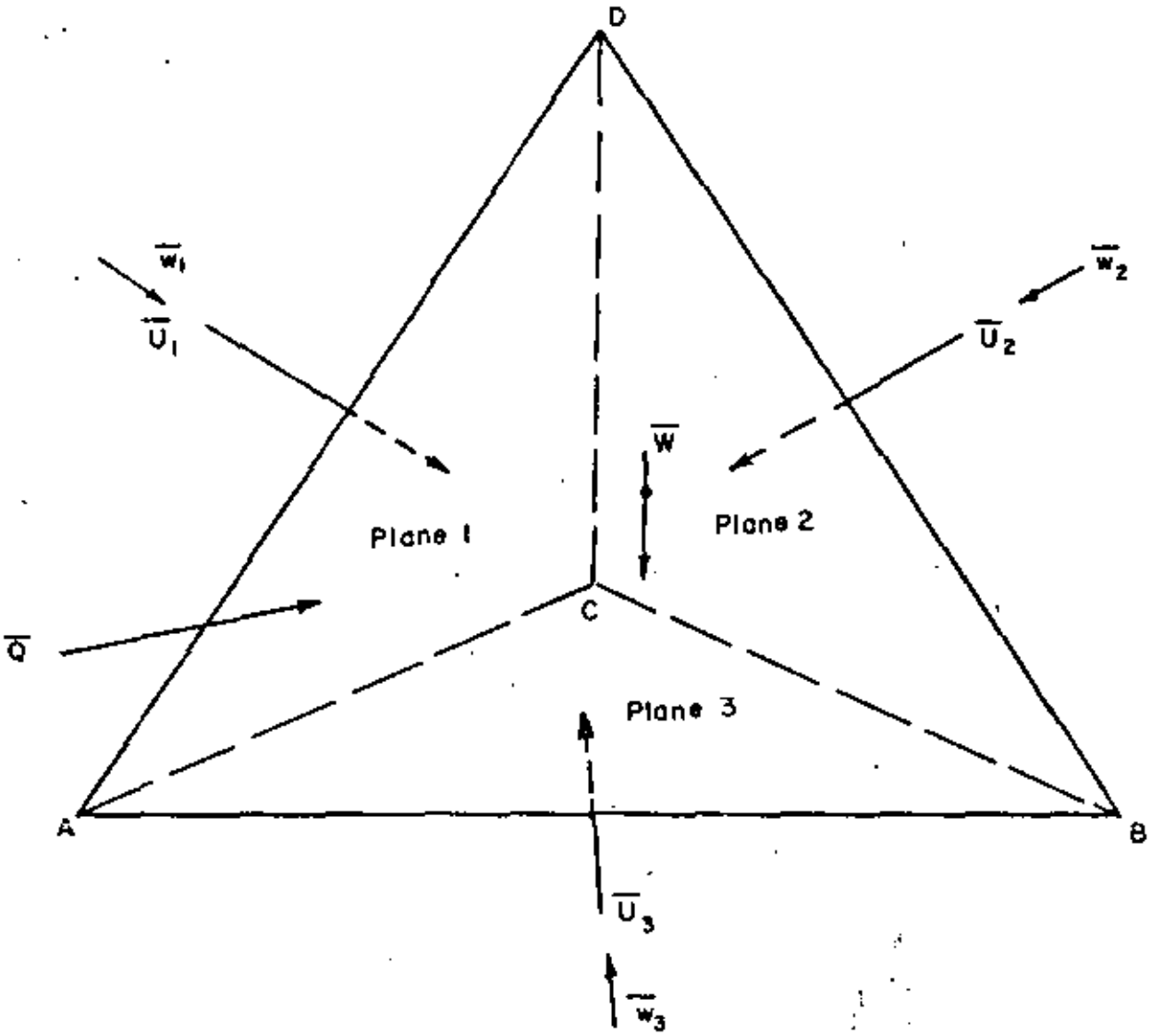

FIG. 3.12 FORCES ON A ROCK WEDGE BOUNDED BY THREE INTERSECTING JOINT PLANES

Sliding failure of the tetrahedral rock mass ABCD, can occur by separation from one or two of the three bounding planes. There are thus six possible modes of sliding failure as shown in Fig. 3.13. The mode of failure in a given case will depend on the geometry of the problem and the magnitude and direction of the resultant of the applied forces, $\bar{R}$, as defined by the equation:

$$\bar{R} = \bar{W} + \bar{Q} + \bar{U}_1 + \bar{U}_2 + \bar{U}_3 \qquad (3.68)$$

Where $\bar{W} = (W_x, W_y, W_z)$ = total weight vector of the tetrahedral volume of rock

$\bar{Q} = (Q_x, Q_y, Q_z)$ = any externally applied force on the rock wedge

$\bar{U}_1, \bar{U}_2, \bar{U}_3$ = hydrostatic uplift or porewater forces that act on planes 1, 2 and 3 resepectively

The first step in the stability analysis of the rock wedge ABCD, is to determine the mode of sliding failure for a given set of input conditions. This can be done as explained in the following section.

3.6.1 Determination of the Mode of Sliding Failure (Fig. 3.14)

Let $\bar{w}_1$, $\bar{w}_2$ and $\bar{w}_3$ represent unit vectors normal to planes 1, 2 and 3 respectively, directed towards the inside of the rock volume. The resultant force $\bar{R}$ lifts the tetrahedron from all three contact faces if all the three following equations are satisfied simultaneously

$$\bar{R} \cdot \bar{w}_1 > 0 \qquad (3.69)$$

$$\bar{R} \cdot \bar{w}_2 > 0 \qquad (3.70)$$

$$\bar{R} \cdot \bar{w}_3 > 0 \qquad (3.71)$$

In such a case equilibrium is not possible unless the joints can take tension or rock bolts are provided to resist the tensile forces across the faces.

NATURE OF SLIDING	CONTACT FACES	OPEN FACES	DIAGRAM
Direction CB	2 and 3	1	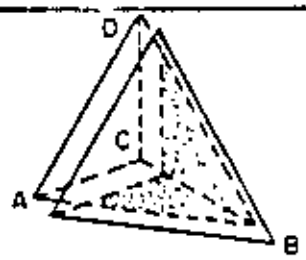
Direction CA	3 and 1	2	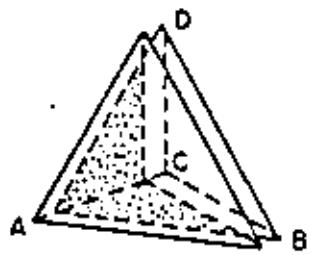
Direction CD	1 and 2	3	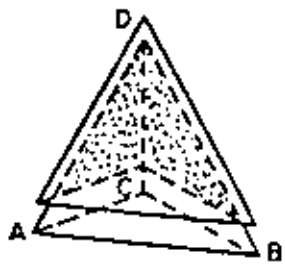
In Plane 3. Direction Between CB and CA	3	1 and 2	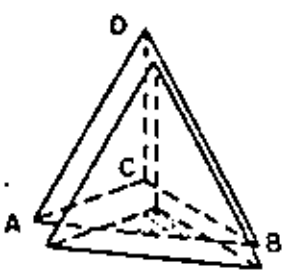
In Plane 1 Direction Between CA and CB	1	2 and 3	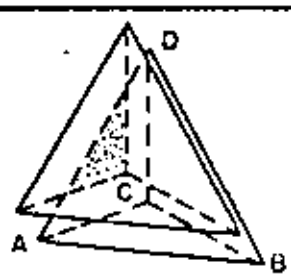
In Plane 2 Direction Between CD and CB	2	3 and 1	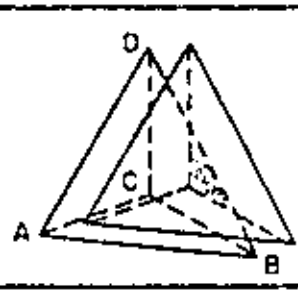

FIG. 3.13 MODES OF SLIDING FAILURE OF A ROCK WEDGE BOUNDED BY THREE INTERSECTING JOINT SETS

If Eqs. 3.69 through 3.71 show that lifting off of the wedge from the support planes does not occur, then further kinematic tests must be made to determine the mode of sliding failure.

The vectors $\bar{x}_{12}$, $\bar{x}_{23}$ and $\bar{x}_{31}$ along the lines of intersection CD, CB and CA are given by the following equations:

$$\bar{x}_{12} = \bar{w}_2 \times \bar{w}_1 \tag{3.72}$$

$$\bar{x}_{23} = \bar{w}_3 \times \bar{w}_2 \tag{3.73}$$

$$\bar{x}_{31} = \bar{w}_1 \times \bar{w}_3 \tag{3.74}$$

Let us now define two new vectors, ${}_1\bar{s}_{12}$ and ${}_2\bar{s}_{12}$ orthogonal to $\bar{x}_{12}$ and lying in planes 1 and 2 respectively as follows:

$${}_1\bar{s}_{12} = \bar{x}_{12} \times \bar{w}_1 \tag{3.75}$$

$${}_2\bar{s}_{12} = \bar{w}_2 \times \bar{x}_{12} \tag{3.76}$$

Similarly the vectors ${}_2\bar{s}_{23}$ and ${}_3\bar{s}_{23}$ normal to $\bar{x}_{23}$ and lying in planes 2 and 3 respectively are given by

$${}_2\bar{s}_{23} = \bar{x}_{23} \times \bar{w}_2 \tag{3.77}$$

$${}_3\bar{s}_{23} = \bar{w}_3 \times \bar{x}_{23} \tag{3.78}$$

The vectors ${}_1\bar{s}_{31}$ and ${}_3\bar{s}_{31}$ normal to $\bar{x}_{31}$ and lying in planes 1 and 3 respectively are similarly given by

$${}_3\bar{s}_{31} = \bar{x}_{31} \times \bar{w}_3 \tag{3.79}$$

$${}_1\bar{s}_{31} = \bar{w}_1 \times \bar{x}_{31} \tag{3.80}$$

The orientations of all the vectors defined by Eqs. 3.72 through 3.80 are shown in Fig. 3.14.

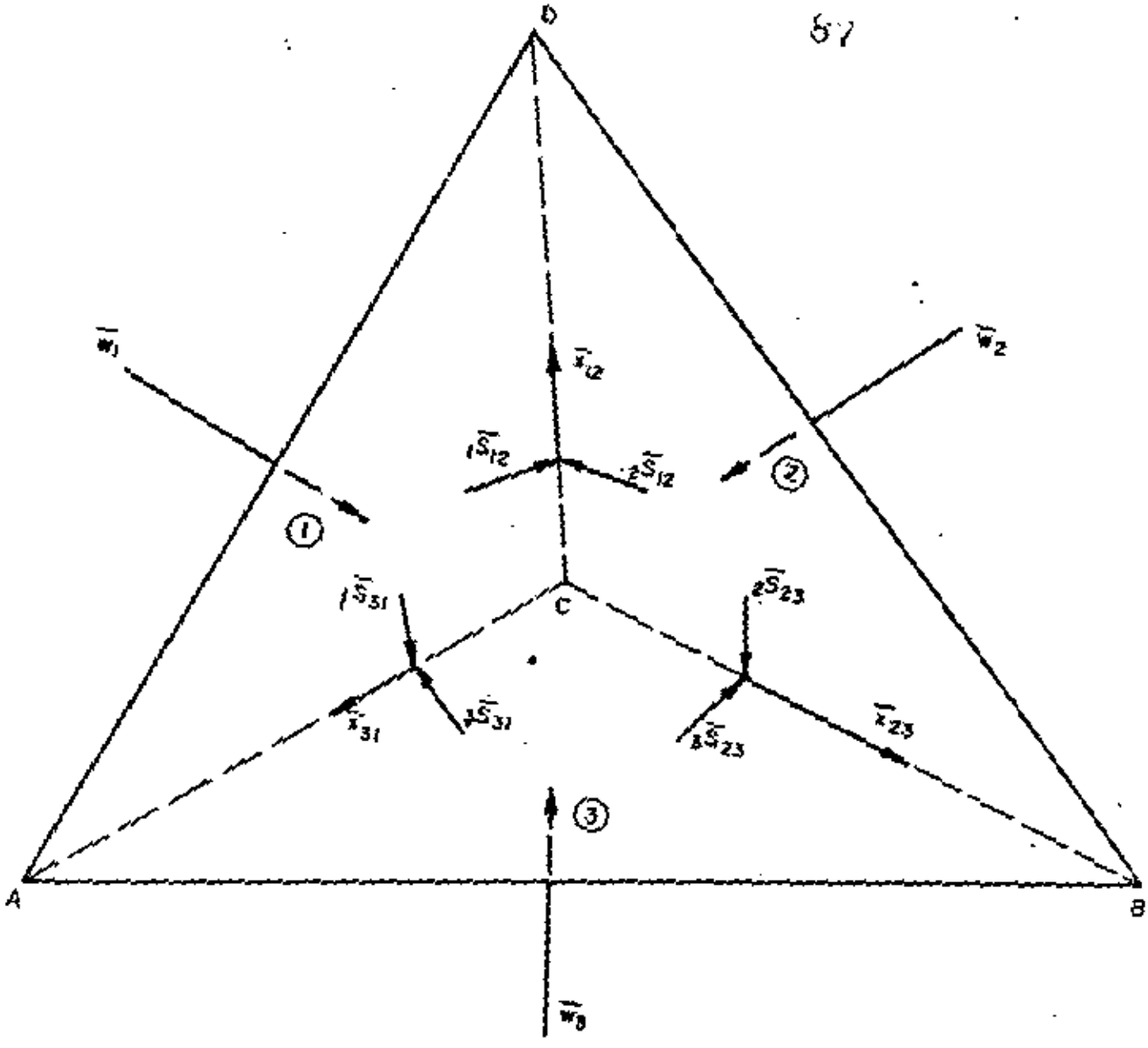

FIG. 3.14 STABILITY OF A ROCK WEDGE BOUNDED BY THREE INTERSECTING JOINT PLANES

If sliding is to occur along the line of intersection $\bar{x}_{12}$, the resultant $\bar{R}$ of the applied forces must have a component along $\bar{x}_{12}$ which tends to move up plane 3. This condition can be represented vectorially by the equation

$$\bar{R} \cdot \bar{x}_{12} \geq 0 \qquad (3.81)$$

In addition the components of $\bar{R}$ on plane 1 and 2 along vectors ${}_1\bar{S}_{12}$ and ${}_2\bar{S}_{12}$ must be directed towards the line of intersection $\bar{x}_{12}$. In other words,

$$\bar{R} \cdot {}_1\bar{S}_{12} \geq 0 \qquad (3.82)$$

$$\bar{R} \cdot {}_2\bar{S}_{12} \geq 0 \qquad (3.83)$$

Eqs. 3.81 through 3.83 must be satisfied simultaneously if the rock wedge ABCD is to slide along $\bar{x}_{12}$ with face 3 open. The conditions to be satisfied for sliding to occur along $\bar{x}_{23}$ and $\bar{x}_{31}$ can be obtained in a similar manner. They are:

For sliding along $\bar{x}_{23}$, $\bar{R} \cdot \bar{x}_{23} \geq 0$ (3.84)

$$\bar{R} \cdot {}_2\bar{S}_{23} \geq 0 \qquad (3.85)$$

$$\bar{R} \cdot {}_3\bar{S}_{23} \geq 0 \qquad (3.86)$$

For sliding along $\bar{x}_{31}$, $\bar{R} \cdot \bar{x}_{31} \geq 0$ (3.87)

$$\bar{R} \cdot {}_1\bar{S}_{31} \geq 0 \qquad (3.88)$$

$$\bar{R} \cdot {}_3\bar{S}_{31} \geq 0 \qquad (3.89)$$

If sliding is to occur on any one plane only, say on plane 1, then $\bar{R}$ must have a component normal to plane 1 directed towards the outside of the rock wedge ABCD. In other words

$$\bar{R} \cdot \bar{w}_1 \leq 0 \qquad (3.90)$$

In addition the components of $\bar{R}$ on plane 1 along ${}_1\bar{S}_{12}$ and ${}_1\bar{S}_{31}$ must be directed away from $\bar{x}_{12}$ and $\bar{x}_{31}$. In other words

$$\bar{R} \cdot {}_1\bar{S}_{12} \leq 0 \qquad (3.91)$$

$$\bar{R} \cdot {}_1\bar{S}_{31} \leq 0 \qquad (3.92)$$

The corresponding equations for cases of sliding on planes 2 and 3 are as follows.

For sliding on plane 2 only:

$$\bar{R} \cdot \bar{w}_2 \leq 0 \qquad (3.93)$$

$$\bar{R} \cdot {}_2\bar{S}_{12} \leq 0 \qquad (3.94)$$

$$\bar{R} \cdot {}_2\bar{S}_{23} \leq 0 \qquad (3.95)$$

For sliding on plane 3 only:

$$\bar{R} \cdot \bar{w}_3 \leq 0 \qquad (3.96)$$

$$\bar{R} \cdot {}_3\bar{S}_{23} \leq 0 \qquad (3.97)$$

$$\bar{R} \cdot {}_3\bar{S}_{31} \leq 0 \qquad (3.98)$$

3.6.2 Calculation of the Factor of Safety for Sliding

After deciding on the mode of sliding failure based on the kinematic tests mentioned above, the next step is to estimate the factor of safety against sliding under the given conditions. The procedure for estimating the factor of safety is basically the same as that explained in Section 3.4.1.3 of this chapter for the case of a rock wedge bounded by two joint planes. Three example problems have been added to illustrate the method of analysis.

In the preceding analysis, of Section 3.6.1, however, it has been tactily assumed that the critical rock wedge is bounded by all the three joint planes and the exterior slope face as shown in Fig. 3.12. When the field conditions

are such that this assumption is valid, the method of stability analysis presented above is directly applicable. But in a majority of cases, it is likely that the critical rock wedge is bounded by two (rather than by all the three) joint planes. Under these conditions the stability analysis has to be performed as explained in Section 3.4.1.3.

3.6.3 Example Problems for Slopes with Three Intersecting Planes of Discontinuity Worked by Vector Analysis

Problem 1

Determine the factor of safety against sliding of the rock wedge ABCD shown in Fig. 3.12. Also estimate the direction and magnitude of the minimu dynamic resistance $\overline{NW}$ which is necessary to just make the potential block ABCD slide.

$\bar{w}_1 = (0.00, 0.72, 0.69)$

$\bar{w}_2 = (0.63, -0.12, 0.77)$

$\bar{w}_3 = (0.00, 0.00\ 1.00)$

$\bar{W} = (0, 0, -36.5 \text{ tons})$ $\bar{Q} = (0, 0, 0)$

$U_1 = 23.6$ tons $U_2 = 8.0$ tons $U_3 = 5.7$ tons

$\phi_1 = 40^\circ$ $\phi_2 = 40^\circ$ $\phi_3 = 40^\circ$

Solution

$$\bar{R} = \bar{W} + \bar{Q} + \bar{U}_1 + \bar{U}_2 + \bar{U}_3 \qquad (3.68)$$

$$= \bar{W} + \bar{Q} + U_1\bar{w}_1 + U_2\bar{w}_2 + U_3\bar{w}_3$$

$= (5.05, 16.04, -8.34)$ all in ton-units

$R = 18.8$ tons

$$\bar{x}_{12} = (-0.638, -0.435, 0.454) \qquad (3.72)$$

$x_{12} = 0.895$

$$\bar{x}_{23} = (0.120,\ 0.630,\ 0) \tag{3.73}$$

91

$$x_{23} = 0.640$$

$$\bar{x}_{31} = (0.720,\ 0,\ 0) \tag{3.74}$$

$$x_{31} = 0.720$$

$$_1\bar{S}_{12} = (-0.626,\ 0.440,\ -0.459) \tag{3.75}$$

$$_2\bar{S}_{12} = (0.280,\ -0.777,\ -0.351) \tag{3.76}$$

$$_2\bar{S}_{23} = (0.485,\ -0.093,\ -0.410) \tag{3.77}$$

$$_3\bar{S}_{23} = (-0.630,\ 0.120,\ 0) \tag{3.78}$$

$$_3\bar{S}_{31} = (0,\ -0.720,\ 0) \tag{3.79}$$

$$\bar{S}_{1\ 31} = (0,\ 0.497,\ -0.518) \tag{3.80}$$

$$\bar{R} \cdot \bar{w}_3 = -8.34 < 0 \tag{3.96}$$

Thus plane 3 is closed and a failure by lifting from the base planes does not occur.

$$\bar{R} \cdot {}_3\bar{S}_{23} = -1.25 < 0 \tag{3.97}$$

$$\bar{R} \cdot {}_3\bar{S}_{31} = -11.55 < 0 \tag{3.98}$$

Eqs. 3.96 through 3.98 thus indicate that sliding can occur only on plane 3.

$$N_3 = \bar{R} \cdot (-\bar{w}_3) = 8.34 \text{ tons}$$

$$\bar{N}_3 = N_3(-\bar{w}_3) = (0,\ 0,\ -8.34)$$

$$\bar{T}_3 = \bar{R} - \bar{N}_3 = (5.05,\ 16.04,\ 0)$$

$$T_3 = 16.8 \text{ tons}$$

$$\text{F.S.} = \frac{N_3 \tan \phi_3}{T_3} = \frac{8.34 \tan 40^\circ}{16.8}$$

$$= 0.42$$

Problem 2

Work out Problem 1 with the following changes:

$U_1 = 12.0$ tons $\quad U_2 = 2.0$ tons $\quad U_3 = 2.0$ tons

Solution

$$\bar{R} = \bar{W} + \bar{Q} + \bar{U}_1 + \bar{U}_2 + \bar{U}_3 \tag{3.68}$$

$$= \bar{W} + \bar{Q} + U_1\bar{w}_1 + U_2\bar{w}_2 + U_3\bar{w}_3$$

$$= (1.26,\ 8.40,\ -24.68)$$

$$\bar{R} \cdot \bar{w}_3 = -24.68 < 0 \tag{3.71}$$

and therefore lifting off of the rock wedge from all the base planes is not possible.

$$\bar{R} \cdot \bar{x}_{23} = 5.45 > 0 \tag{3.84}$$

$$\bar{R} \cdot {}_2\bar{s}_{23} = 9.94 > 0 \tag{3.85}$$

$$\bar{R} \cdot {}_2\bar{s}_{23} = 0.22 > 0 \tag{3.86}$$

The above equations show that sliding can occur only along the line of intersection $\bar{x}_{23}$.

$$T_{23} = \bar{R} \cdot \bar{x}_{23}/x_{23} = 8.50 \text{ tons}$$

$$\bar{T}_{23} = T_{23} \cdot \frac{\bar{x}_{23}}{x_{23}} = (1.60,\ 8.35,\ 0)$$

$$\bar{N}_{23} = \bar{R} - \bar{T}_{23} = (-0.34,\ -.05,\ -24.68)$$

$$= N_2(-\bar{w}_2) + N_3(-\bar{w}_3)$$

$$= N_2(-0.63,\ 0.12,\ -0.77) +$$

$$N_3\ (0,\ 0,\ -1.00)$$

Solving $N_2 = 0.54$ tons $N_3 = 24.26$ tons

$$F.S. = \frac{0.54 \tan 40^\circ + 24.26 \tan 40^\circ}{8.50}$$

$$= 2.44$$

Problem 3

A rock cut slope runs East-West and the three major joint sets intersecting the slope have the following orientations:

Joint Plane	Strike	Dip
1	N47°E	44°SE
2	N20°W	83°SW
3	N69°W	16°SW

The angle of shearing resistance on all the three joint planes is estimated to be 20°. Determine the factor of safety of the slope against a sliding failure.

Solution

Consider the positive x direction to be East, the positive y direction to be North and the positive z direction to be upwards. Then the three joint planes have the following strike and dip angles.

Plane 1	$\beta_1 = 47^\circ$	$\gamma_1 = 44^\circ$
Plane 2	$\beta_2 = 110^\circ$	$\gamma_2 = 97^\circ$
Plane 3	$\beta_3 = 159^\circ$	$\gamma_3 = 164^\circ$

The unit normals to planes 1, 2 and 3 can be defined by Eqs. 2.13, 2.14 and 2.15. When these normals are oriented such that they are directed toward the interior of the rock wedge they are defined by the following equations:

$$\bar{w}_1 = (0.474,\ -0.508,\ 0.719)$$

$$\bar{w}_2 = (-0.933,\ -0.339,\ 0.122)$$

$$\bar{w}_3 = (-0.099,\ -0.257,\ 0.961)$$

$$\bar{x}_{12} = (-0.182,\ 0.729,\ 0.635) \qquad (3.72)$$

$$x_{12} = 0.983$$

$$\bar{x}_{23} = (0.295,\ -0.885,\ -0.206) \qquad (3.73)$$

$$x_{23} = 0.955$$

$$\bar{x}_{31} = (-0.303,\ -0.526,\ -0.172) \qquad (3.74)$$

$$x_{31} = 0.631$$

$${}_1\bar{s}_{12} = (0.847,\ 0.432,\ -0.253) \qquad (3.75)$$

$${}_2\bar{s}_{12} = (-0.304,\ 0.570,\ -0.741) \qquad (3.76)$$

$${}_2\bar{s}_{23} = (-0.178,\ -0.157,\ -0.925) \qquad (3.77)$$

$${}_3\bar{s}_{23} = (0.903,\ 0.263,\ 0.163) \qquad (3.78)$$

$${}_3\bar{s}_{31} = (-0.550,\ 0.309,\ 0.026) \qquad (3.79)$$

$${}_1\bar{s}_{31} = (0.466,\ -0.137,\ -0.403) \qquad (3.80)$$

$$\bar{R} = (0,\ 0,\ -W)$$

$$\bar{R} \cdot \bar{w}_1 = -0.719W < 0$$

$$\bar{R} \cdot \bar{w}_2 = -0.122W < 0$$

$$\bar{R} \cdot \bar{w}_3 = -0.961W < 0$$

Therefore failure by lifting off of all the base planes is not possible as shown by comparison of the above three equations with Eqs. 3.69, 3.70, 3.71. It can easily be verified that all kinematic tests are satisfied only for sliding on plane 3. In other words

$$\bar{R} \cdot \bar{w}_3 = -0.961W < 0 \qquad (3.96)$$

$$\bar{R} \cdot {}_3\bar{S}_{23} = -0.163W < 0 \qquad (3.97)$$

$$\bar{R} \cdot {}_3\bar{S}_{31} = -0.026W < 0 \qquad (3.98)$$

$$N_3 = \bar{R} \cdot (-\bar{w}_3) = 0.961\ W$$

$$\bar{N}_3 = N_3(-\bar{w}_3) = (0.095W,\ 0.247W,\ -0.924W)$$

$$\bar{T}_3 = \bar{R} - \bar{N}_3 = (-0.095W,\ -0.247W,\ -0.076W)$$

$$T_3 = 0.275W$$

$$F.S. = \frac{0.961W \tan 20^\circ}{0.275W} = 1.27$$

The preceding calculations have been carried out under the assumption that the critical rock wedge is bounded by all the three joint planes. As has been pointed out earlier, in a majority of cases, there exists a rock wedge, bounded by only two joint planes, which is more critical than the one considered in the preceding analysis. As a matter of fact, in the present problem, the rock wedge bounded by planes 1 and 2 has a lower factor of safety with respect to sliding. The determination of the mode of failure and the factor of safety against sliding can be done as explained in section 3.4.1.3. The details of this analysis will not be given here except the fact that the sliding tends to occur down the line of intersection of planes 1 and 2 and that the factor of safety is 0.58 as compared to the previous value of 1.27.

3.7 Computer Techniques

The stability of rock slopes bounded by two or three joint sets can also be analyzed using digital computer techniques. This method avoids lengthy hand-calculations and is particularly useful when there is a need for solving a whole series of stability problems.

The basis of the procedure is the same as explained in the previous sub-sections. The essential steps in this procedure are as follows (see flow chart, Fig. 3.15):

1. Using the input data calculate all the required directional vector quantities.
2. Check to see if failure by lifting off the base planes of the rock wedge is possible.
3. If not, determine the probably mode of sliding failure.
4. Calculate the factor of safety for this mode of sliding failure.
5. Check for stability against the possible mode of rotation.
6. Print the results.

A documentation and listing of the computer programs using Fortran IV language is given in Appendix A.

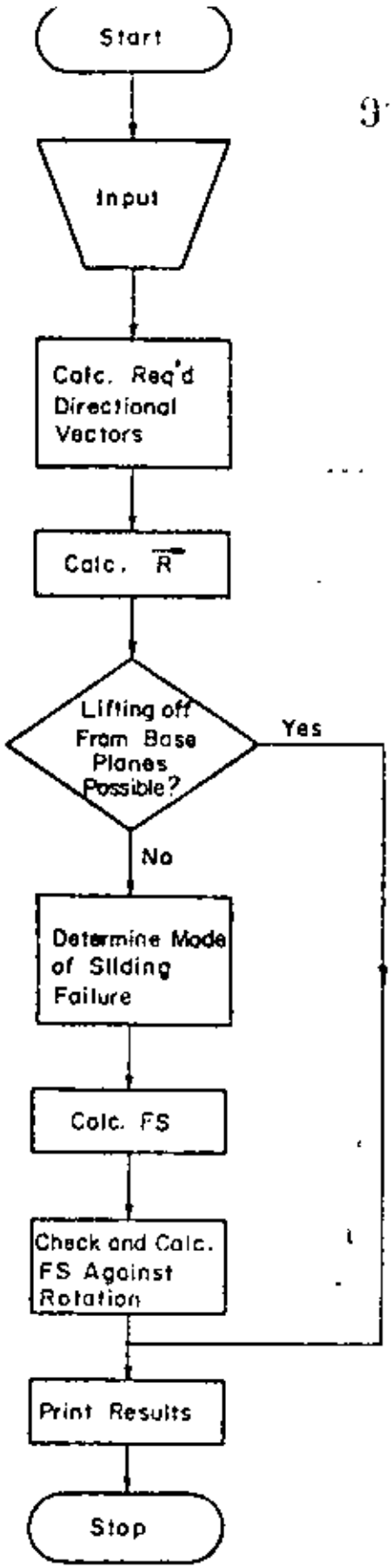

FIG. 3.15 FLOW CHART

Chapter Four

GRAPHICAL SLOPE STABILITY ANALYSIS BY USE OF STEREONETS

4.1 Properties of Spherical Projections

4.1.1 General

The orientation (strike and dip) of planes or lines in space can be represented by the intersection of the plane or line with the surface of a reference sphere through whose center the plane or line passes. As can be seen in Figure 4.1, the intersection of a plane with the sphere is a great circle, while a line which parallels the plane will plot as two points, 180 degrees apart, on the great circle. A plane can also be represented by the intersection of its normal with the sphere (the pole of the plane), which will plot as a point located 90 degrees from the great circle, in both the upper and lower hemispheres of the sphere.

To communicate this information, a two-dimensional representation of the spherical projection is necessary. Several types of projection can be used to transfer great circles and points from the spherical surface to the equatorial plane of the sphere.

The equal angle projection (termed a Wulff net or stereonet) is the method used in this report because of the simplicity in plotting the projections. Each great circle on the sphere plots as an arc of a circle on the equatorial plane of the sphere.

Another type of projection, the equal area projection, is used for compiling statistical information on the frequency and orientation of lines or planes. It therefore should be used to plot and evaluate the

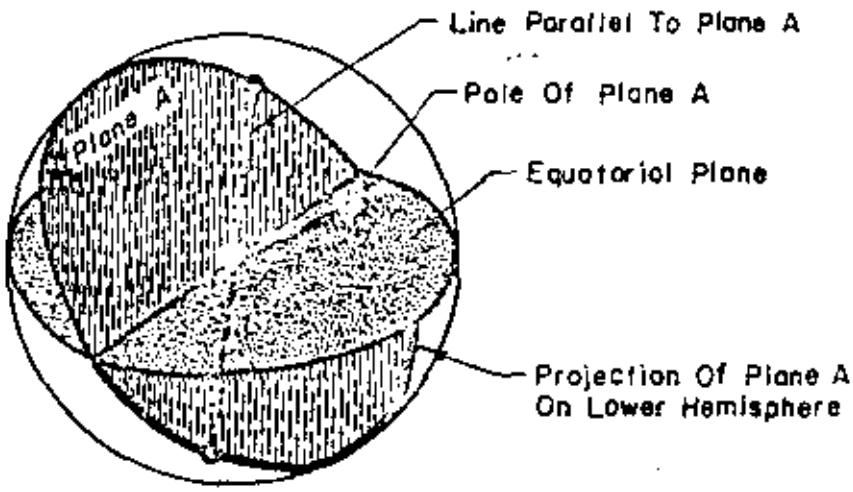

FIG. 4.1 PROJECTION OF PLANE AND LINES ON A SPHERE

raw data from field and borehole mapping of joints and other geologic discontinuities. The equal area projection of great circles from the sphere to the equatorial plane results in a distortion from the circular arc, and therefore is not quite as simple to use for stability analyses as the equal angle projection.

4.1.2 Equal Angle Projections

Figures 4.2 and 4.3 show the lower hemisphere, equal angle method for projecting a point from the surface of the sphere to equatorial plane.

A line is drawn from point P on the sphere to the upper pole, U, of the equatorial plane (dashed line in Fig. 4.2 and 4.3). The intersection of this line with the equatorial plane (P') is the desired projection of point P. In Figure 4.2, the projection of plane A and point P from the lower hemisphere to the equatorial plane is shown; the projection of plane A plots as an arc of a circle (or line of meridian) on the equatorial plane.

The projection of a vertical plane will project as a straight line through the origin of the equatorial plane. A horizontal plane will project as a line of meridian having a radius equal to the radius of the sphere, with the same origin. All points projected from the lower hemisphere will plot within this circle on the equatorial plane. Points from the upper hemisphere projected on the equatorial plane will plot outside the radius of the sphere, as can be seen for the projection, Q', of point Q in Figure 4.3.

A diagram of the stereonet obtained from an equal angle, lower hemisphere projection is shown in Fig. 4.4. The lines of meridian

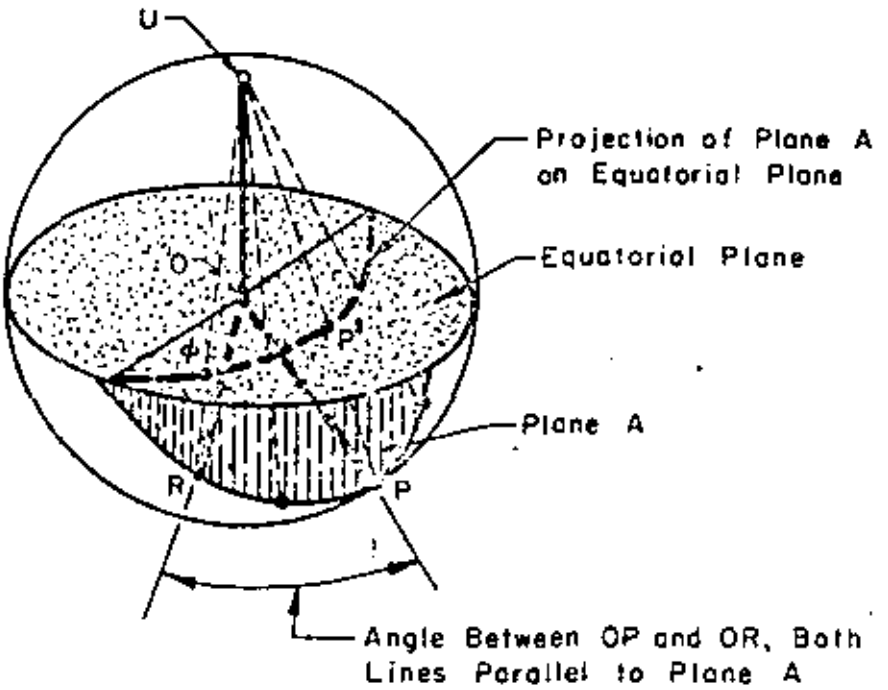

FIG. 4.2 EQUAL ANGLE PROJECTION FROM LOWER HEMISPHERE TO EQUATORIAL PLANE OF THE SPHERE

Q' is a Projection of Point Q (Q is Above the Equatorial Plane) P' is a Projection of Point P (P is Below the Equatorial Plane)

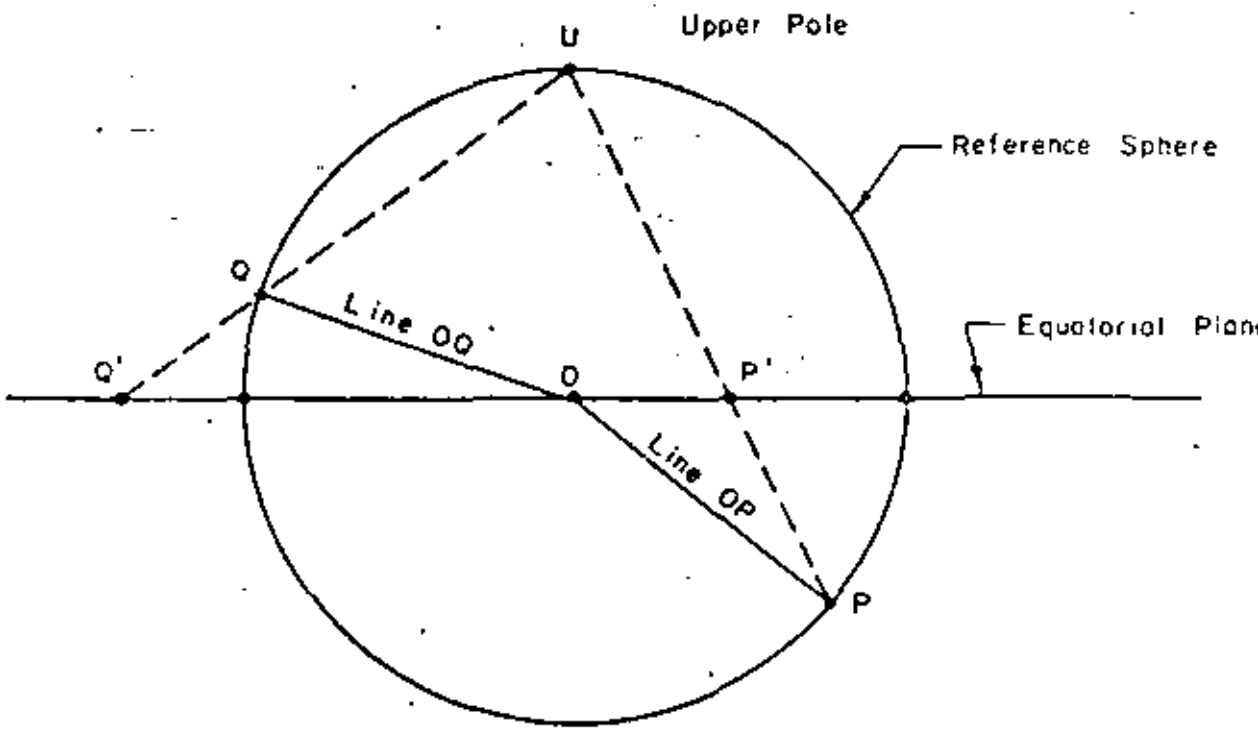

FIG. 4.3 PROFILE OF SPHERE SHOWING METHOD OF EQUAL ANGLE, LOWER HEMISPHERE PROJECTION

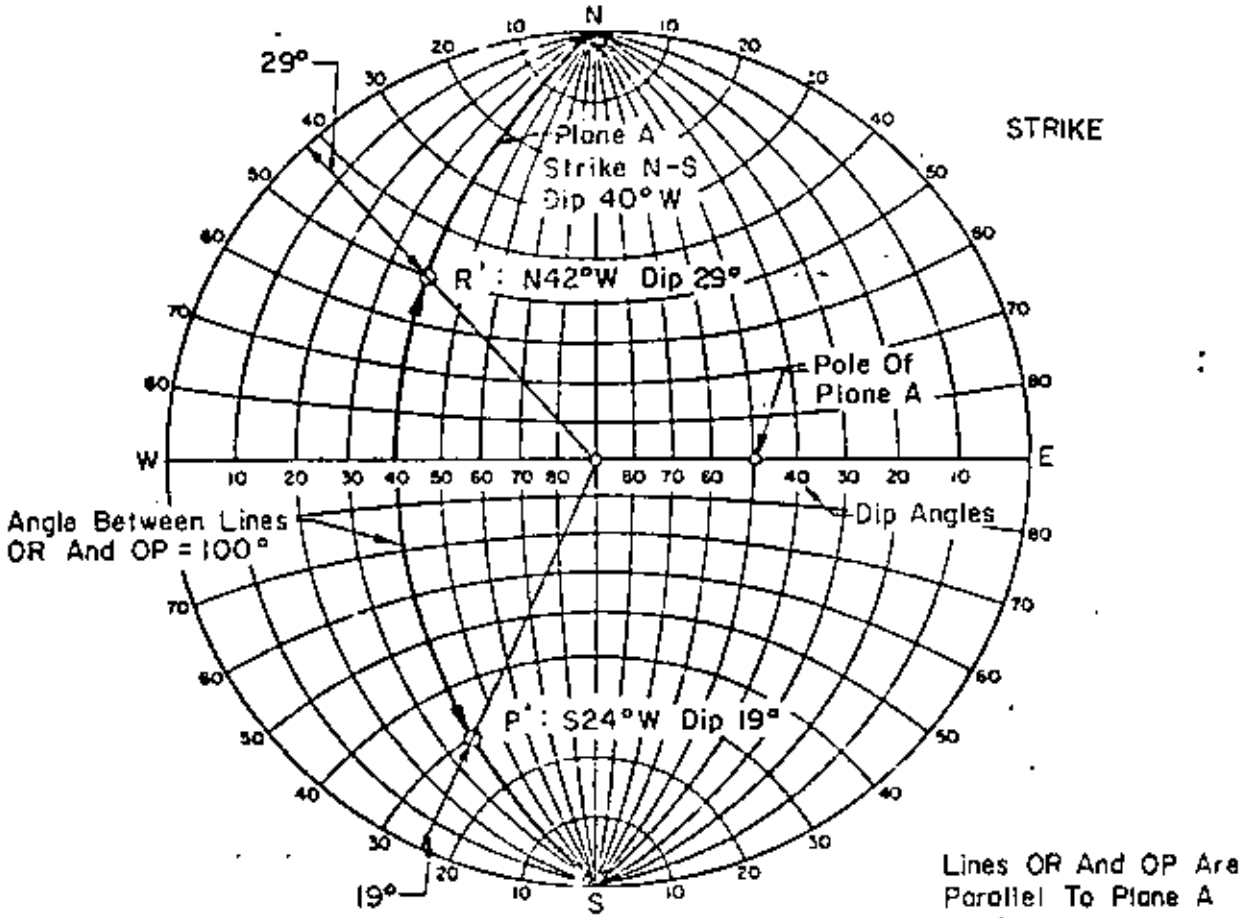

FIG. 4.4 STEREONET (WULFF NET) (EQUAL ANGLE PROJECTION)

through the N and S poles of this diagram represent great circles resulting from the intersection of N-S- striking planes with the reference sphere. Dip angles for these planes are shown on the E-W axis of the stereonet. The meridians for steeply dipping planes will approach straight lines on this plot, while the meridians for flat-lying planes will plot as arcs of circles having radii approaching the radius of the reference sphere. Each of the meridians is divided into 180 degrees by E-W lines of latitude, which plot as arcs of circles on the equal angle stereonet. To represent a plane which strikes other than N-S, the stereonet of Fig. 4.4 must be rotated so that its N-S axis is aligned in the direction of the strike of the given plane. The meridian can then be traced from the stereonet so that it is oriented in its proper strike direction. Note that the true dip of a plane or line should be determined by orienting the E-W axis of the stereonet so that it is in the direction of the dip of the line or plane.

Stereonets similar to that shown in Fig. 4.4 are available from graphic aid suppliers. It is suggested that such a stereonet be used for the example problems of this report by overlaying clear vellum on the stereonet and rotating the stereonet about its center, beneath the sheet of vellum, to plot planes and lines of various strikes and dips.

In Figure 4.4 the great circle projection of Plane A (dipping 40° west and striking N-S) plots as a line of meridian. The pole (or normal) of plane A is located 90° from the plane. Lines parallel to plane A plot as points on this line of meridian. The angle between two such lines, OP and OR is 100° and is found by counting the lines of latitude along the meridian, between points R' and P'.

Figure 4.5 shows the projection of two planes on the stereonet, one striking N-S, the other N 42° E. The orientation of the line of intersection of the two planes is determined from the point of intersection of the two meridians. In this case the line of intersection dips at an angle 24° in a direction of S 32° W. All of this information can be determined by using the stereonet, rotating it as required to plot lines of meridian and read angles. The dip angle is read by rotating the stereonet until either the NS or EW axis coincides with the direction of dip. The dip angle is then read in degrees from the outer edge of the stereonet.

4.2 Use of Stereonet to Evaluate Driving and Resisting Forces on a Potential Sliding Wedge of Rock

The use of the stereonet in stability analyses has been described by John (1968), Goodman (1964). The stereonet can be used to evaluate the stability of a three-dimensional wedge of rock resting on planes having frictional resistances. The method is very similar to the two-dimensional graphical force polygon used to sum forces. However, only the orientation (and not the magnitude) of forces is determined directly from the stereonet. If the resultant driving force acts at an angle further from the normal to the potential failure planes than the angle of the maximum resisting reaction on the planes, then sliding will occur. Note that the location of the forces and reactions is not known, and a summation of moments is not carried out.

The stability analysis is divided into two distinct parts. In the first part the orientation of the maximum resisting reaction on the potential failure planes is plotted on the stereonet. (For sliding on a

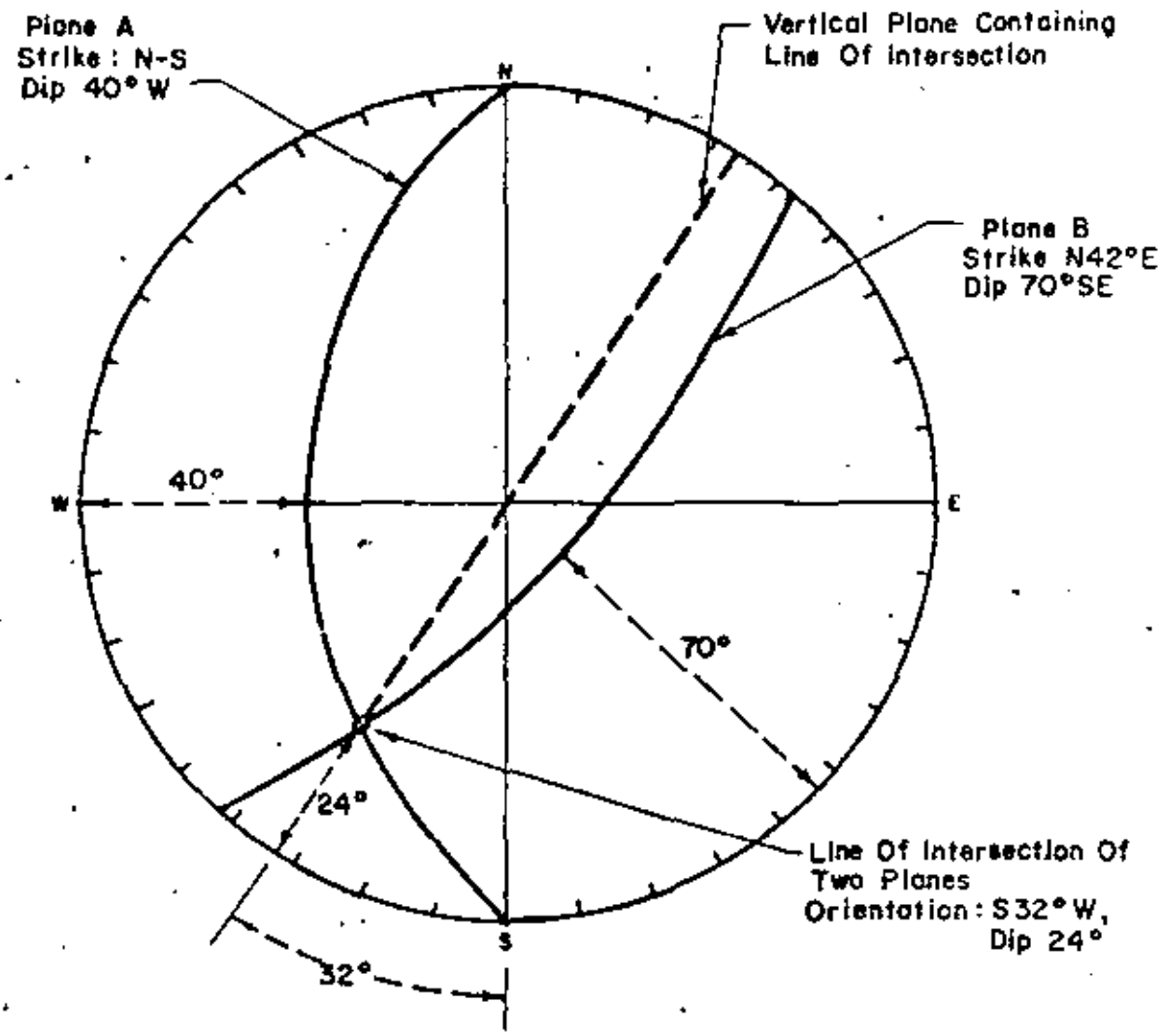

FIG. 4.5 DETERMINATION OF LINE OF INTERSECTION OF TWO PLANES

single plane, the maximum reaction would be oriented at Ø degrees to the normal of the plane.) Zones of stability and instability can thus be outlined on the stereonet, strictly by considering the orientation of the reactions on the potential sliding planes.

The second part involves determination of the orientation of the resultant driving force acting on the wedge. This force may include the weight of the wedge as well as acceleration forces, uplift water pressures on the planes of failure, and driving forces on the wedge from structures such as dam abutments. Graphical addition of vectors is used in conjunction with the stereonet to determine the orientation of the resultant vector force. If the orientation of the resultant driving force falls within the zone of stability on the stereogram, then the wedge is stable; if the orientation of the resultant driving force lies outside the stable zone, then the wedge is unstable.

Not only is the stereonet method of evaluating the stability of a wedge simple and rapid, it also possesses the advantage that a variety of forces required to cause failure or, conversely, to ensure stability can be clearly visualized, without resorting to extensive computations.

4.3 Sliding on a Single Fricitional Plane

The simple case of sliding on a single plane is described, to illustrate the use of the stereonet in stability analysis. Of course, a true two-dimensional problem (where the resultant driving vector force, $\bar{R}$, acts in the direction of the dip) is more simply solved using a conventional two-dimensional force polygon. However, for cases where the driving vector is not in the direction of the dip (such as might occur when an abutment load acts on a wedge), the stereographic method can

be used to solve problems which cannot be readily solved using a two-dimensional force polygon.

4.3.1 Orientation of reaction force on the plane of failure

The reaction force at failure, $\bar{R}_L$ (summation of the normal force, $\bar{N}$, and maximum shear force, $\bar{S}$) is oriented at the angle of friction Ø, from the normal to the plane. Should the tendency for sliding be down-dip, then $\bar{S}$ acts upslope and $\bar{R}_L$ is as shown in Fig. 4.6a. A friction cone can be drawn to show the possible orientations of $\bar{R}_L$ for sliding in other directions. The sides of the cone are oriented at Ø degrees to the normal, as shown in Fig. 4.6a and b. As long as the resultant driving vector, $\bar{R}$, acts at an angle less than Ø degrees to the normal, then sliding will not occur in any direction. When $\bar{R} = \bar{R}_L$, sliding is initiated.

A friction cone will plot as a circle on an equal angle stereonet, as shown in Fig. 4.6c. The position of the normal force is first located on the stereonet. (The position of the normal force is located at the pole of the plane.) The friction circle can then be drawn by marking off 40 degree angles from $\bar{N}$, on great circles passing through $\bar{N}$. (Note that $\bar{N}$ is not in the center of the circle formed by the friction cone.)

4.3.2 Stability of wedge of weight $\bar{W}$ with uplift force, $\bar{U}$, acting on the failure plane

It is immediately apparent that a wedge of weight $\bar{W}$ will not slide on the plane of failure because Ø is 40 degrees and exceeds the slope angle of 30 degrees. This is also apparent from Fig. 4.6c, where the weight vector, $\bar{W}$, falls within the friction cone.

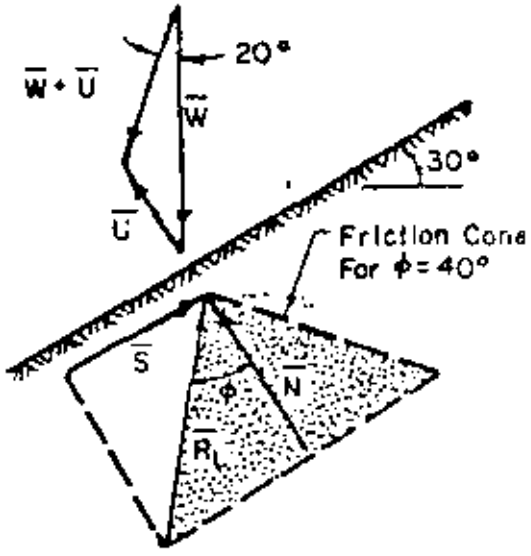

[Given : U = 0.44 W]

(a)

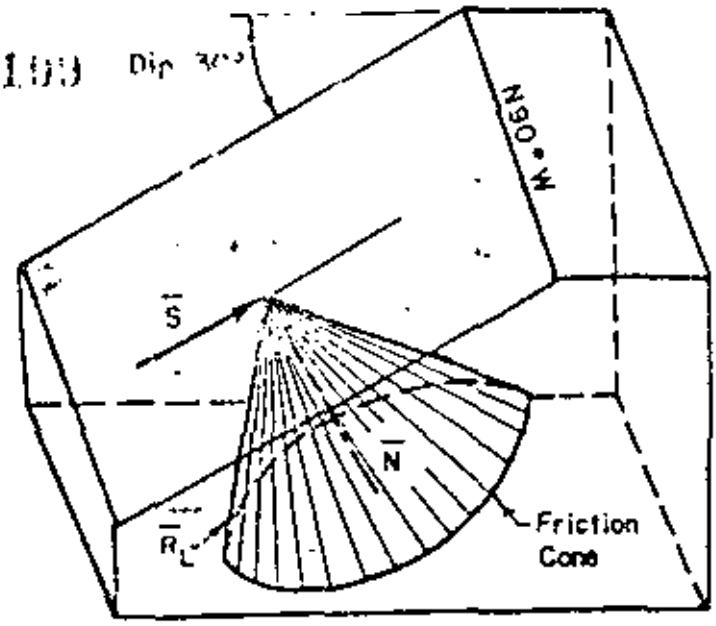

(b)

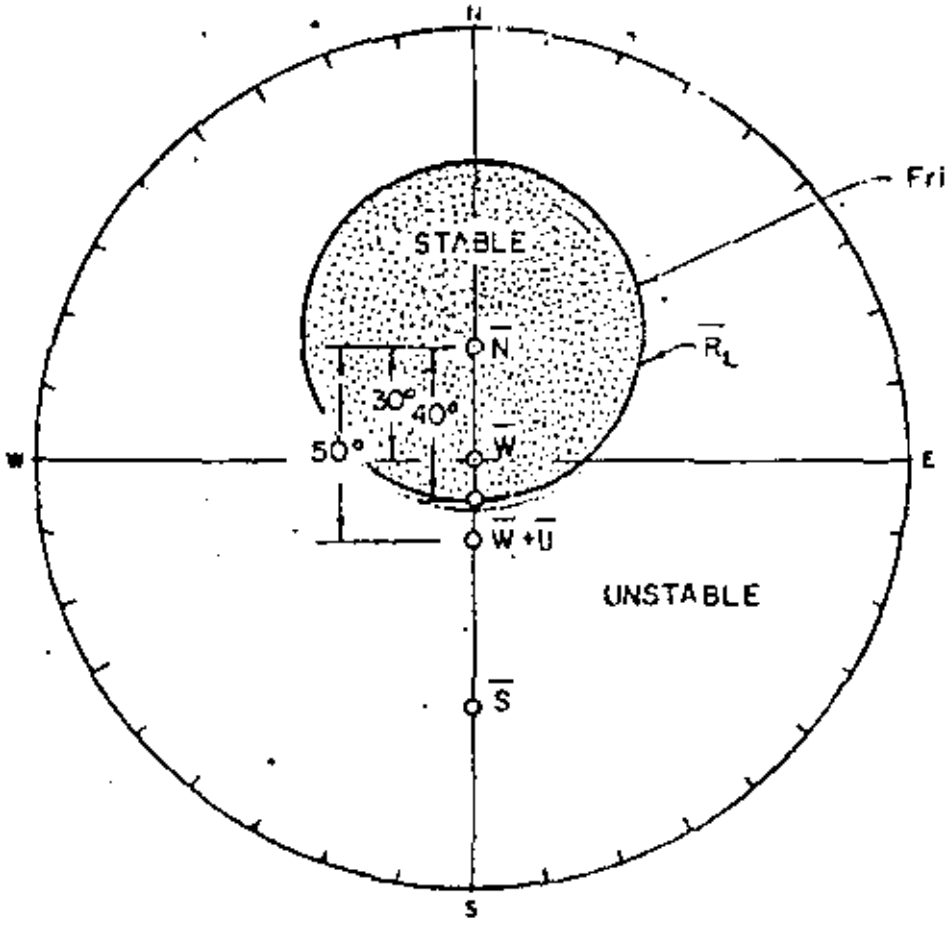

(c)

FACTOR OF SAFETY

1. Due To Weight, $\overline{W}$

$$F.S. = \frac{\tan 40^\circ}{\tan 30^\circ} = 1.45$$

2. Due To $\overline{W}+\overline{U}$

$$F.S. = \frac{\tan 40^\circ}{\tan 50^\circ} = 0.71$$

(d)

FIG. 4.6 SLIDING ON A SINGLE PLANE

If a porewater pressure were acting on the plane of failure, the stability of the wedge would be reduced. The porewater vector force, $\bar{U}$, acts normal to the plane of failure, as shown in Fig. 4.6a. The resultant driving vector, $\bar{R} = \bar{W} + \bar{U}$, can be determined by drawing the two vectors to scale (see Fig. 4.6a) and determining the angle of the resultant. In this case, the magnitude of U is given as 0.44 W and therefore the angle of $\bar{R}$ from the vertical is found to be 20 degrees. $\bar{R}$ is thus located 10^{o} outside the friction circle, in the unstable zone.

The factor of safety for the two cases, with and without the uplift force acting, is shown in Fig. 4.6d. The tangent of the angle between the normal and the resultant driving force determines the denominator in each case.

4.3.3 Graphical procedure for determining the direction of resultant vector force

The summation of a series of vectors cannot be performed using the stereographic projection alone, because there is no method for showing magnitudes of forces on the stereographic projection. However, the orientation of the resultant vector can be determined using the stereographic projection in combination with the graphical addition of vectors, two at a time. Three vectors, $\bar{W}$ and $\bar{U}$ of the preceding example and an additional vector $\bar{A}$, are illustrated in Fig. 4.7. The graphical addition of these vectors is performed as shown in Fig. 4.8. As described in the preceding example, vectors $\bar{W}$ and $\bar{U}$ are added graphically thus determining the orientation of $\bar{W} + \bar{U}$, which is found to be 20 degrees from the vertical (Fig. 4.8a). Vectors $\bar{W}$ and $\bar{A}$ are then added, determining the orientation of $\bar{W} + \bar{A}$, 30 degrees from the vertical (Fig. 4.8b).

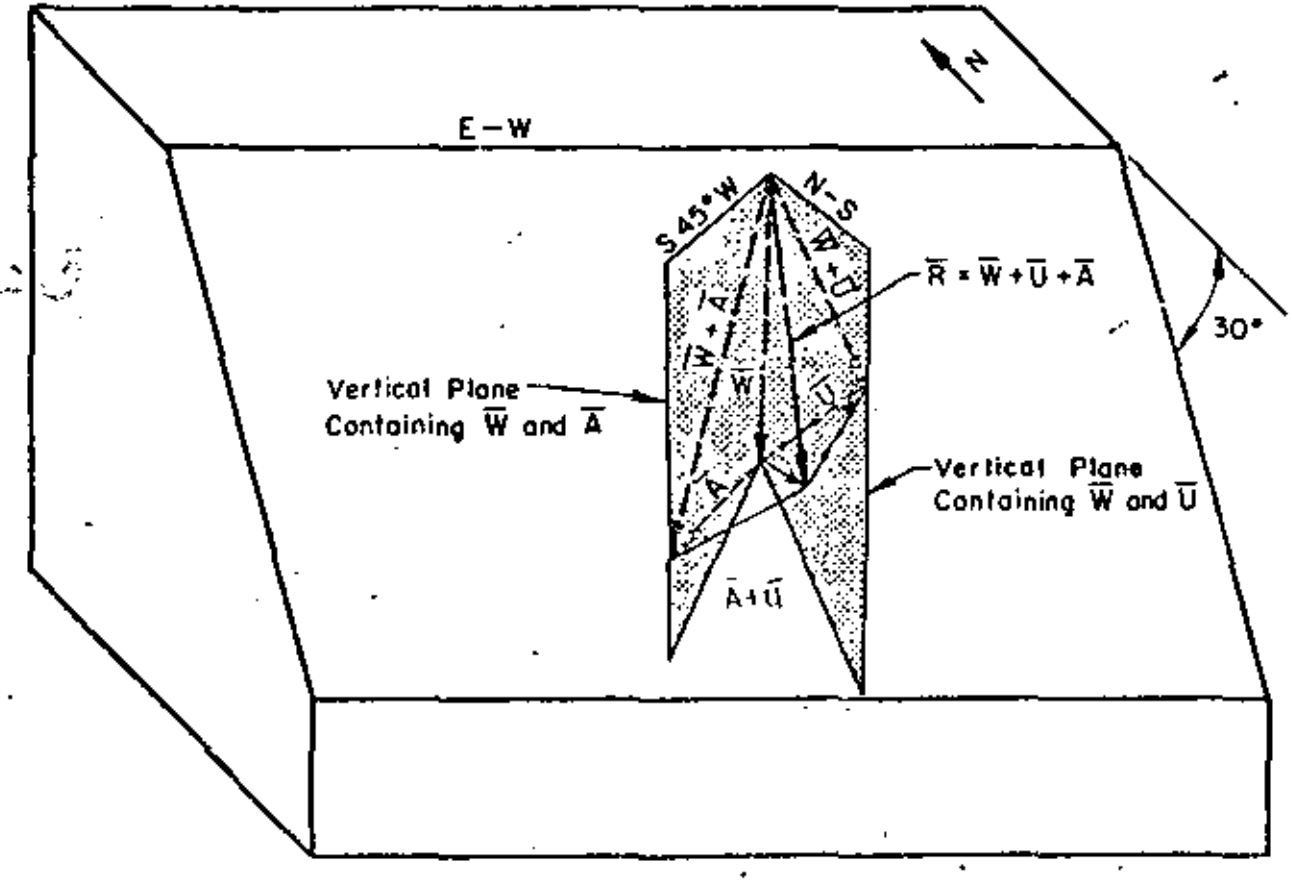

FIG. 4.7 GRAPHICAL SUMMATION OF 3 VECTORS

GIVEN: 1. Weight of Wedge = $\overline{W}$
2. Porewater Force, $\overline{U}$, Equal to 0.44 W, on 30° Plane
3. Force $\overline{A}$, Equal to 0.6 W, Acting S 45° W, Dip 10°

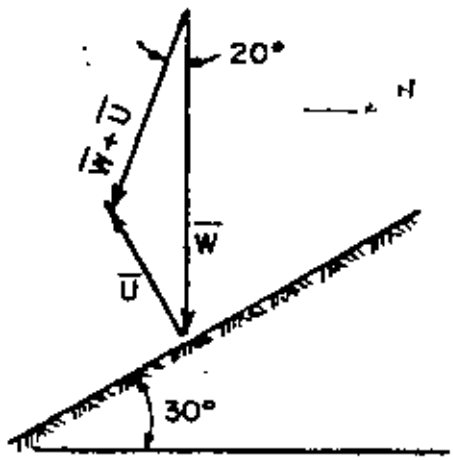

(a) Vertical Plane Oriented N-S Containing Vectors $\overline{W}$ and $\overline{U}$

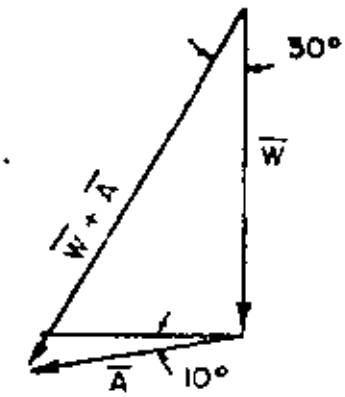

(b) Vertical Plane Oriented S 45° W Containing Vectors $\overline{W}$ and $\overline{A}$

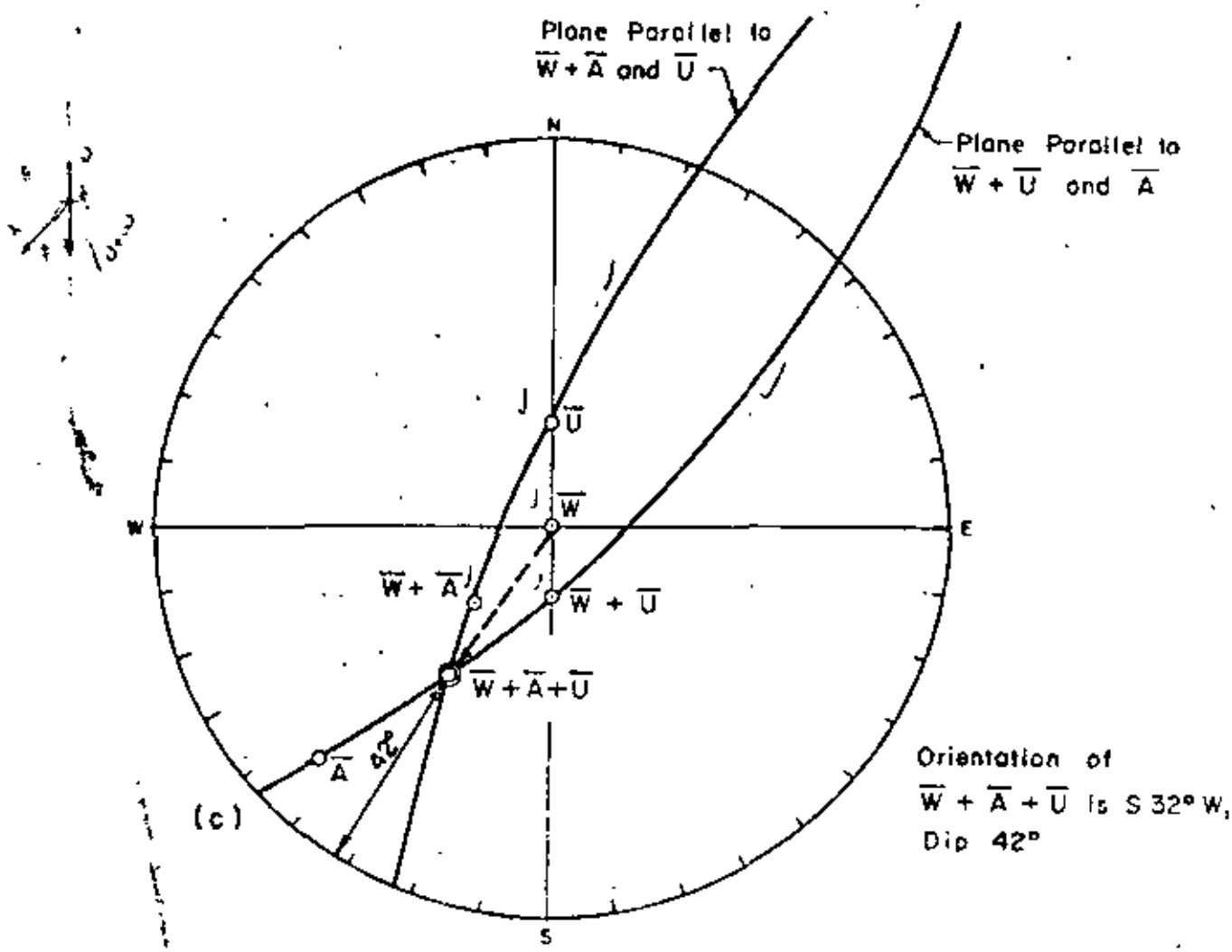

FIG. 4.8 GRAPHICAL DETERMINATION OF ORIENTATION OF RESULTANT VECTOR, $\overline{W}+\overline{A}+\overline{U}$

The orientations of vectors $\bar{W}$, $\bar{U}$, $\bar{A}$, $\bar{W} + \bar{U}$, and $\bar{W} + \bar{A}$ are then plotted on the stereogram (Fig. 4.8c, solid arcs).

Once these vectors have been plotted, the orientation of the resultant vector, $\bar{R} = \bar{W} + \bar{A} + \bar{U}$, can be found using only the stereogram. This is accomplished by finding the line of intersection of two planes. One plane contains $\bar{W} + \bar{A}$ and $\bar{U}$, the other contains $\bar{W} + \bar{U}$ and $\bar{A}$ (Fig. 4.7). The intersection of the two planes is the resultant vector, $\bar{R} = \bar{W} + \bar{A} + \bar{U}$. On the stereogram in Figure 4.8c, a great circle is drawn through $\bar{W} + \bar{A}$ and $\bar{U}$, another great circle is drawn through $\bar{W} + \bar{U}$ and $\bar{A}$. The two great circles intersect at $\bar{R} = \bar{W} + \bar{U} + \bar{A}$, which is thus determined as dipping 42 degrees from the horizontal in a direction of S 32° W.

4.3.4 Determination of direction of movement and factor of safety for case of resultant driving vector, $\bar{W} + \bar{U} + \bar{A}$, acting on the wedge

In Fig. 4.9 the resultant driving vector, $\bar{R} = \bar{W} + \bar{U} + \bar{A}$ has been combined with the friction cone diagram. $\bar{R} = \bar{W} + \bar{A} + \bar{U}$ lies outside of the friction cone, therefore sliding of the wedge will occur. The direction of sliding on the plane will be in the direction of the shear force, S. Sliding is along a line plunging 25° in a S 27° W direction (down an apparent dip slope). Note that this direction is not the same as the S 32° W direction of the resultant driving vector, $\bar{R}$.

The factor of safety is determined from the angular distances along this great circle. From $\bar{N}$ to $\bar{R}_L$, the angle is 40 degrees, while from $\bar{N}$ to $\bar{R}$ the angle is 75 degrees. The factor of safety is therefore:

$$\frac{\tan 40^\circ}{\tan 75^\circ} = 0.22$$

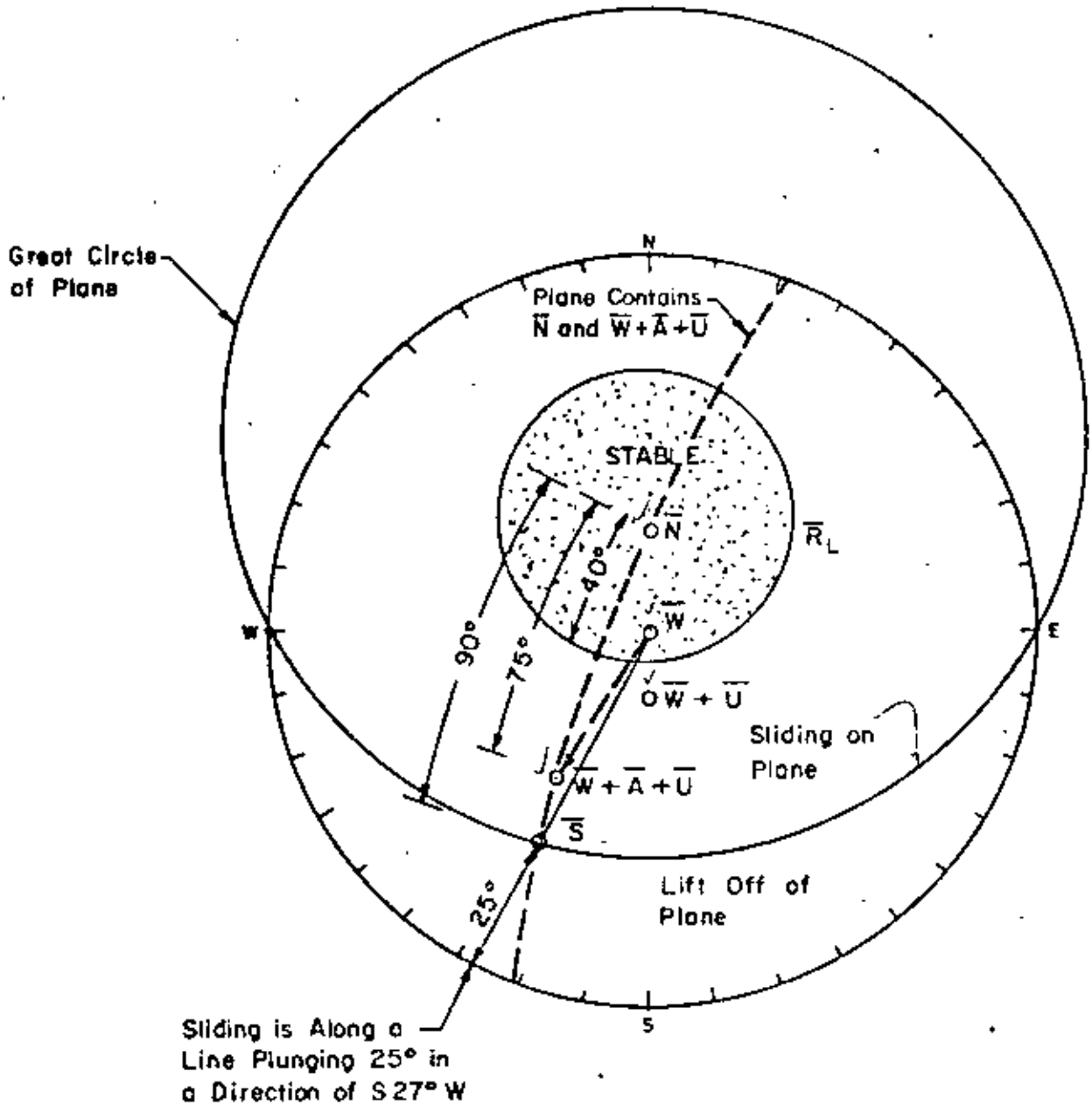

$$F.S. = \frac{\text{Tan } 40°}{\text{Tan } 75°} = 0.22$$

FIG. 4.9 THREE VECTORS ON SINGLE PLANE

4.3.5 Minimum force $\overline{NW}$ required to cause failure

The orientation of the minimum force, $\overline{NW}$, required to cause failure on an otherwise stable slope can be rapidly determined from the stereonet. To determine the magnitude of the minimum force, one auxiliary graphical construction is required (Fig. 4.10).

For the single 30° plane shown in Fig. 4.6, the wedge is stable under its own weight, $\bar{W}$. To reduce the factor of safety to unity, the angle between the weight, $\bar{W}$, and the limiting reaction, $\bar{R}_L$ must be closed. The minimum angle is 10 degrees and will be obtained when the driving forces cause sliding directly down-dip (to the south). Any other direction of sliding will result in a larger angle between $\bar{R}_L$ and $\bar{W}$ and therefore a larger value for $\overline{NW}$.

The minimum force, $\overline{NW}$ will therefore be directed to the south and will be directed upward 10 degrees so that it is normal to $\bar{R}_L$ (Fig. 4.10). The minimum force will be almost horizontal for the case of frictional sliding on a wedge loaded only by its own weight, where the factor of safety is near unity.

4.4 Sliding on Two Frictional Planes

4.4.1 General

The possible modes of failure of a wedge on two planes can be rapidly determined from the stereonet. The orientation of the driving forces determines whether sliding along the line of intersection of the planes or sliding on either one of the planes will occur. An example problem for sliding on two planes has been used to clarify the following discussion. The problem is illustrated in Figs. 4.11 through 4.15.

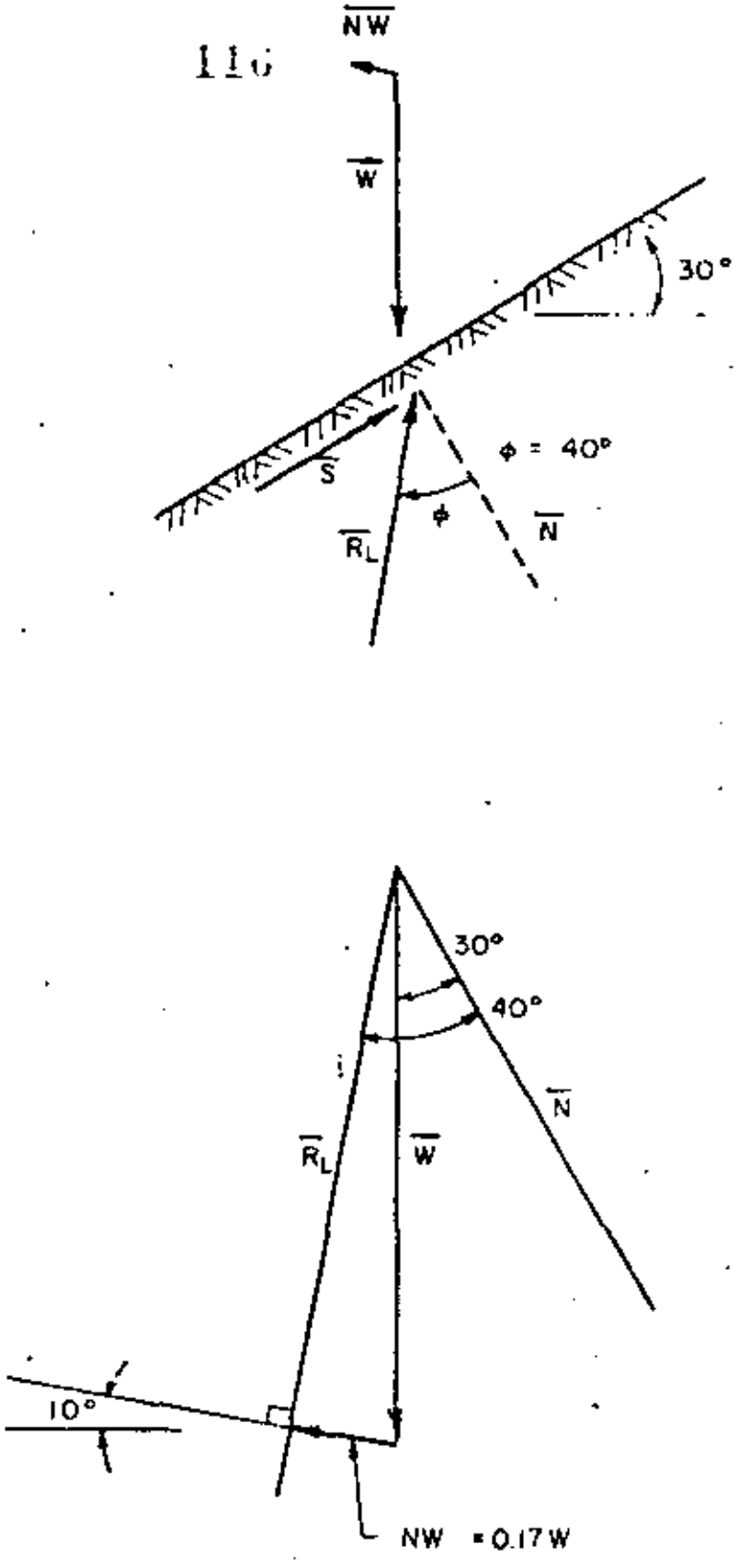

Force Polygon

FIG. 4.10 MINIMUM FORCE REQUIRED TO CAUSE FAILURE

4.4.2 Orientation of line of intersection of the two planes

The orientation of the line of intersection of two potential failure planes is determined using the stereonet as illustrated in Fig. 4.11. The great circles for the two planes are drawn on the stereonet and their intersection is determined as described in section 4.1. For the example problem illustrated in Fig. 4.11, the line of intersection is oriented S 27° W and plunges 40 degrees from the horizontal.

Figure 4.12 is a block diagram of the two planes, showing their line of intersection and the friction cones acting on each plane. For convenience, the friction cones are shown above the sliding plane.

4.4.3 Reaction forces on the failure planes

Stable and unstable zones are separated on the stereonet (Fig. 4.13) by the limiting reaction forces, $\bar{R}_{L_1}$ and $\bar{R}_{L_2}$. The unstable zones include zones for sliding down the intersection, sliding up the intersection, sliding on single planes, and lifting of the wedge off the planes. For the case of sliding on plane 1 alone, the orientation of $\bar{R}_{L_1}$, as defined by the friction cone on plane 1, separates the stable and unstable zones. For sliding along the intersection of planes 1 and 2, the orientation of $\bar{R}_{L_1} + \bar{R}_{L_2}$ separates the stable and unstable zones. The boundary between sliding on the intersection and sliding on plane 1 is the great circle which passes through $\bar{N}_1$ and $\bar{S}_1$, the normal and shear forces, respectively, on plane 1. This great circle represents a plane normal to plane 1 and parallel to the line of intersection.

4.4.4 Method of locating boundary between stable and unstable zones for the case of sliding along the line of intersection

The location of the resultant, $\bar{R}_{L_1} + \bar{R}_{L_2}$, must be determined in

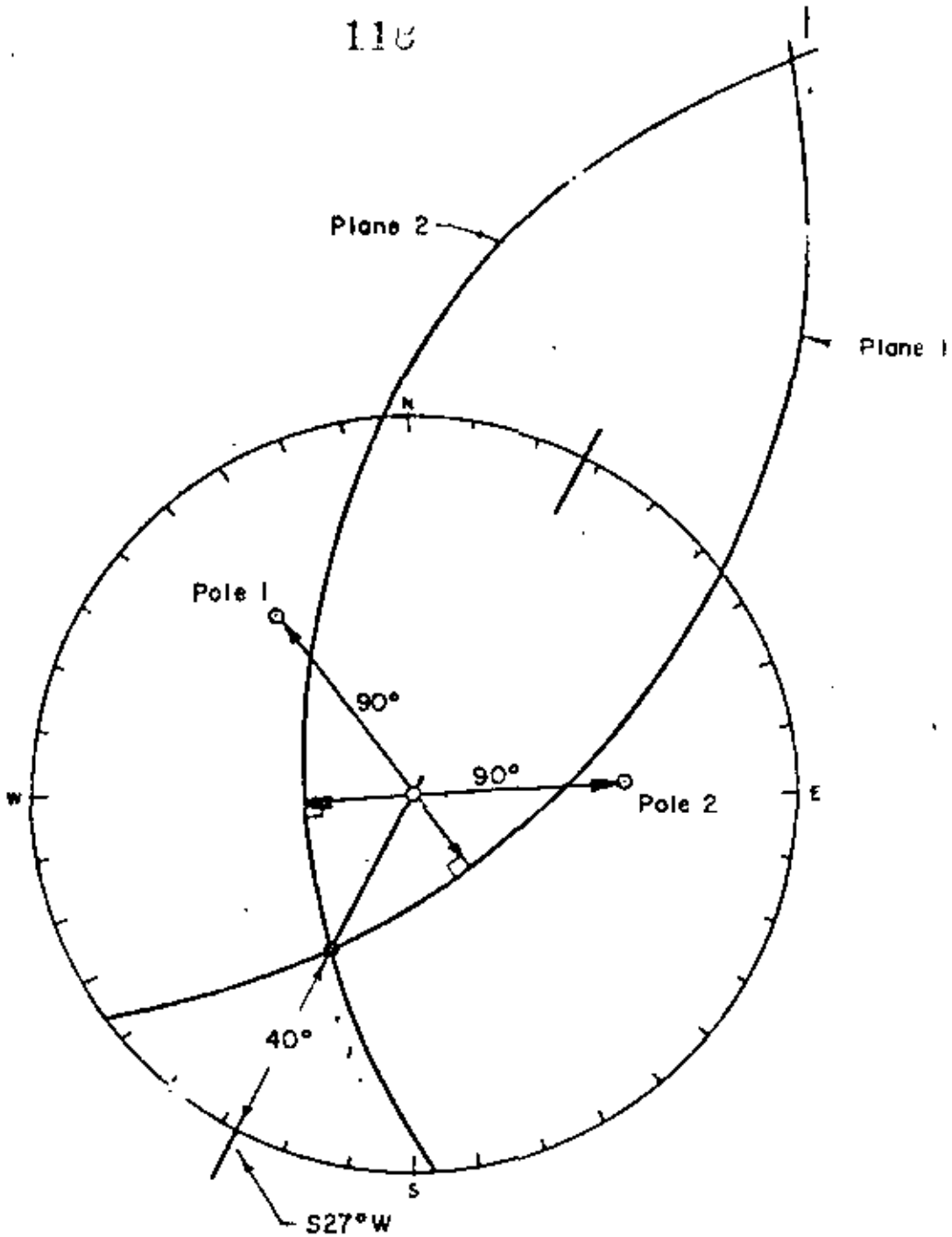

Given :

Plane 1 : Strike N54°E, Dip 62° SE, $\phi = 20°$
Plane 2 : Strike N04°W, Dip 59° SW, $\phi = 40°$

FIG. 4.11 SLIDING ON TWO PLANES : ORIENTATION OF LINE OF INTERSECTION

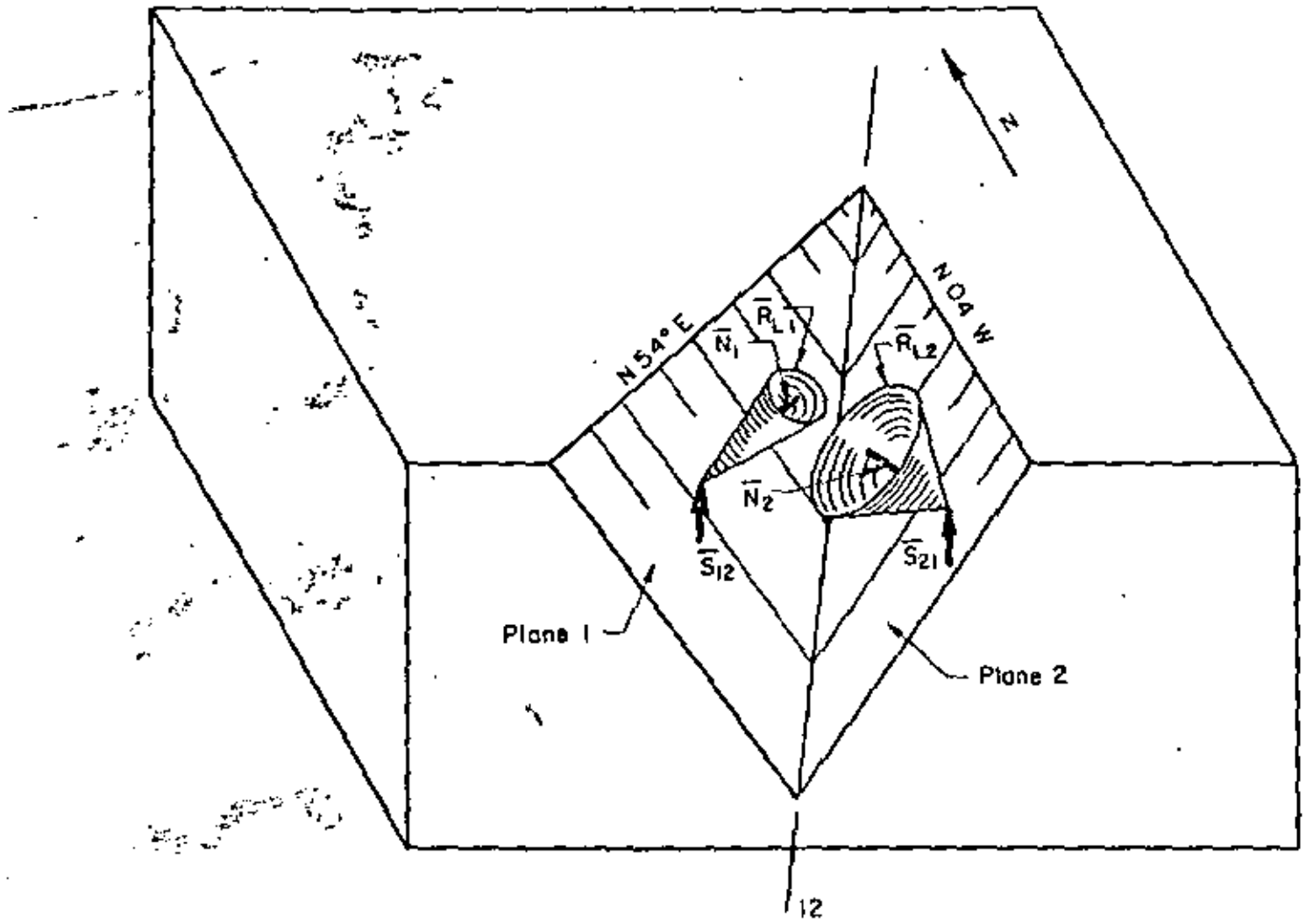

FIG. 4.12 SLIDING ON TWO PLANES : BLOCK DIAGRAM

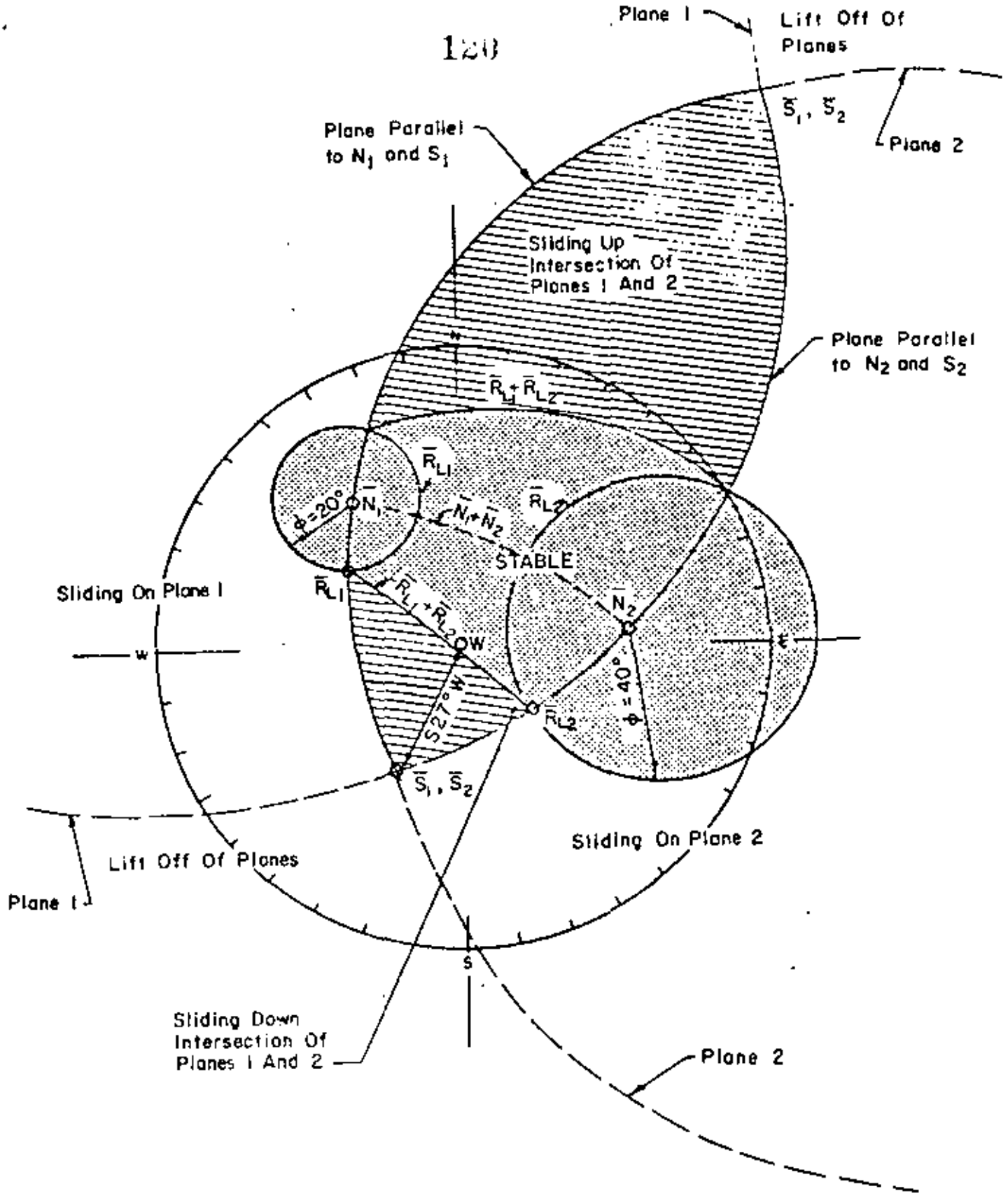

FIG. 4.13 SLIDING ON TWO PLANES : STEREONET

order to outline the stable and unstable zones for the case of sliding along the line of intersection. The shear forces on planes 1 and 2 will act in the direction of sliding, which in this case is parallel to the line of intersection. Therefore, the shear forces, $\bar{S}_1$ and $\bar{S}_2$, will both plot on the stereogram at the same point as does the line of intersection (point $\bar{S}_1$, $\bar{S}_2$ in Fig. 4.13).

The direction of the reaction force on each plane is known, since the direction of its components, the normal and shear forces on that plane, are fixed. The reaction force, $\bar{R}_{L_1}$, must act within the plane in which $\bar{N}_1$ and $\bar{S}_1$ act. Therefore, the direction of the reaction force, $\bar{R}_{L_1}$, can be located by drawing a great circle through $\bar{N}_1$ and $\bar{S}_1$. $\bar{R}_{L_1}$ is located where this circle intersects the friction cone of plane 1. Similarly, $\bar{R}_{L_2}$ is located where the great circle drawn through $\bar{N}_2$ and $\bar{S}_2$ intersects the friction cone of plane 2. No matter what driving forces act on the wedge, as long as the limiting case of sliding along the intersection is considered, then the orientation of both $\bar{R}_{L_1}$ and $\bar{R}_{L_2}$ are fixed.

If $\bar{R}_{L_1}$ and $\bar{R}_{L_2}$ are summed, their resultant, $\bar{R}_{L_1} + \bar{R}_{L_2}$, must act in a plane parallel to $\bar{R}_{L_1}$ and $\bar{R}_{L_2}$. This plane can be located on the stereonet of Fig. 4.13 by drawing a great circle through $\bar{R}_{L_1}$ and $\bar{R}_{L_2}$. For sliding along the intersection of plane 1 and 2, the reaction $\bar{R}_{L_1} + \bar{R}_{L_2}$ will be located somewhere on this great circle, but its position along the great circle will depend on the orientation of the driving forces acting on the wedge, since the orientation of the driving vector affects the relative magnitudes of $\bar{R}_{L_1}$ and $\bar{R}_{L_2}$. Should the orientation of the resultant vector forces lie outside the stable zone outlined by $\bar{R}_{L_1} + \bar{R}_{L_2}$, then sliding will occur on the intersection of the two planes.

In Fig. 4.13, the weight vector, $\bar{W}$, is located just within the stable zone. Only a very small force directed toward the south would be required to move the driving vector out of the stable zone and cause sliding down the line of intersection of planes 1 and 2.

4.4.5 Minimum force ($\overline{NW}$) required to cause sliding of the wedge

In order to cause sliding of the wedge, the resultant driving vector must lie outside the stable zone. The minimum force, $\overline{NW}$ required to cause sliding can be determined by means which is directly analogous to the method for determining the minimum force for sliding on a single plane (Refer to Section 4.3.4). To close the force polygon (and obtain a factor of safety of one) a force must be added which connects the tip of the existing vector (Weight, $\bar{W}$, in this case) to the plane of the reaction, $\bar{R}_{L_1} + \bar{R}_{L_2}$. The minimum force will be the one acting normal to the plane of $\bar{R}_{L_1} + \bar{R}_{L_2}$ as shown in Fig. 4.14.

The orientation of the minimum force can be determined from the stereonet. Its magnitude can be determined by graphical construction of the force polygon (such as Fig. 4.14). In Fig. 4.14, the minimum angle between $\bar{W}$ and $\bar{R}_{L_1} + \bar{R}_{L_2}$, which must be closed for a factor of safety of one, is 4 degrees. The minimum force is also directed upward (in this case at an angle of 4°) in order to intersect the plane of $\bar{R}_{L_1} + \bar{R}_{L_2}$ at right angles. Note that the strike of the minimum force (in this case S40W) is not the same as the strike of the line of intersection (in this case S27W). In general, the minimum force, $\overline{NW}$, will not be oriented directly along the strike of the line of intersection unless the wedge is acted on only by its own weight and the friction angles on the two planes are the same.

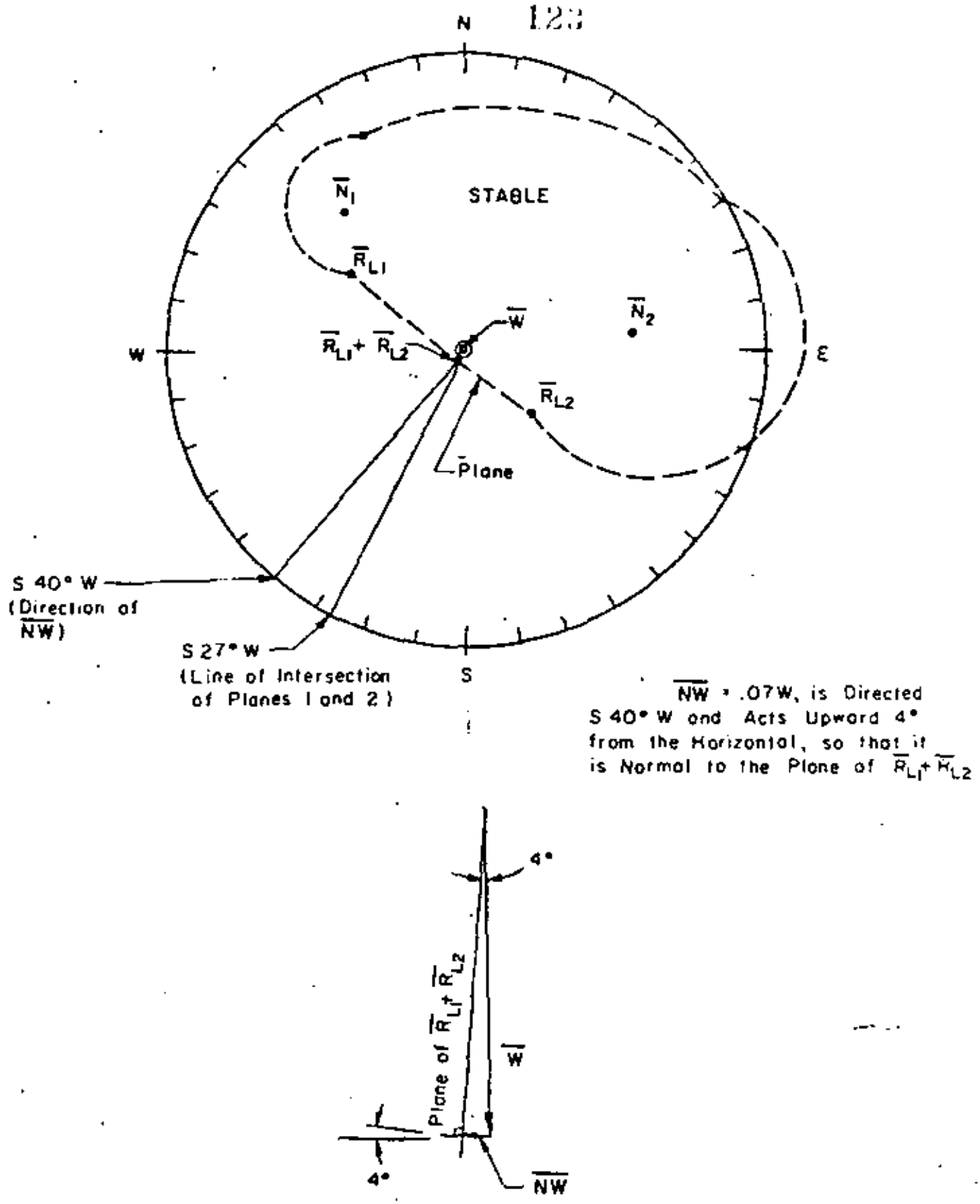

FIG. 4.14 SLIDING ON TWO PLANES: MINIMUM FORCE REQUIRED TO CAUSE SLIDING

It should be noted that the difference in magnitude between the minimum force, $\overline{NW}$, and the force $\overline{NW}$ directed horizontally and parallel to the strike of the line of intersection will be very small in most cases, particularly for cases when the primary force acting on the wedge is its own weight, and the factor of safety is only slightly greater than one. In these cases, a reasonable (but slightly unconservative) approximation is that $\overline{NW}$ acts horizontally, parallel to the strike of the line of intersection.

4.4.6 Factor of safety and minimum forces required to stabilize the wedge

Two separate conditions exist for determination of the factor of safety of the wedge and the forces required to stabilize the wedge. Consider the two conditions illustrated in Fig. 4.15: case 1, where the wedge is acted on by a driving force, $\bar{D}$, causing sliding on a single plane (plane 1), and case 2, where the wedge is acted on by a driving force, $\bar{B}$, causing sliding along the line of intersection of planes 1 and 2.

Case 1: The wedge is acted upon by the driving force, $\bar{D}$, and will slide on plane 1 alone. There will be no normal force on plane 2. In this case, the orientations of both the normal force, $\bar{N}_1$, on plane 1, and the driving force, $\bar{D}$, are known, while the orientation of the shear force, $\bar{S}_1$, and the reaction, $\bar{R}_{L_1}$, on plane 1 remain to be determined. $\bar{S}_1$ and $\bar{R}_{L_1}$ are known to act within the plane of $\bar{N}_1$ and $\bar{D}$. Thus, their position is obtained by drawing a great circle (solid line in Fig. 4.15a) through $\bar{N}_1$ and $\bar{D}$, then locating $\bar{S}_1$ at 90 degrees from $\bar{N}_1$ and locating $\bar{R}_{L_1}$ at ϕ degrees from $\bar{N}_1$, along the great circle. In the example shown, the angle between $\bar{N}_1$ and $\bar{R}_{L_1}$ is $\phi = 20^\circ$, and the angle between

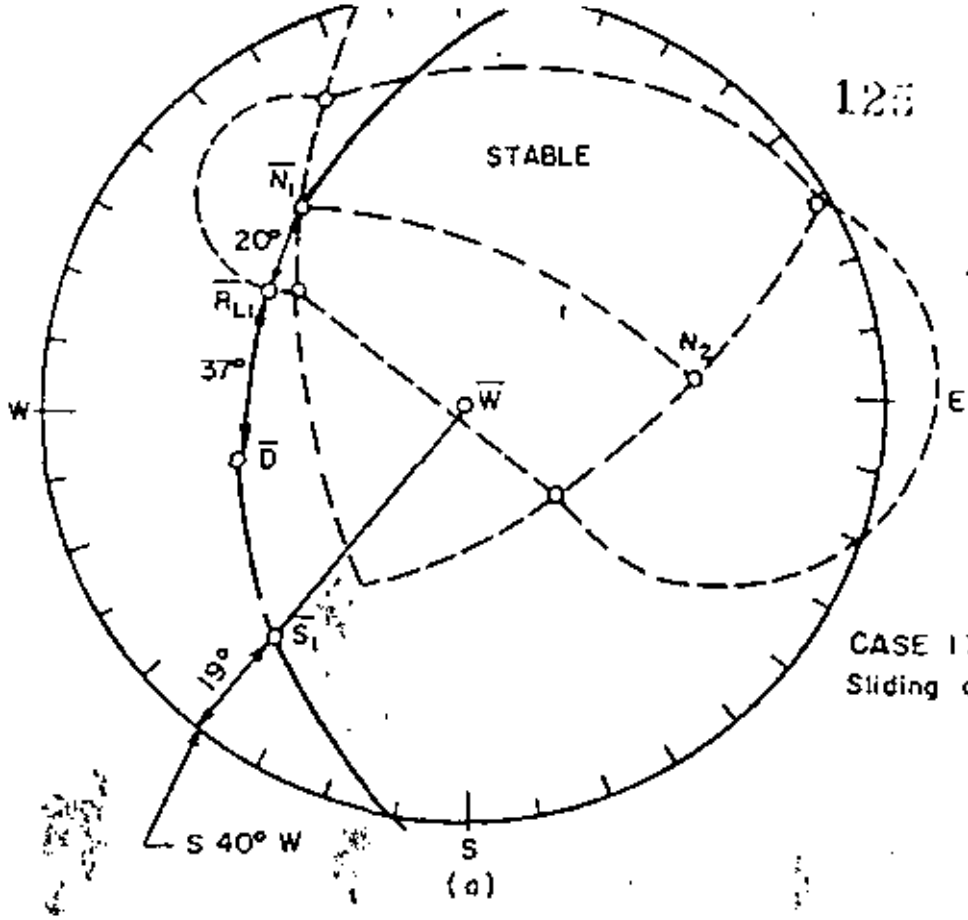

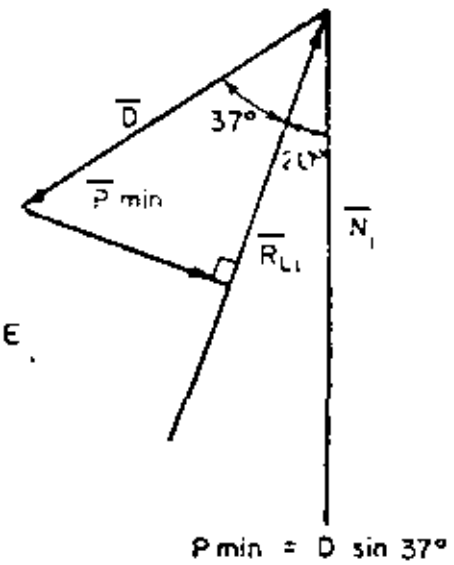

CASE 1:
Sliding on Plane 1

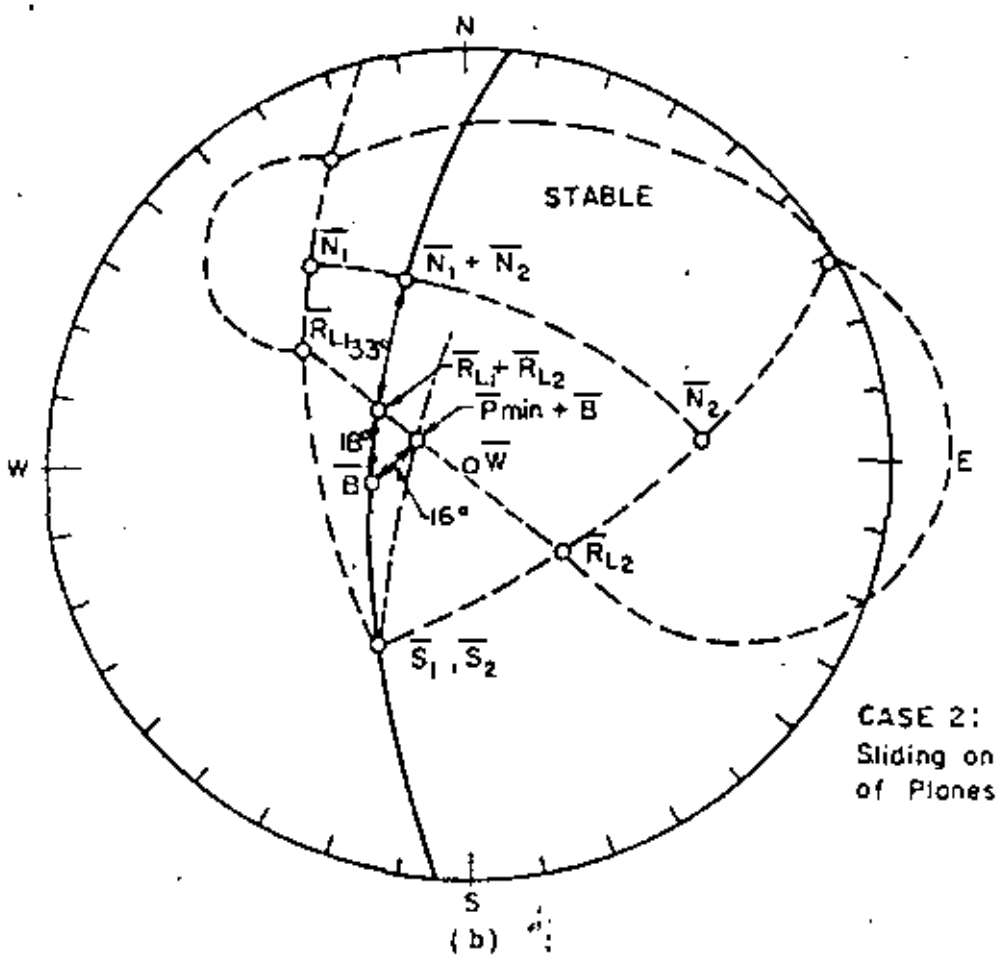

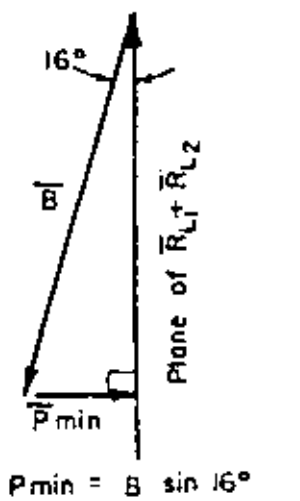

CASE 2:
Sliding on Intersection
of Planes 1 & 2

FIG. 4.15 MINIMUM FORCES REQUIRED TO STABILIZE THE WEDGE

$\bar{R}_{L_1}$ and $\bar{D}$ is 37°. Therefore, the factor of safety is:

$$F.S. = \frac{\text{Maximum shear force available}}{\text{Actual shear force mobilized}} = \frac{\tan 20^\circ}{\tan (20^\circ + 37^\circ)} = 0.24$$

(Refer to Fig. 4.15a.) Sliding of the wedge will be in the direction of the shear force, S, in this case plunging 19° in a direction S 40° W, on plane 1.

The magnitude of the minimum force, $\bar{P}$, required to close the 37° angle between $\bar{R}_{L_1}$ and $\bar{D}$ (and thereby increase the factor of safety to one) can be determined from the graphical construction in Fig. 4.15a. If the magnitude of $\bar{D}$ is known, then the minimum force is:

$$P_{min} = D \sin 37^\circ$$

Case 2: The wedge is acted upon by the driving vector, $\bar{B}$, and will slide on the intersection of planes 1 and 2. The direction of the shear forces, $\bar{S}_1$ and $\bar{S}_2$, are fixed parallel to the line of intersection of planes 1 and 2, while the positions of $\bar{N}_1 + \bar{N}_2$ and $\bar{R}_{L_1} + \bar{R}_{L_2}$ remain to be determined. They can be found by drawing a great circle (solid line in Fig. 4.15b) through $\bar{S}_1$, $\bar{S}_2$ and $\bar{B}$. $\bar{R}_{L_1} + \bar{R}_{L_2}$ is located at the intersection of this great circle and the great circle through $\bar{R}_{L_1}$ and $\bar{R}_{L_2}$. $\bar{N}_1 + \bar{N}_2$ is located at the intersection of the great circle through $\bar{S}_1 + \bar{S}_2$ and $\bar{B}$, and the great circle through $\bar{N}_1$ and $\bar{N}_2$.

The factor of safety in this case is determined by the 51° angle between $\bar{N}_1 + \bar{N}_2$ and $\bar{B}$ and the 33° angle between $\bar{N}_1 + \bar{N}_2$ and $\bar{R}_{L_1} + \bar{R}_{L_2}$. The factor of safety is therefore:

$$F.S. = \frac{\tan (33^\circ)}{\tan (33^\circ + 18^\circ)} = \frac{\tan 33^\circ}{\tan 51^\circ} = .53$$

The direction of sliding is along the line of intersection, S 27° W.

downdip at 40°.

The concept of a factor of safety is somewhat misleading in this case, because the force required to stabilize the wedge does not have to close the 18° angle between $\bar{R}_{L_1} + \bar{R}_{L_2}$ and $\bar{B}$. Instead, the minimum force, P_{min} is B sin 16°. Note that the new resultant driving vector, $\bar{P}_{min} + \bar{B}$, acts in a plane which is different from the plane in which $\bar{B}$ originally acted.

4.5 Sliding of a Wedge Bounded by Three Planes

The case for sliding of a wedge bounded by three or more planes is only slightly more complicated than the case for a wedge bounded by two planes. With three planes another friction circle is added to the stereonet. Depending on the orientation of the driving forces, sliding will occur on any one of the three planes, on any one of the three lines of intersection, or the wedge will lift off the three planes. Methods for determining the minimum forces to cause sliding, for determining factors of safety, etc., are identical to those described for the two plane case (section 4.4). Prior to performing the stability analysis, a basic decision must be made as to which planes are potential sliding planes and which wedges are critical.

Figures 4.16 and 4.17 illustrate the three plane case. The orientations and friction angles for the three planes are given in the block diagram of Fig. 4.16. The corresponding stereonet is illustrated in Fig. 4.17. For this case it is readily apparent that, regardless of the presence of the third plane, the wedge is still closest to a failure by sliding (under its own weight) along the intersection of planes 1 and 2. In order for failure to occur by sliding up plane 3, or by

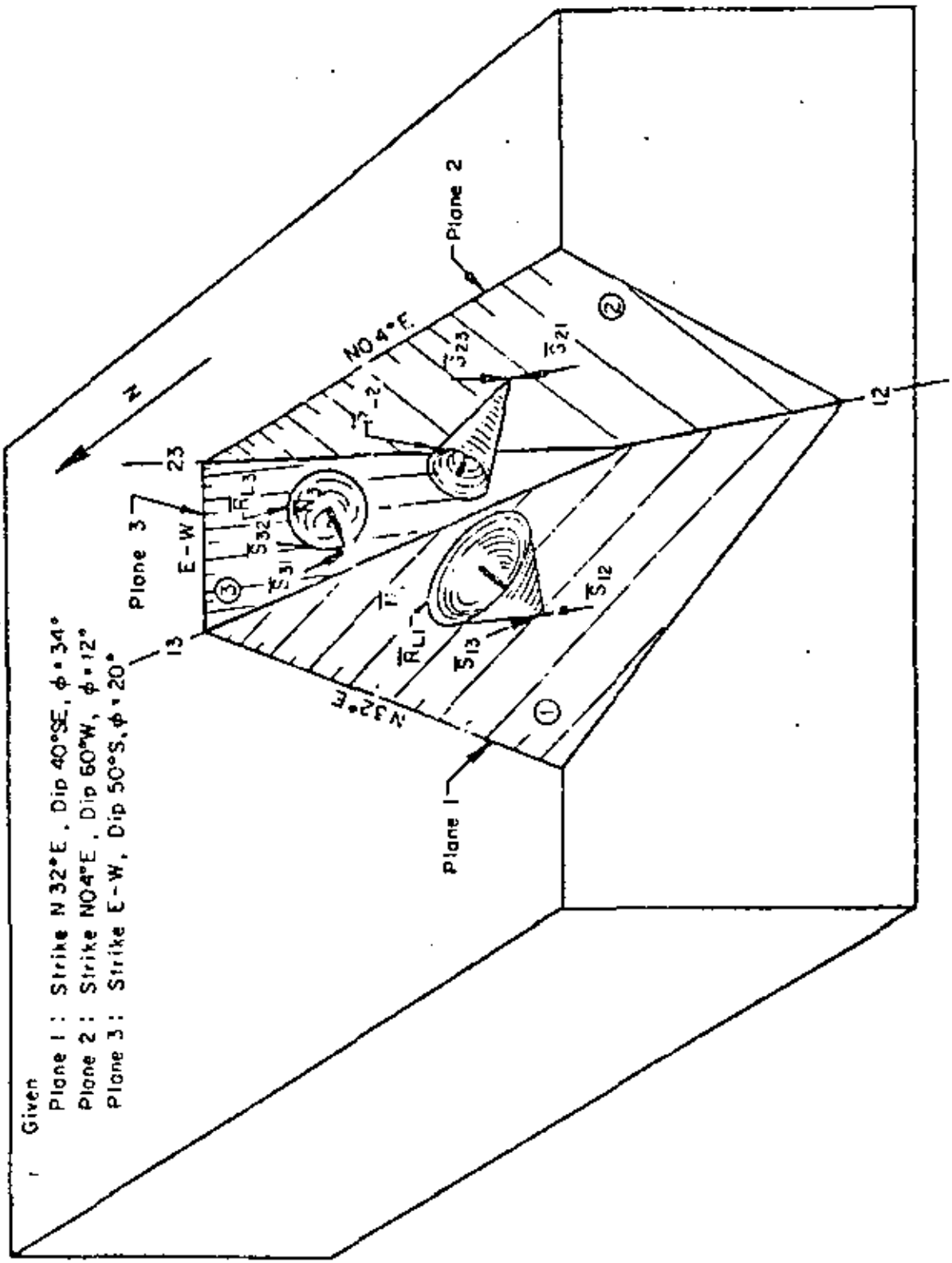

FIG 4.16 WEDGE BOUNDED BY THREE PLANES : BLOCK DIAGRAM

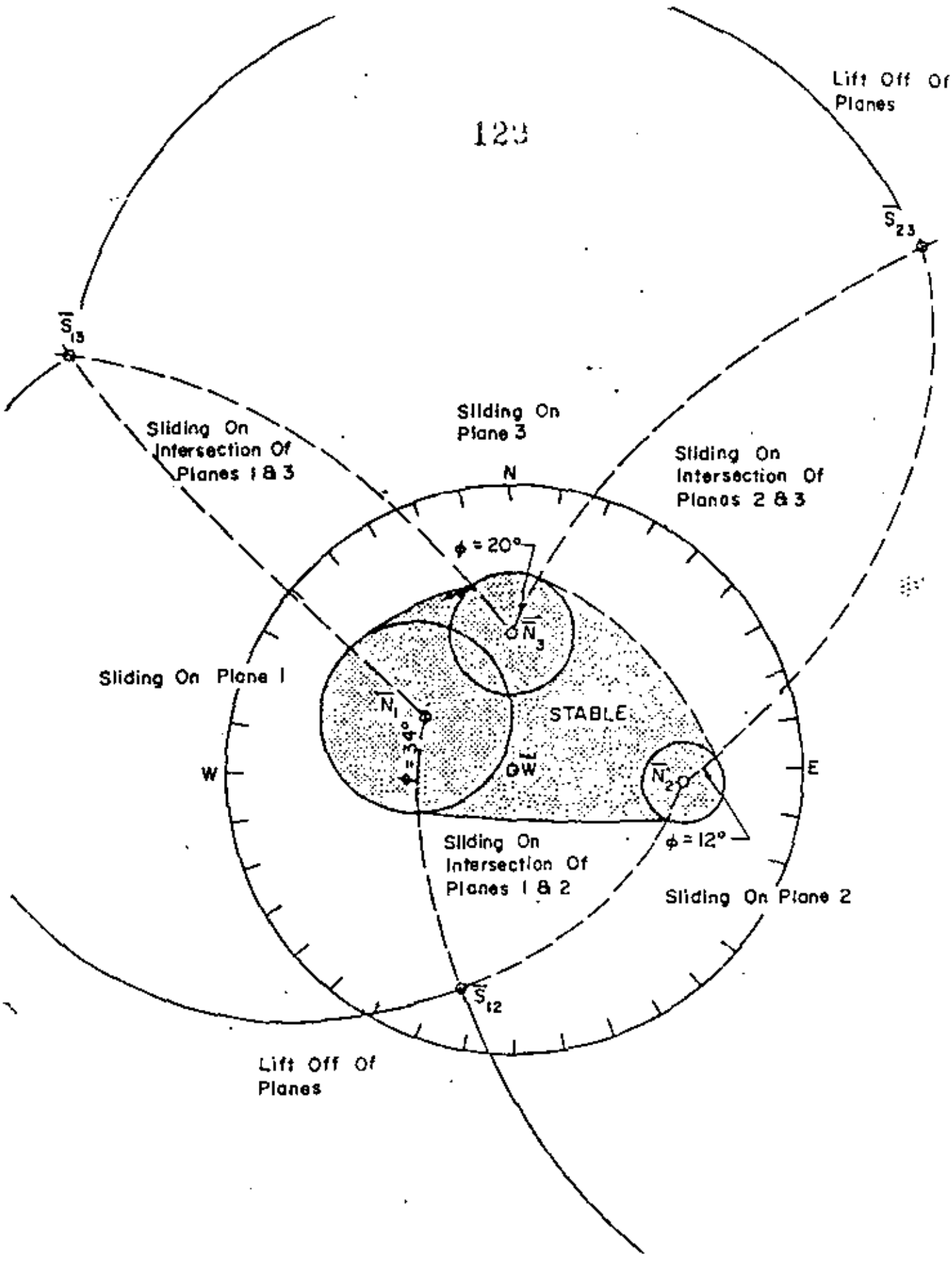

FIG. 4.17 WEDGE BOUNDED BY THREE PLANES: STEREONET

sliding along the intersection of plane 3 and 1, or by sliding along the intersection of plane 3 and 2, an appreciable driving force acting upward (toward the North) would be required.

4.6 Wedge Bounded by Three Planes but Daylighted by Cut Face

Although the wedge bounded by planes 1, 2, and 3 is stable for the condition illustrated in Fig. 4.17, it will not be stable if plane 3 is daylighted at the base and sides of the cut, as shown in Fig. 4.18. Cases similar to this will commonly occur in rock masses where joint sets form multiple wedges, rather than a single wedge.

If planes 1 and 2 are present, as shown in Fig. 4.18a, then wedge A would still be stable under its own weight, as was previously shown in Fig. 4.17. However, if plane 3 is daylighted at the edge of the cut, then plane 2 no longer restrains wedges A and B, thus sliding will occur along the intersection of planes 1 and 3, as indicated in the stereonet of Fig. 4.18b.

Another possible mode of failure would be for wedges A and B (acting as a single wedge) to rotate away from the line of intersection of planes 1 and 3 and slide on plane 3 alone. This is likely to occur if the mass of the wedges is concentrated over plane 3, away from the line of intersection of planes 1 and 3. (Rotational wedge failures are analyzed in section 4.7.)

Another possibility is that wedges A and B would break up and slide as individual blocks, wedge A possibly sliding on the intersection and wedge B sliding on plane 3 alone.

When the planes represent joint sets rather than single discontinuities, then modes of failure similar to those described above become

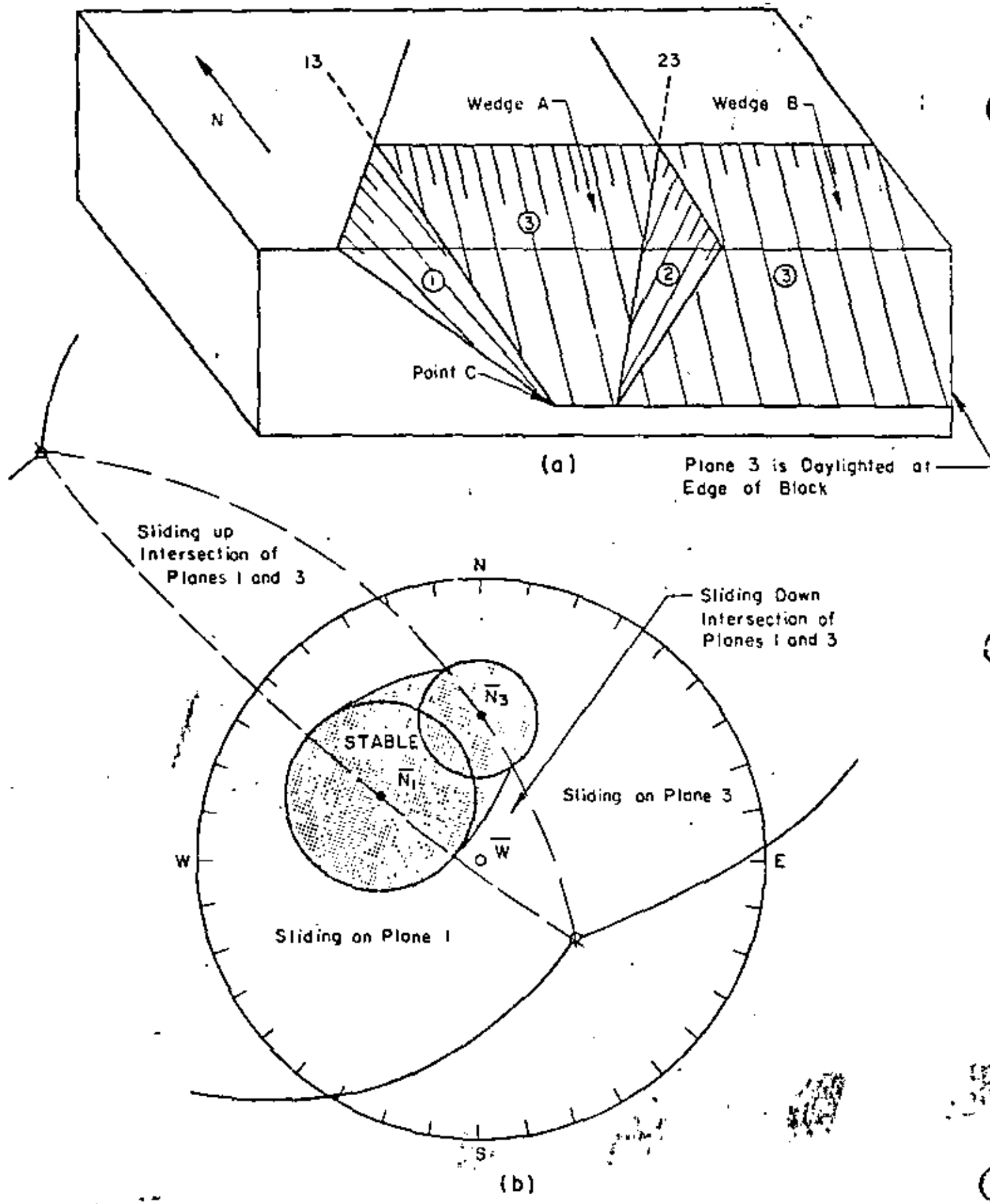

FIG 4.18 WEDGE BOUNDED BY THREE PLANES: PLANE 3 DAYLIGHTED AT EDGE OF BLOCK

quite possible. Some of the joints within a set may daylight on the sides or edges of slopes and allow failure of wedges on single planes rather than multiple planes. Joints of other sets may also free the edges of wedges, facilitating sliding on a single plane. In general, a lower factor of safety will be obtained if the mass has a tendency to move as several rigid bodies broken up by the joint sets, rather than moving as a single rigid body. It is very important that these possibilities be considered during the exploratory phase of the slope stability study, prior to selecting the critical wedges on which the stability analyses will be performed.

4.7 Rotation of Wedge on Plane 3

The factor of safety against rotation of a wedge can be estimated using the stereonet if the point of application of the driving forces on the failure plane is known. Consider the example of Fig. 4.19. The wedge illustrated here is the same as the wedge of Fig. 4.18 except for an increase in the angle of friction on plane 1 from 34° to 40°, so that the wedge is now stable against sliding under its own weight down the intersection of planes 1 and 3. It is assumed for a rotational failure that the wedge rotates about point C, at the base of the slope. It is also assumed that the limiting shear and normal stresses on plane 3 can be summed as forces $\bar{N}_3$ and $\bar{S}_3$, acting at point D (at the point of intersection of the resultant driving vector, $\bar{W}$, with plane 3). This implies that there is no variation in the angle of friction on plane 3. Based on these assumptions the direction of the shear force, $\bar{S}_3$, will be perpendicular to line $\overline{CD}$, as shown in Fig. 4.19.

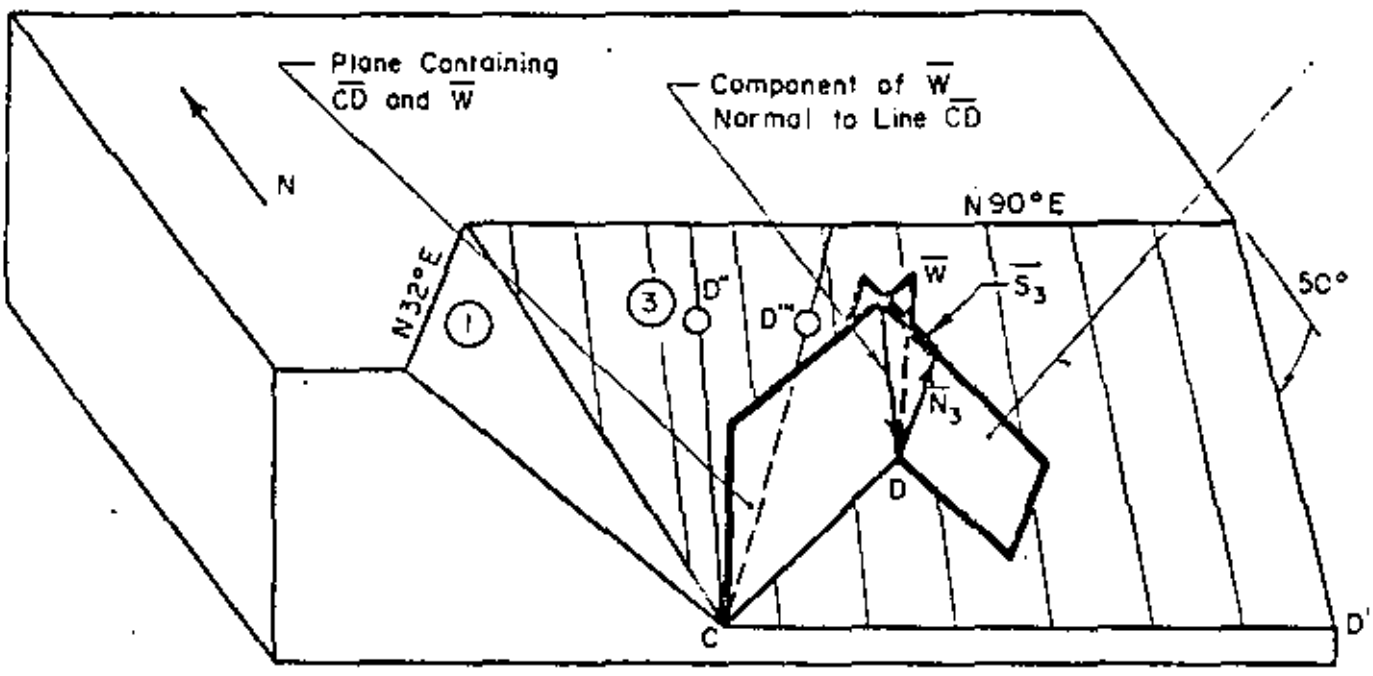

C is Center of Rotation of Wedge

D is Point of Intersection of Driving Force ($\overline{W}$) With Plane 3

(a)

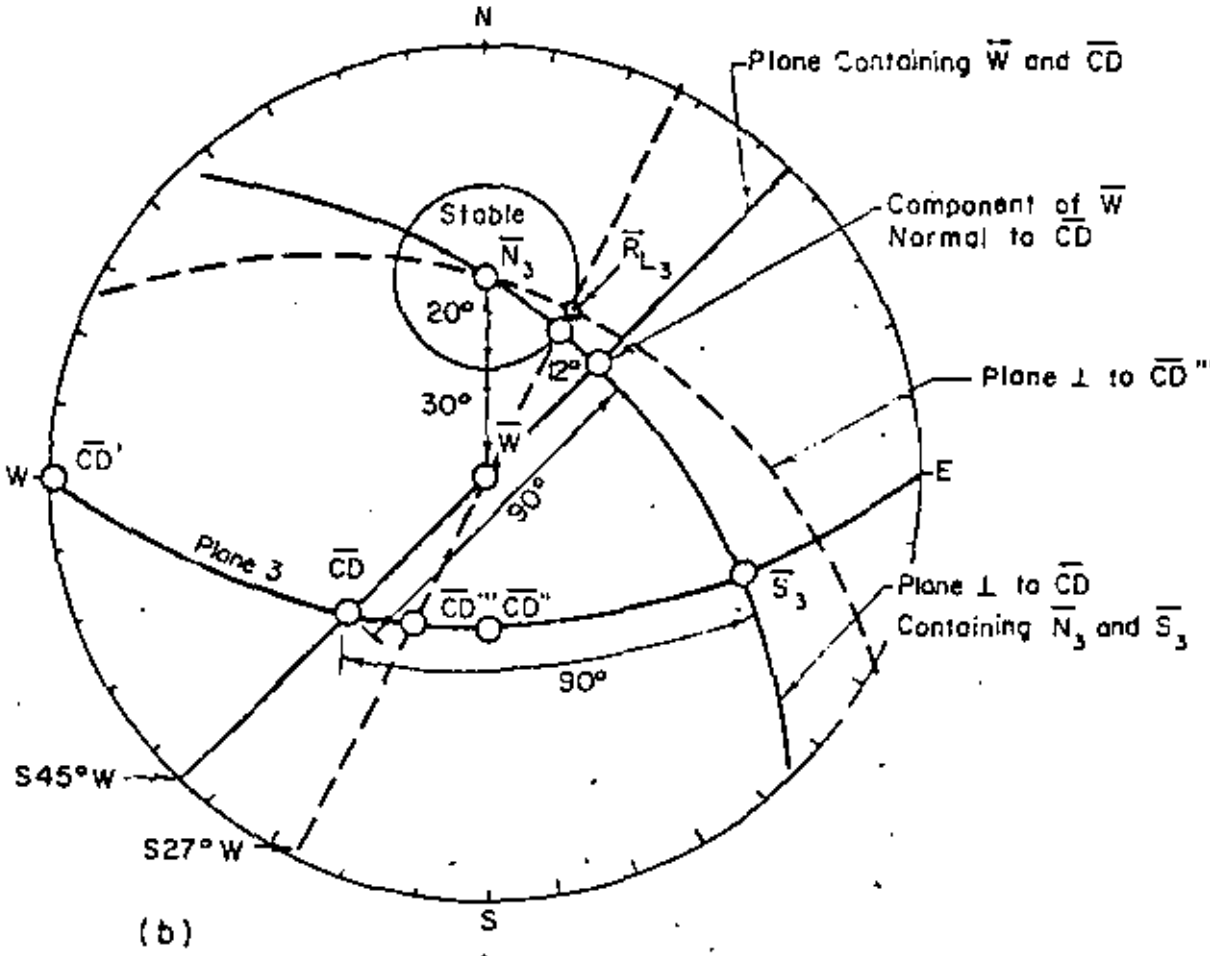

(b)

FIG. 4.19 ROTATION OF WEDGE ON PLANE 3

The given conditions for the wedge of Fig. 4.19a are:

Plane 1: Strike N32°E, dip 40°SE, $\phi = 40^\circ$

Plane 3: Strike E-W, dip 50°S, $\phi = 20^\circ$

In addition, it is assumed that the center of gravity of the wedge is known, so that the orientation of line $\overline{CD}$ is known. Line $\overline{CD}$ is the moment arm from the center of rotation, C, to the point of intersection of the weight vector, $\bar{W}$, with plane 3 (point D). Its orientation is assumed to be S45°W on plane 3.

It is immediately apparent from the given conditions on planes 1 and 3 that the wedge, under its own weight, $\bar{W}$, is stable against sliding on plane 1 alone, since the dip of plane 1 equals the angle of friction on plane 1 (40°). The wedge is therefore also stable against sliding on the intersections of planes 1 and 3.

The wedge is not stable against sliding on plane 3 alone, since the dip of that plane exceeds its angle of friction. If the wedge were to extend an infinite distance to the right of the diagram, then the wedge would behave as if it were sliding on plane 3 alone, since all of the weight of the wedge would be over plane 3 and an infinitesimal portion of the weight would act on plane 1. In this case the moment arm for rotation of the wedge would extend parallel to the strike of plane 3 (line CD'). Thus the shear force, $\bar{S}_3$, would act directly up the dip-slope of plane 3, the identical condition for sliding on a single plane. The factor of safety against rotational sliding would be:

$$F.S. = \frac{\text{RESISTING MOMENT}}{\text{DRIVING MOMENT}} = \frac{\overline{CD'}\ (W \tan 20^\circ)}{\overline{CD'}\ (W \tan 50^\circ)} = \frac{\tan 20^\circ}{\tan 50^\circ} = 0.3$$

the identical factor of safety for sliding directly down plane 3.

Another extreme would be the case where the weight of the wedge was concentrated near the intersection of planes 1 and 3 so that the moment arm extended directly up-slope on plane 3 (line CD''). The limiting shear force, $\bar{S}_3$, in this instance would be directed along the strike of plane 3. The driving force, $\bar{W}$, has no component in this direction, so that rotation would not occur, regardless of the frictional resistance on plane 3. The factor of safety against rotation is therefore:

$$F.S. = \frac{\overline{CD''}(\tan 20^\circ)}{\overline{CD''}(\tan 0^\circ)} = \infty$$

An intermediate case, where line CD is directed S45°W on plane 3, is shown in the stereonet of Fig. 4.19. The rotational stability of the wedge is determined as follows: The great circle representing plane 3 is drawn on the stereonet, as well as the normal force and friction circle for plane 3. Line $\overline{CD}$ is located in its given direction on the stereonet at the intersection of plane 3 and a vertical plane oriented S45°W. $\bar{S}_3$ is then located on plane 3, at a 90° angle from line $\overline{CD}$. A great circle is then drawn through $\bar{S}_3$ and $\bar{N}_3$, representing the plane containing $\bar{S}_3$ and $\bar{N}_3$. This great circle will also be located 90° from $\overline{CD}$, along a great circle (in this case a straight line) passing through $\overline{CD}$ and $\bar{W}$. The component of $\bar{W}$ which is normal to $\overline{CD}$ is located at this point. The factor of safety against rotation is:

$$F.S. = \tan \phi / \tan (\text{angle between } \bar{N}_3 \text{ and the component of } \bar{W} \perp \text{ to } \overline{CD})$$

$$= \frac{\tan 20^\circ}{\tan (20^\circ + 12^\circ)} = \frac{\tan 20^\circ}{\tan 32^\circ} = .58$$

Although the wedge is stable against sliding along the intersection of planes 1 and 3, it is unstable for the case of rotation on plane 3.

However, the factor of safety against rotation (F.S. = 0.58) is still appreciably higher than the factor of safety against sliding on plane 3 alone (F.S. = 0.30).

In order for the factor of safety against rotation on plane 3 to be equal to one, the center of gravity must be located so that line $\overline{CD'''}$ is oriented S27°W on plane 3, as indicated by the dashed line tangent to the friction circle in the stereonet of Fig. 4.19.

CHAPTER FIVE

DYNAMIC STABILITY OF ROCK SLOPES

5.1 Introduction

The stability of rock slopes subjected to dynamic loads has usually been treated as a pseudo-static problem by engineers assessing the "dynamic factor of safety." In this approach, the dynamic forces on a potential sliding mass of weight W are assumed to be equivalent to a horizontal force of $\overline{KW}$ acting through the center of gravity toward the free surface of the slope. The constant K is called the seismic coefficient, the value of which is commonly taken between 0.05 and 0.20 for earthquake design in seismically active areas. If this method is used, the factor of safety is computed by the methods outlined in Chapters 3 and 4 for static problems. The only adjustment which has to be made is that the resultant force R acting on a three dimensional tetrahedron includes not only the weight and pore pressures, but also the force $\overline{KW}$ directed in a horizontal direction. Wittke (1965) has presented this type of analysis to assess the dynamic stability of slopes and has suggested that the horizontal force $\overline{KW}$ be directed along the line of intersection of the two planes on which sliding takes place for the most critical effect. The meaning of the factor of safety calculated for dynamic loading is somewhat nebulous however because the dynamic forces are not constant static forces acting in one direction. The actual factor of safety of a slope subjected to dynamic loading varies with time, and movements of the slope only occur when the factor of safety is momentarily below 1.0. Thus the average factor of safety computed

from a pseudo-static analysis using the seismic coefficient K is not meaningful because the analysis does not indicate the magnitude of the strains or displacements which may develop in the slope. An estimate of the displacement or strain in the slope after shaking enables the engineer to make a judgment on whether the displacements are harmful in terms of either structural damage or are large enough to cause a considerable decrease in shear strength of the slope materials.

In this chapter the basic analysis given by Newmark (1965) for the dynamic analysis of earth slopes is modified to assess the displacement rock slopes might experience under dynamic loadings. A criterion is also given for determining if the computed displacement may be harmful to the stability of the slope.

5.2 Dynamic Analysis of Rock Slopes

The first step in the dynamic analysis of a rock slope is to evaluate the dynamic resistance of the slope. The dynamic resistance is defined as the minimum force applied through the center of gravity of the potential sliding mass which will just begin to move the mass above the assumed failure surface. The dynamic resistance is usually denoted by $\overline{NW}$ (Fig. 3.4a) where N is a coefficient and W is the weight of the potential sliding mass. Physically the dynamic resistance is the minimum shearing resistance which can be mobilized, in addition to that required for static stability, to resist the effects of a dynamic load.

For the three dimensional analysis of rock slopes, as shown in Figs. 3.4 and 3.5, the problem is to find the direction which will minimize N and solve for the magnitude of $\overline{NW}$. Graphical and analytical procedures have been developed for finding the minimum dynamic resistance in

sections 3.2.2 and 3.4.2 respectively.

The quantity Ng is the steady acceleration in the direction of $\overline{NW}$ which will just overcome the resistance of the sliding mass. If the maximum acceleration Ag in the area of the slope is less than Ng then the slope is definitely safe. However, if Ag exceeds Ng, the slope does not necessarily fail because the ground acceleration may only exceed Ng for a very short period of time. During this time, a relative displacement occurs between the portions above and below the failure surface Figure 5.1 shows a plot of the ground motions observed during the 1940 El Centro earthquake. Note that the maximum acceleration, Ag (= $\ddot{y}_o$), of 0.32 g occured only for a short period of time and also note that if a slope in the area of this record had a dynamic resistance, $\overline{NW}$, of 0.2 W that the dynamic resistance would only be exceeded for very short periods of time during 6 pulses. Although some relative displacement would occur during these short times the slope would not necessarily fail. Newmark's method of analysis provides a means of calculating the displacements which occur for the case when A> N.

The following example illustrates Newmark's analysis for the case of a single acceleration pulse acting on the base beneath a sliding mass with a rigid plastic resistance between the base and mass with a resistance of $\overline{NW}$.

Consider the rigid body shown in Fig. 5.2 having a weight W, mass M, and having a motion x. The motion of the ground on which the mass rests is designated by y(t), where y is a function of time t. The relative motion of the mass, compared with that of the ground, is given by u, where

$$u = x - y \qquad (5.1)$$

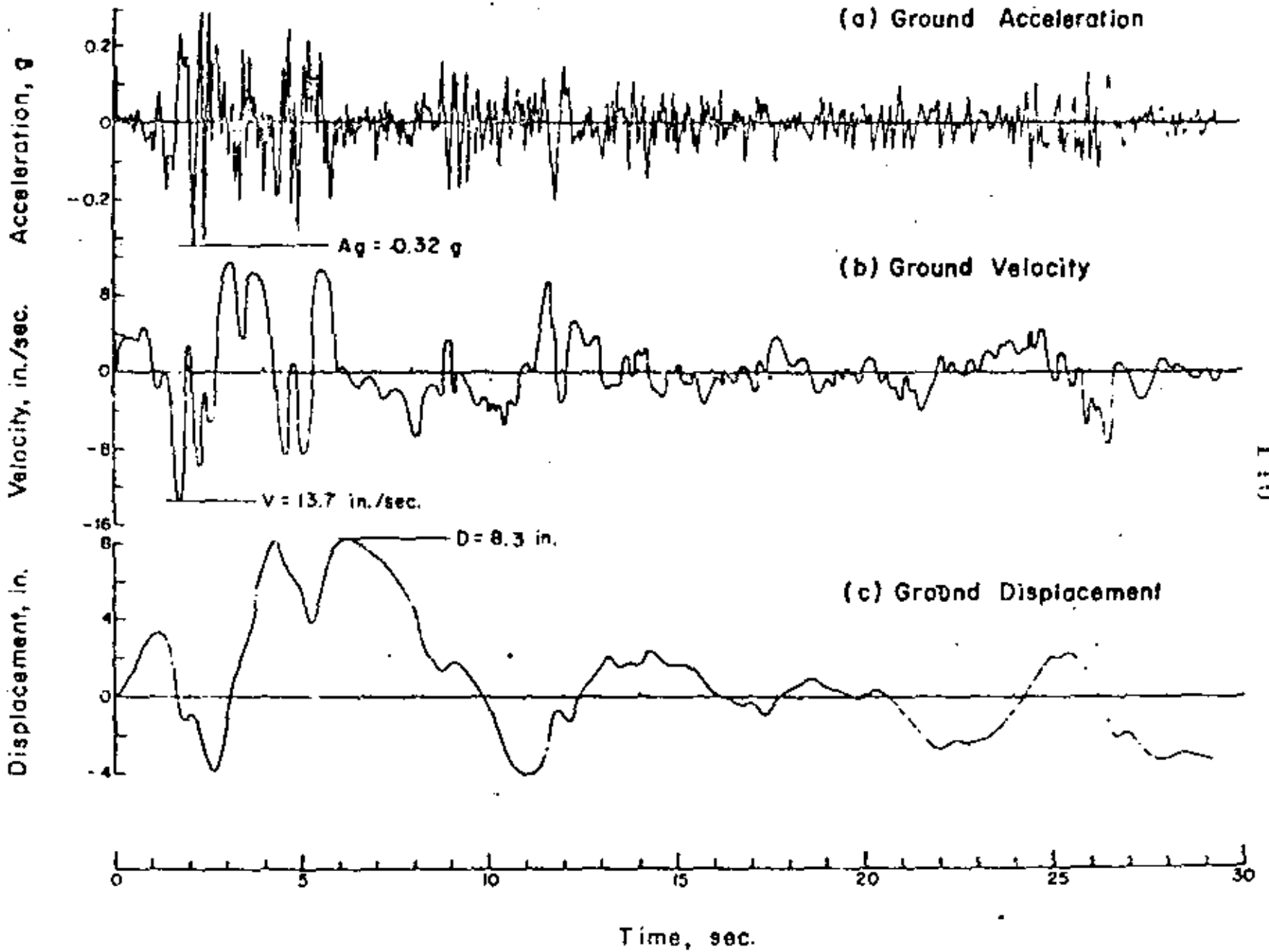

FIG. 5.1 EL CENTRO, CALIFORNIA, EARTHQUAKE OF MAY 18, 1940, N-S COMPONENT

The resistance to motion is accounted for by a shearing resistance, which can be expressed as being proportional to the weight W, and having a magnitude of $\overline{NW}$. This shearing resistance corresponds to an acceleration of the ground of magnitude Ng that would cause the mass to move relative to the ground.

The accelerating forces acting on the mass M are shown in Fig. 5.3. The acceleration considered is a single pulse of magnitude Ng, lasting for a time interval t_o. The resisting acceleration, Ag, is shown by the dashed line in Fig. 5.3. The accelerating force lasts only for the short time interval indicated, but the decelerating force lasts until the direction of motion changes.

In Fig. 5.4 the velocities are shown as a function of time for both the accelerating force and the resisting force. The maximum velocity for the accelerating force has a magnitude V given by the expression

$$V = Agt_o \tag{5.2}$$

After the time t_o is reached, the velocity due to the accelerating force remains constant. The velocitiy due to the resisting acceleration has the magnitude Ngt. At a time t_m, the two velocities are equal and the relative velocity becomes zero, or the body comes to rest relative to the motion of the ground. The formulation for t_m is obtained by equating the velocity V to the quantity Ngt, which results in the expression

$$t_m = \frac{V}{Ng} = \frac{Agt_o}{Ng} = \frac{Agt_o}{Ag} \tag{5.3}$$

The maximum displacement of the mass relative to the ground, u_m, is obtained by computing the shaded triangular area in Fig. 5.4. The

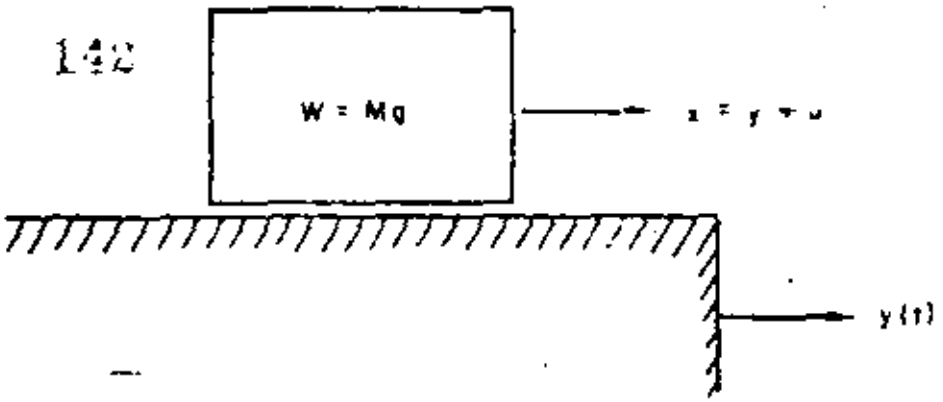

FIG. 5.2 RIGID BLOCK ON A-MOVING SUPPORT.

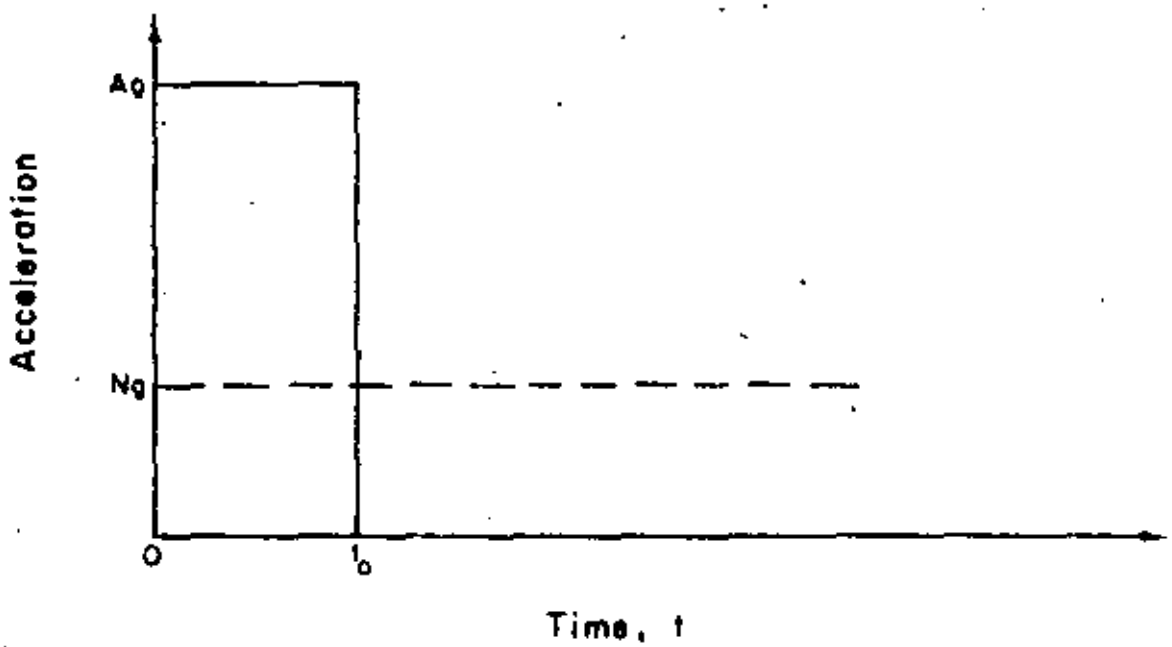

FIG. 5.3 RECTANGULAR BLOCK ACCELERATION PULSE

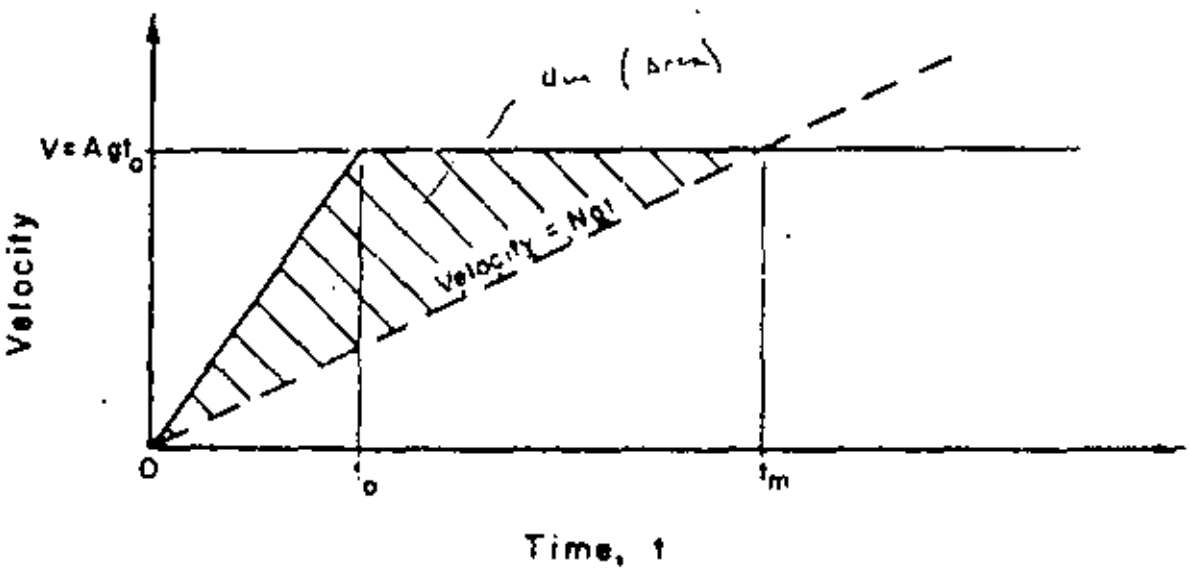

FIG. 5.4 VELOCITY RESPONSE TO RECTANGULAR BLOCK ACCELERATION

calculation is made as follows:

$$u_m = \frac{1}{2} V t_m - \frac{1}{2} V t_o$$

or $$u_m = \frac{1}{2} \frac{V^2}{Ng} - \frac{1}{2} \frac{V^2}{Ag}$$

hence $$u_m = \frac{V^2}{2gN} \left(1 - \frac{N}{A}\right) \qquad (5.4)$$

The acceleration pulse shown in Fig. 5.3 corresponds to an infinite ground displacement. During a real earthquake a mass would undergo a number of pulses occurring in random order, some positive and some negative as shown in Fig. 5.1. If we now consider a second pulse of a negative magnitude that is sufficient to bring the velocity to zero even without the resisting force, then it can be shown that the net displacement occurring with the resistance generally cannot exceed that which would occur without the resistance.

The result of using Eq. (5.4) is to generally overestimate the relative displacement for an earthquake because the equation does not take into account the fact that the pulses occur in opposite directions. However, Eq. (5.4) should give a reasonable order of magnitude for the relative displacement and it does indicate that the displacement is proportional to the square of the maximum ground velocity.

The result derived above is also applicable to the case for a group of pulses in which the resistance in either direction of possible motion is the same. For a situation in which the body has a resistance to motion greater in one direction than in another, one must take into account the cumulative effect of the displacements. A simple example where this effect must be considered is found by rotating Fig. 5.2 clockwise so that the body has a tendency to slide downhill. In this

situation, ground motions in an upslope direction leave the mass without any additional relative motion except where the magnitudes of the motions are extremely large. One may consider this model applicable to a slope.

Similar calculations using wave forms of 4 different earthquake records were made for a resistance of $\overline{NW}$ for downhill movement and an infinite resistance for uphill movement on a digital computer at the University of Illinois. These results are shown in Fig. 5.5. A conservative upper bound to the displacement is given by

$$\delta = \frac{V^2}{2gN} \cdot \frac{A}{N} \text{ for } 0.2 < \frac{N}{A} < 0.4 \qquad (5.5)$$

For $\frac{N}{A} > .4$ a reasonable upper bound is given by

$$\delta = \frac{V^2}{2gN} \left(1 - \frac{N}{A}\right) \frac{A}{N} \qquad (5.6)$$

And for $\frac{N}{A} < 0.2$ a reasonable upper bound for the displacement is given by

$$\delta = \frac{6V^2}{2gN} \qquad (5.7)$$

The simplified calculation presented for one acceleration pulse and the calculation of displacements for actual earthquake records show that the slope movements relative to the base are proportional to the square of the maximum particle velocity, V^2, at a given ratio of N/A. Since the calculations of Newmark, presented in Fig. 5.5, are for four different earthquake records, it is conservative to use the relations given in Eqs. 5.5, 5.6, and 5.7 for ground motions from nuclear explosions because the duration of shaking is significantly shorter.

5.3 Permissible Movement of Rock Slopes

Ultimately, the engineer must decide if the dynamic displacement calculated from Eqs. 5.3 - 5.5 is acceptable. Many slopes in soil and

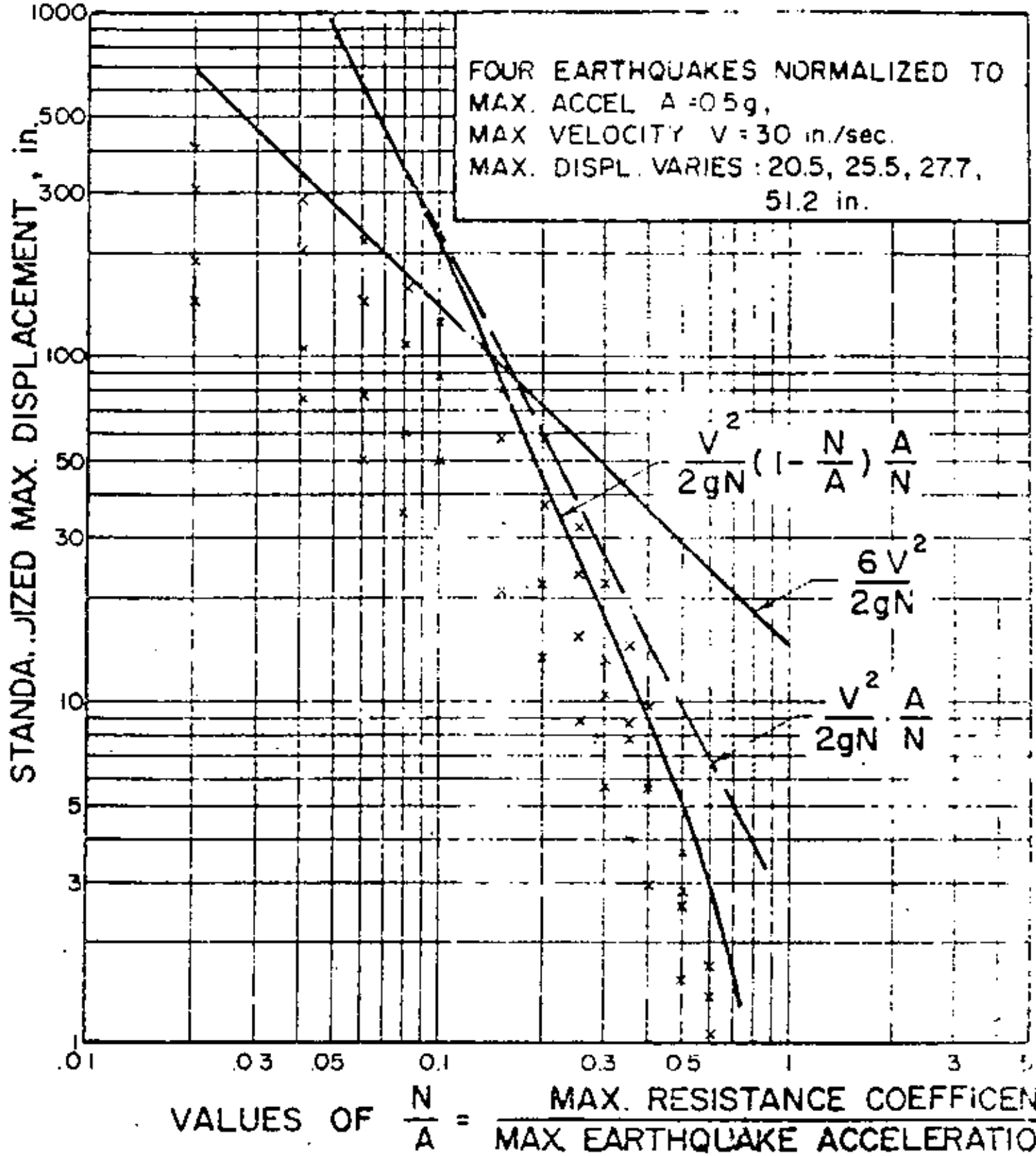

FIG. 5.5 STANDARDIZED DISPLACEMENT FOR NORMALIZED EARTHQUAKES. (UNSYMMETRICAL RESISTANCE)

soft shales have undergone considerable movement (as much as 6-10 ft) under earthquake loading without catastrophic consequences. On the other hand, there have been catastrophic failures of some rock slopes during dynamic loading, such as the Madison Valley, Montana slide and catastrophic slope failures have also been observed in sensitive marine clays in Anchorage, Alaska under earthquake loading. Jointed rock slopes and slopes composed of sensitive marine clays are similar in that they are composed of materials which are strain softening for displacements beyond those required to develop the maximum shearing resistance. A qualitative diagram of shearing strength mobilized versus displacement parallel to the discontinuity is shown in Fig. 5.6b for rough rock surfaces. The peak shearing strength given by point C on this diagram is given by

$$\tau = \sigma_n \tan (\phi_r + i) \qquad (5.8)$$

where i is the geometrical component of resistance given by the roughness along the discontinuities and ϕ_r is the residual angle of shearing resistance.

With further displacement the asperities are sheared off to a certain extent along the discontinuity and eventually at larger displacements the shear strength will be reduced to a value given by

$$\tau = \sigma_n \tan \phi_r \qquad (5.9)$$

where ϕ_r is the residual angle of shearing resistance along the discontinuity. Thus in any given case, the potential fall off in strength between the peak strength and the residual strength is $\sigma_n \tan i$, where i is the angle which the roughness makes with the average direction of movement along the discontinuity, as shown in Fig. 5.6c. The value of

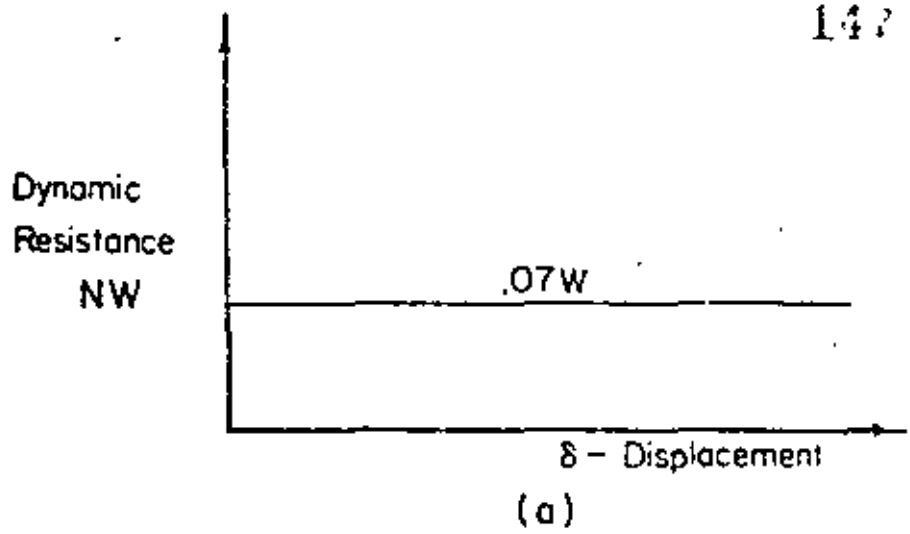

(a)

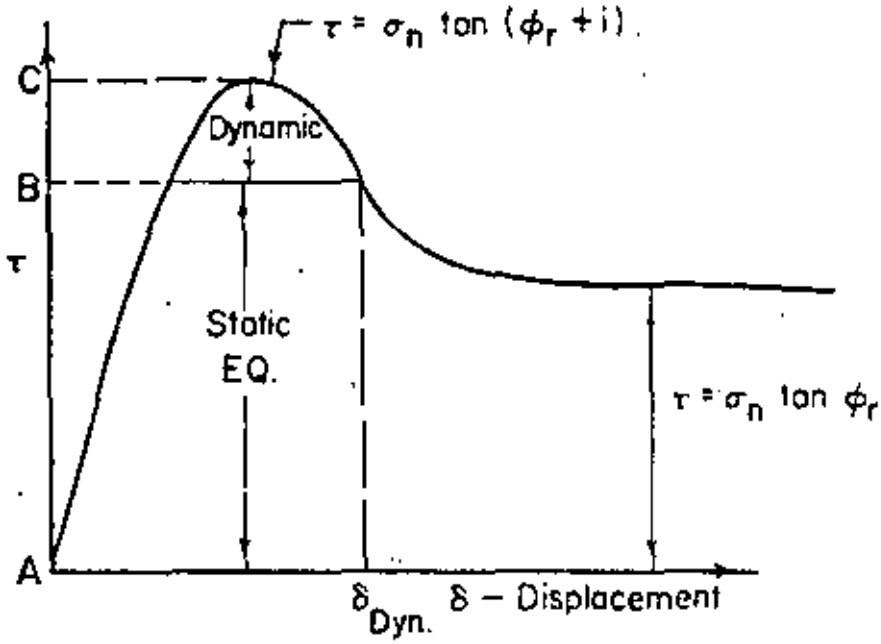

(b)

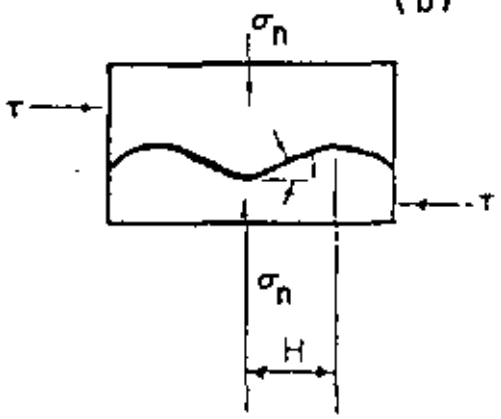

$\delta_{Dyn.} << H$, OK

$\delta_{Dyn.} \cong H$, Static Stability impaired

(c)

FIG. 5.6 RELATIONSHIP BETWEEN PEAK SHEAR STRENGTH AND THE COMPONENT OF STRENGTH DUE TO SURFACE ROUGHNESS

ϕ_r is a function of the type of rock of which the slope is composed and can be relatively easily determined from smooth samples in the laboratory. The selection of the i value, however, is somewhat difficult in that there are usually several groups of undulations on a discontinuitiy which have different i values. For instance, there may be broad undulations (first order irregularities) with wave lengths on the order of 8-10 ft which may have an i associated with them which may only be on the order of 5-15° (Fig. 5.7). Whereas there are shorter undulations (second order irregularities), which may have higher i values (10-46°) as shown in Fig. 5.7. If the dynamic resistance $\overline{NW}$ is calculated on the basis of a peak shearing strength such as point C on diagram 5.6b, then it is of utmost importance to know approximately the wave length of the asperity associated with the value of the angle i chosen in the analysis. For instance, if the value of i is associated with a quarter wave length denoted by H in Fig. 5.6c, then it is obvious that the dynamic displacement as computed by Newmark's method must be less than H or the shear strength value upon which the calculation of $\overline{NW}$ was computed is no longer valid. The displacement in this case would have been enough to roll up and over the asperity shown in Fig. 5.6c and the shear strength would have been reduced to some value lower than the peak shear strength. The full value of i would not be effective because of the lower slope of the surface roughness near the top and possibly because part of the roughness could have been sheared off by the dynamic movement. On the other hand, a value of i used in estimating the peak shear strength used in the calculation of $\overline{NW}$ could be a relatively low value of about 5-10°; and this value of i could be consistent with a length H (Fig. 5.6c)

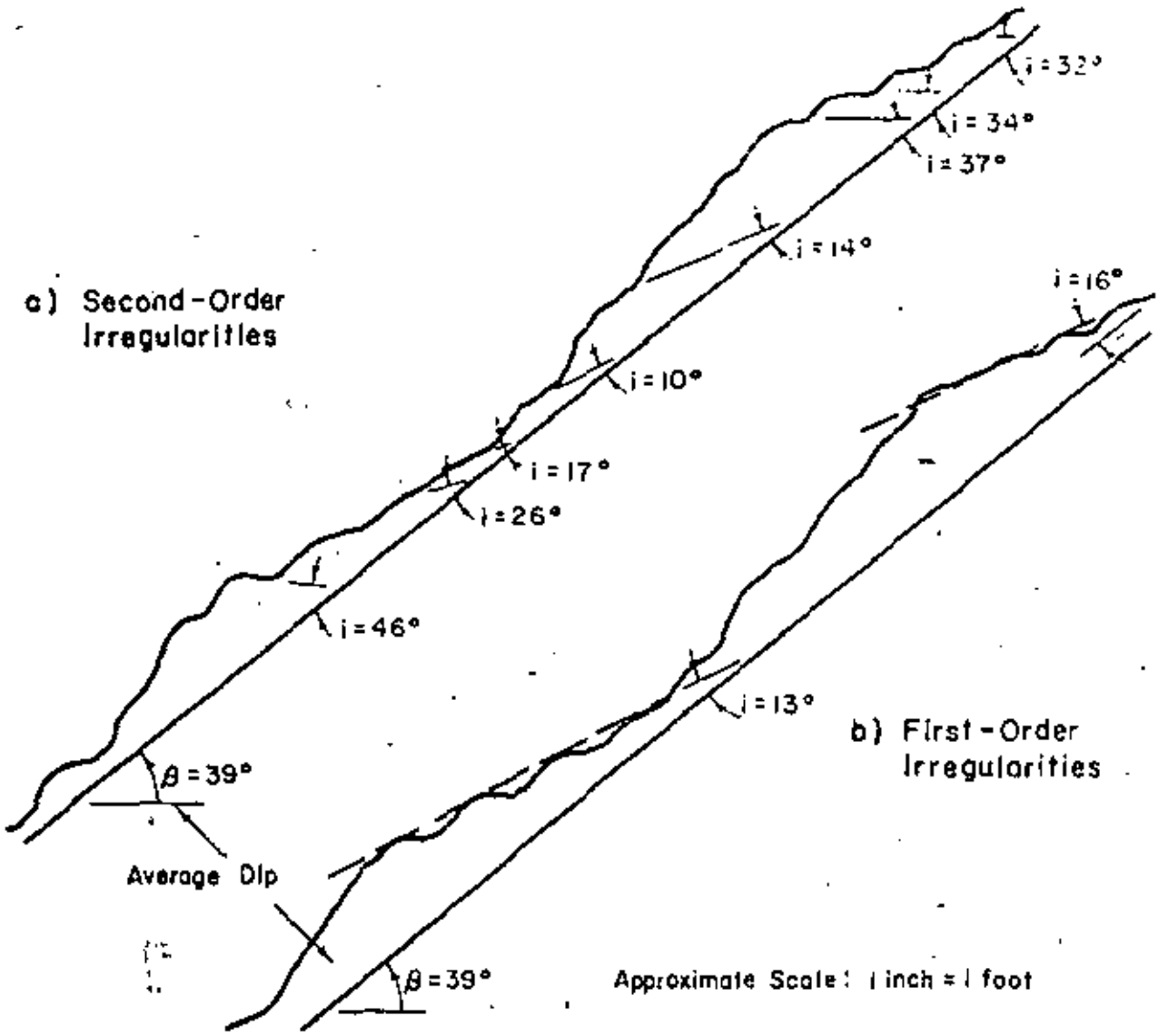

FIG. 5.7 AN EXAMPLE OF A DISCONTINUITY ILLUSTRATING FIRST AND SECOND-ORDER IRREGULARITIES

on the order of 5 or 6 ft. In this case if the calculated dynamic displacement caused by a given earthquake turns out to be something like 6 inches, then we would definitely say that the slope is probably stable or no problems would result from dynamic loading. This is true because the 6 inch displacement will not significantly reduce the strength assumed in calculations of $\overline{NW}$. The relative displacement would have to be on the order of 3 or 4 ft to significantly lower the peak shearing resistance in this case. Thus, in general, the criterion which should be used to decide if a certain displacement is detrimental or not is the wave length of the asperities giving the geometrical component of resistance because this is the resistance which can be destroyed by the dynamic displacement. If preliminary calculations indicate that the dynamic displacements will not be large in comparison with the displacements necessary to significantly lower the shear strength, then the dynamic displacement calculated will probably be acceptable and the slope can be judged safe. However, if the dynamic displacement computed is on the same order of magnitude as the wave length of the discontinuities or the order of displacement necessary to significantly reduce the shear strength along a discontinuity, then the slope may not be safe.

CHAPTER SIX

SUMMARY AND CONCLUSIONS

6.1 Static Stability of Rock Slopes

In this report the methods of analysis for assessing the static stability of rock slopes in three dimensions have been described and a method for calculating the dynamic resistance and displacement of rock slopes subjected to earthquake loading has been given.

The general procedures for determining the static factor of safety of rock slopes analytically by vector analysis and graphically with stereonets are given in Chapter 3 and Chapter 4 respectively. Although the mechanics of the calculation are different in each of these approaches, the same basic steps are followed in each method for determining the static factor of safety. The steps in the analysis are as follows:

(1) the intersection of the various joint sets with each other and with the slope face must be inspected to determine the tetrahedra which may be potential failure wedges. These wedges must then be analyzed in detail.

(2) the forces tending to disturb the equilibrium of the wedge should be added vectorially to give a resultant driving force. These disturbing forces are the weight of the wedge, $\bar{W}$, the external load applied to the wedge by a structure, $\bar{Q}$, and the porewater forces acting on various faces of the tetrahedron given as $\bar{U}_1$, $\bar{U}_2$, and $\bar{U}_3$. This step is illustrated by equations 3.10 and 3.68 for the vector analysis and is shown in Figs. 4.7 and 4.8 for the graphical method using stereonets.

(3) the mode of failure must then be determined. For example a wedge supported on two base planes can either slide along the line of intersection of the two planes, slide on either plane or rotate on either plane. The kinematics of failure will depend upon the orientation of the disturbing force in relation to the orientation of the supporting planes. These kinematic tests for sliding are illustrated by equations 3.16, 3.17, 3.20, 3.21, 3.22 and 3.23 for a tetrahedron supported on two base planes. The kinematic tests for rotation are given in Table 3.1. The orientation of the resultant disturbing force which will cause various modes of failure for a wedge supported on two base planes as shown in Fig. 4.13 by the graphical method using stereonets. Equations 3.81-3.93 are kinematic tests to determine the sliding mode for a tetrahedron bounded by 3 base planes by means of vector analysis. Fig. 4.17 illustrates the method of determining the mode of sliding of a tetrahedron bounded by 3 base planes by utilization of stereonets.

(4) after the mode of failure is determined the maximum shearing resistance which can be mobilized in the direction of movement is compared to the shearing forces necessary for equilibrium to obtain a factor of safety. This step has been illustrated by the many example problems worked in Chapters 3 and 4.

The detailed analyses given in Chapters 3 and 4 can be used to solve most of the problems which arise in the calculation of rock slope stability. A majority of the real problems which arise however are

wedges acted on by their own weight, partially submerged beneath a phreatic surface, and resting on two base planes. The influence of external loads is small relative to the weight of the wedge. For this case, which has been the most common field case encountered by the authors, there are several approximate generalizations which can be made such that all the details of analyses presented in Chapters 3 and 4 are not necessary to obtain a fairly accurate answer to the problem. First of all for a wedge resting on two base planes, acted on by only its own weight, sliding will occur along the line of intersection of the two planes if a line drawn down the dip in both planes tends to intersect the line of intersection. If in either one of the planes a line drawn down the dip is directed away from the line of intersection then sliding will occur on that plane only and the wedge will move away from the line of intersection. If a wedge is acted on by its own weight, it will slide down the maximum dip if sliding occurs on one plane and the factor of safety can be easily computed. If it is determined above that sliding will take place along the line of intersection, the slope of the line of intersection, α, as shown in Fig. 6.1, should be determined immediately by means of graphics. The angle of friction ϕ required for stability will always be equal to or less than α if there are no pore pressures on the joint surfaces. The next step is to determine the angle, β, included between planes 1 and 2 in a plane perpendicular to the line of intersection OA as shown in Fig. 6.1. The smaller angle β, the lower the value of ϕ required for stability. As β approaches zero, the value of ϕ required for stability approaches zero; and, as β approaches 180° the value of ϕ required for stability

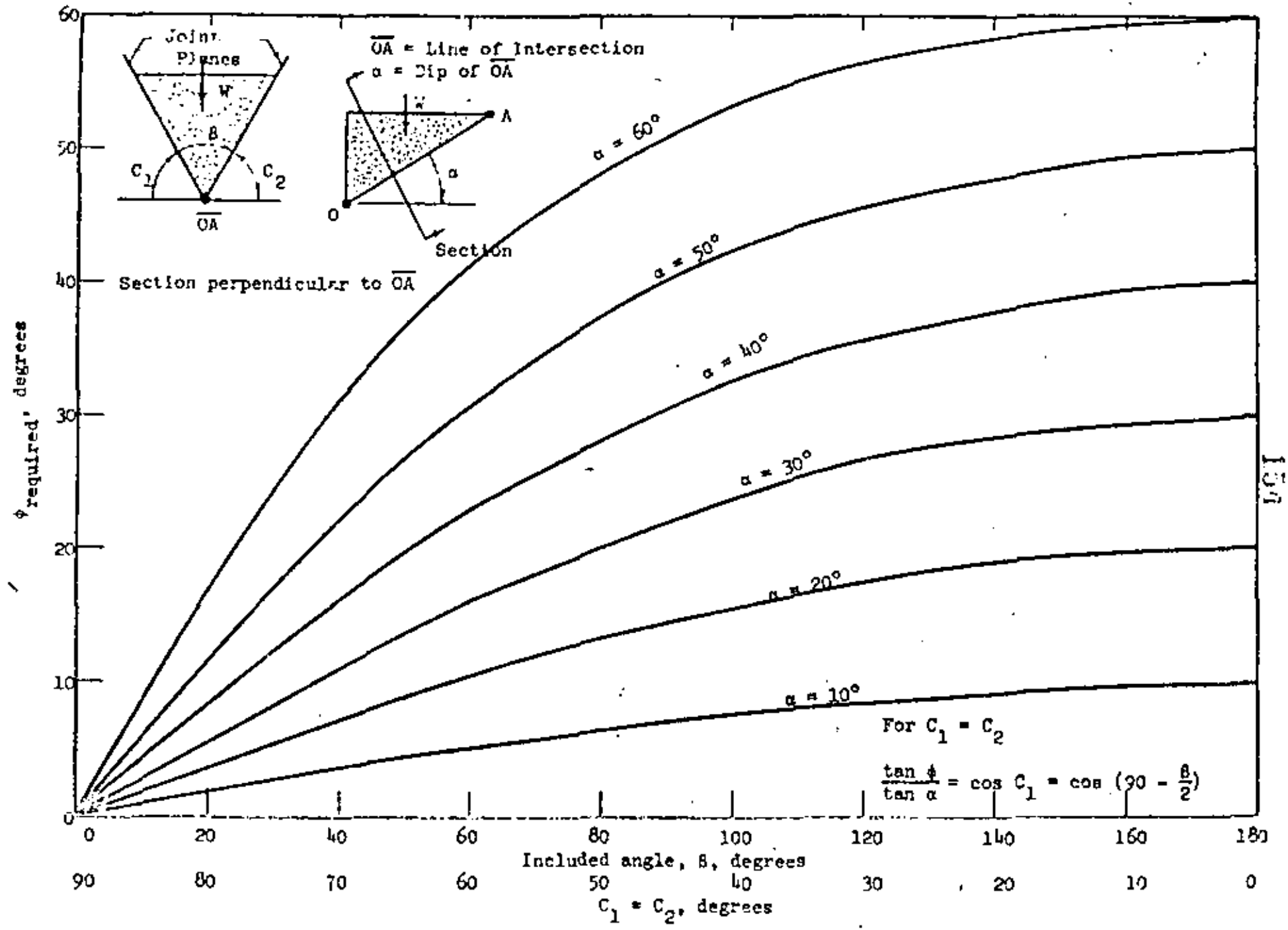

FIG. 6.1. FRICTION ANGLE REQUIRED FOR STABILITY OF WEDGE OF WEIGHT, W, FOR $C_1 = C_2$

approaches α. The next step is to determine the skewness γ of the wedge as shown in Fig. 6.2. For the non-skewed or symmetrical case ($C_1 = C_2$ and $\gamma = 0$, as shown in Fig. 6.1) the ϕ required for a factor of 1.0 for various values of β and α are shown in Fig. 6.1. If the angle of shearing resistance ϕ is the same on both planes 1 and 2, the value of ϕ required for stability is less for the symmetrical case ($C_1 = C_2$, Fig. 2) than for the skewed case ($C_1 \neq C_2$) for the same values of α and β. Figure 6.2 illustrates the effect of skewing the planes on the value of ϕ required for a factor of safety of 1.0. From Fig. 6.2 the value of ϕ required for a factor of safety of 1.0 can be determined from the value of tan ϕ/tan α for various values of β and γ where γ is a measure of the skewness of the wedge as shown in Fig. 6.2. The curve labeled $C_1 = C_2$ ($\gamma = 0$) in Fig. 6.2 summarizes the curves presented in Fig. 6.1 for the symmetrical case. The additional curves presented in Fig. 6.2 illustrate the effect of skewing. These curves illustrate the sensitivity of the value of $\phi_{required}$ to skewing. For values of γ less than 20° the tan $\phi_{required}$/tan α values are increased by only 6 percent above the values for $\gamma = 0$. However if the wedge is skewed 60° ($\gamma = 60^\circ$) then values of tan $\phi_{required}$/tan α are approximately twice the values for $\gamma = 0$. For $\gamma = 40^\circ$ tan $\phi_{required}$/tan α values are increased by approximately 30 percent from the case where $\gamma = 0$.

The five example problems shown below in Table 5.1 illustrate all the conditions which are considered in Fig. 6.2.

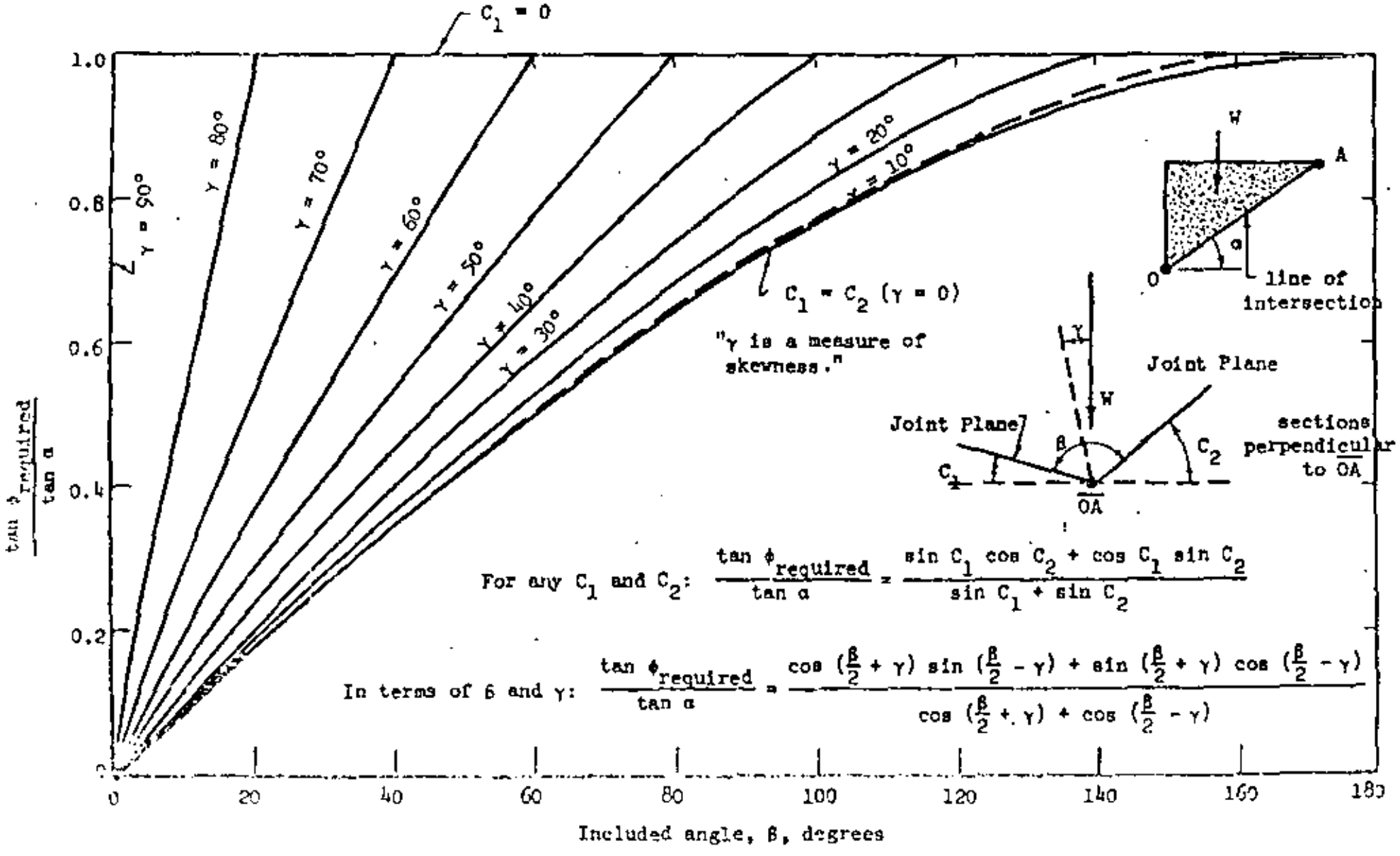

For any C_1 and C_2: $$\frac{\tan \phi_{required}}{\tan \alpha} = \frac{\sin C_1 \cos C_2 + \cos C_1 \sin C_2}{\sin C_1 + \sin C_2}$$

In terms of β and γ: $$\frac{\tan \phi_{required}}{\tan \alpha} = \frac{\cos\left(\frac{\beta}{2} + \gamma\right) \sin\left(\frac{\beta}{2} - \gamma\right) + \sin\left(\frac{\beta}{2} + \gamma\right) \cos\left(\frac{\beta}{2} - \gamma\right)}{\cos\left(\frac{\beta}{2} + \gamma\right) + \cos\left(\frac{\beta}{2} - \gamma\right)}$$

"A" $\phi_{REQUIRED}$ FOR STABILITY OF A WEDGE OF WEIGHT, W FOR VARIOUS VALUES OF β, γ, AND

TABLE 6.1

157

Case 1	$\beta=180°$	$C_1=C_2=0$
Case 2	$C_1=0$	
Case 3	$\beta=0$,	
Case 4	$C_1=C_2$, $\gamma=0$	
Case 5	$C_1\neq C_2$	

Analysis of each of these five cases by the use of stereonets is illustrated in Figs. 6.3, 6.4, 6.5, 6.6, and 6.7.

6.2 Dynamic Stability

The analysis of rock slopes in a static fashion by considering the inertia force as a static load (Wittke, 1965a) is not considered adequate for assessment of the dynamic behavior of rock slopes. In this report a method was given in sections 3.2.2 and 3.4.2 for calculating the dynamic resistance $\overline{NW}$ for a rock slope by means of vector analysis. The calculation of the dynamic resistance by means of stereonets is given in section 4.3.4. The dynamic resistance $\overrightarrow{NW}$ should then be used in the dynamic analysis proposed by Newmark (1965), which is explained and illustrated in Chapter 5. From this analysis the dynamic displacement is computed. This displacement should then be compared with the wavelength of the asperities on the failure planes as shown in Fig. 5.6 to determine if the dynamic displacement would be detrimental to the static stability of the slope. The calculation of the dynamic factor of safety using a pseudo static analysis has little meaning.

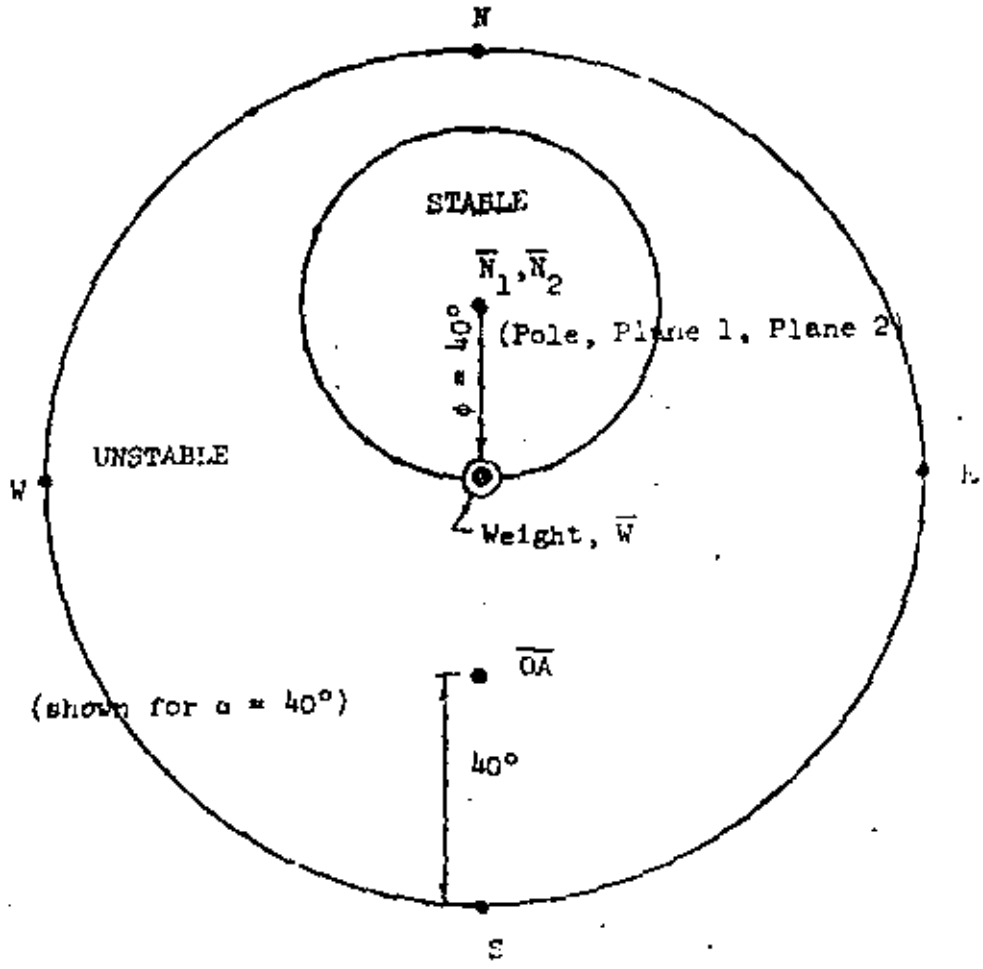

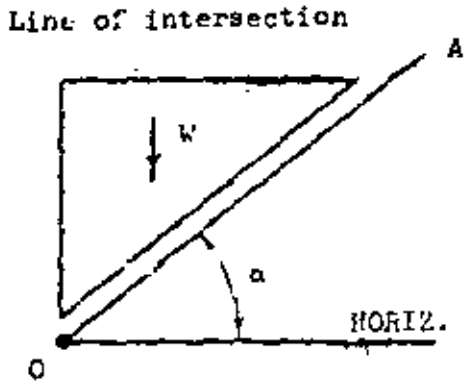

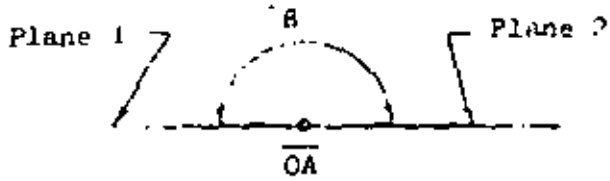

$\beta = 180°$, $C_1 = C = 0$

For factor of safety = 1

$\alpha_{required} = \alpha$

FIG. 6.3. WEDGE ACTING UNDER OWN WEIGHT
CASE 1: SINGLE PLANE, $\beta = 180°$

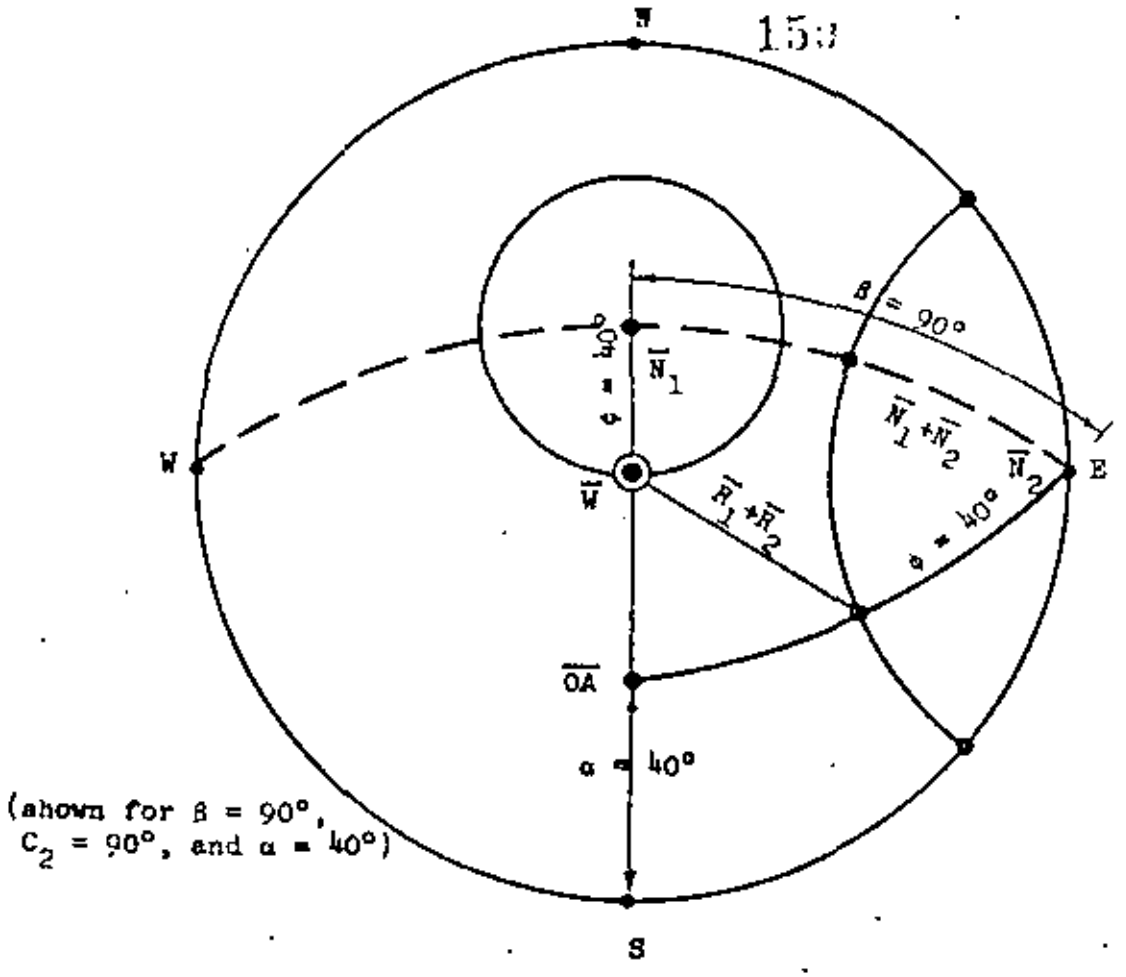

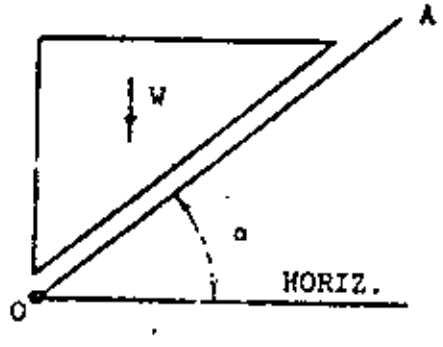

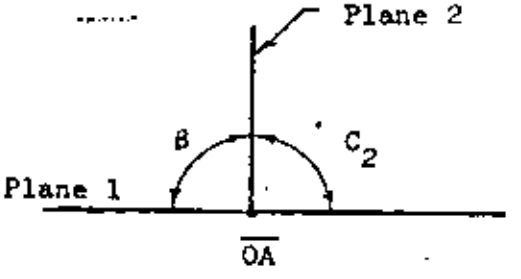

$C_1 = 0$

For F.S. = 1, $\phi_{required} = \alpha$

FIG. [illegible] WEDGE ACTING UNDER OWN WEIGHT
CASE 2: C_1 = 0, β and C_2 = any value
(SINGLE PLANE CASE)

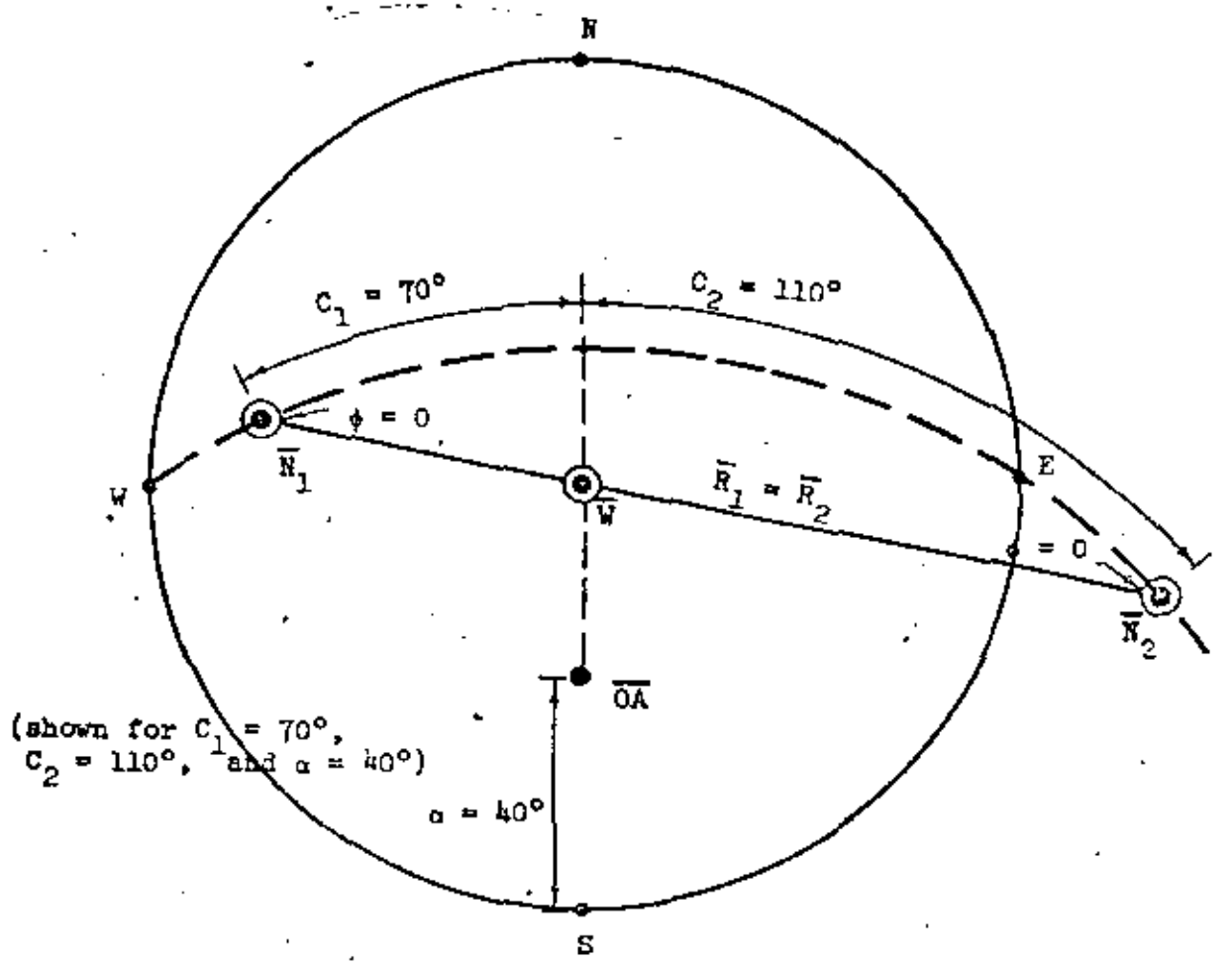

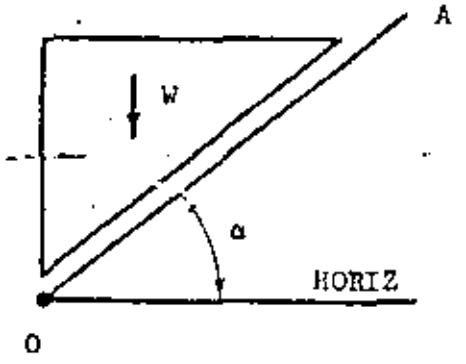

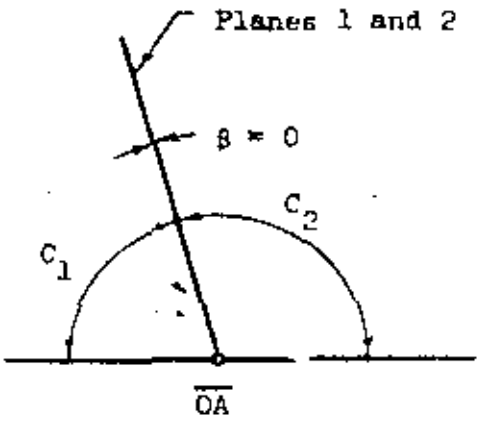

For F.S. = 1

$\phi_{required}$ = 0

FIG. 6.5. WEDGE ACTING UNDER OWN WEIGHT
CASE 3: β = 0; ANY C_1, C_2, α

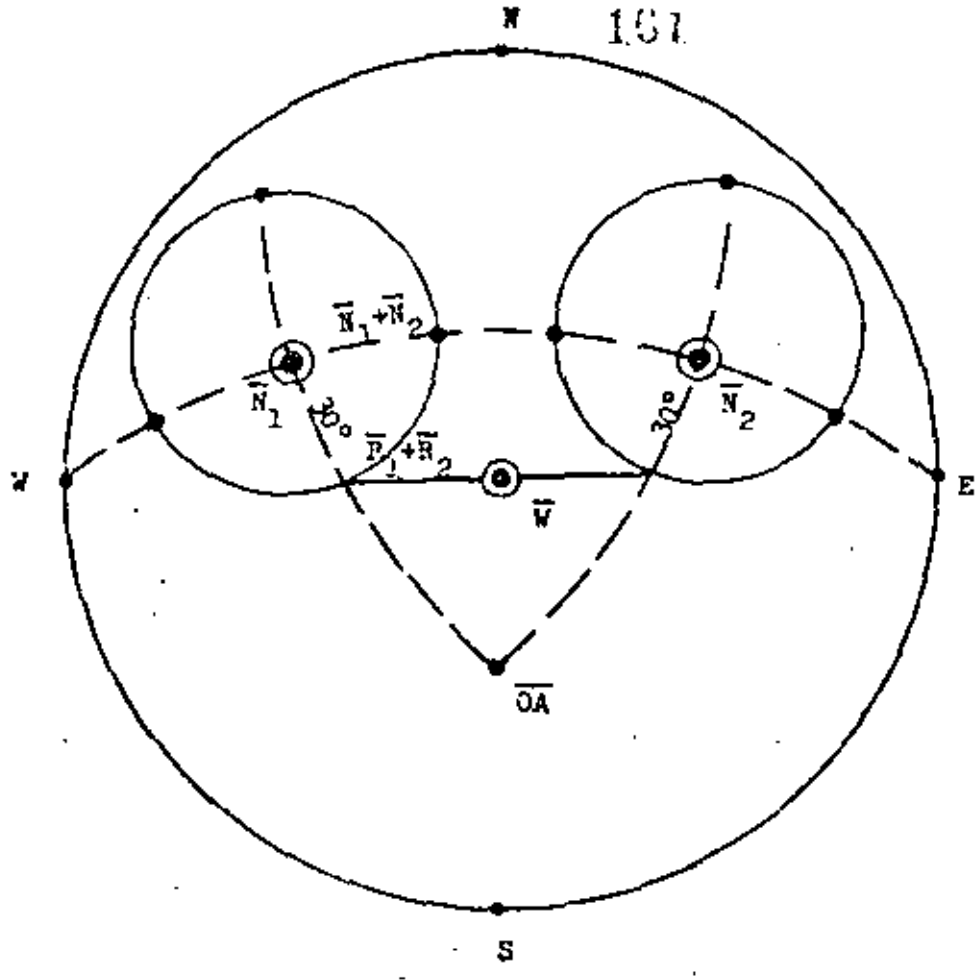

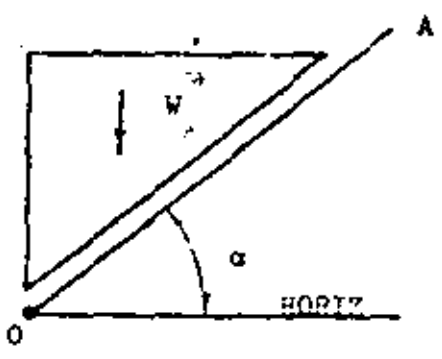

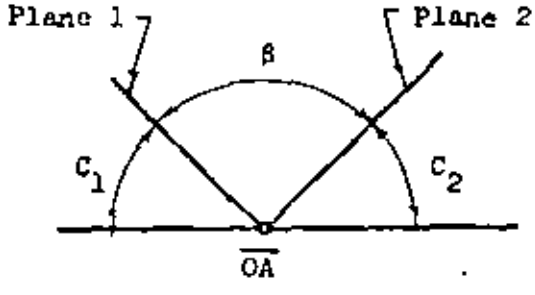

For F.S. = 1 and $\beta > 0$:

ϕ required $< \alpha$

For F.S. = 1, $C_1 = C_2 = 45°$, $\alpha = 60°$

then ϕ required = 30°

FIG. 6.6. WEDGE ACTING UNDER OWN WEIGHT
CASE 4: $C_1 = C_2 \neq 0$, $\beta \neq 0$

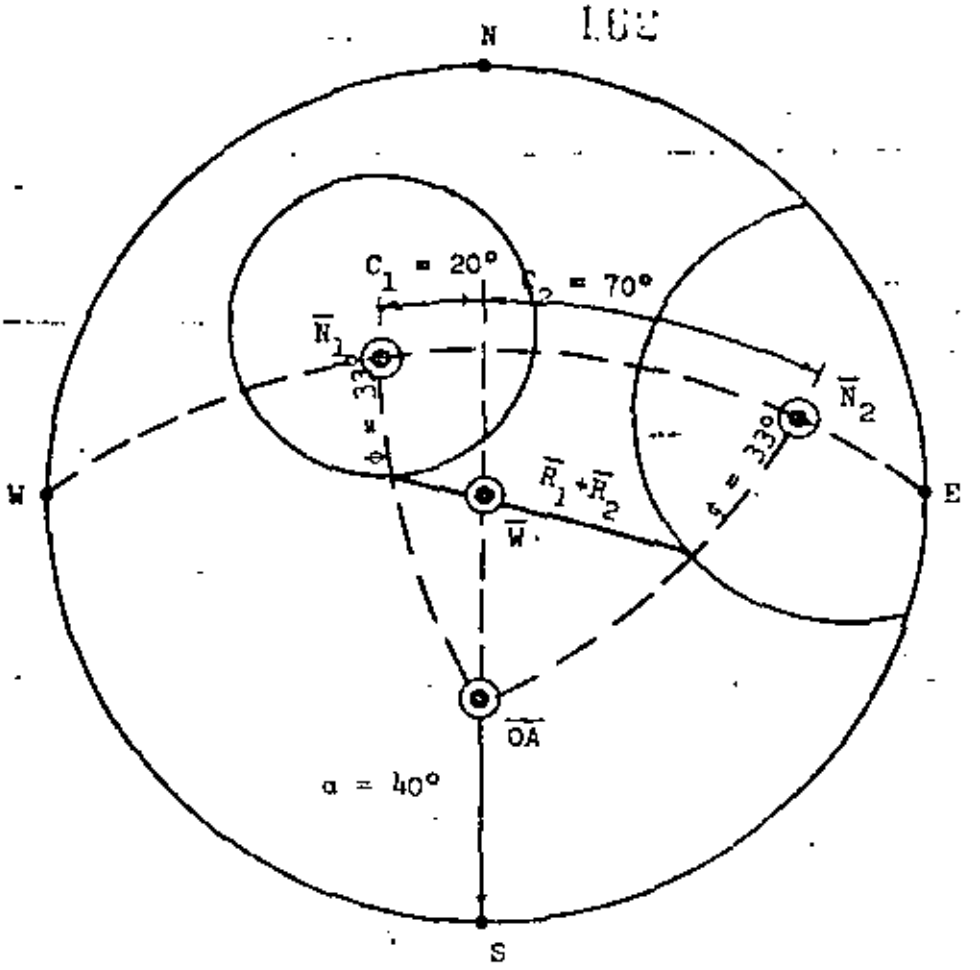

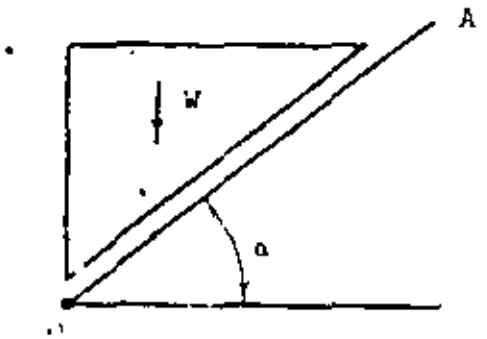

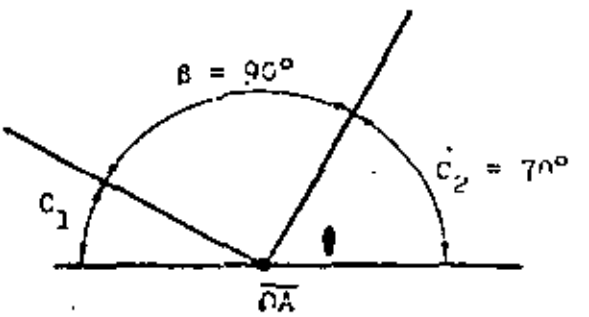

For F.S. = 1 and β = same as Case 4:

$\phi_{required}$ (Case 4) < $\phi_{required}$ (Case 5)

For F.S. = 1, α = 40°, β = 90, C_1 = 20°, C_2 = 70° then $\phi_{required}$ =

FIG. 6.7. WEDGE ACTING UNDER OWN WEIGHT
CASE 5: $C_1 \neq C_2$, $\beta \neq 0$

REFERENCES

Goodman, R. E., (1964), "The Resolution of Stresses in Rock Using Stereographic Projection," International Journal of Rock Mechanics and Mining Science, Vol. 1, pp. 93-103.

Goodman, R. E., and Taylor, R. L., (1967), "Methods of Analysis for Rock Slopes and Abutments: a Review of Recent Developments," Failure and Breakage of Rock, AIME, Chapter 12, pp. 303-320.

John, Klaus W., (1968), "Graphical Stability Analysis of Slopes in Jointed Rock," Journal of the Soil Mechanics and Foundations Divisions, Proceedings, Vol. 94, SM2, pp. 497-526.

Londe, Pierre, (1965), "Une Methode D'Analyse a Trois Dimensions De La Stabilite D'une Rive Rocheuse," Annales Des Ponts Et Chaussees, N° 1 De Janvier-Febrier, pp. 37-60.

Londe, P., (1968), "Stability of Rock Slopes Application to Dams," (in French), Annales de l'Institut Technique du Batiment et des Travaux Publics, Paris No. 69, Nov., pp. 1615-1638.

Londe, P., G. Vigier, R. Vormeringer, (1969), "Stability of Rock Slopes, A Three-Dimensional Study," Proceedings, of ASCE, Vol. 95, No. SM1, January, pp. 235-262.

Newmark, N., (1965) "Effects of Earthquakes on Dams and Embankments," Geotechnique, 15:140-141; 156.

Wittke, W., (1964), "Ein rechnerischer Weg zur Ermittlung der Standsicherheit von Boschungen in Fels mit durchgehenden, ebenen Absonderungsflachen," Principles in the Field of Geomechanics, Rock Mechanics and Engineering Geology, Supplementum I, 14th Symposium of the Austrian Regional Group (i.f.) of the International Society for Rock Mechanics, Salzburg, 27 und 28 September 1963, pp. 101-129.

Wittke, W., (1965a), "Verfahren zur Berechnung der Standsicherheit belasteter und unbelasteter Felsboschungen," Rock Mechanics and Engineering Geology Supplementum II, 15th Symposium of the Austrian Regional Group (i.f.) of the International Society for Rock Mechanics, Salzburg, 25 und 25 September 1964, pp. 52-79.

Wittke, W., (1965b), "Verfahren zur Standischerheitsberechnung starrer, auf ebenen Flachen gelagerter Korper und die Anwendung der Ergebnisse auf die Standischerheitsberechnung von Felsboschungen," Veroffentlichungen, des Institutes fur Bodenmechanik und Grundbau der Technischen Hochschule Friderician a in Karlsruhe, Heft 20.

Wittke, W., (1966), "Berechnungsmoglichkeiten det Standsicherheit von Boschungen in Fels," Deutsche Gesellschaft fur Erd - und Grundbau e.V.

EXCAVACIONES A CIELO ABIERTO

DIVISION DE EDUCACION CONTINUA
FACULTAD DE INGENIERIA U.N.A.M.

CURSOS DE INGENIERIA CIVIL EN EL PROYECTO DE PLANTAS HIDROELECTRICAS.

MATERIA: EVALUACION DE PROYECTOS

PROF. M. EN I. CESAR HERRERA TOLEDO

SEPTIEMBRE, 1981.

III Optimal Resource Allocation, Markets, and Public Policy: An Introduction: Robert C. Lind

INTRODUCTION

The allocation of resources is central to the operation and planning of any economic system. The question of resource allocation arises because, given the existing resources and technology, it is not possible to satisfy all human wants. Therefore, choices have to be made as to what will be produced and to whom it will be distributed. The interest in resource allocation arises from the desire to make these production and distribution decisions so as to maximize, in some sense, the fulfillment of human wants. Therefore, resource allocation is a problem of constrained maximization where the objective is to maximize the fulfillment of human wants, and the constraints are the state of technology and the stocks of available resources.

The first task is to select a criterion by which one allocation can be judged as better than another. In principle, every individual could rank all possible allocations according to his own preferences; however, there would be wide differences among the rankings. More specifically, individuals would almost certainly prefer the allocations that favored them. To obtain a social ranking of alternative allocations, value judgments have to be introduced.

One value judgment which commands wide acceptance is that the social ranking should be based on individual rankings. A related value judgment is that one allocation is better than another if, given this allocation, every individual is at least as well off and some individual is better off than he would have been, given the other allocation. This proposition leads to the concept of Pareto optimality. An allocation is said to be Pareto optimal if there is no other feasible allocation which would make at least one person better off without making someone else worse off.

The concept of Pareto optimality plays a central role in the literature on economic efficiency and optimal resource allocation. One reason for its importance is that the proposition on which it is based commands wide acceptance. However, this concept generally does not determine a unique optimum. Additional value judgments are required to select the best allocation from among the set of Pareto-optimal allocations. These value judgments relate to the distribution of income. A second reason for the importance of Pareto optimality is that, although the concept does not define a unique optimum, the overall optimum will be Pareto optimal. Pareto optimality is therefore a necessary but not sufficient condition for optimal resource allocation.

The theory of optimal resource allocation and the theory of competitive equilibrium are closely related. Specifically, given the requisite conditions for an equilibrium in a perfectly competitive economy, the resulting allocation will be Pareto optimal. However, the theory of optimal resource allocation is in no way dependent upon perfect competition. The theory is developed without reference to any specific institution for allocating resources. The necessary conditions for optimality apply to socialist economies as well as to capitalist economies.

In this chapter the basic conditions for Pareto optimal resource allocation are presented without reference to institutional arrangements for production and distribution. It is then demonstrated that under certain conditions a competitive equilibrium will correspond to a Pareto optimal allocation. In the course of the discussion it will become apparent that the competitive allocation will be one of many allocations which satisfy the conditions for Pareto optimality. To choose among these allocations, value judgments are formally introduced into the analysis by means of a social welfare function. The theoretical and practical difficulties of using a social welfare function to compare allocations are discussed briefly.

The analysis of efficiency is based on an exceedingly simple model economy predicated on certain simplifying assumptions. These assumptions are analyzed and the importance of each assumption is indicated. The model presented does not account for time or uncertainty; however, extensions of the model are outlined which do incorporate these considerations. Also, problems caused by inequalities in wealth and opportunity are discussed.

In addition it is demonstrated that if economies of scale and externalities are present, competitive markets fail to effect a Pareto optimal allocation of resources. In both cases some form of government intervention is required to bring about a Pareto optimal allocation of resources. It will also be shown that markets will fail to bring about a Pareto-optimal allocation when there are monopoly elements in the economy.

The presentation of the theory of optimal resource allocation is traditional in that production and utility functions are defined and a diagrammatic device, the Edgeworth-Bowley box diagram, is used to demonstrate the basic conditions for optimal resource allocation. The advantage of this approach is that it requires only the basic mathematical tool of calculus, and it is consistent with the presentation in most standard economic texts (Bator, 1957;

Henderson and Quandt, 1958; Little, 1950). Therefore, the background of most readers will be sufficient for this presentation. It should be pointed out, however, that an alternative formulation in terms of set theory is in some ways more elegant and more powerful than the one presented. The disadvantage of this alternative is that it requires the use of mathematical concepts which are unfamiliar to a large segment of this audience. For an excellent geometric presentation of this second formulation see Koopmans (1957), and Quirk and Saposnik (1968). For a complete statement and rigorous proof of the basic theorems see Debreu (1959). The presentation is divided into three major sections. The first considers the optimal conditions for productive efficiency; the second, the optimal conditions for distribution of the production. The third considers selection of the commodities to be produced.

OPTIMAL RESOURCE ALLOCATION

Production

To demonstrate the basic ideas of optimal resource allocation consider a hypothetical economy containing two individuals, denoted by A and B, two factors of production, capital and labor, K and L, and two goods for final consumption, X and Y. In addition, suppose that the total amount of capital and labor available is fixed at $\bar{K}$ and $\bar{L}$, respectively, and that these factors are used exclusively to produce consumption goods X and Y. Furthermore, suppose that the amounts of K, L, X, and Y can be varied continuously, that is, they are perfectly divisible.

Now consider the production of the good X. Given any combination of inputs (K, L) applied to the production of X and given the existing technology, there is some maximum amount of X which can be produced. Therefore, we can define a production function for X, f_x, on the space of ordered pairs (K, L), where $f_x(K, L)$ is the maximum amount of X which can be produced with inputs K and L, given the technical possibilities for production. Note that the definition of the production function specifies that the chosen technique of production will be that one which maximizes the output of a commodity given fixed inputs. Upon reflection the reader should see that this condition is necessary for optimal resource allocation if individuals prefer more of a commodity to less of it. It should also be noted that f_x is defined only where K and L are positive because negative inputs of capital and labor do not make sense in this context. In addition we assume that f_x has continuous second derivatives with respect to both K and L. This assumption permits the use of the standard tools of calculus without seriously limiting the validity of the results. If we select a particular value of X, say $\bar{X}$, then we

can implicitly define a locus of points in the input space by the equation $f_x(K, L) = \bar{X}$. This locus of points is called an isoquant or equal output curve. For every value of X we can plot such an isoquant in the input space thereby forming a family of isoquants. Such a family is illustrated in Figure 1. Successively higher isoquants are associated with the production of larger amounts of X.

The shape of the isoquants is of particular importance for the analysis of optimal resource allocation and the theory of competitive markets. If we assume that by increasing either factor of production independently it is possible to increase output, then it follows that each isoquant will be negatively sloped. Furthermore, it is assumed that isoquants are convex to the origin as shown in Figure 1. This assumption has been the subject of much discussion among economists. The basic rationale for the assumption is that the marginal rate at which unit increments in one factor can be substituted for decrements in another, while maintaining the same output, diminishes as the amount of first factor employed increases. More formally, the marginal rate of substitution which is defined to be the absolute value of the slope of the isoquant is assumed to be diminishing. This concept of a diminishing marginal rate of substitution between two factors of production can be illustrated with a simple example. Suppose we consider an earthmoving operation which can be carried out by employing labor and capital in the form of machines. If we were to undertake the job without using any capital, it would require a great deal of labor. Now consider the amount of labor which could be replaced by one machine such that the same output was maintained. The contention is that the first machine can be substituted for

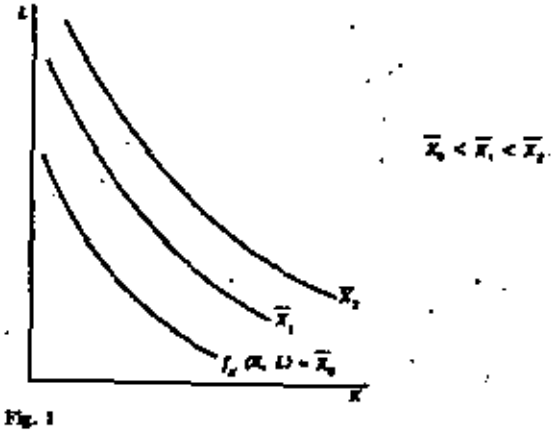

Fig. 1

more labor than can the second machine, the second for more than the third, and so on. Given a large number of machines and very little labor it may be virtually impossible to substitute additional machines for labor while maintaining the same output. Whether a production function is such that there is a diminishing marginal rate of substitution between factors of production depends on the particulars of the specific situation; however, if this condition is not satisfied, competitive markets may fail to allocate resources efficiently. This point is developed subsequently.

To summarize, it will be assumed that there are two production functions f_x and f_y for X and Y, respectively, which are defined on ordered pairs $(K, L) \geq 0$. In addition

$$\frac{\partial f_x}{\partial K}, \quad \frac{\partial f_x}{\partial L}, \quad \frac{\partial f_y}{\partial K}, \quad \text{and} \quad \frac{\partial f_y}{\partial L}$$

are positive, and for any positive outputs $\bar{X}$ and $\bar{Y}$ the loci defined by $f_x(K, L) = \bar{X}$ and $f_y(K, L) = \bar{Y}$ are convex to origin. Furthermore, given an isoquant defined by $f_x(K, L) = \bar{X}$, the marginal rate of substitution (MRS) between factors at a point is defined by

$$\text{MRS} = \left|\frac{dL}{dK}\right| = \frac{\partial f_x / \partial K}{\partial f_x / \partial L}$$

An analogous definition applies to f_y.

Given these concepts and given the simplifying assumption of two outputs and two factor inputs available in fixed supply, it is possible to demonstrate diagrammatically the conditions for productive efficiency by use of an Edgeworth-Bowley box diagram.

In Figure 2 the horizontal edge of the rectangle is of length $\bar{K}$ and represents the total supply of capital available for the production of goods X and Y; the vertical edge is of length $\bar{L}$ and represents the total supply of labor. From the lower left-hand corner of the box are measured the amounts of capital and labor allocated to the production of X, denoted by K_x and L_x, respectively. Similarly, from the upper right-hand corner are measured amounts of capital and labor allocated to the production of Y. Therefore, each point in the box represents an allocation of the total supply of capital and labor to the production of X and the production of Y.

Furthermore, since every point in the box diagram represents an allocation of K and L between the production of X and of Y, isoquants of X and Y can be drawn onto the diagram. The origin for the production of X is the lower left-hand corner of the box and isoquants of X are convex to this origin. Movements upward to the right are associated with ascending levels of the output of X, for example, $\bar{X}^1$, $\bar{X}^2$, $\bar{X}^3$ represent ascending levels of production of X. Similarly, the upper right-hand corner of the box is the origin for Y; isoquants of Y are convex to this origin. The $\bar{Y}^1$, $\bar{Y}^2$, $\bar{Y}^3$ and so on represent ascending levels of the production of Y. Therefore, each point in the box corresponds to a level of production of X and Y; the levels can be determined by looking at the isoquants for X and Y which pass through that point. For example, point R in Figure 2 is associated with outputs of goods X and Y of $\bar{X}^3$ and $\bar{Y}^2$.

Pareto optimality requires the factors of production to be allocated to the production of X and Y in such a way that it is not possible to increase the output of both X and Y by simply reallocating factor inputs. An allocation is said to be productively efficient if there exists no other allocation which produces at least as much of all outputs and more of one output. Clearly, if consumers prefer more rather than less of a commodity, productive efficiency is a necessary condition for Pareto optimality.

Consider again point R in Figure 2. This point does not represent an efficient allocation of the factors of production because more of both X and Y can be produced by any allocation represented by points lying within the shaded area below R. That is, the isoquants of X and Y which pass through any point of the shaded area represent larger amounts of output than do the isoquants passing through R. Furthermore, upon reflection it is clear that the only efficient points in the box are those points at which an isoquant for X is tangent to an isoquant for Y. Point S in Figure 2 represents such a point. A move in any direction from point S will be associated with a decrease in the production of X, Y, or both X and Y. Therefore, the condition for productive efficiency is that the marginal rate of substitution between any two factors of

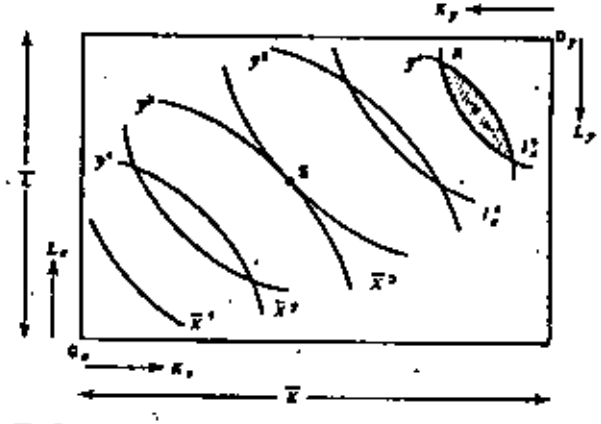

Fig. 2

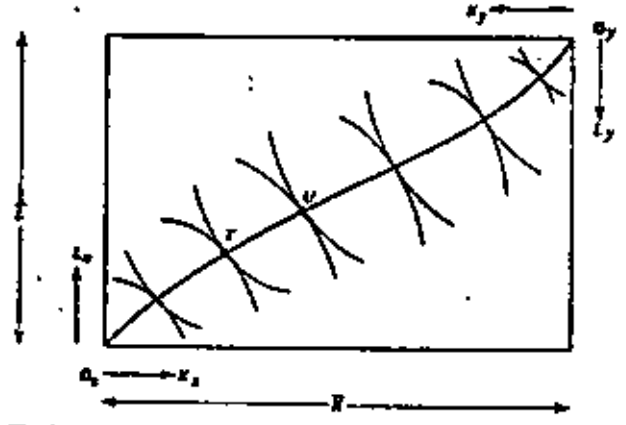

Fig. 3

production is the same in all productive processes which use positive quantities of both factors.* Intuitively one can see that if the factors of production can be substituted at different rates in the two industries, then an opportunity exists for trading factors between the industries so as to increase the production of one good without decreasing the production of the other. Therefore, the efficient points are points of tangency between the isoquants for X and Y. The locus of such points is represented in Figure 3.

From the information contained in Figure 3, it is a simple task to develop the production possibility frontier. Each point on the locus 0_x0_y corresponds to a point in the output space of ordered pairs (X, Y). For example, corresponding to the point T is an output of X and an output of Y. Similarly, the point U corresponds to another pair of outputs, and we know that the output of X associated with U will be greater than that associated with T. The converse is true for Y. Therefore, if we begin at 0_x and proceed to 0_y we can develop a corresponding locus of points in the output space. This production possibility frontier is shown in Figure 4. Point $0'_x$ corresponds to 0_x and point $0'_y$ corresponds to 0_y. Because the points on $0'_x0'_y$ correspond to efficient allocations of factor inputs this curve must have a negative slope. Otherwise, it would be possible to increase the production of both X and Y and one of

* It is possible for an allocation to be efficient even though the marginal rates of substitution of K for L are not the same in the production of X as in the production of Y if this inequality occurs at an allocation on the boundary of the box where one factor is not used in the production of X or Y. Such an allocation does not violate the condition above since the production of either X or Y does not use positive quantities of both K and L.

the points on $0'_x0'_y$ would not correspond to a point on 0_x0_y. The shaded area inside $0'_x0'_y$ represents the set of feasible outputs; however, optimal resource allocation requires that we produce somewhere on the production possibility frontier. This requirement follows from the assumption, which subsequently will be discussed, that people prefer to have more of goods X and Y rather than less.

The absolute value of the slope of $0'_x0'_y$ represents the marginal rate at which X can be transformed into good Y by optimally reallocating factors from the production of X to the production of Y. The absolute value of the slope of $0'_x0'_y$ at a point (X, Y) is commonly referred to as the marginal rate of transformation of X into Y. In addition to having a negative slope the production possibility frontier has been drawn in Figure 4 so that

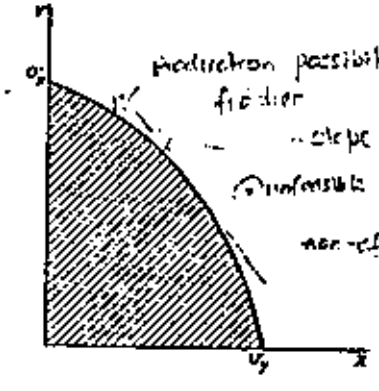

Fig. 4

it is concave to the origin. The concavity means that the marginal rate of transformation of X into Y is increasing as the production of X increases.

This condition can be summarized mathematically. Suppose the locus $0'_x0'_y$ were defined implicitly by the function $Q(X, Y) = C$ where C is a constant or by $Y = q(X)$. Then the marginal rate of transformation is

$$\text{MRT} = \left|\frac{dY}{dX}\right| = -q'(x) = \frac{\partial Q/\partial X}{\partial Q/\partial Y}$$

It is assumed that the marginal rate of transformation is an increasing function of X.

If different factors are differently suited to the production of different goods then it is reasonable to argue that the marginal rate of transformation between

two goods is increasing. This can be explained intuitively in terms of an example.

Suppose there are two goods, wheat and rice, and that the wheat requires a dry climate and one type of land, and rice requires a wet climate and a second type of land. Furthermore, assume that all labor used in the production of both wheat and rice has the same characteristics, and that all land and labor were used in the production of wheat. Now consider the optimal reallocation of land and labor to produce one unit of rice. Obviously, the land which is best suited to rice production would be withdrawn from wheat production. Since this land was not well suited to wheat production a large increase in rice production could be obtained at the cost of a small decrease in the output of wheat. As more land is reallocated from the production of wheat to the production of rice each additional unit will produce a smaller increment of rice while it will cause a greater decrement in wheat production. Therefore, the amount of wheat which must be foregone to produce an additional unit of rice increases with increases in rice production.

If different factors were not better suited to the production of some goods than to others we might have obtained the opposite result. For example, if the factors of production were equally well suited to the production of both X and Y and if there were economies of scale in the production of both goods, the production possibility frontier would be convex to the origin as illustrated in Figure 5. This case is discussed later in the chapter as it creates problems for the efficient operation of competitive markets.

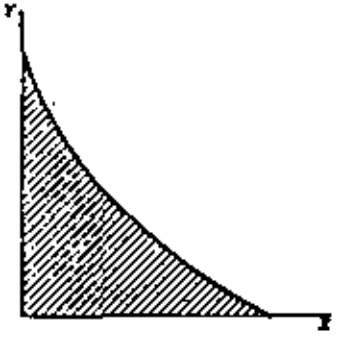

Fig. 5

Distribution

At this point we have considered the problem of allocating factors of production. The total allocation problem involves two additional questions:

first, what bundle of goods should be produced; and second, how should this bundle be distributed between the two consumers. Equivalently, we must consider what point on the production possibility frontier should be selected and how the goods should be distributed between individual A and individual B.

We proceed by assuming that the first choice has been made and discuss the optimal distribution of a fixed bundle of goods. Before we can proceed with the analysis we must introduce the notion of a preference ordering and the concept of a utility function. We assume that each individual is concerned only with the goods he receives. We further assume that his preferences are such that for any two commodity bundles (X^1, Y^1) and (X^2, Y^2) either (X^1, Y^1) is preferred to (X^2, Y^2), (X^2, Y^2) is preferred to (X^1, Y^1), or he is indifferent between (X^1, Y^1) and (X^2, Y^2).

These three alternatives are mutually exclusive and collectively exhaustive. In addition, the individual's preferences are assumed to be transitive. Transitivity means that if (X^1, Y^1) is preferred to (X^2, Y^2) and (X^2, Y^2) is preferred to (X^3, Y^3), then (X^1, Y^1) is preferred to (X^3, Y^3). In addition if $X^1 \geq X^2$ and $Y^1 \geq Y^2$ and if the strict inequality holds for either case, then (X^1, Y^1) is assumed to be preferred to (X^2, Y^2) on the grounds that people prefer to consume more goods to less. A complete discussion of the logical properties of preference orderings is beyond the scope of this chapter; however, for the interested reader a concise and readable treatment of this subject is presented in Quirk and Saposnik (1968).

Given certain conditions the preference ordering of an individual can be represented by a utility function. A function U_A defined on ordered pairs of commodities is a utility function for individual A if for (X^1, Y^1) preferred to (X^2, Y^2), $U_A(X^1, Y^1) > U_A(X^2, Y^2)$ and for (X^1, Y^1) indifferent to (X^2, Y^2), $U_A(X^1, Y^1) = U_A(X^2, Y^2)$. Clearly, U_A is an increasing function of X and Y. However, the utility function is not uniquely determined. If $h(\cdot)$ is any strictly increasing function of a real variable, then the function V_A also satisfies the conditions for a utility function for individual A where $V_A(X, Y) = h[U_A(X, Y)]$. Therefore, it is clear that only the ordinal properties of a utility function are central to the analysis. If $U_A(X^1, Y^1) > U_A(X^2, Y^2)$, this means that (X^1, Y^1) is preferred to (X^2, Y^2) by individual A; however, no other significance can be attached to the difference $U_A(X^1, Y^1) - U_A(X^2, Y^2)$. This difference is not invariant under all strictly increasing transformations of U_A.

Suppose we have a utility function U_A for individual A. Then the relationship $U_A(X, Y) = C$, where C is a constant, implicitly defines a locus of points among which individual A is indifferent. This locus is called an indifference curve. A family of indifference curves for individual A is presented in Figure 6. Points on higher indifference curves are preferred to points on lower curves by individual A. From the assumption of transitivity and the

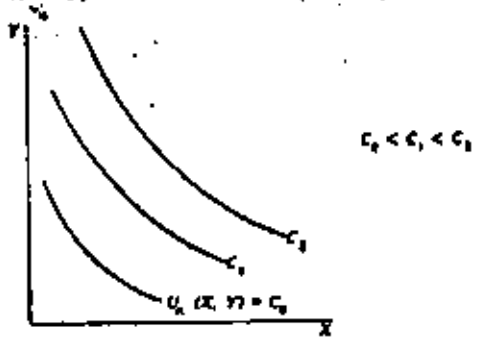

Fig. 6

assumption that individuals prefer more goods rather than less, it follows that indifference curves must be downward sloping from left to right. It also follows that no two indifference curves can cross each other. Furthermore, it follows that indifference curves are invariant to any strictly increasing transformation of the utility function. Again let $U_A(X, Y)$ be a utility function. Let $V_A(X, Y) = h[U_A(X, Y)]$ be a second utility function where $h(\cdot)$ is a strictly increasing function of a real variable. Let $U_A(X, Y) = C$ define an indifference curve under the first utility function. Then for all (X, Y) on this indifference curve, $V_A(X, Y) = h[U_A(X, Y)] = h[C]$, another constant. Therefore, the indifference curves under the first utility function are identical to the indifference curves under the second utility function.

In addition, the indifference curves in Figure 6 have been drawn convex to the origin. This requirement means that the marginal rate at which increments of Y can be substituted for decrements of X so that utility is kept constant decreases as the consumption of X increases. In other words if an individual has an initial endowment of food and clothing he is willing to trade less food for additional clothing as his clothing supply is increased by trading food for clothing. The absolute value of the slope of the indifference curve for individual A is the marginal rate at which he is willing to substitute Y for X given some initial endowment (X, Y). It is generally assumed that this marginal rate of substitution is decreasing as X increases so that indifference curves are convex to the origin as in Figure 6. In addition we assume, for convenience, that the utility function has continuous second-order derivatives.

To summarize, each consumer is assumed to have a preference ordering for commodity bundles (X, Y), and these preference orderings can be expressed in terms of utility functions U_A and U_B. Furthermore, individual utility is assumed to be a function only of the goods allocated to that individual. The indifference curves for each individual are assumed to be

convex to the origin as pictured in Figure 6. Finally, only the ordinal properties of the utility function are significant.

We can now address the problem of how to distribute efficiently a fixed bundle of goods between individual A and individual B. In Figure 7 we have drawn the production possibility curve $0_A'0_B'$, have selected a point, β, on this curve, and have denoted the total output at this point by (X_β, Y_β). To demonstrate the conditions for optimal distribution of the fixed output (X_β, Y_β), we have drawn an Edgeworth-Bowley box diagram in Figure 7. The horizon-

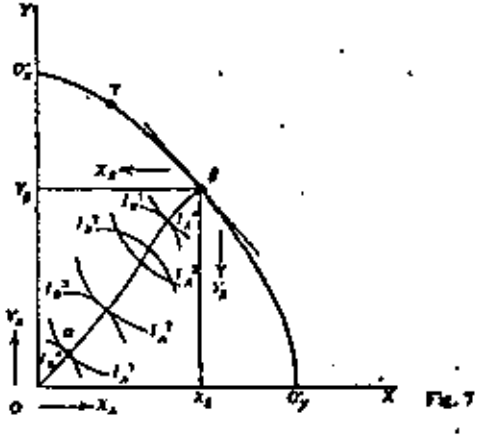

Fig. 7

tal edge of the box is of length X_β; the vertical edge, Y_β. The amount of X and Y allocated to individual A is measured from the origin 0; the amount of X and Y allocated to individual B is measured from the origin β. Every point in the box, $0Y_\beta\beta X_\beta$ represents an allocation of X_β and Y_β between individuals A and B. In addition we can draw in the indifference curves for individuals A and B. The I_A^1, I_A^2, I_A^3, and so on are indifference curves which represent increasing levels of utility for individual A, and I_B^1, I_B^2, I_B^3, and so on represent increasing levels of utility for individual B.

The question that arises is how to allocate (X_β, Y_β) between A and B so that it is not possible for both individuals to move to higher utility levels through trading. By an argument analogous to that for productive efficiency, it can be shown that the locus of efficient points corresponds to the locus of tangency points of the indifference curves for A and B. The locus of efficient distributions is represented by the locus 0β in Figure 7. Therefore, the condition for efficiency in distribution is that, given a particular distribution

of X and Y, the marginal rate of substitution is the same for all individuals who consume positive quantities of both X and Y.* Intuitively one can see that if one individual is willing to trade X for Y at a different rate than is another, there exists an opportunity for a trade which redistributes X and Y so as to make both individuals better off. If this opportunity exists, the initial distribution was not efficient in the Pareto sense.

Choice of Outputs

At this point efficiency has been discussed in terms of allocation of factors of production and of distribution of a fixed bundle of goods. In both cases there was an infinite number of points which satisfied the efficiency conditions. Two questions remain: (1) what bundle of goods should be produced; and (2) which distribution among the efficient distributions of that bundle should be chosen. The answer to these questions involves an introduction of additional value judgments into the analysis. The concept of a social welfare function is introduced to incorporate these value judgments into the analytical framework.

Consider Figure 7 again. Every point on the efficient locus corresponds to a utility level for individual A and a utility level for individual B. By plotting utility levels for A and B for each point on the efficient locus, we can construct a utility possibility frontier. Such a frontier represents a mapping into utility space of efficient distributions of fixed quantities of output. Of course the utility possibility frontier for one output bundle is different from the frontier for another output bundle. In Figure 8 are plotted utility possibility frontiers for several output bundles on the production possibility frontier. The locus $\beta\beta$ corresponds to the output bundle β; the locus $\gamma\gamma$ corresponds to another output bundle γ. Note that each utility possibility frontier must have a negative slope because each point on the locus corresponds to an efficient distribution of a fixed bundle of goods. The grand utility frontier is the outer envelope of all utility possibility frontiers and is represented by UU in Figure 8.

Since an allocation may correspond to a point on a utility possibility frontier while not corresponding to a point on the grand utility frontier, the two efficiency conditions developed previously are not sufficient to guarantee Pareto optimality. In particular, even though resources are allocated optimally for the chosen levels of outputs and though the outputs are optimally distributed, the chosen outputs themselves may not be optimal. Therefore, we must derive conditions to assure that it is impossible to make both individuals better off by reallocating resources from the production of X to the production

* As in the case of productive efficiency, this condition may not hold for points on the boundary of the box.

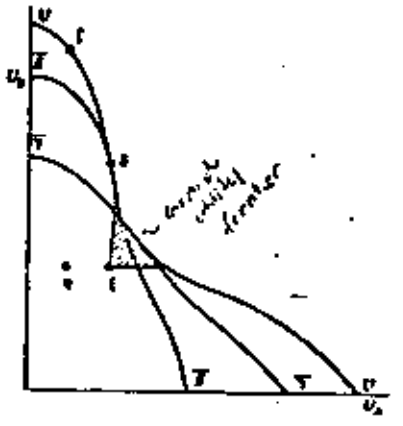

Fig. 8

of Y or vice versa. A condition relating production to distribution must be developed. This condition is that the marginal rate of transformation of X into Y must equal the marginal rates at which A and B are willing to substitute Y for X. This condition is pictured in Figure 7. The only points on the efficient locus 0β which correspond to points on the grand utility frontier are those such as e where the slopes of the indifference curves for A and B at e equal the slope of the production possibility frontier at β.

A simple example will demonstrate that this condition is necessary for Pareto optimality. Suppose that individuals A and B were both willing to substitute two units of X for one unit of Y, and that it was possible to reallocate the factors of production so that one additional unit of Y could be produced at the expense of one unit of X. Then if we produced two more units of Y and two fewer units of X and gave each individual one more unit of Y and one less unit of X, both individuals would prefer this new bundle of goods to the initial one. This conclusion can be drawn from the fact each individual would have been willing to give two units of X for one unit of Y; each, in fact, had to sacrifice only one unit of X for an additional unit of Y; therefore, each is better off with the new allocation than with the old.

To summarize, the conditions which must be satisfied for an allocation of resources to be Pareto optimal are (1) the marginal rate of substitution between any two factors of production must be the same in all productive processes which use positive quantities of both factors, (2) the marginal rate of substitution between two goods in consumption must be the same for all individuals who consume positive quantities of both goods, and (3) the marginal rate of substitution between two goods in consumption must equal the marginal rate of transformation between these two goods. These con-

dition along with the assumptions about the shapes of the isoquants and indifference curves constitute the necessary conditions for Pareto optimality. The conditions are also sufficient for Pareto optimality except in certain cases where there are corner solutions and the equalities above must be replaced by inequalities. This refinement is discussed in Baumol (1957), Debreu (1959), and Quirk and Saposnik (1963).

Again consider the grand utility frontier in Figure 8. It is clear that the points on this frontier correspond to Pareto optimal resource allocations; however, there is an infinite number of such allocations. The problem is how to choose among them. Consider the point at which the utility frontier intersects the vertical axis. Here the allocation of resources is such that the utility of individual B is maximized while individual A has nothing. As we move down the utility frontier individual A's utility increases and individual B's utility decreases until we reach the horizontal axis where the utility for A is the maximum possible while B has nothing. Therefore, resource allocation may be Pareto optimal even though one individual gets everything that is produced. Furthermore, it is clear that the choice of the optimal point on the grand utility frontier is essentially a choice of how income should be distributed between A and B. This choice requires the introduction of a value judgment regarding the appropriate distribution of income.

One tempting line of argument would be to choose that point on UU at which $U_a + U_b$, the sum of the utilities of the two individuals is maximized. However, this procedure could be justified only if we could assign to each individual a cardinal utility function which measured the intensity of his preferences and if the utility functions for both individuals measured intensity of preference on a common scale. While this kind of social calculus once formed the basis of welfare economics, no satisfactory conceptual procedure has been devised to measure intensity of preference. Furthermore, interpersonal comparisons of this type have been abandoned for this reason. To get around these difficulties modern welfare economics assumes only that individuals can rank alternatives in a consistent manner.

Consider again the grand utility frontier in Figure 8. The choice among the points on this frontier involves making a value judgment as to the appropriate utility levels to be assigned to individuals A and B. The social processes by which such a decision might be made and the related question of proper definition of the social welfare function have been discussed in the literature; however, this discussion is beyond the introductory treatment of the subject presented here (Arrow, 1963; Graaf, 1957; Little, 1950; Quirk and Saposnik, 1968).* For the present discussion, assume that alternative points (U_a, U_b)

* Social welfare functions commanding general consent cannot as a practical matter be defined. The concept, however, is useful as a tool in analyzing the issues that are central to optimal resource allocation and to public policy. There exists a special body of literature dealing with questions of how in principle one might construct a social welfare function. The classic work on this topic is Arrow (1963). As a practical matter, policy decisions of this type are made through the political process where bargaining and voting procedures are a central element. No complete model of the political decision making process has been developed with which one could explore the properties of this process, and there is no reason to believe that this process leads to decisions or choices which satisfy any of the properties postulated for social welfare functions. Therefore, while the concept of a social welfare function is instructive, it does not provide an operational tool for choosing among allocations nor does it necessarily correspond to any actual decision process.

in Figure 8 can be ranked according to some ethical criterion. Furthermore, assume that this ranking is transitive and can be expressed by a social welfare function, W, such that if (U_a^1, U_b^1) is socially preferred to (U_a^2, U_b^2) then $W(U_a^1, U_b^1) > W(U_a^2, U_b^2)$. The only condition imposed on W is that it be a strictly increasing function of U_a and U_b. The justification for imposing this condition is the value judgment that social preferences should relate positively to individual preferences. If, given two points η and ξ in Figure 8, such that ξ provides a higher level of utility for individual A and the same level for individual B as does alternative η, then ξ should be socially preferred to η. The assumption that W is an increasing function of U_a and U_b implies that the social optimum among the attainable allocations will correspond to a point on the utility frontier such as point δ in Figure 8. An allocation of productive factors, a production of a particular bundle of goods, and a distribution of goods, corresponds to δ.

Now consider the relationship of Pareto optimality to the optimal allocation of resources from an overall social point of view. Given that the social welfare function has been postulated to be a strictly increasing function of U_a and U_b it follows that the overall social optimum will lie on the grand utility frontier. Therefore, Pareto optimality is a necessary condition for overall welfare maximization or social optimality. At the same time it is important to make it clear that Pareto optimality is not sufficient for social optimality. In fact allocations which are Pareto optimal may be inferior from a social point of view to allocations which are non-Pareto optimal. This fact can be illustrated in Figure 8. The point ξ which lies inside the utility frontier may be superior to the point ζ which lies on the frontier, but which distributes most of the output produced to individual B. That is, ξ may be preferred to ζ because the distribution of income at ξ is considered socially more desirable than at ζ. At the same time it is clear that there are feasible allocations of resources which are superior to ξ; these allocations are represented by the shaded area lying to the right of ξ in Figure 8.

From the foregoing discussion it should be clear that Pareto optimality is desirable, but that other factors such as the distribution of income must be considered in choosing among various resource allocations. In addition it is

clear that an allocation is either Pareto optimal or it is not. The concept of Pareto optimality generally does not provide a basis for choosing among allocations which are not Pareto optimal. In practice this problem often arises since it may be impossible to bring about an allocation of resources that satisfies all the conditions required for Pareto optimality and, at the same time, meets the requirements for an equitable distribution of the income. One is often faced with the task of evaluating alternative policies which are associated with resource allocations which are not Pareto optimal, but which are feasible given all the constraints faced in the real world. The concept of Pareto optimality is of little use for choosing among such allocations. If, however, one accepts the distribution of income as optimal, Pareto optimality becomes a sufficient condition for a social optimum. This last point is expanded in the discussion of optimality and competitive markets.

OPTIMUM RESOURCE ALLOCATION AND COMPETITIVE EQUILIBRIUM UNDER PERFECT COMPETITION

The development of a theory of optimal resource allocation has closely paralleled the development of the theory of perfectly competitive markets. In particular it can be demonstrated that given the conditions which are assumed to hold in perfectly competitive markets, the allocation of resources associated with competitive equilibrium will be Pareto optimal. Furthermore, under appropriate assumptions it can be demonstrated that any Pareto-optimal allocation of resources corresponds to the equilibrium allocation of a perfectly competitive economy given some initial distribution of wealth. In this section the basic assumptions underlying the model of perfectly competitive markets are presented, the argument that competitive equilibrium brings about a Pareto optimal allocation of resources is sketched, and the conditions under which market competition fails to bring about an efficient allocation of resources are discussed.

It is assumed that each producer operates his firm to maximize profit, and that each individual buys goods and sells his services to maximize his utility. From the assumption that producers are profit maximizers it follows that for any fixed bundle of inputs the producer will employ these inputs so as to produce the maximum output. Therefore, a production function defines the relationship between inputs and outputs for each production unit.

In addition it is assumed that each production unit and each individual behaves as a price taker in the sense that market prices are taken as given by each consumer and by each producer. This assumption is based on a concept of markets in which there is a large number of buyers and sellers in each market and in which the transactions of any buyer or seller are an inconsequential fraction of the total transactions of that market. For example, a farmer selling wheat in a national market would not be in a position to influence the market price. Neither would a consumer buying shoes. There has been wide debate over the minimum number of participants and the maximum relative size of the participants consistent with the assumption that prices are taken as given. Clearly, in markets where the industrial giants account for a major fraction of the sales, this assumption is not valid.

A further assumption of the theory of perfectly competitive markets is that the output of any productive unit depends only on the quantity of inputs it uses and on its technical capabilities. The output does not depend upon the production decisions of other firms. This assumption is implicit in the definition of a production function which relates inputs to outputs and which does not depend on the level of production of other commodities. Similarly, the utility of each individual is assumed to depend only on his own consumption. These assumptions were also implicit in the presentation of optimal resource allocation.

Finally, it is assumed, as before, that production functions are such that the isoquants are convex to the origin and that preferences are such that indifference curves are convex to the origin. Production functions are also assumed to exhibit decreasing returns to scale* at some point. This assumption is related to the condition that the production possibility curve be concave to the origin as pictured in Figure 4. This assumption assures that at some level of output the incremental costs of producing an additional unit of output begin to increase. This increase in incremental or marginal costs is a necessary condition for the size and number of firms to be consistent with competitive markets, a point which will subsequently be discussed.

Consider an individual firm which produces a single product X using capital and labor, K and L. Let the production function for this firm be $X = f(K, L)$. In addition the prices for X, K, and L are P_x, P_k, and P_L respectively. The profit of the firm is equal to $P_x X - P_k K - P_L L$. Therefore, the problem of the firm is to maximize $P_x X - P_k K - P_L L$ subject to the constraint that $f(K, L) = X$. The problem of profit maximization can be decomposed into two parts: one is selection of that bundle of inputs which minimizes cost for the chosen level of output; the other is a selection of that level of output which maximizes profit.

It will be demonstrated that if all production units individually were to maximize their profits given a fixed set of prices consistent with the equation of supply and demand in every market, the total production of all commodities would represent a point on the production possibility curve.

Suppose that the production unit under consideration were to produce an

* Technically, decreasing returns to scale means that a proportionate increase in factor inputs will lead to a less than proportionate increase in output.

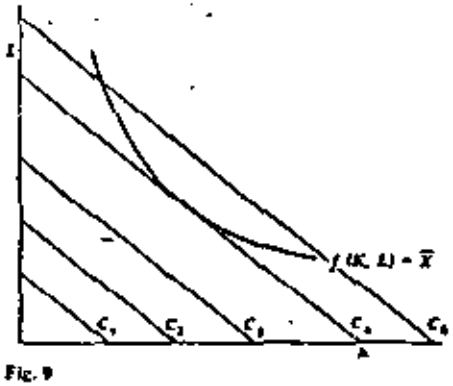

Fig. 9

output $\bar{X}$ at minimum costs. The various combinations of K and L which can be used to produce this output are represented by the isoquant in Figure 9. Equal cost lines have been also plotted in Figure 9. Each line is defined by a cost equation of the form $P_K K + P_L L = C$ where C represents a constant level of cost. The slope of each equal cost line is $-P_K/P_L$. The input combination which minimizes the cost of producing $\bar{X}$ is represented by the point at which the isoquant is tangent to the equal cost line C_4. The absolute value of the slope of the isoquant at any point is the marginal rate of substitution between K and L. Therefore, at the point where costs are minimized the marginal rate of substitution between K and L is equal to the price ratio P_K/P_L.

In Figure 9, we see that the minimum cost of producing $\bar{X}$ is C_4. By using the same procedure, we could find the minimum cost of producing any other level of output X. Therefore, we can represent the minimum cost of producing a given level of X as a function of X, $C(X)$. The revenue derived from the sale of the output X is also a function of X. This revenue is equal to $P_X X$. Therefore, profits will be maximized at that level of output at which $\pi(X) = P_X X - C(X)$ is maximized. Clearly, a necessary condition for X to maximize $\pi(X)$ is that $P_X = dC/dX$. That is, the profit maximizing level of output is that level at which the marginal or incremental cost of producing the last unit produced just equals the price at which that unit can be sold. This condition is illustrated in Figure 10. Notice that the maximum occurs at the point where marginal cost (MC) equals price only if $C(X)$ is concave upward at that point. Notice, also, that if the profit maximizing level of output is to be finite, then the marginal cost of production must at some point become greater than the price. Otherwise, a firm could continue to increase its profit by increasing its output. In such a case, one firm would

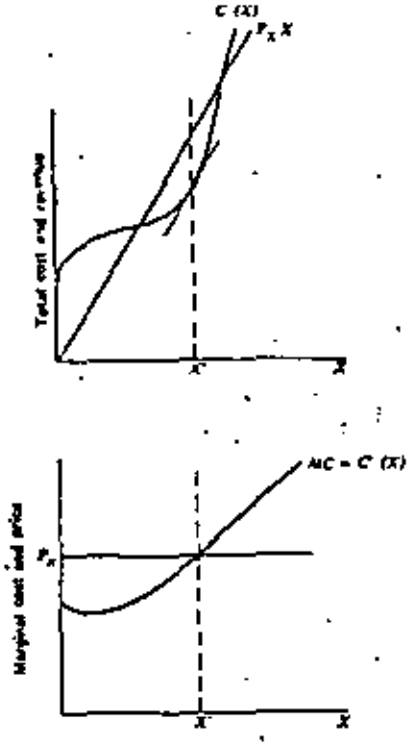

Fig. 10

eventually drive out the competition and would produce for the entire market. This is a basic reason why increasing returns to scale are incompatible with perfect competition.

Now consider the overall allocation of resources in terms of the results of this discussion. Consider a producer of commodity X and a producer of any other commodity Y. If each producer uses both K and L as inputs, the marginal rate of substitution between K and L will equal P_K/P_L for each producer. Therefore, the marginal rate of substitution between K and L will be the same in the production of both X and Y. This equality is one condition required for optimal resource allocation. In addition each firm will produce up to the point at which its marginal cost is just equal to the price of the good that it produces. Therefore, $MC_X = P_X$ and $MC_Y = P_Y$. It follows that if resources were diverted from the production of X to the production of Y, at the margin the rate of transformation between X and Y would be given by

P_x/P_y. For example, suppose $P_x = \$2$ and $P_y = \$1$. Then a decrease in the production of one unit of X would free \$2 worth of resources. These resources would produce 2 units of Y. Therefore, the marginal rate of transformation is 2 for 1. This rate of transformation is just equal to the price ratio, P_x/P_y.

Now consider the behavior of individual consumers. Each consumer begins with a certain quantity of capital and labor which he can sell. He simultaneously decides on how much capital and labor to sell and how much of the commodities X and Y to buy. This decision is made to maximize his utility. To facilitate a graphical presentation in two dimensions, suppose the individual has decided to sell K' units of capital and L' units of labor so that his income is given by

$$I = P_K K' + P_L L'$$

His decision is now to choose a bundle of goods (X', Y') within his budget. In Figure 11, the budget constraint is the line defined by having $I = P_x X' + P_y Y'$ having a slope P_x/P_y. All points below the budget line represent bundles the cost of which is less than his total income; all points on the budget line represent bundles the cost of which equals his income. It is assumed that he will choose that combination of goods within his budget which will maximize his utility. Clearly, this combination is represented by point λ in Figure 11, the point at which the budget line is just tangent to the highest indifference curve which contains a point (X', Y') such that $P_x X' + P_y Y' = I$. Therefore, at λ the marginal rate at which the individual is willing to trade Y for X equals the price ratio P_x/P_y.

Since everyone faces the same set of prices, it follows that the marginal

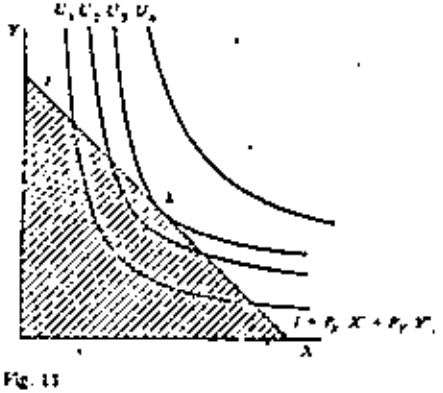

Fig. 11

rate of substitution between X and Y will be the same for every individual who consumes both X and Y. This equality is one of the conditions for Pareto optimality. In addition, since the marginal rate of transformation between X and Y equals P_x/P_y, it follows that the marginal rate of substitution between X and Y in consumption equals the marginal rate of transformation between X and Y in production as shown in Figure 7. Therefore, under the assumptions of perfect competition, the equilibrium resource allocation which obtains through competitive markets will be Pareto optimal and will correspond to a point on the grand utility frontier in Figure 8.

The point on the grand utility frontier which actually will be obtained under perfect competition will depend on the initial distribution of wealth. Recall that an individual's income was determined by the equation $I = P_L L + P_K K$. Therefore, the level of utility that an individual can attain will depend on his original endowment of capital and labor and upon the prices of these two factors. It can be demonstrated that each point on the grand utility frontier corresponds to an allocation of resources which will prevail in competitive equilibrium given some initial distribution of wealth. Therefore, by some redistribution of the initial wealth it is possible to attain any point on the grand utility frontier. It is in this sense that a choice among points on the utility frontier is essentially a choice among different distributions of income.

The discussion to this point has employed the concept of general equilibrium without defining its meaning. The behavior of individuals and of production units has been discussed on the assumption that individuals and production units can buy and sell any amount of each commodity they choose at the given set of prices. Clearly, for an arbitrary set of prices the sum of individual choices will not be consistent with resource endowments. Demands will exceed supplies in some markets and supplies will exceed demands in others. An equilibrium set of prices is one, such that demand and supply are equated simultaneously in all markets. A competitive equilibrium is an allocation of resources associated with an equilibrium set of prices.

One of the primary functions of a competitive market is that it directs production and consumption decisions toward an equilibrium. The process of adjustment toward equilibrium takes place through price changes. If supply exceeds demand for a commodity the price of that commodity will fall; the price decline will effect an increase in the amount demanded by buyers and a decrease in the amount supplied by producers. Both changes will reduce the amount by which the supply exceeds the demand. In the case of an excess of demand over supply the price will be driven up, thereby reducing the excess demand. In summary, competitive markets operate so as to guide production and distribution not only toward an equilibrium state where supplies equal demands, but also toward a Pareto optimal allocation

of resources. If one were to accept the premise that a certain distribution of wealth was ideal from a social point of view, then in equilibrium the competitive market would produce the socially optimal allocation of resources.

The significance of several obvious simplifications must be clarified. First, it was assumed that there were two factors of production, two individuals, and two goods which were produced. This assumption made it possible to present the results graphically. The results can be generalized to the case where there are any finite number of factors, individuals, and consumption goods. Second, it was assumed that the factors of production were in fixed supply and that these factors could not be consumed directly; there were no intermediate goods and no goods which were both consumed and used in production. Again, this assumption was made to facilitate a graphical presentation and does not affect the validity of the results. Third, there were no joint products, that is, each production unit was assumed to produce a single product. This assumption too can be dropped without changing the basic results of the analysis. Fourth, it was assumed that the isoquants and the indifference curves were smooth and convex to the origin. The assumption of a smooth curvature can be relaxed with the result that the conditions for Pareto optimality become a set of inequalities instead of equalities, but this relaxation does not significantly alter basic results. The assumptions concerning the convexity of the indifference curves and the isoquants and the concavity of the production possibility frontier are, however, critical to the analysis. These shapes are related to the mathematical concept of convexity which plays a central role in the formal proof of the general theorems presented. A complete discussion of convexity as it relates to competitive markets and Pareto optimality is beyond the scope of this chapter. The interested reader should refer to Bator (1957), Debreu (1959), and Quirk and Saposnik (1968) for a basic discussion of this issue. One can get an idea of the difficulties which can arise, however, if the assumptions regarding the shapes of various curves are violated. Suppose that isoquants instead of being convex to the origin were concave to the origin. Then the tangency points in Figure 2 would not be optimal. Similarly, the tangency point between the equal cost line and the isoquant, in Figure 9, would not represent the least cost combination for producing that output, but would instead represent the most costly combination. One particularly important situation associated with nonconvexity is that of increasing returns to scale. This situation is discussed in the final section of the chapter.

The analysis of resource allocation has been presented as if production and distribution were carried out under conditions of certainty at a given point in time and space. Clearly, however, production takes place over time, at different locations, under uncertain conditions; the factors of time, location, and uncertainty are critical. The analysis which has been developed can

be extended so as to handle these factors with no effect on the basic results. This extension is accomplished by distinguishing commodities by time, location, and states of the world. Suppose that economic activity takes place over time and that time can be divided into T periods. Then if X is a given commodity, X_1 would represent a quantity of commodity X in period 1. Similarly, one could index the commodity by location so that X_{ij} would represent a quantity of commodity X at time i at location j. Since from an economic point of view, commodities at different locations or at different points in time are not interchangeable, they are treated as different commodities each with its own price.

It is fairly easy to see how one can incorporate time and space into the analysis by differentiating commodities by time and location. The treatment of uncertainty while it is analogous to that of time and location is conceptually more difficult. To introduce uncertainty into the analysis the concept of a state of nature is employed. A state of nature is a complete description of the world such that if the state of nature is known, then the outcomes of all actions are known with certainty. Therefore, given a state of nature, a deterministic model of the economy can be applied. In general, however, there are many possible states of nature and only one will be the true state of nature. Individuals are assumed to assess subjective probabilities as to which state of nature does in fact obtain. Therefore, production and consumption decisions are made on the basis of expectations about the future. Under this analysis commodities are differentiated by time, location, and the state of nature. Individuals are assumed to buy and sell claims much like insurance policies which yield different bundles of commodities given different states of the world. For example, suppose there are two possible states of the world, one in which a given individual will be alive and another in which he will be dead. A life insurance policy is a claim contingent on the state of the world. If the first state obtains, then the policy pays nothing; if the second state obtains and the man dies, the claim pays the amount prescribed by the policy.

The extensions of the model to cover multiple time periods, spatial considerations, and uncertainty simply increase the number of commodities in the economy. This increase creates no analytical problems. However, the difficulty illuminated by the analysis of the extensions is that markets are required for the purchase and sale of contingent claims on commodity bundles at different locations and times. Conceptually, at the beginning of each time period individuals would contract a complete set of transactions for future as well as present production and consumption. Clearly, the set of markets required for the complete set of transactions does not exist. One reason that markets do not exist is that the cost of establishing and carrying out some transactions is so high that markets do not develop.

A more complete discussion of time, space, and uncertainty is beyond the scope of this introductory treatment of resource allocation; however, the interested reader is referred to Debreu (1969) and Radner (1968). The basic conclusion of much of the discussion is that once time, space, and uncertainty have been introduced into the model, the case for the Pareto optimality of competitive markets is weakened because of the difficulties in setting up the requisite markets. Similarly, the economic system which exists in the United States today may fail to achieve optimality not only because of market imperfections to be discussed in the next section, but also because certain markets for insurance and for intertemporal transactions do not exist. When the markets for insurance and capital do exist they often do not meet the conditions of perfect competition.

The theory of resource allocation even as extended to cover a number of periods of time is basically static and does not consider the dynamic aspects of capital formation and economic growth. Recently economists have developed a dynamic theory of optimal resource allocation analogous to the static theory presented here. This work has gone under the heading of optimal economic growth and has employed many of the results of control theory. While the theory of optimal economic growth has been an important contribution to our understanding of efficiency over time, it has not provided a full blown model of economic growth. In particular, processes of innovation and of technical change are not adequately incorporated into this work. In addition, at the present state of development these models are of little value for practical planning.

MARKET FAILURE, EXTERNALITIES, AND INCREASING RETURNS TO SCALE

In addition to problems presented by time and uncertainty, there are two important situations in which competitive markets fail to effect a Pareto optimal allocation of resources. It is in these situations that we find government action which is designed to redress the misallocations. The first case is one in which there are increasing returns to scale in the production of a specific product. The second is the situation in which there are direct, non-market interactions between units. Such interactions are referred to as externalities.

Consider the situation in which there are increasing returns to scale in the production of one commodity. In this case the per unit or average cost of production of the commodity falls as the level of output increases. As a result the marginal cost curve will lie below average cost curve at all levels of output as illustrated in Figure 12. If the firm could sell any level of output

at a fixed price, then the profit maximizing level of output would be either zero or infinity depending upon the price level. Clearly, however, an infinite output is impossible since the market for any product is finite. In such a situation, an aggressive firm will tend to expand rapidly and drive smaller firms out of the market by selling at a lower price based on lower per unit production costs. Once competitors are driven from the market, the remaining firm will behave as a monopolist and the resulting allocation of resources will not be Pareto optimal. More specifically, the price fixed by the monopolist will be above that consistent with Pareto optimality and production will be below the optimum level. This situation is shown in Figure 12.

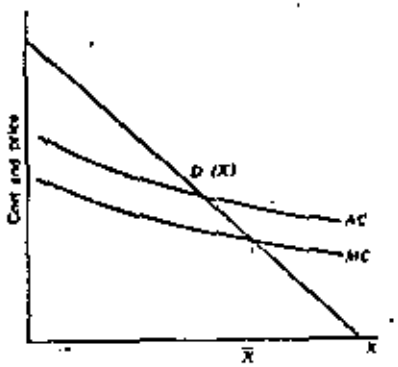

Fig. 12

In Figure 12 the demand curve for a product, represented by $D(X)$, gives that price which will clear the market as a function of the quantity produced. A basic theorem in welfare economics is that for Pareto optimality goods must be priced so that the marginal cost of the last unit produced is equal to the price. If this equality does not hold, then there exists someone who is willing to pay more for an additional unit of production than the additional cost of that production. If the firm were to produce that unit and to sell it at marginal cost the consumer would be better off and the producer would be made no worse off. Therefore, the initial allocation would not have been Pareto optimal. However, if a producer must charge one price for all units sold, a profit maximizing producer facing increasing returns to scale will not set price equal to marginal cost. It can be seen from Figure 12 that whenever there are increasing returns to scale a price equal to marginal cost will result in losses being incurred by the producer. In Figure 12 the demand curve and the marginal cost curve intersect at $\bar{X}$; at this point price is less than average

cost and the producer incurs losses. Clearly, a private monopoly would operate at such a point. In fact, it is clear from Figure 12 that a profit-maximizing monopoly will produce at an output below that which is Pareto optimal and will charge a price above marginal cost.

The case of increasing returns can be illustrated with two examples. First consider the case of supplying water. It would not be efficient for competing companies to serve the same market since there are economies of scale. At the same time a private monopoly may pursue a pricing policy which is contrary to the public interest. In a large number of cases this difficulty has been resolved through public ownership of water companies. A second example is that of the telephone industry. In this case the solution has been to allow a private monopoly to own and operate the system, but for the government to regulate prices.

The second situation in which competitive markets fail to effect a Pareto optimal allocation of resources is where there are externalities, or direct nonmarket interactions of the economic units. In the development of the basic results of this paper, it was assumed that the production relationships in one firm were independent of production decisions by other firms and that the utility levels of one individual were independent of consumption decisions of other individuals. These independence assumptions were implicit in the way production functions and utility functions were defined. Where interdependencies exist, they are called externalities. Pollution is a classical example of an externality. Production which results in pollution may affect both the production function of other firms and the well being of individuals. This nonmarket, direct interaction, between the firm causing pollution and other firms and individuals, violates the independence assumptions of perfect competition. Externalities cause misallocation of resources because the person who creates a cost or a benefit for someone else does not take this cost or benefit into account in planning his production and consumption decisions. For this reason, prices will not direct the market system toward a resource allocation in which the marginal rate of substitution in consumption between any two goods is equal to the marginal rate of transformation in production for the two goods.

An extreme case of an externality in consumption is the case of "public goods." A public good is one where if one person can consume this good, everyone can consume it. National defense is a public good since it is practically impossible to defend only certain individuals. Clean air is a public good since everyone can enjoy it if it exists. Thus the nature of public goods is such that it is impossible to exclude individuals from consuming the good if they do not pay for it. Therefore, it is impossible to sell such goods in the market. There would be no incentive for private firms to produce these goods which cannot be sold. Clearly, many such goods are of value and should be produced. One way around the dilemma is for a governmental unit to purchase these goods publicly and to require that everyone pay for them through taxation.

To summarize, markets will fail to allocate resources efficiently when there are economies of scale or when there are externalities. Most cases in which the government intervenes directly in the allocation of resources involve either externalities or increasing returns to scale. However, the third reason for government intervention is not related to economic efficiency but to income distribution. When the existing distribution of wealth diverges greatly from the socially optimal distribution of wealth, government action may be required to bring the actual distribution closer to the ideal distribution.

REFERENCES

Arrow, K. J. (1963), *Social Choice and Individual Values*, Wiley, New York.

Arrow, K. J., L. Hurwicz, and H. Uzawa (1958), *Studies in Linear and Non-Linear Programming*, Stanford University Press, Stanford, Calif.

Bator, F. M. (1957), "The Simple Analytics of Welfare Maximization," *American Economic Review*, March, pp. 22–59.

Debreu, G. (1959), *Theory of Value*, Wiley, New York.

Graaff, J. de V. (1957), *Theoretical Welfare Economics*, University Press, Cambridge.

Henderson, James M., and Richard E. Quandt (1958), *Microeconomic Theory*, McGraw-Hill, New York.

Koopmans, Tjalling C. (1957), *Three Essays on the State of Economic Science*, McGraw-Hill, New York.

Little, I. M. D. (1950), *A Critique of Welfare Economics*, Clarendon Press, Oxford.

Quirk, James, and Rubin Saposnik (1968), *Introduction to General Equilibrium Theory and Welfare Economics*, McGraw-Hill, New York.

Radner, R. (1968), "Competitive Equilibrium under Uncertainty," *Econometrica*, Vol. 36, No. 1, pp. 31–58.

ANALISIS DE PROYECTOS CON OBJETIVOS MULTIPLES.

INTRODUCCION.-

La mayoría de los proyectos del sector público contemplan objetivos como desarrollo regional, redistribución del ingreso e impacto ambiental, además de la eficiencia económica, que comunmente se considera en los análisis económicos a través de la relación beneficio-costo. La conveniencia de hacer explícitos esos objetivos es evidente, pues intervienen en el proceso de decisión y en la medida que se conozcan podrán ser juzgados.

Algunos economistas piensan que objetivos como la redistribución del ingreso pueden obtenerse de manera más eficiente a través de otros programas, pues nuestra capacidad para evaluar otro tipo de impactos ha sido muy limitada.

El cambio hacia objetivos múltiples proporciona un mecanismo para tratar en forma explícita esos aspectos; de esa manera, independientemente del carácter normativo o descriptivo de los objetivos, es conveniente que sean considerados en el proceso de evaluación.

En estas notas se hace referencia a algunos métodos propuestos para este tipo de análisis, describiendo su campo de aplicación y limitaciones.

ALGUNAS LIMITACIONES DE LA RELACION BENEFICIO-COSTO.-

Con el único fin de destacar las ventajas del enfoque de objetivos múltiples se describen algunas limitaciones de los métodos de análisis económicos, particularmente de la relación beneficio/costo.

a).- La relación B/C puede ser utilizada como una aproximación para seleccionar la escala de un proyecto o bien seleccionar un proyecto de un grupo de ellos.

b).- Atiende solamente al objetivo de " ingreso nacional neto "

(llamado eficiencia económica) y no considera efectos intangibles.

c).- Presentan algunos problemas como son:

1).- Problemas de medición:

Estimación de costos.- Las estimaciones generalmente contienen errores. Entre las fuentes de error destacan:

1).- Los precios de construcción aumentan.

2).- Cambios en las especificaciones de Proyectos; y

3).- Condiciones no previstas.

Fallas de Mercado y Externalidades.

II).-Aspectos conceptuales.

Riesgo e incertidumbre.

Tasa de descuento.- Tiene una influencia dramática en la relación beneficio-costo. La lámina indica algunos efectos resultantes de distintas tasas de descuento.

Horizonte de planeación.- Los problemas de horizonte de planeación y tasa de descuento van acompañados de la mano. Si bien el horizonte de planeación debe ser establecido de manera tal que si se incrementara, no tuviera mayores efectos en la jerarquización; sin embargo, en la práctica muchas veces se establece por experiencia o por razones administrativas.

El efecto combinado de la tasa de descuento y horizonte de planeación puede juzgarse a través del siguiente cuadro.

Tasa de descuento %	Relación Beneficio/Costo. Vida económica 100 años	Vida económica 50 años.
2.0	1.51	1.39
2.5	1.43	1.33
3.0	1.35	1.28
3.5	1.28	1.22
4.0	1.21	1.17
5.0	1.10	1.08
6.0	1.00	1.00

Beneficios secundarios.- Existe controversia respecto a la inclusión o exclusión de los beneficios secundarios. El - principal argumento contra la inclusión presupone una economía - sin desempleo, capacidad de utilización total y movilidad de labor y capital. Si el proyecto no se construye, habrá una salida de recursos económicos. El gasto de esos recursos originarán sus propios beneficios secundarios causados por la interdependencia de actividades económicas.

La atención que se ha prestado a los beneficios secundarios recientemente ha sido considerada ampliamente en la evaluación con objetivos múltiples.

Falta de información sobre redistribución de ingreso. Esta información no queda explícita pues la relación B/C agrega en el análisis.

Omisión de impactos relevantes.- Ejemplo de esto sucede con impacto ambiental.

III.- Aspectos Institucionales.

No considerar algunas alternativas factibles.

Orientación de los especialistas en Planeación:

Las limitaciones anotadas no pretenden desvirtuar el análisis de proyectos con criterio de B/C; por el contrario, se han señalado para destacar las áreas en las que conviene reforzar el análisis, haciendo explícitos elementos - que conlleven a una mejor decisión.

FACTORES Y PESOS.-

Considérese el siguiente problema:

$$\max \{f_1(\underline{x}), \ldots, f_p(\underline{x})\}$$

Sujeto a:

$$g_i(\underline{x}) \leq 0 \qquad i = 1, 2, \ldots, m$$

$$x_j \geq 0 \qquad j = 1, 2, \ldots, n$$

donde $\underline{x} = (x_1, \ldots, x_n)$ es un vector de variables de decisión.

$g_i(\underline{x}) \leq 0$ $i = 1, \ldots, m$ son las restricciones de las x.

$\{f_1(\underline{x}), \ldots, f_p(\underline{x})\}$ es un vector de P objetivos, cada uno de los cuales va a ser maximizado.

Si $P = 1$, hay un solo objetivo y el problema de optimización puede resolverse directamente. De hecho el grado de - dificultades para resolverlo depende de la forma de la función-objetivo y de las restricciones.

La región en el espacio n-dimensional de las variables de decisión en el que cada punto satisface todas las restricciones se llama región factible. Cada punto de esa región está asociado con un vector.

El método de factores pesados, para analizar problemas con objetivos múltiples consiste en combinar todos los - objetivos en una sola función, usando una suma pesada:

$$F(\underline{x}, \underline{w}) = \sum_{k=1}^{p} w_k f_k(\underline{x})$$

donde w_k son coeficientes de peso (o valores relativos).

Usando esta forma lineal, los aspectos que deben estudiarse al desarrollar este enfoque para jerarquizar, se reduce a:

1) La selección de los factores $f_k(\underline{x})$ y

2) La selección de los pesos.

Gran parte de la literatura sobre evaluación de proyectos puede ser organizada en términos de la selección de factores y pesos.

Algunos de los coeficientes resultan del análisis de datos físicos y económicos; otros reflejan valores relativos, - asignados a los distintos objetivos y resultan de juicios de valores.

Para analizar este problema se considerarán dos enfoques distintos. uno que pretende capter en una expresión matemática los factores y pesos; el otro que resulta de un proceso de participación pública y trata de incorporarla en la toma de decisión, es decir la decisión no es el resultado de la aplicación de una fórmula.

III.1 ENFOQUE ALGORITMICO.

La consideración básica de este enfoque es que se pueden incorporar valores en una fórmula y que ésta pueda usarse para desarrollar un algoritmo que jerarquiza acciones.

SELECCION DE OBJETIVOS.

Los métodos que corresponden a este enfoque parten de un conjunto de objetivos ya establecidos, los cuales forman la base para jerarquizar alternativas.

El consejo de Recursos Hidráulicos de Estados Unidos de Norteamérica ha recomendado los siguientes objetivos:

1.- Mejorar el desarrollo económico nacional.
2.- Mejorar la calidad del ambiente.
3.- Mejorar el desarrollo regional.

En los métodos que se describen a continuación se suponen conocidos los objetivos.

Primeramente, para todos los métodos, se requiere conocer una función que represente la manera en que inversiones alternativas contribuyen a los distintos objetivos. La función de transformación representa el límite de un conjunto de contribuciones factibles a los distintos objetivos.

La función de transformación puede generarse mediante un conjunto de soluciones que se obtienen resolviendo el siguiente problema para distintos valores del α

$$\text{Max } f_1(x)$$
$$\text{Sujeto a: } f_1(x) \geq \alpha$$

Para el caso en que P = 2, es decir con dos objetivos.

El método de restricciones consiste en resolver P problemas con objetivo, en cada uno de los cuales se ignoran (P - 1) de los objetivos. Las soluciones son ($x_1^*, \ldots, x_p^*$). Para cada solución se calculan los valores que toman los otros objetivos, por ejemplo $(f_2(x_1^*), \ldots, f_p(x_1^*))$ para x_1^* etc. Para el caso de dos objetivos, el punto A de la figura corresponde a x_1^* y tiene coordenadas $(f_1(x_1^*), f_2(x_1^*)) = (M_1, f_2(x_1^*))$
En forma similar el punto E está en $(f_1(x_2^*), f_2(x_2^*)) = (f_1(x_2^*), M_2)$
donde $f_1(x_2^*)$ es igual a cero.

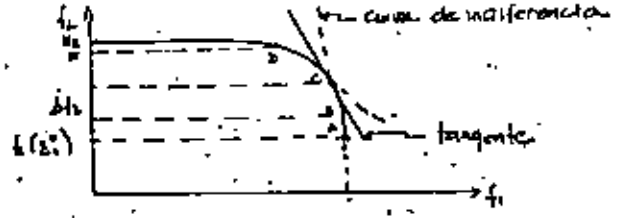

El siguiente paso consiste en dividir el rango de valores de un objetivo, por ejemplo f2 en incrementos de magnitud Δf_2

Se resuelve entonces en forma sucesiva el problema parametrizando un objetivo.

El planteamiento para dos objetivos será:

$$\mu \alpha x \; f_1(x)$$

Sujeto a
$$g_i(x) \leq 0 \qquad i = 1, \ldots, m$$
$$x_j \geq 0 \qquad j = 1, \ldots, n$$
$$f_2(x) \geq f_2(x_1^*) + N * \Delta f_2 \qquad N = 1, 2, \ldots$$

Los puntos resultantes constituyen la curva de transformación..

METODO DEL PROMEDIO PESADO DE FACTORES.-

El método descrito en el capítulo anterior tiene sentido si se cuenta con los objetivos, estos no son muy numerosos, los pesos son conocidos y se obtienen medidas de objetivos independientemente. Estos enfoques han sido di-

difícil llevarlos a la práctica por la complejidad de su desarrollo.

En contraste, han surgido otros métodos que son mas prácticos y que han sido aplicados en diversos problemas y reflejan la concepción de los profesionistas acerca del interés público.

Los métodos aquí considerados, en general tienen la siguiente estructura:

1.- Selección de factores
2.- Descripción de factores en términos cualitativos o cuantitativos.
3.- Escalamiento de factores. Dando a cada factor un valor entre 1 y 10.
4.- Selección de factores de peso.
5.- Cálculo del promedio pesado de factores.

Dependiendo de la aplicación particular del método se buscará maximizar o minimizar la suma.

Como ejemplo de este método se describe a continuación un problema planteado en el Distrito de Tulsa U.S.A.

Se reune a un grupo de personal interdisciplinario que plantea una serie de alternativas para regular una corriente. Una de las alternativas será siempre la consideración de condiciones sin proyectos.

a).- Selección de factores.

Consideran tres objetivos.

I) Calidad del Ambiente.
II) Calidad de la vida.
III) Economía nacional y regional.

Cada objetivo se desagrega en componentes hasta que represente una base adecuada para evaluación. Para el caso de calidad del ambiente resulta:

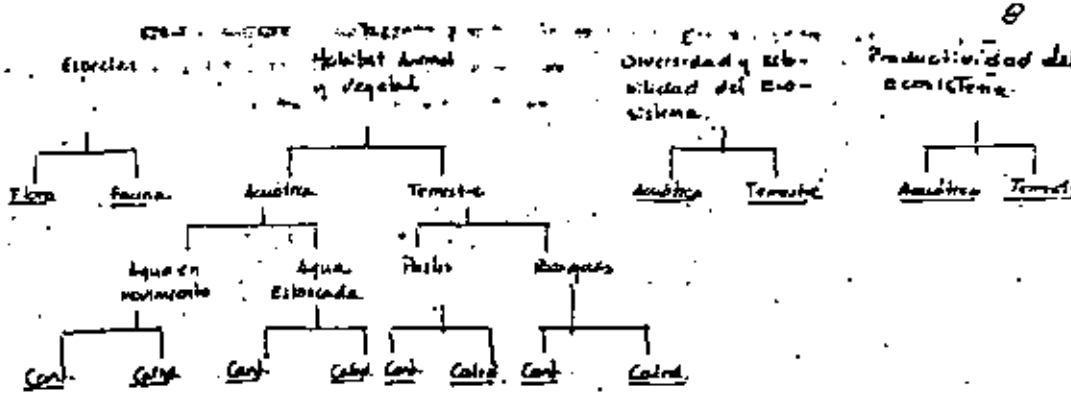

Los términos subrayados constituyen los factores.

b).- Descripción de Factores.

Dependiendo de su naturaleza podrán ser descritos en forma cualitativa o cuantitativa. El resultado de esta etapa es describir como cada acción - alternativa incluye en cada factor.

c).- Escalamiento de Factores.

Consiste en la transformación de cada descripción de los factores a un - índice.

Se utiliza una escala de (-5) a (+5). Se estima la magnitud - del impacto, asignando el valor cero a la situación sin proyecto.

d).- Selección de Factores de peso.

Se asigna un total de 100 puntos a cada objetivo de planeación y se hace proporciones entre factores usando fracciones decimales que representan el valor de las consideraciones.

En el cuadro 2 se muestra un ejemplo para el objetivo de calidad del ambiente.

a).- Cálculo del promedio pesado de factores.

Los valores de cada alternativa se multiplican por sus pesos respectivos y se suman para cada alternativa en cada uno de los objetivos de planeación.

Una crítica al método arriba descrito consiste en el hecho de que se aplica una vez que se han formulado las alternativas en lugar de definir primeramente los factores de mayor importancia para el problema y posteriormente generar alternativas. Estos factores deberán a su vez provenir de un proceso de participación pública y no solo de un grupo interdisciplinario.

III.2 ENFOQUE DE ORIENTACION DE PROCESOS.

En este enfoque, el interés público se manifiesta a través de un proceso de planeación abierto, sin depender de una expresión matemática. El plan óptimo es el que surge del proceso de planeación abierto.

Entre las consideraciones que lleva implícita en este enfoque destacan:

a).- No es posible desarrollar algoritmos que definan la solución óptima con base en su conjunto de valores preestablecidos.

b).- El impacto del proyecto tiene significado solamente con respecto a individuos del grupo que es afectado.

c).- La evaluación de alternativas no puede ser separada de otras actividades de planeación.

Una limitación del método es que no define parámetros que permitan programar los recursos necesarios para implantarlos.

PERFILES DE FACTORES DE LA COMUNIDAD.-

El método consiste en mostrar la información en forma de perfiles de factores. Incluye impactos no monetarios e impactos cuantificables. Es un resumen de los efectos de proyecto.

Al mostrar la información de esa manera, los grupos participantes en la decisión pueden hacer comparaciones entre alternativas, comparando por ejemplo la 1 y la 2 y después la 3 con la mejor de las anteriores, y así sucesivamente.

Una forma de representar estos perfiles se ilustra en el cuadro — , donde aparecen una serie de factores, y representados en porcentaje respecto a un valor máximo o mínimo. El ejemplo corresponde a la selección entre distintas mejoras para una carretera.

Finalmente, correspondiendo el enfoque algorítmico, se presentan los principios propuestos por el Consejo de Recursos Hidráulicos de U.S.A., con relación al agua y suelo.

Básicamente definen dos objetivos y llevan a cabo contabilidades para cada uno de ellos en las distintas alternativas.

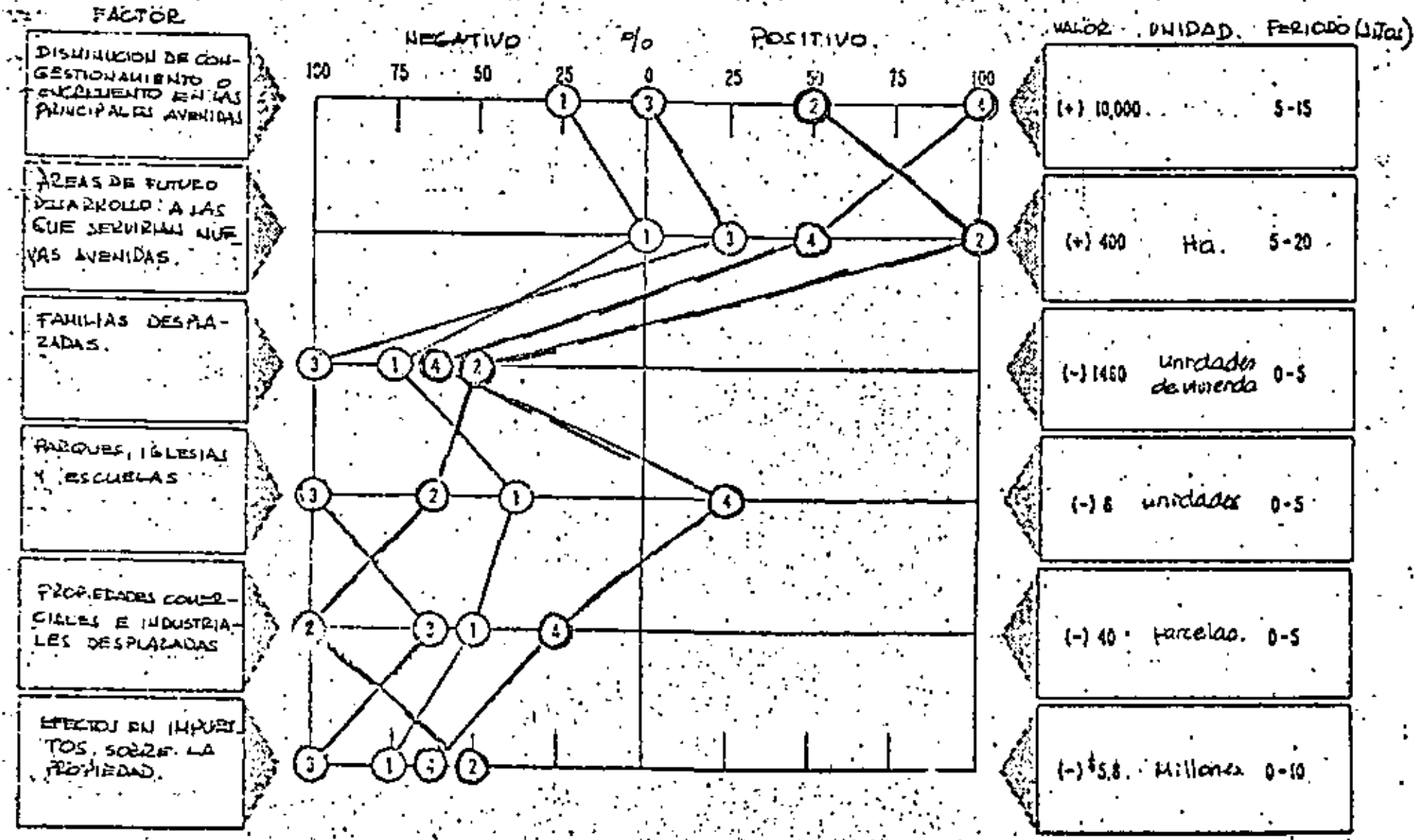

Fuente: C. H. Oglesby, Bruce Bishop, G. E. Willeke
HRR Record 247. pp 1-15.

	PARAMETROS	FACTORES DE PESO			PESOS	DOS SISTEMAS MULTIPLES		CUATRO LAGOS DE P. MULTIPLES.		CINCO LAGOS		PRESERVAR COMO O SILENCIO	
						ESC.	PR. PESADO	ESC.	PR. PESADO	ESC.	PR. PESADO	ESC.	PR. PESADO
I	Especies Unicas	20											
A	Fauna		0.80		16.00	+1	+16.00	+2	+32.00	+3	+48.00	+5	+80.00
B	Flora		0.20		4.00	+2	+8.00	+1	+4.00	-1	+4.00	+5	+20.00
II	Habitat Animal y Vegetal	40											
A	Acuático		0.40										
1	Agua en movimiento			0.90									
a.	Calidad				0.70 — 10.08	+1	+10.08	+3	+30.24	+2	+20.16	+5	+50.40
b.	Cantidad				0.30 — 4.32	+5	+21.60	-2	-8.64	-2	-8.64	0	0.00
2	Agua estancada			0.10									
a.	Calidad				0.70 — 1.12	+2	+2.24	+4	+4.48	+5	+5.60	0	0.00
b.	Cantidad				0.30 — 0.48	+4	+1.92	+5	+2.40	+5	+2.40	0	0.00
B	Terrestre		0.60										
1	Pastos			0.20									
a.	Calidad				0.70 — 3.36	-2	-6.72	-3	-10.08	-3	-10.08	+5	+16.80
b.	Cantidad				0.30 — 1.44	+4	+5.76	-2	-11.52	-5	-28.80	0	0.00
2	Bosques			0.80									
a.	Calidad				0.70 — 13.44	+1	+13.44	+2	+26.88	+3	+40.32	+5	+67.20
b.	Cantidad				0.30 — 1.76	-4	+23.04	-2	-11.52	-5	-28.80	0	0.00
III	Diversidad y Estabilidad del Ecosistema	20											
A	Acuático		0.40		8.00	+3	+24.00	+4	+32.00	+5	+40.00	+1	+8.00
B	Terrestre		0.60		12.00	-2	-24.00	-3	-36.00	-4	-48.00	+5	+60.00
IV	Productividad del Ecosistema	20											
A	Acuática		0.40		8.00	+3	+24.00	+5	+40.00	+4	+32.00	0	0.00
B	Terrestre		0.60		12.00	-4	-48.00	-4	-48.00	-5	-60.00	0	0.00
IMPACTO SOBRE EL AMBIENTE							-17.92		+60.64		+36.16		+302.4
RANGO:							4		2		3		1

CUADRO 2.- ANALISIS DE ALTERNATIVAS, PROCEDIMIENTO UTILIZADO POR EL DISTRITO DE TULSA.

10

MULTIOBJECTIVE WATER-RESOURCES PLANNING

Douglas A. Haith

Departments of Agricultural Engineering and Environmental Engineering
Cornell University

Daniel P. Loucks

Department of Environmental Engineering
Cornell University

10-1 INTRODUCTION

Planning occurs at many levels in any social organization. Even though the scope of the plans will differ, the process of planning at each level is generally the same. Goals are considered, information is gathered and processed, alternative choices are defined and evaluated, and after a number of iterations that may modify the goals, information needs, and alternatives, eventually a decision is made, and a particular choice or plan is implemented. Often the process of planning continues, and plans may be modified after they have been implemented. Hence planning encompasses all activities leading up to a decision among choices and continues during the post-choice stage of implementation and control.[1]

This discussion shall be focused primarily on the "decision-among-choices" part of the planning process. While such decisions are made in public and private organizations, the emphasis in this chapter will be on decision-making in the *public* planning process, i.e., the process in which the final selection of an alternative rests with elected or appointed decision makers or policy makers who in some sense represent the public.

The alternatives formulated by water-resource planners generally attempt, explicitly or implicitly, to achieve various objectives. For the planner, it would be ideal if the choice of one policy over another—or the choice of one investment as compared to another—could be evaluated in terms of a single, well-established objective or goal. In fact, there are always numerous possible goals or objectives that are relevant—many of which are often conflicting—and the importance of each goal is rarely well articulated in advance of the time decisions are made. Public-policy decisions are often made from plans conceived and developed on the basis of a mostly qualitative integration of numerous economic, political, social, and technological objectives. The explicit trade-offs between each of these partially complementary and conflicting objectives are not always clear, and, therefore, the selection and implementation of plans often fail to meet many of the objectives to the extent originally envisioned.

From the start, we should specify several assumptions that are made in this review. The first assumption is that public policy is rarely implemented to satisfy only a single economic objective. The type and scale of public investments in water-resource development and management are usually based on a range of economic, social, and political factors, only some of which can be quantified. Often many important objectives defy quantification, and these, together with the quantifiable objectives, must be considered in the planning and decision-making processes. Thus, like most methods developed to define and evaluate alternative policies, the information obtained from the quantitative techniques discussed in this review can only assist the policy makers and planners; it cannot replace them.

The second assumption is that, among the objectives that can be quantified, the parameters or criteria used to describe them need not be directly comparable. No one has yet suggested a generally acceptable way of assigning a monetary value to environmental quality, for example, that is directly comparable to the monetary value of consumption or regional income and its distribution. Such assignments require the analyst to define the decision maker's welfare or utility function. The assumptions that the analyst or planner must make to derive such a function are unlikely to be those of the decision makers who are ultimately responsible for the establishment of policy. Hence analysts or planners must fall back to what they can do, namely, defining the alternatives available to the decision maker and evaluating each alternative based on each objective, thereby delineating the possible trade-offs between various objectives. These trade-offs among various noncommensurable objectives can be made clear to the decision makers only if each objective is expressed in terms that are meaningful to them.

The third major assumption of this discussion is that the ultimate specification of the relative importance of each objective, or, more accurately, the selection of a policy that in turn *implies* the relative importance of each objective, must take place in the political process. It is a fact that the relative weight given to each objective is ultimately based on political rather than solely eco-

nomic ipl, or technical criteria. These weights are always condit l, depending in part on the decision maker's perception of (1) his policy alterna tives, (2) how each alternative would be implemented if selected, and (3) the likely outcomes. The distinguishing feature of public-policy making is that the power to accept, reject, and implement plans rests with public officials called *policy makers* or *decision makers*. The degree to which each alternative plan is acceptable to, or conforms to the preferences of, those policy makers who have the power of decision is a measure of the plan's political feasibility. Clearly, the policy makers themselves should be involved in this ranking process. The primary motivation behind the development of each of the quantitative methods to be discussed in this review has been to assist economists, engineers, and planners in effectively participating in a responsible political decision-making process.

10-1.1 Water-Resources Planning

Although it has sometimes seemed that in the United States the federal water-resources planning effort has been dedicated to the single goal of national economic development as typified by benefit-cost ratios, this has hardly been the case. More typical, perhaps, have been the attempts to manipulate the ratios of plans serving other objectives.[3] Previous and current federal policy for water-resources planning have recognized more than one national objective,[3,4] and even the rigorous proponents of benefit-cost analysis have indicated that intangible (nonmonetary) benefits, if significant, would compromise a strict benefit-cost criterion for project selection.[5,6]

To a considerable extent, any debate about the virtue of multiobjective water-resources planning has been rendered obsolete, at least in the United States. The National Environmental Policy Act of 1969, with its requirements for environmental impact statements, inserts de facto environmental objectives into planning. The recently enacted "Principles and Standards" of the Water Resources Council specify national economic development and environmental quality as federal water-resources planning objectives.[4]

It seems clear that water-resources planners will give increasing attention to the multiobjective nature of planning. The explicit analysis of varied and often conflicting objectives will be necessary, and alternatives that give varying weights to the various objectives will be required.[7] It is by no means clear, however, how this can be done. While economics has been added to the earlier engineering aspects of water planning, it would appear that ecology, sociology, and political science must be added to the planning effort. Somehow the various objectives and the techniques for plan formulation must be combined into a manageable interdisciplinary enterprise.

The formulation and selection of alternatives are further complicated by uncertainty in the outcome of any public policy due to factors outside the control of the planner or decision maker, and by the limited ability to consider si-

multaneously all relevant information pertinent to the policy even if there were no uncertainty. Even when supplemented with computers, the capacity of a individual planner or group of planners is limited.

10-1.2 The Role of Modeling

In order to deal with the complexities of multiobjective planning, planners are usually forced to construct simplified representations of their problems to enable them to process more efficiently what information they have in order to predict and evaluate the possible outcomes. These simplified representations or models can range from those that are solely conceptual, and wholly contained within the mind of a planner or decision maker, to those that are specified by many sets of algebraic equations, and contained within a program to be solved on high-speed digital computers. These latter models are usually grouped into what are called *mathematical models*.

Mathematical models can provide a useful means of bringing the diverse elements of the planning process together in a conceptual framework that ideally facilitates better understanding of alternatives by both the planner and the decision maker. While most mathematical models are restricted to only those aspects of the evaluation process that are quantifiable, the information derived from them may significantly assist the decision-making process in its selection of a final choice. This is especially true where multiple objectives have been identified. In these situations, usually some alternatives are preferable when particular objectives are considered, while other alternatives are preferable when different objectives are examined. As the number of relevant objectives and alternatives increases, the ability of the planner to manage the problem rapidly decreases. It is here where quantitative modeling techniques and those who know how to use them can be of considerable value as aids to, but not substitutes for, the responsible political decision-making process.

10-2 DESCRIPTIVE MODELS OF THE PLANNING PROCESS

A reasonable model of the water-resources planning process assigns to the planner the function of formulating a set of alternatives. General goals are proposed directly or indirectly by special interests, public decision makers, and the planner. The planner must determine which of these goals are relevant and translate them into operational objectives or design criteria. Specific planning alternatives are generated which accomplish these objectives to varying degrees. One or more of the alternatives is submitted to a policy maker, or policy-making group, that either selects a plan for implementation or rejects the submitted alternative(s). Since policy makers hold elective or appointed roles in a political system, it follows that plan selection is inherently a political decision.[7,8,9,10] Hence in addition to questions of technical and financial feasibility, the problem of *political* feasibility is of critical importance in the pub

planning process. To be successful, water-resources planning must, to an extent, conform to the realities of political decision-making, and an understanding of the policy-making process is a requisite to effective multiobjective planning.

10-2.1 The Policy-making Process

Following the example of Strickland et al.,[11] a discussion of politics can start with some basic assumptions concerning human behavior. First, all individuals have goals. Such goals differ from person to person both in direction and in intensity. The same person may have many goals, some of which conflict with others. Similarly, the goals of one individual may conflict with or be similar to those of others. The relative value or worth of people's goals can be indicated by what they are willing to give up to achieve them. These assumptions imply that conflict has a central role in any social system. Furthermore, individuals are willing to exert some effort to prevent their goals from being frustrated. These implications lead directly to the need for a *political system*. When individuals seek to achieve their objectives through government actions, personal goals become *political goals*, and a *political decision* determines which political goals will be achieved.

Strickland et al.[11] introduce two concepts which clarify the mechanism of political decisions. The first of these is *agency*. Public decision makers are agents of the members of a political system and are authorized to make choices among political goals. Attention focuses on these agents or policy makers, and individuals try to influence them to support various goals. The principal mechanism of influence is through *association*, or more specifically, a political association. A political association attempts to get other people in a political system to accept the political goals of the association's members. One of the principal means of accomplishing this end is to influence the choices of the policy makers.

To summarize, a political system attempts to resolve the conflicting objectives of members of a society. Policy makers are agents of the society and decide which political goals are to be achieved. Supporters of the various political goals try to influence their agents' choices, and association is an important mechanism for such influence.

Inasmuch as political goals exist, then "interests" will exist which support these goals. Whether such interests are represented in a policy maker's decision depends largely on their influence and on his estimate of their potential influence. Organized groups will certainly have their effect, but it is not unreasonable to suppose that the goals of large unorganized segments of society will also be considered. The policy maker's choice will be influenced by interest groups, potential groups, his personal values, and the opinions of friends and political leaders.[11]

A policy maker's decision process can be ideally envisioned as a logical, well-defined process in which he surveys as many possible alternatives as time permits, predicts the consequences of each, and selects the alternative which

most closely corresponds to his perception of the best. This synoptic ideal ignores some of the realities of political decision-making. The first of these is the uncertainty that is present in policy-making. "Uncertainty as to the facts and difficulty in arriving at correct factual judgments are among the most familiar elements in the life of a political decision maker."[13] Furthermore, the essential bargaining aspects of policy making are not included in the above description. If decisions are "by mutual adjustment among partisan advocates, each possessing different, or at least differently weighted, ends and values,"[14] the decision maker must trade off some goals for others. His choice is more compromise than evaluation. Social cooperation among interests and among policy makers who represent these interests is thus a distinctive feature of the policy-making process.[12,13,15]

10-2.2 Planning Strategies

Numerous strategies have been used by planners to deal with realities of policy-making. These strategies are usually modifications and combinations of three basic planning philosophies: target, optimization, and compromise planning.

The target planning philosophy involves the definition of a variety of feasible plans from which one is selected that best meets a predetermined set of objective values or targets that have been articulated by the political leadership. Target planning seeks to find those policies and instruments that will achieve the targets of the decision maker. As such, this method of planning is rational and defensible if the resulting plans are internally consistent, if the data on which the plans are based are reasonably accurate and complete, if the implicit and explicit assumptions in the plans are correct, and if the targets adequately reflect the social needs or goals of the decision makers.

Optimization planning is a refinement of target planning. Both require an a priori knowledge of the decision maker's preferences and desires. This planning philosophy assumes that these desires or preferences are expressed as objectives rather than targets and as such, planners seek to obtain optimal solutions given the available resources, rather than just to satisfy targets. The optimal solution is that plan which satisfies all feasibility constraints and is preferred to all other feasible plans.

Compromise planning is imperfect, but it is also more realistic. It does not assume that the targets or the relative weights given to each possible objective are known in advance of planning. Hence, the emphasis in this type of planning is on the generation of feasible plans and on the active involvement of the responsible decision maker in the selection of the best feasible plan or compromise. This planning philosophy recognizes that, once alternative plans have been defined, it is the responsibility of the political decision maker to analyze and evaluate all the quantitative and qualitative factors that should be analyzed and evaluated in the process of selecting the best plan.

10-3 WATER-RESOURCES PLANNING OBJECTIVES

Although it is generally recognized that objectives other than national efficiency have always been a part of water-resources planning, the Flood Control Act of 1936 saw the beginning of the benefit-cost ratio's role as the primary criterion for selection of federal projects in the United States. In this respect, a distinction is often drawn between planning for multiple *purposes* and multiple *objectives*. A basin plan for navigation and flood control which is evaluated on the basis of a benefit-cost ratio would have two purposes but only one objective—national economic development. Navigation and flood-control benefits and costs are considered as contributory to this single objective. Such distinctions are necessary to obtain benefit-cost ratios.

The new emphasis in multiobjective water-resources planning signals a shift in methods of evaluating plans and comparing objectives. New objectives, particularly those relating to environmental quality, are to be considered and objectives will not be compared solely on the basis of monetary benefits and costs.

10-3.1 Principles and Standards for Planning Water and Related Land Resources

Presidential approval of the U.S. Water Resources Council's "Principles and Standards"[4] culminated a period of debate, agency review, and testing of proposed water-resources planning methods which lasted for many years. The "Principles and Standards" apply to most federally related water-resources planning activities and replace previous federal policy.[3] Agencies are currently developing procedures and guidelines for implementation of the "Principles and Standards."

Two national water-resources planning objectives are established by the "Principles and Standards:"[4]

> 1 *National Economic Development* (NED): "Enhance national economic development by increasing the value of the Nation's output of goods and services and improving national economic efficiency."
> 2 *Environmental Quality* (EQ): "Enhance the quality of the environment by the management, conservation, preservation, creation, restoration, or improvement of the quality of certain natural and cultural resources and ecological systems."

The beneficial and adverse effects of any project or plan are to be displayed in four accounts:

1 NED account
2 EQ account
3 Regional Development (RD) account
4 Social Well-Being (SWB) account

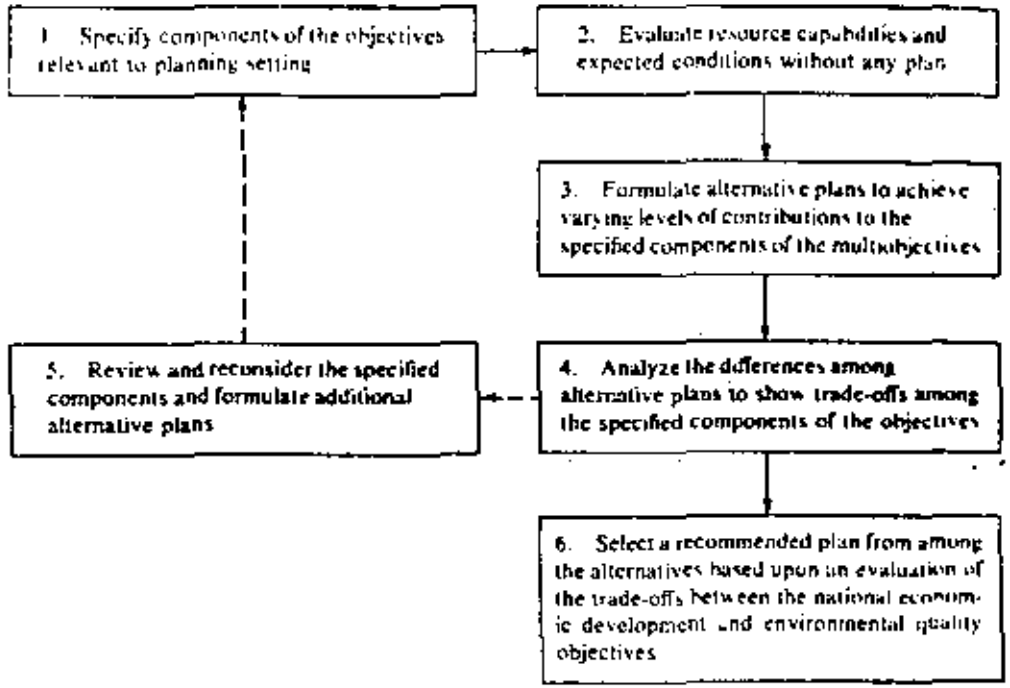

FIGURE 10-1
Plan formulation procedures specified by the *Principles and Standards*.[4]

Impacts are to be quantified in monetary terms for NED, but nonmonetary quantification and "qualitative dimensions" are permissible for the other accounts.

The essence of the planning process envisioned by the "Principles and Standards" is the formulation of at least two plans, one of which emphasizes NED and the other EQ. The procedures for plan formulation are indicated in Fig. 10-1. Regardless of emphasis, the effects of each alternative are to be displayed in the four accounts mentioned earlier. This detailed accounting is to facilitate the identification of trade-offs among objectives. For example, the sacrifice in NED benefits associated with the EQ plan would be seen, or the loss of certain EQ benefits entailed in the NED plan could be identified. The accounting procedure is exceptionally detailed. An illustrative example provided in the "Principles and Standards" indicates 16 pages of accounts for just one plan. Additional plans would require comparable presentation and a final set of comparative tables is required to evaluate trade-offs among alternative plans.

As will be seen shortly, it is useful to consider the formulation and selection aspects of the planning process separately. The "Principles and Standards" are directed primarily toward formulation and can perhaps be considered an example of the compromise planning strategy discussed earlier. The

provision for specific alternatives and the four accounts provide decision makers not only with a range of choice but also with the information necessary for evaluating trade-offs between objectives. Since we have seen that policy makers function by trading off the objectives of some groups for those of others, there is every reason to believe that the planning effort suggested by the "Principles and Standards" should provide useful input to the policy-making process.

The future of the "Principles and Standards" is not certain. Section 80 of the Water Resources Development Act of 1974 (PL93-251) requires a reevaluation of the "Principles and Standards," and there is little question that agencies are having difficulty in implementing all provisions of the new planning requirements.[16,17] One problem, in particular, involves the detailed presentation of plan impacts, which may, paradoxically, constrain effective decision-making. Considering environmental effects, the account for any plan may include dozens or even hundreds of physical and subjective parameters. It thus can become very difficult to evaluate trade-offs among EQ and NED objectives. In addition, there is considerable uncertainty concerning what constitutes a suitable EQ plan. All components of the EQ objective can seldom be emphasized simultaneously, and without quantitative indices for overall evaluation of environmental impacts, any EQ plan will be open to serious challenge. Certainly the formulation of an EQ plan which results in sharply reduced NED benefits compared to the NED plan may cause a bias against the EQ alternatives.

Finally, the "Principles and Standards" can be faulted for their overly normative view of water-resources planning. In particular, there seems to be little recognition of the political aspects of planning. One exception is the test of *acceptability* which refers to "the workability and viability of the plan in the sense of acceptance of the public and compatibility within known institutional constraints."[4] The earlier discussions of political feasibility indicate that such a test may prove to be more critical to the planning process than many of the other factors which are emphasized in the "Principles and Standards."

10-4 QUANTIFICATION OF WATER-RESOURCES PLANNING OBJECTIVES

Although a degree of ambiguity is not without its charms, particularly within a political system, the success of multiobjective water-resources planning rests to a considerable extent on the planner's ability to ascribe operationally meaningful, quantitative parameters to objectives. The systematic evaluation of trade-offs certainly is much more difficult when objectives are intangible or nonquantitative. Obviously the use of mathematical modeling is limited to situations involving quantifiable objectives.

Planning objectives are quantified on either monetary or nonmonetary scales. The measurement of monetary costs and benefits has reached a high

level of refinement, even with objectives for which market prices do not reflect true social benefits and costs or do not exist at all. An example is found in the methods developed for inputting recreation demands and hence monetary benefits associated with recreation use of water-resources projects.[18]

Several attempts have been made to devise single parameters to describe a broad range of environmental quality objectives. The intent is to develop meaningful indicators which include broad ranges of quality aspects. Two examples can be given for air quality and water quality.

The Third Annual Report of the Council on Environmental Quality measures progress in attaining air-quality objectives in terms of several indices. One of these is the Mitre Air-Quality Index (MAQI), which is given by

$$\text{MAQI} = (I_c^2 + I_s^2 + I_p^2 + I_n^2 + I_o^2)^{1/2} \tag{10}$$

where I_c is a carbon monoxide index
I_s is a sulfur dioxide index
I_p is a particulate matter index
I_n is a nitrogen dioxide index
I_o is a photochemical oxidant index

The indices for individual pollutants are defined in such a fashion as to be greater than unity if EPA secondary air-quality standards are exceeded. The MAQI is essentially an objective criterion which could be applied uniformly on a national or regional scale.

Dinius[20] has proposed a very different general indicator for water quality. The Dinius water-quality parameter is highly subjective, in that the judgment of the planner or of water-quality specialists working with the planner is essential in its formulation. Thus, values of the index for different localities or regions are not likely to be comparable. Water quality Q, measured in percent, is given by

$$Q = \frac{w_1 Q_1 + w_2 Q_2 + \cdots + w_n Q_n}{w_1 + w_2 + \cdots + w_n} \tag{10}$$

where Q_i is the ith quality constituent (dissolved oxygen, chlorides, etc.) measured in a scale of 0 to 100
w_i is the weight or relative importance of the ith quality constituent

In a given planning venture, the scales for the Q_i and the weights w_i will be selected by the planner in consultation with water-quality "experts." The water-quality objective for any plan is measured by the levels of Q achieved at various points of interest.

The identification of uniformly acceptable quantitative indicators for nonmonetary objectives of water-resources planning which are meaningful to the planner, the decision makers, and the public is not likely to be achieved in the near future, if at all. The planner does not have to be unduly restricted by this prognosis, however. There is no shortage of possible parameters or methods for quantification. Moreover, attention to, and understanding of, objectives of most concern to the public as reflected in the policy-making proc

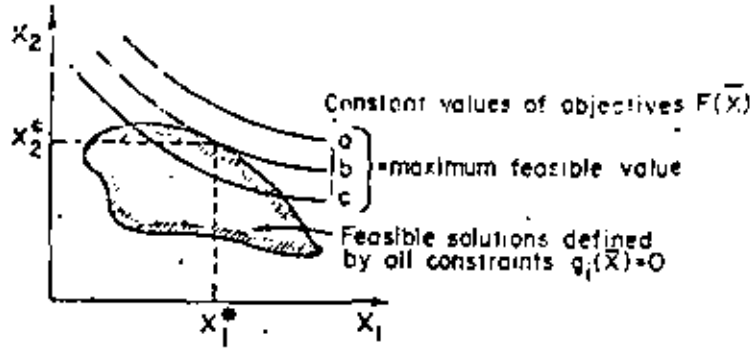

FIGURE 10-2
A two-variable policy program whose optimal solution is X_1^*, X_2^*.

provide a means of selecting numerical indicators appropriate to these objectives. Failure to make this effort will defeat much of the value of multiobjective planning and result in an unjustifiable bias toward the more readily quantifiable objective of economic efficiency.

10-5 MATHEMATICAL MODELS FOR MULTIOBJECTIVE PLANNING

The general multiobjective planning problem is the selection of a vector of decision variables, $X = (x_1, x_2, \ldots, x_k)$, which may represent project or plan outputs, the allocations of scarce resources as inputs, and policies for project or plan operation. Certain technical relationships among variables, $g_i(X) = 0$, $i = 1, 2, \ldots, m$, constrain planning alternatives or define the limits of technical feasibility. Single-objective models built for the purpose of helping in the selection of the best solution assume that the decision makers' preferences are known and can be expressed as a single-objective function $F(X)$ whose value for a particular solution vector X expresses the utility of X for the decision maker. In these situations it is simply a computational problem to find the vector X^* which optimizes $F(X)$ subject to all constraints $g_i(X) = 0$. Assuming only two policy variables X_1 and X_2 and an objective $F(X)$ that is to be maximized, this problem is illustrated in Fig. 10-2.

Most regional development or public investment analyses require a comparison of various solution vectors X based on numerous objectives or goals. Of the objectives that are quantifiable, each can be described by a function $F_j(X)$ that should be either maximized or minimized.† The task now becomes one of appropriately or optimally trading off the value of one objective for another, if by increasing one objective value, one or more other objective values decrease.

†In this discussion each $F_j(X)$ will be assumed a superior objective; i.e., it is to be maximized. Obviously any inferior objective can be changed to a superior one by multiplying by minus one.

Planning thus consists of the selection of a plan

$$X = (x_1, x_2, \ldots, x_k)$$

which is technically feasible, i.e., satisfies all the constraints

$$g_i(X) = 0 \qquad i = 1, 2, \ldots, m$$

and best accomplishes certain objectives whose values are

$$F_j(X) \qquad j = 1, 2, \ldots, n$$

The fundamental characteristic of multiobjective water-resources planning is that the various objectives $F_j(X)$ are frequently both incommensurable and conflicting. Thus if two plans

$$X_1 = (x_{11}, x_{12}, \ldots, x_{1k})$$
$$X_2 = (x_{21}, x_{22}, \ldots, x_{2k})$$

are compared, it may be found that the first plan achieves higher levels of certain objectives and lower levels of other objectives when compared to the second plan. In general, unless $F_j(X_1) \geq F_j(X_2)$ or $F_j(X_2) \geq F_j(X_1)$ for all objectives j, selection of either plan implies a reduction of some objective values for a gain in others.

10-5.1 Trade-Offs and Political Feasibility

Political feasibility can be discussed in the context of the basic planning philosophies discussed in previous sections of this chapter. The use of targets presumes that minimum objective levels T_j have been articulated by, or can be inferred from, the actions of decision makers. Thus, technically feasible plans that achieve targets are assumed to be politically feasible. Such plans are defined by those values of X such that

$$F_j(X) \geq T_j \qquad \forall j \tag{10-3}$$
$$g_i(X) = 0 \qquad \forall i \tag{10-4}$$

Apart from questions of how the targets T_j are to be determined, the target strategy contains some interesting implications. Considering a two-objective planning example if objective targets T_1 and T_2 are specified, and any plan with, say, $F_1(X) < T_1$ is rejected, the implication is that no level of $F_2(X)$ can compensate for the loss $T_1 - F_1(X)$. Below certain minimum levels, no trade-offs of objectives are possible. The political inference is that decision makers wish to provide certain minimum levels of satisfaction to all groups whose objectives are reflected in plans under consideration. While this may or may not be realistic, it provides no clear guideline for comparison of several plans, each of which *exceeds* target levels. The maximization of a single objective, say, $F_1(X)$, subject to constraint equations (10-3) and (10-4), provides this guideline but implies that no increase in targeted objectives over the target levels T_j will compensate for decreases in the primary objective $F_1(X)$.

Optimization planning, as indicated by

Maximize	$F(X)$	(10-5)
Subject to	$g_i(X) = 0 \quad \forall i$	(10-6)

requires that questions of political feasibility and preference be completely described by the objective function $F(X)$. Again, apart from the reasonableness of this assumption, the inference is that trade-offs between objectives are known at all levels of the objectives. For example, again consider two plans for a two-objective planning situation, which have decision vectors X_1 and X_2, respectively. Even though $F_1(X_1)$ may be greater than $F_1(X_2)$, and $F_2(X_1)$ less than $F_2(X_2)$, political preference could be determined by evaluating $F(X_1)$ and $F(X_2)$. If, say, $F(X_1) > F(X_2)$, then the trade-off of $F_2(X_2) - F_2(X_1)$ for $F_1(X_1) - F_1(X_2)$ represents the net increase in political preference, $F(X_1) - F(X_2)$.

It is clear that both target and optimization planning, or any mixture thereof, all require detailed a priori knowledge of policy makers' preferences, and each has inherent assumptions concerning the nature of trade-offs that are possible in the policy-making process. Compromise planning, on the other hand, does not necessarily require either a priori preference data or restrictions on possible trade-offs. In its most basic form, political questions may be avoided entirely, and planning may consist of the technical formulation of a small or large number of alternatives that are submitted to policy makers. The planner's task is considered complete if the plans cover a range of alternatives and if the objectives achieved by each plan are adequately described.

A more sophisticated view of compromise planning, however, incorporates political preferences into the planner's activities. Without making assumptions concerning the exact nature of objective trade-offs, attempts are made to look at a range of possible trade-offs and to screen alternatives for their political feasibility. Modeling techniques appropriate to this approach often require the systematic involvement of responsible decision makers in the planning process and/or the inclusion of the planner in policy-making.

The above form of compromise planning will be emphasized in the remainder of the discussion. Since no preference, value, or utility functions are assumed, this pragmatic approach may be less appealing to those accustomed to well-formulated problems. Nevertheless, for many public-policy decisions, these techniques compare favorably to those previously discussed for assisting in the selection of politically feasible and efficient multiobjective water-resource plans.

It is convenient to view compromise planning as two related processes: the first is plan formulation, or the identification of efficient trade-offs among objectives; the second is plan selection, or the identification of optimal trade-offs.

Th re a number of approaches that can be used to examine the tra offs between separate and noncomparable objectives. If there are only two three objective functions $F_i(X)$ and a relatively few decision variables in the

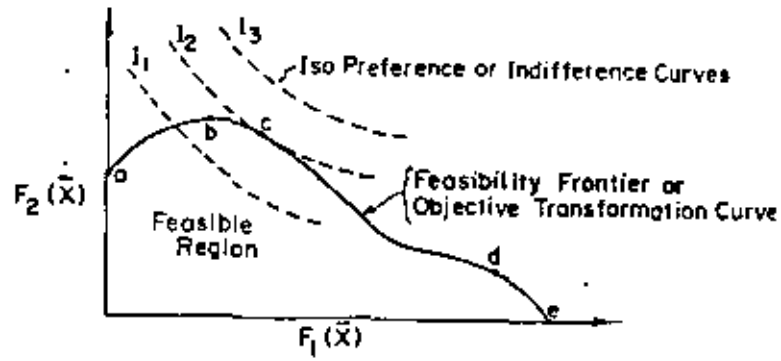

FIGURE 10-3
Feasible solutions for a two-objective problem.

vector X, then it might be possible to simulate all feasible combinations of decision variables in order to plot or graph the values of each of the objective functions associated with each vector X. The envelope of these values would define the efficient vectors X and the trade-offs that are possible among these efficient combinations of X. These concepts are illustrated for a two-objective problem in Fig. 10-3.

Each point within the feasible region in Fig. 10-3 represents a particular set of values for the decision variables in the vector X that satisfy a set of constraints $g_i(X) = 0$, $i = 1, 2, \ldots, m$. The decision vectors that lie on the feasibility frontier, curve *abcde*, are those that define the maximum value of objective $F_2(X)$ given a particular value of objective $F_1(X)$. Of interest to the planner and policy maker are the trade-offs defined by certain combinations of feasible and efficient decision vectors. Each decision vector on the *bcde* portion of the feasibility frontier is efficient, in that there can be no increase in one objective value without a decrease in the other objective value. Solutions on the *ab* portion of the frontier are inferior solutions in the sense that they are dominated by other solutions having higher values for each objective. Inferior-solution vectors are of interest only if some of the objectives are inferior, i.e., if they are to be minimized.† If all objectives are superior, then only the efficient superior solutions need be considered.

Clearly the use of simulation models as a means of defining the feasibility frontier and the corresponding trade-offs between each efficient decision vector becomes less attractive as the number of variables and objectives increases. A simple graphical presentation of the trade-offs between objectives $F_i(X)$ becomes impossible as their number increase beyond three. For these reasons optimization techniques are usually suggested as a means of estimating feasible and efficient decison vectors X.

†Such a situation would be indicated by a negative-sloped decision maker's indifference curve.

It is appropriate here to mention that different models of the same decision problem could result in different feasibility frontiers. Simplifying assumptions, often dictated because of algorithmic, computer, data, or budget limitations, are the primary reason why there is some uncertainty associated with the resulting feasibility frontier. This uncertainty might lead many to argue that the frontier is really a range of points, perhaps best represented by a probability distribution. In addition, politicians whose expectations or aspirations exceed what appears to be feasible might also suggest that one or more restrictions specified in the constraint set are really not constraints, or that they are willing to give up what is required to enlarge the feasible region (as illustrated in Fig. 10-2) to where it includes an otherwise infeasible aspiration or target.† It is also possible that what appears feasible *ex ante* is infeasible *ex post*, or vice versa, regardless of the model used to define feasibility. While all these arguments can be valid in certain situations, we will assume throughout the remainder of the discussion that the planning process can derive a reasonably well-defined and accurate feasibility frontier and, hence, a finite set of efficient alternatives from which a choice can be made.

The goal of plan formulation is the generation of plans that lie on the transformation curve. This can also be interpreted as the identification of efficient trade-offs. Any point on the transformation curve corresponds to a specific trade-off or marginal rate of substitution between the objectives, as indicated by the slope of the curve. Thus, plans *b*, *c*, and *d* in Fig. 10-3 correspond to three different marginal rates of substitution between objectives $F_1(X)$ and $F_2(X)$.

Plan selection is the identification of one of the efficient plans corresponding most closely with policy-making preferences. The indifference curves I_1, I_2, and I_3 are considered as curves of equal political preference. Of course, different individuals or groups may have different sets of indifference curves. The optimal plan for any particular policy maker is the plan on the objective transformation curve that achieves the highest level of political preference, e.g., plan *c* in Fig. 10-3. The optimal trade-off or marginal rate of substitution for the policy maker is indicated by the slope of the transformation curve at that same point *c*.

The remaining sections will discuss modeling techniques that have been proposed for identifying efficient trade-offs as indicated by plans on an objective transformation surface (for *n*-dimensional planning problems) and for estimating optimal trade-offs or plans, i.e., those that attempt to maximize political preferences. Since data generally do not exist to define completely either transformation or isopreference surfaces, the modeling techniques will attempt to approximate the surfaces by considering a relatively small number of efficient planning alternatives. Conceptually, the approaches correspond to the procedure illustrated in Fig. 10-3. However, in practice, the complete mapping of feasible and efficient alternatives is seldom possible or even necessary.

†This argument is essentially over the proper scope of the problem being analyzed.

Any method that is used to define the possible trade-offs between multiple objectives can result in a relatively large number of efficient alternative solutions. As the number of objectives increases, so do the number of alternative solutions usually required to define the possible trade-offs among these objectives. This in turn requires more computer time and expense. Perhaps more importantly, it also requires more of the decision maker's time to examine the numerous solution vectors that define the efficient trade-offs. Decision makers are not always willing to take the time to do this.

Considerable evidence suggests that, contrary to what would appear to be rational behavior, decision makers have typically not yearned for the opportunity of selecting what they judge to be the best from among a large number of alternative efficient solutions to a particular problem. They are more inclined to request from their staff or from an appropriate agency their opinion of the single best solution, and then either accept or reject it. This shifts the burden of trading off the values of conflicting objectives to those technicians proposing the single policy solution. If their trade-offs are considered appropriate by the decision makers, their proposed policy will likely be accepted; otherwise it will probably be rejected. The iterative process of proposing a solution and having it accepted or rejected by the decision makers is one means of focusing in on the trade-offs that are considered acceptable, but not necessarily optimal, by the decision makers.

The selection of the optimal trade-offs between multiple public-policy objectives must, by definition, require the participation of responsible political decison makers. They are required to specify these optimal trade-offs among objectives in a political environment that is dynamic and changing and very demanding of their time. The remainder of this chapter will review some techniques that have been proposed for helping responsible planners and decision makers to estimate efficient alternative solutions and the trade-offs that may be required to obtain a politically acceptable solution.

10-6 FORMULATION OF PLANNING ALTERNATIVES

A variety of modeling techniques are appropriate to the generation of efficient water-resource plans. In general, the approaches may be categorized as optimization or simulation models. Optimization models can be applied to problems in which the technical feasibility restrictions $g_i(X) = 0$ and the objective functions $F_i(X)$ are both explicit and mathematically well defined. Constraints which can be approximated by linear functions are particularly desirable since they facilitate the use of linear and separable programming methods. Recent examples[21,28,33] of the use of optimization models for multiobjective planning should be referred to.

Simulation methods are used extensively in water-resources planning.[34] In its most basic form, simulation modeling consists of finding solutions to the feasibility conditions $g_i(X) = 0$, $i = 1, 2, \ldots, m$, and evaluating objectives

$F_j(X)$, $j = 1, 2, \ldots, n$, in either a deterministic or probabilistic form. The varied nature of simulation models defies simple categorization. An illustration of the flexibility of such models is found in the work of Kane et al.[27,28] Since simulation methods will not, in general, produce Pareto efficient plans, optimization and simulation are sometimes used conjunctively.[27,28] The planning problem is first described by simplified models which are amenable to optimization. The generated plans are then studied using more realistic (and complex) simulation models. The optimization stage is considered as a screening method for identifying promising (Pareto efficient) alternatives, and the simulation stage provides a realistic evaluation of plan feasibility and performance.

Optimization models generally require a number of simplifying assumptions, and as such are seldom exact models of real-world planning situations. As opposed to simulation methods, however, optimization can be used to approximate the feasibility frontier or objective transformation surface. Of course the accuracy of the plans generated will depend on the modeling assumptions, and as previously mentioned, different optimization models of the same problem may not produce identical transformation surfaces.

Perhaps the most common optimization model is the modified target planning model discussed in the previous section. A feasibility frontier is generated by maximizing a single objective $F_1(X)$ while varying the target levels T_j of other objectives $F_j(X)$:

$$\text{Maximize} \qquad F_1(X) \tag{10-7}$$

$$\text{Subject to} \qquad F_j(X) \geq T_j \qquad \forall_j \neq 1 \tag{10-8}$$

$$g_i(X) = 0 \qquad \forall_i \tag{10-9}$$

By selecting different target values T_j, a set of plans could be generated, each of which achieves a maximum level of $F_1(X)$ for a specified set of targets T_j's. See, for example, the work of Miller and Byers.[22]

Numerous variations on target modeling have been prepared and used. A number of studies (e.g., Charnes et al.,[29] Holt et al.,[30] and Theil,[31] to mention only a few) have, in essence, proposed models that minimize the loss, if any, of not meeting targets. Relative loss functions L_j are specified in such a way that any deviation D_j from a target $[D_j = T_j - F_j(X)]$ reflects a penalty for not achieving the target. The problem then is to find a plan X that minimizes the maximum loss:

$$\text{Minimize} \qquad \max_j L_j(D_j) \tag{10-10}$$

An alternative approach, called *goal-programming*,[32] replaces that objective function (10-10) that minimizes the maximum loss by one that minimizes the absolute sum of losses:

$$\text{Minimize} \qquad \sum_j |L_j(D_j)| \tag{10-11}$$

The optimization planning model, Eqs. (10-5) and (10-6), can also be used to formulate alternatives. If the units of each objective $F_j(X)$ are the same, say, dollars, then it is relatively easy to combine separate objectives into a single function. For example, Dorfman and Jacoby[27,33] identify in monetary units the net benefits of a regional environmental quality management program for each of a variety of interest groups within a region. These separate net benefit functions are then weighted relative to one another. Assuming additive values, the trade-offs between objectives are obtained by varying the relative weights in an objective function that maximizes the sum of the weighted individual objectives. Denoting the relative weight of objective $F_j(X)$ by $W_j \geq 0$, the objective function can be written

$$\text{Maximize} \qquad \sum_j W_j F_j(X) \tag{10-12}$$

where the relative weights sum to 1 and the units of each objective $F_j(X)$ are the same. By varying the assumed relative weights, the convex portion of the feasibility frontier can be defined.

The success of any approach used to define the feasibility frontier critically depends on the assumptions of the convexity of the alternative combinations of the different objectives. A convex set of feasible alternatives has the property that a straight-line segment between any two points in the set lies wholly within the interior of the set. For example, the portions *abc* and *de* of the feasibility frontier illustrated in Fig. 10-3 are convex. If parts of the feasibility frontier are not convex (e.g., curve *cd*), or if it is convex but contains inferior points (e.g., curve *ab*), the maximization of various weighted sums of individual objectives will not define all points on the frontier. In these situations, the feasibility frontier can be defined by constraining the values of some of the objectives while maximizing weighted combinations of the others. More efficient adaptive search techniques have also been proposed in the recent operations research literature.

The multiobjective problem becomes more complex when the objectives $F_j(X)$ are not all expressed in the same units. In these cases it is useful to define a scaling function $S_j(F_j(X))$ to ensure that each objective $F_j(X)$ ranges over the same set of numbers, for example, between 0 and 1 as illustrated in Fig. 10-4. The objective $F_j(X)$ in Fig. 10-4 is assumed to range between a minimum value m_j and a maximum value M_j. The maximum value M_j of objective $F_j(X)$ can be obtained from Eq. (10-12) by setting $W_j = 1$ and all other weights to 0. The minimum value m_j can be obtained by setting $W_j = 0$ and selecting the minimum of all solutions $F_j(X)$ generated by various combinations of relative weights associated with the other objectives. In this case the objective function (10-12) is modified to become

$$\text{Maximize} \qquad \sum_j W_j S_j(F_j(X)) \tag{10-13}$$

where again the relative weights W_j range between 0 and 1 and sum to 1, and

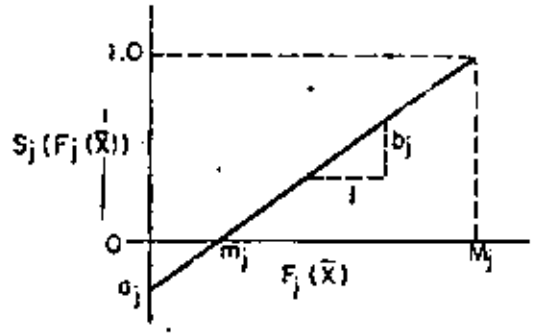

FIGURE 10-4
Scaling objective values.

each scaling function $S_j(\cdot)$ transforms the value of the objective $F_j(\mathbf{X})$ to be within an interval, say, from 0 to 1.

The scaling function can easily be made linear for use in linear programming models. As illustrated in Fig. 10-4, the scaling function can be defined as $a_j + b_jF_j(\mathbf{X})$, where

$$a_j = \frac{-m_j}{M_j - m_j} = \frac{-M_j}{M_j - m_j} + 1 \tag{10-14}$$

$$b_j = \frac{1}{M_j - m_j} \tag{10-15}$$

Using these linear scaling functions, objective function (10-13) is simply

$$\text{Maximize} \quad \sum_j W_j[a_j + b_jF_j(\mathbf{X})] \tag{10-16}$$

where, of course, $\Sigma_j W_j \cdot a_j$ is a constant that can be ignored for the purpose of estimating the trade-offs between separate objectives F_j. Scaling functions may also be used to scale losses in the target optimization models.

The scaling term can be combined with the relative weights so that together they sum to 1. The advantage of this is that different solutions resulting from different weighting strategies can easily be compared. As before, let the value of M_j and m_j represent the maximum and minimum value of the objective $F_j(\mathbf{X})$, respectively. The nonnegative weights $\hat{W}_j$ that sum to 1 and include the previously defined relative weights W_j and the scaling or normalizing constants S_j are defined as

$$\hat{W}_j = \frac{W_j/(M_j - m_j)}{\sum_j [W_j/(M_j - m_j)]} \tag{10-17}$$

The objective function, Eq. (10-13), is then

$$\text{Maximize} \quad \sum_j \hat{W}_jF_j(\mathbf{X}) \tag{10-18}$$

Again, by varying the relative weights $\hat{W}_j$ between 0 and 1 such that $\Sigma_j \hat{W}_j = 1$, the trade-offs between each separate objective $F_j(\mathbf{X})$ can be defined.

10-7 PLAN SELECTION: THE IDENTIFICATION OF POLITICALLY FEASIBLE ALTERNATIVES

In the plan formulation stage of the planning process, numerous, hopefully efficient, alternatives $\mathbf{X}_k$ are produced. Each plan $\mathbf{X}_k$ is a vector of decision variables and accomplishes objective levels $F_j(\mathbf{X}_k)$, $j = 1, 2, \ldots, n$. The generated plans should satisfy technological feasibility $g_i(\mathbf{X}) = 0$, $i = 1, 2, \ldots, m$, and ideally be Pareto optimal or efficient; that is, any increase in one objective value is possible only by decreasing one or more other objective values. If the planner has included objectives which are of concern to policy makers (or the groups which influence the policy-making process), and a broad spectrum of alternatives has been formulated, it is not unreasonable to argue that the planner has performed his function well. He can present these alternatives to decision makers and, after a selection has been made, proceed with plan implementation. The planner could thus avoid more than marginal involvement with questions of political feasibility.

The viability of this approach rests on two assumptions. First, the planner must be capable of formulating Pareto efficient plans that may include a large number of objectives. Second, decision makers must be willing to examine a rather large set of complex alternatives. We have just indicated that there is little reason to believe that either assumption is valid. The formulation of a multiobjective water-resource plan is an expensive, time-consuming process, and even in planning situations that are amenable to mathematical modeling, we have seen that formulated plans may only approach a feasibility frontier. Planning budgets are finite, and policy makers' time is a scarce resource. Thus policy makers may not wish to see a large number of planning alternatives. Efficient use of policy makers' time would dictate the screening of plans so that they may select from a small set of promising alternatives. Hence, it is difficult to eliminate politics from planning. The challenge, perhaps, is to make considerations of political feasibility explicit rather than implicit in the planning process.

The systematic identification of politically feasible water-resource plans can be approached in several ways. If decision makers can be involved in plan formulation, methods are available for estimating their preferences for the various objectives and plans. In this fashion, optimal trade-offs among objectives can be determined with relative certainty, and one or more plans can be identified as being closely aligned with the decision makers' preferences. If policy makers have neither the time nor the inclination for such involvement, optimal trade-offs will be uncertain, and planners must utilize some means of estimating or predicting these trade-offs. Models appropriate to both situations will now be outlined.

10-7.1 Certain Preferences

In Sec. 10-5, plan selection was described as the identification of a plan on an objective transformation curve which achieves the highest level of political feasibility as indicated by a decision maker's isopreference curve (Fig. 10-3). This selection can be effected using indifference analysis as indicated by Raiffa[25] and applied by Haith.[26,27] The procedure is illustrated in an example.

Consider a planning situation in which there are three objectives of concern to a decision maker, described by objective functions $F_1(\mathbf{X}_k)$, $F_2(\mathbf{X}_k)$, and $F_3(\mathbf{X}_k)$. Let the level of objective j achieved by plan $\mathbf{X}_k$, $F_j(\mathbf{X}_k)$ be indicated by F_{jk}. Any plan can thus be specified by the vector (F_{1k}, F_{2k}, F_{3k}). An arbitrary reference level, F_3^* is chosen for objective 3, and the decision maker is asked to specify a level of objective 1, $\tilde{f}_k$ such that he is indifferent between $(\tilde{f}_k, F_{2k}, F_3^*)$ and (F_{1k}, F_{2k}, F_{3k}). In other words, a trade-off is made between the first and third objectives. This is denoted

$$(\tilde{f}_k, F_{2k}, F_3^*) \simeq (F_{1k}, F_{2k}, F_{3k})$$

In an analogous fashion, trade-offs between objectives 1 and 2 are made by selecting a reference level F_2^* and specifying f_k such that

$$(f_k, F_2^*, F_3^*) \simeq (\tilde{f}_k, F_{2k}, F_3^*)$$

Assuming transitive indifferences, we infer that

$$(f_k, F_2^*, F_3^*) \simeq (F_{1k}, F_{2k}, F_{3k})$$

All plans can be evaluated in a similar fashion, using the same reference levels F_2^* and F_3^*. The result is a new set of plans which differ only in the levels of the first objective function $f_1, f_2, f_3, \ldots$. These plans can be ranked according to these values, and the original plans can thus be ordered in terms of the decision maker's priorities. The questions that must be answered to identify trade-offs using indifference analysis are similar to those required by the surrogate worth trade-off method currently being advocated by Haimes and his associates.[28]

In addition to indifference analysis, several other simpler techniques are available for ranking alternatives based on interactions between the planner and the decision maker. These are called *dominance*, *satisficing*, and *lexicography*. They involve the comparison of alternative decision vectors $\mathbf{X}_k$ based on the values of $F_j(\mathbf{X})$ of each separate objective j. Unlike indifference analysis, they do not require the decision maker to specify how much more of one objective value he must have in order to get less of another.

Dominance exists if one alternative results in an equal or higher value for all objectives than do all other alternatives, and if for at least one objective, its value is strictly higher than those of the other alternatives. In other words, for a particular alternative k^* to dominate, $F_j(\mathbf{X}_{k^*}) \geq F_j(\mathbf{X}_k)$ for all objectives j and alternatives k, and for at least one objective, $F_j(\mathbf{X}_{k^*}) > F_j(\mathbf{X}_k)$ for all alternatives $k \neq k^*$. Perhaps more important, if one alternative results in all objective values being equal to or less than the corresponding objective values of all other alternatives, then clearly it is dominated by those alternatives and can be dropped from further consideration. Note that this procedure does not require any specification of the degree of preference for any particular objective values, nor does it require any assessment of the relative importance of each objective value. In fact, the objective values do not even have to be expressed in numerical terms.

While dominance can be a useful method for reducing the size of some decision problems, it is not a very effective method for making the final decision when a number of alternatives remain. For example, all alternatives $\mathbf{X}_k$ that are on the noninferior portion *bcde* of the feasibility frontier in Fig. 10-3 are not dominated; i.e., there exist no other alternatives that have equal or higher values for each of the objectives. Since the formal studies of dominance by Pareto, these nondominated alternatives are often called *Pareto optimal* or Pareto admissible. As implied in Fig. 10-3 there are usually many Pareto optimal or efficient alternatives and each has an objective value that is higher than that of all other alternatives. Although dominance has reduced the number of alternatives from all those that are feasible to those that define the feasibility frontier, the problem of choice among these efficient alternatives remains.

One method of further reducing the number of alternatives is called *satisficing*. As described by Simon,[29] the decision maker supplies the minimal objective values he will accept for each objective. Those alternatives that do not meet these targets are dropped from further consideration. Those that remain are again screened after increasing the minimal acceptable values of one or more objectives. When used in an iterative fashion, the number of alternatives can be reduced down to a single choice. Like dominance, satisficing requires no numerical values for each objective. Nor is any special credit given to alternatives having relatively high values of one or more objectives.

Lexicography involves the ranking of alternatives based on a comparison of objective values for each objective, one at a time, and in order of their importance to the decision maker. Thus the decision maker must specify which objective is most important and then compare the values of this objective for all alternatives. If for this most important objective one alternative has a higher objective value than any of the other alternatives, then it is chosen and the decision process ends. If there is more than one alternative having the highest value of that most important objective, then these and only these alternatives are considered in the next comparison based on the second-most-important objective. The process continues in this lexicographic fashion until either a single alternative emerges or all objectives have been considered.

Each of these techniques, while simple and requiring relatively little information, has a number of limitations. To overcome some of these, other, more complex evaluation techniques have been proposed, necessarily requiring more information and assumptions.

10-7.2 STEM, An Iterative Procedure

Within a mathematical programming framework, Benayoun et al.[9] have proposed a sequential iteration and exploration technique that involves the decision maker. The process "teaches" the decision maker to recognize what he considers as good solutions and important objectives. The final solution selected by the decision maker represents a best compromise among conflicting objectives. Assuming that preferences do not change during the decision-making process, the best compromise is achieved in a relatively small number of iterations. The authors have labeled their approach STEM (step method).

STEM assumes that the decision maker is initially unable to define the relative importance of the separate objectives $F_j(\mathbf{X})$. To teach the decision maker, a number of calculation and decision-making iterations are required, involving essentially a conversation between the analyst and the decision maker. During the decision-making phase of each iteration, the decision maker examines the results of the calculation phase and develops new insights and information about his objectives. This information in turn is used in the calculation phase of the next iteration, thereby providing a guide for the search of the best compromise.

The STEM procedure begins with n alternatives, each of which maximizes one of the n objectives. The first iteration minimizes the maximum weighted difference D between objectives $F_j(\mathbf{X})$ and their respective maximum values M_j:

$$\text{Minimize} \qquad D \tag{10-19}$$

$$\text{Subject to} \qquad D \geq W_j\,[M_j - F_j(\mathbf{X})] \qquad \forall_j \tag{10-20}$$

$$g_i(\mathbf{X}) = \dot{0} \qquad \forall_i \tag{10-21}$$

Constraints (10-20) simply ensure that D is no less than each weighted difference between the maximum and the actual value of each objective, and, as before, constraints (10-21) are all the other constraints specific to the problem being solved. The weights W_j indicate the relative magnitude of the deviations from the optimum. These weights include scale or normalizing terms. The weights W_j can be defined as a quotient of a sensitivity parameter γ_j and a scaling parameter α_j:

$$W_j = \frac{\gamma_j}{\alpha_j} \tag{10-22}$$

Recalling that M_j is the maximum value of $F_j(\mathbf{X})$ and denoting m_j as the minimum value assumed by $F_j(\mathbf{X})$, the numerator of Eq. (10-22)

$$\gamma_j = \begin{cases} \dfrac{M_j - m_j}{M_j} & \text{if } M_j > 0 \\[2ex] \dfrac{m_j - M_j}{m_j} & \text{if } M_j \leq 0 \end{cases} \tag{10-23}$$

indicates the relative range of the values assumed by objective $F_j(\mathbf{X})$. If, for various solution vectors $\mathbf{X}$, the value of $F_j(\mathbf{X})$ does not vary much from the optimum solution M_j, the objective is not sensitive to a variation in the weighting values W_j, and therefore a relatively small weight can be assigned to this objective. As the variation in $F_j(\mathbf{X})$ becomes larger with changes in the decision vector $\mathbf{X}$, the weight W_j will become correspondingly greater. (Note that this relative weight has nothing to do with the relative political importance of the corresponding objective.)

The denominator or α_j term of Eq. (10-22) is used to scale each objective and ensure that the sum of the relative weights W_j equals 1. Initially this constant equals

$$\alpha_j = (M_j + K) \sum_i \frac{\gamma_i}{M_i + K} \tag{10-24}$$

where if any $M_j \leq 0$, $K = 1 - \min_j M_j$; otherwise $K = 0$. On succeeding iterations the relative weights of the objectives whose values are satisfactory are set to 0, and thus α_j is changed accordingly by summing only over those objectives whose values are unsatisfactory. By normalizing the values of each objective, and ensuring that the relative weights sum to 1, different solutions obtained from different sets of relative weights can easily be compared.

The solution to the first iteration is a plan $\mathbf{X}_0$ which yields a vector of objective values, $\mathbf{Z}_0 = [F_1(\mathbf{X}_0), F_2(\mathbf{X}_0), \ldots, F_n(\mathbf{X}_0)]$. The decision maker compares these results with the ideal objective vector $\mathbf{Z} = [M_1, M_2, \ldots, M_n]$. If the values of some components of $\mathbf{Z}_0$ are satisfactory and others are not, the decision maker must accept a certain reduction in the value of one or more satisfactory objectives in order to improve the unsatisfactory ones in the next iteration. Hence, the decision maker must identify the satisfactory objective values $F_j^*(\mathbf{X}_0)$ that can be reduced and the permissible amount of the reduction, ΔF_j^*. Prior to the next iteration the relative weights W_j^* of the satisfactory objectives are set equal to 0, the feasible region is modified by the additional constraints

$$F_j^*(\mathbf{X}) \geq F_j^*(\mathbf{X}_0) - \Delta F_j^* \qquad \forall j^* \tag{10-25}$$

$$F_j(\mathbf{X}) \geq F_j(\mathbf{X}_0) \qquad \forall j \neq j^* \tag{10-26}$$

and the α_j terms used in Eq. (10-24) are increased to ensure that the relative weights of the nonsatisfactory objectives sum to 1.

The next iteration begins with the solution of the modified programming problem [Eqs. (10-19), (10-20), (10-21), (10-25), and (10-26)] and ends with a further adjustment in the relative weights and constraint set. This sequence of iterations continues until either all or none of the components of the objective vector $\mathbf{Z}$ are satisfactory. If all the components are satisfactory, the decision vector $\mathbf{X}$ represents the best compromise. If none of the components is satisfactory, there is no solution to the problem. For an n-objective problem the total number of iterations required to obtain either a best compromise solution,

or no solution, is no more than n providing the decision maker does not change his preferences during the iterative process. The latter assumption, of course, is rather heroic, but its violation would not detract significantly from the potential usefulness that an iterative procedure similar to STEM might have in the decision-making process.

The analyst using STEM can further assist the decision maker by presenting the results of a sensitivity analysis on the different objective functions in the neighborhood of the solution X for each iteration. Also, during each calculation phase several discrete reductions between 0 and the maximum acceptable reduction ΔF_j^* of each satisfactory objective can be evaluated. When the best compromise solution has been obtained, the relative weights that would yield this solution can be calculated a posteriori if desired, by the simultaneous solution of Eqs. (10-27) and (10-28):

$$\text{Constant} = W_j(M_j - F_j(\mathbf{X})) \qquad \forall j \tag{10-27}$$

$$\sum_j W_j = 1 \tag{10-28}$$

The iterative STEM procedure can be illustrated by a simple numerical example. In this example the STEM procedure will be modified to examine inferior objectives, i.e., ones that are minimized. Suppose there are two municipal waste-water treatment facilities that must be built in a small river basin in order to improve stream quality. The treatment efficiency of each facility, X_1 and X_2, must be determined.

For planning purposes three objectives are identified. Each of the two municipalities wishes to minimize its treatment costs, or equivalently, its required treatment efficiency. Since the federal government is subsidizing a specified (and equal) fraction of the cost of each facility, it is interested in minimizing the total cost. Assuming that the cost of X_1 is half that of X_2 for each value of X_1 and X_2, the three objectives are

Minimize	X_1	(F-1)
Minimize	X_2	(F-2)
Minimize	$X_1 + 2X_2$	(F-3)

These objectives are subject to a variety of constraints $g_i(X_1, X_2) = 0$ that define all feasible combinations of X_1 and X_2. Included among these constraints are the effluent or stream-quality standards applicable to the basin. These feasible combinations are illustrated by the shaded region in Fig. 10-5*a*. Also illustrated are the minimum values of each of the three objectives. Clearly, not all objectives can be minimized simultaneously, and it is up to the local river basin commission to achieve an acceptable compromise among the three interest parties, if possible. An analyst on the river basin commission staff begins the STEM procedure by calculating a payoff matrix of the values of the jth objective when the kth objective is minimized. In this case these values

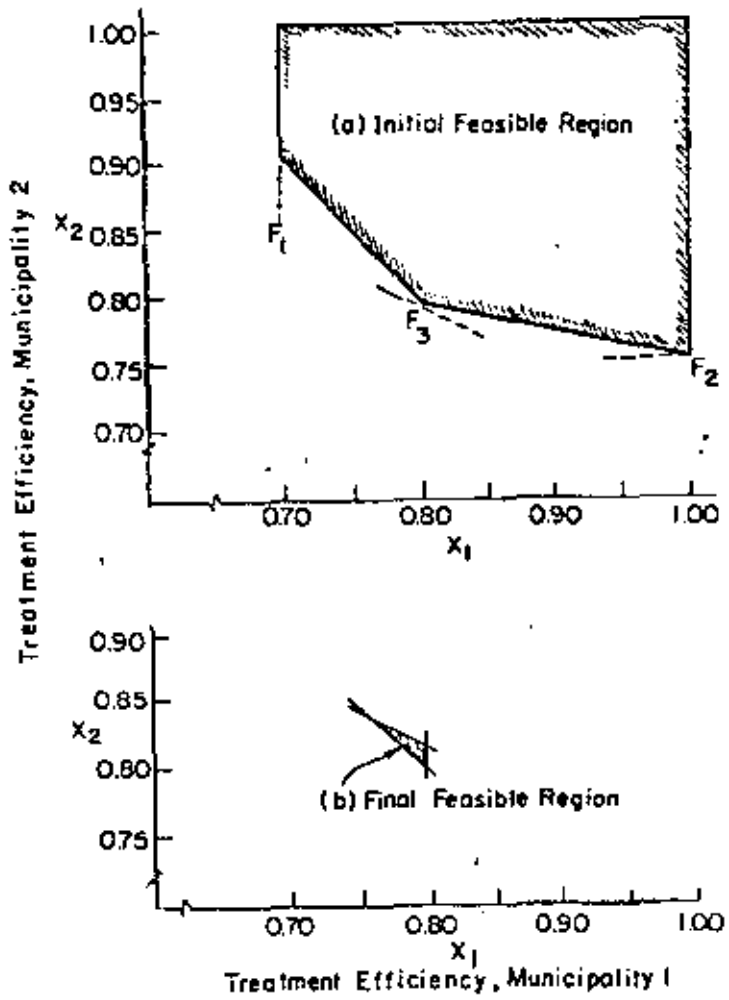

FIGURE 10-5
Feasible combinations of treatment efficiencies.

can be observed from Fig. 10-5*a*:

Objective F_j	j \ k	1	2	3
	1	0.70	1.00	0.80
	2	0.90	0.75	0.80
	3	2.50	2.50	2.40

Using the values in the payoff matrix, the weights W_j ined by Eqs. (10-22), (10-23), and (10-24) for each of the three objectives j are 0.60, 0.37,

and 0.03, respectively. Using these weights in constraints (10-20), the values of X_1 and X_2 that minimize the maximum weighted difference between the objective $F_i(X)$ and its minimum value v_i are 76 and 84, respectively. Hence the values of the three objectives are 0.76, 0.84, and 2.44, respectively. This efficient solution is then presented to the representatives of the two municipalities and the federal government.

Suppose that the representative from municipality 2 (which would have to treat at a higher efficiency than municipality 1) is not satisifed with this solution because of the difference in required treatment efficiencies between the two municipalities. The representative from municipality 1 must then state how much, if any, he is willing to increase treatment efficiency in order to achieve a more equitable solution. Assuming that he is willing to increase treatment efficiency by 4 percent, the next iteration of STEM begins by considering only those combinations of X_1 and X_2 defined by all constraints $g_i(X_1, X_2) = 0$ and the additional constraints (10-25) and (10-26), modified, of course, for inferior objectives:

$$X_1 \leq 0.76 + 0.04$$
$$X_2 \leq 0.84$$
$$X_1 + 2X_2 \leq 2.44$$

These feasible combinations are illustrated in Fig. 10-5*b*.

The relative weight of the first objective (F-1) whose value has been increased and is satisfactory is now set equal to 0. The weights W_2 and W_3 of the remaining objectives equal 0.92 and 0.08, respectively. These weights are then used to recalculate an efficient solution. In this case the solution that minimizes the maximum difference between the objective values and their minimum feasible values is also the solution that minimizes the total cost, namely, $X_1 = X_2 = 0.80$. Clearly all three interested parties are satisfied with this objective, unless, of course, the representative from municipality 1 changes his mind.

The STEM algorithm just discussed corresponds to an educational process that leads to a best compromise. As was illustrated, the process involves the reduction of some superior objective values (or an increase in some inferior objectives) in order to achieve more acceptable values of other objectives.

10-7.3 Uncertain Preferences

If policy makers cannot or will not become involved in the iterative processes described above, the planner is placed in the difficult position of attempting to estimate or infer the policy makers' preferences. These preferences must be considered as uncertain quantities, and the planner is forced to rely to a considerable extent on his judgment for their determination. Personal judgment has always played a role in planning, of course, and estimates of political feasibility have often been made implicitly by planners. The two approaches that have been proposed for analyzing situations in which the preferences are uncertain go somewhat beyond such implied determinations. Each attempts to model the policy-making process, and the planner is forced to be quite explicit in providing the (judgmental) data that is required. The methods are experimental and are subjective in nature. Users of mathematical models frequently attribute undue accuracy and objectivity to the results of their efforts. Such optimism should obviously be avoided when dealing with models of the political process.

One of the two approaches is a probabilistic form of indifference analysis that assumes the trade-offs can be described by subjective probabilities that are determined by the planner's judgment. Techniques for assigning such probabilities are available,[35,36] and in general, they provide a means for explicit and consistent quantifications of personal judgment. The procedure is applicable also to decision-making problems involving small or large policy-making groups.

The other approach can be termed *policy simulation*. Buckley and McLaughlin[41] have developed such a simulation procedure for estimating political feasibility. They have focused on the agencies which influence the policy-making process rather than on the policy makers themselves. By simulating the agencies' reactions to a proposed multiobjective water-resource plan, conflicts among groups are identified, probable coalitions in support of and in opposition to the plan are formed, and the plan is either accepted or rejected according to the levels of political power possessed by both coalitions.

Buckley and McLaughlin utilized this simulation procedure to compare the political feasibility of alternative water-development plans for the Maule River Basin, Chile. This method was also adopted by Burke et al.[42] to analyze the hypothetical water-quality problem proposed by Dorfman and Jacoby.[33]

SUMMARY

The National Water Commission has noted that multiobjective water-resources planning has "yet to be successfully fashioned and implemented in the field."[43] There are two main reasons why implementation has been difficult. Quantification of nonmonetary planning objectives has not been easy, and thus far there have been few methods and established precedents or guidelines for planners to follow. Yet guidelines and methods are beginning to appear in the literature. The primary purpose of writing these notes has been to provide planners with a review of some of these methods and guidelines.

The methodologies that have been reviewed in this chapter represent only a few of a relatively large class of procedures designed to assist the planner in the definition and evaluation of multiple-objective policies. Each of these methodologies, to a greater or lesser extent, provides a mechanism for estimating the trade-offs between conflicting objectives. Some go beyond this to predict what the politically optimal trade-offs may be. Most would agree that, for a multiple-objective solution to be optimal, the choices between conflicting objectives must reflect the best interests of society. Those who are responsible for expressing and articulating these interests are the political decision makers.

Thus it is inescapable that responsible politicians must become involved in the process of selecting the optimal trade-offs between multiple objectives. In the planning process, the relative weights that define these trade-offs are considered to be unknown variables. The precise values of these relative weights will be known only after the political process has selected its final solution. The relative weights of different objectives, as well as the instruments that contribute to meeting these objectives, should reflect conscious political decisions with respect to these political questions at the time those decisions are made. They involve political preferences concerning the future and therefore must be revised as frequently as new policies or new investments are made. To permit project formulators or evaluators to select the final values of these relative weights is to turn over political decisions to technicians.

On the other hand, the political decision-making process often encourages technicians to assign values to the relative weights. One reason for this is the politician's reluctance to learn the methodology of policy analysis and evaluation or to spend the time answering seemingly "academic" questions that would eventually lead to a set of well-defined relative weights. Another reason is that political leaders rely on the support of distinct interest groups that are often in conflict with one another. In such situations it is obviously to the advantage of political leaders not to be too explicit in quantifying political value judgments regarding trade-offs between conflicting objectives. Technicians, of course, all too often encourage politicians not to intervene in making value judgments in areas in which they consider themselves competent. But it is precisely in these areas that they themselves have bias or special interests.

It is clear that what is needed is a methodology that does not require explicit intervention by the political decision makers, yet does make use of value judgments that must be defined by the political decision-making process. The only way that this can be done is to have policy makers recognize that the assignment of values to the relative weights of various objectives is their responsibility, and that they must devote more time to acquiring the skills necessary to articulate those values in advance of specific decision-making.† If the decision makers could indicate even a reasonable range of appropriate values for the relative weights of each objective, planners could present to the decision makers policy alternatives and their trade-offs that reflect only these ranges of politically determined weights.

In the meantime, perhaps the best procedure for planners to follow is to consider the relative weights as unknown, to identify the values of the weights that make significant differences in the values of the objectives, and to define the policies that are efficient for different ranges of weights. These alternative policies, together with their policy implications, can then be submitted to the responsible decision makers. Such a planning procedure, it is hoped, would ensure that the political leadership is aware of the relevant alternatives and the efficient trade-offs among multiple goals. At the same time it would stress the importance of the politician's role in the assignment of relative priorities and in the definition of the best compromise solution. Finally, such a procedure would form the basis for a systematic determination of the relative priorities among various goals by the political process, leading, it is hoped, to a time when they will be at least approximately specified in advance of particular policy formulation and evaluation. If estimates of the values of relative weights are ever to be known in advance of policy planning, it will be necessary for technicians to take the initiative and force responsible decision makers to reveal their value judgments. Rather than presenting to them a single project plan or policy that represents a best compromise between conflicting objectives, planners should put political choice in the hands of those responsible for making those choices—the politicians who are accountable to the people affected by those choices. Through the further development and use of analytical planning techniques similar to those reviewed in this discussion, technicians can begin to enlighten those who would suggest that public-policy evaluation and analyses should not be political.

†Compared to the static assignment of values for relative weights, policy makers can be expected to have even more difficulties in articulating the future changes in the values of the relative weights. These too have to be determined. To the planner, the horizon of each objective is unknown, as well as its relative weight.

ACKNOWLEDGMENTS

This chapter is a condensed and revised version of some notes prepared for a short course on multiobjective water-resources planning at the University of Nebraska in July 1973. In addition to the work drawn from the cited literature, some of the material contained herein comes from a more detailed study (by DAH) of certain aspects of multiobjective water-resources planning. Other portions have been abstracted from a paper prepared (by DPL) for a book on national economic planning models compiled by the Development Research Center of the World Bank. The writers have benefited considerably from the comments many have made on earlier drafts, yet remain responsible for any opinions or inadvertent errors. We also gratefully adknowledge the financial support provided by the Office of Water Research and Technology, U.S. Department of the Interior, as authorized under the Water Resources Research Act of 1964, as amended.

REFERENCES

1. SIMON, H. A., "Models of Man," John Wiley & Sons, Inc., New York, 1957.
2. WHITE, G. F., "Strategies of American Water Management," The University of Michigan Press, Ann Arbor, 1969.
3. *Policies, Standards, and Procedures in the Formulation, Evaluation, and Review of Plans for Use and Development of Water and Related Land Resources*, Senate Document No. 97, 87th Cong., May 1962.

11316 DELPHIC PREDICTIONS AND CROSS SIMULATION

KEY WORDS: Environmental impact statements; Forecasting; Planning; Probability theory; Regional planning; Transportation; Urban development; Urban planning

ABSTRACT: The writers review two techniques that are potentially useful tools in urban and regional planning. These techniques are the Delphi method for obtaining subjective predictions about a changing future through a panel of experts and Cross-Impact Simulation for combining a number of discrete subjective forecast with a number of similar related forecasts to produce alternative descriptions of the future. The potential of this class of techniques for planners and engineers who are involved in managing the future is pointed out. The use of the techniques is specifically relevent to situations where subjective judgments have to be made about complex interrelated events. The paper presents mathematical examples of the utilization of these two complimentary methods.

REFERENCE: Dajani, Jafir S., and Gilbert, Gorman, "Delphic Predictions and Cross Impact Simulation," *Journal of the Urban Planning and Development Division*, ASCE, Vol. 101, No. UP1, Proc. Paper 11316, May, 1975, pp. 49-59

JOURNAL OF THE URBAN PLANNING AND DEVELOPMENT DIVISION

DELPHIC PREDICTIONS AND CROSS IMPACT SIMULATION

By Jafar S. Dajani, M. ASCE[1] and Gorman Gilbert[2]

INTRODUCTION

Forecasting future events is a basic component of any design or planning effort. Forecasting techniques in most common use by engineers and planners at the present time are concerned with forecasting the value of a single measurable entity at some future time. Examples of such situations are population and economic forecasts, in which the implicit assumption of a continuation of, or a marginal predictable change in present trends is usually assumed. The outcomes of such forecasts are, of course, a future that provides for more of the same.

Two variations of the previous theme are becoming increasingly apparent. The first is that a continuation of past trends is becoming increasingly improbable due to a continuously accelerating rate of change in every aspect of life. This increasing rate of change results in a significant reduction in the amount of information about the future available to the forecaster. The second is the fact that forecasting a singular entity is a meaningless exercise in an increasingly complex world in which most entities are interrelated in more than one way. Thus, it becomes imperative that the forecaster simultaneously considers a number of these interrelated entities in efforts to predict the future value of any one of them. The present paper reviews two forecasting techniques designed to handle these two problems: (1) The Delphi method for making subjective predictions about a changing future; and (2) The Cross Impact Simulation, which uses the results of the Delphi Technique to estimate the future value of any of a number of interrelated entities. This paper presents the application of these techniques in forecasting complex, interrelated, and sometimes subjective combinations of events for design and planning purposes.

Note.—Discussion open until October 1, 1975. To extend the closing date one month, a written request must be filed with the Editor of Technical Publications, ASCE. This paper is part of the copyrighted Journal of the Urban Planning and Development Division, Proceedings of the American Society of Civil Engineers, Vol. 101, No. UP1, May, 1975. Manuscript was submitted for review for possible publication on June 3, 1975.

[1]Asst. Prof. of Civ. Engrg. and Policy Scis., Duke Univ., Durham, N.C.

[2]Asst. Prof., Dept. of City and Regional Planning, Univ. of North Carolina, Chapel Hill, N.C.

DELPHI TECHNIQUE

In some cases estimates or forecasts have to be made on the basis of very little information. The only source of knowledge might be some "experts" who do not agree among themselves about the value that should be assumed by the estimate or forecast. The term, experts, is loosely used to denote scientists attempting to make predictions about future developments in their fields, businessmen attempting to predict the volume of sales of a new product, policy analysts trying to map alternative futures, or residents of a community trying to determine the goals of the community and thus offer guidelines for planning and design. The opinions of these experts are usually subjective, albeit guided by some objective background. They can be described as informed judgments. The use of experts for estimating and forecasting is not new. A number of methods could be used to obtain expert opinion. At one extreme is the use of a single expert. The other extreme is the use of a committee, which is based on the premise that many opinions are better than one. However, committees are known to have many disadvantages and can indeed be counter-productive. They often reflect the opinion of a vocal minority. A dominant individual with an imposing personality might have a significant influence on the committee's decisions. Participating individuals are often unwilling to abandon previously announced positions, to publicly contradict individuals of higher positions, or to take positions on issues before it is known in what direction the majority is going. Members having a vested interest may succeed in obtaining a favorable outcome that has no claim to validity. These shortcomings of the committee approach to handling problems of subjective estimation, "guesstimation," and forecasting have led to the development of the Delphi technique. This technique was pioneered by Olaf Helmer at the RAND Corporation and is designed to encourage consensus development among experts and to sharpen their own thinking with respect to estimation efforts (1,5). These objectives are achieved through avoiding any direct exchange of ideas among the experts, but instituting a strong well-designed feedback system. The elimination of direct exchange is intended to insure anonymity of opinions, and thus eliminate the risks of personality dominance and the desire for conformity and acceptance among peers. The members of a panel of experts never meet. They communicate with a coordinator, but never with each other, through letters of electronic media.

The participants in a Delphi experiment are first asked to "brainstorm" about different questions that have a bearing on the entity or entities being forecast. They may, for example, be asked what developments they may expect to occur in a certain field, or what possible future impacts a certain action might have or what set of alternative futures might be feasible. On the basis of their answer, the experiment coordinator selects specific areas for attack, and formulates questions to ask the panelists. These questions should be straightforward, with a clearly defined answer. They may pertain to the specific timing of an event, the specific value of an entity, the probability of occurrence of an event, the feasibility or desirability of certain actions, etc. The participants are asked to give their best informed judgment in answering their questions and the reasons for their opinions. These reasons are submitted in writing, edited by the experiment coordinator, and fed back to the panelists, while the question is asked again. Consecutive iterations of this process tend to narrow down the spread of responses and approach a consensus.

To illustrate the use of this technique, suppose that a panel of seven experts is called upon to estimate the year in which their town will need a new water supply source and suppose that these experts have equal expertise and knowledge

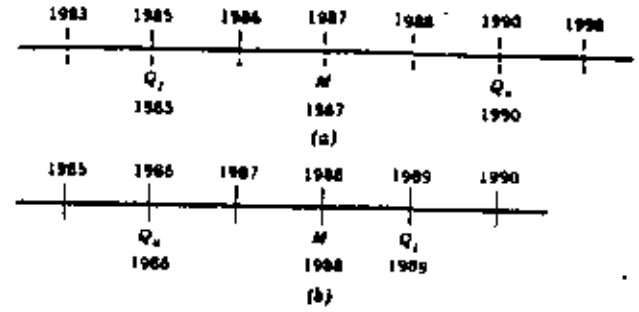

FIG. 1.—Interval Scale

Event	Year	Probability	E_1	E_2	...	E_j	....	E_n
E_1	Y_1	P_1		$+\Delta_{2/1}$ % $+\Delta Y$				
E_2	Y_2	P_2						
⋮	⋮	⋮						
E_j	Y_j	P_j		$-\max \beta$ $+\max \gamma$				
⋮	⋮	⋮						
⋮	⋮	⋮						
E_n	Y_n	P_n						

FIG. 2.—Typical Cross Impact Matrix

Event	Probability	Year	E_1	E_2	E_3	E_4
Shopping center built	0.40	1980		+0.05 −5 yr	+0.10 −10 yr	+0.05 −2 yr
$P_A = 50000$	0.50	1985	0 +2 yr		0 0	0 0
Female lawyer hired	0.75	1985	−0.10 +10 yr	0 0		+0.05 −5
$P_B = 100000$	0.50	1990	+0.05 0	0 0	−0.05 +5 yr	

FIG. 3.—Cross Impact Matrix for Transportation Study

about local development patterns and ground and surface-water supplies. Each member of the panel is first asked to estimate the year in question. The estimates can be shown on an interval scale as shown in Fig. 1(a). The interval scale in Fig. 1(a) shows three points designated as M, Q_u, and Q_l. The first point

M = the median of the responses, i.e., there are as many panelists who believe that the event will occur after 1987 as those who believe that it will occur before 1987; Q_l = the lower quartile; and Q_u = the upper quartile. The point, Q_l is the median of all predictions earlier than 1987, while Q_u is the median of all predictions of occurrence after 1987. The lower and upper quartiles are thus 1985 and 1990, respectively. Other quartiles can be used, depending on the expected spread of the final forecast.

The values of Q_l, M, and Q_u are now communicated to the panelists, who are asked to revise their original estimates and, if the new estimate lies outside the interquartile range, Q_l to Q_u, to briefly explain, in writing, why it should be outside the range of 75% of the panelists' first round estimates. The results of this second round of predictions are then fed back to the panelists, together with an edited statement of the reason for making a prediction that is above (or below) the upper (or lower) quartile. The figures obtained in the second round are typically less dispersed and thus represent an improvement in consensus. The representation of these results on interval scale might be as shown in Fig. 1(*b*).

This second round result might be deemed acceptable in this case. If not, however, it could be repeated for a third round, or as many rounds as may be thought necessary to achieve an acceptable level of consensus. The median of the final round can be assumed to be an estimator of the entity being sought. The dispersion of other estimates can give an indication of the probability distribution around the median as a point estimate.

The basic model presented previously is the classic version developed by the Delphi originators. There are a number of possible variations that could be incorporated into the model. One of these variations is the association of weights with predictions, and thus, the use of a weighted average of estimates as the point estimates. These weights could be selected by the panelists themselves on the basis of their evaluation of their own relative competence and expertise in the specific question area. Another variation pertains to the extent of feedback given to the participants. In some Delphi experiments, it was found that complete feedback of the type shown previously tends to produce an overconvergence of opinion, which might be the result of overt group pressures. To remedy the situation, partial feedback information can be channelled to the participants. This might include the fact that they are (or are not) in one of the two extreme quartiles, and thus an attempt must be made to have them converge in the absence of perfect information (6). A third variation has panelists give estimates of the most probable, optimistic, and pessimistic estimates, or of the median, upper quartile (or other fractile), and lower quartile (or other fractile). In these cases the medians for each of the three estimates are calculated, and those with median estimates falling outside the interquartile range are asked to explain their estimates. A fourth variation applies to experiments in which obtaining a consensus is not necessarily the main objective, but is rather superceded by the desire to understand the nature of an existing distribution of group opinions. In such cases the criterion for discontinuing Delphi rounds may not be the achievement of an acceptable level of convergence of opinion, but rather the achievement of a stable situation in which the change in the distribution of opinions between rounds is at an acceptable minimum. This change in distribution may be measured by the percentage change between panelists holding similar opinions in two consecutive rounds. When the percentage change is at an acceptable minimum, the experimenter can be more confident that he is obtaining a good image of opinion distributions, rather than a short-lived consensus.

The Delphi technique need not be used exclusively for estimating the value of some readily measurable entity. Estimates also can be made of any entity for which some measurement scale can be developed. Some entities as the feasibility or desirability of an event, for example, can be estimated by assigning them to a scale between $-\alpha$ and $+\alpha$, in which 0 = the indifference point; $-\alpha$ = the point of extreme infeasibility or undesirability; and $+\alpha$ = the point of extreme feasibility or desirability. This is similar to the usual measures of probability, which range from zero to unity. The method also can be used to estimate functional relationships, e.g., estimating the curve of benefits obtained from a certain investment over time. This is achieved by simply obtaining estimates for each of a number of future years. The data thus obtained can be plotted against time for the median, upper quartile, and lower quartile. The three resulting curves will represent the most probable, an optimistic, and a pessimistic time-dependent stream of benefits.

Cross Impact Simulation

Forecasting methods of common use by engineers and planners are usually concerned with forecasting or estimating a single entity at a time. They discard any direct interrelationship between the entity being forecast and other entities, or at best attempt to include it in a one-way fashion. In other words, they may consider the effect of A on B without considering the feedback loop between B and A. Even less attention is paid to chain relationships with built-in feedback. An interest in developing a methodology that can trace through such chains of interrelationships has led to the development of cross impact analysis by Gordon and his associates, following the development of the Delphi technique (2,3). This resulted from criticisms directed at the Delphi technique, on the basis of its panel of experts handling one forecast or estimate at a time. The use of cross impact analysis is not limited to the interaction among different Delphic predictions, but is applicable whenever a systematic approach is desired for combining a number of forecasts of discrete events. It utilizes a simple version of simulation that could be done either manually or with the aid of electronic computers. It can lead to the development of scenarios and to the analysis of policy alternatives. These terms will be presented and explained later in this paper. The following examination of the general formulation of cross-impact analysis will be divided into three areas: (1) the input; (2) the format; and (3) the mechanics.

Inputs.—Two types of inputs are required for conducting a cross-impact analysis: (1) Event descriptions; and (2) event interactions. An event is completely described by the probability of its attaining a certain value by a certain time. The value could be defined as a binary number, having a value of unity in case of the occurrence of the event and a value of zero in case of its nonoccurrence. Since most forecasts include information about the value of an entity or event at some future date and with some probability distribution for attaining that value, the description of the event should be readily obtainable from these

forecasts. However, the analyst can fix any of these descriptors and allow variations in the other two. This is both desirable and practical since it is in conformity with the output of most single entity forecasting procedures (including the Delphi). He might select to concern himself with forecasting "the date when an event attains a given value with a variable probability," or "the probability of an event attaining one of a number of values at given date," or "the value attained by the event by any one of a number of dates with variable probabilities." This, in effect, means that for events with a binary outcome, the forecaster will concern himself with predicting the date of occurrence and its probability. A remote date with low probability indicates a situation approaching an outcome of zero. The inputs to the analysis will thus be as many date-probability combinations as the forecaster finds necessary. If the event is, for example, "complete replacement of the internal combustion engine by a different technology," then the forecaster might use the median time estimate of a Delphic experiment, which has a 50% probability attached to it. He also may want to use the upper quartile time estimate with a cumulative probability of 75% or the lower quartile with a cumulative probability of 25%, or he may design his experiment so as to provide a probability spread associated with each of a number of time forecasts. If the event can attain other than binary values, e.g., "x% replacement of all internal combustion engines on the road," then the procedure outlined previously may be repeated for each of a number of values of x. As will be seen later, the larger the number of events described, the more complex the problem becomes and the more imperative the use of electronic computers becomes.

The second input is that of event interactions. These are described in three different ways, all related to the event descriptions mentioned previously. Event interactions can be described by mode and intensity. The mode by which the occurrence or nonoccurrence of one event can influence another is by enhancing or diminishing its probabilities of occurrence and by advancing or delaying its time of occurrence. The intensity of the change caused by the occurrence or nonoccurrence of the first event, on the occurrence of the second, can be estimated as a percentage increase or decrease in the probability of the second event's occurrence and as a number of years by which its occurrence is hastened or delayed. This number of years should include any time lag between the occurrence and the initiation of the impact.

Format.—Once all the event values, probabilities, and times are found, and the mode and intensity of interevent interactions are known, the problem can be cast into its standard format, i.e., a cross impact matrix. This is an $n \times n$ matrix; in which n = the number of events. If all the events are expected to occur initially at the same year, then they can be listed in random order. This order can be decided by the roll of a dice or by the use of a random number generator. If, on the other hand, they are expected to occur at different future dates, then they should be arranged in chronological order. Any number of events with the same future occurrence date can be randomly arranged between the immediately preceding and succeeding events. There are $n(n-1)$ interactions describing the effects of the occurrence of some event on another, assuming that there is no effect on the occurrence of one event resulting from its own occurrence. The same number of interactions exist describing the effect of the nonoccurrence of an event over the occurrence of another. Thus, all interaction

modes and intensities can be described by two matrices: (1) An occurrence matrix; and (2) a nonoccurrence matrix. Both matrices will have no entries along their diagonals. Each entry a_{ij} in the occurrence matrix would indicate the mode and intensity (both probability change and time change) of the effect of the occurrence of an event listed in row i on the event listed in column j. The effect of the nonoccurrence of the event in row i on the occurrence of the event in row j is entered as a'_{ij} in the nonoccurrence matrix.

An alternative simplified format would capitalize on the fact that the occurrence of a later event is usually not expected to have an effect on an earlier event and that a scrutiny of events occurring simultaneously might lead to the discovery of small differentials in time, based on possible interrelationships. If no such logical ordering is possible, then a random ordering would do. By making this assumption, the number of cells in the occurrence matrix is cut in half, and only $[n(n-1)]/2$ cells are needed. These are the cells above the diagonals. The same can be said about the nonoccurrence matrix, which can be represented by cells below the diagonal. These cells contain data about the expected effect of the nonoccurrence of the event, j, in the column on the occurrence of the event, i, in the row. Fig. 2 shows a typical such matrix, similar to that presented by Martino (4). In this matrix the entry, a_{12} (first row, second column) indicates that the occurrence of E_1 will enhance the probabilities of the occurrence of E_2 by Δp% and delay its expected time by ΔY years. The entry, a'_{21}, on the other hand, indicates that the nonoccurrence of E_2 will reduce the probabilities of occurrence of E_1 by the maximum possible amount, i.e., drive it to 0%. It will delay the expected time of occurrence by the maximum possible amount, which could be set at any large number of years. In other words, unless E_2 occurs, E_1 will never occur. Thus, the impact of the occurence of a certain event could be found by following the appropriate row above the diagonal, while the impact of its nonoccurence could be found by following the appropriate column below the diagonal.

Mechanics.—To demonstrate the mechanics of cross impact analysis, let us consider the following illustrative example. Assume two settlements A and B are considering the construction of a mass transit link between them and assume that the following forecasts have been made: (1) The link will become economically feasible by 1985 with a probability of 0.75; (2) settlement A will have a population of 50,000 by 1985, with a probability of 0.50; (3) settlement B will have a population of 100,000 by 1990 with a probability of 0.5; and (4) a large regional shopping center will be built between the two settlements by 1980 with a probability of 0.4. Also assume that the modes and intensities of interactions between these four predictions are as given by the cross impact matrix given in Fig. 3. The second and third rows and columns could have been interchanged. Their relative position is random since they are not forecast to have any significant interaction.

To proceed with the mechanics of the analysis, a random number generator is used. As a number is picked, the probability of an event's occurrence is compared to that number and it is thus decided whether it would occur in the first round of the analysis. Probabilities and times of occurrence of other events are accordingly determined. If, for example, the first two figures of a random number are between 0 and 39, then we can consider the first event to have occurred, while if these numbers are between 40 and 99, we can consider

it not to have materialized. Using a random numbers table, assume that it is found that the first random variable is 37. Thus, the first event does occur and its occurrence hastens the expected time of E_2 by 5 yr and increases the probability of its occurrence by 0.05. It also increases the probability of occurrence of E_3 to 0.85, speeds up its occurrence by 10 yr, and increases the probability that E_4 will materialize by 1990 to 0.55 and hastens its occurrence by 2 yrs. This procedure is repeated for the remaining three events and then the whole cycle is repeated a large number of times. The results obtained by three rounds are shown in Table 1. Each round represents one possible future situation or scenario. The first round represents one in which events 1, 3, and 4 occurred. In the second round, all four events occurred, while in the third round events 1, 3, and 4 occurred. The probability of a scenario occurring can thus be found once a large number of rounds is completed, by dividing the number of rounds in which it has actually occurred by the total number of rounds completed. Thus, in the example given previously, the probability of the scenario, YNYY = 2/3 (N = the nonoccurrence of an event; Y = its occurrence; and the location of letters corresponds to the number of the event). At the end of a large number of rounds it is also possible to replace the original individual entity forecast (given in the input to the analysis) by a revised combined forecast that takes into account the effect of the interaction of events. This forecast can be found by averaging the probabilities and associated times resulting from each round. In the example given previously, the continuous interaction has resulted in an improvement in the probability of having a mass transit link become feasible. While it initially looked like there was a 0.75 probability that it would become feasible by 1985, it now seems that there is a 0.85 probability that it will become feasible by the year 1975. This is due to the effect of the occurrence of the regional shopping center (which happened to have a very high frequency in our limited experiment). Note that the revised probability and time of E_4 are obtained by averaging the figures obtained from the third step in the simulation, since it is assumed that the occurence or nonoccurence of an event has no effect on the characteristics of that event.

A few further comments on the mechanics are in order. There are two types of limiting cases in the analysis. One of those deals with placing an upper and lower limit on the probability of occurrence of an event. It naturally makes no sense to increase a present probability of 0.90 by 0.20 and obtain a probability of 1.10. Neither does it make any sense to end up with a negative probability. This problem could be circumvented in a number of ways, all of which are arbitrary. One approach is to limit these probabilities to their maximum or minimum values and not to perform any calculations that will cause them to violate these limits. Another approach is to apply the percentage change resulting from the impact of one event over the other to the difference between the actual probability of the affected event and the upper or lower limit, whichever is applicable. This implies that the percentage change reduced the difference between the actual probability and the limit exponentially. Thus, an enhancing probability change of intensity, 0.20, applied to an initial probability of 0.6 would increase it to 0.60 + 0.20(1 − 0.60) or to 0.68, while a diminishing intensity of −0.20 would decrease it to 0.6 (0.6 × 0.2) = 0.48. A similar problem arises with time forecasts. If a future event is subjected to a number of delaying influe , its date of occurrence might approach the present or might ever

TABLE 1.—Example of Cross Impact Simulation

Event	First Round				Second Round				Third Round				Revised probability	Revised time
	Random number				Random number				Random number					
	37	70	08	38	19	41	36	16	18	84	21	05		
E_1	Y	0.40[a]	0.40	0.40		0.40	0.40	0.40		0.40	0.40	0.40	0.40	
	0.55	1980	1980	1980	Y	1980	1980	1980	Y	1980	1980	1980	0.40	1980
E_2	1980		0.55	0.55	0.55		0.55	0.55	0.55		0.55	0.55		
	0.85	N	1980	1980	1980	Y	1980	1980	1980	N	1980	1980	0.55	1980
E_3	1975	0.85	0.85	0.85	0.85	0.85	0.85	0.85	0.85	0.85		0.85		
	0.55	1975	1975	1975	1975	1975	Y	1975	1975	1975	Y	1975	0.85	1975
E_4	1988	0.55	Y	Y	0.55	0.55	0.60	0.55	0.55	0.55	0.60	Y		
		1988	0.60		1988	1988	1983	Y	1988	1988	1983		0.60	1983

[a] As an example, this means that the probability that event E_1 will occur by the year 1980 is 0.40.

go into the past. Should such a situation arise, the analyst might want to impose a lower limit on the expected time of occurrence. However, if the situation persists he should consider revising his original forecasts for entries into the cells of the cross impact matrix.

Cross impact analysis is at best an exercise in systematic subjectivity. The quality of the results obtained from the analysis is dependent on the quality of the inputs. The analyst must not place blind faith in its results, but must consider the method nothing more than an aid for systematic judgment. As the number of interacting events increases, so does the total number of required calculations and so does the number of possible independent scenarios. This number is actually equal to 2^n; in which n = the number of interacting events. Thus for our four event situation, there is a total of 16 possible outcomes that will occur with different probabilities. If 10 interacting events are analyzed, the total number of possible futures jumps to 2^{10} or 1,024. Such situations naturally warrant the use of an electronic computer, which lends itself to the efficient handling of such repetitive tasks. However, a neatly printed computer output does not improve the quality of the results, nor does it guarantee a "correct" analysis!

It is often desirable to make a combined forecast of a future set of interacting events, under certain policy assumptions. If, for example, it were decided that the shopping center be built at location C by a certain year or if a land-use policy that would limit the growth of settlement B to a certain population by a certain year were set, what would happen to the feasibility of the mass transit link? Such hypothetical questions can be answered with cross impact analysis by correspondingly changing the individual time and probability forecasts to reflect the proposed policy action. Note that the policy action does not have to be of the definitive type given in the two examples given previously, where the occurence or nonoccurence of an event are the only two possibilities. It might be a tax or land improvement policy that would simply change the predicted time and probability of future events and thus require a new cross impact matrix. The modes and intensities of event interactions also must be revised to reflect the new policy. It also would be of interest to compare the outcomes of situations with and without a certain policy or with different levels of policy implementation. Thus, the impact of implementing these policies can be forecast. It would be useful to test the impact of combinations or sequences of policies on the given set of interacting events.

The term, scenario, has been used repeatedly in this section. Its introduction herein is not because of its unique association with cross impact analysis, but because it is a method for analyzing and presenting combined forecasts that could be useful when used in conjunction with cross impact analysis. This method has been developed by Herman Kahn at the Hudson Institute and is directed at viewing and combining various forecasts in a systematic way. Typically, it follows a route similar to that of cross impact analysis by analyzing the changes that are expected to result from single forecasts or from strategy and policy decisions and obtaining different possible combinations of policies and outcomes. Each scenario is written up in such a way as to convey to the decision maker a total image of a possible future. The decision maker is assumed not to be interested in discrete events and specific estimates, but rather in a qualitative descriptive map of discrete situations. These maps can be readily

obtained from a cross impact analysis, but also can be obtained from other methods of varying degrees of rigor.

Conclusions

This paper has presented the two related techniques of Delphi and cross impact simulation within the context of urban and regional forecasting. The application of these methods has not yet become widespread in this field, yet they have promising implications. The main advantages that can be expected from the use of these methods are the incorporation of the following into a presently simplistic forecasting technique: (1) Subjective judgments; (2) presently unforeseeable technological and institutional changes; and (3) complex interrelationships and feedback structures. Such a development will lead to the projection of a number of alternative futures with probabilistic structures. These futures can form the basis for the generation of more policy responsive plans and for a more realistic planning and decision-making environment.

Appendix I.—References

1. Dalkey, N. C. and Helmer, O., "An Experimental Application of the Delphi Method to the Use of Experts," *Management Science*, Vol. 9, No. 3, 1963.
2. Gordon, T. J., Enzer, S., and Rochberg, R., "An Experiment in Simulation Gaming for Social Policy Studies," *Technological Forecasting*, Vol. 1, 1970, pp. 241-261.
3. Gordon, T. J. and Hayward, H., "Initial Experiments with the Cross Impact Matrix Method of Forecasting," *Futures*, Vol. 1, Dec., 1968.
4. Martino, J. P., *Technological Forecasting for Decision Making*, American Elsevier, New York, N.Y., 1972.
5. Pill, J., "The Delphi Method: Substance, Context, a Critique and Annotated Bibliography," *Socio-Economic Planning Sciences*, Vol. 5, No. 1, 1969.
6. Rutherford, et al., "Goal Formulation for Socio-Technical Systems," *Journal of the Urban Planning and Development Division*, ASCE, Vol. 99, No. UP2, Proc. Paper 9985, Sept., 1973, pp. 157-169.

Appendix II.—Notation

The following symbols are used in this paper:

- a_{ij} = measure of mode and intensity of effect of occurrence of event i on event j;
- a'_{ij} = measure of mode and intensity of nonoccurrence of event i on event j;
- E = event;
- M = median of Delphic prediction;
- P = probability;
- Q_1 = median of all predictions occurring earlier than overall median;
- Q_u = median of all predictions occurring after overall median; and
- Y = year.

6.4. System optimisation *(contibuted by J. Kuiper)*

This section deals with the techniques of analysis that can be used for minimising the total costs, and then maximising the total net benefits of a multi-purpose water resource system. The system will consist of three upstream reservoir sites which will provide a

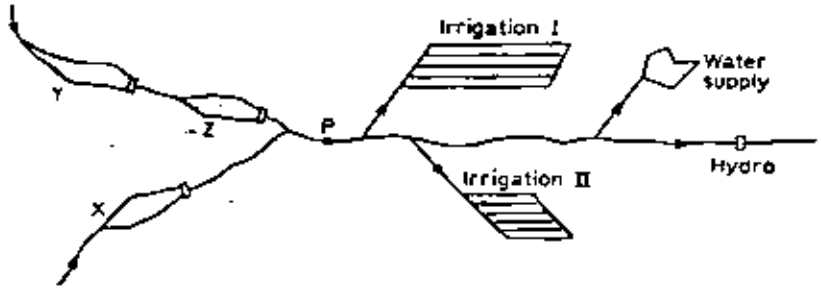

Fig. 6.8 Location of reservoirs and water development projects

dependable flow, and four downstream projects which are competing to use this water: two irrigation projects, a municipal water supply project, and a hydro project. These are shown in Fig. 6.8.

The objective in designing this system will be to find the combination of projects and level of development of each project which will maximise the total net benefits of the whole system. In order to do this, we will separate the problem into its two components: finding the minimum cost of a dependable flow and the maximum benefits of a dependable flow, and then combine the benefit and cost functions to obtain that level of development which has the maximum net benefits. In the first part of this section we will discuss the techniques for minimising the cost of storage for a certain level of dependable flow, using both the equalisation of marginal costs method, and the two project comparison method. In the second half we will consider the maximisation of benefits for a certain level of flow, and then finally we will combine the two to obtain the optimum plan for development.

In this water resource system, we have three upstream storage

reservoirs for the purpose of providing a dependable flow of water to the downstream projects. Our purpose will be to minimise the total cost of these three reservoirs for any level of dependable flow. The dependable flow on the main river will be a function of the total storage capacity developed in the upstream reservoirs. This total storage can be distributed among any of the upstream reservoir sites, and we shall assume that storage in all these sites is equivalent and interchangeable. This equivalence occurs because we are only interested in augmenting the flow at point P, and so from a downstream point of view it does not matter from which of the upstream reservoirs storage releases are made during periods of low flow, as long as the total storage release is the same.

The assumption of equivalence of storage will only be true if the outlet and channel capacity of each reservoir is large enough to handle the expected releases from that reservoir, and if no reservoir is so large that it cannot be filled. Specifically, it should not be so large that it may not be full while other reservoirs are full and spilling water in excess of downstream requirements. We shall assume that these two limitations do not occur in this case, and therefore we can consider storage in all the upstream reservoir sites as equivalent and interchangeable.

The problem then becomes one of minimising the total cost of a fixed volume of total storage. The total system cost is the sum of the separate project costs shown in Fig. 6.9. The simple technique for finding the least cost combination of two projects with the

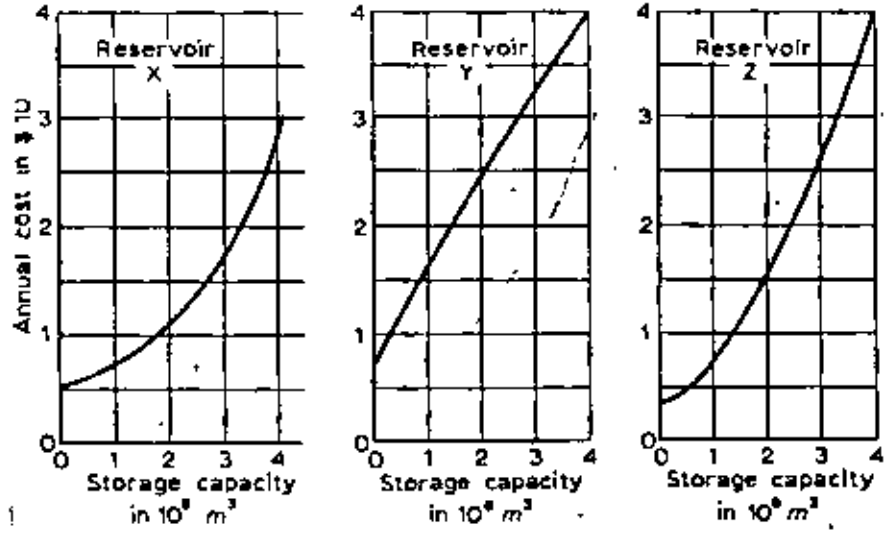

Fig. 6.9 Annual cost of storage reservoirs X, Y and Z

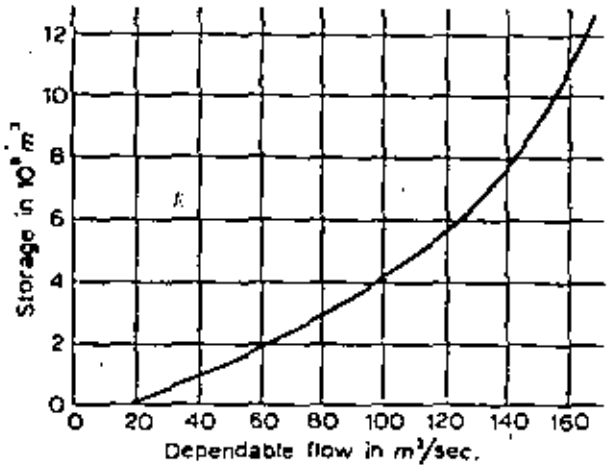

Fig. 6.10 Relation between reservoir storage and dependable flow at point P

total output fixed as discussed in the previous section, can be readily adapted to solve a problem with three or more projects, although the technique becomes rather laborious when many projects are involved.

Let us first illustrate the two project method with a simple two project example. The two projects will be reservoirs X and Z, shown in Figs. 6.8 and 6.9, and the total output will be the total required storage capacity. The total required storage S_{xz} of the system XZ is then fixed, and if we vary the storage S_x of project X we can define S_z, the storage requirement of project Z, in terms of S_{xz} and S_x:

$$S_x + S_z = S_{xz} = \text{total storage}$$

or:

$$S_z = S_{xz} - S_x$$

We can now compute the total cost of the combination by finding the cost $C_x(S_x)$ of project X at a particular level of storage S_x, and adding to it the cost $C_z(S_z)$ of project Z at a particular level of storage S_z, defined by $S_z = S_{xz} - S_x$. In mathematical terms:

$$C_{xz} = C_x(S_x) + C_z(S_z)$$

The total cost can then be defined in terms of S_x if total storage S_{xz} is specified and the costs of reservoirs X and Z are given, as in Fig. 6.9. For example, at the total storage level of $S_{xz} = 6{\cdot}0 \times 10^6 m^3$, we can compute the following costs for various combinations of X and Z:

S_x	S_z	C_x	C_z	C_{xz}
$2 \times 10^6 m^3$	$4 \times 10^6 m^3$	$1{\cdot}1 \times 10^6$ \$	$4{\cdot}0 \times 10^6$ \$	$5{\cdot}1 \times 10^6$ \$
3	3	1·7	2·6	4·3
4	2	2·8	1·5	4·3

We can plot these points on a graph to obtain Fig. 6.11. From this graph it can be seen that the least cost combination for a total storage requirement of $6{\cdot}0 \times 10^6 m^3$ is $S_x = 3{\cdot}5 \times 10^6 m^3$ and $S_z = 6{\cdot}0 - S_x = 2{\cdot}5 \times 10^6 m^3$, at a total cost of $4{\cdot}1 \times 10^6$. If we repeat this procedure for different levels of total storage S_{xz}, and

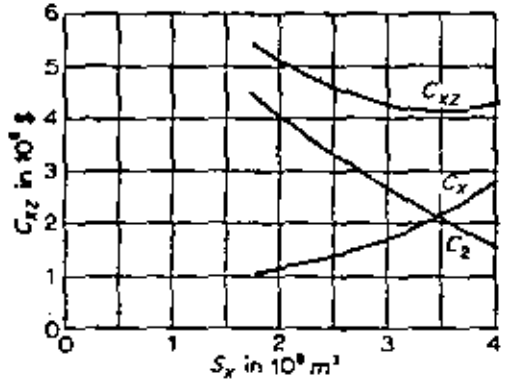

Fig. 6.11 Annual cost of reservoir combination X and Z
$S_{xz} = 6{\cdot}0 \times 10^6 m^3$
$S_z = S_{xz} - S_x$
$= 6{\cdot}0 - S_x$
$C_{xz} = C_x + C_z$

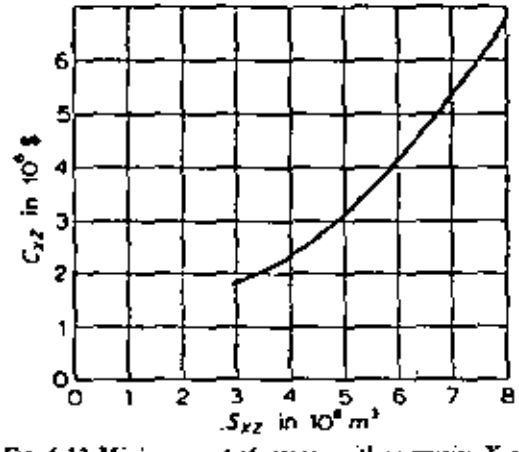

Fig. 6.12 Minimum cost of storage with reservoirs X and Z
$C_{xz} = f(S_{xz})$

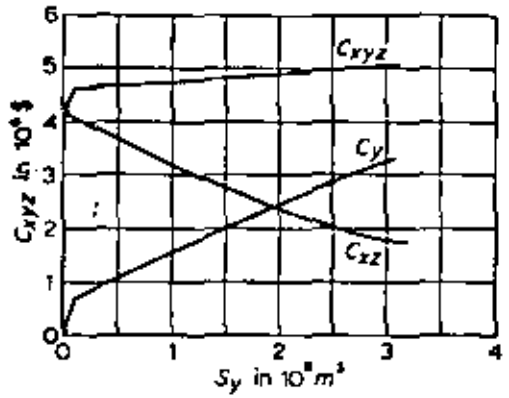

Fig. 6.13 Annual cost of reservoir combination X, Y and Z
$S_{xyz}=6{\cdot}0\times10^8 m^3$
$S_{xz}=6{\cdot}0-S_y$
$C_{xyz}=Cy+Cxz$

if for each total storage level we plot the minimum cost C_{xz} we can obtain $C_{xz}=f(S_{xz})$ as shown in Fig. 6.12. For each level of total storage S_{xz}, we can also plot the least cost combination of S_x and S_z, and the curve of these points for various levels of S_{xz} is shown in Fig. 6.16. With these curves we can then immediately find the least cost combination of storage reservoirs for any given level of total storage.

The simple two project least cost computation method can also be adapted to three projects if we consolidate two of the projects, regard this pair as one project, and then compare it with a third project by the two project method. In this example where we are dealing with storage capacity we could first find the least costly combination of reservoirs X and Z for various levels of storage S_{xz}, and then we could consolidate this pair and regard the resultant cost curve $C_{xz}(S_{xz})$ as belonging to one project XZ. We could then compare project XZ to project Y, and use the two project method to find the least costly combination of reservoirs Y and XZ. The project XZ can then be separated into its two components using Fig. 6.16. A simple calculation for $S_{xyz}=6{\cdot}0\times10^8 m^3$ is shown below:

S_{xz}	S_y	C_{xz}	C_y	C_{xyz}
$3\times10^8 m^3$	$3\times10^8 m^3$	$1{\cdot}8\times10^6$ $	$3{\cdot}3\times10^6$ $	$5{\cdot}1\times10^6$ $
4	2	2·4	2·5	4·9
5	1	3·2	1·6	4·8
6	0	4·1	0·0	4·1

These points are plotted in Fig. 6.13 and it is found that the least costly combination at this storage level is $S_y=0$, $S_{xz}=6{\cdot}0$, and from Fig. 6.16 we can find that for $S_{xz}=6{\cdot}0$, $S_x=2{\cdot}6$, and $S_z=3{\cdot}4\times10^8 m^3$. At this storage level we can conclude that it is uneconomical to develop the project reservoir Y.

The least cost combination can be found in this way for various levels of total storage S_{xyz}, and the resultant least cost storage

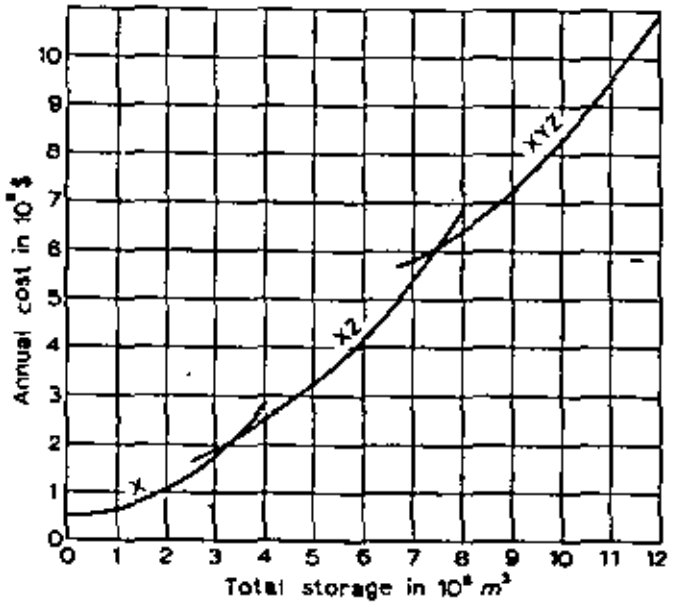

Fig. 6.14 Minimum total cost curves for reservoirs X, Y and Z

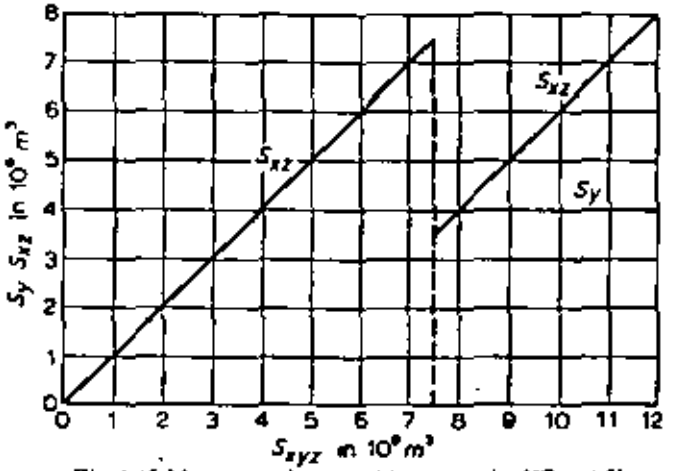

Fig. 6.15 Most economic composition reservoirs XZ and Y

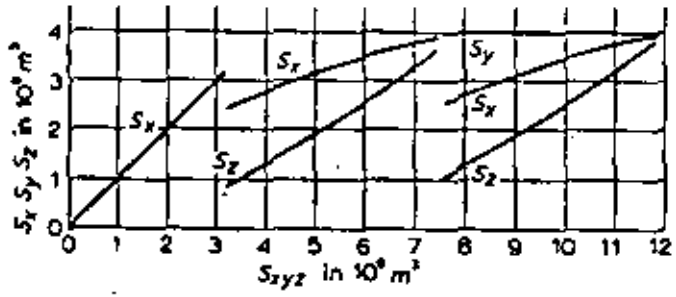

Fig. 6.16 Most economic composition reservoirs X, Y and Z

curve can then be plotted, as shown in Fig. 6.14. For each level of total storage we can again plot the least cost combination of project Y and XZ, as shown in Fig. 6.15, and if we separate XZ we can obtain S_{xz} in terms of S_x, S_y, and S_z as shown in the separation curve in Fig. 6.16.

If more than three projects were involved in this system, we could consolidate the combination XYZ and compare it to a fourth project, and then we could consolidate that optimum combination and compare it to a fifth project by the two project method, etc.

In this way, by consolidating pairs of projects using the two project method, we can reduce the number of units in a system to any lower number, and when there are finally only two units left we can combine these also with the two project method to find the least cost combination. The consolidated units may then be separated using the composition curves to find the least cost combination in terms of all the original projects. This method is simple and effective, but it becomes rather laborious if it must be done by hand when many projects are involved in a system.

A more efficient way of minimising the total cost of a large system of reservoirs would be to use the equalisation of marginal costs technique. The total cost will be at a minimum for a particular combination of projects when the marginal or incremental cost of storage capacity is equal for each project in that combination. The marginal cost in this case is the increment in cost of a project due to an increment in storage capacity, and will be expressed in dollars per acre foot. If this equality did not occur, and if for example the marginal cost of project X in a system was higher than that of project Y, then the total cost of the system could be reduced by decreasing the size of high cost X a few units and increasing that of lower cost Y, until the minimum total cost is achieved at that point where the marginal cost of incremental storage capacity for each project is equal.

If all the possible projects or reservoir sites in a system are not required to meet the total storage requirements, then we may discard some and select only the cheapest sites. In general, we should select those sites with the lowest average costs first for limited developments, and then as the size of the development increases we can add projects of increasingly higher average costs, as well as increasing the capacity of each separate project in the system. Thus the priority of inclusion in the system is usually based on average project costs. This ranking should not be taken for granted however, and it should be checked by investigating all reasonable permutations and combinations, especially where projects may differ greatly in size.

We see therefore, that we must calculate two different costs, the average costs and the marginal costs, when selecting a system or combination of projects with a minimum total cost. We select

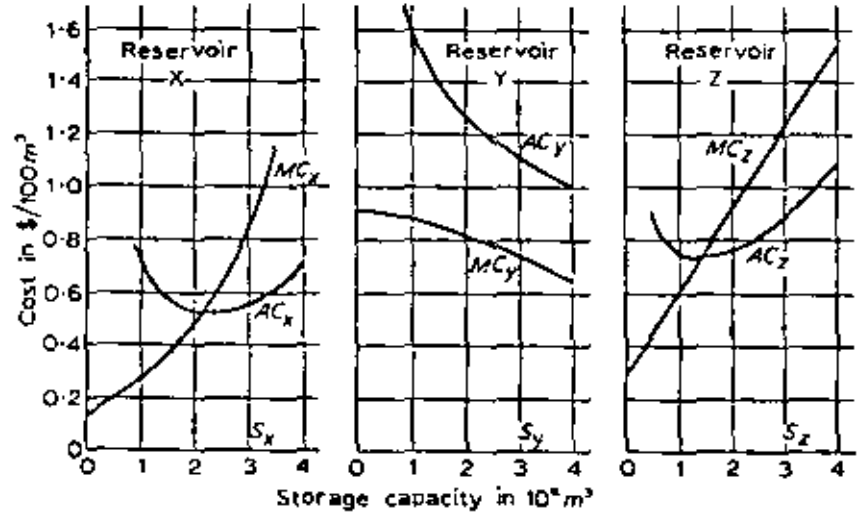

Fig. 6.17 Average and marginal costs of reservoirs X, Y and Z

projects for that system according to their average costs, and once the projects have been selected, we shall adjust them in size according to their marginal costs.

The average and marginal costs of each project have been calculated and these are shown with graphs in Fig. 6.17. For one project:

$$Average\ Cost = \frac{Total\ Cost}{Total\ Storage\ Capacity}$$

or in symbols:

$$AC(S) = \frac{C(S)}{S}$$

and: $$Marginal\ Cost = \frac{Increment\ in\ Total\ Cost}{Increment\ in\ Total\ Storage}$$

or: $$MC = \frac{C(S_2) - C(S_1)}{S_2 - S_1}$$

MC will represent the slope of the cost curve midway between S_1 and S_2.

From Fig. 6.17 we can see that project X has the lowest average costs, project Z the next lowest average costs, and project Y the highest average costs. In choosing a minimum cost combination then, we would choose only project X for a very small development, a combination of projects X and Z for larger developments, and a combination of projects X, Z, and Y for still larger developments.

For small developments with only project X, the total cost is equal to the cost of project X. This storage cost curve is shown in Fig. 6.14. For larger developments using a combination of project X and Z, we must calculate another cost curve. Our intention is to minimise total cost for a given total storage. Rather than fixing storage and finding cost, let us work backwards which is easier, by picking an equal marginal cost for each project, finding each project storage and total cost at this marginal cost, and then adding projects to find total system storage and cost. In mathematical terms, this procedure is:

Pick a combination of projects X, Y, Z.
Pick a marginal cost MC.
Find project storage S_x and cost C_x at this MC.
Repeat for S_y and S_z.
Total Storage $= S_x + S_y + S_z = S_{xyz}$.
Total Cost $= C_x + C_y + C_z = C_{xyz}$.
Plot $(S_{xyz}; S_x, S_y, S_z)$ for total storage S_{xyz}.
Plot (S_{xyz}, C_{xyz}) for system (XYZ).
Increase MC and repeat.

The following table illustrates how this procedure is followed for combination (XZ).

MC \$/100m³	S_x $10^8 m^3$	S_z $10^8 m^3$	S_{xz} $10^8 m^3$	C_x 10^6\$	C_z 10^6\$	C_{xz} 10^6\$
0·5	2·20	0·70	2·90	1·15	0·55	1·70
0·7	2·75	1·30	4·05	1·50	0·95	2·45
1·0	3·30	2·25	5·55	1·95	1·75	3·70
1·2	3·55	2·85	6·40	2·20	2·45	4·65
1·5	4·00	4·00	8·00	2·80	4·00	6·80

These five points are plotted on Fig. 6.14 and a curve is drawn through them. It is found for example that above a total storage of $3·3 \times 10^8 m^3$ combination XZ is less costly than project X alone, and that combination XZY is least costly in the range of $7·5–12 \times 10^8 m^3$. The above table can also be plotted on a graph as in Fig. 6.16, and then the least costly combination of project X and Z can be found for any total value of storage, S_{xz}. From Fig. 6.14 we can then find the best project combination for a particular range of total capacity, and from Fig. 6.16 we can find the exact optimum size of each project in the combination for a particular level of storage. Although only two projects are used in the above illustration, the same techniques would be used for three or more projects. If the storage requirements are $6 \times 10^8 m^3$ for example, the best combination will be projects XZ at a total cost of $\$4·15 \times 10^6$, as shown in Fig. 6.14. From Fig. 6.16, we find that at this total storage level $S_x = 3·4$ and $S_z = 2·6 \times 10^8 m^3$.

This technique of analysis may seem rather elaborate for a system involving only a few projects, and if only two or even three reservoirs are involved, similar results could be obtained by the simple two project method discussed previously. However, when many projects are involved more sophisticated techniques such as the one just used are required, and the great advantage of these is that they will give an exact solution for problems involving a great number of projects.

We will now go on to show how these same techniques that were used to minimise total costs for a fixed level of output can also be used to maximise total benefits for a fixed level of input, or dependable flow, for this simplified water resource system. In order to maximise the benefits of a multi-purpose water resource development, we must first define and evaluate the benefits of each project in this system. The benefit or value of water in a water resource project is a function of several variables. Some of the most important ones are

(a) quantity of water supplied;
(b) quality of water;
(c) reliability of supply;

(d) time of year (seasonal demand);
(e) year in a timespan (growing annual demand).

Other outside factors such as technology and the demand for water derived products such as hydro power and irrigated crops also affect the value of water, but we shall assume that these are fixed and given, or independent for this problem. Of the variables listed above, the quantity of water is usually the most important variable in determining the value of water. The quality of water is also important for such projects as municipal water supply.

The reliability of supply is important in all projects and we must realise that it is impossible to obtain 100% reliability, especially for large projects such as irrigation and water power. The value of a water supply will therefore depend also on its reliability, and this should really be taken into account in evaluating the benefits of a project, although it is often difficult to do so. The value of water also depends upon when it is made available and used. Irrigation for example requires water only during the summer growing season. Other projects, such as municipal and industrial water supplies, may increase in size as the demand increases over time, and therefore the value of such water will depend on time as well as quantity, quality and reliability, etc.

Although this list of variables is by no means complete, it does illustrate the complexity involved in attempting to maximise the benefits of a water resource development. In order to simplify this analysis, we will consider only one of the most important variables in this section, i.e. the quantity of water supplied. The results of such a simplified analysis will not be conclusive. However, the techniques developed may be useful in solving the more complicated real problem through the use of modifications and supplementary analysis.

We will assume then that the value or benefit of a water supply for a certain project is a function only of the quantity of water supplied to that project. The value of water to a project can be defined as the net benefits of this project attributable to its water supply. The value of water will then correspond to the demand for water, where the maximum price which one is willing to pay for a certain quantity of water is equal to the net benefits or value derived from that water.

Let us illustrate this by introducing four competing water development projects downstream of the three reservoir sites discussed previously, as shown in Fig. 6.8. The value of water to each of these four projects is shown in Fig. 6.18. Irrigation project I is a large development in an arid plain some distance from the river, with high initial costs for the construction of a main canal.

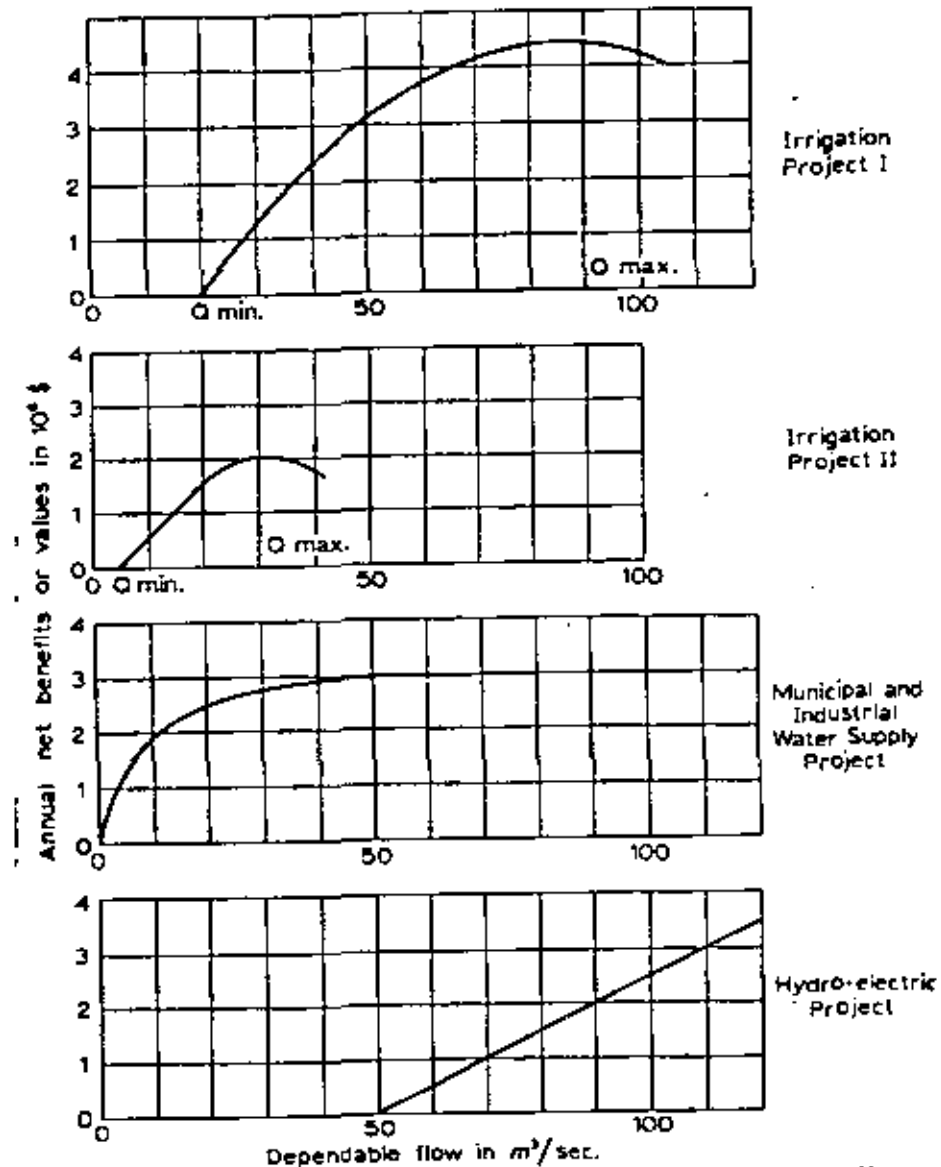

Fig. 6.18 Annual net benefits of water development projects as a function of dependable flow

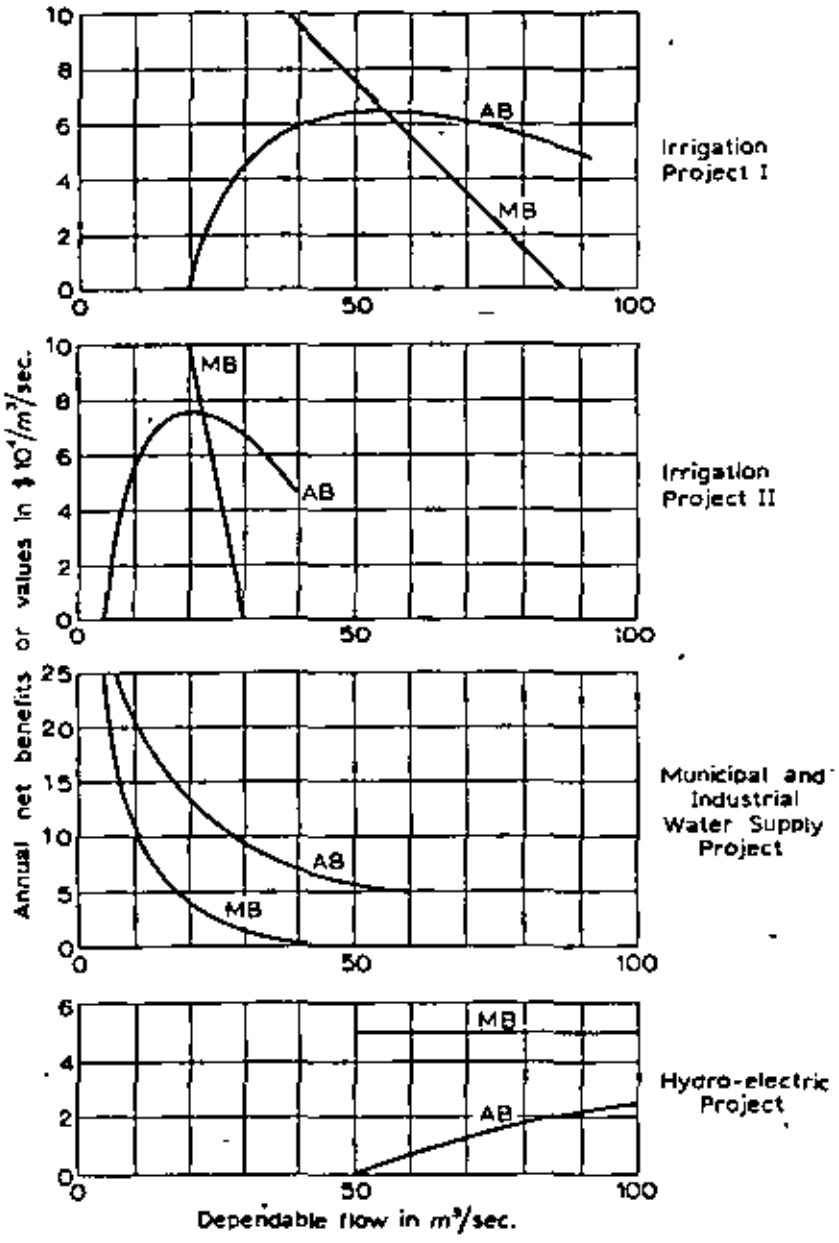

Fig. 6.19 Average and marginal benefits of water development projects as a function of dependable flow

The benefits of irrigation will not cover the high initial costs below a certain level of development, labelled Q_{min}. Beyond that level the net benefits, after all costs of irrigation have been subtracted, are shown on the graph. There is also an upper limit of development, labelled Q_{max}, beyond which further development would be unprofitable because of the limited supply of suitable land for irrigation, and perhaps the limited demand for irrigated crops.

Another irrigation project, No. 2, is also shown in Fig. 6.18. This project is located in the valley and has low initial development costs. However, the amount of irrigable land is limited to the valley, and the project is much smaller than No. 1. A municipal and industrial water supply value curve is also shown. This project has very high net benefits or value even at low levels of development. As the quantity of water supply increases, net benefits also increase, but they level off after a point and further increases in supply do not cause a significant increase in net benefits. The fourth project is a hydro power development. This project also requires a certain minimum flow to cover the high initial costs of the construction of the dam. Beyond this minimum flow, the net benefits will increase lineally with the quantity of flow available. In all four cases, we will assume that the projects are so arranged that water used by one project cannot be re-used by another project.

The objective now is to maximise the total net benefits of these four projects for a fixed level of total water supply. This can be done with the same two project method that was used previously to minimise costs for a fixed level of output, except that in this

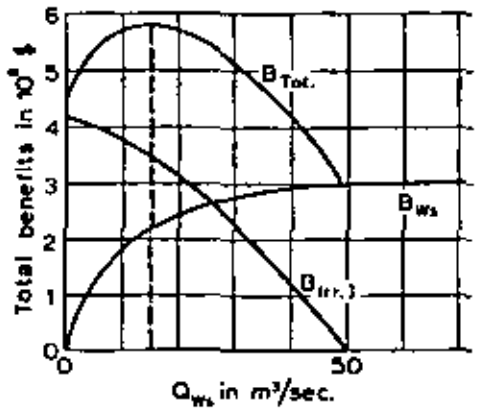

Fig. 6.20 Total annual benefits of Irrigation Project 1 and Water Supply Project
$Q_{IRR1} + Q_{WS} = 70 m^3/s$
$B_{TOT} = B_{IRR1} + B_{WS}$

case we will maximise benefits for a fixed level of total flow. To illustrate this procedure, let us compare the irrigation project 1 with the municipal and industrial water supply. The table below shows a sample calculation for a total fixed flow of 70 m^3/s.

Irrigation 1		*Water supply*		*Total*
Flow in m^3/s	*Benefit in $10^6$$*	*Flow in m^3/s*	*Benefit in $10^6$$*	*Benefits in $10^6$$*
0	–	70	3·05	3·05
10	–	60	3·00	3·00
20	0	50	2·95	2·95
30	1·30	40	2·90	4·20
40	2·35	30	2·80	5·15
50	3·15	20	2·55	5·70
60	3·80	10	1·95	5·75
70	4·20	0	0	4·20

This joint benefit function is plotted in Fig. 6.20. It can be seen that maximum total benefits for this combination occur at $Q_{wat.\,supp.} = 15\ m^3/s$, $Q_{irr} = 55\ m^3/s$. These calculations can be made for various levels of flow, as was done when total costs were minimised previously, and at each level of flow the optimum combination of two projects with maximum total net benefits can be found. When more projects are introduced, pairs can be consolidated and compared to third, and then to fourth projects, and the techniques are exactly the same as those used previously.

This problem can be solved more easily however by using the

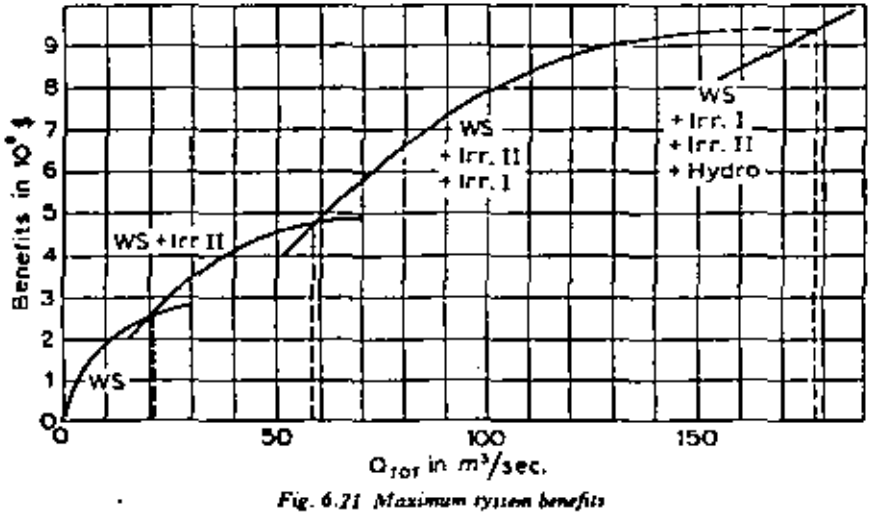

Fig. 6.21 Maximum system benefits

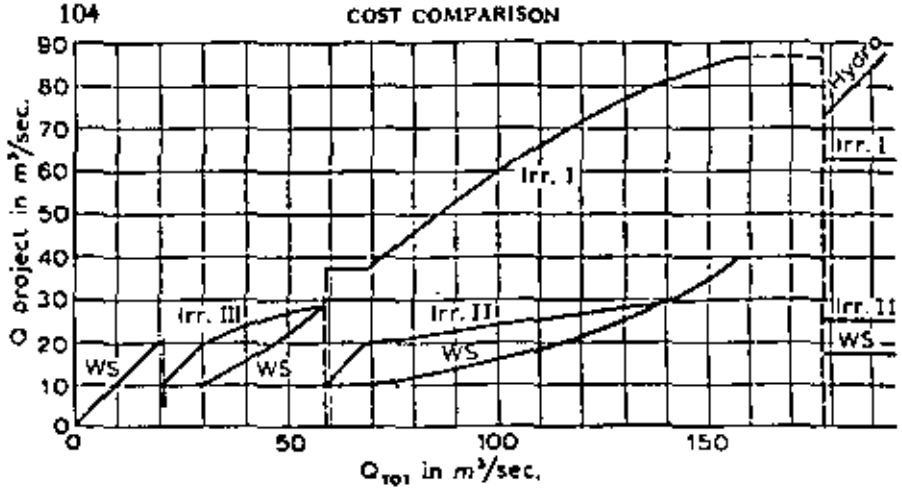

Fig. 6.22 Most economic system comparison

equalisation of marginal benefits technique. With this method, marginal net benefits of water for each project are set equal for an optimum combination. We must therefore calculate the marginal benefits of each project for each level of development, and these are shown in addition to the average benefits in Fig. 6.19. We can now choose combinations of projects on the basis of the highest average benefits. For low levels of development the municipal and industrial water supply project alone will provide the greatest net benefits. For larger levels of development, a combination of the water supply project and irrigation project 2 would be best; for still higher levels a combination of water supply, irrigation 2, and irrigation 1; and for still higher levels a combination of all projects including hydro would have the largest net benefits. Once the marginal net benefits of each project are known we can combine projects of equal marginal benefits to obtain the system with maximum total net benefits. The procedure is the same as that which was used previously for minimising total costs, as shown below:

1. For a given combination of projects, pick a certain marginal benefit MB_a.
2. Find Q_t at MB_a, or $Q_t(MB)$ for each project.
3. Find B_t at each Q_t, or $B_t(MB)$.
4. Add Q_t's to find total system input:
$$Q_T(MB) = \quad Q_t(MB)$$
5. Add B_t's to find total system output:
$$B_T(Q_T) = \quad B_t(Q_t)$$
6. Plot (B_T, Q_T) and $(Q_T, Q_t \ldots)$ for each MB, and repeat with decreased MB.

7. Repeat procedure for each different system or combination of projects.

These calculations are shown in the following table and the results are plotted out in Figs. 6.21 and 6.22.

Combination WS+IRR 2

MB 10^6\$/cms	Q_{ws} m³/s	$Q_{IRR\,2}$ m³/s	Q_{tot} m³/s	B_{ws} 10^6\$	$B_{IRR\,2}$ 10^6\$	B_{tot} 10^6\$
10	10	5	15	2·0	0	2·0
or 10	10	20	30	2·0	1·5	3·5
8	12	22	34	2·1	1·7	3·8
6	15	24	39	2·3	1·8	4·1
4	19	26	45	2·5	1·9	4·4
2	25	28	53	2·7	2·0	4·7
0	50	30	80	3·0	2·0	5·0

Combination WS+IRR 2+IRR 1

MB 10^6\$/cms	Q_{ws} m³/s	$Q_{IRR\,2}$ m³/s	$Q_{IRR\,1}$ m³/s	Q_T m³/s	B_{ws} 10^6\$	$B_{IRR\,2}$ 10^6\$	$B_{IRR\,1}$ 10^6\$	B_T 10^6\$
10	10	5	38	53	2·0	0	2·2	4·2
or 10	10	20	38	68	2·0	1·5	2·2	5·7
8	12	22	48	82	2·1	1·7	3·0	6·8
6	15	24	58	97	2·3	1·8	3·7	7·8
4	19	26	68	113	2·5	1·9	4·1	8·5
2	25	28	78	131	2·7	2·0	4·4	9·1
0	40	30	87	157	2·9	2·0	4·5	9·4

Combination WS+IRR 2+IRR 1+HYDRO

MB 10^6\$/cms	Q_{ws} m³/s	$Q_{IRR\,2}$ m³/s	$Q_{IRR\,1}$ m³/s	Q_H m³/s	Q_T m³/s	B_{ws} 10^6\$	$B_{IRR\,1}$ 10^6\$	$B_{IRR\,2}$ 10^6\$	B_H 10^6\$	B_T 10^6\$
5	17	25	63	50	155	2·4	1·8	4·0	0	8·2

or $Q_T = 105 + Q_H$

$B_T = 8·2 + (Q_H - 50)/20$

Combination WS—see Fig. 6.18.

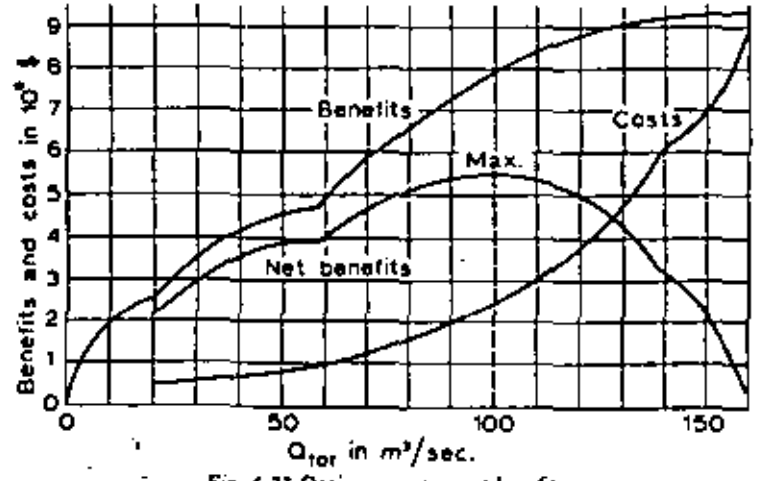

Fig. 6.23 Optimum system net benefits

It can be seen from Fig. 6.21 that the transition for maximum net benefits between combination *WS* and *WS+IRR 2* occurs at 21 m³/s; the transition to *WS+IRR 2+IRR 1* is at 58·5 m³/s; and hydro is only profitable when Q_T is greater than 178 m³/s. At each total level of flow, the optimum components are indicated in Fig. 6.22. It can be seen that wherever the marginal benefits of a project are constant, the development of that project is linear, and when hydro is finally introduced, all other projects remain at a fixed level while only hydro expands with increasing Q_T.

We can now compare the total benefits of this system at each level of flow with the costs of providing this flow, and then find the level of flow which will yield the maximum net benefits. This has been done in Fig. 6.23. The cost of providing a certain dependable flow is obtained by using the dependable flow-storage curve, shown in Fig. 6.10, with the storage-cost curve in Fig. 6.14. It can be seen that the optimum system design is at 100 m³/s. At this point we will have the following components:

Total Dependable Flow = 100 m³/s
Total Required Storage (Fig. 6.10) = 4×10^8 m³

	Storage 10^8 m³	*Cost* 10^6\$
Total Costs: (Figs. 6.16 and 6.9)		
Reservoir X	2·7	1·45
Reservoir Y	—	—
Reservoir Z	1·3	0·95
Total	4·0	2·40
	Flow m³/s	*Value* 10^6\$
Total benefits: (Figs. 6.22 and 6.18)		
Irrigation 1	60	3·75
Irrigation 2	24	1·8
Water supply	16	2·35
Hydro	—	—
	100	7·9
Net System Benefits		5·5

This is the optimum design for this simplified system of reservoirs and water development projects, and no other design will yield higher net benefits.

The conclusions of this analysis depend, of course, on the assumptions which were made, and many of these are open to criticism. In a real study it is unlikely that all projects would be independent of each other, as they were in this case, or that each project would consume all the water used so that it could not be used again downstream. The benefit cost analysis of a project should also be done on the basis of present values rather than

annual benefits and costs which were used in this case, because in reality the benefits of a project are seldom constant over time.

However, the purpose of this example is to illustrate the basic techniques of analysis which can be used when the problem is reduced to one of its most important variables: the quantity of water available. Other variables such as time and reliability are also important, and these may be introduced with modifications to the basic analysis. Other inputs in addition to water may also enter the system, and then more general optimality conditions may be used.

Some of these are:

1. $MC_i/MB_j = MP_{ij}$
2. $MC_i/MC_h = MRS_{hi}$
3. $MB_j/MB_k = MRT_{kj}$

Where: MC_i = marginal cost of one unit of input i.

MB_j = marginal benefit of one unit of output j.

MP_{ij} = marginal productivity, or increase in output of j due to one unit increase of input i.

MRS_{hi} = marginal rate of substitution between inputs i and h, such that output remains the same.

MRT_{kj} = marginal rate of transformation between outputs k and j, or number of additional units of output k which can be produced by a one unit decrease in output j.

These marginal relationships will lead to a local optimum, but total benefits and costs must still be used to compare all the local optimums and obtain a global or overall optimum. Although these optimality conditions may appear bewildering at first sight, a closer examination will reveal that they are simply mathematical expressions of common sense when all inputs and outputs have a well defined price, and a simple conventional analysis will often achieve the same result.

TECNICA SUECA DE VOLADURAS

por Rune Gustafsson

163

Editado por
SPi. Nora. Suecia

Impreso en Suecia por
Nora Boktrycken AB
Nora 1.977

Colaborador en la traducción: Benito Bravo

CONTENIDO

1. PROLOGO

La primera edición de este libro fué publicada en idioma sueco en el año 1.972. Posteriormente fué traducido al inglés y se publicó en 1.973 con el título "Swedish Blasting Technique". La edición inglesa ha sido distribuida prácticamente a todos los países del mundo. No obstante, y debido a la demanda solicitada por los países de habla hispana, se publica ahora en castellano en una edición prácticamente igual a la última editada en Suecia en 1.976.

El contenido de este libro ha sido adaptado para su utilización como libro de texto en escuelas y en cursos organizados para ingenieros y técnicos en voladuras. Mi intención ha sido más bien la de simplificar relaciones y procedimientos de cálculo, en lugar de presentar la técnica de voladura de rocas en forma de una ciencia teórica complicada. No obstante, las bases empíricas descritas para los cálculos pueden resultar igualmente útiles a aquellos que estén interesados en los aspectos teóricos.

Estoy muy agradecido por los consejos y ayudas recibidos de mis colegas de Nitro Consult y del Departamento de Servicio e Investigación de Nitro Nobel AB. Particularmente doy las gracias a Conny Sïöberg, de Nitro Consult, a Mats Johansson, Bernt Larsson, Birger Roos, Bertil Davidson, Björn Engsbraten, de Nitro Nobel y también a P. A. Persson, Nils Lundberg y Aigot Persson, Swedish Detonic Research Foundation. La Sección relativa al NONEL" GT ha sido escrita por Gösta Liltner, ingeniero con gran experiencia en este sistema nuevo y simplificado de encendido no-eléctrico. La Sección que lleva por título "La Seguridad en los Trabajos de voladura" ha sido escrita por Gösta Silfverbrand, del Departamento Sueco de Seguridad e Higiene.

En lo relativo a la traducción al castellano, hay que agradecer especialmente la asistencia recibida por parte de HISPANO-SUECA DE INGENIERIA S.A., de Madrid, empresa altamente especializada en todo tipo de trabajos de excavación en roca, tanto como contratistas como asesores. Su experiencia sobre voladuras, así como su grado de especialización han sido de gran utilidad en el conjunto de opiniones manifestadas sobre el tema.

Dentro de HISPANO SUECA DE INGENIERIA S.A. agradezco a su Director Técnico, A. Iglesias, el apoyo prestado, así como a A. Abuja y J. Martín del Departamento Técnico.

Ha sido muy aleccionador el comprobar la utilidad práctica del libro como manual al ser empleado por técnicos dentro de los campos de las obras públicas, industria y minería.

Durante mis trabajos como asesor en voladuras he intercambiado puntos de vista muy interesantes con técnicos procedentes de las empresas constructoras, propietarias y consultoras. Es para mí un honor el trabajar en este campo donde se manifiesta un enorme interés por todos los que en él estamos en relación con la técnica de voladuras y en el cual existen continuos avances hacia nuevos e interesantes problemas.

Espero sinceramente que esta edición española proporcionará a sus lectores una visión de la técnica sueca de voladuras de la cual, me atrevo a decir, que ha ganado por sí misma una excelente reputación en los trabajos de voladuras llevados a cabo por todo el mundo.

Nora, Suecia, Enero 1.977
Rune Gustafsson

2. INTRODUCCION

2.1 DESARROLLO DE LA TECNICA DE VOLADURAS

El empleo de explosivos para voladuras en roca empezó a ponerse en práctica a comienzos del siglo XVII. En Alemania se introdujo la pólvora en minería, donde se había venido utilizando el método de rotura por contracción. Este procedimiento consistía en un calentamiento y subsiguiente riego de agua, produciendo tensiones en la roca con la aparición de fisuras en su estructura; con mazos, punterolas y cuñas se conseguía después su rotura. Este sistema estuvo empleándose en las minas suecas hasta casi finales del siglo XIX. La mina de plata de Nasa fueron el primer lugar en Suecia donde se utilizó la pólvora después de haber sido introducida por Ingenieros de Minas alemanes en 1.632.

Cuando Alfred Nobel en 1.864 comenzó la fabricación de un aceite explosivo basado en la Nitroglicerina líquida, el producto ganó rápidamente un campo de aplicación sumamente extenso, conquistando el mercado mundial con una velocidad que en aquella época era desacostumbrada. Este nuevo aceite explosivo empezó a elaborarse pronto en fábricas de todo el mundo. Un recuerdo de aquella época es el hecho de que el nombre de "Nobel" se encuentra en las marcas comerciales de muchos fabricantes de explosivos, sin que las empresas en la actualidad tengan intereses comunes.

Después de algunos años, Nobel vió que era más conveniente absorber la Nitroglicerina en algún material, con lo que podría realizarse el encartuchado del explosivo. El aceite tenía el inconveniente de que podía penetrar en las fallas y fisuras de la roca, lo que entrañaba riesgos en los trabajos posteriores. El aceite explosivo era incluso sensible al impacto y se solidificaba rápidamente a bajas temperaturas. Los primeros cartuchos de Nitroglicerina explosiva se prepararon dejando que la Nitroglicerina fuera absorbida por kieselgulr (también conocida como diatomeas, un residuo silíceo, con aplicación en materiales aislantes, refractarios, etc.). Este primer tipo de explosivo en cartuchos fué seguido por explosivos plásticos, en los que el kieselgulr se sustituyó por Nitrocelulosa. Este fué el material conocido como dinamita, en el cual ciertas proporciones de Nitroglicerina fueron gradualmente reemplazadas por Nitrato Amónico y otras sustancias explosivas.

Durante el período 1.872—80 se realizaron los trabajos de excavación de los legendarios túneles a través de los Alpes utilizando la dinamita inventada por Alfred Nobel. Los tipos usados en diferentes países han cambiado con los años, y hoy día están formados normalmente por un gran porcentaje de nitrato amónico o substancias similares, además de nitroglicerina.

En Estados Unidos el empleo de mezcla de explosivos del tipo ANFO (nitrato amónico/fuel-oil) y tipo hidrogeles (slurries), han conquistado una gran parte del mercado a partir de finales de los años 50. Hasta ahora se observa una evolución diferente en Europa, donde lo más generalizado son los explosivos en cartuchos, basándose por lo general en nitroglicerina y nitrato amónico.

La evolución de los sistemas de perforación ha influído en gran manera sobre el desarrollo de los explosivos y con ello en la técnica de voladuras. En Estados Unidos se han venido empleando, especialmente en las voladuras a cielo abierto, diámetros cada vez mayores. Estos grandes diámetros han proporcionado una premisa técnico-económica para favorecer el uso de explosivos de mezcla más baratos.

Posiblemente sea demasiado pronto para apreciar con claridad la evolución de los explosivos en Europa, pero probablemente las condiciones para el empleo de hidrogeles sean menores. En el caso de grandes proyectos de voladura quizás pueda estimarse que los explosivos del tipo hidrogel lleguen a tener en el futuro una aplicación más generalizada que en la actualidad.

Los "Slurries" tienen muchas ventajas en los países donde existen grandes depósitos minerales y la minería tiene un fuerte impulso. Durante los años 70 en los Estados Unidos y Canadá este sistema se desarrolló con el nombre de "explosivos tipo hidrogel, capaces de ser iniciados con detonador normal". El desarrollo de los hidrogeles con sus diferentes características de grado de sensibilidad, velocidad de detonación, etc., les proporciona buenas posibilidades de utilización, en relación con los explosivos a base de nitroglicerina.

En Suecia se ha comenzado con el uso de los hidrogeles en trabajos subterráneos, pero es demasiado pronto para estimar sus posibilidades de desarrollo, ya que, ni las características de la roca, ni las propiedades de los actuales explosivos a base de nitroglicerina pueden ser comparados entre los Estados Unidos y Escandinavia.

El desarrollo en Suecia de los sistemas de carga con cartuchos fabricados a base de nitroglicerina, ha proporcionado a este tipo de explosivo un mayor campo de aplicación que en los Estados Unidos, donde normalmente los cartuchos tienen una mayor rigidez. Una amplia gama de cargas alargadas y de tipo especial ha sido adaptada para cubrir la variada demanda del mercado en Suecia.

Esto quiere decir que el adaptar el explosivo, tipo hidrogel, al mercado sueco exigiría unas condiciones de desarrollo de las unidades y equipos de carga. Con este explosivo habría que conseguir una elevada potencia por unidad de peso a causa de la dureza de la roca y también unas buenas cara-

terísticas de detonación en diferentes condiciones. No obstante, existe un gran campo de aplicación de los mismos.

El desarrollo de los métodos de iniciación ha sido, en lo que se refiere a la técnica de voladuras, de al menos, igual importancia que el mismo explosivo. El sensacional invento de Alfred Nobel — el detonador — ha sido ensombrecido de alguna manera por la atención prestada a los aceites explosivos, como un nuevo elemento técnico. Desde que a mediados del siglo XIX Bickford descubrió en Inglaterra la mecha de seguridad, los métodos eléctricos de encendido conquistaron el mercado de Escandinavia durante las tres últimas décadas y lo mismo ha sucedido en cierta manera en otros países europeos. El incremento del márgen de seguridad respecto a igniciones prematuras ha supuesto una importante contribución al éxito de los sistemas eléctricos. La utilización de sistemas de ignición no eléctricos ha sido tradicionalmente muy elevada en los Estados Unidos y Canadá. Por ésto será interesante seguir los trabajos de investigación que sobre este sistema se han desarrollado recientemente en Suecia. En los países donde se utiliza a gran escala este sistema de ignición no eléctrico, los técnicos en voladuras opinan que existe una gran posibilidad de que éste llegue a ser el tercero en importancia con la mecha de seguridad y los sistemas eléctricos de encendido.

Solamente en estos últimos años, desde el tiempo que vienen utilizándose los explosivos, han surgido métodos competitivos para la rotura de rocas. Hoy día en la construcción de túneles se emplean máquinas que perforan todo el a sección completa. Se han obtenido resultados satisfactorios en rocas de constitución blanda, mientras que en rocas duras el procedimiento resulta mas caro que mediante el uso de explosivos. Durante la última década el desarrollo de la técnica de voladuras en túneles ha sido muy rápido y sobre todo, las voladuras con precaución en zonas edificadas, ha hecho que este método sea muy competitivo. Mediante voladuras controladas con explosivos especiales e instrumentos para la medida del efecto de las mismas ha mejorado considerablemente la aplicación de las nuevas técnicas. Las voladuras controladas han hecho posible realizar excavaciones en zonas edificadas sin daños en su entorno. El avance de la técnica de voladuras con un conocimiento mejor de los efectos de los explosivos y una mejor calidad de los productos, permite obtener grandes voladuras de roca con un costo cada vez menor. En una época en que los problemas ecológicos y del medio ambiente son de ámbito internacional, la adaptación de la técnica de voladuras con un menor factor de alteración de dichos medios es muy importante. En este aspecto merece especial atención la posibilidad de realizar instalaciones mediante voladuras en roca, teniendo como objetivo la mejora del medio ambiente, existiendo en la actualidad una tendencia a emplearlas en excavaciones subterráneas, si bien nos encontramos en los comienzos de esta nueva técnica.

Desde un punto de vista internacional, la técnica de voladuras de rocas para trabajos mineros o de edificación está alcanzando cada vez mayor importancia. En el caso de países en los cuales actualmente están en fase de trabajos intensivos de edificación, el tema de las voladuras incide en los trabajos en un gran porcentaje, existiendo por tanto una gran demanda con alto nivel de preparación en voladuras. Tal sucede con las arterias de comunicación, plantas industriales, minería, etc. donde realmente se muestra el valor constructivo de dicha técnica.

2.2 TABLA DE UNIDADES Y FACTORES DE CONVERSION

		Factor de conversión
Longitud		
Milímetro (mm)	1 m = 100 cm	1 pulgada = 25,4 mm
Centímetro (cm)	1 m = 1000 mm	1 yarda = 0,9144 m
Metro (m)		1 pié = 0,3048 m
Kilómetro (km)	1 km = 1000 m	1 km = 0,6214 millas terrestres
		(1 milla terrestre = 1,609 km)
Peso		
Gramo (g)		1 onza = 28,35 gramos
Kilogramo (kg)	1 kg = 1000 g	1 libra = 0,4534 kg
Tonelada métrica (t)	1 t = 1000 kg	(1 kg = 2,205 libras)
		1 tonelada corta = 0,9072 t
		1 tonelada larga = 1,016 t
		1 t = 1,102 ton corta / 0,9842 ton larga
Velocidad		
Milímetros por segundo (mm/seg)		1 pié/seg = 0,3048 m/seg
Metros por segundo (m/seg)		1 m/seg = 3,281 pié/seg
Presión		
Kilopondio por centímetro cuadrado (kp/cm²)		1 p.s.i. (libra/pulgada²) = 0,07301 kg/cm²
(Conocido por Kilogramo fuerza por centímetro cuadrado = kg/cm²)		1 kg/cm² = 14,22 p.s.i.
Volumen		
Metro cúbico (m³)		1 yarda cúbica = 0,7646 m³
		1 pié cúbico = 0,02832 m³
		1 m³ = 1,308 yarda³ = 35,31 pié³
Peso por unidad de volumen		
Kilogramo por metro cúbico (kg/m³)		1 libra/yarda³ = 0,593 kg/m³
		(1 kg/m³ = 1,685 libra/yarda³)
Area		
Centímetro cuadrado (cm²)		1 pulgada² = 6,452 cm²
Metro cuadrado (m²) = 10.000 cm²		1 pié² = 929 cm²
		1 yarda² = 0,836 m²
		(1 m² = 1,196 yarda²)

2.3 NOMENCLATURA

Esta sección es un resúmen de los conceptos normalmente usados en los trabajos de voladuras.

Aceleración	Unidad de medida de vibración en g. (1g = 9,81 m/seg².).
Altura del hastial	Distancia del piso del túnel al punto de arranque de la bóveda.
Amplitud	Unidad de medida de vibración (Altura del sismograma).
Arranque de niveles por socavación ascendente	Sistema minero de explotación y relleno con escombro
Atacador	Herramienta utilizada para compactar los cartuchos, normalmente de madera o plástico.
Avance	Longitud de túnel realizada por unidad de tiempo.
Avance por voladura	Longitud de túnel realizada por voladura.
Banco	Macizo rocoso que presenta al menos dos caras descubiertas.
Barra, Barrena	Pieza de acero roscada en los extremos o con punta cortante.
Barrenos de contorno	Taladros en el contorno final o próximos a él.
Barreno decapitado, descabezado	Sección de roca abierta por un tiro fallido y su incidencia en el taladro.
Barreno de destroza	Taladro con *piedra* libre (usualmente en interior).
Barreno de exterior	Taladro vertical o inclinado realizado desde la superficie.
Barreno perdido, fallido	Fallo total o parcial de una carga despues de la voladura.
Barreno, taladro	Una unidad en el esquema de perforación.
Boca, tallante	Parte de la barrena que dispone de elementos de corte.
Bloque	Fracción de roca de gran tamaño, procedente de una voladura.
Borde del banco	La linea frontal superior de un banco.
Caja, área, pecho	Método de edificación
Carga con separadores	Normalmente empleada en la carga de columna y consistente en la introducción de tacos de madera o separadores entre cartuchos o fracciones de los mismos para conseguir menor concentración por metro.
Carga de columna	Explosivo situado en la zona de columna de un barreno y por encima de la carga de fondo.

Neutralización de detonadores

Los detonadores dañados se neutralizarán destruyéndolos, introduciéndolos en un costado de un cartucho, que se deja sobre el suelo en un lugar libre de piedras. El encendido se hace por medio de un detonador no dañado y con mecha de al menos 0,6 m de longitud. La zona de peligro ha de ser vigilada cuidadosamente.

Los detonadores eléctricos u ordinarios con aberturas obturadas pueden ser destruidos introduciéndolos en una carga en un barreno. Los detonadores abiertos no pueden ser destruidos de esta forma, pues habría riesgo de explosión. Está prohibido intentar neutralizar los detonadores arrojándolos al agua.

Neutralización de explosivos, pólvora de mina, y mecha detonante

No se quemará el explosivo dañado o sobrante en cantidades superiores a 5 kg de cada vez. Se opera sobre un lecho de virutas de madera o un material similar empapado en parafina (keroseno). El encendido se realiza contra el viento y con ayuda de una mecha de al menos 1 metro, naturalmente sin detonador conectado en su extremo. La combustión sólo puede hacerse sobre un suelo libre de piedras, por ejemplo un suelo arcilloso, un pantano, o sobre el hielo de un lago. La zona de peligro ha de ser guardada cuidadosamente, pues pueden producirse explosiones; en tal caso, el explosivo que haya sido dispersado por los alrededores se recogerá y cuidará.

Los explosivos de tipo pulverulento o plástico, en pequeñas cantidades y con un contenido máximo de nitroglicerina del 40 % pueden ser sumergidos en grandes cursos de agua o en lagos profundos. Los cartuchos han de sacarse de sus paquetes, y las cargas largas entubadas han de ser cortadas en porciones.

La pólvora de mina es inactivada sumergiéndola en grandes cursos de agua o en lagos profundos.

La mecha detonante deteriorada puede ser quemada del mismo modo que un explosivo.

La destrucción de explosivos o de materiales de encendido en las formas que se han citado más arriba sólo puede ser llevada a cabo por el Jefe de voladuras o su delegado. Si se trata de grandes cantidades de explosivos a destruir, la operación debe ser realizada por un experto.

Saneo y refuerzo de la roca

Con el fin de evitar daños personales y materiales por desprendimientos de roca, son necesarias ciertas medidas de saneo y refuerzo de la misma. La necesidad de tales medidas viene determinada por la magnitud de las presiones y de la resistencia de la roca, las cuales dependen a su vez de las condiciones geológicas imperantes. Las presiones en la roca dependen también del tipo de terreno, la profundidad, la forma y dimensiones de sus cavidades, su emplazamiento relativo y su extensión con relación a la superficie. La resistencia de la roca posee también influencia sobre el modo de realizar la voladura.

Geología

La resistencia de la roca puede variar considerablemente y viene determinada especialmente por las posibles venas de pizarra y esquisto, así como por la estratificación, y además por la composición mineralógica y el tamaño de los granos. La roca que contenga pizarra, esquistos o esté estratificada, resiste cargas menores en sentido paralelo a la estratificación, que en sentido perpendicular. La resistencia depende asimismo de los componentes minerales; los minerales blandos, como talco, clorita y mica, hacen disminuir esta resistencia. Una roca de grano fino suele ser más resistente que otra de la misma composición mineral y grano grueso.

Las masas rocosas contienen generalmente irregularidades que en muchas ocasiones afectan a su resistencia; estas irregularidades van asociadas al sistema de grietas originado en el curso del enfriamiento inicial de la roca, así como al material alterado en la masa por efecto de las fallas. Las voladuras provocan también agrietamientos. Las corrientes intensas de agua pueden arrastrar material fuera de las grietas, y reducir con ello la resistencia de la roca.

La erosión química y mecánica es también importante. Debe prestarse un cuidado especial al hecho de que la superficie de roca está con frecuencia muy erosionada y agrietada.

Saneo

Las observaciones geológicas proporcionan una base para estimar los riesgos de desprendimientos locales. Las fisura, y las filtraciones intensas de agua, deben ser tomadas en consideración.

Uno puede apreciar las características de la estructura de la roca, así como las posibles zonas de debilidad, a través del polvo de perforación, el ruido, y la velocidad de penetración de la perforadora.

El supervisor de los trabajos debe fijar con claridad los nombres de las personas que llevarán a cabo y serán responsables del saneo de la roca. Esta operación se realiza con barras de acero macizas o — para disminuir el peso — tubulares, que deben mantenerse bien aguzadas. Golpeando la roca puede averiguarse si es compacta o está fisurada; para esta operación es preferible emplear una barra maciza.

En lugares en los que el techo y las paredes no sean accesibles desde el suelo, el saneo habrá de realizarse desde plataformas, que a menudo son móviles.

En las operaciones de saneo deben observarse las siguientes normas, basadas en la experiencia:

Comenzar los trabajos de saneo desde un lugar seguro.

Utilizar una barra aguzada de longitud adecuada.

Usar casco y botas protectoras.

Operar desde una superficie firme y asegurarse de que el cuerpo está bien equilibrado.

Hacer palanca con la barra hacia arriba.

No operar si hay alguien lo bastante cerca para estar en peligro.

Prestar atención a las grietas, diaclasas, y vetas.

Prestar atención a los restos de barrenos (que pueden contener explosivo).

En las Instrucciones mineras y en la Instrucciones de Voladuras se incluyen normas sobre los trabajos de saneo.

Refuerzo de la roca

Cuando en el seno de la roca se abre, mediante voladuras una cámara subterránea, la distribución de tensiones en la roca se modifica; las tensiones ejercidas inicialmente sobre la roca volada han de ser transferidas a la roca de alrededor de la cavidad que acaba de crearse. La roca trata de relajar sus tensiones en la zona inmediata a la cavidad expandiéndose hacia el interior de la misma.

La redistribución de tensiones puede originar movimientos de la roca, el aflojamiento de ciertas partes en dirección a las superficies libres, así como el ensanchamiento de las grietas preexistentes y la formación de otras nuevas. La distribución de presiones se modifica nuevamente, y en el curso de la estabilización hasta la nueva posición de equilibrio, la zona de perturbaciones se expande gradualmente durante un periodo de tiempo que varía con las características de la roca, etc. Esto pone de manifiesto que los trabajos de refuerzo de la roca han de efectuarse en una fase la más temprana posible, y que estos refuerzos deben tomar la forma de sustentaciones directamente asociadas a la roca.

Los elementos para refuerzo de la roca toman las forma de estructuras de madera, acero o hormigón, que se aseguran por medio de elementos de anclaje. Pueden también emplearse combinaciones de los diversos métodos. Frecuentemente es difícil decidir el método a adoptar, pues esta elección depende no sólo de las características de la roca y del aspecto económico, sino también del tiempo disponible, la durabilidad estimada, los equipos mecánicos utilizables, etc. En los últimos años, la inyección y proyección de hormigón se han convertido en un método de refuerzo de la roca de aplicación normal.

REGISTRO DE LITERATURA

"The Modern Technique of Rock Blasting" by U. Langefors and B. Kihlström.
"Handbok I Bergsprängningsteknik" by Sten Brännfors.
"Detonics of High Explosives" by C. H. Johansson and P. A. Persson.
"Tryckluftshandboken". Atlas Copco.
The Swedish Board of Occupational Safety and Health: "Anvisningar angående skydd mot yrkesfara vid sprängningsarbete nr 3" (Blasting Instructions, No. 3).
The Swedish Board of Occupational Safety and Health: Instructions concerning protective measures underground "Gruva, Stenbrott och Bergbygge".
"Berghållfasthetens beroende av sprängningen" by U. Langefors.
"Fullskaleförsök med gleshålssprängning" by P. A. Persson.
"Blaster's Handbook", fifteenth edition, Du Pont.
"Neuzeitliche Sprengtechnik" by Bierman.
"Theory and Practice of Blasting" by Dr. Kumao Hino.
"Le Mine nei lavori minerari e civili" by Tullio Seguti.
"Rivningsalternativ — gamla byggnader kan sprängas bort" by R. Gustafsson and L. G. Bergling.
"Försiktig sprängning av rörgravar" by R. Gustafsson, B. Larsson, M. Johansson and L. G. Bergling.
"Sprängning av betongcistern med vattentryck" by R. Gustafsson and C. Sjöberg.
"Luftstötsvågors skadeverkan vid sprängning" by Nils Lundborg.
"Ljudtrycksvågors utbredning vid detonation av laddningar på marken och dess störande inverkan på människor och bebyggelse" by Aget Persson and Lars-Åke Almgren.
"Explosive Excavation Technology" by Stanley M. Johnsson.
Army and engineer nuclear crating group. Livermoore, California, June 1971.

Carga de fondo	Explosivo concentrado en el fondo de un barreno.
Carga específica	Kilos de explosivo por m³ de roca volada.
Cargas conformadas	Explosivo colocado sobre los bloques destinados a su taqueo (Vulgarmente "Planchas").
"Cerdo"	Expresión inglesa, en argot, para denominar el aire comprimido utilizado en una pala cargadora en interior.
Chimeneas	Labor de excavación vertical o con un ángulo inferior a 45° con la vertical.
Collarín, culata	Parte de la barrena donde se aloja la perforadora.
Comienzo	Inicio de una labor, perforación, etc.
Corte	Frente abierto de un banco.
Cuele noruego	Tipo de cuele en túnel con ángulo de taladros en dos direcciones.
Cuele en abanico	Tipo de cuele con disposición de los barrenos en cuñas sucesivamente mayores.
Cuele, corte	Sección abierta en la roca en una voladura.
Cuele en cuña o en V	Tipo de cuele con disposición de los barrenos en forma de V.
Cuele paralelo	Tipo de cuele en túnel con los barrenos paralelos.
Cuele quemado	Tipo de cuele paralelo.
Cuele quemado "Cathole"	Tipo especial de cuele paralelo (vulgarmente en inglés)
Datos de voladuras	Notas tomadas con detalle despues de realizar una voladura.
Desescombro	Término canadiense de la extracción de los productos de las voladuras. (El término sudafricano es "Lashing").
Detonador de medio segundo, retardo	Cápsula detonante con retardo de 0,5 seg.
Detonador de milisegundo, Micro-retardo	Cápsula detonante con retardo de 100 ms (1 ms = 0,001 seg).
Explosores	Aparatos usados para iniciar detonadores eléctricos.
Explosivo sensible a un detonador	Tipo de explosivo capaz de ser iniciado con un detonador normal.
Emboquille	Alineación del equipo de perforación antes del comienzo de un taladro.
Ejecución de chimeneas	Sistema utilizado para realizar chimeneas.
Error de perforación	Desviación del taladro respecto al esquema teórico.
Espaciamiento (E)	Distancia entre barrenos de una misma hilera.
Esponjamiento	Aumento del volúmen de la roca despues de volada en comparación con su volúmen "in situ".

Falla, error, falta	Alteración geológica de la roca.
Fallo de encendido	Fallo total o parcial de una voladura.
Flecha	Altura de la bóveda en el eje del túnel.
Fondo del barreno	Parte inferior del barreno.
Fragmentación	Tamaños de la roca volada.
Frecuencia	Unidad de medida de la vibración (períodos/segundo).
Frente, Cabeza	Superficie libre de una excavación.
Frente de avance	Cara libre cuando se perfora un frente.
Galería de avance	Galería realizada con sección reducida, previa a la ejecución de un túnel.
Galería en corona	Normalmente ejecutada en cámaras o túneles a lo largo de su bóveda.
Gran diámetro	Taladros con diámetro mayor de 40 mm.
Galería entibada con madera	Labor en túnel o galería, con sostenimiento de madera.
Galería perforada	Expresión minera en inglés para indicar frecuentemente un túnel o labor subterránea.
Hidrogel	Explosivo a base de substancias gelificantes y agua, con componentes en suspensión.
Hidrogel (slurries)	Papilla explosiva, normalmente conteniendo TNT (trinitrotolueno).
Inclinación del taladro	Angulo entre la dirección del barreno y la línea vertical.
Inyección	Relleno de fisuras en roca con cemento u otros materiales.
Inyección de cemento y hormigón	Forma de refuerzo en roca.
Limpieza de banco	Realizar el desescombro del banco despues de la voladura o limpiar su superficie de tierra y piedras.
Limpieza de montera	
Desmonte	Retirar el material suelto depositado sobre la roca.
Línea de pega	Cables usados para conectar la pega al explosor.
"Línea sastre"	Fila de tiros paralelos realizada con barrenos muy próximos, 10—30 cm.
Marca de rotura	Indicio de grietas que aparece normalmente en la dirección longitudinal de una hilera de barrenos en cantera.
Margen para emboquille	Sobrancho necesario en los barrenos de contorno para poder realizar la perforación de la siguiente pega, en los túneles.

Minero	Personal especializado en trabajos de minería.
Plan de tiro	Esquema indicando perforación, carga y secuencia de encendido, así como las medidas a aplicar durante la voladura.
Pega, voladura	Etapa en la ejecución de una voladura.
Pendiente, inclinación	Relación entre la longitud y la diferencia de cotas en un terreno.
Perforación específica	Metros de perforación por m³ de roca.
Perforación con recubrimiento (voladura)	Método especial generalmente usado en voladuras submarinas.
Perforación a sección completa	Avance de un túnel con máquinas integrales sin explosivos.
Perforadora, martillo	Máquina de perforación.
Perno, bulón	Anclaje para refuerzo de la roca normalmente con longitud mayor de 1 m.
Perno cementado	Anclaje de refuerzo de la roca con acero y mezcla de arena-cemento-agua.
Piedra, Línea de menor resistencia, carne, peso	Distancia del barreno a la cara libre, medida perpendicularmente a éste (V).
Piso del banco	Superficie inferior de un banco.
Pérdida de corriente	Fuga de corriente en un detonador, debida a daños en el mismo o en sus cables.
Piso, suelo	Superficie inferior en un túnel, cámara o banco.
Pico, tocón	Saliente de roca por encima del fondo teórico.
Polvo de perforación	Pequeñas partículas de roca procedentes de la ejecución de un barreno.
Precorte	Barrenos de contorno volados antes del resto de la voladura, con características especiales y que producen una grieta o corte en el terreno.
Proyección	Lanzamiento de piedras en una voladura.
Recorte, voladura suave	Pega de barrenos de contorno, especialmente dispuestos de forma que se consigue una mejor terminación de la superficie con menor aparición de grietas.
Retacado	Zona sin cargar en un barreno y normalmente rellena de tierra, polvo, etc.
Roca suelta	Roca desprendida a causa de grietas o fallas.
Saneo	Desprender trozos de roca suelta normalmente después de una voladura.
Sobreexcavación	Rotura de la roca en la zona superior de los barrenos en una voladura.
Sobreperforación	Perforación realizada por debajo del nivel teórico.

Subniveles con perforación ascendente	Sistema de explotación minera con voladuras en bancos que disponen, al menos, de una superficie libre.
Sucio, Residuo, escombro, barro, lodo	Escombro que permanece en el frente después de realizar el desescombro.
Suspendida	Roca colgada por encima del nivel vertical.
Taqueo, voladura secundaria	Romper bloques procedentes de una pega con explosivo.
Tiro de corona, emboquillador	Tiro de destroza próximo al techo de un túnel o primera barrena de una serie (vulgarmente en inglés).
Túnel de acceso	Túnel que comunica la superficie con una cámara u otro túnel.
Velocidad de detonación	Referido al explosivo en m/seg.
Velocidad de propagación	Espacio recorrido por unidad de tiempo por la onda de choque en un medio determinado.
Velocidad de la vibración	Unidad de medida de la vibración (mm/seg).
Vibración del suelo	Efecto de la transmisión de la onda de choque a través del terreno.
Voladura en banco	Efectuar voladuras en un banco.
Voladura con barrenos espaciados	Taladros especialmente dispuestos principalmente en voladuras en banco.
Voladura en cámara	Antiguo método de voladura con ensanchamiento sucesivo del barreno. (Vulgarmente "Rehova").
Voladuras con micro-retardo	Empleo en excavaciones de detonadores de milisegundo.
Voladura con precaución	Voladura especialmente realizada, debido a su proximidad a edificaciones.
Voladura de precaución	Voladura especialmente realizada, teniendo en cuenta la roca circundante.
Zapatera	Barreno inferior horizontal o casi horizontal.

3. EXPLOSIVOS

3.1 PROPIEDADES DE LOS EXPLOSIVOS

Para conseguir que un explosivo sea eficiente se exigen determinadas condiciones, ya que es imprescindible que detone completamente bajo circunstancias difíciles, como son: introducido en un taladro, sumergido en agua, etc. y todas las substancias necesarias para este proceso deben estar incluidas dentro del mismo explosivo, por ejemplo, no puede tomar el oxígeno del aire, como lo hace la gasolina para su combustión.

Cuando un explosivo detona en un taladro, el proceso resultante desarrolla una gran cantidad de energía por unidad de tiempo, siendo por kilógramo aproximadamente 1/10 de lo contenido en 1 kg. de gasolina, pero con un período de reacción mucho menor y por lo tanto, la energía desarrollada por unidad de tiempo a traves del explosivo resulta mucho más elevada.

Ejemplo: Un coche circulando a 100 km/hora consume 10 l. = aproximadamente a 10 kg. de gasolina a la hora. A un explosivo en forma de carga concentrada en un taladro de 100 mm. de diámetro, le corresponde una concentración de 10 kg/m.
La velocidad de detonación del explosivo es del orden de 5 km/seg.
Esto significa que 10 kg detonan en $\frac{1}{5.000} = 0{,}0002$ seg.

El caudal de energía (relativa) por unidad de tiempo

Gasolina	*Explosivo*
$10 \times 10 = 100$	$\frac{1 \times 10 \times 60 \times 60}{0{,}0002} = 180.000.000$

En las paredes del taladro se desarrolla una presión del orden de 100.000 atmósferas (kg/cm²) y la temperatura durante el proceso de detonación es de miles de grados centígrados.

Las características más importantes de un explosivo pueden ser subdivididas en cuatro importantes grupos:

Efecto explosivo
Seguridad en el manejo
Sensibilidad a la iniciación y estabilidad en la detonación
Almacenaje

Efecto explosivo

Se entiende por efecto explosivo la capacidad del mismo para desarrollar un trabajo en determinadas condiciones. Es muy difícil encontrar un concepto único que en este sentido cubra todas las características de los diferentes explosivos. Una forma de comparar éstos, es mediante la potencia del mismo por unidad de peso en lo concerniente a su poder; indicando más adelante cómo calcular la potencia por unidad de peso.

Los factores más importantes que tienen influencia en el efecto explosivo podrían ser:

Características de los gases producidos durante la explosión
Temperatura
Volúmen
Presión
Velocidad de detonación del explosivo

Se pueden realizar medidas comparativas del efecto de un explosivo, mediante el ensayo del bloque de plomo, haciendo detonar una pequeña cantidad en un cilindro de este material.

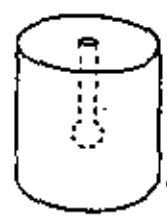

Fig. 3.1.1

La capacidad del hueco producido, expresado en centímetros cúbicos, nos da una indicación del efecto explosivo.

Otros métodos de medida, incluyendo el mortero balístico, se han usado más ampliamente en los últimos años que el del bloque de plomo.

También durante los últimos años se han realizado ensayos para determinar el poder de diferentes explosivos con cargas sumergidas que, al detonar, se encuentran suspendidas libremente en el agua y se registra el volúmen y presión del gas liberado.

El factor de energía de un explosivo puede ser calculado y se mide usualmente en *Tn.m/Kg*. Los fabricantes normalmente indican la potencia explosiva de sus productos, comparada con la goma pura (explosivo gelatinoso), viniendo expresada su potencia por unidad de peso o de volúmen.

Según Langefors, la potencia por unidad de peso se calcula por la relación 5/6 e + 1/6 v, en donde

e = factor energía — Factor de energía $= \frac{A}{500}$

v = factor volúmen — Factor de volúmen $= \frac{V}{850}$

siendo V = volúmen del gas a 0° C y 1 atmósfera.

A = Factor de trabajo — Factor de trabajo $= \frac{425 \times Qv}{1000}$

Qv = Calor de explosión en K cal/Kg.

Estos cálculos están basados en el hecho de que es conocida la composición química del explosivo considerado. Qv se determina mediante el cálculo del calor de explosión resultante de las substancias combinadas.

Debe tenerse presente que el efecto de un explosivo depende de las características de la roca, así como del esquema de voladura utilizado y el grado de retacado de los barrenos, siendo por tanto la mejor forma de comparar los efectos de los diferentes explosivos, hacer ensayos con voladuras reales.

Una alta velocidad de detenación en un explosivo es de vital importancia cuando se utiliza como carga rompedora, tanto en taqueos como en demoliciones, ya que es necesario producir grandes tensiones.

El efecto de la velocidad de detonación en el caso de voladuras normales en roca es motivo de discusión, dado que la experiencia parece demostrar que una alta velocidad es una ventaja cuando se produce en tipos de roca en las cuales la onda de choque tiene un alto poder de propagación, mientras que en rocas blandas y fisuradas los explosivos que liberan mayor cantidad de gases, actúan mejor, a pesar de tener menor velocidad de detonación.

El balance de oxígeno es otro factor importante que debe ser incluido en la composición básica de las substancias integrantes, puesto que, un defecto de oxígeno produce monóxido de carbono y un exceso del mismo da origen a óxidos de nitrogeno. En orden a evitar que estos gases se formen en grandes cantidades, es necesario usar explosivos equilibrados en oxigeno con una buena mezcla, buen encartuchado y una correcta iniciación.

Dada la importancia que tiene la formación de humos en las labores subterráneas, existe actualmente una gran demanda de explosivos de alta calidad con bajo contenido de gases tóxicos.

El volúmen de los gases puede ser calculado a partir de las substancias que componen el explosivo.

En la práctica se ha comprobado que los problemas de ventilación varían, según el tipo de explosivo utilizado, por ejemplo, un explosivo que produzca un gran volúmen de gases, puede formar un tapón tan denso en el frente de

trabajo que haga difícil la evacuación y dilución de los mismos; por tanto con cada explosivo debería proporcionarse un factor o índice que facilitara su elección para un cálculo correcto de la ventilación, sobre todo en voladuras subterráneas.

La experiencia demuestra que el comparar distintos tipos de explosivos basados en resultados de ensayos directos, debe ser realizado con sumo cuidado, ya que existen diferentes puntos de vista, por lo que insistimos en que la estimación más correcta es la obtenida mediante ensayos con voladuras reales. Esto es válido en la estimación del efecto de voladura, tanto en lo concerniente a la potencia como a la composición de los gases.

Seguridad en el manejo

Una característica esencial que debe poseer todo explosivo es que pueda ser transportado y utilizado de forma segura, sin riesgos para las personas encargadas de su manejo.

Antes de ser aprobados por las autoridades suecas competentes, los explosivos son sometidos a múltiples pruebas, siendo una de las principales el ensayo al choque o al impacto, consistente en dejar caer un peso sobre el explosivo desde una cierta altura, determinando así su sensibilidad al impacto.

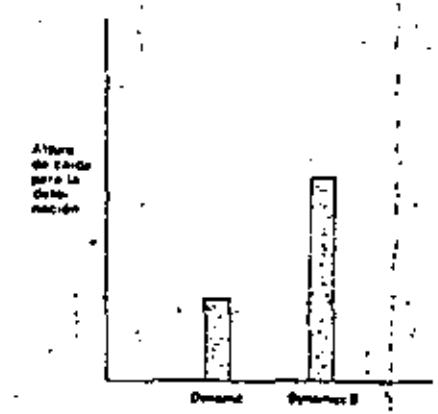

Fig. 3.1.3 Ensayo de impacto

Los explosivos están sujetos así mismo a otros ensayos, como son los de fricción y penetración.

La Fig. 3.1.3 muestra la diferencia entre la "Dynamit" convencional y "Dynamex B", al ser disparado un proyectil sobre el explosivo.

Como resúmen puede decirse que los explosivos están sujetos a ensayos que

corresponden a posibles cambios ambientales y tensiones como las que pueden presentarse en la práctica.

Los ensayos necesarios en este sentido han sido realizados en los bancos de pruebas del Detonic Research Laboratory en Vinterviken.

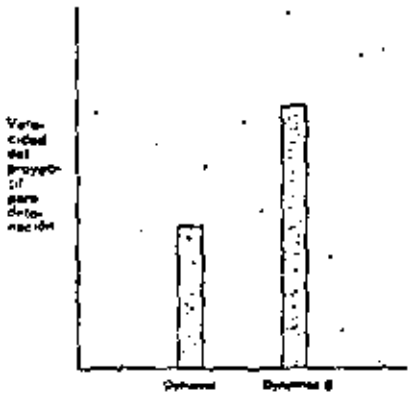

Fig. 3.1.3 Ensayo con disparo

Sensibilidad a la iniciación y estabilidad en la detonación

Los explosivos deben ser fácilmente iniciados y ser estables desde el punto de vista de la detonación. Normalmente un explosivo es iniciado con un detonador, pero ciertos tipos son tan inertes que requieren un poder mayor de iniciación. Los explosivos, tipo ANFO (nagolita) se inician usando como cebo Dynamex (goma) o un detonador potente, y también es frecuente utilizar cordón detonante de carga reforzada a lo largo del barreno. Los explosivos, tipo Hidrogeles (slurries) son iniciados por medio de un multiplicador para su cebado, consistente en un explosivo de alta velocidad de detonación. Conviene indicar que el resultado de una voladura depende en gran manera de una correcta iniciación.

La estabilidad en la detonación implica el que, una vez iniciada ésta, no se detenga por ninguna causa hasta que la carga total haya detonado, siendo este requisito difícil de satisfacer, dada la alta velocidad y la presión a la que se produce, aunque los trabajos de investigación han producido grandes resultados dentro de esta rama especial de la técnica de los explosivos.

Almacenaje

En muchos casos un explosivo se almacena durante largo tiempo, siendo importante que no esté sujeto a cambios que puedan menguar su capacidad de trabajo.

Los explosivos *plásticos*, llamados Dynamex (gomas), etc. pueden sufrir un proceso de envejecimiento, debido a la desaparición total o parcial de las burbujas de aire incorporadas en el explosivo durante su fabricación, implicando éste una mengua de sus características de propagación, aunque el efecto explosivo permanezca inalterado.

Los explosivos plásticos no deben estar sujetos durante su almacenaje a altas temperaturas, dado que pueden ablandarse y la formación de sales en la substancia explosiva puede penetrar a través de la envoltura de los cartuchos, deformándose y dificultando su utilización.

Los explosivos *pulverulentos* encartuchados son frecuentemente más sensibles a la humedad durante su almacenaje. En el caso de una atmósfera húmeda o temperaturas extremadamente elevadas, se pueden formar sales sobre los cartuchos endureciéndolos, no existiendo en este caso fenómeno de envejecimiento.

Los explosivos de *mezcla* pueden en ciertos casos segregarse, por lo cual cambian completamente sus características, si bien los explosivos manufacturados actualmente están fabricados de tal forma que ésto no suceda.

Es importante que los polvorines o almacenes de explosivo se mantengan limpios y secos, procurando utilizar en primer lugar los explosivos más antiguos, de tal forma que el tiempo de almacenaje se mantenga.

Las cuatro características más importantes de los explosivos, descritas anteriormente, pueden ser ampliadas con las siguientes:

	Alta	*Baja*
Aptitud a la propagación	Ventaja: Menor riesgo de interrupción de la voladura.	Ventaja: Menor riesgo de autoencendido, por ejemplo, en voladuras submarinas; menor riesgo de vibración del terreno.
Densidad	Ventaja: Alta concentración de carga por metro lineal.	Ventaja: Buena distribución de la carga, cuando sea necesario.
Resistencia al agua	Ventaja: La carga puede realizarse bajo el agua.	Ventaja: Se destruye rápidamente por el agua.

4. ENCENDIDO

4.1 METODOS DE ENCENDIDO

Un factor decisivo en el desarrollo de la técnica de voladuras ha sido la elección de un sistema racional y seguro, que produzca la detonación de un explosivo — proceso de iniciación —.

El empleo de la mecha de seguridad, desarrollada por Bickford en Inglaterra en 1.840, contribuyó en gran manera a mejorar dicho factor.

El descubrimiento del detonador por Alfred Nobel fué ensombrecido en parte por su éxito en la fabricación de un explosivo casi perfecto. El detonador de micro-retardo ha permitido controlar importantes factores, como son: fragmentación, proyección y vibraciones del terreno al realizar grandes voladuras.

Es interesante hacer notar que en Escandinavia la iniciación eléctrica se utiliza con mayor frecuencia que en muchos otros países, por ejemplo, en voladuras submarinas se ha considerado desde un principio que la utilización de un sistema eléctrico de encendido es el método más adecuado, debido a sus posibilidades de control, mientras que los países anglosajones utilizan cordón detonante con frecuencia, no consiguiendo por nuestra parte el mismo grado de confianza este método de iniciación. No obstante, el cordón detonante ha sido siempre, en ciertos trabajos, un excelente suplemento de los metodos eléctricos.

Ultimamente con el desarrollo del sistema NONEL se preven grandes posibilidades de utilización del tipo de encendido no eléctrico.

Los métodos de encendido pueden clasificarse en cuatro importantes grupos:

Iniciación con mecha
Iniciación eléctrica
Cordón detonante
Sistema NONEL (ver pag. 54)

La iniciación con mecha se utiliza normalmente para hacer detonar una sola carga, pero anteriormente ha sido ampliamente utilizada en trabajos subterráneos. Es obvio que en grandes voladuras este sistema es inadecuado.

Las siguientes cifras indican el desarrollo de los métodos de iniciación en Suecia, deducidas de la cantidad de detonadores utilizados:

Año	Iniciación eléctrica %	Iniciación con mecha %
1.944	5	95
1.954	23	77
1.970	83	17
1.974	89	9

La mecha de seguridad está formada principalmente por un núcleo de pólvora negra, rodeada por varias capas de hilados, estando bien aislada de la humedad y otros agentes externos por medio de diferentes envueltas de material aislante.

La mecha de seguridad debe poseer un tiempo de combustión bien controlado. En Suecia la tolerancia admitida es del 5 %, con un tiempo de combustión de 2 minutos por metro. Si durante el almacenaje la mecha es dañada por la humedad o por otro agente, puede variar su tiempo de combustión.

Debe evitarse que la mecha entre en contacto con aceite, petróleo (keroseno) y gasolina, ya que el material aislante puede disolverse y producir daños en el núcleo de pólvora negra.

La unión de la mecha a su detonador debe ser realizada con gran cuidado.

Un detonador ordinario está formado por una cápsula de aluminio que contiene materiales explosivos (ver fig. 4.1.1).

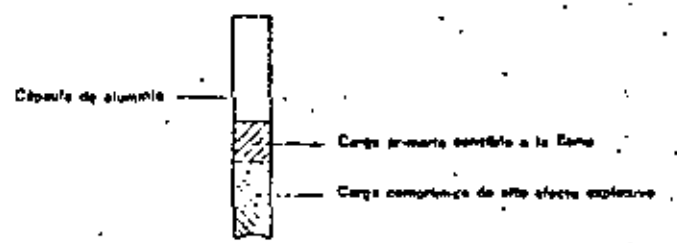

Fig. 4.1.1

La carga superior del detonador es muy sensible a la humedad y por esta razón la unión a la mecha debe realizarse de forma que no penetre agua ni humedad en el detonador, utilizando tenazas especiales. Si se trata de un gran número de detonadores, es preferible realizar el trabajo con una máquina especial de engarzar.

Reglas prácticas para realizar la unión mecha-detonador:

- Realizar un corte recto y limpio en la mecha
- Limpiar cualquier residuo de polvo existente en el detonador
- Introducir la mecha hasta el fondo del detonador — debe quedar en contacto con la carga —
- Realizar la unión muy cuidadosamente — apretar varias veces con las tenazas —
- En caso de barrenos con agua, aislar la unión entre el detonador y la mecha con grasa o, como otra alternativa, presionar con los dedos la mecha para empujar el compuesto aislante hacia la junta.

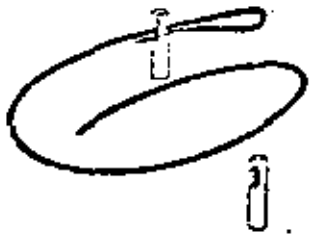

Fig. 4.1.2

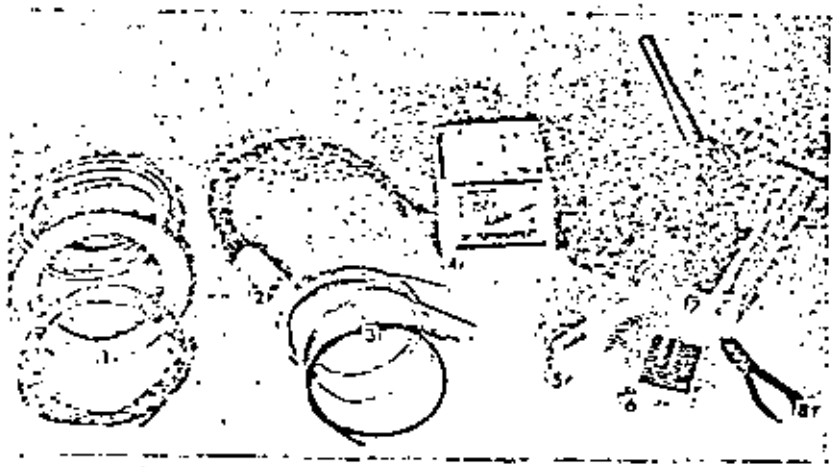

Fig. 4.1.3: 1. Mecha de seguridad. 2. Conectador múltiple. 3. Mechas unidas al detonador. 4. Encendedor especial de mecha. 5. 10 detonadores. 6. 50 detonadores. 7. Máquina de engarzar. 8. Tenazas.

La mecha de seguridad puede ser iniciada con una cerilla o utilizando encendedores especiales de mecha. Desde el punto de vista de seguridad, debe utilizarse una mecha de aviso que sea de una longitud de 0,60 m. más corta que la mecha menor existente en la voladura.

El encendido de un gran número de mechas desde un mismo punto puede realizarse utilizando cordón de ignición con conectadores; un conectador se acopla al final de la mecha, la cual queda unida al cordón de ignición que puede ser encendido con una cerilla. Se pueden iniciar varias mechas al mismo tiempo usando un conectador múltiple, que consiste en un manguito de cartón con la carga de ignición colocada en el fondo.

Iniciación eléctrica

La enorme ventaja de la iniciación eléctrica es que cada detonador por separado y la pega completa pueden ser comprobados antes de realizar la voladura.

Al contrario de lo que sucede con la iniciación con mecha, el momento de la detonación está siempre bajo control.

Un detonador eléctrico instantáneo actúa tan pronto como reciba la corriente eléctrica de encendido. Salvo los componentes eléctricos, un detonador de este tipo está diseñado en principio de la misma forma que un detonador ordinario.

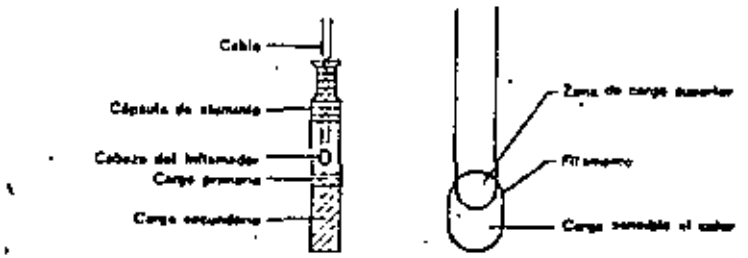

Fig. 4.1.4

Los detonadores micro-retardo disponen de un elemento retardador que les permite detonar con diferentes intervalos de tiempo entre los distintos números.

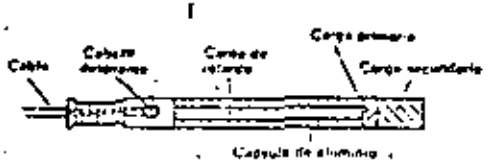

Fig. 4.1.5

En Suecia para clasificar un detonador como de microretardo, es necesario que tenga un tiempo de retardo entre distintos números menor de 100 milisegundos (ms).

Un detonador de retardo tiene 500 ms, de tiempo de intervalo entre dos números consecutivos. Este tipo de detonador se utiliza en voladuras en túneles, donde, debido a la constricción de los barrenos, puede ser ventajoso un mayor intervalo desde el punto de vista técnico.

La posición de los números de los diferentes detonadores en una pega (esquema de encendido), es muy importante. A continuación se indican algunos ejemplos.

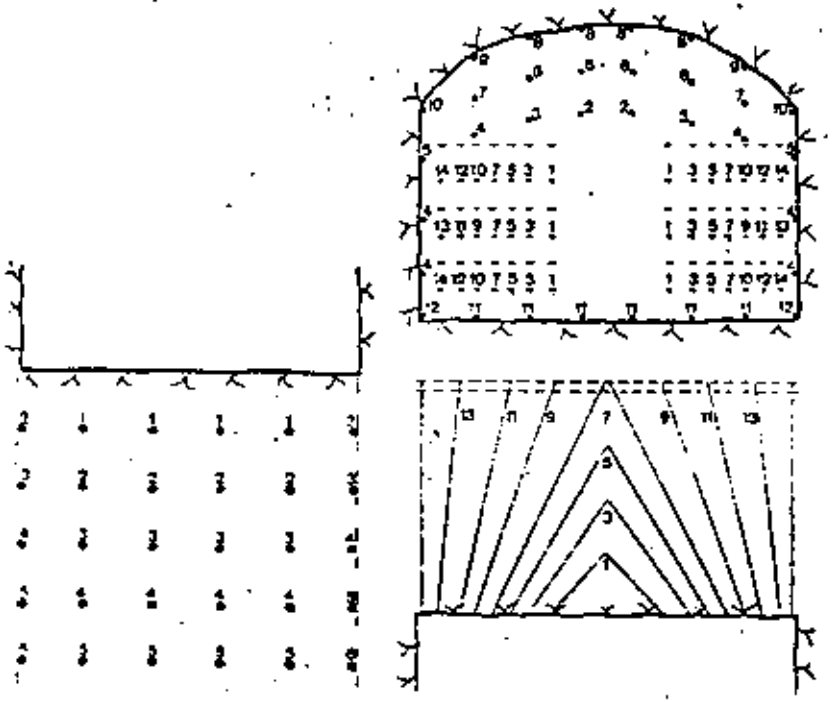

Esquema de encendido en voladura en banco

Esquema de encendido en voladura en túnel

Fig. 4.1.6

4.2 ENCENDIDO — SISTEMAS DE COMPROBACION

Los detonadores eléctricos que se usan en Suecia son los siguientes:

Denominación	Grupo	Tipo	Color de los cables	Retardo no.	Tiempo de retardo ms	Longitudes normales m
Instantáneos	I	TE	Amarillo-blanco	—	—	1, 2, 3, 4 y 6
„	II	VA	Gris-blanco	—	—	2, 4 y 6
Micro-retardo	I	TE	Amarillo-verde	0—18	30	2, 4 y 6
„	II	VA	Gris-verde	1—20 [1]	25 [2]	2, 4 y 6
„	II	VA	Gris-verde	24—80 [3]	100	2, 4 y 6
Medio segundo	I	TE	Amarillo-rojo	1—12	500	4 y 6
„	II	VA	Gris-rojo	1—12	500	4 y 6

[1]) Se dispone de medios números entre 1 y 10, 1 ½, 2 ½, etc.
[2]) Tiempo de retardo con medios números = 13 ms.
[3]) Esta amplia serie está asociada directamente con la serie normal de microretardo. Los números de retardo son 24, 28, 32, etc. hasta el número 80.

La serie VA dispone de dos tipos de detonadores especiales conocidos como VA-G, los cuales poseen un gran aislamiento en los terminales, debido a que están introducidos en un manguito protector de polietileno.

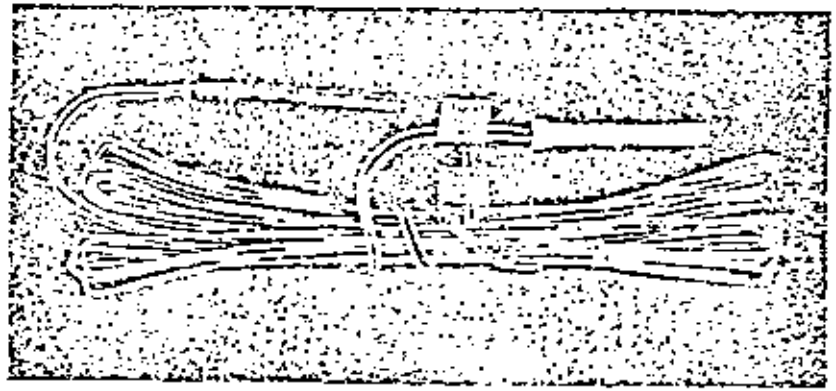

Fig. 4.2.1 Detonador VA con manguito protector

El detonador tipo VA-OD está diseñado para voladuras submarinas en las que normalmente los detonadores están sujetos a situaciones muy especiales. Además de un fuerte aislamiento, estos detonadores poseen un doble manguito de protección.

En otoño de 1.972 se normalizó la protección aislante de los terminales de los detonadores. El tipo VA dispone de un manguito de conexión que, no sólo realiza el papel de aislante, sino que trabaja como un elemento de unión. Este manguito es de gran utilidad para prevenir los contactos fortuitos de los terminales, por ejemplo, durante el momento de la conexión. Así mismo, el riesgo de ignición prematura durante el transporte puede considerarse mínimo.

Los detonadores del tipo VA pueden ser suministrados con longitudes de cable de 10, 12, 20, 27 y 35 m. Es importante que estas longitudes sean las adecuadas en función de la profundidad del taladro.

Para iniciar un explosivo tipo Prillit o ANFO se utilizan multiplicadores, consistentes en HEXOTOL, muy adecuados para ser utilizados como cebo.

Comprobación del sistema de encendido

En Suecia la comprobación de detonadores, en series o individualmente, solo puede ser realizada mediante la utilización de instrumentos adecuados que hayan sido aprobados por la Dirección General de Seguridad e Higiene del Trabajo.

Estos aparatos de comprobación están diseñados de tal forma que no existe riesgo de ignición prematura durante su utilización.

El comprobador de circuito es un sencillo aparato que solamente indica si el circuito está intacto o si existe una rotura, teniendo gran utilidad en la comprobación de cargas individuales, por ejemplo, durante las operaciones de tacqueo.

La corriente se suministra por medio de una pequeña pila de mercurio que permite realizar alrededor de diez mil medidas.

Cuando la resistencia del circuito es superior a 140 ohms, la medida obtenida no ofrece total garantía.

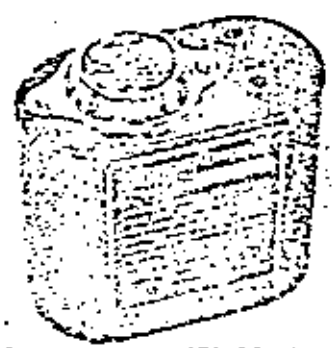

Fig. 4.2.2 Comprobador de circuito

El *Ohmímetro* es un instrumento muy completo que, no solamente comprueba el circuito, sino que proporciona información sobre la resistencia de los detonadores y del sistema de encendido. La medición de la resistencia se efectúa normalmente en cada operación de voladura en la que se utilicen más de dos detonadores.

Análogamente al comprobador de circuito, el Ohmímetro envía una pequeña corriente de medida a través de los cables, siendo esta corriente varios cientos de veces menor que la necesaria para iniciar un detonador individualmente.

Fig. 4.2.3 Ohmímetro

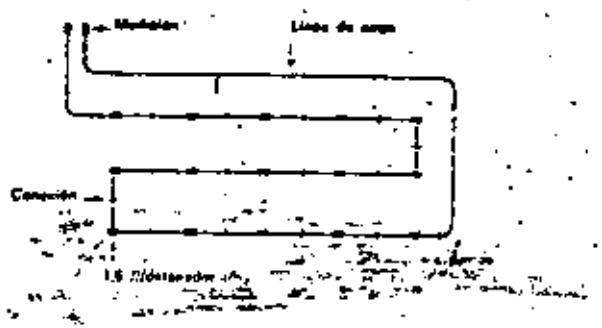

Resistencia por detonador: 1,6 Ω (ohmios)
Número de detonadores: 15
Resistencia en serie: 15 × 1,6 = 24 Ω

En el caso de grandes pegas, los detonadores deben ser conectados formando varias series paralelas, con el fin de reducir la resistencia.

Cada serie debe ser comprobada entonces con gran exactitud, así como la pega completa despues de haber conectado todas las series.

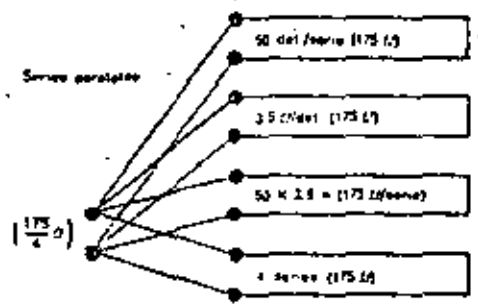

Datos:

Número total de detonadores en la pega: 200
Resistencia de cada detonador: 3,5 Ω
Explosor capaz para: 50 detonadores
Número de series: $\frac{200}{50} = 4$
Resistencia de la línea de pega: 5 Ω

Mediciones:

Resistencia por serie : 50 × 3,5 = 175 Ω (± 5 % desviación)

Resistencia despues de la conexión en paralelo:

$$\frac{\text{Resistencia por serie}}{\text{Número de series}} = \frac{175}{4} = \text{aproximadamente } 44\ \Omega$$

Resistencia de la línea de pega = 5 Ω (medida antes de la conexión)
Resistencia total obtenida: Resistencia después de la conexión en paralelo + resistencia de la línea de pega = 44 + 5 = 49 Ω

Siempre debe comenzarse con la comprobación del número de detonadores en cada serie y el número total admitido por la capacidad del explosor.

El *comprobador de puesta a tierra* (medidor de pérdidas de corriente) se utiliza en zonas donde existe riesgo de fugas de corriente a tierra. Generalmente suelen producirse en el caso de voladuras submarinas, principalmente en agua salada y también con masas minerales conductoras.

Si existen cables dañados en los detonadores, se pueden producir pérdidas de corriente que impiden la correcta iniciación de algunos detonadores de la pega. Estos daños en los cables pueden ser determinados con la utilización del comprobador de puesta a tierra.

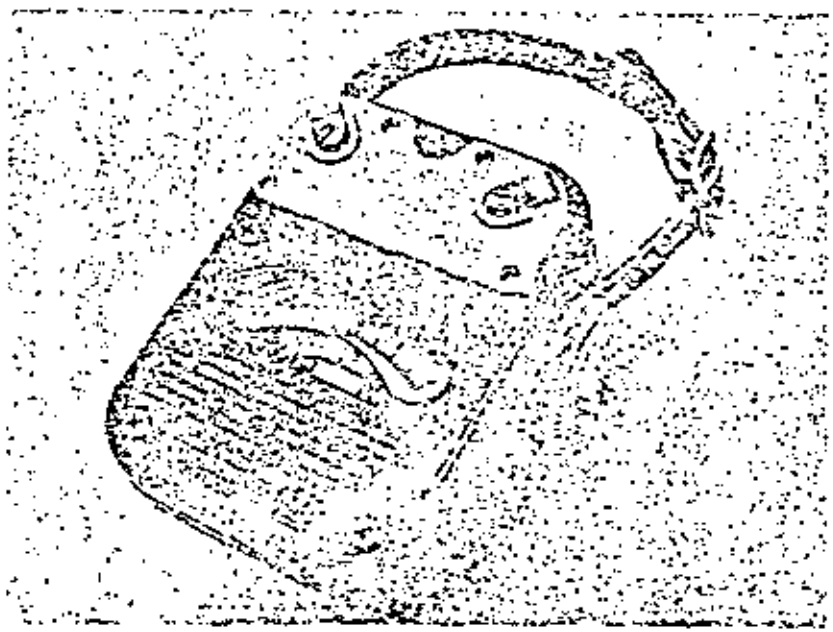

Fig. 4.2.4 Comprobador de puesta a tierra

Este instrumento mide la pequeña cantidad de corriente producida por la acción galvánica de un metal conductor (cables de los detonadores) y un medio salino. La corriente medida suele ser del orden de milésimas de amperio y puede tener diferente signo: + o —. En teoría ésto significa que dos pérdidas de corriente con signos opuestos pueden suprimirse unas a otras durante las medidas de comprobación.

El comprobador de puesta a tierra no tiene batería.

El medidor o *comprobador de aislamiento* proporciona una medida directa, en ohmios, de la resistencia a tierra de las series o parte de las series de una pega, lo cual permite estimar el riesgo existente a través de cables dañados.

El comprobador de aislamiento fabricado por Nitro Nobel permite realizar mediciones directas en zonas de voladuras sin que exista ningún riesgo. Este comprobador es un instrumento de corriente alterna con un voltaje limitado.

En Suecia la utilización de los explosores y aparatos de medida debe ser limitada a los tipos oficialmente aprobados. El encendido por medio de baterías está completamente prohibido en Suecia, debido al gran riesgo que implica; muchos accidentes han tenido lugar a causa de su utilización.

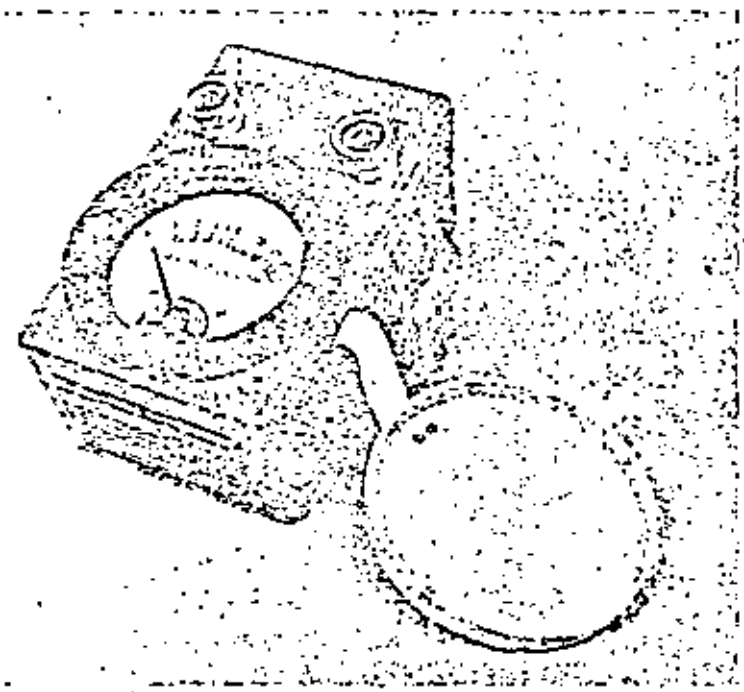

Fig. 4.2.5 Medidor de aislamiento

Los explosores de condensador, de manejo más simple y seguro, mayor capacidad de encendido y de características de descarga más adecuadas, son los de mayor utilización. El desarrollo de detonadores más seguros, con un alto márgen respecto a igniciones prematuras, ha hecho por otra parte necesaria la utilización de explosores de mayor capacidad.

Nitro Nobel dispone de una extensa gama de explosores de alta calidad.

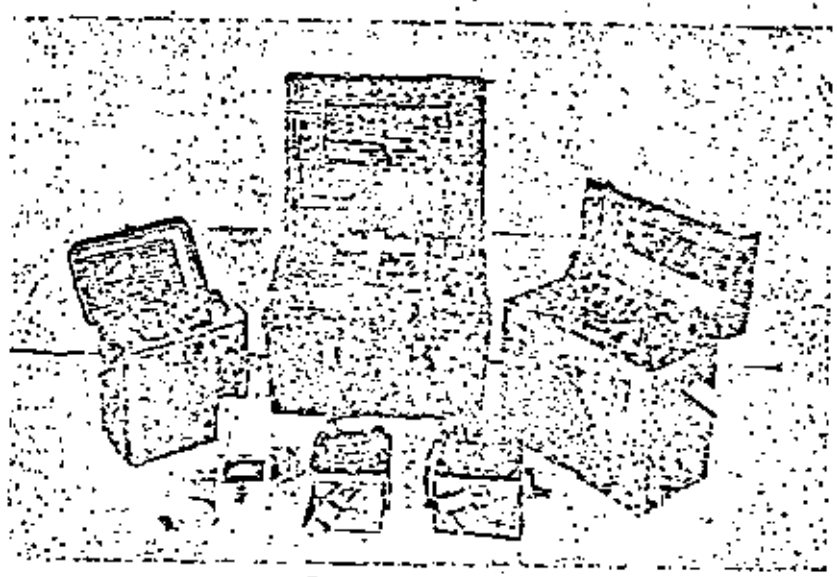

Fig. 4.2.6 Explosores

Número máximo de detonadores de sensibilidad normal.

Explosor	Voltaje	Resistencia línea de pega Ohmios	Número de detonadores	Número de detonadores por serie	Número de series en paralelo
CI 50	340	10	50	50	1
CI 15 VA	620	10	150	150	1
		2	480	80	6
		5	480	80	6
		10	400	80	5
CI 100 VA (anteriormente 2400)	1100	10	300	300	1
		2	3000	120	25
		5	2400	120	20
		10	1800	120	15
CI 275 VA	2800	10	700	700	1
		2	9000	300	30
		5	7500	300	25
		10	6000	300	20

Explosor	Voltaje	Resistencia línea de pega Ohmios	Número de detonadores*	Número de detonadores por serie	Número de series en paralelo
CI 700 VA	2500	10	650	650	1
		2	24000	300	80
		5	18000	300	60
		10	12000	300	40
Número máximo de detonadores del tipo VA					
CI 50 VA	340	2	2	2	1
		5	2	2	1
		10	2	2	1
CI 15 VA	620	10	15	15	1
CI 100 VA	1100	5	50	50	1
		2	120	30	4
		5	100	25	4
		10	80	20	4
CI 275 VA	2800	5	120	120	1
		2	300	50	6
		5	275	55	5
		10	240	60	4
CI 700 VA	2500	2	700	50	14
		5	550	50	11
		10	450	50	9
CI 700 VA + C 300 VA	2500	2	1500	60	25
		5	1000	50	20
		10	750	50	15

La utilización de altos voltajes implica la necesidad de un buen aislamiento en los detonadores, uniones y cables de encendido.

Donde exista riesgo de que las uniones entren en contacto con materiales conductores, etc. los cables de los detonadores deben estar unidos entre sí por medio de conectadores, a menos que los detonadores utilizados sean del tipo VA, con manguito protector incorporado.

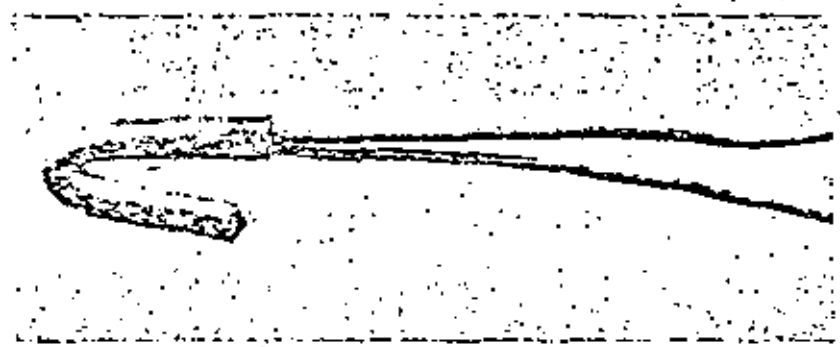

Fig. 4.2.7 Conectador

Así mismo es de gran importancia que la línea de pega y los hilos de conexión no se encuentren dañados y que sean de buena calidad.

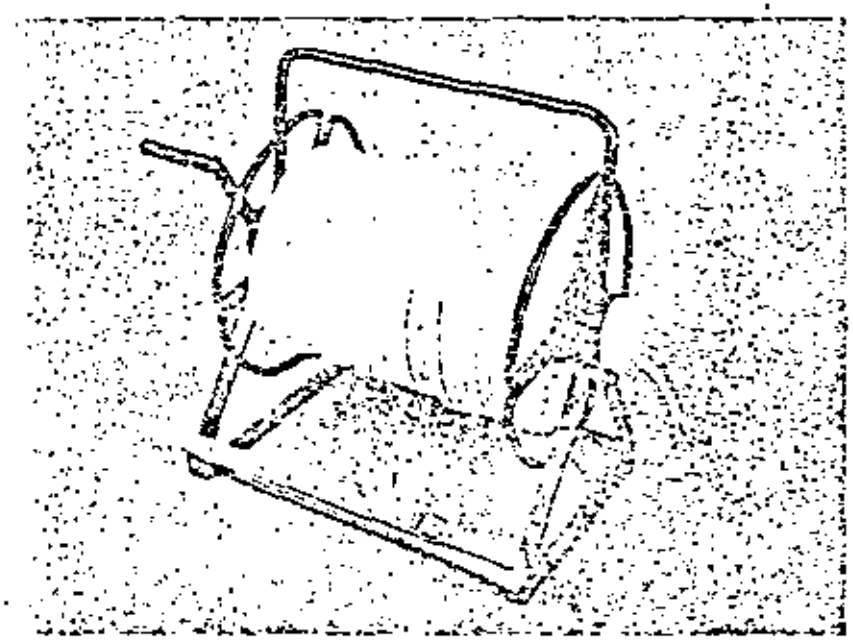

Fig. 4.2.8 Línea de pega

Mecha detonante

Este cordón o mecha detona con una velocidad de 6.000—6.500 m/s aproximadamente y se inicia por medio de un detonador; a su vez la mecha detonante actúa como iniciador de la mayor parte de los explosivos, recomendándose su uso bajo los siguientes aspectos:

Donde el encendido eléctrico no está admitido.

Como suplemento de la iniciación eléctrica en condiciones difíciles — profundidad, barrenos rotos y delicados.

En la iniciación de cargas alargadas en barrenos profundos, donde normalmente se encuentran unidas al cordón.

En voladuras de hileras múltiples. El retardo entre hileras puede obtenerse usando elementos especiales de retardo, tipo relés.

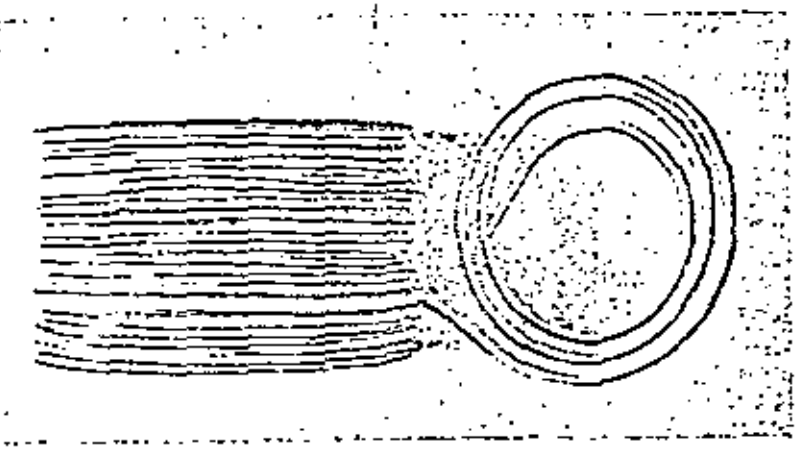

Fig. 4.2.9 Mecha detonante

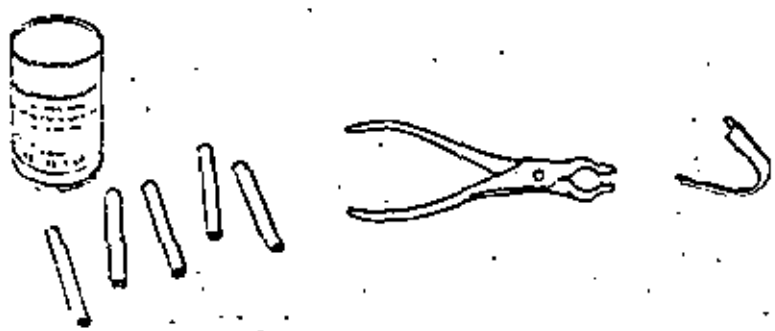

Fig. 4.2.10 Relés, grapas y elementos de sujección.

- La conexión se realiza en ángulo recto.
- La distancia entre líneas paralelas es, al menos, de 0,2 m.
- La distancia entre el elemento de retardo y la línea paralela es, al menos, de 1,0 m.
- No se deben emplear lazos ni producir torceduras.

El cordón detonante es relativamente sensible a la humedad y por esta razón debe ser manipulado durante la operación de carga de forma que la protección aislante no sea dañada. Si se utiliza en un barreno con agua, los terminales del cordón deben ser aislados con el fin de evitar la entrada de la misma, principalmente en grandes profundidades donde existen altas presiones.

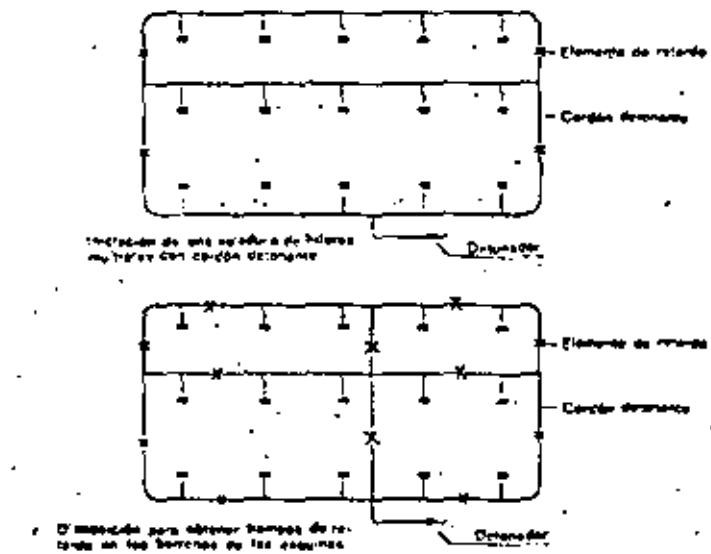

Fig. 4.2.11

4.3 ENCENDIDO IMPREVISTO

El encendido imprevisto de detonadores eléctricos puede producirse por varios factores:

Tormentas

Potenciales de tierra a través de líneas de alta tensión y cables eléctricos.

Contacto directo con objetos conductores.

En tiempo de tormenta y cuando haya riesgo de caída de rayos deberán desalojarse los lugares de trabajo donde existan pegas cargadas y mantener la zona bajo vigilancia. Nitro Nobel ha perfeccionado un detector de tormentas que advierte con antelación la proximidad de las mismas e incluso indica cuándo existe peligro inminente.

Este detector proporciona actualmente dos tipos de medidas, ya que cuenta con un sistema luminoso y mide los potenciales de campo.

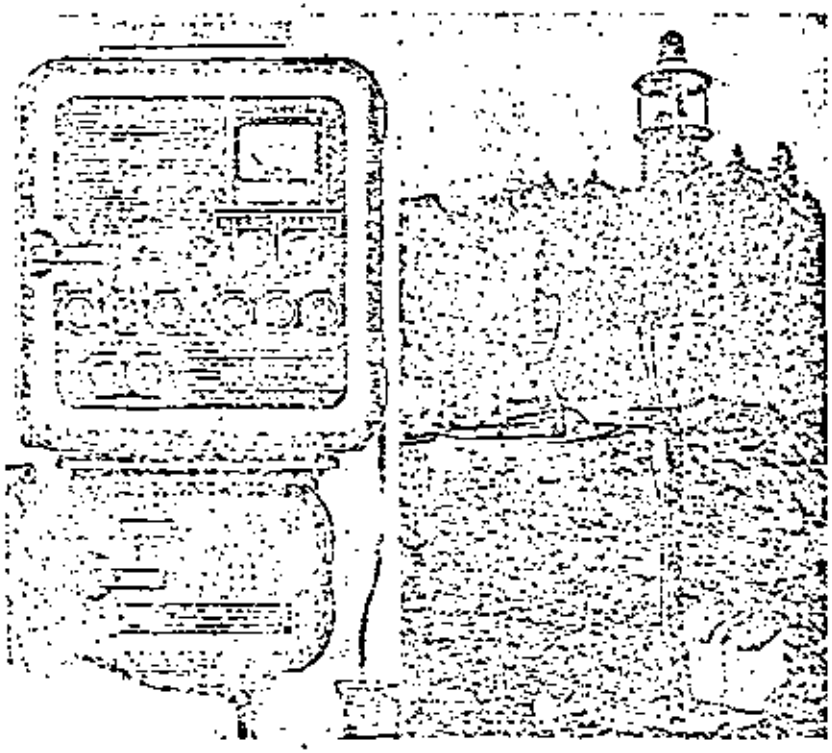

Fig. 4.3.1

El detector lleva incorporada una luz intermitente de aviso y una sirena que empieza a funcionar en el momento de peligro. En tiempo de tormentas hay que tomar todo tipo de precauciones desde el punto de vista de seguridad, ya que pegas enteras han sido iniciadas por la caída de un rayo.

Las líneas de alta tensión constituyen un riesgo debido a la inducción e influencia capacitiva. Las distancias de seguridad para distintos tipos de detonadores y voltajes están especificadas en las Normas de Voladuras No. 3 de la Dirección General de Seguridad e Higiene del Trabajo, en Suecia.

Voltaje kV	Distancia de seguridad en metros Tipo de detonadores Grupo I TE, S	Grupo II VA
3—6	20	—
10	50	—
20—50	100	—
50	200	—
70		—
130		10
220		10
400		16

Las distancias medidas son horizontales y pueden considerarse válidas para líneas subterráneas. En las proximidades de líneas de alta tensión y subterráneas se emplean acoplamientos especiales. (Ver Normas de Voladuras, para más detalles).

En determinadas condiciones las *emisores de radio* pueden significar un riesgo para la ignición prematura de los detonadores eléctricos.

El siguiente cuadro pretende ofrecer un resúmen de las normas de seguridad existentes. (Ver Normas de Voladuras para información mas detallada).

Potencia W	Frecuencia MHZ (Megaciclos)	Distancia de seguridad para detonadores tipo Grupo I TE, S m	Grupo II VA m
5	independiente	—	—
< 50	> 30	15 [1])	—
25	< 30	30	—
50	< 30	50	—
100	< 30	70	—
110			—
250	< 30	100	X

Potencia W	Frecuencia MHZ (Megaciclos)	Distancia de seguridad para detonadores tipo Grupo I TE, 8 m	Grupo II VA m
500	< 30	— 150	X
1000	< 30	200	X
2500	< 30	300	X
5000	< 30	400	X
10000	< 30	600	X
25000	< 30	1000	X
50000	< 30	1500	X
100000	< 30	2000	X
250000	< 30	3000	X

1) 15 m. desde carreteras con circulación de coches (emisora portátil).

X) En el caso de potencias superiores a 110 W y frecuencias menores de 30 MHZ (megaciclos), la distancia de seguridad para detonadores tipo VA depende de las características de la emisora y número de detonadores por pega. (Véase Normas para Voladuras.)
superior a = >
inferior a = <

4.4 NONEL GT. UN SISTEMA DE ENCENDIDO NO-ELECTRICO TOTALMENTE NUEVO

Nitro Nobel introdujo el sistema NONEL en 1.973. Desde entonces ha sido desarrollado y simplificado hasta conseguir el NONEL GT en 1.976.

En este nuevo sistema de encendido se utilizan los mismos componentes que en el anterior NONEL, con la innovación de ser el conectador y el detonador unidades separadas, consiguiendo mayor flexibilidad, economía y seguridad en el sistema.

Descripción del sistema

Los detonadores NONEL GT están formados por:

— Un tubo NONEL de longitud adecuada con el extremo final sellado.
— Un detonador de las siguientes características.

Detonador	No. de intervalos	Retardo ms	Intervalo entre Nos. ms	Longitud normal m
3—20	18	75—500	25	4,2, 4,8, 6,0, 15,0
24, 28, 32				
36, 40, 44	6	600—1100	100	4,2, 4,8, 6,0
50, 56, 62				
68, 74, 80	6	1250—2000	150	4,2, 4,8, 6,0

Los detonadores NONEL GT pueden también suministrarse en otras longitudes, en fracciones regulares de 0,6 m con longitud mínima de 2,40 m.

Los *conjuntos iniciadores* se utilizan para conectar la pega y consisten en:

— Un tubo NONEL de longitud adecuada y normalmente con un extremo sellado.
— Un conectador con un detonador instantáneo (cebador) en uno o ambos lados del tubo.

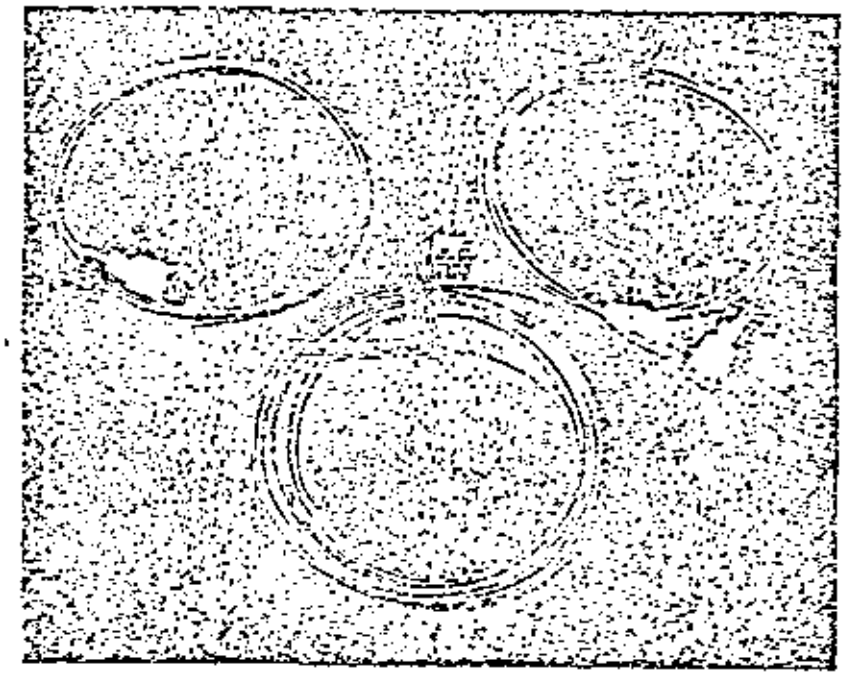

Fig. 4.4.1 GT1, 2,4 m. Detonador NONEL GT 4,8 m, GT2 2,4 m

Actualmente se dispone de los siguientes conjuntos iniciadores:

Designación	Conectador	Longitud normal m
GT1	1 amarillo	1,8, 3,0, 4,8
GT2	2 amarillo	2,4
Cebador	1 amarillo	30, 50, 100

Los conjuntos iniciadores pueden suministrarse en otras longitudes, desde 1,2 m, aumentando en fracciones de 0,6 m.

Normas de conexión del sistema NONEL GT:

Para obtener el máximo grado de seguridad y economía es necesario conseguir que el conjunto iniciador actúe en condiciones óptimas.

Fig. 4.4.2 Fase 1: Retirar el precinto e insertar el tubo del detonador, por parejas, en el conectador

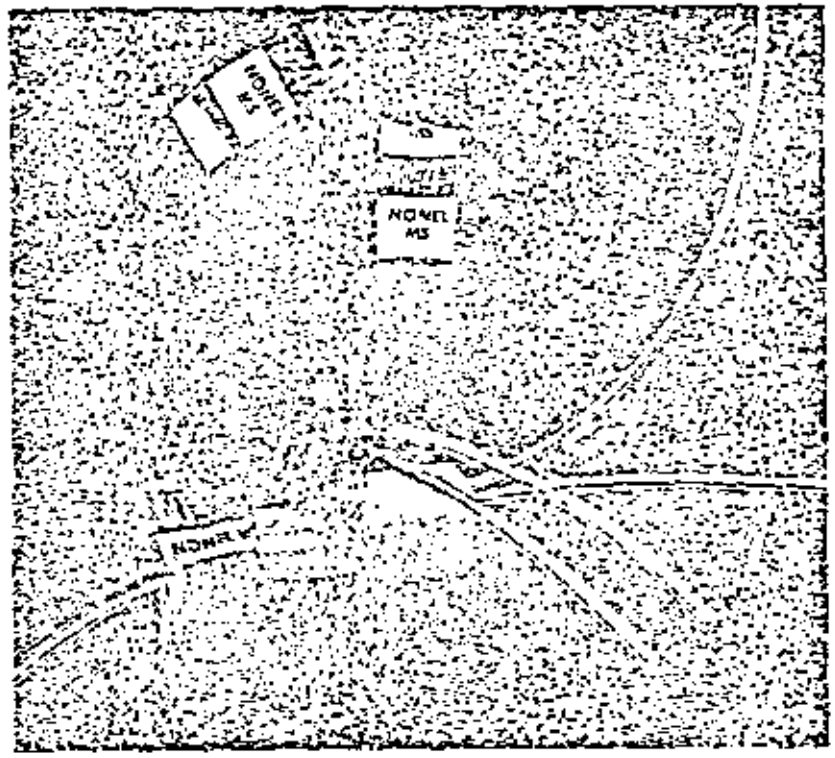

Fig. 4.4.3 Fase 2: Asegurar mediante un nudo la zona de empalme anterior

La función del conjunto iniciador (ver fig. 4.4.4)

El conectador está diseñado de tal forma que las longitudes del tubo conectado están siempre en contacto con el detonador cebador. Esto significa que un conectador NONEL, debido a sus características constructivas, no se ve influenciado por factores externos, como puede ser el grado de adiestramiento del personal.

Cuando el tubo NONEL (1) es iniciado una onda de choque o impulso se desplaza a través del mismo con una velocidad de 2000 m/seg. haciendo detonar el cebador (2), que propaga dicha onda a través del tubo NONEL

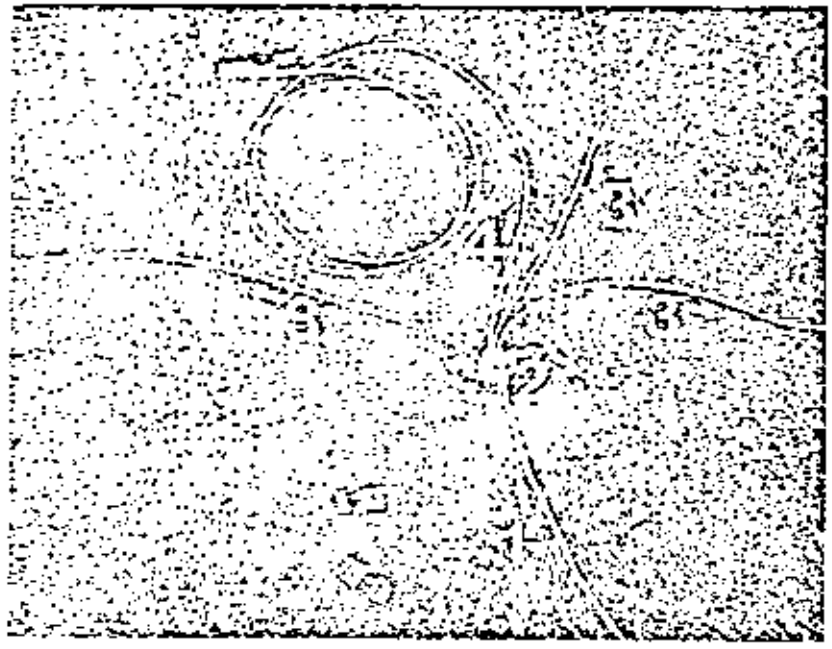

Fig. 4.4.4 Fases 3 y 4: En la siguiente operación de acoplamiento tomar otro detonador juntamente con el siguiente conjunto iniciador

insertado en el conectador en las dos direcciones, hacia uno o más detonadores (3) y también hacia el siguiente conjunto iniciador (4), repitiéndose el proceso.

La velocidad de propagación dentro del tubo NONEL proporciona al sistema un tiempo de retardo extra de 0,5 ms por metro, factor que hay que tener en consideración cuando se conectan grandes pegas. Es importante que todos los detonadores sean iniciados antes de que la roca comience a desplazarse, particularmente en el caso de voladuras subterráneas. Las porciones de tubo que no sean necesarias para la conexión deben ser situadas detrás del conectador, donde no contribuyan al retardo del sistema.

Nunca deben cortarse partes del tubo sobrante, ya que, si el precinto se rompe, el sistema se hace sensible a la humedad.

Algunos ejemplos de conexión con NONEL GT

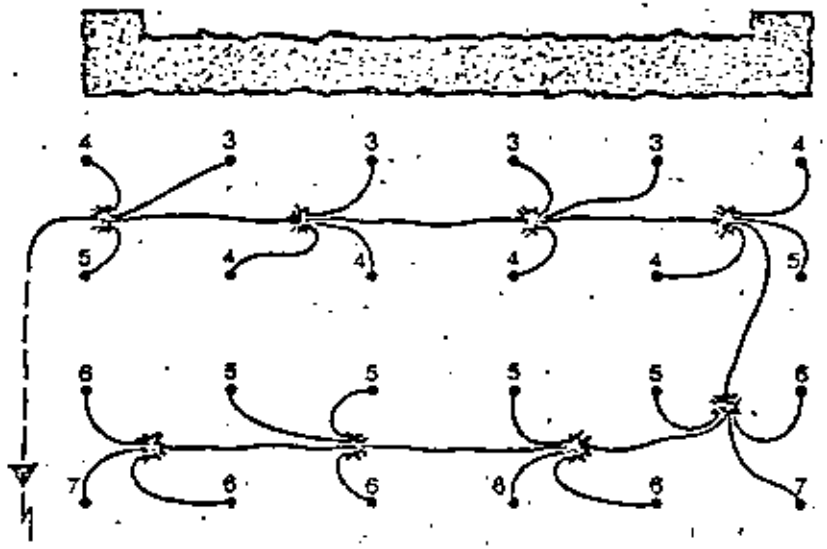

Fig. 4.4.5 En el caso de pequeñas voladuras en banco (incluso las realizadas en zanjas), la conexión se realiza en zig-zag comenzando por la primera hilera de barrenos

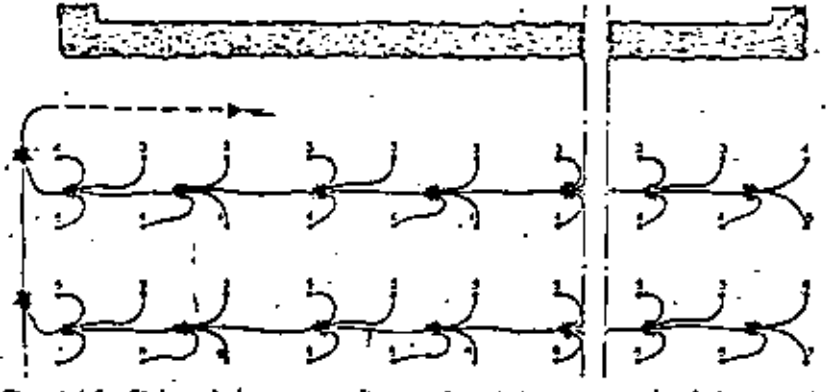

Fig. 4.4.6 Si la voladura es amplia, puede existir una irregularidad motivada por los tiempos de intervalo, debilitando el sistema de acoplamiento. En tales casos es recomendable que cada hilera de barrenos sea conectada en la misma dirección, iniciándose conjuntamente por medio de una "línea maestra" que une las hileras por el borde exterior de la pega.

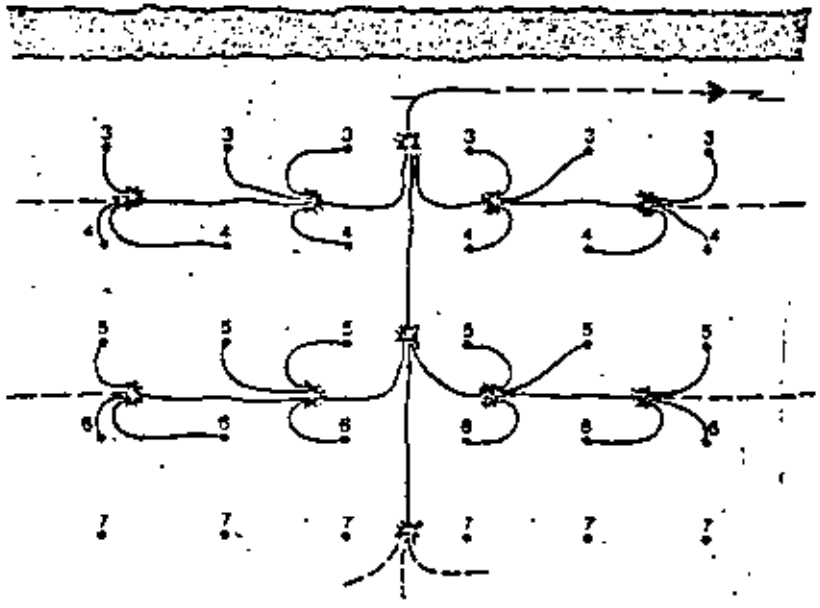

Fig. 4.4.7 Este "línea maestra" puede ser situada también simétricamente, según el ejemplo

Es importante que la conexión se realice totalmente de acuerdo con la secuencia de encendido de la pega. En caso de defecto en el sistema de acoplamiento la iniciación de la voladura cesa en ese punto, pudiendo ser subsanado el defecto con facilidad para volver a iniciar le pega rápidamente, si la conexión estaba correctamente realizada, cosa que no es posible si, por ejemplo, la conexión se ha empezado en la parte opuesta de la pega.

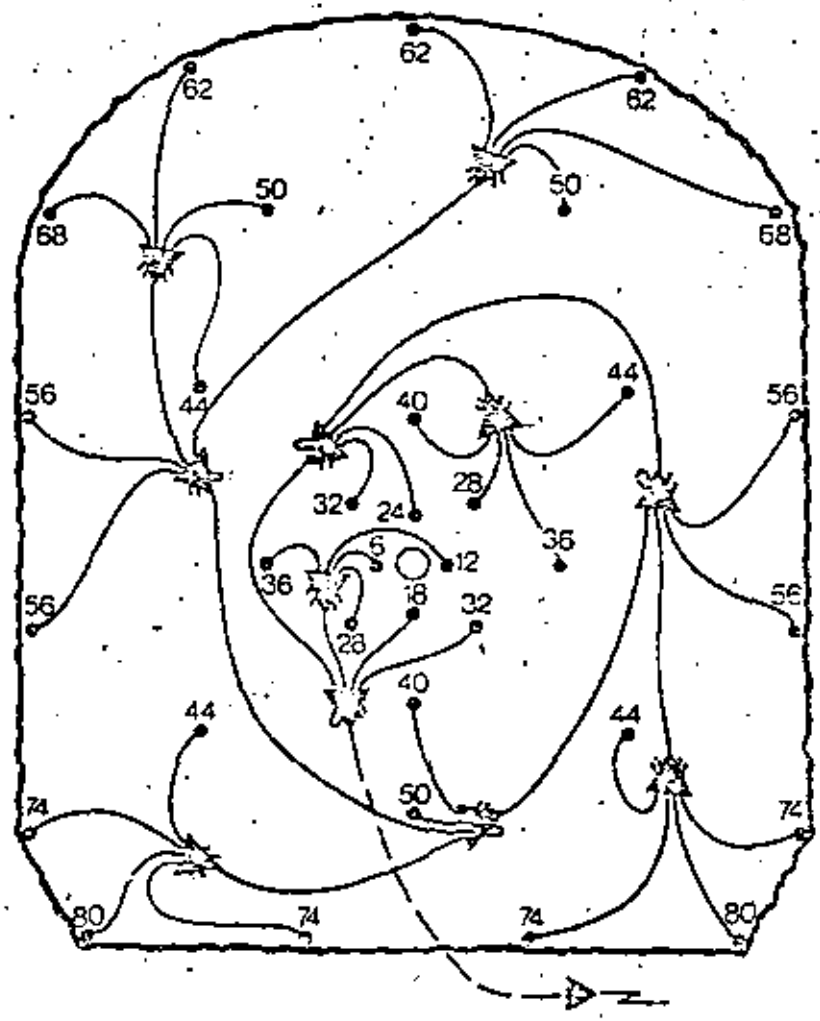

Fig. 4.4.8 En pequeñas voladuras en túnel la iniciación se realiza en el cuele y como en el caso anterior, la conexión debe seguir la secuencia de encendido tan lejos como sea posible, pudiendo tomar, por ejemplo, la forma de espiral. La conexión se termina con los barrenos de corona, teniendo en cuenta que el conectador debe situarse de forma que no esté en contacto con el suelo. En este caso podría utilizarse un conjunto iniciador GT2.

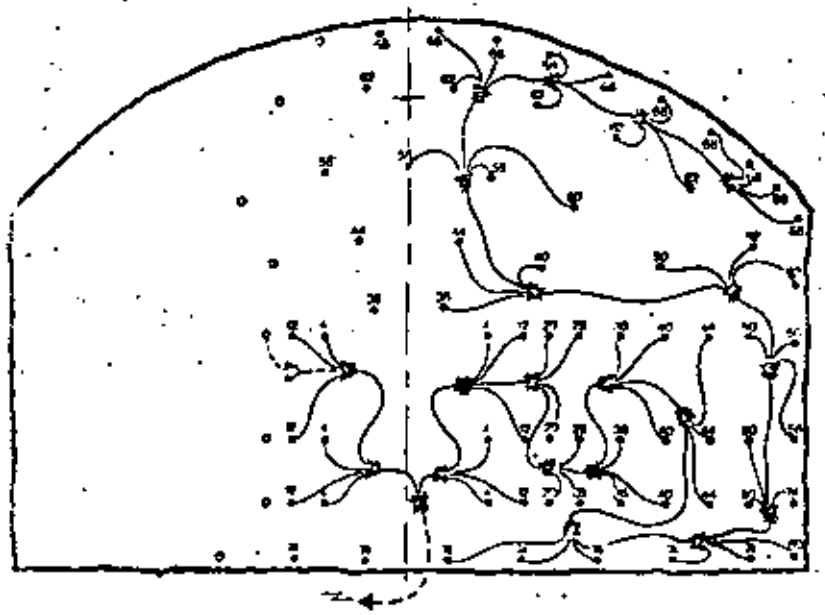

Fig. 4.4.9 En voladuras en túneles de sección amplia, utilizando, por ejemplo, un cuele en cuña, la conexión debe dividir el circuito en dos mitades, cada una de las cuales debe seguir la secuencia de encendido prevista, comenzando con la primera carga y terminando a nivel de corona. La conexión de los dos circuitos se realiza en el centro por medio de un conjunto de iniciación corto, procurando que el conectador no quede en contacto con el suelo. El conjunto iniciador GT1 es muy adecuado para estos trabajos.

Algunas reglas generales de utilización del sistema NONEL GT

Lo mismo que sucede con otros sistemas de encendido no-eléctricos, el sistema NONEL no puede ser comprobado mediante la utilización de aparatos de medida, siendo por lo tanto de gran importancia los siguientes puntos para conseguir un buen resultado.

— Un sistema de conexión sencillo permite realizar fácilmente un control visual.
Se deben utilizar detonadores y conjuntos iniciadores que dispongan de longitudes de tubo acordes con la profundidad del barreno y su situación, lo que al mismo tiempo es más económico.

— No romper las empaquetaduras de protección, a menos que sea absolutamente necesario.

— Debe utilizarse material en buenas condiciones y comprobar que no se ha dañado durante las operaciones de carga y conexión.

— Conectar los detonadores cebadores tan próximos a los barrenos, como sea posible pero al menos 1,5 m del detonador de retardo.

— Acortar el sistema de conexión situado en el suelo tanto como sea posible, pero sin forzar el tubo.

— No conectar la voladura antes de que los equipos de perforación y carga, así como el personal no necesario se hayan retirado.

— Utilizar la capacidad total de los conjuntos iniciadores para cuatro conexiones en cada punto.

Las voladuras con el sistema NONEL pueden ser iniciadas:

A. Mediante una pistola con cápsulas de fogueo (a través de un conjunto iniciador de 30, 50 o 100 metros de tubo).

B. Utilizando un detonador de mecha ordinario, el cual se conecta a la pega por medio de un conjunto iniciador extra de 5 metros de longitud aproximadamente.

C. Con un detonador eléctrico conectado de la misma forma anterior.
Hay que tener en cuenta que el detonador eléctrico hace del sistema NONEL un conjunto sensible a los fenómenos eléctricos, por lo cual debe ser conectado en el momento del disparo, una vez despejada la zona.

5. VOLADURAS EN BANCO

5.1 CALCULO DE LA CARGA

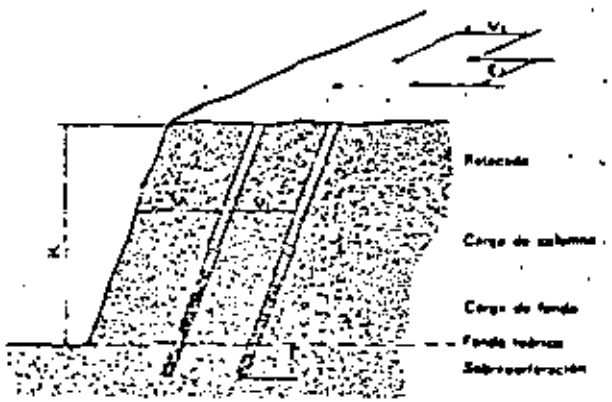

Fig. 5.1.1

Nomenclatura:

V_{max} = *Piedra* máxima en metros
V_t = *Piedra* práctica en metros
E_t = Espaciamiento práctico en metros
K = Altura de banco en metros
U = Sobreperforación en metros
Q_b = Carga de fondo en Kg.
Q_p = Carga de columna en Kg.
q = Carga específica en Kg/m^3.

(V_t debe ser realmente medida perpendicularmente al taladro, pero, por razones prácticas, utilizaremos aquí la distancia medida horizontalmente.)

Dentro de los tipos de voladuras, las ejecutadas en bancos pueden considerarse como las más usuales y se pueden definir como voladuras realizadas con barrenos normalmente verticales en una o en varias hileras, con salida hacia una superficie libre.

Los taladros pueden tener el fondo encerrado o libre, lo cual implica, en este último caso, que el barreno termina por encima de la superficie libre horizontal.

De hecho, casi todos los tipos de voladura pueden ser considerados de alguna forma como voladura en banco.

Las voladuras en trinchera son similares, pero el grado de fijación de la roca es superior, requiriéndose por lo tanto un incremento de la carga específica y una mayor perforación.

En el caso de voladuras en túnel, existe solamente una cara libre — el frente del túnel. Despues de haber volado el cuele, la roca que permanece presenta la forma de voladura en banco contra el hueco formado, denominándose destroza.

Los diferentes tipos de roca con características tan dispares como son la resistencia a la tracción, compresión y cizalladura afectan al resultado de una voladura, dado que esta resistencia debe ser vencida, si se pretende romper la roca por el efecto del explosivo.

Un factor que tiende a dificultar este aspecto es el hecho de que las rocas mantienen muy pocas veces su homogeneidad dentro de cada tipo. Las grietas y fallas pueden cambiar total o parcialmente su resistencia en relación con el efecto del explosivo. En zonas con existencia de fallas — donde la resistencia de la roca en su conjunto depende de la fricción entre distintos planos — existe una amplia gama de características en las voladuras, comparado, por ejemplo, con zonas de roca dura y homogénea con una resistencia a la tracción de 200 kg/cm^2.

Las rocas que contienen pizarra y con huecos que pueden proporcionar a los gases formados en la voladura la posibilidad de penetrar por los mismos sin producir ningún efecto, pueden ser difíciles de volar, a pesar del hecho de tener propiedades resistentes más bajas.

La base teórica disponible para el cálculo de la carga se fundamenta en valores empíricos proporcionados por los ensayos de voladuras y por los resultados prácticos que se han ido acumulando.

La unidad que parece influir con mayor simplicidad las características de la roca a la voladura (con un explosivo determinado) es la que manifiesta la relación entre la cantidad de explosivo de una determinada potencia y el volúmen de roca arrancado.

Esta es la *carga específica* en Kg/m^3.

Usando un sistema de cálculo basado en la carga específica, es posible determinar la carga adecuada para un tipo de roca considerado, a pesar de que existan variaciones en sus características a la voladura. En los cálculos que siguen se utiliza el explosivo tipo Dynamex B, que tiene las siguientes características:

Velocidad de detonación:	5.500 metros/segundo
Factor de energía:	Aprox. 500 ton. m/kg
Potencia relativa:	100

La carga específica es una excelente unidad para el cálculo de las cargas, pero la distribución del explosivo en la roca es de suma importancia.

A igualdad de carga específica, una voladura realizada con barrenos muy próximos y de pequeño diámetro proporciona una mejor fragmentación que, si se utilizan barrenos de gran diámetro y con esquema más amplio.

Si los cálculos se basan en una carga específica de 0,40 Kg/m³ (Dynamex B) necesaria para romper la *piedra* en el fondo, (de acuerdo con Langefors), entonces se puede calcular el espaciamiento que debe ser utilizado con diferentes diámetros. Estos cálculos se refieren a cargas con un grado de retacado de 1,25 Kg/dm³ (Ver Sección Carga).

Es de gran importancia para obtener el resultado deseado en una voladura, conseguir en la práctica la concentración de carga estimada teóricamente.

En el caso de voladuras en banco se considera que la zona del fondo, al existir una mayor constricción, requiere una determinada carga específica para desprender la roca. Por encima de esta zona, la carga de columna, se requiere una concentración de carga considerablemente menor para desprender la *piedra*. En la práctica, se utiliza con frecuencia un exceso de carga para compensar las desviaciones del barreno y conseguir una mayor potencia necesaria para el esponjamiento y lanzamiento de la roca hacia adelante.

El sistema de encendido utilizado es de gran importancia. Las voladuras realizadas con tiempos de retardo muy pequeños implican en principio que la roca se rompa en etapas, con diferencia de tiempo de milésimas de segundo entre barrenos adyacentes.

El efecto de tiempos de retardo muy cortos entre barrenos adyacentes se traduce en una colaboreción entre sí para la rotura de la roca, consiguiendo además mantenerla unida durante la voladura, produciendo menor efecto de proyección. Si se utilizan tiempos de retardo de varios segundos, el proceso de la voladura tendría un carácter completamente distinto, obteniendose una gran proyección o una mala rotura de la roca, con aumento de la fragmentación y obtención de grandes bloques.

Una voladura de hileras múltiples con microretardos normalmente tiene un exceso de carga por encima del valor mínimo necesario para una sóla hilera de barrenos.

La expresión *exceso de carga* no debe significar, como frecuentemente sucede, una carga sobrante, cuando se está comparando con un mínimo determinado.

Hace muchos años los especialistas en voladuras estaban obligados a calcular individualmente cada carga proporcionándoles un conocimiento completamente distinto del actual en lo relativo al efecto ejercido por el explosivo, ya que el amplio campo de aplicación de las voladuras con microretardo implica el que actualmente exista un enmascaramiento de dicho efecto. No obstante, hoy día existe personal altamente especializado trabajando en voladuras con precaución, demoliciones, etc.

La cantidad de explosivo utilizado debería ser muy próxima a la mínima necesaria para desprender la roca, significando ésto que el efecto obtenido puede ser estudiado de una forma completamente distinta. Por ejemplo, en canteras de las que se pretende obtener bloques de granito y diabasa, el personal suele estar muy adiestrado para determinar los posibles planos de rotura de la roca.

Mucho se ha dicho sobre voladuras, tanto en teoría como en la práctica. La capacidad de que dispone el personal adiestrado de recordar datos basados en la experiencia para su aplicación diaria en el trabajo, es una forma de teoría muy avanzada. Realmente pueden considerarse análogos los datos basados en la experiencia y los valores empíricos, que han sido recogidos a lo largo de los años y que han proporcionado la base para el desarrollo de las relaciones y fórmulas para los cálculos de las cargas.

Cuando se utilizan tablas y cálculos en los trabajos de voladuras, deben ser adaptadas para cada caso en particular a las condiciones existentes, teniendo este aspecto mayor importancia en el caso de voladuras con precaución que en el caso de voladuras destinadas a producción. Un cálculo teórico no puede predecir todos los detalles que tendrán lugar durante las operaciones de perforación y voladura, ya que básicamente dependerán de las variaciones de las características en la roca, así como de las fallas, grietas y zonas débiles existentes.

La acumulación de una buena experiencia práctica y una sólida formación teórica, constituyen la mejor combinación para todo profesional.

Cálculo de la carga

Los resultados obtenidos con los cálculos básicos de Langefors han sido tan buenos que no hay razón para utilizar nuevas fórmulas empíricas, si bien se incluyen los factores que determinan las relaciones geométricas de las voladuras, manteniendo los relativos a la constricción de los taladros y a la voladura de una o más hileras.

(El procedimiento de cálculo de las cargas se ha desarrollado por fases.)

Cálculo de la carga (de acuerdo con Langefors)

V_{max} = *Piedra* máxima en metros
V_1 = *Piedra* práctica en metros

F	=	Error de perforación
E_t	=	Espaciamiento práctico en metros
U	=	Sobreperforación en metros
H	=	Longitud del barreno en metros
K	=	Altura de banco en metros
Q_b	=	Carga de fondo en Kg.
Q_p	=	Carga de columna en Kg.
Q_{tot}	=	Carga total en Kg/barreno
ζ	=	Carga específica en Kg/m³
d	=	Diámetro del barreno en mm.
Q_{kb}	=	Concentración de carga de fondo en Kg/m.
Q_{kp}	=	Concentración de carga de columna en Kg/m.
h_b	=	Altura de carga de fondo en metros
h_p	=	Altura de carga de columna en metros
h_a	=	Retacado en metros
b	=	Perforación específica en m/m³
B	=	Anchura de la pega en metros

V_{max} = 45 × d

Piedra máxima teórica = 45 × diámetro del taladro

U = 0,3 × V_{max}

Sobreperforación = 0,3 × *piedra* máxima teórica

H = K + U + 0,05 (K + U)

Profundidad del taladro = Altura de banco + Sobreperforación + 5 cm/m debido a la inclinación 3:1 del taladro.

F = 0,05 + 0,03 × H

Error de perforación = 5 cm. de error de emboquille + 3 cm/m de taladro

V_1 = V_{max} — F

Piedra práctica = *Piedra* máxima — Error de perforación

E_t = 1,25 × V_1

Espaciamiento práctico = 1,25 × *Piedra* práctica

Q_{kb} = $\frac{d^2}{1000}$ concentración de carga de fondo = $\frac{(\text{diámetro taladro})^2}{1000}$

h_b = 1,3 × V_{max}

Altura de carga de fondo = 1,3 × *Piedra* máxima teórica

Q_b = h_b × Q_{kb}

Carga de fondo = Altura de carga de fondo × concentración de carga de fondo

Q_{kp} = 0,4 — 0,5 × Q_{kb}

Concentración de carga de columna = (0,4 a 0,5) × concentración de la carga de fondo

h_p = H — (h_b + h_a)

Altura de la carga de columna = profundidad del taladro — (Altura de la carga de fondo + retacado)

h_a = V_1 (en ciertos casos V_{max}).

Retacado = *Piedra* práctica (en ciertos casos la *Piedra* teórica)

El siguiente ejemplo nos indica cómo se realizan los cálculos.

Datos: Altura de banco K = 12 m.
Anchura de la pega B = 20 m.
Diámetro de perforación = 64 mm.

1. V_{max} = 45 × d
   V_{max} = 45 × 64 = 2,880 mm = 2,88 m.
2. U = 0,3 × V_{max}
   U = 0,3 × 2,88 = 0,864 m. (0,9 m.)
3. H = K + U + 0,05 (K + U)
   H = 12 + 0,9 + 0,05 (12 + 0,9) = 13,54 m. (13,6 m.)
4. F = 0,05 + 0,03 × H
   F = 0,05 + 0,03 × 13,6 = 0,46 m.
5. V_1 = V_{max} — F
   V_1 = 2,88 — 0,46 = 2,42 m. (2,40 m.)
6. E_t = 1,25 × V_1
   E_t = 1,25 × 2,40 = 3,00 m.

   Número de espacios $\frac{B}{E_t} = \frac{20}{3} = 6,6$ (7)

   E_t = $\frac{B}{\text{Número de espacios}} = \frac{20}{7}$ = 2,86 m.
7. Q_{kb} = $\frac{d^2}{1000}$

   Q_{kb} = $\frac{64^2}{1000} = \frac{4.100}{1.000}$ = 4,1 Kg/m.
8. h_b = 1,3 × V_{max}
   h_b = 1,3 × 2,88 = 3,74 (3,7 m.)
9. Q_b = h_b × Q_{kb}
   Q_b = 3,7 × 4,1 = 15,2 Kg

10. $Q_{pb} = 0,4 - 0,5 \times Q_{bc}$
$Q_{pb} = 0,5 \times 4,1 = 2,05$ (2,0 Kg/m.)

11. $h_a = V_1$
$h_a = 2,40$ m.

12. $h_p = H - (h_t + h_a)$
$h_p = 13,6 - (3,7 + 2,40) = 7,5$ m.

13. $Q_p = h_p \times Q_{pb}$
$Q_p = 7,5 \times 2,0 = 15,0$ Kg

14. $Q_{tot} = Q_b + Q_p$
$Q_{tot} = 15,2 + 15,0 = 30,2$ Kg

15. $q = \dfrac{\text{Barrenos/hilera} \times Q_{tot}}{V_1 \times K \times B}$

$q = \dfrac{8 \times 30,2}{2,40 \times 12 \times 20,00} = 0,42$ Kg/m³

16. $b = \dfrac{\text{Barrenos/hilera} \times H}{V_1 \times K \times B}$

$b = \dfrac{8 \times 13,6}{2,4 \times 12 \times 20} = 0,19$ m. perforación/m³

Resúmen de datos importantes

Altura de banco	Prof. del taladro	Piedra	Espaciamiento	Carga de fondo	Carga de Columna		Carga específica	Perforación específica
m	m	m	m	Kg	Kg	Kg/m	Kg/m³	m/m³
12,0	13,6	2,40	2,86	15,20	15,00	2,00	0,42	0,19

(Para el Plan de Tiro ver la sección Métodos de Encendido.)

Los cálculos mencionados anteriormente pueden considerarse normales en rocas de características también normales. Si no se realizan las operaciones de desescombro entre cada voladura, se necesita frecuentemente una carga específica más elevada, particularmente en el caso de voladuras en las que exista mayor constricción de los barrenos (ver Sección Espònjamiento). En el caso de voladuras con precaución en zonas habitadas no se utilizan normalmente grandes diámetros de perforación y la carga específica es menor en ciertos casos.

Si el centro de gravedad de la roca está localizado a una altura considerablemente mas elevada que el nivel del terreno, debe disminuirse la carga específica, si se trata de evitar un lanzamiento hacia arriba. Las tablas siguientes de perforación y carga están calculadas conforme al método descrito anteriormente.

La adaptación de los cálculos a los casos prácticos pueden realizarse fácilmente, teniendo en cuenta lo indicado en las Secciones Fragmentación, Esponjamiento y Proyección.

Realizar una voladura de prueba de una o más hileras es un buen camino para obtener una impresión de las características de la roca. Cuando se desea aprovechar al máximo los diámetros de los barrenos, como en el caso de voladuras para producción, pueden ajustarse fácilmente los cálculos cambiando el factor k, en la relación:

$V_{max} = k \times d$

Un cambio de este factor de k = 45 a otros valores modifica la carga específica en el fondo, variando totalmente la voladura, pudiendo realizarse los cálculos de carga de la misma manera, lo que significa que el sistema puede ser adaptado a todos los tipos de roca con independencia de sus características a la voladura.

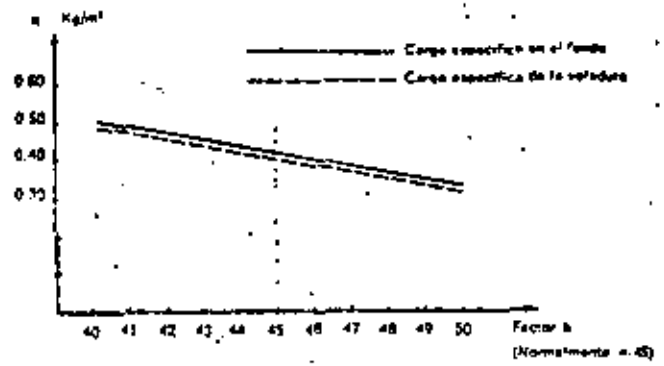

Fig. 5.1.2

Los esquemas de encendido pueden ser realizados usando distintas combinaciones, siendo importante que el tiempo de retardo entre barrenos adyacentes sea elegido de forma que no se produzcan proyecciones imprevistas; además cada barreno debe tener rotura libre en el momento de la explosión.

Una hilera de barrenos con el mismo tiempo de intervalo tiene mejor posibilidad de rotura, ya que cooperan uno con otro en la rotura de la *piedra*. No obstante, la fragmentación puede ser menor, debido a que el tiempo de retardo entre barrenos adyacentes, en este caso, es solamente el correspondiente a la dispersión dentro de cada número.

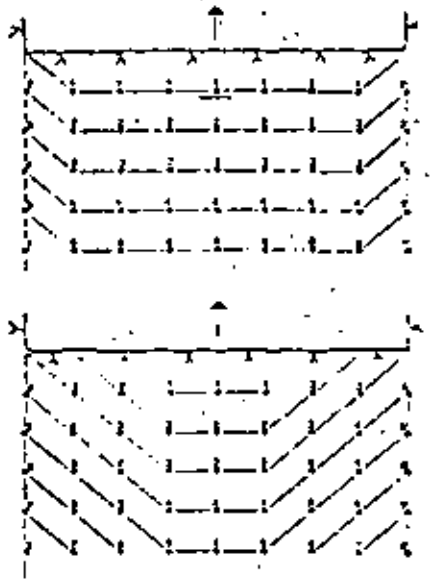

Fig. 5.1.3 Esquema de tiro en voladura en banco

El cuele en cuña produce normalmente buena fragmentación y buena acumulación de escombro, existiendo también disminución de la constricción de los barrenos en su contorno.

El tiempo de intervalo es extremadamente importante desde el punto de vista de la fragmentación. (Ver Sección Fragmentación.)

Cuando se realizan voladuras próximas a edificios o instalaciones donde puede existir riesgo de vibraciones, el esquema de encendido debe ser adaptado a dichas exigencias. (Ver Sección 13.3 Voladuras con Precaución.)

Tablas para voladuras en banco con distintos diámetros de perforación

En las páginas siguientes se incluyen tablas para voladuras en banco, utilizando distintos diámetros y alturas. Las tablas representan el caso normal de voladura, sin ninguna especificación especial respecto a vibraciones. En el caso de voladuras para producción, por ejemplo, excavaciones a cielo abierto, en muchos casos puede resultar económicamente ventajoso incrementar la carga específica con objeto de obtener mejor fragmentación. Cuando exista constricción en los barrenos, como, por ejemplo, en voladuras en trinchera para carreteras, también se necesita mayor carga específica para desplazar la roca hacia adelante. (Ver Sección 5.3 Esponjamiento.)

A continuación se indican algunas consideraciones importantes para la utilización de las tablas, que deben analizarse detenidamente.

Aptitud de la roca a la voladura

Algunos tipos de roca pueden presentar más dificultad que otros para ser volados, dependiendo de sus características de resistencia, existencia de fallas, composición pizarrosa, etc. No obstante, los valores representados en las tablas incluyen el suficiente incremento de carga por encima de la carga límite de rotura. Si se vuela una sola hilera de barrenos en gneis o granito sueco, el nivel límite de carga esta alrededor de 0,20 Kg/m³. En voladuras de hileras múltiples en banco se requiere en la práctica un valor de 0,35—0,45 Kg/m³ para compensar los errores de perforación y el esponjamiento. Los métodos de cálculo ofrecen la posibilidad de cambiar el factor k en la relación $V_{max} = k \times d$, distribuyendo los barrenos convenientemente, dependiendo de la aptitud de la roca a la voladura.

Concentración de carga

Las tablas están calculadas para el explosivo Dynamex B y un grado de retacado en el fondo de 1,25 Kg/dm³. Si la concentración de carga difiere sensiblemente de este valor, la perforación debe adaptarse de forma que se obtenga en el fondo la misma carga específica. Cuando los cartuchos son retacados con atacador, la carga de fondo debe ser cuidadosamente realizada si se quiere obtener el grado de retacado de 1,25 Kg/dm³, lo cual es imposible cuando se introducen varios cartuchos antes de retacar. El siguiente ejemplo indica la importancia de conseguir una correcta concentración en el fondo.

Diámetro del barreno: 64 mm.
Altura de banco: 8,0 m.
Profundidad del barreno: 9,3 m.

Encartuchado tipo	Método de carga	Concentración de carga Kg/dm³	Kg/m
Dynamex B 55 × 400	Introducían de los cartuchos en el taladro, dejándoles caer sin retacar Baja temperatura	1,05	3,40

Encartuchado tipo	Método de carga	Concentración de carga Kg/dm³	Kg/m
Dynamex B 55 × 400	Cartuchos rajados Retacado mediante atacador pesado Temperatura + 15 a 25° C	1,25	4,10
Dynamex B 29 × 200	Cargadora neumática manual	1,25	4,10
Dynamex B 29 × 200	Cargadora neumática tipo Robot	1,35	4,30

Podemos observar que mediante distintos métodos de carga pueden obtenerse diferencias de hasta 25 o 30 % en la concentración de la carga de fondo, debiendo tener en cuenta estas consideraciones cuando se calculan las cargas para su aplicación en la práctica. Dado que es antieconómico el no utilizar el máximo el volúmen del taladro, las tablas están basadas en la concentración de 1,25 Kg/dm³ que puede considerarse como un valor relativamente elevado.

Error de perforación

La *piedra* máxima teórica V_{max} de las tablas ha sido reducida por un factor, debido al error de perforación, estimado en 5 cm + 3 cm/m de taladro. Normalmente este valor es sobrepasado en la práctica. No obstante, durante los últimos años se han desarrollado aparatos de alineación, consiguiendo mayor precisión en la perforación, de forma que los resultados obtenidos están próximos al valor de dicho factor.

El error de perforación debe considerarse pura y simplemente como un factor práctico, considerado necesario para compensar las desviaciones encontradas en la practica, en relación con los datos aportados por la teoría.

Potencia por unidad de peso del explosivo

Según se indica anteriormente, las tablas han sido calculadas, de acuerdo con las características del explosivo, tipo Dynamex B. Si se utiliza un explosivo de menor potencia, el esquema de perforación debe ser más cerrado, es decir, los barrenos deben estar situados más próximamente y lo mismo sucede al conseguir una concentración de carga inferior a la calculada. La potencia por unidad de peso sirve de base para comparar el efecto de distintos explosivos. (Ver Sección 3.1 Explosivos), y, aunque pueda ser calculada de acuerdo con sus componentes, su determinación está basada en los resultados de pruebas reales de voladuras en roca. Se ha demostrado que explosivos con la misma potencia por unidad de peso que el Dynamex B producen efecto

distinto en la roca; por ejemplo, el Reolit A no posee la misma capacidad de lanzamiento o proyección hacia adelante de la roca durante la voladura, a pesar de que el desprendimiento y la fragmentación es normal, pudiendo ser debido al hecho de que el Reolit A tiene menor velocidad de detonación; pero también a su diferente sistema de fabricación, lo que se traduce en distintas formas de operar con sus ventajas y desventajas. La práctica de voladuras, con un estudio cuidadoso de los resultados, proporciona la mejor base de estimación de los efectos.

Tabla de perforación y carga para diámetro del taladro de 34 a 27 mm. Serie 11.

Inclinación del taladro: 3:1.

Altura de banco K m	Profundidad taladro H m	Piedra máxima V_{max} m	Piedra práctica V_t m	Espaciamiento práctico E_t m	Carga de fondo Q_b kg	Carga de columna Q_p kg	Carga de columna Q_{pk} kg/m	Carga total Q_{tot} kg/barreno	Carga específica q kg/m³
0,5	0,8	0,50	0,50	0,65	0,075	—	—	0,075	0,46
0,8	1,1	0,60	0,60	0,75	0,15	—	—	0,15	0,41
1,0	1,4	0,80	0,80	1,00	0,30	—	—	0,30	0,38
1,2	1,6	0,90	0,90	1,10	0,45	—	—	0,45	0,38
1,5	1,9	1,00	1,00	1,25	0,55	0,10	0,40	0,65	0,35
1,7	2,2	1,00	1,00	1,25	0,60	0,15	0,40	0,75	0,35
2,0	2,5	1,10	1,00	1,25	0,70	0,20	0,40	0,90	0,35
2,5	3,0	1,20	1,10	1,35	1,00	0,30	0,40	1,30	0,35
3,0	3,6	1,35	1,20	1,50	1,60	0,30	0,50	1,90	0,35
3,5	4,1	1,30	1,10	1,35	1,40	0,60	0,50	2,00	0,38
4,0	4,6	1,30	1,10	1,35	1,40	0,85	0,50	2,25	0,38
4,5	5,1	1,25	1,05	1,30	1,30	0,90	0,40	2,20	0,36
5,0	5,6	1,25	1,05	1,30	1,30	1,10	0,40	2,40	0,36
5,5	6,2	1,20	1,00	1,25	1,10	1,40	0,40	2,50	0,36

Si no se realiza el desescombro entre voladuras, es necesario incrementar la concentración de carga de columna; por ejemplo, con un incremento hasta 0,7 Kg/m. en un banco de 5 m. de altura, la carga específica aumentaría hasta 0,50 Kg/m³. La carga específica indicada en las tablas es la correspondiente a cada barreno considerado individualmente, si bien en una voladura la carga

es mayor, debido a la influencia de los barrenos extremos y se puede calcular mediante la siguiente relación:

$$q_{real} = \frac{q_{teor} \times \text{número de barrenos/hilera}}{\text{Número de barrenos/hilera} - 1}$$

por ejemplo: K = 4,00 q = 0,38 10 barrenos/hilera

$$q_{real} = \frac{0,38 \times 10}{10 - 1} = 0,42 \text{ Kg/m}^3$$

Tabla de perforación y carga para diámetro del taladro de 40 a 29 mm. Serie 12.

Inclinación del taladro: 3:1.

Altura de banco K m	Profundidad taladro H m	Piedra máxima V_{max} m	Piedra práctica V_t m	Espaciamiento práctico E_t m	Carga de fondo Q_b kg	Carga de columna Q_p kg	Carga de columna Q_{pk} kg/m	Carga total Q_{tot} kg/barreno	Carga específica q kg/m³
0,5	0,8	0,50	0,50	0,65	0,075	—	—	0,075	0,46
0,8	1,1	0,60	0,60	0,75	0,15	—	—	0,15	0,41
1,0	1,4	0,80	0,80	1,00	0,30	—	—	0,30	0,38
1,2	1,6	0,90	0,90	1,10	0,45	—	—	0,45	0,38
1,5	1,9	1,00	1,00	1,25	0,50	0,10	0,40	0,60	0,35
1,7	2,2	1,00	1,00	1,25	0,60	0,15	0,40	0,75	0,35
2,0	2,5	1,10	1,10	1,25	0,70	0,20	0,40	0,90	0,35
2,5	3,0	1,20	1,10	1,35	1,00	0,33	0,50	1,35	0,36
3,0	3,6	1,40	1,25	1,50	1,70	0,35	0,50	2,05	0,36
3,5	4,2	1,58	1,40	1,75	2,50	0,55	0,70	3,05	0,35
4,0	4,7	1,58	1,40	1,75	2,50	0,90	0,70	3,40	0,35
4,5	5,2	1,53	1,35	1,70	2,30	1,25	0,70	3,55	0,35
5,0	5,7	1,53	1,35	1,70	2,30	1,60	0,70	3,90	0,35
5,5	6,2	1,49	1,25	1,55	2,10	1,75	0,60	3,85	0,35
6,0	6,7	1,44	1,20	1,50	1,85	1,95	0,55	3,80	0,35
6,5	7,2	1,44	1,20	1,50	1,85	2,20	0,55	4,05	0,35
7,0	7,8	1,40	1,15	1,40	1,75	2,35	0,50	4,10	0,36
7,5	8,3	1,35	1,05	1,30	1,60	2,10	0,40	3,70	0,36
8,0	8,8	1,35	1,00	1,25	1,60	2,10	0,40	3,70	0,36
8,5	9,3	1,31	1,00	1,25	1,40	2,40	0,40	3,80	0,36

Tabla de perforación y carga para diámetro del taladro de 45 mm.

Inclinación del taladro: 3:1.

Altura de banco K m	Profundidad taladro H m	Piedra máxima V_{max} m	Piedra práctica V_t m	Espaciamiento práctico E_t m	Carga de fondo Q_b kg	Carga de columna Q_p kg	Carga de columna Q_{pk} kg/m	Carga total Q_{tot} kg/barreno	Carga específica q kg/m³
1,0	1,4	1,00	0,80	1,00	0,40	—	—	0,40	0,50
2,0	2,4	1,00	1,00	1,25	0,55	0,40	0,50	0,95	0,33
3,0	3,6	1,50	1,35	1,65	1,05	0,60	0,60	2,65	0,39
4,0	4,8	2,03	1,80	2,25	5,20	0,40	1,00	5,60	0,35
5,0	5,9	2,03	1,80	2,25	5,20	1,50	1,00	6,70	0,33
6,0	6,9	2,03	1,75	2,15	5,20	2,50	1,00	7,70	0,34
7,0	8,0	2,03	1,70	2,10	5,20	3,50	1,00	8,80	0,35
8,0	9,0	2,03	1,70	2,10	5,20	4,60	1,00	9,80	0,34

Tabla de perforación y carga para diámetro del taladro de 48 mm.

Inclinación del taladro: 3:1.

Altura de banco K m	Profundidad taladro H m	Piedra máxima V_{max} m	Piedra práctica V_t m	Espaciamiento práctico E_t m	Carga de fondo Q_b kg	Carga de columna Q_p kg	Carga de columna Q_{pk} kg/m	Carga total Q_{tot} kg/barreno	Carga específica q kg/m³
1,0	1,4	1,00	0,80	1,00	0,40	—	—	0,40	0,50
2,0	2,4	1,00	1,00	1,25	0,55	0,50	0,50	1,05	0,42
3,0	3,6	1,50	1,35	1,65	2,05	0,70	0,70	2,75	0,41
4,0	4,8	2,00	1,80	2,25	5,20	0,40	1,00	5,60	0,35
5,0	5,9	2,16	1,90	2,35	6,45	1,40	1,15	7,85	0,35
6,0	7,0	2,16	1,90	2,35	6,45	2,65	1,15	9,10	0,35
7,0	8,1	2,16	1,85	2,30	6,45	3,90	1,15	10,35	0,35
8,0	9,1	2,16	1,80	2,25	6,45	5,05	1,15	11,50	0,35
9,0	10,1	2,16	1,75	2,15	6,45	6,20	1,15	12,65	0,37
10,0	11,2	2,16	1,75	2,15	6,45	7,45	1,15	13,90	0,37

Tabla de perforación y carga para diámetro del taladro de 51 mm.
Inclinación del taladro: 3:1.

Altura de banco K m	Profundidad taladro H m	Piedra máxima V_{max} m	Piedra práctica V_t m	Espaciamiento práctico E_t m	Carga de fondo Q_b kg	Carga de columna Q_p kg	Carga de columna Q_{pk} kg/m	Carga total Q_{tot} kg/barreno	Carga especifica q kg/m³
1,0	1,4	1,00	0,80	1,00	0,40	—	—	0,40	0,50
2,0	2,4	1,00	1,00	1,25	0,55	0,50	0,60	1,05	0,42
3,0	3,6	1,50	1,50	1,65	2,10	0,70	0,70	2,80	0,41
4,0	4,8	2,00	1,80	2,25	5,20	0,40	1,00	5,60	0,35
5,0	6,0	2,30	2,10	2,60	7,80	1,30	1,30	9,10	0,33
6,0	7,0	2,30	2,05	2,55	7,80	2,50	1,30	10,30	0,33
7,0	8,1	2,30	2,00	2,50	7,80	4,00	1,30	11,80	0,34
8,0	9,1	2,30	2,00	2,50	7,80	5,30	1,30	13,10	0,33
9,0	10,2	2,30	1,95	2,40	7,80	6,80	1,30	14,60	0,35
10,0	11,2	2,30	1,90	2,35	7,80	8,20	1,30	16,00	0,36
12,0	13,3	2,30	1,85	2,30	7,80	11,00	1,30	18,80	0,37
14,0	15,4	2,30	1,80	2,25	7,80	13,80	1,30	21,60	0,39

En el caso de voladuras de hileras múltiples con barrenos sujetos a constricción, es necesario incrementar la carga; igualmente sucede, si no se realiza el desescombro entre voladuras (ver Sección titulada Esponjamiento).

Los valores de las tablas se han determinado, suponiendo que la carga de fondo tiene un grado de retacado de 1,25 Kg/dm³, lo que significa que debe utilizarse una cargadora neumática. En el caso de bancos bajos es preferible la utilización de barrenos de pequeño diámetro, pero por razones prácticas se han incluido en la tabla anterior. La voladura de banco bajos, debido a la concentración de carga en el fondo, no deben realizarse con diámetros grandes cuando existe riesgo de proyección.

Tabla de perforación y carga para diámetro del taladro de 64 mm.
Inclinación del taladro: 3:1.

Altura de banco K m	Profundidad taladro H m	Piedra máxima V_{max} m	Piedra práctica V_t m	Espaciamiento práctico E_t m	Carga de fondo Q_b kg	Carga de columna Q_p kg	Carga de columna Q_{pk} kg/m	Carga total Q_{tot} kg/barreno	Carga especifica q kg/m³
2,0	2,4	1,00	1,00	1,25	0,60	0,50	0,60	1,10	0,48
3,0	3,6	1,50	1,35	1,65	2,10	1,00	0,30	3,10	0,46
4,0	4,8	2,00	1,80	2,25	5,20	1,50	0,90	6,70	0,41
5,0	6,0	2,50	2,20	2,75	7,80	2,70	1,50	10,50	0,35
6,0	7,2	2,88	2,60	3,25	15,30	1,70	2,00	17,00	0,34
7,0	8,3	2,88	2,55	3,20	15,30	4,00	2,00	19,30	0,34
8,0	9,3	2,88	2,55	3,20	15,30	6,00	2,00	21,30	0,33
9,0	10,4	2,89	2,50	3,10	15,30	8,30	2,00	23,60	0,34
10,0	11,4	2,88	2,50	3,10	15,30	10,30	2,00	25,60	0,33
11,0	12,5	2,88	2,45	3,05	15,30	12,60	2,00	27,90	0,34
12,0	13,5	2,88	2,40	3,00	15,30	14,70	2,00	30,00	0,35
13,0	14,6	2,88	2,40	3,00	15,30	16,70	2,00	32,00	0,34
14,0	15,6	2,89	2,35	2,90	15,30	19,00	2,00	34,30	0,36
15,0	16,7	2,98	2,30	2,85	15,30	21,30	2,00	36,60	0,37

La voladura de bancos bajos por debajo de $2 \times V_{max}$ de altura no se recomienda con grandes diámetros, debido al control de la misma; no obstante, por razones prácticas los bancos bajos son volados frecuentemente con grandes diámetros y por esta rezón estos casos se incluyen en las tablas. El riesgo de proyección es relativamente grande y por tal motivo la voladura de bancos bajos con grandes diámetros debe realizarse solamente cuando no existan exigencias que limiten las proyecciones.

Tabla de perforación y carga para diámetro de taladro de 75 mm.

Inclinación del taladro: 3:1.

Altura de banco K m	Profundidad taladro H m	Piedra máxima V_{max} m	Piedra práctica V_t m	Espaciamiento práctico E_t m	Carga de fondo Q_b kg	Carga de columna Q_p kg	Carga de columna Q_{pk} kg/m	Carga total Q_{tot} kg/barreno	Carga especifica q kg/m³
4	4,8	2,00	1,80	2,25	5,20	2,50	1,20	7,80	0,48
5	6,0	2,50	2,20	2,75	7,80	5,60	2,00	13,40	0,44
6	7,2	3,00	2,60	3,25	15,30	4,70	2,60	20,00	0,39
7	8,5	3,37	3,00	3,75	24,60	2,10	2,80	26,70	0,34
8	9,6	3,37	3,00	3,75	24,60	6,20	2,80	30,80	0,34
9	10,6	3,37	3,00	3,75	24,60	9,00	2,80	33,60	0,33

Altura de banco K m	Profundidad taladro H m	Piedra máxima V_{max} m	Piedra práctica V_t m	Espaciamiento práctico E_t m	Carga de fondo Q_b kg	Carga de columna Q_p kg	Q_{pk} kg/m	Carga total Q_{tot} kg/barreno	Carga específica q kg/m³
10	11,7	3,37	2,95	3,70	24,60	12,20	2,80	36,80	0,34
11	12,7	3,37	2,90	3,60	24,60	15,10	2,80	39,70	0,35
13	14,8	3,37	2,85	3,55	24,60	21,10	2,80	45,70	0,35
14	15,9	3,37	2,80	3,50	24,60	24,40	2,80	49,00	0,36
15	16,9	3,37	2,80	3,50	24,60	27,20	2,80	51,80	0,35
16	18,0	3,37	2,75	3,45	24,60	30,40	2,80	55,00	0,36
17	19,0	3,37	2,75	3,40	24,60	33,20	2,80	57,80	0,36
18	20,0	3,37	2,70	3,35	24,60	36,10	2,80	60,70	0,37
19	21,1	3,37	2,70	3,30	24,60	38,90	2,80	63,50	0,37
20	22,2	3,37	2,65	3,30	24,60	42,40	2,80	67,00	0,38

En el caso de grandes alturas de bancos, existe una gran diferencia entre una voladura de dos filas en una cantera y una voladura en cuele, donde la roca esté sujeta a gran constricción (ver Sección 5.3 Esponjamiento).

Tabla de perforación y carga para diámetro de taladro de 100 mm.

Inclinación del taladro: 3:1.

Altura de banco K m	Profundidad taladro H m	Piedra máxima V_{max} m	Piedra práctica V_t m	Espaciamiento práctico E_t m	Carga de fondo Q_b kg	Carga de columna Q_p kg	Q_{pk} kg/m	Carga total Q_{tot} kg/barreno	Carga específica q kg/m³
10	11,7	4,50	4,00	5,00	58,00	9,00	5,00	67,00	0,33
12	14,0	4,50	4,00	5,00	58,00	21,00	5,00	79,00	0,33
15	17,2	4,50	3,90	4,85	58,00	37.50	5,00	95,50	0,34
20	22,4	4,50	3,80	4,75	58,00	69,00	5,00	127,00	0,35
25	27,7	4,50	3,60	4,50	58,00	89,00	5,00	147,00	0,36
30	22,9	4,50	3,50	4,35	58,00	118,00	5,00	176,00	0,38

La elección de la carga específica depende frecuentemente de la fragmentación deseada. Puede ser económico utilizar en canteras cargas específicas del orden de 0,50 Kg/m³.

La elección de una carga específica baja del orden de 0,20 a 0,25 Kg/m³ era una costumbre muy extendida antiguamente y que aún se practica en la actualidad, lo que lleva consigo que la *piedra* en el fondo no se desprende totalmente, siendo necesario ayudar a este desprendimiento mediante tiros horizontales o voladuras suplementarias.

Desde el punto de vista económico es importante estudiar todos los factores que intervienen, al planificar los trabajos.

Tabla de perforación y carga para diámetro de taladro de 250 mm.

Inclinación del taladro: 3:1.

Altura de banco K m	Profundidad taladro H m	Piedra máxima V_{max} m	Piedra práctica V_t m	Espaciamiento práctico E_t m	Carga de fondo Q_b kg	Carga de columna Q_p kg	Q_{pk} kg/m [1]	Carga total Q_{tot} kg/barreno	Carga específica q kg/m³
15	18,1	7,5	6,9	8,6	430	70	17	500	0,56
20	24,1	10,0	9,2	11,5	625	150	30	775	0,37
25	29,8	11,2	10,3	12,9	910	260	38	1170	0,37

[1]) Los cálculos de concentración de la carga de columna han sido incrementados desde el valor del 50 % al de 60 % de la concentración de la carga de fondo para compensar el esponjamiento en el caso de *piedras* tan elevadas. Si se pretende obtener una buena fragmentación, la práctica aconseja elevar la carga de columna para obtener una carga específica mayor.

Hay que observer que la *piedra* máxima teórica no se alcanza hasta una altura de banco de 25 m. En caso de bancos menores, por ejemplo, 15 m., hay que considerarlo como banco bajo, si se trata de utilizar al máximo el diámetro de perforación.

Cuando se utiliza Reolit A, el taladro es llenado por completo, resultando una elevada concentración de carga, tanto en el fondo como en la columna; ésto significa que en voladuras de bancos de 15 m. se puede diseñar un esquema de 8 × 10 m. que es considerablemente mayor que el reflejado en la tabla.

Los explosivos, tipo Slurries, pueden considerarse más rentables para utilizarlos con estos grandes diámetros de perforación, dado que la carga se efectúa rápidamente bombeando el explosivo en el interior de los barrenos.

5.2 FRAGMENTACION

El término fragmentación se utiliza en relación con el tamaño de los bloques despues de volar la roca, si bien, al no existir un criterio generalizado de medida, no es sencillo definirla con más detalle. En muchos casos este término se utiliza en relación con el tamaño medio y otras veces viene referido al tamaño mayor de los bloques.

Existe una teoría, basada más en la fé que en la ciencia, según la cual, la velocidad de detonación puede muy bien ser de la misma magnitud que la velocidad con la cual se propaga la onda de choque a través de la roca. Esto significaría que una velocidad alta de detonación sería favorable en el caso de rocas duras. De acuerdo con esta teoría, el explosivo, tipo Dynamex, es adecuado para estas rocas.

El tamaño de la roca es un factor muy importante y ejerce gran influencia sobre los trabajos posteriores a la voladura, tanto desde el punto de vista práctico como económico (ver Sección 5.8 Estudio económico de voladuras).

Por ejemplo, en el caso de voladuras en cantera, la fragmentación está influenciada por los siguientes factores:

Número de bloques por unidad de volumen.
Capacidad de machaqueo.
Capacidad de desescombro.
Desgaste de máquinas y materiales

No es exagerado decir que la fragmentación es el factor más importante en toda voladura de producción.

El Departamento sueco de Centrales Hidroeléctricas ha desarrollado un sistema para su definición, mediante un *coeficiente de fragmentación*.

El coeficiente de fragmentación relativa se define como el tamaño de malla, en relación con una cierta abertura a través de la cual puede pasar el 50 % del material. El método de medida requiere una descripción más detallada, por lo que aquí se menciona como idea general.

Langefors ha establecido la posibilidad de medir el volumen de los bloques más grandes, obteniendo así una medida relativa de la fragmentación.

El estudio de voladuras por medio de fotografías tomadas durante diferentes fases, permite determinar gráficamente la distribución de la fragmentación.

Con objeto de determinar con mayor exactitud la influencia que ciertos factores tienen sobre la fragmentación, deben realizarse estudios muy amplios; más adelante, y en relación con este aspecto, se indican ciertos métodos destinados a mejorar la fragmentación y que han sido llevados a la práctica desde hace algunos años.

La dificultad de obtener una relación entre la fragmentación por un lado y la perforación y carga por otro, es debida al gran número de variables que intervienen en la práctica. La composición de la roca y la aparición de grietas, fallas y zonas débiles tienen gran influencia, así como la forma de utilización del explosivo y sus características, ya que un explosivo que produzca buenos resultados en roca sana y homogénea puede no ser efectivo en rocas blandas y fisuradas.

Tipo de roca	Velocidad propagación de onda de choque m/seg.	Explosivo	Velocidad de detonación m/seg.
Granito homogéneo, Gneis	5.000—6.000	Dynamex	5.500
Caliza dura	3.000—4.500	Nabit	3.500
Caliza blanda	1.000—2.500	Prillit	2.400

Desde que estas ideas fueron adelantadas en la primera edición, 1.972, en los Estados Unidos se han desarrollado ampliamente los trabajos de investigación para determinar la relación entre la velocidad de detonación de un explosivo y la velocidad de propagación de la onda de choque, desde el punto de vista del efecto explosivo. Los resultados indican que es ventajoso, si ambos valores están próximos.

El contenido energético y el volumen de gases tienen gran importancia desde el punto de vista del efecto explosivo (ver Sección 3, Explosivos). Debe recordarse también que los explosivos lentos son ricos en gases, lo cual es una ventaja en el caso de rocas fisuradas. Cuando se utilizan diferentes tipos de explosivos conviene señalar que el *poder de un explosivo por unidad de peso* es importante y no debe olvidarse al comparar sus efectos.

En rocas fisuradas las voladuras deben ser planificadas cuidadosamente, teniendo en cuenta la dirección de la estratificación.

En el caso de estratificación tendiendo a la horizontalidad, es ventajoso que la inclinación de los taladros permita atravesar los planos de contacto de los estratos; de esta forma el explosivo actúa en mejores condiciones.

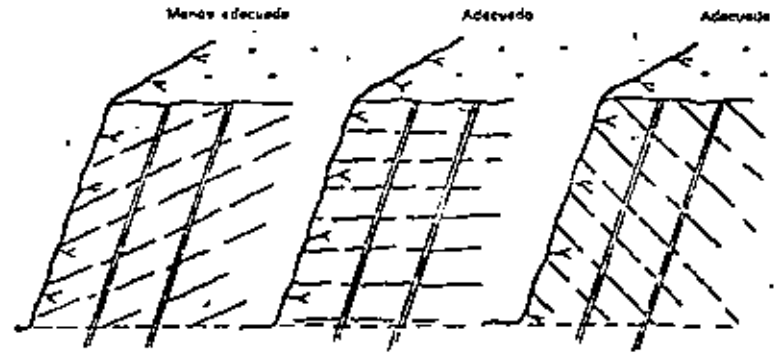

Fig. 5.2.1

Si la estratificación tiende a la verticalidad, es preferible disponer las voladuras de forma que la *piedra* rompa en ángulo recto con su dirección; en

estos casos es frecuente obtener una rotura irregular en el fondo. No obstante, este criterio no es aplicable a todos los casos, ya que a veces se han obtenido excelentes resultados con barrenos dispuestos de forma que la *piedra* rompa en la dirección de los estratos.

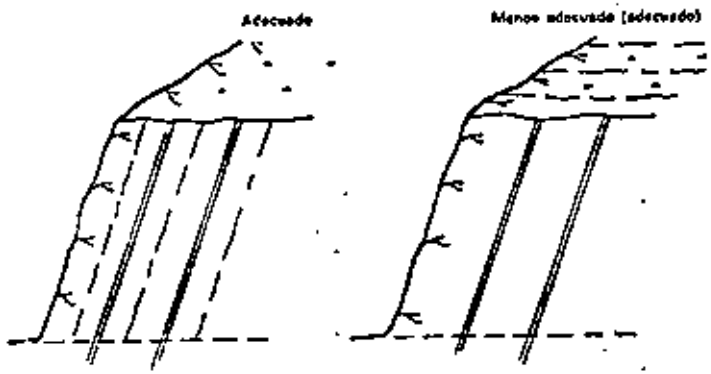

Fig. 5.2.2

La composición de la roca tiene gran influencia en la fragmentación, al variar sus características resistentes. Muchos tipos de roca se fragmentan como terrones de azucar, aunque la carga varie considerablemente. En otros casos no se obtiene el grado deseado de rotura, a pesar de utilizar grandes cargas.

Los factores que tienen mayor influencia bajo el punto de vista de la técnica de voladuras son:

La carga específica.
La perforación específica.

Un incremento de la carga específica, manteniendo constante el esquema de perforación, produce un aumento de la fragmentación y, dado que normalmente se desea utilizar al máximo los barrenos, frecuentemente se incrementa la carga de columna.

En un barreno se distinguen tres zonas que tienen gran influencia en la fragmentación:

Carga de fondo.
Carga de columna.
Retacado.

La zona de carga de fondo tiene una carga específica tan elevada y el explosivo actua en tan buena disposición, que la fragmentación es normalmente muy satisfactoria. No obstante, si la estratificación es muy acusada, puede dar origen a la formación de bloques. En las zonas más próximas al taladro, donde la presión es superior a la resistencia a la compresión, la roca llega a pulverizarse.

Ejemplo

Diámetro del barreno mm	Concentración de carga Kg/m	Sección circular quebrantada mm diam.
30	0,9	35
50	2,5	70
100	10,0	150

Las cifras que indica la tabla se han basado en un tipo de roca de gran resistencia. En rocas menos resistentes la zona quebrantada es mayor, pero sin llegar a pulverizarse completamente.

En la zona de carga de columna el quebrantamiento producido es menor, debido a que la concentración de carga y la constricción de los barrenos son más reducidas.

Al aumentar la concentración de carga aumenta también la tensión sobre la roca y por esta razón la fragmentación es mayor (ver el diagrama).

Si la roca fuera completamente homogénea, ésto es, sin fallas, grietas o fisuras, la fragmentación podría ser calculada entonces con gran exactitud. El diagrama 5.2.3 proporciona valores indicativos, ya que las características de la roca varian de un caso a otro. No obstante, el gráfico puede proporcionar una idea relativa de fragmentación, puesto que puede preverse que la relación es análoga para diferentes tipos de roca con un desplazamiento de valores. La representación gráfica es mas bien un conjunto de líneas curvas en lugar de las rectas que se observan en el diagrama.

La zona de retacado tiene un efecto desfavorable en la fragmentación. Los barrenos con grandes retacados son propensos a producir bloques.

Las medidas que pueden tomarse para mejorar los resultados son las siguientes:

Una longitud mayor de carga de columna.
Ejecución de barrenos auxiliares en la zona de retacado.

Cargas más altas de las normalmente recomendadas requieren mayor superficie de evacuación. En ciertos casos la colocación de pequeñas cargas de explosivo en la zona de retacado puede favorecer la fragmentación.

Una estimación de la longitud del retacado puede realizarse en base a la concentración de carga utilizada.

Concentración de carga en la carga de columna extra. Kg/m	Tipo de carga	Retacado necesario m
1,00	29 mm Dyn	1,80
0,65	25 mm Dyn	1,50
0,50	22 mm Dyn	1,40
0,40	22 mm Nabit	1,25
0,16	17 mm Gurit	0,80

En el caso de *piedras* mayores de 3 m, es difícil obtener buenos resultados con la intercalación de cargas en la zona de retacado, dado que normalmente éstas son demasiado débiles en relación con el volumen de roca existente entre taladros.

La perforación de barrenos auxiliares favorece la fragmentación, pero, análogamente al caso anterior, si la distancia entre barrenos es grande, este efecto no se produce; por otro lado una perforación excesiva es antieconómica y en muchos casos es más rentable el tolerar un cierto número de bloques.

La perforación específica es de gran importancia en la fragmentación. El diagrama 5.2.3 muestra que con una misma carga específica la fragmentación disminuye al aumentar la *piedra*.

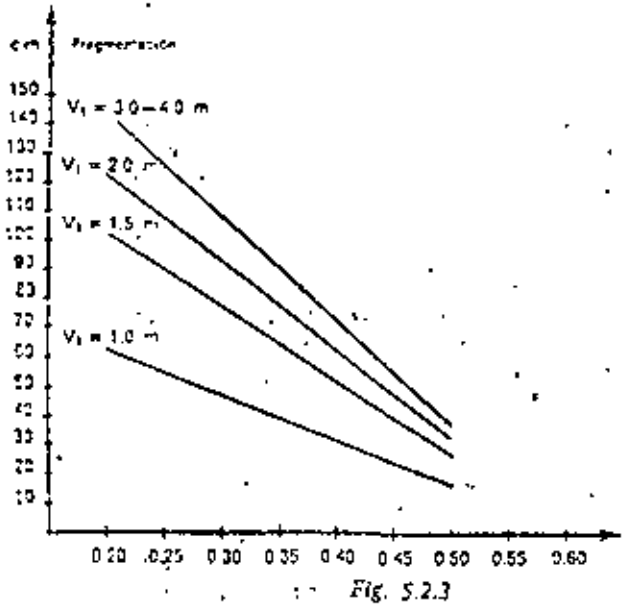

Fig. 5.2.3

En el caso de *piedras* pequeñas la distribución de la carga es mejor y la posibilidad de formación de bloques está limitada por el especiamiento entre barrenos. La utilización de grandes diámetros con cargas concentradas produce gran proporción de material fragmentado, pero también se obtienen bloques de gran tamaño.

La fragmentación es mayor cuando se utilizan diámetros pequeños.

El diagrama muestra así mismo que en el caso de *cargas límites* existe la mayor diferencia entre las distintas *piedras*, y que, a mayor carga específica, mayor es la fragmentación.

Además de la carga específica, la precisión en la perforación es de gran importancia, ya que, si los barrenos están mal distribuídos o los errores de perforación son elevados, entonces la fragmentación es considerablemente menor.

Los diagramas 5.2.4 y 5.2.7 indican los resultados de los trabajos realizados por Bernt Larsson para determinar la relación existente entre la carga específica y la influencia en la fragmentación de la perforación específica. Larsson ha incluído también las constantes de la roca, relativas a la voladura, así como sus características desde el punto de vista de la fragmentación.

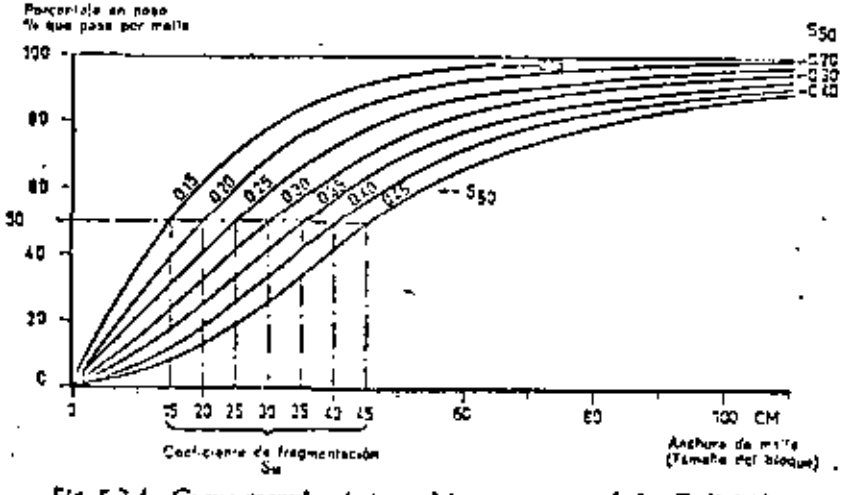

Fig. 5.2.4 Curva granulométrica teórica para roca volada. Definición del coeficiente de fragmentación S_{50}

El diagrama 5.2.4 es muy interesante e indica la curva granulométrica o curva de fragmentación para una voladura en banco, que, de acuerdo con Larsson, siempre tiene una forma parecida a la representada.

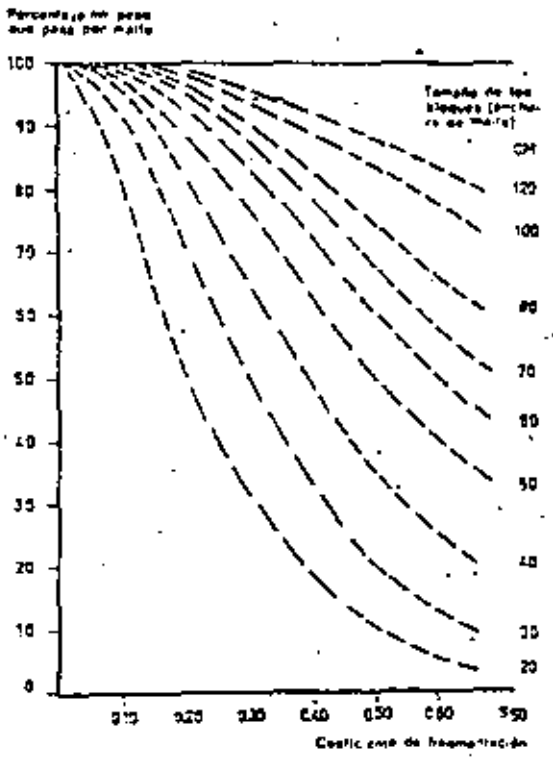

Fig. 5.2.5 Fragmentación teórica obtenida en una voladura, en función del coeficiente de fragmentación S_{50}

Los diagramas 5.2.5 y 5.2.6 proporcionan una idea más clara del concepto de fragmentación a través del coeficiente de fragmentación, ofreciendo en la práctica buenas posibilidades para determinar que coeficiente debe ser elegido para obtener el mejor resultado posible.

En el completo diagrama 5.2.7 Larsson ha reunido las cargas específicas de uso más corriente, mientras que el diagrama 5.2.3 proporciona los datos necesarios al utilizar cargas específicas comprendidas entre 0,20 y 0,30 Ke/m³ en voladuras de hileras múltiples.

El ejemplo que Larsson representa en el diagrama 5.2.7 da un coeficiente de fragmentación de 0,26. Si el mismo ejemplo se representa en el diagrama 5.2.3 de Gustafsson, se obtiene un resultado de 0,29 aproximadamente, lo

cual coincide prácticamente en el intervalo 0,40—0,50 Kg/m³, aunque el diagrama 5.2.3 en su conjunto de valores más elevados.

Una vez más debe subrayarse que los diagramas de fragmentación son módulos que a través de su diseño dan la posibilidad de controlar la influencia de la carga y del esquema en la fragmentación.

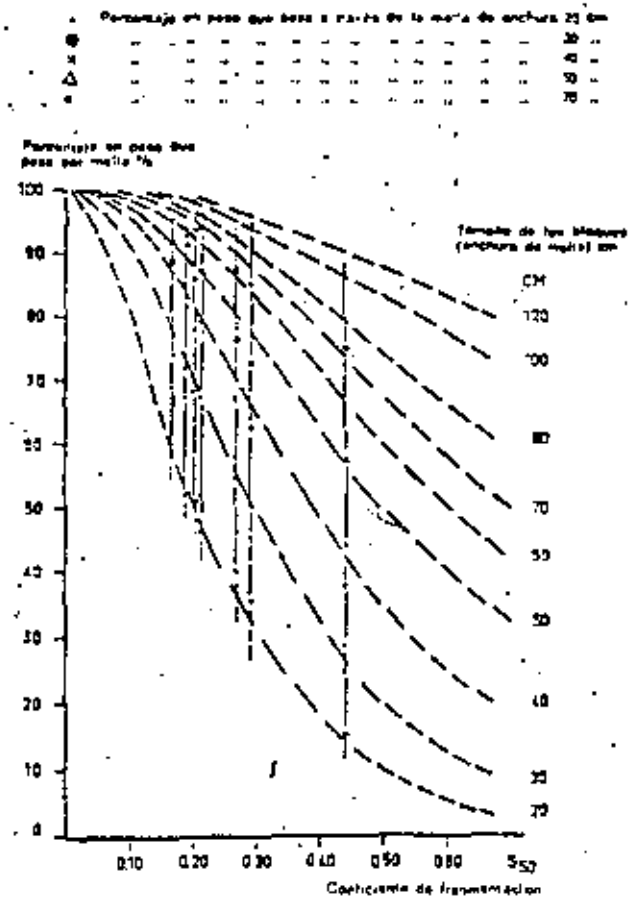

Fig. 5.2.6 Distribución de la fragmentación en voladuras en función del coeficiente de fragmentación S_{50}

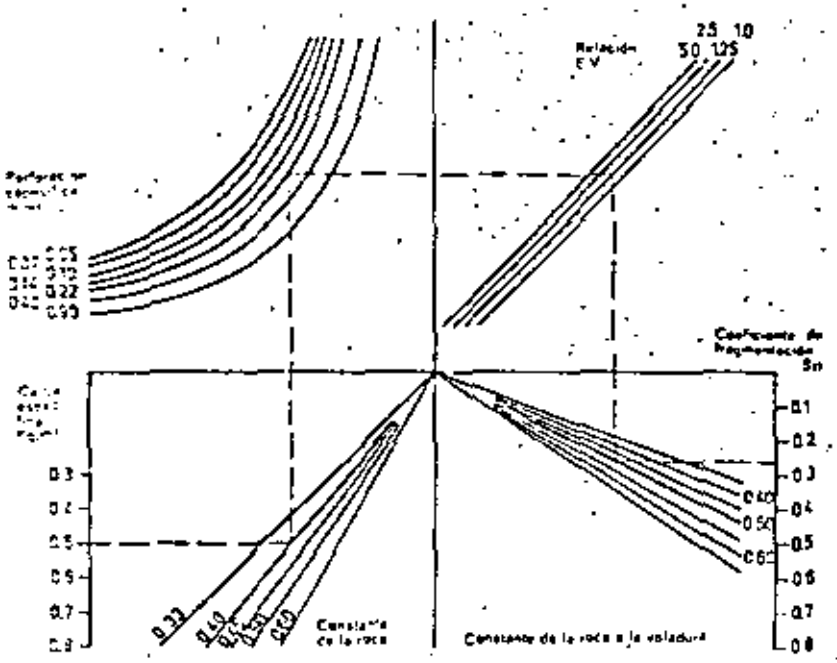

Fig. 5.2.7 Cálculo del coeficiente de fragmentación S_m basado en los datos técnicos de la voladura

Efecto de la secuencia de encendido y del tiempo de intervalo en la fragmentación

El tiempo de intervalo ejerce gran efecto en el proceso de voladura y por esta razón es muy importante desde el punto de vista de la fragmentación.

En el caso de *piedras* pequeñas la roca se desplaza hacia adelante más rápidamente; si los tiempos de retardo son pequeños, la roca no tiene posibilidad de desplazarse antes de que detonen las cargas en los barrenos adyacentes. Esto puede constituir una ventaja cuando la roca está fisurada, pero por otro lado existe el riesgo de que la roca rompa por sus planos naturales, sin que los gases del explosivo tengan la posibilidad de actuar suficientemente. Los intervalos de tiempo demasiado cortos entre barrenos adyacentes pueden impedir que la roca disponga de tiempo para su esponjamiento, dificultando la salida de las siguientes hileras. La roca se desplaza más lentamente en el caso de grandes *piedras* y ésto significa que el tiempo disponible para la formación de grietas y la penetración de los gases es tambien mayor.

En su libro "Rock Blasting" Langefors establece la siguiente relación:

$t = K\ V$

donde K es una constante de magnitud 3—5.

t = tiempo de retardo en milisegundos

La experiencia obtenida por Jenelid indica que el valor de 5 es válido para la constante en el caso de grandes *piedras* (5—8 m).

En nuestra opinión consideramos que esta relación es más adecuada para la voladura de una o posiblemente dos hileras. En el caso de voladuras de hileras múltiples es más adecuada la siguiente:

$t = K\ V$

donde K es aproximadamente 12.

El efecto del tiempo de retardo en una voladura puede ser estudiado a través de películas de diferentes procesos, así como por comparación de diferentes secuencias de encendido.

Métodos especiales para mejorar la fragmentación

La Swedish Detonic Research Foundation, en base a los modelos de plástico de Langefors, comenzó una serie de pruebas en granito homogéneo, bajo la dirección P. A. Persson, en las cuales se estudió la influencia del espaciamiento en la fragmentación.

La teoría básica indica que un cambio en la relación entre *piedra* y espaciamiento, desde su valor normal E/V = 1,25 a valores considerablemente más elevados, mejoraría la fragmentación. Los resultados de las pruebas demostraron que con la perforación y carga específica constantes, la fragmentación crecía significativamente cuando la relación E/V se incrementaba hasta valores de E/V = 8.

Desde entonces el método ha sido tratado a mayor escala en una cantera experimental, obteniéndose buenos resultados, que continúan en la actualidad.

El planteamiento del esquema y la secuencia de encendido debe ser llevada a cabo, teniendo en cuenta ciertos factores; el esquema en la primera fila debe ser realizado de forma normal, ya que pueden existir barrenos con *piedras* muy pequeñas, incrementando el riesgo de proyección. Este método implica una cierta anchura de banco, si se pretende que sea práctica su utilización.

La figura representada a continuación muestra un esquema de perforación, y encendido con un espaciamiento amplio entre barrenos.

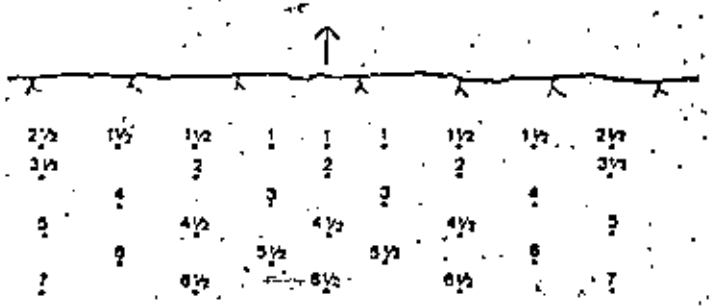

Fig. 5.2.8

Resultados obtenidos:

Método	Zona de voladura	Número de pegas	Perforación específica media m/m³	Carga específica media Kg/m³	Promedio de bloques/ 1000 m³	Promedio de carga Tm/día
Convencional	I	7	0,17	0,53	121	—
Espaciamiento amplio	I	3	0,15	0,48	63	—
Convencional	II	6	0,16	0,49	169	1.550
Espaciamiento amplio	II	6	0,18	0,63	97	1.988

(Tabla obtenida de una conferencia dada por el Dr. P. A. Persson, Swedish Detonic Research Foundation.)

Métodos para la obtención de bloques de gran tamaño

En cierto tipo de obras, para la construcción de puertos, escolleras, etc. se necesita obtener menor fragmentación, debido a la demanda de bloques de determinado tamaño.

La dificultad de obtener menor fragmentación puede ser muchas veces análoga a la necesaria para la obtención de bloques de tamaño pequeño, siendo la roca con sus características la que normalmente es culpable de esta dificultad. Si la roca es homogénea, la obtención de grandes bloques es con frecuencia más sencilla.

Existen algunos métodos para conseguir menor fragmentación:

Carga específica baja
Espaciamiento desfavorable para la rotura, E/V menor de 1
Voladura instantánea
Voladura de una hilera cada vez
Combinación de estos métodos, dependiendo de las circunstancias.

Una carga específica baja, en el límite necesario para la rotura de la piedra, produce normalmente grandes bloques. El diagrama indica que, cuando la carga de columna se disminuye, el tamaño de los fragmentos aumenta en gran manera. Si la voladura se realiza con valores límites de carga específica de 0,20—0,25 Kg/m³ total, es preferible realizar voladuras de una sola hilera, debiendo admitirse que en el fondo será necesario realizar alguna voladura secundaria.

Si se elige la piedra de forma que sea considerablemente mayor que el espaciamiento, los bloques obtenidos serán mayores. Las líneas de tensión resultantes en la roca se distribuyen con más facilidad hacia la parte superior entre los barrenos, obteniéndose un efecto análogo al del recorte, cuando E/V adopta un valor de 0,8. En este caso particular que estamos considerando, un valor más favorable para la relación E/V es el de 0,5 aproximadamente.

Ejemplo: Voladura en banco utilizando barrenas de la serie 12.
$V_1 \times E_1 = 1{,}2 \times 1{,}5$ m. $E/V = 1{,}25$

En el caso de querer obtener grandes tamaños, el esquema debe modificarse a
$V_1 \times E_1 = 2{,}0 \times 0{,}9$ m. $E/V = 0{,}45$

Las voladuras instantáneas proporcionan normalmente tamaños mayores que las de microretardo, ya que existe menor efecto de rotura entre barrenos; la combinación de este sistema con el anterior, es decir, con la relación E/V = 0,5 aproximadamente, da excelentes resultados.

5.3 ESPONJAMIENTO

En la Sección Cálculo de la Carga se menciona en varios sitios la necesidad de una carga extra debido al esponjamiento. Cuando la roca ha sido volada necesita mayor espacio que cuando se encontraba en su estado natural. Si no se dispone de dicho espacio, delante o a un lado de la zona que se va a volar, la roca se ve forzada hacia la superficie libre superior, pudiendo tambien suceder que se comprima contra la roca procedente de voladuras anteriores.

Cuando se realiza una voladura con fondo encerrado, existe mayor fricción entre la superficie del fondo y las paredes laterales.

Los diferentes tipos de voladura en los que hay que tener en cuenta el esponjamiento son los siguientes:

Voladuras en banco con frentes estrechos y de mucha profundidad
Voladuras sucesivas en banco sin desescombro intermedio
Voladuras en zanja
Voladuras en túnel
Voladuras por subniveles (sub-level caving)

En los cálculos de carga utilizados normalmente para las voladuras en zanja y en túneles se incluye una sobrecarga suficiente y necesaria para el esponjamiento, basada en experiencias adquiridas en trabajos realizados. Las dificultades para estimar diversos factores, especialmente dicha sobrecarga, han complicado el proceso de cálculo en muchos casos.

Debido a que en las voladuras en banco los factores que afectan el proceso son más sencillos de calcular, la determinación de la carga se ha centrado en este tipo de voladura. Conviene subrayar que las tablas de cálculo llevan incluida esta sobrecarga.

La compensación de carga necesaria debida al error de perforación, debe tenerse en cuenta, aunque en la práctica se realice una perforación muy exacta, sobre todo en bancos de hileras múltiples con barrenos profundos, con el fin de compensar el esponjamiento.

Los distintos tipos de roca presentan así mismo diferentes grados de esponjamiento, particularmente las rocas blandas tienen menor grado, lo que hace que en ciertas condiciones sean difíciles de volar.

Cuando en este capítulo se hace mención de la carga necesaria para el esponjamiento, se refiere a los casos en los cuales los cálculos normales de la misma no son suficientes. Los tiempos de retardo y la secuencia de encendido tienen una influencia considerable en el esponjamiento de una voladura. Cuando las condiciones son tales que el fondo se halla sujeto a constricción, los tiempos de retardo excesivamente cortos pueden contrarrestar el efecto de esponjamiento, debido a que la roca no tiene tiempo para desplazarse suficientemente hacia adelante y dejar espacio a la roca procedente de la siguiente hilera.

Por otra parte, tiempos de retardo excesivamente largos, principalmente entre barrenos de la misma hilera, pueden ser desfavorables desde el punto de vista de rotura de la *piedra*. Si el retardo entre barrenos adyacentes es demasiado grande, no existe colaboración entre ellos para el lanzamiento de la roca hacia adelante (Ver tambien la sección titulada "Fragmentación").

La inclinación de los taladros tiene así mismo gran importancia en el esponjamiento. Por razones naturales un taladro inclinado proporciona mayor fuerza de levantamiento de la roca que uno vertical; siendo muchas veces totalmente inapropiada su utilización en casos donde el fondo está sometido a fuerte constricción.

Langefors ha desarrollado cálculos teóricos sobre la fuerza de levantamiento de los explosivos al variar la inclinación del barreno. Los cálculos se basaron en una energía específica del explosivo de 500 Tm m/kg y se estimó que 80 Tm m/kg eran necesarias para el desplazamiento de la roca; con una dirección de proyección del 2:1, el 20 % de la energía se asociará con el componente del levantamiento.

La carga específica adicional necesaria en el fondo del barreno para obtener un esponjamiento suficiente es equivalente a 0,04 × altura del banco (K).

Con menor inclinación, la carga requerida para el esponjamiento aumenta rápidamente y, según Langefors, se llega al valor de 0,09 × K con una inclinación del 3:1.

La siguiente fórmula, adquirida con la práctica, nos indica la carga específica que se necesita en una voladura en banco cuando no se realiza el desescombro de la voladura anterior.

$$q_{esponj} = q_{normal} + 0{,}03\ (K - 2 \times V_{max}) + \frac{0{,}40}{B}$$

Se observa en esta relación que la compensación de carga, debida al esponjamiento, no se aplica en bancos menores de $2 \times V_{max}$.

La aplicación de este fórmula es de gran interés en la ejecución de zanjas, ya que la influencia del factor $\frac{0{,}40}{B}$ es importante.

En los casos donde el frente de voladura es muy estrecho en relación con el diámetro de perforación, la expresión $\frac{0{,}40}{B}$ puede ser remplazada por

$$\frac{0{,}40}{\text{No. de taladros/fila} - 1}$$

Ejemplo 1. Se necesita realizar una excavación en trinchera mediante voladuras sucesivas, sin efectuar desescombro entre ellas.

Datos:

K = 12 m

d = 64 mm

$q_{tabla} = 0{,}35$ kg/m³

$q_{normal} = 0{,}39$ kg/m³

B = 27 m

$$q_{normal} = 0{,}39 + 0{,}03\ (12 - 2 \times 2{,}88) + \frac{0{,}40}{27}$$

$$q_{normal} = 0{,}39 + 0{,}19 + 0{,}01 = \underline{0{,}59\ \text{kg/m}^3}$$

Ejemplo 2. Se quiere realizar una excavación de frente muy estrecho, perforando con barrenas de la serie 12, mediante voladuras sucesivas, sin efectuar desescombro entre ellas.

Datos:

K = 7 m

$q_{tabla} = 0{,}36$ kg/m³

B = 6 m

$$q_{normal} = 0{,}36 + 0{,}03\ (7 - 2 \times 1{,}40) + \frac{0{,}40}{6}\left(\frac{6\ 0{,}40}{6 - 1}\right)$$

$$q_{normal} = 0{,}36 + 0{,}13 + 0{,}07 = \underline{0{,}56\ \text{kg/m}^3}$$

Se ha confeccionado una tabla en la cual se refleja la carga específica necesaria debida al esponjamiento. *Debe subrayarse* el hecho de que cargas específicas elevadas requieren zonas apropiadas que permitan dicho esponjamiento y tomar medidas especiales de seguridad, salvo que este tipo de voladuras sea realizado en el interior de cámaras subterráneas.

La siguiente tabla indica la carga específica necesaria en voladuras en banco, donde el esponjamiento puede producirse hacia la superficie, con una inclinación de los taladros del 3:1.

La anchura de las voladuras se ha fijado en 15 m lo cual tiene gran importancia cuando las voladuras en banco tienden a aproximarse al límite de las voladuras en trinchera o cuando tienen un número excesivamente bajo de barrenos por fila.

Altura de banco K m	Serie 11	Serie 12	Diámetro del taladro en mm 43	48	51	64	75	100
4	0,45	0,41						
5	0,46	0,45	0,41					
8		0,55	0,53	0,52	0,51	0,48	0,47	
10				0,60	0,59	0,54	0,54	
12					0,64	0,62	0,58	
15						0,72	0,65	0,55 [1]
18							0,79	0,65 [1]
20							0,86	0,71 [1]
25								0,87 [1]
30								1,04 [1]

1) Los valores para 100 mm de diámetro deberían incrementarse realmente en 0,10 kg/m³, dado que una anchura de banco de 15 m es excesivamente pequeña para el espaciamiento normal, el cual ha influido también en los valores obtenidos en los otros diámetros mayores.

Por la tabla se puede deducir lo inadecuado que resulta la realización de voladuras en bancos muy altos sin realizar desescombro.

Cuando se realizan voladuras de muchas filas, es decir, con frente profundo, se necesita una cierta cantidad de carga para el esponjamiento, aunque la *piedra* en el fondo esté realmente rota. Cuando se produce la detonación de las cargas en los barrenos y la roca comienza a desplazarse hacia adelante, se hace cada vez más difícil el esponjamiento.

Una simple regla puede aplicarse, considerando que la voladura debe calcularse como si fuera a esponjar hacia la superficie a partir de la fila de taladros en los cuales la distancia al frente es mayor que la anchura.

Ejemplo

K = 10 m

d = 51 mm

B = 12 m

Profundidad del frente = 25 m

No. de filas	q	V_1
1—5	0,36	1,90
6—13	0,58	1,25 [1]

1) Incrementando la carga de columna se puede aumentar la *piedra* a 1,75 m.

Los cambios en los esquemas de tiro no se producen lógicamente con tanta brusquedad como figura en la tabla anterior, debiendo interpolarse para valores intermedios. La conclusión práctica es: evitar la realización de voladuras cuya profundidad es superior a su anchura.

Muchas veces, debido a la tendencia a obtener la mayor capacidad posible de los equipos, se eligen diámetros de perforación mayores que los recomendados en la tabla. En estos casos los factores económicos deben ser reconsiderados con objeto de obtener la mejor solución global.

5.4 PROYECCIONES

Por Proyección se entiende usualmente el lanzamiento inesperado de trozos de roca, procedentes de una voladura. Cuando se habla de lanzamiento de piedras pequeñas procedentes de la zona superior de una voladura se emplea a menudo el término "dispersión". Desde el punto de vista de la técnica de voladuras pueden diferenciarse 3 formas distintas de proyección:

Proyección hacia adelante de toda la voladura.
Proyección producida por rotura de barrenos por carga indebida.
Proyección hacia la superficie debida a la presión de los gases.

Las causas de la proyección pueden ser varias. Algunas de las principales y más frecuentes son:

Fallas, grietas y zonas débiles que han disminuido localmente la resistencia de la roca.

Una mala disposición de los barrenos puede producir altas concentraciones de carga.

La secuencia de encendido mal realizada puede dar lugar a barrenos sin salida adecuada o tiempos de encendido excesivamente largos.

Empleo de cargas demasiado altas.

Como se ha indicado anteriormente en el capítulo Cálculo de Cargas, la utilización de detonadores de micro-retardo ha permitido la ejecución de grandes voladuras con un control mejor de las proyecciones. Para establecer el justo tatal del problema de proyecciones procedentes de una voladura es

preciso considerar el tema relacionado con el material usado en la protección. (Ver cap. 8. Protecciones.) La protección se considera como una medida de seguridad adicional contra las posibles proyecciones que pueden surgir, pese a todas las demás medidas que hayan sido tomadas. Pese a que la técnica de voladuras ha mejorado y el conocimiento sobre los explosivos y las rocas ha aumentado considerablemente, siguen produciéndose aún hoy proyecciones en las voladuras y frecuentemente con pérdidas materiales y daños personales.

El problema de las proyecciones es una parte de la técnica de voladuras que ha quedado un tanto relegada y sobre la que deberían realizarse trabajos de desarrollo e investigación. Es obvio que en casos donde exista un gran riesgo de proyección, los métodos de voladura deberán elegirse cuidadosamente, de tal forma que los daños resultantes sean mínimos. Si se han adoptado todas las medidas que contrarrestan el riesgo de proyección y se ha realizado una protección correcta de la zona, los riesgos pueden considerarse limitados.

Proyección frontal de la voladura

Cuando se realiza una voladura normal en banco se produce un desplazamiento del centro de gravedad de la misma hacia adelante. A mayor altura de banco corresponderá un desplazamiento mayor de la roca volada. La carga específica desempeña un papel muy importante. Una carga específica próxima a la carga límite produce un desplazamiento menor de la roca, no obstante, cargar por debajo de los valores límite es un sistema no recomendable. Existe una opinión errónea, y sin embargo muy extendida, de que una carga débil soluciona todos los problemas relacionados con la proyección. El factor mas importante en una voladura es conseguir una planificación correcta de la misma, puesto que un barreno que no rompa suficientemente o tenga un fallo en su encendido, puede originar una considerable proyección, dado que, al no tener suficiente ángulo de rotura, la presión de los gases se producirá hacia la superficie.

Admitido que la roca se desplazará hacia adelante en la voladura, hay que planificar los trabajos y la dirección del efecto de rotura de forma que pueda tolerarse un cierto lanzamiento hacia el frente. Si no resulta posible por razones prácticas el modificar la dirección del efecto de rotura y tampoco puede permitirse ningún lanzamiento frontal, es conveniente volar primeramente una o dos filas con cargas mas débiles, próximas al límite de carga de rotura, de tal forma que la roca volada posteriormente pueda servir de pantalla para el resto de la voladura. Así mismo hay que tener presente el factor de esponjamiento de la roca a efectos de la proyección frontal admitida. (Ver cap. 5.3 Esponjamiento.)

En zonas de voladuras situadas a nivel considerablemente mas alto que el del terreno resulta difícil evitar que la roca desprendida se deslice, con el

consiguiente aumento de la proyección frontal. En bancos con la disposición anterior, frecuentemente se efectúan voladuras con fondo libre, requiriendose en estos casos una carga considerablemente menor que la que indican las tablas. Esta es debido a que existe una menor constricción, pero tambien a la ayuda proporcionada por la fuerza de gravedad en la caida de la roca y a que no se necesita ninguna fuerza para producir el esponjamiento ni para la proyección frontal de la misma. Se puede aplicar para estos casos la siguiente regla práctica para obtener la carga necesaria que prevenga el deslizamiento y la proyección frontal:

Las cargas de fondo se dimensionan de acuerdo con la *piedra real*, sin ningún suplemento debido a la desviación de la perforación, etc. la concentración de carga de columna se determina de forma que la carga especifica en ella esté comprendida entre 0,20 y 0,25 kg/m³.

Proyecciones producidas por la rotura de barrenos por carga indebida

Estudios realizados en diferentes voladuras indican que en muchos casos las proyecciones provienen de la primera fila de barrenos y frecuentemente de la zona que corresponde a la carga de fondo, sobre todo en perforación con gran diámetro, pues cuanto mayor sea éste, mayor es el riesgo de proyecciones. Esto se aplica en lo concerniente no sólo a la proyección producida por la rotura del barreno, sino tambien a la producida hacia la superficie, debiendo tenerse en cuenta estas consideraciones cuando se realizan voladuras próximas a zonas habitadas.

Las proyecciones causadas por las cargas de fondo en la primera fila de una voladura pueden ser debidas a dos importantes factores:

Errores cometidos durante la perforación.
Fallas o grietas del terreno que facilitan la rotura del barreno al disminuir la resistencia de la roca.

Si los barrenos se disponen de forma que la *piedra* resulte considerablemente menor que la calculada para la carga, el riesgo de proyección será grande, especialmente cuando se emplean barrenos de gran diámetro.

Ejemplo: La perforación se ha realizado con taladros de 64 mm. La *piedra* calculada es 2,40 m. pero, por un error en la inclinación del frente del banco, ha quedado reducida a 1,40 m.
Carga especifica calculada en la parte del fondo 0,55 kg/m³.
La carga especifica real obtenida, debido al error, es aproximadamente 1,0 kg/m³.

Está claro que una sobrecarga local, como en este caso, puede ocasionar importantes proyecciones, especialmente si coincide con una roca muy fisurada. En voladuras con barrenos de diámetro pequeño este riesgo es menor.

Ejemplo: La perforación se ha realizado con barrenas de la serie 11. La piedra calculada es 1,20 m. Debido a la irregularidad del banco, la piedra real obtenida en el fondo es de 0,80 m.
La carga especifica de fondo calculada es de 0,50 kg/m³ y *la carga especifica real* resulta aproximadamente 0,75 kg/m³.

El ejemplo demuestra que incluso aqui, la carga especifica es tan alta que entraña evidentes riesgos de proyección. La diferencia en riesgo de lanzamiento entre pequeños y grandes diámetros depende principalmente de la concentración de carga por metro.

Taladro diámetro pequeño	Taladro diámetro grande	Concentración de carga kg m.
32		1,0
36		1,3
	64	4,1
	75	5,6

Si en barrenos de gran diámetro existe una concentración de carga en zonas debilitadas, por errores durante la perforación o por corresponder a terrenos fisurados, los efectos de proyección pueden ser muy acusados. Se ha dado el caso en que bloques de hasta 0,5 m³ han sido proyectados centenares de metros, mientras que con la utilización de pequeños diámetros estos hechos no pueden producirse.

Medidas preventivas de proyección debida a la rotura de los barrenos

La proyección procedente de la primera fila de una voladura puede ser evitada con una correcta planificación de la misma. Si la primera fila, en el caso de líneas múltiples, no da origen a proyecciones, el riesgo existente para el resto de los barrenos es considerablemente menor, con la condición de que la secuencia de encendido haya sido correctamente planteada. Sobre éste último punto insistiremos mas adelante.

La proyección procedente de la primera fila de una voladura puede ser evitada de la siguiente forma:

Con una carga muy cuidadosa.
Dejando material volado en el frente de la voladura.

La perforación y la carga de explosivo en la primera fila es particularmente importante, ya que los barrenos deben emboquillarse en el borde del banco y éste se encuentra normalmente alterado por las voladuras anteriores. En estos casos cada tiro debe ser planificado de modo que la *piedra* obtenida en el fondo sea la adecuada.

En lo referente a la carga de explosivo, *cada barreno de la primera fila debe ser estudiado individualmente*. Los cálculos utilizados normalmente en las voladuras de banco, que incluyen cargas adicionales por errores de perforación, esponjamiento, etc., se aplican a los barrenos de una voladura que no presenten riesgos de proyección, pero no a los barrenos de la primera fila.

La primera fila debe cargarse de la siguiente forma:

La carga de fondo se calcula de acuerdo con la *piedra* práctica y sin tener en cuenta los suplementos debidos a desvíos en la perforación; por la cual el valor actual de V en el fondo se estima con gran precisión.

Ejemplo: $V = 1{,}0$, $Q_b = 0{,}55$

La carga de columna debe adaptarse a la *piedra* actual, dependiendo de las irregularidades que presente el frente. La carga específica puede disminuirse hasta 0,20—0,25 kg/m³.

Ejemplo: $V = 1{,}0$ $E = 1{,}3$, la carga de columna utilizada es $Q_{pc} = 0{,}26—0{,}32$ kg/m.

Otra forma de prevenir la proyección procedente de la zona de carga de fondo es dejar parte del escombro de las voladuras anteriores depositado a pié de banco (ver fig. 5.4.1) y cubriendo perfectamente dicha zona. Si el escombro

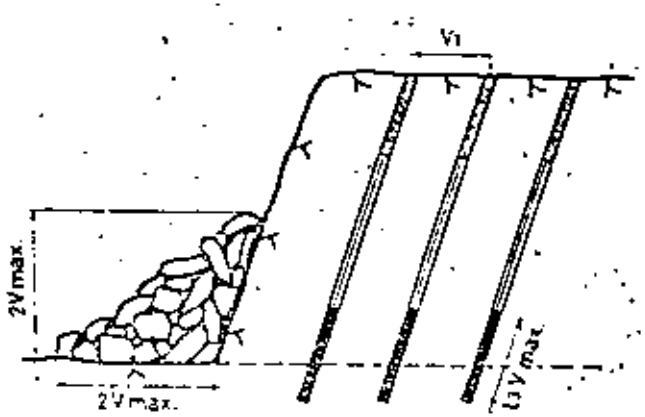

Fig. 5.4.1

se deposita como muestra la figura, los barrenos pueden ser cargados de la forma habitual. Representando una ventaja con relación a la elección de cargas próximas al límite de rotura de la roca.

El valor $2 \times V_{max}$ puede ser utilizado independientemente de que los barrenos hayan sido realizados con pequeños o grandes diámetros. La resistencia que ofrece el escombro depositado queda absorbida por el suplemento necesario para el esponjamiento que se incluye al dimensionar las cargas de explosivo.

Influencia de la secuencia de encendido en el riesgo de proyección

El diseño de la secuencia de encendido es de una gran importancia. Según se indicó anteriormente, los detonadores de micro-retardo poseen la ventaja, durante el proceso de la voladura, de mantener la roca agrupada de tal forma que la roca volada por los barrenos del frente actúa en etapas como una protección material de los barrenos iniciados en la siguiente hilera. Si el tiempo de retardo entre hileras o entre barrenos de una misma hilera es demasiado alto, este efecto protector desaparece. Estudios de películas de voladuras demuestran que, cuanto menor sea el tiempo de retardo, se obtiene mejor agrupación de la roca. Este aspecto concierne a todos los tipos de proyección, tanto en la superficie como en otras zonas de una voladura.

EL RETARDO ENTRE BARRENOS ADYACENTES EN UNA VOLADURA NO DEBE SER MAYOR DE 100 MILISEGUNDOS.

La secuencia de encendido debe realizarse de forma que las condiciones anteriores se lleven a cabo. Cuando la *piedra* es menor de 1 m, y también en el caso de bancos bajos, la secuencia de encendido debería ser estudiada de forma que los tiempos de retardo fueran incluso menores.

No debe haber constricción en los barrenos durante el momento de la detonación, ya que en caso contrario existe un gran riesgo de proyecciones. Con pequeños tiempos de retardo entre hileras existe mayor posibilidad de mantener en su sitio los materiales usados como protección durante el proceso de una voladura.

Proyección hacia la superficie debida a la presión de los gases

Al realizar los cálculos de carga de explosivo en un barreno, se determina una zona sin cargar en una distancia igual a la *piedra*. Si se disminuye considerablemente el retacado, el riesgo de proyección aumenta, debido a que la carga de columna puede tender a lanzar la roca hacia la superficie. El retacado está constituido normalmente por arena o polvo procedente de la perforación. Es también de gran importancia el asegurarse de que la superficie

del terreno esté libre de piedras o materiales sueltos que puedan ser despedidos durante la voladura.

El riesgo de que trozos pequeños de roca puedan ser proyectados, debido a la presión de los gases, es mayor en las rocas fisuradas, pero un excesivo retacado pueda favorecer dicha proyección ya que, si la carga no es capaz de romper la roca en la superficie y se forman en su lugar grandes bloques, la presión de los gases empujará partículas de roca por los huecos existentes. Este efecto contrario de rotura se observa frecuentemente en el caso de grandes retacados, lo que significa que las proyecciones pueden provenir de cualquier barreno situado en el centro de una pega y son debidas sin duda a la carga de columna. Una carga de fondo muy elevada y un gran retacado, dan origen frecuentemente a voladuras cuyo resultado es muy desfavorable y que suele traducirse en fuertes proyecciones. Es preferible cargar los barrenos en mayor altura con una carga baja, pero que pueda romper la roca en la zona superficial.

Finalmente debe señalarse que una voladura normalmente calculada, en la cual la carga no es excesivamente alta ni demasiado reducida y no se encuentra desigualmente repartida, proporciona la mejor protección contra las proyecciones.

5.5 VOLADURAS EN BANCOS BAJOS

Aunque no se ha determinado directamente el límite de apreciación entre voladuras en bancos normales y en bancos bajos, usualmente se consideran bajos aquellos que tienen una altura menor de 1,0—2,0 m., debido a que este tipo de banco exige un coste de voladura por metro cúbico mas elevado (ver Sección 5.8 Estudio económico de voladuras).

Desde el punto de vista de la pura técnica de voladuras, el límite entre bancos normales y bajos depende del diámetro de perforación utilizado, por

ejemplo, en el caso de una voladura en la cual se utiliza un diámetro de 100 mm., los bancos de 5 m. pueden ser considerados como bancos bajos. La relación entre el diámetro de perforación utilizado y la altura de banco, determina dicho concepto, ya que, si en la práctica fuera posible utilizar un diámetro de perforación de 10 mm., entonces el término de banco bajo no existiría. Técnicamente, lo correcto sería definir como bancos bajos aquellos en los cuales su altura es inferior a $2 \times V_{min}$.

En las tablas de perforación y voladura se han incluido los datos correspondientes a bancos bajos cuando se utilizan grandes diámetros, resaltando no obstante las dificultades para obtener una correcta distribución de la carga. Es posible que además de la relación existente entre el diámetro del taladro y la altura de banco, influyan otros factores. Es bien conocido el hecho de que la dureza de la roca aumenta cuando disminuye su volúmen y Langefors señala que en voladuras en banco existe un fuerte incremento de la carga específica en el caso de *piedras* muy pequeñas.

Las voladuras en bancos bajos se efectúan normalmente en banqueo vertical. A causa del reducido esquema necesario y el gran porcentaje de sobreperforación, la perforación vertical es, desde el punto de vista puramente geométrico, menos indicada que la realizada horizontalmente. No obstante existen algunas dificultades para la realización de taladros horizontales, ya que hoy día no hay equipos de perforación que se adapten bien a esta forma de trabajo.

Se pueden volar grandes superficies con este sistema, pero es necesario realizar el *descombro* antes de cada voladura; además existe mayor dificultad de obtener una correcta distribución de la carga para evitar proyecciones. No obstante, este método tiene grandes posibilidades y debería ser investigado a fondo.

En bancos bajos con perforación vertical es importante que los taladros tengan una inclinación al menos de 3:1.

Dado que con este sistema disminuyen las posibilidades de rotura en el fondo del barreno, existe un aumento del riesgo de proyección debido al efecto de rotura hacia la superficie, pudiendo ocurrir lo mismo, si el espaciamiento de los taladros es grande en relación con la altura del banco, cosa muy frecuente en la práctica, por lo que no se recomienda utilizar este procedimiento en zonas habitadas (ver Sección 5.9 Proyecciones). En el caso de bancos con muy poca altura no se necesita perforar por debajo del fondo teórico y es necesario tomar medidas extraordinarias de precaución. Empresas Constructoras sin experiencia en voladuras determinan grandes zonas de excavación con alturas de bancos de pocos centímetros, resultando muy problemática su ejecución, si se pretende no profundizar por debajo del nivel teórico.

La siguiente tabla, prevista para pequeños diámetros, proporciona los datos necesarios:

Inclinación de los taladros 3:1

Altura de banco	Profundidad de taladros	Piedra	Espaciamiento	Carga de fondo	Carga de columna
0,2	0,6	0,40	0,50	0,035	—
0,3	0,6	0,40	0,50	0,035	—
0,4	0,7	0,45	0,55	0,050	—
0,5	0,8	0,50	0,65	0,100	—
0,8	1,1	0,60	0,75	0,15	—
1,0	1,4	0,80	1,00	0,30	—
1,5	1,9	1,00	1,25	0,55	0,05
2,0	2,5	1,00	1,25	0,70	0,25

La secuencia de encendido es de extrema importancia en los bancos bajos, porque a causa de su poca altura la roca se desplaza mas rápidamente hacia adelante y ésto implica necesariamente tiempos de encendido mas pequeños entre barrenos adyacentes. Ahora bien, si este tiempo es demasiado corto, el efecto deseado no se produce y aumenta el riesgo de proyección. Esto quiere decir que en voladuras en bancos bajos deberían usarse los detonadores con el menor tiempo de retardo y los números de éstos deben colocarse por filas, de tal manera, que los intervalos entre éstas sean los menores posibles.

En muchos casos, pudiendo volar por debajo del fondo teórico, es una ventaja tanto técnica como económica perforar los barrenos mas largos con una *piedra* mayor.

Ejemplo:

Altura de banco: 0,5 m.

	Caso normal m	Perforación bajo fondo teórico m
Altura de banco	0,5	0,5
Profundidad del barreno	0,8	1,4
Piedra	0,5	0,8
Metros perforados/m^3	4,9	3,5
No. barrenos/m^3	3,1	1,3

Naturalmente, el desescombro se realiza hasta la línea teórica de fondo. Esto viene facilitado por el hecho de que encima de dicha línea solamente aparecen muy pocas puntas de roca, disminuyendo por tanto la necesidad de voladuras posteriores. Sin embargo no siempre es posible excavar por debajo, debido a razones técnicas de construcción.

5.6 ELECCION DEL DIAMETRO DE PERFORACION

El diámetro de perforación determina en gran manera el resultado de una voladura en banco; además de la planificación de máquinas y equipos, la elección del diámetro de perforación está influenciada por los siguientes factores:

Aspecto económico de la voladura
Fragmentación
Riesgo de proyección
Formación de grietas en su contorno
Frecuencia de aparición de bloques

En el caso de grandes proyectos de voladura la elección del diámetro de perforación es de la máxima importancia (ver Sección 5.8 Estudio económico de voladuras). Si éste es grande con relación a la altura del banco, puede producir una disminución en el espaciamiento de los barrenos hasta tal punto que resulte antieconómico. Desde el punto de vista técnico de voladuras, si se pretende utilizar al máximo el diámetro de perforación para la explotación en banco, la altura de éste debería ser como mínimo $2 \times V_{min}$. Este criterio proporciona los siguientes valores para diferentes diámetros:

Diámetro perf. mm.	Altura mínima de banco m.	Altura aconsejable de banco m.
Barrenas serie 11 34—26	0—3,0	0—4,0
35	3,2	3,2—5,0
Barrenas serie 12 40—28	3,5	3,5—5,0
38	3,5	3,5—5,0
41	3,7	3,7—8,0
45	4,0	4,0—8,0
51	4,6	4,6—10,0
64	5,8	5,8—12,0
75	6,7	6,7—15,0
100	9,0	9,0—20,0

Dado que la *fragmentación* disminuye cuando aumenta el diámetro, (ver Sección 5.2 Fragmentación), su elección es en determinados casos de suma importancia, por ejemplo en el caso de voladuras con destino a una planta de machaqueo, un tamaño inadecuado puede originar un taqueo inadmisible.

El riesgo de proyección aumenta con el diámetro de perforación (ver Sección 5.4 Proyección), y, como ya se indicó, el problema debe ser estudiado muy cuidadosamente cuando se realizan voladuras en zonas edificadas o habitadas.

La formación de grietas en el contorno del fondo del barreno aumenta con el diámetro y, en el caso de que sea necesario obtener una superficie muy cuidada, este aspecto es un factor determinante.

La frecuencia de aparición de bloques depende, como en los casos anteriores, del diámetro de perforación elegido, así como del concepto de "bloque" para cada caso en particular, teniendo en cuenta las distintas fases posteriores, como son la carga y el transporte, machaqueo, etc.

Los factores descritos anteriormente, que influyen en la determinación del diámetro de perforación, pueden crear una impresión negativa en lo que al uso de grandes diámetros se refiere, aunque evidentemente no sea esa la intención, ya que los grandes diámetros normalmente proporcionan un mejor resultado desde el punto de vista económico y en muchos casos constituyen una condición fundamental para obtener un mejor rendimiento.

5.7 TAQUEO

El taqueo — también denominado voladura secundaria — es la forma de designar las voladuras destinadas a romper bloques de piedra demasiado grandes para ser transportados o machacados. La manipulación de los bloques es una cuestión de costosa economía, y por esta razón, las voladuras se planifican de modo que no se produzca en ellas un número demasiado abundante de bloques de excesivo tamaño (véase la sección 5.2 Fragmentación). En esta sección no se trata de la voladura de bloques sueltos de los que se encuentran ocasionalmente en el terreno (véase sección 16.1 Voladura de bloques Sueltos naturales); tampoco se citan otros métodos, aparte de las voladuras, utilizados para el tratamiento de estos bloques, aun cuando se dispone en la actualidad de varios de estos procedimientos para la fragmentación de grandes bloques.

Los grandes bloques producidos por una voladura anterior han sufrido tensiones y fuerzas muy intensas, y por ello son a menudo más fáciles de romper que los encontrados ocasionalmente y de procedencia natural. Los bloques resultantes de una voladura presentan con frecuencia profundas fisuras, lo que facilita su tratamiento ulterior. Antes de perforar e introducir la carga en uno de estos bloques, deberá examinársele cuidadosamente para asegurarse de que no contiene algún taladro cargado con una fracción de explosivo procedente de las voladuras anteriores; si es posible, debe dársele la vuelta para inspeccionarlo por todos los lados. A la hora de decidir la ubicación de las perforaciones que vayan a hacerse, es preciso tomar en consideración las fisuras y diaclasas existentes en el bloque.

Fig. 5.7.1

Cabe diferenciar dos métodos de taqueo:

— El empleo de cargas conformadas ("planchas").
— Cargas introducidas en barrenos taladrados en el bloque.

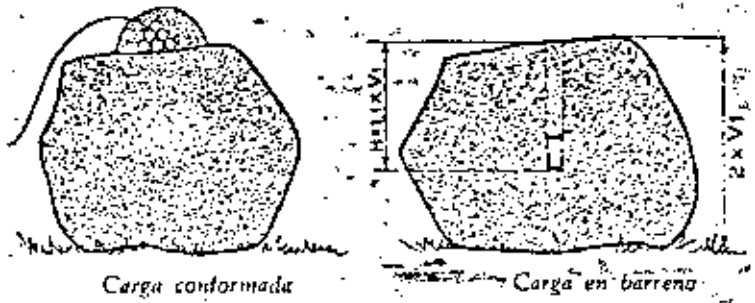

Carga conformada *Carga en barreno*

Fig. 5.7.2

Las cargas conformadas están constituidas por cargas completamente libres de confinamiento, y sólo pueden ser utilizadas a grandes distancias de los edificios. Se conocen casos en los que voladuras de este tipo han tenido efectos molestos a una distancia de hasta 1 km. La onda de presión de aire que hace vibrar los vidrios de las ventanas implica, el que cargas de este tipo sean consideradas como molestas mucho antes de que se alcance el umbral de tensión necesario para producir daños: ésto significa que el método sólo puede ser utilizado lejos de áreas edificadas.

La carga es aplicada encima del bloque, de tal modo que el explosivo quede bien en contacto con la superficie de roca. Una sencilla regla empírica para el cálculo de la carga es utilizar una carga específica de 1,0 kg/m³. La carga necesaria puede variar, dependiendo de la forma del bloque: un bloque redondo es más difícil de romper con cargas de este tipo que otro delgado y de gran área.

El explosivo "Carga conformada A" posee una velocidad de detonación de unos 7000 m/seg., lo que proporciona un excelente impacto. La existencia de este práctico explosivo ha conllevado una tendencia al incremento de las voladuras con cargas de superficie en Suecia. Las cargas de esta clase son de empleo práctico y económico, especialmente en relación con la voladura de bloques o piedras sueltas.

En minas subterráneas, las cargas de superficie han desempeñado siempre un papel importante en las zonas de arranque de mineral. Una "Carga conformada B" está concebida asimismo para proporcionar una elevada velocidad de detonación con un excelente efecto de impacto. La "Carga conformada B" posee un mejor balance de oxígeno que la "Carga conformada A", lo que la hace más adecuada para utilización subterránea.

También se han efectuado ensayos con buenos resultados empleando cargas conformadas del tipo Reomex. La idea que mueve a desarrollar las cargas conformadas de Reomex es la de obtener unos mejores resultados en lo que concierne a los gases, para las voladuras subterráneas.

Sobre la superficie del terreno, no hay duda ninguna sobre el hecho de que la "Carga conformada A" es la más eficaz.

Sobre la carga debe aplicarse un material de retacado, como arcilla húmeda, etc. No puede usarse ningún material de protección. Cuando las ondas de choque generadas por el explosivo alcanzan las superficies libres, son reflejadas, con lo que se producen tensiones de tracción capaces de resquebrajar el bloque. El explosivo debe ser de alta velocidad de detonación, y el bloque estar situado en posición despejada para que la reflexión no sufra perturbaciones.

Las cargas en el interior de taladros se usan mucho más que las cargas externas que se acaban de describir. Se perfora el taladro hasta una profundidad cuidadosamente calculada en el seno del bloque. Si la *piedra* resulta demasiado pequeña en alguna dirección, el resultado de la voladura empeora, al haber grandes porciones que no son escindidas. La distribución de taladros deberá adaptarse a la forma del bloque. Si éste es muy grande, pueden necesitarse varios taladros, entre los que se distribuye la carga. El valor de la carga específica es adaptado al lugar en que se efectúa la voladura. La Tabla siguiente muestra las características del taqueo allí donde son permisibles las proyecciones.

Tamaño del bloque m³	Espesor m	Profundidad de perforación m	Número de taladros	Carga kg/taladro
0,5	0,8	0,44	1	0,030
1,0	1,0	0,55	1	0,060
2,0	1,0	0,55	2	0,060
3,0	1,5	0,83	2	0,090

La Tabla se ha calculado del modo siguiente:

Carga específica: 0,060 kg/m³

Profundidad del taladro: 1,1 × mitad del espesor = 1,1 × V,

Si se emplean varios barrenos en un mismo bloque, el encendido ha de hacerse mediante detonadores instantáneos. En el caso de voladuras con precaución, puede resultar más conveniente utilizar varios barrenos con cargas pequeñas. Las cargas serán completamente retacadas con arena o polvo de perforación. En áreas edificadas, es fundamental disponer una protección completa.

Fuera de zonas edificadas, por ejemplo en el taqueo de bloques en una cantera, pueden utilizarse valores de la carga más altos que los de la Tabla, siempre que la voladura se efectúe con unas condiciones suficientemente buenas de supervisión y evacuación.

Con todo, el valor de la carga específica empleada es suficiente generalmente para romper la piedra. Existen series de ensayos en las que se demuestra que, en ciertos tipos de roca, se han fragmentado satisfactoriamente bloques con cargas de 0,030 kg/m³.

Durante este año se está procediendo a la realización de una serie de ensayos de taqueo con taladros sumamente cortos, cuyo objetivo es encontrar un método económico para estas voladuras secundarias. Los ensayos indican que las voladuras resultan relativamente satisfactorias, pero el método sólo es adecuado por ahora para las voladuras de producción, en donde pueden seguirse las medidas de seguridad mencionadas hasta que se haya adquirido experiencia suficiente. En este terreno es todavía necesario un mayor desarrollo de la técnica, pues el manejo de los bloques sueltos es un proceso relativamente caro.

5.8 ESTUDIO ECONOMICO DE LAS VOLADURAS

La economía de las voladuras es un asunto complicado con muchas facetas, que no puede ser estudiado aquí con detalle. Los diferentes modos de calcular los costes de las voladuras en banco forman una técnica que es familiar a los ingenieros que se ocupan de estos temas, y para la cual se han desarrollado diferentes métodos.

Los costes dependen siempre de las condiciones básicas prevalecientes en el lugar donde están siendo calculados. La subdivisión entre costes fijos y variables puede variar en gran medida.

En esta sección se estudian los factores que poseen influencia sobre el aspecto financiero de las operaciones de voladuras en banco.

Es importante tomar en consideración todos los factores, y no únicamente el arranque o desprendimiento de la roca con los explosivos: una voladura con barrenos muy espaciados y una baja carga específica puede resultar barata, pero los costes de taqueo, carga, y machaqueo de los fragmentos pueden ser considerablemente más altos en términos relativos.

Para el cálculo de costes han de tomarse en consideración los factores siguientes:

1. Coste de perforación.
2. Coste de los explosivos.
3. Coste de la carga de los barrenos y de la voladura.
4. Tratamiento de los bloques.
5. Coste del desescombro.
6. Coste del machaqueo.

1. El coste de perforación varía con las diferentes características de la roca de que se trata, las fallas existentes, etc. El diagrama de la Fig. 5.8.1 muestra el coste de perforación por litro de taladro para diferentes diámetros del mismo. En él se pone de manifiesto que este coste es menor en el caso de barrenos de gran diámetro. Dado que puede cargarse la misma cantidad de energía por unidad de volumen de barreno, los taladros de gran diámetro serán más económicos que los de pequeño diámetro.

2. El coste de los explosivos varía con el tipo utilizado y con el diámetro del barreno. Un cálculo comparativo entre explosivos diferentes ha de incluir su potencia por unidad de peso para llegar a conclusiones correctas. El diagrama de la Fig. 5.8.2 muestra el coste de diversas alternativas posibles bajo las mismas condiciones.

Ejemplo:

Coste del explosivo con consideración de la fuerza de arranque:

$$K = 3 \times V_{max} \qquad d = 75 \text{ mm}$$

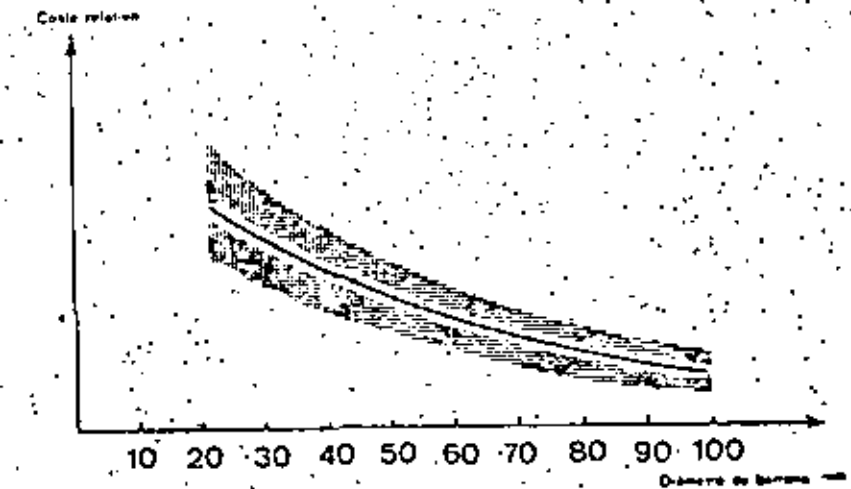

Fig. 5.8.1

En el diagrama 5.8.2 se ilustran los costes para un determinado diámetro de barreno y altura del banco. Si se modifican estos dos parámetros, ello afecta tanto a los costes como a la diferencia entre las diversas alternativas.

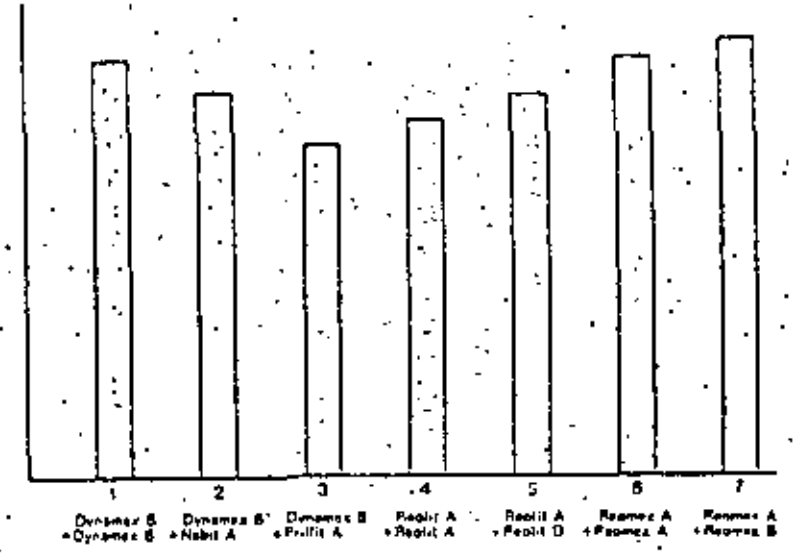

Fig. 5.8.2

La figura pretende ante todo mostrar el coste de diversos explosivos por unidad de energía; no muestra el coste de la voladura, ya que no se incluye el coste de perforación. Los explosivos alternativos, por otro lado, han sido calculados sobre la base de una pega normal de barrenos de gran diámetro, de modo que se ofrezcan unas alternativas razonables de carga. Una variante con una carga de fondo rica en energía y una carga de columna económica, como en la alternativa 3, puede ser la más favorable. La alternativa 4, con papillas, muestra quizá un cuadro ligeramente favorable. En la práctica hay tendencia a obtener una elevada carga específica llenando el barreno con un explosivo que proporcione una densidad de carga de 1,50 kg/dm³.

3. Los costes por metro cúbico de la operación de carga de los barrenos son evidentemente inferiores en el caso de un trabajo extenso con taladros de gran diámetro que en el caso de barrenos de pequeño diámetro con una carga limitada en cada uno.
En la Fig. 5.8.3 se muestra un diagrama que ilustra la diferencia de costes de la operación para diferentes diámetros de barreno, suponiéndolos aplicados en condiciones técnicamente normales. El diagrama incluye los costes de carga y los de voladura.
En el caso de barrenos de diámetro muy grande, por ejemplo 250 mm, y tratándose de papillas explosivas bombeadas, el coste de carga y voladura es casi despreciable calculado por metro cúbico de roca volada. Cada

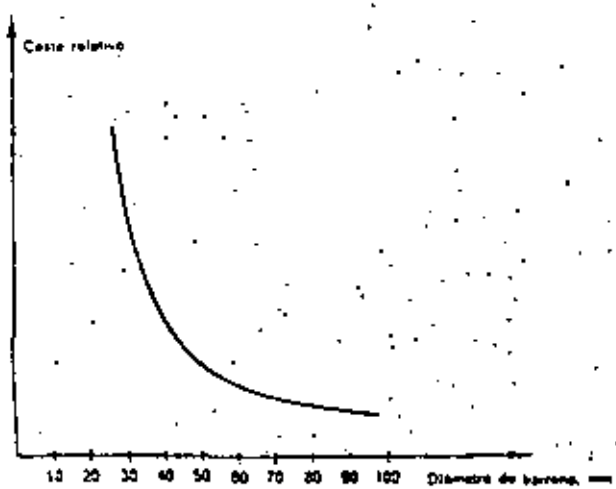

Fig. 5.8.3 Coste de carga y de voladura

barreno desprende de 1000 a 1500 m³ de roca, y la carga de los mismos lleva unos 10 minutos.
El coste de voladura disminuye al aumentar el diámetro del barreno.
En la Fig. 5.8.4 se muestran los costes relativos de voladura con diferentes diámetros de barreno. Se han utilizado las mismas cargas específicas y tipos de explosivo.

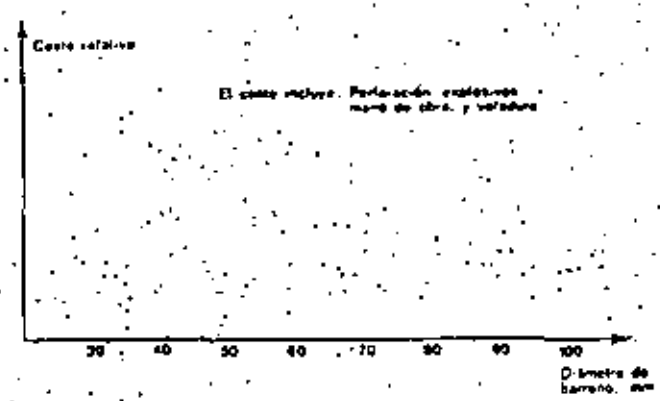

Fig. 5.8.4

4. El taqueo constituye una parte considerable de los costes totales de las voladuras. La definición de bloque varía según los casos, y depende de las máquinas de desescombro empleadas y el volumen de la pala cargadora, así como de las dimensiones de la boca de alimentación de la planta de machaqueo, en el caso de que la roca vaya a ser triturada.
Como el equipo utilizado en los trabajos de voladura se selecciona normalmente de modo que los diversos elementos se ajusten en el sistema, la frecuencia con que se producen bloques es normalmente elevada, incluso con barrenos densamente distribuidos y de pequeño diámetro.
El coste del taqueo oscila corrientemente entre 4 y 8 coronas suecas por bloque, siendo el valor normal de 5 a 6 coronas suecas. Con una frecuencia de presentación de un bloque por cada 10 metros cúbicos, ésto significa que el coste aproximado es de 0,50 a 0,60 coronas por m³, lo que, en el caso de voladuras de producción, constituye una parte considerable del coste de arranque de la roca.
La frecuencia con que se presentan los bloques depende la mayoría de las veces del grado de fragmentación: con un menor tamaño medio de fragmentación, el número de bloques por unidad de volumen disminuye.
El taqueo de los bloques puede llevar consigo, en algunos casos, costes indirectos, como la evacuación en relación con la voladura, etc.

5. Analogamente, los costes de desescombro dependen del volumen de la cuchara y del tipo de maquinaria empleada. El coste por unidad de volumen disminuye rápidamente con el volumen de la pala. Otro factor que influye poderosamente en la *capacidad de desescombro* es la *fragmentación*. En la Fig. 5.8.5 se ilustra la influencia de la fragmentación sobre la capacidad de carga de los escombros.

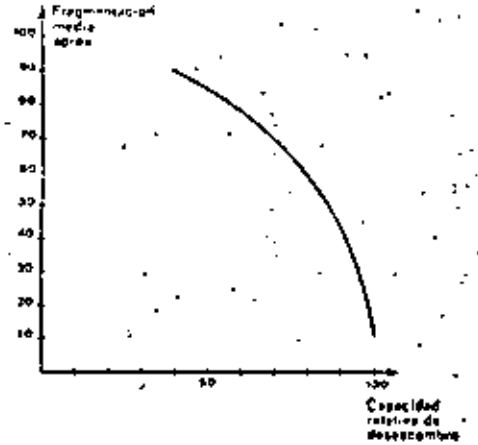

Fig. 5.8.5 Diagrama correspondiente a una cargadora de ruedas relativamente grande

Los diferentes tipos de maquinaria de desescombro dependen, en mayor o menor grado, de la fragmentación. Esta tiene una importancia considerablemente mayor si se emplean cargadoras de ruedas que con excavadoras. Si la rotura en la parte inferior del barreno es incompleta, la capacidad de desescombro puede disminuir mucho más en términos relativos de lo indicado en la figura para diversos tipos de fragmentación. Una fragmentación deficiente se traduce siempre en un mayor desgaste de las máquinas, y hace crecer el riesgo de interrupciones operacionales.

6. El machaqueo constituye un coste difícil de considerar en general. En el caso de grandes instalaciones permanentes, los costes fijos forman una proporción considerable del total. La influencia de las partes desgastables en el coste por unidad de volumen depende de la capacidad de la instalación. No es nada infrecuente que una planta de machaqueo forme un cuello de botella en el ciclo de producción de material pétreo. La capacidad de penetración a la planta de machaqueo por unidad de tiempo puede, en tales casos, adquirir una importancia financiera tan grande que hace pasar a segundo plano otros factores.

Si se hace la suma de toda la cadena que influye sobre los costes en las voladuras en banco, se encuentra que los costes por unidad de volumen disminuyen conforme los métodos empleados se hacen más extensivos y a mayor escala. Se comprueba asimismo que la fragmentación constituye un factor clave a este respecto, pues influye con especial intensidad sobre los costes.

Los ahorros conseguidos por metro perforado, y los explosivos que producen una gran fragmentación, pueden sin embargo conducir a un resultado insatisfactorio desde un punto de vista financiero global. Para cada caso existe un método óptimo. La influencia que ejerce cada uno de los factores en juego puede variar dependiendo de las condiciones de cada caso, pero también hay factores que no pueden ser influenciados, como las características de la roca frente a la voladura y sus propiedades de perforación.

La Fig. 5.8.6 constituye un resumen de esta sección. Sin pretender en

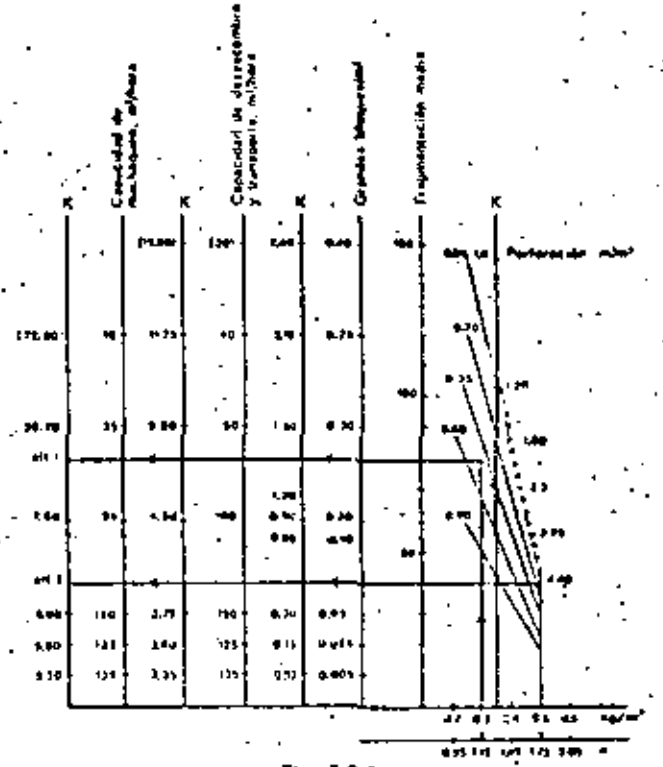

Fig. 5.8.6

absoluto mostrar una imagen correcta del aspecto económico de una voladura en todas las condiciones, la figura proporciona una idea de la influencia de los diversos factores sobre el resultado global de la voladura en banco.

K es la línea de coste, que puede ser calculada para cada caso individual. La suma de K = coste total. Cada caso concreto exige la introducción de las líneas de coste y las relaciones de fragmentación correctas.

El modelo va dirigido a mostrar que la economía de las voladuras está influenciada por una multitud de factores. Si, en un caso particular en que el machaqueo constituye un cuello de botella en el proceso de producción, se ha de hacer una evaluación de las pérdidas, los demás factores conformadores del coste total llegan a perder casi toda su importancia.

La fragmentación no puede probablemente ser nunca demasiado fina. Siempre que las pegas realizadas hayan sido efectuadas de un modo técnicamente correcto desde el punto de vista de la seguridad, el uso de altas cargas específicas mejora el aspecto económico global en la mayoría de los casos.

Se incluye a continuación un ejemplo que ilustra la aplicación del diagrama:

Alternativa 1. q = 0,30 kg/m³; b = 0,35 m perf./m³
(normalmente con un diám. de 45 mm)

Alternativa 2. q = 0,50 kg/m³; b = 0,09 m perf./m³
(con un diám. aprox. de 100 mm)

	Alternativa 1			Alternativa 2	
Costes =		1,15 × K	Voladura	aprox.	1,75 × K
	aprox.	2,30 × K	Perforación	aprox.	1,20 × K
	aprox.	1,40 × K	Taqueo	aprox.	0,40 × K
	aprox.	7,00 × K	Desescombro y transporte	aprox.	3,95 × K
	aprox.	16,00 × K	Machaqueo	aprox.	6,45 × K
		27,85 × K			13,75 × K

Debe observarse que no han sido incluidos los costes imputables a pérdidas de producción.

La diferencia entre uno y otro caso reside en la fragmentación: valor medio aproximado de 80 y 35 cm, respectivamente.

El diagrama pone de manifiesto que la fragmentación arroja diferencias menores entre los diferentes diámetros de barreno al aumentar la carga específica.

El diagrama está proyectado esencialmente como un modelo para la estimación de costes en voladuras de producción.

- Cada lugar de voladura tiene su línea o curva de fragmentación.
- Cada sistema de producción requiere sus líneas de costes.
- En cada caso, la capacidad de producción de cada parte del sistema proporciona unos valores específicos.

La Fig. 5.8.6 muestra la posibilidad existente en cada caso particular de confeccionar un modelo económico que ponga de manifiesto como se influyen entre sí los diversos factores en las voladuras de producción. El ejemplo ilustra, por su parte, la diferencia entre una fragmentación completamente inaceptable y una fragmentación normal.

La Fig. 5.8.7 muestra un ejemplo en el que la diferencia de fragmentación entre los dos casos no es tan grande, sino que en ambos puede considerarse como aceptable. Este ejemplo viene a recalcar aún más la importancia de efectuar un estudio cuidadoso de la fragmentación en relación con las voladuras de producción, así como de su influencia sobre la economía del conjunto. Como indica la figura, las *diferencias de fragmentación* tienen mayor significado desde el punto de vista financiero que el coste total de los explosivos utilizados.

El capítulo 6, Carga de barrenos, describe asimismo la influencia de diversos métodos de carga sobre los costes de la voladuras.

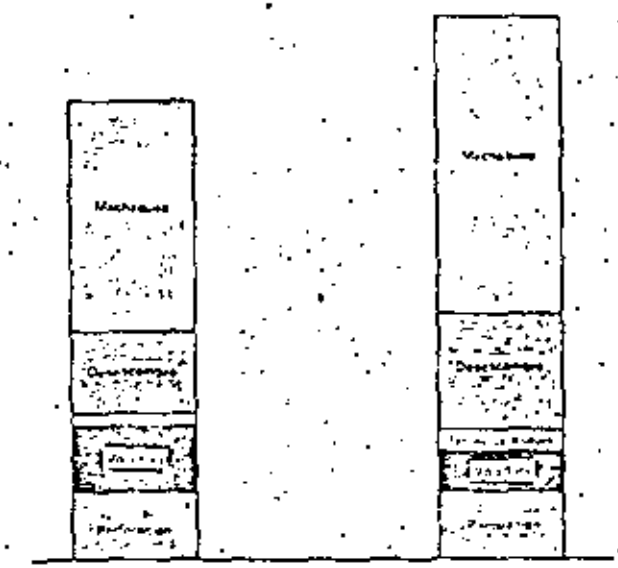

Fig. 5.8.7 Coste total de las voladuras para producción con diferentes grados de fragmentación

6. CARGA DE LOS BARRENOS

6.1 METODOS DE CARGA

Fig. 6.1.1 Carga con atacador

La creciente efectividad y rendimiento de las voladuras de producción ha hecho aumentar la importancia de los métodos para introducir el explosivo en los barrenos de un modo más rápido y eficiente. Los avances en la tecnología de las perforadoras han hecho posible reducir los tiempos de perforación, lo que ha dado aún más importancia a la consecución de unas operaciones de carga con mayor eficacia, de modo que pueden utilizarse con mayor amplitud costosos equipos mecánicos. La demanda de unos métodos de carga más eficientes ha influido sin duda en los éxitos registrados por diversos explosivos, aun cuando tales logros no hayan sido imputados directamente a las posibilidades de cargar los explosivos en cuestión. Esto es aplicable en gran medida a los explosivos de nitrato amónico y a las papillas, que pueden ser cargados a granel hasta alcanzar altos niveles de capacidad de carga.

El hecho de que en Suecia ha sido posible cargar explosivos de nitroglicerina de alta energía con aparatos de aire comprimido ha hecho competitivos a este tipo de explosivos, lo cual ha de ser tomado en consideración cuando se estudia el desarrollo de los explosivos en otros países en los que, en muchos casos, sólo ha podido disponerse de dinamita rígida.

El método sueco de carga con Dynamex B ha resultado muy competitivo a nivel internacional, lo que viene a recordar otro importante efecto que se consigue con este método: el buen aprovechamiento del barreno, con una elevada concentración de energía en el fondo del mismo. Puede asimismo conseguirse una carga digna de confianza en barrenos rotos, que son difíciles de cargar con cartuchos rígidos y de gran diámetro.

Otro modo de lograr unos métodos racionales de carga consiste en diseñar las unidades de explosivo de modo que permitan directamente una operación rápida. Las cargas alargadas enfundadas en plástico, por ejemplo, pueden ser cargadas rápidamente en las voladuras de construcción de túneles. Además, se consigue una concentración de carga equilibrada que reduce la cantidad total necesaria, impidiendo la fisuración innecesaria de la roca circundante.

La sensibilidad de los explosivos de nitroglicerina no ha permitido el desarrollo de métodos de carga a granel. En el caso del Reumex, en cambio, su composición y grado de sensibilidad sí han hecho posible esta modalidad de carga, lo que facilita la carga efectiva de un explosivo sofisticado de alta energía, y parece tener unas posibilidades de desarrollo particularmente grandes.

Todavía hay grandes cantidades de explosivo que son cargadas con atacador, lo cual resulta lo más práctico en el caso de barrenos poco profundos y de pequeño diámetro.

6.2 CARGA CON ATACADOR

Los atacadores utilizados deben ser de madera o de plástico, si bien en barrenos en roca alterada se suele colocar en la punta un casquillo de cobre, prohibiéndose terminantemente el uso del hierro. Se recomienda que un atacador no sea demasiado ancho en relación con el diámetro del taladro, ya que puede producir daños y roturas en el cordón detonante o en los cables de los detonadores durante los trabajos de carga.

Si se quiere obtener un buen grado de retacado cargando con atacador, debe realizarse la operación individualmente con cada cartucho, y es una

ventaja disponer de explosivo encartuchado con diámetro tan próximo al de perforación como sea posible.

En el caso de barrenos profundos frecuentemente se introducen y compactan varios cartuchos al mismo tiempo, lo cual da origen a una disminución de la concentración de carga de un 20—30 %, y ésto puede influir de forma importante en los resultados de la voladura. De acuerdo con Cook, una reducción del 10 % en la concentración de carga puede significar en ciertos casos una caída de presión del 30 % en el taladro.

El detonador debe ser correctamente colocado en el interior del barreno durante el proceso de carga, ya que, si se coloca en diagonal con respecto al eje del cartucho, puede dar lugar a una iniciación incompleta; además puede

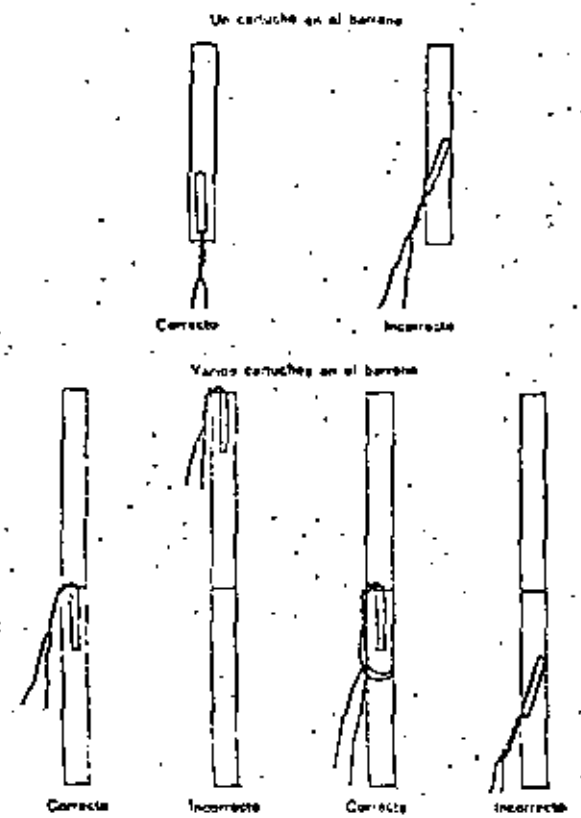

Fig. 6.2.1

engancharse mas fácilmente contra las paredes del barreno y producir su rotura al realizar la carga y, dado que la cabeza del detonador puede permanecer intacta, no hay garantía de que sea observado cuando se comprueba la pega.

Si el espesor del cartucho delante de la parte posterior del detonador no es suficiente, la iniciación puede resultar incompleta, aplicándose particularmente este caso en los explosivos que presentan una mayor dificultad a aquella.

En el caso de utilizar detonadores de retardo de medio segundo y, si el detonador está colocado diagonalmente en el interior del cartucho, puede ser expulsado durante la iniciación de los barrenos con retardos de intervalos mas bajos.

Un atacador pesado está hecho de madera con lastre de plomo fundido que le proporciona suficiente peso. La madera utilizada debe ser resistente al desgaste, por ejemplo, de roble, previamente torneada y sumergida en agua durante varios días, despues de lo cual se coloca el lastre con una anilla a la que se puede atar una cuerda o roble.

El atacador pesado es una herramienta excelente para reconocer taladros y tambien para compactar barrenos de gran diámetro. El explosivo encartuchado en plástico en grandes diámetros generalmente se compacta mal en barrenos menores de 15 m. de profundidad; pero si se utiliza un atacador pesado, los cartuchos en el fondo del taladro pueden ser compactados de forma que se logre un aprovechamiento mejor de los mismos.

6.3 CARGADORAS DE AIRE COMPRIMIDO

Los dispositivos de carga con aire comprimido han sido utilizados en Suecia durante unos 20 años. La primera variedad de los mismos consistía en tuberías de aluminio conectadas entre sí, y los cartuchos eran inyectados en el barreno con una presión de aire de 3 kp/cm².

Desde entonces, se ha sustituido el tubo de carga por un tubo de plástico de diseño especial con tratamiento antiestático. La cargadora incluye una válvula operada con el pie, una válvula de reducción con el tubo de aire, obturador, tubo de conexión, y manguera de carga (Fig. 6.3.1).

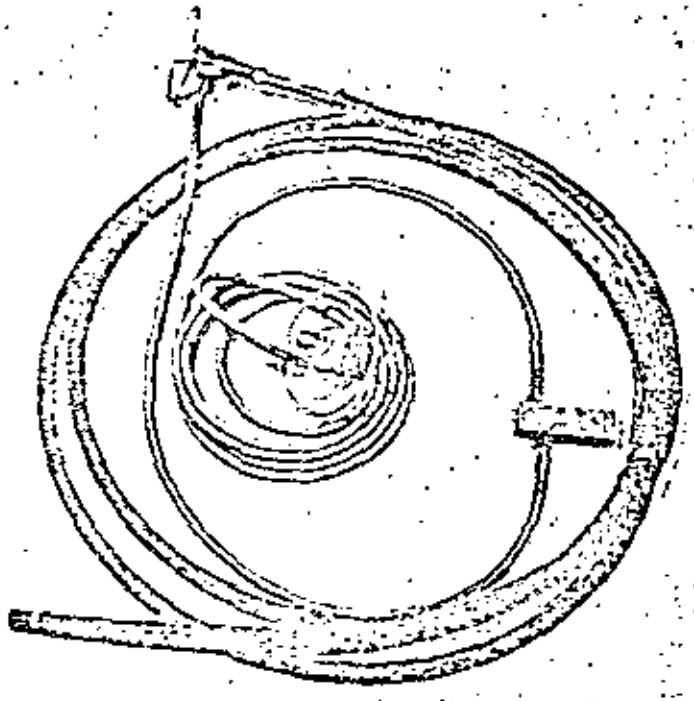

Fig. 6.3.1

En el extremo de la manguera de carga va acoplada una boquilla que lleva incorporadas unas cuchillas que rasgan el papel alrededor del cartucho cuando éste es impulsado. La manguera de carga está estriada en sentido longitudinal en su interior, con objeto de facilitar un aumento de la presión en el conducto si un cartucho queda atascado. La boquilla va provista de un manguito de protección que puede ser reemplazado cuando está desgastado. Lo mismo cabe decir de las cuchillas. La boquilla completa ha de ser también sustituida cuando esté gastada.

La manguera de plástico ha de poseer el diámetro exterior correcto en relación con el barreno. Nitro Nobel recomienda las dimensiones siguientes:

Diámetro del cartucho mm	Manguera de plástico Diámetro interior mm	Diámetro exterior mm	Diámetro del taladro mm mínimum	Diámetro del taladro mm máximum
22	25	30	37	48
25	26	34	40	51
29	30	39	45	75
40	41	51	58	100

Se ha comprobado que la operación funciona mejor si se agregan unos 20 a 40 cartuchos cada vez. El detonador se introduce en un cartucho que es impulsado hacia adelante hasta el extremo de la manguera, y los cables del mismo se sacan de ella desde el interior del barreno. Se mueve hacia adelante y hacia atrás la manguera, con pequeños movimientos que exigen la mínima cantidad de trabajo y aseguran un buen grado de compactación. En el caso de un barreno lleno de agua, puede colocarse alrededor de la manguera un disco de goma o de un material similar, con objeto de proteger al operador del agua pulverizada.

Consideraciones prácticas:

- Almacenar las mangueras de carga extendidas, o arrolladas en un círculo de gran diámetro.
- Asegurarse de que la boquilla y las cuchillas están en buen estado.
- Comprobar que la alimentación de aire es satisfactoria y que la presión, pasada la válvula de seguridad, es de 3 kp/cm².
- Restaurar los cartuchos aplastados antes de introducirlos en el aparato.
- Almacenar el explosivo en un lugar caliente antes de la carga con tiempo frío.
- Utilizar una manguera del diámetro adecuado para el barreno de que se trate.
- Si se forma un tapón, utilizar únicamente el tipo autorizado de bomba especial de agua.

Cuando se emplea una cargadora de aire comprimido, la concentración de carga debe ser:

Diámetro del barreno mm	Concentración de carga kg/m (1,25 kg/dm³)
35	1,2
40	1,6
45	2,0
48	2,3
51	2,6
64	4,1
75	5,6

En el caso de un retacado muy preciso, puede lograrse una concentración más alta. Esta depende también de la rigidez del explosivo; con temperaturas del aire bajas, el explosivo aumenta su rigidez, y la concentración de la carga puede disminuir.

Cargadora semiautomática

Esta máquina permite la introducción continua de cartuchos a la misma velocidad con que son cargados en el barreno por la manguera. En lugar de

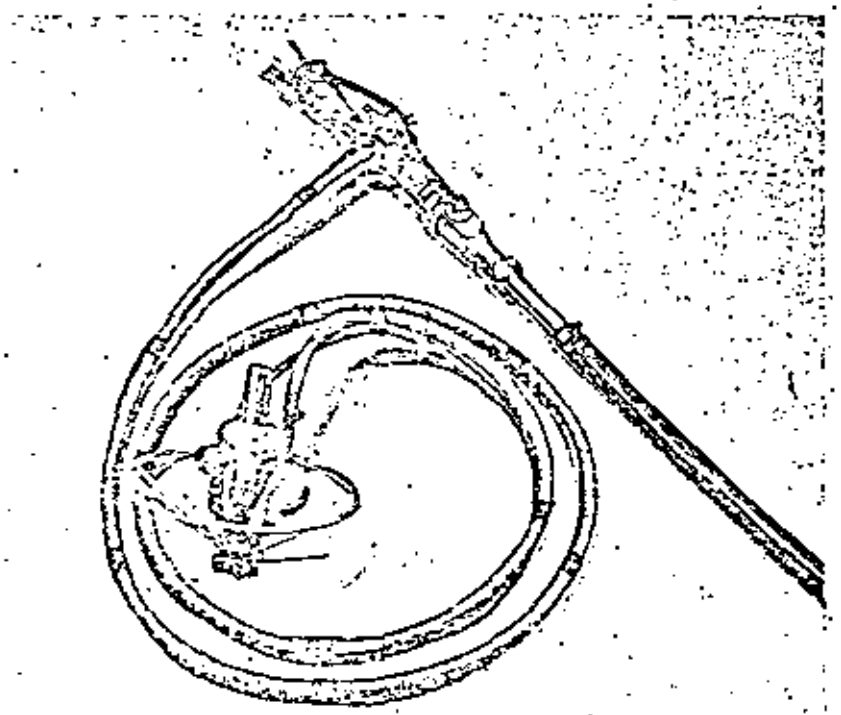

Fig. 6.3.2 Cargadora semiautomática

utilizar una válvula, los cartuchos pasan a través de una esclusa neumática entre dos lengüetas. La presión de aire es mantenida en el tubo mientras se introducen los cartuchos. La cargadora semiautomática permite una capacidad de carga considerablemente más elevada que el tipo normal.

Consideraciones prácticas:

- Introducir los cartuchos con un ritmo regular de modo que tengan tiempo para llegar al final de la manguera.
- Utilizar un soporte para el obturador.
- Manejar la máquina con cuidado y mantenerla limpia y bien engrasada.
- Asegurarse de que reciba suficiente aire comprimido.

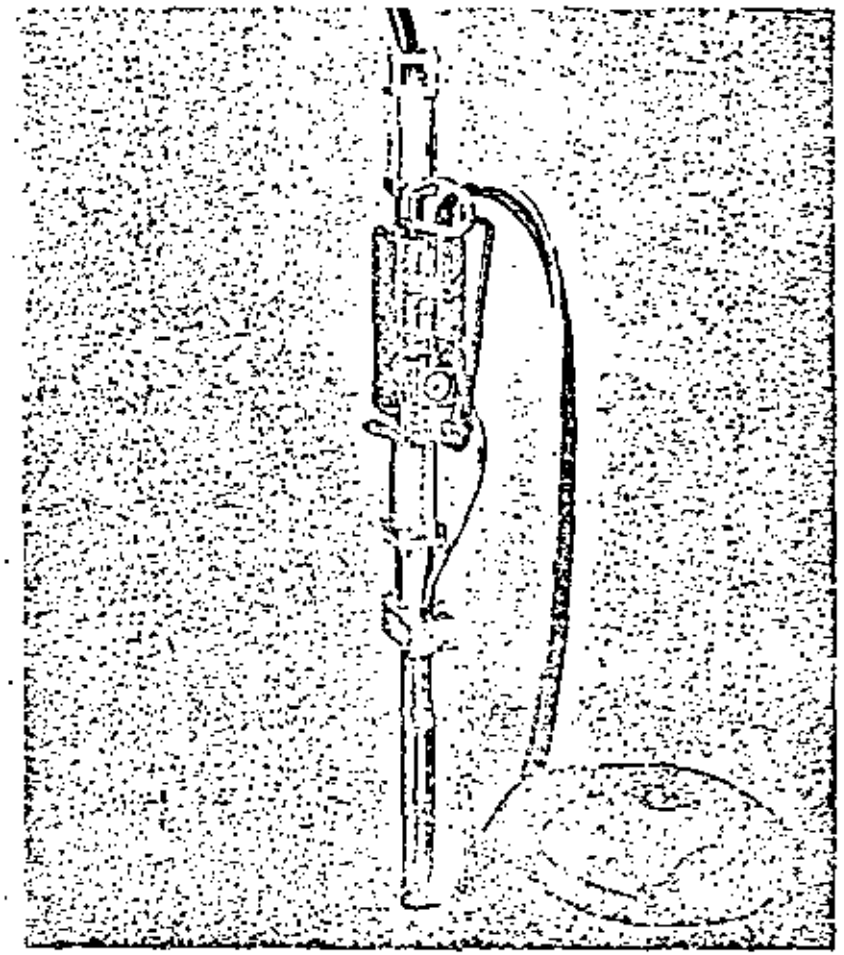

Fig. 6.3.3 Cargadora automática

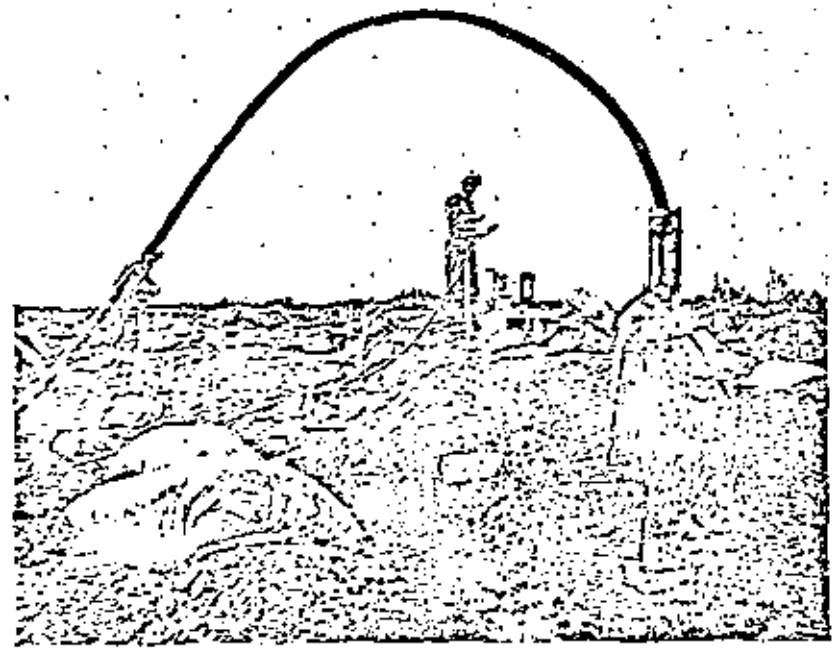

Fig. 6.3.4 Cargador automático

Las *cargadoras automáticas* han sido utilizadas principalmente debajo de la superficie para cargar barrenos de gran longitud, pero también se han probado en los últimos años en voladuras en banco.

Esta máquina realiza el retacado con un tubo o manguera de carga. Su principio básico es una mordaza neumática que mantiene firmemente en posición a la manguera mientras se mueve hacia atrás y adelante, accionada mediante un cilindro automático de doble acción.

Si se varía la presión del aire en el elemento de agarre, varía también la fricción entre la manguera y la mordaza, y con ello el grado de retacado de la carga. Utilizando una cargadora automática, un hombre puede realizar la operación con un obturador semiautomático. Esto implica que la capacidad de carga alcanzada es muy buena. El conjunto de ambos elementos constituye un sistema de carga que proporciona unas buenas posibilidades de realizar la operación con alto rendimiento y plena utilización del volumen del barreno.

Además, la cargadora automática constituye un método más favorable desde el punto de vista operacional, especialmente en el caso de barrenos llenos de agua o de gran longitud dirigidos hacia arriba.

La Tabla siguiente muestra las posibilidades de utilización de los barrenos para diferentes diámetros de los mismos y distintas concentraciones de carga. El ejemplo está basado en una profundidad de perforación de 12 m, con un error de perforación de 3 cm/m, y un error de emboquille de 5 cm.

Diámetro del barreno	Carga manual, en cartuchos o fundas de plástico		Cargadora de aire comprimido		Cargadora neumática automática	
	Aprox. 1,15 kg/dm³		Aprox. 1,25 kg/dm³		Aprox. 1,40 kg/dm³	
mm	Conc. kg/m	Piedra V_1	Conc. kg/m	Piedra V_1	Conc. kg/m	Piedra V_1
38	1,3	1,2	1,4	1,3	1,6	1,4
45	1,8	1,5	2,0	1,6	2,2	1,7
48	2,1	1,7	2,3	1,8	2,6	1,9
51	2,4	1,8	2,6	1,9	2,9	2,0
64	3,8	2,4	4,1	2,5	4,6	2,6
75	5,1	2,8	5,6	3,0	6,3	3,2
88	7,1	3,4	7,7	3,6	8,6	3,8
100	9,2	3,9	10,0	4,1	11,2	4,3

Esta Tabla muestra claramente la influencia de las concentraciones de carga sobre la posibilidad de aumentar la *piedra* del barreno. La mejor forma de calcular la diferencia, sin embargo, es calcular las áreas correspondientes a cada barreno:

Diámetro del barreno mm	Carga manual, en cartuchos o fundas de plástico $V_1 \times E_1$	Cargadora neumática automática $V_1 \times E_1$	Incremento de área por barreno %
38	1,8	2,4	33
45	2,8	3,6	28
48	3,6	4,6	28
51	4,0	5,0	25
64	7,2	9,0	25
75	9,8	12,3	25
88	14,4	18,0	25
100	19,1	23,2	21

Los cálculos indican que el área por barreno aumenta de un 20 a un 30 % aproximadamente, utilizándolo al máximo, con relación a la carga manual con cartuchos o en tubos de plástico. Esto lleva consigo la correspondiente reducción en el coste de perforación, además de un mayor volumen de roca desprendido por barreno y unidad de tiempo.

La reducción de coste por metro cúbico de roca puede calcularse sobre la base del valor de la perforación específica y del coste de perforación por metro, a partir del ejemplo anterior y para una profundidad del taladro de 12 m. Puede calcularse la cuantía de la perforación necesaria por metro cúbico de roca volada suponiendo para la sobreperforación un valor normal de 0,3 V_{max}:

Diámetro de los barrenos mm	Perforación espec. Carga en cartuchos o tubo de plástico m perf./m³	Cargadora neumática automática m perf./m³	Coste de perforación supuesto Coronas/m	Reducción de coste Coronas/m
38	0,61	0,46	7—9	1,05—1,35
45	0,40	0,31	7—9	0,63—0,81
48	0,31	0,24	8—10	0,56—0,70
51	0,28	0,22	8—10	0,48—0,60
64	0,16	0,13	12—15	0,36—0,45
75	0,12	0,09	13—16	0,39—0,48
88	0,08	0,06	14—17	0,28—0,34
100	0,06	0,04	15—19	0,30—0,38

El coste de perforación puede evidentemente variar en el caso de valores no incluidos en las tablas. Por otra parte, ha de tomarse debidamente en consideración el hecho de que la situación del barreno influye también sobre la fragmentación. Para una misma carga específica, se obtiene una mejor fragmentación con barrenos menos espaciados. Por esta razón, si los barrenos se perforan alejados unos de otros, por disponerse una concentración más elevada en la carga de fondo, debe mantenerse un valor elevado de carga específica aumentando también la carga de columna.

Carga bajo el agua

Cuando se realizan operaciones de voladura bajo el agua, es muy importante que se utilicen máquinas cargadoras: el resultado de la voladura depende de la posibilidad de obtener exactamente la concentración de carga prevista.

Las operaciones de carga son más dificultosas por la contrapresión que ejerce el agua. Cuando se trabaja a profundidad considerable, esta contrapresión puede ser compensada sumergiendo la válvula de reducción en el

agua. La compensación será de 1,0 kp/cm² por 10 m de profundidad de agua. Ljungberg recomienda que la presión en la boquilla de la manguera de carga sea de 1,5 a 2,0 kp/cm². Esto significa que la válvula de reducción ha de ser bajadade5 a 8 metros por debajo de la superficie del agua cuando se está efectuando la carga a 20 m de profundidad.

El método seco de voladuras subacuáticas está basado fundamentalmente en realizar la carga con máquinas neumáticas. Para las voladuras de esta clase, la carga específica es corrientemente de 1,0 a 2,0 kg por m³ de roca, con lo que esta operación se constituye en una parte importante del trabajo a realizar en la voladura. Una ventaja adicional consiste en que los barrenos son cargados en condiciones de plena confianza, pues la manguera puede ser introducida hasta el fondo del barreno antes de comenzar a cargar, lo que garantiza que el barreno queda cargado hasta la profundidad deseada. Sobre todo en el caso de roca con barrenos rotos, resulta difícil cargar éstos completamente, usando cargas envasadas y de gran diámetro. En cuanto a los detonadores, se introducen a través del tubo o manguera de carga.

Es particularmente importante cuando se opera bajo el agua emplear una presión de carga convenientemente adaptada, y deben efectuarse ensayos a este respecto haciendo bajar la válvula de reducción a diferentes profundidades.

En ciertos tipos de roca con grandes oquedades, la carga puede realizarse usando cargas alargadas rígidas que se introducen en los barrenos. El encendido de estas cargas se efectúa entonces con ayuda de mecha detonante, que está herméticamente protegida contra la humedad.

Carga de Reomex con cargadora neumática

En 1.973 se comenzó a cargar el hidrogel explosivo Reomex con ayuda de cargadoras neumáticas. El obturador semiautomático TA32R ha sido proyectado especialmente para los cartuchos de Reomex de 32 × 300 mm.

El obturador semiautomático puede ser combinado con un dispositivo automático para voladuras subacuáticas o en banco. Como el Reomex tiene una densidad menor que el Dynamex, se obtiene un grado de compactación más bajo. La densidad del Reomex A es de 1,20 kg/dm³, y la del Reomex B, de 1,10 kg/dm³.

Diámetro de los barrenos mm	Carga con cargadora neumática y un alto grado de compactación Reomex A kg/m	Reomex B kg/m
48	2,0	1,8
64	3,6	3,3
75	4,9	4,5

El Reomex bien retacado presenta una buena resistencia frente al agua, lo que es una gran ventaja, en el caso, por ejemplo, de voladuras subterráneas en las que barrenos de gran longitud han de permanecer frecuentemente cargados durante un periodo de tiempo relativamente largo.

Carga de Reomex a granel

La carga a granel de los explosivos es un método que presenta muchas ventajas. Con anterioridad se efectuaba la carga a granel de explosivos de mezcla del tipo Prilit, no habiendo sido posible hacer lo mismo con productos de alta energía, como los explosivos de nitroglicerina, por razones de seguridad. El Reomex es un hidrogel explosivo sensible a la iniciación con detonador, con muchas características sobresalientes que pueden hacer de él un explosivo muy completo, especialmente en trabajos subterráneos. Tanto el Reomex A como el Reomex B pueden ser cargados a granel con ayuda de una bomba especialmente diseñada capaz de desplazar el producto, relativamente rígido.

Como no se emplea ningún material de retacado, la *totalidad* del barreno es llenada de explosivo, y ésto facilita una utilización completa del barreno a pesar de que este explosivo es menos potente que el Dynamex B. En la Tabla siguiente se muestra la fuerza de rotura de la roca en barrenos cargados con Reomex, en relación con los mismos barrenos cargados con Dynamex B mediante máquina.

Diámetro de los barrenos	Dynamex B		Reomex A		Reomex B	
	Conc.	Fuerza rotura	Conc.	Fuerza rotura	Conc.	Fuerza rotura
mm	kg/m	F.rel./m	kg/m	F.rel./m	kg/m	F.rel./m
38	1,44	144	1,38	132	1,27	98
48	2,30	230	2,21	212	2,02	156
64	4,10	410	3,94	378	3,61	278

La fuerza rompedora por metro de barreno ha sido calculado del modo siguiente: Potencia por unidad de peso × Concentración de carga por metro = Fuerza rompedora relativa por metro (F.rel./m).

La capacidad de carga que se logra con Reomex a granel es extremadamente alta: pueden alcanzarse valores de hasta 25 kg/min. trabajando bajo tierra, incluso en condiciones no ideales.

Este sistema de carga, completamente nuevo en Suecia, presenta grandes posibilidades por su capacidad y su ventajosa manipulación desde el punto de vista operacional.

Fig. 6.3.5 Carga de Reomex bajo la superficie

Cargadoras para explosivos en forma de materiales sueltos (ANFO)

Los explosivos en forma granular, corrientemente los de nitrato amónico, requieren unas máquinas cargadoras especiales, entre las que pueden diferenciarse dos tipos: de cuba de presión, y de eyector.

Las máquinas del primer tipo son especialmente adecuadas para explosivos cristalinos de nitrato amónico. La capacidad de carga lograda con ellas puede ser muy buena.

Los eyectores funcionan aspirando el explosivo de un recipiente, a través de un conducto; el explosivo es inyectado a continuación al interior del barreno a través de la manguera de carga.

Existen también máquinas combinadas de presión y eyector.

En relación con el empleo de las máquinas cargadoras de explosivos pulverulentos, es importante asegurarse de que la manguera de carga utilizada sea de un tipo autorizado.

El método empleado para el transporte del explosivo por la conducción implica un riesgo considerable de acumulación de energía estática, por lo que las mangueras de carga utilizadas han de ser conductoras de la electricidad. De acuerdo con las normas del Departamento sueco de Higiene y Seguridad en el Trabajo, la manguera de carga para los trabajos con explosivos ANFO ha de tener una resistencia eléctrica de al menos 1 $k\Omega/m$, y de 30 $k\Omega/m$ como máximo.

Este sencillo y racional método de carga ha supuesto una valiosa contribución al éxito de los explosivos de nitrato amónico. Existen asimismo equipos para el transporte del explosivo a lugares subterráneos de difícil acceso y donde han de efectuarse operaciones de carga.

Se está trabajando en el desarrollo de procedimientos para una más completa adaptación de los equipos de carga a los diversos tipos de explosivos de nitrato amónico que se producen en la actualidad. Además del nitrato amónico cristalino y en gránulos, se emplean también mezclas de ambos tipos. Existe también un explosivo de nitrato amónico (Prillit) que contiene una cierta proporción de aluminio pulverizado y que también puede ser cargado con máquinas neumáticas.

En el caso de voladuras para producción, usando diámetros de barrenos de más de 150 mm, el explosivo de elección más racional es una papilla (Reolit): ello se fundamenta en gran medida en el hecho de que se han desarrollado hoy en día unos eficaces métodos de carga para el bombeo de las papillas explosivas. En el caso de barrenos de gran diámetro, más de 250 mm, puede alcanzarse una capacidad de carga de 150 kg/min. Si los barrenos están rotos, pueden ser entubados con una delgada funda de plástico.

Naturalmente, el explosivo utilizado ha de poseer una consistencia adecuada que lo haga apto para el bombeo. En el caso de voladuras a gran escala a

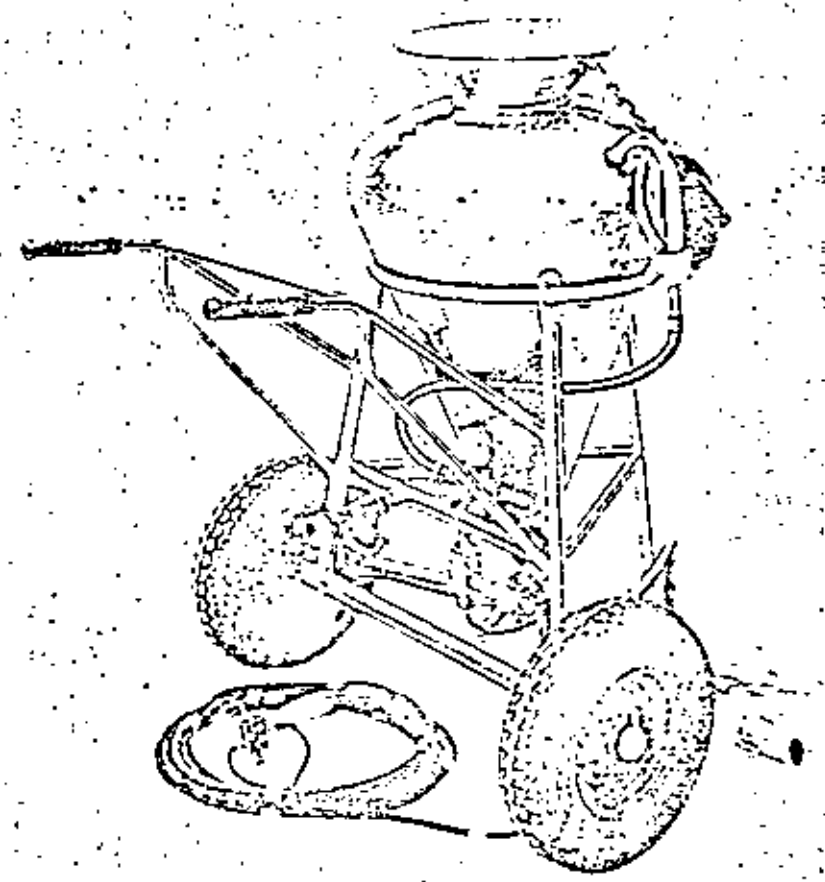

Fig. 6.3.6 Máquina cargadora para Prillit

nivel de la superficie y con un empleo de cantidades considerables de explosivo, es recomendable establecer una pequeña planta de producción de los mismos próxima al lugar de las voladuras.

En tales casos, para que el sistema citado resulte ventajoso, el consumo de explosivo debe ser cercano a las 2000 t/año.

El sistema de las papillas explosivas ha sido también ensayado para trabajos de edificación, empleando barrenos de 64 a 75 mm de diámetro; sin embargo, el procedimiento no ha resultado apropiado para este tipo de voladuras, pues la carga por barreno es demasiado pequeña para cargar con bombas, y los explosivos de este tipo son más difíciles de adaptar a carga manual que optar por el empleo de explosivos en cartuchos.

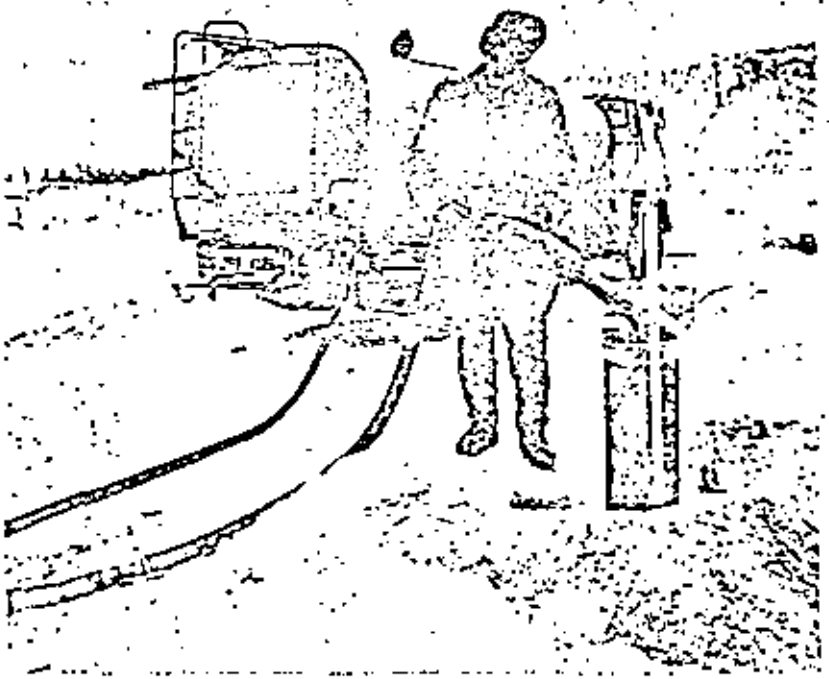

Fig. 6.3.7 Inyectando Reolit con bomba

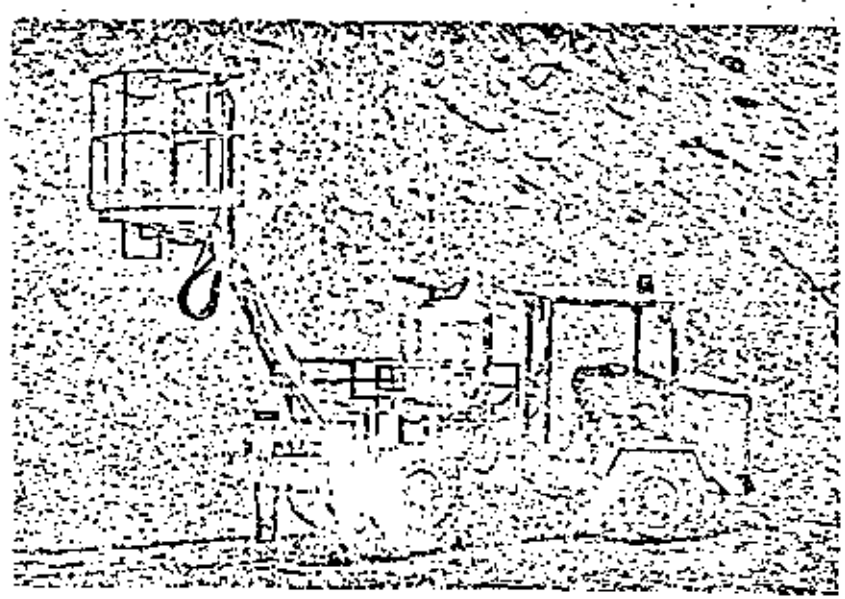

Fig. 6.3.8 Moderno camión de carga

7. VOLADURAS EN ZANJA

7.1 METODOS DE CALCULO DE CARGAS

La voladura de zanjas constituye una parte importante de la tecnología de los explosivos. En Suecia, se ha registrado en los últimos años un aumento en la cuantía de las zanjas abiertas con explosivos, al haberse realizado numerosas obras de construcción e instalación de servicios zonales de calefacción y de drenaje y alcantarillado en áreas edificadas (véase la sección 13.4, Voladura controlada de zanjas).

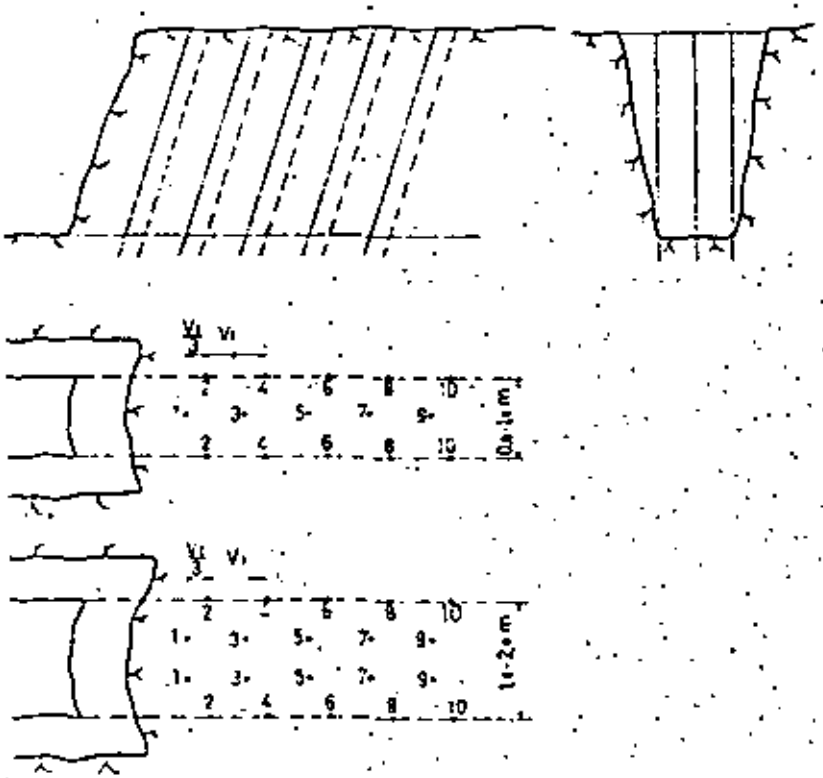

Fig. 7.1.1

La voladura de zanjas implica generalmente voladuras en banco con una anchura no superior a 2 m. La frontera entre voladuras en banco y voladura en zanjas puede ser un poco difusa; lo importante es ser consciente de las diferencias en la perforación y en la carga que han de ser observadas en el caso de excavaciones poco profundas. La voladura en zanjas requiere unos barrenos con espaciamiento denso, así como un alto nivel de carga específica (kg/m³), que depende de las tensiones existentes en la roca. El grado de fricción contra las superficies de roca es considerable, y se requieren unas cargas suplementarias para lograr el esponjamiento de la masa (véase la sección 5.3, Esponjamiento). En las voladuras en zanjas, la inclinación de los barrenos posee una importancia capital: una inclinación acusada de los barrenos hace disminuir la tensión en la roca, con lo que se facilita el efecto rompedor en el fondo, y el esponjamiento. Esto es especialmente aplicable al caso de zanjas o trincheras profundas.

La perforación y la carga pueden realizarse de acuerdo con la Tabla que se incluye a continuación, adecuada para barrenos de la serie 11, 34—29 mm.

Profundidad de la zanja	Prof. barrenos	V_{area}	V_1	Carga de fondo, kg/barreno. Anchura del fondo: 3 barrenos 0,8—1,0 m	4 barrenos 1,5—2,0 m	Carga de columna, kg/barreno. Concentración aprox. de carga: 0,25 kg/m
m	m	m	m			
0,4	0,6	0,4	0,4	0,05	0,05 [1]	—
0,6	0,9	0,6	0,6	0,10	0,10 [1]	—
0,8	1,1	0,7	0,7	0,15	0,15 [1]	—
1,0	1,4	0,8	0,8	0,15	0,20 [1]	0,10
1,2	1,6	0,9	0,8	0,15	0,25 [1]	0,20
1,5	1,9	0,9	0,8	0,20	0,30 [1]	0,25
2,0	2,4	0,9	0,8	0,25	0,35 [1]	0,40
2,5	3,0	0,9	0,75	0,30	0,45	0,45
3,0	3,5	0,9	0,75	0,40	0,55	0,60
3,5	4,0	0,9	0,70	0,50	0,65	0,70
4,0	4,5	0,9	0,70	0,60	0,90	0,80

[1]) Se emplean 3 barrenos en zanjas menores de 2,5 m de profundidad y 1,5 m de anchura. En ciertos tipos de roca difíciles de volar, puede ser necesario incrementar la carga cuando se utilizan 3 barrenos en trincheras menores de 2,5 m de prof.

En esta Tabla, se ha calculado el valor de la *piedra* práctica tomando en consideración el error de perforación y la necesidad de esponjamiento.

La carga de columna tiene una concentración reducida para disminuir la

sobreexcavación. Es difícil realizar las voladuras en zanjas de modo que se obtenga la sección teórica deseada.

Los barrenos están situados verticalmente y en sentido longitudinal a lo largo de la zanja (Fig. 7.1.1). Como normalmente es deseable una cierta inclinación de los lados de la zanja, una cierta proporción de la acción de arranque tiene lugar fuera de la hilera de barrenos que está dentro de la sección teórica.

La reducida concentración de carga se consigue mediante el empleo de carga con separadores, consistente en medios cartuchos de Dynamex espaciados por separadores de madera de unos 10 cm de longitud.

En estos casos es importante asegurarse de que la carga de columna no sea retacada de tal modo que se obtenga una concentración de la misma considerablemente mayor. También pueden usarse como cargas de columna cargas alargadas de Gurit de 17 mm, con lo que se produce menor sobreexcavación.

En roca difícil de romper, las cargas alargadas de Gurit pueden resultar poco potentes para las *piedras* más grandes. Se incluye seguidamente un resumen de las diferentes concentraciones de carga que pueden ser consideradas:

Piedra m	Carga	Concentración kg/m de Dynamex
0,6	Gurit de 17 mm	0,18
0,7	Gurit de 17 mm + ¼ cartucho de Dynamex	0,21
0,7	½ cartucho Dynamex + separadores madera de 10 cm	0,25
0,8	Gurit de 17 mm + ½ cartucho de Dynamex	0,23
0,8	½ cartucho Dynamex + separadores madera de 10 cm	0,25

No deben usarse separadores de madera de longitud superior a 10 cm (4"), sobre todo en tiempo frío, pues ello implica una considerable disminución de las propiedades de propagación del explosivo.

Es también importante que se coloque un tapón sobre la carga de columna antes de añadir el material de retacado.

El esquema de encendido toma en principio la forma de la Fig. 7.1.1.

El cálculo de las cargas puede también hacerse a partir de la carga específica necesaria (véase la sección 13.4, "Voladura controlada en zanjas").

En muchos casos puede ser conveniente realizar las voladuras de excavación de zanjas en forma de trabajo preliminar para voladuras en banco. Una vez abierta mediante voladuras una zanja en un emplazamiento adecuado, puede determinarse la dirección de rotura para las pegas en banco.

Si las voladuras se realizan fuera de áreas edificadas, o si puede tolerarse una cierta cantidad de proyecciones y vibraciones del terreno, pueden utilizarse barrenos de un diámetro mayor que la serie usual de pequeño diámetro.

Tabla de perforación y carga para diámetro del taladro de 50 mm.

Profundidad de la zanja	Prof. barrenos	V_{max}	V_1	Carga de fondo, kg barreno. Anchura del fondo: 3 barrenos 1,0 m	3 barrenos 1,5—2,0 m	Carga de columna, kg barreno. Concentración aprox. de carga 0,40 kg m⁻¹
m	m	m	m			
0,6	0,9	0,6	0,6	0,15	0,20	—
1,0	1,4	0,8	0,8	0,20	0,25	0,20
1,5	2,0	1,4	1,1	0,30	0,40	0,35
2,0	2,5	1,4	1,1	0,40	0,55	0,50
2,5	3,1	1,4	1,1	0,50	0,65	0,75
3,0	3,6	1,4	1,1	0,60	0,75	0,90
3,5	4,1	1,4	1,1	0,75	0,95	1,10
4,0	4,6	1,4	1,1	0,90	1,15	1,30

1) En zanjas de 2 m de anchura hay que aumentar la concentración de carga de columna a 0,50 kg/m.

La magnitud de la *piedra* práctica ha sido reducida a 1,1 m para disminuir las tensiones. En los casos en que existe un campo libre para las voladuras, es posible aumentar este valor hasta 1,2 m, y con ello incrementar también la carga en la correspondiente magnitud.

En cualquier caso, las voladuras de zanjas con barrenos de gran diámetro sólo pueden efectuarse cuando no haya edificios en las proximidades, pues el riesgo de vibraciones del terreno y de proyecciones es considerablemente mayor que con el método convencional.

La Tabla anterior puede ser también utilizada con barrenos de un diámetro aproximado de 40 mm, en cuyo caso puede ser necesario disminuir ligeramente la carga de columna.

En las voladuras de zanjas, la zona de retacado de los barrenos no debe ser demasiado larga, especialmente en roca de resistencia elevada, pues existiría el peligro de que la roca de la superficie resistiera la explosión aun cuando la zona del fondo fuera desprendida.

Por lo que se refiere al empleo de materiales de protección en las voladuras de zanjas, es éste un factor muy importante (véase el capítulo 8, "Protección"). Cuando se trabaja en áreas edificadas, es preciso tomar precauciones especiales (véase la sección 13.4, "Voladura controlada en zanjas").

El ejemplo siguiente es una ilustración de la aplicación de las Tablas anteriores:

Se ha de efectuar un trabajo de voladuras de zanjas a gran escala, con algunos tramos muy próximos a diversas instalaciones, si bien la mayor parte del trabajo se hace en condiciones completamente libres.

Anchura de la zanja: 1,5 m.
Profundidad de la zanja en la zona de instalaciones: 1,0—2,0 m.
Profundidad de la zanja en la zona libre: 2,5 m aproximadamente.

Se ha decidido utilizar perforaciones de pequeño diámetro en la zona de instalaciones, y un equipo de perforación para diámetros de 50 mm fuera de esta zona.

Los cálculos de perforación y de carga se realizan basándose en las Tablas anteriores y para los diámetros de barreno correspondientes:

Situación	Diámetro barrenos mm	Profdad. zanja m	Profdad. barrenos m	Piedra práctica m	Carga de fondo kg	Carga de fondo kg	Carga de columna kg/m
Dentro del área de instalaciones	Serie 11	1,0	1,4	0,8	0,20	0,10	0,25
	Serie 11	1,5	1,9	0,8	0,30	0,25	0,25
Fuera del área de instalaciones	50 mm	2,5	3,1	1,1	0,65	0,75	0,40

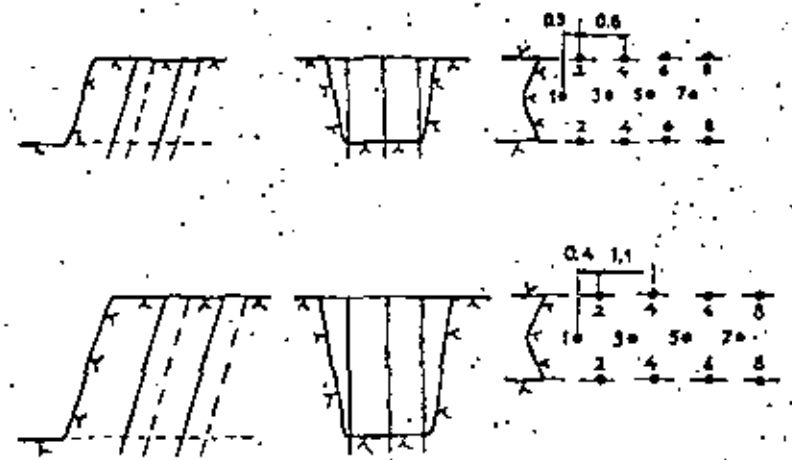

Fig. 7.1.2

7.2 VOLADURA EN ZANJAS. MEJORAS EN LA EJECUCION

Cuando se están excavando zanjas por medio de explosivos, es importante que las operaciones de perforación y carga de barrenos se efectúen de tal modo que resulte el menor volumen posible de sobreexcavación. Este volumen no sólo significa una mayor cantidad de material que retirar, sino también mayores costes de relleno. No es en absoluto infrecuente en los métodos convencionales de voladura de zanjas que se produzcan volúmenes de sobreexcavación de hasta el 100 % del volumen teórico proyectado. Las voladuras controladas hacen posible reducir esta sobreexcavación en una gran proporción.

Si las voladuras en zanjas se realizan de acuerdo con el método que se ha descrito en la sección 7.1, los barrenos quedan distribuidos de tal manera que es posible repartir a cada uno de ellos una carga igualmente grande. Sin embargo, si los barrenos están distribuidos en una hilera con la misma *piedra*, las cargas de los mismos pueden ser repartidas de otro modo que resulte ventajoso desde muchos puntos de vista.

En la llamada *voladura suave* o *recorte*, se da a los barrenos la misma *piedra* disponiéndolos en una hilera ininterrumpida. Si los barrenos se distribuyen en la hilera de la forma que se muestra en el ejemplo siguiente, los centrales pueden llevar cargas más potentes, al tiempo que se reduce la carga en los del contorno, rebajando así la sobreexcavación. Ha resultado también ventajoso cargar hasta arriba los barrenos del contorno con Gurit, lo que asegura el corte a lo largo del contorno teórico. Los altos niveles de carga exigen, sin embargo, un material de protección muy pesado y que sirva también contra las esquirlas.

Este último método presenta además otras ventajas:

— El plan de perforación es más regular, lo que facilita el trabajo de situar y orientar los barrenos.

— Los barrenos de contorno pueden ser cargados a niveles altos con explosivo poco potente (Gurit, por ejemplo), y el resultado es un buen recorte de la roca de la superficie a lo largo del contorno teórico.

La Tabla siguiente es aplicable a barrenos de la serie 11, de 34 a 29 mm. Se emplea una inclinación de los mismos de 3:1, y una anchura de zanja de 1 metro, con filas de barrenos de tres en fondo.

Profdad. de la zanja	Profdad. de los barrenos	$V_{max.}$	V_n	Carga de fondo kg barreno		Carga de columna			
				Barrenos centrales	Barrenos contorno	Barrenos centrales		Barrenos contorno	
m	m	m	m	kg	kg	kg	kg.m	kg	kg.m
0,4	0,6	0,4	0,40	0,05	0,05	—	—	—	—
0,6	0,9	0,6	0,60	0,12	0,09	—	—	—	—
0,8	1,1	0,7	0,70	0,18	0,13	—	—	—	—
1,0	1,4	0,8	0,70	0,20	0,15	0,10	0,35	0,15	0,18
1,2	1,6	0,9	0,70	0,20	0,15	0,25	0,35	0,20	0,18
1,5	1,9	0,9	0,70	0,25	0,20	0,30	0,35	0,25	0,18
2,0	2,4	0,9	0,75	0,30	0,25	0,45	0,35	0,30	0,18
2,5	3,0	0,9	0,75	0,35	0,30	0,65	0,35	0,45	0,18
3,0	3,5	0,9	0,75	0,45	0,40	0,80	0,35	0,50	0,18
3,5	4,0	0,9	0,70	0,55	0,50	0,95	0,35	0,55	0,18
4,0	4,5	0,9	0,70	0,65	0,60	1,10	0,35	0,65	0,18

Además de la necesidad de una correcta inclinación de los barrenos, el paralelismo de los mismos y una perfecta alineación o emboquille, es muy importante que la perforación se ejecute hasta la *profundidad especificada*. Naturalmente, ésto es aplicable a todas las voladuras en roca, pero especialmente al caso de las zanjas, por encontrarse en ellas la roca con una constricción muy severa en los lados. La carga de fondo es relativamente pequeña (= corta), y ésto lleva consigo la posibilidad de que, en un barreno que haya sido perforado con una profundidad excesiva, la carga puede quedar por debajo del nivel de corte del fondo, y no llegar a romper por completo la roca.

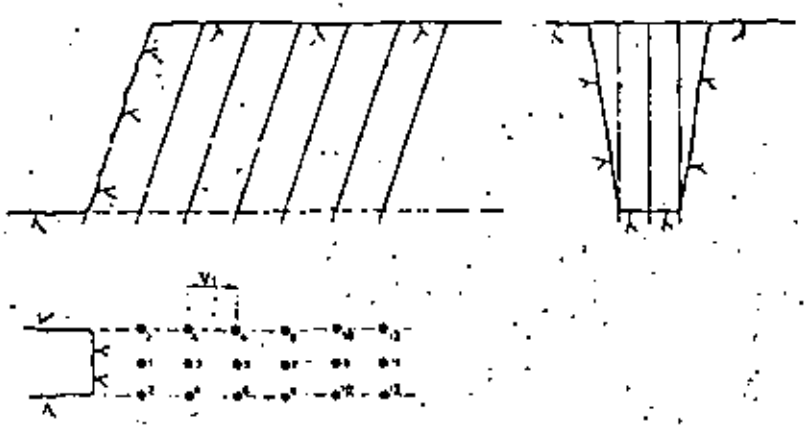

Fig. 7.2.1 Distribución de los barrenos en zanjas para conseguir un buen acabado

Una carga de columna adecuada para los barrenos centrales es la formada por Nabit A de 22 mm, que da una concentración de 0,40 kg/m si es apilada sin retacar, lo cual corresponde a 0,38 kg/m de Dynamex B. Los barrenos de contorno se cargan con Gurit de 17 mm. Estos elevados niveles de carga exigen el empleo de una protección pesada y que sea al mismo tiempo eficaz contra las esquirlas. El único material de retacado que se utiliza en este caso con las cargas alargadas de Gurit consiste en unos tacos de contención que mantienen las cargas en su posición. Los barrenos centrales se rellenan con un retacado de arena, como en el caso de las voladuras convencionales de zanjas. En las hileras de barrenos con rotura libre — la primera hilera de la pega — la carga de los mismos es inferior a la cantidad indicada en las Tablas.

La carga específica en el barreno es semejante a la empleada en el método descrito en la sección 7.1; la diferencia reside en que, en este caso, la concentración de carga se distribuye de modo diferente, con el resultado de una

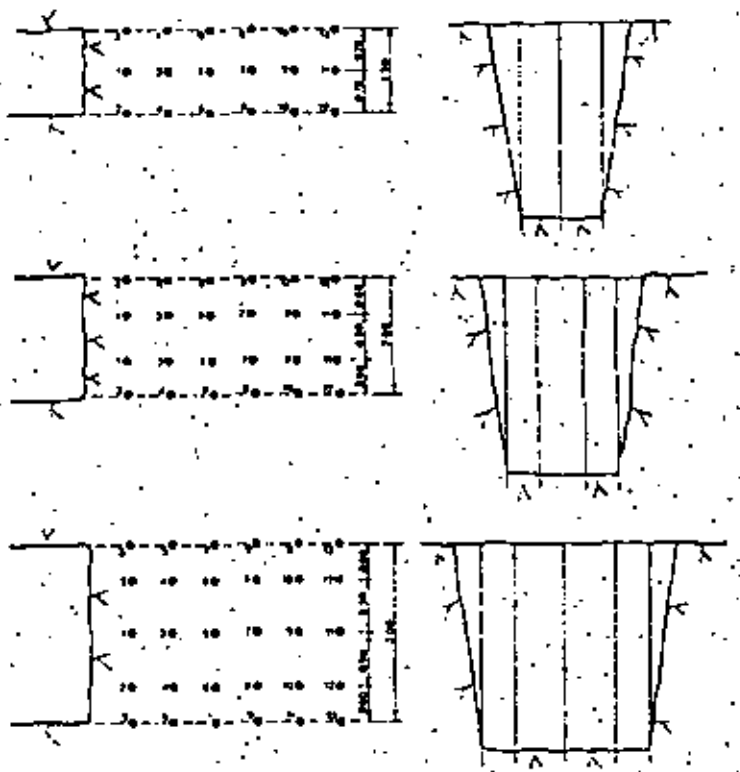

Fig. 7.2.2 Distribución de los barrenos en zanjas con varias anchuras

menor sobreexcavación. Otra ventaja reside en que el esquema de perforación es más regular, lo que facilita el emboquille y orientación de los taladros.

La Tabla siguiente es aplicable a barrenos de la serie 11, de 34—29 mm, con una inclinación de 3:1. Se considera una anchura de zanja de 1,5 m, con hileras de tres barrenos en fondo, siendo también aplicable a zanjas de 2,0 m de anchura con hileras de cuatro barrenos en fondo, o de 3 m de ancho con hileras de cinco barrenos en fondo.

Profdad. de la zanja	Profdad. de los barrenos	V_{max}	V_t	Carga de fondo kg barreno		Carga de columna			
				Barrenos centrales	Barrenos contorno	Barrenos centrales		Barrenos contorno	
m	m	m	m	kg	kg	kg	kg m	kg	kg/m
0,4	0,6	0,4	0,40	0,05	0,05	—	—	—	—
0,6	0,9	0,6	0,60	0,12	0,09	—	—	—	—
0,8	1,1	0,7	0,70	0,18	0,15	—	—	—	—
1,0	1,4	0,8	0,80	0,25	0,20	0,10	0,35	0,15	0,18
1,2	1,6	0,9	0,80	0,30	0,25	0,25	0,35	0,20	0,18
1,5	1,9	0,9	0,80	0,35	0,30	0,30	0,35	0,25	0,18
2,0	2,4	0,9	0,80	0,40	0,35	0,60	0,50	0,30	0,18
2,5	3,0	0,9	0,75	0,50	0,45	0,85	0,50	0,45	0,18
3,0	3,5	0,9	0,75	0,60	0,55	1,05	0,50	0,50	0,18
3,5	4,0	0,9	0,70	0,70	0,65	1,25	0,50	0,55	0,18
4,0	4,5	0,9	0,70	0,95	0,90	1,45	0,50	0,65	0,18

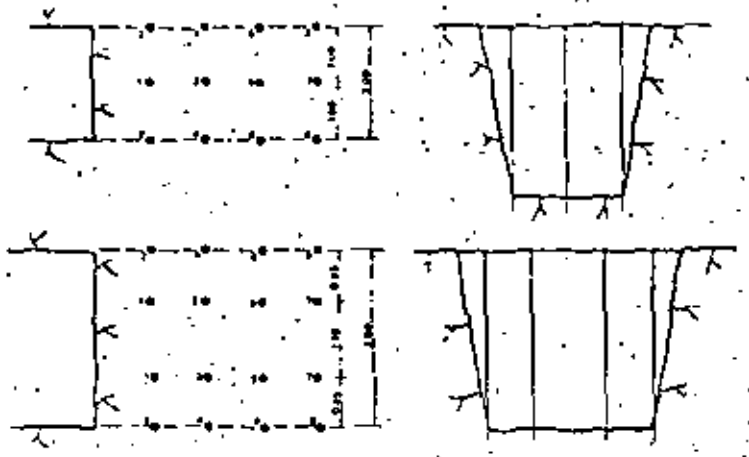

Fig. 7.2.3 Distribución de los barrenos en voladuras en zanjas al emplear 40 mm y 50 mm ø de perforación

Mediante este método es más fácil distribuir el total de la carga específica, especialmente en el caso de una zanja de 1,5 m de anchura, en el que la potente carga de columna a mayor profundidad compensa los requerimientos de carga con hileras de solamente 3 barrenos en fondo.

Para anchuras de zanja de 2,0 m — y fundamentalmente de 3 m — las cargas de columna en los barrenos centrales pueden ser reducidas, si se trata de rocas de un tipo fácil de volar y la profundidad de la zanja es de menos de 2,5 m.

La Tabla siguiente corresponde a barrenos de 40 mm de diámetro, y es aplicable a zanjas de 2,0 m de anchura con hileras de tres barrenos en fondo, y a zanjas de 3,0 m de anchura con hileras de cuatro barrenos en fondo.

Profdad. de la zanja	Profdad. de los barrenos	V_{max}	V_t	Carga de fondo kg barreno		Carga de columna			
				Barrenos centrales	Barrenos contorno	Barrenos centrales		Barrenos contorno	
m	m	m	m	kg	kg	kg	kg m	kg	kg.m
0,6	0,9	0,6	0,6	0,20	0,20	—	—	—	—
1,0	1,4	0,8	0,8	0,30	0,25	0,20	0,50	0,20	0,40
1,5	2,0	1,4	1,1	0,45	0,40	0,50	0,50	0,45	0,40
2,0	2,5	1,4	1,1	0,60	0,55	0,70	0,50	0,60	0,40
2,5	3,1	1,4	1,1	0,70	0,65	1,00	0,50	0,85	0,40
3,0	3,6	1,4	1,1	0,80	0,75	1,20	0,50	1,00	0,40
3,5	4,1	1,1	1,1	1,00	0,95	1,40	0,50	1,15	0,40
4,0	4,6	1,4	1,1	1,20	1,00	1,60	0,50	1,40	0,40

La Tabla siguiente corresponde a barrenos de 50 mm de diámetro, y es aplicable a zanjas de 2,0 m de anchura con hileras de tres barrenos en fondo, y a zanjas de 3,0 m de anchura con los barrenos en hileras de cuatro en fondo.

Profdad. de la zanja	Profdad. de los barrenos	V_{max}	V_t	Carga de fondo kg barreno		Carga de columna			
				Barrenos centrales	Barrenos contorno	Barrenos centrales		Barrenos contorno	
m	m	m	m	kg	kg	kg	kg.m	kg	kg.m
0,6	0,9	0,6	0,6	0,20	0,20	—	—	—	—
1,0	1,4	0,8	0,8	0,30	0,25	0,20	0,50	0,20	0,40
1,5	2,0	1,4	1,1	0,45	0,40	0,50	0,50	0,45	0,40
2,0	2,5	1,4	1,1	0,65	0,60	0,70	0,50	0,60	0,40
2,5	3,1	1,4	1,1	0,75	0,70	1,15	0,60	0,85	0,40
3,0	3,6	1,4	1,1	0,85	0,80	1,50	0,60	1,00	0,40
3,5	4,1	1,4	1,1	1,10	1,05	1,80	0,60	1,15	0,40
4,0	4,6	1,4	1,1	1,30	1,10	2,10	0,60	1,40	0,40

8. PROTECCION

8.1 MATERIALES DE PROTECCION

Una vez que se han tomado todas las medidas precisas para eliminar las proyecciones en las voladuras, puede también hacerse desaparecer cualquier peligro residual mediante el empleo de una protección perfectamente dispuesta. Esta protección puede estar compuesta por materiales de diversos tipos, y debe satisfacer algunas de las condiciones siguientes:

Resistencia considerable
Capacidad de unión de los elementos
Flexibilidad
Peso
Relativamente compactos
Permeabilidad a los gases
Capacidad de cubrir una gran área
Posibilidad de fijarse en su posición

Normalmente se establece una distinción entre dos tipos de material de protección:

Material de protección pesado
Material de protección contra esquirlas

El material de protección pesado debe evitar la proyección de grandes fragmentos de roca, así como impedir en cierta medida que la roca se mueva demasiado hacia adelante. El material de protección contra esquirlas debe impedir esencialmente la proyección o diseminación de fragmentos de la superficie de la pega. Los dos tipos de material de protección se emplean conjuntamente con frecuencia, el primero para evitar las proyecciones de mayor magnitud, y el segundo para detener las pequeñas piedras que hayan pasado a través del material pesado o provengan de las zonas de la pega no cubiertas por la protección pesada.

Hay muchos materiales diferentes que pueden ser utilizados como pantallas protectoras en las voladuras. Constantemente se desarrollan nuevos materiales con características diversas. Entre los materiales de protección más usuales en la actualidad cabe hacer la subdivisión siguiente:

Material pesado	*Material ligero (contra esquirlas)*
Pantallas de caucho	Pantallas de fieltro industrial
Rollizos atados en un conjunto	Pantallas Nitro de alambre de acero
Pantallas de alambre	Pantallas Columbus
Pantallas de argollas de hierro	Pantallas de trapos
	Mallas de armadura
	Mallas de alambre
	Lonas
	Tejidos de plástico-nylon

Las pantallas de caucho, confeccionadas generalmente con viejos neumáticos de automóviles, constituyen el tipo de protección más usado en Suecia. Las piezas grandes, en especial, con áreas de 10 a 12 m², proporcionan una excelente protección con su peso y durabilidad.

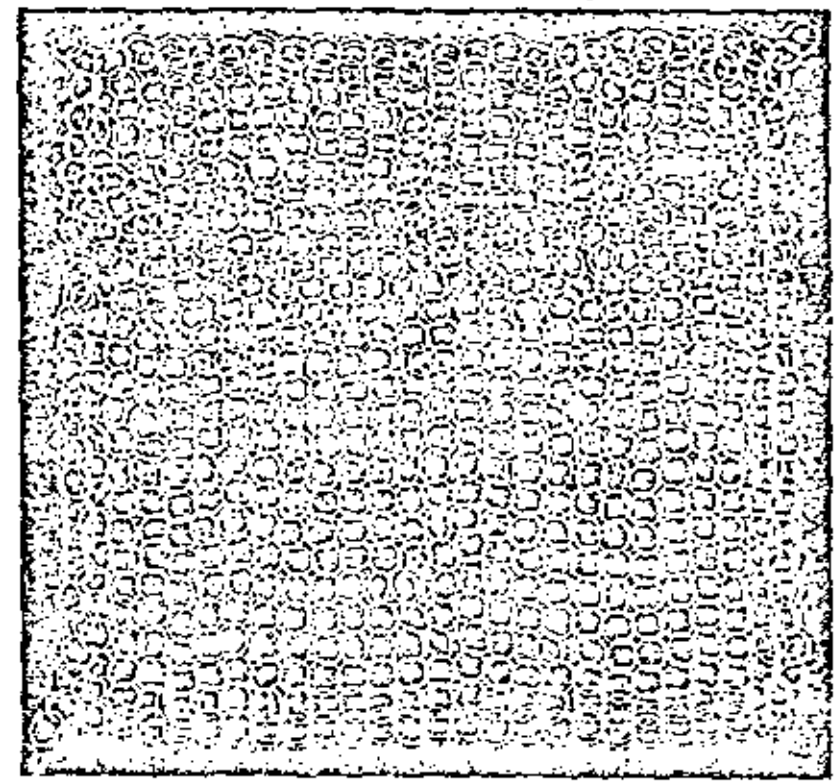

Fig. 8.1.1 Pantalla Nitro

Debe existir la posibilidad de ensamblar conjuntamente las pequeñas unidades portátiles. La pantalla Nitro, con sus 9 m² de área, posee la capacidad de mantener unidos los elementos al mismo tiempo que proporciona protección frente a las esquirlas. Las pantallas fabricadas con rollizos atados se utilizaron más extensamente en el pasado: no obstante, son apropiadas para la protección de bocas de túneles, o para otros trabajos con explosivos en los que se requiera alguna forma de protección colgante.

El fieltro industrial, un producto de las fábricas de papel, es un material muy bueno para la protección contra esquirlas; puede recubrir una gran área y es también de bastante duración. Unas simples mallas de alambre, preferiblemente en varias capas, proporcionan una buena protección contra el lanzamiento de piedras pequeñas. Es preciso asegurarse cuidadosamente de que ningún empalme entre los cables de los detonadores eléctricos entre en contacto con material conductor en las pantallas de protección; estos empalmes deben ser aislados. Algunas pantallas de caucho llevan sus partes metálicas aisladas con un material plástico, lo que resulta muy conveniente. Las pantallas de alambre han demostrado, tanto en ensayos como a lo largo de su utilización práctica, que poseen unas buenas características; a pesar de su peso relativamente elevado por unidad de superficie, presentan buenas propiedades desde el punto de vista de la permeabilidad a los gases.

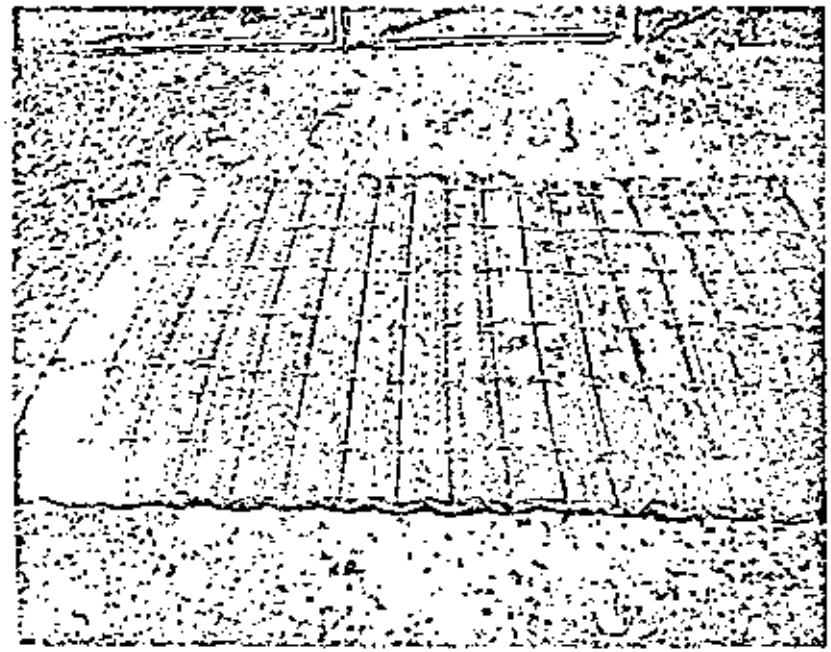

Fig. 8.1.2 Pantalla de caucho

Antes de comenzar la recogida de los escombros, hay que tener la precaución de retirar los materiales protectores, pues de otra forma se deterioran muy rapidamente. Incluso materiales relativamente sensibles, como el fieltro industrial, son recuperables y reutilizables.

Se ha discutido ampliamente sobre las formas más adecuadas de material de protección, y se han sostenido puntos de vista diferentes: algunos afirman que el factor más importante es la medida en que los materiales permiten el paso de los gases, mientras que otros sostienen que el único factor de importancia es el peso: ninguna de estas opiniones es totalmente correcta. En el caso de voladuras controladas en áreas muy sensibles, es preciso emplear protección pesada, pero también resulta útil el material ligero, permeable a los gases, para rebajar las distancias de proyección en los casos en que ésta puede ser tolerada en cierto grado.

ES DE IMPORTANCIA ESENCIAL SEGUIR EN TODO LAS NORMAS GENERALES (REGULACIONES SOBRE VOLADURAS), PERO NO DEBEN OLVIDARSE TAMPOCO LAS REGULACIONES LOCALES.

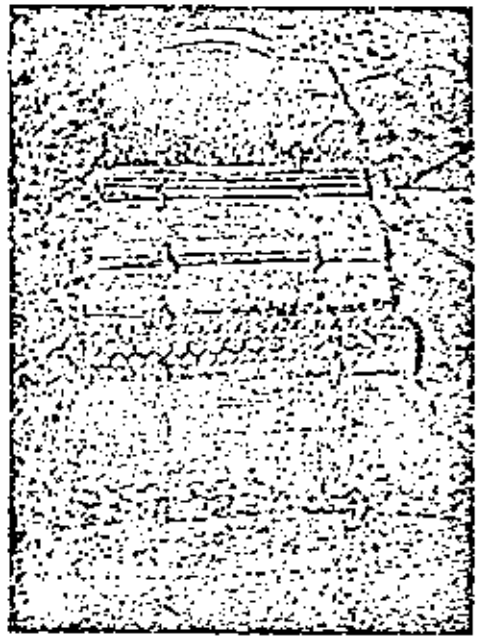

Fig. 8.1.3 Pequeñas pantallas unidas

8.2 MODO DE EMPLEO DE LOS MATERIALES DE PROTECCION

Debe emplearse protección frente a las voladuras cuando existe riesgo de daños personales o materiales: éste es el principio básico que orienta las regulaciones actualmente en vigor en Suecia (Instrucción sobre Voladuras, puntos 97—100). Ello significa que las personas encargadas de la voladura deben decidir si existe algún riesgo a este respecto. En varios lugares de Suecia, cuando se obtiene un permiso para voladuras, va acompañado de algunos condicionamientos sobre material de protección y la cuantía de su utilización. Desde el punto de vista de la seguridad, sería más conveniente que las regulaciones sobre protección fueran un poco más específicas, detallando la cuantía de la misma para los diferentes tipos de voladuras. Al estimar el riesgo de proyecciones, es evidentemente importante la distancia desde el lugar de la explosión a las edificaciones. Al mismo tiempo, somos conscientes del hecho de que ha habido casos de lanzamiento de piedras a centenares de metros, y conozco personalmente un ejemplo en que las piedras fueron proyectadas a más de 1 km. En los trabajos en que hayan de eliminarse las proyecciones, es importante la elección del método de voladura (véase la sección 5.4, "Proyecciones"). Cuanto mayor sea el diámetro de los barrenos, mayor es también el área en que existe riesgo.

Los datos que se incluyen a continuación pueden servir de orientación a la hora de estimar la protección necesaria:

Tipo de voladura	*Material de protección*
1. En la inmediata proximidad de edificios, vías públicas, líneas eléctricas, etc.:	
Voladura en zanjas	Pesado + Ligero
Voladuras en banco	Pesado + Ligero
Voladuras en bancos bajos	Pesado + Ligero
2. A una distancia de 50 a 100 m de las instalaciones indicadas arriba:	
Voladura en zanjas	Pesado + Ligero
Voladura en bancos bajos	Pesado + Ligero
Voladuras en banco	Pesado (primeras operaciones, zonas débiles, fallas, la primera y última fila de barrenos) + Ligero
3. A más de 100 m de las instalaciones indicadas arriba:	
Voladura en zanjas	Pesado (completo en ciertas situaciones difíciles; por lo demás, parcial) + Ligero
Voladura en bancos bajos	Ver arriba
Voladura en banco	Ver arriba
4. Túneles en áreas edificadas	Pesado + Ligero (bocas del túnel completas)

Cuando se efectúan voladuras en la proximidad de líneas eléctricas y otras instalaciones delicadas, ha de entrarse en contacto con los propietarios de las mismas, para conocer sus puntos de vista sobre el modo de realizar la protección. En el caso de voladuras próximas a las líneas aéreas de energía de ferrocarriles eléctricos, se aplican a veces regulaciones especiales sobre la protección y el modo de efectuar las voladuras.

Ejemplos de aplicación de protección

Se va a proceder a la voladura de una *zanja* a unos 45 m de unas casas de campo.

La protección, de acuerdo con el punto 1, se efectuará empleando material pesado y ligero. Una combinación apropiada puede consistir en pantallas de caucho como material pesado, con fieltro industrial como material ligero colocado sobre el primero. Si las pantallas de caucho son del tipo de pequeña dimensión, que puede ser trasladado manualmente, pueden colgarse elementos de pantalla Nitro sobre las de caucho para mantenerlas unidas. Las grandes pantallas de caucho, con un área de unos 12 m², proporcionan una excelente protección en casos como éste, pero requieren un dispositivo mecánico para levantarlos, lo que no siempre está disponible.

Se va a proceder a la voladura de un gran cerro, mediante *voladuras en banco*, a una distancia de unos 110 m de unas edificaciones. Por ciertas razones, no ha sido posible conseguir alejar completamente de los edificios la proyección de piedras.

La protección se dispone de acuerdo con el punto 3.

Se permite que siempre quede escombro de la voladura precedente frente a la primera hilera de barrenos para servir de protección (véase la sección 5.4, "Proyecciones"). La protección ligera empleada consiste en una malla de alambre relativamente tupida con un cierto solapamiento más allá de los bordes de la pega. En una zona de las voladuras, en la que existe un área de roca fragmentada, se la cubre con un material de protección pesado, consistente en rollizos de madera atados entre sí. Al encender las primeras pegas donde la roca se encuentra a un nivel bajo, se utilizan pantallas de caucho como protección sobre las hileras primera y última.

Consideraciones prácticas sobre protección

Las pantallas pesadas deben disponerse preferiblemente con un cierto solapamiento de unas con otras, para que no queden huecos en el material de protección. Las pantallas pequeñas, manejables manualmente, pueden ser ensambladas entre sí, pero ésto implica al mismo tiempo que la retirada de las pantallas antes de comenzar las labores de desescombro se convierta en una tarea más costosa. Es posible empalmar entre sí los elementos de modo que resulte fácil separarlos. Un elemento ligero de protección del tipo Nitro y de gran dimensión puede constituir una buena ayuda para mantener unidas las pantallas pequeñas.

Cuando la superficie de la roca está inclinada, puede ser conveniente fijar las pantallas al borde posterior para evitar que deslicen. Esto es especialmente aplicable al material pesado. El sistema de fijación usado, sin embargo, no debe ser tan sólido que desgarre las pantallas; si se utiliza alambre, debe ser también considerablemente más débil que el material de las pantallas. Es una gran ventaja disponer de pantallas que puedan ser reparadas. También es importante que la retirada de las pantallas se haga con los debidos cuidados antes de comenzar el desescombro, pues con ello su vida aumentará varias veces con relación a los casos en que se le deja deteriorar.

Es preciso desarrollar la investigación en el campo de las proyecciones y de los materiales de protección para que las voladuras puedan llegar a efectuarse prácticamente sin riesgo alguno de proyección de cualquier tipo. Pero la utilización plena de los elementos de que se dispone ya hoy debe permitir una reducción considerable de los daños y accidentes originados por las proyecciones.

9. VOLADURAS EN TUNELES

9.1 CALCULOS DE CARGAS

La construcción de túneles excavados mediante voladuras es una técnica que ha experimentado un desarrollo extremadamente rápido en los últimos años. La nueva maquinaria ha llevado consigo la introducción de métodos más racionales.

El empleo de cargas alargadas y de máquinas cargadoras para explosivos de ANFO ha hecho que las operaciones de carga se realicen mucho mas rapidamente.

Como resultado de la experiencia recogida en las voladuras en túneles, al calcular la alineación y la carga de los barrenos se utiliza un esquema de per-

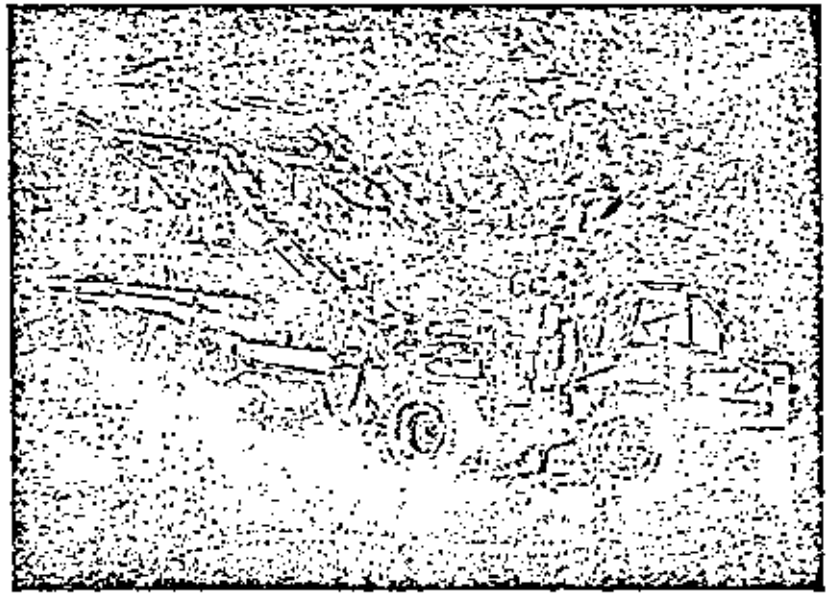

Fig. 9.1.1

foración adecuado al área de que se trate. En general, los cálculos se han hecho de un modo menos sistemático que, por ejemplo, los de voladuras en banco.

La información teórica básica para las voladuras en túneles está fundamentada generalmente en una comparación con las voladuras en banco, con la adición de unos factores correspondientes al aumento de carga necesario en las voladuras en túneles.

La única superficie libre en estas voladuras es el frente de ataque del túnel, lo que significa que las pegas se efectúan en condiciones de gran confinamiento. Cuanto más pequeña sea el área del frente, más confinada está la roca, y ésto implica que la carga específica aumenta al disminuir el área.

El principio de las voladuras en túneles reside en la apertura de una cavidad inicial mediante un cuele, y la subsiguiente destroza de la totalidad de la sección rompiendo hacia dicha cavidad.

La destroza puede ser comparada perfectamente con las voladuras en banco, pero exige cargas considerablemente mayores, por las desviaciones de perforación, las necesidades del proceso de esponjamiento, la ausencia de inclinación de los barrenos, la falta de cooperación entre barrenos adyacentes, y también la influencia de la gravedad según la ubicación de los mismos.

Con el transcurso de los años, se han ido desarrollando un gran número de cueles de diferentes tipos. Dado que los cálculos utilizados para los diferentes cueles varían considerablemente por la diversidad total de sus configuraciones, los tipos más corrientes de cueles serán tratados por separado en secciones especiales. En esta sección se tratará del cálculo de la carga para otros barrenos de la pega.

Se supondrá que en la roca se ha abierto una cavidad de 1,4 × 1,4 m. Este es el área que generalmente requieren los barrenos de destroza para tener rotura libre hacia dicha abertura. En el caso de grandes diámetros de barreno, puede ser preciso aumentar sus dimensiones hasta 2 × 2 m, para que los tiros de destroza tengan rotura libre. La rotura libre en este caso puede ser calculada como 0,7 × anchura de la abertura. Todos los barrenos del contorno, como los de techo, hastiales, y piso, han de ser orientados de modo que proporcionen un margen para emboquille de la pega siguiente, con objeto de mantener la sección del túnel de acuerdo con la proyectada. Este margen implica que se da a los barrenos una inclinación que los hace llegar más allá del contorno; el ángulo utilizado depende del espacio necesario para emboquille, lo cual a su vez es función del equipo de perforación que se emplee.

En ciertos tipos de cuele, como el cuele en abanico, por ejemplo, los barrenos del mismo más los de contracuele comprenden la mayor parte de la sección del túnel.

Los principios de cálculo descritos en esta sección están basados simplemente en la experiencia obtenida en diferentes condiciones específicas.

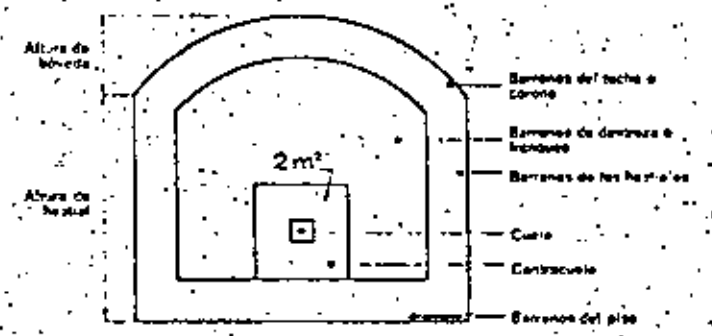

Fig. 9.1.2

La Fig. 9.1.3 muestra las cargas específicas que se utilizan normalmente en las voladuras en túneles. Esta figura, y la 9.1.4, indican los valores normales en túneles; existen muchos ejemplos con valores que se desvían de los señalados, debido a la forma del túnel, condiciones de la roca, etc. En muchos casos se aprecian unas diferencias en el número de barrenos según el diámetro de los mismos que son menores que las indicadas en la Fig. 9.1.4.

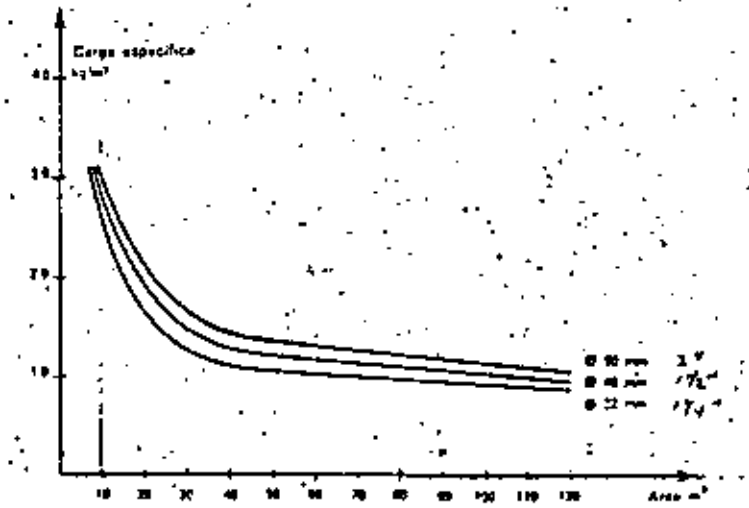

Fig. 9.1.3

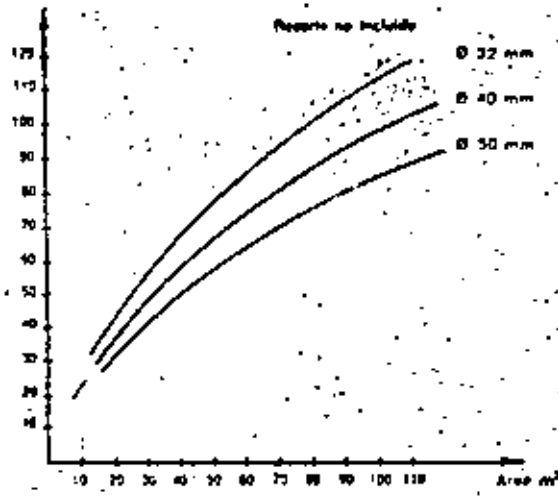

Fig. 9.1.4 Número de taladros para diferentes secciones de túnel

Cálculo de los barrenos de destroza con rotura en dirección horizontal o hacia arriba

Se llenan los barrenos con una carga de fondo concentrada hasta un tercio de su profundidad total. La *piedra* no debe ser mayor que (profundidad del barreno − 0,40)/2 (ésta es una precondición, no una base para el cálculo).

Para el espaciamiento de los barrenos se toma un valor igual a 1,1 × *piedra*. En la parte del fondo se requiere la carga específica siguiente:

Diámetro de los barrenos mm	Carga específica kg/m³
aprox. 30	1,1
40	1,3
50	1,5

Para la concentración de la carga de columna se adopta un valor de 0,50 × carga de fondo en kg/m.
Zona de retacado = 0,5 × *piedra*.

El espaciamiento de los barrenos puede calcularse a partir de la carga específica necesaria en la zona del fondo:

Diámetro barrenos mm	Area barreno m²	Piedra m	Espaciamiento barrenos m
32	0,91	0,90	1,00
35	1,00	0,95	1,05
38	1,15	1,00	1,15
45	1,44	1,15	1,25
48	1,57	1,20	1,30 *)
51	1,71	1,25	1,35 *)

*) Este espaciamiento puede conseguirse normalmente sólo en el caso de secciones de túnel de gran área. En el caso de áreas menores, el espaciamiento ha de adaptarse a las condiciones geométricas, disminuyendo su magnitud.

La concentración y la potencia de las cargas de fondo y de columna pueden calcularse a partir de las relaciones mencionadas anteriormente:

Diámetro barrenos mm	Profdad. barrenos m	Piedra m	Espaciamiento m	Carga de fondo kg	Carga de fondo kg/m	Carga de columna kg	Carga de columna kg/m	Zona de retacado m
33	1,6	0,60	0,70	0,60	1,10	0,30	0,40	0,30
32	2,4	0,90	1,00	0,80	1,00	0,55	0,50	0,45
31	3,2	0,90	0,95	1,00	0,95	0,85	0,50	0,45
38	2,4	1,00	1,10	1,15	1,44	0,80	0,70	0,50
37	3,2	1,00	1,10	1,50	1,36	1,15	0,70	0,50
45	3,2	1,15	1,25	2,25	2,03	1,50	1,00	0,55
48	3,2	1,20	1,30	2,50	2,30	1,70	1,15	0,60
48	4,0	1,20	1,30	3,00	2,30	2,45	1,15	0,60
51	3,2	1,25	1,35	2,50	2,60	1,95	1,30	0,60
51	4,0	1,25	1,35	3,40	2,60	2,70	1,30	0,60

El margen de 33—38 mm cubre las series 11 y 12 de perforación, así como las barrenas integrales y bocas de 33 y 38 mm, respectivamente. Los valores de la piedra y espaciamiento de los barrenos son los que se utilizan en la práctica. Se incluye en los cálculos el error de perforación.

La Tabla pone de manifiesto que el error de perforación y las necesidades de esponjamiento al aumentar la profundidad de los barrenos son compensados por las mayores cargas de fondo. La plena utilización de los diámetros mayores implica grandes cargas por barreno, lo cual es desventajoso desde el punto de vista de la tecnología de las rocas.

Cálculo de la carga para los barrenos del piso

La *piedra* y el espaciamiento en estos barrenos inferiores pueden ser calculados del mismo modo que para los barrenos de franqueo mencionados más arriba. Es importante, sin embargo, incluir en las dimensiones de la *piedra* los márgenes para emboquille, con lo que la alineación de los barrenos del piso ha de hacerse teniendo en cuenta los dos valores: por ejemplo, con una *piedra* de 1,00 m y un margen para emboquille de 0,20 m, los barrenos habrán de emboquillarse a 1,00—0,20 = 0,80 m por encima del punto de emboquille de los barrenos inferiores.

La zona de retacado se toma de una longitud igual a 0,2 × *piedra*. La concentración de la carga de columna se hace llegar hasta un 70 % de la concentración de la carga de fondo.

Diámetro barrenos mm	Profdad. barrenos m	Piedra m	Espaciamiento m	Carga de fondo kg	Carga de fondo kg/m	Carga de columna kg	Carga de columna kg/m	Zona de retacado m
33	1,6	0,60	0,70	0,60	1,10	0,70	0,75	0,10
32	2,4	0,90	1,00	0,60	1,00	1,00	0,70	0,20
31	3,2	0,90	0,95	1,00	0,95	1,30	0,65	0,20
38	2,4	1,00	1,10	1,15	1,44	1,40	1,00	0,20
37	3,2	1,00	1,10	1,50	1,36	1,80	0,95	0,20
45	3,2	1,15	1,25	2,25	2,03	2,60	1,40	0,25
48	3,2	1,20	1,30	2,50	2,30	3,00	1,60	0,25
48	4,0	1,20	1,30	3,00	2,30	4,25	1,60	0,25
51	3,2	1,25	1,35	2,70	2,60	3,20	1,80	0,25
51	4,0	1,25	1,35	3,40	2,60	4,75	1,80	0,25

Cálculo de la carga para los barrenos de destroza con rotura hacia abajo

Como estos barrenos necesitan una menor fuerza de esponjamiento, y son además ayudados por la acción de la gravedad, la carga específica en la zona de fondo puede reducirse a:

Diámetro de los barrenos mm	Carga específica kg/m³
30	1,0
40	1,2
50	1,4

El espaciamiento puede aumentarse hasta un valor de 1,2 × *piedra*. Por lo demás los cálculos se efectúan del mismo modo que para los barrenos de franqueo citados más arriba. En el caso de túneles con secciones de pequeña

área, la *piedra* y el espaciamiento de los barrenos se reducen de acuerdo con las condiciones geométricas del caso.

En la Tabla siguiente se incluyen las magnitudes geométricas y de carga correspondientes a estos barrenos de destroza. Los valores indicados para el espaciamiento son aplicables siempre que la concentración de carga en el fondo alcance también el valor señalado. Si el método de carga utilizado se traduce en una concentración menor, el espaciamiento deberá reducirse de modo que se obtenga la carga específica requerida.

Diámetro barrenos mm	Profdad. barrenos m	Piedra m	Espaciamiento m	Carga de fondo kg	Carga de fondo kg/m	Carga de columna kg	Carga de columna kg/m	Zona de retacado m
33	1,6	0,60	0,70	0,60	1,10	0,30	0,40	0,30
32	2,4	0,90	1,10	0,80	1,00	0,55	0,50	0,45
31	3,2	0,85 *)	1,10	1,00	0,95	0,85	0,50	0,45
38	2,4	1,00 *)	1,20	1,15	1,44	0,80	0,70	0,50
37	3,2	1,00 *)	1,20	1,50	1,36	1,15	0,70	0,50
45	3,2	1,15 *)	1,40	2,25	2,03	1,50	1,25	0,55
48	3,2	1,20 *)	1,45	2,50	2,30	1,70	1,15	0,60
48	4,0	1,20 *)	1,45	3,00	2,30	2,45	1,15	0,60
51	3,2	1,25 *)	1,50	2,70	2,60	1,95	1,30	0,60
51	4,0	1,25 *)	1,50	3,40	2,60	2,70	1,30	0,60

*) En túneles cuya sección tenga un área mayor de 70 m², los valores de la *piedra* y el espaciamiento pueden ser ampliados considerablemente en muchos casos, ya que los barrenos rompen con mucha mayor facilidad. En estas circunstancias, las voladuras pasan a ser similares a las voladuras en banco.

En la mayor parte de los casos, puede aumentarse el valor de la *piedra* en un 10 %, con lo que el espaciamiento entre barrenos se hace también considerablemente mayor.

El espaciamiento de los barrenos de franqueo puede aumentarse hasta áreas mayores en relación con la de la sección del túnel. Puede afirmarse asimismo que, en muchas ocasiones en que la roca es fácil de volar, el espaciamiento indicado en la tabla puede ser excesivamente pequeño; por otra parte, es frecuente que la concentración de carga lograda en el fondo de los barrenos sea menor que la que figura en la tabla; ello implica que, en el caso de roca fácil de romper, pueden utilizarse los espaciamientos de la tabla aun cuando la concentración de carga sea inferior.

Cálculo de la carga en los barrenos de los hastiales

Normalmente, a lo largo del techo y los hastiales de la sección de los túneles, las voladuras son del tipo de recorte, (véase sección 9.5 "Recorte"). Los cálculos que se hacen aquí se refieren a los casos en que no se hacen voladuras de esta clase.

La *piedra* de los barrenos, con inclusión del margen para emboquille, se toma igual a 0,9 × *piedra* de los barrenos de franqueo.

Espaciamiento = 1,2 × V.

La longitud de la carga de fondo se reduce a 1/6 de la profundidad del barreno.

Zona de retacado = 0,5 × *piedra*. La concentración de la carga de columna se hace igual a 0,40 × concentración de la carga de fondo.

Ejemplo:

Diámetro barrenos	Profdad. barrenos	Piedra	Espaciamiento	Carga de fondo		Carga de columna		Zona de retacado
mm	m	m	m	kg	kg/m	kg	kg/m	m
33	1,6	0,55	0,65	0,30	1,10	0,45	0,45	0,30
32	2,4	0,80	0,95	0,40	1,00	0,65	0,40	0,40
31	3,2	0,80	0,95	0,50	0,95	0,90	0,40	0,40
38	2,4	0,90	1,10	0,60	1,44	0,85	0,60	0,45
37	3,2	0,90	1,10	0,75	1,36	1,20	0,55	0,45
45	3,2	1,00	1,20	1,10	2,03	1,80	0,80	0,50
48	3,2	1,10	1,30	1,20	2,30	2,00	0,90	0,55
48	4,0	1,10	1,30	1,50	2,30	2,50	0,90	0,55
51	3,2	1,15	1,40	1,40	2,60	2,10	1,00	0,60
51	4,0	1,15	1,40	1,70	2,60	2,70	1,00	0,60

Cálculo de la carga en los barrenos del techo

El espaciamiento es el mismo que para los barrenos de los hastiales. La carga de columna se reduce a 0,30 × concentración de la carga de fondo.

Diámetro barrenos	Profdad. barrenos	Piedra	Espaciamiento	Carga de fondo		Carga de columna		Zona de retacado
mm	m	m	m	kg	kg/m	kg	kg/m	m
33	1,6	0,55	0,65	0,30	1,10	0,35	0,35	0,30
32	2,4	0,80	0,95	0,40	1,00	0,50	0,30	0,40
31	3,2	0,80	0,95	0,50	0,95	0,70	0,30	0,40
38	2,4	0,90	1,10	0,60	1,44	0,70	0,45	0,45
37	3,2	0,90	1,10	0,75	1,36	0,90	0,40	0,45
45	3,2	1,00	1,20	1,10	2,03	1,30	0,60	0,50

Diámetro barrenos	Profdad. barrenos	Piedra	Espaciamiento	Carga de fondo		Carga de columna		Zona de retacado
mm	m	m	m	kg	kg/m	kg	kg/m	m
48	3,2	1,10	1,30	1,20	2,30	1,45	0,70	0,55
48	4,0	1,10	1,30	1,50	2,30	1,95	0,90	0,55
51	3,2	1,15	1,40	1,40	2,60	1,70	0,80	0,60
51	4,0	1,15	1,40	1,70	2,60	2,25	0,80	0,60

RESUMEN DE CARACTERISTICAS DE LOS BARRENOS

Barrenos de destroza o franqueo con rotura horizontal o hacia arriba

d (mm)	q (kg/m³)
30	1,1
40	1,3
50	1,5

$h_a = H/3$

$V_1 \leq \frac{H - 0{,}40}{2}$ (condición, no base de cálculo)

$E = 1{,}1 \times V$

$Q_{pk} = 0{,}50 \times Q_{ak}$

$h_a = 0{,}5 \times V$

Barrenos del piso

Ver arriba

$h_a = 0{,}2 \times V$

$Q_{pk} = 0{,}70 \times Q_{ak}$

Barrenos de fraqueo son rotura hacia abajo

Ver los barrenos de franqueo anteriores

$E = 1{,}2 \times V$

Barrenos de los hastiales

Ver los barrenos de franqueo con rotura hacia abajo

$V = 0{,}90 \times V_{\text{barrenos franq. rot. hacia abajo}}$

$Q_{pk} = 0{,}40 \times Q_{ak}$

$h_a = H/6$

Barrenos del techo

Ver barrenos de franqueo con rotura hacia abajo y barrenos de hastiales

$V \quad = V_{\text{barrenos hastiales}}$

$Q_{cc} \quad = 0{,}30 \times Q_{\text{hast}}$

En la sección 9.6, "Ejemplos de cálculo", puede verse con detalle la utilización de las diversas relaciones.

Hay dos modos de preparar los planes de perforación en los túneles: uno de ellos consiste en calcular los espaciamientos y carga de cada barreno de acuerdo con las bases de cálculo que se acaban de explicar; la manera más sencilla de proceder es utilizar directamente las Tablas, y distribuir los distintos tipos de barreno por el área del frente. Puesto que en el caso de túneles de pequeña sección, los barrenos del cuele y los del contracuele forman una proporción considerable del área del frente, este caso particular puede tomarse directamente de la sección 9.2.

9.2 CUELES DE TIROS PARALELOS Y CALCULO DE LA CARGA EN LOS BARRENOS DE CONTRACUELE

Como ya lo indica su propio nombre, en este tipo de cuele todos los barrenos son paralelos entre sí. La rotura tiene lugar en dirección a un barreno sin carga que sirve de abertura inicial. Los primeros barrenos adyacentes al barreno vacío requieren una gran precisión en la perforación y en la carga. Más abajo se indican los espaciamientos alrededor de este barreno.

Fig. 9.2.1

Como el barreno vacío es normalmente de un diámetro mayor que los del resto de la pega, los cueles de tiros paralelos son denominados algunas veces cueles de gran diámetro.

Los cueles quemados fueron los predecesores de los cueles paralelos. En el cuele quemado, los barrenos son paralelos, pero en el centro se utiliza el barreno de igual diámetro que los demás. Este barreno se llena con una carga potente, y los cuatro barrenos situados a su alrededor se dejan sin carga, aunque algunas veces se dejaba vacío el barreno central y se cargaban los otros cuatro. En cualquier caso, los cueles quemados producen generalmente un avance menor que los cueles paralelos del tipo de gran barreno central, por lo que en esta sección se tratará solamente de este último tipo de cuele.

La perforación del barreno central de gran diámetro y de los barrenos adyacentes, así como su carga, ha de efectuarse con precisión. Para diferentes valores de estos diámetros, se requieren también diferentes espaciamientos; las características de la roca a la voladura pueden también hacer preciso un reajuste de los espaciamientos y las cargas a fin de obtener una satisfactoria rotura. Si la carga empleada fuera demasiado pequeña, el cuele no rompería correctamente, y si fuera demasiado grande, la roca podría sinterizarse y el cuele se malograría.

Existen muchas variantes ya bien experimentadas de cueles paralelos de funcionamiento satisfactorio. Una regla sencilla para el cálculo de la *piedra* entre el barreno de gran diámetro y el más próximo a él es la siguiente:

Piedra = 0,7 × Diámetro barreno central

$V \quad = 0{,}7 \times d_{\text{central}}$

En el caso de dos barrenos de gran diámetro, esta última relación se modifica en la forma:

$V = 0{,}7 \times 2\,d_{\text{central}}$

La relación puede ser también utilizada para los barrenos del contracuele, correspondiendo la anchura de la superficie libre al diámetro del barreno central, según la relación:

$V = 0{,}7 \times B$

La zona de roca desprendida ha de ser de anchura suficiente para que los barrenos de destroza tengan la posibilidad de romper en ángulo recto, lo que implica $2 \times V_{\text{barr destroza}}$

La *piedra* de los barrenos del cuele no ha de ser confundida con la distancia entre centros de los mismos normalmente utilizada. La tabla siguiente puede servir de guía:

Diámetro del barreno grande mm	Diámetro barrenos pequeños mm	Piedra mm	Distancia entre centros mm
57	32	40	85
76	32	53	107
76	45	53	113
2 × 57	32	80	125
2 × 57	45	80	131
2 × 76	32	106	160
2 × 76	45	106	167
100	45	70	143
100	51	70	146
125	51	88	176

En el caso de roca fácilmente volable, puede ser preciso aumentar la distancia entre centros.

La experiencia permite asignar, para los barrenos del cuele más próximos al central, las cargas siguientes:

Diámetro barrenos mm	Concentración de carga kg/m	Diámetro adecuado para el barreno grande mm
32	0,25 *)	57 — 2 × 76
35	0,30 *)	76 — 2 × 76
38	0,36 *)	76 — 2 × 76
45	0,45	2 × 76 — 125
48	0,55	2 × 76 — 125
51	0,55	2 × 76 — 125

(*) Normalmente puede usarse Nabit de 22 mm, aunque corresponde a una carga de Dynamex de 0,38 kg/m.

Por otra parte, con el objeto de mantener la concentración de carga dentro de unos valores necesariamente bajos, pueden usarse separadores de madera entre los cartuchos:

Composición de la carga	Concentración de carga kg/m
⅓ cartucho Dynamex 22 mm + separador madera 10 cm	0,21
½ cartucho Dynamex 22 mm + separador madera 10 cm	0,25
½ cartucho Dynamex 25 mm + separador madera 10 cm	0,31
1 cartucho Dynamex 22 mm + separador madera 10 cm	0,35
1 cartucho Nabit 22 mm	0,38

Como ya se señaló anteriormente, puede ser preciso ajustar las cargas en razón de las características de la roca. En el caso de una roca que se aglomere con facilidad, el cálculo preciso de la carga se hace especialmente necesario.

Tipos diferentes de cueles paralelos

El "*cuele Coromant*" es bien conocido: los barrenos se distribuyen en él de tal modo que se logre una utilización óptima del cuele en el momento de la detonación. Con el objeto de conseguir una buena precisión en la perforación, los fabricantes han desarrollado un tipo especial de equipos de guía de las perforadoras. Las plantillas de perforación permiten taladrar simultaneamente dos barrenos de gran diámetro formando una acanaladura en el frente. Los barrenos del cuele se perforan también con ayuda de plantillas.

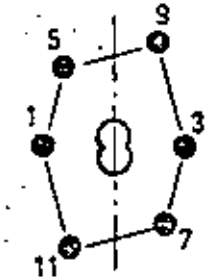

Fig. 9.2.2

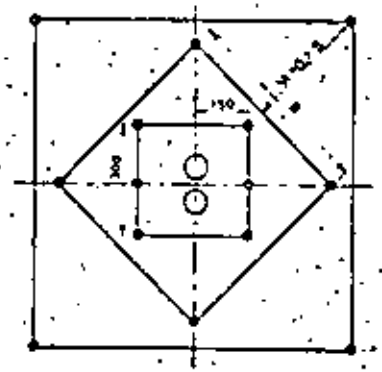

Fig. 9.2.3

Los barrenos de contracuele, situados fuera de éste, son adaptados al área de la sección transversal del túnel.

También ha sido empleada en numerosas ocasiones una forma de cuele análoga al tipo anterior, con dobles barrenos de gran diámetro.

En la figura se puede ver también la disposición de los barrenos del contracuele, debido a la gran constricción de los mismos su carga es de valor elevado:

Piedra	Carga de fondo	Carga de columna, en kg/m para los diámetros:			
m	kg	32 mm	38 mm	45 mm	48 mm
0,20	0,25	0,30	0,45	0,60	0,75
0,30	0,40	0,30	0,45	0,60	0,75
0,40	0,50	0,35	0,50	0,70	0,80
0,50	0,65	0,50	0,70	1,00	1,15
0,60	0,80	0,50	0,70	1,00	1,15
0,70	0,90	0,50	0,70	1,00	1,15

Zona de retacado = 0,5 × V

Los barrenos de descarga con una *piedra* de más de 0,70 m se cargan del mismo modo que los barrenos de destroza con rotura horizontal (véase sección 9.1).

La Fig. 9.2.4 muestra un cuele con gran barreno central, y la zona de ampliación del cuele para diversos diámetros de barrenos. Los barrenos más exteriores de la zona de ampliación pueden ser considerados como de destroza, pero han sido adaptados geométricamente en cierta medida para que encajen más fácilmente en la figura.

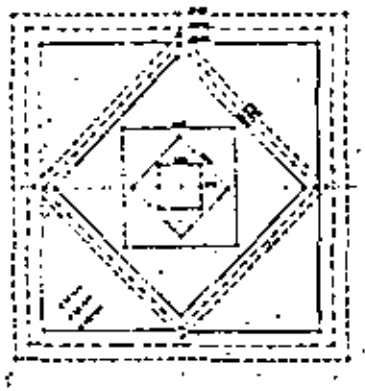

Fig. 9.2.4

Independientemente de que un cuele de barreno central de gran diámetro lleve, por ejemplo, un barreno central de 125 mm o dos de 76 mm, el área del cuele será aproximadamente de 0,30 × 0,30, lo que significa que en la mayoría de los casos, este modelo puede ser empleado sin necesidad de una mayor adaptación.

La superficie del cuele y del contracuele, de 2,00 × 2,00 m para barrenos de unos 32 mm, puede situarse generalmente fuera del alcance de la *piedra* de los barrenos del piso.

Pueden formarse cueles paralelos de gran barreno central de muchas formas diferentes. En la Fig. 9.2.5, por ejemplo, se ilustra el cuele "Fagersta".

Fig. 9.2.5

Con una profundidad de perforación de 2,4 m o menos, se usa generalmente un barreno de gran diámetro. En la figura se muestran los espaciamientos adecuados para un diámetro de los barrenos de 45 mm.

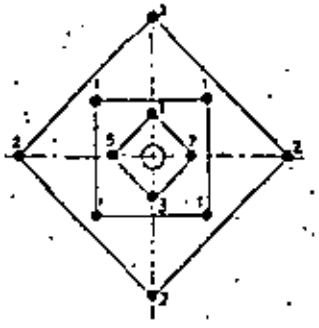

Fig. 9.2.6

Para concluir, puede afirmarse que los cueles de tiros paralelos con grandes barrenos centrales vacíos poseen una amplia variedad de aplicaciones. Pueden ser utilizados en túneles con secciones cuya área varíe desde la más pequeña a la más grande. En los últimos años, en efecto, los cueles paralelos han entrado también en uso, en gran cantidad, aun en los casos de túneles de gran sección.

Para obtener resultados satisfactorios, los cueles de esta clase exigen una gran precisión en la perforación y en la carga.

En la sección 9.6 se describe el modo de proceder para el cálculo de los cueles paralelos en un túnel.

9.3 CUELE EN CUÑA O EN V.-CALCULO DE LAS CARGAS EN LOS BARRENOS DEL CONTRACUELE

De todos los tipos de cuele en ángulo utilizados en las voladuras de túneles, el más usual es el denominado cuele en cuña o en V. En la Fig. 9.3.1 se ilustra la disposición del mismo.

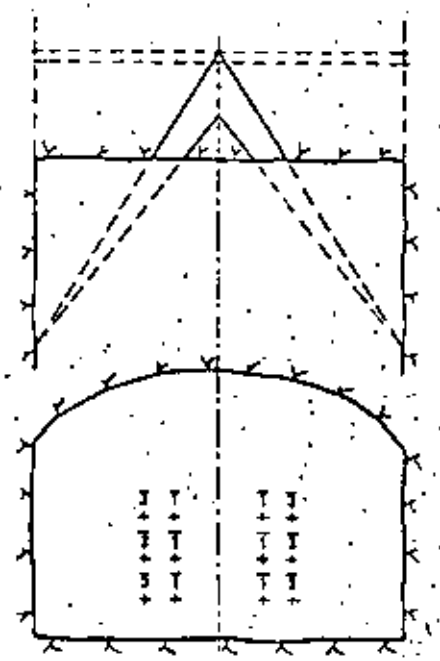

Fig. 9.3.1

Los cueles en V necesitan una cierta anchura de túnel para lograr un buen avance. En túneles estrechos, el ángulo de la cuña se reduce, y su voladura se hace son ello más dificultosa. Este fenómeno se origina por el alto grado de confinamiento en que se encuentra el cuele en tales casos. La precisión de la perforación es otro factor que posee una gran influencia sobre el resultado de la voladura; cuanto más se acerque la realidad al esquema de perforación teórico, mayor será la cooperación entre los barrenos de cara al efecto rompedor.

Para el cálculo de las cargas, se admitirá en esta sección que el ángulo del vértice interior de la cuña es como mínimo de 60°. Si el ángulo fuera menor, habrá de incrementarse la carga por barreno, o incluso utilizar otra cuña en profundidad o encima de la primera.

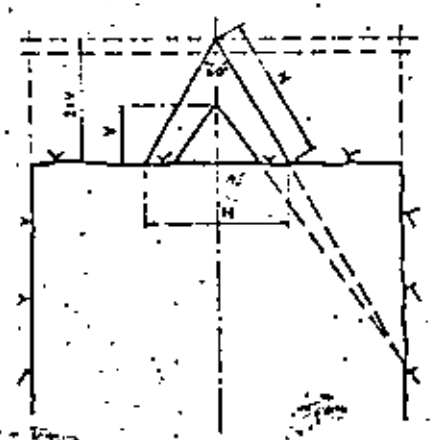

Fig. 9.3.2

La *piedra* para cada cuña depende de la cantidad de explosivo que puede cargarse en los barrenos con arreglo a su diámetro. La Tabla que se incluye a continuación puede servir como orientación para los cálculos de perforación y carga:

Diámetro barrenos	Altura total del cuele	Piedra	Concentración de la carga de fondo	Número de cuñas en sentido vertical
mm	m	m	kg/m	
aprox. 30	1,5	1,0	0,9	3
38	1,6	1,2	1,4	3
45	1,8	1,5	2,0	3
51	2,8	2,0	2,6	3

La carga de fondo ha de ser al menos igual a un tercio de la profundidad del barreno ($h_a = H/3$). Un ángulo más agudo en el vértice requiere una carga más potente. En cuanto a la concentración de la carga de columna, ha de ser igual a 0,5 × carga de fondo. La longitud de la zona de retacado debe ser igual a 0,3 × V, pero debe asimismo ser adaptada al espaciamiento de los barrenos, de modo que no haya un exceso de carga en la parte de columna.

Los barrenos de contracuele, exteriores al cuele, se perforan también en ángulo, para mejorar el efecto rompedor. En la Fig. 9.3.3 se muestra un esquema de la disposición de estos barrenos.

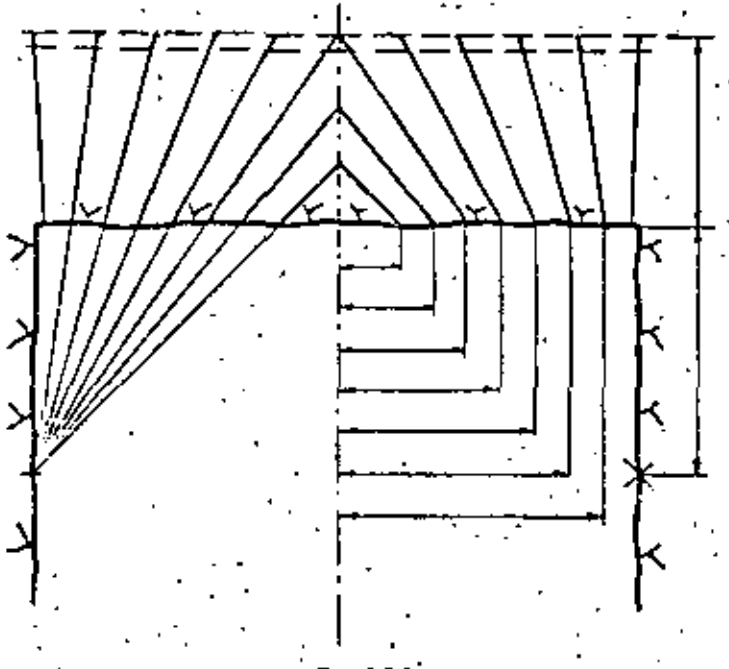

Fig. 9.3.3

Los barrenos de contracuele se perforan y cargan según las orientaciones proporcionadas por la Tabla siguiente:

Diámetro barrenos mm	Piedra m	Carga de fondo kg/m	Carga de columna kg/m	Zona de retacado m
aprox. 30	0,80	0,90	0,36	0,40
38	0,90	1,40	0,55	0,45
45	1,00	2,00	0,80	0,50
48	1,10	2,30	0,90	0,55
51	1,20	2,60	1,00	0,60

Altura de la carga de fondo = ⅓ × Profundidad del barreno.

Concentración de la carga de columna = 0,40 × Concentración de la carga de fondo.

La *piedra* no debe ser de una magnitud superior a $\frac{\text{profdad. barreno} - 0{,}4}{2}$

Esto implica que, en el caso de pegas de pequeña profundidad, la *piedra* ha de disminuirse de valor.

Los barrenos del cuele y contracuele deben ser iniciados en la mayor medida posible por medio de detonadores de microrretardo. Un encendido con simples retardos de medio segundo significaría una menor cooperación entre los barrenos desde el punto de vista del efecto rompedor. El retardo entre las diversas cuñas no debe ser demasiado corto; si el retardo no permite el esponjamiento de la roca, la rotura puede ser deficiente. En la Fig. 9.3.4 se muestra una secuencia de encendido apropiada para un cuele en V, con un microrretardo de 25 ms entre cada dos números de retardo.

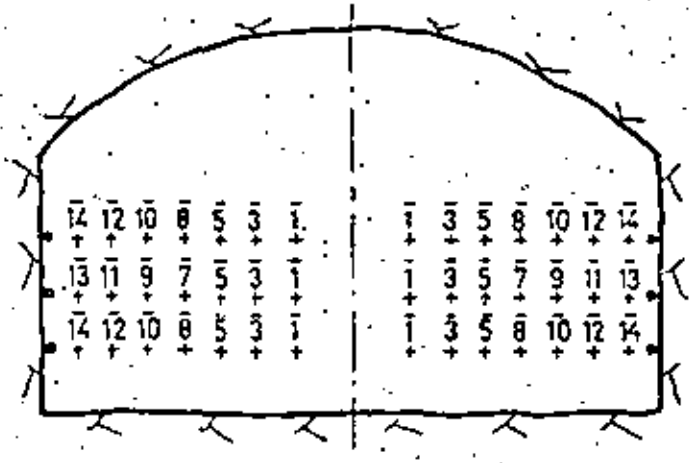

Fig. 9.3.4

Con el fin de lograr la precisión exigida por los cálculos, la ubicación y orientación de los barrenos ha de efectuarse de un modo sistemático. El esquema de perforación ha de hacerse teniendo en cuenta el espacio requerido por el equipo de perforación.

Los demás barrenos de la pega además de los del cuele y contracuele se calculan de acuerdo con la sección 9.1, "Cálculos de cargas".

9.4 CUELES EN ABANICO Y OTROS TIPOS DE CUELE

Como su nombre indica, este tipo de cuele tiene sus barrenos dispuestos de modo que forman un abanico. En la Fig. 9.4.1 se muestra un esquema del mismo.

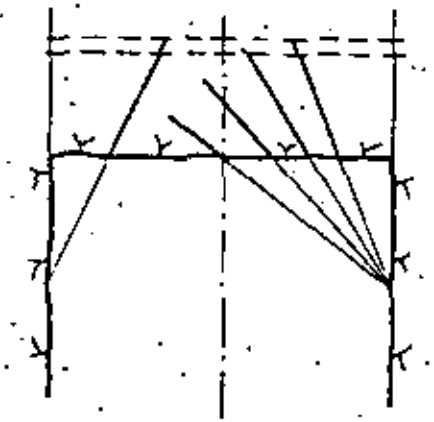

Fig. 9.4.1

Al igual que los cueles en V, el cuele en abanico necesita una cierta anchura de túnel para que el avance conseguido por pega sea aceptable. El cuele en abanico podría llamarse también cuele de destroze, pues su funcionamiento se basa en la destroza de la roca en dirección a la superficie libre, el frente de ataque del túnel. Como las condiciones de confinamiento no son severas, el cuele en abanico es de arranque relativamente fácil en comparación con la mayoría de los otros tipos.

La distribución irregular de la perforación, así como la necesidad de una planificación de profundidades de los barrenos, y un emboquille de los mismos, bien precisos, han hecho que su utilización en la actualidad sea menor que en el pasado. El cuele en abanico, por otra parte, puede ser adaptado a las diaclasas visibles existentes en la roca de modo que se facilite la rotura, pues la roca se desprende con mayor facilidad a lo largo de ellas.

Los valores orientativos para la perforación y carga del cuele en abanico pueden obtenerse de la misma Tabla dada anteriormente para los barrenos de contracuele del cuele en V.

En cuanto a los barrenos de contracuele del cuele en abanico, las características aplicables son las siguientes:

Diámetro barrenos mm	Piedra m	Altura del cuele m	Carga de fondo kg/m	Carga de columna kg/m	No. de barrenos por hilera	Zona de retacado m
aprox. 30	0,80	1,50	0,90	0,35	3	0,50
40	0,90	1,60	1,60	0,65	3	0,55
45	1,00	1,80	2,00	0,80	3	0,60
48	1,10	1,90	2,30	0,90	3	0,65
51	1,20	2,00	2,60	1,00	3	0,75

La *piedra* no debe ser mayor de la mitad de la profundidad del barreno menos 0,40 m.

La carga de fondo se toma igual a ⅓ de la profundidad del barreno. En voladuras con precaución o controladas puede reducirse la carga (véase sección 13.5).

Concentración de la carga de columna = 0,40 × Concentración de la carga de fondo.

El mecanismo rompedor en los cueles en abanico es completamente diferente del de los cueles en V, y ésto tiene su influencia sobre la disposición de la secuencia de encendido. La iniciación con microrretardos es la más adecuada para los barrenos del cuele y contracuele (véase Fig. 9.4.2).

En los últimos años se ha puesto nuevamente en uso el "cuele sastre", que fue un predecesor del cuele paralelo con gran barreno central.

En la Fig. 9.4.3 puede verse su distribución.

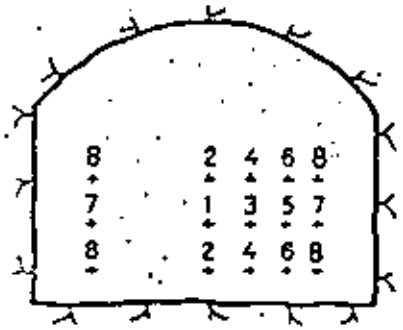

Fig. 9.4.2

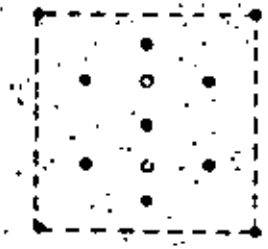

Fig. 9.4.3

Con perforaciones de pequeño diámetro, lo más adecuado resulta utilizar siete barrenos. La distancia entre estos barrenos puede calcularse mediante la expresión:

$E_{entre\ b} = 3 \times$ Diámetro del barreno

Diámetro barrenos mm	Distancia entre centros mm	Número de barrenos	Carga kg m
aprox. 30	90	7	0,45
38	115	6	0,70
45	135	6	1,00
48	144	5	1,15
51	153	5	1,30

Los barrenos del cuele más próximos al mismo han de situarse con un valor $V = 0{,}7 \times$ número de barrenos $\times$ d.

La zona de retacado debe ser lo menor posible.

Los cueles de esta clase originan una acusada onda de choque del aire a través de los barrenos que los forman, con cargas relativamente potentes, y que configuran una hendidura en la roca, en dirección a la cual puede hacerse luego la destroza. Incluso es normal la proyección de pequeños fragmentos de roca. Los barrenos de contracuele, se cargan de acuerdo con la cuantía de su *piedra*.

El cuele "sastre" o "cremallera" ha resultado útil en su aplicación práctica, fundamentalmente para las perforaciones con maquinaria de túneles.

El cuele noruego pertenece también a un tipo antiguo de cuele que fue el predecesor de los cueles quemados y de los cueles paralelos de barreno grande.

En los casos de una anchura limitada del túnel en relación con las necesidades de espacio del equipo de perforación, el cuele noruego puede dar un avance por pega más satisfactorio que el cuele en V. Desde el punto de vista de la tecnología de las voladuras, la concepción del cuele es más correcta, pues los barrenos tienen posibilidades de romper tanto en forma de cuña como en forma de abanico; el inconveniente es la complicación de su preparación, un esquema de la cual se muestra en la Fig. 9.4.4.

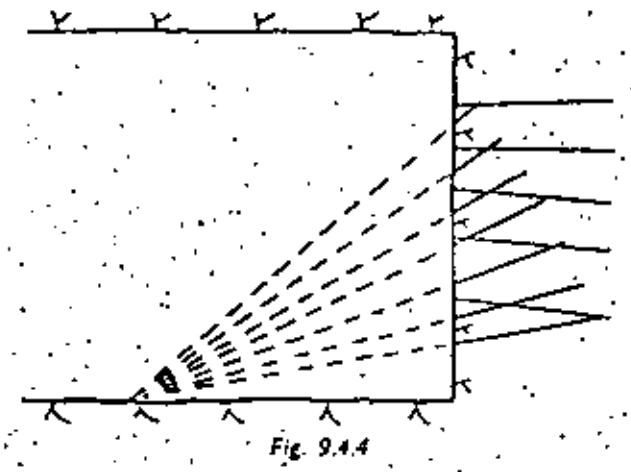

Fig. 9.4.4

Carga de fondo = ⅓ de la profundidad del barreno. Concentración de la carga alargada = 0,5 × Concentración de la carga de fondo.

El cuele denominado "Surte" o "Blásut" está basado en hacer un precorte en la pared del túnel; a continuación se procede a la destroza de la sección, con barrenos inclinados diagonalmente hacia la abertura del precorte. El precorte es en este caso más potente que uno normal. Los cueles de este tipo resultan apropiados para el uso de jumbos de perforación; sus inconvenientes consisten en la carga relativamente potente que ha de ser detonada muy próxima al contorno final, y la onda de choque producida en el aire al efectuar la voladura.

Los tipos de cuele que se han descrito a propósito de las voladuras en túneles son los cueles más usuales en la actualidad; dentro de cada tipo principal existen a su vez muchas variantes. Muchos expertos en voladuras tienen sus propios tipos favoritos de cuele que funcionan a su satisfacción.

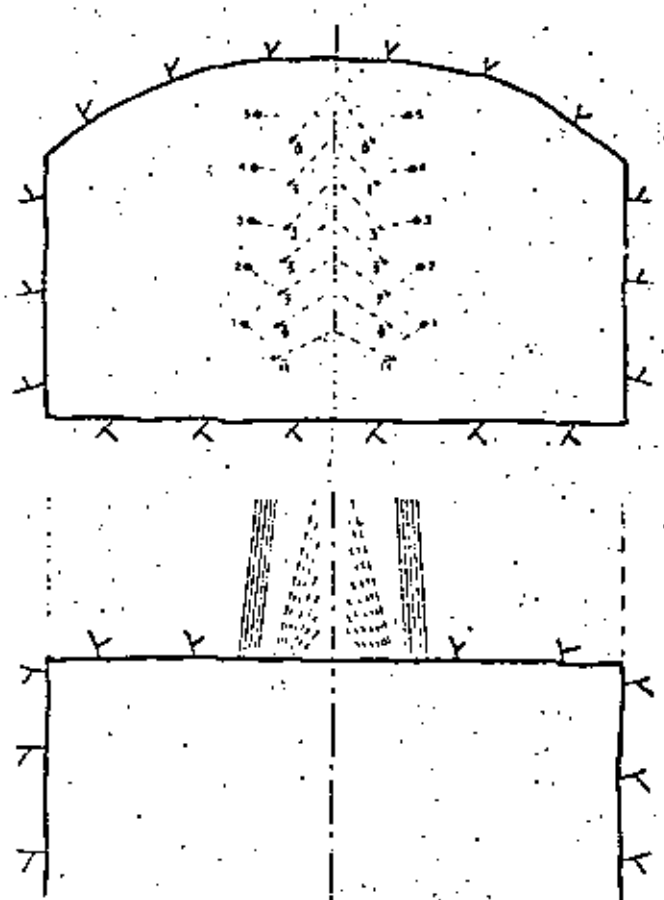

Fig. 9.4.5

Un principio importante a observar consiste en la conveniencia de hacer cueles con márgenes pequeños a su alrededor, pues el resultado de toda la voladura depende de la buena rotura del cuele.

Se están haciendo experimentos con cueles de nuevo tipo, y puede esperarse el desarrollo de nuevas variantes con arranque más fiable y mayores avances por pega. Los progresos que ya se han registrado en este campo han sido bastante rápidos.

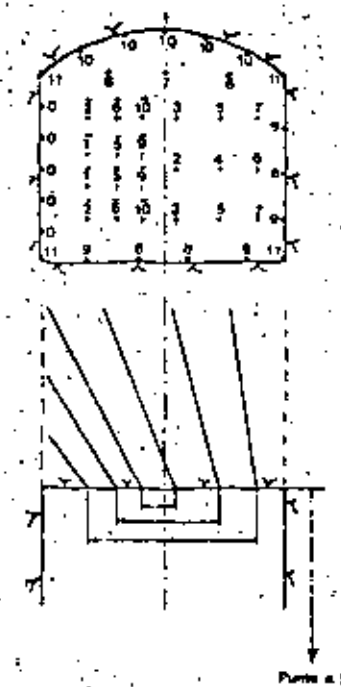

Fig. 9.4.6 - "Cuele Bildsut". Diametro de los barrenos 45—48 mm (Diseñado por L. G. Bergling)

9.5 RECORTE

En el curso de las últimas décadas, el recorte ha llegado a ser prácticamente un método estandarizado para las voladuras en túneles (véase sección 10.1). En las voladuras en túneles, el recorte proporciona las ventajas siguientes:

Mayor resistencia de la roca circundante
Menor necesidad de refuerzo
Zona agrietada más reducida alrededor del contorno final
Menor necesidad de hormigón para inyecciones
Menor sobreexcavación
Trabajo de saneo más fácil

En el caso de roca de baja resistencia, sobre todo, el recorte tiene una gran importancia de cara al resultado final, y ejerce una influencia favorable en el aspecto económico de la voladura (véase sección 9.7).

Fig. 9.5 1 Recorte en el techo de un túnel de acceso (Foto: Gerhard Bronsan)

En los trabajos en túneles, es preciso prestar una especial atención a que la alineación y emboquille de los barrenos del contorno final se haga con la máxima precisión. Con el objeto de evitar que la sección del túnel vaya haciéndose progresivamente menor con los sucesivos avances, es preciso dar un margen para emboquille a los barrenos del contorno final; ello implica una irregularidad del contorno de roca, y debe ser de una cuantía lo más pequeña posible. El mínimo margen para emboquille depende de las necesidades de espacio del equipo de perforación utilizado. En la práctica, un nivel de precisión aceptable puede ser el mínimo margen de emboquille + 3 cm/m de barreno.

La concentración de carga en los barrenos del contorno debe ser la más pequeña posible.

Los explosivos especiales del tipo Gurit han supuesto mucho en el desarrollo de la técnica de recorte. En barrenos de gran diámetro pueden utilizarse cargas dobles de Gurit o unidades más potentes de carga, del tipo Nabit.

En la Tabla incluida a continuación se indican los valores básicos apropiados para estas voladuras:

Diámetro barrenos mm	Concentración de carga kg m Dyn.	Unidad de carga	Piedra m	Espaciamiento barrenos m
25—32	0,08	Gurit de 11 mm	0,30—0,45	0,25—0,35
25—43	0,18	Gurit de 17 mm	0,70—0,80	0,50—0,60
45—51	0,18	Gurit de 17 mm	0,80—0,90 *)	0,60—0,70
51	0,30	Nabit de 22 mm	1,00	0,90
64	0,36	Nabit de 22 mm	1,00—1,10	0,80—0,90

(*) Puede parecer que los valores de los espaciamientos no son lógicos, pero en roca que no sea difícil de volar, normalmente son satisfactorios empleando Gurit. Generalmente, y por razones económicas, es preferible evitar espaciamientos excesivamente reducidos entre barrenos de gran diámetro.

La carga de fondo se limita corrientemente a un cartucho de diámetro apropiado al barreno. En los hastiales se acostumbra a usar dos cartuchos.

Diámetro barrenos	Carga de fondo Barrenos del techo	Carga de fondo Barrenos de hastiales
mm	kg	kg
aprox. 30	0,1	0,2
aprox. 40	0,175	0,35
aprox. 50	0,33	0,66

Una vez situados los barrenos en la pega, se incluye el margen para emboquille en la prolongación de los barrenos de recorte.

El esquema de encendido debe proyectarse de tal forma que los barrenos de recorte tengan rotura libre en el momento de su detonación.

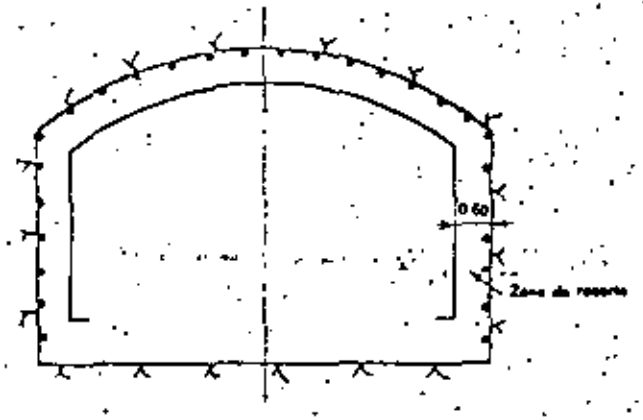

Fig. 9.5.2

En el ejemplo de la Fig. 9.5.2 se muestra el esquema de un recorte con $V_1 = 0{,}80$ m y un margen para emboquille de 20 cm.

El empleo de unas cargas potentes en los barrenos de franqueo inmediatos a la zonas de recorte puede ejercer una influencia desfavorable sobre el resultado de dicho recorte. En el caso de roca de mala calidad puede ser especialmente recomendable reajustar la perforación y carga de estos barrenos de franqueo de modo que pueda obtenerse otra hilera de recorte, pero con una carga más potente.

En túneles de gran sección, estos barrenos no se encuentran generalmente en condiciones de una constricción tan grande, por lo que no son tan difíciles de volar.

La magnitud de la formación de grietas en la roca circundante por efecto de la voladuras es un problema que ha sido considerado en la sección 11.1, "Voladura de cámaras subterráneas".

La siguiente Tabla indica los valores-guía para la carga de los barrenos de franqueo inmediatos al contorno final:

Diámetro barrenos mm	Carga de fondo kg	Carga de columna kg/m	Unidad de carga
aprox. 30	0,30 *)	0,40	Nabit de 22 mm o equivalente
aprox. 40	0,45	0,60	Dynamex de 25 mm o equivalente
aprox. 50	0,75	1,00	Dynamex de 32 mm o equivalente

(*) Como los barrenos de franqueo inferiores inmediatos a los hastiales son de voladura difícil, la carga en ellos ha de aumentarse hasta el doble del valor indicado en la Tabla.

Cada vez ha ido adquiriendo mayor importancia la posibilidad de disminuir la magnitud de los agrietamientos más allá del contorno final de la sección. La penetración del agua a los túneles, con la consiguiente necesidad de inyecciones, se han convertido en uno de los problemas más importantes en las voladuras en túneles bajo zonas edificadas. Los técnicos están consagrando una gran atención a la realización de las voladuras de modo que la formación de grietas quede limitada. Durante mucho tiempo se ha recurrido al recorte en el techo y los hastiales, pero en los últimos años, se ha comenzado también a prestar atención a la necesidad de una voladura más controlada en los barrenos del piso; como estos barrenos llevan normalmente cargas mayores que el resto de la pega, ello se ha traducido en acusados agrietamientos que conllevan la penetración al túnel de agua procedente de las capas inferiores. El subsiguiente y necesario trabajo de impermeabilización ha sido de más difícil ejecución que en el techo y los hastiales. Así pues, siempre que se desee reducir lo más posible la entrada de agua al túnel, los barrenos del piso deberán perforarse y cargarse de forma controlada. La Tabla siguiente proporciona unos valores que pueden servir de guía para lograr este propósito:

Diámetro barrenos mm	Carga de fondo kg	Carga de columna kg/m	Unidad de carga	Piedra m	Espaciamiento m
aprox. 30	0,30	0,50	Dynamex de 22 × 200 mm	0,70	0,60
aprox. 40	0,45	0,65	Dynamex de 25 × 1000 mm	0,80	0,65
aprox. 50	0,75	0,90	Dynamex de 29 × 1000 mm	0,90	0,70

El plan de encendido se proyecta de tal modo que los barrenos del piso tengan pronto rotura libre, disminuyendo así la carga necesaria para levantar la roca desprendida que hay sobre ellos. El empleo de cargas rígidas (cargas alargadas) disminuye el riesgo de un innecesario exceso de carga. Debe hacerse notar que el control de la voladura se consigue en este caso dismi-

nuyendo la carga concentrada en el fondo y la concentración de carga en la columna. La carga específica, por otro lado, muestra tendencia a aumentar. El espaciamiento denso contribuye también a regular la formación de grietas en la dirección deseada.

El encendido no puede hacerse normalmente con microrretardos, aunque es posible aplicarlo en los casos en que el recorte vaya a hacerse por separado después del resto de la pega, alcanzándose entonces unos mejores resultados; sin embargo, tal procedimiento es dificultoso desde el punto de vista técnico. No obstante, en roca de mala calidad, pueden existir motivos suficientes para proceder así.

Puede lograrse un resultado aproximadamente igual si se perforen los barrenos de recorte de modo que la zona de recorte quede 0,5 m detrás del resto de la pega; los fondos de los barrenos poseen entonces rotura libre, lo que disminuye el grado de confinamiento y mejora los resultados.

El *precorte* no ha sido utilizado tan ampliamente en las voladuras en túneles. En Noruega y en Suecia se han hecho ensayos con precorte de la sección del túnel y voladura posterior del núcleo de la pega con barrenos con cargas potentes, y sin utilizar cuele alguno. Los resultados obtenidos indican que el método puede ser factible, pero se precisa un mayor desarrollo del mismo.

Unas cargas excesivamente concentradas en los cueles o en los barrenos de una pega no resultan demasiado convenientes desde el punto de vista de la ingeniería de minas, y lo mismo se ha señalado ya varias veces en esta sección a propósito de las voladuras en túneles. Puede no ser recomendable rebajar el nivel técnico para obtener unos métodos de operar más racionales pero con un resultado final que, en conjunto, sea más deficiente.

9.6 EJEMPLOS DE CALCULO. CUELE PARALELO. CON BARRENOS DE 31 MM DE DIAMETRO

Con base en los distintos métodos que se han descrito en este capítulo, pueden hacerse los cálculos de una pega; en el primer ejemplo, se procede de acuerdo con dichos métodos. Se ha incluido también un ejemplo que ilustra el modo de calcular un plan de perforación mediante las Tablas calculadas en la sección 9.1. El modelo para el cuele y contracuele se toma de la sección 9.2.

Condiciones: Profundidad de perforación: 3,2 m
Explosivo: Dynamex B
No se efectúa recorte
Dos barrenos centrales de 76 mm en el cuele
Area: 37 m² aproximadamente.
Avance previsto por pega, 90 %: 2,9 m aproximadamente

A fin de obtener el mínimo número de barrenos, se calculan por separado los barrenos del cuele y contracuele, con objeto de que puedan luego ser combinados con los demás.

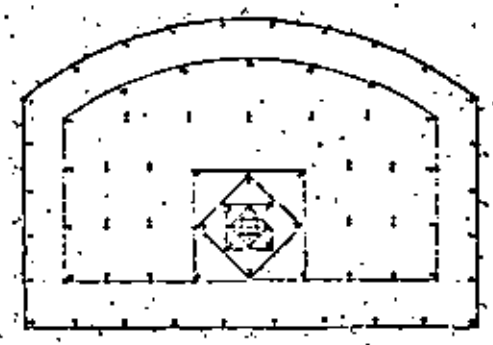

Fig. 9.6.1

1. Como los barrenos del cuele y contracuele han sido situados con relación a la *piedra* del piso, los primeros que se calculan son los barrenos del piso. De acuerdo con la Tabla, $V_t = 0{,}90$ m
$E_t = 0{,}95$ m
Tomando en consideración el margen para emboquille, la *piedra* en el fondo de los barrenos es igual a 0,90 — margen para emboquille. En el caso de perforación con equipo manual, ésto es igual aproximadamente a $0{,}90 - 0{,}10 = 0{,}80$ m

El espaciamiento de los barrenos se adapta a la anchura del túnel. Número de espacios $= \frac{8,0}{0,95} = 8,4$ y por consiguiente se toman 9 espacios

$E_1 = \frac{8,0}{9} = 0,89$ m

Los barrenos del piso se cargan con una carga de fondo igual a la calculada según la fórmula $\frac{1}{3} \times H \times \frac{d \times d}{1000}$, siendo H la profundidad del barreno y d su diámetro:

$\frac{1}{3} \times 3,2 \times \frac{31 \times 31}{1000} = 1,03$ kg = aprox. 1,00 kg (véase la Tabla)

Zona de retacado = 0,2 × *Piedra* = 0,2 × 0,90 = 0,18; aprox. 0,20 m
Longitud de la carga de columna = Profundidad del barreno — (Longitud de la carga de fondo + zona de retacado) = 3,2 — (1,1 + 0,2) = 1,9 m
Concentración de la carga de columna = 0,70 × Concentración de la carga de fondo = $0,70 \times \frac{31 \times 31}{1000} = 0,67$; 0,70 kg aprox.
Peso de la carga de columna = 1,9 × 0,70 = 1,33; 1,3 kg aprox.
Carga de los barrenos del piso = 1,0 + 1,3 = 2,3 kg/barreno
Como los barrenos del techo y de los hastiales son determinados por el contorno, son los que se calculan en los pasos siguientes.

2. *Cálculo de los barrenos de los hastiales*

Piedra = 0,9 × $V_{\text{barr. destroza}}$ ($V_{\text{barr. destroza}} = V_{\text{barr. piso}}$)
$V_{\text{barr. hastiales}} = 0,90 \times 0,90 = 0,81$; 0,80 m aprox.
Piedra con margen para emboquille 0,80 — 0,10 = 0,70 m
$E_1 = 1,2 \times V_{\text{barr. hastiales}}$
$E_1 = 1,2 \times 0,80 = 0,96$ m
El espaciamiento de los barrenos ha de adaptarse a las condiciones geométricas del problema. Deben repartirse de forma regular desde el piso a los arranques de bóveda, substrayendo la zona de barrenos de piso: 4,00 — 0,80 = 3,20 m

Número de espaciamientos $= \frac{3,2}{0,96} = 3,3$; aproximadamente 4

$E_2 = \frac{3,2}{4} = 0,80$ m

Altura de la carga de fondo = 1/6 de la profundidad del barreno
Carga de fondo = ½ de la carga de fondo de los barrenos de destroza = 0,50 kg

Altura de la carga de fondo $= \frac{3,2}{6} = 0,53$; aprox. 0,50 m
Zona de retacado = 0,5 × *Piedra* = 0,5 × 0,80 = 0,40 m

El margen para emboquille queda incluido en esta longitud
Longitud de la carga de columna = Profundidad del barreno — (Longitud de la carga de fondo + Zona de retacado) = 3,2 — (0,5 + 0,4) = 2,3 m
Concentración de la carga de columna = 0,40 × Concentración de la carga de fondo = 0,40 × 0,95 = 0,38 ; aprox. 0,40 kg/m
Peso de la carga de columna = 2,3 × 0,40 = 0,92 ; aprox. 0,90 kg
Carga de los barrenos de hastiales = 0,50 + 0,90 = 1,40 kg/barreno

3. *Cálculo de los barrenos del techo*

Espaciamiento = El mismo que para los barrenos de hastiales
Carga de fondo = La misma que en los barrenos de hastiales = 0,50 kg
Concentración de la carga de columna = 0,30 × Concentración de la carga de fondo = 0,30 × 0,95 = 0,29 ; aprox. 0,30 kg/m
Peso de la carga de columna = 2,3 × 0,30 = 0,69 ; aprox. 0,70 kg
Carga de los barrenos del techo = 0,50 + 0,70 = 1,20 kg/barreno

4. *Cuele con barrenos de contracuele situados a una altura de perforación adecuada sobre los barrenos del piso*

Resulta práctico situar primero el cuele y contracuele y acoplarlo luego al área implicada de una forma adecuada.
Carga del cuele:
Carga de fondo = 0,1 kg Dynamex por barreno
Concentración de la carga de columna = 0,25 kg/m
Longitud de la carga de columna = 3,2 — (0,1 + 0,1) = 3,0 m (Zona de retacado la más corta posible)
Peso de la carga de columna = 3,0 × 0,25 = 0,75 kg
Carga de cada barreno del cuele = 0,10 + 0,75 = 0,85 kg/barreno

5. *Cálculo de la carga del contracuele*

Primer cuadrado V = 0,20 m

Carga de fondo, según la Tabla = 0,25 kg
Concentración de la carga de columna = 0,30 kg/m
Zona de retacado = 0,5 × V = 0,10 m
Longitud de la carga de columna = 3,2 — (0,25 + 0,10) = 2,85 m
Peso de la carga de columna = 0,30 × 2,85 = 0,85 kg
Carga por barreno = 0,25 + 0,85 = 1,10 kg/barreno

Segundo cuadrado V = 0,40 m

Carga de fondo, según la Tabla = 0,45 kg
Concentración de la carga de columna = 0,35 kg/m

Zona de retacado = 0,5 × V = 0,20 m
Longitud de la carga de columna = 3,2 — (0,50 + 0,20) = 2,50 m
Peso de la carga de columna = 2,5 × 0,35 = 0,88 = aprox. 0,90 kg
Carga por barreno = 0,45 + 0,90 = 1,35 kg/barreno

Tercer cuadrado V = 0,55 m

Carga de fondo, según la Tabla = 0,75 kg
Concentración de la carga de columna = 0,50 kg/m
Zona de retacado = 0,5 × V = 0,5 × 0,65 = 0,32 = aprox. 0,30 m
Longitud de la carga de columna = 3,2 — (0,90 + 0,30) = 2,0 m
Peso de la carga de columna = 2,0 × 0,5 = 1,00 kg
Carga por barreno = 0,75 + 1,00 = 1,75 kg/barreno

Los barrenos del cuarto cuadrado se calculan como barrenos de destroza

De acuerdo con la Tabla:
Carga de fondo = 1,00 kg
Carga de columna = 0,85 kg (Concentración = 0,50 kg/m)
Carga por barreno = 1,85 kg/barreno

6. *Cálculo de los barrenos de destroza con rotura hacia arriba — horizontal*

De acuerdo con la correspondiente Tabla, para un diámetro de 31 mm y una profundidad de perforación de 3,2 m, los valores característicos son los siguientes:
Piedra V_1 = 0,90 m
Espaciamiento E_1 = 0,95 m
Carga de fondo = 1,00 kg
Concentración de la carga de fondo = 0,95 kg/m
Carga de columna = 0,85 kg
Concentración de la carga de columna = 0,50 kg/m
Los barrenos se adaptan para que se ajusten a la sección del túnel, de acuerdo con las zonas de barrenos de contorno.
V_1 se toma igual a 0,77 m
E_1 se toma igual a 1,00 m

7. *Cálculo de los barrenos de destroza con rotura hacia abajo*

La Tabla correspondiente da los valores:
V_1 = 0,90 m
E_1 = 1,10 m Se toma E_1 = 1,00 m
Q_b = 1,00 kg
Q_{bk} = 0,95 kg/m
Q_p = 0,85 kg
Q_{pk} = 0,50 kg/m

8. *Resumen de los datos más importantes:*

Barreno No.	Clase de barreno	Profdad. barreno m	No. de barrenos	Carga de fondo kg	Carga de columna kg	kg.m	Carga empleada kg/barr.	kg.
Micro./1—11	Cuele	3,2	6	0,10	0,75	0,25	0,85	5,10
Retar./1	Contrac.	3,2	4	0,25	0,85	0,30	1,10	4,40
Retar./2	Contrac.	3,2	4	0,45	0,90	0,35	1,35	5,40
Retar./3	Contrac.	3,2	4	0,75	1,00	0,50	1,75	7,00
Retar./4	Contrac.	3,2	4	1,00	0,85	0,50	1,85	7,40
Retar./5—11	Franqueo	3,2	30	1,00	0,85	0,50	1,35	55,50
Retar./11	Hastial	3,2	8	0,50	0,90	0,40	1,40	11,20
Retar./11—12	Techo	3,2	10	0,50	0,70	0,30	1,20	12,00
Retar./11—12	Piso	3,2	10	1,00	1,30	0,70	2,30	23,00
		256,0 m	80					131,00

Volumen = 37 × 2,9 = 107,3 m³
Carga específica = 1,22 kg/m³
Perforación específica = 2,38 m/m³

Ejemplo de cálculo con los mismos datos que el anterior pero haciendo uso de las Tablas de la sección 9.1 y el modelo de cuele y contracuele de la sección 9.2.

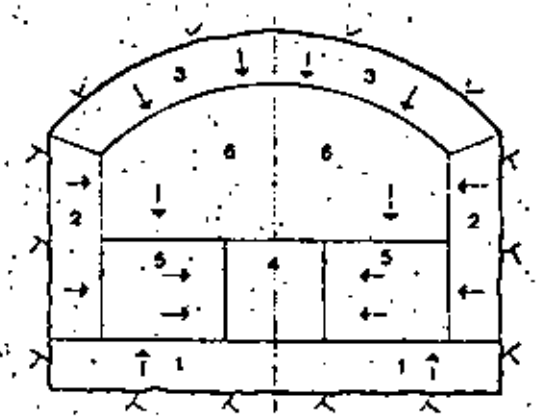

Fig. 9.6.2 1 Barrenos del piso; 2 Barrenos de hastiales; 3 Barrenos del techo; 4 Barrenos del cuele y contracuele; 5 Barrenos de destroza con rotura horizontal; 6 Barrenos de destroza con rotura hacia abajo

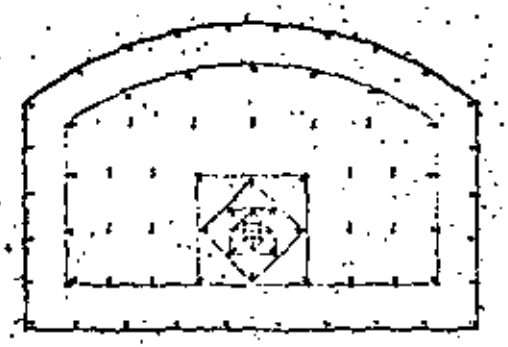

Fig. 9.6.3

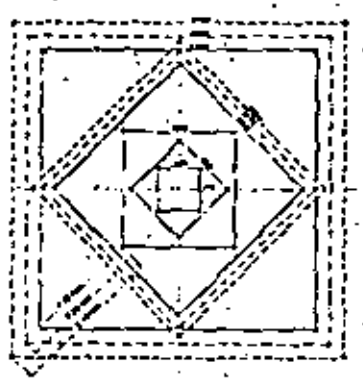

Fig. 9.6.4 Zona del cuele y contracuele

La Fig. 9.6.2 muestra el orden en que pueden irse ajustando a la sección los diversos tipos de barrenos. Las zonas correspondientes a los de contorno se forman con el valor de la *piedra* y el margen para emboquille. Los barrenos del cuele y contracuele se ecoplan encima de los barrenos del piso. Al situar los barrenos de destroza con rotura horizontal, puede ser conveniente desplazar hacia un lado los barrenos de contracuele, a fin de aprovechar mejor los mismos. En túneles de sección pequeña es posible que sea preciso hacer ciertos reajustes en las zonas del cuele y contracuele.

1. Ajuste de los barrenos del piso: Se utiliza la Tabla correspondiente a estos barrenos.

El margen para emboquille es de unos 0,10 m, con equipo de perforación manual.

Piedra con margen para emboquille: $0{,}90 - 0{,}10 = 0{,}80$ m

Espaciamiento, según la Tabla = 0,95 m

Espacios a través de la anchura del túnel $= \frac{8{,}0}{0{,}95} = 8{,}4 = 9$ aprox.

Espaciamiento $= \frac{8{,}0}{9} = 0{,}89$ m

Utilícese la carga indicada en la Tabla.

2. Ajuste de los barrenos de hastiales: Se utiliza la Tabla correspondiente.

Piedra, con margen para emboquille: $0{,}80 - 0{,}10 = 0{,}70$ m

El espaciamiento es de 0,95 m según la Tabla, a lo largo de toda la altura del hastial menos la *piedra* de los barrenos del piso: $4{,}0 - 0{,}80 = 3{,}2$ m

$\frac{3{,}2}{0{,}95} = 3{,}4 =$ aprox. 4

Espaciamiento $= \frac{3{,}2}{4} = 0{,}80$ m

Utilícese la carga indicada en la Tabla.

3. Ajuste de los barrenos del techo: Se utiliza la Tabla correspondiente.

Piedra, con margen para emboquille $= 0{,}80 - 0{,}10 = 0{,}70$ m

El espaciamiento dado por la Tabla es de 0,95 m, a lo largo de la bóveda, de unos 8,5 m de longitud: $\frac{8{,}5}{0{,}95} = 9$

Espaciamiento $= \frac{8{,}5}{9} = 0{,}93$ m

Utilícese la carga indicada en la Tabla.

4. Ajuste de la zona del cuele y contracuele: Se utiliza el modelo correspondiente.

El cuele está situado corrientemente en el centro de la sección del túnel, a fin de conseguir un esquema de perforación más regular.

El cuele y la zona de contracuele han de cargarse tal como se indica en la Tabla. Los cuatro barrenos más exteriores se cargan como barrenos de destroza.

5. Ajuste de los barrenos de destroza con rotura horizontal: Se utiliza la Tabla correspondiente.

Piedra = 0,90 m

Espaciamiento = 0,95 m

La *piedra* y el espaciamiento se ecoplan sobre la sección libremente

$V_1 = 0{,}77$ m $\quad E_1 = 1{,}0$ m

Utilícese la carga indicada en la Tabla.

6. Ajuste de los barrenos de destroza con rotura hacia abajo: Se utiliza la Tabla correspondiente.
   Piedra = 0,90 m
   Espaciamiento = 1,10 m
   La *piedra* y el espaciamiento se acoplan sobre la sección libremente. Los barrenos de destroza más altos inmediatos a los hastiales son de rotura más fácil, y pueden espaciarse más, de modo que los espaciamientos se acoplen a la geometría del problema.
   Utilícese la carga indicada en la Tabla.

Resumen de los datos más importantes:

Barreno No	Clase de barreno	Profdad. barreno m	No. de barrenos	Carga de fondo kg	Carga de columna kg	Carga de columna kg/m	Carga empleada kg/barr.	Carga empleada kg
Micro./1—11	Cuele	3,2	6	0,10	0,75	0,25	0,85	5,10
Retar./1	Contrac.	3,2	4	0,25	0,85	0,30	1,10	4,40
Retar./2	Contrac.	3,2	4	0,45	0,90	0,35	1,35	5,40
Retar./3	Contrac.	3,2	4	0,75	1,00	0,50	1,75	7,00
Retar./4	Contrac.	3,2	4	1,00	0,85	0,50	1,85	7,40
Retar./5—11	Franqueo	3,2	30	1,00	0,85	0,50	1,85	55,50
Retar./11	Hastial	3,2	8	0,50	0,90	0,40	1,40	11,20
Retar./11—12	Techo	3,2	10	0,50	0,70	0,30	1,20	12,00
Retar./11—12	Piso	3,2	10	1,00	1,30	0,70	2,30	23,00
		256,0 m	80					131,00

Volumen = 37 × 2,9 = 107,3 m³
Carga específica = 1,22 kg/m³
Perforación específica = 2,39 m/m³

Ejemplo de cálculo: Túnel con cuele en V y barrenos de 45 mm de diámetro.

Condiciones: Profundidad de perforación = 3,6 m
Explosivo: Dynamex como carga de fondo
Dynamex o Nabit como carga de columna
Gurit para recorte
Area aproximada = 74 m²
Anchura = 10 m
Margen para emboquille = 20 cm
Espacio necesario para el equipo de perforación = 5,5 m

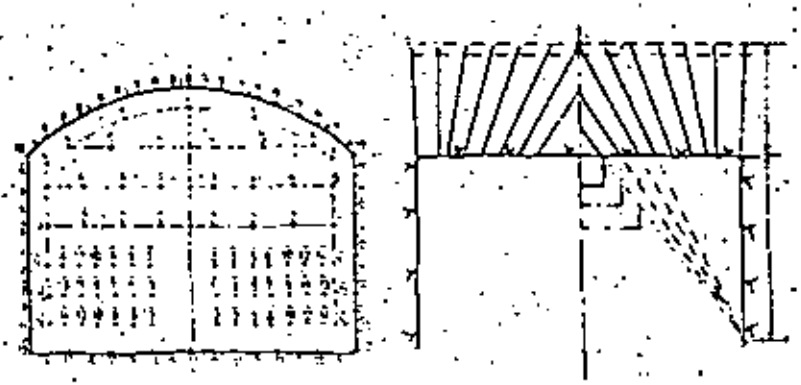

Fig. 9.6.5

1. Dado que la posición de los barrenos del cuele y contracuele depende de la situación de los barrenos del piso, son éstos los que han de ser calculados en primer lugar (véase sección 9.1):
   De acuerdo con la Tabla, para barrenos de 45 mm, el espaciamiento será:
   V_1 = 1,15 m
   E_1 = 1,25 m
   Si se toma en cuenta el margen para emboquille, los barrenos del cuele y contracuele pueden situarse a 1,15 — margen para emboquille = 0,95 m por encima del piso.
   El espaciamiento ha de ser adaptado a la anchura del túnel:
   Número de espaciamientos = $\frac{10,0}{1,25}$ = 8, lo que significa 9 barrenos al nivel del piso.
   Longitud de la carga de fondo = ⅓ de la profundidad del barreno.
   Longitud de la carga de fondo = ⅓ × 3,6 = 1,2 m
   Concentración de la carga de fondo = $\frac{d \times d}{1000} = \frac{45 \times 45}{1000}$ = 2,02 = = aprox. 2,0 kg/m
   Peso de la carga de fondo = 1,2 × 2,0 = 2,4 kg
   Longitud de la carga de columna = Profundidad del barreno — (Longitud de la carga de fondo + Zona de retacado).
   Zona de retacado = 0,2 × V = 0,2 × 1,15 = 0,23; aprox. 0,2 m
   Longitud de la carga de columna = 3,6 — (1,2 + 0,2) = 2,2m
   Concentración de la carga de columna = 0,70 × Concentración de la carga de fondo = 0,70 × 2,0 = 1,4 kg/m
   Peso de la carga de columna = 2,2 × 1,4 = 3,08 = aprox. 3,1 kg.
   Carga de los barrenos del piso = 2,4 + 3,1 = 5,5 kg/barreno

2. Para los *barrenos de hastiales*, la *piedra* viene determinada en este caso por el recorte (véase sección 9.5), que se hace utilizando Gurit como explosivo, y viene exigido por las demandas especiales del caso. Por tanto, según la Tabla correspondiente, la *piedra* será de 0,80 m. Deduciendo el margen para emboquille, la *piedra* hacia el interior del contorno será igual a 0,80 — 0,20 = 0,60 m.
   El espaciamiento 0,60 m ha de ser adaptado a la altura de los hastiales:
   Número de espaciamientos = $\frac{6,0}{0,60}$ = 10, lo que significa 11 barrenos.
   De acuerdo con la Tabla, la carga de fondo para el recorte es aproximadamente de 0,35 kg/barreno.
   La carga de columna es con Gurit de 17 mm — 0,46 m/unidad.
   Zona de retacado = 0,5 × Piedra = 0,5 × 0,80 = 0,40 (si se emplea Gurit, puede reducirse esta zona a 0,2 m).
   Longitud de la carga de columna = 3,6 — ($\frac{0,35}{2,0}$ + 0,2) = aprox. 3,2 m.
   Número de unidades de Gurit = $\frac{3,2}{0,46}$ = 6,96, es decir, 7 unidades, con un peso de 0,11 kg/unidad.
   Carga de los barrenos de hastiales = 0,35 + 0,77 = 1,12 kg/barreno.
3. Los *barrenos del techo* se perforan con el mismo espaciamiento. La única diferencia reside en que la carga de fondo se reduce a 0,175 kg/barreno.
   Carga de los barrenos de techo = 0,175 + 0,77 = 0,945 = aprox. 0,95 kg/barreno.
   Se necesita un total de 17 barrenos.
4. Ahora pueden ya calcularse y situarse los barrenos del cuele y contracuele (véase sección 9.3).
   De acuerdo con la Tabla para los cueles en cuña, la *piedra* máxima para una cuña con barrenos de 45 mm de diámetro es de 1,5 m. Esto implica $\frac{3,6}{1,5}$ = 2,3 cuñas. Se toman dos cuñas con un barreno auxiliar.
   La altura de la cuña ha de ser como máximo de 1,8 m, con tres cuñas dispuestas verticalmente. Si es posible, las cuñas se harán de tal modo que el ángulo del vértice interior sea de 60° o más. Debe tenerse también en cuenta el espacio requerido por el equipo de perforación; en este caso 5,5 m.
   En este ejemplo, el ángulo de la cuña es muy próximo a los 60°.
   Los barrenos se cargan hasta ⅓ de su profundidad.
   Zona de retacado = 0,3 × V.
   La concentración de la carga de columna se toma igual a 0,5 × Concentración de la carga de fondo, la cual está completamente compactada en el barreno.

Primera cuña

Longitud de la carga de fondo = ⅓ × 4,2 = 1,39 ; aprox. 1,4 m.
Concentración de la carga de fondo = 2,0 kg/m.
Peso de la carga de fondo = 1,4 × 2,0 = 2,8 kg/barreno.
Zona de retacado = 0,3 × V = 0,3 × 1,5 = 0,45 ; aprox. 0,50 m.
Longitud de la carga de columna = 3,6 — (1,4 + 0,50) = 1,7 m.
Concentración de la carga de columna = 0,5 × 2,0 = 1,0 kg/m.
Peso de la carga de columna = 1,7 × 1,0 = 1,7 kg.
Carga por barreno = 2,8 + 1,7 = 4,5 kg.

Segunda cuña

Longitud de la carga de fondo = ⅓ × 2,6 = 0,86 = aprox. 0,90 m.
Peso de la carga de fondo = 0,90 × 2,00 = 1,80 kg/barreno.
Longitud de la carga de columna = 2,6 — (0,90 + 0,50) = 1,2 m.
Peso de la carga de columna = 1,2 × 1,00 = 1,2 kg.
(Esto proporciona un cierto exceso de carga en la columna, pero si se desea evitar las proyecciones, puede reducirse la carga de columna en las dos cuñas.)
Peso de la carga = 1,8 + 1,2 = 3,0 kg/barreno.

Barreno auxiliar

Longitud de la carga de fondo = ⅓ × 1,7 = 0,56 = aprox. 0,60 m.
Peso de la carga de fondo = 0,60 × 2,00 = 1,20 kg.
No es necesaria carga de columna.

5. Los barrenos del contracuele pueden perforarse, de acuerdo con la Tabla para cueles en cuña de la sección 9.3, con una *piedra* de 1,00 m, valor teórico inicial que ha de adaptarse a las condiciones geométricas del problema particular.
   En este caso: semianchura del túnel — zona de barrenos de hastiales = 5,0 — 0,6 = 4,4 m. Número de espacios = $\frac{4,4}{1,00}$ = 4,4, y se toma un número de 5, pues los barrenos de contracuele deben estar más bien sobrecargados.
   $V_1 = \frac{4,4}{5}$ = 0,88 m.
   La profundidad de los barrenos de contracuele varía entre 4,1 y 3,6 m. Cuando la perforación haya sido efectuada con espaciamientos muy pequeños, puede calcularse la carga de fondo para una profundidad de barreno de 3,6 m.

Carga de fondo = 1/3 × 3,6 × 2,00 = 2,40 kg/barreno.
Zona de retacado = aprox. 0,50 m.
Puede permitirse que los primeros barrenos de contracuele tengan zonas de retacado más largas.
Longitud de la carga de columna = 3,6 — (1,2 + 0,50) = 1,9 m.
Concentración de la carga de columna = 0,40 × Concentración de la carga de fondo = 0,40 × 2,00 = 0,80 kg/m.
Peso de la carga de columna = 1,9 × 0,80 = 1,52 = aprox. 1,50 kg/barreno.
Carga de los barrenos de contracuele = 2,40 + 1,50 = 3,90 kg/barreno.

6. Los *barrenos de destroza* están dirigidos todos hacia abajo en este caso. De acuerdo con la sección 9.1, pueden tomarse los valores siguientes:

V_1 = 1,15 m.
E_1 = 1,35 m.
El espaciamiento ha de ser adaptado a la anchura 4,4 × 2 = 8,8 m.

Número de espaciamientos = $\frac{8,8}{1,35}$ = 6,5 = aprox. 7 y 8 barrenos por hilera.

$E_1 = \frac{8,8}{7}$ = 1,26 m.

Peso de la carga de fondo = 1/3 × 3,6 × 2,00 = 2,4 kg/barreno.
Zona de retacado = 0,55 m.
Longitud de la carga de columna = 3,6 — (1,2 + 0,55) = 1,85 m.
Concentración de la carga de columna = 0,50 × Concentración de la carga de fondo.
Peso de la carga de columna = 1,85 × 1,00 = 1,85 kg.
Carga de los barrenos de destroza = 2,40 + 1,85 = 4,25 kg/barreno.
La carga de columna ha de adaptar su valor a las unidades adecuadas, según las condiciones existentes.

Resumen de los datos más importantes:

Barreno No.	Clase de barreno	Profdad. barreno m	No. de barrenos	Metros perforados m	Carga de fondo kg	Carga de columna kg	Carga de columna kg/m	Carga empleada (kg) Dyn.	Carga empleada (kg) Gurit
Micro. 1—2	Cuele	1,70	3	5,10	1,20			3,60	
Micro. 3	Cuele	2,60	6	15,60	1,80	1,20	1,00	18,00	
Micro. 5	Cuele	4,20	6	25,20	2,80	1,70	1,00	27,00	

Barreno No.	Clase de barreno	Profdad. barreno m	No. de barrenos	Metros perforados m	Carga de fondo kg	Carga de columna kg	Carga de columna kg/m	Carga empleada (kg) Dyn.	Carga empleada (kg) Gurit
Micro. 7—16	Contrac.	3,6—4,1	30	114,00	2,40	1,50	0,80	117,00	
Retar. 2—6	Destroza	3,60	26	93,60	2,40	1,85	1,00	110,50	
Retar. 7—11	Hastiales	3,60	20	72,00	0,32	0,77	0,24	7,00	15,40
Retar. 8—9	Techo	3,60	17	61,20	0,175	0,77	0,24	3,00	13,10
Retar. 11—12	Piso	3,60	9	32,40	2,40	3,10	1,40	42,50	
			117	419,10				335,60	28,50 21,10 Dyn.)

Volumen = 74 × 3,24 = 240 m³

Carga específica = $\frac{356,70}{240}$ = 1,48 kg/m³

Perforación específica = $\frac{419,10}{240}$ = 1,75 m/m³

Si se utilizan cargas de columna que no sean de Dynamex, han de escogerse de forma que se adecúen a la concentración de la carga de columna.
Sobre los resultados de los cálculos cabe hacer los comentarios siguientes:
La perforación específica es alta, debido al empleo del recorte y a una anchura adversa del túnel para los barrenos de contracuele.
La carga específica es también elevada, debido a la reducida *piedra* de los barrenos de contracuele en razón de la anchura del túnel. En la mayoría de los casos puede aumentarse el valor de la *piedra*, según el punto 5, disminuyendo a cuatro el número de hileras: $V_1 = \frac{4,4}{4}$ = 1,10 m. Puede asimismo eliminarse alguno de los barrenos de destroza de encima del cuele, reduciéndose así el número de barrenos en una proporción significativa.
Puede ser conveniente comenzar las voladuras en un túnel con un esquema de perforación que contenga unos ciertos márgenes de aproximación; posteriormente podrán reducirse las cargas y el número de barrenos, según las características de la roca a la voladura. Sin embargo, generalmente no merece la pena mantenerse estrictamente en el límite mínimo de rotura aceptable.

9.7 ESTUDIO ECONÓMICO DE LAS VOLADURAS

[illegible] de actualidad a unos valores [illegible] [illegible] [illegible] [illegible] [illegible] [illegible] [illegible] [illegible] puede suponer un ahorro significativo [illegible] [illegible]. En esta sección se pretende [illegible] [illegible] los factores influyentes en el aspecto [illegible] [illegible] 5.8 y a propósito de las voladuras en banco, se trata de los [illegible] [illegible] [illegible] de [illegible] de las [illegible]

[illegible] el método de [illegible] de cálculo [illegible] desde el punto de vista económico. Por ejemplo, [illegible] que si se sustituye [illegible] determinado producto utilizado [illegible] multiplicada por el [illegible] de [illegible] el ahorro conseguido [illegible] de [illegible].

[illegible] de cálculo [illegible] totalmente aplicable a todas las [illegible], pero cuanto mayor sea el número de factores implicados en el [illegible] menor será el campo de aplicabilidad de dicho método.

En el caso de las voladuras en túneles puede afirmarse que la influencia [illegible] cada variable se extiende [illegible] el trabajo que [illegible] [illegible] del túnel o mina y [illegible] [illegible] del mineral.

[illegible]

[illegible] la concentración de la carga de fondo [illegible]

[illegible] [illegible] [illegible] [illegible] [illegible] [illegible] [illegible] [illegible] [illegible] [illegible]

[illegible] en la cadena productiva [illegible] [illegible] [illegible] [illegible] [illegible]

[illegible] la [illegible] experimentación [illegible] [illegible] de la perforación, del diseño [illegible] [illegible] mismos [illegible] mismo tiempo [illegible] el [illegible] [illegible] en forma de [illegible] [illegible] mucho [illegible] una [illegible] [illegible] diseño de las máquinas [illegible]

[illegible] para [illegible] [illegible] en [illegible] [illegible] es más acertado calcular el [illegible] desde el punto de vista [illegible].

[illegible] [illegible] en este [illegible] de la carga de voladura [illegible].

La elección del diámetro de los barrenos posee una gran [illegible] económica. [illegible] [illegible] en banco, [illegible] utilizar barrenos de diámetro [illegible] en el caso de [illegible], el factor de limitación [illegible] [illegible] [illegible] [illegible] [illegible] pueden perforarse en general mucho más rápidos [illegible] de gran diámetro que cuando son [illegible] [illegible] mm.

[illegible] [illegible] [illegible] [illegible] [illegible] [illegible] del diámetro [illegible] [illegible] [illegible] [illegible] [illegible] [illegible]

barrenos de pequeño diámetro realizados con perforadoras sostenidas manualmente a barrenos de gran diámetro (48—51 mm) realizados con Jumbos de perforación, y actualmente se tiende a barrenos de menor diámetro (32—45 mm) realizados con este tipo de máquinas. Esto último supone que se están manteniendo las ventajas de los barrenos de pequeño diámetro, al tiempo que se desarrollan métodos de perforación más racionalizados. A este respecto, debe hacerse también una evaluación de las mejoras obtenidas en los resultados, desde el punto de vista de la técnica minera, en el caso de barrenos de pequeño diámetro, con menores concentraciones de carga por metro de barreno.

Un cálculo de los costes de perforación por metro de túnel, basado en el coste por metro perforado, para diferentes dimensiones de barrenos y secciones, proporciona una cierta información fundamental para una estimación de costes. Sin embargo, como ya se ha señalado anteriormente, no puede decirse que el cálculo proporcione el material básico para una estimación extensiva, pues ha de estudiarse también el resultado global.

9.8 CALCULO DE ESQUEMAS DE PERFORACION MEDIANTE COMPUTADOR

En los últimos años la técnica de los computadores electrónicos ha sido puesta al servicio de la preparación de esquemas de perforación para voladuras en túneles. Han trabajado en este terreno Atlas Copco, Nitro Consult, y el Laboratorio de Investigaciones de Nitro Nobel.

Ocurre con frecuencia en los cálculos a propósito de las voladuras en túneles que la posibilidad de estudiar un número elevado de posibles alternativas quede limitada por la gran cantidad de trabajo que ello supondría. La utilización de computadores viene a hacer posible realizar una rápida revisión de las diferentes posibilidades de diámetros de barrenos, explosivos, profundidades de perforación, etc., y del efecto de estos factores sobre los resultados previstos. El programa de cálculo se hace a partir de unas relaciones conocidas; se tratará de desarrollar estas relaciones y fijar en el programa los precios de las unidades componentes, como el coste por metro de perforación, etc.

El programa de computador ha de poseer la flexibilidad suficiente para que, por ejemplo, un contratista particular pueda manejar un programa basado en las condiciones aplicables a su caso concreto. Las condiciones comprenden la forma geométrica y el área del túnel, los explosivos a emplear, los diámetros de los barrenos, el avance deseado por pega, y las características de la roca de que se trate frente a la voladura. También es posible incluir o no el recorte.

Cuando se trabaja con planes de perforación programados con computador, pueden variarse las constantes de voladura de los túneles cuando sea necesario, de modo que pueda escogerse el esquema de perforación más adecuado para el caso en estudio.

Las dificultades de elaboración de esquemas de perforación programados mediante computador estriban en la posibilidad de lograr un programa que incluya las diversas alternativas posibles normalmente al proyectar un túnel. Las relaciones que forman la base del programa son unas fórmulas empíricas que describen las condiciones de rotura, necesidades de carga, etc. para cada barreno que ocupa una determinada posición en la pega. La falta de algunas correlaciones ha llevado consigo la necesidad de ciertas modificaciones.

El material básico para los cálculos referentes a los túneles incluido en este capítulo ha sido reunido con objeto de que proporcione la información necesaria para el cálculo de las voladuras en túneles desde el primero al último barreno, de modo análogo a como se hizo para las voladuras en banco.

A medida que se va adquiriendo una mayor experiencia en las voladuras en túneles, las posibilidades de contar con un programa de computador plenamente comprensivo se van haciendo más grandes.

De haber sido en un principio un simple auxilio técnico en la elaboración de esquemas de perforación-carga-encendido, los programas del computador pueden ir siendo perfeccionados gradualmente hasta convertirse en un auxiliar de primer orden para el trabajo de cálculo, de planificación, y operaciones prácticas.

10. RECORTE

10.1 RECORTE CONVENCIONAL

El recorte es un método especial de voladura que tiene por objeto proteger la superficie de roca remanente alrededor de la pega; se trata no solamente de obtener una superficie lisa, sino también de proteger la roca del agrietamiento, pues la eliminación de las fisuras lleva consigo muchas ventajas. En los últimos diez años, la técnica del recorte ha ampliado su campo de aplicación. Han de distinguirse dos diferentes tipos de recorte; el recorte convencional y el precorte. Como este último método difiere netamente del convencional desde el punto de vista técnico, se le trata en un apartado especial.

Los dos métodos son utilizados cuando interesa dar un tratamiento cuidadoso a la roca circundante; no obstante, el orden de utilización varía considerablemente según los casos. En trabajos subterráneos, el recorte convencional es notablemente más frecuente que el precorte.

El recorte se realiza en la práctica mediante el empleo de un explosivo con una reducida concentración de carga por metro, y otras características que se traduzcan en un efecto más suave. En las zonas de roca en las que se va a efectuar el recorte, el esquema de perforación es considerablemente más denso de lo normal. Una condición esencial que ha posibilitado el éxito de la técnica del recorte ha sido el desarrollo de un explosivo apropiado; en Suecia se han utilizado durante muchos años las cargas alargadas (entubadas) de Gurit, las cuales se han revelado como un excelente instrumento de trabajo para los recortes. Las características de este explosivo son:

Velocidad de detonación:	4000 m/seg.
Volumen de gases:	404 litros/kg
Factor de trabajo:	349 ton metros/kg
Potencia por unidad de peso:	74
Concentración de la carga:	0,245 kg/m (17 mm)
Concentración de la carga:	0,11 kg/m (11 mm)

Las cargas alargadas de Gurit han sido utilizadas con considerable éxito en roca de diferentes tipos en lugares esparcidos por todo el mundo.

Estos son los trabajos en los que se emplea actualmente el recorte:

Túneles
Cámaras subterráneas
Desmontes para carreteras
Taludes para cimentaciones de edificios
Voladuras controladas
Zanjas para conducciones
Voladura de bloques de piedra en canteras

Estos tres últimos casos serán tratados en una sección especial al describir la técnica del recorte aplicada a diversos casos prácticos.

Las ventajas que proporciona el recorte son las siguientes:

Superficies de roca más lisas
Superficies de roca más sanas — Menor necesidad de refuerzo
Menor sobreexcavación
Menores necesidades de hormigón de revestimiento
Menores pérdidas en el caso de conducciones de agua
Concordancia muy precisa con la sección teórica en trabajos complicados de cimentaciones
Menor agrietamiento — Menor penetración de agua

Geotécnicos y geólogos se muestran de acuerdo en que el recorte constituye una contribución muy importante de cara a la posibilidad de conseguir la construcción de estructuras de roca con buenas características resistentes. En el caso de voladuras subterráneas, es extremadamente importante que la roca circundante quede libre de fisuras, pues en caso contrario pierde la totalidad o una parte de sus propiedades de autosostenimiento. Las voladuras de potencia innecesariamente elevada hacen asimismo aumentar el riesgo de penetración de agua, lo que a su vez puede producir un descenso del nivel freático en los estratos superiores.

Los expertos en el campo de las inyecciones subrayan la importancia de realizar las voladuras de tal modo que se eviten las fisuras lo más posible. Aun cuando las personas dedicadas al estudio de la roca estén de acuerdo sobre la importancia del recorte, existen también opiniones contrarias a él; sostienen que el recorte produce unos resultados aparentemente buenos a causa de la superficie lisa obtenida, pero que esta superficie ha de ser reforzada posteriormente. Este juicio significa que la apariencia lisa de la superficie es engañosa a la hora de estimar el estado de la roca. Es éste un punto de vista razonable, pero que considero erróneo. Cuanto más deficiente sea la calidad de la roca, más necesario es el recorte. Como los folletos y publi-

caciones técnicas muestran generalmente los resultados mejores y más atractivos, puede ser decepcionante que, trabajando en una roca no homogénea, se obtenga un resultado en el que quizás no pueda apreciarse ni la traza de una sola perforación; en tales casos debe recordarse que, trabajando en roca de mala calidad, se llega a resultados considerablemente mejores (como es, por ejemplo, la menor sobreexcavación), que los obtenidos en roca homogénea, comparando ambos casos en términos relativos. El peor aspecto de la superficie final es lo que influye sobre la evaluación que en esas ocasiones se hace del resultado. En resumen, puede afirmarse que el recorte hace que se obtengan siempre unos mejores resultados en lo que concierne al contorno y a la roca circundante, aun cuando puede seguir siendo necesario reforzar la roca en las proximidades de fallas, diaclasas, y zonas de debilidad, si bien el recorte, al mantener la curvatura, puede contribuir a que la roca se sostenga por un tiempo. Con todo, el refuerzo preciso será menor, y la aplicación de hormigón proyectado de modo casi inmediato, antes de que la roca haya tenido tiempo de moverse, es un método excelente para ser combinado con el recorte, permitiendo abordar incluso situaciones en que la roca se encuentra en condiciones muy difíciles.

La influencia de las voladuras subterráneas en la roca circundante, juntamente con las leyes de la Mecánica de Rocas, constituye un interesante sector de la técnica minera que se ha convertido en el centro de la atención en el curso de los últimos años, siendo éste un terreno en el que cabe esperar un continuo desarrollo tecnológico.

Las consideraciones a las que se ha hecho mención más arriba se refieren principalmente a la aplicación del recorte en túneles y cámaras subterráneas; sin embargo, esta técnica tiene asimismo un amplio campo de aplicación en superficie. A medida que los proyectistas han ido descubriendo las posibilidades de obtener mejores contornos de acabado gracias al empleo del recorte, la técnica se hizo más y más utilizada. En muchos casos, la aplicación del recorte tiene repercusión fundamentalmente en el aspecto económico de la obra; los responsables de éste no siempre se muestran muy propicios a utilizar un método de voladuras más caro únicamente por la satisfacción de contemplar una superficie de roca más lisa y atractiva, y mucho menos si han de hacerse posteriormente rellenos, con lo que la superficie de roca desaparece de la vista. Los estudios realizados han demostrado sin embargo que, incluso en el caso de voladuras en zanjas, el recorte puede resultar económicamente ventajoso por la disminución que lleva consigo en la cuantía de la sobreexcavación y del material de relleno necesario; la modalidad normalmente empleada es el precorte.

Como se indicó ya anteriormente, el recorte se efectúa mediante explosivos especiales y esquemas de perforación densos. En la Tabla que se incluye a continuación pueden verse las características recomendadas:

Diámetro barrenos mm	Concentración de la carga kg. m Dyn.	Unidades de carga	Piedra V_t m	Espaciamiento E_t m
25—32	0,08	Gurit de 11 mm	0,45	0,35
25—43	0,18	Gurit de 17 mm	0,70—0,80	0,50—0,60
48—51	0,18 (*)	Gurit de 17 mm	0,80—0,90	0,60—0,70
48	0,30	Nabit de 22 mm	1,0	0,8
64	0,38	Nabit de 22 mm	1,0—1,1	0,8—0,9

(*) En tipos de roca fácilmente volable.

Los valores de la Tabla muestran que la relación entre *piedra* y espaciamiento es $E/V = 0{,}8$ aproximadamente. Con este espaciamiento se controla la formación de grietas de modo que se concentran a lo largo de la traza del contorno final. La Tabla muestra asimismo que si se emplean barrenos de mayor diámetro, el recorte puede realizarse con cargas más potentes. La regularidad de la superficie, y el resultado en conjunto son, sin embargo, generalmente mejores con barrenos estrechos y cargas ligeras. La distribución de barrenos puede necesitar alguna corrección para ajustarse a las condiciones particulares de la roca en cuestión.

La precisión de la perforación tiene la máxima importancia para el resultado final.

La iniciación de las hileras de barrenos de un recorte debe efectuarse con el menor lapso posible de tiempo entre las diversas hileras. Dado que, en los recortes, los barrenos de contorno forman una sucesión de números de retardo más altos que los de los barrenos de una pega, esto puede ser difícil de conseguir en muchos casos.

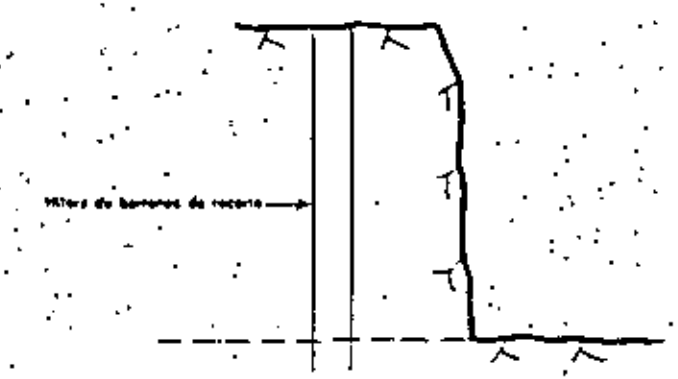

Fig. 10.1.1

Antes de pasar a estudiar la forma en que se realizan los recortes según los diferentes casos, ha de hacerse resaltar un punto importante: el recorte significa también una voladura en la que los barrenos de contorno, con cargas ligeras, tienen una *piedra* prácticamente libre (Fig. 10.1.1).

Las voladuras en que los barrenos de contorno llevan los mismos retardos, y son iniciados al mismo tiempo que el resto de la pega, no pueden ser consideradas como verdaderos recortes, excepto en el caso de voladura subterránea. Cuando un barreno de contorno cargado con Gurit detona sin tener rotura libre, una parte considerable de la energía del explosivo se invierte en una sacudida contra el interior de la masa de roca, con lo que el recorte que se obtiene es deficiente. En voladuras sobre la superficie, a menudo resulta difícil en la práctica romper la roca inmediata al contorno final en una pega independiente; sin embargo, si se quiere obtener un buen resultado, es preciso efectuar el recorte de este modo.

Recorte en excavaciones en trinchera

Los barrenos del contorno se perforan con la distribución que se muestra en la Fig. 10.1.2. En los barrenos de recorte se colocan cargas de fondo con Dynamex en la parte inferior, adaptándose la cuantía de la carga a la profundidad del barreno y al esquema de perforación. La carga de fondo puede calcularse con ayuda del ejemplo siguiente:

$H = 8$ m
$V_1 = 0{,}30$ m
$E_1 = 0{,}60$ m
$V_1 \times E_1 = 0{,}60 \times 0{,}60$, a la inversa en el cálculo normalmente utilizado para voladuras en banco $0{,}50 \times 0{,}80$, lo que da $V_1 = 0{,}60$ m.
Error de perforación $= 0{,}05 + 0{,}03 \times 8 = 0{,}29$; aproximadamente 0,30 m.
$V_{real} = 0{,}60 + 0{,}30 = 0{,}90$ m.
En el caso de 0,90 m, se requiere una carga de fondo de 0,40 kg
Esto significa que la carga de fondo en cada barreno será de 0,40 kg.

En el caso de voladuras profundas en construcción de carreteras, la carga de fondo puede ser aumentada en muchas ocasiones, siempre que esta carga en la parte inferior del barreno no dañe la roca del contorno final; no obstante, deberán evitarse las cargas excesivamente potentes.

Es también importante asegurarse de que los barrenos de la pega inmediatos a la hilera de recorte no poseen una concentración excesivamente potente en la carga de columna, pues de ser así, el resultado del recorte puede quedar destruido antes de que los barrenos de contorno hayan tenido tiempo de romper. En la excavación de trincheras para carreteras, con frecuencia no

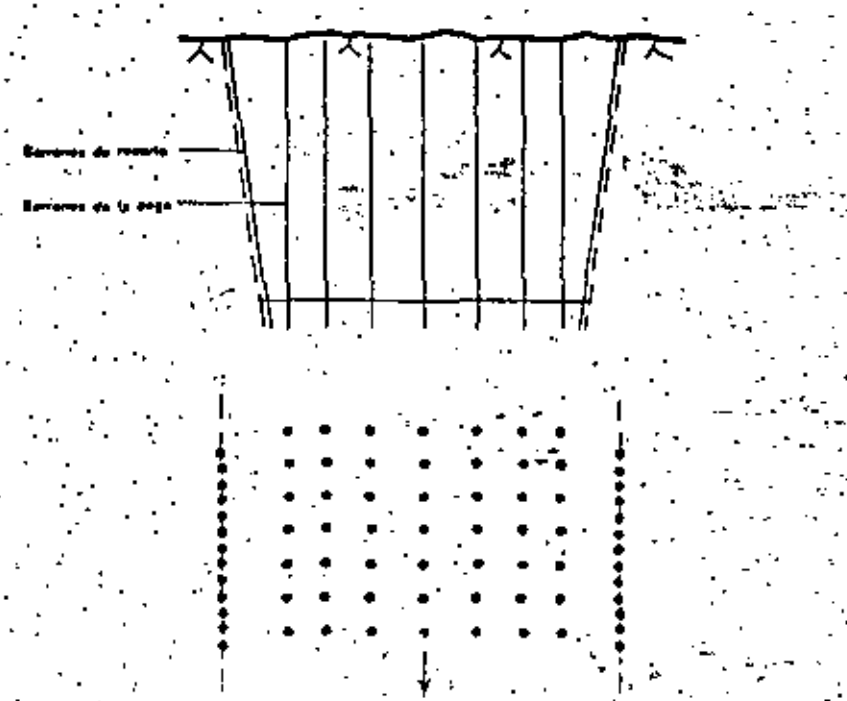

Fig. 10.1.2

conviene en la práctica volar el contorno por separado, por lo que puede ser preferible el precorte al recorte convencional.

Es importante comprobar que las operaciones de carga de columna de los barrenos se efectúan con todo cuidado, de forma que las cargas constituyan una cadena ininterrumpida, evitando también que puedan ser disparadas fuera de los barrenos por la detonación de los adyacentes; si no se utiliza un material de retacado normal, han de asegurarse las cargas por medio de tapas especiales, tacos, etc.

Recorte para cimentaciones de edificios

Cuando se efectúan voladuras para la construcción de edificios o de otras instalaciones, es muchas veces deseable evitar desprendimientos o arranque de la roca exterior a la sección teórica. En muchos casos, las voladuras han de realizarse muy próximas a construcciones preexistentes que descansan sobre la roca (véase capítulo 13).

En tales ocasiones, es fundamental realizar el recorte de modo que los barrenos de contorno tengan *piedra* libre. Normalmente, pueden detonarse las pegas hasta una cierta distancia del contorno final, tras lo cual se inician los barrenos de recorte y los auxiliares que puedan existir, con *piedra* libre frente a ellos (Fig. 10.1.1).

Existe una forma avanzada de recorte que es denominada "línea sastre" (véase capítulo 13).

Si, en ciertos casos especialmente sensibles, puede proyectarse la voladura de modo que los fondos de los barrenos de recorte tengan *piedra* libre, el resultado del recorte quedará mejorado (véase Fig. 10.1.1).

Recorte en túneles

Para los espaciamientos y cargas de columna pueden utilizarse los valores de la Tabla.

La carga de fondo se limita normalmente a un solo cartucho, lo que significa 0,1 kg de carga en el caso de un barreno de unos 30 mm de diámetro, y 0,3 kg en el caso de un barreno de 48 mm.

La precisión de la perforación es de extrema importancia para lograr un buen resultado.

En las voladuras en túneles, debe darse a los barrenos una inclinación o margen para emboquille que abra un espacio que posibilite la perforación de la pega siguiente de modo que se mantengan las dimensiones proyectadas de la sección. La cuantía de este margen para emboquille depende del equipo de perforación empleado, pero también es función en gran medida del tipo y alineación de los barrenos. Inicialmente, las grandes perforadoras utilizadas requerían un gran espacio, pero los equipos más mecanizados de los últimos años han hecho que disminuya en magnitud esta necesidad. Ha habido discusiones sobre cómo podría definirse adecuadamente la precisión de perforación exigible para los barrenos de contorno de un túnel. A este respecto he sugerido "el menor margen para emboquille posible + 3 cm/m de barreno"; ésto significa que con un margen mínimo posible de 12 cm, el máximo valor aceptable sería de 21 cm en el caso de una pega con barrenos de 3,2 m.

Además de la perforación y carga de los barrenos de contorno, el encendido es también un factor de importancia. En túneles, frecuentemente es necesario utilizar el número alto de retardo de la pega en los barrenos de contorno, lo que implica que, si se usan detonadores de retardo (de medio segundo), hay un lapso considerable de tiempo entre la iniciación de los barrenos de recorte que resulta inconveniente. En casos especialmente sensibles, se han detonado los barrenos del recorte por separado, después de la pega principal, haciendo así posible el empleo de detonadores de microrretardo. En este terreno se están haciendo avances en Suecia utilizando detonadores con retardos de aproximadamente 100 ms, que están resultando muy apropiados para el trabajo subterráneo.

El método de voladura de la totalidad de la pega del túnel también es importante desde el punto de vista de los resultados del recorte. Las grandes cargas con iniciación instantánea dejan sentir mucho sus efectos sobre su entorno, abriendo grietas y diaclasas preexistentes. La carga de los barrenos de franqueo inmediatos a los de contorno ha de hacerse con especial cuidado para no comprometer el resultado del recorte; una carga de fondo demasiado potente ejerce su efecto mucho más allá del contorno final. Esto es especialmente aplicable a los barrenos de gran diámetro.

Un medio de definir el cuidado con que se realiza un recorte consiste en determinar las vibraciones del terreno a una cierta distancia del contorno del túnel; la extensión del agrietamiento de la roca alrededor del contorno es proporcional a la frecuencia de estas vibraciones (véase sección 13.1).

Recorte en cámaras subterráneas

Las estructuras del tipo de cámaras o naves subterráneas pueden ser de una gran variedad (véase sección 11.1). Normalmente, las cámaras subterráneas poseen extensiones de techo libre más grandes que los túneles ordinarios, por lo que es frecuente que las demandas de recorte y de refuerzo de la roca sean mayores que en ellos. Al proyectar cámaras subterráneas, sin embargo, existe la posibilidad de escoger un área de roca adecuada, lo que en cambio puede ser difícil de conseguir en el caso de un túnel, estructura larga y estrecha, sin que alguno de sus tramos haya de cruzar roca de mala calidad. Los trabajos de construcción de cámaras subterráneas consisten muchas veces en una combinación de voladuras en banco y voladuras en túnel.

Pueden aplicarse las recomendaciones hechas para el recorte en túneles y excavaciones en trinchera. En los últimos años se ha convertido en algo cada vez más frecuente en las cámaras subterráneas que se opere en bancos con barrenos horizontales. Esto implica que los barrenos del recorte son asimismo horizontales, pero ello no tiene por que ser un inconveniente si se adoptan unos valores adecuados para el espaciamiento y la concentración de carga.

Más aún que en el caso de los túneles, es preciso tener presente en las voladuras en cámaras subterráneas que las grandes cargas con iniciación instantánea pueden comprometer el resultado de un recorte. Por otro lado, el empleo de bancos altos y de barrenos de gran diámetro puede hacer aumentar de tal modo la necesidad de reforzar la roca, que el aspecto financiero global se resienta notablemente.

También en este caso puede estimarse el cuidado con que se ha realizado una voladura por las vibraciones del terreno. En el caso de las minas, situadas a mayores profundidades, lo que implica presiones más elevadas en la

roca y mayores demandas de refuerzo, se ha consagrado ultimamente una mayor atención al estudio de los problemas relacionados con los efectos de las voladuras sobre su entorno rocoso.

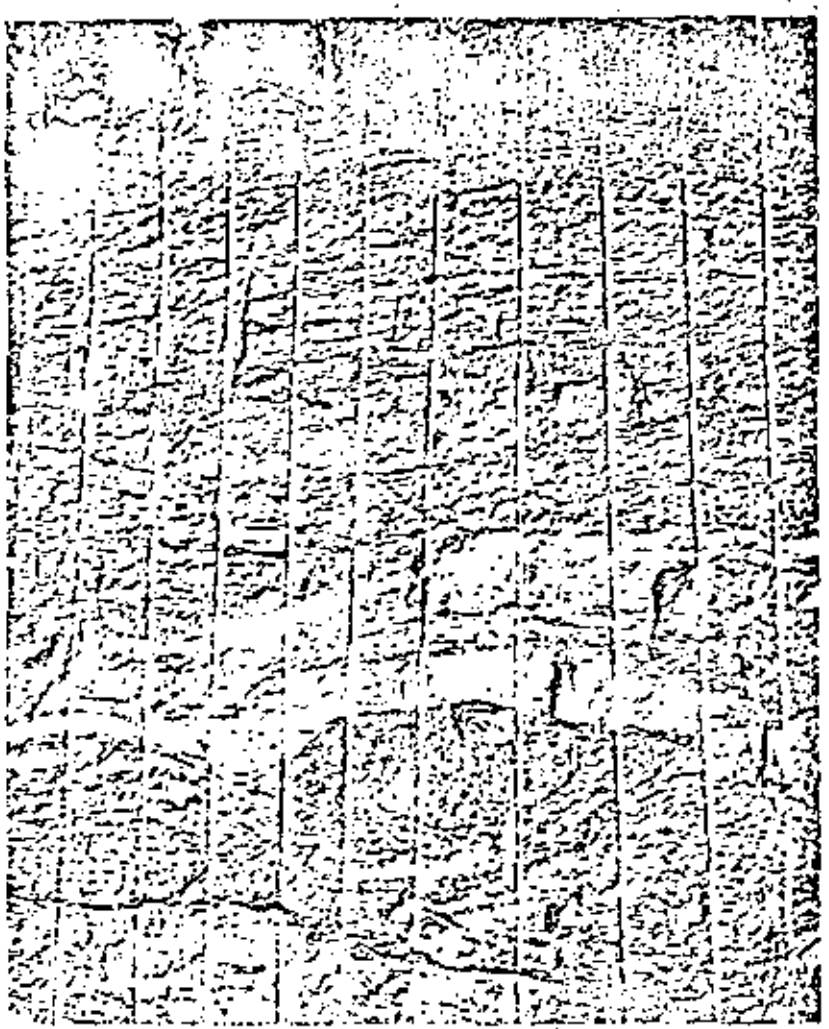

Fig. 10.1.3 Precorte de un desmonte para una carretera en un área edificada (Karlshamn, Suecia). Jefatura de Carreteras, Distrito Sur. Foto: Gerhard Broman.

10.2 PRECORTE.

El objetivo del precorte es conseguir las mismas ventajas que con el recorte, pero, a diferencia de éste, en el precorte se hacen detonar primero los barrenos del contorno, antes de encender la pega propiamente dicha. El precorte produce una grieta entre los barrenos de contorno; en la subsiguiente voladura en banco, la roca se desprende a lo largo de esta grieta. Como los barrenos están muy próximos entre sí, las grietas se forman siguiendo las hileras de barrenos, y los mismos barrenos constituyen el inicio del agrietamiento. Esto significa que la inclusión de barrenos vacíos entre los cargados, puede hacer mejorar los resultados cuando sea preciso (Fig. 10.2.1).

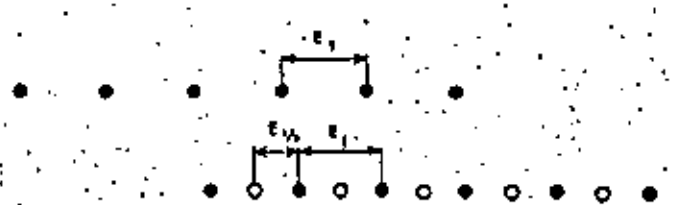

Fig. 10.2.1

Es extremadamente importante en el precorte emplear los espaciamientos y cargas correctas para el tipo de roca de que se trate. Las características de la roca tienen una mayor influencia sobre los resultados que en la mayoría de los demás métodos de voladura.

La orientación de los estratos puede implicar que la roca se hienda fácilmente según la estratificación, pero perpendicularmente a esta dirección, los barrenos habrán de estar considerablemente más juntos para la misma carga. Es ésta una situación normal en canteras en las que se arrancan grandes bloques de piedra. A pesar de la homogeneidad de la roca, el material puede comportarse de modo completamente diferente cuando ha de fisurarse en distintas direcciones. En un precorte puede apreciarse que, en los barrenos más exteriores, las grietas se desvían de la dirección señalada por los barrenos para seguir la dirección natural de fisuras de la roca; si se perforan los barrenos lo suficientemente próximos entre sí, esta tendencia puede ser contrarrestada y forzar la formación de grietas según las líneas de barrenos.

También para el precorte resulta ser la Gurit un excelente explosivo.

En la Tabla siguiente se indican los valores aproximados para perforación y carga:

Diámetro barrenos mm	Concentración de carga kg.m Dyn.	Unidades de carga	Espaciamiento E_1 m
25—32	0,08	Gurit de 11 mm	0,20—0,30
25—32	0,18	Gurit de 17 mm	0,35—0,60
40	0,18	Gurit de 17 mm	0,35—0,50
51	0,36 medio barreno	2 Gurit de 17 mm	0,40—0,50
	0,18 medio barreno	Gurit de 17 mm	
64	0,38	Nabit de 22 mm	0,60—0,80

Los barrenos se cargan aproximadamente hasta un 75 % de su profundidad total. En roca muy fisurada, puede reducirse la carga hasta el 55 %. Si en el curso de la perforación se descubre una diaclasa claramente marcada, puede resultar ventajoso alojar la carga más allá de la diaclasa.

El único material de retacado empleado consiste en los tapones para evitar el lanzamiento al exterior de las cargas alargadas de Gurit, dispositivos que pueden ser necesarios en el caso de iniciación con microrretardos.

La precisión de la perforación es de gran importancia para el resultado del precorte. El encendido puede tener también una gran influencia.

Si no hay impedimentos que no permitan vibraciones del terreno, se utiliza el encendido instantáneo. Los ensayos realizados con cordón detonante han demostrado un aumento del efecto de precorte de las cargas, lo que ha hecho posible el uso de espaciamientos más grandes.

Si ha de tenerse cuidado con las vibraciones del terreno, se hace preciso el encendido con microrretardos. La formación de grietas es algo más deficiente que en el caso de iniciación instantánea, a menos que se reduzca el espaciamiento de los barrenos. Si se usan detonadores de microrretardo, deben ser de un tipo que tenga tiempos de retardo y de ignición mínimos; si el tiempo de retardo es excesivamente grande, no se consigue ningún precorte.

La iniciación con microrretardos puede hacerse de diversas formas. Con base a la carga admitida para el caso de detonación instantánea, se elegirá un margen de números de retardo tal que la carga por retardo no sea demasiado grande (Fig. 10.2.2). También puede hacerse la subdivisión de la carga

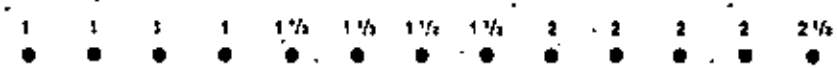

Fig. 10.2.2

total mediante una combinación de encendido con microrretardos y con cordón detonante (Fig. 10.2.3). Se conectan entre sí los barrenos con cordón detonante formando varios grupos, los cuales son iniciados mediante detonadores de microrretardo con números sucesivos. La carga por grupo ha de adaptarse

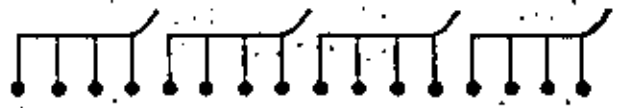

Fig. 10.2.3

a las vibraciones del terreno permisibles, pues detona instantáneamente. Mediante el uso de cargas instantáneas distribuidas en grupos y gracias a la acción del cordón detonante, este procedimiento da generalmente buenos resultados. Las cargas son iniciadas en este caso desde arriba.

El explosivo de Gurit se conecta al cordón detonante en toda su longitud, para asegurar un buen encendido. En el caso de iniciación eléctrica instantánea, los detonadores se sitúan generalmente en el fondo del barreno. En el precorte se utiliza una cierta carga de fondo que influye también sobre los resultados obtenidos. Si el precorte se realiza en varios bancos dentro del mismo contorno de roca, debe evitarse el empleo de cargas de fondo potentes.

Los valores aproximados que se dan a continuación son los utilizables como cargas de fondo en el precorte:

Profundidad del barreno m	Carga de fondo kg
menos de 2,0	0,05
2,0— 4,0	0,10
4,0— 6,0	0,20
6,0—10,0	0,30

Antes de hacer las perforaciones de precorte para una longitud grande, puede ser conveniente realizar una voladura de muestra a lo largo de una distancia más corta y normalmente es posible examinar el resultado del precorte después de la voladura. Al evaluar el resultado de la carga de prueba, recuérdese que la fisura es más marcada cuando la voladura abarca una longitud grande que en el caso de una distancia más corta. Esto significa que la voladura de muestra debe cubrir una longitud de unos 5 metros; si el agrietamiento resulta demasiado pobre, normalmente queda la posibilidad de cargar de nuevo los barrenos.

Precorte en excavaciones en trinchera

En muchas excavaciones en trinchera para carreteras puede verse, por toda Suecia, el resultado de un precorte logrado (véase Fig. 10.2.5). Normalmente, lo más ventajoso es realizar el precorte de los barrenos del contorno

antes de la perforación y disparo de la pega. El precorte de los barrenos de contorno al mismo tiempo que el resto de la pega, puede dar resultados más deficientes. En ciertos casos, con excavaciones profundas inclinadas hacia los lados, puede ser necesario operar de este modo para evitar complicaciones en la perforación y voladura.

El precorte puede despizarar capas superficiales de la roca suelta, y ésta es la razón por la que no es recomendable perforar los barrenos de la pega antes de llevar a cabo el precorte.

Los barrenos de la pega inmediatos a la línea de precorte poseen espaciamientos iguales a la mitad de los empleados en el interior de la pega; ésta es una regla sencilla adecuada para barrenos de diferentes diámetros. Por lo que respecta al encendido de la pega principal, puede ser conveniente que los barrenos de precorte lleven una pequeña carga de fondo para facilitar el desprendimiento de la roca en la zona de fondo.

Precorte en cimentaciones de edificios y otras instalaciones

El precorte no se ha utilizado mucho en la proximidad de edificaciones. Aun cuando haya sido posible controlar las vibraciones del terreno, la onda de choque y el peligro de proyecciones han actuado como influencia disuasorias (véase capítulo 8). Sin embargo, es posible utilizar un material de protección. Cuando se hagan demandas especiales sobre los contornos, puede mejorarse el resultado del precorte utilizando barrenos-guía descargados entre los barrenos con carga. Normalmente no es preciso perforar los barrenos descargados en toda su profundidad; con frecuencia es suficiente con pasar más allá de la zona superficial que contiene las fallas o diaclasas.

Cuando se realizan voladuras para instalaciones y se desea seguir el contorno teórico proyectado, el precorte controlado proporciona la posibilidad de conseguir un ventajoso resultado.

Precorte subterráneo

El precorte ha tenido una menor utilización subterránea; no obstante, se han obtenido buenos resultados en pozos verticales.

Se ha demostrado que es muy posible realizar el precorte del contorno de un túnel. En los túneles se emplea un método de voladura diferente del normal, con objeto de evitar que el trabajo de perforación aumente excesivamente. Las voladuras de ensayo con barrenos provistos de cargas potentes, en una pega con capacidad para arrancar la roca a lo largo de la cara de precorte, han demostrado ser una posible dirección de desarrollo del método. Ensayos realizados con precorte en minas a profundidades considerables han hecho surgir la teoría de que los empujes de la roca prohiben la utilización del precorte, opinión que no comparto.

Precorte en zanjas y en pozos

Puede utilizarse el precorte en voladuras para excavación de zanjas y obras similares en que se desee reducir la cantidad de roca excavada en exceso sobre la sección teórica. Con distancias tan cortas entre los lados del barreno ha parecido conveniente que en estos casos se precorte un lado de cada vez. Esta norma sería aplicable hasta una distancia de unos 5 m en roca moderadamente fisurada. En el caso de una profundidad de barreno inferior a 1,5 m, puede ser necesario reducir los espaciamientos indicados en la Tabla incluida más arriba.

En la excavación mediante explosivos de pozos de pequeña sección, el precorte es un posible método a considerar (Fig. 10.2.4). Se precortan los lados del pozo uno tras otro, y luego se vuela la zona central. Si los lados de la sección del pozo son de 1 metro como mínimo, puede utilizarse un cuele en abanico para esta voladura. En caso de una sección menor, ha de usarse un cuele paralelo con un barreno central de gran diámetro para la voladura del núcleo (véase sección 9.2). El procedimiento descrito para la voladura de pozos requiere una gran cantidad de material de protección.

Pozo para un pilar de 1,0—1,5 m de profundidad

Los lados se precortan uno de cada vez Los taladros son usados nuevamente para la voladura

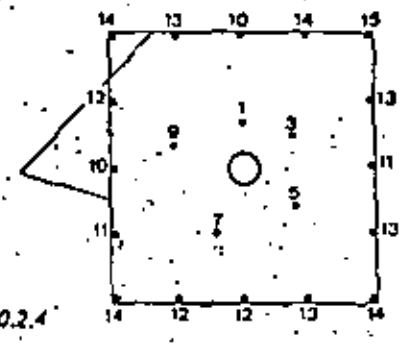

Fig. 10.2.4

Si se ha de realizar un precorte a lo largo de un contorno circular, el espaciamiento dado en la Tabla ha de ser disminuido.

A modo de conclusión puede afirmarse que los campos de aplicación del precorte son muchos, y que, aun en el caso de roca de relativa mala calidad, su resultado es generalmente un contorno final considerablemente mejor que con las voladuras ordinarias.

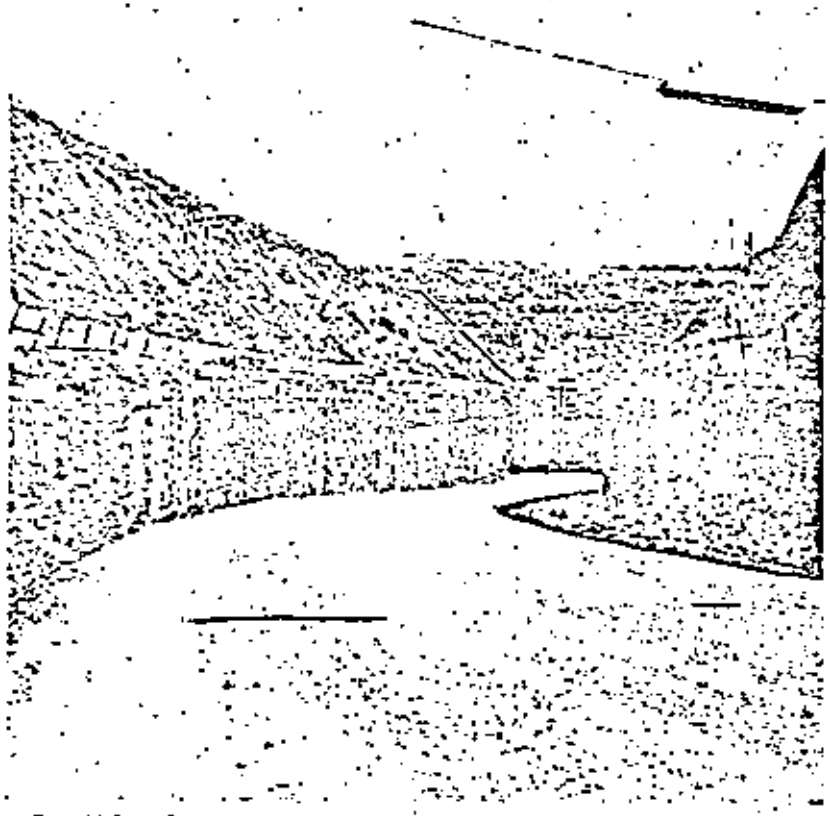

Fig. 10.2.5 Precorte de excavaciones en trinchera para una carretera Jefatura de Carreteras, Distrito Sur. Foto: Atelje Floberg, Karlskrona.

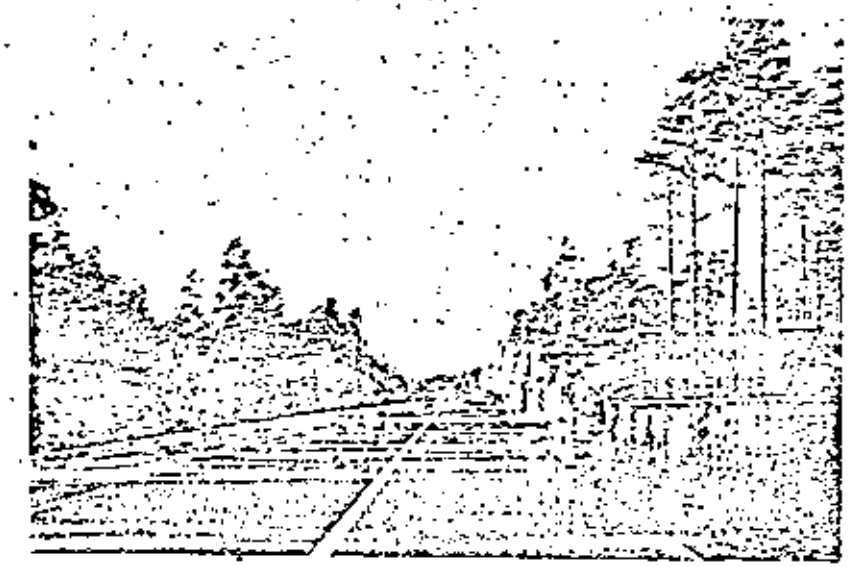

Fig. 10.2.6 Precorte de una excavación en trinchera. Consultor de voladuras: Nitro Nobel Service Department.

10.3 RECORTE ESPECIAL

En esta sección se describen unos métodos especiales de recorte de los que no poseo personalmente experiencia práctica. Se los ha usado principalmente en los Estados Unidos, y se los incluye asimismo en proyectos internacionales en los que están implicados consultores norteamericanos. Las fotografías de este tipo de voladuras muestran unos resultados excelentes. Los métodos que se describen aquí son:

Perforación de límite.
Voladura amortiguada.

El método de perforación de límite recuerda algo a las hileras de barrenos muy juntos utilizados en voladuras controladas próximas a edificaciones. Los barrenos se dejan en este método sin cargar, y actúan como señaladores de la dirección de la grieta a lo largo de la cual se desprende la roca cuando se hacen detonar los barrenos de la pega. El efecto es probablemente superior en roca de baja resistencia que en las rocas de Suecia.

Los barrenos utilizados en el contorno son generalmente bastante anchos: 50—75 mm de diámetro. El espaciamiento entre ellos se ha fijado en 2—4 veces el diámetro, es decir, entre 10 y 30 cm. Los barrenos con carga se sitúan a una distancia igual a la mitad del espaciamiento de los barrenos de la pega, como en el caso del precorte. Las cargas de los barrenos más próximos de la pega han de reducirse, para no dañar el contorno final. En casos en los que la roca no es apropiada para la aplicación de este método, a veces se han detonado unas cargas ligeras antes de la pega, es decir, en la misma forma de un precorte; el inconveniente consiste, evidentemente, en el coste de perforación.

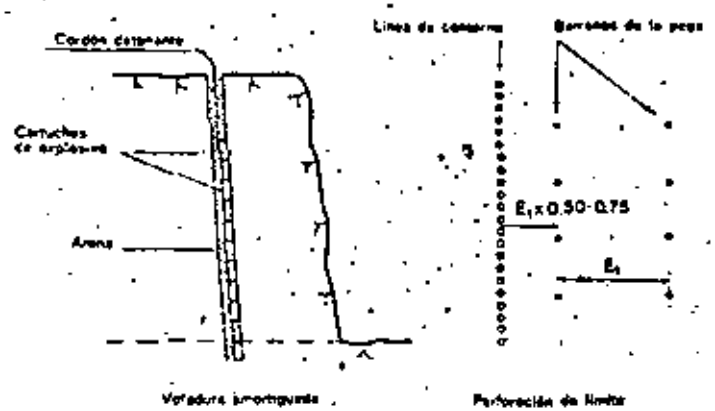

Fig. 10.3.1

Parece probable, que una combinación de perforación de límite con el precorte podría ser un buen método a aplicar en los casos en que se desea obtener superficies extremadamente lisas. El precorte a que me refiero en este caso es con barrenos auxiliares sin carga entre los barrenos cargados.

La voladura amortiguada es una forma de recorte utilizable en casos en que los barrenos del contorno tienen rotura libre; los barrenos se cargan con cartuchos de explosivo conectados a cordón detonante, y a continuación se rellenan enteramente con arena. Debe hacerse lo posible por que el lapso de encendido entre los barrenos sea el mínimo. Como en el recorte normal, se requiere una cierta carga de fondo para esta zona.

Cuando se están haciendo voladuras según líneas curvas, puede resultar adecuada una combinación de voladura amortiguada con la perforación de límite.

El Manual de Voladuras cita los siguientes valores aproximados para este método de recorte:

Diámetro barrenos mm	Espaciamiento m	Zona de retacado m	Concentración de carga kg m
50—64	0,90	1,20	0,12—0,40
75—88	1,20	1,50	0,20—0,80
100—112	1,50	1,80	0,40—1,20
125—138	1,80	2,10	1,20—1,50
150—165	2,10	2,70	1,50—2,20

El método puede resultar de interés cuando se realiza un recorte con barrenos de gran diámetro. Parece que, en lo que respecta a concentraciones de carga, los valores más a la derecha de la Tabla, los más altos, son los más apropiados para los tipos de roca que se encuentran en Suecia.

Los dos métodos especiales de recorte que se han descrito pueden servir para impulsar a los técnicos de voladuras a efectuar ensayos prácticos y adaptar diversos métodos a las formas más adecuadas para los tipos de roca implicados en cada caso.

11. VOLADURAS EN CAMARAS SUBTERRANEAS

11.1 ALMACENAMIENTO SUBTERRANEO

En el curso de los últimos años se ha registrado un considerable incremento en el uso de naves y cámaras subterráneas con fines de almacenamiento. Los refugios contra bombardeos aéreos, e instalaciones similares, están emplazados generalmente en roca firme por razones evidentes. La lista siguiente muestra algunas de las variedades de utilización de las cámaras subterráneas excavadas en roca:

Almacenamiento de petróleo
Cámaras frigoríficas
Refugio aéreo
Instalaciones militares
Instalaciones de depuración de aguas residuales
Almacenes para diversos productos.
Garajes y estacionamientos subterráneos.

Puede pensarse en un mayor y significativo incremento en el uso de cámaras subterráneas; las intensas discusiones sobre el medio ambiente de los últimos años han proporcionado impulsos que apuntan en esta dirección. Es posible que además del almacenamiento de elementos contaminantes, y de productos contaminados para un posterior tratamiento, incluso industrias agresivas para el medio ambiente pueden ser emplazadas bajo tierra.

Estudios realizados en Norteamérica han puesto de manifiesto la posibilidad de reutilización de la mayoría de los productos contaminados, combinando así el cuidado del medio ambiente con el rendimiento productivo. Podemos, por tanto, esperar que masas de roca no utilizadas hasta el presente brinden unas posibilidades ilimitadas para productos muy importantes.

Desde el punto de vista de la tecnología de las voladuras, existe la posibilidad de dar a la cámara subterránea la forma adecuada para el volumen deseado. Hay ciertos factores que afectan de modo importante al proyecto, como son:

La profundidad de la cámara bajo la superficie — Los accesos.
La amplitud de la cámara — La resistencia de la roca.

Si la profundidad a que está situada la cámara es excesiva, el acceso a la misma se hace más difícil durante las operaciones de voladura, y también más tarde cuando esté en servicio. Pero, por otra parte, no es conveniente por razones técnicas situar la cámara a una profundidad demasiado pequeña, pues generalmente la roca alcanza su menor resistencia cerca de la superficie.

No puede darse a las cámaras subterráneas una anchura excesiva, pues la roca no tendría capacidad para sostener el techo con ayuda de su sola resistencia. En una cámara subterránea en condiciones normales, y a diferencia de lo que ocurre en minería, no existen problemas de empujes o tensiones de la roca. En roca de buena calidad, normalmente es posible una luz de unos 20 metros.

La situación de las cámaras subterráneas con relación a las condiciones geológicas de la roca es naturalmente un factor de importancia vital. En obras de gran envergadura se realizan primero reconocimientos y estudios geológicos completos que proporcionan la base para determinar el emplazamiento de las cámaras subterráneas y también, en muchos casos, su diseño. En los últimos años se han perfeccionado los métodos empleados para la inspección del medio rocoso, pero un estudio preliminar aun más detallado, con la cooperación de geólogos y técnicos de voladuras, puede proporcionar una mejor base para las decisiones concernientes al método de voladura a utilizar.

Los métodos de reconocimiento de la roca han de ser desarrollados para llegar a estimaciones más cuantificadas aun cuando haya de incluirse en ellas un margen de seguridad. La clasificación de la roca en varias denominaciones

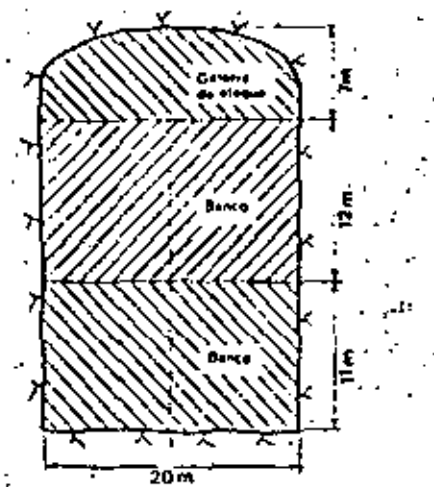

Fig. 11.1.1 Método de galería de ataque superior y bancos

Altura del banco m	Profdad. barrenos m	Piedra m	Espaciamiento m	Carga de fondo kg	Carga de columna kg	kg/m	Carga específica kg m³
12	13,3	1,85	2,20	7,8	11,9	1,25	0,45

La carga específica de 0,45 kg/m³ puede aumentarse hasta 0,62 kg/m³ en caso necesario, haciendo que la carga de columna llegue a 2,0 kg/m.

Si se han de detonar pegas de más de cinco filleras, la carga de columna puede incrementarse de forma gradual a partir de la sexta fillera. La zona de retacado no tiene que ser de longitud superior a unos 0,8 m, excepto si hay peligro de daños por proyecciones dentro del área de la obra.

Zona de recorte

Con barrenos de 51 mm, el Nabit de 22 mm puede ser adecuado como carga de columna.

El espaciamiento puede obtenerse de la Tabla de recorte (sección 10.1).

Altura del banco m	Profdad. barrenos m	Piedra m	Espaciamiento m	Carga de fondo kg	Carga de columna kg	Composición
12,0	12,8	1,00 *)	0,80	1,00	4,70	Nabit 22 mm

(*) Teoricamente la piedra es de 1,2 m en el ejemplo, pero hay también una cierta sobreexcavación en las pegas. La carga de fondo se calcula con 0,50 como *piedra* y error de perforación.
0,05 + 0,03 × 12,8 = 0,40 aproximadamente.

Para los barrenos de gran longitud que se utilizan en este caso, lo más seguro es utilizar mecha detonante para iniciar las cargas alargadas de Nabit, pues la carga del contorno está sometida a la influencia de los barrenos de la pega más próximos.

En las pegas de barrenos horizontales, el recorte se realiza también con perforación horizontal como en el caso de las voladuras ordinarias en túneles.

La magnitud del margen para emboquille en la perforación posee un efecto significativo sobre los resultados del recorte.

Método de voladura por separado de la zona central

El método de la zona central (Fig. 11.1.3) es el otro procedimiento utilizado en las voladuras de excavación de cámaras subterráneas.

Primeramente se abren una galería de ataque superior (por corona) y otra inferior (por solera), y a continuación se procede a la voladura de la zona

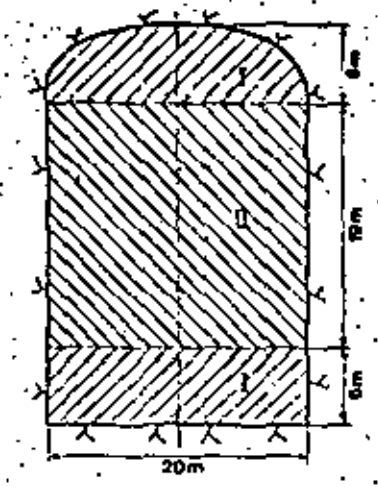

Fig. 11.1.3 Voladura por separado de la zona central

central de roca restante. Este método requiere un mayor trabajo en túnel pero, por otra parte, la zona central es más fácil de volar al no estar constreñida. Un inconveniente del método es la dificultad de acceso para los trabajos de saneo y refuerzo, necesitándose galerías destinadas a este fin en la zona del techo y en la del piso.

Las galerías de ataque superior e inferior se abren mediante los métodos normales de voladura en túneles (ver capítulo 9).

Voladura de la zona central

Como los barrenos no tienen confinamiento por la parte inferior, la carga puede ser distribuida regularmente en toda su longitud. El menor gredo de confinamiento implica que la carga puede ser disminuida hasta unos 0,30 kg/m³.

Ejemplo. Ha de volarse una zona central de una sección, con recorte de las paredes laterales. Las dimensiones de dicha zona son de 19,0 m de altura y 20 m de anchura. Se utilizarán barrenos de 51 mm.

Las cargas se calculan sobre la base de la concentración utilizada en kg/m, así como del valor 0,30 kg/m³.

Carga kg/m	Composición	Area/barreno m²	Piedra m	Espaciamiento m
2,6 *)	Dynamex	8,7	2,65	3,30
1,6	Dyn. 40 mm	5,3	2,05	2,55
2,1	Prillit			
1,8 **)	Prillit	6,0	2,20	2,75

(*) Utilizando cargadora neumática.

(**) Nuevo cálculo referido a la potencia con Dynamex.

La perforación debe llegar hasta una distancia de 0,5 m del techo de la galería inferior. Si algún barreno se abre camino hasta el espacio ya libre,

En la Fig 11.1.4 se indican otros métodos de voladura.

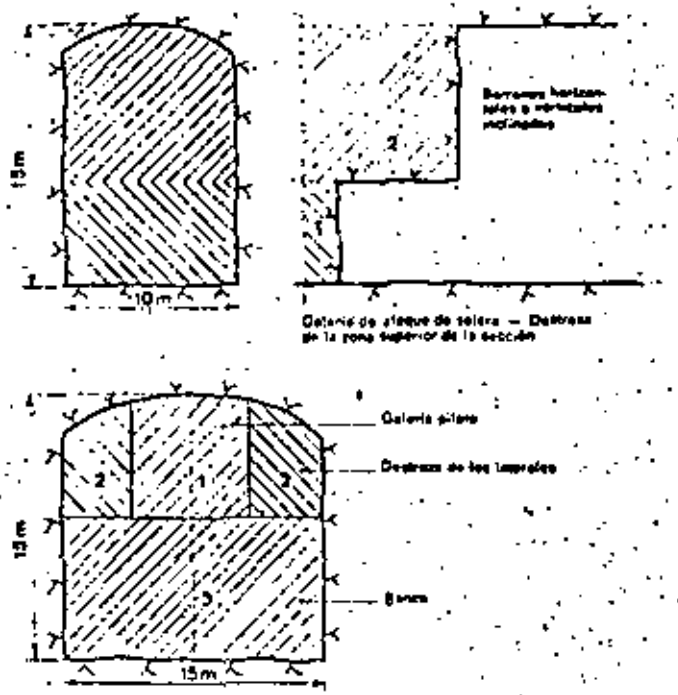

Fig. 11.1.4

ha de ser taponado de algún modo. Cuando se utiliza Prillit, puede ser conveniente asegurar el drenaje de los barrenos. En barrenos profundos lo más seguro es utilizar dos detonadores en cada uno. El recorte se realiza con la misma distribución de barrenos que en el ejemplo precedente. La carga de fondo se reduzca a 0,2 kg de Dynamex en función de cebo.

Además de los dos métodos de voladura descritos, existen muchas posibilidades de combinación a partir de ellos. En el caso de roca de mala calidad, puede resultar difícil hacer uso de grandes superficies libres de roca sin efectuar un refuerzo o sostenimiento de las mismas por fases. Los modernos métodos permiten, no obstante, el empleo de grandes luces si se limita el avance por pega.

Como la técnica minera es muy importante en las voladuras en cámaras subterráneas, los conocimientos sobre los efectos de las mismas en la roca circundante son sumamente significativos; ésto es aplicable no sólo a la voladura de los barrenos del contorno final, sino a la planificación de todo el conjunto. Si la carga de los barrenos de la pega es tal que origina fisuras más allá del contorno final, el empleo del recorte por sí solo no sirve de ayuda.

Se ha señalado ya anteriormente que el grado de cuidado puesto en las voladuras en cámaras subterráneas puede ser medido a través de la magnitud de las vibraciones del terreno a una cierta distancia del contorno de la excavación. Nuestras propias investigaciones, así como las llevadas a cabo en otros países, han demostrado que la extensión de la zona fisurada es proporcional a la velocidad de las vibraciones del terreno.

Lo importante a estos efectos es reducir lo más posible las cargas de acción coordinada (véase la sección 13.1).

Si se hace la hipótesis de que la formación de grietas se produce a una velocidad de vibración de $v = 300$ mm/seg., lo que ha resultado concordar con la realidad, puede calcularse la amplitud de la zona agrietada para diversas magnitudes de carga. El valor de 300 mm/seg. incluye las zonas de debilidad e inicios de grietas existentes normalmente en la roca; si la roca fuera enteramente homogénea, podría usarse un valor considerablemente más alto.

Influencia de los barrenos de recorte sobre la zona fisurada

Las bajas concentraciones de carga empleadas y la proximidad del contorno significan que no puede calcularse la totalidad de la carga del barreno como carga coordinada. A efectos comparativos, se han hecho asimismo cálculos para barrenos de gran diámetro con altas concentraciones de carga.

La concentración de carga en kg/m sirve como el indicador más correcto en el cálculo de las cargas en los recortes:

Composición de la carga	Concentración de carga kg/m	Profundidad zona agrietada, en m
Gurit de 11 mm	0,08	0,24
Gurit de 17 mm	0,18	0,42
Nabit de 22 mm	0,38	1,5
Barrenos de 40 mm enteramente cargados	1,00	2,0
Barrenos de 51 mm enteramente cargados	2,60	2,8
Barrenos de 75 mm enteramente cargados	5,60	4,6

En una roca completamente homogénea, puede esperarse que no se produzca prácticamente ningún agrietamiento más allá del contorno final si se utilizan cargas alargadas de Gurit.

En resumen: Los cálculos efectuados y descritos demuestran que el recorte origina una formación limitada de grietas más allá del contorno final. Asimismo ponen de manifiesto que unas cargas potentes en los barrenos de una pega pueden afectar a la roca del interior del contorno; ésto no debe ser interpretado en el sentido de que el recorte es por ello superfluo. La formación de grietas en este caso se refiere a fisuras finas en la proximidad de las cargas concentradas, donde la roca está con frecuencia completamente confinada.

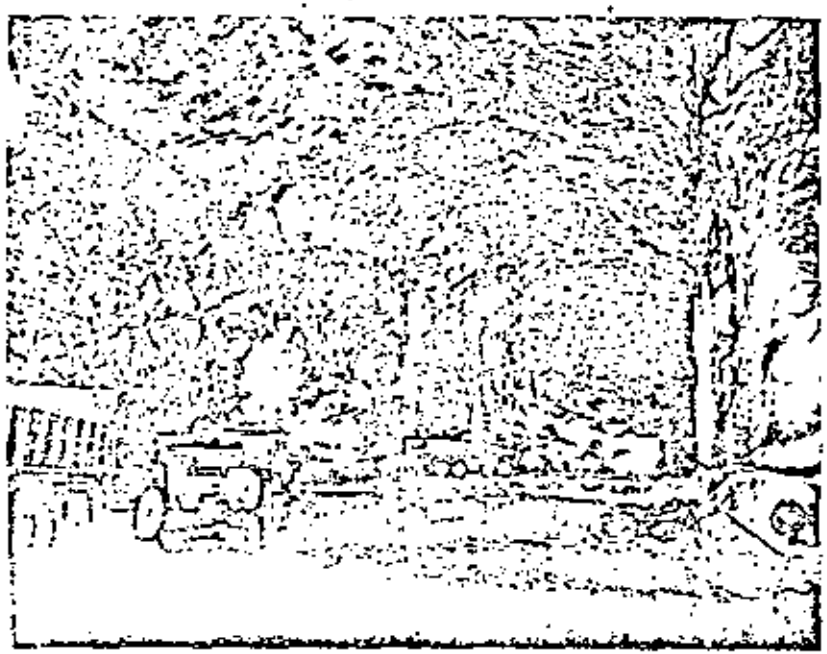

A distancias mayores del contorno final puede esperarse en la práctica que la influencia de unas concentraciones de carga más potentes incluso, disminuya con la distancia de un modo relativamente rápido.

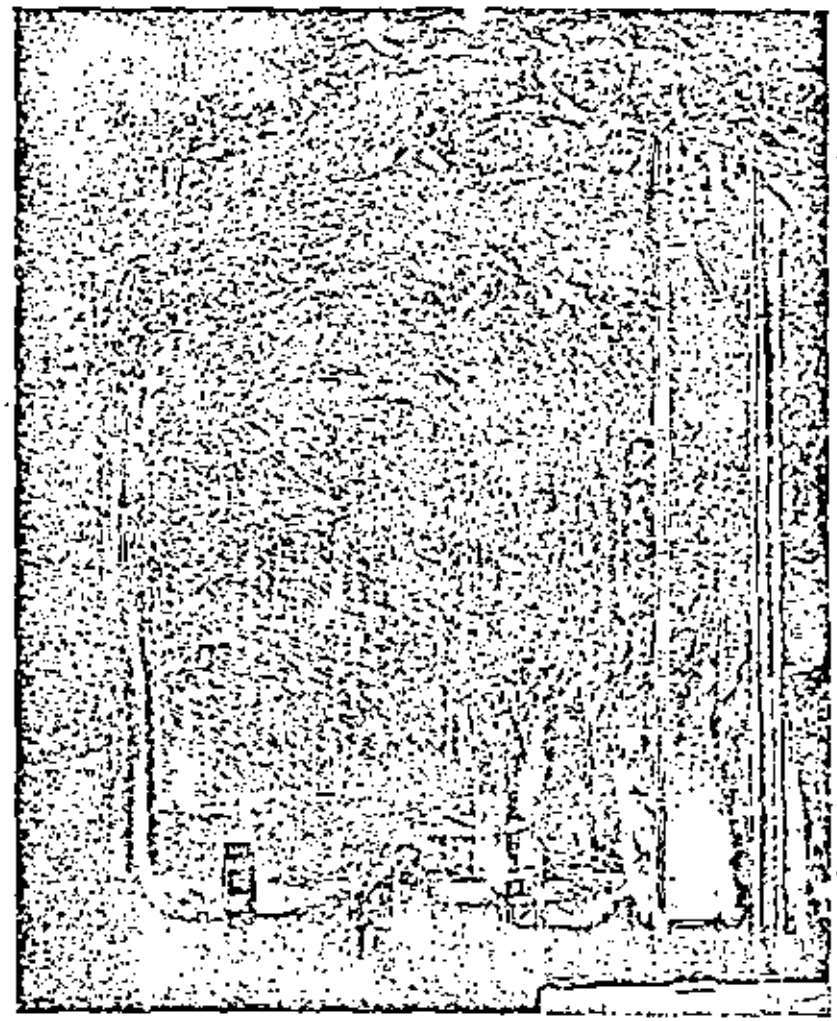

Figs. 11.1.5 y 11.1.6 Cámara subterránea para almacenamiento de petróleo. Lugar: Värtaverket, Estocolmo. Contratista: AB Skånska Cementgjuteriet. Foto: Gösta Nordin.

11.2 VOLADURAS MINERAS, CAMARAS CON BANQUEO DESDE NIVELES. EJEMPLOS DE VOLADURAS MINERAS

El método de cámaras con banqueo desde niveles es un método de explotación que se utiliza en minas en las que el mineral y las rocas que lo rodean poseen unas buenas características resistentes. El mineral se encuentra normalmente formado un ángulo acusado de inclinación con la horizontal, con contornos limitae verticales o subverticales separándolo de la roca estéril.

Después de extraído el mineral, es frecuente que los huecos dejados formen cámaras subterráneas.

La perforación se realiza corrientemente desde galerías de preparación en la forma de cueles en abanico con perforación hacia arriba, hacia abajo, o en ambos sentidos. Generalmente es conveniente evitar la carestía que supone una longitud excesiva de galerías, por lo que los barrenos pueden ser relativamente largos.

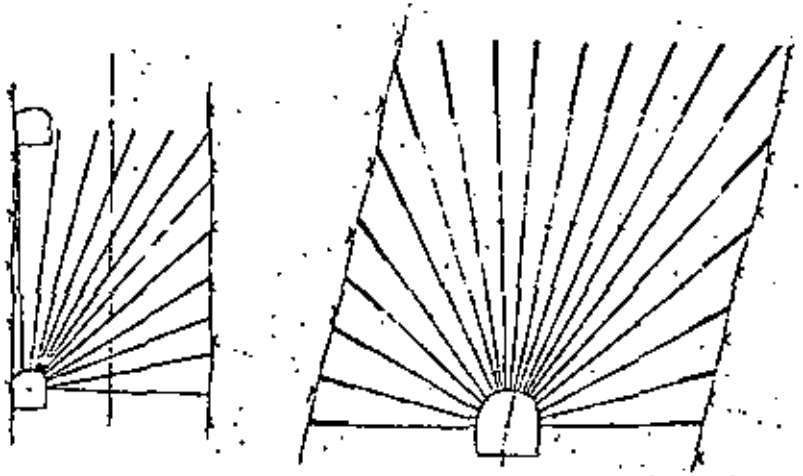

Fig. 11.2.1

El emboquille y orientación correctos de los barrenos es de la mayor importancia para el resultado de la voladura, sobre todo para la fragmentación obtenida. Como elementos auxiliares a este respecto cabe citar los niveles de burbuja, transportadores de ángulos, etc.

Al efectuar las voladuras, las hileras de barrenos tienen generalmente rotura libre, pues los ciclos de voladura se adaptan a los trabajos de desescombro llevados a cabo más abajo. La roca arrancada es recogida en depósitos situados a un nivel inferior y en donde se efectúa el desescombro. Este puede hacerse mediante dragalina directamente desde los depósitos, pero también es posible un desescombro mecánico desde galerías laterales.

La fragmentación tiene una gran importancia en estos casos, pues el empleo posterior de cargas conformadas para el taqueo de los bloques grandes implica interrupciones de todo el ciclo de producción, sin contar la influencia del grado de fragmentación sobre las operaciones de desescombro. Si se quiere que la explotación por cámaras con pegas en abanico sea lo más eficaz posible, la estimación del grado de fragmentación y la adaptación de la voladura a este objetivo constituyen factores de gran importancia. En principio, puede hacerse uso del mismo modelo que se describió en la sección 5.8, "Estudio económico de las voladuras".

Las condiciones específicas propias de cada mina en particular implican que toda generalización a este respecto ha de hacerse con las debidas precauciones.

La perforación de cueles en abanico se ha desarrollado como consecuencia del deseo de limitar la magnitud de las labores de preparación. Desde el punto de vista de la técnica de voladuras, los cueles en abanico no resultan tan acertados, pues la distancia entre los barrenos se va haciendo progresivamente mayor, y la mitad inferior de los mismos no puede ser aprovechada de forma adecuada. Los barrenos paralelos ofrecen una mejor posibilidad de lograr mayor precisión y carga, con una fragmentación más provechosa y resultados globales superiores (véase sección 11.1).

Con los avances habidos en los últimos años en el campo de las voladuras de galerías, puede resultar ventajoso, en el caso de filones de mineral estrechos, considerar la posibilidad de realizar la voladura del filón en toda su anchura mediante barrenos paralelos.

Cálculo de cargas

El método de cámaras con pegas en abanico (subniveles con perforación ascendente) puede muy bien compararse, desde el punto de vista de la técnica de voladuras, a las voladuras en banco sobre la superficie. La voladura comprende generalmente un número limitado de hileras de barrenos, y las dimensiones geométricas de la pega y sus condiciones de confinamiento limitado implican normalmente que este método de explotación no sea difícil de llevar a la práctica. Puede considerarse generalmente que una carga específica de 0,40 kg/m³ es suficiente. Si se establece la comparación con la voladura de la zona central en una cámara subterránea, resulta que ésta última precisa solamente 0,30 kg/m³; pero es preciso tener en cuenta que su grado de constricción es menor y el emplazamiento de los barrenos más ventajoso.

11.2 VOLADURAS MINERAS, CAMARAS CON BANQUEO DESDE NIVELES. EJEMPLOS DE VOLADURAS MINERAS

El método de cámaras con banqueo desde niveles es un método de explotación que se utiliza en minas en las que el mineral y las rocas que lo rodean poseen unas buenas características resistentes. El mineral se encuentra normalmente formado un ángulo acusado de inclinación con la horizontal, con contornos limitae verticales o subverticales separándolo de la roca estéril.

Después de extraído el mineral, es frecuente que los huecos dejados formen cámaras subterráneas.

La perforación se realiza corrientemente desde galerías de preparación en la forma de cueles en abanico con perforación hacia arriba, hacia abajo, o en ambos sentidos. Generalmente es conveniente evitar la carestía que supone una longitud excesiva de galerías, por lo que los barrenos pueden ser relativamente largos.

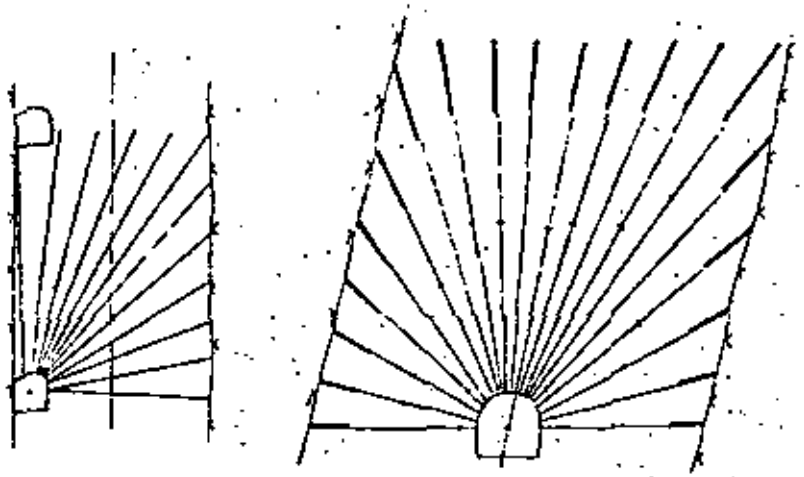

Fig. 11.2.1

El emboquille y orientación correctos de los barrenos es de la mayor importancia para el resultado de la voladura, sobre todo para la fragmentación obtenida. Como elementos auxiliares a este respecto cabe citar los niveles de burbuja, transportadores de ángulos, etc.

Al efectuar las voladuras, las hileras de barrenos tienen generalmente rotura libre, pues los ciclos de voladura se adaptan a los trabajos de desescombro llevados a cabo más abajo. La roca arrancada es recogida en depósitos situados a un nivel inferior y en donde se efectúa el desescombro. Este puede hacerse mediante dragalina directamente desde los depósitos, pero también es posible un desescombro mecánico desde galerías laterales.

La fragmentación tiene una gran importancia en estos casos, pues el empleo posterior de cargas conformadas para el taqueo de los bloques grandes implica interrupciones de todo el ciclo de producción, sin contar la influencia del grado de fragmentación sobre las operaciones de desescombro. Si se quiere que la explotación por cámaras con pegas en abanico sea lo más eficaz posible, la estimación del grado de fragmentación y la adaptación de la voladura a este objetivo constituyen factores de gran importancia. En principio, puede hacerse uso del mismo modelo que se describió en la sección 5.8, "Estudio económico de las voladuras".

Las condiciones específicas propias de cada mina en particular implican que toda generalización a este respecto ha de hacerse con las debidas precauciones.

La perforación de cueles en abanico se ha desarrollado como consecuencia del deseo de limitar la magnitud de las labores de preparación. Desde el punto de vista de la técnica de voladuras, los cueles en abanico no resultan tan acertados, pues la distancia entre los barrenos se va haciendo progresivamente mayor, y la mitad inferior de los mismos no puede ser aprovechada de forma adecuada. Los barrenos paralelos ofrecen una mejor posibilidad de lograr mayor precisión y carga, con una fragmentación más provechosa y resultados globales superiores (véase sección 11.1).

Con los avances habidos en los últimos años en el campo de las voladuras de galerías, puede resultar ventajoso, en el caso de filones de mineral estrechos, considerar la posibilidad de realizar la voladura del filón en toda su anchura mediante barrenos paralelos.

Cálculo de cargas

El método de cámaras con pegas en abanico (subniveles con perforación ascendente) puede muy bien compararse, desde el punto de vista de la técnica de voladuras, a las voladuras en banco sobre la superficie. La voladura comprende generalmente un número limitado de hileras de barrenos, y las dimensiones geométricas de la pega y sus condiciones de confinamiento limitado implican normalmente que este método de explotación no sea difícil de llevar a la práctica. Puede considerarse generalmente que una carga específica de 0,40 kg/m³ es suficiente. Si se establece la comparación con la voladura de la zona central en una cámara subterránea, resulta que ésta última precisa solamente 0,30 kg/m³, pero es preciso tener en cuenta que su grado de constricción es menor y el emplazamiento de los barrenos más ventajoso.

Si los filones de mineral son estrechos, aumenta la constricción, y con ello la carga específica necesaria. En la sección 5.3, "Esponjamiento", se describe un factor a añadir a la carga específica dependiendo de la anchura de la pega:

$$q_{real} = \frac{0,40}{B} \quad \left(\text{o bien } q_{real} = \frac{0,40}{\text{No de barrenos por hilera} - 1}\right)$$

siendo B = anchura de la pega.

Si se adopta una carga específica de 0,40 kg/m³ como valor orientativo adecuado para la explotación normal en cámaras con pegas en abanico, puede establecerse la siguiente correlación:

$$q_{real} = 0,40 + \frac{0,40}{B}$$

Esta relación permite formar la Tabla siguiente:

Anchura de la pega m	Carga específica necesaria kg/m³
3	0,53
5	0,48
10	0,44
20	0,41
30	0,42
40	0,41

En los casos en que el mineral previamente arrancado impide la rotura libre, ha de aumentarse la carga específica en el factor 0,03 × altura de la sección del obstáculo.

Ejemplo

Se ha de realizar una explotación en cámaras con pegas en abanico. La anchura del filón mineral es de 18 m y la altura entre niveles 15 m.

El mineral ya arrancado por voladuras anteriores cubre una altura de unos 10 m.

$$q_{real} = 0,40 + \frac{0,40}{18} + 0,03 \times 10 = 0,72 \text{ kg/m}^3$$

Como la distancia entre los barrenos es relativamente grande, hay riesgo de que se produzcan fragmentos de gran tamaño. Aun cuando se coloque la misma carga específica en el fondo de los barrenos, la fragmentación es más deficiente debido a la menor perforación específica (véase sección 5.2).

Así pues, sería preferible aumentar la carga específica en las extremidades de los barrenos de modo que se obtenga una fragmentación más regular. Sugiero utilizar una carga específica de 0,50 kg/m³ en 1/5 de la longitud del barreno en los casos normales, reduciéndola a 0,37 kg/m³ en el resto del barreno.

Las cargas pueden ser calculadas a partir de la concentración de carga posible para el diámetro de los barrenos utilizados.

Diámetro barrenos mm	Concentración de carga kg/m	Carga específica kg/m³	Volumen/metro de barreno en el fondo m³
35	1,20	0,50	2,4
41	1,70	0,50	3,4
48	2,30	0,50	4,6
51	2,60	0,50	5,2

Si se conoce el volumen por metro de perforación en el fondo del barreno puede calcularse el espaciamiento. Para evitar la sobreperforación puede ser conveniente modificar el valor de la relación *piedra*/espaciamiento desde la cifra normal de 0,8 a 0,5.

Los estudios realizados en los últimos años han indicado que la fragmentación suele mejorar cuando se aumenta el espaciamiento en relación con la *piedra*.

V × 2V = Volumen en el fondo de los barrenos.

2V² = Volumen en el fondo de los barrenos.

Puede, por consiguiente, calcularse ya el espaciamiento entre los barrenos:

Diámetro barrenos mm	Piedra m	Espaciamiento m
35	1,1	2,2
41	1,3	2,6
48	1,5	3,0
51	1,6	3,2

Ejemplo:

Se va a realizar una explotación por el método de cámaras con pegas en abanico en las condiciones siguientes:

Diámetro de los barrenos: 38 mm
Altura de banco: 17 m (hacia arriba)
Anchura del filón de mineral: 20 m
No quedará mineral previamente arrancado que impida la rotu re.

Procedimiento de cálculo:

1. Cálculo de la carga específica:

$$q_m = 0{,}40 + \frac{0{,}40}{20} = 0{,}42 \text{ kg/m}^3$$

(0,50 kg/m³ en el fondo de los barrenos)

2. Cálculo del volumen por barreno en el fondo:

$$\text{Concentración de carga} = \frac{d \times d}{1000} = \frac{38 \times 38}{1000} = 1{,}40 \text{ kg/m}$$

$$\text{Carga específica} = 0{,}50 \text{ kg/m}^3$$

$$\text{Volumen por barreno} = \frac{1{,}40}{0{,}50} = 2{,}8 \text{ m}^3$$

3. El espaciamiento se calcula basándose en el volumen por barreno que se acaba de hallar:

$$2V^2 = 2{,}8$$
$$V_t = 1{,}2 \text{ m (aprox.)}$$
$$E_t = 2 \times V_t = 2 \times 1{,}2 = 2{,}4 \text{ m}$$

En cada barreno, la carga en el extremo, como carga de fondo, ha de llenar al menos 1/5 de la longitud (véase Fig. 11.2.1).

La carga de columna, que normalmente llena también el barreno, se distribuye de tal forma que se obtenga una carga específica adecuada; en este caso 0,37 kg/m³.

Las zonas de retacado se calculan aproximadamente en 230 m de barreno.

El volumen residual de mineral es aproximadamente $16 \times 16 \times V_t = 307$ m³.

La carga necesaria en las zonas de columna: $0{,}37 \times 307 = 115$ kg.

Es recomendable elegir una concentración de carga inferior a la del caso de un barreno completamente cargado, pues en la zona de columna es difícil distribuir la carga.

Si se elige una concentración de carga de 1,0 kg/m la zona de columna cargada será de $\frac{115}{1{,}0} = 115$ m de longitud.

La zona no cargada restante, zona de retacado, es de unos 230 m de longitud, con lo que la extensión cargada es aproximadamente de un 50 % de la longitud de la columna.

Con una carga de 1/1 — 40 % — 40 % — 1/1 y así sucesivamente se consigue, con aproximación más o menos grosera, la carga deseada (véase Fig. 11.2.1). La zona de retacado en los barrenos totalmente cargados es de unos 0,5 m.

El procedimiento de cálculo mostrado ilustra la dificultad de distribuir correctamente la carga en una pega en abanico con barrenos de gran longitud.

Los barrenos paralelos presentan unas ventajas tan grandes, que se recomienda utilizarlos siempre que sea posible desde el punto de vista de la técnica minera.

El empleo de barrenos con amplios espaciamientos implica asimismo un mejor aprovechamiento de los mismos (véase la sección 5.2).

El encendido se efectúa mediante detonadores de microrretardo, con lo que la abertura inicial toma la forma de un cuele en cuña o en V.

En el caso de minerales conductores de la electricidad, han de hacerse comprobaciones de las pérdidas a tierra de corriente, además de las mediciones de resistencia.

Para garantizar que la perforación y la carga se realizan de modo que proporcionen los resultados apetecidos, es esencial una cuidadosa planificación de las voladuras y ejecución del proyecto.

11.3 VOLADURAS MINERAS, MÉTODO DE NIVELES HUNDIDOS. EJEMPLOS DE VOLADURAS MINERAS

El método de niveles hundidos se utiliza ampliamente en las minas suecas. La base del método consiste en abrirse paso hasta el mineral mediante galerías separadas por pilares. Los túneles de acceso se excavan a diferentes niveles.

Cuando se vuelan el techo y los pilares, puede procederse al desescombro de la roca arrancada. El relleno con roca estéril se realiza al mismo tiempo que continúa la extracción de mineral. Esto implica que después del desescombro de una pega de mineral, la roca estéril se introduce en la cavidad; en la práctica se produce antes una mezcla de mineral y estéril, con lo que una cierta cantidad de este último es recogido juntamente con el mineral, lo que significa una pérdida.

En esta sección no se trata del método de niveles hundidos desde el punto de vista de la ingeniería de minas, sino más bien en lo que respecta a la influencia de las diversas técnicas de voladura sobre los resultados obtenidos.

Por otra parte, es preciso recordar que los aspectos puramente de técnica minera, en lo concerniente al emplazamiento de las galerías, la inclinación de los estratos, la *piedra* en relación con el espesor de éstos, etc. son siempre de una importancia vital a la hora de considerar los resultados globales del método.

El método de niveles hundidos, junto con el de cámaras con banqueo desde niveles, puede ser comparado con las voladuras en banco sobre la superficie. En el caso de niveles hundidos, la posibilidad de rotura de la pega se ve perjudicada por la contrapresión ejercida por la roca ya fragmentada situada

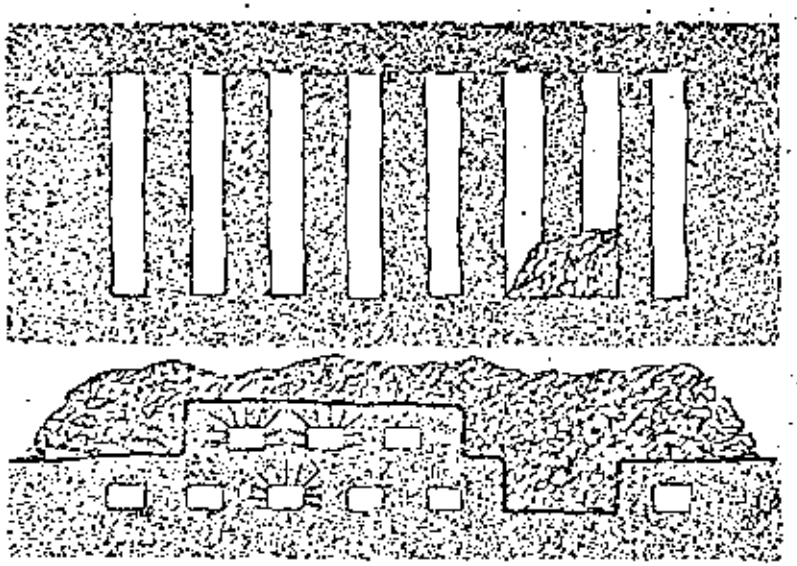

Fig. 11.3.1

encima. Ciertamente, las pegas no tienen un confinamiento especialmente acusado, excepto en el caso de filones muy estrechos, pero no obstante la roca posee escasa posibilidad para desplazarse hacia adelante. Sin embargo, el mineral puede moverse hacia abajo en el hundimiento, y este desplazamiento se ve acelerado por la presión del material ya roto.

En la Fig. 11.3.1 se muestra el método de explotación por niveles hundidos.

El método plantea unas grandes exigencias en lo que respecta a la fragmentación; además de la disminución de la capacidad de desescombro, si en la voladura se producen muchos bloques grandes, es el mismo proceso de hundimiento el que se ve interrumpido.

La perforación se realiza en este método en forma de abanico, con los barrenos abriéndose hacia el interior de los pilares o macizos adyacentes, y dirigiéndose hacia arriba en el macizo suprayacente. Si la galería de perforación no está centrada con respecto a este pilar superior, las longitudes de perforación habrán de ajustarse de modo que se logre una distribución uniforme en el seno de la roca intacta. Igual que en el caso de cámaras con banqueo desde niveles, la perforación en abanico presenta muchas desventajas desde el punto de vista de la tecnología de voladuras. Si fuera posible perforar paralelamente los barrenos sin dejar de observar los criterios técnicos de la ingeniería de minas, la fragmentación obtenida sería mucho mejor con una perforación menor, debido a la mejor distribución de la carga.

Cálculos de carga

En las voladuras en banco ordinarias, la carga específica necesaria es aproximadamente de 0,40 kg/m³.

La fuerza suplementaria que se precisa para el esponjamiento en el método de niveles hundidos es proporcional a la potencia del estrato. El rozamiento contra los lados de la pega, por otra parte, puede exigir una cierta compensación de carga, y en el caso de filones estrechos tiene su importancia.

Puede hacerse uso de las mismas bases de cálculo que en el caso de cámaras con banqueo desde niveles; sin embargo, el suplemento para esponjamiento aparece siempre presente, lo que hace que la carga específica sea normalmente considerada mayor.

$$q_{esp} = 0{,}40 + 0{,}03 \times (\text{espesor del estrato} + \text{macizo superior}) + \frac{0{,}40}{\text{anchura de la pega}}$$

$$q_{esp} = 0{,}40 + 0{,}03 \times \text{máxima profundidad de perforación} + \frac{0{,}40}{\text{anchura pega}}$$

Ejemplo: Método de niveles hundidos con una anchura de 7 m. Máxima profundidad de perforación = 6,0 m.

$$q_{esp} = 0{,}40 + 0{,}03 \times 6{,}0 + \frac{0{,}40}{7}$$

$$q_{esp} = 0{,}40 + 0{,}18 + 0{,}06 = 0{,}64 \text{ kg/m}^3$$

La carga se divide regularmente a lo largo del espesor del estrato.

La distribución de los barrenos se calcula del mismo modo que en las voladuras en banco. Como en éste la profundidad de perforación es menor, puede modificarse la relación piedra/espaciamiento hasta darle un valor de 0,70, con lo que E = 1,4 V.

Diámetro barrenos mm	Concentración de carga kg/m	Carga específica kg/m³	Volumen por barreno *) m³	Piedra m	Espaciamiento m
35	1,2	0,65	1,8	1,15	1,60
35	0,80 **)	0,65	1,2	0,95	1,30
48	2,3	0,65	3,5	1,60	2,20
48	1,6 **)	0,65	2,5	1,35	1,80

(*) Volumen por metro de barreno en el fondo.

(**) Con ANFO o Prillit, refiriendo el cálculo a la potencia del Dynamex.

El espaciamiento ha de ser ajustado a las condiciones geométricas existentes, por lo que respecta a la anchura de la pega y a la altura del estrato.

Por lo demás, el método de cálculo puede ser utilizado para alturas de estrato, diámetros de barrenos, y explosivos diversos.

La iniciación se realiza con detonadores de microrretardo, y la abertura inicial toma la forma de orificios en el macizo aún intacto.

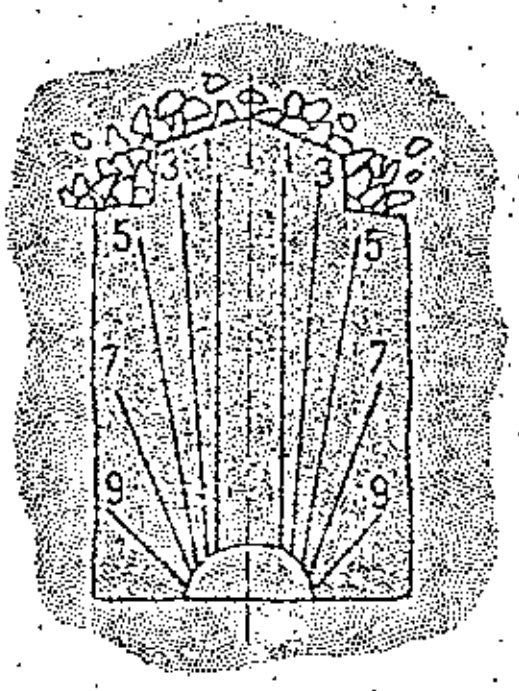

Fig. 11.3.2

Puede resultar interesante una comparación entre los costes de varios explosivos convencionales con los de ANFO o Prilit. Por explosivos convencionales se entiende aquí el Dynamex o similares.

Siempre es difícil hacer un cálculo de costes de un modo genérico, pues las condiciones varían en cada caso particular.

A partir de la Tabla anterior puede hacerse un sencillo cálculo para barrenos de 48 mm:

Precios básicos (1977): Dynamex aprox. 5,50 coronas/kg
ANFO aprox. 2,50 coronas/kg
Coste de perforación 7—10 coronas/m

Alternativas	Carga específica kg/m³	Coste explosivos Cors./m³	Perforación específica m perf./m³	Coste de perforación Cors./m³	Coste total Cors./m³
Dynamex	0,65	3,57	0,29	2,03—2,90	5,60—6,47
ANFO	0,79	1,97	0,43	3,01—4,30	4,98—6,27

Este cálculo sencillo muestra unas diferencias pequeñas entre ambas alternativas, pero es preciso tomar en consideración más factores implicados en el problema.

12. EXCAVACION DE CHIMENEAS CON BARRENOS DE GRAN LONGITUD

12.1 METODOS DE VOLADURA

El término "chimenera" sirve para designar aquellas labores que son verticales o poseen una pendiente de más de 45°. La excavación de chimeneas se considera una de las labores de mayor dificultad en minería subterránea. El método más antiguo, utilizando un "cajón" implica la erección por fases de una pared de troncos de madera simultáneamente al avance de la excavación. Al efectuar la voladura, la roca arrancada cae entre la pared de troncos y la roca sólida. A lo largo de un costado del "cajón" se construye una pasarela de servicio. Después de detonar cada pega, la roca arrancada se extrae a través de una abertura destinada a este fin, con el objeto de disponer una altura de trabajo conveniente. El método requiere una gran cantidad de trabajo de construcción y demolición, así como una gran cantidad de transporte de material. Sin embargo, aún está en uso.

En la *chimenea abierta* el trabajo de construcción se limita a la pasarela de servicio y a la base de una sencilla plataforma sobre la que trabaja el personal de perforación. Se precisa una cierta inclinación en la chimenea. El método se utiliza frecuentemente en chimeneas de una longitud menor de unos 60 metros, pues en otros casos el transporte se hace dificultoso. Aun con los métodos modernos puestos últimamente en práctica, este sistema resulta competitivo, si bien requiere un personal experimentado.

Los *elevadores de chimeneas* se utilizan muy ampliamente.

El Alimak desliza a lo largo de unas guías empernadas a la pared de la chimenea, y consta de una jaula con una plataforma. Desde una posición protegida de la jaula puede efectuarse el trabajo de saneo, y las labores de perforación pueden así mismo llevarse a cabo en condiciones de seguridad y de mayor comodidad. Este tipo de elevador se ha utilizado en chimeneas verticales e inclinadas. El sistema de guías se va prolongando por fases y ha de ser protegido en las voladuras. La ventilación después de éstas se realiza así mismo desde el extremo del sistema de guías.

La jaula Jora va suspendida de un cable que pasa a través de un orificio perforado antes de comenzar la excavación de la chimenea. Este taladro puede ser utilizado también como parte del cuele cuando se dispara una pega.

La jaula del elevador puede ser controlada desde su interior. En el caso de chimeneas inclinadas, ha de empernarse un elemento de guiado a la pared de suspensión. Las labores de perforación y carga se realizan desde el techo de la jaula. El saneo puede realizarse en condiciones de seguridad desde el interior de la jaula a través del techo. Cuando se va a proceder a la voladura se extrae el cable por el orificio después de haber descendido el elevador. El taladro de gran diámetro resulta también ventajoso desde el punto de vista de la ventilación.

Sistema de ejecución con barrenos profundos

En el curso de la última década, se ha hecho cada vez más frecuente la perforación de barrenos de gran profundidad para la excavación de chimeneas. Este método se basa en perforar barrenos a través de toda la longitud de la chimenea, después de lo cual se realiza la voladura por fases (cargas colgadas).

Para obtener un buen resultado se precisa una gran exactitud en la perforación y carga de los barrenos. Cuando se comenzó a emplear este método en Suecia, el mayor problema residía en las desviaciones de la perforación. Desde entonces se han perfeccionado los equipos de guiado de la maquinaria de perforación, y se han desarrollado perforadoras adecuadas para este tipo de trabajo.

Desde el punto de vista de la seguridad, este método es ventajoso, pues todo el trabajo de perforación y carga se realiza desde un lugar protegido. Los inconvenientes surgen de los problemas relacionados con las voladuras totalmente confinadas.

Pueden distinguirse dos variantes principales del método:

Voladura hacia barrenos de gran diámetro.
Voladura con cuele en cráter.

La *voladura hacia barrenos de gran diámetro* fue el método utilizado primeramente, y sigue siendo todavía el más frecuente. Los barrenos de la pega suelen ser relativamente anchos, de 51—75 mm de diámetro. El gran barreno central se ensancha hasta 102—203 mm por medio de barrenas especiales. Actualmente es normal que en los trabajos de perforación se comience por usar una barrena ancha y se introduzca luego una ordinaria. Se emplean unos tubos especiales de guiado para obtener una mayor precisión en la perforación. El equipo de Atlas Copco designado con el nombre de "Simba 5" es especialmente adecuado para este objetivo. Es importante que el equipo de perforación se mantenga solidamente en posición durante el trabajo.

Como resultado de los avances registrados en este campo, unas desviaciones de perforación del orden de 0,5 % son ahora valores totalmente realistas.

En la Fig. 12.1 se muestra el plan de perforación para una chimenea de 4 m² de sección con barrenos de 64 mm y un barreno central de 127 mm de diámetro.

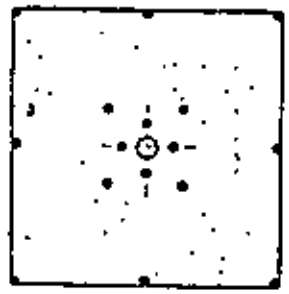

Fig. 12.1

La voladura se realiza por fases. Si se detonan todos los barrenos de modo que se pretenda conseguir un avance por pega normal para esta sección, existe el riesgo de que los barrenos queden bloqueados, y ello obstaculice la continuación de las voladuras.

Barreno No.	Profundidad de voladura adecuada m	No. de barrenos por pega
1—4	2	1
5—8	3	1
9—12	4	4
13—16	8	4

La secuencia de encendido se ajusta con respecto al error de perforación de modo que los barrenos con la menor *piedra* real sean los primeros en ser iniciados. Para las operaciones de carga es importante disponer de un esquema de perforación en el que se marquen los errores de perforación, y llevar en un registro los datos correspondientes a cada barreno.

En la Fig. 12.2 se muestra el procedimiento seguido para la voladura.

La carga se efectúa descendiendo los explosivos desde la superficie superior. Es importante que las cargas del cuele sobresalgan ligeramente por debajo del barreno, a fin de asegurar una rotura completa. Las cargas alargadas de Dynamex resultan apropiadas para este fin. Acoplando un manguito de retención a la extremidad inferior del tubo de carga, puede comprobarse si éste ha traspasado la boca del barreno al tirar de él hacia atrás. Para determinar

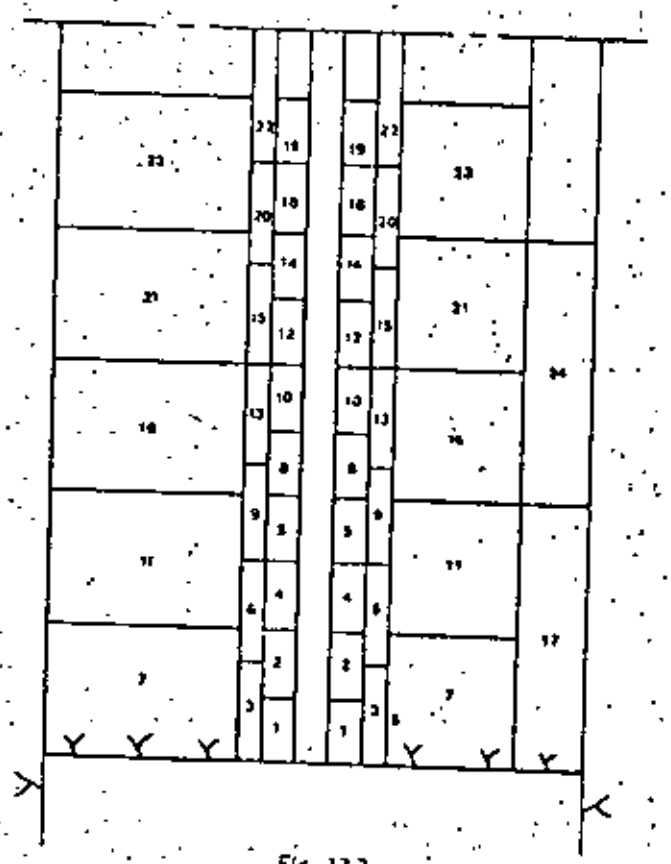

Fig. 12.2

el grado de rotura alcanzado puede utilizarse aire comprimido, el cual, al ser insuflado al interior del barreno, puede dar una idea de la distancia hasta la que éste ha roto. Para conectar entre sí las cargas alargadas resulta adecuada la mecha detonante, que proporciona además una mejor iniciación. No es recomendable emplear material de retacado, pues se puede sinterizar y complicar las operaciones ulteriores de carga.

El método puede parecer muy complejo, pero al evitar las voladuras con confinamiento total se requiere trabajar con precisión. A medida que se va adquiriendo experiencia sobre las propiedades de la roca frente a las voladuras y el riesgo de bloqueo de los barrenos, pueden irse emprendiendo operaciones de voladura de mayor amplitud.

Cálculo de las cargas

En las voladuras con barrenos profundos se requieren unas concentraciones de carga relativamente altas; esto se justifica en parte por el hecho de que los barrenos están abiertos en las dos direcciones, lo que hace que disminuya la presión de los gases, así como por el empleo de mayores diámetros de barreno en relación con la *piedra*. El peligro de que se produzca la sinterización del material en la zona del cuele no es tan grande como en el caso de las voladuras ordinarias en túneles, aun cuando la carga sea mayor.

Barrenos del cuele:

En la Tabla siguiente se incluyen las características de perforación y carga de los barrenos de la zona del cuele:

Diámetro barrenos mm	Diámetro barreno central mm	Distancia entre centros mm	Concentración de carga kg m	Composición de la carga
51	127	210	0,67	Dynamex 25 mm
64	127	220	1,00	Dynamex 32 mm
64	152	250	1,00	Dynamex 32 mm
75	127	230	1,40	2 Dynamex 25 mm
75	152	265	1,40	2 Dynamex 25 mm

Barrenos de franqueo:

Diámetro barrenos mm	Piedra máx. aderuada m	Concentración de carga kg m	Composición de la carga
51	1,0	0,9	Dynamex 29 mm
64	1,1	1,1	Dynamex 32 mm
75	1,2	1,2	2 Dynamex 25 mm

En los barrenos de franqueo en los que, por razones geométricas, no puede lograrse la *piedra* prescrita, la carga debe poseer la concentración correspondiente al diámetro de barreno de que se trate.

En chimeneas de gran longitud puede incorporarse al esquema de perforación otra disposición cuadrada con cuatro barrenos (Fig. 12.1); con ello los ángulos de rotura no son tan agudos y ésta se produce con más facilidad. Preferentemente la *piedra* no deberá ser mayor que la anchura de la abertura contra la cual rompe el barreno.

El *recorte* puede ser utilizado en los trabajos de excavación de chimeneas con barrenos profundos. Dado que se usan barrenos de gran diámetro, no es recomendable desde un punto de vista económico perforarlos demasiado próximos entre sí. En la Tabla siguiente se incluyen algunos valores que pueden servir de orientación para el recorte:

Diámetro barrenos mm	Espaciamiento m	Piedra m	Concentración de carga kg m	Composición de la carga
51	0,70	0,90	0,50	Dynamex de 22 mm
64	0,80	1,00	0,70	Dynamex de 25 mm
75	0,90	1,10	0,90	Dynamex de 29 mm

La iniciación de los barrenos de recorte se efectúa con pocos números de retardo, de modo que se obtenga un efecto de corte.

También es posible el *precorte*, y aproximadamente con el mismo espaciamiento entre barrenos; sin embargo, este procedimiento exige unas limitadas desviaciones de perforación. El precorte se realiza en un lado cada vez, y en caso de pozos largos, puede ser preciso dividir cada lado en varias fases con objeto de evitar unas cargas excesivamente elevadas con detonación instantánea.

Voladura con cuele en cráter

En las voladuras con cuele en cráter por el sistema de barrenos profundos, la voladura se realiza hacia la superficie libre inferior de la chimenea. No se necesita un barreno de gran diámetro en el centro, y tampoco se exige una precisión tan grande en la perforación. La diferencia entre este método

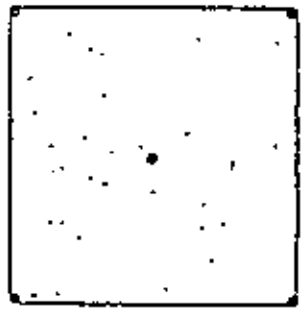

Fig. 12.3.

y el anterior consiste en la zona de ampliación o ensanchamiento del cuele. En las voladuras con cuele en cráter, se abre inicialmente una cavidad de aproximadamente 1 m³, y a continuación se realiza la destroza del resto de la sección en la forma usual. En la Fig. 12.3 se muestra el esquema de perforación para la apertura del cuele.

Los barrenos se detonan por fases, con cargas concentradas (Fig. 12.4). La operación de carga se realiza con máquinas neumáticas o con cartuchos

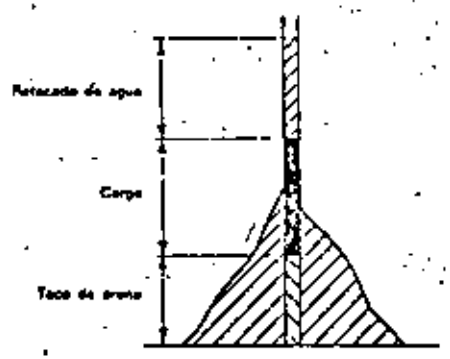

Fig. 12.4

especiales que se adaptan estrechamente al diámetro del barreno. Antes de comenzar la operación, se tapona por un extremo el barreno y se utiliza arena como material de retacado. Por encima de la carga, el material de retacado debe consistir en agua. Ha de encenderse un barreno de cada vez. Una vez adquirida una cierta experiencia sobre las características de la roca frente a la voladura, pueden encenderse varios barrenos al tiempo; la iniciación se realiza entonces con números alternos de microrretardo.

La profundidad ocupada por la carga depende de la concentración que puede conseguirse, la cual, a su vez, es función del diámetro del barreno.

Según la teoría de Livingstone, la profundidad de carga que puede adoptarse es la siguiente:

$$L_{opt} = 0{,}5 \times S \times \sqrt[3]{\frac{3 \cdot p}{2}} \times 10 \times d$$

siendo S = Factor de energía = 1,5 (dependiendo del explosivo utilizado y del tipo de roca).

p = grado de compactación de la carga en kg/dm³.

d = diámetro del barreno en mm.

La teoría del cráter de Livingstone se refiere sólo al barreno central. Las cargas de los demás barrenos se distribuyen de tal modo que la *piedra* sea inferior a la profundidad de la carga del barreno central. Esta profundidad se va aumentando por escalones de 10—20 cm. Los barrenos no deberán estar demasiado próximos entre sí, pues ésto podría implicar el riesgo de que se produjera sinterización del material con las altas concentraciones de carga empleadas.

De acuerdo con la experiencia obtenida en la investigación minera, las cargas apropiadas para los distintos diámetros son las siguientes:

Diámetro del barreno mm	Carga por barreno kg
50	0,80
64	1,35
75	2,60
100	6,10

Como la rotura del barreno del cráter posee la mayor importancia puede ser recomendable utilizar un diámetro de barreno más grande que en el resto de lo barrenos de la chimenea.

Desde el punto de vista de la ingeniería de minas, el método del cráter es más agresivo para la roca circundante que el método descrito en primer lugar. Es éste un factor que debe ser tomado en consideración a la hora de situar la zona de ensanchamiento del cuele en la pega.

En 1975 Björn Andersson recogió en un informe toda una amplia suma de experiencias prácticas obtenidas en la excavación de chimeneas con perforación de barrenos de gran profundidad. El informe se refería a chimeneas de hasta 50 m de longitud. Mediante ensanchamiento cilíndrico del cuele ha sido posible un avance de 10 m de cada vez y, en ciertos casos, de hasta 12 m.

El anillo interior (Fig. 12.5) se enciende con microrretardos, y el exterior, con retardos simples (de medio segundo). Como ambos anillos son encendidos al tiempo, se obtiene un diámetro de 1,2 m. La carga se realiza desde abajo, mediante una escalera extensible que puede ser subida por la chimenea con ayuda de un sistema neumático de elevación. Andersson considera posible llegar a una longitud de 100 m con un alto grado de precisión.

Ciertos detalles técnicos de perforación adquieren la mayor importancia:

— Debe ponerse un gran cuidado al iniciar la perforación.
— Es preciso eliminar todas las holguras de los equipos mecánicos.
— Han de usarse barrenas guía.
— La diferencia entre el diámetro de la boca y el de la barrena ha de ser mínima.

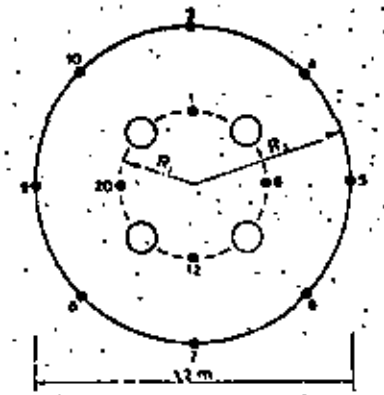

Fig. 12.5 Plan de perforación y encendido con ensanchamiento cilíndrico del cuele

Si se tienen en cuenta estas observaciones, es posible alcanzar una precisión en la perforación bastante menor del 0,5 % de desviación por barreno.

Otro método que puede utilizarse es la combinación de los barrenos profundos con la perforación de un gran taladro central. El número de barrenos estrechos disminuye considerablemente si se emplea un taladro de 0,6—0,9 m.

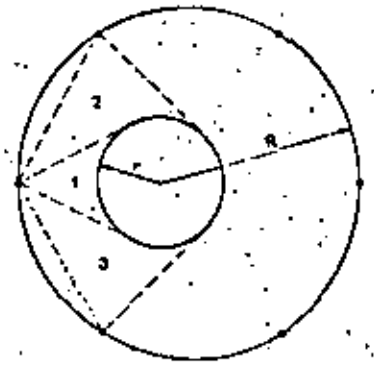

Fig. 12.6 Plan de perforación y encendido mediante la utilización de un gran taladro central

El método de los barrenos profundos ha sido también adaptado para cuando se perfora hacia abajo. Esto implica que la combinación de perforaciones hacia arriba y hacia abajo puede conseguir una chimenea de 100 m de longitud, desde un mismo punto, usando barrenos de 50 m.

Para mejorar aun más la precisión de la perforación, se ha colocado en cada barrena un muelle en espiral, el cual centra a ésta en el interior del barreno, lo que se traduce en un avance más preciso de la perforación y una vida más larga para la propia barrena.

Las bocas recambiables han supuesto asimismo un importante perfeccionamiento para este método de perforación.

Con las mejoras y avances de este tipo, la excavación de chimeneas mediante perforación de barrenos profundos se ha convertido en la actualidad en un método competitivo, cuyo perfeccionamiento se ha basado en una extensiva y cuidadosa planificación y realización del proyecto.

13. VOLADURAS CONTROLADAS

13.1 VIBRACIONES DEL TERRENO

En Suecia, el término "voladuras con precaución" o "voladuras controladas" se refiere especialmente a las que se efectúan en áreas edificadas, salvaguardando la integridad de los edificios, instalaciones, y servicios circundantes. En las últimas décadas se ha registrado un gran incremento de las voladuras en zonas edificadas; se construyen túneles para ferrocarriles subterráneos, tráfico automovilístico, drenajes, y medios de comunicación, como cables telefónicos y de energía eléctrica; la ubicación de todos estos servicios en el interior de la roca firme ha proporcionado unas considerables ventajas. Sobre la superficie, el valor del espacio en las ciudades se está haciendo cada vez más alto. Cuando se procede a derruir antiguas zonas residenciales, se ha hecho ya usual emplear los explosivos, y utilizar luego en gran medida el subsuelo.

Los conductos subterráneos para instalaciones de calefacción de todo un distrito urbano, así como para otros servicios, se construyen en gran proporción mediante voladuras, y muy frecuentemente en la proximidad de otras edificaciones.

En todos estos tipos de operaciones en áreas edificadas, deberá recurrirse a una voladura controlada, de forma que las proyecciones, las ondas de choque aéreas, y las vibraciones del terreno, no produzcan daños ni riesgos en los edificios próximos.

Hoy día se sabe ya mucho más sobre la tecnología de las voladuras en roca, y la posibilidad de controlarlas con ayuda de ciertos tipos de mediciones ha aumentado consecuentemente. En Suecia se dispone hoy de una amplia gama de experiencias obtenidas en voladuras en las que se han tomado mediciones de las vibraciones del terreno.

Existe además un campo aún más amplio de conocimientos en lo relativo a la correlación entre las cargas y la influencia de la distancia sobre la intensidad de las vibraciones del terreno. Ya en 1956 Langefors y Kihlström adelantaron una relación teórica entre carga y distancia, por un lado, e intensidad de las vibraciones del terreno, por el otro.

En los últimos años, las mediciones se han concentrado en la velocidad de las vibraciones del terreno, en tanto que anteriormente fue la aceleración la magnitud que se consideró de gran importancia a la hora de estimar el riesgo de que se produjeran daños.

En nuestra opinión, la velocidad de vibración del terreno constituye un excelente parámetro para ser usado como criterio de posibilidad de daños. Utilizamos la correlación siguiente, en la cual se ha supuesto que las vibraciones son ondas de tipo aproximadamente senoidal:

$$v = 2 \pi f A$$

siendo v = velocidad de vibración en mm/seg.
f = frecuencia en ciclos/seg.
A = amplitud en mm

El diagrama de la vibración puede ser también utilizado para calcular la aceleración de la misma:

$$a = 4 \pi^2 f^2 A$$

siendo a = aceleración con relación a m/seg² (1 g = 9,81 m/seg²)
A = amplitud en mm

Para medir todos estos valores se dispone de diversos instrumentos.

El cizallamiento o corte que se produce en un edificio a través del cual pasan las vibraciones del terreno depende no sólo de la velocidad de dicha vibración, sino también de la velocidad de propagación de las ondas en el terreno situado bajo la cimentación del edificio. Calculamos el ángulo de cizallamiento como directamente proporcional al riesgo de daños:

$$\gamma = \frac{v}{c}$$

siendo γ = ángulo de cizallamiento en mm/m
v = velocidad de vibración en mm/seg.
c = velocidad de propagación en m/seg.

La Tabla siguiente es un resumen de los valores normalmente admisibles que se utilizan para estimar el riesgo de daños por vibraciones del terreno en edificios residenciales normales; en ella se muestra que aun cuando la velocidad de vibración sea de un valor permitido, la dimensión de los daños probables viene determinada por el ángulo de cizallamiento.

En el caso de edificios antiguos, de peor calidad de construcción, se acostumbra a disminuir la velocidad de vibración admisible desde v = 70 mm/seg. a v = 50 mm/seg. Hemos llegado a alcanzar en algunos casos una velocidad v = 100 mm/seg. sin que se produjera ningún daño en los edificios.

En el caso de voladuras aisladas, una estructura robusta de hormigón puede soportar valores de más de 200 mm/seg.

El estudio de la influencia de las vibraciones del terreno sobre los edificios constituye por sí solo una ciencia, en la cual interviene tanto la técnica de voladuras como los conocimientos sobre técnica de la construcción.

Como los edificios se agrietan siempre en alguna medida, con frecuencia resulta muy difícil determinar si unas grietas son consecuencia de la voladura o no. Incluso los más expertos técnicos de la construcción consideran sumamente difícil definir una grieta u otras formas de daño como típicos de las voladuras.

Graduccion del riesgo de daños en edificios residenciales ordinarios en relacion con la velocidad de vibracion del terreno y el materiel sobre el que estan cimentados los edificios

Velocidad de propagación de la onda, c (m/seg.)	1000—1500 Arena, grava, arcilla bajo el nivel freático	2000—3000 Morrenas, pizarra, caliza blanda	4500—6000 Granito, Roca, caliza dura cuarcita, arenisca, diabasa	Efecto sobre edificios normales	Nivel de carga para c = 4200—6000 m/seg.
Velocidad de vibracion, v (mm/seg.)	9	18	35	Sin grietas apreciables	0,008
	13	25	50		0,015
	18	35	70		0,03
	30	55	100	Grietas finas y caída de yeso (valor límite)	0,06
	40	80	150	Agrietamiento	0,12
	60	115	225	Agrietamiento severo	0,25

La evaluación de la resistencia de los distintos materiales del edificio y los cálculos teóricos hechos sobre esta base no proporcionan indicaciones válidas. Los cálculos de este tipo implicarían que el materiel puede tolerar sin daños valores elevados de la vibración del terreno. Un edificio ha de ser considerado como un conjunto complejo, con unas características resistentes de los materiales que varían cuando se considera el conjunto como un todo, y en el cual debe incluirse también el hecho de que las vibraciones locales del terreno dentro del edificio pueden originar asentamientos desfavorables que generen tensiones considerables.

Este estado de la cuestión ha de ser incluido en la visión del problema a la hora de calcular los valores admisibles de la vibración. Los que figuran en la Tabla pueden considerarse totalmente empíricos, pero disponiendo de una base experimental de mediciones constituida por más de 100.000 lecturas, no se nos puede acusar de trabajar sobre hipótesis poco sólidas.

Los problemas de vibraciones del terreno pueden conducir fácilmente a consideraciones teóricas en las cuales se acepten o rechacen los diversos métodos y valores resultantes. La forma de proceder más correcta sería hacer uso de las mediciones para llegar a conocer el carácter de las vibraciones producidas en el terreno por las voladuras, y hacer entonces un estudio de los valores para los cuales se inicia la formación de grietas.

A medida que aumenta el material obtenido, puede proporcionar indicaciones sobre la necesidad o no necesidad de ajustar los valores iniciales en algún sentido determinado. Especialmente en el caso de realizar voladuras en la proximidad de instalaciones y servicios de diversos tipos, los valores obtenidos a partir de la experiencia son con frecuencia las únicas bases de estimación. Si no se dispone de ningún material experimental de esta clase, debe hacerse un reconocimiento detallado de dicha instalación o servicio, así como un estudio de la sensibilidad a las vibraciones del contenido de la instalación o servicio. Este trabajo habrá de hacerse conjuntamente con los fabricantes y proyectistas implicados. Pero, aun con estudios de este tipo, frecuentemente resulta difícil llegar a criterios de tensiones que puedan ponerse en relación con los valores de vibración del terreno normalmente medidos. Finalmente suele ser preciso decidirse sobre un valor que sea razonable y que, sobre la base de la experiencia recogida en las instalaciones y servicios más similares a los del problema tratado, aparezca aplicable. Si la única base utilizada son los valores admisibles dados por los proyectistas, calculados teóricamente por ellos, es muy fácil que se llegue a magnitudes de un orden completamente erróneo. Las personas que trabajan en el problema necesitan para sus estimaciones disponer de unos valores comparativos. De nuevo se demuestra que el modo más fiable de evaluar los valores admisibles de las vibraciones del terreno es de carácter empírico, sin hacer uso de demasiadas teorías.

Como ejemplo puede citarse el caso de las estimaciones hechas sobre los valores admisibles en relación con las operaciones de voladura efectuadas con ocasión de la construcción de todas las estaciones de televisión de Suecia. Después de un estudio del tema, decidimos admitir un valor de v = 35 mm/seg., lo que resultó ser muy adecuado; cuando este valor era excedido, se producían algunas pequeñas perturbaciones. En un par de estaciones nos vimos obligados a complementar la prescripción de este valor admisible de la velocidad con el establecimiento de un límite admisible para la aceleración, igual a 3,0 g. A este respecto, conviene recordar que la aceleración resulta con frecuencia una magnitud importante cuando las voladuras se efectúan

muy cerca de instalaciones que contengan relés, instrumentos muy sensibles, etc.

Cuando se realizan voladuras en la cercanía de instalaciones de computadores, el fabricante estipula una aceleración admisible de 0,25 g en ciertas condiciones; ello implica que las voladuras ordinarias se hacen de más difícil realización, e incluso imposibles en ciertos casos. Nitro Consult ha desarrollado un método especial de amortiguación para las instalaciones de computadores, de forma que las voladuras puedan ser llevadas a cabo como en el caso de un edificio normal de oficinas.

Puede resultar de interés pasar revista brevemente a los niveles de vibración permitidos en otros países. En los Estados Unidos, la máxima velocidad de vibración usada es de 50 mm/seg. en cualquiera de las tres direcciones del espacio. Además se han confeccionado tablas de distancia-carga para voladuras de diversos tipos. Por ejemplo, para el caso de las canteras se dan los siguientes valores de la carga, que pueden compararse con el nivel 0,015 prescrito en Suecia para una velocidad de vibración de v = 50 mm/seg.

Distancia m	Valores de carga americanos (kg. carga coordinada)	Valores de carga suecos (nivel 0,015) (kg. carga coordinada)
30	34	2,6
60	41	7,5
90	53	14
150	80	29
210	118	47
365	350	102

En el caso de distancias más cortas y cuando la voladura se realiza en la inmediata proximidad de instalaciones y edificios, se utiliza otra Tabla:

Distancia m	Valores de carga americanos (kg. carga coordinada)	Valores de carga suecos (kg. carga coordinada)
1,8—3,0	0,11	0,015—0,08
4,5—15	1,3—4,5 *)	0,15—0,9
18—60	6,8—23 **)	1,2 —7,5

(*) 1/3 de libra por pie de distancia
(**) 3/4 de libra por pie de distancia

Los valores americanos son considerablemente más altos que los suecos. Por otra parte, para la carga se emplea un nivel de 0,03, y una velocidad admisible de la vibración de 70 mm/seg. El nivel 0,03 tiene unos valores dos

veces más elevados que el 0,015, pero siguen siendo inferiores a los americanos; la razón de ello reside en el hecho de que las condiciones rocosas imperantes en Estados Unidos son completamente diferentes a las que prevalecen en Suecia; los tipos de roca son considerablemente más blandos, lo que implica una menor velocidad de propagación de las ondas de vibración del terreno, pero al mismo tiempo — y ésto es lo más importante de todo — las vibraciones se amortiguan más rapidamente, y la velocidad de vibración se hace pequeña por la baja frecuencia.

En Canadá, en donde las condiciones de la roca son semejantes a las existentes en Suecia, las velocidades de vibración admisibles usadas son de hasta v = 80 mm/seg.

En Gran Bretaña se ha recurrido a la amplitud de las vibraciones para definir los niveles admisibles, pero actualmente también se considera que la velocidad de vibración proporciona el mejor criterio para la estimación de los riesgos de producir daños. Se utiliza el mismo valor que en Estados Unidos, es decir, v = 50 mm/seg.

Puede ser interesante conocer las amplitudes que se utilizan como límites admisibles; para edificaciones normales de vivienda este valor es de 200 µ (0,2 mm), y para casas en malas condiciones, 100 µ (0,1 mm).

Si en Suecia hubiéramos de usar la amplitud como criterio de permisibilidad, nos veríamos forzados a emplear unos valores variables con la distancia, a causa de las altas frecuencias que aparecen en las rocas duras. Para una velocidad de vibración de v = 70 mm/seg., y una amplitud de 100 µ, la frecuencia no puede ser superior a 100 c.p.s., valor que se alcanza a menudo en granito y gneis a distancias inferiores a 25 metros.

Interesa señalar aquí que la amplitud ha sido empleada también como criterio de posibilidad de daños en Noruega, en donde, sin embargo, la amplitud admisible se ha disminuido a 150 µ (0,15 mm) para viviendas normales. En realidad, el criterio de la velocidad de vibración es el más utilizado en Noruega en la práctica, y con los mismos valores que en Suecia.

Alemania se encuentra en una posición muy peculiar, con unos valores admisibles que pueden ser considerados excesivamente bajos y nada realistas; el tipo de roca no es muy diferente del existente en Gran Bretaña, pero los valores utilizados son mucho menores. Como estos valores son objeto actualmente de intensas discusiones por parte de los técnicos alemanes, prefiero no citarlos aquí en este momento.

Aparte del ejemplo mencionado en último lugar, existen unas correlaciones lógicas evidentes entre las diferentes velocidades admisibles de vibración y los valores de las cargas en los distintos países. Es preciso tener siempre en cuenta que las condiciones varían en gran medida, puesto que la roca afectada posee características diferentes. Con los valores suecos este aspecto de la cuestión ha sido tenido en cuenta de una forma más completa, pues de-

pendiendo de las condiciones del terreno se aplican diversos valores admisibles. Asimismo ha de prestarse la debida atención a las características de las instalaciones o edificios afectados. Dependiendo de las condiciones climatológicas, la resistencia material de un bloque de viviendas puede variar de forma acusada con relación a diversos tipos de diseño del mismo.

En países en los que se están haciendo estudios con objeto de llegar a especificar los valores admisibles, no es por consiguiente recomendable basarse en la literatura y la experiencia proveniente de otros países; en lugar de ello, es preciso llevar a cabo exhaustivas investigaciones sobre la propagación de las vibraciones del terreno para diversas cargas, a distancias variables, y con diferentes condiciones de la roca. Una estimación general de la resistencia material de los edificios implicados puede entonces proporcionar la base para el establecimiento de unas Tablas de cargas-distancias, y de los valores admisibles de las vibraciones. Tras unos años de experiencia empírica, pueden reajustarse estos valores si se considera necesario.

El número de voladuras realizadas en Suecia en áreas edificadas ha aumentado considerablemente; a pesar de ello, se ha registrado un claro descenso de los daños ocasionados por vibraciones del terreno; es ésta evidentemente una valiosa confirmación práctica indicadora de que se ha escogido el nivel de tensión correcto, sin por ello perder de vista la importancia de los aspectos económicos en las operaciones de voladura.

13.2 METODOS DE MEDIDA DE LAS VIBRACIONES DEL TERRENO Y SU RELACION CON LA CARGA

Gráficos de vibraciones

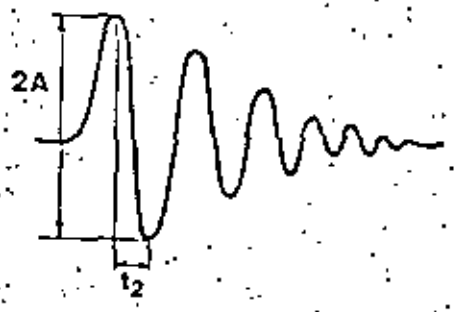

A = amplitud

t_2 = semilongitud de onda (ver la evaluación)

Tipos diversos de gráfico

Baja frecuencia

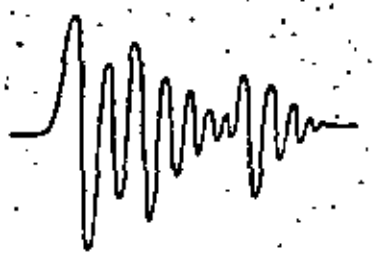

Alta frecuencia

Fig. 13.2.1.

Métodos de medida de las vibraciones del terreno

Para medir la magnitud de las vibraciones del terreno se dispone de diversos tipos de instrumentos, los cuales pueden subdividirse en dos grupos principales:

Instrumentos mécanicos
Instrumentos eléctricos

Los instrumentos mecánicos utilizados en Suecia son:

El vibrógrafo Cambridge
El Combigrafo
El Ampligrafo

El *vibrógrafo Cambridge* es el instrumento más antiguo, y se utiliza actualmente menos que en el pasado. El instrumento consta de un peso suspendido de un muelle conectado a una aguja registradora que marca la vibración sobre una banda de celuloide. Como esta banda puede ser desplazada hacia adelante a una velocidad conocida y con marcas de tiempo, puede calcularse la frecuencia de vibración. En principio el instrumento funciona de modo que la superficie inferior, que puede estar cargada, está sometida a la vibración, en tanto que el peso suspendido del muelle se mantiene inmóvil. En tal caso el movimiento que se registra en la banda de celuloida queda algo amplificado. En el caso de aceleraciones elevadas, es preciso utilizar una carga suspendida del muelle para que el instrumento no pierda contacto con la superficie inferior.

Al igual que el instrumento citado anteriormente, el *Combigrafo* puede medir la frecuencia de las vibraciones del terreno, a partir de la cual pueden calcularse la velocidad y aceleración de las mismas. El principio de funcionamiento del Combigrafo es el mismo que el del vibrógrafo Cambridge, pero con importantes diferencias de diseño. Por ejemplo, el Combigrafo puede sujetarse a las paredes mediante pequeños pernos para asegurar un emplazamiento firme.

El Combigrafo marca la traza de la vibración sobre un disco de papel parafinado, con lo que se consigue una gráfica de lectura clara a la hora de hacer la evaluación.

La evaluación se hace normalmente con ayuda de una potente lente de aumento. Para llegar a un resultado correcto es necesaria una cierta experiencia en la lectura de estas gráficas.

El instrumento registra la curva con una amplificación de cinco veces. Da una vuelta en 12 segundos, es decir, 5 revoluciones por minuto. El disco se hace girar por medio de un pequeño motor sincrónico de 220 v. y 50 c.p.s.

La evaluación se realiza del modo siguiente:

Amplitud: $A_{mm} = \frac{A_{leído}}{5 \times 2}$

siendo 5 el grado de amplicación y 2 el factor para la división de la doble amplitud.

Ejemplo: A través de la lente se ha tomado una lectura de 0,2 mm (200 μ).

$$A_{mm} = \frac{0,2}{5 \times 2} = 0,02 \text{ mm} = 20 \ \mu$$

Frecuencia

$$f = \frac{\pi \, d}{12 \times 2t_1} \text{ ciclos/seg.}$$

siendo d = diámetro del círculo de ordenada cero en mm

12 = tiempo preciso para el registro de una vuelta completa en segundos

t_1 = semilongitud de onda (normalmente es más fácil de medir que la totalidad de la longitud de onda)

Ejemplo: El instrumento registra con un diámetro de referencia de 70 mm, y la semilongitud de onda, leída con la lente de aumento, resulta ser de 0,2 mm.

$$f = \frac{\pi \times 70}{12 \times 2 \times 0,2} = 45 \text{ ciclos/seg.}$$

Una vez evaluadas A y f, la velocidad de vibración y la aceleración se obtienen mediante las relaciones:

$v = 2 \pi f A$
$a = 4 \pi^2 f^2 A$

El Combigrafo posee también un registro a largo plazo que funciona permanentemente. El diagrama de registro permanente consiste en un disco de papel con 8 hojas, que duran para una semana de funcionamiento, y en el que se incluyen unas marcas de tiempo, con lo que el tiempo de vibración puede ser determinado con precisión de 1 minuto. En el registro permanente solamente se miden amplitudes de vibración, lo que es suficiente a efectos exploratorios. Aun efectuando un control de las vibraciones del terreno, con frecuencia ocurre que se presentan reclamaciones a propósito de las voladuras, porque se está operando de tal modo que los trabajos de medición no han

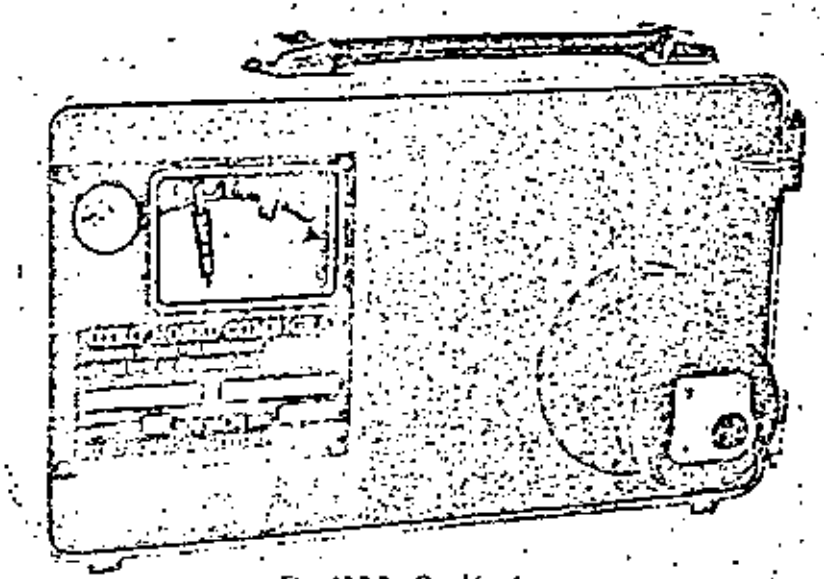

Fig. 13.2.2 Combígrafo

servido de beneficio alguno, aun cuando se hayan tomado muchas mediciones. Es muy conveniente, por otra parte, registrar todas las pegas efectuadas; la magnitud de las amplitudes de vibración puede facilitar la estimación del peligro relativo correspondiente a cada registro.

El *Ampligrafo* está diseñado basándose en el mismo principio que el Combígrafo, pero sin incluir la sección de registro rápido; ésto implica que solamente puede ser empleado para mediciones de exploración. Si las amplitudes registradas indican un valor que puede considerarse comparable a una velocidad de vibración muy próxima al límite admisible, las mediciones de registro de frecuencias pueden llevarse a cabo con el Combígrafo. Cuando se están tomando mediciones de las vibraciones del terreno en relación con la hinca de pilotes, de tablestacas, o de los efectos del tráfico, el instrumento de registro permanente resulta muy práctico. En vibraciones de este tipo, la variación de frecuencia no es tan grande.

Resulta muy conveniente y adaptable un sistema de medición formado por pequeñas unidades mecánicas. Para comprobar el área que rodea el espacio de una voladura, se utiliza un par de Combígrafos en los puntos más sensibles, y Ampligrafos en los demás puntos. Si en alguno de estos puntos aparece un valor elevado de la vibración, deberán tomarse en él mediciones

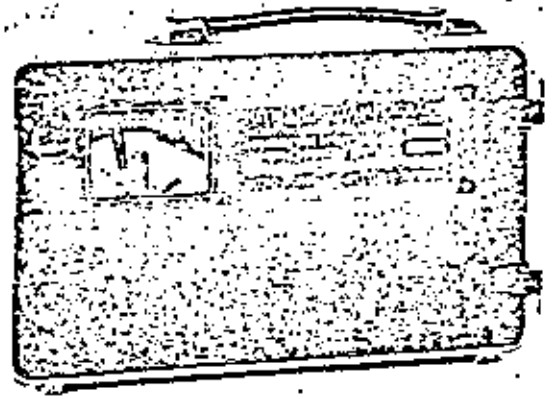

Fig. 13.2.3 . Ampligrafo

con Combígrafo. Las vibraciones del terreno están todo el tiempo bajo control, lo cual resulta valorable tanto desde un punto de vista técnico como psicológico.

Los instrumentos eléctricos empleados en Suecia para mediciones de las vibraciones del terreno son los siguientes:

Indicadores ultravioleta
Vibracorder

Los *indicadores ultravioleta* constituyen un tipo de instrumento que se utiliza en muchos lugares en todo el mundo. Consisten en unos geófonos (sensores) que detectan las vibraciones y las transforman en impulsos eléctricos, los cuales son transportados a través de cables hasta una unidad central de registro, la cual marca las vibraciones, por intermedio de unos galvanómetros de espejo, sobre una película fotosensible que puede hacerse pasar a diferentes velocidades. Normalmente la velocidad de vibración es

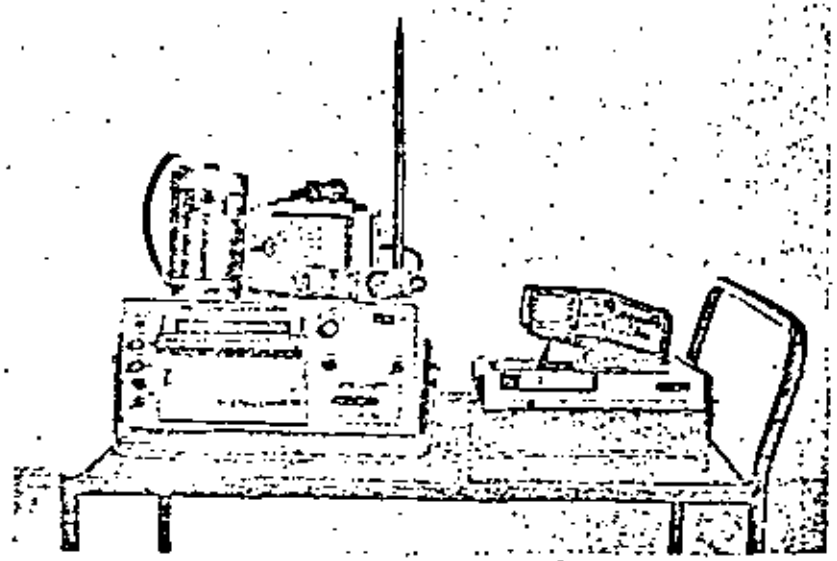

Fig. 13.2.4

registrada directamente, y a continuación pueden evaluarse la frecuencia, aceleración, y amplitud a partir de la gráfica de la vibración.

Además de estos valores, existe también la posibilidad de medir la velocidad de propagación de la onda de choque en el terreno. Los instrumentos de este tipo ofrecen un amplio abanico de posibilidades de medición, pero requieren un trabajo a lo largo de un cierto periodo de tiempo para que la instalación de los cables y geófonos pueda hacerse de un modo racional.

El *Vibracorder* es un instrumento desarrollado por Nitro Consult. Está basado en el mismo principio que los indicadores ultravioleta, pero evalúa por sí solo las figuras que se deseen, y es también del tipo de registro a largo plazo. Puede medir o la velocidad o la frecuencia de la vibración, según se desee, en cuatro puntos que pueden estar situados hasta a varios centenares de metros de la unidad central de registro. También se emplean cables y sensores, pero los primeros han de ser de un tipo especial. La unidad central de registro consta de dos registradores, un sistema electrónico, y una fuente auxiliar de energía para el caso de un corte en la red principal; cuando esto ocurre, la batería auxiliar se conecta automáticamente, y puede alimentar el instrumento durante 24 horas. El Vibracorder resulta práctico, pues puede

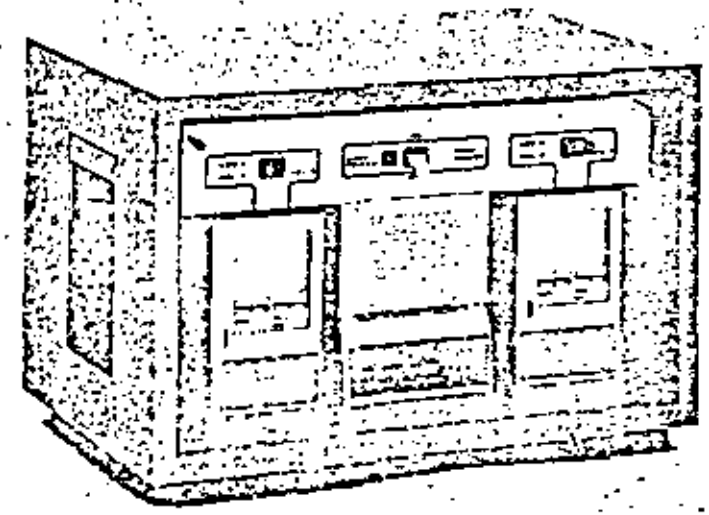

Fig. 13.2.5 Vibracorder

instalarse en las mismas oficinas, desde donde se toman las lecturas correspondientes a cada pega. El papel de registro ha de ser sustituido todos los meses, pero se recomienda una inspección más frecuente del instrumento por un técnico experto.

El papel de registro lleva incluidas unas marcas de tiempo que facilitan la documentación de cada pega.

En las mediciones de vibraciones del terreno que se llevan a cabo en Suecia, normalmente lo que se toma en consideración es la componente vertical de la vibración; una excepción a esta norma la constituye el caso en que se miden los movimientos horizontales resultantes de las ondas de choque del aire. Es sabido que, en muchos países, se miden varias componentes de la vibración, y a veces sus resultados son utilizados para definir los valores admisibles. Resulta dudoso, sin embargo, que se obtenga así un valor verdadero, puesto que, es de suponer que haya un cierto desfase entre las componentes.

Como se señaló ya anteriormente, el factor más importante no es el tratamiento de las magnitudes medidas, sino la consecución de una experiencia en métodos e instrumentos de medida que permita estimar los riesgos de daños con un buen grado de precisión.

A la hora de proyectar voladuras en las que aparezcan problemas de vibraciones del terreno, es importante tener presente la correlación entre estas últimas y los valores de distancia y carga. Hemos hecho uso de la fórmula de Langefors para varios niveles de carga:

$$\text{Nivel} = \frac{Q}{R^{3/2}}$$

Q = carga de detonación instantánea en kg
R = distancia en m

La velocidad de vibración puede calcularse mediante la fórmula:

$$v = k \sqrt{\frac{Q}{R^{3/2}}}$$

v = velocidad de vibración en mm/seg.
k = constante (aproximadamente 400 para rocas duras en Suecia).

La relación anterior puede ser empleada para confeccionar unas sencillas Tablas que pueden servir de material de base para planificar las voladuras:

Distancia	Carga en kg (detonación instantánea)						
m	Nivel: 0,008	0,015	0,03	0,06	0,12	0,25	0,50
0,5				0,02	0,04	0,08	0,16
1	0,008	0,015	0,03	0,06	0,12	0,25	0,50
2	0,025	0,05	0,09	0,2	0,4	0,7	1,4
3	0,040	0,08	0,16	0,33	0,65	1,3	2,6
4	0,06	0,12	0,25	0,5	1,0	2,0	4,0
5	0,09	0,18	0,36	0,73	1,4	2,8	5,6
6	0,12	0,23	0,47	0,95	1,9	3,8	7,2
7	0,14	0,27	0,57	1,15	2,3	4,6	9,2
8	0,18	0,36	0,72	1,45	2,9	5,8	11,6
9	0,2	0,42	0,85	1,70	3,4	6,8	13,6
10	0,25	0,5	1,0	2,0	4,0	8,0	16,0
12	0,3	0,6	1,3	2,5	5,2	10,5	21
14	0,4	0,8	1,6	3,2	6,4	13,0	26
16	0,5	1,0	2,0	3,9	7,8	15,5	31
18	0,6	1,2	2,4	4,7	9,4	19	38
20	0,7	1,4	2,8	5,6	11	22	44
25	1,0	2,0	4,0	8,0	16	32	64
30	1,3	2,6	5,2	10,4	21	42	84
35	1,6	3,2	6,5	13	26	52	104
40	2,0	4,0	8,0	16	32	64	128

Distancia	Carga en kg (detonación instantánea)						
m	Nivel: 0,008	0,015	0,03	0,06	0,12	0,25	0,50
45	2,4	4,8	9,5	19	38	76	152
50	2,8	5,5	11	22	44	88	176
55	3,3	6,5	13	26	52	104	208
60	3,8	7,5	15	30	60	120	240
65	4,3	8,5	17	34	68	136	272
70	4,8	9,5	19	38	76	152	304
75	5,3	10,5	21	42	84	169	336
80	5,8	11,5	23	46	92	184	368
85	6,4	12,8	25,5	51	102	204	409
90	7,0	14,0	28	56	112	224	448
95	7,6	15,2	30	61	122	244	488
100	8,5	16,5	33	66	132	264	528
110	9,3	18,5	37	74	148	296	592
120	10,5	21,0	42	84	168	336	672
130	11,7	23,5	47	94	188	376	752
140	13,2	26,3	52,5	105	210	420	840
150	14,5	29,0	58	116	232	464	928
160	16,0	32,0	64	128	256	512	1024
170	17,5	35,0	70	140	280	560	1120
180	19,0	38,3	76,5	153	306	612	1224
190	20,7	41,5	83	166	332	664	1328
200	22,5	45,0	90	180	360	720	1440

En la Tabla siguiente, los niveles de carga están calculados para dar las vibraciones que se incluyen:

Nivel	Velocidad de vibración mm/seg.		
$Q R^{-3/2}$	Granito	Morrenos	Arcilla
0,008	35	18	9
0,015	50	25	13
0,03	70	35	18
0,06	100	55	30
0,12	150	80	40
0,24	225	115	60
0,50	300	150	75

En el caso de voladuras controladas, el esquema de encendido ha de prepararse de tal modo que la carga de detonación instantánea sea lo menor posible.

Si se emplea iniciación con microrretardos, las vibraciones del terreno se reparten por toda la roca. La distribución del encendido dentro del mismo número de retardo es de gran importancia.

La coordinación dentro del mismo retardo o entre los diversos números de retardo depende de la frecuencia de las vibraciones del terreno. Generalmente aplicamos la siguiente regla práctica:

Tipo de detonador	Número de retardo	Coordinación dentro del retardo
TE/MS	1—12	1/2
TE/MS	13—18	1/3
VA/MS	1—10 *)	1/2
VA/MS	11—20	1/3
VA/MS	24—80	1/4
TE, VA/HS	1—12	1/6
Detonadores instantáneos		1

(*) Existen medios números entre el 1 y el 10: 1 ½, 2 ½, etc.

La Tabla ha sido confeccionada basándose en los tiempos de ignición de cada tipo de detonador. En el caso de frecuencias bajas, la coordinación puede ser superior, según Langefors.

Tipo de detonador	Número de retardo	Coordinación dentro del retardo
	Menos de 60 ciclos/segundo	
TE/MS	1—12	1
TE/MS	13—18	1/2
VA/MS	1—10	1
VA/MS	11—20	1/2
VA/MS	24—80	1/3
	Menos de 20 ciclos/segundo	
TE/MS	1—18	1
VA/MS	1—20	1
VA/MS	24—80	1/2

Para las frecuencias más bajas, teóricamente debe haber también coordinación entre diferentes números de retardo. Y digo "teoricamente", porque en la práctica la primera Tabla puede usarse para frecuencias superiores a 60 ciclos/seg.

Las bajas frecuencias se producen cuando la voladura es a una distancia relativamente grande, o en rocas blandas. En el caso de grandes distancias, la velocidad de vibración suele ser considerablemente menor que la indicada

por la relación de Langefors, y en el caso de tipos de roca blanda, el amortiguamiento es también considerable, con lo que una carga coordinada teoricamente elevada no origina ninguna vibración de magnitud especialmente grande en estos casos.

Las velocidades de vibración relativamente pequeñas medidas a grandes distancias implicarán la no aplicabilidad de la relación de Langefors. En cambio, un incremento de los valores de la Tabla a distancias grandes significaría que la magnitud de las ondas de choque aéreas sería mayor, con el consiguiente riesgo de daños.

Las *mediciones de las ondas de choque aéreas* se han comenzado a realizar en los últimos años, aplicándolas principalmente a mediciones en el encendido de grandes pegas, o las ondas de choque en las bocas de túneles.

Las mediciones se han realizado por medio de un equipo microfónico conectado a un indicador ultravioleta. El campo de medición ha sido de 0,1 a 15 milibares. Las mediciones han mostrado una buena concordancia con las medidas de la vibración de registro horizontal. Es evidente, por otra parte, la gran importancia que poseen las condiciones climatológicas, como la dirección del viento y la presión atmosférica.

El método ha sido desarrollado por la Swedish Detonic Research Foundation en Vinterviken.

En un campo de sensibilidad más grosera, por ejemplo la medición de las ondas de choque aéreas en el interior de una cámara subterránea excavada en la roca, se ha utilizado un equipo mecánico con un campo de medición de entre 20 y 100 milibares. El Swedish Detonic Research Laboratory ha diseñado un instrumento mecánico conocido con el nombre de Barógrafo.

Existen también registros permanentes como en el caso del Combigrafo.

Los problemas concernientes a la medición de las ondas de choque aéreas tienen su interés, y en Suecia estamos adquiriendo datos en este campo a través de la experiencia. Hasta ahora se han efectuado mediciones en muchas canteras, en túneles y en cámaras subterráneas en la roca, así como en muchas voladuras sobre la superficie.

En el caso de voladuras controladas, la planificación de la perforación y la carga ha de basarse en las cargas de detonación instantánea que puedan ser usadas. Una vez estudiados los resultados de las mediciones tomadas de las vibraciones del terreno, pueden ajustarse las cargas para obtener unos valores adecuados.

Esto es aplicable en principio a todos los tipos de operaciones de voladuras en los que hayan de limitarse las vibraciones del terreno. En el caso de voladuras en túneles, por ejemplo, ésto significa que puede ser necesario reducir el avance por pega, y adoptar un esquema de perforación más denso, a fin de reducir la magnitud de las cargas utilizadas.

En el caso de las voladuras en banco y en zanjas, la perforación ha de

seguir una distribución más densa y, en ciertas condiciones, la roca ha de ser dividida en más bancos. Por lo que respecta a la reducción de la magnitud de las cargas, otra posibilidad consiste en utilizar los mismos barrenos con cargas parciales.

En la actualidad es posible preplanificar completamente las voladuras basándose en la carga admisible a emplear. Pueden prepararse diversas alternativas, y aplicarlas en relación con las diferentes distancias y grados de sensibilidad a las vibraciones.

Es un dato conocido que las vibraciones del terreno son percibidas subjetivamente por los seres humanos como desagradables y peligrosas mucho antes de que exista riesgo real de daños. El estudio realizado a este respecto por Reihar y Meister concuerda muy bien con la realidad. En este estudio se demuestra la capacidad humana para percibir vibraciones extremadamente pequeñas de menos de v = 5 mm/seg.

La consecución de un campo más amplio de conocimientos sobre las posibilidades de las voladuras controladas es un objetivo extremadamente importante. El público en general debe asimismo ser informado más extensamente, con objeto de que comprenda las perturbaciones que originan las voladuras, y se limite asimismo el número de reclamaciones inmotivadas por daños que suelen plantearse.

13.3 VOLADURAS CONTROLADAS EN BANCO — DIFERENTES SISTEMAS

En las voladuras en banco ordinarias, normalmente se trata de utilizar lo más posible los barrenos, con cargas de fondo concentradas; si se desea conseguir una fragmentación especialmente buena, puede aumentarse considerablemente la carga de columna.

En el caso de voladuras controladas en el interior de un área edificada, debe prestarse atención a las edificaciones próximas, así como a los servicios, instalaciones, y, claro está, personas de los alrededores.

Las voladuras deberán proyectarse de modo que no causen daños en los edificios por vibraciones del terreno o proyección de rocas. Las ondas de choque aéreas pueden suponer asimismo un riesgo. Las piedras lanzadas al aire son evidentemente peligrosas como posibles causantes de daños.

Los problemas relativos a las vibraciones del terreno han sido descritos en detalle en las secciones 13.1 y 13.2. Los de las proyecciones, y los medios de limitarlos o evitarlos, se tratan en detalle en la sección 5.4 y sumariamente en la sección 13.6.

El tema de esta sección es esencialmente el de los métodos de cálculo de las cargas en las voladuras controladas en banco. Se supondrá al describir el procedimiento de cálculo que se está familiarizado con el método empleado para calcular las cargas en las voladuras en banco normales (véase sección 5.1). El método que se expone más abajo intenta sistematizar el procedimiento de cálculo para las condiciones de barrenos con espaciamiento más denso y carga limitada que han de satisfacerse en la voladura controlada.

La base de los cálculos es una carga específica por barreno de 0,35 kg/m³. Puede ser preciso modificar este valor dependiendo de las propiedades de la roca, su emplazamiento, la posibilidad o no de una rotura fácil por desplazamiento hacia abajo del centro de gravedad, etc. Las modificaciones de la carga específica, sin embargo, no alteran el procedimiento de cálculo.

En las voladuras controladas, a menudo son las vibraciones del terreno las que delimitan la carga por barreno; una vez determinado el valor admisible de la vibración, la carga permitida para obtener un nivel de carga apropiado se toma de la Tabla de distancias-cargas de la sección 13.1.

Se usan también las Tablas para bancos de la sección 5.1, para dimensionar las cargas de fondo.

Procedimiento de cálculo

(No es necesario hacer uso de las fórmulas que se incluyen, pero pueden servir para facilitar los cálculos y esquemas).

1. A partir de las vibraciones del terreno admisibles y de la distancia de que se trate, se toma de la Tabla de distancias-cargas la máxima carga coordinada.

2. Con ayuda de las Tablas para voladuras en banco se hace un estudio sobre la posibilidad de realizar estas voladuras según el procedimiento normal, sin necesidad de una perforación más densa de los barrenos; se comienza partiendo de la altura del banco y se comprueba el valor de la carga necesaria en los casos normales.

3. Si se comprueba que la carga en el punto 1 no es suficientemente grande para las voladuras en banco normales, se comienzan los cálculos según el procedimiento siguiente:
El espaciamiento se calcula basándose en el valor de 0,35 kg/m³ como carga específica para cada barreno.

$$\text{m}^3/\text{barreno:}\quad \frac{\text{Carga admisible}}{\text{Carga específica}} = \frac{Q_{max}}{0{,}35}$$

Así se obtiene el volumen de roca correspondiente a la carga de cada barreno. Se calcula entonces la superficie que puede cubrir cada una de ellas:

$$m^2/\text{barreno}: \frac{\text{Volumen por barreno}}{\text{Altura del banco}} = \frac{m^3/\text{barreno}}{\text{Altura banco}}$$

Una vez conocida la superficie por barreno, es fácil calcular el espaciamiento:

Piedra práctica V_1
Espaciamiento práctico E_1
El espaciamiento se toma $E_1 = 1{,}25 \times V_1$
$m^2/\text{barreno} = V_1 \times 1{,}25 \times V_1 = 1{,}25 \times V_1^2$
Generalmente V_1 puede ser calculado mentalmente después de determinar los m^2/barreno.

4. El paso siguiente consiste en calcular la sobreperforación. Obsérvese que en el punto anterior lo que se calculó fue el espaciamiento *práctico*. La sobreperforación, por su parte, se calcula con base a la *piedra* teórica máxima (la sobreperforación es el exceso de perforación por debajo del nivel teórico calculado). Para que el cálculo sea correcto, a la *piedra* práctica ha de añadirse un margen aproximado de error de perforación:
Sobreperforación = (V_1 + error de perforación aproximado) × 0,3
Sobreperforación = (V_1 + 0,03 × altura del banco) × 0,3

5. Puede ahora pasarse a calcular la profundidad de los barrenos:
Profundidad barreno = Altura del banco + Sobreperforación + Suplemento por la inclinación del barreno
H = K + U + Suplemento por la inclinación del barreno

6. Una vez conocida la profundidad de los barrenos, puede calcularse el error de perforación:
Error de perforación = 0,05 + 0,03 × profundidad del barreno
F = 0,05 + 0,03 × H

7. Ha de calcularse la piedra teórica máxima, para poder dimensionar la carga de fondo.
$V_{max} = V_1 + F$

8. El espaciamiento práctico se ajusta a la anchura de la pega, y se calcula seguidamente el número de barrenos:

$$\text{Número de espacios entre barrenos} = \frac{\text{Anchura de la pega}}{E_1} = \frac{B}{E_1}$$

$$E_{1\ corr} = \frac{B}{\text{Número de espacios}}$$

Número de barrenos por hilera = Número de espacios + 1

9. La carga de fondo se obtiene de la Tabla para voladuras en banco, adoptando el valor V_{max} como la magnitud apropiada de la *piedra*.

10. $$\text{Longitud de la carga de fondo} = \frac{\text{Peso de la carga de fondo}}{\text{Diám. barreno} \times \text{Diám. barreno}/1000}$$

$$h_b = \frac{Q_b}{d \times d/1000}$$

11. Longitud de la carga de columna = Profundidad del barreno — (Longitud de la carga de fondo + Zona de retacado)
$h_p = H - (h_b + h_r)$
La zona de retacado se toma normalmente de longitud = V_1 (pero usualmente con un límite mínimo de 1,0 m).

12. Peso de la carga de columna = Carga admisible — Peso de la carga de fondo
$Q_p = Q_{admd} - Q_b$

13. $$\text{Concentración de la carga de columna} = \frac{\text{Peso de la carga de columna}}{\text{Longitud de la carga de columna}}$$

$$Q_{pk} = \frac{Q_p}{h_p}$$

14. Peso de la carga por barreno = Carga de fondo + Carga de columna
Peso de la carga por barreno = $Q_b + Q_p$

15. Peso de la carga por hilera = carga/barreno × no. de barrenos por hilera

16. Se calcula el volumen por hilera de barrenos. Es mejor calcular la carga específica y la perforación para toda una hilera completa.
Volumen por hilera = V_1 × anchura del banco × altura del banco
$m^3/\text{hilera} = V_1 \times B \times K$

17. $$\text{Carga específica} = \frac{kg/\text{hilera}}{m^3/\text{hilera}}$$

$$q = \frac{kg/\text{hilera}}{\text{volumen/hilera}}$$

18. Número de metros perforados por hilera = Número de barrenos × profundidad del barreno

19. $$\text{Perforación específica} = \frac{\text{Metros perforados por hilera}}{\text{Volumen por hilera}}$$

$$m/m^3 = \frac{m/\text{hilera}}{m^3/\text{hilera}}$$

20. Resumen de los datos fundamentales:

Altura banco	Profdad. barrenos	Piedra	Espaciamiento	Carga de fondo	Carga de columna		Carga especif.	Perfor. especif.
K	H	V_1	E_1	Q_b	Q_p	Q_{pl}	q	b
m	m	m	m	kg	kg	compos. kg/m	kg/m³	m/m³

Ejemplo 1

Condiciones: Se ha de efectuar la voladura controlada de un banco situado a 11 m de un edificio cimentado sobre el subsuelo de roca. El buen estado del edificio hace posible admitir una velocidad de vibración de hasta v = 70 mm/seg.

Datos:

Altura del banco = 3,5 m
Diámetro de los barrenos: Barrenas de la serie 11; 34—30 mm
Inclinación de los barrenos = 3:1
Anchura de la pega = 15 m

Se sigue el procedimiento de cálculo que se acaba de describir:

1. La máxima carga coordinada, según la Tabla de distancias-cargas, será de 1,2 kg para una distancia de 11 m y un nivel de carga 0,03 al cual corresponde un valor máximo de v = 70 mm/seg.

2. De acuerdo con la Tabla de voladuras en banco para la serie 11, se necesitan 2,0 kg de carga para una voladura normal y una altura de banco de 3,5 m. En este caso ha de reducirse el valor del espaciamiento.

3. Con base en los 0,35 kg/m³ de carga específica, se hacen los siguientes cálculos de espaciamiento:

$$m^3/\text{barreno} = \frac{\text{Carga admisible}}{\text{Carga específica}} = \frac{1,2}{0,35} = 3,4\ m^3/\text{barreno}$$

$$m^2/\text{barreno} = \frac{m^3/\text{barreno}}{\text{Altura del banco}} = \frac{3,4}{3,5} = 0,97 = \text{aprox. } 1,0\ m$$

$V_1 = 0,9$ m
$E_1 = 1,1$ m
$m^2/\text{barreno} = 1,25 \times V_1^2$
$V_1 = 0,9$

4. Sobreperforación = $(V_1 + 0,03 \times \text{altura del banco}) \times 0,3 =$
$= (0,9 + 0,03 \times 3,5) \times 0,3 = 0,315$; aprox. 0,30 m

5. Profundidad de los barrenos = Altura del banco + Sobreperforación + + Suplemento por la inclinación de los barrenos
H = 3,5 + 0,3 + 0,05 × 3,8 = 3,99 = aprox. 4,0 m.

6. Error de perforación = 0,05 + 0,03 × profundidad del barreno =
= 0,05 + 0,03 × 4,0 = 0,17 ; aprox. 0,20 m

7. $V_{max} = V_1$ + error de perforación F
$V_{max} = 0,90 + 0,20 = 1,10$ m

8. Número de espacios entre barrenos = $\frac{\text{Anchura de la pega}}{E_1}$ =

$$= \frac{15,0}{1,10} = 13,6 = \text{aprox. } 14$$

$$E_{1\ mm} = \frac{15,0}{14} = 1,07\ m$$

Número de barrenos por hilera = 14 + 1 = 15

9. Según la Tabla de voladuras en banco para las barrenas de la serie 11, la carga de fondo, para una *piedra* de 1,1 m, será igual a 0,70 kg.

10. Longitud de la carga de fondo = $\frac{\text{Peso de la carga de fondo}}{d \times d/1000}$ =

$$= \frac{0,70}{30 \times 30/1000} = 0,78 = \text{aprox. } 0,8\ m$$

11. Longitud de la carga de columna = profundidad del barreno — (Longitud de la carga de fondo + Zona de retacado) =
= 4,0 — (0,8 + 1,0) = 2,2 m

12. Peso de la carga de columna = Carga admisible — Peso de la carga de fondo = 1,2 — 0,70 = 0,50 kg

13. Concentración de la carga de columna = $\frac{\text{Peso de la carga de columna}}{\text{Longitud de la carga de columna}}$

$$= \frac{0,50}{2,2} = 0,23\ kg/m$$

Ha de escogerse una carga de columna adecuada entre las que figuran en la Tabla:

Composición de la carga	Concentración de la carga kg/m	kg/m Dynamex
Dynamex de 22 mm	0,50	0,50
Nabit de 22 mm	0,40	0,38
Gurit de 17 mm	0,24	0,18
Gurit de 11 mm	0,11	0,09
Carga espaciada, con separador de 10 cm y ½ cartucho de Dynamex de 22 mm	0,25	0,25
Gurit 17 mm + 1 cartucho Dyn.	0,32	0,27
Gurit 17 mm + ½ cartucho Dyn.	0,28	0,23
Gurit 17 mm + ⅓ cartucho Dyn.	0,27	0,22
Gurit 11 mm + ½ cartucho Dyn.	0,18	0,15

Puede comprobarse en la Tabla que existen muchas posibilidades distintas a la hora de elegir una carga de columna. En este caso resultan muy adecuadas las cargas de Gurit.

Se tomará como carga de columna en este ejemplo Gurit de 17 mm alternada con ½ cartucho de Dynamex, lo que da una concentración de 0,23 kg/m de Dynamex.

La carga estará compuesta por cuatro cargas alargadas de Gurit de 0,46 m de longitud cada una = 1,84 m

Peso: $4 \times 0{,}11 = 0{,}44$ kg

Tres medios cartuchos de Dynamex de 0,10 m de longitud cada uno = = 0,30 m

Peso: $3 \times 0{,}05 = 0{,}15$ kg

Longitud de la carga = 2,14 m. Peso = 0,59 kg

Zona de retacado = 4,0 — (0,80 + 2,14) = 1,06 m

14. Peso de carga por barreno = Carga de fondo + Carga de columna = = 0,70 + 0,59 = 1,29 kg (1,2 kg Dynamex)

15. Peso de carga por hilera = Carga/barreno × no. de barrenos/hilera = = 1,29 × 15 = 19,35 kg (18,00 kg Dynamex)

16. Volumen por hilera = V_1 × anchura del banco × altura del banco = = 0,90 × 15,0 × 3,5 = 47,5 m³

17. Carga específica = $\frac{\text{kg/hilera}}{\text{Volumen por hilera}} = \frac{19{,}35}{47{,}5} = 0{,}41$ kg/m³ (0,38 kg/m³ de Dynamex)

18. Longitud total perforada por hilera = Número de barrenos por hilera × profundidad de los barrenos = 15 × 4,00 = 60 m

19. Perforación específica = $\frac{\text{Longitud perforada por hilera}}{\text{Volumen/hilera}} = \frac{60{,}0}{47{,}5}$ = 1,26 m/m³

20. Resumen de los datos fundamentales:

Altura banco m	Profund. barrenos m	Piedra m	Espaciamiento m	Carga de fondo kg	Carga de columna kg	Carga de columna kg/m	Carga específica kg/m³	Perforación específica m/m³
K	H	V_1	E_1	Q_b	Q_p	$Q_{p/l}$	q	b
3,5	4,0	0,90	1,10	0,70	0,59	0,23	0,41 (0,38)	1,26

El mismo método de cálculo puede ser también utilizado para barrenos de mayor diámetro y mayores distancias. En la inmediata proximidad de edificios no suelen emplearse en absoluto barrenos de diámetro grande; no sólo originan mayores vibraciones del terreno, sino también mayor peligro de proyecciones (véase sección 5.4).

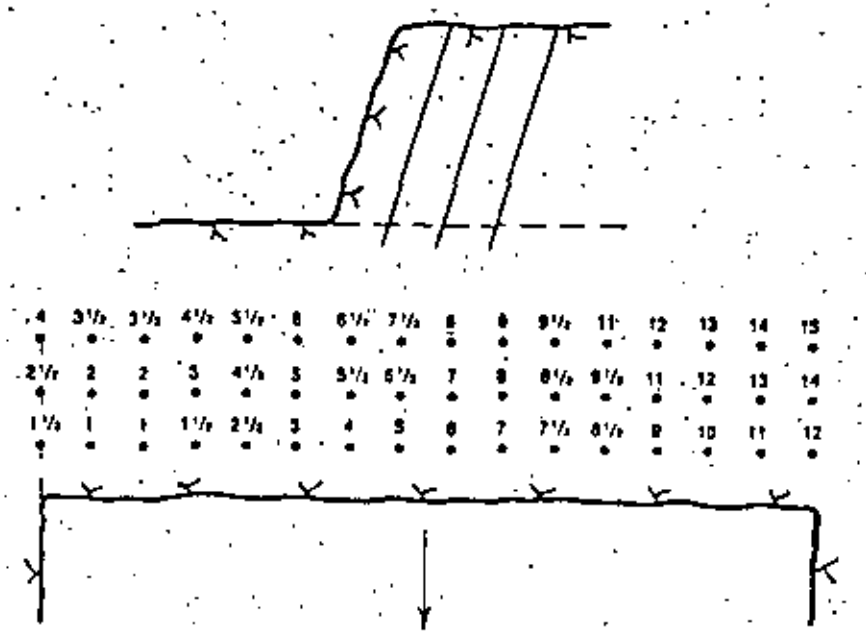

Fig. 13.3.1

Este método de cálculo proporciona asimismo una distribución de la carga en el barreno que es preferible a una carga de fondo concentrada con una larga zona de retacado; este último tipo de distribución puede dar una menor carga específica, pero suele ser más peligrosa por lo que respecta a las vibraciones del terreno y las proyecciones.
El esquema de encendido es importante en las voladuras controladas; no sólo debe ser ajustado de modo que la carga coordinada sea lo más pequeña posible, sino que además, el retardo entre barrenos adyacentes ha de ser cuidadosamente elegido para evitar el riesgo de proyecciones.
Si la roca presenta una superficie libre en un lado de la carga, ésto proporciona un frente que facilita la elaboración del plan de encendido para el retardo más breve posible entre los barrenos adyacentes. El plan de encendido no debe contener barrenos confinados en el momento de la detonación.

Cargas separadas en el mismo barreno

Las cargas coordinadas pueden ser también reducidas dividiendo la carga de cada barreno en varias unidades separadas, con tacos de arena entre ellas. La longitud de éstos, para barrenos de pequeño diámetro, debe ser aproximadamente de 1 m, para garantizar que no se produzca una propagación indeseada.

1—2. Se procede del mismo modo que en el ejemplo anterior.

3. Como criterio de determinación de la *piedra* V_{max} se toma el valor de la máxima carga admisible; de acuerdo con la Tabla correspondiente a barrenos de la serie 11, a una carga coordinada de 1,2 kg le corresponde un $V_{max} = 1,20$ m.

4. Sobreperforación $= 0,3\ V_{max}$
$U = 0,3 \times 1,20 = 0,36 =$ aprox. 0,40 m

5. Profundidad del barreno = Altura del banco + Sobreperforación + Suplemento por la inclinación del barreno
$H = 3,5 + 0,40 + 0,05 \times 3,90 = 4,10$ m

6. Error de perforación $= 0,05 + 0,03 \times$ profundidad del barreno
$F = 0,05 + 0,03 \times 4,10 = 0,17 =$ aprox. 0,20 m

7. *Piedra* práctica = V_{max} — error de perforación
$V_1 = 1,20 - 0,20 = 1,00$ m

8. Espaciamiento $= 1,25 \times 1,00 = 1,25$ m

9. Número de espacios entre barrenos $= \frac{15,0}{1,25} = 12,0$
Número de barrenos por hilera $= 12 + 1 = 13$

10. Longitud de la carga de fondo $= \frac{\text{Peso de la carga de fondo}}{d \times d/1000} =$
$= \frac{1,20}{29 \times 29/1000} = 1,43 =$ aprox. 1,4 m

11. Zona residual del barreno = Profundidad del barreno — (Longitud de la carga de fondo + Longitud del taco de arena) =
$= 4,10 - (1,40 + 1,00) = 1,70$ m
Esta zona puede ser considerada como un nuevo barreno.

12. Error de perforación $= 0,05 + 0,03 \times H$
$F = 0,05 + 0,03 \times 1,7 = 0,10$ m

13. $V_{max} = V_1 +$ Error de perforación
$V_{max} = 1,00 + 0,10 = 1,10$ m

14. La carga de fondo necesaria se calcula con referencia al valor de V_{max} según la Tabla, resulta ser de 0,70 kg. Dado que el barreno tiene rotura libre por el fondo, se necesitan sólo ¾ de la carga $= ¾ \times 0,70 = 0,50$ kg.

15. Longitud de la carga de fondo $= \frac{\text{Peso de la carga de fondo}}{d \times d/1000} =$
$= \frac{0,50}{31 \times 31/1000} =$ aprox. 0,50 m

16. Zona de retacado = Profundidad del barreno — Longitud de la carga de fondo $= 1,7 - 0,50 = 1,2$ m
Si el barreno hubiese sido más profundo, se habría aún aplicado $1,20 - 0,50 = 0,70$ kg para la carga de columna. A partir del valor de la piedra se habría entonces escogido una carga de columna adecuada en relación con la carga de fondo.

17. Peso de la carga por barreno $= 1,20 + 0,50 = 1,70$ kg

18. Peso de la carga por hilera = Peso de la carga por barreno × Número de barrenos por hilera $= 1,70 \times 13 = 22,1$ kg/hilera

19. Volumen por hilera = $V_1 \times$ Anchura del banco × Altura del banco =
$= 1,00 \times 15,0 \times 3,5 = 52,5\ m^3$

20. Carga específica $= \frac{\text{kg/hilera}}{\text{volumen/hilera}} = \frac{22,1}{52,5} = 0,42\ kg/m^3$

El plan de encendido toma la forma que se muestra a continuación:

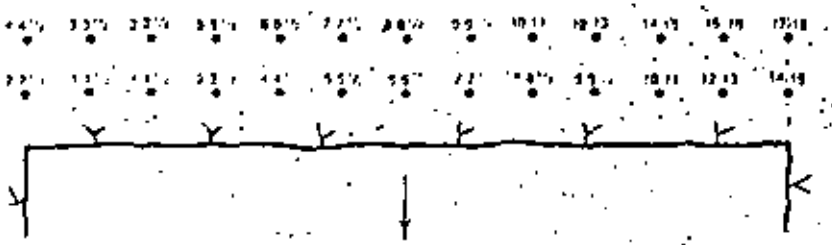

Fig. 13.3.2

Esquema de un barreno con carga parcial (cargas separadas) y taco de arena.

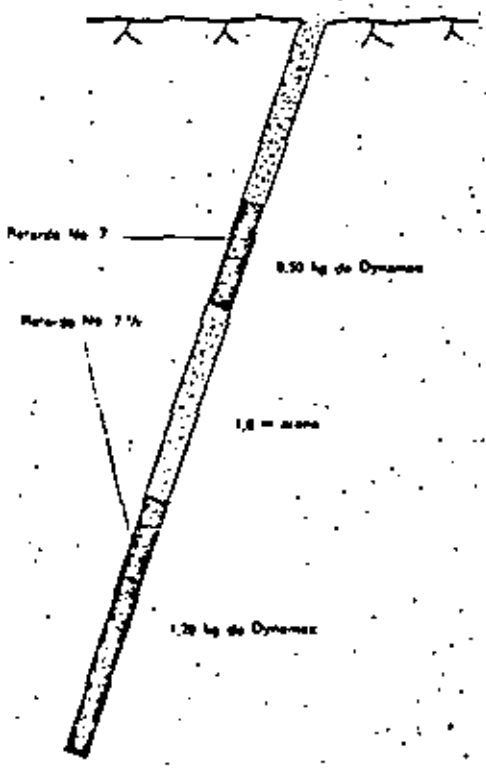

Fig. 13.3.3

En la primera hilera de barrenos, la carga se ajusta especialmente en su tramo superior a la *piedra* real, con lo que generalmente puede reducirse la carga.

21: Perforación por hilera = Número de barrenos por hilera × Profundidad del barreno = 13 × 4,1 = 53,3 m

$$\text{Perforación específica} = \frac{\text{Perforación por hilera}}{\text{Volumen por hilera}} = \frac{53,3}{52,5} = 1,01 \text{ m/m}^3$$

Resumen de los datos fundamentales

Altura banco	Profdad. barrenos	Piedra	Espaciamiento	Carga de fondo	Carga de columna		Carga específica	Perforación específica
K	H	V_1	E_1	Q_b	Q_p	Q_{pL}	q	b
m	m	m	m	kg	kg	kg/m	kg/m³	m/m³
3,5	4,1	1,00	1,25	1,20	—	—		
				0,50	—	—	0,42	1,01

Voladuras en la zona próxima a edificios, servicios, o instalaciones

Cuando la voladura ha de efectuarse a una distancia de muy pocos metros de un edificio, el peligro de que se produzcan daños es máximo. La perforación y carga debe realizarse aquí con un cuidado especial, para no arruinar en los últimos metros el resultado de una operación que ha estado controlada.

A distancias de menos de 5 m, la onda de choque en el terreno sólo es amortiguada en cuantía insignificante, por lo que, en general, no debe pensarse que los valores de la Tabla vayan a ser demasiado desfavorables.

Las fisuras y diaclasas de la roca pueden dar origen a sorpresas imprevistas en su entorno inmediato, al ser desplazadas las capas superficiales de la roca por las fuerzas originadas al penetrar los gases resultantes de la explosión en dichas fisuras y diaclasas.

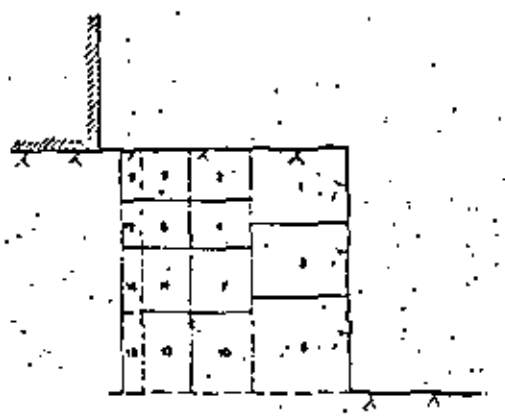

Fig. 13.3.4

Es importante que las pegas que se detonen muy próximas a edificaciones tengan rotura libre, pues ello reduce el peligro de levantamiento de la roca superficial. Esta misma norma es aplicable a los recortes, en los que no se obtiene un buen resultado si los barrenos del contorno no tienen la posibilidad de romper fácilmente.

En los barrenos de la zona más sensible, las cargas de columna deben ser débiles, de modo que desprendan la roca evitando la rotura hacia atrás.

El ejemplo que se expone a continuación se refiere a la voladura de los últimos cinco metros más próximos a una casa cimentada sobre roca firme. La velocidad de vibración admitida es v = 70 mm/seg. La altura del banco es de 5 m.

Tramo entre 5 y 3 m

Carga adecuada 0,2 kg/barreno

Piedra: $V_1 = 0{,}6$ m
Espaciamiento: $E_1 = 0{,}8$ m
Altura del banco: $\frac{5}{3} = 1{,}65$ m
Profundidad de los barrenos: 2,0 m
Carga de fondo: 0,10 kg Dynamex
Carga de columna: 0,22 kg de Gurit de 17 mm (0,16 kg Dynamex)
Número máximo de hileras de barrenos: 3
Esto implica que en esto tramo se realiza un recorte normal.

Tramo entre 3 y 2 m

Carga aproximada 0,15 kg/barreno

Piedra: $V_1 = 0{,}5$ m
Espaciamiento: $E_1 = 0{,}7$ m
Altura del banco: $\frac{5}{4} = 1{,}25$ m
Profundidad de los barrenos: 1,6 m
Carga de fondo: 0,05 kg Dynamex
Carga de columna: 0,22 kg Gurit de 17 mm (0,16 kg Dynamex)
Número máximo de hileras de barrenos: 2.
Lo elevado de la carga hace necesario emplear elementos de *protección*, pero es importante desprender la roca.

Tramo entre 2 y 1 m

Carga aproximada: 0,1 kg/barreno

Piedra: 0,4 m
Espaciamiento: 0,5 m
Altura del banco: 1,25 m
Profundidad de los barrenos: 1,6 m
Carga de fondo: 0,05 kg
Carga de columna: 0,10 kg de Gurit de 11 mm (0,07 kg de Dynamex)
Número máximo de hileras de barrenos: 2

Tramo entre 1,0 y 0,5 m — zona con espaciamientos muy densos

Este tramo toma la forma de una roza con gran densidad de perforación; espaciamientos de 0,15 m o tal vez 0,20 m. El mismo método se utiliza incluso en el caso de que la voladura continúe justamente hasta el límite del edificio.
Piedra: 0,5 m
Espaciamiento: 0,15 m
Altura del banco: 1,25 m
Profundidad de los barrenos: 1,6 m
Carga de fondo: 0,025 kg Dynamex
Carga de columna: 0,15 kg de Gurit de 11 mm (0,10 kg Dynamex).
Número de hileras de barrenos: 1

Obsérvese que los barrenos de este último tramo están completamente cargados, por lo que es esencial una protección total. La onda de choque del terreno ve reducida su intensidad al ser cortada la roca.

La medición de unos valores elevados de vibración del terreno en un punto muy próximo a una voladura que se realice muy cerca de un edificio tiene un significado totalmente distinto del caso en que tales valores son medidos a una distancia mayor. Las cargas pequeñas dan un amortiguamiento más rápido de la onda de choque, y no afectan al conjunto del edificio de la misma manera.

En la figura se muestra la conveniencia de preparar la voladura de modo que las pegas tengan rotura libre en la zona de fondo. No se recomienda emplear tacos de arena, al menos en el caso de distancias inferiores a 4 m.

Como resumen, y basándome en la experiencia recogida, me gustaría subrayar el hecho de que la ejecución del trabajo con unos cuidados que pueden incluso parecer exagerados está siempre justificada, dentro del área más inmediata a los edificios a que nos hemos referido, si es que se quieren evitar con un margen holgado de seguridad todo tipo de daños.

13.4 VOLADURA CONTROLADA EN ZANJAS

Las voladuras para excavación de zanjas se realizan en su mayor proporción en el interior de áreas edificadas. En muchos casos, las zanjas han de llegar justamente hasta el límite de un edificio, o discurrir a lo largo de uno de sus costados. En la sección 7.1 se consideró la excavación de zanjas mediante voladuras normales, sin especial consideración de las vibraciones originadas en el terreno.

Dado que, en relación a su volumen, las voladuras en zanjas han originado daños en gran escala, debe prestarse una atención especial a la planificación de las mismas en zonas edificadas. Es posible que los riesgos que encierran estas voladuras hayan sido subestimados.

En 1970, Nitro Consult llevó a cabo una serie de estudios con el objeto de determinar los factores que influyen sobre la magnitud de las vibraciones del terreno en las voladuras en zanja. Al mismo tiempo se elaboró un resumen de datos correspondientes a unas 80 mediciones con cargas y distancias conocidas, el cual mostró una buena concordancia con la relación teórica que se había utilizado. Pudo apreciarse que el amortiguamiento de las vibraciones del terreno que con frecuencia se produce en las voladuras, raramente podía observarse en el caso de las voladuras en zanja; por lo que concierne a las vibraciones del terreno, el confinamiento de los barrenos se mostraba muy desfavorable.

En el resumen de dichos resultados, que se muestra aquí en forma de un diagrama, se indica asimismo la inclinación de los barrenos. El diagrama muestra que la velocidad de vibración depende de esta inclinación en el caso de *piedra* constante y cargas coordinadas (cargas de detonación instantánea). Debe hacerse notar que las cargas coordinadas empleadas en los ensayos *excedían a las admisibles* para distancias de 2,0 m, lo que explica los elevados valores registrados incluso en el caso de inclinación favorable de los barrenos.

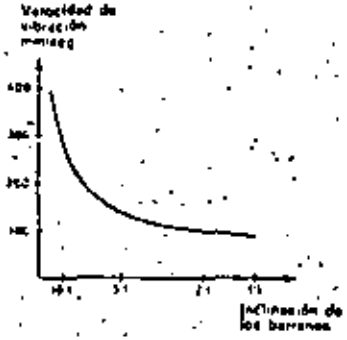

Fig. 13.4.1

Los resultados de la medición en la serie de ensayos realizados muestran una buena concordancia con la Tabla de distancias-cargas para una inclinación normal de los barrenos (3:1). En el caso de inclinaciones más acusadas, u otras condiciones de constricción (barrenos fallidos, etc.) puede obtenerse un aumento significativo de la velocidad de vibración.

El cálculo de la carga en la voladura controlada en zanjas puede hacerse por el mismo procedimiento que en las voladuras en banco. También aquí la base del cálculo es la carga específica en kg/m³.

Para el empleo de dicho procedimiento de cálculo se han confeccionado las Tablas siguientes:

Anchura de la zanja: 0,8—1,0 m. No. de barrenos por ancho de zanja: 3

Barrenas de la serie 11; 34—30 mm. Inclinación barrenos 3:1.

Piedra práctica V_1 m	Carga de fondo en kg barreno para diversas profundidades. Profundidad de la zanja m					Carga de columna Concentración kg m	Composición
	1,0	1,5	2,0	2,5	3,0		
0,40	0,05	0,10	0,15	0,20	0,25	0,08	Gurit 11 mm (**)
0,50	0,08	0,13	0,18	0,23	0,28	0,12	Gurit 11 mm + ¼ cartucho Dynamex 22 mm
0,60	0,10	0,15	0,20	0,25	0,30	0,18	Gurit 17 mm
0,70	0,12	0,17	0,23	0,28	0,35	0,23	Gurit 17 mm + ½ cartucho Dynamex 22 mm
0,80 (*)	0,13	0,20	0,27	0,32	0,40	0,25	½ cartucho Dynamex + separador de madera de 10 cm, o bien Gurit 17 mm + ½ cartucho de Dynamex
Carga específica en kg/m³ para una sección teórica rectangular	0,80	0,90	1,00	1,10	1,20		

(*) $V_1 = 0{,}75$ m para una profundidad de zanja de 2,5—3,0 m.

(**) Encima de las cargas alargadas de Gurit debe ir colocado un tapón antes de añadir el material de retacado. Por lo que respecta a las vibraciones del terreno, una carga relativamente elevada resulta favorable, pero requiere el empleo de un material de protección eficaz.

En la Fig. se muestra la distribución apropiada de los barrenos.

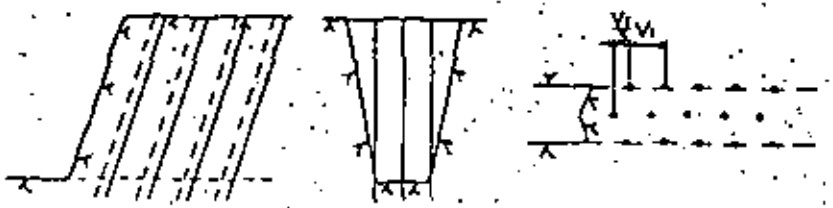

Fig. 13.4.2

Anchura de la zanja: 1,5—2,0 m No de barrenos por ancho de zanja: 3 y 4

Barrenas de la serie 11; 34—30 mm. Inclinación barrenos 3:1.

Piedra práctica V_1 m	Carga de fondo en kg/barreno para diversas profundidades de la zanja m					Carga de columna Concentración kg/m	Composición
	1,0	1,5	2,0	2,5	3,0		
0,40	0,08	0,13	0,18	0,23	0,30	0,08	Gurit 11 mm **).
0,50	0,11	0,16	0,21	0,27	0,35	0,12	Gurit 11 mm + ¼ cartucho Dynamex
0,60	0,15	0,19	0,24	0,31	0,40	0,18	Gurit 17 mm
0,70	0,18	0,24	0,29	0,37	0,47	0,23	Gurit 17 mm + ½ cartucho Dynamex
0,80 *)	0,22	0,30	0,37	0,45	0,55	0,25	½ cartucho Dynamex + separador de madera de 10 cm, o bien Gurit 17 mm + ½ cartucho de Dynamex
Carga específica en kg/m³ para una sección teórica rectangular	0,75	0,78	0,81	0,84	0,87		

(*) Para una profundidad de la zanja de 2,5—3,0 m, la *piedra* disminuye hasta $V_1 = 0,75$ m.

(**) Debe colocarse un taco por encima de las cargas de Gurit antes de añadir el material de retacado.

Estas Tablas facilitan el cálculo de la perforación y la carga en los casos en que han detonarse en consideración las vibraciones del terreno, lo que implica que frecuentemente ha de reducirse la carga por barreno en relación con los valores normales. La carga más reducida lleva consigo la necesidad de reducir también el espaciamiento de los barrenos.

La base para los cálculos es la máxima carga de detonación instantánea (carga coordinada) que puede emplearse. En las secciones 13.1 y 13.2 se han descrito los problemas relativos a las vibraciones del terreno.

Ejemplo

Se ha de efectuar una voladura para una zanja a una distancia de 5 metros de un edificio de buena calidad de construcción, cimentado sobre roca firme.

La vibración permisible es $v = 70$ mm/seg., lo que implica que puede emplearse el nivel de carga 0,03 (véase la Tabla de distancias-cargas).

La zanja debe tener una anchura de 2,0 m en su fondo, y una profundidad aproximada de 2,0 m.

Procedimiento de cálculo

1. La Tabla de distancias-cargas, para el nivel 0,03, da una carga admisible de 0,36 kg.
2. Se hace entonces una comprobación para averiguar si pueden utilizarse voladuras ordinarias. La Tabla para zanjas del capítulo 7.1 muestra que, con una profundidad de 2,0 m y una anchura de 2,0 m, la cantidad de explosivo necesaria es de $0,35 + 0,35 = 0,70$ kg/barreno.
   Esto significa que no pueden realizarse voladuras normales, por lo que habrán de perforarse los barrenos con menores espaciamientos, y usar cargas más reducidas.
3. Se determina el número de barrenos por ancho de zanja: Para una anchura de 2,0 m, hacen falta 4 barrenos.
4. Se determina la carga específica necesaria: Según la Tabla, para una profundidad de 2,0 m, la carga específica adecuada es aproximadamente de 0,81 kg/m³.
5. Se calcula la *piedra* basándose en la carga posible por barreno y en la carga específica necesaria:
   Carga admisible por barreno: 0,35 kg
   Carga específica: 0,81 kg/m³
   Número de barrenos: 4
   Carga por hilera de barrenos: $4 \times 0,35 = 1,44$ kg

$$\frac{\text{Carga por hilera}}{\text{Anchura} \times \text{Profundidad zanja} \times V_1} = \text{Carga específica}$$

$$\frac{1,44}{2,0 \times 2,0 \times V_1} = 0,81$$

Piedra $V_1 = 0,44$ m = aprox. 0,4 m.

6. La profundidad de los barrenos se toma de la Tabla de la sección 7:1: Para una profundidad de zanja de 2,0 m, la profundidad de perforación necesaria es de 2,4 m.

7. La carga de *fondo* se calcula con ayuda de la Tabla: Para una *piedra* de 0,4 m, el valor que indica la misma es de 0,18 kg.

8. Cálculo de la magnitud y concentración de la carga de columna:
   Carga de columna = Carga admisible por barreno — Carga de fondo = = 0,36 — 0,18 = 0,18 kg
   De acuerdo también con la Tabla, la concentración de la carga de columna para una *piedra* de 0,4 m es de 0,08 kg/m.

9. Una composición apropiada de la carga puede consistir en Gurit de 11 mm.
   La longitud de la carga será $\frac{\text{Concentración de la carga}}{\text{Peso de la carga}} = \frac{0,18}{0,08} = 2,3$ m
   Dado que la zona de retacado ha de ser como mínimo igual a la *piedra*, la longitud de la carga de columna ha de ser corregida al valor:
   Profundidad del barreno — (Longitud de la carga de fondo + Zona de retacado) = 2,4 — (0,2 + 0,4) = 1,8 m (cuatro tubos de carga de 0,46 m cada uno).

Resumen de los cálculos:

Profdad. zanja m	Profdad. barrenos m	Piedra m	Espaciamiento m	Carga de fondo kg	Carga de columna kg	Composición
2,0	2,4	0,4	0,67	0,18	0,20 *)	Gurit de 11 mm

(*) Cada carga alargada de Gurit pesa 0,05 kg. Normalmente se cuenta con el hecho de que con Gurit se originan unas menores vibraciones que con una cantidad equivalente de Dynamex.

Siguiendo el mismo principio básico mostrado en este ejemplo pueden realizarse los cálculos para diferentes profundidades de zanja, cargas admisibles, etc.

Puesto que toda reducción considerable de la carga de fondo implica un significativo incremento en el trabajo de perforación, en ciertos casos puede

Fig. 13.4.3

ser conveniente servirse de otras alternativas distintas a la que se acaba de exponer. Existen otros dos métodos aplicables:

Dividir la carga del barreno mediante tacos separadores de arena.
Dividir la zanja en varios bancos.

Estudios recientemente realizados muestran que la longitud que debe tener un taco de arena para evitar la propagación indeseada entre las cargas es considerablemente mayor que los valores que hasta ahora se aplicaban, debiendo ser como mínimo de 1,0 m incluso en el caso de barrenos de pequeño diámetro.

La necesidad de que exista además en el barreno una zona de retacado obliga a no permitir el empleo de cargas con tacos de arena para barrenos de profundidad inferior a 2,0 m, es decir, *profundidades de zanja de menos de 1,5 m.*

Para las mismas condiciones de partida que en el ejemplo anterior, los cálculos de la carga por el método de los tacos de arena pueden efectuarse del modo siguiente:

1—2. Se procede del mismo modo que en el ejemplo anterior.

3. La *piedra* V_1 puede determinarse a partir de la máxima carga admisible y con ayuda de las Tablas de esta sección. Para la carga admisible de 0,36 kg, la Tabla correspondiente a 2,0 m de anchura y profundidad de zanja da una *piedra* de 0,80 m.

4. La profundidad de los barrenos se determina a partir de la Tabla de la sección 7:1: Para una zanja de 2,0 m de profundidad, los barrenos serán de 2,4 m.

5. Se determina seguidamente la carga por encima del tapón de arena tomando como referencia la longitud residual de barreno considerada como si fuera la profundidad total del mismo:

Longitud residual = Profundidad del barreno — (Longitud de la carga de fondo + Longitud del taco de arena) = 2,4 — (0,4 + 1,0) = 1,0 m.
La carga de fondo, para una profundidad de barreno de 1,0 m (que correspondería aproximadamente a una profundidad de zanja de 0,8 m), y 0,8 m de *piedra*, es, según la Tabla, de 0,22 kg.
En los casos en que *el fondo del barreno no esté confinado* (frente libre), la carga puede ser *reducida aproximadamente a ¾ del valor* indicado en la Tabla. En este caso la carga de fondo será igual a ¾ × 0,22 = 0,17 kg/barreno, o aproximadamente 0,20 kg/barreno.

6. Se verifica si se necesita carga de columna, y consecuentemente, si el valor de la carga admisible es tal que permita más carga, o que sea necesario un reajuste del valor de la carga admisible y del emplazamiento de los barrenos.
La zona de retacado será 1,0 — Longitud de la carga de fondo (por encima del taco de arena).
Zona de retacado recomendable = 1,0 — 0,20 = 0,80.
De la carga admisible quedan ahora solamente 0,36 — 0,20 = 0,16 kg.
En este caso no hay espacio para más carga de columna, pero si el barreno fuese de mayor longitud, habría sido posible cargar una zona suplementaria de 0,16/0,25 = aproximadamente 0,60 m.

Resumen de los cálculos:

Carga parcial	Profdad. zanja	Profdad. barreno	Piedra	Espaciamiento	Carga de fondo	Carga de columna	
	m	m	m	m	kg	kg	Comp.
I	2,0	2,4	0,8	0,67	0,36	—	—
II	aprox 0,8	1,0	0,8	0,67	0,20	—	—

Si ello es posible, frecuentemente resulta ventajoso aumentar algo la carga de fondo con objeto de compensar la relativamente grande zona del barreno sin carga debido al taco de arena. Por otra parte, si la roca es difícil de volar, la *piedra* puede reducirse.

Debe tenderse a que el retacado entre las cargas situadas en un mismo barreno sea lo más corto posible. El esquema de tiro que se muestra en la Fig. 13.4.4, con detonadores de microretardo del tipo VA, en donde el intervalo de retardo entre los medios números es de 13 ms, resulta una disposición apropiada. Si los detonadores empleados tienen retardos más largos, puede ser recomendable emplear dos detonadores con el mismo número de retardo en el mismo barreno.

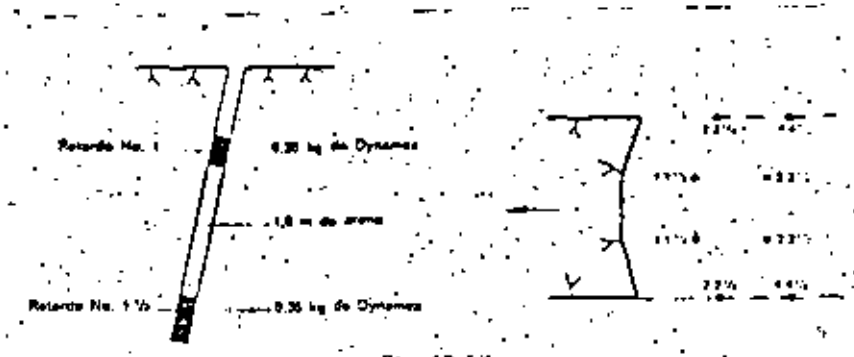

Fig. 13.4.4

En roca dura y con zanjas estrechas, el método de *cargas separadas con tacos de arena puede no resultar adecuado.*
La subdivisión de la zanja en varios bancos puede ser llevado a la práctica según el procedimiento siguiente:

1—2. Se procede del mismo modo que en el primer ejemplo.

3. Se utiliza la Tabla de la sección 7.1 para hacer una estimación de la profundidad (altura de banco) que puede darse a cada fase, a partir de la carga admisible y con la mínima cuantía posible de perforación:
Carga admisible: 0,36 kg.
Según la Tabla, la profundidad máxima: 1,2 m, requiere 0,15 + 0,20 = = 0,35 kg/barreno.
En este caso la zanja puede ser dividida en dos bancos, con una profundidad de 1,0 m cada uno.

Resumen de los cálculos:

Profdad. zanja	Profdad. barrenos	Piedra	Espaciamiento	Carga de fondo	Carga de columna	
m	m	m	m	kg	kg	Concentración
1,0 (2 bancos)	1,4	0,8	0,67	0,15	0,10	0,25 kg/m

Si el desescombro se realiza por fases, ambos bancos pueden ser utilizados a un mismo tiempo.

Los tres ejemplos expuestos muestran cómo pueden adoptarse métodos diferentes para el cálculo y la realización de la voladura controlada en zanjas. — El método de los tacos de arena con cargas separadas se ha hecho conside-

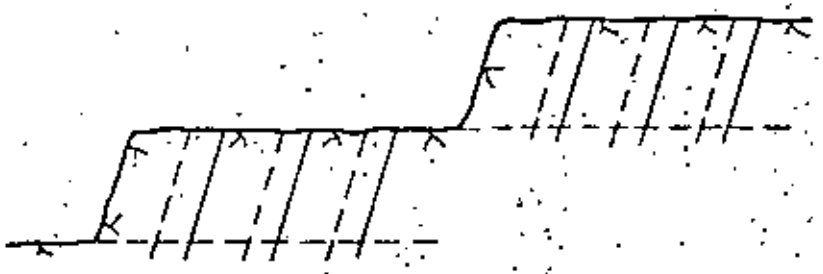

Fig. 13.4.5

rablemente más complicado a medida que se han ido adquiriendo más conocimientos sobre la longitud necesaria de los tacos de arena. En tipos de roca duros y tenaces, el método puede ser difícil de aplicar sin una considerable compensación de carga. Por otra parte, este método no es recomendable cuando la voladura se efectúa a menos de 4 metros de cimentaciones existentes.

En la proximidad inmediata de las cimentaciones, existe el peligro no sólo de vibraciones del terreno, sino también el que se deriva de la penetración de los gases resultantes de la explosión al interior de las grietas que puedan existir, con el consiguiente posible desplazamiento o levantamiento de zonas de la superficie de la roca. Si estos fenómenos afectan a la cimentación de un edificio, los daños pueden ser graves.

Cuando se están realizando voladuras de este tipo, es importante que las cargas de columna estén formadas por cargas débiles de tipo Gurit.

Una larga zona de retacado, por su parte, resulta completamente inconveniente, y puede dar a las cargas la posibilidad de provocar el levantamiento de la superficie de roca circundante, fenómeno que es deseable evitar.

13.5 VOLADURA CONTROLADA EN TUNELES

Al hablar de voladura controlada a propósito de los túneles, se hace referencia a las voladuras que se realizan en los túneles de tal modo que se reducen los riesgos de vibraciones del terreno, ondas de choque aéreas, o proyección de piedras. Este tipo de voladuras constituye una parte importante de la tecnología de las mismas, pues es una proporción muy grande de túneles la que se construye bajo zonas edificadas.

Cuando un túnel pasa por debajo de edificios o de otras instalaciones sensibles, las vibraciones del terreno constituyen el problema fundamental. Además, al abrir un túnel se producen ondas de choque aéreas y proyección de fragmentos de roca, en muchos casos en lugares descubiertos sin ninguna protección.

Por lo que respecta a las operaciones iniciales de voladura en túneles, con frecuencia surgen problemas mineros, derivados del limitado recubrimiento de roca y de la necesidad de refuerzo y sostenimiento de la misma. Cuando se realizan las operaciones iniciales de voladura en un túnel situado en el interior de un área edificada, conviene poner en práctica las siguientes medidas:

Voladuras controladas, limitando la profundidad de los barrenos, la cuantía de las cargas, y el número de barrenos por pega.

Utilización de encendido con microrretardos.

Empleo de material de protección colgado.

Medición de las vibraciones del terreno y de las ondas de choque aéreas.

En un principio fue el cuele en abanico el más utilizado en las voladuras controladas iniciales para la apertura de un túnel; sin embargo, se ha demostrado que los cueles paralelos de gran barreno central, y preferiblemente con dos grandes barrenos centrales, resultan muy eficaces. En cuanto a la perforación, su profundidad se limita a una longitud de entre 1,0 y 1,6 m, dependiendo de la ubicación del lugar de la voladura y de las condiciones técnicas de la roca. La primera pega consiste en un cuele formado por un solo barreno; a continuación suelen detonarse dos barrenos de cuele por pega. En el momento debido, se aumenta el número de barrenos del contracuele y de destroza por pega, dependiendo este incremento del peso del material de protección y de su capacidad para mantenerse fijo en su posición durante la voladura. No es recomendable aumentar demasiado el número de barrenos por pega, ya que, en un lugar suficientemente sensible, un par de barrenos en exceso es bastante para levantar el material de protección. Ha de procederse con precauciones incluso después del primer avance, de modo que el material de protección empleado sea capaz de interceptar las ondas de choque del aire y las proyecciones.

Lo más seguro es utilizar el encendido con microrretardos. Empleando encendido con retardos simples, existe el riesgo de que el primer retardo levante el material de protección, tras lo cual pueden producirse proyecciones.

El material de protección empleado ha de tener un cierto peso. Se recomienda el uso de pantallas petadas de caucho o pantallas colgadas de rollizos. Para interceptar las esquirlas de roca y proporcionar protección contra las ondas de choque atmosféricos, es conveniente utilizar como elementos suplementarios lonas alquitranadas o fieltro industrial.

Debe usarse material de protección en todas las pegas hasta que el túnel haya avanzado la distancia suficiente como para que las ondas de choque aéreas no posean ya efecto alguno, lo cual puede suponer, en el caso de túneles estrechos, longitudes considerables.

Si se realizan mediciones de las vibraciones y ondas de choque aéreas, las voladuras pueden ser ajustadas de acuerdo con los valores que se obtengan. Como la onda de choque atmosférica origina vibraciones en los edificios próximos, la componente horizontal de la onda de choque puede ser de la mayor importancia en las voladuras de este tipo.

La magnitud de la onda de choque aérea puede calcularse teoricamente a partir de las cargas, los intervalos de retardo, y la distancia. La estimación más difícil es la del factor de confinamiento que ha de incluirse cuando el explosivo está contenido en el interior de un barreno. A medida que se dispone de más datos empíricos recogidos a través de mediciones de estas ondas de choque, la precisión de los cálculos de esta clase puede ir siendo mejorada.

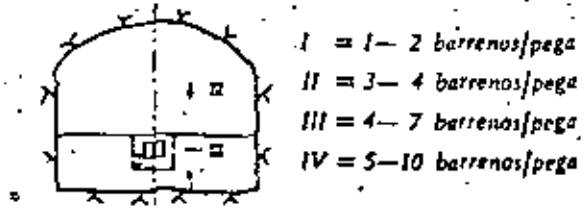

Fig. 13.5.1

En la figura se muestra el esquema operativo para la apertura de un túnel en un área edificada y muy próximo a los edificios. Los barrenos están distribuidos con pequeños espaciamientos, con lo que la carga en cada uno de ellos puede ser limitada.

En el caso de problemas de vibraciones del terreno, a menudo es preciso perforar los barrenos con una distribución densa, y limitar el avance por pega, a fin de reducir la cuantía de la carga de detonación instantánea (véase la sección 13.1).

En los cálculos de voladuras en túnel con limitaciones impuestas por las vibraciones, el procedimiento seguido en principio es el mismo que para las voladuras en banco y en zanjas. A partir de la carga admisible de detonación instantánea, los valores de la profundidad de perforación, carga por barreno, y los planes de perforación y tiro se reajustan de forma que las vibraciones del terreno satisfagan las demandas impuestas. En el caso de voladuras en túnel, normalmente puede adaptarse el plan de perforación a condición de que la carga coordinada no exceda a la carga por barreno. La diseminación de los números de retardo reparte las vibraciones del terreno por toda la roca circundante.

Tipo de detonador	Número de retardo	Coordinación dentro del retardo
TE/MS	1—12	1/2
TE/MS	13—18	1/3
VA/MS	1—10 (*)	1/2
VA/MS	11—20	1/3
VA/MS	24—80	1/4
TE, VA/HS	1—12	1/6
Instantáneo 0		1

(*) Existen medios números entre 1 y 10: 1 ½, 2 ½, etc.

Algunos cueles, como por ejemplo los cueles en V, no resultan adecuados en los casos de problemas por vibraciones del terreno cuando existe riesgo de coordinación de las cargas de un gran número de barrenos del cuele. Lo mismo cabe decir de los cueles "quemados" de diversos tipos. El cuele en abanico sí puede ser utilizado, fundamentalmente en túneles de gran sección; para secciones más estrechas, en las que resulta complicado perforar los barrenos en ángulo, pueden usarse perfectamente cueles paralelos de gran barreno central. Anteriormente se pensaba que este tipo de cueles originaba unas vibraciones muy intensas; los resultados de las mediciones llevadas a cabo a lo largo de un periodo de cinco años han demostrado que ésto no es cierto si el cuele funciona correctamente.

En voladuras que hayan de hacerse con una especial precaución, es preferible perforar dos grandes barrenos centrales en el cuele; éste reduce el confinamiento y con ello el peligro de roturas fallidas. Existe también la posibilidad de disminuir la distancia entre los centros del barreno central y los otros barrenos del cuele, reduciendo así la carga por metro. Sin embargo, ésto no es generalmente necesario; la reducción de la profundidad de perforación suele ser bastante.

El cálculo del cuele en abanico de la sección 9.4 incluye un importante exceso de carga, que normalmente está motivada por la zona de contracuele del túnel. En voladuras controladas, es preciso en muchos casos quedarse mucho más cerca del límite de rotura. Cuando la sección del túnel sea grande, puede ser necesario dividirla en una serie de voladuras, con objeto de evitar un plan de tiro con cargas coordinadas excesivamente grandes.

Los cálculos de una voladura controlada con cuele en abanico pueden hacerse basándose en los mismos valores utilizados para las voladuras en zanjas.

Profundidad de la carga m	Carga específica kg m³
1,0	0,80
1,2	0,90
2,4	1,00
3,2	1,20

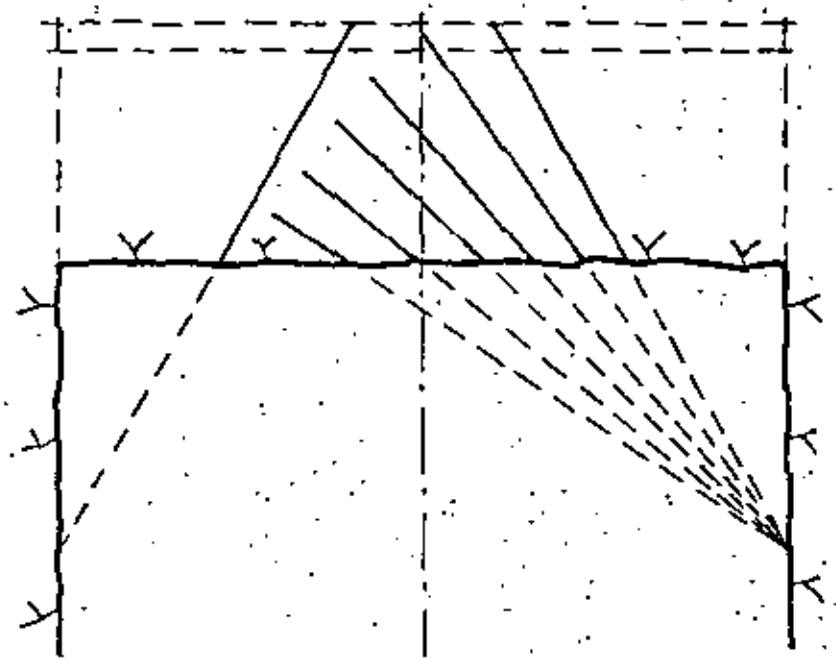

Fig. 13.5.2

En la voladuras controladas se emplean generalmente barrenos de pequeño diámetro. Para barrenos de 30 mm puede hacerse uso de la siguiente Tabla:

Profdad. pega m	Piedra m	Carga de fondo kg	Carga de columna kg/m	Altura del cuele m	No. barrenos por hilera	Zona de retacado m
1,2	0,50	0,10—0,20	0,16	1,2	3	0,4
1,6	0,70	0,25—0,40	0,40	1,5	3	0,5
2,4	0,70	0,25—0,60	0,40	1,5	3	0,5
3,2	0,50	0,40—0,65	0,40	1,6	3	0,5

Los valores de las cargas se ajustan de acuerdo con la experiencia, para obtener la menor carga posible con un efecto de rotura aceptable.

En las voladuras controladas, los barrenos de destroza han de ser tan poco profundos, o la *piedra* tan pequeña, que no puede aplicarse el procedimiento de cálculo mostrado anteriormente en el capítulo 9 para las voladuras en túneles.

En la Tabla que se incluye a continuación se recogen los valores que pueden servir de guía para la perforación y la carga:

Clase de barreno	Profdad. barreno m	Piedra m	Espaciamiento m	Carga de fondo kg	Carga de columna kg	Carga de columna kg/m	Zona de retacado m
Destroza	1,0	0,40	0,50	0,15	0,11	0,18	0,40
Piso	1,0	0,40	0,50	0,20	0,11	0,18	0,30
Destroza	1,6	0,40	0,50	0,20	0,22	0,18	0,40
Destroza	1,6	0,50	0,60	0,30	0,22	0,18	0,40
Destroza	1,6	0,60	0,70	0,40	0,32	0,24	0,40
Destroza	1,6	0,70	0,85	0,60	0,20	0,30	0,40
Piso	1,6	0,70	0,85	0,60	0,30	0,40	0,20

Frecuentemente se ha encontrado más racional evitar unos avances por pega excesivamente cortos, perforando en lugar de ello los barrenos con un espaciamiento más denso y una carga reducida en cada uno.

Cuando se realizan voladuras en la inmediata proximidad de instalaciones particularmente sensibles, puede ser conveniente seguir de modo continuado todo el proceso a través de mediciones de las vibraciones del terreno.

En muchos casos se ha encontrado que los valores reales de las vibraciones del terreno han sido más favorables que los deducidos de las relaciones teóricas.

Si la voladura se ajusta a los resultados de las mediciones tomadas, ello implica la consecución de una velocidad óptima de excavación sobre la base del nivel de tensiones admisible a que se ha hecho mención anteriormente.

13.6 MEDIDAS PARA EVITAR LAS PROYECCIONES

Los problemas relativos a las proyecciones debidas a las voladuras en el interior de áreas edificadas exigen que se les preste la mayor atención. Son varios los factores que influyen sobre el riesgo de proyecciones imprevistas:

Fallas, grietas, y zonas de debilidad naturales de la roca
Precisión de la perforación
Distribución y magnitud de la carga
Configuración del plan de encendido
Protección

Además del empleo de los materiales de protección ordinarios, pueden tomarse otras medidas destinadas a este mismo fin:

Dejar roca previamente arrancada ante la primera hilera de barrenos.

Emplear un cálculo especial de cargas para la primera hilera de barrenos.

En las secciones 5.4, 8.1, y 8.2 puede encontrarse una descripción más detallada de las causas de las proyecciones y las posibilidades de evitarlas. En el capítulo 8, Protección, se sugieren los materiales adecuados para diversos trabajos de voladura.

Es preciso señalar que, si bien el mayor riesgo de daños por proyecciones corresponde al caso de que la voladura se efectúe en un área edificada, también es preciso evitar las proyecciones en las voladuras para producción minera.

El área que ha de ser evacuada en cada caso depende de los métodos utilizados.

En Suecia, cuando se realizan voladuras en un área edificada, es preciso seguir no sólo las instrucciones del Departamento de Seguridad e Higiene del Trabajo, sino también las normas y regulaciones locales.

Si se toman en consideración todos los factores que pueden dar origen a proyecciones en el momento de planificar y de realizar voladuras en áreas edificadas, y se ponen en práctica las necesarias medidas de protección, debe ser posible efectuar dichas voladuras con un riesgo de proyecciones muy reducido. Para reducir aún más este riesgo, es preciso disponer de mayores conocimientos sobre la tecnología de las voladuras, así como un mayor trabajo de investigación y desarrollo.

13.7 PLANIFICACION DE VOLADURAS EN AREAS EDIFICADAS

La ejecución de voladuras en zonas edificadas requiere una planificación especialmente cuidadosa que comprenda todos los factores que han de ser tomados en consideración. Cuando se están proyectando voladuras para producción, el objetivo principal es la comparación entre los diversos métodos y el cálculo de capacidades, para delimitar desde el punto de vista económico las diferentes alternativas. En las voladuras en zonas edificadas, es preciso tener en cuenta si existe responsabilidad frente a los daños que pudieran sufrir las personas o propiedades del entorno.

Durante la fase de proyecto, muchos contratistas efectúan un estudio de los alrededores del lugar de la voladura, e incluyen los resultados de este estudio a la hora de negociar el contrato.

Además de este reconocimiento de los edificios e instalaciones sensibles de las cercanías, se está haciendo cada vez más corriente el determinar los niveles de vibración del terreno permisibles. También se presentan demandas sobre la apariencia de los contornos de roca y otros factores similares. Todo ello facilita la planificación y los cálculos de costes a los subcontratistas, los cuales, por razones de coste y de tiempo, no siempre pueden realizar un reconocimiento detallado del lugar.

En muchos casos, sin embargo, no se dispone de ninguna información sobre el trabajo que se va a realizar, y ha de hacerse a pesar de ello alguna estimación antes de hacer una oferta o — en el caso de que el contratista encargado de la construcción realice él también el trabajo de voladuras — durante la fase de elaboración del proyecto.

Si en todo el trabajo de planificación se emplea un proceder sistemático, existe un menor riesgo de olvidar algún factor importante.

Las normas que se incluyen a continuación pueden ser utilizadas como lista de comprobación antes de efectuar unas voladuras en zona edificada en la que hayan de tenerse en cuenta los edificios e instalaciones sensibles de los alrededores.

Antes de calcular una oferta o en las fases iniciales del proyecto

1. Estudiar los documentos y los planos — Exigir aclaraciones en caso necesario.
2. Inspeccionar el lugar de las voladuras.
3. Estimar los niveles de vibración permisibles para diversas estructuras y edificios. En el caso de algunos objetos especiales, puede ser necesario hacer un estudio para determinar el nivel de vibraciones permisible que resulta apropiado.

4. Hacer una estimación de las mediciones de vibración que van a precisarse y del área que debe ser inspeccionada.
5. Comprobar si existen líneas de conducción de energía eléctrica, cables telefónicos, o sistemas de calefacción, agua, o drenaje, afectados por la voladura proyectada.
6. ?Se necesita algún dispositivo de protección especial?
7. ?Se necesita algún dispositivo de protección contra el ruido?
8. ?Es necesario especificar los momentos adecuados para realizar las voladuras?
9. ?Se requiere utilizar el recorte?
10. Comprobar si la pólizas de seguros contratadas cubren los posibles daños. En caso de necesitarse algún suplemento o asesoramiento, consúltese con la compañía de seguros.
11. ?Es necesario algún refuerzo especial de la roca, o de todo el conjunto?
12. ?Proporciona la roca alguna indicación sobre sus propiedades frente a la perforación y voladura?
13. Considerar los caminos de retirada de la roca arrancada, y los puntos de ataque.

Después de que la inspección preliminar del escenario de la voladura haya proporcionado algunas orientaciones, pueden hacerse cálculos más precisos sobre costes y plan de voladuras:

1. Seleccionar las máquinas que van a utilizarse.
2. Elaborar un plan en el que se especifiquen los niveles límite de carga por lo que respecta a las vibraciones del terreno, de acuerdo con las tablas de distancias y cargas.
3. Preparar los puntos de ataque más idóneos, así como las direcciones de rotura y las fases de trabajo.
4. Calcular el emplazamiento de los barrenos en los diversos tramos.
5. Dividir la zona en diferentes pegas.
6. Elegir un explosivo adecuado.
7. Estimar la magnitud de los dispositivos y materiales de protección necesarios.
8. Estudiar el empleo que se va a dar a la roca arrancada.

Cuando las operaciones llegan a una etapa en la que se otorga una concesión a un subcontratista, o en que el contratista de la construcción se prepara a comenzar su trabajo, es necesario tomar nuevas medidas:

1. Solicitar los permisos de voladuras y almacenamiento de explosivos.
2. Realizar una inspección de los edificios e instalaciones, y ensayos de presión de los gases de escape en las chimeneas.
3. Concluir los trámites de seguros que sean necesarios.
4. Elaborar un plan de tiro de acuerdo con las exigencias de las leyes de construcción.
5. Comenzar un libro-registro que debe ser rellenado con toda la información concerniente a cargas, encendido, y materiales de protección. Debe ser posible registrar las condiciones de las diversas pegas.
6. Preparar las mediciones de la vibración en los edificios circundantes, y las posibles mediciones especiales para instalaciones sensibles.
7. Desarrollar los sistemas de aviso y señalización de los lugares de disparo y los dispositivos de protección necesarios.
8. Informar a las personas que habiten en la inmediata proximidad de la voladura del hecho de que va a realizarse un trabajo de este tipo.
9. Informar e instruir al personal implicado antes de comenzar las operaciones de voladura.
10. Confeccionar un plan de transportes.

13.8 ASPECTO FINANCIERO DE LAS VOLADURAS CONTROLADAS

La voladura controlada en bancos, zanjas, y túneles, presenta evidentemente unos costes más elevados que las voladuras convencionales, en las que no se impone ninguna limitación.

En el caso de voladuras a cielo abierto, en que es preciso tomar en consideración las vibraciones del terreno y el riesgo de proyecciones, los principales factores que elevan el coste de la voladura son los siguientes:

Aumento de la perforación específica.
Aumento de los costes de la operación de carga.

Mayor número de operaciones de voladura.
Mayor número de barrenos por unidad de volumen de roca.
Materiales de protección.
Otras medidas protectoras.
Inspecciones.
Mediciones de la vibración del terreno.
Costes de los seguros.
Trabajo de supervisión y planificación más intensivo.

Las voladuras controladas pueden ofrecer también algunos aspectos favorables desde el punto de vista económico:

Menor sobreexcavación.
Fragmentación más pequeña.

Puede resultar difícil hacer un cálculo del incremento de costes de la voladura controlada usando un método general, pues las condiciones determinantes varían en cada caso particular. Los factores que influyen sobre el coste del trabajo puro de voladura pueden ser evaluados con base en:

Las cargas coordinadas admisibles.
La perforación específica.
Las cargas específicas.
El número de barrenos.
Las áreas de limpieza en los bancos.
Los materiales de protección.
La capacidad de trabajo por unidad de tiempo.

En la Fig. 13.8.1 se muestra la influencia de las limitaciones concernientes a las vibraciones del terreno sobre el trabajo puro de voladura. En el diagrama se presupone el empleo de barrenos de pequeño diámetro y una altura de banco limitada. Puede apreciarse que a una distancia de menos de 10 m de edificios e instalaciones, los costes son particularmente elevados. Si esta parte del trabajo constituye solamente una fracción de una obra mucho mayor en la que las voladuras junto a edificaciones forman únicamente una proporción limitada del volumen total de voladuras a efectuar, el cuadro sería completamente diferente.

Es preciso señalar, sin embargo, que en la inmediata proximidad de edificios e instalaciones el control de la voladura posee la máxima importancia; caso de no ser éste suficiente, es el resultado total del conjunto de la operación el que puede quedar completamente arruinado.

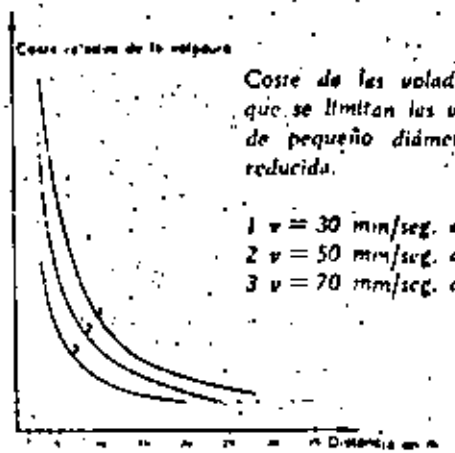

Coste de las voladuras controladas en las que se limitan las vibraciones, con barrenos de pequeño diámetro y altura de banco reducida.

1 v = 30 mm/seg. admisibles
2 v = 50 mm/seg. admisibles
3 v = 70 mm/seg. admisibles

Fig. 13.8.1

Casos prácticos

Se trata de la voladura controlada realizada en un caso en que las condiciones imperantes fueron modificadas posteriormente debido a una instalación sensible a las vibraciones. Unos cálculos precisos realizados para determinar el efecto de la limitación de vibraciones sobre las operaciones de voladura, con una altura de banco de 2,5 m y una distancia de 1,25 m, arrojaron el siguiente resultado:

Velocidad de vibración admisible (mm/seg.)	Coste relativo
Voladura libre	a
70	2 × a
50	3 × a
35	4 × a

En el caso de voladuras en túneles dentro de un área edificada, las restricciones a la vibración implican un incremento de los costes de voladura.

Los costes suplementarios debidos a primas de seguros, inspecciones, y control de las vibraciones del terreno, pueden añadir sumas considerables. Una variación del nivel freático puede traducirse en daños de difícil predicción.

Sin embargo, el rápido desarrollo de las técnicas de inyección ha supuesto la posibilidad actual de construir túneles a prueba de filtraciones.

La excavación de túneles a sección completa con equipos integrales, ha sido ensayada en Suecia en varios lugares. La elevada resistencia de los tipos de roca que se encuentran en Suecia hace difícil la excavación por estos métodos mecánicos; los ejemplos observables en algunos países, como Italia, muestran que la perforación integral del túnel a través de rocas más blandas se ve interrumpida frecuentemente al llegar a zonas de roca más dura, en las que ha de recurrirse a los explosivos. Los contratistas suizos registran unos costos altos de excavación cuando se trabaja en gneis.

A pesar de las dificultades que se encuentran actualmente en la excavación mecánica integral a plena sección a través de rocas duras, los desarrollos tecnológicos se traducirán probablemente en el hecho de hacer competitivo este método de perforación de túneles.

Cuando se habla de las ventajas de la excavación por medios integrales de los túneles en áreas edificadas, no deben ser olvidadas las posibilidades que ofrecen también las voladuras controladas. Actualmente el objetivo consiste en no sobrepasar un nivel de tensiones que evite los daños por vibraciones del terreno, pero si fuera necesario, por razones técnicas o de otro tipo, las voladuras se podrían efectuar con un nivel de precaución que no diera origen a daños en la roca y edificios adyacentes, sin dejar de ser económicamente competitivo.

Un recorte cuidadoso, usando barrenos de pequeño diámetro y evitando las cargas excesivas en los barrenos de la pega, puede limitar la fisuración de la roca a una distancia inferior a 0,5 m más allá del contorno final.

Desde el punto de vista técnico, todo ésto significa que difícilmente podrán las voladuras hacer necesario un trabajo de refuerzo de la roca, o provocar un descenso de la capa freática, en los casos en que la perforación integral a sección completa no produzca estos inconvenientes.

Otro hecho que debe ser tenido asimismo en cuenta es que, debido a la situación de responsabilidad existente en las voladuras en túneles, los daños que aparezcan en los edificios circundantes son atribuidos con toda facilidad a las consecuencias de las operaciones de voladura sin que pueda demostrarse ninguna relación directa entre ambos fenómenos.

Ejemplo

En una zona edificada, ha de excavarse con explosivos un túnel con una sección de 4,5 m². El túnel pasa por debajo de edificios en todo su recorrido. El nivel de vibración permitido es $v = 50$ mm/seg. El espesor del recubrimiento del túnel oscila entre 10 y 35 m. Los 4,5 km de longitud del mismo se subdividen de la forma siguiente:

Espesor del recubrimiento m	Longitud de túnel m	Coste de voladura (coste normal = a)
10	500	2,30 × a
15	500	2,00 × a
20	500	1,30 × a
25	1000	1,15 × a
30	1000	a
35	1000	a

$$\text{Coste total} = \frac{(500 \times 2{,}30 + 500 \times 2{,}00 + 500 \times 1{,}30 + 1000 \times 1{,}15 + 1000 \times 1 + 1000 \times 1) \times a}{4500}$$

$$a \times \frac{5950}{4500} = 1{,}32 \times a$$

Este cálculo pone de manifiesto que los costes puros de voladura aumentan en un 32 % debido a la técnica de voladuras controladas empleada. A ésto debe añadirse el coste de las inspecciones, primas de seguros, gastos extraordinarios fijos, y mediciones de la vibración.

Puede resultar de interés la cuestión de qué grado de precaución puede aplicarse a la voladura en un túnel, manteniendo los costes dentro de unos niveles realistas. En la Fig. 13.8.2 se muestra un diagrama de costes correspondiente a voladuras controladas en un túnel, realizadas con una precaución extremada, comparados con los de la perforación integral a sección completa en rocas duras. La curva superior de los gráficos incluye los costes de inspección, gastos de seguros, y mediciones de vibración.

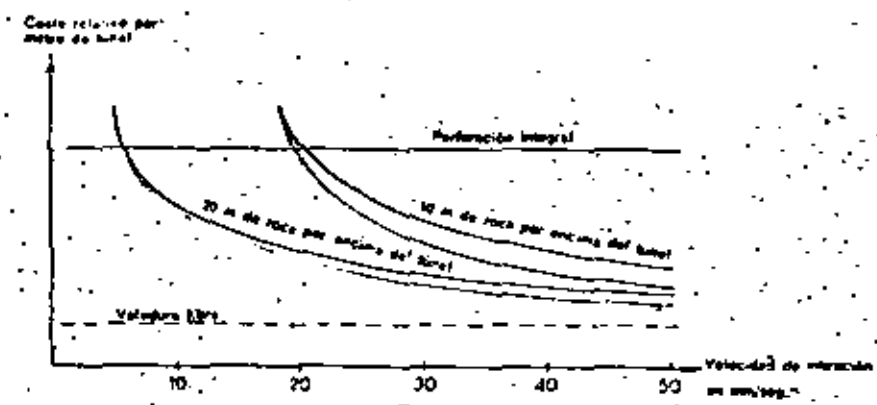

Fig. 13.8.2

El diagrama muestra que las voladuras resultan competitivas hasta niveles de tensión muy bajos. El cálculo de la influencia de las voladuras está basado tambien en los Tablas clásicas de material estadístico concerniente a las voladuras en túneles con cargas pequeñas.

El efecto de las voladuras sobre la roca circundante en este tipo de operaciones controladas es tal que no es preciso recurrir a trabajos de refuerzo.

En esta sección se han dado unas cuantas ideas y puntos de vista en torno al tema del coste de las voladuras controladas. Mientras se trate de costes deberá tenerse cuidado con las generalizaciones, pues cada caso particular muestra variaciones en la práctica, debido a las diferentes condiciones imperantes.

13.9 ONDAS DE CHOQUE AEREAS CAUSADAS POR VOLADURAS

Las voladuras originan una onda de presión que se propaga a través del entorno, y cuya intensidad depende de la magnitud de la carga, así como también, en una gran proporción, del grado de confinamiento de la misma. Es evidente que una cierta cantidad de carga confinada en un barreno origina una onda de presión considerablemente menor que cuando la misma carga se detona colocada libremente sobre el suelo.

Las mediciones realizadas con cargas libres de varios tamaños han demostrado que las condiciones climatológicas predominantes en el momento de la detonación son sumamente importantes. La dirección y velocidad del viento, la temperatura y la presión del aire, ejercen una gran influencia sobre la propagación de las ondas de presión; incluso el tiempo que haga, por ejemplo cielo cubierto o casi despejado, debe ser tomado en consideración a la hora de hacer una estimación sobre la propagación de las ondas de presión.

Las depresiones atmosféricas pueden originar amplificaciones locales de la onda de presión, con riesgo de llegar a valores de la presión superiores a los que normalmente podrían preverse a una determinada distancia.

En esta sección se trata de las ondas de choque inducidas en el aire por *voladuras al nivel de la superficie*. Cuando las voladuras se efectúan en el interior de túneles o cámaras subterráneas, las condiciones prevalecientes resultan ser totalmente distintas; la onda de presión queda confinada, y normalmente se concentra en una dirección particular; ésto significa una amplificación de la presión con respecto a las voladuras realizadas en la superficie. En

las voladuras muy próximas a estructuras situadas en el interior de instalaciones subterráneas es preciso tomar grandes precauciones; para comprobar el riesgo de daños en estos casos es posible hacer mediciones de la onda de choque aérea, al igual que en las voladuras sobre la superficie, en las que estas mediciones son el medio más seguro de evaluar la influencia de la explosión sobre el entorno a través de la onda de choque (ver final sección 13.2).

Sin embargo, a la hora de estimar los valores admisibles, se echa en falta la existencia de unos datos empíricos tan completos como los recogidos a propósito de los niveles admisibles de vibración del terreno.

En Suecia y en otros países se han hecho estudios sobre el efecto en los edificios de los impactos supersónicos provocados por los aviones. La Swedish Detonic Research Foundation ha llevado a cabo extensas investigaciones, y ha diseñado asimismo equipos de medición de las ondas de choque atmosféricas.

En las medidas de estas ondas originadas por las voladuras, la unidad de presión generalmente utilizada es el milibar (mbar):

1 bar = 1000 mbar
1 bar = 1,02 atmósferas
1 atm. = 1 kp/cm²
1 mbar = 10 kp/m² (no exactamente)
1 kp/cm² = 14,2 libras/pulgada²

La máxima presión reflejada puede calcularse mediante la fórmula: (aplicable a presiones inferiores a 14 mbar)

$$\overline{P}_r = 1400 \frac{Q^{1/3}}{R} \text{ mbar}$$

en donde Q = cantidad de carga en kg
R = distancia en metros

Para la máxima presión estática se aplica la relación siguiente:

$$P_r = 700 \frac{Q^{1/3}}{R} \text{ mbar}$$

Las dos fórmulas son aplicables al TNT, lo que implica que en los explosivos convencionales del tipo Dynamex ha de reducirse el valor de la carga al 80 % al introducirla en la fórmula. Las fórmulas se aplican a *cargas libres*.

El confinamiento de los explosivos en los barrenos posee una importancia extrema. Si la longitud del tramo de retacado es pequeña, la presión aumenta. Un buen material de retacado puede, por el contrario, reducir el valor de la

misma en gran medida, así como el empleo de protección sobre la pega. En los casos en que la roca esté muy diaclasada, las ondas de presión pueden propagarse lateralmente a través de la roca, que es arrancada por fases; ésto puede apreciarse cuando una cierta pega origina una potente onda de choque aérea capaz de romper los vidrios de las ventanas.

Para poder calcular la presión originada cuando se realizan voladuras en roca, es preciso estimar un valor para el factor de confinamiento. En el caso de voladuras ordinarias en banco y en zanjas, las mediciones muestran que este factor es de 150 o más. Esto significa que, para explosivos convencionales, los valores de la carga en las fórmulas anteriores han de reducirse 150 veces, incluyendo también esta cifra los explosivos normales del tipo del Dynamex. Las fórmulas para voladuras normales en roca son, por consiguiente:

$$\overline{P.} = 1400 \frac{\left(\frac{Q}{150}\right)^{1/3}}{R} \text{ mbar}$$

$$P. = 700 \frac{\left(\frac{Q}{150}\right)^{1/3}}{R} \text{ mbar}$$

La experiencia recogida en cuanto a roturas de ventanas y otras formas de daños en los edificios indica que en muchos casos pueden apreciarse presiones considerables sin que se observen daños. Pero siempre que se opera en zonas edificadas, el objetivo debe ser eliminar completamente los daños.

La onda de presión tiene una elevada velocidad inicial, tras lo cual disminuye y se hace muy próxima a la del sonido.

En el caso de distancias cortas, las cargas son pequeñas, y ésto hace que disminuya el periodo de crecimiento de la presión, lo cual implica que es razonable permitir un valor más elevado en la inmediata proximidad.

Los valores admisibles sugeridos para la onda de presión de reflexión son los siguientes:

Distancias de menos de 100 m: 10 mbar.
Distancias de más de 100 m: 5 mbar.

En la Tabla siguiente se indican unos valores-guía para la máxima carga coordinada que puede admitirse si se quieren eliminar los daños producidos por la onda de choque aérea. A efectos comparativos se incluye asimismo en la Tabla el límite de carga admisible para un nivel 0,03, que corresponde a un valor normal de 70 mm/seg. para la velocidad de vibración del terreno:

Distancia m	Carga coordinada kg		Carga correspondiente al nivel 0,03 (*) kg	Presión de reflexión admisible mbar
50	6,8		11,0	10
100	33,0	(54,0 **)	33,0	10
200	90,0 **)	(54,0 ***)	90,0	5
300	180		160	5
400	440		240	5
500	850		340	5
600	1480		440	5
800	3500		680	5
1000	6800		950	5

(*) En la práctica, no se ha apreciado que una carga correspondiente al nivel 0,03 origine ondas de choque desfavorables.

(**) En este caso el factor de dimensionamiento ha sido el nivel de carga para las vibraciones del terreno.

(***) La carga es en este caso de 54,0 kg debido a la admisibilidad de una transición a 5 milibares. La carga coordinada, sin embargo, ha sido calculada como no favorable desde el punto de vista de la onda de choque aérea.

Por lo que respecta a las ondas de choque, y en el caso de encendido con microrretardos, todas las cargas comprendidas en un intervalo se consideran como coordinadas a distancia superior a 100 metros. Esto es también aplicable en teoría, en muchos casos, para las vibraciones del terreno. En la práctica, sin embargo, generalmente es posible en ambos casos hacer una reducción a ½ ó ⅓ de las cargas comprendidas en dicho intervalo. Para distancias menores la carga coordinada se calcula del mismo modo que cuando se trata de vibraciones del terreno, es decir, igual a ½ ó ⅓ de las cargas comprendidas en el intervalo de retardo en los casos normales.

La Tabla anterior muestra que, en el caso de viviendas normales, la onda de choque aérea implica generalmente menos problemas que las vibraciones del terreno. Normalmente la carga deberá ser determinada por los niveles admisibles en función de las vibraciones del terreno, pues este nivel de carga no puede ser excedido si hay edificios o instalaciones junto al lugar de la voladura. Simultaneamente con las mediciones de presión se han tomado registros de las vibraciones en sentido horizontal en los edificios, habiéndose con ello puesto de manifiesto la buena concordancia existente entre los valores de la vibración y los de la onda de presión. Puede afirmarse que, si no

se miden unas vibraciones horizontales peligrosas, la onda de choque aérea no implicará normalmente riesgo de que se produzcan daños; no obstante, como las desviaciones locales pueden ser más grandes que las que aparecen en el caso de las vibraciones del terreno, es preciso comprobar los valores de la onda de choque, al menos en el caso de extensas operaciones de voladura en la inmediata proximidad de edificios. Generalmente, la onda de choque aérea es experimentada como de efectos muy desagradables por las personas afectadas por ella en el interior de edificios. A medida que se va adquiriendo más experiencia sobre estas ondas de choque, irá siendo posible especificar las cantidades y los niveles admisibles de carga con un mayor grado de precisión.

14. VOLADURAS SUBMARINAS

14.1 CALCULO DE CARGAS

Se habla de voladura submarina cuando la totalidad o la mayor parte de la pega está cubierta por el agua.

El emplazamiento de los barrenos por debajo de la superficie del agua hace más complicadas las operaciones de carga de los mismos. La precisión de perforación, en cuanto al emboquille y dirección de los barrenos, se hace asimismo más difícil de comprobar.

Cuando las cargas han de permanecer un periodo considerable de tiempo bajo el agua, se plantean unas exigencias especiales en cuanto a los explosivos y dispositivos de disparo empleados.

En cuanto al caso de iniciación eléctrica, es preciso un trabajo de control completo, con mediciones de los detonadores por separado y de las series en conjunto. No basta con medir simplemente las resistencias, sino que también han de tomarse medidas de las pérdidas de corriente.

Desde el punto de vista de la tecnología de las voladuras, las voladuras normales bajo el agua pueden ser comparadas a las voladuras en banco. La

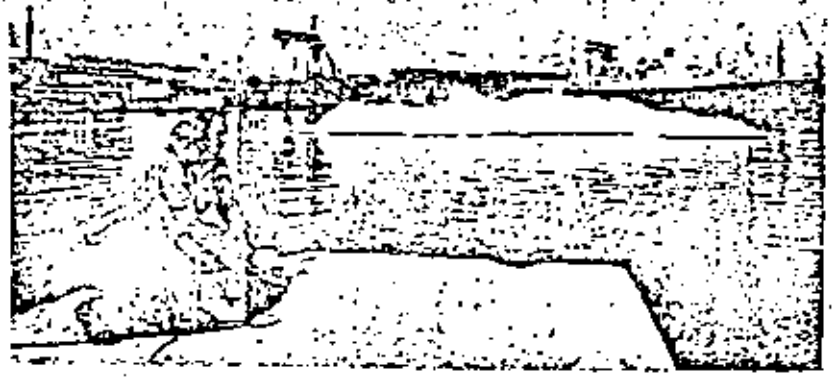

única diferencia consiste en el peso del agua, que ejerce un efecto retardador, tanto más intenso cuanto mayor sea la profundidad. Además, en la práctica hay desviaciones con respecto a los valores proyectados de la carga y los espaciamientos debido a las complicadas condiciones imperantes en los trabajos bajo el agua. El fallo de barrenos aislados, o la propagación entre distintas cargas puede dar origen a una fragmentación insatisfactoria (grandes bloques de roca).

A la hora de efectuar el desescombro, lo cual se hace normalmente mediante dragado, el grado de fragmentación tiene una gran importancia. El taqueo de los grandes bloques bajo el agua plantea generalmente problemas prácticos.

Para evitar la formación de repiés en el fondo de la pega, cuando se trabaja bajo el agua se utiliza una sobreperforación de magnitud considerablemente superior a la normal. Por otra parte, cuanto más profunda es la voladura, mayor es el suplemento de carga necesario para compensar la acción de los factores adversos. Si la roca está cubierta de arcilla, se hace necesario un nivel de carga ligeramente superior al preciso cuando la roca está cubierta unicamente por agua.

El procedimiento de cálculo que se expone a continuación está basado en la experiencia práctica, e incluye la carga extra necesaria en las diversas condiciones con que se realiza normalmente una voladura bajo el agua.

Cálculo de cargas

1. Para una voladura normal en banco se necesita una carga específica aproximada de 0,45 kg/m³ si se quiere asegurar una buena fragmentación. Como es de prever que se produzca el fallo de uno o dos barrenos, en las voladuras submarinas esta carga se duplica hasta 0,90 kg/m³, con lo que, si un barreno no detona pero sí lo hacen los circundantes, la carga específica continúa siendo de 0,45 kg/m³.
   La verticalidad de los barrenos implica una capacidad de rotura más deficiente en la parte del fondo. Sobre todo en el caso de voladuras de mucha profundidad de perforación, el fondo de la pega muestra tendencia a levantarse.
   Con barrenos verticales, la carga específica debe aumentarse en un 10 % aproximadamente, hasta 1,0 kg/m³.

2. La presión del agua sobre la pega es compensada aumentando la carga específica en un valor igual a 0,01 × altura de agua.

3. Si la roca está cubierta de arcilla, puede aumentarse la carga específica en 0,02 × espesor de arcilla. Para tramos de roca, la relación normal es 0,03 × K (K = altura del banco).

4. Debido a la carga específica que se necesita, el espaciamiento de los barrenos se calcula con relación a la concentración de carga posible por metro de barreno. Si se emplea una cargadera neumática, las concentraciones de carga pueden calcularse como en el caso de las voladuras en tierra: $\frac{d^2}{1000}$ * Cuando se utilizan cargas ya envasadas de gran diámetro, el espaciamiento ha de adaptarse a la carga por metro que da la unidad de explosivo empleada. Los barrenos se disponen en un esquema cuadrado, con V = E.

5. La sobreperforación se hace igual a la piedra (U = V_1), siendo su valor mínimo de 0,8 m.

6. Profundidad de los barrenos = Altura del banco + Sobreperforación.

7. La zona de retacado se hace igual a ⅓ de la *piedra* ($h_r = \frac{1}{3} \times V_1$), siendo su valor mínimo de 0,5 m.

Fórmulas de carga:

$q_{real} = 0{,}90 + 0{,}01 \times K_{agua} + 0{,}02 \times K_{arc} + 0{,}03 \times K_{roca}$

$q_{teor} = 1{,}00 + 0{,}01 \times K_{agua} + 0{,}02 \times K_{arc} + 0{,}03 \times K_{roca}$

Ejemplo:

Se ha de efectuar una voladura submarina con las características siguientes:
Diámetro de barrenos: 51 mm
Profundidad de agua: 15 m
Altura del banco: 6 m
Se utilizarán barrenos verticales, y la carga se realizará por medios mecánicos.

1—3. Cálculo de la carga específica necesaria:

$q_{real} = 1{,}00 + 0{,}01 \times 15 + 0{,}02 \times 0 + 0{,}03 \times 6$

$q_{teor} = 1{,}00 + 0{,}15 + 0 + 0{,}18 = 1{,}33$ kg/m³

4. La concentración obtenida en la carga es $\frac{51^2}{1000} = \frac{51 \times 51}{1000} = 2{,}6$ kg/m

Espaciamiento:

$$\text{Superficie por barreno} = \frac{\text{Concentración de carga}}{\text{Carga específica necesaria}}$$

m²/barreno: $\frac{2{,}6}{1{,}33} = 1{,}95$ m²

$V \times E = 1{,}95$

$V = 1{,}4$ m aprox. ($V = \sqrt{1{,}95}$)

$E = 1{,}4$ m aprox.

5. Sobreperforación = V
   U = 1,4 m

6. Profundidad de los barrenos = Altura del banco + Sobreperforación
   H = 6,0 + 1,4 = 7,4 m

7. Zona de retacado = ⅓ × V
   h_z = ⅓ × 1,4 = aprox. 0,5 m.

Resumen de los datos fundamentales:

Altura de banco m	Profdad. barrenos m	Piedra m	Espaciamiento m	Carga kg	Concentración de carga kg/m	Carga específica kg/m³
6,0	7,4	1,4	1,4	18,0	2,6	1,53 *)

(*) La carga específica se ha calculado sobre el volumen teórico.

Una parte de la voladura puede ser realizada desde la superficie del terreno, perforando a través de una capa de tierra de 8 m de espesor. La altura de banco en esta parte es de 12,0 m de roca.

La carga específica necesaria en esta parte de la voladura será:

$q_{ver} = 1{,}00 + 0{,}01 \times 0 + 0{,}02 \times 8 + 0{,}03 \times 12$
$q_{ver} = 1{,}00 + 0 + 0{,}16 + 0{,}36 = 1{,}52$ kg/m³

Como se ha visto posible perforar sin dificultad con una inclinación de los barrenos igual a 3:1, la carga específica puede ser reducida a:

$q_{ut} = 0{,}90 + 0{,}16 + 0{,}36 = 1{,}42$ kg/m³

Es preciso subrayar que este tipo de procedimientos de voladura ha de ser empleado a una distancia considerable de áreas edificadas o de otras instalaciones sensibles, pues las proyecciones imponen la necesidad de evacuar una extensa área cuando se efectúa la voladura.

Cuando se realizan voladuras junto a instalaciones como las de los muelles, la carga específica puede reducirse de valor, siempre que se consiga una precisión especial en el emboquille y la carga de los barrenos. Es preciso asimismo prestar la debida atención a la "onda de marea" provocada por la voladura.

En la Tabla que se incluye a continuación se indican los valores guía para la perforación y la carga en los casos en que no existen factores de limitación, como las vibraciones del terreno, o los riesgos de proyecciones o de "ondas de marea":

Diámetro barrenos mm	Altura de banco m	Profundidad barrenos m	Profundidad de agua m	Piedra m	Espaciamiento m	Carga kg	Carga específica teórica kg/m	Carga específica teórica kg/m³
30	2,0	2,9	2,0—5,0	0,90	0,90	2,1	0,9	1,14
	5,0	5,8	2,0—5,0	0,85	0,85	4,8	0,9	1,20
	2,0	2,8	5,0—10,0	0,85	0,85	2,1	0,9	1,16
	5,0	5,8	5,0—10,0	0,85	0,85	4,8	0,9	1,25
40	2,0	3,2	2,0—5,0	1,20	1,20	4,5	1,6	1,11
	5,0	6,2	2,0—5,0	1,15	1,15	9,3	1,6	1,20
	7,0	8,1	2,0—5,0	1,10	1,10	12,3	1,6	1,26
	7,0	8,1	5,0—10,0	1,10	1,10	12,3	1,6	1,31
51	2,0	3,2	2,0—10,0	1,20	1,20	5,0	2,6 [3])	1,16
	3,0	4,5	2,0—10,0	1,50	1,50	10,4	2,6	1,19
	5,0	6,5	2,0—10,0	1,45	1,45	15,6	2,6	1,25
	10,0	11,5	2,0—10,0	1,35	1,35	26,0	2,6	1,40
70	2,0	3,2	2,0—10,0	1,20	1,20	10,0	4,9 [3])	1,16
	3,0	4,5	2,0—10,0	1,50	1,50	19,0	4,9	1,19
	5,0	7,0	2,0—10,0	1,95	1,95	30,4	4,9	1,25
	10,0	11,9	2,0—10,0	1,85	1,85	55,4	4,9	1,40
	10,0	11,8	20,0	1,80	1,80	55,4	4,9	1,50
	15,0	16,7	20,0	1,70	1,70	78,9	4,9	1,65
100	2,0	3,2	5,0—10,0	1,20	1,20	16,0	6,4 [3])	1,16
	3,0	4,5	5,0—10,0	1,50	1,50	23,7	6,4	1,19
	5,0	7,3	5,0—10,0	2,25	2,25	42,2	6,4	1,25
	10,0	12,1	5,0—10,0	2,10	2,10	73,0	6,4	1,40
	15,0	17,0	5,0—10,0	2,00	2,00	103,7	6,4	1,55
	15,0	17,0	20,0	1,95	1,95	103,7	6,4	1,65
	20,0	21,9	25,0	1,85	1,85	136,3	6,4	1,85

La Tabla es aplicable a barrenos verticales.

[1]) La reducida altura de banco permite una piedra limitada.

[2]) Igual que [1]). En este caso se aplica a un área mayor con pequeña altura de banco.
La profundidad de perforación por debajo del nivel teórico de la pega ha de quedar al mismo nivel de los otros barrenos si la profundidad de éstos varía.

[3]) En barrenos de gran diámetro se emplean generalmente unidades de carga ya preparadas, lo que implica que el barreno no es aprovechado al máximo.

La Tabla muestra también los diámetros de barreno que pueden resultar apropiados para los diferentes valores de altura del banco y de profundidad de agua.

Diámetro barrenos mm	Altura de banco apropiada m
30	0—3 (*)
40	2—5
51	3—8
70	5—15
100	6—20

(*) Si el espaciamiento es demasiado pequeño, hay un mayor riesgo de propagación entre las cargas de los distintos barrenos.

Apertura de salida o cuele

En muchos casos no existe una dirección natural de rotura para las primeras hileras de barrenos, por lo que se hace necesario proporcionar una salida a los mismos. Como el resultado de la voladura depende por completo del éxito de esta operación, tanto la perforación como la carga han de llevarse a cabo con un ancho margen de seguridad. Si la roca está a nivel o la altura del banco es pequeña, la apertura debe iniciarse fuera del tramo donde ha de hacerse la voladura.

La verticalidad de los barrenos es también en este caso fuente de más dificultades.

En la Fig. 14.1.1 se muestra esquemáticamente el fundamento de la ampliación o apertura del cuele.

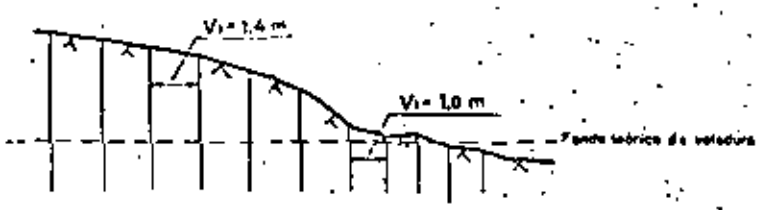

Fig. 14.1.1

14.2 METODOS DE VOLADURAS SUBMARINAS

Las voladuras submarinas pueden efectuarse de muchas maneras diferentes. La perforación puede ser realizada por un buzo que trabaje bajo el agua, pero también puede ser llevada a cabo enteramente desde la superficie, y lo mismo cabe decir de la carga. Es corriente utilizar plataformas o balsas de perforación de diversos diseños. Los métodos empleados pueden variar dependiendo de las condiciones predominantes en el lugar de la voladura.

Tanto la perforación como la carga se convierten en operaciones más complicadas en los lugares en los que hay grandes olas; en estos casos las plataformas de perforación deben sostenerse sobre unos pies que lleguen hasta el fondo, o deben usarse grandes y pesadas balsas. Con olas fuertes puede resultar difícil la utilización de balsas.

La plataforma o balsa debe ser fácil de trasladar de un lugar a otro, y de retirar de los pasos cuando haya de dejarse vía libre a un barco. Es sumamente importante que la balsa o plataforma de perforación sea situada nuevamente en el lugar correcto después de haber disparado una pega.

Si la precisión de la perforación no es buena, las posibilidades de rotura tampoco lo son, y la fragmentación será demasiado escasa.

Las voladuras submarinas pueden dividirse en dos tipos principales, según el procedimiento seguido:

Voladura subacuática con ayuda de buzos.
Método "OD" (de perforación con recubrimiento).

Existen variantes de ambos métodos en las que, por ejemplo, la perforación se efectúa desde una balsa, con la ayuda de buzos para el emboquille y la carga de los barrenos.

La voladura con ayuda de buzos es la más adecuada en el caso de operaciones de extensión limitada, o cuando se impongan severas exigencias sobre el ajuste al contorno teórico final bajo el agua. Desde una balsa la perforación suele realizarse mediante perforadoras manuales o fijas; las perforadoras manuales pueden ser empleadas cuando las profundidades de agua y de roca no son grandes. Los buzos ayudan a establecer la alineación de los barrenos. Como en muchos casos el campo de visión bajo el agua no es bueno, el buzo necesita ayudarse con diversos medios para orientarse, que pueden consistir en cuerdas tensas con respecto a las cuales se toman las medidas, o plantillas de acero o algún dispositivo similar. Los barrenos son tapados cuidadosamente a medida que son perforados. No pueden cargarse barrenos a menos de 2 m de un punto en donde se esté perforando, y asimismo no puede efectuarse una perforación a menos de 2 m de un barreno cargado.

Empleando barrenos de gran diámetro, la conexión entre ellos y la superficie puede establecerse mediante un tubo o manguera de plástico a través de

la cual se efectúa la carga. Para conectar la manguera al barreno se necesita la ayuda de un buzo. En el caso de aguas poco profundas y de operaciones pequeñas, este trabajo puede ser perfectamente llevado a cabo por hombres rana, los cuales también pueden cargar los barrenos de la forma ordinaria, con un atacador.

El método de perforación a través del recubrimiento o método "QD" (también llamado en Suecia método Lindö) fue introducido con ocasión de las operaciones de voladura del canal Lindö, cerca de Norrköping, a comienzos de la década de 1960. El método fué desarrollado por las compañías suecas AB Skånska Cementgjuteriet, Atlas Copco, y Nitroglycerin AB (conocida ahora con el nombre de Nitro Nobel AB).

En el lugar en que había de construirse el canal, no sólo había roca sino también una gruesa capa de arcilla. En vez de proceder al desmonte de la capa de arcilla hasta dejar la roca al descubierto, se realizó la perforación a través de la arcilla y la roca usando un equipo especial.

Se diseñaron unos detonadores especialmente robustos (detonadores OD). La carga se llevó a cabo con máquinas neumáticas. Los sistemas de carga y de encendido fueron comprobados cuidadosamente. Las pegas utilizadas tenían aproximadamente unas 50 toneladas de explosivo.

Tras este satisfactorio comienzo el método ha sido utilizado en muchos lugares en Suecia y otros países. Está asimismo recomendado en los casos en que la perforación puede efectuarse desde una plataforma o una balsa.

Los principios básicos del método son los siguientes:

La perforación se ejecuta con ayuda de perforadoras potentes; el diámetro de los barrenos es normalmente de 51—70 mm, pero son posibles diámetros todavía mayores.

Para penetrar a través de la capa de terreno suelto hasta unos pocos decímetros en la roca firme se emplea un tubo de preperforación. En el caso de perforación bajo el agua sin capa de arcilla sobre la roca, se hace penetrar de modo análogo el tubo de preperforación en el emplazamiento del punto de emboquille del barreno. Seguidamente se realiza la perforación a través del interior del tubo, con un equipo de menor diámetro y de tipo extensible.

Una vez terminada la perforación, se extrae la barrena y se introduce una manguera de plástico por el tubo de preperforación hasta la parte superior del barreno; se saca entonces este tubo, y la manguera queda ahora formado la conexión entre el barreno y la superficie. La carga puede efectuarse cuando se juzgue conveniente.

Si la perforación se realiza de manera que queden satisfechos los requerimientos de seguridad, la carga puede hacerse luego a través del tubo de preperforación, sin necesitarse la manguera.

La carga se realiza mediante máquinas neumáticas, ajustándose estrictamente a la concentración deseada.

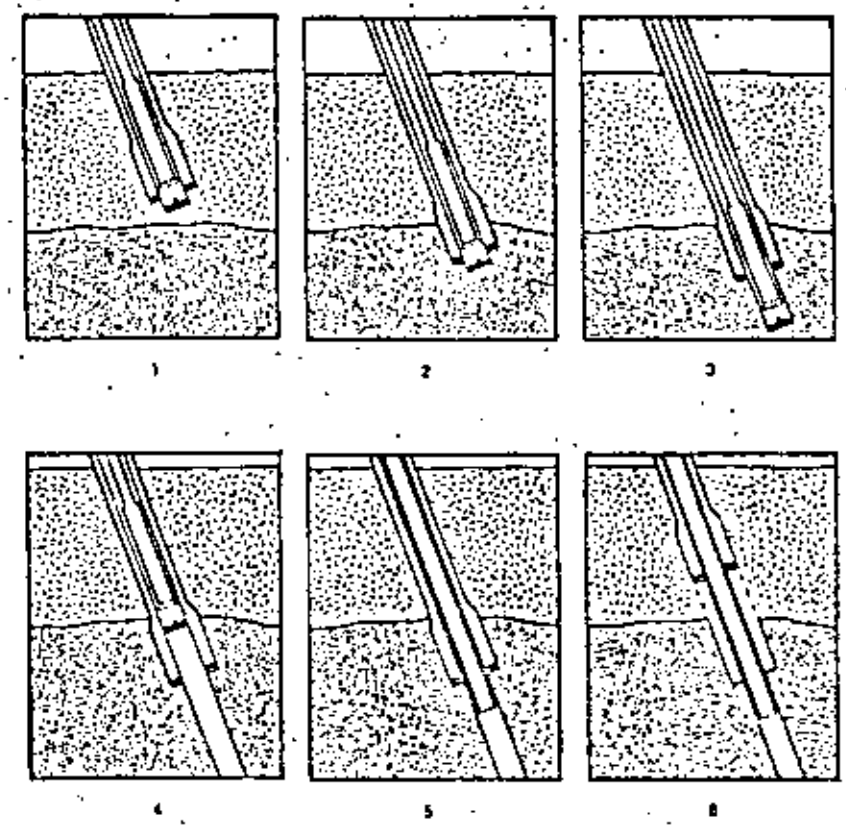

1 El tubo de preperforación y la barrena extensible penetran a traves de la capa de suelo

2 El tubo de preperforación penetra unos decímetros en la roca

3 Perforación del barreno en la roca con una barrena extensible

4 Extracción de la barrena

5 Se introduce hasta abajo una manguera de plástico que se ajusta firmemente contra la roca.

6 Se extrae el tubo de preperforación y puede procederse a la carga del barreno a través de la manguera de plástico.

Fig. 14.2.1

En cada barreno debe haber al menos dos detonadores, que se conectan a series diferentes con el fin de obtener una mayor garantía de detonación completa en los barrenos. Durante la carga y durante las operaciones posteriores de conexión, ha de comprobarse la resistencia de cada detonador. Además de esta comprobación, han de controlarse también las pérdidas de corriente. Los detonadores dañados han de ser sustituidos.

En los últimos años, y en ciertos casos, la resistencia eléctrica del terreno ha sido tenida también en cuenta; en este campo se continúa ahora investigando y aún no se ha llegado a unos resultados definitivos, pero en su debido momento estas investigaciones permitirán desarrollar unos métodos de control más perfectos.

El conjunto de los detonadores se subdivide en varias series mediante conexiones en series paralelas (véase la sección 4.2).

A fin de obtener un margen de seguridad aún mayor, el número de detonadores de cada serie puede ser reducido con relación a los que se utilizan en una voladura normal con el mismo explosor.

En la Fig. 14.2.1 se ilustra el procedimiento seguido en el método de perforación con recubrimiento (sistema OD).

14.3 DISPOSICIONES ESPECIALES

Información suplementaria en relación con el proyecto de voladuras submarinas

— Elección de los explosivos
— Dispositivos de detonación y comprobación del sistema de encendido
— Carga e inspección de la carga
— Vibraciones del terreno
— "Ondas de marea"

El *explosivo* utilizado en una voladura bajo el agua ha de ser capaz de permanecer sumergido en ésta después de cargado durante el lapso de tiempo preciso hasta su detonación. El *Dynamex A* está garantizado para soportar el agua al menos durante una semana, pero hay muchos casos en los que una pega o partes de una pega han de permanecer cargadas un período de tiempo considerablemente mayor. La dinamita con 60 % de nitroglicerina tiene garantizada una resistencia al agua de una duración mínima de tres semanas.

La resistencia de un explosivo frente a la acción del agua varía en gran medida, dependiendo de las condiciones predominantes en cada caso. Los plazos garantizados por el fabricante del explosivo se consideran aplicables a las condiciones más desfavorables que puedan presentarse.

Los estudios realizados han puesto de manifiesto el hecho de que explosivos cargados por medios mecánicos en barrenos relativamente intactos toleran el agua durante períodos de tiempo varias veces superiores a los garantizados. En el caso de barrenos rotos y agrietados, en cambio, el agua puede atacar al explosivo por los lados, y sus efectos son más rápidos, especialmente si el barreno no está lleno por completo. Lo más importante es la iniciación del explosivo; si los detonadores están situados en un explosivo muy insensible a la acción del agua existe una probabilidad considerablemente mayor de un buen encendido en el caso de que, por diversas razones, no haya sido posible disparar la pega en el momento proyectado.

La relativamente baja capacidad de propagación del Dynamex es una gran ventaja en voladuras submarinas, donde normalmente es deseable evitar que se produzca tal fenómeno. El peligro de propagación disminuye al aumentar la profundidad bajo el agua. Si en una roca agrietada y muy diaclasada se utiliza un explosivo con una considerable capacidad de propagación, el resultado de la voladura será más deficiente desde el punto de vista de la rotura y la fragmentación.

La *detonación* es un factor importante en las voladuras submarinas. Como el proceso de detonación requiere un encendido con microrretardos para que funcione correctamente desde el punto de vista tecnológico, los detonadores eléctricos resultan preferibles a la mecha detonante. No obstante, la mecha detonante con extremos provistos de un buen aislamiento puede constituir un buen complemento en barrenos en los que la roca está rota y es difícil realizar satisfactoriamente la carga.

Los detonadores OD van provistos de un sólido aislamiento que proporciona una buena protección frente a las considerables tensiones a que está sujeto el sistema de encendido en las voladuras submarinas. En cada barreno deben usarse como mínimo dos detonadores; normalmente se les sitúa en la parte inferior del barreno por medio de un atacador o de la manguera de un cargador mecánico. Si la inspección del sistema de encendido mostrara que un detonador no se encuentra en buen estado, deberá colocarse uno nuevo en la parte superior del barreno.

Con ocasión de las operaciones de carga de los barrenos, se comprobarán debidamente las resistencias eléctricas y pérdidas de corriente del sistema de iniciación eléctrica.

Los detonadores de cada barreno deberán marcarse cuidadosamente, y anotarse en un libro-registro.

En cuanto a las conexiones, si puede procederse de modo que los empalmes estén *por encima de la superficie del agua*, ello supondrá una gran ventaja. En caso de que sea necesario que haya empalmes bajo el agua, deben ir alojados en una caja o manguito de protección que impida absolutamente la entrada de agua. Los manguitos de conexión y la cinta aislante ordinarios no son suficientes. Cuando los empalmes hayan de ir bajo el agua, conviene que los cables de los detonadores sean lo suficientemente largos como para que puedan conectarse conjuntamente varios detonadores en un punto; es también recomendable limitar lo más posible el tiempo que una caja de empalmes permanece bajo el agua.

Los hilos de los detonadores que pueden ser empalmados por encima del agua suelen disponerse en una o más pequeñas boyas, cuerdas, etc.

Por diversas razones, a veces es necesario evitar que haya cables de detonadores flotando en el agua; en tales casos pueden sujetarse dichos cables a una boya que se mantiene a un metro sobre el fondo, aproximadamente. Cuando llegue el momento de las conexiones, se libera la boya, y ésta hace subir los hilos de los detonadores hasta la superficie.

Como ya se ha señalado anteriormente, en ciertos casos se mide también la resistencia a tierra; una medición directa de esta resistencia eléctrica facilita la estimación de las pérdidas de corriente (pérdidas a tierra) que pueden ser toleradas. Un valor elevado del porcentaje de pérdidas de corriente puede indicar que la carga y las conexiones no han sido realizadas con el suficiente cuidado y precisión.

La carga es una operación difícil en las voladuras bajo el agua. El mejor resultado se obtiene generalmente con cargador neumático, llegándose a elevadas concentraciones de carga.

Durante la carga, la presión sobre los cartuchos para impulsarlos a través del tubo es contrarrestada por la presión contraria del agua. No está permitido aumentar la presión del aire en el tubo de carga, por lo que, para una profundidad de agua de 20 m, la presión de carga disminuye de 3,0 a 1,0 atmósferas (kg/cm^2); a esta presión la operación no puede realizarse. Para compensar la contrapresión del agua se ha de bajar la válvula de seguridad hasta una profundidad aproximada de 15 m.

Se ha encontrado asimismo que no resulta conveniente utilizar un tubo de carga excesivamente estrecho en relación con el diámetro del barreno. Además, la capacidad de carga aumenta con las dimensiones del cartucho.

En las voladuras bajo el agua es especialmente importante que todos los componentes del cargador neumático se encuentren en buen estado, sin partes deterioradas que obstaculicen el proceso de carga.

Si la roca está notablemente fracturada, o si, en rocas blandas, existen oquedades, el proceso de carga mecánica puede complicarse mucho. En estos casos puede ser conveniente utilizar cargas alargadas rígidas.

En barrenos con grandes oquedades, la carga mecánica no funciona bien, pues los incrementos de presión necesarios para forzar la salida de los cartuchos a través del tubo se ven obstaculizados; además, resulta difícil verificar la concentración de carga, con lo que pueden obtenerse grandes excesos locales de carga que pueden dar origen a propagaciones indeseadas. Puede haber asimismo tramos del barreno que queden sin cargar.

En muchos casos puede ser recomendable el uso de cargas entubadas relativamente largas. La operación de carga puede efectuarse por medios mecánicos, a través de tubos de plástico que se introducen en los barrenos; estos tubos de plástico pueden cargarse también con cartuchos de gran diámetro.

Debe llevarse un registro de la magnitud y la concentración de la carga en cada barreno. Dada la importancia que poseen todos y cada uno de los barrenos, el procedimiento seguido al efectuar la carga resulta de gran trascendencia a pesar de todas las dificultades encontradas.

Las *vibraciones del terreno* pueden ser medidas y controladas del mismo modo que en las voladuras por encima de la superficie (véase la sección 13.1). En las voladuras submarinas, sin embargo, hay un mayor peligro de propagaciones, las cuales son desfavorables desde el punto de vista de las vibraciones. La capa de arcilla situada sobre la roca puede originar estos efectos sobre las cimentaciones de edificios próximos que la atraviesen.

Las "*ondas de marea*" provocadas por voladuras bajo el agua pueden causar problemas en algunos casos a instalaciones próximas, como pueden ser las esclusas. No obstante, los explosivos confinados en barrenos originan unas ondas considerablemente menores que las cargas no confinadas.

La presión máxima puede ser reducida considerablemente por medio de una "cortina de aire", producida por uno o más tubos de plástico perforados y dispuestos sobre el fondo, a través de los cuales se bombea aire, que sale de los mismos en forma de burbujas que suben hasta la superficie. En los últimos años se han expresado ciertas dudas sobre la eficacia del sistema de la cortina de aire; se considera que únicamente reduce los valores punta de la presión, por lo que su efecto no es muy beneficioso, pues el impulso de la onda de choque pasa inalterado.

En las voladuras submarinas, la dificultad consiste en evaluar el grado de confinamiento de las cargas de los barrenos comparadas con las cargas suspendidas y no confinadas.

Langefors ha publicado unos diagramas elaborados por Enhamre y a partir de los cuales pueden calcularse la presión máxima y el impulso con base en la carga y la distancia.

Los diagramas se refieren a cargas suspendidas libremente.

Según W. Kohlrusz, Bierman ha desarrollado el concepto de "Blubbergrenzen", que es la profundidad de agua a la cual los gases producidos por la detonación de una carga libremente suspendida se abren camino de un solo golpe hasta la superficie:

Profundidad de agua m	Carga de TNT necesaria kg
1,4	1
3,0	10
7,0	100

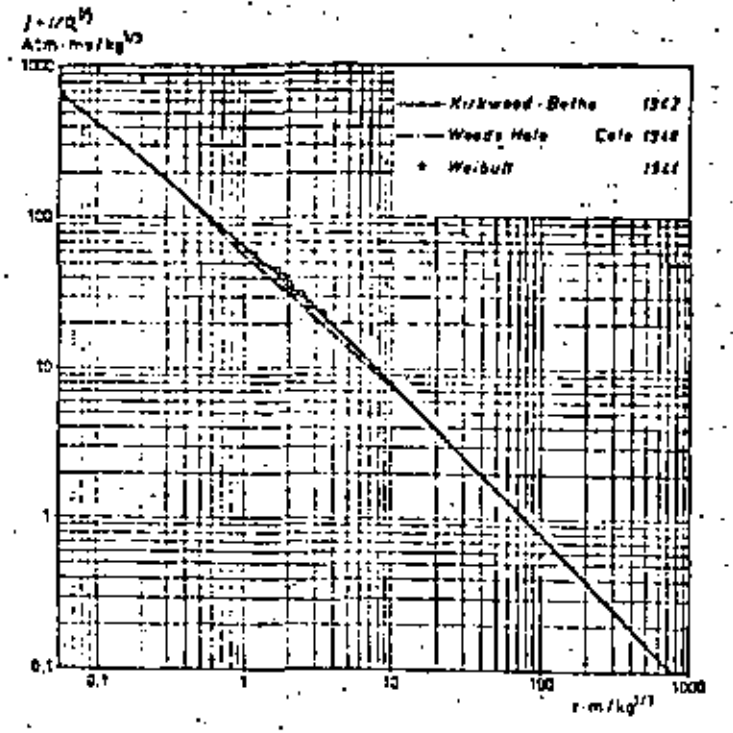

Fig. 14.3.1 Impulso reducido j para el cálculo del impulso i = j × Q⅓ originado por una carga Q suspendida libremente en agua (según Enhamre)

Este cuadro muestra la gran importancia de la profundidad cuando se realizan voladuras muy próximas a diversas instalaciones. Muestra al mismo tiempo una buena concordancia con el diagrama de presión de Enhamre, de acuerdo con el cual el "Blubbergrenzen" es de 200 kg/cm².

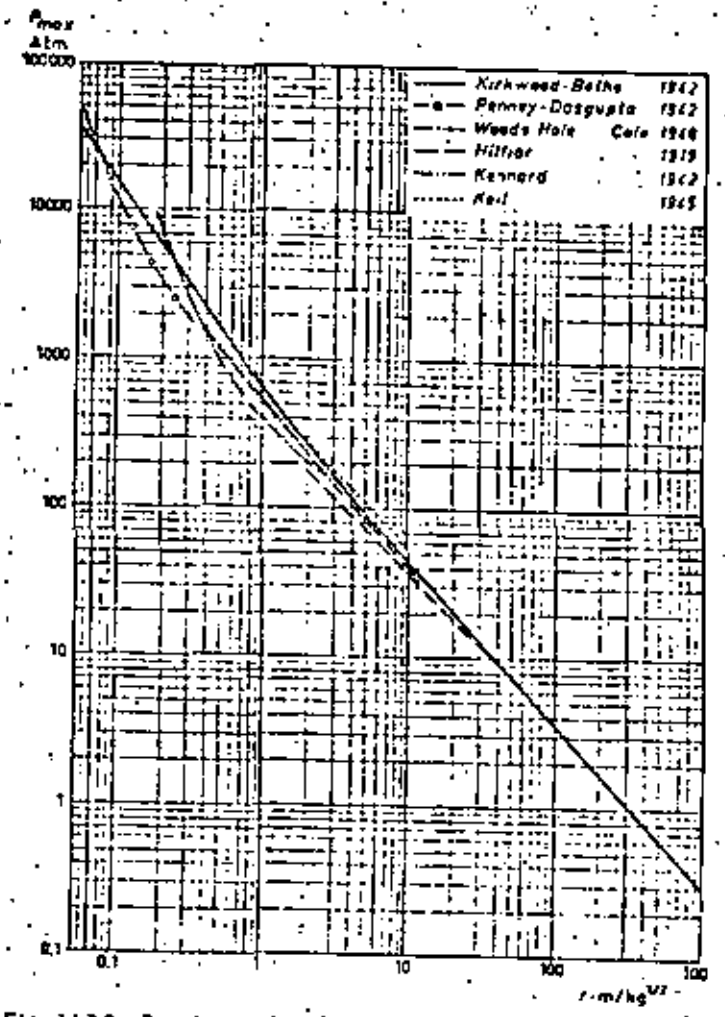

Fig. 14.3.2 Presión máxima P_{max} originada por una carga Q suspendida libremente en agua a una distancia R = r × Q⅓ (según Enhamre)

Langefors establece en un 10 % la probable presión máxima originada por cargas encerradas en barrenos con respecto a la debida a cargas suspendidas libremente. Este valor parece concordar bien con la experiencia práctica sobre el factor de confinamiento para las ondas de choque aéreas.

En la práctica parece como si los valores teoricamente calculados dieran origen a unos efectos sobre las instalaciones adyacentes menores de los esperados. Probablemente es importante tener en cuenta el efecto amortiguador del agua y la duración sumamente corta del período de carga de la onda. Los gases producidos por la voladura pueden posiblemente interferir en el proceso de formación de la onda de presión en un sentido favorable a la reducción de la misma. Esto implica que la pega debe disponerse preferentemente de modo que el retardo que detone en primer lugar posea una carga lo más baja posible, y el grueso de la carga debe trasladarse al último retardo.

El mejor método para conseguir una estimación más digna de confianza del efecto ejercido a este respecto por las voladuras submarinas, lo proporcionarán unas mediciones empiricas extensivas de las ondas de choque del agua originadas con ocasión de las voladuras en roca.

15. DEMOLICION DE EDIFICIOS E INSTALACIONES

15.1 DEMOLICION DE EDIFICIOS

Los explosivos han resultado ser un método competitivo para los trabajos de demolición en antiguas zonas residenciales. Los métodos convencionales a menudo implican un riesgo cuando el trabajo se realiza junto a vias de tráfico y lugares utilizados por muchos peatones.

La voladura de edificios en zonas habitadas o edificadas es un método que no ha sido utilizado durante muchos años. Se utilizó por primera vez en Gothenburg, con ocasión de la demolición de un edificio situado sobre un estrato deslizante de arcilla. El edificio había comenzado a inclinarse de tal modo que se consideró demasiado arriesgado utilizar un método convencional para su derribo. Tras un trabajo de planificación muy extenso, se efectuó la voladura con un resultado muy satisfactorio. Se midieron las vibraciones en los edificios circundantes en el curso de la voladura, sin que se pudieran observar valores nocivos, ni siquiera en edificios situados tan solo a 4 m de distancia.

A partir de entonces se han llevado a cabo muchas voladuras en edificios con muy buenos resultados. La voladura descrita fue preparada por Nitro Consult, y esta compañía destacó también a su personal al lugar del trabajo para comprobar las operaciones de perforación y carga.

En la voladura de edificios hay varios principios básicos fundamentales:

1. Han de destruirse los elementos vitales de sustentación, de modo que el propio peso del edificio haga por sí solo la mayor parte del trabajo.
2. Las cargas han de subdividirse para que proporcionen una rotura completa.
3. Se realiza el encendido con microrretardos, y los números de los diversos intervalos se disponen de forma que proporcionen la dirección de caída o de rotura deseada.

Hay asimismo ciertas medidas de seguridad que son esenciales en zonas edificadas:

1. Las cargas han de ser recubiertas con materiales de protección.
2. Se efectuarán mediciones de la vibración del terreno en los edificios o instalaciones circundantes.

3. Durante el proceso de voladura deben hacerse riegos de agua para que no se levante polvo.
4. El área que circunda el lugar de la voladura ha de ser evacuada y supervisada del mismo modo que en las voladuras en roca.
5. Si se usan en cierta cantidad cargas de superficie, deben medirse también las ondas de choque aéreas.

Aparte de los principios fundamentales, no es recomendable establecer ningún método para la voladura de edificios con carácter general. Cada edificio

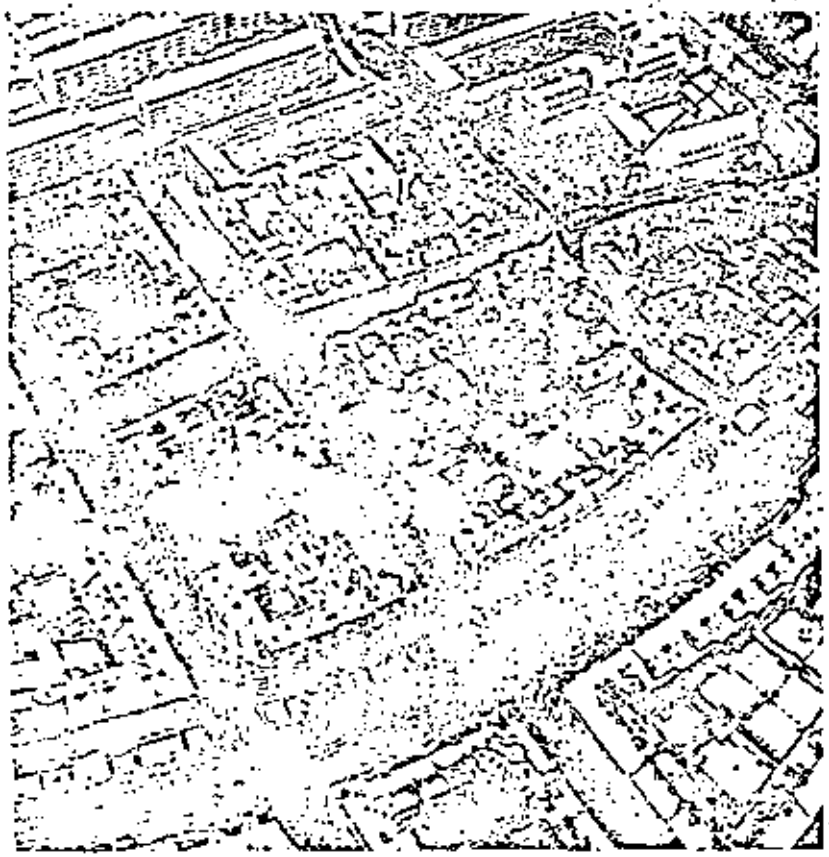

Fig. 15.1.1 El lugar de la voladura desde el aire. Foto: FIT-bild, Gothenburg.

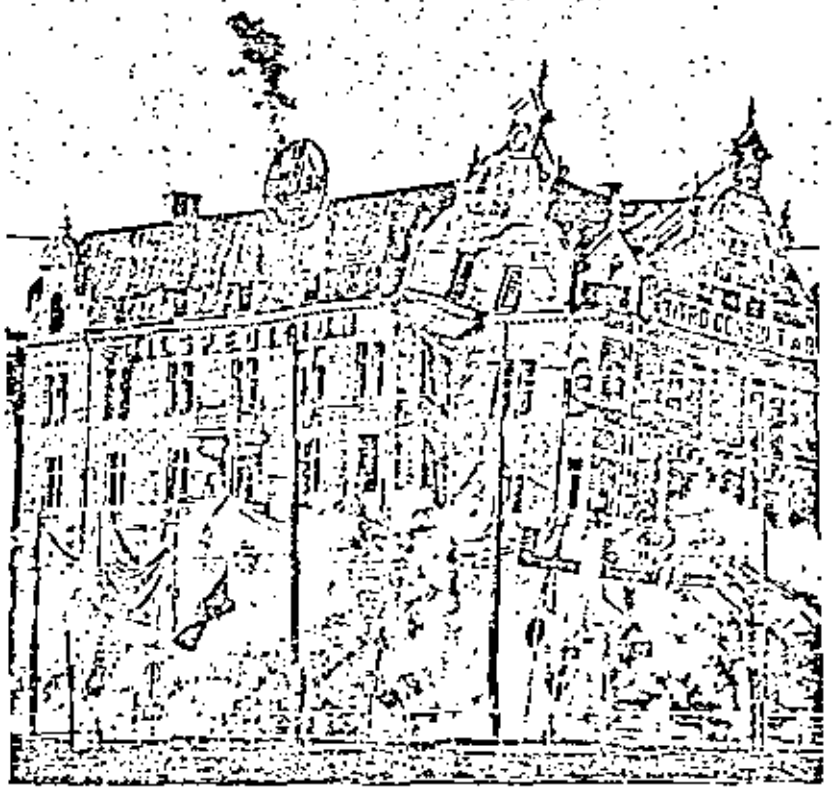

Fig. 15.1.2 Voladura de un edificio en Gothenburg situado en una calle principal con tráfico intenso.
Fotos: Bo Timback, Säwedalen y Jens Karlsson, Kungsbacka.

constituye un caso especial, que exige unos cálculos completos y la adaptación de barrenos y cargas para sus particularidades; la diferencia entre un edificio con muros portantes de ladrillo y otro con pilares de hormigón, por ejemplo, es realmente muy grande.

En una ocasión hemos volado un edificio con una estructura portante consistente en sólidas vigas de acero; este trabajo requirió el uso de cargas de superficie, para los cuales hubimos de desarrollar un sistema de protección tras una serie de experimentos, hasta que nos aventuramos a realizar esta voladura, en pleno centro de una ciudad.

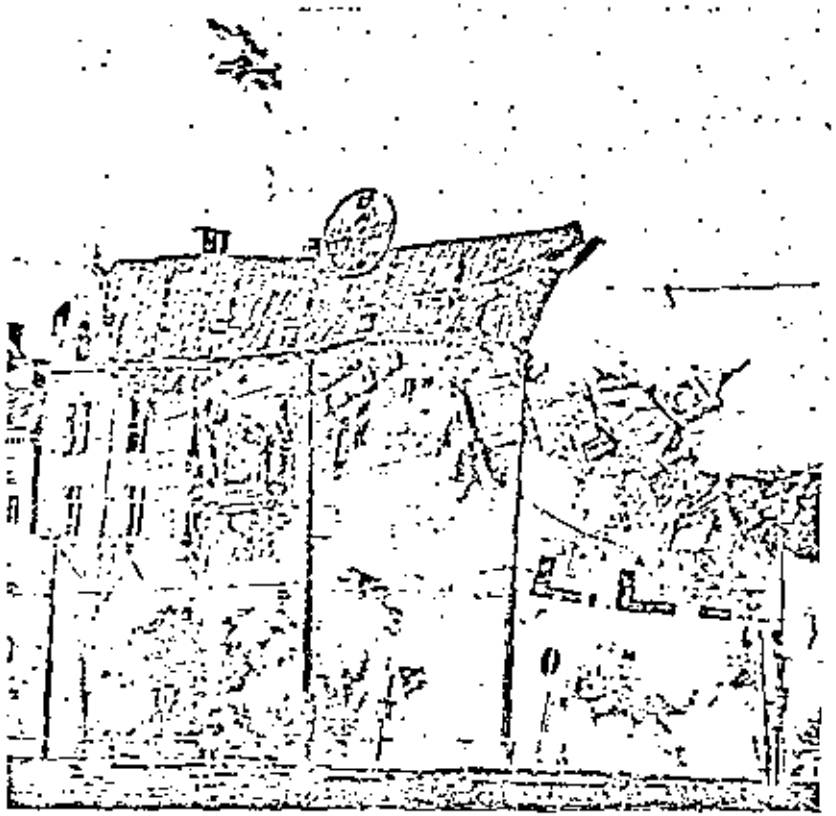

Fig. 15.1.3 El edificio que se muestra fue derribado mediante una voladura, a pesar de que se halla en una calle con tráfico muy intenso en pleno centro de Gotteeburg. Una línea de tranvía con servicios muy frecuentes pasa frente al edificio. Un derribo por métodos convencionales hubiera ocasionado considerables cortes de tráfico y grandes gastos, por las medidas de seguridad necesarias. La mayor parte del explosivo usado se colocó en el sótano, bajo el nivel del suelo, donde algunos de los muros tenían 1,2 m de espesor. La cantidad total de explosivo utilizado fue de 200 kg aproximadamente, repartido entre 600 barrenos. La perforación se realizó con perforadoras convencionales de tipo manual. En cada barreno se colocó gran cantidad de material de retacado consistente en cartuchos de arena y tacos de papel.

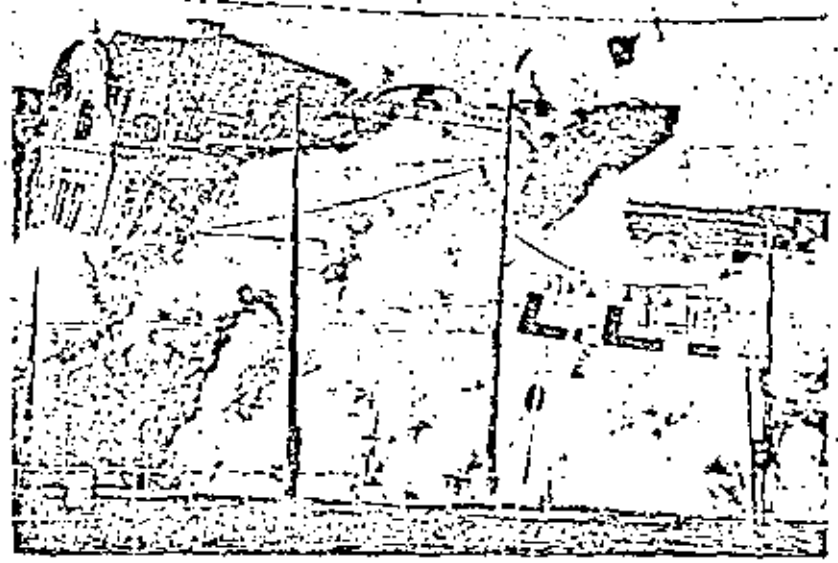

Fig. 15.1.4 Como se ve en la fotografía, el edificio muestra tendencia a caer hacia dentro, lejos de la calle. Esto depende de la configuración del plan de encendido, que determina la situación del centro de gravedad de la obra de fábrica. En el encendido se utilizaron 18 números de una serie de microrretardos.

Para evitar las proyecciones, se erigieron pantallas de troncos contra el edificio hasta una altura de unos 2 metros por encima del nivel de la calle. Se emplearon además mallas de alambre y lonas viejas como protección adicional contra las esquirlas. Los materiales usados con este fin deben proporcionar un 100% de protección, pues había personas relativamente muy cerca del lugar de la voladura. No se produjo proyección de ningún tipo.

Comparado con los métodos convencionales de demolición, la voladura de edificios presenta las ventajas siguientes:

Mayor seguridad cuando se trabaja junto a vías de tráfico, etc.
Origina perturbaciones sólo durante un tiempo limitado.
Produce polvo solamente durante un tiempo limitado.
Puede ser controlada.
Permite posteriormente el uso de métodos de desescombro m[illegible]tionales.

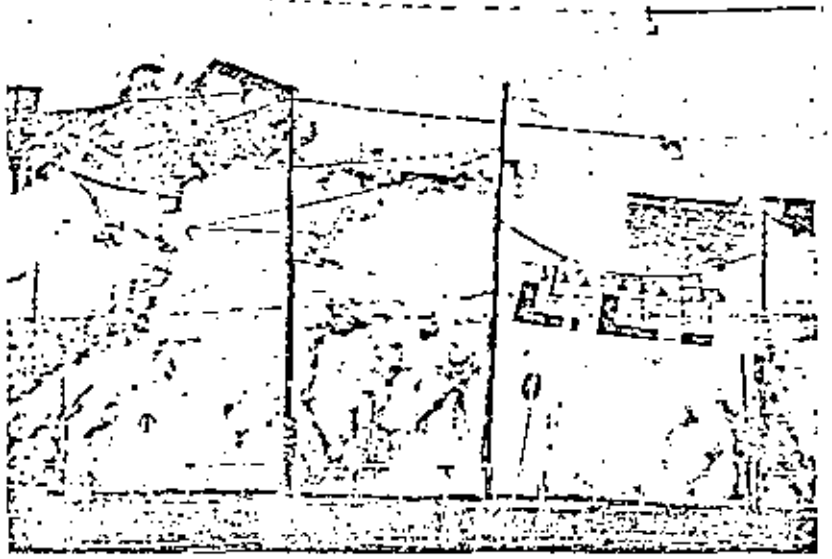

Fig. 15.1.5 Como puede verse en las fotografías, se produjo una densa nube de polvo en la explosión. Sin embargo, esta nube se disipó con relativa rapidez y no causó mayores problemas. Obsérvese que el riego de agua puede tener unos efectos acusados como reductor del polvo.

Una voladura de este tipo requiere una planificación exhaustiva, en especial en lo que respecta al sistema de encendido. El plan horario establecido para la evacuación de la zona, la interrupción del tráfico, etc. debe ser cuidadosamente observado de acuerdo con las partes implicadas, y la persona responsable de la voladura debe poseer siempre una imagen clara de la situación.

Si se toman en consideración todos los factores implicados en el problema, puede comprobarse asimismo que el método es también más económico.

Estructuras especiales, como las chimeneas, pueden ser voladas en principio del mismo modo que los edificios. En este caso suele ser de importancia ajustar la voladura a una cierta dirección de caída prefijada, lo cual resulta completamente factible.

Fig. 15.1.6 Estas fotografías muestran la voladura de una casa situada sobre una capa deslizante de arcilla. La demolición por métodos convencionales se consideró peligrosa, pues la casa había comenzado a inclinarse considerablemente.

Fig. 15.1.7 La parte del edificio volada no tenía construcciones de ningún tipo a su izquierda. Sin embargo, fue preciso abrir con explosivos unas hendiduras en el edificio de la derecha para asegurar que no impediría el colapso de la casa que iba a derribarse. Detrás hay casas habitadas a una distancia de 18 metros, y la casa a demoler se inclinaba en esta dirección. Como puede verse en la fotografía, se estudió un esquema de encendido tal, que la dirección de caída fue en realidad hacia el patio y lejos de las casas habitadas (chimeneas). Se utilizaron también algunas cargas suplementarias para romper unos puntales armados de hierro en el edificio. Se dispuso una protección muy cuidadosa, y no hubo proyecciones.

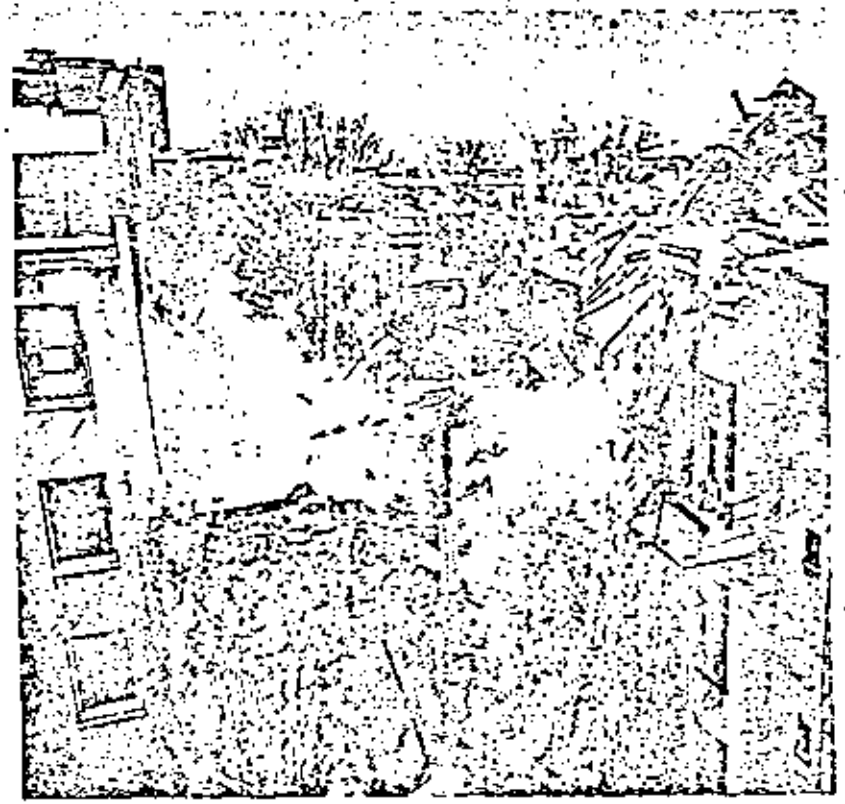

Fig. 15.1.8 En esta fotografía, la casa se ha derrumbado ya varios metros. El edificio cae con una rapidez inusitada debido a los considerables márgenes usados por lo que respecta a los barrenos y el explosivo.
La cantidad total de explosivo empleada fue de unos 75 kg de Dynamex B, repartido entre unos 1000 barrenos.
La conexión de los detonadores en varias series diferentes hizo precisa una cuidadosa planificación y una gran precisión. En este caso la perforación también se realizó con perforadoras convencionales de tipo manual.

Fig. 15.1.9 Final de la voladura. Puede verse que el centro de gravedad del material demolido ha sido desplazado hacia el interior, en dirección al patio, sentido opuesto a aquél hacia el que se inclinaba anteriormente la casa. La compañía que encargó la voladura quedó sumamente satisfecha con la solución dada a este problemático trabajo de demolición. La técnica de las voladuras cubre un amplio campo de posibilidades, y una voladura de este tipo es especialmente estimulante para los técnicos que se ocupan de estos trabajos.

15.2 VOLADURAS EN HORMIGON

En este apartado puede incluirse un amplio campo de operaciones de voladura completamente diferentes unas de otras. No es posible establecer unas normas generales para las voladuras de hormigón, pues la resistencia de este material puede variar considerablemente. Además, la forma geométrica de la construcción de hormigón posee una gran importancia. Si se establece una comparación entre el caso de la losa de un puente, para el que se necesita un esquema de perforación muy denso con barrenos poco profundos, y el de un muro de hormigón de unos 0,25 m de espesor, puede comprobarse que la cuantía de la carga necesaria varía enormemente; la losa puede requerir una carga específica de 5,0—10,0 kg/m³, en tanto que el muro necesita solamente 0,65—0,75 kg/m³ o incluso menos.

Las dimensiones y cuantía de las armaduras influyen sobre las características de las estructuras de hormigón frente a las voladuras; generalmente resulta difícil realizar éstas de forma que las armaduras se rompan; en muchos casos es preciso complementar la voladura del hormigón con el corte de las armaduras.

La Tabla siguiente es una sistematización de los cálculos de cargas para la voladura de estructuras de hormigón. Se supone en ella que el hormigón alcanza una dimensión mínima de 1,0 m en todas direcciones:

Material volado	Carga específica necesaria kg/m³	Espaciamiento, en red cuadrada $V_t \times E_t$ m	Explosivo empleado
Hormigón en masa de mala calidad	0,25—0,30	0,70—0,80	Gurit de 17 mm *)
Hormigón en masa de buena calidad y resistencia	0,30—0,40	0,60—0,70	Gurit de 17 mm
Hormigón armado solamente en la superficie	0,60—0,75	0,50—0,60	Gurit de 17 mm + ½ cartucho de Dynamex entre las cargas alargadas
Hormigón armado con armaduras densas	0,80—1,00	0,50—0,55	Gurit de 17 mm + 1 cartucho de Dynamex entre las cargas alargadas

Material volado	Carga específica necesaria kg/m³	Espaciamiento, en red cuadrada $V_1 \times E_1$ m	Explosivo empleado
Hormigón especial armado de uso militar	1,5—2,0	0,40—0,50 0,50—0,55	Nabit de 22 mm Dynamex de 22 mm

(*) En el caso de estructuras compactas se precisa una cierta carga de fondo, que puede calcularse como en el caso de las voladuras en banco, para los valores correspondientes de *piedra* y *profundidad* de barrenos.

Cuando las voladuras se realizan en hormigón débil, puede ser preferible que la iniciación de las cargas alargadas de Gurit se haga con mecha detonante.

El encendido de las pegas se realiza mediante microrretardos normales. En los casos en que no pueden permitirse proyecciones, y debido a la constricción que proporcionan las armaduras, debe disponerse una extensa protección (véase capítulo 8); se necesitan materiales de protección pesados y ligeros.

Las estructuras altas y estrechas requieren otras magnitudes de carga. En tales casos el objetivo suele ser el de conseguir una rotura suficiente para facilitar posteriormente las operaciones de corte y desescombro. En la Tabla siguiente se dan valores correspondientes al caso de muros de altura superior a 1,0 m y constreñidos únicamente por su base:

Objeto volado	Espesor del muro m	Espaciamiento E_1 m	No. de hileras de barrenos	Explosivo empleado
Muros de hormigón no armados	0,20	0,60	1	Gurit de 11 mm
	0,30	0,90	1	Gurit de 17 mm
	0,40	0,65	1	Gurit de 17 mm
Muros de hormigón armado con armaduras exteriores	0,20	0,50	1	Gurit de 11 mm
	0,30	0,70	1	Gurit de 17 mm
	0,40	0,55	1	Gurit de 17 mm
	0,50	0,40	1	Gurit de 17 mm
	0,60	0,70	2	Gurit de 17 mm
	0,70	0,60	2	Gurit de 17 mm
	0,90	0,50	2	Gurit de 17 mm

El encendido de las cargas se hace con microrretardos y con ½—1 cartucho de Dynamex. Ha de usarse una cuidadosa protección.

Es preciso subrayar que resulta esencial hacer una voladura experimental de un corto tramo de hormigón, después de lo cual las cargas y los espaciamientos serán modificados si se estima necesario.

En los casos en que se emplean dos hileras de barrenos, la disposición de éstos es la que se indica:

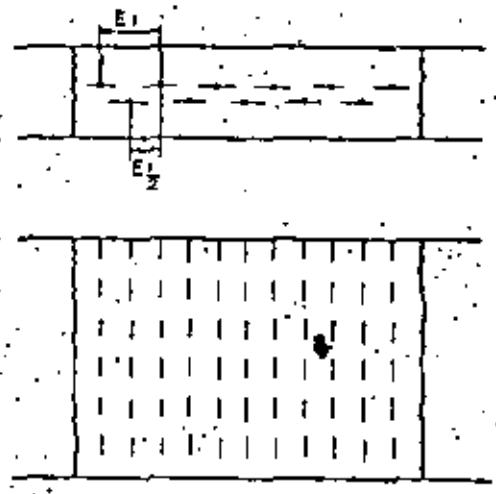

Fig. 15.2.1

Voladura de pilares de hormigón

Para efectuar la demolición completa de pilares de hormigón mediante perforación y explosivo, y debido a las distintas dimensiones en el caso de edificios, pueden ser necesarias considerables alturas de voladura para lograr el efecto de demolición deseado. En esta sección se trata de la carga que es necesaria para que el hormigón quede completamente fragmentado independencia de su apoyo.

La Tabla siguiente se refiere a pilares de hormigón armado:

Lado, sección cuadrada m	Profundidad barrenos m	Espaciamiento E_1 m	No. de hileras de barrenos	Carga, Dynamex kg
0,30	0,20	0,30	1	0,05
0,40	0,30	0,30	1	0,10
0,50	0,40	0,35	2	0,085
0,60	0,45	0,35	2	0,125
0,70	0,55	0,35	2	0,17

Frente a las cargas se coloca una gran cantidad de material de retacado. En el caso de dos hileras de barrenos, la disposición de los mismos es la que se muestra a continuación:

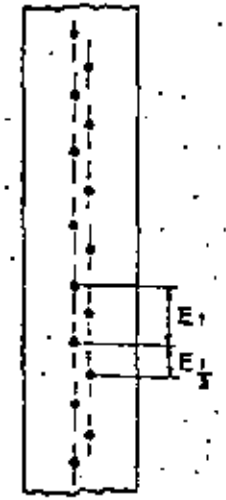

Fig. 15.2.2

Se precisa una protección cuidadosa. En voladuras en las que el resultado global depende de la voladura de unos pilares de hormigón, tanto las cargas como el retacado se aumentarán notablemente.

Voladura de muros o losas de hormigón mediante barrenos poco profundos

En ciertos casos no resulta posible en la práctica la voladura de estructuras delgadas de hormigón mediante barrenos perforados a lo largo de su superficie. En el caso de losas de hormigón cimentadas en el propio terreno, por ejemplo, ha de recurrirse a unos barrenos superficiales, de muy poca profundidad. Por esta circunstancia, es posible perforarlos con un espaciamiento relativamente pequeño.

En hormigón de gran resistencia puede ser necesario abrir mediante voladuras unas hendiduras a través de las cuales se cortan las armaduras, tras lo cual puede procederse al levantamiento y retirada de los trozos en que ha quedado dividida la estructura. La apertura de hendiduras se ajusta a los requerimientos de los dispositivos de levantamiento de que se disponga. En hormigón de baja resistencia, en cambio, los barrenos pueden tener espaciamientos mayores y se consigue una fracturación total.

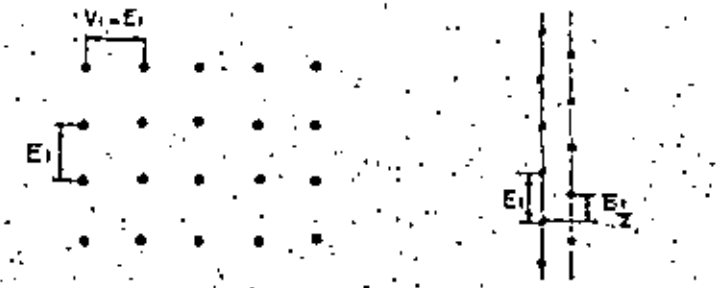

Fig. 15.2.3

I Hormigón de baja resistencia o sin armar

Espesor de hormigón m	Profundidad barrenos m	Espaciamiento $V_1 \times E_1$ m	No. de hileras de barrenos	Carga, Dynamex kg
0,30	0,20	0,40	—	0,03 (fracturación)
0,40	0,30	0,50	—	0,06
0,50	0,40	0,50	—	0,075

II Hormigón armado de alta resistencia

0,30	0,20	0,20	2	0,03 (apertura de grietas)
0,40	0,30	0,20	2	0,04
0,50	0,40	0,20	2	0,05

Se hacen primeramente unas voladuras experimentales, pues la resistencia del hormigón y la influencia de las armaduras son de gran importancia. Pueden ser precisas cargas más potentes. El empleo de una cuidadosa protección es de importancia esencial.

15.3 VOLADURA DE PUENTES

También en este terreno las voladuras han resultado una alternativa competitiva. Se trata de un campo en el que las voladuras son una aplicación militar ya tradicional. En una operación no militar, sin embargo, la voladura de un puente ha de satisfacer unas demandas totalmente diferentes. Las cargas usadas no deben dañar el entorno a través de las proyecciones, vibraciones del terreno, u ondas de choque aéreas que originen. Generalmente no es posible utilizar cargas externas separadas.

Los puentes pueden ser de diseños muy variados, y en consecuencia los métodos de voladura han de adaptarse al caso concreto de que se trate. Al igual que en el caso de la voladura de edificios, puede no ser recomendable establecer un procedimiento de voladura sin hacer antes un estudio más detallado de cada caso particular. No obstante, puede establecerse una diferenciación entre dos variantes principales:

Voladuras para demolición completa, con la mayor fracturación posible.
Voladura de tramos de puente para ser retirados por etapas.

El primer método es el más ventajoso para las voladuras, pero como es frecuente que el puente en cuestión se halle en un lugar muy al descubierto, en muchos casos puede ser necesario recurrir a la voladura por fases. En la sección 15.2, Voladuras en hormigón, se especifican las cargas y espaciamientos necesarios. La calzada es volada mediante el método de las hendiduras con barrenos poco profundos, en tanto que los estribos y las pilas son volados siguiendo las Tablas para pilares y estructuras compactas de hormigón.

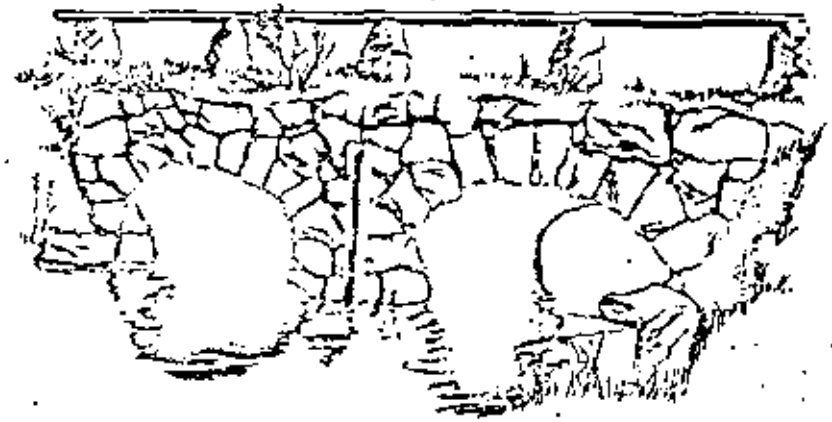

Fig. 15.3.1 Antiguo puente de piedra

Cuando se usa el primer método con rotura total, se necesita disponer de un amplio margen de seguridad que garantice la destrucción completa de las partes vitales, de modo que no se impida el colapso de la estructura. Hay que diferenciar dos tipos de puentes:

Puentes de piedra
Puentes de hormigón

Los puentes de piedra suelen ser relativamente antiguos; están formados por pilares, estribos, y arcos hechos con piedras unidas mediante un mortero. En muchos casos se incluye también hormigón en masa. Estos puentes pueden ser de gran resistencia, como ha quedado demostrado con ocasión de bombardeos y voladuras.

Como los elementos portantes suelen constituir una parte importante del volumen del puente, es difícil hacer una voladura que ocasione el colapso total desde unos pocos puntos vitales. Aun cuando esto fuera posible, lo más probable es que la fragmentación resultara tan deficiente que hiciera difícil el subsiguiente trabajo de desescombro.

Para los trabajos de perforación en puentes de este tipo puede usarse una potente perforadora desde la calzada que cruza el puente. La voladura se realiza con encendido de microrretardos, y una carga específica comprendida entre 0,40 y 0,80 kg/m³. Debe disponerse protección en los puntos al descubierto, y adaptarse asimismo las cargas.

En el caso de un puente como el que se muestra en la figura, la voladura puede ser dividida en varias fases si ello se estima conveniente.

Demolición de puentes de hormigón

Si la voladura se efectúa de modo que el puente se ve sometido a grandes tensiones durante el proceso de colapso e impacto contra el terreno, puede lograrse una considerable fracturación. La perforación y carga de los pilares y estribos debe hacerse dejando grandes márgenes que aseguren la rotura. Es preferible sobrecargar y aumentar la protección y las distancias de seguridad. Los tableros, las vigas de borde, y los arcos han de volarse de modo que se rompan por los puntos vitales.

El encendido se dispone de forma que durante el proceso de voladura y colapso el puente se ve sometido a las máximas tensiones posibles.

Con relación al impacto contra el terreno, la erección de bancos o espaldones por debajo del puente a distancias adecuadas entre sí puede provocar un aumento de las tensiones cuando el puente choca contra el suelo.

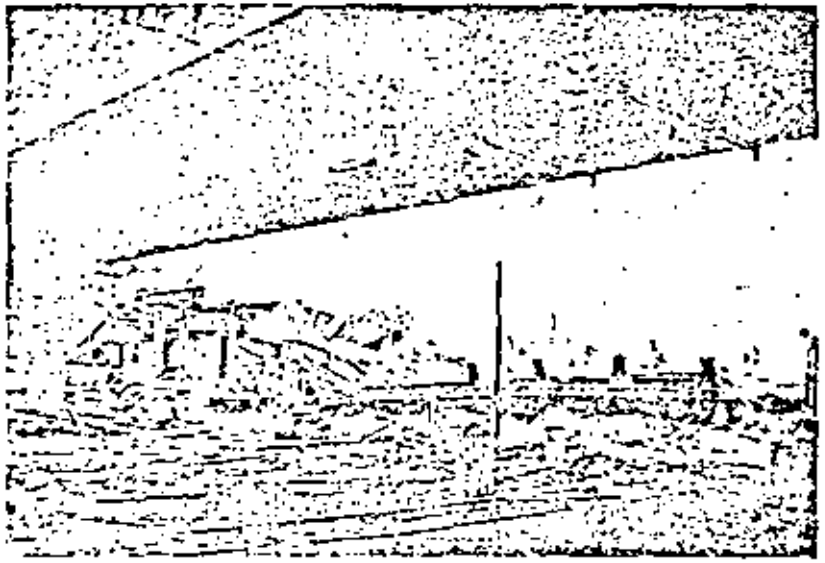

Fig. 15.3.2 Voladura de un puente en Malmö. Contratista: Nils P. Lundh. Consultor de voladura: L. G. Bergling.

15.4 VOLADURAS MEDIANTE PRESION DE AGUA

Los edificios de tipo completamente cerrado pueden ser volados utilizando la presión del agua.

Los métodos usuales de voladura resultan en muchos casos difíciles de aplicar, especialmente en edificios de hormigón diseñados de tal modo que no puede aprovecharse el efecto del propio peso. Se necesita entonces una gran cantidad de trabajo de perforación, y aún es preciso cortar una gran cantidad de armaduras a la hora del desescombro.

La voladura de edificios mediante presión de agua se efectúa llenando el edificio total o parcialmente de agua, y haciendo entonces detonar unas cargas libremente suspendidas; la presión producida sobre los muros por la onda de impacto del agua puede ser realmente muy grande; su magnitud puede calcularse teoricamente para poder evaluar las cargas.

Resulta difícil establecer un procedimiento general de cálculo de las cargas, pues el diseño de los edificios y las circunstancias externas varían de uno a otro caso. En los cálculos ha de tomarse en cuenta el volumen del edificio y la presión necesaria para romper los muros.

El método no es tan violento como parece; no origina vibraciones del terreno u ondas de choque aéreas especialmente grandes. Además, las proyecciones no constituyen un problema importante. Es preciso, sin embargo, disponer las cosas para que el agua pueda fluir libremente hacia afuera.

Este método resultará práctico también para estructuras de hormigón relativamente pequeñas, siempre que puedan ser llenadas de agua, en cuyo caso evitará la necesidad de recurrir a un extenso trabajo de picar y cortar que requiere un gran esfuerzo y mucho tiempo.

Según nuestros datos, hasta ahora este método es nuevo en Suecia. Anteriormente ha sido utilizado en Dinamarca con buenos resultados, y presenta muchas facetas interesantes para un más amplio uso en el futuro.

16. VOLADURAS ESPECIALES

16.1 VOLADURA DE BLOQUES SUELTOS NATURALES

La voladura de bloques sueltos, o taqueo, se refiere en este caso a la rotura de piedras naturales que pueden hallarse libres o parcialmente enterradas en el suelo (véase también la sección 5.2 para el taqueo de bloques resultantes de una voladura anterior).

El taqueo puede realizarse con una carga externa (carga conformada), o con una carga situada en el interior de un barreno taladrado en el bloque.

La carga de los barrenos puede hacerse de acuerdo con las indicaciones de la Tabla siguiente:

Volumen del bloque m^3	Espesor m	Profundidad de perforación m	Número de barrenos	Carga kg barreno
0,5	0,8	0,44	1	0,05
1,0	1,0	0,55	1	0,10
2,0	1,0	0,55	2	0,10
3,0	1,5	0,87	2	0,15

La Tabla está calculada para una carga específica de 0,1 kg/m³ (ver Fig. 16.1.1).

En el caso de varios barrenos en un mismo bloque, se emplea el encendido instantáneo. Sobre la carga ha de aplicarse un material de retacado correctamente dispuesto. A la hora de situar los barrenos y de estimar la cantidad de carga a emplear es importante prestar atención a las grietas y diaclasas existentes en el bloque.

Cuando el taqueo se realiza en la proximidad de edificios, la carga debe ser reducida a 0,03 kg/m³.

Los bloques completa o parcialmente enterrados suelen ser mucho más difíciles de volar que los situados totalmente por encima de la superficie (Fig. 16.1.2).

Las cargas han de ser estimados con relación al grado de empotramiento en el bloque. A continuación se dan unos valores que pueden servir de orientación:

Volumen del bloque m^3	Espesor m	Parte enterrada m	Profundidad de perforación m	Número de barrenos	Carga kg barreno
1,0	1,0	0,5	0,6	1	0,15
1,0	1,0	1,0	0,6	1	0,20

Cuando el bloque está completamente enterrado, se aumenta la carga a 0,2 kg/m³, y la profundidad de perforación se incrementa asimismo hasta 1,2 × ⅓ del espesor del bloque.

Las cargas conformadas solamente pueden ser empleadas lejos de áreas edificadas, debido a las ondas de choque aéreas que se producen (Fig. 16.1.3).

Para bloques enteramente situados encima de la superficie, la carga necesaria en general es de 1,0 kg/m³. La carga se coloca de forma que tenga un buen contacto con la superficie del bloque. Ha de utilizarse también abundante material de retacado sobre la carga, del tipo de arcilla húmeda o similar.

Cuando se utilizan cargas de superficie es sumamente importante elegir un explosivo adecuado. La Carga conformada A (Nitroseismex) es un explosivo que ha sido adaptado para este tipo de voladura en su diseño y su elevada velocidad de detonación. El Nabit es mejor que el Dynamex como carga de superficie.

Puede resultar muy difícil el taqueo de bloques enterrados mediante cargas conformadas. Esto es debido al hecho de que la onda de choque resultante de la detonación del explosivo no puede reflejarse contra las superficies libres.

Si es absolutamente necesario hacer el taqueo de un bloque con una carga conformada, puede colocársela bajo el bloque, que rompe entonces con mayor facilidad. La aplicación de la carga puede hacerse más fácil si el orificio abierto en el terreno junto al fondo del bloque es ensanchado haciendo detonar ¼—½ cartucho de explosivo.

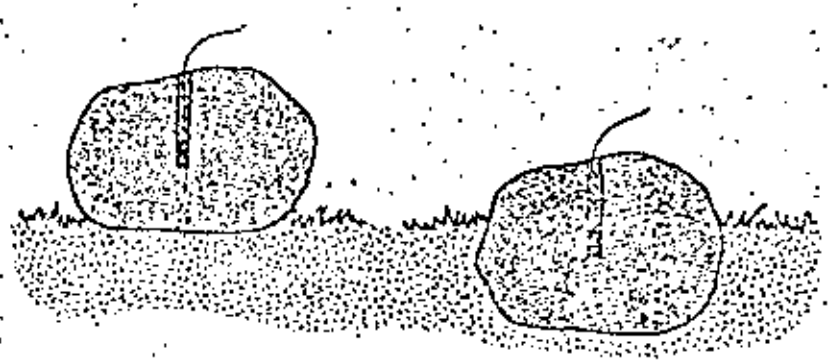

Fig. 16.1.1

Fig. 16.1.2

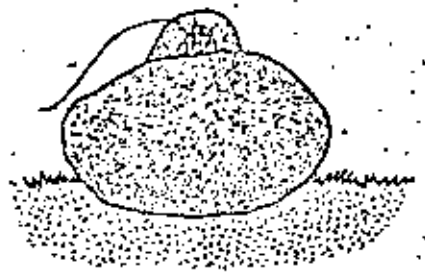

Fig. 16.1.3

16.2 VOLADURA DE METALES

Los explosivos han sido utilizados frecuentemente para romper el hierro y el acero. En los últimos años se ha desarrollado un procedimiento de mezcla de metales por medio de explosivos; se le conoce con el nombre de "metal-cladding" (revestimiento metálico), y en la actualidad está siendo ya utilizado en procesos de producción. El procedimiento se basa en el principio de que la presión extremadamente elevada producida en la detonación es capaz de "soldar" entre sí materiales diferentes de tal modo que la unión entre ellos está constituida por un material común con componentes de los dos materiales originales (Nitro Metall ha desarrollado un explosivo tipo "metal-cladding").

Por lo que respecta a las aplicaciones militares, existen muchos conocimientos sobre la voladura de estructuras diversas de hierro y acero. Dado que en las operaciones de voladura no militares no se tiene generalmente la posibilidad de evacuar un área de seguridad suficientemente grande, normalmente no es posible llegar a los mismos niveles de carga que en las Tablas militares.

Como el objetivo de la voladura es diferente, los cálculos militares de las cargas incluyen un suplemento de carga suficiente para cada caso.

Otra dificultad que se plantea al volar metales consiste en la variación de las características resistentes de los materiales; existe por ejemplo, una gran diferencia entre el hierro colado y el hierro forjado. Las diversas clases de acero poseen diferentes características de volabilidad.

Las voladuras experimentales pueden proporcionar experiencia sobre las características de los diversos materiales, de modo que pueda hacerse uso de una serie bien equilibrada de cargas.

En las voladuras en hierro y acero es preciso llamar la atención sobre el peligro de proyecciones, que es considerable, tanto con cargas en barrenos como con cargas de superficie. Debe disponerse una cuidadosa protección con material pesado y ligero (anti-esquirlas).

Puede establecerse una subdivisión entre dos métodos principales de voladura de metales:

Voladura con cargas de superficie (cargas conformadas)
Voladura con cargas confinadas

En las voladuras con cargas de superficie se aprovecha la fuerza de impacto del explosivo, razón por la que una elevada velocidad de detonación constituye una característica importante en el explosivo que vaya a emplearse. Los explosivos en forma de pasta resultan muy adecuados para estos fines, tanto en lo que respecta a las características de detonación como a la consistencia, pero también pueden utilizarse explosivos convencionales del tipo del Dynamex y Nabit.

Un par de casos prácticos pueden servir para ilustrar la dificultad de establecer normas generales de carga para las voladuras de hierro y acero:

1. Radios de un volante, de hierro colado; diametro: 15 cm
   Carga necesaria: 0,20 kg de dinamita
   Carga por unidad de superficie: 0,11 kg/dm²
2. Viga de acero DIP 26
   Carga límite necesaria: 0,50 kg de pasta explosiva
   Carga por unidad de superficie: 0,42 kg/dm²

La carga necesaria por unidad de superficie puede ser una constante de voladura apropiada, pero la forma del material que va a volarse es también significativa. Un objeto delgado y ancho, por ejemplo, es más fácil de volar que otro más masivo.

Deben hacerse *voladuras de ensayo* para determinar la cuantía de la carga necesaria. En las cargas de superficie debe aplicarse un material de retacado del tipo de la arcilla. Cuando las voladuras se efectúan en lugares en los que existe riesgo de daños por onda de choque aérea, el retacado deberá complementarse con un material que amortigüe dichas ondas de choque. El material de protección para combatir las proyecciones debe ser asimismo muy robusto. En el caso de cargas sobre el terreno, puede ser recomendable el empleo de una "jaula" de troncos con un material de protección contra esquirlas sobre su parte superior. El material de protección pesado no debe ser completa-

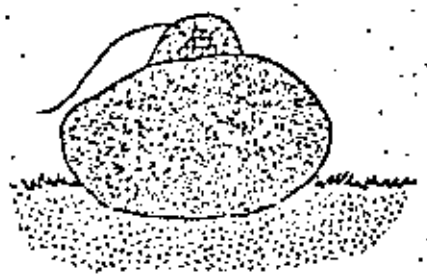

Fig. 16.1.3

16.2 VOLADURA DE METALES

Los explosivos han sido utilizados frecuentemente para romper el hierro y el acero. En los últimos años se ha desarrollado un procedimiento de mezcla de metales por medio de explosivos; se le conoce con el nombre de "metal-cladding" (revestimiento metálico), y en la actualidad está siendo ya utilizado en procesos de producción. El procedimiento se basa en el principio de que la presión extremadamente elevada producida en la detonación es capaz de "soldar" entre sí materiales diferentes de tal modo que la unión entre ellos está constituida por un material común con componentes de los dos materiales originales (Nitro Metall ha desarrollado un explosivo tipo "metal-cladding").

Por lo que respecta a las aplicaciones militares, existen muchos conocimientos sobre la voladura de estructuras diversas de hierro y acero. Dado que en las operaciones de voladura no militares no se tiene generalmente la posibilidad de evacuar un área de seguridad suficientemente grande, normalmente no es posible llegar a los mismos niveles de carga que en las Tablas militares. Como el objetivo de la voladura es diferente, los cálculos militares de las cargas incluyen un suplemento de carga suficiente para cada caso.

Otra dificultad que se plantea al volar metales consiste en la variación de las características resistentes de los materiales; existe por ejemplo, una gran diferencia entre el hierro colado y el hierro forjado. Las diversas clases de acero poseen diferentes características de volabilidad.

Las voladuras experimentales pueden proporcionar experiencia sobre las características de los diversos materiales, de modo que pueda hacerse uso de una serie bien equilibrada de cargas.

En las voladuras en hierro y acero es preciso llamar la atención sobre el peligro de proyecciones, que es considerable, tanto con cargas en barrenos como con cargas de superficie. Debe disponerse una cuidadosa protección con material pesado y ligero (anti-esquirlas).

Puede establecerse una subdivisión entre dos métodos principales de voladura de metales:

Voladura con cargas de superficie (cargas conformadas)
Voladura con cargas confinadas

En las voladuras con cargas de superficie se aprovecha la fuerza de impacto del explosivo, razón por la que una elevada velocidad de detonación constituye una característica importante en el explosivo que vaya a emplearse. Los explosivos en forma de pasta resultan muy adecuados para estos fines, tanto en lo que respecta a las características de detonación como a la consistencia, pero también pueden utilizarse explosivos convencionales del tipo del Dynamex y Nabit.

Un par de casos prácticos pueden servir para ilustrar la dificultad de establecer normas generales de carga para las voladuras de hierro y acero:

1. Radios de un volante, de hierro colado; diametro: 15 cm
   Carga necesaria: 0,20 kg de dinamita
   Carga por unidad de superficie: 0,11 kg/dm²
2. Viga de acero DIP 26
   Carga límite necesaria: 0,50 kg de pasta explosiva
   Carga por unidad de superficie: 0,42 kg/dm²

La carga necesaria por unidad de superficie puede ser una constante de voladura apropiada, pero la forma del material que va a volarse es también significativa. Un objeto delgado y ancho, por ejemplo, es más fácil de volar que otro más masivo.

Deben hacerse *voladuras de ensayo* para determinar la cuantía de la carga necesaria. En las cargas de superficie debe aplicarse un material de retacado del tipo de la arcilla. Cuando las voladuras se efectúan en lugares en los que existe riesgo de daños por onda de choque aérea, el retacado deberá complementarse con un material que amortigüe dichas ondas de choque. El material de protección para combatir las proyecciones debe ser asimismo muy robusto. En el caso de cargas sobre el terreno, puede ser recomendable el empleo de una "jaula" de troncos con un material de protección contra esquirlas sobre su parte superior. El material de protección pesado no debe ser completa-

mente impermeable a la onda de choque aérea. Cuando se usan cargas de superficie, *los objetos de acero no protegidos pueden ser lanzados a centenares de metros.*

En el caso de grandes piezas de acero o de otro metal, puede resultar difícil utilizar unas cargas suficientemente grandes para romperlas; en tales casos, la voladura debe hacerse con *cargas confinadas.*

Aun cuando se use este último método, las características resistentes del material son de importancia decisiva para la magnitud de la carga necesaria.

Ha ocurrido a menudo en voladuras de hierro que se han obtenido unos resultados de eficacia nula, o bien indicadores de un exceso de carga; ésto confirma la necesidad de realizar ensayos para obtener la carga apropiada.

Por ejemplo, en la voladura de bloques o lingotes con una superficie mínima o lingote. Este método es *inadecuado;* es mejor abrir una hendidura o roza de aproximadamente 0,7 m² y longitud variable, se ha utilizado el método de voladura en cámara, con una carga concentrada en el centro del bloque formada por varios taladros, cuyas cargas pueden ser iniciadas simultaneamente. Este efecto de cuele en roza debido a una hilera de barrenos implica que la carga necesaria puede disminuirse considerablemente. El bloque o lingote se corta a lo largo de la línea de barrenos, y normalmente las demás partes del mismo no se rompen.

Es conveniente abrir los taladros perforando el metal con un soplete de oxígeno. Antes de introducir la carga es importante controlar estrechamente la temperatura del barreno; la máxima admisible es de 50°C, lo que significa que es preciso enfriar el bloque o lingote después de hacer las perforaciones, a menos que esta operación se haya realizado el día anterior. Los materiales de protección han de ser del tipo pesado y del ligero (anti-esquirlas).

Caso práctico:

Se va a volar un lingote de acero cuyas dimensiones son 0,8×0,85×2,00 m.

Se abren dos rozas de cinco barrenos cada una, con distancias de 12,5 cm entre centros de barrenos.

Profundidad de perforación: 0,60 m; aproximadamente el 75 % del espesor del material.

La carga por barreno es de 120 g, y pudo ser rebajada posteriormente a 100 g de Dynamex.

La iniciación se efectúa mediante detonadores instantáneos de tipo VA.

Material de protección: 1 pantalla de rollizos de madera, de 15 m² × 6" y 15 pantallas de alambre de 2 × 1 m, una protección adecuada para una voladura efectuada en un área de estampación de acero.

Este procedimiento se encontró muy apropiado en ulteriores trabajos de voladura, pero otros materiales diferentes precisan cargas distintas.

En Estados Unidos, Alemania, e Italia, se han efectuado voladuras a gran escala en fundiciones. La rotura de salamandras con escoria en la zona superior se ha realizado con ayuda de explosivos, perforadoras, y sopletes de oxígeno. Las altas temperaturas imperantes hacen preciso adoptar medidas especiales.

No debe realizarse la voladura en un material muy caliente antes de haber efectuado estudios especiales y obtenido el permiso correspondiente de la autoridad responsable de las regulaciones de voladuras.

16.3 VOLADURA EN TIERRAS

Por voladuras en tierras se entiende aquí la utilización de explosivos con el objeto de *aflojar o disgregar un suelo,* y hacer con ello más fácil la excavación o carga del mismo. En las graveras, la capacidad de carga aumenta considerablemente tras la voladura.

Una regla sencilla de dimensionamiento consiste en utilizar una carga específica de 0,1 a 0,2 kg/m³.

La carga necesaria se sitúa en la parte que quiere moverse y como la creación de líneas de barrenos exigiría una gran cantidad de trabajo de perforación, se intenta utilizar lo más posible los barrenos sirviéndose de voladuras en cámara para ensancharlos. Debe darse tiempo para que se enfríe la cavidad abierta con estas voladuras antes de efectuar la carga; la máxima temperatura admisible es de + 50°C.

Las cavidades de carga pueden ser planificadas para barrenos horizontales o verticales o para tubos de carga, dependiendo de los equipos de que se disponga.

El departamento de Servicios de Nitro Nobel AB ha desarrollado un método de perforación que puede ser aplicado también en un arenal para eliminar *los taludes colgantes* o en desplome, que constituyen un peligro considerable, por lo que resulta ventajoso volarlos.

En los suelos son posibles muchos métodos de perforación, que posibilitan el empleo de explosivos en tierra y arenas.

En la *excavación de hoyos para implantación de postes,* las voladuras de aflojamiento del terreno facilitan en grado considerable el trabajo posterior de excavación; se perfora un barreno o se introduce un tubo de carga hasta

la profundidad deseada, y se escoge una carga adecuada. Las voladuras de ensayo llevadas a cabo por el Departamento de Servicios de Nitro Nobel AB han demostrado que unos tres cartuchos de Nobit constituyen una carga de fondo adecuada, con cargas alargadas de Gurit de 17 mm formando la carga de columna.

Se han obtenido buenos resultados empleando explosivos para la apertura de hoyos en la plantación de árbole. frutales; el explosivo afloja la tierra circundante, lo que resulta ventajoso desde el punto de vista del crecimiento de la planta. Un hoyo de unos 80 cm de profundidad y una carga consistente en 0,15 kg del Nabit son suficientes para conseguir este aflojamiento. Si el terreno es pedregoso, debe usarse material de protección cuando las voladuras se llevan a cabo en áreas edificadas.

También puede emplearse un explosivo cuando se trata del rejuvenecimiento de árboles frutales, para aflojar asimismo el terreno circundante. Las cargas se colocan (según el Departamento de Servicios de Nitro Nobel AB) en el terreno bajo los puntos más exteriores de las ramas del árbol. Los hoyos son de 0,60—0,80 m de profundidad y se cargan con 0,05—0,1 kg de Nabit. En el caso de árboles aislados, se colocan cuatro cargas regularmente distribuidas; en el caso de hileras de árboles, se utilizan tres cargas, dos de ellas a lo largo de las alineaciones, y una entre cada dos árboles de la misma hilera.

16.4 VOLADURA EN TERRENOS CONGELADOS PERMANENTEMENTE

La voladura de estratos o capas de terreno permanentemente congelados y de profundidad variable ("permafrost") es una operación acerca de la cual es difícil aventurar cualquier tipo de instrucción con carácter general. No se trata de un terreno en absoluto uniforme, sino que puede presentar considerables variaciones tanto en lo que respecta a su composición como al grado de congelación. La magnitud de estas voladuras suele adaptarse en la práctica a las máquinas empleadas para cargar y retirar el terreno después de volado; cuando se utilizan máquinas potentes, un ligero aflojamiento puede ser suficiente para que éstas puedan trabajar. La profundidad hasta la que llega la congelación varía según los lugares; en las zonas árticas puede profundizar hasta más de dos metros bajo la superficie del terreno. Las voladuras de estos terrenos congelados pueden realizarse según dos métodos diferentes:

Voladura con cargas situadas en el terreno congelado.
Voladura con cargas situadas bajo el terreno congelado.

Las voladuras con cargas situadas bajo el terreno congelado constituyen el método que resulta mejor cuando se trata de capas congeladas de profundidad reducida. La carga se coloca bajo dicha capa de modo que la presión a que da origen al hacer explosión pueda forzar el terreno hacia arriba. La aplicación de las cargas puede hacerse de diferentes modos; pueden introducirse unos tubos horizontales hasta debajo de la capa congelada, si existe ya una abertura; si no puede llegarse desde arriba a ninguna abertura o cavidad, es preciso perforar primeramente la capa congelada, tras lo cual puede prepararse una cavidad de carga por medio de una voladura en cámara; la carga empleada será la más pequeña posible para limitar el tamaño de la cavidad formada bajo la capa congelada, pues si fuera demasiado grande ello perjudicaría el resultado de la voladura subsiguiente; puede bastar con medio cartucho. Cuanto más duro sea el material situado bajo la capa congelada, mayor será la carga necesaria para la cavidad, y mejores serán también las condiciones para conseguir unos resultados satisfactorios. Si el terreno que hay bajo la capa congelada consiste en arcilla blanda, el resultado puede ser más deficiente, sobre todo si la primera es relativamente profunda. La carga a utilizar puede calcularse en función de la profundidad de la capa congelada:

Profundidad de congelación m	Profundidad de emplazamiento de la carga m	Carga kg barreno
0,2	0,4	0,07
0,4	0,6	0,20
0,6	0,8	0,30
0,8	1,1	0,60
1,0	1,4	1,00

Muchas veces puede ser complicado perforar a través del terreno congelado. Si se utilizan potentes equipos de perforación con perforadoras de gran diámetro, puede no ser necesario recurrir a las voladuras en cámara; en lugar de ello se perforan barrenos hasta una profundidad igual a 1,5 veces la de la capa congelada. La distancia entre barrenos se toma igual a 2 veces esta profundidad, cuando hayan de perforarse varios. La forma de iniciación más adecuada es mediante detonadores de microrretardo, pero también pueden usarse detonadores eléctricos instantáneos.

Voladuras con cargas situadas en el terreno congelado

En el caso de que la profundidad de la capa congelada sea superior a 1 m, se hace progresivamente más difícil emplazar las cargas bajo esta capa. Esto es especialmente cierto en el caso de que el material situado bajo la capa congelada no ofrezca ninguna resistencia. Con capas congeladas de gran profundidad resulta más ventajoso perforar y cargar dentro de la propia capa congelada de un modo aproximadamente igual al de las voladuras ordinarias en roca. Los barrenos no atraviesan toda la capa, sino que terminan a unos 0,2 metros por encima de la cavidad que hay debajo de la misma. El efecto de la voladura es menor si los barrenos atraviesan toda la capa congelada. Para planificar la perforación y la carga puede servir de ayuda la Tabla que se incluye a continuación, si bien, como ya se ha señalado, las características del terreno congelado frente a la voladura pueden variar considerablemente.

Profundidad de congelación	Profundidad de perforación	Piedra	Espaciamiento de los barrenos	Carga
m	m	m	m	kg
0,8	0,6	0,6	0,6	0,15
1,0	0,8	0,8	0,8	0,30
1,2	1,0	1,0	1,0	0,50
1,4	1,2	1,2	1,2	1,00
1,6	1,4	1,3	1,3	1,35
1,8	1,6	1,4	1,4	1,80
2,0	1,8	1,5	1,5	2,50

Las cifras de carga señaladas para profundidades del terreno congelado superiores a 1,2 m indican que son necesarios barrenos de mayor diámetro que los de la serie normal de barrenos pequeños para poder alojar la carga necesaria; de otro modo, los barrenos habrán de ser perforados con un espaciamiento más denso y la misma carga específica en kg/m³. Esto mismo debe hacerse también si las voladuras han de efectuarse junto a edificios donde exista peligro de proyecciones. Pueden emplearse Dynamex o Nabit. Los explosivos ricos en gases, como el Nabit, son muy eficaces en materiales como los terrenos congelados. El encendido se realiza con detonadores de microretardo del mismo modo que en las voladuras ordinarias en banco. Pueden utilizarse detonadores eléctricos instantáneos, pero no resultan adecuados en los casos en que las vibraciones del terreno o las proyecciones supongan un riesgo.

La voladura de las capas de terreno permanentemente congeladas implican ciertos riesgos. Las proyecciones son enormemente más difíciles de controlar, y las vibraciones del terreno pueden suponer un problema cuando las voladuras se efectúan en la proximidad de edificios o de otras instalaciones sensibles a las mismas.

Los métodos que se han descrito para la voladura del terreno congelado no deben ser aplicados de modo general en áreas edificadas. En estas zonas, el espaciamiento entre barrenos ha de hacerse menor, de modo que pueda disminuirse el valor de la carga en cada uno de ellos. Además, debe disponerse una protección análoga a la que se emplea en los trabajos de voladura en bancos bajos (véase el capítulo 8).

Las capas congeladas pueden inducir unas acusadas vibraciones del terreno, y producir daños cuando hay edificios a menos de unos 10 metros (véase la sección 13.1). Un edificio rodeado por terreno congelado está más sometido al efecto de las vibraciones, debido al buen contacto entre edificio y terreno bajo la cimentación. Hasta cierto punto puede compararse este caso con el de voladuras en roca junto a un edificio asentado sobre el mismo macizo. En las voladuras en roca próximas a edificios, por otra parte, es fácil calcular una carga apropiada que garantice que los edificios no sufran daños.

La experiencia recogida en lo que respecta a las vibraciones en las voladuras de terreno congelado muestra que los valores experimentan variaciones mayores que en las voladuras en roca; es por tanto recomendable comenzar las voladuras limitando las cantidades de carga de detonación instantánea, y medir constantemente la magnitud de las vibraciones que se originan; si son muy pequeñas, puede aumentarse el volumen de las cargas. En las voladuras en roca, normalmente basta con medir la componente vertical de las vibraciones, pero en las voladuras de terreno congelado debe medirse también la componente horizontal pues, debido al contacto más estrecho entre edificio y terreno al que ya se hizo mención más arriba, esta componente puede ser considerablemente mayor que la vertical. Esto es aplicable sobre todo cuando la distancia entre la voladura y la edificación es pequeña.

Los riesgos citados aquí han tenido como consecuencia el que en muchos lugares se haya prescindido de la voladura del terreno congelado en el interior de zonas edificadas. Sin embargo, incluso en estas zonas, si es realizado de una forma correcta y con suficiente control de las vibraciones y material de protección, el método es completamente aplicable.

16.5 VOLADURAS EN PEDRAPLENES

Estas voladuras tienen como objetivo mover los materiales sueltos situados bajo un terraplén o un pedraplén, de modo que los materiales de relleno que forman estos últimos se asienten más fácilmente hasta la profundidad deseada.

Así pues, puede establecerse una diferenciación entre dos métodos distintos:

Voladura bajo pedraplenes.
Voladura en arcilla antes de verter el relleno de piedras.

Ambos métodos pueden ser aplicados en construcción de carreteras, así como debajo de terraplenes o rellenos en los que se desea garantizar que el material vertido apoya sobre una base suficientemente firme.

Voladura bajo un pedraplén

En este caso, las cargas han de colocarse bajo las piedras después de formar el dique o pedraplén. Esto puede hacerse perforando, o hincando tubos, a través del material de dique, o bien introduciendo unos tubos oblicuos desde los lados del mismo; este método es el más sencillo si no hay obstáculos para su realización práctica.

En arcillas blandas, es fácil introducir tubos de tipo extensible a través del terreno, con ayuda de una excavadora mecánica.

La distancia entre los tubos inclinados se ajusta de acuerdo con las cargas que caben en los mismos y con la carga total necesaria.

El cálculo de la carga se hace del modo siguiente:

Carga específica = 0,1 kg/m³
Volumen = Anchura del dique × (Espesor de asentamiento + 2,0)
Las cargas deben llenar como mínimo la mitad de la longitud de tubo situada bajo el nivel de la superficie.

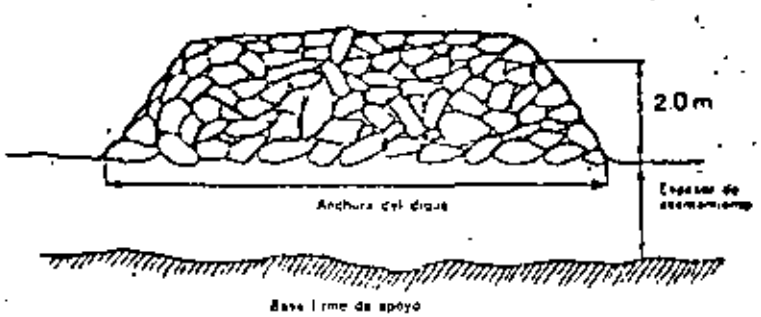

Fig. 16.5.1

Ejemplo:

Se va a efectuar una voladura bajo un dique de escollera cuya anchura en la base es de 20 m, y separado por un espesor de 6 m de una base firme de apoyo.

1.° La carga necesaria se calcula por metro lineal de dique:
Carga necesaria = 0,1 × Anchura del dique × (Espesor de asentamiento + 2,0)
Carga necesaria = 0,1 × 20 (6,0 + 2,0) = 16 kg/m

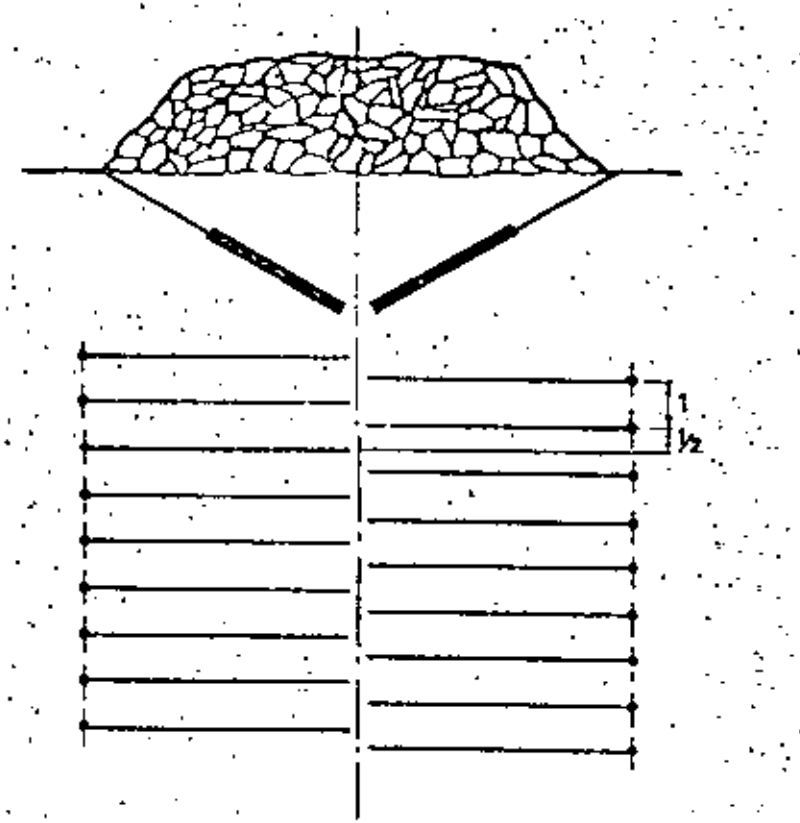

Fig. 16.5.2

2. Si se hincan tubos desde ambos lados del dique, dirigidos con una cierta inclinación hacia el centro del mismo, la longitud de tubo hasta el eje central es de unos 14 m, y la longitud de carga será de unos 7 metros por tubo. Como son dos tubos, la longitud cargada será aproximadamente de 14 m por hilera.

3. A partir de la longitud cargada puede calcularse el espaciamiento en la hilera (entre cada dos tubos) para diversos diámetros de tubo, así como las concentraciones de carga:

Diámetro interior de los tubos mm	Concentración de carga kg/m	Carga por hilera kg/hilera	Espaciamiento en la hilera m
40	1,6	22,4	1,40
50	2,5	35,0	2,20
60	3,6	50,4	3,15
70	4,9	78,4	4,90

Si las dos filas de tubos que bordean el dique se disponen de modo que los extremos interiores de los tubos sigan una distribución alternada, con distancias iguales a la mitad del espaciamiento entre los extremos de tubos consecutivos de distinto lado (Fig. 16.5.2), se consigue un mejor reparto de la carga.

El encendido se hace con detonadores eléctricos instantáneos. Si hay peligro por vibraciones, puede recurrirse al encendido con microrretardos.

La *voladura antes de verter el relleno de piedras* es el otro método que puede aplicarse.

Los cálculos de la carga se hacen basándose en la carga específica necesaria, y a partir del volumen de terreno que ha de ser movido.

Carga necesaria = 0,1 × Volumen de terreno a mover.

Las cargas son aplicadas en el interior de tubos, hincados formando una retícula cuadrada en el área de terreno que quiere aflojarse. La carga se coloca en la mitad inferior de cada tubo.

Como se presentan muchos casos en los que la vegetación es espesa, puede ser preciso cargar cada dos tubos hasta ¾ de su longitud, con lo que la longitud cargada puede establecerse, como media, en $\frac{0,50 + 0,75}{2} = 0,63$, es decir, el 63 % del tubo.

Ejemplo:

Se trata de mover una capa de tierra suelta hasta una profundidad de 7 m. Los tubos de que se dispone tienen un diámetro interior de 55 mm, y una longitud de 7 m.

1. Se cargan los tubos en una longitud media del 63 % = 0,63 × 7 = 4,41 = = aprox. 4,4 m.

2. Concentración de carga utilizando cargadora

$$= \frac{d \times d}{1000} = \frac{55 \times 55}{1000} = \text{aprox. } 3,0 \text{ kg/m}$$

3. La carga media por tubo será 4,4 × 3,0 = 13,2 kg.
De cada dos tubos, uno se carga con 3,5 × 3,0 = 10,5 kg, y el otro, siguiendo una distribución alternada, con 5,25 × 3,0 = 15,75 kg.

4. Los tubos se disponen de modo que proporcionen la carga específica necesaria:

$$\text{Volumen/tubo} = \frac{\text{Carga/tubo}}{\text{Carga específica necesaria}}$$

$$\text{m}^3\text{/tubo} = \frac{13,2}{0,1} = 132 \text{ m}^3$$

$$\text{Area/tubo} = \frac{\text{Volumen/tubo}}{\text{Longitud tubo}}$$

$$\frac{132}{7} = 18,8 \text{ m}^2\text{/tubo}$$

$$V \times E = 18,8$$

$$V = E$$

$$V = \text{aprox. } 4,3 \text{ m } (\sqrt{18,8})$$

La iniciación se hace mediante detonadores eléctricos instantáneos, o bien en caso necesario con microrretardos, como en el primer método.

El aflojamiento del terreno, es decir, la voladura, no debe hacerse con demasiada anticipación al vertido del relleno, pues la arcilla recupera gradualmente sus características resistentes iniciales.

Cuando se detonan cargas encerradas en tubos de hierro, existe siempre el peligro de que algún trozo de éstos sea proyectado, lo que indica la necesidad de evacuar la zona cuando se efectúa la voladura.

En la figura se muestra la distribución de los tubos y las cargas:

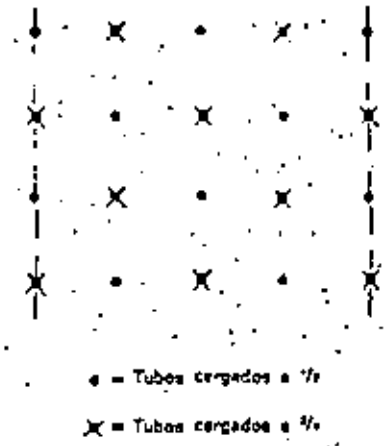

Fig. 16.5.3

16.6 VOLADURAS PARA ZANJAS DE DRENAJE

Durante muchos años se han utilizado los explosivos en Suecia en relación con el drenaje de áreas forestales. Hasta mediados de 1972 se venía empleando una dinamita de zanjas especial, con características específicas para los fines a que era destinada. En la actualidad se ha dejado de fabricar dinamita de zanjas en toda Escandinavia, por lo que ha sido necesario desarrollar un método nuevo para estas voladuras.

En conjunto, el método utilizado en las voladuras para zanjas forestales en tierra seca es el mismo que se aplicaba anteriormente.

Las cargas se colocan a intervalos de 0,60—0,80 m. En tierra húmeda resulta adecuado el Dynamex B, mientras que en tierra seca puede usarse Nabit. Una zanja de dimensiones normales requiere unas cargas de aproximadamente 0,25—0,30 kg cada una. Cada carga se sitúa algo más abajo de la mitad de la profundidad deseada para la zanja.

Como las condiciones del terreno varían considerablemente, el espaciamiento entre barrenos, su profundidad, y la cantidad de carga son factores que se ajustan en cada caso para obtener los mejores resultados. Se recomiendan voladur[illegible] ensayo sobre una pequeña longitud.

La iniciación ha de ser instantánea para garantizar una correcta proyección de la tierra; puede utilizarse mecha detonante o detonadores eléctricos instantáneos; la primera puede ser encendida mediante un detonador ordinario o eléctrico.

En el caso de iniciación eléctrica instantánea, se coloca un detonador en cada carga. Cuando se emplea mecha detonante, se tiende una mecha a todo lo largo de la futura zanja, y se colocan ramificaciones desde esta línea principal a cada carga. Es importante asegurarse de que las conexiones están en ángulo recto. No debe haber pliegues en la mecha. En caso de que la tierra esté húmeda, las conexiones deben ser dotadas de aislamiento, y el intervalo de tiempo antes del disparo debe ser lo más corto posible.

Las distancias de seguridad en las voladuras para zanjas son las establecidas en las Normas de Voladuras publicadas por las autoridades suecas. Para suelo pedregoso esta distancia es de 250 m y en turba, de 150 m y su observancia es muy necesaria.

Si ha de excavarse una zanja ancha, puede necesitarse unir varias cargas de Dynamex B, que son iniciadas mediante detonadores eléctricos instantáneos, si bien puede emplearse también mecha detonante. Los manojos de cartuchos, cada uno formado por 1 kg aproximadamente, se colocan a intervalos de 1,0 m. Con ello la anchura de la zanja será de 3 a 3,5 m.

También pueden utilizarse las cargas unidas, de magnitud adecuada, en voladuras para presas, diques, etc. en terreno apropiado. Cuanto mayor sea la anchura requerida, más grande habrá de ser la carga.

También se emplean explosivos para ensanchar canales y zonas de amarre para pequeñas embarcaciones.

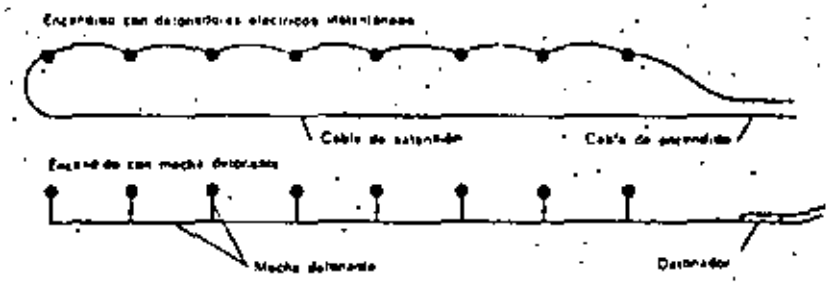

Fig. 16.6.1

16.7 VOLADURAS EN HIELO

El medio más seguro para volar hielo consiste en colocar la carga debajo de éste. La profundidad de la carga bajo el hielo debe ser de 1,25 m, excepto cuando la profundidad de agua debajo del hielo sea inferior a 2,5 m, caso en que las cargas deberán situarse a la mitad de dicha profundidad. En la Tabla siguiente se recogen los datos correspondientes a la experiencia militar en voladura de hielo:

Espesor de hielo m	Anchura abierta m	Carga kg	Espaciamiento m
Hasta 0,40	5	1	4
„ 0,40	6	2	5
„ 0,40	8	3	8
0,40—0,60	8	4	8
0,60—1,00	8—10	5	8

Si la profundidad del agua es menor de 2,5 m, el espaciamiento entre las cargas se reduce, en la forma que se muestra en la Tabla:

Profundidad de agua m	Espaciamiento en m, para una carga de 3 kg	4 kg	5 kg
2,0	5	7	8
1,5	4	6	8
1,0	4	5	6
0,5	3	4	5

Las cargas se colocan bajo el hielo a través de un agujero de carga abierto en éste. Es importante asegurar las cargas para que no puedan ser arrastradas por las corrientes.

En el caso de voladuras junto a instalaciones, puede ser preciso aislar éstas por medio de una voladura controlada, formando canales en el hielo mediante perforación de orificios o con otros medios mecánicos. La onda de choque del agua, por otra parte, puede dar origen a grandes presiones, incluso a distancias relativamente lejanas. Se dice que se han volado grandes bloques de hielo a la deriva mediante potentes cargas de superficie, pero personalmente no poseo ninguna experiencia de ello ni tengo otras que pueda mostrar. Es esencial disponer de un amplio espacio abierto, por las ondas de choque aéreas que pueden producirse.

16.8 VOLADURA DE BLOQUES DE PIEDRA EN CANTERAS

En las canteras de todo el mundo se vuelan cantidades considerables de roca de diversos tipos que es empleada en las industrias de la construcción. El granito se utiliza para la producción de piedras para bordillos y pavimentación. El mármol no sólo se usa en las industrias de construcción, sino también en escultura, y lo mismo cabe decir del granito y otras rocas.

La diferencia más significativa entre las voladuras en canteras y las ordinarias consiste en que la roca circundante no debe sufrir daños, ni la roca arrancada debe agrietarse. Es ésta una técnica basada en cierto grado en la tecnología de las voladuras, pero que exige también esencialmente el conocimiento de las características de la roca de que se trate, el cual se adquiere gradualmente de una larga experiencia práctica en canteras.

En los capítulos 10 y 11 puede encontrarse información sobre el problema de la extensión de los agrietamientos en la roca circundante cuando se realiza una voladura. La onda de choque que se propaga por el interior de la roca da origen a unas grietas iniciales, que se ensanchan cuando los gases de la detonación penetran en ellas.

Durante muchos años se utilizó en las canteras la pólvora de mina, pues posee una baja velocidad de detonación, y por ello es de efectos suaves sobre la roca. En los últimos años se han llevado a cabo en Suecia un número considerable de voladuras en canteras con cargas alargadas de Gurit, lo que ha puesto de manifiesto la posibilidad de emplear Gurit sin dañar la roca circundante.

Las voladuras se han hecho con cargas alargadas de Gurit de 17 y de 11 mm. Por razones evidentes no pueden aplicarse métodos de voladura exactamente iguales cuando se emplean explosivos tan diferentes como la pólvora de mina y Gurit. En el primer caso se perfora un número limitado de barrenos muy próximos entre sí, cuya acción se ejerce en una cierta dirección a través del efecto de zona. Utilizando cargas alargadas de Gurit, en cambio, se ha empleado el precorte en gran escala, con lo que superficies de roca más grandes se han hecho accesibles a trabajos ulteriores (ver fotografía). En uno y otro caso se aprovechan las superficies naturales de discontinuidad horizontal, que permiten la rotura de zonas enteras de roca sin que se produzca desmenuzamiento alguno.

Si en una cantera quiere dividirse un bloque de piedra en partes más pequeñas, es fundamental que éste se encuentre completamente libre por todas sus caras; ésto significa que la explotación se planifica de modo que la roca arrancada tenga el máximo número posible de caras libres. Si existen superficies horizontales de discontinuidad a distancias adecuadas entre sí, la explotación de la cantera se ve facilitada en grado considerable.

En muchos casos, las superficies libres se obtienen por medio de diversos

procedimientos; en las canteras de granito se hacen cortes en la roca mediante perforación térmica ("jet piercing"); estos cortes tienen unos centímetros de anchura, y la combustión se efectúa con ayuda de una mezcla de oxígeno y parafina (keroseno). En lugar de oxígeno puede emplearse también aire comprimido. El uso de este método presupone una cierta cantidad de cuarzo en la roca.

En las canteras de mármol se abren rozas con taladros mediante equipos mecanizados de perforación. En las canteras italianas de esta roca se emplea mucho un sistema de aserrado en curva, consistente en un perfil en forma de lazo que puede tallar en el mármol, por erosión, unas delgadas estrías, pudiendo aplicarlo a menudo a varios bancos de una misma cantera.

Las cuñas constituyen otro procedimiento ampliamente usado en las canteras, fundamentalmente para la subdivisión de bloques sueltos.

Como en las canteras la roca es un producto de valor, los métodos de explotación utilizados han de tener sobre este material los menores efectos posibles. Las voladuras normales con explosivos convencionales del tipo del Dynamex destruirían un gran volumen de la roca adyacente. Las cargas alargadas de Gurit, en cambio, poseen un efecto muy suave sobre la roca circundante, especialmente si ésta es homogénea y con inicios de fisuración natural de magnitud reducida, lo que es muy normal en las canteras.

La perforación de hileras de barrenos con espaciamiento reducido orienta las fuerzas de rotura que se produzcen en la roca como consecuencia de una voladura hacia unas líneas de fracturación representadas por los barrenos, evitándose con ello una acción más intensa sobre la roca circundante.

Los espaciamientos indicados seguidamente pueden servir como orientación:

Tipo de roca	Carga	Espaciamiento entre barrenos, m
Granito	Gurit de 17 mm	0,35—0,40
Granito	Gurit de 11 mm	0,15—0,25
Diabasa	Gurit de 17 mm	0,35—0,40
Diabasa	Gurit de 11 mm	0,15—0,25
Mármol	Gurit de 11 mm	0,20—0,25

De hecho, considerar unos tipos de roca tan amplios como en esta Tabla es generalizar demasiado. Los espaciamientos y las cargas habrán de adaptarse a los resultados de las voladuras de ensayo en cada caso particular.

Aun cuando en las canteras se encuentran las rocas de mayor homogeneidad que pueden verse, las propiedades a la voladura pueden variar dentro de una misma cantera por efecto de la estructura rocosa; las fisuraciones se producen en una roca con mucha mayor facilidad a lo largo de los "granos" que a su través.

Los barrenos se cargan con Gurit aproximadamente hasta un 75 % de su profundidad total. El detonador ha de conectarse directamente en Gurit, pues no puede usarse nada de Dynamex. No debe usarse material de retacado alguno, con la excepción de las tapas de las cargas alargadas. Un encendido con microretardos, con los menores intervalos posibles entre barrenos, es el de efectos más suaves sobre la roca circundante. Esto implica, sin embargo, que en rocas muy duras puede ser necesario adoptar un espaciamiento menor que el indicado en la Tabla, pues las cargas poseen un menor efecto de arranque que si la iniciación fuera instantánea.

Es importante observar las recomendaciones siguientes:

La *piedra* delante de los barrenos no debe ser pequeña.

Si se pretende arrancar completamente un bloque de roca, no debe estar parcialmente constreñido.

La precisión de perforación ha de ser buena.

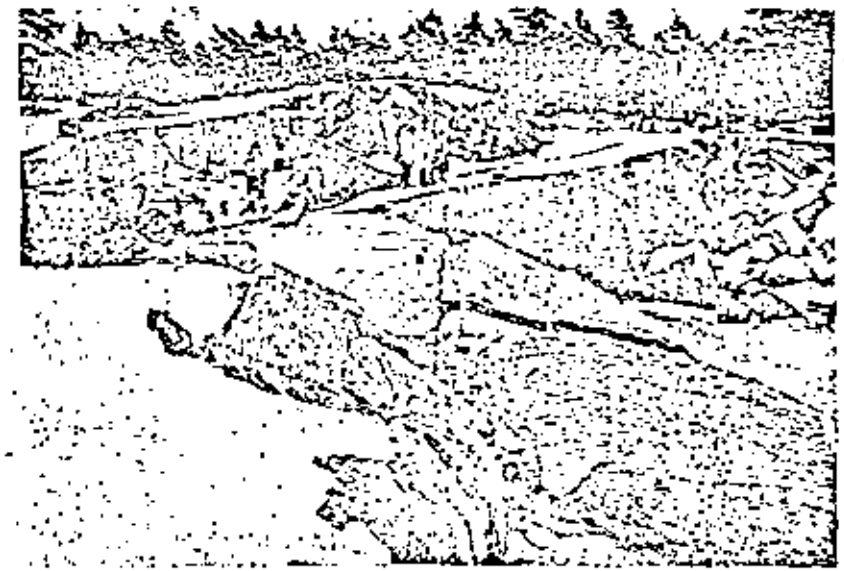

Fig. 16.8.1 Voladuras en una cantera de granito. (Nilsson och Söner, Mistorhult, Suecia.)

Con ayuda de medios como las cargas alargadas de Gurit, debe ser posible desarrollar métodos más racionales de voladura en las canteras. En las voladuras de ensayo puede ser conveniente comenzar por zonas en las que la roca sea de menos valor.

Una vez calculado el espaciamiento y las cargas adecuadas, se planificarán las voladuras de forma que las condiciones geométricas sean las más favorables para la rotura con la menor constricción posible.

Los métodos de medida para la determinación de la propagación de la onda de choque en el terreno, y los métodos de control de la formación de grietas hacen hoy posible comprobar los efectos de las voladuras sobre la roca circundante.

16.9 VOLADURA DE RAICES

Las raíces y tocones pueden ser volados por dos métodos diferentes; el más sencillo consiste en colocar una carga bajo el mismo, con lo que, si el resultado es correcto, el conjunto es volado completamente. Sin embargo, este método requiere disponer de un espacio libre a su alrededor, pues las proyecciones son difíciles de controlar.

Un método menos violento consiste en perforar un taladro en el tocón y quizás en las raíces gruesas, y romperlo así en trozos que puedan ser retirados. Con este método es posible disponer alguna protección.

Con *cargas bajo las raíces*, es importante que la carga esté situada en el lugar correcto y que su cantidad sea también la apropiada. Si el primer tiro fracasa, suele producir una oquedad tan grande que hace imposible cualquier voladura posterior.

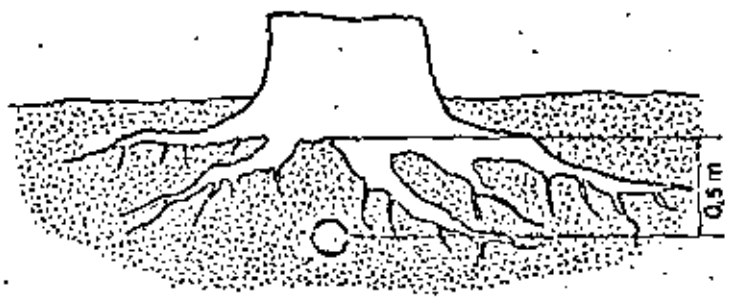

Fig. 16.9.1

La carga se coloca a unos 0,5 m bajo las raíces. La cantidad de Dynamex B o Nabit usada debe ser igual a 0,2—0,3 kg por decímetro de diámetro del tronco. Algunas veces puede resultar difícil colocar toda esta carga bajo las raíces sin abrir primero una pequeña cámara con ayuda de ½ de cartucho introducido en un orificio hecho con una palanca. Es importante que los cartuchos estén bien agrupados para que detonen todos juntos. Después de colocada la carga en posición, la cámara y el orificio abierto con la palanca se rellenan de nuevo.

La voladura es más fácil si el terreno bajo el tronco es duro. Las raíces situadas en terrenos pantanosos pueden ser muy difíciles de volar; sin embargo, no debe usarse una carga excesivamente grande, pues abre grandes hoyos en los lugares donde estaban; ésto es aplicable especialmente cuando la voladura de troncos se realiza con ocasión de la construcción de carreteras para trabajos forestales. Como ya se ha señalado anteriormente, las proyecciones son difíciles de controlar, por lo que la distancia de seguridad debe ser grande.

La voladura con cargas pequeñas introducidas en orificios taladrados en el tronco es un método considerablemente más suave. Estos barrenos se abren con una barreno de madera, y pueden localizarse y taladrarse desde arriba o desde un lado, dependiendo del crecimiento y tamaño del tronco. La perforación desde arriba generalmente es preferible desde el punto de vista de la voladura, pero puede resultar algo difícil en algunos troncos. También puede perforarse en las raíces gruesas. Las raíces pueden también volarse utilizando 1 ó 2 cartuchos como cargas conformadas (de superficie); sin embargo, es preciso tener cuidado con las cargas conformadas en zonas edificadas debido a la onda de choque aérea. Las cargas en el tronco pueden consistir en 1 ó 2 cartuchos de Dynamex B o Nabit, dependiendo del tamaño del mismo. En las raíces se usan de ½ a 1 cartucho, dependiendo de su grosor.

La carga requerida puede variar considerablemente, pues la resistencia material de los diversos tipos de madera puede ser muy diferente según que sea nueva o seca. El modo más adecuado de iniciar las cargas es con detonadores eléctricos instantáneos. En la proximidad de edificios, es importante disponer cuidadosamente la protección.

7.1. LA SEGURIDAD EN LOS TRABAJOS DE VOLADURA

Protección industrial

El objetivo de la protección industrial es el proporcionar unas condiciones de trabajo higiénicas y seguras a los trabajadores. Los aspectos legales de este campo son referidos normalmente a la legislación sobre protección industrial; en Suecia, la legislación consiste fundamentalmente en la "Swedish Labour Welfare Act" y los reglamentos publicados por las autoridades en asociación con esta ley. Estas regulaciones incluyen fundamentalmente las Ordenanzas de Seguridad Industrial, normas prohibiendo el empleo de personas jóvenes en determinados trabajos, y normas relativas a los exámenes médicos, así como inspecciones médicas regulares para evitar la aparición de determinadas enfermedades laborales. Hay también leyes especiales para diversos campos. Por lo que respecta a los trabajos de voladura, las más importantes son las Normas sobre uso de explosivos junto con los boletines del Ministerio sueco de Comercio concernientes a las aplicaciones prácticas. Otras formas de legislación incluyen los reglamentos generales y reglamentos de construcción.

Para que sirva de ayuda en la aplicación de la "Swedish Labour Welfare Act" (Ley de Bienestar en el Trabajo), el Departamento de Higiene y Seguridad en el Trabajo proporciona consejo e instrucciones. Para los trabajos de voladura, el Departamento ha publicado unas Instrucciones de Voladuras, No. 3. Otras disposiciones incluyen las Instrucciones para Trabajos en la Roca, No. 67, Instrucciones para elevadores de mina, No. 32, así como Instrucciones acerca de la Inspección de cámaras subterráneas, No. 33, y Medidas protectoras relativas a ciertos elevadores en chimeneas de minas, No. 56.

Regulaciones

Según el § 7 de la Swedish Labour Welfare Act, el empresario tiene la obligación de prestar atención a todos los aspectos relacionados con la naturaleza y condiciones del trabajo, edad y experiencia de los trabajadores, así como otros criterios que son evidentemente necesarios para evitar que los empleados sufran daños en su salud como consecuencia del trabajo, o sean heridos en accidentes.

De acuerdo con el § 1 de la Swedish Labour Welfare Act, el empresario tiene la obligación de asegurarse de que sus empleados están informados de los peligros especiales que supongan daños para la salud o accidentes asociados a su trabajo y cuando sea necesario, entregar las normas y regulaciones que deben ser observadas por los trabajadores para eliminar tales riesgos.

Cuando exista peligro de enfermedad o daños en un determinado trabajo, los supervisores o capataces no pueden declinar la responsabilidad en nadie que no posea experiencia en dicho trabajo. En trabajos en los que unos conocimientos o una experiencia insuficientes puedan implicar riesgo de daños o enfermedad, además de lo dicho más arriba, no deben utilizarse personas que carezcan de la experiencia necesaria sin la instrucción y dirección precisas.

De acuerdo con el § 7 de la Ley citada, el trabajador tiene la obligación de utilizar los dispositivos de seguridad existentes, seguir cuidadosamente las instrucciones de la Ley y los boletines basados en ella, y observar además el cuidado necesario y poner de su parte la atención precisa para evitar enfermedades o daños.

El Departamento de Seguridad e Higiene en el Trabajo está encargado de la inspección necesaria para asegurar el cumplimiento de la Swedish Labour Welfare Act y los boletines publicados asociados a esta Ley, así como, bajo la dirección del Departamento, los inspectores industriales y en el caso de trabajo subterráneo, los inspectores de minas.

Según el § 5 de la Swedish Labour Welfare Act, el empresario ha de informar sin retardo al inspector industrial (o inspector de minas) de cualquier accidente que haya ocurrido en el trabajo que está siendo realizado y que haya ocasionado daños mortales o graves, o haya afectado simultáneamente a varios trabajadores, así como otros accidentes o posibles circunstancias que puedan ser consideradas suficientemente importantes como para ser puestas en conocimiento del inspector correspondiente.

Las autoridades de policía han de ser informadas en los casos necesarios, tal como establece el § 56 de las Normas suecas sobre explosivos.

Según el § 6 de las Normas y Regulaciones Generales, no puede efectuarse ninguna voladura dentro de un área urbana, sea una ciudad, un pueblo, u otra zona edificada en la que sean aplicables las ordenanzas urbanas, sin obtener un permiso de las autoridades de policía.

La Ley de Construcción sueca, así como los diversos reglamentos de construcción incluyen ciertas regulaciones relativas a los trabajos de voladura.

Instrucciones

Los patrones tienen el deber de proporcionar a cada empleado que tome parte en los trabajos de voladura una copia de las Instrucciones de Voladura, a no ser que el empleado en cuestión tenga ya una. Este debe firmar un recibo o confirmación de estar ya en posesión de la copia.

Competencia del personal

Con relación a la seguridad, es sumamente importante que el personal empleado posea la experiencia práctica necesaria, y una buena suma de conocimientos, sobre el trabajo de voladura. Ciertas características que debe reunir el personal empleado en trabajos de voladura son las de responsabilidad, pulcritud, y buen juicio.

El supervisor o capataz debe comprobar de una u otra forma que el personal empleado en trabajos de voladura posee los conocimientos necesarios para realizar su trabajo con seguridad, remediando cualquier defecto en este sentido por medio del correspondiente adiestramiento. A la hora de elegir entre diversos métodos de voladura, el supervisor o capataz debe tomar en consideración la competencia del personal de que dispone en relación a cada uno de ellos.

Para trabajar en condiciones de seguridad es importante que el supervisor o capataz tenga la competencia necesaria para la dirección de las operaciones, y el jefe de voladuras debe asimismo ser lo suficientemente competente para dirigir los trabajos sobre el terreno.

Planificación de las operaciones de voladura

Las Normas de Construcción suecas establecen que cuando se efectúan voladuras junto a edificios, vías de tráfico, instalaciones, u otros servicios, de forma que puede existir algún riesgo de daños, el trabajo ha de ser dirigido por una persona competente de acuerdo con un plan de tiro predeterminado. Este plan ha de incluir la información necesaria sobre las operaciones de perforación, carga, protección, y encendido proyectadas, así como las medidas relativas a la evacuación y vigilancia del escenario de la voladura. El plan de tiro ha de conservarse en este lugar, y sus especificaciones han de ser transmitidas a las personas empleadas en el trabajo en cuestión.

Cuando sea necesario, han de tomarse las medidas oportunas para evitar las vibraciones del terreno. Durante el trabajo ha de llevarse un libro-registro de tiro, que se guardará en la zona de las voladuras.

Evacuación y vigilancia del lugar de la voladura

Cuando se efectúan voladuras en la proximidad de edificios, carreteras públicas, líneas de energía, y otras instalaciones o servicios en los que exista riesgo de daños materiales o personales, la roca ha de ser sanead̄a con la suficiente extensión, y las cargas han de ser cubiertas con materiales de protección de modo que en el curso de las voladuras no sean proyectadas piedras, tierra, etc. sobre los alrededores.

A este respecto habrá de prestarse la debida consideración a las condiciones especificadas en el permiso de voladura obtenido de las autoridades de policía en los casos en que tal permiso sea necesario, por ejemplo en las voladuras en áreas edificadas en las que se aplican los reglamentos de la construcción.

Dentro de un cierto radio a partir del lugar de la voladura — la zona de peligro — existe riesgo de daños personales y materiales que pueden ser causados por las piedras proyectadas al aire y las ondas de choque aéreas. Para evitar estos daños, la zona de peligro ha de ser evacuada y vigilada.

El jefe de voladuras o su delegado es responsable de garantizar que la zona de peligro ha sido evacuada, y está guardada por un número suficiente de personas con banderas rojas desplegadas (de al menos 30 × 30 cm) cuando vaya a hacerse la voladura. Estas personas están autorizadas para — y tienen obligación de ello — detener a cualquiera que vaya a entrar en la zona de peligro, y deben detener asimismo todo el tráfico que penetre en dicha zona. Los guardas no dejarán sus puestos hasta no recibir la señal correspondiente.

Es preciso comprobar que los guardas están bien instruidos sobre sus obligaciones, y asegurarse de que la zona de peligro ha sido evacuada y están en sus puestos antes de encender la pega.

Las personas que hayan de permanecer en edificios muy próximos al lugar de la voladura cuando se realice ésta deben ser advertidas en el debido momento de que no deben permanecer cerca de ventanas o puertas que miren hacia este lugar. Estas medidas de seguridad no pueden ser reemplazadas por una nota anunciando que se realizará una voladura después de un cierto tiempo o en un determinado momento.

Debe prestarse asimismo la atención debida a las personas que vivan en las cercanías publicando un aviso con la antelación suficiente para que puedan prepararse para la explosión, proporcionando asimismo una información clara e inequívoca sobre las señales y gritos que se usarán con ocasión de la voladura. Las Instrucciones de Voladuras incluyen información sobre estas señales.

Los explosivos sobrantes han de ser controlados, y conducidos a un lugar seguro antes de detonar la pega. La maquinaria y el material han de ser retirados o protegidos. Recuérdese que incluso unos daños poco importantes en la maquinaria pueden ocasionar accidentes debidos a las esquirlas producidas, etc.

Las personas que se protejan detrás de un muro deben permanecer pegadas a él. No debe abandonarse un lugar protegido para observar la explosión.

En canteras, etc. en donde se efectúan voladuras de modo regular y es difícil conseguir una evacuación satisfactoria de la zona de peligro, puede ser necesario disponer casetas de refugio en número suficiente. Una zona de trabajo de este tipo debe ser inaccesible a personas no autorizadas en la extensión que sea precisa.

Cuando se procede a voladuras de excavación de zanjas, debe proporcionarse

a tiempo información sobre el trabajo que se está realizando mediante los tablones de avisos de los pueblos vecinos, y mediante información directa a las fincas próximas. En esta información debe darse la situación y extensión de la zona de peligro, la hora a la que se va a realizar la voladura, y el tipo de señales y gritos que van a usarse. Para información sobre señales, consúltense las Instrucciones de Voladuras.

Si un sendero, camino de bicicletas, o camino de caballerías frecuentado cruza la zona de peligro, deben apostarse guardas en el mismo en el límite de la zona de peligro antes de encender la pega, o instalar señales claras de advertencia. Si es una carretera, deben ponerse siempre guardas antes de la voladura.

Cuando las voladuras son subterráneas, es preciso colocar guardas en las carreteras y senderos que lleven hacia el lugar de las mismas y en zonas en las que haya peligro de que la onda se propague o de que se desprendan piedras, etc. por efecto de las vibraciones del terreno asociadas a la voladura.

En lugares subterráneos especiales en donde la voladura no afecte otros trabajos ni rutas de transporte, éstas pueden llevarse a cabo sin necesidad de colocar guardas siempre que se bloqueen los accesos y se instalen señales claras de aviso. La persona responsable de la voladura lo es también del bloqueo de dichos accesos.

La distribución de responsabilidades

Es de importancia esencial que el empresario explique por intermedio del supervisor o capataz cómo se divide la responsabilidad entre sus empleados, y que se proporcione una información clara a este respecto. Esto debe hacerse antes de comenzar el trabajo.

En el curso de las operaciones debe seguirse un plan de tiro bien establecido; es importante no desviarse del mismo sin consultar al director del proyecto.

Las Instrucciones de Voladuras incluyen una información más detallada sobre la distribución de responsabilidades.

Retorno al lugar de la voladura

Nadie, con la única excepción del jefe de voladuras o su delegado, puede volver al lugar de ésta antes de que se dé la señal de retorno.

Cuando la voladura ha tenido lugar y no existe ya más peligro, este hecho ha de ser establecido por la misma persona que dió la señal de aviso, es decir, el jefe de voladuras o su delegado.

Cuando se produce la voladura, las cargas que detonan deben ser contadas, a ser posible por más de una persona, si ello es factible. Si existe alguna razón para sospechar que ha ocurrido algo anormal, que una carga no ha detonado o lo ha hecho después de lo previsto, que la mecha no ha tenido tiempo de quemarse, etc. nadie puede retornar al lugar de la voladura hasta 5 minutos después del momento en que la explosión debería haber ocurrido. En el caso de encendido con mechas, y usando longitudes superiores a 2 metros, este lapso de tiempo ha de ampliarse hasta 10 minutos como mínimo.

Si se observa un gas marrón o amarillo de olor penetrante y se oye un sonido siseante, la carga puede haber comenzado a quemarse en vez de detonar, y existe el peligro de una explosión retardada.

En voladuras subterráneas debe dejarse el tiempo suficiente para ventilación y disipación de los gases antes de retornar al frente de trabajo. Si se riega con agua el montón de roca volada pueden dispersarse con mayor rapidez los gases y el polvo.

Antes de dar la señal de retorno, el jefe de voladuras debe examinar rigurosamente el lugar y comprobar si existen algunas cargas residuales que sean visibles. Los detonadores que no han hecho explosión pueden ser detectados observando si hay cables aparentemente intactos. Antes de reanudar el trabajo en la zona, debe hacerse un cuidadoso saneo de la roca.

Tiros fallidos y cargas que se queman o no hacen explosión
Razones por las que no se produce la detonación, etc.

Si la carga y el encendido se realizan con todo cuidado, éste es el mejor modo de asegurar que la carga en cuestión detona propiamente. Las razones más usuales de los fallos de barrenos o de que las cargas comiencen a arder o quemarse, según las Instrucciones de Voladuras, son las siguientes:

a. Relativas al explosivo o la pólvora de mina:
   El explosivo o la pólvora están húmedos o son defectuosos.

b. Relativas a la mecha:
   La mecha está húmeda o es defectuosa.
   La mecha ha sido cortada oblicuamente.
   La mecha no se ha introducido enteramente en el detonador hasta llegar a su carga, debido, por ejemplo, a una conexión defectuosa.
   En el material de retacado hay gravilla o piedras afiladas que han dañado la mecha.
   La mecha no ha sido encendida.

c. Relativas a los detonadores:
   El detonador es muy poco potente o está dañado.
   Ha quedado serrín dentro del detonador.
   El detonador ha sido instalado descuidadamente, y ha penetrado agua, dañando el extremo de la mecha o la carga del detonador.
   El detonador se ha separado de la carga durante las operaciones de carga del barreno.

d. Relativas a las cargas:

Las cargas han quedado separadas unas de otras por piedras o grava. Hay demasiado espacio entre unas cargas y otras.

e. Relativas al material de retacado:

Un explosivo difícil de iniciar no tiene material de retacado ninguno, o muy poco.

f. Relativas a los dispositivos de iniciación eléctrica:

Los cables eléctricos están dañados.
Los cables han sido conectados mal unos con otros.
Los cables han estado en contacto con railes, tuberías, etc.
Los cables utilizados no son adecuados.
El explosor utilizado, o la fuente de energía empleada, es demasiado débil o está dañado, o ha sido usado incorrectamente.

g. Otras razones:

Temperatura demasiado alta en un barreno o cámara.
La carga o parte de ella, el detonador, o la mecha, han sido rotos o expulsados fuera por la detonación de las cargas adyacentes.

Estudio y recogida de información sobre las cargas fallidas

Toda carga fallida ha de ser examinada por el jefe de voladuras o su delegado. La carga ha de ser recuperada inmediatamente bajo la dirección del jefe de voladuras, o si ésto no es posible, ha de ser marcada claramente su posición y, en caso necesario, ser vigilada. Si es preciso, el jefe de voladuras debe informar también al turno siguiente de la carga fallida, su posición y su composición; magnitud de la carga, dirección del barreno y profundidad, posición del detonador, etc. Si no se encuentra o no se inactiva la carga fallida, el jefe de voladuras del turno siguiente ha de continuar el examen hasta conseguirlo.

Una operación de voladura con un barreno fallido residual, no debe ser aprobada.

Recuperación e inactivación de una carga fallida

Está prohibido perforar a través del material de retacado que cubra una carga fallida.

Siempre que se trabaje en una carga fallida, el personal debe ser lo más reducido posible, y deben aplicarse las máximas precauciones. Sólo pueden extraerse los detonadores en caso de que estén sueltos.

Si en una carga fallida no hay ningún detonador, y el material de retacado consiste solamente en agua o no existe, el procedimiento a seguir es el siguiente:

a. Primeramente se intenta sacar la carga con un atacador.
b. Si no es posible extraerla de este modo, se intenta lo mismo con agua a presión.
c. Si no se dispone de agua a presión, se intenta la misma operación con aire comprimido; éste debe hacerse con todo cuidado y usando gran cantidad de agua.
d. Si el explosivo no puede ser expulsado del barreno con agua o aire comprimido, se intenta volarlo con ayuda de un nuevo cartucho. Esto debe hacerse con el máximo cuidado; el explosivo puede haberse inflamado y producirse una explosión retardada; por esta razon ha de esperarse el tiempo suficiente antes de dar la señal de retorno. Si la nueva voladura no tiene éxito, hay que enfriar la zona con agua o aire antes de hacer otro intento.
e. Como último recurso pueden perforarse unos taladros auxiliares, con cuidados extremos. No deben perforarse demasiado cerca de la carga fallida, y ha de prescindirse de este recurso cuando la carga se ha realizado con máquina, pues el explosivo pueda haber sido presionado hasta introducirse en las fisuras próximas. La perforación se efectuará desde un lugar protegido y en la zona de peligro se apostarán guardas.

Si existe peligro de que en la carga se encuentre incluido un detonador, no se la golpeará con el atacador, pero si pueden utilizarse los otros métodos citados. Si es necesario perforar taladros auxiliares, no hay que llegar nunca con la perforación junto al cartucho. Sólo pueden usarse en la inyección de aire tubos de cobre.

Precauciones con el explosivo que no ha detonado

Tras un tiro auxiliar, o en otras ocasiones en las que hay razones para suponer que una carga ha sido lanzada fuera de un barreno y no ha detonado, para ver si el explosivo expulsado del barreno está entre los materiales volados o lo ha hecho sólo parcialmente, debe efectuarse un reconocimiento completo. Los explosivos que se encuentren se recogerán inmediatamente y pasarán al cuidado del jefe de voladuras o su delegado. Si hay razones para pensar que ha quedado explosivo en algún lugar inaccesible entre los escombros, el personal de desescombro ha de ser informado de ello. El montón de roca volada será regado con agua, y los explosivos que se encuentren al cargar el mismo para su retirada o durante otra operación, serán llevados al jefe de voladuras.

Engineering of Rock Blasting on Civil Projects

A. J. Hendron, Jr.*

Introduction

Controlled blasting is used at some time during most civil engineering projects where there is rock excavation. Controlled blasting is often necessary because the blasting must take place in the near proximity of adjacent structures. In other instances, the blasting is controlled because a smooth perimeter is desired to minimize rock support and overbreak. The construction of tunnels and shafts for subways, rock excavations for foundations, and the excavation of road cuts for interstate highways sometimes require blasting operations which must be conducted in an urban environment. Unfortunately, blasting operations produce unwanted sounds and vibration along with their beneficial effects. Thus, in the writing of specifications for blasting in an urban environment, potential damage to adjacent structures by ground vibrations must be considered, possible damage to windows from airblasts must be considered, potential damage and safety problems from fly rock must be considered, and the discomfort to people from ground vibrations, airblast, and noise must be taken into account. In some instances the potential interruption in service of delicate equipment housed in adjacent structures must be considered; this equipment may be electronic computers or other electronic gear with sensitive relays in the circuits.

The contractor or the owner's engineer is faced with determining the maximum weight of explosives which may be detonated without damage to structures on adjacent property. If the weight of explosive is overestimated, the resulting damage to adjacent structures may result in costly losses. But, if the engineer or contractor is too conservative, and the weight of explosive

*Professor of Civil Engineering, University of Illinois at Urbana-Champaign, Urbana, Ill.

becomes too restrictive, progress of the project may be curtailed, and the cost of excavation will increase accordingly.

Because people are so sensitive to sounds and vibrations produced by blasting, complaints and damage claims quite commonly arise within the range of perceptibility of these effects, even when no actual structural damage is done. This situation is likely to become even more critical in the future because of the recent emphasis placed on pollution of the environment, which has resulted in efforts to isolate the individual from intrusions of noise and vibration.

Blasting rounds are controlled on many civil engineering projects in order to achieve a smooth wall around the perimeter of the excavation with a minimum of overbreak. Smooth wall excavations minimize the rock support and can be utilized to minimize the amount of concrete used on structures such as spillways. In open excavations, such as portal cuts for tunnels, spillway cuts, highway cuts, and basement excavations in metropolitan areas, controlled blasting techniques such as presplitting, cushion blasting, or line drilling can be used to advantage. Smooth walls in underground excavations, such as underground powerhouses and tunnels, can be achieved by a technique called smooth wall blasting. Properly executed smooth wall blasting results in less temporary support and more economical permanent liners in tunnels. Deep (50–70 ft) basement excavations in metropolitan areas are very special cases which must be treated with extreme care. In many instances they are located within several feet or inches from existing structures and the construction procedure requires blasting immediately adjacent to the structures as well as the installation of high-capacity rock anchors for stability. In this situation it is most important to install the anchors as soon as possible and to carefully control the unsupported length and height of the open excavation. Although blasting vibrations need to be considered, they are an item of secondary priority in comparison to the consideration of the overall stability of the cut. Thus, the inspection forces in the field must allocate their time and energies accordingly.

To achieve the desired result, the engineer must know the technical state-of-the-art for all of the types of controlled blasting mentioned above. But, equally important, the construction specifications and bid documents must be written in such a way that it is possible to achieve the desired result. The specifications must be written in such a way that the contractor knows beforehand what is expected. This will permit the contractor to be responsive and include the proper items and expenses in his bid for the controlled rock excavation. Much controversy has resulted from specifications for controlled blasting because many of them have been so vague that the contractor could not ascertain before bidding the nature of the procedures which would be required by the engineer. It should also be pointed out that the specifications should not be so restrictive that they eliminate the contractor's ingenuity and

restrict any contributions he may make to the job from his past experience and ingenuity. For some problems, such as the excavation of high vertical walls adjacent to occupied buildings, the engineer and owner may justifiably feel that other measures are necessary in addition to a well-written and technically sound specification accompanied by diligent inspection. Since the final result is primarily influenced by the knowledge, experience, and responsible performance of the contractor, the engineer may indeed make his most valuable contribution to the job by writing a good prequalification specification which the contractor must satisfy to become a bidder. This mechanism has been used with success on projects where the owners have been both private parties and government agencies.

In this chapter, the technical aspects and the current state-of-the-art in controlled blasting will be reviewed. In addition, guidelines will be set forth and suggestions will be made on how to incorporate these ideas into the specifications so that the desired results will be achieved.

Vibration Criteria

General

The problem of predetermining the quantity of explosives which may be used without damaging an existing structure may be resolved into two parts. First, the engineer must be able to predict the intensity of ground vibration as a function of charge weight, distance from the detonation, and properties of the transmitting medium. Second, it is necessary to know the level of ground vibration which can be tolerated by different types of structures without causing damage. The available information relating to both parts of this problem is discussed below.

Ground Vibrations from Blasting

Part of the energy released in the detonation of a blasting round is transmitted directly into the surrounding rock mass in the form of stress waves. The ground motions observed at a given point are dependent on the weight of explosive detonated per delay, the distance from the detonation point to the observation point, and the transmission characteristics of the rock mass. Since an acceptable theoretical approach has not yet been developed for calculating ground motions in rock, the scaling of field measurements is used almost exclusively for predicting ground motions from explosions. Available data for estimating these motions have been measured from quarry blasting, construction blasting, and blasting in open pit mines. Similar measurements have been obtained in connection with nuclear and chemical explosions tests conducted for the development of design procedures for protective military structures [12].

The empirical scaling of shock phenomena from explosions involves the comparison of dynamic measurements obtained at various distances from a wide range of charge sizes. Ambraseys and Hendron [1] have suggested the use of cube-root scaling to compare particle velocity measurements made from different-sized explosions. Such a correlation of data is shown in Fig. 1, where the measured particle velocity is plotted versus the scaled range, which

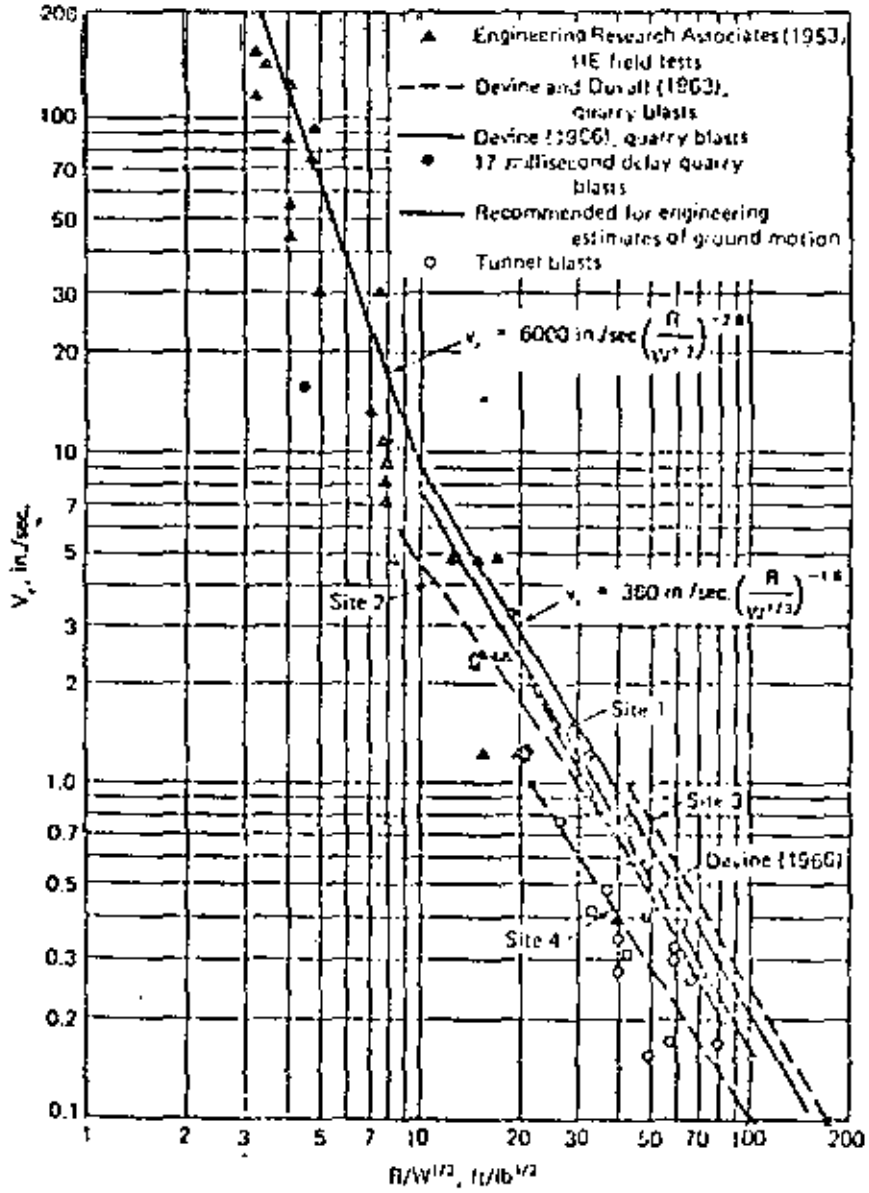

Fig. 1. Maximum particle velocity versus scaled range according to cube root scaling

is the slant range in feet divided by the cube root of the maximum weight of charge per delay in lb[1/3]. In this figure, experience from many jobs is shown. For preliminary estimates of maximum radial particle velocity, it is suggested that, for scaled ranges greater than 10 ft/lb$^{1/2}$, the upper-bound line on Fig. 1 be used. This line is described by the following equation:

$$v = 360 \frac{\text{in./sec}}{\text{sec}} \left(\frac{R}{W^{1/3}}\right)^{-1.6}, \quad (1)$$

where R is in feet, and W is the maximum charge per delay in pounds.

Other investigators, such as Oriard [18,19], Devine and Duvall [1], and Devine [7], prefer to use square-root scaling rather than the cube-root scaling as shown in Fig. 1. Thus, for preliminary estimates of maximum particle velocity, Oriard [18,19] uses the upper bound of previous measurements, shown by line B in Fig. 2. In Fig. 2 the maximum particle velocity is plotted against the scaled range according to square-root scaling. Line D in Fig. 2

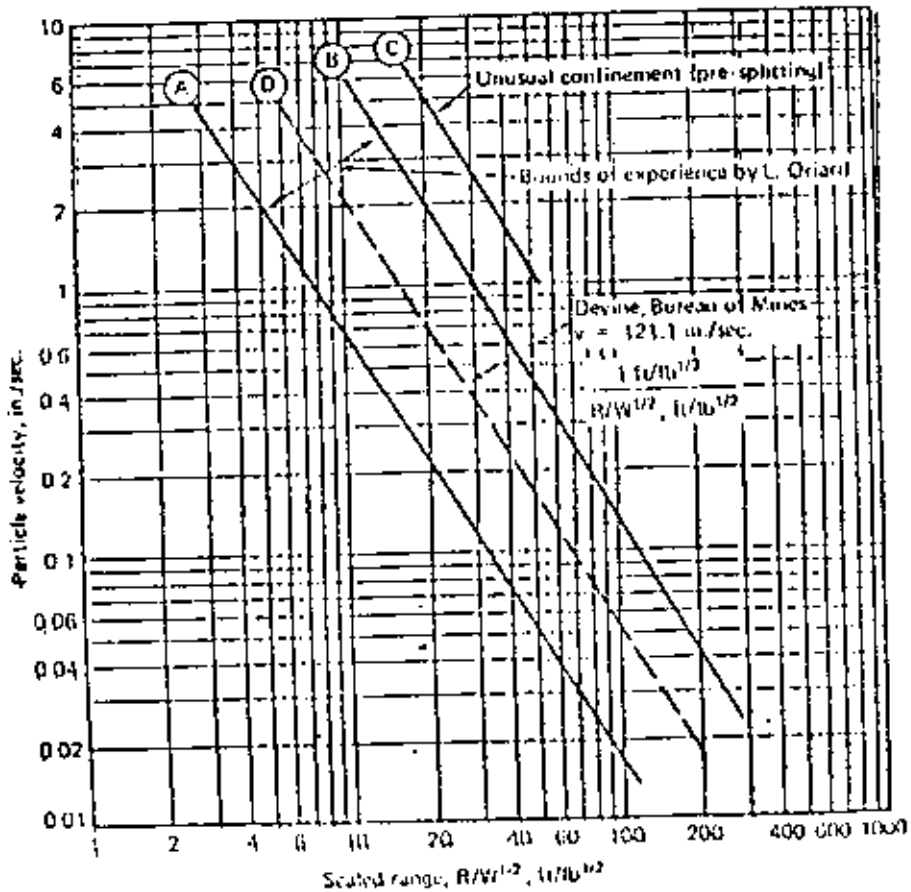

Fig. 2. Maximum particle velocity versus scaled range, according to square-root scaling

represents the best fit to many measurements of radial particle velocity obtained from quarry blasts by Devine [6]. It should be noted that line D falls nearly in the middle of the range of Oriard's experience, which falls between lines A and B. The range shown between lines A and B is typical for data obtained from downhole blasting and represents the scatter that is typical from vibrations produced by blasting. In such cases where there is unusual confinement, such as in the first holes which are detonated in the cut round of a tunnel or the holes which are detonated simultaneously down a presplit line, line C shown in Fig. 2 gives an appropriate estimate of the maximum particle velocity as a function of scaled range.

The relative merits of cube-root and square-root scaling will not be debated in this chapter, but the differences which result in practical applications will be discussed below. The relations between the maximum charge per delay and range which produce given maximum particle velocities are shown in Fig. 3 for various scaling techniques. Note that line 4 in Fig. 3 is the

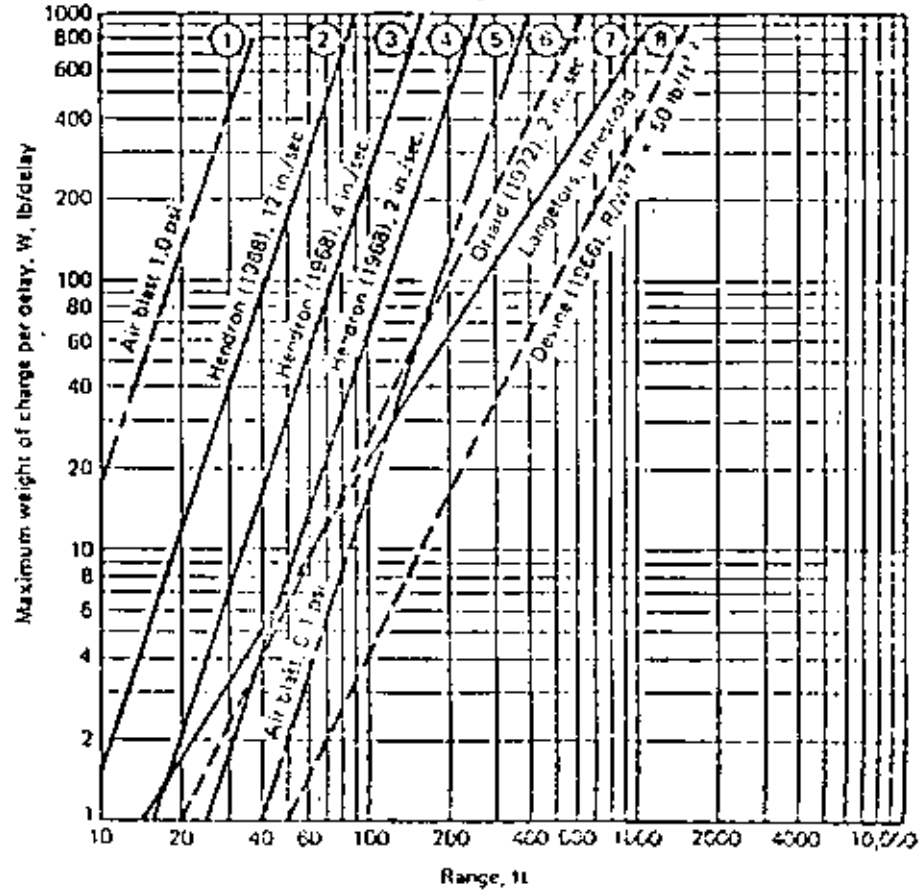

Fig. 3. Relation between charge per delay and range for various levels

relationship between the maximum charge per delay and range which gives a maximum particle velocity of 2 in./sec according to the data scaled by cube-root scaling in Fig. 1 [1]. The relationship given by line 6 in Fig. 3 is the combination of maximum charge weights per delay and range which will result in a maximum particle velocity of 2 in./sec according to square-root scaling from curve *B* in Fig. 2 [18,19]. It should be noted that the differences between lines 4 and 6 are not significant for practical applications where the range is between 20 and 100 ft. In general, the relationship given by square-root scaling (line 6) becomes increasingly more conservative, with respect to the relationship given by cube-root scaling (line 4), as the range increases. For ranges closer than about 45 ft, the relationship given by cube-root scaling (line 4) is more conservative for determining allowable charges per delay than the relationship derived from square-root scaling (line 6).

In all instances, the reader is cautioned to explore thoroughly the responses of the project site in question and to study the relationship between different scaling techniques and the type of seismic waves under consideration, i.e., whether it is a body wave or surface wave. The degree of conservatism is further related to the manner in which preliminary test blasts are related to the production blasts being evaluated. For example, consider a small test shot at close range designed to produce the limiting vibration (maximum particle velocity) at the same scaled range as a larger production blast at a greater absolute range. Scaling to the production blast by cube-root scaling is more liberal than square-root scaling. The designer who wishes to be conservative may choose to use square-root scaling. The decision should be influenced by the number of tests available and the scatter in the results.

In the above discussion emphasis is given to maximum peak particle velocity because controlled studies of the damaging effects of blasting vibrations have indicated that peak particle velocity is the best index for blasting vibration damage to residential structures [4,10,14]. The development of peak particle velocity damage criteria will be traced in the next section. There are many problems to which the maximum particle velocity criteria do not apply and for which it is necessary to know the response spectrum of the blast-induced ground motions because the response spectrum pertains to the whole frequency range of response rather than the limited frequency range represented by the velocity bound. To be useful, the response spectrum of a blasting vibration must be easily predictable. Therefore, a method was developed [8,13] to predict response spectra from preliminary blasting and geologic information. The resulting method is similar to that used to predict smoothed earthquake response spectra [17] and is based on predicting peak ground acceleration, particle velocity, and displacement from attenuation relationships developed from scaling field data. The expected peak ground motions are then amplified to yield the idealized response spectrum bounds.

The attenuation of scaled field measurements of peak ground motion

(particle displacement, δ, particle velocity, v, and particle acceleration, a) with increasing scaled distance, $R/(\rho c^2)^{1/3}/W^{1/3}$, is presented in Fig. 4, where R is the range in feet, ρ is the mass density per unit of volume in slugs per cubic foot, c is the seismic velocity in feet per second, and W is the maximum weight of explosive per delay in pounds. The basis in dimensional analysis for the scaling used is given by Hendron and Ambraseys [1], Newmark [16], Dowding [8], Hendron and Dowding [13], and Hendron [12]. The plots shown in Fig. 4 were derived from 12 separate field studies involving open cut, tunnel, and shaft blasts with maximum explosive weights per delay ranging from 2.4 to 19,625 lb [8,13]. The average scaled-distance-attenuation relationships shown in Fig. 4 for peak values of blast-generated displacements, velocities, and accelerations may be expressed as

$$\delta = \frac{3}{1000}\ \text{in.}\left[\frac{100\ \text{ft}}{R}\right]^{1.4}\left[\frac{10{,}000\ \text{ft/sec}}{c}\right]^{1.4}\left[\frac{W}{10\ \text{lb}}\right]^{0.7}\left[\frac{5.25}{\rho}\right]^{0.7}, \tag{2}$$

$$v = \frac{3}{4}\ \frac{\text{in.}}{\text{sec}}\left[\frac{100\ \text{ft}}{R}\right]^{1.1}\left[\frac{W}{10\ \text{lb}}\right]^{0.7}\left[\frac{5.25}{\rho}\right]^{0.7}, \tag{3}$$

$$a = \frac{2}{3}\ g\left[\frac{100\ \text{ft}}{R}\right]^{1.9}\left[\frac{c}{10{,}000\ \text{fps}}\right]^{1.4}\left[\frac{W}{10\ \text{lb}}\right]^{0.7}\left[\frac{5.25}{\rho}\right]^{0.7}, \tag{4}$$

Proper units for ρ are obtained by dividing the unit weight of the rock in pounds per cubic foot by the acceleration of gravity (32.2 ft/sec), although ρ will vary so little in rock that this factor can safely be ignored. The maximum values given by Eqs. (2), (3), and (4) are a conservative estimate for motions produced by bench blasts to a free face or by the later delays in a tunnel round. These values should be doubled for a conservative estimate of the motions produced by confined blasts such as presplit rounds, the cut portion of a tunnel round, or the initial cuts in an open excavation.

A study of the actual response spectra of many construction blasts [8] has shown that the following procedure can be used for constructing a smooth response spectrum for the ground vibrations produced by such blasts:

1. Estimate ρ, c, $W^{1/3}$, and R and obtain δ, v, a from Eqs. (2), (3) and (4).
2. The peak ground motions should be plotted on tripartite paper to yield a trapezoidal ground motion spectrum.
3. The principal spectrum frequency, ω_0, is defined as the center of the ground motion spectrum.
4. The response spectrum for frequencies lower than $\frac{1}{3}\omega_0$ can be obtained by multiplying the ground displacement by the appropriate amplification factor A_δ.
5. The response spectrum for frequencies between $\frac{1}{3}\omega_0$ and $1\frac{1}{2}\omega_0$ can be obtained by multiplying the maximum ground velocity by the appropriate amplification factor A_v. If the blast is detonated with delays at a

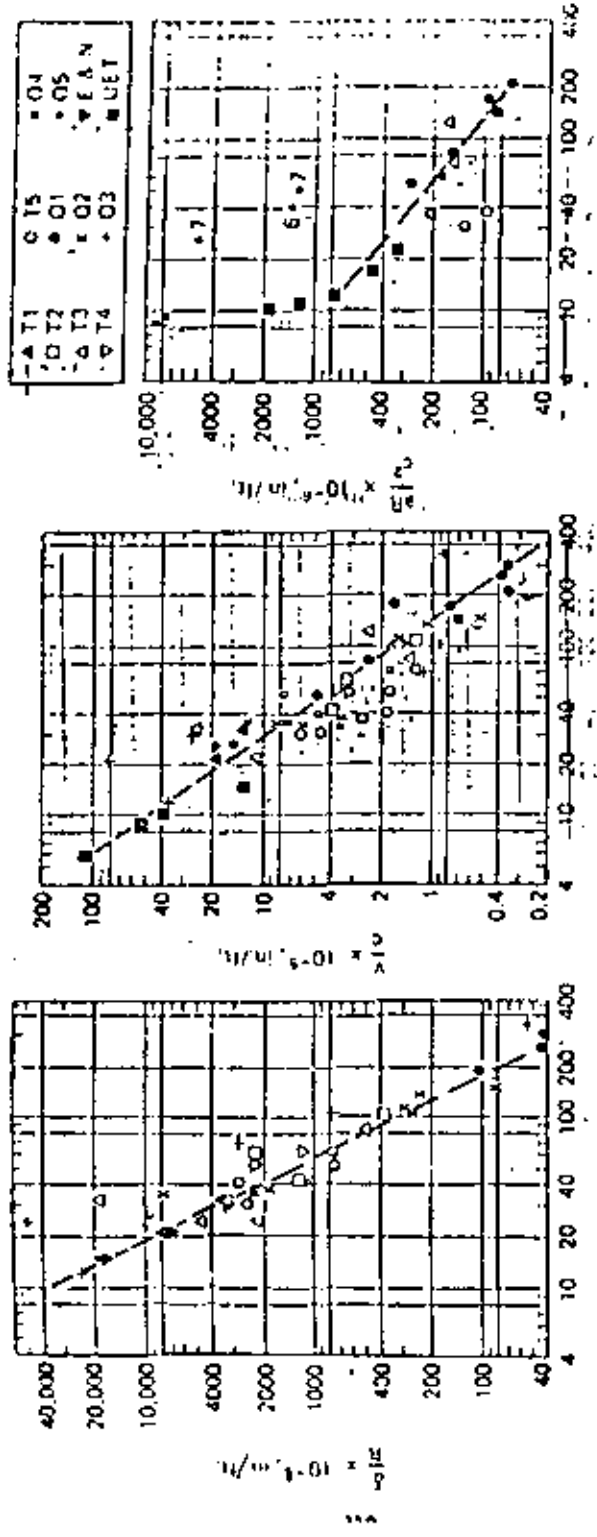

Fig. 4. Scaled field measurements of radial particle displacement, velocity, and acceleration versus scaled range

constant interval, the velocity bound must include the frequency corresponding to the delay interval.

6. The response spectrum for frequencies greater than $2\omega_0$ is obtained by multiplying the maximum ground acceleration by the appropriate amplification factor A_a.

7. The amplified spectrum displacement, velocity, and acceleration bounds should be connected to complete the spectrum.

The amplification factors A_d, A_v, and A_a are given in Fig. 5 (after Dowding [8]) as a function of scaled range for 3% critical damping. Note that the factors A_v and A_a do not vary with scaled range, whereas the value of A_d varies with scaled range. It should also be noted that the value of A_d is dependent on whether the blast is a single or multiple delay blast. Experience has shown that the upper relationship for A_d should be used if the number of delays is greater than 3. If the response spectrum is desired for values other than 3% of critical damping, the values of A_d, A_v, and A_a from Fig. 5 should be multiplied by the following factors:

% Critical Damping	A_d	A_v	A_a
2	1.05	1.10	1.20
5	0.83	0.76	0.72
10	0.65	0.52	0.42

Observations by Dowding [8] on a significant number of structures subject to blasting vibrations indicate that most structures behaved as if 3% of critical damping was appropriate for the intensity of motions produced by blasting vibrations less than 2 in./sec.

As an example of the procedure described above, the response spectrum (for $\beta = 3\%$) for the ground motions 220 ft from a blast consisting of seven 200-lb delays at 34-msec intervals will be calculated. The seismic velocity will be assumed to be 13,000 ft/sec, and the soil overburden at the point of interest is assumed to be negligible. From Eqs. (2), (3), and (4) the maximum ground displacement, velocity, and acceleration are 0.007 in., 1.0 in./sec, and 0.65 g, respectively. When the ground motions are plotted on tripartite paper as shown in Fig. 6, the principal spectral frequency, ω_0, is found to be 30 cps. The frequency corresponding to the delay interval is 29 cps and is located within the frequency limits of the velocity bound. Therefore, the velocity bound need not be extended to cover the frequency corresponding to the delay interval. The appropriate amplification factors for the multiple delay, constant-interval shot are $A_d = 1.2$, $A_v = 3.8$, and $A_a = 2.5$, for $\frac{R}{W^{1/3}} = 35$ ft/lb$^{1/3}$, from Fig. 5. In Fig. 6 the amplified velocity b[illegible] extends

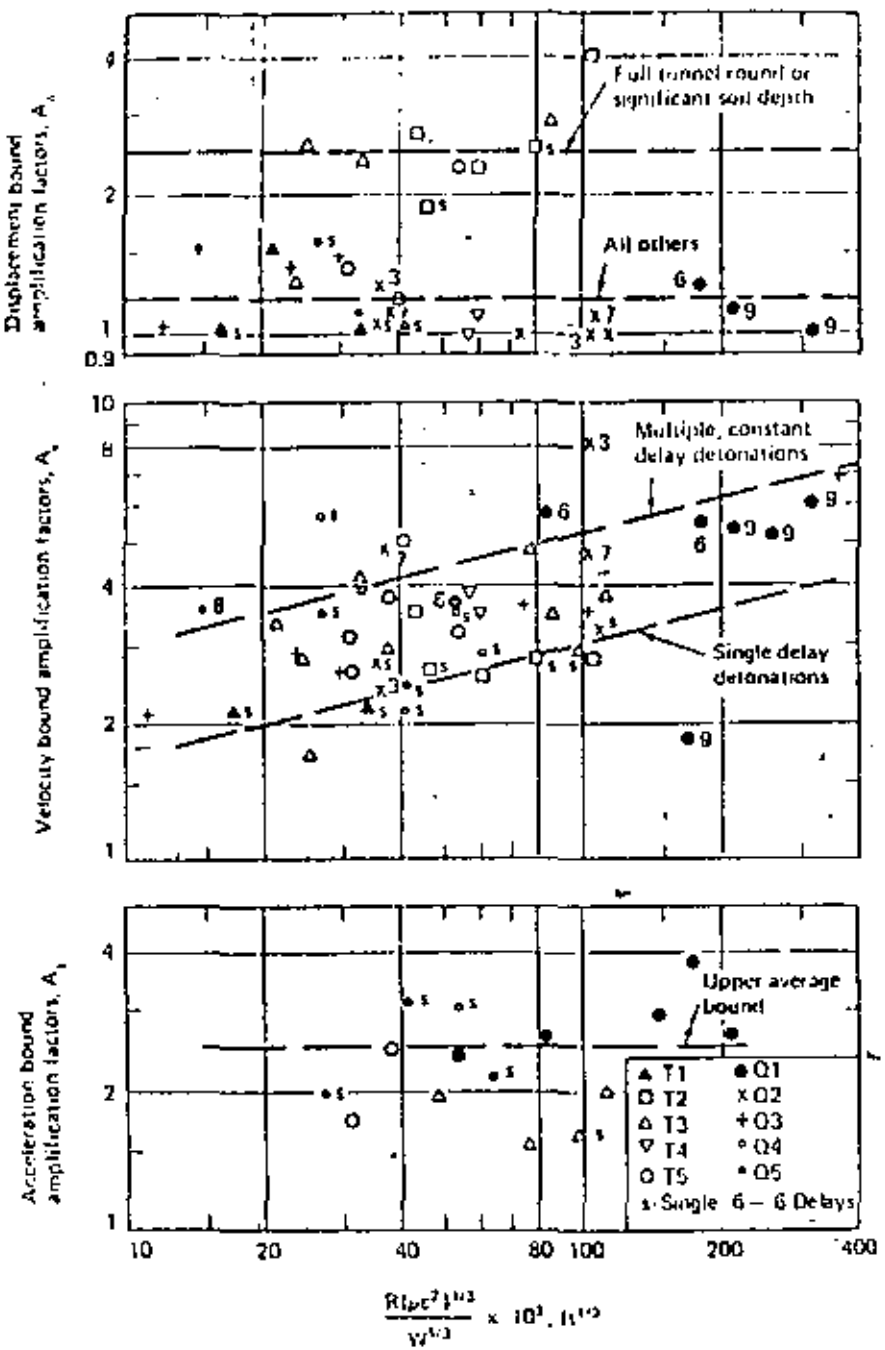

Fig. 5. Displacement-, velocity-, and acceleration-bound amplification factors versus scaled range ($\beta = 0.03$)

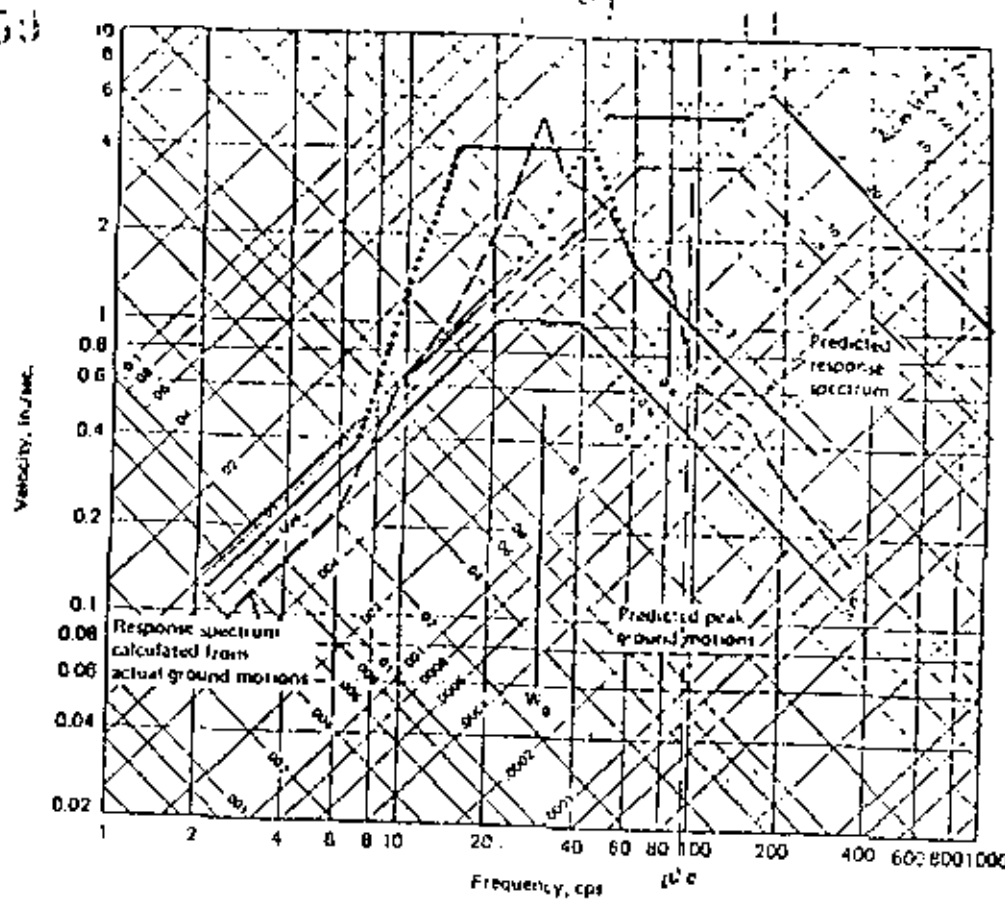

Fig. 6. Comparison of the simplified, predicted response spectra with the actual calculated response spectra

from 15 to 45 cps, the amplified displacement bound applies to frequencies below 7 cps, and the amplified acceleration bound applies to frequencies above 60 cps. These bounds are then connected by the inclined dotted lines (Fig. 6) to form the complete 3% critically damped response spectrum. The dashed irregular line in Fig. 6 is the actual response spectrum calculated from the ground motions from a blast corresponding to the assumptions of the hypothetical case. This example was taken from field study Q2 as described by Dowding [8].

Damage Criteria

The intensity of ground motion which can be tolerated by various structures must be determined by the engineer before estimates of permissible charge weights can be determined. Obviously, the level of ground motion

required to damage structures is not the same for different types of structures. In addition, the "acceptable" damage level may depend more on the use of a structure rather than the actual integrity of the structure. For example, a given set of ground motions may not structurally affect either a residence or a steel framed warehouse, but the home may be "damaged" because the distortion resulted in plaster cracks objectionable to the owner. Thus, the limiting ground motions which cause various types of damage can be established only by experience from cases where the ground motions are measured near the structure and the resulting damage can be correlated with the magnitude of the motions.

Crandell [3] reported the results of a comprehensive study in which over 1000 residential homes, two-story business buildings, schools, and churches were investigated before and after blasting. On the basis of this study, Crandell presented the first damage criterion which was based on measurements of ground motions in the vicinity of the structure. He found that the energy ratio, defined as the square of the ratio of maximum acceleration in feet per square second to frequency in cycles per second, could be correlated with damage. An energy ratio of 3 or below was considered safe, and the danger of producing damage was considered highly probable for energy ratios greater than 6. If harmonic motion is assumed for the ground vibrations, the following relations exist among maximum acceleration a_{max}, maximum particle velocity v_{max}, maximum displacement δ_{max}, and frequency f:

$$v_{max} = 2\pi f \delta_{max}, \tag{5}$$

$$a_{max} = 4\pi^2 f^2 \delta_{max}, \tag{6}$$

$$a_{max} = 2\pi f v_{max}. \tag{7}$$

Thus from Eq. (7) it is apparent that the energy ratio is proportional to the square of the maximum particle velocity v_{max}. A damage criterion based on energy ratio is therefore the same as a criterion based on maximum particle velocity. Calculations show that energy ratios of 3 and 6 correspond to maximum particle velocities of 3.3 and 4.7 in./sec, respectively.

Langefors et al. [15] reported the results of an investigation similar to Crandell's, except that they measured displacement and frequency in the vicinity of the structure rather than acceleration and frequency as measured by Crandell. They found that damage to structures could be correlated with the product of maximum displacement and frequency. Since maximum particle velocity is proportional to the product of maximum displacement and frequency, this damage criterion is also equivalent to a maximum particle velocity criterion. Based on these data, Langefors et al. concluded that maximum particle velocities below 2.8 in./sec would not produce damage. Edwards and Northwood [10] concluded from similar studies that a particle velocity criteria could be used for damage control and that a maximum particle velocity of 2 in./sec would not produce damage.

Duvall and Fogelson [9] statistically analyzed the vibration measurements and damage correlations made by Edwards and Northwood [10], Langefors et al. [15], and Thoenen and Windes [23]. Although the three studies analyzed were made at different times in three different countries, they showed remarkable agreement. The statistical analysis showed that for a maximum particle velocity of 7.6 in./sec the probability of producing major damage (fall of plaster, serious cracking) is 50% and that the probability of producing minor damage (fine plaster cracks, opening of old cracks) is slightly less than 50% at a particle velocity of 5.4 in./sec. In all 124 cases analyzed, damage was not observed from blasting vibrations if the particle velocity was below 2 in./sec. The damage criteria given above are recommended because they resulted from a thorough analysis of a considerable body of damage data on residential-type structures.

Langefors and Kihlstrom [14] also give particle velocity criteria for damage to tunnels in rock. A particle velocity of 12 in./sec is given as a criterion for the fall of rock in unlined tunnels, and a particle velocity of 24 in./sec is correlated with the formation of new cracks in rock. These criteria are consistent with the experience of the author for unlined tunnels near nuclear detonations. Unlined tunnels rarely experience visible damage at ranges where the free-field ground motions are on the order of 1–2 ft/sec, unless a loosened piece of rock is detached from the roof by the shaking.

The observations of Langefors and Kihlstrom [14] concerning rock tunnels are not contrary to the results of the Underground Explosion Tests (UET) which were conducted by Engineering Research Associates [11] for the Corps of Engineers during the period from 1948 to 1952.

In the underground explosion tests a considerable number of TNT explosions were detonated at scaled depths of about 0.38 ft/lb$^{1/3}$ in sandstone, granite, and limestone. The most comprehensive set of these tests was conducted in sandstone, and one of the variables in this series of tests included a study of damage to unlined tunnels which were mined to pass directly below the point of detonation. Generally, the tunnel size was selected to be in proportion to the cube root of the corresponding charge weight used in the test. A full-scale tunnel was taken to be approximately 30 ft in diameter and the corresponding full-scale charge weight for a tunnel of this size was 320,000 lb. A brief summary of the underground explosion tests is given in Table 1.

From the UET program, four zones of failure were empirically defined from the observations of damage to unlined tunnels. Zone I was described as tight closure of the tunnel. Zone I failure appeared for a length along the tunnel roughly as shown in Fig. 7. Zone II was also a region of fairly tight closure, but the degrees of tightness decreased progressively with range; thus, zones I and II were sometimes difficult to distinguish, and in many reports no effort was made to delineate between them. Zone III was characterized by continuous damage to the tunnel surface, but this damage [illegible] with

Table 1
Brief Summary of UET Tests

Rock Type	No. of Tests	Weight of TNT (lb)
Limestone	2	320
Granite	10	320
	2	2,560
Sandstone	8	320
	1	1,050
	3	2,560
	1	10,000
	3	40,000
	1	320,000

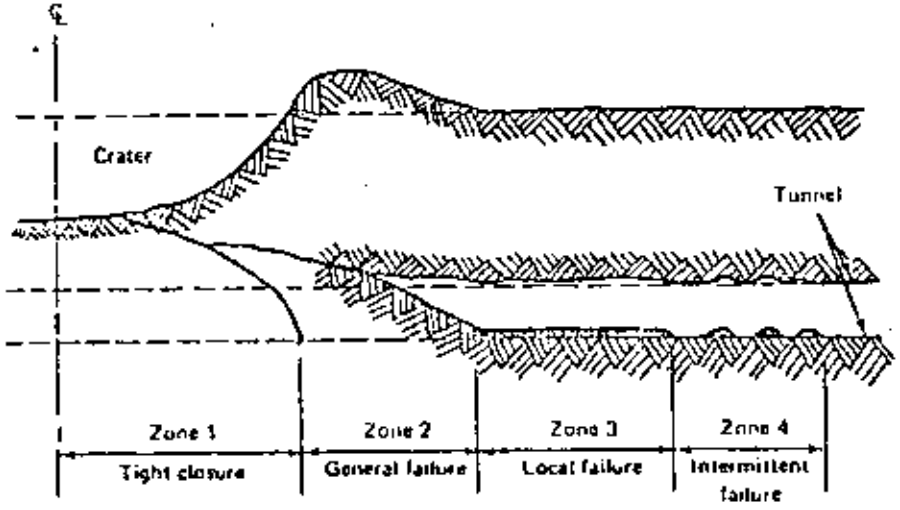

Fig. 7. Damage zones from UET program

increase in distance from the explosion. Finally, zone IV encompassed a region of intermittent failure of the tunnel surface with its maximum extent being the limit of observable damage. Table 2 gives a summary of the empirical designation of damage zones for all the tests conducted over unlined tunnels in sandstone. It should be noted at the bottom of Table 2 that the average scaled distances for zone I, zone II, zone III, and zone IV damage limits are 1.3, 2.0, 3.3, and 5.1 ft/lb$^{\frac{1}{3}}$, respectively. The peak radial strains measured as a function of scaled range for explosions in sandstone are shown by the line given in Fig. 8. The measured peak radial particle velocities versus scaled range are shown by the lines given in Fig. 9. A general summary of the behavior of unlined tunnels in sandstone in the Underground Explosion Tests is given in Table 3. In Table 3 it is shown that the outer limit of zone I corresponds to a

Table 2
Scaled Damage Distance in Tunnels

Round	Scaled Distance (ft/lb$^{\frac{1}{3}}$) from Charge to Tunnel Portal	Scaled Distance (ft/lb$^{\frac{1}{3}}$) from Charge to Tunnel Face	Scaled Distance (ft/lb$^{\frac{1}{3}}$) from Charge to Nearest Point of Tunnel	Number of Observers	Scaled Damage Distances, R/W$^{\frac{1}{3}}$ (ft/lb$^{\frac{1}{3}}$) Zone I		Zone II		Zone III		Zone IV	
807	13.4	1.8	1.19	3	1.2	1.3	1.9	—	2.7	—	3.1	—
808	7.4	7.8	1.75	3	—	—	1.8	1.8	2.2	2.2	3.8	4.8
809	7.5	4.6	1.32	2	—	—	—	—	—	—	4.3	—
810	16.5	7.2	3.29	3	—	—	—	—	4.0	3.3	5.2	4.5
811	10.2	13.6	1.82	2	—	—	2.4	2.0	3.5	3.6	5.0	5.3
812	5.3	17.6	1.32	4	—	—	1.6	1.1	2.5	2.6	4.0	4.0
813	9.0	5.8	1.71	2	—	—	2.0	2.1	3.4	3.4	4.8	4.5
814	—	6.4	2.76	3	—	—	3.8	2.8	4.2	3.1	8.7	—
814"A"	4.4	7.2	3.51	3	—	—	—	—	3.7	3.7	—	5.3
815	—	1.9	1.17	4	1.2	1.3	1.7	—	4.0	—	6.4	—
816	—	8.0	1.43	4	1.5	1.5	1.9	2.0	3.7	3.5	7.3	—
817	4.8	—	1.75	5	—	—	2.6	2.2	3.6	—	—	—
817"A"	2.5	3.4	1.75	5	—	—	1.8	1.9	—	2.8	—	—
817"B"	2.1	1.2	0.85	5	—	—	1.3	—	—	—	—	—
					Average						Average	
					1.3	1.4	2.0	2.0	3.4	3.1	5.3	4.7
					1.3		2.0		3.3		5.1	

free-field strain of about 1%. The outer limit of zone III corresponds to a radial strain of about 0.0012, and the other limit of zone IV corresponds to a free-field radial strain of about 0.0004.

From Table 3 it is apparent that particle velocities on the order of 3–6 fps were associated with the limit of occasional rock drops from the roof in an unlined tunnel. This type of failure would not occur in a lined tunnel. Thus, it seems that the UET test data indicate that the Langefors and Kihlstrom [14] damage criteria for tunnels in rock (10 in./sec) is conservative enough to be used in practice for both lined and unlined tunnels.

For residential-type structures the writer has used 2 in./sec as a damage criterion for controlling blasting operations. The relationship between charge weights per delay and distance for 2 in./sec from Ambraseys and Hendron [1] and Oriard [18,19] are given in Fig. 3. Note that the Ambraseys-Hendron and Oriard curves for 2 in./sec (Fig. 3) fall very close to the Langefors-Kihlstrom threshold relationship given by line 7 in Fig. 3. This criterion has not resulted in damage and also allows the contractor to excavate the rock as long as the blasting operation is greater than about 30 ft from the structure in question. For distances closer than about 30 ft it is usually found that a

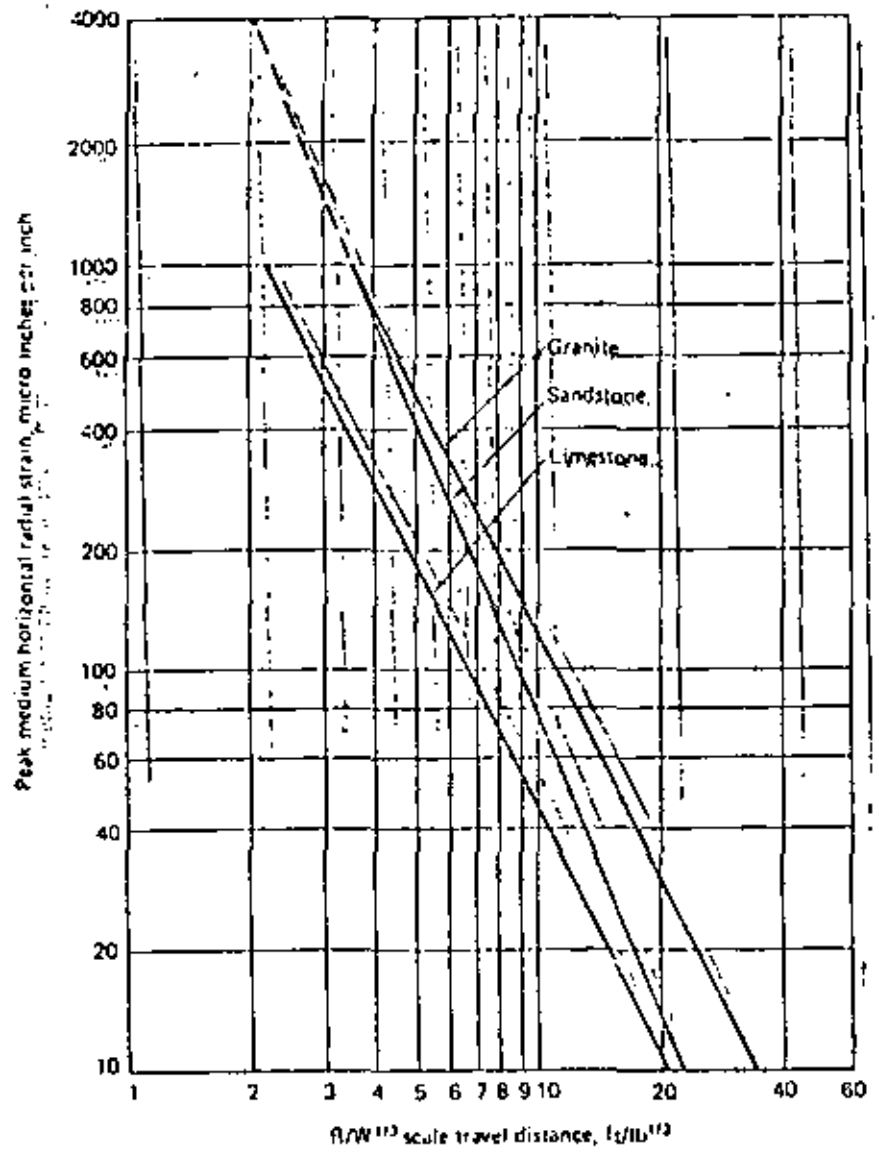

Fig. 8. Variation of average peak medium horizontal radial strain with scale travel distance in granite, limestone, and sandstone

2-in./sec criterion will severely restrict the contractor's operations. It has been the experience of the writer that these structures can tolerate a higher particle velocity without damage for small charges close to the structure because the m[illegible] occurs at a high frequency (40-150 cps), whereas the empirical criteri[illegible] of 2 in./sec was developed for more distant blasts where the pre-

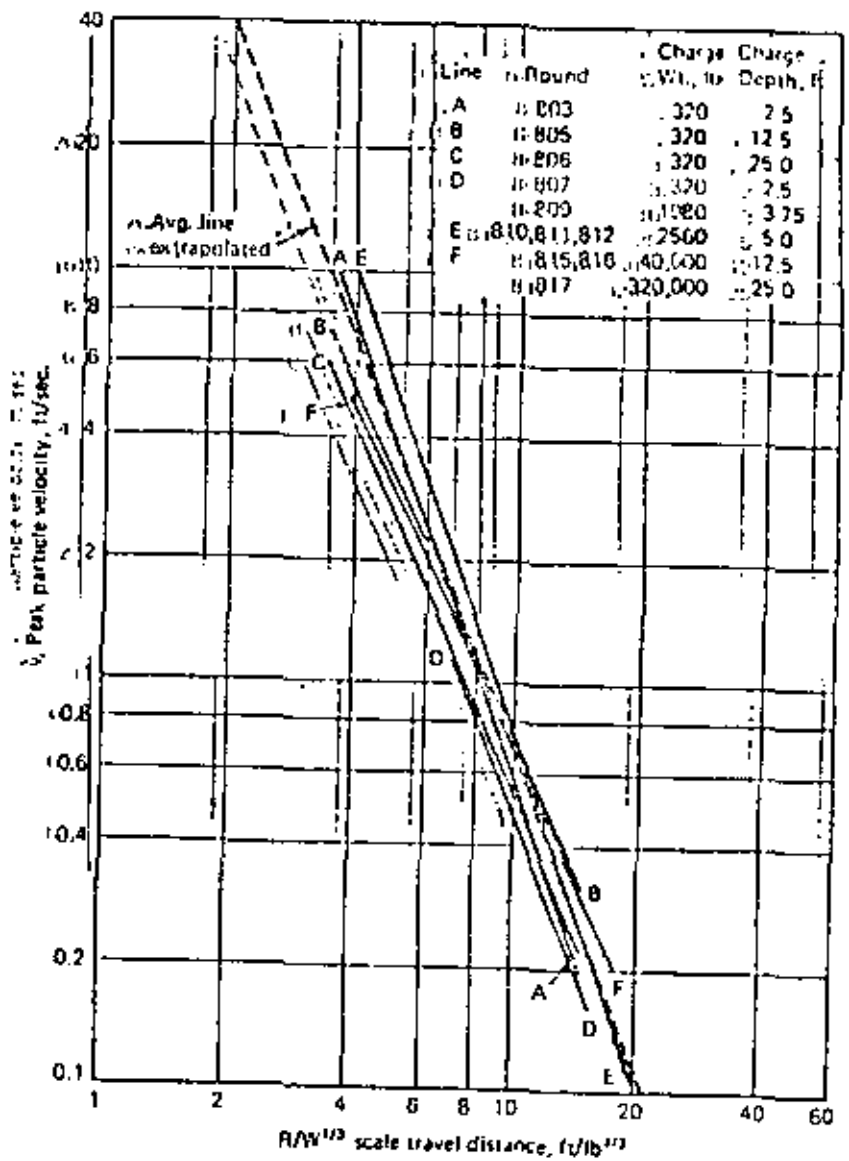

Fig. 9. Variation of peak particle velocity with scale travel distance

dominant ground motion frequencies were more nearly coincident with the frequency (about 10 cps) of the single-story structures studied. In such instances the response spectrum of the blasting vibrations can be used as a basis for determining permissible charge weights per delay for close-in blasts.

The application of the response spectrum for determ[illegible] the allowable charge per delay for close-in blasting as discussed above is illustrated by the

Table 3
Summary of UET Tests, Sandstone

	Zone I	Zone II	Zone III	Zone IV
Scaled range, $R/W^{1/3}$, ft/lb$^{1/3}$	1.1	2.0	3.3	5.1
Free-field radial strain	0.012	0.004	0.0012	0.0004
Free-field radial particle velocity, fps		40	13	3–6

following case history of a job in New York City. For a 4 lb/delay blast at a distance of 25 ft from a brick apartment building, a particle velocity of 3.5 in./sec was measured at the base of the exterior wall. This value, of course, was in excess of the 2 in./sec specified but did not cause damage to the building. If the peak ground vibrations for this case are computed from Eqs. (2), (3), and (4) for $c = 10{,}000$ fps, the maximum ground displacement, particle velocity, and acceleration are 0.0006 in., 3.4 in./sec, and 6.5 g, respectively. The response spectrum calculated from the procedure described previously is shown in Fig. 10. It was determined that the structure had a frequency of less than 10 cps and that the responses of masonry walls between columns and floors were at about 30 cps. Thus, from Fig. 10 it is apparent that the response of the structure and wall was governed by the displacement bound to the spectrum. Thus, the structure should not be damaged or the wall cracked if the response spectrum of subsequent blasts did not exceed the displacement bound in Fig. 10. Thus, for blasts closer than 25 ft, charge-distance relations were determined from Eq. (2) such that a displacement of 0.0066 in. would not be exceeded. This charge per delay-distance relationship is shown in Table 4 along with the expected maximum particle velocity. This guideline was used for the remainder of the job and enabled the contractor to excavate the rock with no damage to the building.

For blasting near reinforced tie back retaining walls, bridge abutments, bridge piers, engineered industrial buildings, and semigravity dam sections a maximum velocity criterion of 4 in./sec has been successfully used by the writer for blasts greater than 25–30 ft from the structure. The weight of charge per delay as a function of distance which can be used in such instances is given by curve 3 in Fig. 3. For distances closer than 25–30 ft the charges can be increased above those given by curve 3 of Fig. 3 on a case-by-case basis by using the response spectrum approach with the pertinent properties of the structure involved. The application of the approach as indicated above for a semigravity dam section led to the charge per delay-distance relationship as shown in Table 5 for distances closer than 50 ft.

For unusual problems without precedent the response spectrum approach may be the only available method upon which engineering decisions can be based. Such an example is the consideration of damage or loss of service of

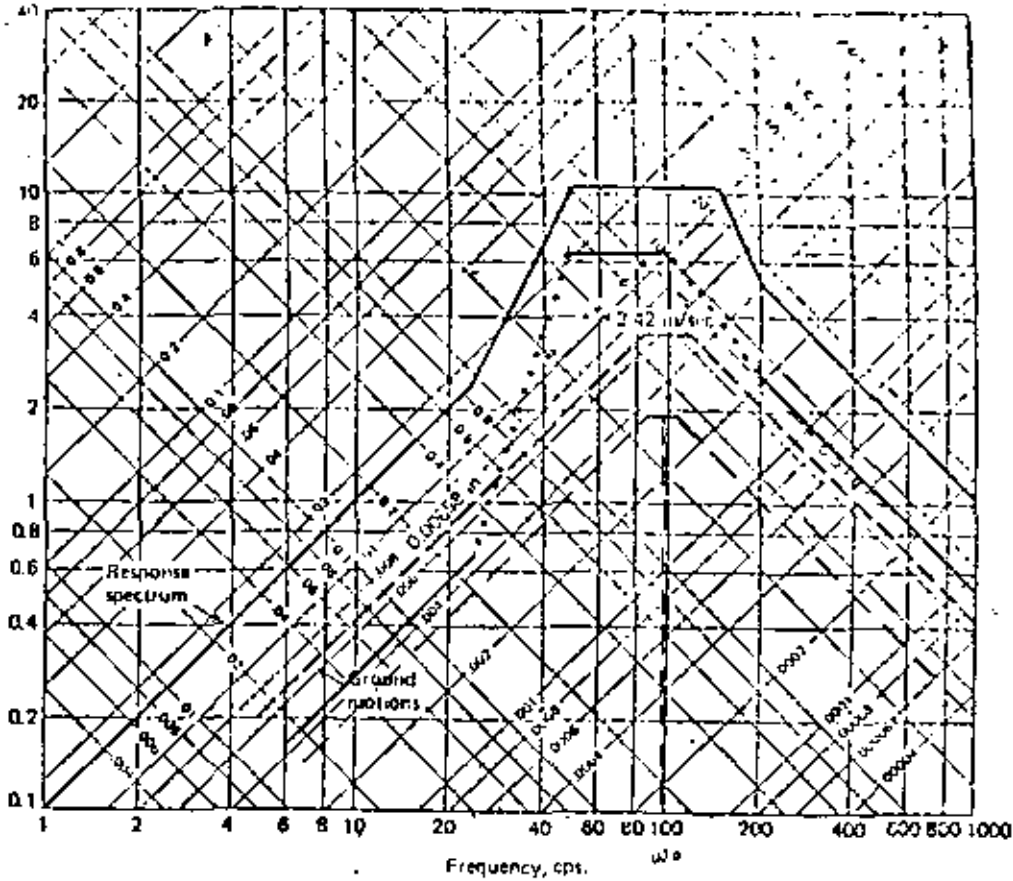

Fig. 10. Predicted response spectrum at 25 ft. from a 4 lb /delay blast

Table 4

Distance (R) to Blast (ft)	Maximum Permissible Charge Per Delay (lb/delay)	Maximum* Permissible Particle Velocity (in/sec)
<5	—	—
5–10	0.5	12.0
10–15	1.0	6.7
15–20	2.0	5.2
20–25	3.0	4.1
25–30	4.0	3.4
30–35	5.0	2.9
>35		2.0

Table 5

R (ft)	W (lb/delay)
150	200
125	125
100	80
75	50
50	20
30	10
20	5
10	2

use the response spectrum of the expected motions in conjunction with the frequencies of the racks or mounts containing the equipment. The fragility level of the equipment can then be used to determine the acceptable base motion input into the system. In the absence of specific fragility data, the peak acceleration transmitted to the equipment through the racks, mounts, or suspended floors should be less than 1 g.

Airblast Effects

In typical downhole blasting operations, airwaves are not likely to endanger any structures. Occasionally, however, such a hazard may exist. Examples are operations where surface charges are detonated, where large quantities of primacord are exposed at the surface, where no stemming is used (such as tunnel or shafting rounds), or where demolition is above ground. Ordinary structures, such as single-story homes, could have new plaster cracks formed with airblast overpressures on the order of 1 psi. Overpressures on the order of 1 psi would also most certainly break all windows. The data shown in Fig. 11 indicate that nearly all windows less than 60 ft² in area, if properly mounted, are safe from breaking at airblast pressures less than about 0.1 psi. There have been observations in practice, however, where occasional windows have been broken at pressure levels corresponding to about 0.1 psi where the windows have been poorly mounted.

In Fig. 12, relationships are given between peak overpressure in psi and the scaled range in ft/lb$^{1/3}$ for blasts at various depths of burial. The three shaded curves represent data from experiments with spherical charges in clay and in rock at scaled depths of burial of $\frac{1}{2}$ ft/lb$^{1/3}$ and 1 ft/lb$^{1/3}$. Also shown on the same diagram are data from single delay quarry blasts and multiple delay quarry blasts. It should be noted that the data from the single delay and multiple delay quarry blasts fall quite close to the data from the single spherical charges detonated at a scaled depth of 1 ft/lb$^{1/3}$ if the quarry blast

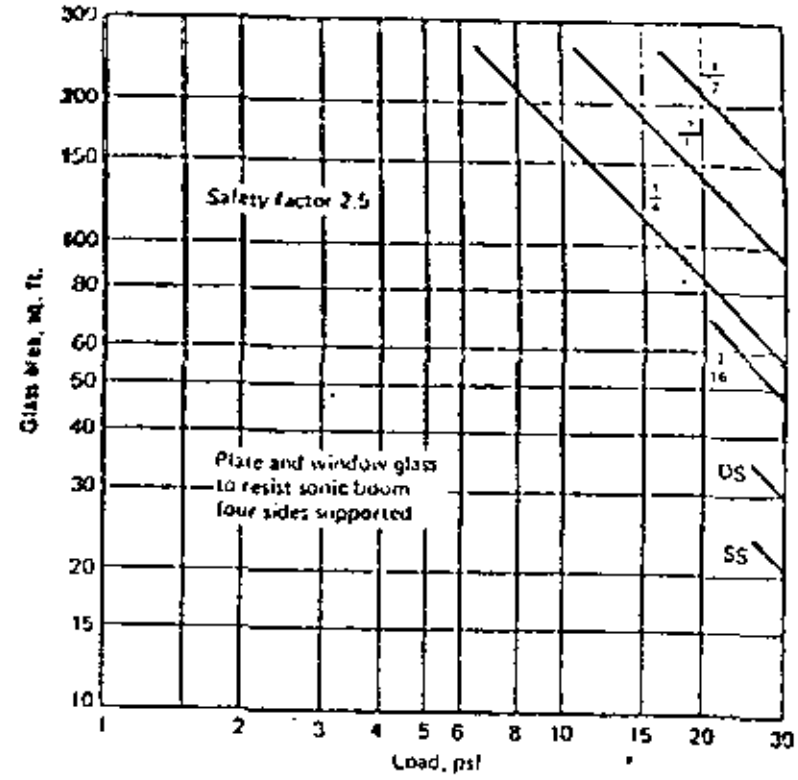

Fig. 11. Relation between window area and safe sonic boom pressure for various glass thickness. (After PPG Industries, 1969)

data are scaled using the weight of charge in the group of holes which are shot on the same delay interval closest to the point where the airblast was measured. The solid line given in Fig. 12 is a suggested approximate relationship to determine the overpressure for the various scaled ranges from the group of holes with the maximum charge per delay. Note that an overpressure of 1 psi occurs at a scaled range of 4 ft/lb$^{1/3}$ and that an overpressure of 0.1 psi occurs at a scaled range of 40 ft/lb$^{1/3}$. Figure 12 should not be used to predict airblast from shafting or tunnel rounds or for bench blasting with primacord rather than electric blasting caps.

In Fig. 3, the relationship between the maximum charge per delay and the scaled range which yields an airblast pressure of 1 psi is shown by line 1. The relationship between maximum charge per delay and the range which yields an airblast pressure of 0.1 psi is given by line 5. The relationship given by line 1 shows that an airblast pressure of 1 psi occurs at much closer ranges than the ground velocities which are likely to damage a structure. Thus, plaster cracking should never be caused by airblast for downhole blasting with electric caps and most probably would be caused by ground vibration. It does

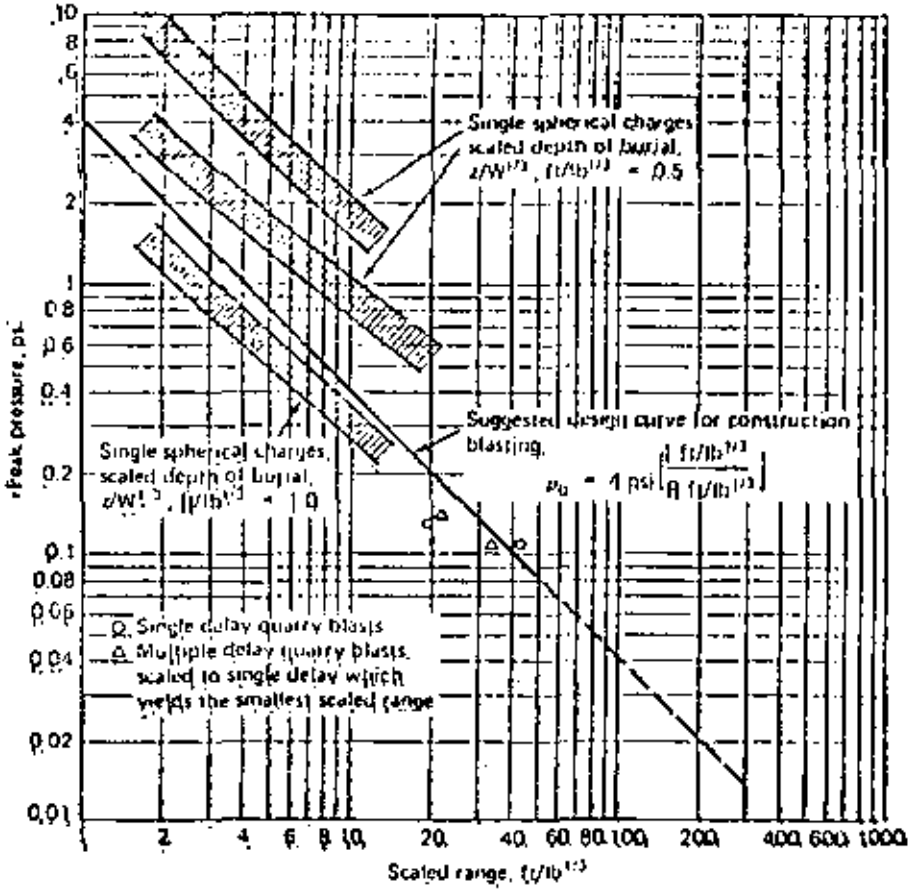

Fig. 12. Peak overpressure versus scaled range for buried explosions

appear, however, that the relationship shown on line 5 (Fig. 3), for 0.1 psi, that airblast pressures of 0.1 psi can extend out as far as ranges corresponding to a ground velocity of 2 in./sec. Thus, occasional windows could be broken, if very poorly mounted, at ranges corresponding to a ground velocity of 2 in./sec.

Human Response

A simple statement regarding the potential hazard of vibrations to structures does not begin to describe or satisfy the overall problem of blasting in a populated area. One of the chief difficulties is the sensitivity of people to sounds and vibrations and their lack of knowledge of the normal static nonvibratory physical forces which are involved in their daily lives. Consequently, one must at least consider the reaction of people as well as the response of the structures.

The response of humans to vibration has been studied by Reiher and Meister [22]. They studied the response of people to steady-state vibrations. Crandell [4] published curves on the level of human response to transient vibration. And more recently, Rathbone [21] and Bollinger [3] discussed the perceptibility of people to transient motion. A simplified summary of the response of people to steady-state motion is given in Fig. 13(a). The response of people to transient vibratory motion, without noise, is given in Fig. 13(b). Note that people can notice transient motions as low as 0.06 in./sec, that the

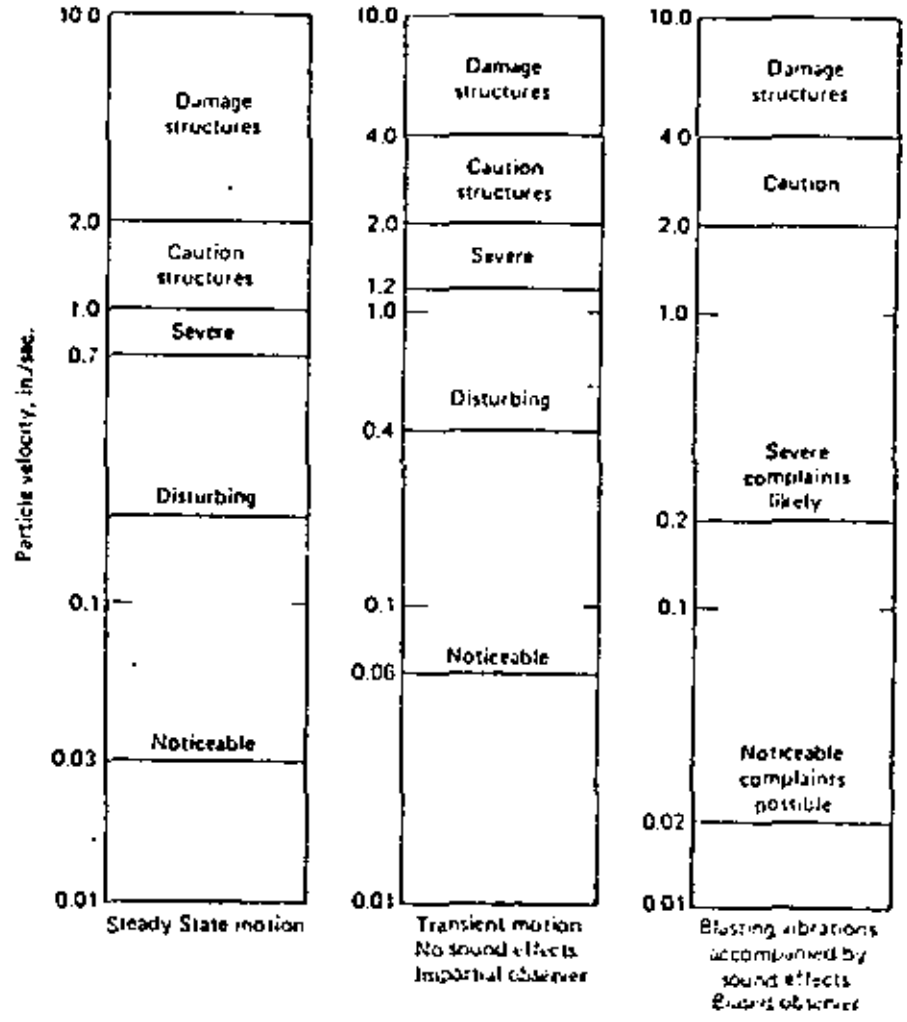

Fig. 13. Human response to vibrations

motion becomes disturbing at 0.4 in./sec, and that it feels severe to people at 1.2 in./sec. In actual practice, however, all rules for predicting motion response fall apart when sound effects accompany the motion and when the motion is of short duration. In some instances, the average person forms a judgment based largely on his psychoacoustic responses and is usually unaware of the important distinction between the characteristics of the motion alone and the sound effects that accompany that motion. One type of sound effect is produced by a blast which generates a very large noise at the source of the explosion. Such a blast is often regarded as severe and damaging when damage did not occur and when motion was not perceptible. To the average layman, the loud noise is sufficient to prove severity. Similarly, a blast may be accompanied by an inaudible airwave that has sufficient energy to cause loose windows and doors to rattle. The motion may be imperceptible, but the building occupant can be expected to judge the intensity of the blast by what he heard. Simply stated, he thinks the building was subject to strong vibration because he heard the sound of vibration of parts of the structure.

In Fig. 18(c), a simplified guideline is given for human response for blasting vibrations accompanied by sound effects for an observer who is slightly biased and is cognizant of the fact that blasting is going on in the area. For this combination, the blasting is noticeable at 0.02 in./sec and is often judged to be severe, and complaints are likely at a particle velocity as low as 0.2 in./sec. It may be in planning some blasting operations that these factors, rather than structural damage considerations, may govern.

Controlled Perimeter Blasting

General

Line drilling, cushion blasting, and presplitting are controlled blasting techniques for producing smooth walls on the perimeter of surface excavations in rock. Smooth wall blasting is a procedure used to produce smooth perimeters in tunnel excavations. A general description of the methods and guidelines for practical application of these methods are given below.

Line Drilling

Line drilling consists of a single row of closely spaced, unloaded, small-diameter holes along the perimeter of the excavation, as shown in Fig. 14. The line of line drill holes provides a plane of weakness to which the production blast can break. Line drill holes should be about 2 to 3 in. in diameter, and the spacing between holes should be 2–4 times the hole diameter. The distance between the line drill holes and the adjacent row of holes is usually 50–75 % of the normal burden. The spacing of holes in the row adjacent to the perimeter is also commonly reduced to 50–75 % of the normal spacing, and the load-

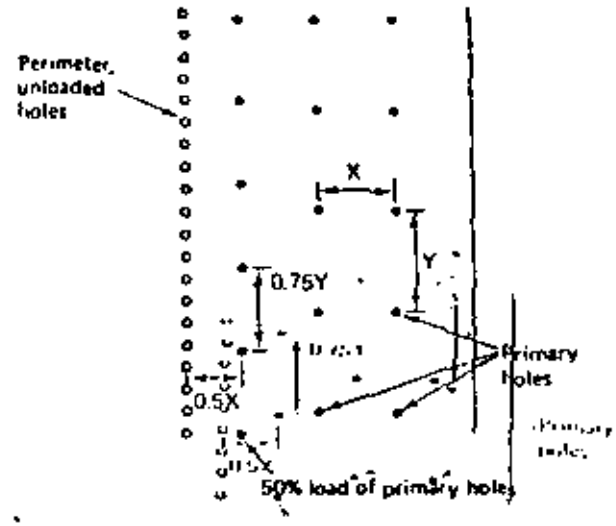

Fig. 14. Typical hole pattern for line drilling. (After Du-Pont Blasters Handbook, 1966)

ing of holes in this row is about 50 % of the loading used in the primary holes. One of the most important factors affecting the results on a job where the line drilling technique is used is the drill hole alignment. Holes should not deviate out of a vertical plane more than 6 in. Drilling accuracy usually is the main factor which controls the maximum depth to which one set of line drilled holes should be drilled.

Line drilling is used on nearly all perimeters immediately adjacent to existing structures in an urban environment. In some instances the unloaded perimeter holes may be drilled very close to form an open slot. This is done by inserting steel pipe into the last hole drilled and drilling the next hole adjacent to the pipe. This is called channel drilling.

Cushion Blasting

Cushion blasting involves the use of a single row of holes along the perimeter of the excavation. Cushion blast holes are loaded with light, distributed charges which are stemmed and fired after the primary excavation is removed. The holes are fired with a minimum delay between holes such that the detonation tends to shear the rock between holes and give a smooth wall. After the primary cut is removed, a minimum burden should be left in front of the final excavation line, as shown in Fig. 15. The burden will vary with the hole diameter being used. Table 6 gives guidelines for drill hole spacing and loadings for various drill hole diameters. Note that the spacing between holes should always be less than the burden. The loadings given in Table 6 may be obtained by stringloading dynamite cartridges with primacord downlines

by stringloading dynamite cartridges with primacord downlines

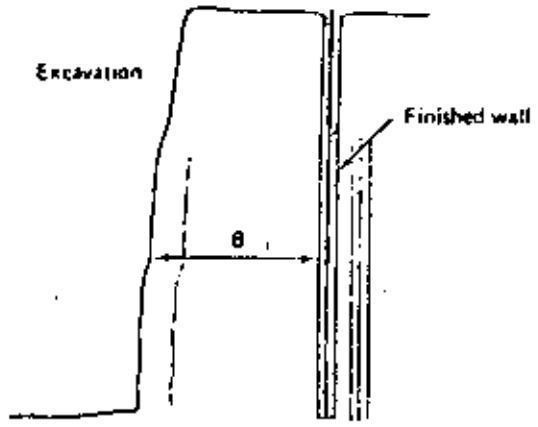

Fig. 15. Typical layout for cushion blasting. (After DuPont Blasters Handbook, 1966)

as shown in Fig. 15. Two to three times the loading used in the upper part of the hole should be used at the bottom of the hole to ensure shearing at the bottom of the hole. Sand or pea gravel is commonly used to stem the hole. The top 2 or 3 ft of the hole should be completely stemmed and not loaded. Primacord trunklines are normally used to get a minimum delay between holes, but if noise and ground vibrations must be controlled, MS delays can be used.

Table 6*

Hole Diameter (in.)	*Spacing (ft)*	*Burden (ft)*	*Hole Loading (lb/ft)*
2–2½	3	4	0.08–0.25
3–3½	4	5	0.13–0.50
4–4½	5	6	0.25–0.75

*After *Blasters Handbook* [2].

Presplitting

Presplitting consists of a single row of holes, 2 to 4 in. in diameter, drilled along the perimeter of the excavation. In most cases, all the holes are loaded. Presplitting is different from line drilling and cushion blasting because the holes are fired before the adjacent primary excavation is blasted, as shown in Fig. 16. In presplitting, the row of holes is shot simultaneously, and the web between holes is subjected to tensile stresses which cause cracking along the line of presplit holes on the perimeter of the excavation. This presplit surface

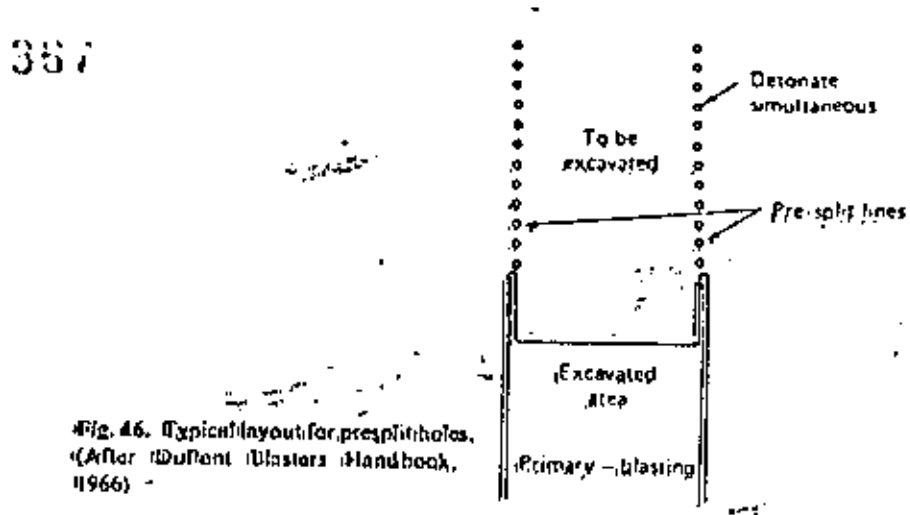

Fig. 16. Typical layout for presplit holes. (After DuPont Blasters Handbook, 1966)

is the smooth surface desired for the final excavation, if the proper hole loadings and hole spacings are used.

Presplit holes are string loaded, similar to cushion blasting holes, to obtain the average loadings shown in Table 7. The holes are usually fired simultaneously with a primacord trunkline, but if noise or ground vibrations are a consideration, sections of the presplit line can be fired with MS delays. The average spacings of presplit holes as a function of drill hole diameter are given in Table 7. All presplit holes should be completely stemmed, as in cushion blasting and should be loaded to about twice the average loading in the bottom few feet of the hole to ensure shearing at the bottom of the hole.

Table 7
Typical Loads and Spacings for Presplitting

Hole Diameter (in.)	*Spacing (ft)*	*Explosive Charge (lb/ft)*
2–2½	1½–2	0.08–0.25
3–3½	1½–3	0.13–0.50
4	2–4	0.25–0.75

*After *Blasters Handbook* [2].

The depth that can be presplit at one time is primarily dependent on drilling accuracy. Depths of 20–40 ft are commonly used for drill hole sizes ranging from 2 to 4 in. The author has found that 3-in.-diameter holes on a 2-ft spacing loaded at about 0.25 lb/ft give good results for fairly average rock conditions.

Presplitting should not be used adjacent to existing structures because the gas pressures tend to heave the rock at shallow depths. The confin-

and large number of holes detonated simultaneously also produce intense vibrations close to the presplit line.

Smooth Wall Blasting

Smooth wall blasting is used in tunnels to obtain a smooth perimeter. The technique is very similar to cushion blasting in that holes are drilled at a fairly close spacing around the periphery; these holes are lightly loaded and shot simultaneously to remove the final burden in the tunnel round. A typical tunnel round, designed to produce smooth walls, is shown in Fig. 17. In Fig. 17, the number by each drill hole denotes the number of the standard tunnel

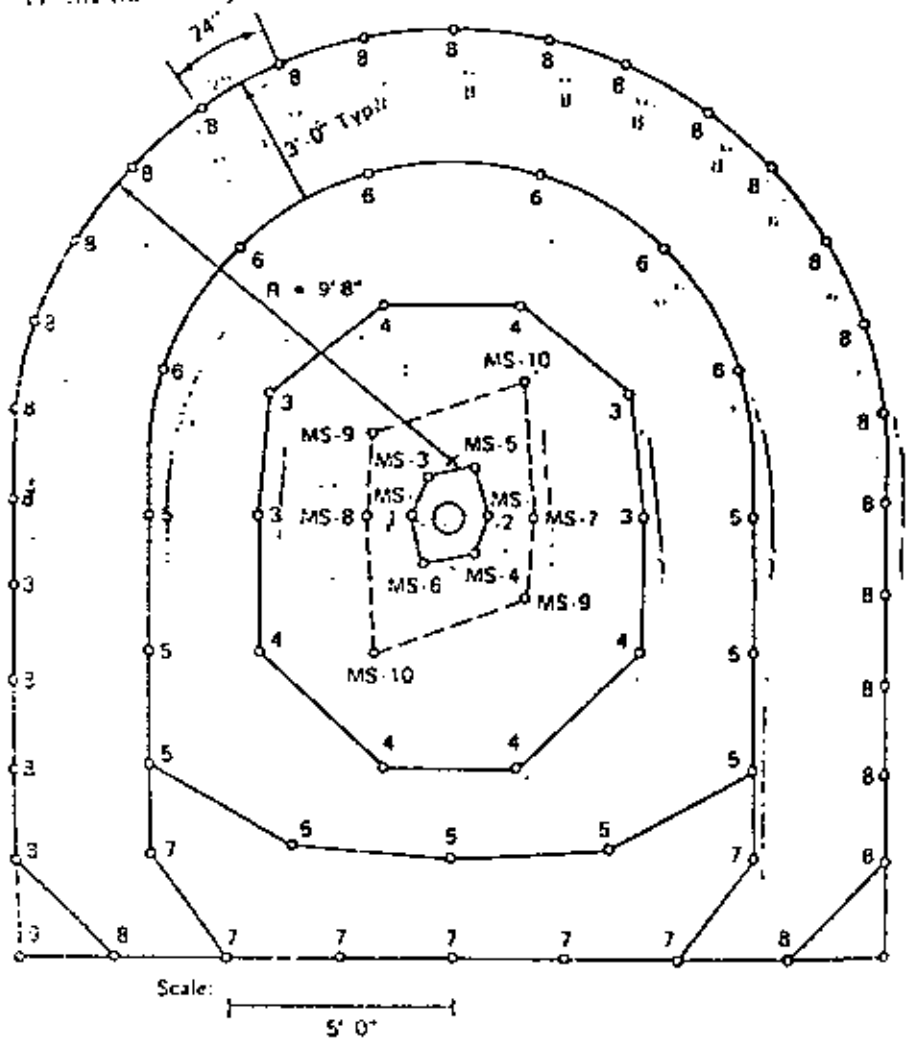

Fig. 17. Typical smooth wall tunnel round. (After Deere, 1972)

delay interval on which the hole is to be fired. If the letters MS are placed before the number, the hole is to be fired on that particular delay interval using millisecond delays. For the round shown in Fig. 17, the perimeter holes are shot simultaneously on the number 8 standard tunnel delay. The tunnel round should be designed such that the perimeter holes are fired on the lowest number delay possible. In general, the scatter in firing times increases as the delay number increases for electric caps; thus, the perimeter holes will be fired more nearly simultaneously if the delay used in the perimeter holes is as small as possible. One method of designing a tunnel round to reduce the delay number used on the perimeter holes is to use millisecond delays in the cut portion of the tunnel round. Note in Fig. 17 that the first 10-msec delay intervals were used to detonate the 12 holes used in the double spiral cut [14].

For smooth wall blasting, the spacing of the perimeter holes should be about 15 times the drill hole diameter, and the perimeter holes should be loaded with light, distributed charges ranging from ¼ to ½ lb/ft of hole. Small-diameter cartridges are commercially available which will give these loadings. The burden on the perimeter holes at the time of firing should always be greater than the spacing of the perimeter holes. A burden of 1.5 times the spacing of the perimeter holes is commonly used but may have to be altered slightly for various rock conditions. For the round shown in Fig. 17, a hole spacing of 2 ft was used on the perimeter holes and a burden of 3 ft was employed.

Blasting Specifications

General

Blasting specifications for a civil engineering project are usually written in two parts. The first part of the specification covers the general blasting procedures, and a second part entitled Specific Requirements usually covers such special topics as the controlled blasting techniques discussed in this chapter. The items which should be included in these two parts of the blasting specifications are discussed below.

Specifications on General Blasting Procedures

The specifications on general blasting procedure usually include those items which apply to all blasting operations. For example, in this section it is usually required that the contractor provide the services of at least one person qualified in the use of explosives for designing each blast and directing the execution of the blast. The qualifications of such persons are commonly required to be transmitted to the engineer for approval. If for one reason or another the blasting operations affect other aspects of a construction job, there should also be a requirement in these general specifications that the contractor must notify the engineer within some stated minimum time before

Blasting is to commence. This notification will permit the rescheduling of other operations and enable the engineer to control the use of such items as two-way radios which may be hazardous in the vicinity of electric blasting caps.

It is also common to specify in the general blasting specifications that the contractor submit the design of a blast to the engineer for approval before drilling and loading is begun. Such a plan should include the following information:

1. Number, location, diameter, and depth of drill holes shown on a plan drawn to scale.
2. Type and grade of explosive, size of cartridge, and weight of explosive in each hole.
3. Total amount of explosives in the blast and maximum pounds of explosive per delay interval.
4. Delay arrangement scheme showing delay interval proposed for each hole. Type and brand of delays should also be shown.
5. Character and source of firing current, size and length of lead lines, current requirement, and the combined resistance of the complete blasting circuit.

In each specification, it should be stated specifically what "approval" of the blasting plan by the engineer implies. Although the engineer may be extremely interested in inspecting the blasting plans regarding the adequacy of a round for obtaining a smooth perimeter, he may not be concerned about the design of a production blast to obtain adequate breakage so that the excavated rock can be handled by the type of equipment the contractor has on the job. Thus, as an example, a statement can be added to the specification stating that "approval of the blast design and plan by the engineer shall not relieve the contractor of his responsibility for the accuracy or adequacy of the plan for obtaining adequate breakage." Other examples may also be cited, but the significant point is that the specifications should clearly state the division of responsibility between the engineer and the contractor if the blasting plan is "approved."

Safety precautions should also be covered in the general specifications. The contractor is usually made completely responsible for safety in this portion of the specifications. All items regarding the safe handling, storage, and firing of explosives which are required in addition to the applicable federal, state, and municipal statutes should be covered. Such items may include the restriction of two-way radios, special precautions if stray currents have been detected on the site, procedures for clearing a danger area before blasting, and provisions for special inspection of equipment required if certain free-running blasting agents are used in place of cartridged explosives, and many other

items too numerous to mention. One of the most important items to include in this section is the requirement of blasting mats if structures and people will be close enough such that fly rock is a problem.

Specific Blasting Specifications

Specific requirements, which are necessary for achieving the desired results and which affect the contractor's costs, should be clearly stated in this section of the specifications. Specifications for vibration control, line drilling, presplitting, cushion blasting, and smooth wall blasting should be covered in this section of the specification. In addition, in many civil engineering jobs, limits may also be placed on some aspects of the production blasting. For example, if the engineer may wish to specify "small hole" blasting, there should be a statement in this section of the specification requiring that the blast holes be less than a certain diameter; that maximum diameter may be about 4 to 5 in. If a maximum diameter is not stated, the contractor may bid the job on the basis of large blast holes on large spacings, and restriction to smaller holes at a later date could possibly cause a contractual dispute.

Such items as the maximum depth of lift and the maximum depth of subdrilling permitted should also be treated in this portion of the specification. On jobs involving the installation of high-capacity tendons to tie back vertical cuts adjacent to structures the maximum depth of lift is extremely important since it governs the maximum unsupported height of cut immediately after each bench blast near the perimeter.

It has been the experience of the writer that the best way to cover vibration limitations *for blasts greater than about 30 ft away from a structure* is to specify the allowable vibration limit, not the quantity of explosive, and to specify the critical locations which will be monitored and the methods of monitoring. Specifying explosive quantities is not desirable. If the engineer is too liberal, he may actually exceed the vibration limits and get damage. It is more likely that the engineer will be too conservative and large sums of money will be wasted because his quantity limits are unnecessarily low. It is more desirable to let the contractor and his consultants demonstrate a little ingenuity. They may know of techniques for accomplishing the work more efficiently than the engineer anticipated and still stay within the limit the engineer really wants, namely a vibration limit (usually in terms of a maximum particle velocity). The writer has found it useful, however, to include a table in the specifications giving the approximate pounds per delay which will correspond to the specified velocity at various distances. Although this table may not be binding on either party, it does prevent the contractor from being totally surprised at the small charges required for some jobs. This type of contractor should be eliminated by a prequalification specification, however, if the owner's lawyers will permit.

When vibration limits are given in the specifications which are not to be

exceeded at various locations of structures around the perimeter of the job, the owner should also make available in the bid documents any vibration data from test blasts in the immediate area. This will enable the contractor and his consultants to make the best prebid estimate of the procedures which they will use. If prebid test blasts are not available, then the specifications should provide for the job to be started with four or five test blasts for which the contractor should be paid. This will allow him to approach the vibration limits gradually and will enable him to adjust his production patterns on the basis of vibration data obtained on the site. Usually the engineer will provide the equipment and personnel to monitor the initial locations. But, on some jobs, it may be desirable for the contractor to make the vibration measurements. If this is the case, the specifications must specify the type of equipment, frequency response, etc., which will be satisfactory for accurately measuring the ground vibrations expected.

As shown previously in this chapter, it may be necessary to allow higher particle velocities as blasting gets closer than 30 ft from a structure. In such cases the engineer and the contractor should work out the charge-distance relations, as in Table 4, on the basis of seismograph measurements from initial blasts at distances farther than 30 ft from the structures of concern. Until this information is obtained the values in Table 4 or Table 5 could be used as a guide.

For the controlled perimeter blasting methods of line drilling, presplitting, and cushion blasting, the specifications should cover the following items:

1. The diameter, depth, and spacing of the perimeter holes should be specified for all three types of controlled blasting (line drilling, cushion blasting, and presplitting). This enables the contractor to estimate drilling costs.
2. An approximate range should be given of the charge per foot of hole for the presplit and cushion blast perimeter holes. For line drilling, it should be stated that the perimeter holes are unloaded.
3. Stemming materials should be specified for the presplit and cushion blast holes.
4. Hole alignment tolerances should be given for the perimeter holes for all three methods of controlled blasting (holes should not deviate more than 6 in. out of plane).
5. Simultaneous firing of the perimeter holes should be specified for cushion blasting and presplitting, unless simultaneous firing produces too much ground vibration. If ground vibrations control, then the perimeter holes should be shot with MS delays.
6. The approximate range of burden values should be suggested for cushion blasting.

The spacing and loading of the two holes adjacent to the perimeter holes should be suggested for line drilling.

For smooth wall blasting in tunnels, the following items should be included in the specifications:

1. The diameter and spacing of the perimeter holes should be specified.
2. The approximate burden on the perimeter holes should be suggested (1.1 to 1.5 times the spacing of the perimeter holes).
3. It should be required that all the perimeter holes, except the lifters, be fired on the last delay period used in the round.
4. The approximate loading in the perimeter holes should be suggested in the specifications.

Conclusions

In this chapter, the technical aspects of controlling construction blasting to prevent damage to adjacent structures from ground vibrations and airblast has been discussed. Controlled blasting techniques available for producing smooth perimeters on both surface and tunnel excavations have also been reviewed. In addition, the items which should be covered in a good blasting specification have been set forth. The author feels that one of the most significant things that the reader should have learned from this chapter is that most of our knowledge about controlled blasting is empirical. Enough experience has been accumulated, however, that we are technically capable of achieving good controlled blasting for almost all situations where controlled blasting is required. In most situations where experience with controlled blasting has been poor, it can usually be traced to vague specifications which did not state either the result to be achieved or the detailed method to accomplish the desired result. The objective of this chapter was to give some of the detail which must be considered before a good specification can be written. It should be obvious that the specification writer must have at his disposal a knowledge of many of the construction details of blasting to permit the writing of an acceptable specification.

The writer has also found that a knowledge of the response spectrum of ground motions produced by blasting vibrations is valuable for making design decisions affecting the specifications for those cases where we are presently lacking precedent.

References

1. Ambraseys, N. R., and A. J. Hendron, Jr., "Dynamic Behavior of Rock Masses," *Rock Mechanics in Engineering Practice*, K. G. Stagg and O. C. Zienkiewicz, eds., Wiley, New York, 1968, pp. 203–27.
2. *Blasters Handbook*, E. I. du Pont de Nemours and Company, Inc., Wilmington, 1966.

3. Bollinger, G. A., "Blast Vibration Analysis," manuscript to Sprengnether Instrument Company. (Private communication.)
4. Crandell, F. J., "Ground Vibration Due to Blasting and Its Effect Upon Structures," *J. Boston Soc., Civil Eng.* Vol. 36, No. 2, 1949, pp. 206–229.
5. Deere, D. U., personal communication, 1972.
6. Devine, J. R., "Avoiding Damage to Residences from Blasting Vibrations," *Highway Research Record No. 135*, Highway Research Board, National Research Council, National Academy of Sciences, Washington, D.C., 1966.
7. Devine, J. F., and W. I. Duvall, "Effect of Charge Weight on Vibration Levels for Millisecond Delayed Quarry Blasts," *Earthquake Notes Seism. Soc. Am.*, Vol. 34, No. 2, 1963, p. 17.
8. Dowding, C. H., "Response of Buildings to Ground Vibrations Resulting from Construction Blasting," Ph.D. thesis, University of Illinois, Urbana, 1971.
9. Duvall, W. I., and D. E. Fogelson, "Review of Criteria for Estimating Damage to Residences from Blasting Vibrations," *Report of Investigations 5968*, Bureau of Mines Report, Denver, 1962, 19 pp.
10. Edwards, A. T., and T. D. Northwood, "Experimental Studies of the Effects of Blasting on Structures," *The Engineer*, Vol. 210, Sept. 30, 1960.
11. Engineering Research Associates, "Underground Explosion Test Program, Final Report," Vol. II: Rock, 1953.
12. Hendron, A. J., Jr., "Scaling of Ground Motions from Contained Explosions in Rock for Estimating Direct Ground Shock from Surface Bursts on Rock," *Technical Report No. 15*, Omaha District, Corps of Engineers, Omaha, 1973.
13. Hendron, A. J., Jr., and C. H. Dowding, "Ground and Structural Response Due to Blasting," *Proceedings, 3rd Congress of the International Society of Rock Mechanics*, Vol. II-B, National Academy of Sciences, Washington, D.C., 1974, pp. 1359–1364.
14. Langefors, U., and B. Kihlstrom, *The Modern Technique of Rock Blasting*, Wiley, New York, and Almqvist & Wiksell, Stockholm, 1963, 405 pp.
15. Langefors, U., B. Kihlstrom, and H. Westerberg, "Ground Vibrations in Blasting," *Water Power*, Feb. 1958, pp. 335–338, 390–395, 421–424.
16. Newmark, N. M., "Problems in Wave Propagation in Soil and Rock," *Proceedings of International Symposium on Wave Propagation and Dynamic Properties of Earth Materials*, University of New Mexico Press, Albuquerque, 1968, pp. 7–26.
17. Newmark, N. M., and W. J. Hall, "Seismic Design Criteria for Nuclear Reactor Facilities," *Proceedings, 4th World Conference on Earthquake Engineering, Santiago, Vol. 2*, IAEA, 1969, pp. 37–50.
18. Oriard, L. L., "Blasting Effects and Their Control in Open Pit Mining," Symposium and Specialty Seminar on Stability in Open Pit Mines, University of British Columbia, Vancouver, Nov. 1971.
19. Oriard, L. L., "Blasting Operations in the Urban Environment," *Bull. Assoc. Eng. Geol.*, Winter 1971.
20. PPG Industries, "Glass Product Recommendations, Structural," *PPG Industries Technical Service Report No. 101*, Pittsburgh, 1969.
21. Rathmell, T. C., "Human Sensitivity to Product Vibration," *Product Eng.*, Feb.

22. Reiher, H., and F. J. Meister, "Die Empfindlichkeit des Menschen gegen Erschutterungen (Human Sensitivity to Vibration)," *Forsch. Gebiete Ing.*, Vol. 2, No. 11, 1931, pp. 381–386.
23. Thoenen, S. R., and S. L. Windes, "Seismic Effects of Quarry Blasting," *Bulletin 442*, Bureau of Mines, Denver, 1942, 83 pp.

EXCAVACIONES SUBTERRANEAS

CHAPTER 3
DESIGN

3-1. General.

a. This chapter will present the simplified methods most commonly used in the design of tunnels at the time of this writing. Appendix K presents more elaborate approaches to tunnel design using continuum mechanics and finite element methods of analysis which are coming into use. The more elaborate methods, although not in general use for arriving at an actual design, can be used for arriving at a better understanding of how the rock and the support system interact and for estimating the combined effects of rock quality, joint spacing, and joint orientation on support requirements.

b. Rock can act either as a continuum or a discontinuum. A continuum is a material in which average values of physical properties such as stress or density can be used in physical models to define the mechanical behavior of the material. The approaches to support design are entirely different for each type of medium. The continuum approach to tunnel analysis can be used directly only when the material meets the assumptions for a continuum. This may be true in massive, unfractured rock or even in very poor rock, but the majority of rock masses are broken by numerous rock defects and hence behave as a discontinuum. There are also some indications that problems in rock masses of intermediate strengths can be solved through the use of continuum mechanics methods. As further discussed in Appendix K, this requires the use of appropriate "average" constants to describe the rock mass and a carefully reasoned justification, preferably backed up by evidence obtained from field observations and measurements. In applying the simplified design methods discussed in this chapter, the rock is considered to act as a discontinuum. However, the support system is designed with the use of empirical or semi-empirical methods which do not directly incorporate predicted stresses or displacements in the rock medium or the medium-support system interaction. Because of limitations inherent in any of the design methods discussed in this manual, personal evaluations and solutions based on judgement and experience still play an important role in the design process.

c. It should be noted that the excavation and construction methods used can significantly affect the support system requirements. Support loadings can be minimized by the use of construction methods (such as machine mining or controlled blasting) which cause minimum overbreak or damage to the rock near the tunnel surface. Geologic conditions also change from one section of a tunnel to another. As a result, support system requirements may need to be altered during tunnel construction. The support system should therefore be capable of responding to these changes by providing for variations in the strength or type of system.

3-2. Factors Affecting the Design.

a. Basic Factors. Factors which should be considered in the design of a rock support system using methods described in this chapter are listed below:

(1) Geologic conditions.

(2) Size of opening with respect to spacing of rock joints.

(3) Shape of opening.

(4) Orientation of opening with respect to orientation of rock joints.

(5) Material properties. (Does the rock swell, slake, or crumble?)

(6) Construction procedure.

(7) Ground water.

(8) Earthquake effects.

b. How Factors Affect Design. A brief discussion of how these factors affect the design is presented below:

(1) Geologic Conditions. The geologic conditions (particularly the orientation, spacing and frequency of the joints and bedding planes that control the shape and size of rock blocks) serve as a basis for classifying the rock, for determining rock loads on steel set supports or concrete lining, for determining the spacing, strength and length or rock reinforcement elements, for determining shotcrete thickness and for selecting the support system itself. The need for supplementary support materials or methods can also be anticipated on the basis of geologic data. These include the use of chain link fencing or wire mesh on the rock surface, lagging between steel sets, or the use of spiling at the tunnel face.

(2) The Size of the Opening with Respect to the Rock Joint Properties. Experience has shown that the degree of stability of a tunnel through a particular jointed rock formation tends to decrease as the tunnel size increases. The ratio of joint spacing to tunnel size is considered to be an important parameter although rock quality, joint orientation and condition of joints must all be considered in making determinations with regard to the effect of tunnel size on support system requirements. In using simplified design methods based on the qualitative rock classification given in paragraph 2-4a, the effect of size may be accounted for by adjusting the classification at a particular site. For example, the same rock at a particular site might be classified as moderately blocky or seamy for a 7-foot diameter tunnel but the classification adjusted to very blocky and seamy for a 30-foot diameter tunnel. Although determinations are usually based on personal judgement and experience, relationships

based on statistical analyses of historical tunneling data are being developed (Wickham, Tiedmann, Skinner[65]) which will aid in making adjustments for the effects of tunnel size.

(3) Shape of the Opening. The shape of the opening can be based on either the function of the tunnel or on the rock conditions at the tunnel site. Normally, vehicular tunnels are horseshoe shaped, whereas water tunnels are either horseshoe or circular. Tunnels through dams upstream of the embankment cutoff, where the tunnel is subject to external reservoir head, should be of circular cross section. If the material to be mined is swelling or squeezing rock or rock of poor quality, a circular section or perhaps an elliptical section should prove safest for support. Where the possibility of using a mining machine exists, tunnels should be designed with a cross section that would fit this method of excavation. At the present time, machines which mine a circular cross section are most common. Machines are also available which will mine other shaped sections.

(4) Orientation of the Opening with Respect to Orientation of Bedding and Joints. The bedding can vary from flat to vertical, and the jointing will normally divide the rocks into blocks. The difference in loading between vertical and horizontal bedding may not be significant. However, the more steeply bedded rocks may trap water at the contacts between different types of rock. These areas should be approached carefully. Interpretation of borings that are vertical can be misleading in steeply bedded rocks and in these cases, the use of angled holes intersecting the bedding surfaces at steeper angles should be considered. The effect of geologic discontinuities and tunnel orientation on tunnel behavior is further discussed by Cording and Maher[22].

(5) Material Properties. The type and nature of rock and state of stress can have an influence on the shape of the opening as well as the method of support. Rocks that apply large lateral loads to steel supports require invert struts at the base of horseshoe ribs. If possible, the use of circular or elliptical shaped sections would be more desirable. The design of tunnels in swelling rock is discussed in detail by Einstein and Bischoff[31]. Some rocks deteriorate on contact with the air and will require protection during tunneling operations. This is normally done using shotcrete or some other coating material which will seal the surface. Also, the filler in some joints contain filling with very little strength, while others have fillings which actually cement the rock together. Some rock may not provide adequate anchorage for expansion shell rock bolts and will require a grouted anchorage or an alternate support system.

(6) Construction Procedure. The procedures used in excavating the tunnel can have a significant influence on the selection and design of tunnel support systems. The varying degrees of damage and overbreak resulting from the use of conventional blasting methods, smooth wall blasting methods, or machine mining methods will affect the design of

the support system. The volume of damaged and loosened rock remaining in place, which in turn will load the initial support (steel sets, rock bolts or shotcrete), may be twice as large as a result of using conventional rather than smooth wall blasting techniques. Machine mining methods will result in less overbreak than with blasting methods and create minimum disturbance to the rock at depth. However, the machine itself may become an obstacle to the early installation of long rock bolts or shotcrete. The use of shotcrete alone for initial support is not recommended when large overbreak exists at the tunnel periphery because the resulting non-uniform stress concentrations can seriously degrade the stabilizing influence of the shotcrete. Under certain geologic conditions, the direction of excavation advance may have a pronounced effect on the support system design. For example, rock would have a much greater tendency to loosen and fall into the opening if rock joints crossed the tunnel route at approximately 90 degrees and dipped downward at 45 degrees toward the opening rather than away from the opening. Likewise, rock reinforcement would be more effective in controlling rock loosening and movement in the latter case. Reinforcing elements could be installed more normal to the joint planes while the rock between joints was still confined by unexcavated rock forward of the tunnel face. In general when tunneling in rock, initial support should be installed immediately behind the tunnel face regardless of whether the support consists of rock bolts, shotcrete or steel sets. In this manner, further rock loosening is prevented or minimized and maximum advantage is taken of the rock's inherent ability to support itself.

(7) Ground Water. Consideration should be given to the quantity, quality and temperature of the ground water that may be encountered during tunneling. Support problems are most likely to develop if large water inflows under high pressures are encountered during tunneling through poor rock. If the water is to be discharged into a stream, then its quality and temperature must be known to avoid environmental problems. Also, the possible effect of draining water from existing aquifers should be carefully studied to avoid litigation that may arise as a result of lowering the water table.

(8) Earthquake Effects. Experience indicates that most well-designed hard rock tunnels withstand the dynamic effects of earthquakes. Historically, well-designed deep tunnels that do not cross capable faults have sustained only limited damage even when located near the epicenters of major earthquakes. Damage has, however, been reported where displacements and/or stress concentrations have occurred along capable faults. Tunnels located through faults, where displacements can be anticipated, are beyond the scope of this manual and special design features are necessary to accommodate movement. For most rock tunnels the area of maximum vulnerability to earthquake effects are in areas of shallow cover, particularly near the portal. In such areas, displacements can occur during an earthquake when the overlying material deforms along faults, joints, weathered rock or other weak anomolies. Slides can also take place in the overlying overburden.

The amount of displacement depends upon the magnitude of the earthquake, the location of the tunnel from epicenter, and whether the residual strength after the earthquake is sufficient to resist the static loads. A detailed discussion on dynamic stability, however, is not within the scope of this manual. Literature contains little data on experience records of tunnels that have experienced earthquakes. However, some general conclusions have been stated as a result of research studies (Duke and Leeds[29], Atchley and Dobbs[9]). These have been summarized and supplemented by Cooke[20], and are listed below.

(a) The probability of occurrence of earthquake damage to tunnels is small.

(b) Damage is inevitable if fault movement occurs across the tunnel.

(c) Fault movement is rare, and is conceivable only on capable faults.

(d) In regions of high Modified Mercalli Intensity, VIII - XII, damage is probable to tunnels in incompetent rock and near the surface.

(e) There is no recorded damage to tunnels in hard rock.

(f) Earthquake vibrations are less severe in intensity as depth increases, and considerably less severe than in weathered rock or alluvium overburden near the surface.

(g) There is virtually no risk of earthquake damage to tunnels located in hard rock provided capable faults are not crossed.

c. Evaluation and Interpretation. The factors cited in paragraph 3-2.a. should be evaluated before proceeding with the design of the rock support system. This must be done during the time geological investigations are made. The number of borings required to supply this information must be determined individually for each site by cooperation between the designers and the geologists. Interpretation of data from the borings is the responsibility of the geologist but maximum benefit accrues to the support system design when interpretations are jointly applied by the engineering geologist and the structural engineer responsible for the design of the support system. It is also quite helpful if the designer can actually view the cores and photographs of cores. This will provide him with a better feel for the imperfections in the rock than would only a review of the boring logs.

3-3. Load Determination Using Empirical Methods.

a. General.

(1) In Szechy[59], several existing theories and methods of tunnel lining design are presented and then summarized as follows:

resented,
r than

d of
installa-
lication
e of
capacity
mind
ased on
ard to

5B, the
taken
general.
use

all

of

most tunnel
was developed
tion of hundreds
erzaghi[60]), have
thods which
ecommendations
aghi's recommenda-

ll be loaded by
e system, the
teel set supports
rs immediately
of factors which
nts, depth of
thod, and the
essive loosen-
ports
excavation and
he above
ces due to
ing as well
s are redis-
tion, rock
n and steel
ds on the
round the

"From the wide variety of rock pressure theories presented, a series of sound and intuitive assumptions, rather than satisfying uniform results may be concluded. The theoretical consideration of factors such as method of excavation, rigidity of supports, time of support installation, consolidation process of deformation, stratification and relative location of overlying layers, magnitude of residual stresses, etc., seems to lie beyond the capacity of both elastic and plastic theories. Bearing in mind their inherent defects, practical design may be based on the following rock pressure theories, with due regard to circumstances and local conditions."

(a) "Up to a depth of cover of (H) equal to 2.5B, the full weight of the material above the crown must be taken into account." (Note: This statement applies in general. However, a conservative design would result with the use of this loading in good rock.)

(b) "For depth of cover (H) exceeding 2.5B in all kinds of material, the use of Terzaghi's theory is permissible. H = Depth of cover measured from roof of tunnel. B = Diameter of the opening."

(2) The above approach is the one generally used by most tunnel designers for estimating rock loads. Although this method was developed empirically, its use has resulted in the successful completion of hundreds of tunnels. Terzaghi's qualitative rock load concepts (Terzaghi[60]), have also served as a basis for the development of alternate methods which relate rock loads to quantitative rock quality indices. Recommendations made with some of these alternate methods, as well as Terzaghi's recommendations, are given in the paragraphs that follow.

(3) When based on the assumption that the system will be loaded by a definite volume of loosened rock lying directly above the system, the design of tunnel support systems is generally limited to steel set supports or concrete linings. The initial rock loosening which occurs immediately as the tunnel opening is excavated is related to a number of factors which include rock quality, orientation and condition of rock joints, depth of damage or disturbance to rock created by the excavation method, and the orientation and condition of rock fractures. Further progressive loosening can then occur to increase the load on the steel set supports initially installed depending on the elapsed time between excavation and installation of the supports, as well as on the effect of the above factors. After installation, the supports act to resist forces due to the weight of loosened rock attempting to move into the opening as well as to resist other rock deformations that result as stresses are redistributed in the rock around the opening. Following installation, rock movements due to creep of the wood blocking between the rock and steel sets may result in additional rock loosening to increase loads on the supports and result in further redistribution of stresses around the

opening as the opening reaches stability. No direct application of Terzaghi's rock load concept is made when designing shotcrete or rock reinforcement systems, although attempts have been made to relate the support capabilities of these systems to the support provided by steel sets. Shotcrete and rock reinforcement systems (which are discussed later in the text) act to prevent or greatly reduce rock loosening and movements which may progressively lead to rock failure and instability, and therefore make greater use of the rock's inherent strength to provide stability than do steel set supports. As mentioned previously, rock load concepts are used when designing final concrete lining support. Concrete lining design is also covered later in the text.

b. Terzaghi's Rock Load Concept. In this concept, (Terzaghi[60]) the support system is assumed to carry a certain height, H_p, of loosened rock above the crown of the tunnel. The concept is strictly applicable only to rocks where this loosening can occur and where the loosened rock is the primary contribution to the load on the support. This is usually the case in jointed rocks which are non-coherent to begin with or which lose coherence with time. Where loosening is prevented (such as when shotcrete or rock bolts are installed immediately behind the face), the added rock load caused by the loosening process is partly or completely eliminated. Terzaghi's rock load concept was developed before machine tunneling and rock reinforcement construction methods were introduced or adopted and therefore generally reflects the magnitude of rock loads that would develop in conventionally excavated tunnels. Ordinarily, the rock surfaces of a machine-driven tunnel will not require as much support because the rock disturbances are minimized. Terzaghi's rock load recommendations are given as a function of rock condition (classification) in Table 3-1. Commenting on the table, Terzaghi writes:

> "Our knowledge of the intensity of rock loads on tunnel supports is derived chiefly from the results of tests which were carried out (in the late 1920's) in various railroad tunnels in the eastern Alps. In these tests, wooden blocks with known strength were inserted between the individual members of timber sets and the load (H_p) on the timbering was estimated from the visible manifestations of the progressive failure of the blocks."

c. Alternate Methods for Estimating Rock Loads. Deere, et al[28], includes correlations of different classification systems along with recommended rock load factors for design. Table 3-2 shows comparisons in terms of average fracture spacings, rock quality designation (RQD), and Terzaghi's rock classification. Included are qualitative relationships that exist between the RQD and the support required for tunnels (20' to 40' diameter) in rock. Recommended support system requirements are related to RQD and also to the method of excavation in Table 3-3. The rock load factors recommended in the table for tunnels excavated by conventional drilling and blasting methods are approximately 20 percent

Table 3-1. Estimate of Rock Load

(After Proctor and White[47])

Rock load H_p[a] in feet of rock on roof of support in tunnel with width B (ft) and Height H_t (ft) at depth of more than 1.5 $(B + H_t)$.[b]

	Rock Condition	Rock Load H_p in Feet	Remarks
1.	Hard & intact	zero	Light lining, required only if spalling or popping occurs.
2.	Hard stratified or schistose[c]	0 to 0.5 B	Light support.
3.	Massive, moderately jointed	0 to 0.25 B	Load may change erratically from point to point.
4.	Moderately blocky and seamy	0.25 B to 0.35 $(B+H_t)$	No side pressure.
5.	Very blocky and seamy	$(0.35 \text{ to } 1.10)(B+H_t)$	Little or no side pressure.
6.	Completely crushed but chemically intact	$1.10\ (B+H_t)$	Considerable side pressure. Softening effect of seepage towards bottom of tunnel requires either continuous support for lower ends of ribs or circular ribs.
7.	Squeezing rock, Moderate depth	$(1.10 \text{ to } 2.10)(B+H_t)$	Heavy side pressure, invert struts required. Circular ribs are recommended.
8.	Squeezing rock, Great depth	$(2.10 \text{ to } 4.50)(B+H_t)$	
9.	Swelling rock	Up to 250 ft. irrespective of value of $(B+H_t)$	Circular ribs required. In extreme cases use yielding support.

[a]Vertical load acting on tunnel supports per foot of tunnel length = $(H_p)(B)(\gamma)$, when γ = density of rock, lbs/ft^3.

[b]The roof of the tunnel is assumed to be located below the water table. If it is located permanently above the water table, the values given for types 4 to 6 can be reduced by fifty percent.

[c]Some of the most common rock formations contain layers of shale. In an unweathered state, real shales are no worse than other stratified rocks. However, the term shale is often applied to firmly compacted clay sediments which have not yet acquired the properties of rock. Such so-called shale may behave in the tunnel like squeezing or even swelling rock. (The tunnels of the Missouri River Dams were driven through clay shales that behaved more like blocky and seamy rock due to numerous joints, slickensides and bentonite seams that reticulated the shale mass.) If a rock formation consists of a sequence of horizontal layers of sandstone or limestone and of immature (weak) shale, the excavation of the tunnel is commonly associated with a gradual compression of the rock on both sides of the tunnel, involving a downward movement of the roof. Furthermore, the relatively low resistance against slippage at the boundaries between the clay and hard rock is likely to reduce very considerably the capacity of the rock located above the roof to bridge. Hence, in such rock formations, the roof pressure may be as heavy as in a very blocky and seamy rock. (This was the condition at Ft. Peck and Oahe tunnels which were driven through clay shales.)

age rock load factors that would be estimated by the use
The influence of the excavation method is reflected by
ors for machine excavated tunnels which are approximately
er than for tunnels excavated by conventional drilling
In Table 3-3, guidelines are also given which apply to
shotcrete or rock reinforcement systems when used in lieu
supports for each rock condition listed.

of Rock Load Concepts for Support System Design. It is
even though widely used there are shortcomings to Terzaghi's
ept. One is that the classification is qualitative and
ely dependent on the judgement and personal observations
ing geologist. Another is that the rock loads were
om observations of wood blocks which failed. Terzaghi
iod of load increase on a set placed behind a face and
se in load as the face is advanced and the rock load is
to the tunnel walls. Wood blocks could not give any
the magnitude of these latter loads. However, a conserva-
nerally results with the use of the rock load concept.
ated below the water table in blocky and seamy rock,
sts that the concept may be quite conservative. Expected
sed in design should be based on Table 3-1 with Tables 3-2
additional guides. In all cases, the reference sources
ables should be consulted for further discussion on the
limitations of the tables.

Support Design.

eral.

the early days of tunneling in the United States, when
required they were generally made of wood since it was
p and labor costs for installation were low. The first
upports were not installed until the late 1920's and early
use has rapidly increased since that time. The reasons
increase are the following:

el can be installed much faster than timber. In most rock,
ous to install support as soon as possible.

lled carpenters are required to install timber supports
be installed with relatively unskilled labor.

er men are required to install steel supports.

ber rots and decays behind a concrete lining which results
on the lining.

installed as temporary excavation support can be
art of the reinforcement in a permanent lining.

Table 3-2. Rock Loads and Classification
(From Deere, et al[28])

383

Fracture Spacing (cm)	Fracture Spacing (ft, in)	RQD(%)		Rock Load, H_p Initial	Rock Load, H_p Final	Generally no side pressure. Erratic load changes from point to point.	Remarks
	2'	98	1. Hard and Intact	0	0		Lining only if spalling or popping
50		95	2. Hard Stratified or Schistose	0	0.25B		Spalling common
	1'	90	3. Massive, moderately jointed	0	0.5B		Side pressure if strata inclined, some spalling
20		75	4. Moderately blocky and seamy	0	0.25B to 0.35C		
	6"						
10	4"	50	5. Very blocky, seamy and shattered	0 to 0.6C	0.35C to 1.1C		Little or no side pressure
		25	6. Completely crushed		1.1C		Considerable side pressure. If seepage, continuous support.
5	2"	10					
		2					
	1"		7. Gravel and sand	0.54C to 1.2C	0.62C to 1.38C		Dense
2				0.94C to 1.2C	1.08C to 1.38C		Side pressure $P_h = 0.3\gamma\ (0.5H_t + H_p)$ Loose
	Weak and coherent		8. Squeezing, moderate depth		1.1C to 2.1C		Heavy side pressure. Continuous support required.
			9. Squeezing, great depth		2.1C to 4.5C		
			10. Swelling		up to 250'		Use circular support. In extreme cases: yielding support

Notes: 1) For rock classes 4, 5, 6, 7, when above ground water level, reduce loads by 50%.
2) For sands (7), H_{pmin} is for small movements (-0.01 C to 0.02C) H_{pmax} for large width movements (-0.15 C).
3) B is tunnel width, C = B + H_t = width + height of tunnel (in feet). For circular tunnel, C = 2B = 2H_t
4) γ = density of medium, lbs/ft^3.

Table 3-3, Sheet 1. Support Recommendations for Tunnels in Rock (20-ft. to 40-ft. diameter) Based on RQD
(From Deere, et al[28])

Rock Quality	Tunneling Method	Alternative Support Systems		
		Steel Sets[2]	Rock Bolts[3]	Shotcrete
EXCELLENT[1]				
RQD > 90	A. Boring Machine	None to occ. light set. Rock load (0.0-0.2)B.	None to occasional	None to occ. local application
	B. Conventional	None to occ. light set. Rock load (0.0-0.3)B.	None to occasional	None to occ. local application 2 in. to 3 in.
GOOD[1]				
75 < RQD < 90	A. Boring Machine	Occ. light sets to pattern on 5-ft to 6-ft ctr. Rock load (0.0 to 0.4)B.	Occasional to pattern on 5-ft to 6-ft centers	None to occ. local application 2 in. to 3 in.
	B. Conventional	Light sets, 5-ft to 6-ft ctr. Rock load (0.3 to 0.6)B.	Pattern, 5-ft to 6-ft centers	Occ. local application 2 in. to 3 in.

Table 3-3, Sheet 2. Support Recommendations for Tunnels in Rock (20-ft. to 40-ft. diameter) Based on RQD
(From Deere, et al[28])

Rock Quality	Tunneling Method	Alternative Support Systems		
		Steel Sets[2]	Rock Bolts[3]	Shotcrete
FAIR				
50 < RQD < 75	A. Boring Machine	Light to medium sets, 5-ft to 6-ft ctr. Rock load (0.4-1.0)B.	Pattern, 4-ft to 6-ft ctr.	2 in. to 4 in. on crown
	B. Conventional	Light to medium sets, 4-ft to 5-ft ctr. Rock load (0.6-1.3)B.	Pattern 3-ft to 5-ft ctr.	4 in. or more crown and sides
POOR[2]				
25 < RQD < 50	A. Boring Machine	Medium circular sets on 3-ft to 4-ft ctr. Rock load (1.0-1.6)B.	Pattern, 3-ft to 5-ft ctr.	4 in. to 6 in. on crown and sides. Combine with bolts.
	B. Conventional	Medium to heavy sets on 2-ft to 4-ft ctr. Rock load (1.3-2.0)B.	Pattern, 2-ft to 4-ft ctr.	6 in. or more on crown and sides. Combine with bolts.

Table 3-3, Sheet 3. Support Recommendations for Tunnels in Rock (20-ft. to 40-ft. diameter) Based on RQD (From Deere, et al[26])

Rock Quality	Tunneling Method	Alternative Support Systems		
		Steel Sets[2]	Rock Bolts[3]	Shotcrete
VERY POOR[3]				
RQD < 25 (Excluding squeezing or swelling ground.)	A. Boring Machine	Medium to heavy circular sets on 2-ft ctr. Rock load (1.6 to 2.2)B.	Pattern, 2-ft to 4-ft ctr.	6 in. or more on whole section. Combine with medium sets.
	B. Conventional	Heavy circular sets on 2-ft ctr. Rock load (2.0 to 2.8)B.	Pattern, 3-ft center.	6 in. or more on whole section. Combine with medium to heavy sets.
VERY POOR[4]				
(Squeezing or swelling.)	A. Boring Machine	Very heavy circular sets on 2-ft ctr. Rock load up to 250-ft.	Pattern, 2-ft to 3-ft ctr.	6 in. or more on whole section. Combine with heavy sets.
	B. Conventional	Very heavy circular sets on 2-ft ctr. Rock load up to 250-ft.	Pattern, 2-ft to 3-ft ctr.	6 in. or more on whole section. Combine with heavy sets.

Notes:
1) In good and excellent quality rock, the support requirement will be, in general, minimal but will be dependent upon joint geometry, tunnel diameter, and relative orientations of joints and tunnel.
2) Lagging requirements will usually be zero in excellent rock and will range from up to 25% in good rock to 100% in very poor rock.
3) Mesh requirements usually will be zero in excellent rock and will range from occasional mesh (or straps) in good rock to 100% mesh in very poor rock.
4) B = tunnel width.

(f) Wet tunneling conditions do not affect the strength of steel supports. However, when using timber in wet conditions, it is recommended that the allowable unit stress be reduced by 30 percent (U.S.D.A.[62]).

(g) Less excavation is required with steel supports since they require less space than wood and can be incorporated in the final lining.

(2) Steel ribs for ground support are usually fabricated from wide flange structural steel beams. A rough rule of thumb is that 1 inch of rib depth is required for each 3 feet of tunnel diameter (nominal diameter of excavated section), (Woodruff[67], Vol. 2, p. 391). Table 3-4 shows structural shapes commonly used in various sized tunnels.

Table 3-4. Structural Shapes Commonly Used In Tunneling
(After Woodruff[67])

Excavated Nominal Diameter	Structural Shape Commonly Used
Up to 8'	S4 x 7.7
8' to 14'	W4 x 13
14' to 20'	W6 x 20
above 20'	W8 x 31
Large diameter or heavy ground	W10 shapes or larger

(3) Since tunnel design is based largely on successful experience, it is desirable that the designer of steel supports does not depart too far from practices which have been successfully used in the past; therefore, new designs should be compared to the guidance given in Table 3-4. To further aid in comparing a new support system design to existing successful systems, the charts shown in Appendix F have been compiled based on projects constructed for the most part by the Corps of Engineers. The charts include brief geologic descriptions of the rocks encountered, the finished tunnel diameter and other pertinent details. Rough bore diameter can be obtained by adding the liner thickness to the finished tunnel diameter. The design of a support system is affected mostly by variations in rock type and diameter of opening. Because only limited information is available, no measure of the performance of the supports (whether barely adequate, ample or excessive) is given. Also, in many cases information on the rock quality is not available. The charts should be especially helpful when preparing preliminary estimates or design memoranda.

(4) The ... essentially ... that follows on steel set support design is ... reference should ... Proctor and White[47]. Chapters 9 and 10 of that ... consulted if a more detailed discussion is desired.

b. Load ... estimated by ... In steel set support design, the rock load ... the set (rib) ... discussed in paragraph 3-3 is transferred to ... sent the locati... of spaced blocking points. The points repre- ... the outside of ... blocks which are inserted between the rock and ... ing distributio... during erection in the tunnel. The assumed load- ... load due to the ... shown at the left side of Figure 3-1 where the ... acts vertically ... of a uniform height (H in the figure) of rock ... represent the ro... full width of the tunnel. The shaded areas ... are shaded with ... produces this loading. Individual areas which ... rock which is a... of vertical or horizontal lines represent the ... The uniform loa... load the set at individual blocking points. ... although rock f... sion is considered to be satisfactory for design, ... leaves a void a... unsupported tunnels is not uniform but instead ... "U." It can be ... tunnel ususlly shaped like an inverted "Y" or a ... active rock forc... that the maximum thrust induced in the rib by the ... against the rock ... one blocking point will cause the rib to press ... the active rock ... other blocking points with a force greater than ... mobilized by the ... those points. Sufficient passive force is then ... ing point to rest... combine with the active rock force at each block- ... The rib is there... rib pressure and reach a state of equilibrium. ... that causes maxi... proportioned for the single concentrated rock load ... external radial ... thrust. Figures 3-1 and 3-2 illustrate that ... with active rock ... consisting of passive resistance forces combined ... ing points for d... can be considered equal at corresponding block- ... load the sets. ... quantities and configurations of rock acting to ... when a uniform l... external forces on the set can be the same ... is assumed, the ... assumed or when a triangular or oblique loading ... associated with t... stresses must also be the same. Any errors ... uniform load assu... which are not considered significant and the ... should be sufficiently valid for design.

c. Forces ... is continuous, be... Bending Stresses in Blocked Ribs. Unless blocking on a rib ... reduce the load c... stresses as well as thrusts are induced which ... as the square of t... capacity of the rib. The bending moment varies ... first made of one... blocking point spacing. In design, a layout is ... to the crown joint... of a rib set. Blocking points are required close ... the arch and leg... with one at the spring line or the junction between ... spaced. The bendi... intermediate blocking points are assumed equally ... straight line betw... moment is determined by the rise in arc from a ... radius of the rib. ... blocking points, and is thus dependent on the ... ... these reasons there is no set blocking pattern ... ... all ribs. However, a blocking spacing of 2 feet ... ... minimum and 5 feet 6 inches a maximum. A block- ... ... commonly used on tunnels with a radius of from

(4) The discussion that follows on steel set support design is essentially taken from Procter and White[7]. Chapters 9 and 10 of that reference should be consulted if a more detailed discussion is desired.

b. Load Assumptions. In steel set support design, the rock load estimated by the procedures discussed in paragraph 3-3 is transferred to the set (rib) at a number of spaced blocking points. The points represent the location of wood blocks which are inserted between the rock and the outside of the set during erection in the tunnel. The assumed loading distribution is as shown at the left side of Figure 3-1 where the load due to the weight of a uniform height (H_1 in the figure) of rock acts vertically over the full width of the tunnel. The shaded areas represent the rock which produces this loading. Individual areas which are shaded with the use of vertical or horizontal lines represent the rock which is assumed to load the set at individual blocking points. The uniform load assumption is considered to be satisfactory for design, although rock failure in unsupported tunnels is not uniform but instead leaves a void above the tunnel usually shaped like an inverted "V" or a "U." It can be shown that the maximum thrust induced in the rib by the active rock force at any one blocking point will cause the rib to press against the rock at all other blocking points with a force greater than the active rock force at those points. Sufficient passive force is then mobilized by the rock to combine with the active rock force at each blocking point to resist the rib pressure and reach a state of equilibrium. The rib is therefore proportioned for the single concentrated rock load that causes maximum rib thrust. Figures 3-1 and 3-2 illustrate that external radial forces (consisting of passive resistance forces combined with active rock forces) can be considered equal at corresponding blocking points for different quantities and configurations of rock acting to load the sets. Since the external forces on the set can be the same when a uniform load is assumed or when a triangular or oblique loading is assumed, the internal stresses must also be the same. Any errors associated with this approach are not considered significant and the uniform load assumption should be sufficiently valid for design.

c. Forces and Stresses in Blocked Ribs. Unless blocking on a rib is continuous, bending stresses as well as thrusts are induced which reduce the load carrying capacity of the rib. The bending moment varies as the square of the blocking point spacing. In design, a layout is first made of one-half of a rib set. Blocking points are required close to the crown joint with one at the spring line or the junction between the arch and leg. The intermediate blocking points are assumed equally spaced. The bending moment is determined by the rise in arc from a straight line between the blocking points, and is thus dependent on the radius of the rib. For these reasons, there is no set blocking pattern that should be used for all ribs. However, a blocking spacing of 2 feet should be considered a minimum and 5 feet 6 inches a maximum. A blocking spacing of 4 feet is commonly used on tunnels with a radius of from

330

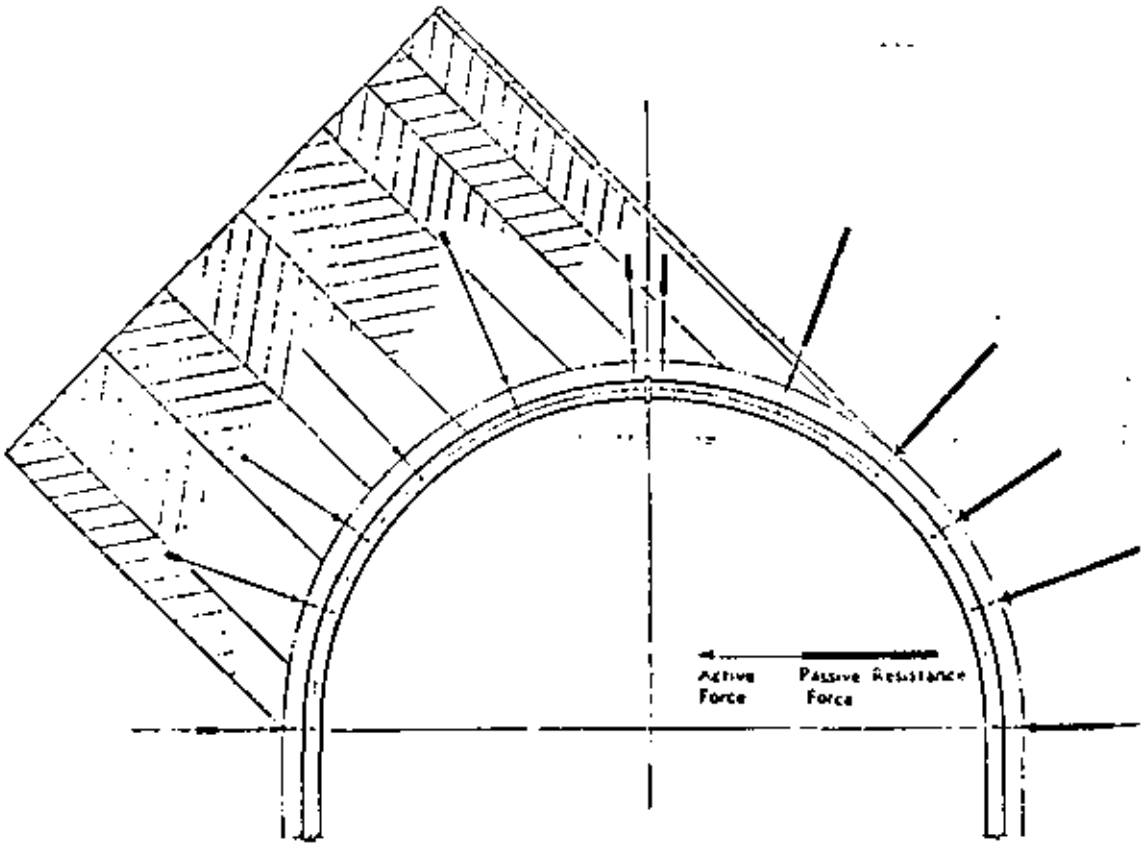

(From Proctor and White[47])

Figure 3-2. Oblique load assumption. When loads act obliquely, they set up forces at the blocking points in the same manner as uniform vertical loads. The figure shows an assumption wherein the load is acting at 45° to the vertical. Such a condition might occur where the strata are inclined steeply or where a fault occurs at one side of the roof. Total forces set up at the blocking points are the same as for the uniform load assumption shown in Figure 3-1.

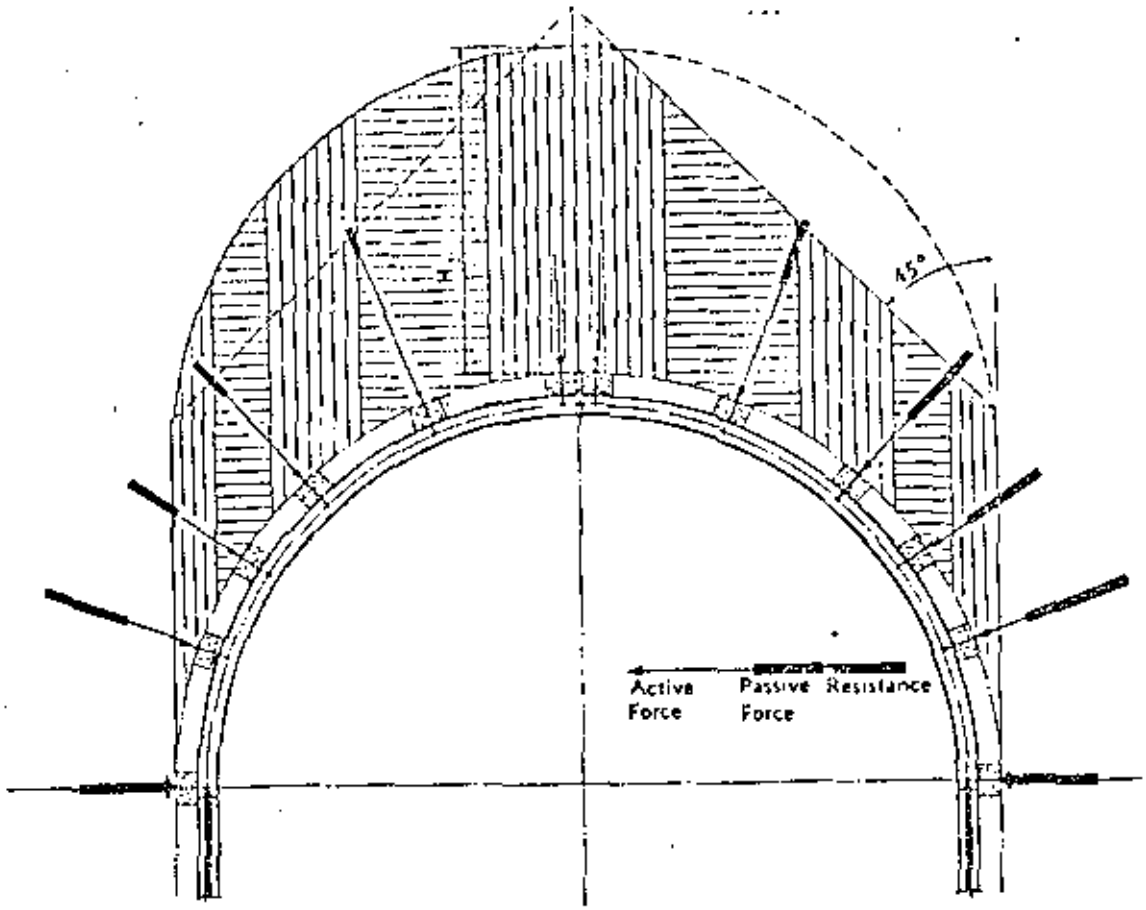

(From Proctor and White[47])

Figure 3-1. The total combined active and passive forces at corresponding blocking points are the same in each loading assumption.

7 to 14 feet. Blocking points are very rarely placed in the same location in the field as shown on drawings. Irregularities are usually present in the excavated surface and blocking points are located where a suitable rock surface is available. Figure J-4 shows how blocking is sometimes done under field conditions. The design spacing should be the maximum spacing of the blocks. The effect on rib stress due to changes in the blocking point spacing is shown in Figure 3-3. The cost of labor and materials should be considered when designing blocking. The more blocks installed the more the cost. A contractor will usually block rock that looks loose but has a tendency to leave out blocks whose need is not so apparent, although the maximum spacing is critical to the design. A maximum spacing should therefore be specified in the contract documents.

d. Loads to Ribs. Each blocking point transfers part of the rock load to each rib. The load is assumed equal to a volume of rock that would be inside vertical planes extending upward from midway between blocking points and successive ribs. Vertical height would be equal to the load assumed using Table 3-1. Little or no shear is transmitted through the blocking points to the rib. Therefore, it can be assumed that the blocking points form a pinned connection (Figure 3-4) and that the loads are transmitted normal to the axis of the rib. When the ribs are installed, the rock is self supporting, either because its stand-up time has not been exceeded or because it has been reinforced with rock bolts or shotcrete. Wedging of the blocks then prestresses the rib and develops a passive force in the rock, normal to the center line of the rib (Figure 3-5a). As the vertical active rock load begins to act on the rib, the line of action of the passive force in the rock rotates until equilibrium is reached (Figure 3-5b and c). With additional increases in rock load, this line of action passes the horizontal and ultimately becomes parallel to the tangent of the rib at that point (Figure 3-5d). Further increases in rock load cause the blocking point to move slightly inward as the rib deflects while mobilizing a great enough force to establish equilibrium (Figure 3-5e). Figure 3-6a and 3-6b show that the magnitude of the force exerted by the rib is maximum or minimum (with the same active rock load) when the direction of the passive rock force is assumed as horizontal or as parallel to the tangent to the overbreak line at the blocking point, respectively. However, it is assumed that the passive rock force can rotate until it becomes parallel to the tangent at a blocking point only if the blocking points are less than 25 degrees from a vertical line. This is based on the arbitrary assumption that friction of the rock cannot supply a passive force whose direction is more than 25 degrees from the horizontal (Figure 3-6c).

e. Stresses in Ribs. The stresses in the ribs are caused by the loads applied at the blocking points. These loads are resisted by the thrusts in the rib. The thrusts can be determined by means of a force polygon (see Appendix G for examples). The total load applied to each leg is approximately equal to the radius of the rib times the rock load

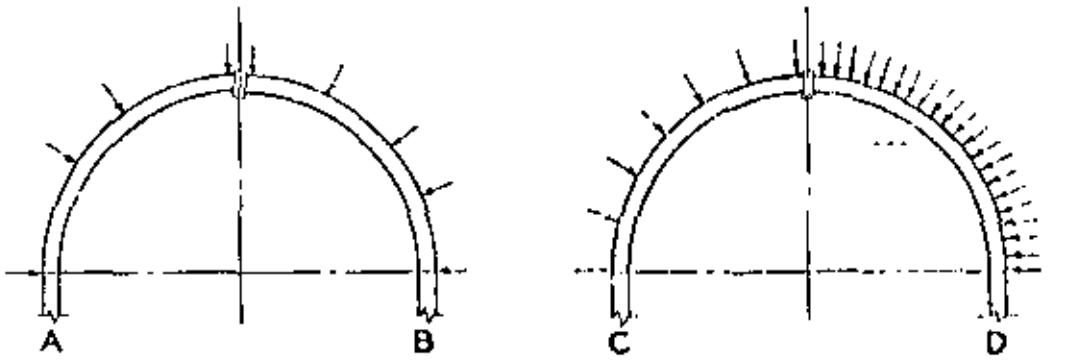

(From Proctor and White[47])

Figure 3-3. Effect on rib stress of changes in blocking point spacing.

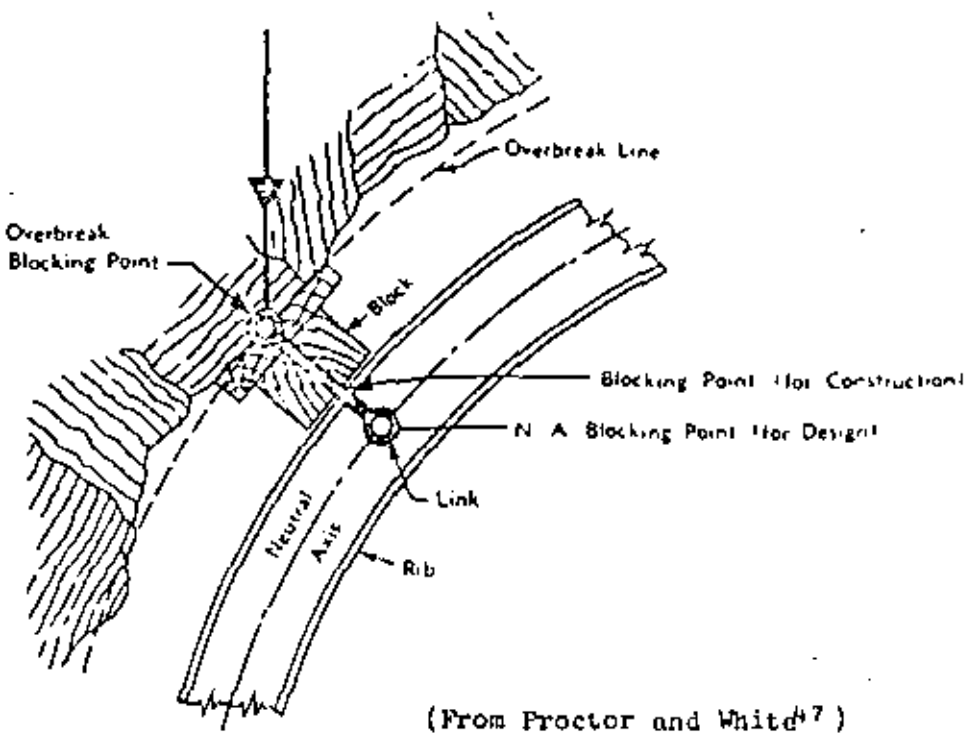

(From Proctor and White[47])

Figure 3-4. Transfer of force from rock to rib. Every block is considered to be a link as it has very little resistance to shear deformation. Forces are considered to be applied in a direction normal to the tangent of the rib at the neutral axis.

The active force F_r exerted by the prestressed rib is met by an equal and opposite passive force F_p induced in the rock.

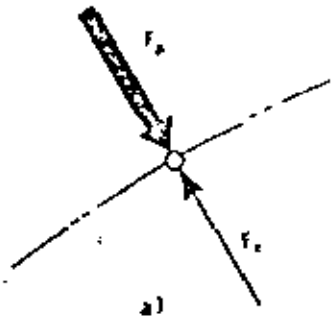

The rock begins to develop weight. It exerts an active vertical force W on to the block. The resultant of the two active forces W and F_r induces an equal and opposite passive force F_p.

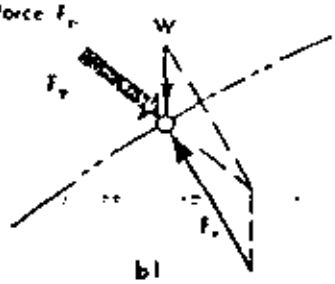

The active rock force W increases. Since the resultant of W and F_r induces an equal and opposite passive force, F_p, the magnitude of F_p changes and its direction passes through the horizontal.

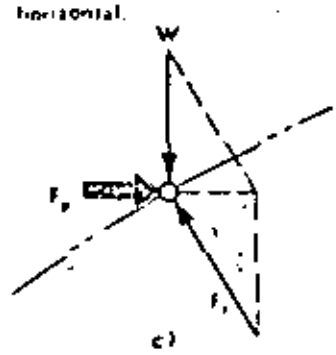

With increasing active rock force W, the direction of F_p ultimately becomes parallel to the tangent. This is as far as it can rotate as the rock cannot supply a force whose line of action lies outside the rock.

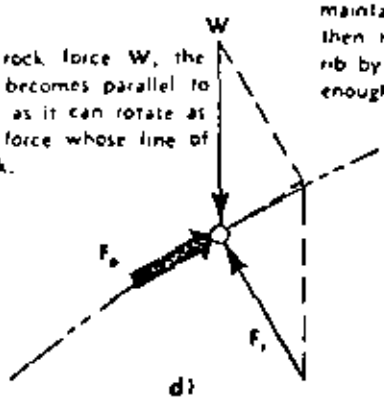

With further increases of the active rock force W and the direction of passive force F_p fixed, F_r is not of sufficient magnitude to maintain the equilibrium. The blocking point then moves slightly toward the rib until the rib by deflecting slightly can mobilize a great enough Force F_r to establish equilibrium.

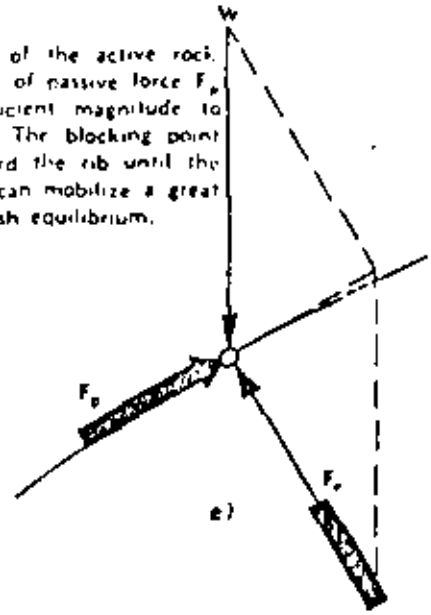

(From Proctor and White[47])

Figure 3-5. Forces acting at overbreak blocking point.

applied to the rib per unit of horizontal projection. Where the rib is bent to more than one radius, the maximum combination of radii and load per unit of horizontal projection will approximately be equal to the thrust. When active rock loads are not sufficient to close the force polygon, passive resistance will be developed to maintain equilibrium and close the polygon (Figure 3-7). Bending moments and deflections in the ribs are discussed below:

(1) If the steel set consists of curved segments which are pin-connected at the blocking points, the bending moment in the rib would be zero at the blocking points. The moment in the segment would be at maximum value midway between successive blocking points and be equal to the product of the thrust (T) and the rise (h) of the arc.

$$M_t = Th \qquad (3\text{-}1)$$

Since the ribs are continuous over several blocking points, there is a moment (M_b) at the blocking points which acts counter to M_t. The maximum moment midway between blocking points then becomes:

$$M_m = M_t - M_b \qquad (3\text{-}2)$$

The bending moments in Equation 3-2 may be computed by the theory of curved bars. The distribution of moments over the full arch is similar to that over a uniform continuous beam. If the rib is continuous, fixed at both ends and bears against equally spaced blocking points, the maximum bending moment occurs at each blocking point and is approximately

$$M_{max} = M_b = 0.67\ M_t = 0.67\ Th \qquad (3\text{-}3)$$

If the rib is hinged, the maximum moment is at the blocking point nearest the hinge and is approximately equal to

$$M_{max} = M_b = 0.86\ M_t = 0.86\ Th \qquad (3\text{-}4)$$

These equations are also valid approximations if the space between intermediate blocking points is less than that between a hinge and adjacent blocking point. The maximum fiber stress in a curved portion of the rib is then equal to the sum of the compressive stresses due to thrust and bending.

(2) The straight leg of a continuous rib represents a slender column acted upon by the arch thrust and bending moment at the spring lines. The moment at the spring line, due to continuity of the leg with the arch portion, may be approximated by

$$M_2 = 0.67\ M_t \qquad (3\text{-}5)$$

The moment is maximum at the top, decreasing uniformly to zero at the foot. This bending moment causes the leg to deflect toward the middle of the

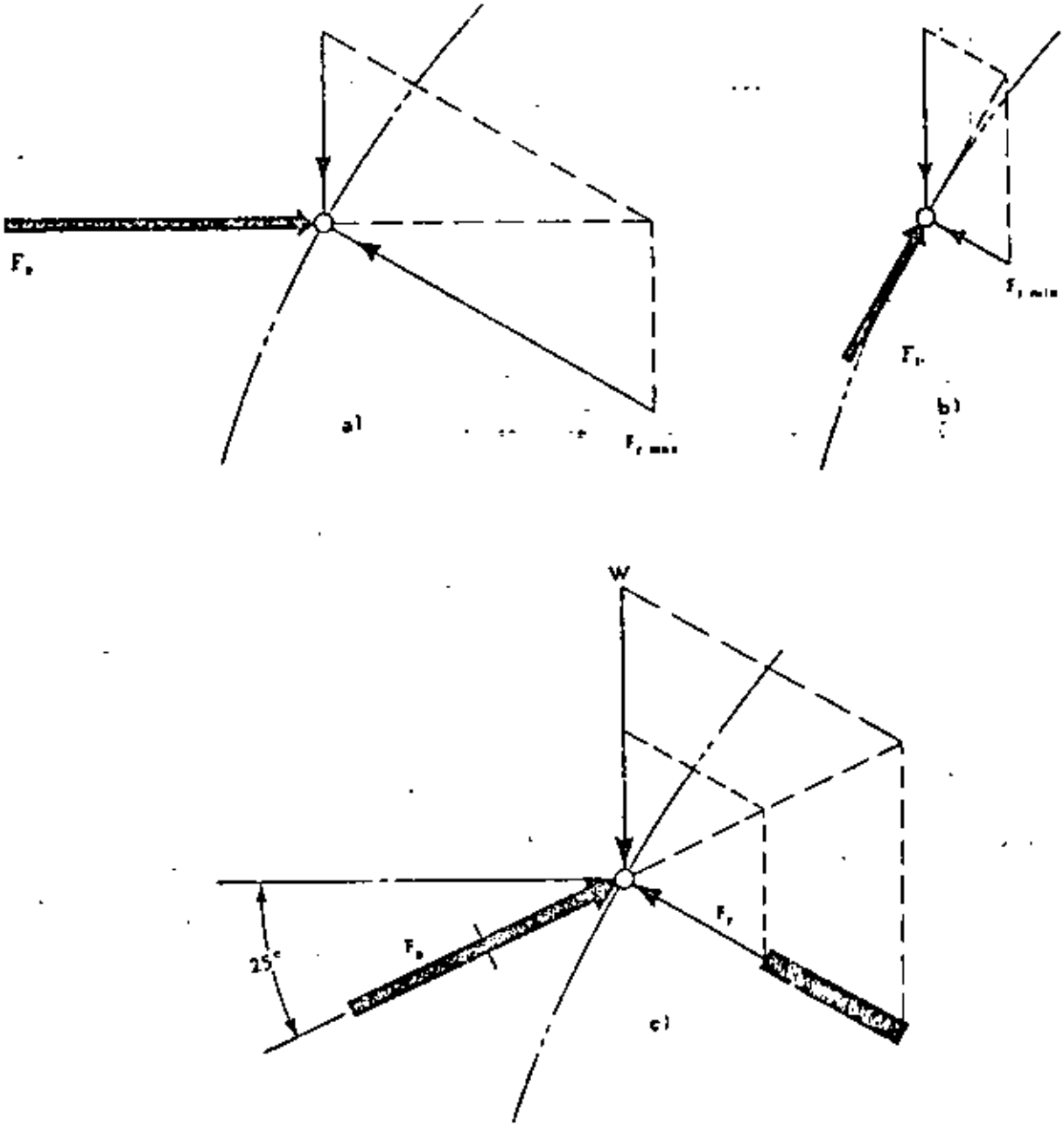

(From Proctor and White[47])

Figure 3-6. Limits to directions of forces acting at overbreak blocking point. It is assumed that because of friction, the rock can supply a force F_p whose direction is not more than 25° from the horizontal.

tunnel a distance d_1 as shown in Figure 3-8. The point of maximum deflection occurs at 0.422 ℓ below the top of the leg where ℓ is equal to the length of the leg. The leg is also loaded by the thrust from the arch. This force causes axial compression and also an additional moment since the leg is already deflected due to the moment M_2. The resulting increase in deflection from d_1 to d_2 is usually quite small with the length of legs encountered in tunneling. The increase in bending moment is only about 3 percent. The maximum deflection occurs somewhere between 0.422 ℓ and 0.5 ℓ below the top of the leg. The total bending moment at this point is:

$M_c = (1.0 - a) \times 0.67\ M_t + Td_2$, where the value of a ranges between 0.422 and 0.5.

$M_t = Th$. If a is set equal to 0.422, then:

$$M_c = 0.38\ Th + Td_2 \qquad (3\text{-}6)$$

At the upper end of the leg, the moment is equal 0.67 Th. For the lengths of legs usually encountered in tunnels, $0.38\ h + d_2$ is less than 0.67 h. The moment in the leg is less than for the arch rib, therefore, the arch portion governs the design. This analysis does not consider blocking on the straight leg and no blocking should be allowed on the leg unless an invert strut is used. The computations for the stresses in a straight leg are shown in Example No. 3, Appendix C. If side pressure is encountered, the addition of an invert strut or use of full circle ribs should be considered. For details of ribs, see Figures 4, 5 and 6 of Appendix G and Plates 14 and 15 of Appendix I.

f. Yielding Arches. The yielding arch is composed of a channel having a special U or W-shaped cross section. The ends of the segments overlap and are held together by using U-bolt clamps. The yielding arches are used to control deformations of tunnel walls. By allowing deformations to occur, the loading on the ribs will be smaller than if deformations were not allowed. Deere, et al[28] state that "Conditions that would appear to benefit most from the use of yielding arches are swelling, squeezing or broken or disturbed ground where large displacements are expected and can be tolerated prior to stability." Yielding arches have had very little application on Corps of Engineers projects, therefore associated detailed design procedures will not be covered in this manual. Should additional information on yieldable arches be desired, Woodruff[67] covers this subject in Chapter 4 of Volume No. 2.

3-5. Design of Rock Reinforcement Systems.

a. Terminology. The term "rock reinforcement" refers to the placement of rock bolts, rock anchors, or tendons at a fairly uniform spacing to consolidate the rock and reinforce the rock's natural tendency to support itself. As a result of long established usage, the term "rock support" also refers to the placement of rock reinforcement as well as to shotcrete, steel and wood set supports, or concrete lining. When

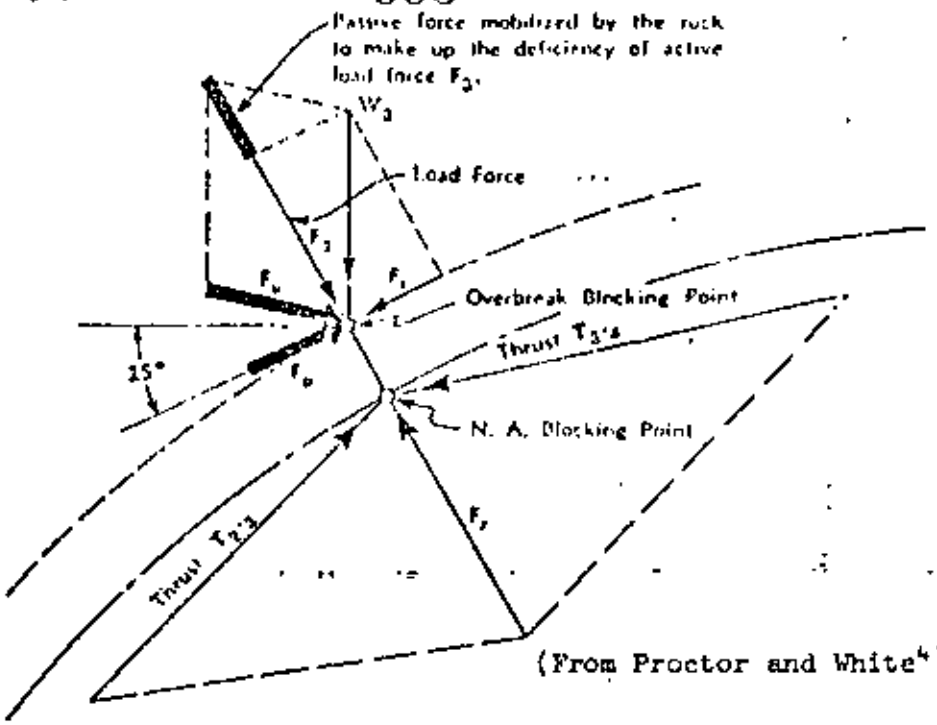

Figure 3-7. Action of forces at blocking point 3. The rib force F_r is the resultant of the two thrust forces T. It is transmitted radially by the block to the rock where it is met by the active load force F. This in turn is the radial component of the active vertical load force W. If F is less than the rib force F_r, the rock mobilizes additional passive force by changing the direction and magnitude of passive force Fp so that the resultant of F_p and W is equal to F_r.

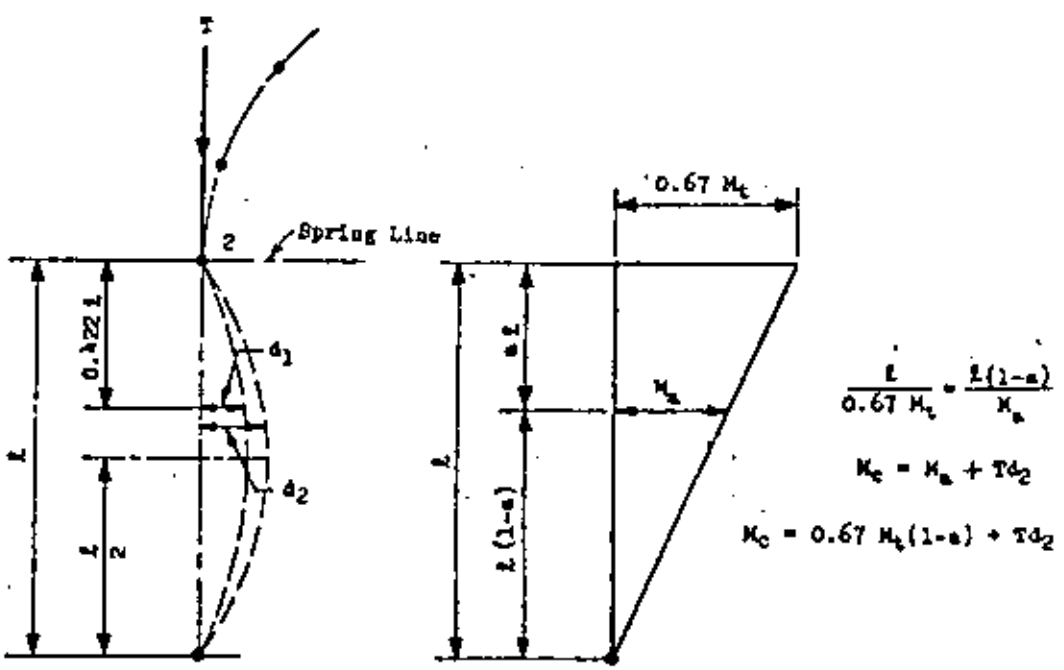

Figure 3-8. Deflection and moment in leg.

used in its narrower sense, however, the term "rock support" refers only to internal support systems (such as set supports or concrete lining) which provide support only after rock movement, loosening of rock blocks, or rock failure occurs. Other terms related to rock reinforcement on civil engineering projects are defined below.

(1) Element. This is a general term for rock bolts, tendons and rock anchors.

(2) Rock Bolt. A rock bolt is a tensioned reinforcement element consisting of a rod, a mechanical or grouted anchorage, and a plate and nut for tensioning by torquing the nut or for retaining tension applied by direct pull.

(3) Rock Anchor. A rock anchor is an untensioned reinforcement element consisting of a rod embedded in a mortar or grout filled hole.

(4) Rock Dowel. This is synonymous with rock anchor.

(5) Recessed Rock Anchor. This is a rock anchor placed to reinforce the rock behind the final excavation line after a portion of the tunnel cross-section is excavated but prior to excavating to the final line.

(6) Prestressed Rock Anchor or Tendon. These are tensioned reinforcing elements, generally of higher capacity than a rock bolt, consisting of a high strength steel tendon (made up of one or more wires, strands or bars) fitted with a stressing anchorage at one end and a means permitting force transfer to the grout and rock at the other end.

(7) Pattern Reinforcement or Pattern Bolting. This refers to the installation of reinforcement elements in a regular pattern over the excavation surface.

(8) Spot Reinforcement or Spot Bolting. This refers to the installation of reinforcement elements in localized areas of instability or weakness as determined during excavation. Spot reinforcement may be in addition to pattern reinforcement or internal support systems.

b. General. The first use of rock reinforcement in civil engineering tunnels took place in the early 1950's. As a result of favorable experience on projects since then and due to improvements in design and construction procedures, rock reinforcement is now accepted as an alternate or partial alternate to other support systems. In its various forms, rock reinforcement is in common use on projects with open cuts, portals, tunnels, shafts, and large chambers as well as for stabilizing existing slopes and strengthening weak foundation rock. Some form of surface treatment in the form of wire mesh, chain link fabric, mine ties, steel strapping or shotcrete is considered as part of the reinforcement, particularly in closely jointed rock. Surface

treatment is required to restrain rock loosened to shallow depths and prevent further loosening at greater depths which could lead to local or general fallout of rock. Rock reinforcement is commonly used as initial support, either alone or in conjunction with shotcrete or steel sets. If the function of the tunnel and the rock quality permits, rock reinforcement is used as sole support, particularly in larger tunnels or underground chambers. Rock reinforcement is more appropriate for use in better quality rock, but can also be used in poor to fair rock if protection against falling rock is provided for workers installing the reinforcement. Although economics play an important part in the support system selection process, the following advantages of rock reinforcement over other support systems should be considered during the selection process.

(1) An immediate compressive force or restraint is applied to the rock which reduces deformation and results in early stabilization of the rock mass around the opening. Restraint to rock movement is applied where it is needed most, i.e., at depths in the rock where planes of weakness exist and where rock loosening first begins.

(2) Rock reinforcement is adaptable (as is shotcrete) to any configuration or size of tunnel whereas sets must be fabricated to fit a particular configuration. Also, the quantity of reinforcement can be readily varied to fit rock conditions.

(3) Less space is required and obstructions are less than with sets. This provides for greater maneuverability of tracked vehicles, provides for better lighting and ventilation, reduces susceptibility to damage as a result of blasting or movement of equipment, and may contribute to a reduction in opening size needed to achieve the necessary working clearances.

(4) Drilling operations for blasting can be carried out during placement of the reinforcement.

(5) In large tunnels or chambers, rock reinforcement may be installed after only a portion of the top heading width is excavated to strengthen the opening before excavating to the full width.

(6) Recessed reinforcement may be installed prior to reaching the final excavation line by first excavating a large pilot tunnel. This provides instant restraint at the time final enlargement is made.

(7) Rock ahead of the heading may be reinforced by angling grouted bars ahead of the face (similar to spiling) to provide support in badly fractured rock.

(8) Progressive rock loosening is minimized and rock blocks or wedges formed by intersecting joints are tied together by rock reinforcement. If concrete lining is needed, less load will be transmitted to the lining since the rock's competency to support itself has been improved.

c. Function of Rock Reinforcement.

(1) Rock reinforcement is intended to prevent progressive loosening of the jointed medium and thus upgrade the capability of the jointed medium to sustain load. Installation should therefore be made as soon as possible as the excavation advances to hold loosening to an absolute minimum. The benefit received from the reinforcing element is greatest if the major portion of the yield force in the element is developed to resist movements along discontinuities. The element must be ductile enough to absorb unavoidable movements without failure. With the possible exception of temporary safety bolting, all reinforcing elements must be permanently bonded to the rock by filling the voids around the bars and anchorages with grout or mortar. This provides positive bond between the bars and the rock necessary to control rock movement and provides the corrosion protection necessary for a permanent installation (except in an extremely corrosive environment where corrosion resistant steel bars may be required).

(2) The installation of chain link fabric over the surface of the rock is highly desirable to prevent the fall of shallow pieces of rock from surfaces between the rock bolts and to supplement the function of the reinforcing elements.

d. Tensioned Rock Bolts. The primary advantage of rock bolts over anchor bars is due to initial stress in the bar which acts to prevent rock loosening rather than to inhibit loosening. Where bolting is required, bolts should be installed and tensioned as soon as possible after excavation or as close as possible to a tunnel heading (within two to fifteen feet of the heading). Experience has shown that the specification of two-thirds to three-quarters of the yield load of the bolt assembly is a practical range for initial tension, if the rock will allow it. Direct pull tensioning with hydraulic devices or application of torque to the nut with impact wrenches may be used to tension bolts. Direct pull tensioning is more reliable and preferable. If torquing is used, effective lubrication of threads with a molybdenum disulfide base lubricant should be used to achieve effective tensioning under the applied torque. Bolts preferably should be retensioned at least once before grouting. Release of the tension on a bolt is poor practice and should be avoided unless special safety precautions are taken.

(1) Grouting of Bolts. In addition to providing corrosion protection, grouting prevents any progressive slippage of mechanical anchorage during blasting and provides dependable bond between the bar and the rock. The importance of bond and the elimination of anchorage slippage makes early grouting very desirable. Polyester resin grout or Portland cement grout mixes, which contain accelerators, may be used within the cycle of blasting operations to achieve appreciable bond strength before the grouted bolts experience the effects of blasting. The bearing plate at the rock surface should be placed on a quick-setting mortar pad. This provides a level bearing surface for the plate and seals the drill hole around the bolt.

(2) Anchorages. Until a reinforcing element has been fully grouted and the grout has set, the anchorage determines the percentage of total restraining force in the element available for resisting rock movement. It is therefore desirable to achieve anchorage strength in excess of the ultimate strength of the element. This is not always possible because anchor strengths vary considerably with the type of rock being reinforced and type of anchorage being used. Anchorages in general use are either of the mechanical type or grouted end type. The mechanical types make use of an expanding element that is forced against the walls of the borehole to deform the rock and to provide frictional resistance to pullout. Grouted end anchorages rely on a bonding medium between a portion of the reinforcing element and the rock to develop the desired anchorage strength. Types of rock bolt anchorages are discussed below.

(a) The most common bolt anchorages of the mechanical type are the slot and wedge type and the expansion shell type. The use of the slot and wedge type was once very common; but in recent years, most of the bolts used in this country in connection with civil engineering works are of the expansion shell type. With the wedge type, anchorage is obtained by inserting the wedge into the slotted end of the bolt and expanding the slot by driving the wedge against the end of the drill hole. Bolts with wedge type anchorage hold best in hard, sound rock. To assure good anchorage, the hole length must be accurately drilled to within one inch and heavy driving equipment is needed. The expansion shell type obtains anchorage by the action of a cone or wedge drawn through the shell to expand the shell against the sides of the hole. Application of torque to the bolt prior to tensioning is required to expand the shell; or, with some types, shell expansion and tensioning can be accomplished in one operation (either by direct pull or by applying torque to the bolt nut). Hole diameter is more critical than with the slot and wedge and should not be more than 1/16-inch larger than the shell diameter. The expansion shell type offers a great advantage in that the hole may be of any depth greater than the length of the bolt. The equipment used for setting the anchorage is portable. Another advantage is that expansion shell bolts are available with a hollow core or integral vent tube which facilitates pumping of neat cement grout. Shells hold best in hard rock, but special types have been developed for use in softer rocks.

(b) A grouted end anchorage consists simply of a deformed bar embedded in grout placed at the blind end of the drill hole. Length of embedment varies with type and condition of rock and can be determined by conducting pull tests. In hard rock, three feet of grout embedment will develop the breaking strength of a 1-inch diameter bar; four feet of embedment will develop the breaking strength of a 1-3/8-inch diameter bar. With Portland cement grouts, a set-up time of four to eight hours is necessary before the bar is tensioned. However, polyester grouts are available to develop sufficient strength within five to thirty minutes. Once the grout is set, the anchorage is subject to less creep than that experienced with mechanical anchorages. A grouted end anchorage is suitable for use in almost any rock type and holds well even in badly

fractured rock. The ultimate strength of commonly used reinforcing elements installed in down-holes can be developed by simply embedding the lower end of the element in grout placed by gravity flow at the bottom of the hole. For up-holes, special techniques and aids have been developed to keep the grout at the upper end of the hole. Several processes (some patented) using perforated sleeves, prepackaged resin cartridges, grout transfer tubes, and pressure grouting with pumps through small-diameter tubes are being used successfully. These are now also used in many down-hole installations. Two of the most commonly used methods are described below.

(c) One method of forming a grouted end anchorage utilizes perforated half sleeves to retain mortar at the desired location. The half-sleeves are packed with mortar, tied together, and the bar inserted through the sleeve to extrude the mortar through the perforations and completely fill the voids to provide continuous bond along the embedment length. Once the end anchorage is set, the bar can be tensioned and grouted full length by pumping neat cement grout through pre-placed plastic tubes (usually 1/4" inside diameter). The most recent developments in grouted anchorages have been in connection with the formulation and packaging of polyester resin grouts which develop ultimate element strengths within minutes of installation. If properly installed, these systems incorporate most of the characteristics considered desirable for rock reinforcement. In forming this type of anchorage, a predetermined amount of resin packaged in sausage-like cartridges is placed at the blind end of the hole. A deformed reinforcing bar is then inserted and spun through the cartridges to mix hardener and catalyst in the cartridges. Depending on the formulation selected, the bar can then be tensioned within five to thirty minutes. Full length grouting can also be accomplished at the time of tensioning by using a mix of cartridges. Fast-set resin is placed to develop the desired anchorage strength and slow-set resin is placed for the remainder of the bar which sets up after tensioning is complete.

(3) Bolts and Accessories. Steel bars used to connect the anchorage to the bearing plate at the collar of the hole are either smooth rods or deformed bars, solid or hollow (groutable), threaded one or both ends, or threaded one end and headed at the other, depending on the type of anchorage and the type of hardware at the collar. Specified minimum yield strengths of commonly used bars usually vary between 30,000 and 75,000 psi with tensile strengths ranging from 60,000 psi to 100,000 psi. A minimum elongation in 8-inch gage length of 8 percent is considered acceptable for the high strength steel ranging up to 17 percent minimum for the lower strength steel. Groutable types used with mechanical anchorages are manufactured to simplify the task of pumping liquid grout to completely fill the annulus around the rock bolt. These are either hollow-core deformed bars or smooth bars equipped with an integral grout/vent tube. Deformed bars are ordinarily used to form grouted end anchorages because a shorter bond length is

required than with smooth bars. For the resin anchor types, deformed bars or specially designed smooth bars must be used to achieve good mixing of the resin components. Specially-manufactured deformed bars with a continuous rolled-in pattern of thread-like deformations along its entire length are also available. The deformations serve as threads to fit specially supplied anchorage nuts which are tightened to hold a prestress load applied by direct pull. Types of bolts commercially available, along with other pertinent information, are shown in Table 3-5.

(a) Bearing Plate and Mortar Pad. Bearing plates are used to spread out and transfer the concentrated bolt load to the rock around the collar of the hole. The bearing capacity of the rock and the prestress load in the elements will govern the size of the bearing plate but 6" x 6" x 3/8" to 8" x 8" x 3/8" for 1" bars or 8" x 8" x 1/2" for 1-3/8" bars have been found satisfactory in hard rock. The bearing plate should be seated on a pad of quick-setting mortar to provide a uniform bearing surface and to adjust the angle of the plate with the bolt to a more normal position.

(b) Other Accessories. Bevel washers are used between the bearing plate and a hardened washer to create a uniform bearing surface for the nut as near normal as possible to the bolt axis. This combination, along with treatment of contact surfaces with a molybdenum disulfide base lubricant, will result in increased efficiency during the bolt tensioning operation. Other accessories include small diameter plastic grout tubes for pumping grout, perforated sleeves for retaining stiff grout in holes, couplings for splicing bars and a variety of other accessories which are described in manufacturer's catalogs.

e. Untensioned Reinforcement Elements. Fully grouted untensioned elements (rock anchors) behave much as grouted tensioned rock bolts do, except that an initial prestress is not applied to rock. Instead, forces in the bar to restrain further rock movement are developed in the bar as initial rock movements take place. This makes the earliest possible installation of anchor bars desirable. Anchoring through burden (installation of recessed rock anchors) that is to be removed by later blasting is a desirable application because the initial movements resulting from the removal of rock by blasting develop the force in the bars. Rock anchors are also highly desirable for use in soft rock or in highly fractured or sheared hard rock where point anchorages do not hold well. Critical points in the installation of rock anchors include the necessity of having the drill hole around the bar completely filled with grout and the use of quick setting grout. Deformed bars should be used in rock anchor installations. Full length grouting is accomplished by methods similar to those described for forming grouted end anchorages. Material and equipment which is generally used for grouting around reinforcement elements is listed in Table 3-6.

Table 3-5. Commercially Available Rock Bolts with Mechanical Anchorage

Manufacturer/ Distributor	Type of Anchorage	Bolt Sizes Available: Smooth Bar Headed Bolts	Threaded Bolts with Nuts: Solid Bar	Threaded Bolts with Nuts: Groutable	Remarks
Williams Form Engrg, Grand Rapids, MI	Expansion shell	---	1/2" to 2" in 1/8" increments	No. 8, No. 11 No. 16 (hollow, deformed)	Specializes in rock bolts for use in civil engineering works.
CF&I Steel Corporation Pueblo, CO	Expansion shell, "Pattin"	5/8" to 1"	5/8" to 1"	---	In Eastern US, shells supplied by Pattin Mfg. Co., Marietta, OH.
	Slot & wedge	---	1"	---	
Bethlehem Steel, Bethlehem, PA	Expansion shell	5/8" to 1"	---	---	
	Slot & wedge	---	1" to 2-1/2"	---	
Republic Steel, Cleveland, OH	Expansion shell	5/8" & 3/4"	---	---	
	Slot & wedge	---	1"	---	
Titan (M.M. McElvaine, Ltd. San Francisco, CA)	Expansion shell	5/8" & 3/4"	1"	No. 8 (hollow, deformed)	Not stocked in USA. Available thru Distributor from Australian manufacturer.
	Slot & wedge	---	1" to 2-1/4"	---	
Howlett (Fox Industries, Berkeley, CA)	Expansion shell (Bethlehem K-4)	---	---	1" (smooth bar)	Manufactured with grout/vent tube installed in groove along bolt.
Ohio Brass Co., Mansfield, OH	Expansion shell for 5/8" & 3/4" diameter bolts	---	---	---	Supplies shells only.
Birmingham Bolt Co., Birmingham, AL	"Cone" Expansion shell	---	---	---	For use in soft rock with 3/4" & 1" diameter bolts.

Table 3-6. Commercially Available Equipment and Materials for Installing Grouted Reinforcing Elements

Manufacturer	Item	Bonding Medium	Type and Size of Reinforcing Element Recommended
Sika Chemical Corp., Passaic, NJ	Perfo sleeves	Portland cement or gypsum mortar	Smooth or preferably deformed bars, 3/4" to 1-3/8" dia. (Nos. 6 to 11)
Robbins & Myers, Inc., Springfield, OH	Moyno grout pump	Neat cement or gypsum grout, chemical grouts	Smooth or deformed bars, all sizes.
Williams Form Engineering, Grand Rapids, MI	Williams grout pump	Neat cement or gypsum grout. Chemical grouts	Offered as part of Williams Groutable Rock bolt system. Can be used similar to Moyno pump.
Ranco Industrial Products, Cleveland, OH	Sulfa-Set, F-181	Neat gypsum grout or mortar.	Use with Perfo sleeves or grout pump and elements listed with each.
American Cyanamid Co., Wayne, NJ	ROC-LOC 540 Mining Kit	Polyester resin. Placed via transfer tube.	Any size deformed bar or threaded smooth bar.
Celtite, Inc., Cleveland, OH	Celtite System	Polyester resin. Prepackaged in cartridges.	Deformed bars, No. 6 through No. 11, No. 14.
Inland Ryerson, Melrose Park, IL	Dywidag Thread-Bar Rock Bolt	Celtite resin cartridges.	Dywidag high alloy deformed "threadbar." 5/8" dia. (230 ksi), 1", 1-1/4" 1-3/8" dia. (all 150 ksi).
Conmat, Inc., Allentown, PA	Celtite resin anchor system. Dywidag Thread-Bar Rock Bolts	Celtite resin cartridges.	Deformed bars, No. 6 through No. 11, No. 14. Dywidag Threadbar, 22 mm, Grade 60.
DuPont Company, Wilmington, DE, 19898	FASLOC resin anchored bolt system	Polyester resin prepackaged in cartridges.	Specially manufactured deformed bar headed bolt, 3/4" diameter.
Bethlehem Steel, Bethlehem, PA	Resin-anchor roof bolt.	Epoxy resin and stone aggregate in glass cartridges.	Specially manufactured smooth bar bolt with threaded ends. 5/8" to 1-1/4" diameter.

f. High Capacity Reinforcement Elements.

(a) Background and Function. During the last few years, high strength (25 to 1,100 kips) and long length tendons have been utilized extensively by various organizations to solve special rock reinforcement problems. Tendon systems appear to have good possibilities for increased usage when considering high capacity reinforcement systems. This type of reinforcement system is intended to function the same as rock bolts by applying a prestress load and restrain rock movements to upgrade the capacity of the jointed or layered medium to sustain load. These systems can also be used to anchor a structure to rock. Many times the above functions and others are combined simultaneously. The benefits received from the supporting element is greatest if the major portion of the yield force (approximately 70 percent) is developed, but the element must be ductile enough to absorb further unavoidable movements without failure.

(b) Anchorage and Installation. The anchorage of most high capacity reinforcement systems, regardless of the type of rock, is obtained by grouting a portion of the tendon or rock bolt. Field testing of the anchorage is almost mandatory. If both ends of the tendon or rock bolt can be made accessible, bearing plates can be used on both ends. The basic installation procedure involves drilling the hole, water pressure testing of holes to determine potential grout leakage through rock seams, consolidation grouting if necessary, placement of grout for obtaining anchorage, tensioning the element, and placement of secondary grout to fill the annular space over the stressing length. Usually, full bonding of tendons to the rock is desirable so that rock movements will be immediately resisted by the short length of tendon located on each side of planes of weakness where movement occurs. More specialized equipment and material are required to install tendon systems than are required for ordinary rock bolt systems.

g. Design Procedures. The design of rock reinforcement systems is based primarily on experience and emperical rules that establish the size, length, and spacing of reinforcement elements. A detailed discussion of rock reinforcement experience, concepts, installation procedures and design procedures is beyond the scope of this manual. However, emperical rules are given in Tables 3-7 and 3-8 which provide guidance for selecting size, length and spacing of reinforcing elements. Bar sizes of one-inch diameter and one and three-eighths inch diameter are in common use. Spacings normally range between three and six feet underground and up to ten feet on slopes. Cost savings can sometimes be made by varying the bar size and spacing to achieve the same average confinement on the rock provided other design requirements are met.

h. Anchorage Tests. During preliminary design stages, the results of past experience in similar rock types are useful for making preliminary estimates of anchorage strengths. However, anchorage

Table 3-7. Minimum Length and Maximum Spacing for Rock Reinforcement

Parameter	Empirical Rules	Notes
Minimum Length	Greatest of: a. Two times the bolt spacing b. Three times the width of critical and potentially unstable rock blocks c. For elements above the springline: 1. Spans less than 20 feet - one-half span 2. Spans from 60 feet to 100 feet - one-fourth span 3. Spans 20 feet to 60 feet - interpolate between 10 to 15 feet lengths respectively d. For elements below the springline: 1. For openings less than 60 feet high-use lengths as determined in c. above. 2. For openings greater than 60 feet high - one-fifth the height	
Maximum Spacing	Least of: a. One-half the bolt length b. One and one-half times the width of critical and potentially unstable rock blocks c. Six feet	Greater spacing than 6 feet would make attachment of surface treatment such as chain-link fabric difficult.

Table 3-8. Minimum Average Confining Pressure for Rock Reinforcement

Parameter	Empirical Rules	Notes
Minimum Average Confining Pressure at Yield Point of Elements	Greatest of: I. Above Springline — a. Pressure equal to a vertical rock load of 0.20 times the opening width	This assumes the elements will behave in a ductile manner. a. For example if the unit weight of the rock is 144 pounds per cubic foot and the opening span is 75 feet the internal confining pressure is 15 pounds per square inch.
	b. Six pounds per square inch	b. For the maximum spacing of 6 feet this requires a yield strength of approximately 32,000 pounds.
	II. Below Springline — a. Pressure equal to a vertical rock load of 0.1 times the opening height	a. For example if the unit weight of the rock is 160 pounds per cubic foot and the cavity height is 144 feet the required confining pressure is 16 pounds per square inch
	b. Six pounds per square inch	b. See note b. under I. above.
	III. At Intersections — a. Twice the confining pressure as determined above	a. This reinforcement should be installed from the first opening excavated prior to forming the intersection. Stress concentrations are generally higher at intersections, and rock blocks are free to move toward both openings.

strengths to provide design information must eventually be determined by conducting pull tests at the site. During construction, the specifications should also call for pull tests and for adjustments in installation procedures or material, if required. The test program should be carefully planned and as a minimum should provide data to answer the following questions.

(1) Is the rock capable of holding the anchorage?

(2) Which anchorage or combination of anchorages is best suited for the rock conditions?

(3) Will the installation procedure used assure efficient bolt installation of satisfactory and uniform strengths?

i. Instrumentation. Instrumentation should be planned at the time the rock reinforcement system is designed. Although a variety of rock mechanics instruments are available, the most useful measurements are usually those that give a good indication of rock deformation and movement. Instrumentation is most valuable for monitoring deformation or movement during construction to indicate variations from the assumptions made during design. In addition to providing information for making adjustments in the rock reinforcement system or in the excavation procedures, instrumentation provides data for the control of safety and stability during and after excavation.

j. Equivalence of Support Systems. Although highly desirable, procedures have not yet been developed for accurately assessing and evaluating the relative strengths of alternate support systems such as shotcrete, rock reinforcement and steel set supports. However, general strength relationships have been developed on the basis of experience and are shown in Table 3-3. Progress is also being made in developing empirical and analytical procedures for determining the equivalence of various support systems. These are discussed by Barton, Lien and Lunde[11,12] and Bischoff and Smart[14]

3-6. Shotcrete Support Design.

a. General.

(1) Shotcrete is defined by the American Concrete Institute as mortar or concrete conveyed through a hose and pneumatically projected at high velocity onto a surface. The force of the jet impinging on the surface compacts the material. A relatively dry mixture is generally used, and the material is capable of supporting itself without sagging or sloughing, even for vertical and overhead applications (ACI[4]).

(2) Shotcrete has been in use for more than 50 years for various types of construction. However, it has only recently been applied to tunnels and other underground support, following the development of

high volume equipment and accelerating admixtures which cause the concrete to set up very rapidly. The state-of-the-art is best described in the proceedings of an Engineering Foundation Conference (ACI[5]).

(3) The Europeans first used shotcrete for tunnel support. The first large application on this continent was the lining of the Vancouver railroad tunnel (Mason[43]). This was followed by the Washington, D.C. Metro System project (Bawa[13]) and others. Within the Corps of Engineers, the most noteworthy example has been the New Melones Dam in the South Pacific Division, Sacramento District (CE[26]).

(4) Shotcrete, applied immediately after excavation, seals and ties down the rock and provides a thin, strong, flexible membrane. It frequently speeds up the tunneling operation and may result in cost savings as compared with other tunnel support methods. It is best suited for tunnels excavated by drilling and blasting. Where appropriate, it should be listed as one of the bidding alternates.

(5) The basic design concepts of shotcrete tunnel support were developed mainly by Rabcevicz[48,49] and Rabcevicz and Colser[50]. Specific tunnel designs have been prepared by Alberts and Backstrom[7], Sutcliffe and McClure[57], Evans[33] and others. The geology and its relation to structural considerations have been further developed by Heuer[35] and Cording[21]. Like many other aspects of tunnel work, current design formulas for shotcrete linings are far from exact. The design should be tempered with judgment, taking into account the rapidly developing body of information from experience records.

(6) In Corps of Engineers tunnel construction, shotcrete will generally be used for initial support, prior to placing the permanent concrete lining. Occasionally, it may be used for final support as well. It is also frequently used essentially in a non-structural capacity to seal rock surfaces and to keep them from air slaking, while at the same time preventing fallouts.

b. Support in Various Types of Rock.

(1) Ground Conditions. There are three basic ground conditions for which shotcrete may be considered for support:

(a) In blocky hard rock, where there are loosening pressures in the crown but little or no side pressure.

(b) Where the opening is subjected to squeezing accompanied by large pressures in the crown and sidewalls, and sometimes by significant pressures in the invert.

(c) In swelling soils.

(2) In Hard, Blocky Rock. This is the most likely application of shotcrete in Corps of Engineers work. Alberts and Backstrom[7] offer the

following reasonable explanation of the behavior of shotcrete in this case, "A shotcrete support yields slightly during the first few hours; but while the loosening pressures increase, the shotcrete is gaining strength. A state of equilibrium is reached and a ground arch above the tunnel roof is developed. A thin shotcrete layer, a mere skin, applied immediately after blasting, can therefore transform a rock of minor strength into a stable mass. A shotcrete lining does not generally support loads by transferring them to the tunnel floor as steel ribs do; it helps the rock to carry itself." To assure a lining adequate against loosening pressures, the rock should generally have a stand-up time of at least 4 hours to permit the shotcrete to be applied and gain appreciable strength before any load is applied.

(3) Design of Shotcrete for Tunnel Support. The shotcrete section is designed as follows:

(a) To protect against crown fallouts where the rock would punch through the shotcrete, loadings are assumed as either equal to the weight of one or more loose rock blocks or as a uniform pressure over a certain width of the tunnel. The thickness of shotcrete must be such that the shear strength around the perimeter of the assumed areas is adequate to support the loading, as shown in Figure 3-9.

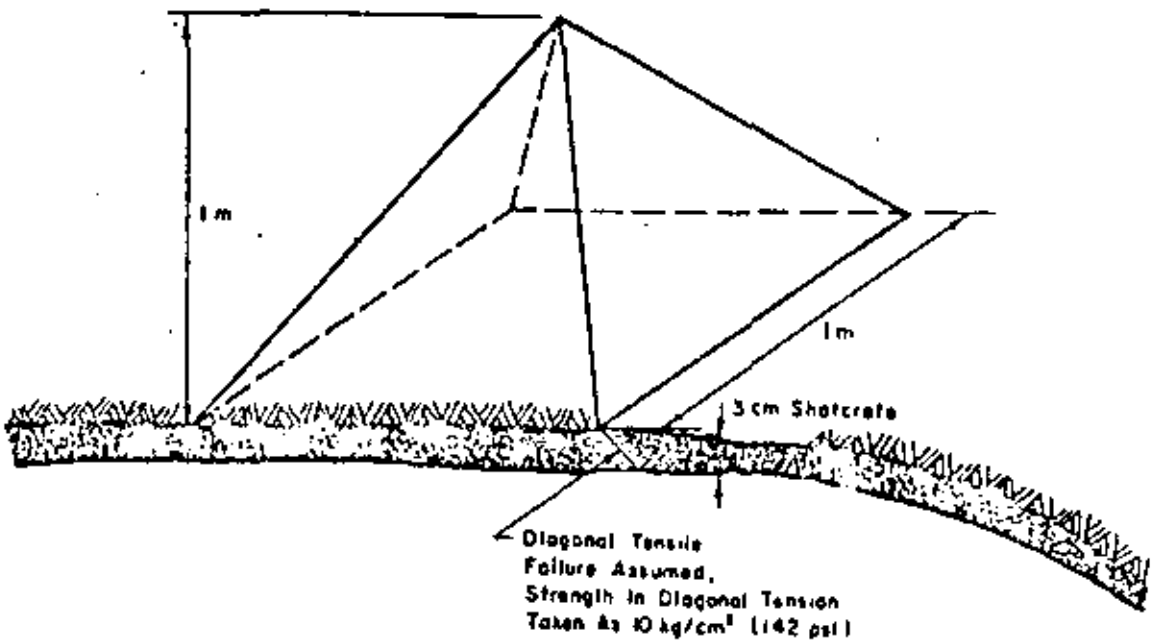

Weight of Pyramid = 900 kg
Shotcrete Resistance = 4 x 1 m x 3 cm x 10 kg/cm² = 12000 kg
Factor of Safety Against Fallout = $\frac{12000}{900}$ = 13

(From Deere, et al[28])

Figure 3-9. Resistance of a 3 centimeter-thick layer to roof fallout.

(b) The shotcrete section is also designed to support the rock loads given in Table 3-2. The values in this table are based on the assumption that the rock can loosen. When the rock is supported with shotcrete, this loosening is partially prevented and the loading will be somewhat less. Therefore, the values in the table are conservative. Nevertheless, they should be used where data on actual loads is not available (which is usually the case). Usually the resisting force is assumed to be the shotcrete-rock bond in a narrow band along the tunnel springline (Evans[33]).

(c) The design should also take into account previous experience with shotcrete tunnel linings. Experience has shown that the thickness of shotcrete should be at least 4 inches at the crown and 2 inches at the springline, then tapering to zero below the springline. Under unfavorable conditions (in large tunnels, in poor rock, and where the possibility of significant side pressures exist), minimum thicknesses should be at least 6 inches at the crown, 4 inches at the springline and tapering to zero near the invert.

(d) In squeezing rock, sidewall and invert (as well as crown) support are required. In this case, a complete ring of shotcrete should be used.

(e) Swelling soils impose large forces on tunnel linings, and the use of a thin shotcrete membrane is normally not recommended. If shotcrete is considered, a complete ring should be used and a most careful design prepared. "Pre-swelling" the soil and reinforcing the shotcrete have been tried with some success.

(4) Shotcrete Combined with Other Support Systems. There may be local areas of weaker rock where the shotcrete alone will not provide the needed carrying capacity. In such cases, rock bolts designed to take the additional load may be used. Rock bolts may also be used advantageously with shotcrete to limit deformation in swelling ground. Where steel sets are used in very weak rock, placement of shotcrete between the sets is sometimes advisable to give additional support, provide lateral stiffness to the sets, or to protect against fallout. The shotcrete thickness should be adequate to support the loads imposed, and should not be less than 2 inches.

(5) Use of Shotcrete as a Permanent Lining. In Corps of Engineers work, conventional concrete is generally preferable to shotcrete because it provides a larger safety factor against overloading, better hydraulic properties, and possibly better durability. However, shotcrete is attractive for certain applications, such as diversion tunnels and railroad tunnels. Where shotcrete is used for such structures, conservative loadings should be assumed and special attention should be given to drainage and the possibility of swelling ground.

(6) Use of Wire Mesh in Shotcrete Linings. The use of wire mesh in shotcrete linings is very controversial. Many designers feel it

adds conservatism to the design, and favor its use in permanent linings and other jobs where an additional safety factor is needed. However, it should be recognized that it is difficult to install mesh just back of the heading. Also, the vibration of the mesh resulting from coarse aggregate striking at a high velocity may adversely affect the quality of the placed shotcrete.

(7) Drainage. Drains should be provided to divert any running water which might prevent a good shotcrete application. Also, permanent drains should be used where necessary to prevent the buildup of large durability problems (especially where the lining is subject to freezing). It is usually impossible to predict in the design stage exactly where all drains will be needed. Therefore, provisions should be made for installing additional drains as the need arises during construction.

3-7. Permanent Tunnel Linings.

a. General.

(1) Permanent lining is provided in most tunnels to maintain the integrity of the section, to resist the residual rock load, to resist internal pressure, and to provide a smooth-surfaced conduit for hydraulic purposes. The character of the rock and the ultimate use of the tunnel will dictate the lining design. The thickness of the lining will be governed by the ultimate load it must carry and by construction requirements. The thickness of the lining at the crown should be sufficient to provide room for the concrete placing pipe. This will seldom be less than ten inches. Where thin lining is all that is required to carry the external loads, working room may be provided by excavating an enlargement or chase at the crown of the rock arch. In some cases, no lining at all may be required.

(2) Where tunnel linings are required, the design rock loading is generally based on experience and on the use of empirical guidelines described in paragraph 3-3. Limited field observations in tunnels have qualitatively demonstrated that increasing lining thickness can often be self-defeating in that it causes the lining to receive even greater load. In contrast, more flexible linings allow "arch action" of the ground to carry the load around the opening. In reality, the ground itself is the most effective load carrying member of the system; the function of the lining should be one of preserving the ground strength by resisting deformations to well below those values which would initiate progressive failure. However, in large openings or areas where the lateral stresses are small (usually when tunnels are located at shallow depths), the possibility of large blocks transmitting the load directly to the lining exists. In these cases, the lining thickness should be adequate to resist shear and movement stresses caused by this loading.

(3) Although not usually considered as a design loading, grouting operations can substantially stress the lining and should be closely controlled to avoid overstressing.

(4) Factors for consideration in designing tunnel linings include the type of ground, its time-dependent properties, and the extent to which its strength is reduced by the tunneling method employed (such as blast damage). Since previous experience is an important consideration, the data presented in Appendix F on existing tunnel linings can be used as a guide when designing concrete linings.

b. Concrete Lining Design.

(1) Principle Considerations. Concrete linings are placed to prevent the rock from ravelling and to support any additional loads which may develop after construction of the lining. Linings are also placed to provide smooth walls to reduce hydraulic friction. Loadings will develop from the elastic and creep properties of the rock, the stiffness of the lining, subsequent construction activities such as embankment placement over the tunnel area or nearby tunneling, and as a result of pressure from water sources. In some rock formations, no lining will be required. Where water velocity through a tunnel is greater than 8 to 10 feet per second, linings are required regardless of the rock type.

(2) Monolith Joints. The length of a tunnel monolith is normally based on the limitations of concrete placement procedures and equipment, including the practical length of form that can be handled economically. Monoliths have usually been placed in lengths of 20 to 40 feet with the expectation that shrinkage cracking will then be partially controlled. However, continuously placed lining may be satisfactory where leakage would not be objectionable or detrimental. Circumferential cracking in continuously placed lining can be expected to occur at approximately 10 foot intervals. Monolith joints are provided with waterstops whether or not longitudinal reinforcement is discontinuous at the joint.

(3) Water Load and Stress in Lining. Concrete linings are generally designed to resist external hydrostatic loads equal to the full ground water load or the head of the reservoir if the tunnel is to be subjected to reservoir pressure. It may not be practical to design to resist the full hydrostatic load if unreasonably thick linings are required to resist external pressures because of depth or size of tunnel. In this case, water pressure must be reduced by installing drains behind and through the lining or by constructing a separate drainage tunnel above the main tunnel. Linings can be classified as either thin or thick shells, depending on the ratio of lining thickness to the tunnel radius. Stress induced in a circular tunnel lining by hydrostatic water load can be determined as shown below. Compressive stress is considered as negative stress and tensile stress as positive stress.

(a) If the lining thickness is equal to or less than one-tenth the tunnel radius, the lining is treated as a thin shell. For thin shells (see Roark[54], Table XIII, Case 1),

$$f_c = \frac{-pR}{t} , \tag{3-7}$$

where f_c = stress in concrete lining, psi
p = external water pressure, psi
R = radius to circumferential centerline of lining, in
t = lining thickness, in

(b) If lining thickness is greater than one-tenth the tunnel radius, the lining is treated as a thick shell. For thick shells (see Roark[54], Table XIII, Case 3d),

$$f_c = \frac{-pR_2^2(R_1^2 + r^2)}{r^2(R_2^2 - R_1^2)} \tag{3-8}$$

where R_1 = radius to inner surface of lining, in
R_2 = radius to outer surface of lining, in
r = radius to point in lining under consideration, in

Hoop stress is maximum at the inner surface of a thick shell and is determined from:

$$f_c(\text{maximum}) = \frac{-2pR_2^2}{R_2^2 - R_1^2} \tag{3-9}$$

(4) Rock Load. The actual loads which will be transmitted by the rock to the lining cannot be exactly forecast. However, for the purpose of lining reinforcement design, an unbalanced vertical rock load of a magnitude ranging from one-half to one of the load used for designing steel set supports is recommended. If wood sets are used as initial support, then the design load for concrete lining should be equal to that used for the initial support design. When rock reinforcement, shotcrete or a combination of these systems are designed as initial support with sufficient strength to provide for long term stability, smaller loads will develop on concrete lining installed as final support. An unbalanced vertical rock load is therefore recommended whose value ranges from one-quarter to three-quarters of the design rock load estimated in accordance with procedures outlined in paragraph 3-3 for steel set supports. The amount of load reduction allowed must be based on careful evaluation of all geological investigation results and other data gathered prior to and during the design phase. Monitoring of rock movements and deformation during construction should be required to determine the adequacy of the initial support system prior to placing the concrete lining.

(5) Determination of Bending Moments for Design. This discussion is primarily limited to the design of concrete linings of circular cross-section, since this configuration is in common use on Corps of Engineers projects. Two methods of determining bending moments induced in the lining by an unbalanced vertical rock load are presented. The rock load will tend to deflect the lining to cause a shortening of diameter in the vertical direction and a lengthening in the horizontal direction. As the horizontal diameter increases, the rock is compressed and passive forces are developed in the rock to limit further deflection of the lining. In determining bending moments in the lining, a conservative approach can be taken by neglecting the passive forces in the rock. The lining is then treated as a free-standing cylinder. This method is discussed first.

(a) This procedure is taken from Roark[54], Table VIII, Case 11. Figure 3-10 shows the general loading case. Bending moment at the centerline of crown or invert is calculated with the use of Equation 3-10.

$$M_1 = wR^2 \left[0.3183(0.5\theta + \theta s^2 + 1.5\, sc) - 0.5 s^2\right] \qquad (3\text{-}10)$$

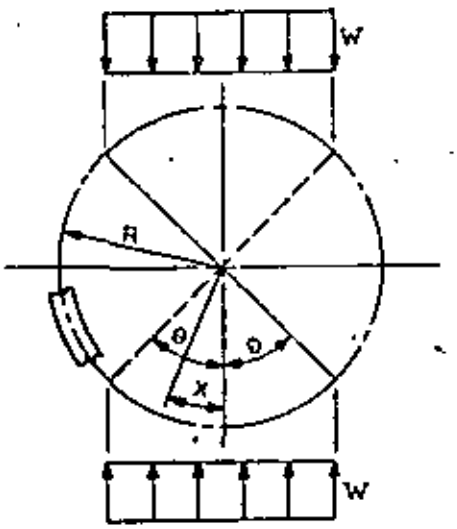

Figure 3-10.

Notation follows:

M_1 = bending moment at centerline of crown or invert, in-lb
w = applied load, lb per lineal inch
R = radius to circumferential centerline of lining, in
θ = angle which defines load span, radians
X = angle to point in lining being considered, radians
s = sin θ
c = cos θ
z = sin X

positive moment shown, reverse is negative moment

For computing the moment (M) at points around the lining ranging from $X = 0$ to $X = \theta$,

$$M = M_1 - 0.5 z^2 wR^2 \qquad (3\text{-}11)$$

In lining design, the load (w) is assumed as acting across the full width of the tunnel, i.e., $\theta = 90^\circ$ in Figure 3-10. For this case,

$$M_1 = 0.25\, wR^2 \qquad (3\text{-}12)$$

and $$M = wR^2(0.25 - 0.5z^2) \qquad (3\text{-}13)$$

With the use of Equation 3-13, the maximum moments will occur at invert and the crown (X = 0, 180°) and be equal to $0.25\ wR^2$. Moment will also be maximum but opposite in direction at the springline (X = 90°) and be equal to $-0.25\ wR^2$.

(b) Maximum moments computed by the above procedure represent upper limits to values of bending moments which may develop in the concrete lining as the result of an unbalanced rock load. However, the equations are useful during preliminary design or for determining whether the lining design is governed by rock loading rather than by other considerations. If the interaction of the lining and surrounding rock is taken into account, reduced bending moments can be computed, dependent on the passive resistance offered by the rock and the rigidity of the lining. Approximate methods suitable for design purposes are available, although the reaction of the rock to deformation of the lining is difficult to evaluate. One such procedure (Bougayeva's Method) based on the analysis of an elastically embedded ring is taken from Szechy[59] and outlined below. In evaluating the reaction of the rock, use is made of the coefficient of subgrade reaction, a term borrowed from soil mechanics. This term is also commonly referred to as the foundation modulus and is expressed as the external force in pounds per square inch required to cause a total deflection or deformation of one inch in the subgrade (foundation) or medium surrounding the tunnel. The distribution of subgrade reactions assumed for an elastically embedded ring subjected to a uniform vertical load is shown in Figure 3-11. Moments are computed in accordance with Szechy[59], Chapter 4, beginning with Equation 3-14 shown below.

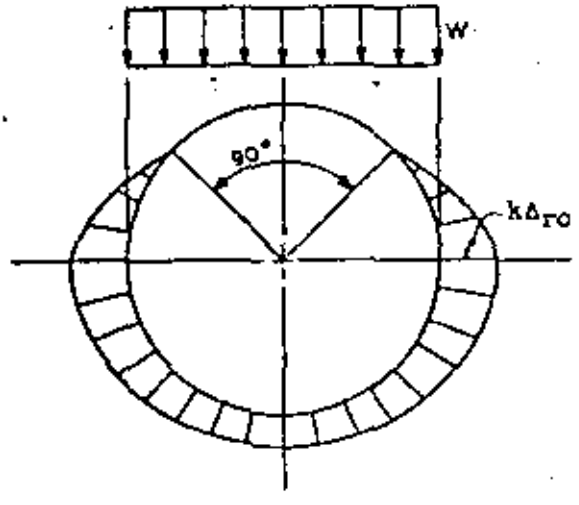

w = unit load

k = coefficient of subgrade reaction (foundation modulus)

Δ_{ro} = deformation of medium

(After Szechy[59])

Figure 3-11.
Distribution of medium reaction.

$$M = wRR_2[A\alpha + B - C_1 n(1+\alpha)], \text{ where } M = \text{moment, in-lb,} \qquad (3\text{-}14)$$

$$n = \frac{1}{m+0.06416} \qquad (3\text{-}15)$$

$$m = \frac{EI}{bkR_2R^3}$$, if lining thickness is considered, (3-16)

and $$m = \frac{EI}{bkR^4}$$, if lining thickness is neglected (3-17)

Additional notation follows:

w, R and R_2 as previously defined

b = width of the ring = breadth of beam used for computing moment of inertia of lining section, in

E = modulus of elasticity of lining material, lb/in^2

I = moment of inertia of lining section, in^4

k = coefficient of subgrade reaction (foundation modulus), $lb/in^2/in$. (Use lb/in^3 in Equations 3-16 and 3-17)

$$\alpha = 2 - \frac{R_2}{R}$$

A, B and C_1 are constants which vary around the ring in accordance with values tabulated below.

ϕ	A	B	C_1
0	0.1628	0.0872	-0.0070
$\pi/4$	-0.0250	0.0250	-0.00084
$\pi/2$	-0.1250	-0.1250	0.00825
$3\pi/4$	0.0250	-0.0250	0.00022
π	0.0872	0.1628	-0.00837

For purposes of lining design, the relatively small difference between R and R_2 can be neglected. Then $R_2 = R$ and $\alpha = 1$. Equation 3-14 can now be rewritten as:

$$M = wR^2(A + B + \frac{2C_1}{m+0.06414})$$ (3-18)

With the use of Equation 3-18, a moment diagram can be plotted which is similar to that shown in Figure 3-12, dependent on the value of m. A value of m = 0.00178 was used in Szechy[59] for computing values shown for illustrative purposes in the diagram.

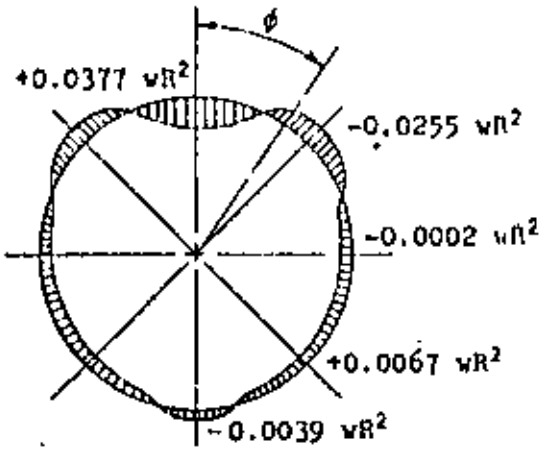

(After Szechy[59])

Figure 3-12. Moment diagram.

NOTE: Value for m is based on following properties of ring & surrounding medium. Values given in Szechy[59] have been converted to British units of measurement.

E = 10×10^6 t/m² = 14.223×10^6 lb/in²

I = 0.000144 m⁴ = 345.954 in⁴

k = 10,000 t/m³ = 361.27 lb/in³

R = 3.0 m = 118.11 in

b = 1.0 m = 39.37 in

where t = metric ton (1000 kilograms) and m = meter

The maximum moment occurs at the crown. After substituting the appropriate values for A, B and C_1, Equation 3-18 becomes:

$$M_{max} = wR^2[0.25 - \frac{0.014}{m+0.06416}] \qquad (3\text{-}19)$$

In Equation 3-19, the effect of varying m (which is a function of the rigidity of the ring and foundation modulus of the medium) can be seen in Figure 3-13. As the amount of lateral support ranges from full restraint to no support, the crown moment increases from 0.032 to 0.25 wR^2 or by a factor of approximately eight. As can be seen in the figure, the moment increases rapidly for small values of m, then increases slowly until m = 1. From m = 1 to m = infinity, the moment increases slightly from 0.237 wR^2 to 0.25 wR^2. Since the value of m can be varied in Equation 3-17 by varying only the value of the foundation modulus (holding other factors constant), it is evident from Figure 3-13 that a small amount of lateral support can significantly reduce bending moments in a flexible ring.

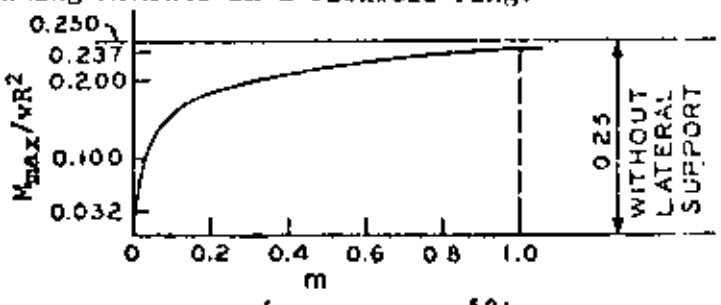

(After Szechy[59])

Figure 3-13. Variation of crown moment as a function of rigidity of the ring and the foundation modulus.

The effect on crown moment of varying only the value of the foundation modulus of the medium in which a particular ring is embedded is shown in Figure 3-14. It is evident that most of the benefit in reducing the moment is limited to smaller values of foundation modulus. Therefore, the determination of the foundation modulus is not critical beyond a certain value, dependent on the flexibility of ring. A method for determining the foundation modulus of the rock medium is discussed below.

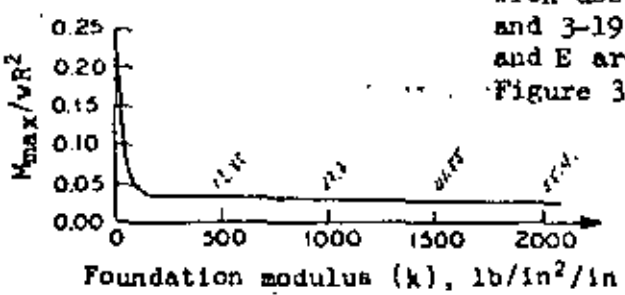

NOTE: Value of M_{max}/wR^2 computed with use of Equations 3-17 and 3-19. Values of I, R, and E are as given in Figure 3-12.

(After Szechy[59])

Figure 3-14. Effect of value of foundation modulus on crown moment.

(6) Method for Determining Value of Foundation Modulus. Listings of values of foundation modulii of various rock masses are not readily available. Approximate values, generally suitable for tunnel lining design purposes can be found if the modulus of deformation of the rock mass is known. The modulus of deformation is similar to the modulus of elasticity except that the rock deformation measured under load includes the effect of geologic discontinuities in the rock mass. Methods of estimating the value of modulus of deformation by conducting large scale field tests or possibly by conducting laboratory tests are discussed in Chapters 2 and 5, Stagg and Zienkiewicz[55]. In the laboratory, the modulus of elasticity of intact rock specimens establishes the upper bound for the modulus of deformation of the rock mass for the case where joints are very tight and widely spaced. Table 3-9 lists values of the modulus of deformation for a number of rock types based on data gathered at various projects. The table is useful as a guide and also shows possible ranges of modulus of deformation for different rock masses. Once an estimate of the modulus of deformation is made, the foundation modulus (coefficient of subgrade reaction) can be estimated in the following manner. Equation 3-20 is a modification of an equation presented in Deere, et al[28], Appendix 3, page 8, for estimating rock deformation due to the application of a uniform internal pressure on the walls of an opening in an elastic medium.

Table 3-9. Estimated Values of Modulus of Deformation for Various Rock Types

Location	Rock Type	Modulus of Deformation 10^6 lb/in^2		
		Ave	Max	Min
	Quartzite	1.6	5.[illegible]	0.3
Church Hill Falls	Granodiorite	2.4	5.8	0.6
	Diorite & Diorite Gneiss	6.0	7.0	0.5
	Biotite Schist	0.9	2.6	0.3
	Chlorite Schist	1.3	2.6	0.4
	Graphite Schist	0.3	0.4	0.1
	Augen Gneiss	0.9	1.0	0.5
	Granite Gneiss	4.2	9.0	0.5
	Siltstone	1.1	2.2	0.9
Dex Project, Iran	Limestone Cobble Conglomerate	1.4	1.8	1.0
	Limestone	0.2	0.3	0.1
Yellowtail Dam	Limestone		5.0	3.0
	Argillite	1.8	3.6	0.5
Glen Canyon Dam	Sandstone		1.3	0.9
	Amphibolite	1.3	1.7	0.7
	Scoriaceous Basalt	0.6	1.2	0.1
	Vesicular Basalt	1.2	1.6	0.6
Hokes Canyon Tunnel	Clayey Siltstone		0.018	0.005
Rock River Junction on I-80	Shale		0.014	0.012

$$\Delta_{ro} = \frac{PR_2(1 + \nu_r)}{E_d} \qquad (3\text{-}20)$$

where P = internal pressure, psi

R_2 = radius to excavated surface of opening, in

ν_r = Poisson's ratio for rock

E_d = modulus of deformation for rock, psi

If Δ_{ro} is set equal to one inch, then the foundation modulus (k) can be calculated from:

$$\text{P/inch of deformation} = k = \frac{E_d}{R_2(1+\nu_r)} \qquad (3\text{-}21)$$

If Poisson's ratio is unknown, a value of 0.25 may be used in accordance with the recommendation made in Stagg and Zienkiewicz[55], page 395. Although errors are introduced with the use of Equations 3-20 and 3-21 by assuming that a discontinuous medium acts as a continuous one, the magnitude of error probably does not exceed the limits of accuracy of the methods employed for estimating values of E_d. Also, it can be shown that values of E_d greater than $.05 \times 10^6$ to 0.1×10^6 psi will result in no significant reduction in the crown moment value. This range of values is greatly exceeded for most of the rock types shown in Table 3-9. For example, for the ring properties used as a basis for plotting the curve in Figure 3-12, a value of $k = 340$ lb/in^2/in can be calculated by Equation 3-21 if $E_d = .05 \times 10^6$ psi. Figure 3-14 shows that almost no further moment reduction will result with larger values of k. Similar plots can be drawn for rings possessing different degrees of rigidity and similar comparisons made. During construction of a tunnel, it is necessary that voids between the tunnel lining and the rock face be completely filled with grout along the entire tunnel length. Grouting will also be necessary to consolidate damaged or loosened rock behind the lining. Otherwise bending moments in excess of those calculated by the above procedure may develop.

(7) Computation of Stresses.

(a) Once bending moments have been calculated, the resulting stress in the concrete lining can be determined from:

$$f_c = \frac{M}{S} \quad \text{where} \qquad (3\text{-}22)$$

f_c = stress in concrete at extreme fiber of section, psi

M = bending moment, in-lb

S = section modulus, in^3

(b) The rock load will also impose an axial load on the lining. The resulting stress (f_w) is assumed to act uniformly across the lining section and is determined from:

$$f_w = \frac{wR_2}{R_2 - R_1}, \text{ where} \qquad (3\text{-}23)$$

w = unit rock load, lb/in of span

R_2 = radius to outer surface of lining, in

R_1 = radius to inner surface of lining, in

The combined axial and bending stress (f_{co}) acting on the concrete lining section due to rock load is then found from:

$$f_{co} = f_c + f_w \qquad (3\text{-}24)$$

(8) Design Guidance.

(a) The lining should be designed to resist the external hydrostatic water load acting alone, the rock load acting alone, and the combined effects of external water and rock loads. For practical reasons, concrete linings are seldom constructed to thicknesses of less than nine inches.

(b) In tunnels subject to water flow, design stresses for use in tunnel concrete lining design should be in accordance with EM 1110-2-2902. Otherwise concrete with f'c = 3,000 psi is considered acceptable.

(c) Reinforced concrete linings should be provided with longitudinal steel reinforcement on the inner face (farthest from the rock) of the lining. Area of steel (A_s) should be equal to approximately one-quarter percent of the design cross sectional area of the tunnel lining or $A_s = 0.0025\pi(R_2^2 - R_1^2)$, within the limits of a minimum of #6 bars at 18" o.c. and a maximum of #9 bars at 12" o.c. Concrete cover over reinforcement should be a minimum of three inches. Where high velocity flow (greater than 30 feet per second) is expected, where the water may carry a high silt load, or where water has properties which may damage concrete (such as high sulfate or acid levels, salt water, etc.), the minimum cover over reinforcement should be four inches.

(d) Shear stress should not be critical in tunnels unless the tunnel cross section includes long straight side walls. Shear stresses should be computed as outlined in EM 1110-2-2902.

(e) Concrete tunnel linings located in zones of strong seismicity should be reinforced. Areas of strong seismicity are defined as areas where accelerations of 0.2g or greater can be expected, or in Zones 3

and 4 of the Seismic Zone Map of the United States. Reinforced concrete linings should also be used in those areas of Seismic Zone 2 which may experience a high frequency of earthquakes. A seismic zone map is included in TM 5-809-10.

(f) The design of concrete linings of circular cross section is discussed further in Appendix H where a number of design examples are presented.

(9) Design of Non-Circular Tunnels. If properties of the surrounding medium are not directly taken into account, stresses in linings of non-circular tunnels may be determined in accordance with the column analogy analysis presented in EM 1110-2-2902. When medium properties are taken into account, stress analysis may be accomplished with the use of numerical methods discussed in Appendix K, Chapter 6 (p. K-95). Other methods involve treatment of the medium as a continuum to allow closed-form mathematical solutions. One such method (the Zurabov-Bougayeva method) is presented in Chapter 4 of Szechy[59] for a monolithic horseshoe section in an elastic medium. The assumed distribution of subgrade reactions due to a uniform external vertical load on the section is shown in Figure 3-15.

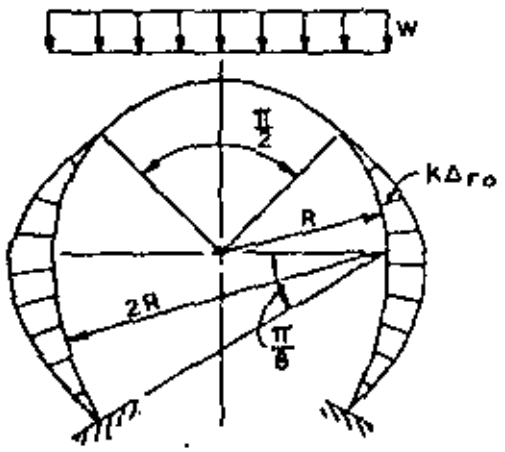

w = unit load

k = coefficient of subgrade reaction (foundation modulus)

Δ_{ro} = deformation of medium

Figure 3-15. Distribution of medium reaction, horseshoe section. (After Szechy[59])

With the use of a numerical example, equations are developed in Szechy[59] for determining moments around a horseshoe lining. The structure is solved first for the condition of fixed ends and no lateral ground support and then for the condition of fixed ends and lateral ground support. The conditions of elastically constrained ends with and without lateral support are also investigated. Moments were computed for these conditions and are summarized in Figure 3-16 for a tunnel section and surrounding medium assigned definite properties, size and configuration. In addition to information shown in Figure 3-15, the following values were assigned:

foundation modulus of medium, k = 50 kg/cm^3 (1806.38 lb/in^3)

R = 3.0 meters (118.11 in)

moment of inertia for one-meter wide strip of section in longitudinal direction, I = 0.0104 meter^4 (24,986 in^4 for one-meter wide or 634.65 in^4 for one-inch wide strip)

modulus of elasticity of lining material, E = 3 x 10^6 ton/meter^2 (4.26 x 10^6 lb/in^2)

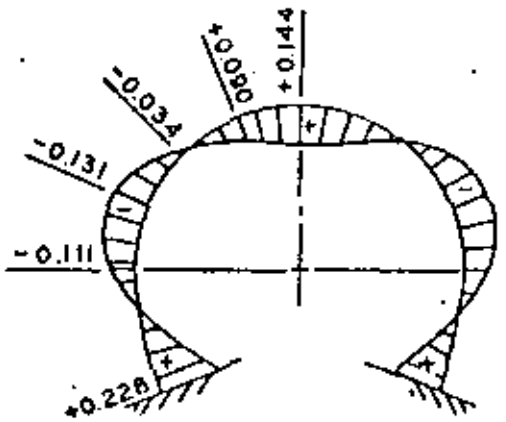

a. Rigidly-fixed ends, no lateral support.

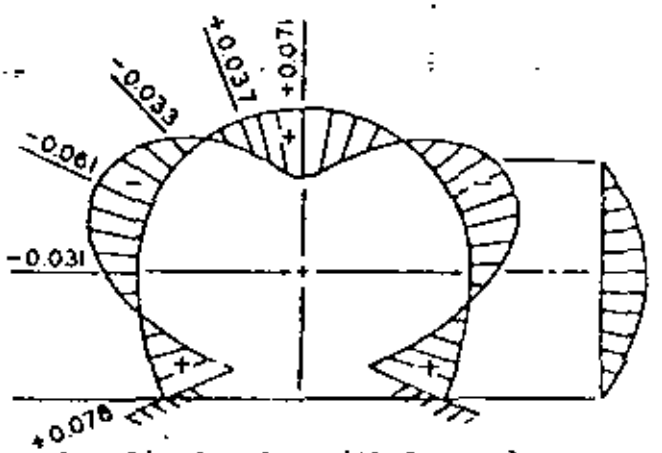

b. Fixed ends, with lateral support.

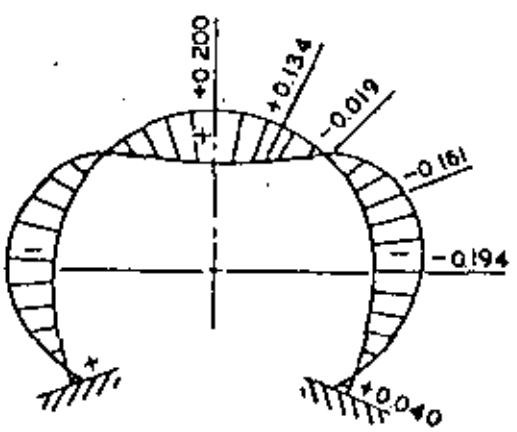

c. Elastically constrained ends, no lateral support.

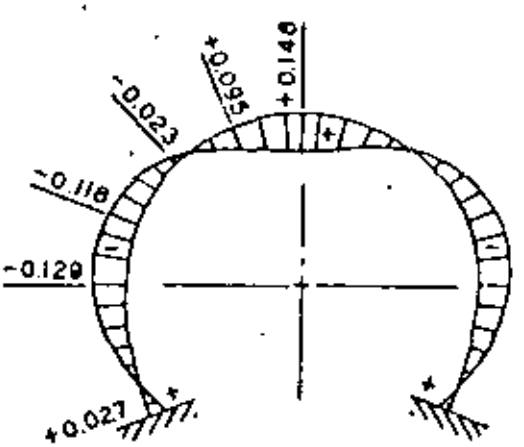

d. Elastically constrained ends, with lateral support.

(After Szechy[59])

NOTE: All moments and ordinates to be multiplied by wR^2.

Figure 3-16. Moments due to vertical load for various conditions.

Just as with the circular cross section discussed in paragraph 3-7b(5)(b), p. 3-44, the bending moments for variable structural rigidity and foundation modulus are a function of the ratio EI/bkR^4. The authors in Szechy[59] conclude that the foundation modulus value may generally be neglected if EI/bkR^4 is less than 0.1. The section in that case can be treated as being free-standing. Because solutions of non-circular sections are made simpler if values for size, configuration and material properties are known, a further detailed discussion and design example are included in Appendix H, paragraph H-6.

c. Steel Lining Design.

(1) General.

(a) Tunnel linings designed to resist internal water pressure usually require steel either in the form of conventional reinforcement or as a lining around which the concrete lining is cast. If the pressure tunnel serves as a conduit leading to a hydraulic turbine, the tunnel as a whole forms a penstock. In this case, plate steel lining usually is provided downstream from the impervious zone of the embankment. Free-standing penstocks, that is, those erected within a completed tunnel or conduit, are pressure vessels in a pure sense and design and construction will conform closely to the requirements given in ASME[6]. While the function and many of the details of construction and erection for integrally embedded steel liner are quite similar to those for a free-standing penstock, the loading conditions are somewhat different. When completed, the steel lining, the concrete encasement, and the surrounding rock act together to resist internal pressures. The degree to which the rock participates is extremely variable, being dependent upon the modulus of deformation of the rock medium, which in turn is affected by the presence of micro-fissures, faults, and variations in rock from point to point.

(b) The modulus of deformation of rock surrounding the tunnel opening can be determined by chamber tests. The tests are conducted by sealing a short length of chamber at tunnel depth, applying a hydrostatic pressure, and measuring changes in diameter as the pressure is changed. Alternatively, similar data can be obtained from uniaxial jacking tests; but, the loaded area is limited to the size of bearing plates used under the jacks rather than to the entire periphery of the tunnel as in hydrostatic chamber tests. In a series of chamber tests made in France around the year 1960, it was found that 25 to 96 percent of the pressure was transferred to the rock through the lining. However, it should be recognized that the results of chamber or jacking tests apply only to the area tested. Therefore, variations in the modulus of deformation along the length of the tunnel should be expected.

(c) It is usually dangerous to have water escaping from a pressure tunnel. Water escaping into an abutment or slope can cause

slope failures and other serious problems. In designing tunnel linings to resist internal water pressure, the steel liner and the concrete reinforcement are considered to act independently and also together. Liner plate and reinforcement must be designed to satisfy all conditions outlined below. When the steel liner is considered acting independently, the allowable liner stress is taken at 80 percent of the yield strength or 50 percent of the ultimate strength, whichever is less. When considered acting with the concrete reinforcement, allowable stresses in the liner and reinforcement are limited to 50 percent of the yield strengths of the respective steels. When the concrete reinforcement is considered independently, the allowable stress is taken at the yield point of the steel. Reduction or even elimination of reinforcement can be considered if intact rock of sufficient depth to provide a cover equal to or more than the maximum internal pressure (in feet of head) is available. In this case, the allowable stresses are taken as 50 percent of the yield strength of the respective steels.

(d) External hydrostatic pressure can develop directly behind the steel liner if the concrete lining develops cracks. Cracks in the concrete could be due to shrinkage or to an internal pressure which exceeds the tensile strength of the concrete. Therefore, in the event the pressure tunnel is unwatered, the external water pressure may exceed the critical buckling strength of the lining. Excessive external pressure can also develop on the steel lining during construction as a result of grouting pressures. To resist buckling, anchors into the concrete should be provided so that the steel lining is stiffened by a portion of the concrete shell. These anchors are welded to the outer surface of the shell and are usually spaced at three to four-foot intervals depending on the predicted external load, the liner thickness, and the liner radius.

(e) The most frequent cause of leakage from a steel lining is due to the existence of grout holes which are not completely sealed. Therefore, it is essential that grout holes and sealing plugs be carefully detailed and fabricated. This can best be done by adopting a pattern of grout holes in advance and by requiring the preparation of sealing plugs in the shop. The prepared grout hole in the liner can be so devised that grout will be admitted between the steel and concrete linings to fill existing voids. In filling around a cylindrical steel lining, air is often entrapped at the invert; therefore, invert grout holes should always be provided. If left unplugged during concreting until concrete appears at the surface, grouting of the invert probably will not be necessary. A detailed description of procedures for fabricating and erecting steel liners is contained in a publication of the Bureau of Reclamation[18].

(2) Design to Resist Internal Pressure.

(a) Steel Liner. When considered acting independently, the steel

lining is designed to resist the entire internal pressure at 80 percent of its yield strength or 50 percent of its ultimate strength, whichever is the lesser value. The lining will be a thin shell and its thickness can be determined from the following:

$$t = \frac{PR_1}{f_s} \qquad (3\text{-}25)$$

where f_s = 80% of the yield strength or 50% of the ultimate strength, lb/in^2

P = internal pressure, lb/in^2

R_1 = inside radius of the liner, in

t = thickness of the liner, in

This will usually control the liner thickness; however, the minimum thickness for handling should also be investigated. A publication of the Bureau of Reclamation[18] gives the following formula for determining minimum thickness (t_{min}) for handling a steel penstock:

$$t_{min} = \frac{D + 20}{400} \qquad (3\text{-}26)$$

where D = internal diameter of the liner, in

The computed thickness may be reduced if adequate stiffeners (external anchors which also serve as stiffeners or temporary internal stiffeners) are provided to prevent deformation during fabrication, handling and erection, which will usually be the case. The method of fabrication should also be considered since the liner sections will probably be assembled prior to attachment of external anchor/stiffeners. For example, sections could be assembled and the cylinders kept in a vertical position until the stiffeners are welded in place.

(b) Concrete Reinforcement. When the rock surrounding the tunnel is not assumed to resist any of the internal pressure, sufficient reinforcement is provided to resist the full internal pressure. For this condition, the allowable stress in the reinforcement is taken as equal to the yield point of the steel. The most conservative assumption is that the internal pressure acts to the excavated rock surface, including an allowance for overbreak. The required area of reinforcing is computed as follows:

$$A_s/in = \frac{PR_2}{f_s} \qquad (3\text{-}27)$$

where A_s/in = area of steel, in^2, required per inch of tunnel length

f_s = the yield strength of the reinforcement, lb/in^2

P = internal pressure, lb/in^2

R_2 = radius to the outside of the concrete lining or to the excavated rock surface, in

(c) Steel Lining and Concrete Reinforcement Combined. When the steel liner and reinforcement are considered acting together, the allowable stresses are limited to 50 percent of the respective yield strengths of the liner plate and reinforcement. A method for estimating the distribution of load (resulting from internal pressure) on the steel lining and reinforcing steel is outlined below. In this case, it is considered that surrounding rock is carrying none of the load due to internal pressure. Figure 3-17 and the following notation supplement the discussion and equations that follow.

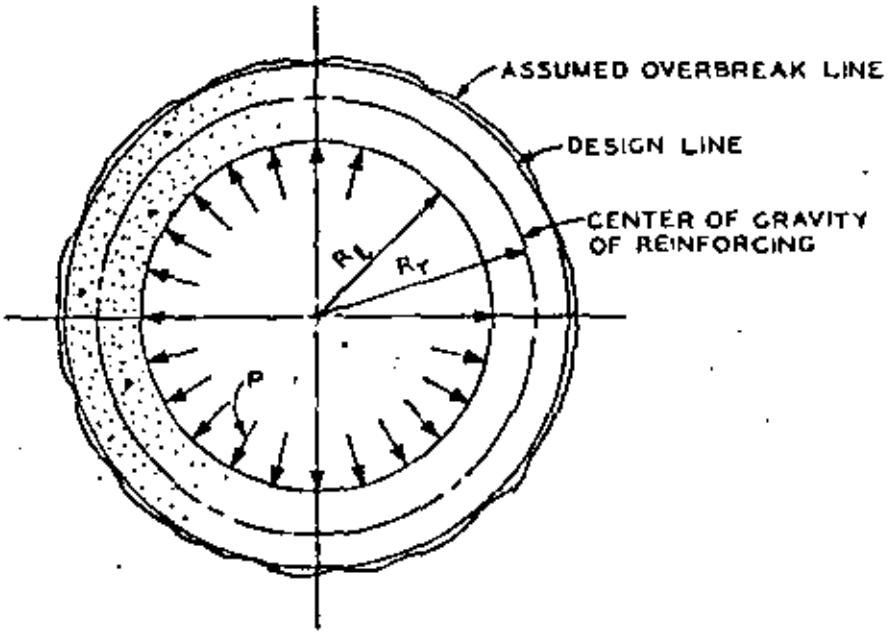

Figure 3-17. Lining subjected to internal pressure.

R_r = radius to center of gravity of reinforcing steel, in

R_L = radius to inside face of steel liner, in

P = internal pressure, lb/in^2

P_L = portion of internal pressure resisted by steel liner, lb/in^2

P_r = portion of internal pressure resisted by reinforcing steel, lb/in^2

E_c = modulus of elasticity of concrete, lb/in^2

A_s = area of reinforcing steel, in^2, per inch of tunnel length

E_s = modulus of elasticity of steel, lb/in^2

t = liner plate thickness, in

L = distance between outside face of steel liner and center of gravity of reinforcing steel, in ($L = R_r - R_\ell + t$)

Δr = radial extension of reinforcement, due to radial load, in

Δc = radial shortening, due to radial load, of intervening concrete between the steel liner and the reinforcement, in

Δ_ℓ = radial extension of steel liner, due to radial load, in

ν_s = Poisson's ratio of steel

ν_c = Poisson's ratio of concrete ($\nu_c = \sqrt{f'_c/350}$, See Timoshenko and Woinowsky-Krieger[61], p. 97)

In estimating the distribution of load, the following equations are used:

Assume $\Delta_\ell = \Delta_r - \Delta_c$ (3-28)

$$\Delta_r = \frac{P_r - R_r^2}{A_s E_s} \quad (3\text{-}29)$$

$$\Delta_c = \frac{P_r L (1 - \nu_c^2)}{E_c} \quad (3\text{-}30)$$

$$\Delta_\ell = \frac{P_\ell R_\ell^2 (1 - \nu_s^2)}{t E_s} \quad (3\text{-}31)$$

Substituting in Equation 3-28,

$$\frac{P_\ell R_\ell^2 (1 - \nu_s^2)}{t E_s} = \frac{P_r R_r^2}{A_s E_s} - \frac{P_r L (1 - \nu_c^2)}{E_c} \quad (3\text{-}32)$$

Also, $P_r = P - P_\ell$ (3-33)

Equations 3-32 and 3-33 can now be solved simultaneously for values of P_r and P_ℓ.

(d) Steel Lining, Concrete Reinforcement and Rock Combined. If the rock is used in the design to resist a portion of the radial load due to internal pressure, it is recommended that smooth wall blasting or machine mining be required in the specifications. When assuming that the rock is resisting a portion of the internal load, the load assigned to the rock should not exceed the gravity load of the rock directly above the tunnel. It is necessary that values for foundation modulus of the rock medium (see paragraph 3-7) be determined along the length of the tunnel before distributing the load between the rock, reinforcing steel and liner. The minimum value of foundation modulus can then be used in the design. A procedure similar to that discussed above for liner and reinforcement combined is discussed below. Notation is the same with the following additions:

P_{ro} = portion of load resisted by rock, lb/in^2

k = foundation modulus of rock medium, lb/in^2 per inch of deformation

Δ_{ro} = deformation of rock due to radial load, in

For purposes of estimating the allocation of radial internal load, it is assumed that the radial extension of the reinforcement minus the shortening of the intervening concrete equals the extension of the liner. This was also the basis for developing the relationships expressed in Equation 3-32. It is further assumed that the rock deformation is also equal to the radial extension of the reinforcement. The rock deformation can also be expressed as a function of the radial load on the rock and the foundation modulus.

$$\Delta_{ro} = \Delta_r \tag{3-34}$$

$$\Delta_{ro} = \frac{P_{ro}}{k} \tag{3-35}$$

With the use of Equations 3-29, 3-34 and 3-35,

$$\frac{P_{ro}}{k} = \frac{P_r R_r^2}{A_s E_s} \tag{3-36}$$

Also, $$P = P_l + P_r + P_{ro} \tag{3-37}$$

Equations 3-32, 3-36 and 3-37 can now be solved simultaneously for values of P_l, P_r and P_{ro}. In this case, allowable stresses equal to 50 percent of the respective yield strengths of the liner and reinforcing steels are used in the design.

(e) Steel Lining and Rock Combined. In the event reinforcing is not required, Equation 3-30 may be rewritten to set L = thickness of concrete lining and $P_r = P_{ro}$.

$$\Delta_c = \frac{P_{ro}\, t_c\, (1 - \nu_c^2)}{E_c} \qquad (3\text{-}38)$$

where, t_c = concrete lining thickness

Δ_c = radial shortening of concrete lining thickness

Assume, $\Delta_\ell = \Delta_{ro} - \Delta_c$ (3-39)

With the use of Equations 3-31, 3-38 and 3-39,

$$\frac{P_\ell\, R_\ell\, (1 - \nu_s^2)}{t\, E_s} = \frac{P_{ro}}{k} - \frac{P_{ro}\, t_c\, (1 - \nu_c^2)}{E_c} \qquad (3\text{-}40)$$

Also, $P = P_{ro} + P_\ell$ (3-41)

Values for P_{ro} and P_ℓ can now be found from Equation 3-40 and 3-41. The allowable stress for determining liner plate thickness is taken as 50 percent of the yield stress. As previously indicated, P_{ro} should not exceed the gravity load of the rock directly above the tunnel.

(3) Design to Resist External Pressure.

(a) The stresses caused by an external load, on an assumed tunnel lining cross section of concrete and steel acting together, can be determined from procedures for designing concrete linings, paragraph 3-7. Should the concrete lining develop cracks, due to shrinkage or because the tensile strength of the concrete is exceeded as a result of internal pressure transmitted by the steel lining, an external load may develop directly behind the steel lining. The external load may be due to either ground water or grouting pressures. The critical external load is found from the principles of elastic stability.

(b) To determine the critical load, the lining is considered as a thin tube under uniform external pressure as shown in Figure 3-18.

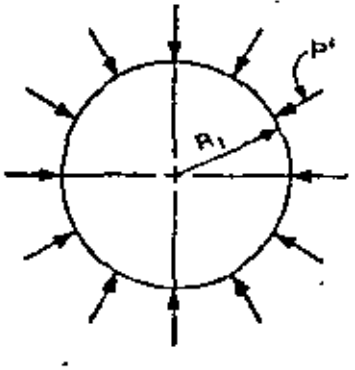

Figure 3-18. Uniform external pressure on thin tube.

In the figure, p' represents the external pressure at which elastic buckling occurs. The liner should be stiffened at intervals to provide a critical pressure (p') for elastic stability that is greater than the expected external design pressure. In accordance with Roark[54], page 354, case 31, the approximate formula for determining the critical pressure for a short tube of length L_1 with the ends held circular but not otherwise constrained, or a long tube held circular at intervals L_1 is:

$$p' = \frac{0.807\, E_s\, t^2}{L_1\, R_1} \sqrt[4]{\left(\frac{1}{1 - \nu_s^2}\right)^3 \frac{t^2}{R_1^2}} \qquad (3\text{-}42)$$

where E_s = modulus of elasticity of steel, lb/in^2

t = thickness of the liner, in

R_1 = radius to the inside of the liner, in

ν_s = Poisson's ratio for steel

L_1 = spacing of anchors, in

A minimum factor of safety of 2 should be provided between the maximum external pressure, either due to grouting or water, and the critical buckling pressure.

(c) Figure 3-19 shows forces and moments developed on a stiffened liner. Anchor reactive force (P_a) is the force per inch of stiffener required to keep the cylinder circular. In Figure 3-19, where only one section with two end stiffeners embedded is considered in the diagram, the reactive force equals $P_a/2$. The discussion presented below is based on Timoshenko and Woinowsky-Krieger[61], Chapter 15. The following equation is for a shell with built-in edges.

$$M_o = \frac{pX_2\,(2\alpha)}{2\beta^2}\text{, see p. 480, Eq. 292 of above ref.} \qquad (3\text{-}43)$$

where, $$\beta = \sqrt[4]{\frac{3(1 - \nu_s)^2}{R_1^2 t^2}} \qquad (3\text{-}44)$$

setting $\nu = 0.30$ for steel, $$\beta = \frac{1.2854}{\sqrt{R_1 t}} \qquad (3\text{-}45)$$

$$2\alpha = \beta L_1\text{, and} \qquad (3\text{-}46)$$

$$X_2\,(2\alpha) = \frac{\sinh 2\alpha - \sin 2\alpha}{\sinh 2\alpha + \sin 2\alpha} \qquad (3\text{-}47)$$

Also from page 480 of the above reference, the following equation is useful:

$$M_o = \frac{P_a X_2 (2\alpha)}{4\beta X_3 (2\alpha)} \qquad (3\text{-}48)$$

where, $$X_3 (2\alpha) = \frac{\cosh 2\alpha - \cos 2\alpha}{\sinh 2\alpha + \sin 2\alpha} \qquad (3\text{-}49)$$

Solving Equations 3-43 and 3-48 for P_a,

$$\frac{P_a X_2(2\alpha)}{4\beta X_3(2\alpha)} = \frac{p X_2(2\alpha)}{2\beta^2} \qquad (3\text{-}50)$$

and, $$P_a = \frac{2p X_3(2\alpha)}{\beta} \qquad (3\text{-}51)$$

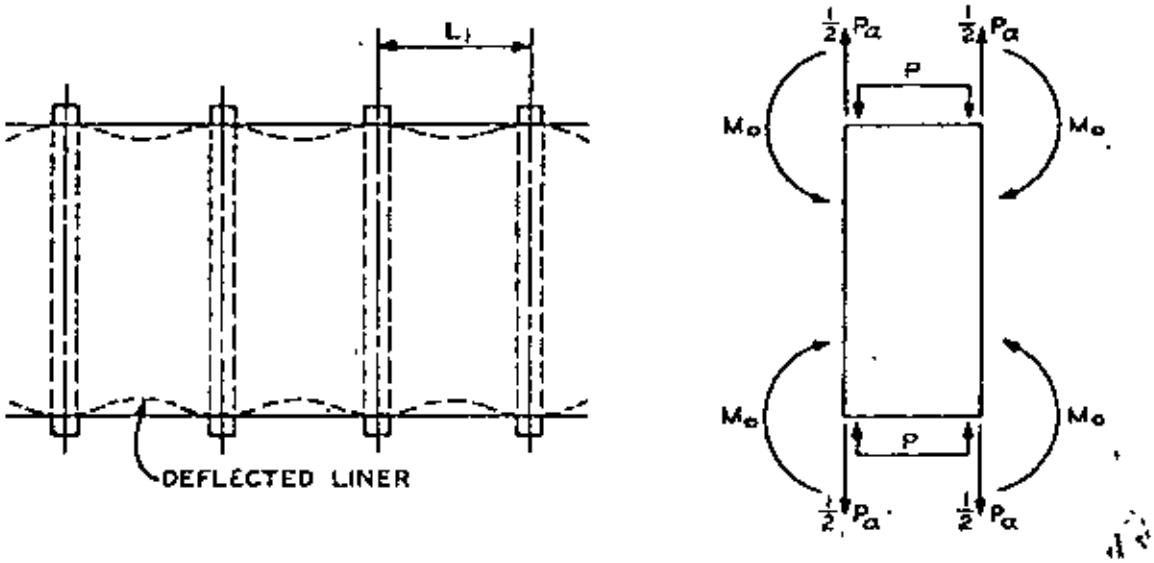

L_1 = spacing between stiffeners, in
p = external pressure on the lining, lb/in^2
P_a = anchor reactive force on the stiffener, or P_a = the magnitude of the forces per unit length of the circumference of the tube, lb/in
M_o = fixed end moment of the liner at the stiffeners, in-lb

Figure 3-19. Forces and moments on stiffened thin tube.

For shorter shells, the values of the factors $X_2(2\alpha)$ and $X_3(2\alpha)$ can be taken from Timoshenko and Woinowsky-Krieger[61], Table 85, page 478. The factors $X_2(2\alpha)$ and $X_3(2\alpha)$ for values of 2α larger than 5.0 approach unity. In Figure 3-19, the forces at the stiffeners are shown equal to 1/2 P_a. For a continuous liner with a series of equally spaced stiffeners, the web of each stiffener and the weld to the liner should be designed to take a load equal to P_a since forces on the liner on each side of a stiffener will contribute to the total load. For details of steel liners, see Figure I-16. See Appendix H for design examples.

3-8. Design of Intersections.

a. Initial Support. Intersections will require initial support in the same way as tunnels. Loadings on the support system are usually the same as for a tunnel. When steel set supports are used, the form used to shape a member may be elliptical. To analyze this type of member, a force polygon may be constructed (see Appendix G) to determine the thrusts in the members. If ring beams (circular steel set supports) are framed into a supporting linear beam, the reactions from the ring beams (determined by the usual analyses) become the applied loads on the supporting beam. Procedures for designing steel set supports at intersections are the same as used for tunnels. Examples of the geometry of intersection supports are shown in Figure I-15.

b. Lining. The main considerations in the design of branch outlets and wyes are the provision of sufficient structural strength to withstand the internal and external pressure, and the minimization of hydraulic losses.

(1) Penetration of a tunnel lining for a pipe or opening causes a reduction in the lining strength at the penetration. The area around the penetration should be reinforced to be equal in strength to the lining in the typical tunnel section. It should be noted that the nearer to 90 degrees the intersection is made, the smaller the penetration opening required in the tunnel lining. However, hydraulic losses are increased when the intersection angle approaches 90 degrees. Hydraulic losses can be greatly minimized by using a branch outlet which forms a frustum of a cone and converges six to eight degrees, rather than a cylindrical branch outlet. An example of this is shown in the bottom section of Figure I-5. Difficulties are encountered when reinforcing branch outlets if the intersection forms a sharp angle. A minimum angle of 60 degrees is therefore recommended.

(2) Where branch outlets are made in a penstock that is not embedded in concrete, the intersection can be reinforced with heavy steel plates. However, when the intersection is to be made underground, it becomes difficult to install the plates in the limited working space and it also requires a larger excavation which often leads to support problems. For these reasons, it is recommended that intersections made underground be strengthened with reinforced concrete. When using

working stress design, the stress in the concrete should be limited to 0.45 times its compressive strength and the reinforcing steel stress limited to 0.50 times its yield strength. When using ultimate strength design, a load factor of 1.8 should be used. These allowable stresses are considered conservative, as the rock cover will limit the deflections and also the stresses. To avoid congestment of reinforcement and minimize concrete placement difficulties, excavation openings should be as large as practicable and the use of large size bars, bundled reinforcement and rolled sections should be considered.

(3) Stress analyses of branch outlets and wyes can be accomplished using finite element techniques or approximate methods. Analysis based on theory of elasticity becomes too involved to be of much practical value. Approximate methods are available which are sufficiently accurate for planning purposes or if access to finite element programs is not available. An approximate method of stress analysis is illustrated below.

c. Stress Analysis of Branched Outlets. The reinforcement for a branch outlet should be proportioned to carry the unsupported loads, the areas of which are shown shaded in Figure 3-20 and 3-21. The total load to be carried by the reinforcement is equal to the product of the internal pressure and the unsupported areas projected to the plane of the outlet. The forces to be considered in design are illustrated diagrammatically in Figure 3-22.

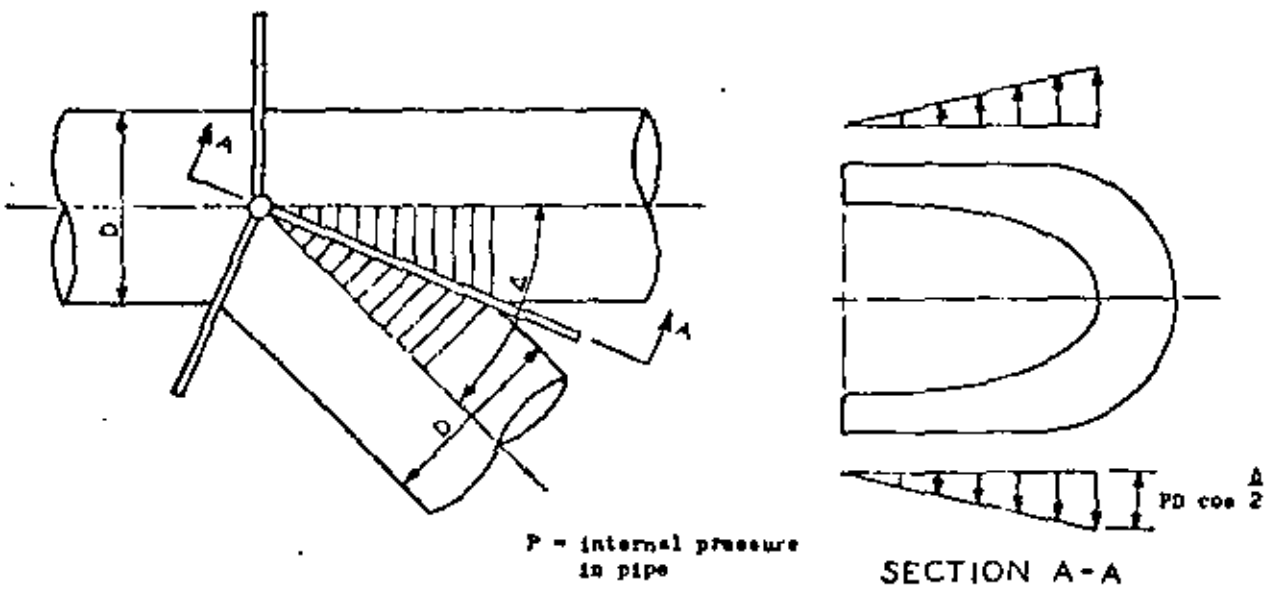

Figure 3-20. Unsupported areas in wye.

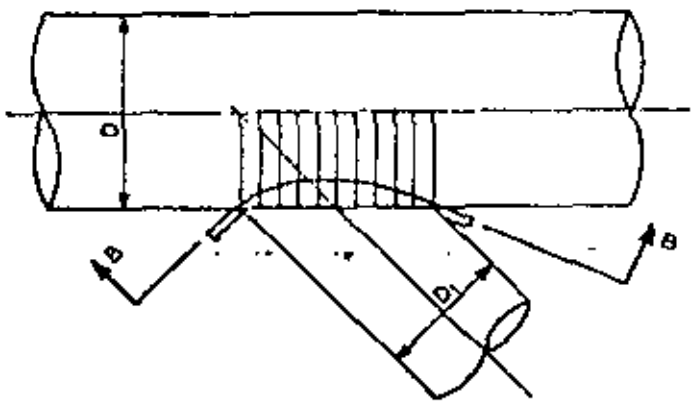

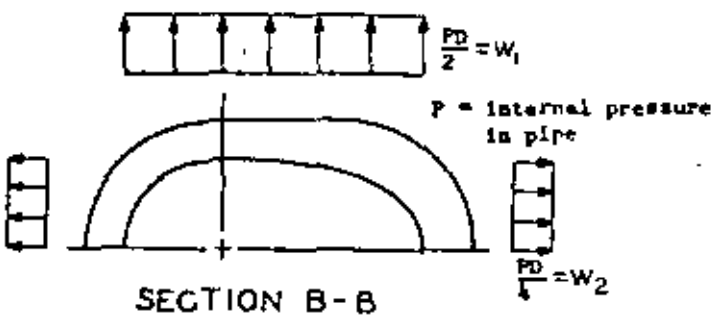

Figure 3-21. Unsupported areas in branch outlet.

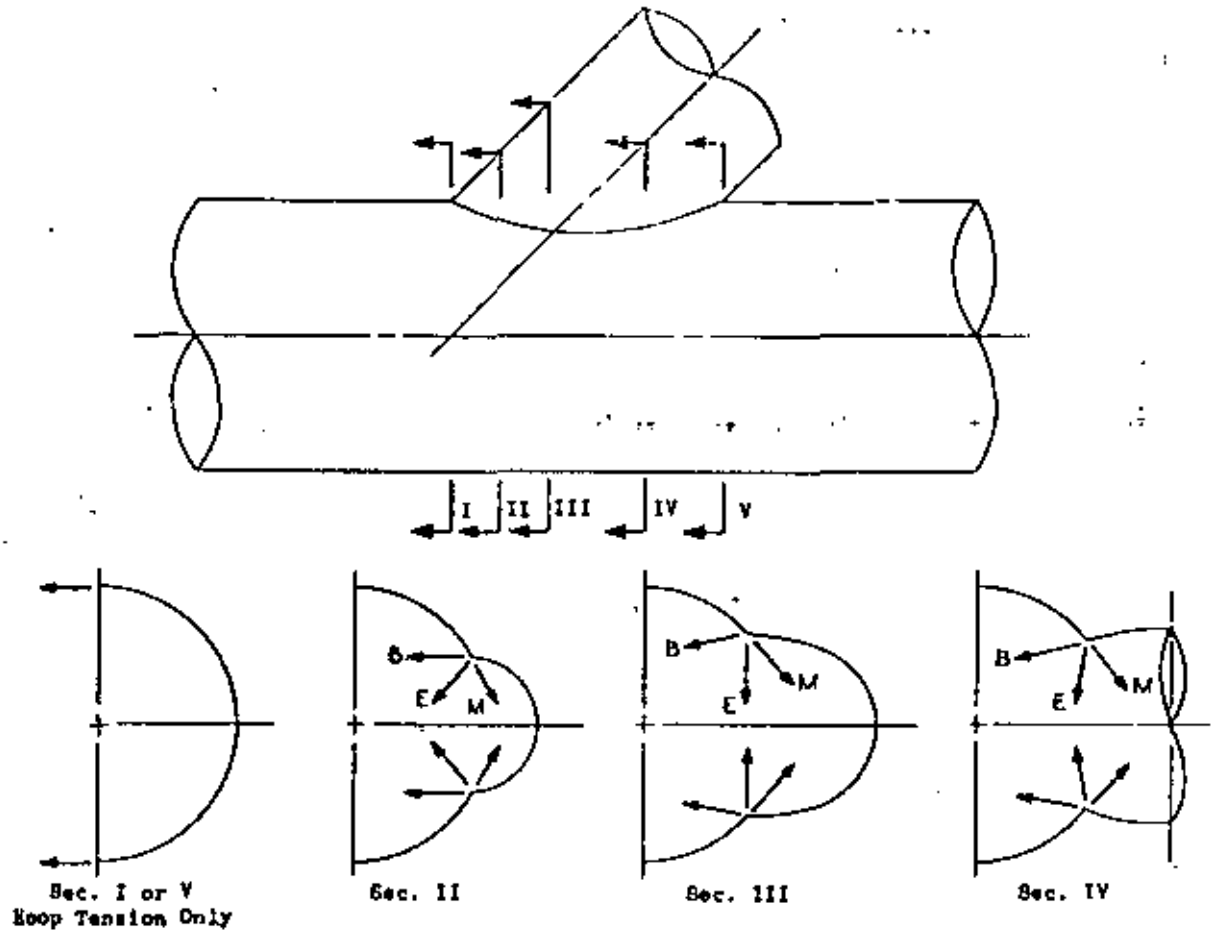

NOTE: At each point along the joints, the unbalanced tension is the vector sum of the stress in main and branch pipes. M = equilibrant of tension in main liner, B = equilibrant of tension in branch liner, E = total equilibrant.

Figure 3-22. Design forces in branched outlet.

Procedures for reinforcement of branch outlets are suggested in Swanson, et al[58]. Although based on steel plate reinforcement, the procedure may also be used in the analysis of reinforced concrete linings. The following extracts are from the above-referenced report.

(1) One Plate Design. The reinforcement consists of a ring girder placed around the joint. Although the girder does not lie in a plane, this analysis is considered valid when the ratio of diameters of branch and main pipe are between 0.3 and 0.6. Moments and stresses are computed with the following equations and the use of Figure 3-23.

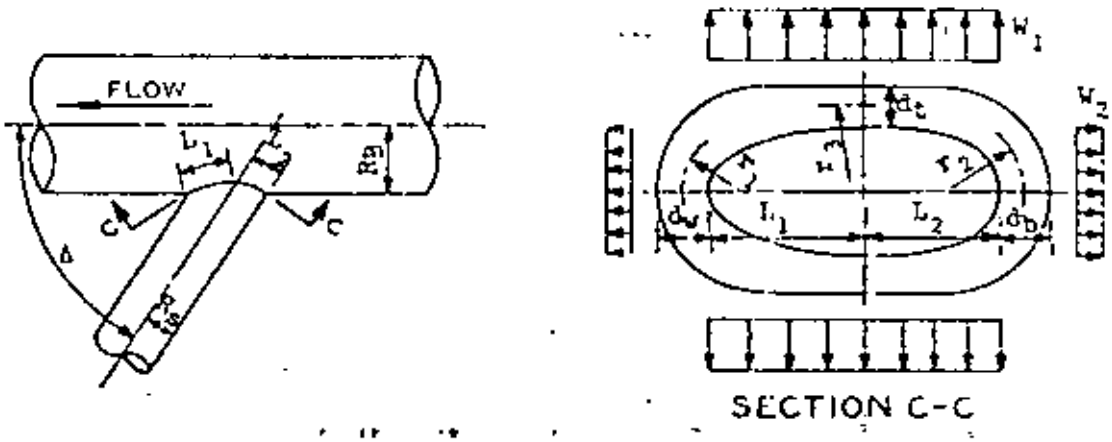

(From Swanson, et al[58])

Figure 3-23. One plate design.

$$W_1 = PR_B, \text{ where } P = \text{internal pressure} \tag{3-52}$$

$$W_2 = 1/2\ W \tag{3-53}$$

At crown: $$\text{Moment } (M_1) = \left(W_2 - \frac{W_1}{\sin^2\Delta}\right) \frac{R_B^2}{4} \tag{3-54}$$

$$\text{Thrust } (T_1) = W_2 R_B \tag{3-55}$$

$$r_3 = \frac{L_2^2}{R_B} + \frac{d_t}{2} \tag{3-56}$$

$$f_s(\max) = K \frac{M_1 c}{I} \quad \frac{T_1}{A}, \tag{3-57}$$

where K is Seely's constant, dependent on the curvature of the collar and c = distance from the neutral axis to the extreme fiber.

At sides: $$\text{Moment } (M_2) = \left(\frac{W_1}{\sin^2\Delta} - W_2\right) \frac{R_B^2}{4} \tag{3-58}$$

$$\text{Thrust } (T_2) = W_1 R_B \tag{3-59}$$

$$r_1 = \frac{R_B^2}{L_1} + \frac{d_w}{2} \tag{3-60}$$

$$r_2 = \frac{R_n^2}{L_2} + \frac{d_b}{2} \qquad (3\text{-}61)$$

$$f_s = \frac{KM_2c}{I} + \frac{T_2}{A} \qquad (3\text{-}62)$$

In Figure 3-23, d_t = depth of collar at junction of reinforcing plates, d_w = depth of collar at acute crotch of reinforcing plates, and d_b = depth of collar at obtuse crotch of reinforcing plates.

(2) Two-Plate Design. Two girders are attached, following the joint between main and branch pipes and meeting at crown and invert. (Figure 3-22). Each girder is designed for the water pressure acting on the part of the joint it supports, and (unless the angle of intersection is 90°) a reaction force "y" is calculated to make the deflections of the two girders at the apex (or open end of the girders) equal. Each girder may be sized by any convenient method of column analogy or the methods outlined in Swanson, et al[58]. Note that the depth of collar plates is not necessarily constant.

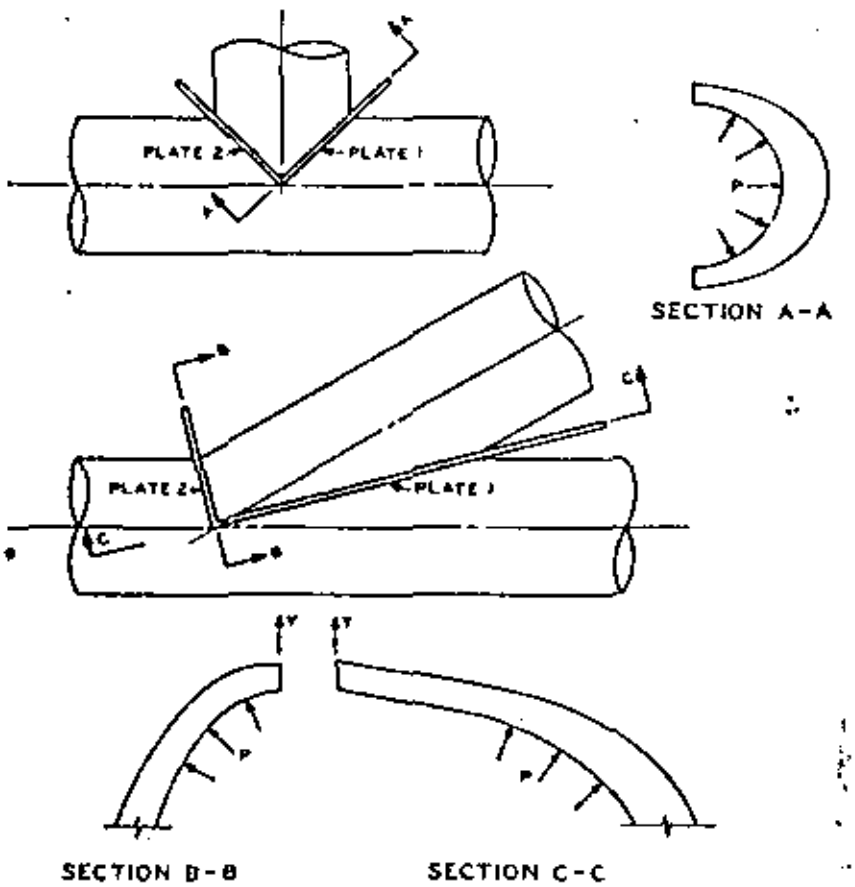

Figure 3-24. Two-plate design.

(3) Three-Plate Design. This is similar to two-plate design except that a third plate girder is joined to the other two which passes around the solid section of the main pipe. The stem of the Y thus formed is welded to the two crotch plates at crown and invert, but not to the pipe shell. It is recommended that this type of reinforcement be designed as for the two-plate design. The third plate is added to limit deflections, and is simply made equal in depth to the crotch plates where the three join.

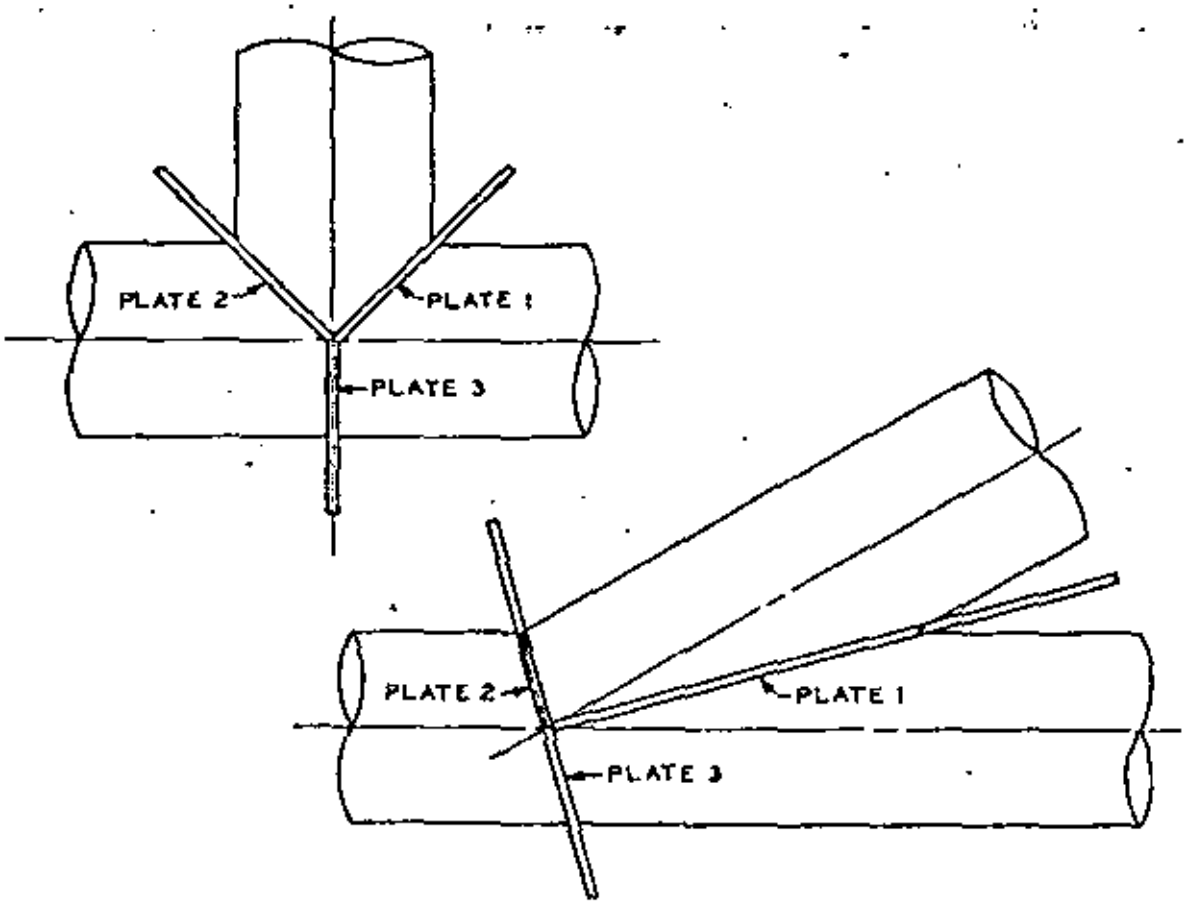

Figure 3-25. Three-plate design.

(4) Simplified Approach. For preliminary design or estimating, the following method of analysis may be useful. The single plate of Figure 3-21 may be considered as a circular ring girder provided that the intersection angle between branches is near 90°. It is further assumed that the girder acts as though it lies in one plane. This is considered approximately correct for a reinforced concrete girder since the reinforcement is embedded in concrete which is confined by rock and cannot be twisted or deflected laterally. The internal load is shown as uniform and unidirectional in Figure 3-26. This is considered to be a conservative assumption. The development of equations for analyses of the circular ring is presented below.

(a) In this development, the thickness of the ring in Figure 3-26 is neglected.

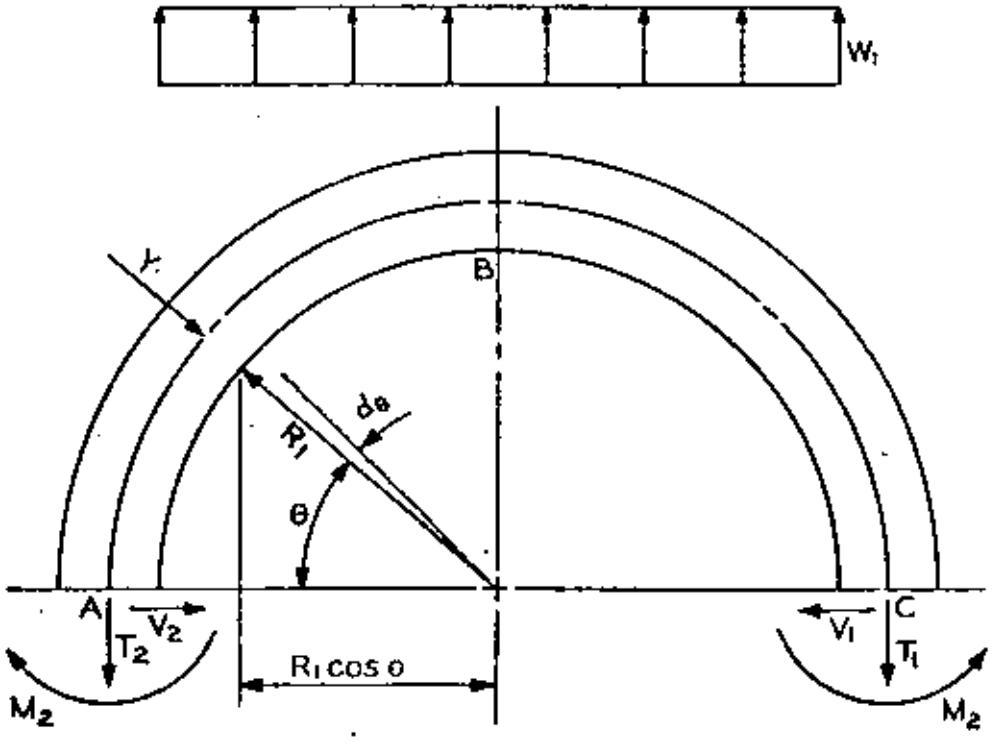

Figure 3-26. Circular girder.

Since horizontal load = 0, $V_1 = V_2 = 0$.

$T_1 = T_2 = W_1R_1$. $T_1 + T_2 = 2\,W_1R_1$

Moment (M_θ) due to internal load at any point,

$$M_\theta = W_1R_1(1 - \cos\theta)\left[\frac{R_1(1 - \cos\theta)}{2}\right] = \frac{W_1R_1^2}{2}(1 - \cos\theta)^2$$

Total moment (M) at any point,

$$M = M_2 - T_2R_1(1 - \cos\theta) + M_\theta$$

$$M = M_2 - T_2R_1(1 - \cos\theta) + \frac{W_1R_1^2}{2}(1 - \cos\theta)^2 \qquad (3\text{-}63)$$

The angular rotation of the member at points A and C will be zero under this loading condition.

$$\int_0^\pi \frac{M ds}{EI} = \int_0^\pi \frac{MR_1 d\theta}{EI} = 0$$

$$\int_0^\pi \left[M_2 - T_2R_1(1 - \cos\theta) + \frac{W_1R_1^2}{2}(1 - \cos\theta)^2\right] R_1 d\theta = 0$$

$$M_2R_1\pi - \frac{W_1R_1^3\pi}{4} = 0$$

$$M_2 = \frac{W_1R_1^2}{4} \qquad (3\text{-}64)$$

(b) At points other than the springline, a radial force is possible (Figure 3-27).

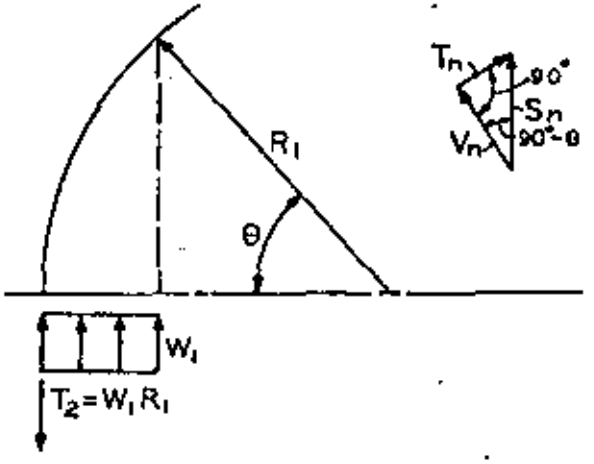

Figure 3-27. Radial force.

$$S_n = T_2 - W_1R_1(1 - \cos\theta)$$

$$S_n = W_1R_1 \cos\theta \qquad (3\text{-}65)$$

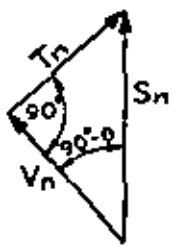

$$T_n = S_n \cos\theta = W_1R_1 \cos^2\theta \qquad (3\text{-}66)$$

$$V_n = S_n \sin\theta = W_1R_1 \sin\theta \cos\theta$$

$$V_n = W_1R_1 \frac{\sin 2\theta}{2} \qquad (3\text{-}67)$$

V_n is maximum when $\frac{dV_n}{d\theta} = W_1R_1 \cos 2\theta = 0$,

Therefore, V_n is maximum when $\theta = \frac{\pi}{4}$ or 45°

At crown (or invert) $\theta = \frac{\pi}{2}$ or 90°, and

$$T_n = W_1R_1 \cos^2 90° = 0$$

$$V_n = W_1R_1 \frac{\sin 180°}{2} = 0$$

The above equations can also be found from Roark[54], Case 11, Table VIII.

(c) In the development that follows, the thickness of the ring shown in Figure 3-26 is now considered. The distance from the inner surface to the centerline of the member is denoted as Y, as shown.

Moment due to internal load at any point,

$$M = W_1R_1(1 - \cos\theta)\left[\frac{R_1}{2}(1 - \cos\theta) - Y\cos\theta\right] \qquad (3\text{-}68)$$

$$ds = (R + Y)\, d\theta$$

$T_1 = T_2 = W_1R_1$ (as stated above)

$V_1 = V_2 = 0$ (as stated above)

Angular rotation at points A and C equals zero, $\Delta\theta = 0$

$$\int_0^{\pi} \left\{M_2 - T_2(R_1 + Y)(1 - \cos\theta) + W_1R_1(1 - \cos\theta)\left[\frac{R_1}{2}(1 - \cos\theta) - Y\cos\theta\right]\right\}(R_1 + Y)\, d\theta = 0.$$

$$(R_1 + Y)\int_0^{\pi} \left[M_2 - W_1R_1(R_1 + Y)(1 - \cos\theta) + \frac{W_1R_1^2}{2}(1 - \cos\theta)^2 - W_1R_1Y(\cos\theta)(1 - \cos\theta)\right] d\theta = 0$$

$$(R + Y)\ M_2 = -W_1R_1 \left(\frac{R_1}{4} + \frac{Y}{2}\right) = 0 \ \ldots$$

$$M_2 = \frac{W_1R_1}{4}(R_1 + 2Y) \qquad (3\text{-}69)$$

As before, the general moment equation is:

$$M = \frac{W_1R_1}{4}(R_1 + 2Y) - W_1R_1(R_1 + Y)(1 - \cos\theta) + \frac{1}{2}W_1R_1^2(1 - \cos\theta)^2 - W_1R_1Y \cdot \cos\theta\,(1 - \cos\theta) \qquad (3\text{-}70)$$

To determine points of maximum and minimum moment, set $\frac{dM}{d\theta} = 0$.

$$W_1R_1(R_1 + Y)\sin\theta + W_1R_1^2(1 - \cos\theta)(\sin\theta) + W_1R_1Y\sin\theta - W_1R_1Y\sin 2\theta = 0.$$

$$-\sin\theta\cos\theta\,(W_1R_1^2 + 2W_1R_1Y) = 0$$

Maximum or minimum moment occurs when $\sin\theta$ or $\cos\theta = 0$. This occurs when θ is equal to 0°, 90° or 180°.

To determine the inflection points, the second derivative of the moment equation is set equal to zero.

$$\frac{d^2M}{d\theta^2} = 0$$

$$\cos 2\theta\,(W_1R_1^2 + 2W_1R_1Y) = 0$$

The inflection points therefore occur at $\theta = 45, 135°$

When the angle of the branch outlet is small and a more accurate analysis than the circular ring assumption is desirable, procedures described in EM 1110-2-2902 can also be used.

3-9. Portal Design.

a. General. Tunnel portals present the following special problems:

(1) They are usually located as near the surface of a valley wall as possible in order to reduce the amount of open cut excavation. Therefore, the rock is likely to be more weathered and of poorer quality than the main tunnel.

(2) The construction of the portal face affects the slope stability to a significant degree because the toe of the slope is unloaded.

(3) At the time of the portal opening, the individual supervisors and workers may not previously have worked together as a crew or had opportunity to develop an understanding of rock behavior at a particular site with the excavation methods being employed.

(4) Historically, portals have often been troublesome and failures have occurred due either to design or construction deficiencies. The most common design error involves the omission of restraint against outward movement of the rock surface. The movement may be visualized as arising from elastic behavior (release of stress) or due to slight movements of rock blocks. Since a limited area is involved, the cost of reinforcement of the surface will be relatively small. Therefore, a conservative approach should be taken by the portal designer. Line drilling or pre-splitting of the rock to be excavated will minimize the damage to the rock left in place. The following paragraphs discuss types of portals and offer general guidelines for portal design which are based on experience and are considered to represent good practice.

b. Basic Portal Criteria. The most important requirement for establishing a portal is that there must be adequate rock cover over the crown of the opening to permit the rock to form a self-supporting arch. The amount of cover required is dependent on the rock at the site. For most projects, the rock at the portal is likely to be the poorest quality at the site. Therefore, a rock cover of two diameters or more is advisable. Consideration may be given to reducing the cover in intact, relatively joint-free, strong rock. Geological explorations must therefore be made in sufficient detail to establish a tentative portal location that has adequate rock cover. It is also desirable to have a horizontal berm, if the topography is favorable, at about two diameters above the crown of the opening. The purpose of this berm is to catch surface rock falls and also to provide a working area for installation of any required vertical rock reinforcement as discussed below. The berm also serves to drain surface water runoff away from the portal area and provides a convenient area to install instrumentation for monitoring rock movement.

c. Stability of Portal Face. The stability of the portal face involves the same considerations as any slope stability problem and is analyzed accordingly. Although the width of a portal cut for a single tunnel is normally relatively small, the effect of the tunnel opening at the toe of the slope must be considered. A two-dimensional slope stability analysis for a single tunnel is considered conservative. Methods of predicting slope stability include soil and rock mechanics methods or a combination of both.

(1) Soil Mechanics. Woodruff[67] states that "when the dimensions of a slope are large as compared with the dimensions of the units of material composing the slope, then conditions favor the analysis of slope stability by the principles of soil mechanics." Since slope stability analyses using soil mechanics methods are discussed in detail in several soil mechanics books, the detailed procedures will not be included here. Until recently, most portal slopes have been analyzed using soil mechanics methods. However, if the slope material is a rock formation containing adversely oriented planes of weakness such as bedding, jointing, faults, or schistocity, failure will probably occur along the orientation established by the rock weakness regardless of relative rock block size. In such cases, the principles of rock mechanics should be used in the analysis.

(2) Rock Mechanics. When a rock slope is composed of rock blocks which are large relative to the height of the bank or slope, principles of rock mechanics should be used to assess the stability of a portal face. In order to predict slope stability using rock mechanics methods, a detailed field investigation is required. Joints, faults, and bedding planes must be located, mapped and their extent determined by methods described in Chapter 2. Shear strengths along the planes of weakness should be determined by laboratory tests and compared to the applied shearing stresses. The rock mass will have the greatest structural strength when pre-existing planes of weakness are oriented approximately normal to the directions of the maximum shearing stress. The rock mass will have the least strength when pre-existing planes of weakness are oriented approximately parallel to the maximum shearing stress.

(3) Combined Rock and Soil Mechanics. In some instances, a combination of the two methods may be required. If the slope is composed of fractured materials, failure may occur along a circular arc as described in texts on soil mechanics. Should the same slope have adversely oriented planes of weakness, then failure may occur as plane shear. Muller[44] states that rock stability and the maximum permissible angle of slope are governed by a number of factors. These are the type and strength of rock, stratifications and foliations, mechanical fragmentation, chemical defects, positional relations between slope plane and structural elements, the time factor, water in rock joints, and the effect of vibrations. The engineer working with the geologist can and should exercise control over several of the factors during the design stage. The portal can usually be oriented advantageously and the time factor can be controlled to some extent by avoiding delays in installation of necessary rock reinforcement or portal structures. The design should also specify controlled blasting to minimize vibration and drainage of the portal area through the use of horizontal drill holes.

d. Earthquake Loadings. Rock and earth slopes that are stable under static conditions have failed when subjected to earthquakes,

Barney[10]. The state-of-the-art for design of slopes to withstand earthquake effects is changing rapidly. The current Corps of Engineers procedure involves application of an additional horizontal force whose value is related to the seismic zone location as described in EM 1110-2-1902. For projects located in seismic zones 2, 3 and 4 which have portal slopes consisting of saturated cohesionless material or rock slopes containing critically oriented weak anomalies, a detailed study of earthquake effects is required if slope failure would preclude the operation of the project. Such studies for cohesionless materials would be similar in scope to those now being utilized for embankment dams constructed by hydraulic means or constructed on a saturated cohesionless foundation as discussed in WES[64].

e. Types of Portals and Portal Treatments. The type of portal support treatment used is dependent on results of the portal face stability analysis. Portal types can generally be classified into the following categories.

(1) No Support of Portal. This can be accomplished only with strong, intact rock that is free of structural defects in the portal area.

(2) Portal Canopy Only. A canopy can be constructed of timber or steel set supports and is used where the rock is generally strong and intact but where surface blocks or pieces of rock above the portal are relatively loose and likely to fall. This treatment is used mainly for personnel safety and does not contribute to the stability of the portal.

(3) Rock Reinforcement. This type of portal treatment has been successfully used in moderately blocky and seamy rock (see Table 3-1). Reinforcement consists of vertical rock anchors installed from a horizontal berm approximately two diameters above the crown and extending downward to the crown. The anchors are not tensioned but are grouted full length and installed before the portal face is excavated. As the portal face is excavated, horizontal rock bolts are placed, tensioned and grouted. With this type of treatment, a component of the restraint or load applied by the reinforcement acts on all joints regardless of their orientation and portal stability is greatly enhanced. The bolts and anchors are installed on a regular pattern usually four feet on center. Since the major cost of the treatment is related to hole drilling, No. 11 (1-3/8" diameter) rock bolts or anchors are normally used. Overbreak is also minimized during portal face excavation. During initial tunneling operations, a portion of the rock immediately above the crown will be carried by the vertical rock anchors. If the rock at the portal is weathered, closely jointed, or subject to slaking, the rock reinforcement is normally augmented with chain link fabric installed over the face, with shotcrete, or with a concrete headwall. An example of this type

of construction is shown in Figure I-11.

(4) Rock Reinforcement and Portal Structure. In the event that the slope stability analysis shows possible instability of the portal face, even with the rock reinforced as described above, portal treatment can be augmented with a concrete portal structure. This will consist of a headwall spanning two sidewalls which act as buttresses, and which must be designed to resist the forces in excess of those resisted by the reinforced rock structure (the reinforced rock mass may be considered to act as a gravity type rock structure). With this type of construction, the rock bolt reinforcement must maintain face stability until the concrete structure is built.

(5) Cut and Cover Section. If the quality of the rock is so poor that construction of the above types of portals cannot be completed without risking a general slope failure in the portal area, a cut and cover section must be used. With this technique, a cut and cover section is constructed as far as practical and necessary into the slope and is then backfilled. This method is desirable where the stability of the entire slope is questionable since the backfill tends to load the toe of the slope to provide stability. Figures J-1 and J-2 are photographs which show construction of this type of portal. Figure I-10 shows a plan and profile of the portal used on the upstream end of the same tunnel.

(6) Shaft as Tunnel Portal. One or more shafts are sometimes used as tunnel access where it is desirable to tunnel from more than two headings. Shaft and intersection excavation and support are discussed in paragraphs 3-10 and 3-8, respectively.

f. Drainage at Portal. It is desirable to provide drainage at all portals. Slope stability analyses using either soil or rock mechanics principles will usually indicate a significant increase in the factor of safety if adequate drainage is provided. Drainage will consist of provisions to guide surface runoff away from the portal area and will include horizontal holes into the portal face. If installed outside the tunnel periphery, drain holes will continue to operate and be effective throughout the construction period and will also serve as exploration holes to further assess the quality of the portal rock before tunneling begins.

g. Portal Entry Design. Steel set supports placed just inside the tunnel portal should be designed to support the weight of rock extending to the berm above the tunnel, if a berm is used. Recommendations for determining the rock load with the use of Table 3-1 are valid only if the height of rock cover is greater than 1.5 times the sum of width and the height of the tunnel. It is considered good practice to use steel set supports of a circular shape which extend a minimum of two tunnel diameters from a portal, if possible. Horizontal rock bolts should be installed at close spacing around

the tunnel periphery and fully grouted, prior to making portal entry. The rock bolts will tend to prevent excessive overbreak in the portal area during the first crucial rounds of tunnel excavation and help maintain stability.

3-10. Design of Shafts.

a. Initial Support. Shafts will require initial rock support (steel set supports, rock reinforcement or shotcrete) similar to that used for tunnels. Design procedures are also similar for a shaft and a tunnel except that treatment is carried for a full 360 degrees in a shaft. The main difference is in determining the loads to be applied to the supports. Just as with tunnels, support loads are found by the methods described in paragraph 3-3. A percentage of the loads estimated for tunnels is used for loads on shaft support. In most rocks, 50 percent of the tunnel load is adequate for shafts. If the shaft is to be placed in a rock containing montmorillonite or other material that tends to swell or when squeezing rock is expected then the full load estimated for a tunnel in the same material should be used for a shaft. The direction of the bedding will also tend to influence the load that is taken by the initial support system. When the bedding is horizontal, the smaller values obtained from Table 3-1 for the particular rock condition should be used. As the dip of the bedding increases, so will the rock load; therefore, values near the top of the range for the particular rock condition should be used. If the shaft is mechanically mined, the recommended loading can be decreased. At this time, observed data are not available for making a firm recommendation on loading; however, Table 3-3 does provide some guidance on rock load relationships between machine and conventional mining methods. Although recommendations for loading on the initial support system may be considered conservative, the additional cost will be small since shafts used on Corps of Engineers projects are usually not deep. More lagging should also be used in shafts than in tunnels because all loose rock falls to the bottom of the shaft. Chain link fabric or shotcrete may be considered in lieu of lagging.

b. Linings. Shafts are lined in the same manner as tunnels and should be designed as outlined in paragraphs 3-7 and 3-8. Shafts located upstream from the impervious core are rarely steel lined. However, downstream shafts for surge tanks should follow the same criteria as for penstock tunnels.

3-11. Tunnel Drainage.

a. Drainage System. The drainage system required in a tunnel will depend on the type of tunnel, its depth, and ground water conditions. Some tunnels may not require special drainage. Others may require drainage to limit the pressure behind the lining or to remove water due to condensation and leakage through the tunnel joints. A detailed design procedure for drains will not be attempted

here; however, a brief description will be included to indicate what is involved in providing drainage for the various types of tunnels.

(1) Pressure Tunnels. Drainage for pressure tunnels may be required if normal outlets through gates or power units do not accomplish complete unwatering of the tunnel. The drains are then located at the low point of the tunnel and are provided with a shut-off valve. In some cases, it is desirable to provide drainage around a pressure tunnel. This may be done to limit the external head on the lining or to limit pressures in a slope in the event leakage developed through the lining. Drainage may be provided by drilling holes from the downstream portal or by a separate drainage tunnel. An example of a separate drainage tunnel is shown in Figures I-8 and I-9.

(2) Outlet Tunnels. Drainage for outlet tunnels may be required to completely unwater the tunnel if some point along the tunnel is lower than the outlet end. To limit the external head, drains can be provided that lead directly into the tunnel. In this manner, the outlet tunnel also serves as a drain tunnel.

(3) Vehicular Tunnels. Drainage for vehicular tunnels will usually consist of weep holes to limit the pressure behind the lining and an interior drain system to collect water from condensation and leakage through the joints in the lining. Interior drainage can be either located in the center of the tunnel between vehicular wheel tracks or along the curbs. If the tunnel is located in areas where freezing temperatures occur during part of the year, precautions should be taken to prevent freezing of the drains. If the tunnel is long, protection against freezing need not be installed along the entire length of tunnel, depending on the climate and depth at which the tunnel is located.

(4) Drain and Access Tunnels. Drainage from these tunnels may require a sump and pump, depending on the location of the outlet end. Drain tunnels usually have drain holes that extend from the tunnel through the strata to be drained.

(5) Waterstop. To prevent uncontrolled water seepage into a concrete lined tunnel, the construction joints are waterstopped. EM 1110-2-2102 covers the types and use of waterstop.

b. Grouting. Grouting in connection with tunnel construction is covered in paragraph 20 and Plate 5 of EM 1110-2-3501. Recommendations are made below regarding special grouting treatment typically required to prevent drainage problems in various types of tunnels or shafts. Ring grouting (i.e., grouting through radial holes drilled into the rock at intervals around the tunnel periphery) is used to reduce the possibility of water percolating from the reservoir along

the tunnel bore and for consolidation grouting along pressure tunnels. Contact grouting refers to the filling of voids between concrete and rock surfaces with grout.

(1) Outlet Works Tunnels. As a minimum, the crown of outlet works tunnels should be contact grouted for their entire length. Grouting to prevent water from percolating along the tunnel bore should consist of a minimum of one ring, interlocked with the embankment grout curtain. If the impervious core of the embankment extends upstream from the grout curtain and sufficient impervious material is available between the tunnel and the base of the embankment, the location near the upstream edge of the impervious core also should be ring grouted. The ring grout holes should extend into the rock approximately one tunnel diameter.

(2) Pressure Tunnels. Pressure tunnel linings are designed in two ways. Either the concrete and steel linings act together to resist the entire internal pressure or concrete and steel linings and the surrounding rock act together to resist the internal pressure. Contact and ring grouting for pressure tunnels is done the same as for outlet tunnels except one additional ring should be grouted at the upstream end of the steel liner. Consolidation grouting of the rock around the lining of a pressure tunnel and the filling of all voids is a necessity if the rock is to take part of the radial load. Consolidation grouting of the rock behind the steel liner is good practice and should be done whether or not the rock is assumed to resist a portion of the internal pressure.

(3) Shafts. Shafts are normally grouted the same as tunnels except that grouting is done completely around the shaft in all cases.

3-12. Design Loads for Supports and Linings in Tunnels and Large Chambers at Shallow Depths. At shallow depths, the compressive stresses due to gravity may be so small that rock blocks will have a tendency to fall out of the face, the crown and the side walls. Under these circumstances, the design is controlled more by the equilibrium of individual blocks, without the benefit of large normal forces to develop frictional resistance, than by the magnitude of the external pressure. Methods for evaluating design loads based on knowledge of the actual geometry of rock joints around the underground opening are discussed in Cording and Deere[24]. It is fairly difficult to accurately determine the jointing but approximations can be made through the use of exploration techniques such as oriented core, full core recovery samplers, inspection adits and possibly calyx holes. An estimate must also be made of the shear strengths along the joint surfaces. Rock loads can then be estimated by considering various combinations of joints which can form critical large wedges or rock at failure along the joints. Methods for minimizing support loads by using excavation and support procedures which prevent

extensive loosening of rock blocks are also discussed in the above reference. Additional discussion on the support of large caverns is contained in Cording, Hendron and Deere[23].

INSTRUMENTACION

CONTENIDO

1. INSTRUMENTACION DE MECANICA DE ROCAS

1.1 Introducción

El objeto de la instalacion de instrumentos de medición en los macizos rocosos es el de verificar el comportamiento previsto o calculado, por efecto de la ejecución de obras de ingeniería tales como: cimentaciones, excavaciones subterráneas o a cielo abierto y estabilidad de taludes naturales o artificiales, por otro lado, constituyen elementos de alarma contra posible falla.

Para esto es necesario utilizar dispositivos de medición superficiales, así como, instalar aparatos dentro de barrenos para medir desplazamientos longitudinales y transversales.

2. DISPOSITIVOS DE MEDICION DENTRO DE BARRENOS

2.1 Extensómetros longitudinales

2.1.1. Extensómetro tipo Comisión Federal de Electricidad.

Miden desplazamientos relativos entre 4 "puntos fijos" localizados a diferentes niveles dentro de una perforación y el dispositivo de medición colocado en la superficie del terreno. Los desplazamientos son transmitidos por alambres de acero al dispositivo de medición, el cual tiene montados 8 resortes de tensión constante de 4.5 kg de capacidad, montados en cilindros embalados. El alambre pasa enrollándose en una polea cuyo eje está acoplado a un potenciómetro eléctrico radial. Este dispositivo tiene una precisión de ± 0.25 mm.

Los alambres y los puntos fijos se encuentran dentro de tubos de PVC, Ø 2". La tubería se llena con aceite diesel para proteger

los alambres de la corrosión.

El tubo de PVC Ø 2" se introduce en barrenos Ø 4" y se cementa a las paredes del barreno con mortero de cemento-arena-bentonita. En la Fig. 1 se presenta esquemáticamente este dispositivo. Requiere calibración.

2.1.2. Extensómetros longitudinales Tipo Terrametrics

Estos extensómetros miden también desplazamientos diferenciales entre "puntos fijos" colocados dentro de barrenos a diferentes niveles y el dispositivo de medición que se encuentra en la superficie. Los "puntos fijos" están constituidos por crucetas de picos que se abren mecánicamente y se encajan en la roca. Los desplazamientos se transmiten a través de alambres que conectan los puntos fijos con los extremos de una soleras que trabajan en voladizo. Estas soleras están instrumentadas con celdas de deformación eléctricas (strain gages). Requiere calibración. Geosistemas, S.A. ha modificado el sistema de medición utilizando extensómetros mecánicos de carátula (micrómetros) para medir los desplazamientos que son amplificados trabajando la solera de apoyo de los alambres como palanca. En la Fig. 2 puede verse el dispositivo. No se recomienda el uso de este dispositivo cuando tiene los "straingages" y se utiliza en ambiente húmedo pues se pierde el aislamiento eléctrico de las celdas.

2.1.3. Extensómetros de barra

Estos extensómetros miden también desplazamientos relativos entre "puntos fijos" dentro de barrenos y la superficie donde se encuentra el dispositivo de medición. Los desplazamientos se

transmiten a través de barras de acero llenas o huecas. El medidor puede ser mecánico o eléctrico. Tiene buena aceptación, pues no tiene el problema de fluencia que se presenta en los extensómetros a base de alambres. En la Fig. 3 puede verse esquemáticamente un extensómetro con 4 barras independientes. Existen diseños de este dispositivo que permite alojar 2 barras dentro de un barreno.

2.2.- Extensómetros longitudinales de deformación transversal

2.2.1. Inclinómetros

Los inclinómetros están constituidos por tubos de aluminio o de PVC, que tienen 4 ranuras a 90°. Se utilizan para medir desplazamientos verticales y horizontales dependiendo del tipo de sonda utilizada.

En rocas se utilizan únicamente para medir desplazamientos horizontales utilizando sondas de alta precisión.

Tipos de sondas:

Sonda Slope Indicator de péndulo y potenciómetro eléctrico
Sonda Slope Indicator de acelerómetros.
Sonda Geosistemas de péndulo instrumentada con strain gages
Sondas de medición magnéticas

Las sondas se calibran en un goniómetro obteniéndose de esta manera el número de unidades por grado de inclinación. Conocida esta constante los desplazamientos horizontales pueden integrarse a lo largo del tubo del inclinómetro.

En la Fig. 4 se presenta esquemáticamente este dispositivo.

2.2.2. Extensómetro transversal

Estos extensómetros están diseñados por Slope Indicator, para medir desplazamientos sobre un plano perpendicular al eje del instrumento, de 3 a 6 puntos localizados a diferentes elevaciones dentro de una perforación.

Los puntos de medición (elementos sensibles) están constituidos por un potenciómetro longitudinal montado en un péndulo accionado por una muelle de horquilla que obliga a mantener en contacto al potenciómetro con un alambre revestido de plata, que se mantiene tensado entre dos "puntos fijos" que se ubican fuera de la zona de influencia de los desplazamientos ocasionados por las excavaciones. Los desplazamientos de los elementos sensibles son relativos a estos puntos fijos, y se miden indirectamente por la posición que guarda la resistencia respecto al alambre plateado.

Tanto el alambre plateado como los elementos sensibles quedan introducidos en tubos de PVC de 4" de diámetro, el cual se llena con aceite dieléctrico de transformador para mejorar el aislamiento eléctrico del potenciómetro. Este aparato requiere calibración y tiene una precisión aproximadamente de 0.1 mm. En la Fig. 4-a se presenta esquemáticamente este dispositivo.

3. MEDICIONES SUPERFICIALES

3.1. Extensómetro longitudinal portátil

3.1.1. Extensómetro de cinta o alambre invar, portátil

Este dispositivo se utiliza para realizar mediciones de desplazamientos sobre la superficie de terreno, entre bases metálicas o de concreto fijas al terreno.

Los desplazamientos se miden indirectamente por medio de potenciómetros eléctricos. La cinta o el alambre invar son mantenidos en tensión por resortes de tensión constante (tipo cuerda de reloj). Requiere calibración previa. El tamaño máximo de la cinta o alambre es del orden de 10 m. La precisión es de 0.1 mm a 0.2mm. En la Fig. 5 se presenta esquemáticamente este dispositivo.

3.1.2. Extensómetro de cinta con resorte de tensión variable

Este extensómetro es muy sencillo y mide desplazamientos entre bases fijas al terreno. Se utiliza una cinta graduada de 20 m, calibrada por tensión y temperatura. La tensión es proporcionada por un resorte helicoidal de tensión variable también calibrado. La lectura se realiza visualmente en la cinta al pasar por una marca, de manera que puede leerse con precisión 0.5 mm. En la Fig. 6 se presenta esquemáticamente este dispositivo.

3.2. Extensómetro "invar wire" tipo Cambridge

Este extensómetro ha sido desarrollado por la Universidad de Cambridge para la medición superficial dentro de galerías de desplazamientos horizontales que ocurren en la corteza terrestre por efecto de atracción lunar (marea terrestre).

El dispositivo mide desplazamientos entre dos puntos fijos en la superficie de roca, ligados por un alambre invar de ϕ=0.5 mm tensionado constantemente por una pesa, los desplazamientos son amplificados por un sistema de palanca articulada, midiéndose los desplazamientos por medio de un LVDT. Cuando el desplazamiento es tal que el LVDT está operando fuera de su intervalo lineal, op

un servomotor que hace girar un tornillo sin fin que desplaza un contrapeso para aumentar o disminuir la tensión en el alambre, hasta que el LVDT registra nuevamente en el intervalo lineal.

En la Fig. 7 se presenta esquemáticamente este dispositivo. Es de alta precisión, del orden de 0.05 mm y después del rayo Lasser es el dispositivo más económico.

3.3. Mira móvil de colimación

Esta mira se utiliza para medir desplazamientos superficiales horizontales entre bases sujetas al terreno. La medición se utiliza empleando colimadores o tránsitos que definen una línea entre las bases extremas de referencia. En las bases intermedias se coloca esta mira constituida por una regla graduada de acero inoxidable y buena calidad sobre la que se desplaza una mira usual de telemetría de tipo "mariposa". Haciendo coincidir la línea de colimación con la marca de la "mariposa", las lecturas de la posición relativa de la "mariposa" se leen en la regla graduada en forma visual. Su precisión es del orden de 0.2 mm. En la Fig. 8 se presenta un dibujo de este dispositivo.

3.4. Telurómetros

Los telurómetros se utilizan para la medición de puntos localizados en la superficie del terreno a distancias entre 500 m a 2 km. El sistema utilizado es de trilateración y se utiliza principalmente para el control de estabilidad de taludes en presas o en minas explotadas a cielo abierto. Ver Fig. 8-a.

3.4.1. Telurómetro a base de ondas de radio

Este telurómetro tiene una precisión del orden de 2 mm en 1 km. La medición entre dos puntos se realiza determinando el tiempo que tarda una onda de radio en recorrer la distancia de ida y vuelta entre dos estaciones. Requiere calibración por temperatura y altitud.

3.4.2. Telurómetro a base de rayos infrarrojos

Este telurómetro tiene una precisión también del orden de 2 mm en 1 km, funciona también midiendo el tiempo de ida y vuelta del rayo entre dos puntos fijos. Requiere corrección por temperatura y densidad del aire, pero esta operación la realiza automáticamente con una computadora electrónica. Es el aparato comercial de mayor precisión para medición de grandes distancias después del rayo Lasser.

3.5. Rayo Lasser

El rayo Lasser se emplea también en la medición superficial entre bases fijas al terreno para distancias superiores a 500 m, es el dispositivo de mayor precisión existente en la actualidad pues no es afectado por temperatura y densidad del aire. Aun no está desarrollado comercialmente y por eso ha tenido poco uso. Se le ha utilizado en mediciones de desplazamientos de la corteza terrestre por efecto de atracción lunar en California, U.S.A. En la Fig. 9 se presenta este dispositivo.

3.6. Nivelación de precisión con aparato fijo

También es usual el uso de niveles de precisión para medición desplazamientos verticales superficiales tanto en excavaciones

subterráneas como a cielo abierto. Para contro. de taludes de c. nales de presas y tajos de explotación minera a cielo abierto. Estos aparatos deben tener por lo menos una precisión de 0.1 mm, los hay de 0.01 mm pero por consiguiente es más lenta y cara la medición pues requiere hacerse en intervalos cortos de tiempo, pues también la corteza queda afectada por desplazamientos verticales por la acción de mareas terrestres. (Se ha medido que toda la América se desplaza aproximadamente 2 cm en dirección vertical diariamente, lo cual da lugar a desplazamientos horizontales relativos de 0.5 mm en 10 m).

3.7. Nivel de precisión de manguera

Este dispositivo se utiliza fundamentalmente en la medición de asentamientos diferenciales en estructuras para edificios urbanos e industriales. Utiliza el principio de vasos comunicantes y la medición del nivel se realiza con tornillos micrométricos. Su precisión es del orden de 0.1 mm, requiere corrección por temperatura. En la Fig. 10 se presenta esquemáticamente este dispositivo.

3.8. Vertedores

Estos dispositivos se utilizan en la medición de desplazamientos verticales de estructuras de edificios urbanos e industriales, tanques y presas. El sistema opera a base de vasos comunicantes: el vertedor que es un pequeño recipiente cilíndrico con la cara superior vertedora y la inferior conectada a una manguera que en su otros extremo está conectada a un recipiente de agua (bureta) con un indicador de nivel graduado. Este indicador de nivel puede colocarse en una superficie considerada fija, pero si tam-

es móvil, entonces por medio de nivelación a puntos fijos se puede conocer los desplazamientos relativos y totales entre el punto del vertedor, el punto del medidor y el punto base fijo. La precisión es del orden de 0.2 mm, tiene gran aceptación por ello, por su bajo costo y facilidad de instalación.
En la Fig. 11 se presenta un esquema de su funcionamiento.

4. MEDICION DE VIBRACIONES

4.1. Efectos de explosivos en estructuras y cimentaciones

Con objeto de estudiar los efectos que causan el uso de explosivos sobre estructuras y cimentaciones superficiales y subterráneas se han utilizado vibrógrafos para medir la velocidad, aceleración y desplazamiento de la partícula. Con estos dispositivos puede determinarse los valores límites que deben alcanzar estos parámetros cuando se usan explosivos cercanos a las estructuras mencionadas. De este tipo son el Amplígrafo de Nitro Consult, y el Vibrógrafo SV2 y SV3 de Slope Indicator Co.
En las Figs. 12 y 13, pueden verse estos dispositivos.

5. MEDICION DE CARGAS EN ANCLAS

5.1 Celdas de presión hidráulica

Estas celdas de presión hidráulica se utilizan para la medición de la evolución de cargas en anclas, pueden ser del tipo gato plano Freyssinet con agujero al centro, o de pistón perforado como el realizado por Geosistemas, S.A. En la Fig. 14 se presenta la celda Geosistemas. Estas celdas requieren calibración y no son afectadas de manera importante por humedad y temperat

5.2. Celdas instrumentadas con "strain gages"

Este tipo de celda es de alta precisión, pero no es buena para utilizarse en ambientes húmedos. Requiere calibración previa. En la Fig. 15 se presenta un dibujo de la misma, marca KYOWA.

6. MEDICION DE FRACTURAMIENTO

6.1 Métodos acústicos

Crandell ha diseñado un dispositivo de medición de ruidos de alta precisión el cual puede colocarse dentro de barrenos realizados en túneles. El aumento de ruido representa avance del fracturamiento, de modo que estadísticamente puede preverse el colapso de la caverna. Se ha observado en ensayes de laboratorio que cuando la carga de compresión alcanza un 80% de la carga de ruptura se produce un cambio importante en aumento de ruido, el cual continúa en forma intermitente hasta la falla. Este dispositivo ha tenido poco uso, pues es muy difícil evitar el ruido normal existente en los túneles por las actividades desarrolladas dentro del mismo.

En la Fig. 16 se presenta este dispositivo.

6.2.- Método de refracción microsísmica

Obert y Duvall han desarrollado un dispositivo de medición de vibraciones proveniente de avance de fracturamiento, son geófonos de alta precisión. Tiene las mismas limitaciones de uso del dispositivo de Crandell.

En la Fig. 17 se presenta este dispositivo.

7.- MEDICIONES REALIZADAS EN LA P.H. LA ANGOSTURA, CHIS.

La Comisión Federal realizó mediciones de desplazamientos en las estructuras componentes más importantes de la Obra. Se realizaron mediciones superficiales y dentro de perforaciones.

7.1.- Túneles de Desvío

Los túneles de desvío localizados uno en cada margen del Río Grijalva, tienen 14.5 m de diámetro interior y aproximadamente 650 m de longitud.

El diámetro revestido es de 13 m.

En cada túnel se instalaron dos secciones de control consistentes cada una de tres aparatos. Un extensómetro longitudinal de alambres y potenciómetros, localizado en el eje vertical del túnel con 4 puntos de medición y dos extensómetros transversales laterales tipo Slope Indicator de elementos sensibles a base de potenciómetros longitudinales.

La localización de estos aparatos se presenta en la Fig. 19.

Los resultados de las mediciones de los extensómetros longitudinales y transversales se presentan en las Figs. 19 y 20.

En la Fig. 21 se representa de manera diferente las mediciones obtenidas con estos paratos en el túnel de desvío No. 2 de la margen derecha.

En la Fig. 20 puede verse un desplazamiento diferido con el tiempo en la zona de la clave del túnel el cual se suspendió después de colocar el revestimiento de concreto.

En la Fig. 20, puede apreciarse que en la 1a. etapa de excava-

ción los desplazamientos horizontales de la mitad superior hacia afuera del túnel y hacia aguas abajo, que es la dirección que traía el avance de la excavación. Los desplazamientos horizontales son registrados en ambos túneles mayores del lado del cantil del río, donde el confinamiento es menor.

7.2. Canales vertedores

La presa tiene dos canales vertedores cuyas dimensiones son: 25 m en la plantilla, 50 m en la corona, 50 m de profundidad y longitud aproximada de 900 m.

Para estudiar los desplazamientos de los taludes se instalaron tres líneas de referencias superficiales paralelas a la traza de uno de los canales. Las mediciones entre bases en dirección perpendicular al corte de los taludes se realizó mediante extensómetro portátil con cinta invar de 5 m de longitud, así como por sistema de colimación y mira móvil. Además se instrumentaron tres secciones de control a lo largo de ambos canales constituidas por 4 extensómetros longitudinales de alambre y potenciómetros eléctricos en ambas paredes de cada canal.

La posición de las referencias superficiales se presenta en la Fig. 21 y los resultados de medición en una de las secciones de control con bases superficiales se presenta en la Fig. 22.

Los resultados de las mediciones con extensómetros e inclinómetros en las tres secciones de control pueden verse en las Figs. 23, 24 y 25.

Superficialmente con el sistema de bases fijas al terreno y extensómetro portátil de cinta no se detectaron desplaza-

mientos importantes que implicaran falla total del talud. Unicamente se registraron desplazamientos importantes (1.5cm) en zonas de falla local del talud. Los taludes de ambos canales han permanecido estables desde su excavación hace aproximadamente 5 años hasta la fecha.

Los resultados comparativos entre los desplazamientos horizontales de la pared del talud en las secciones de control, medidos con extensómetros longitudinales e inclinómetros son congruentes, habiéndose registrado desplazamientos de las paredes de los canales hacia adentro del canal, del orden de 2.5 cm. En estas mediciones puede observarse claramente el efecto de los explosivos durante la excavación, pues en ocasiones los desplazamientos de las paredes de la roca son hacia el macizo rocoso por el efecto de cargas de precorte y cargas de fondo en los barrenos. Tampoco en estas secciones de control se presentó ni se ha presentado tendencia a falla total del talud.

7.3.- Casa de máquinas

La casa de máquinas de la P.H. La Angostura está alojada en una caverna de las siguientes dimensiones: 20 m de ancho, 40 m de alto y 120 m de largo. El comportamiento de bóveda y paredes fue estudiado mediante la instalación de extensometros longitudinales con potenciómetro eléctrico sobre la bóveda y con extensómetros transversales tipo Slope Indicator e inclinómetros en paredes y crimpano del lado del río.

Los instrumentos se colocaron en tres secciones transversales al eje de la caverna utilizando galerías excavadas exprofeso y ubicadas a 11 m por arriba de la bóveda de la caverna.

Cada galería contenía 5 extensómetros longitudinales hacia abajo del piso de las galerías y 5 extensómetros longitudinales hacia arriba del techo de la galería. Cada extensómetro constaba de 5 puntos fijos y sus longitudes hacia arriba eran variables entre 50 m y 110 m. En cada extremo de estas galerías se colocaron inclinómetros paralelos a los paredes de la excavación y en los extremos de dos ellas se instalaron extensómetros transversales para verificar los desplazamientos obtenidos con los inclinómetros.

En la Fig. 19 puede verse la localización de los instrumentos en la casa de máquinas.

De acuerdo con los resultados de la medición del estado de esfuerzos interno de la roca se verificó la existencia de un esfuerzo tectónico horizontal paralelo al río de 80 kg/cm^2, o sea perpendicular a las paredes de la casa de máquinas, ello obligó a utilizar un anclaje sistemático en ambas paredes a base de anclas de tensión de concha expansora tensadas a 10 ton.

En la Fig. 26 se presentan los desplazamientos verticales medidos sobre la bóveda, en la galería 2, en la que puede verse que los desplazamientos hacia abajo fueron muy pequeños, del orden de 1 mm, y que se presentan algunos desplazamientos hacia arriba

En las Figs. 27, 28 y 29, se presentan los desplazamientos horizontales medidos en las tres galerías con los inclinómetros y extensómetros transversales, para la última etapa de excavación, en las que puede observarse una buena concordancia de las medi

ciones realizadas con ambos aparatos. Los desplazamientos máximos observados se presentan en la parte inferior y son del orden de 6 mm y corresponden más bien a los desplazamientos calculados por el método del elemento finito por el Instituto de Ingeniería para esfuerzos horizontales de peso propio, mientras que los desplazamientos verticales observados corresponden a los teóricos calculados si existiera un esfuerzo tectónico horizontal de 80 kg/cm^2.

El autor interpreta que ello puede deberse a que en todo lo alto de las paredes el esfuerzo tectónico horizontal no se transmite en toda su intensidad por las discontinuidades ocasionadas por los tünes de presión del lado aguas arriba y por los pozos de oscilación del lado de aguas abajo, mientras que sobre la bóveda la roca presenta continuidad horizontal y por tanto buena transmisión del esfuerzo tectónico que origina desplazamientos verticales hacia arriba en la bóveda de la caverna.

En la Fig. 30 se presenta la comparación de los desplazamientos de las paredes calculados y medidos, presentada por Jesús Alberro del Instituto de Ingeniería, al Congreso Internacional de Denver, 1974.

8.- RECONOCIMIENTOS

Los trabajos de instalación de instrumentos y procesamiento de datos de los trabajos realizados por la Comisión Federal de Electricidad en Angostura, fueron realizados por los Ings. Javier Hernández Utrilla, Carlos Bernal Montemayor, Raúl Ramírez Aranda y Mario Fernández Bifuentes.

9. BIBLIOGRAFIA

Catálogo Terrametrics

Catálogo Slope Indicator

Catálogo Kyowa

Catálogo Geositemas

Rock Mechanics and the design of structures in rock.-Obert y Duvall

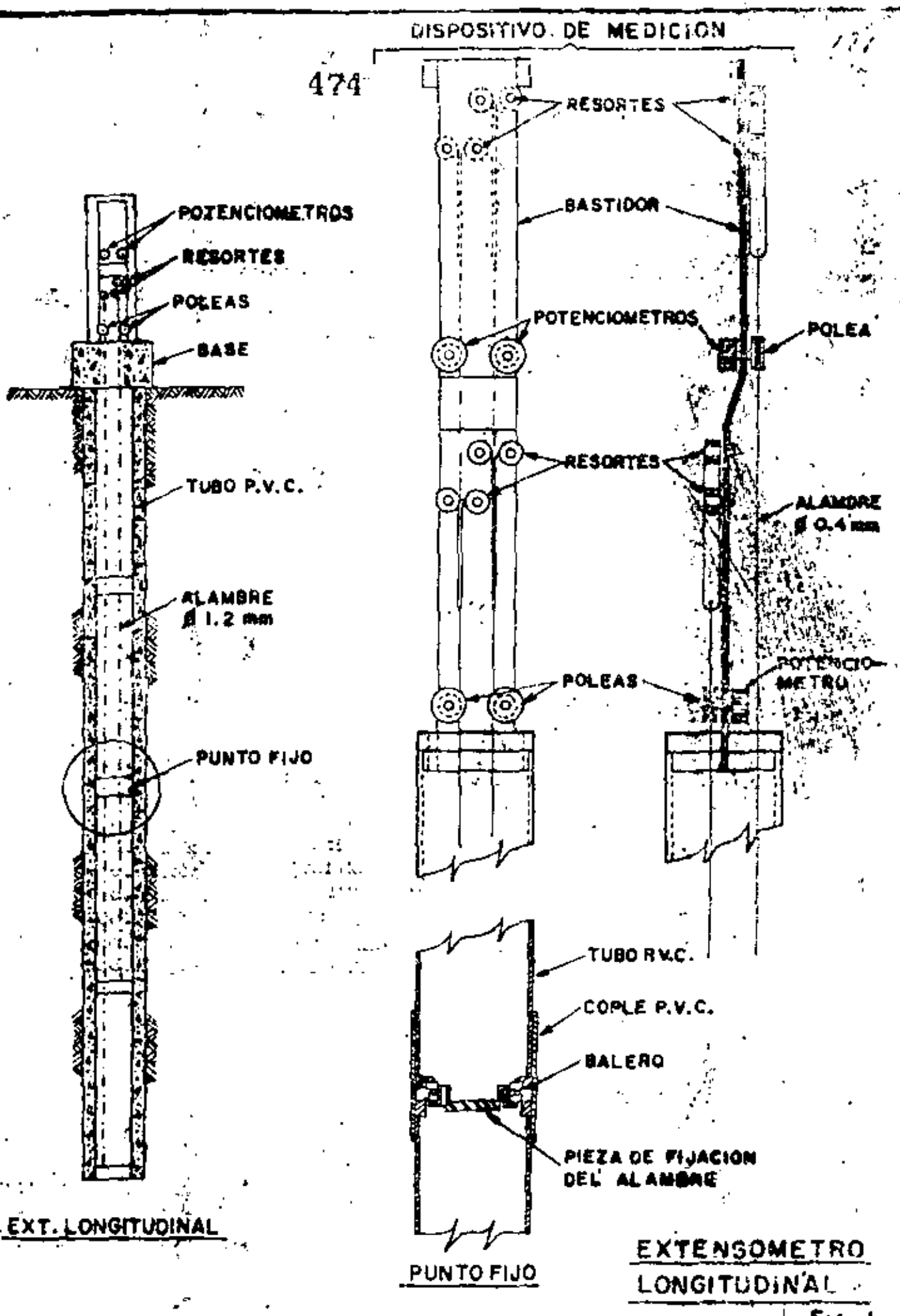

EXTENSOMETRO LONGITUDINAL

FIG. 1

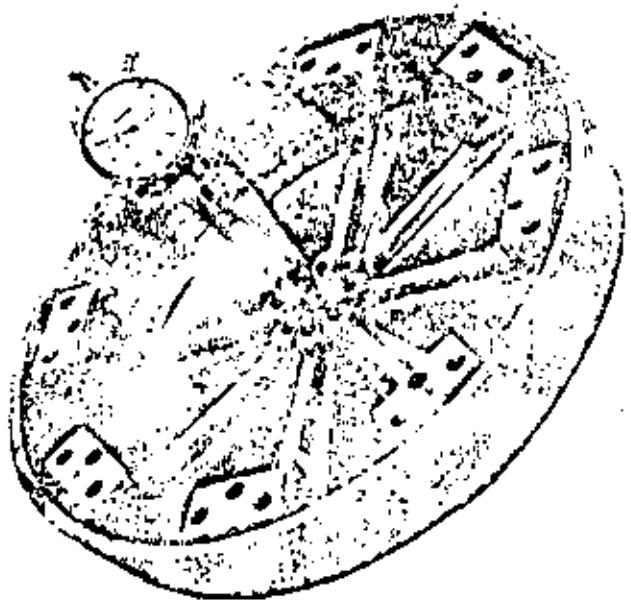

Bocina del extensómetro mecánico de posición múltiple.
Mod. GS-EM8

EXTENSOMETROS LINEALES Y DE POSICION MULTIPLE

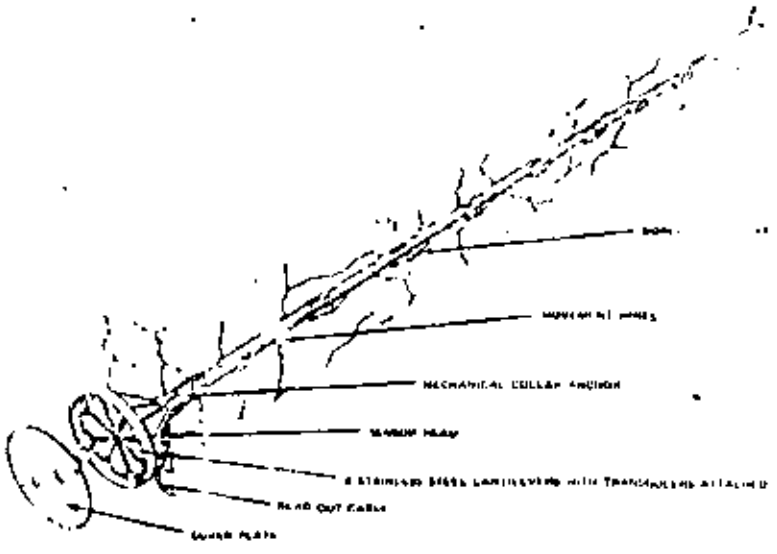

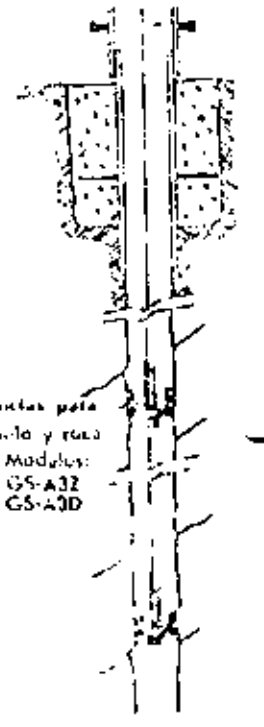

Anclas para suelo y roca
Modelos:
GS-A32
GS-A3D

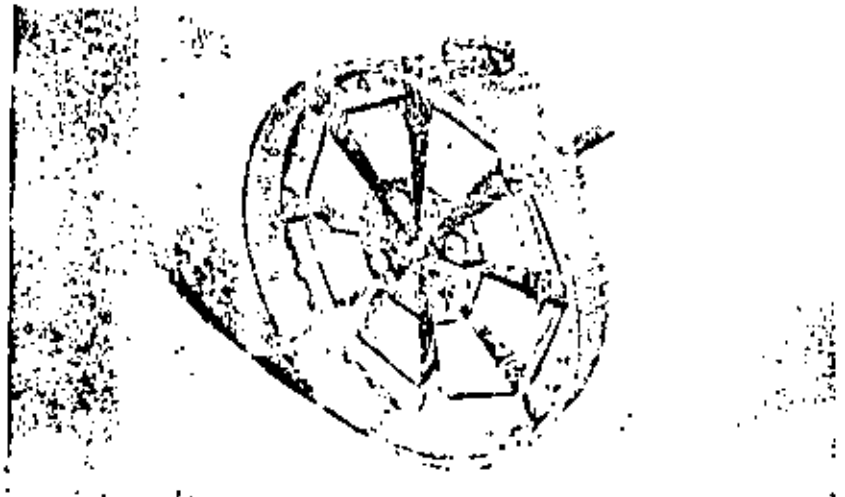

Detalle de la fijación del ancla en la boca del barreno

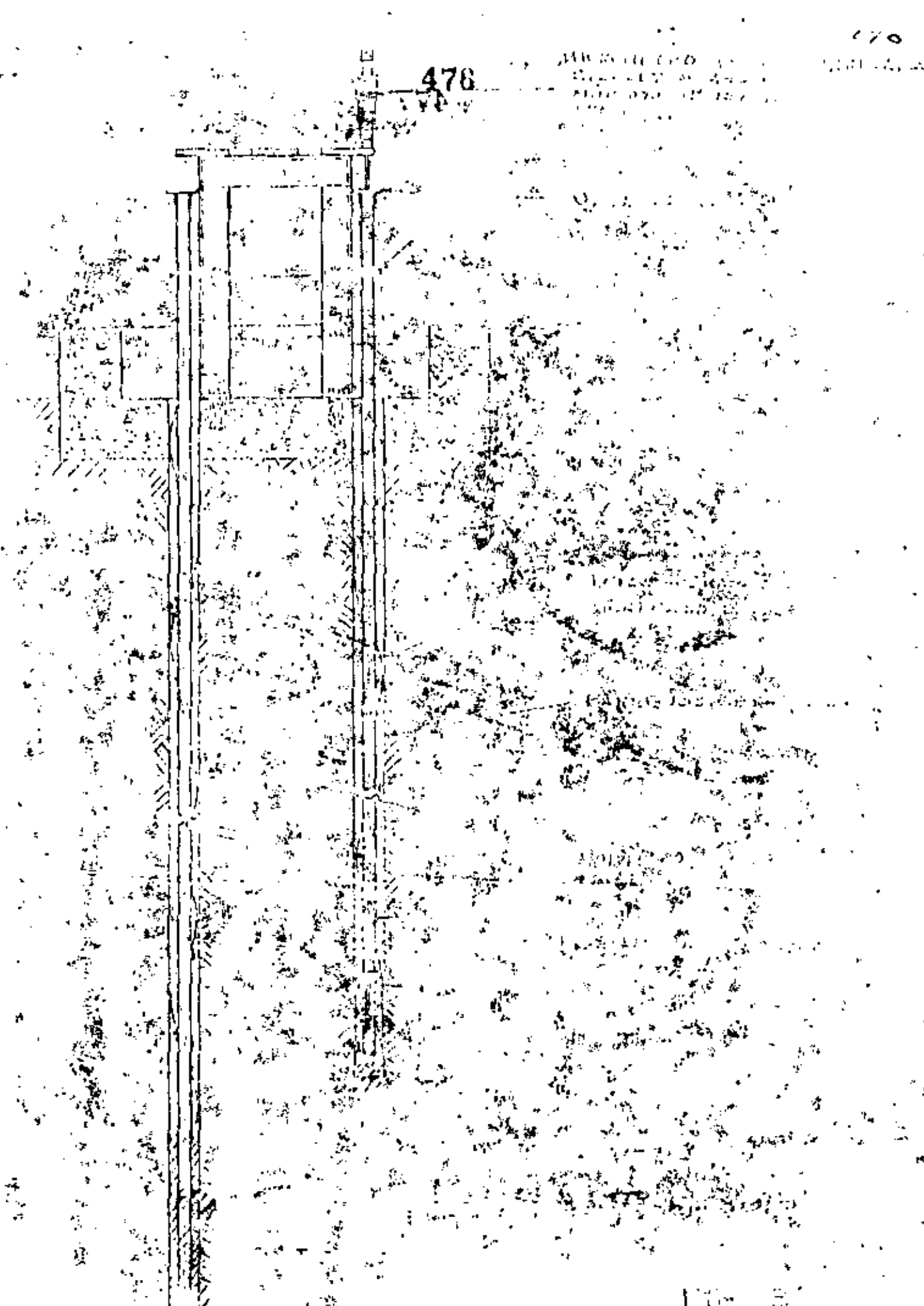

DIGITAL INCLINOMETER

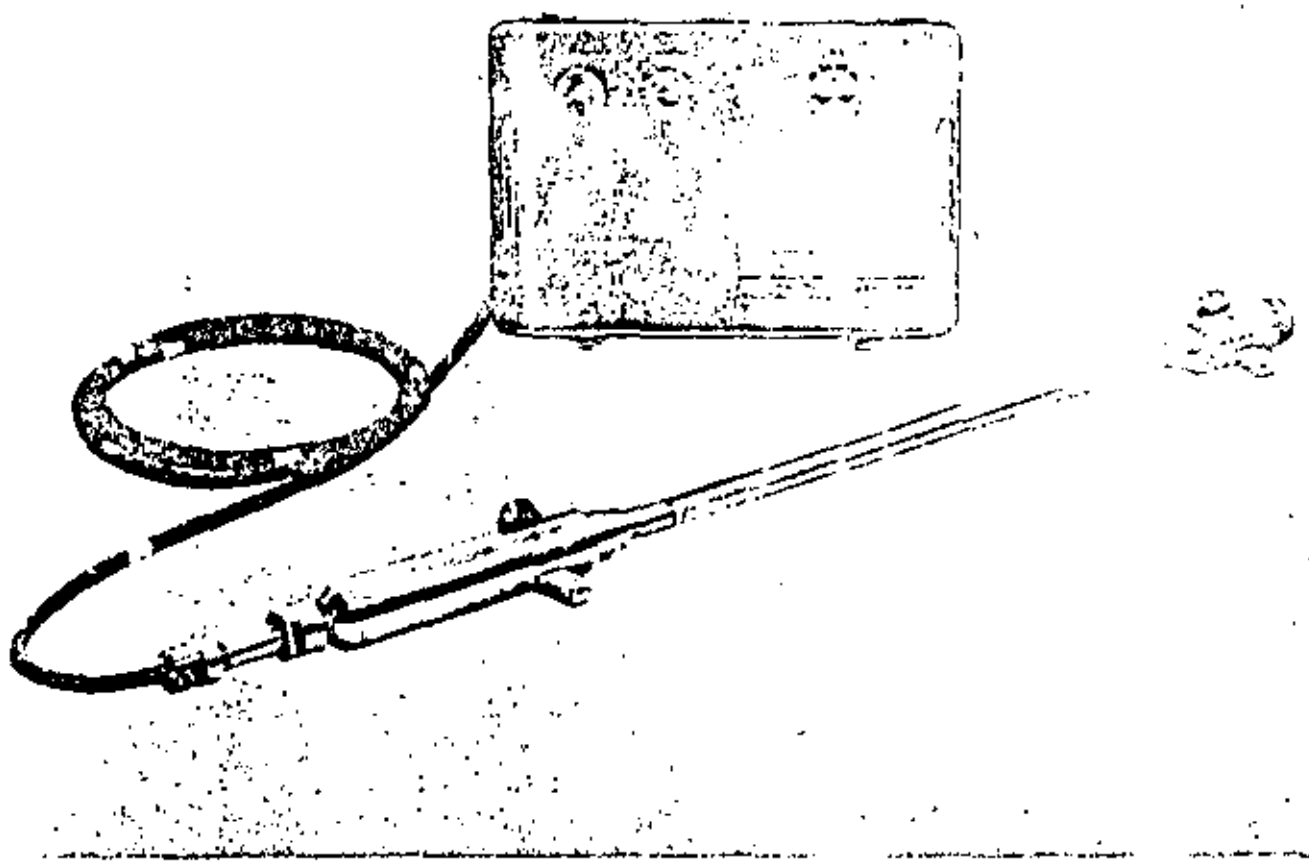

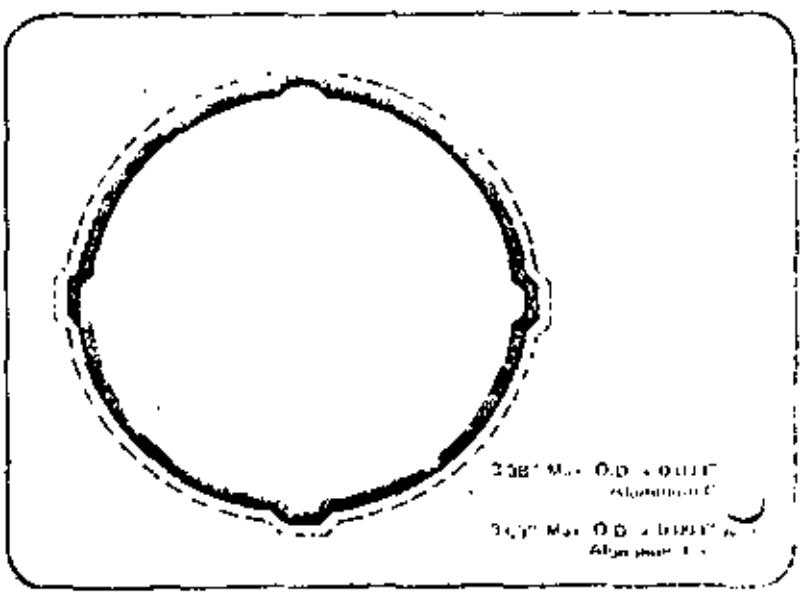

Aluminum Casing

Fig. 4

INCLINOMETER

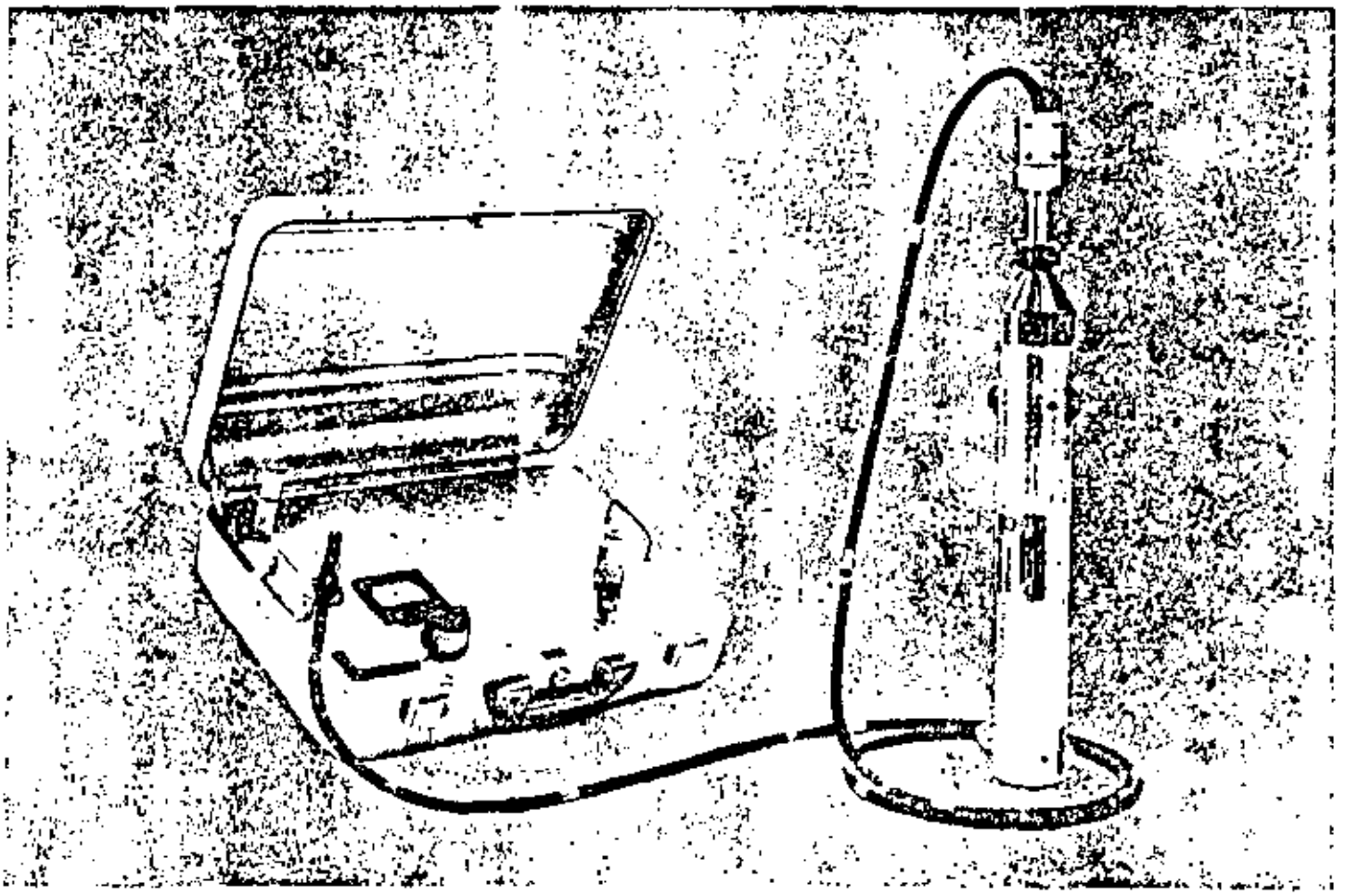

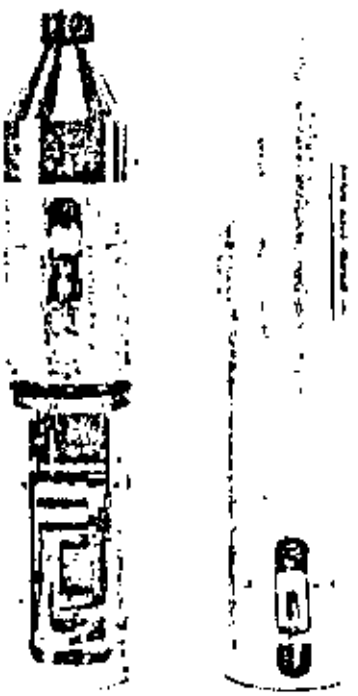

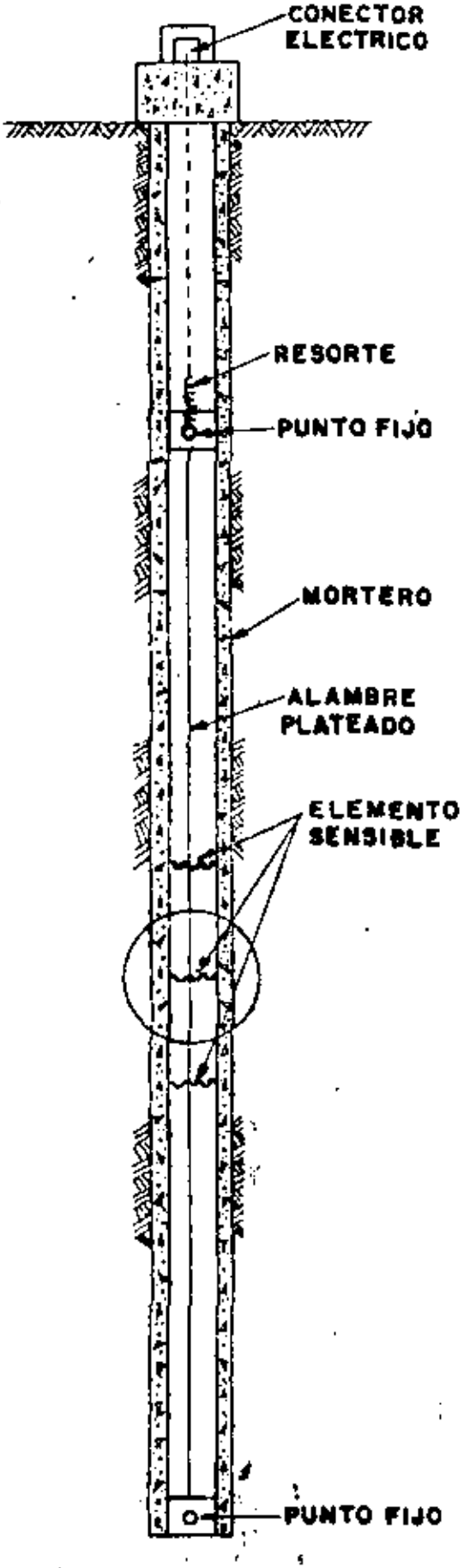

EXT. TRANSVERSAL

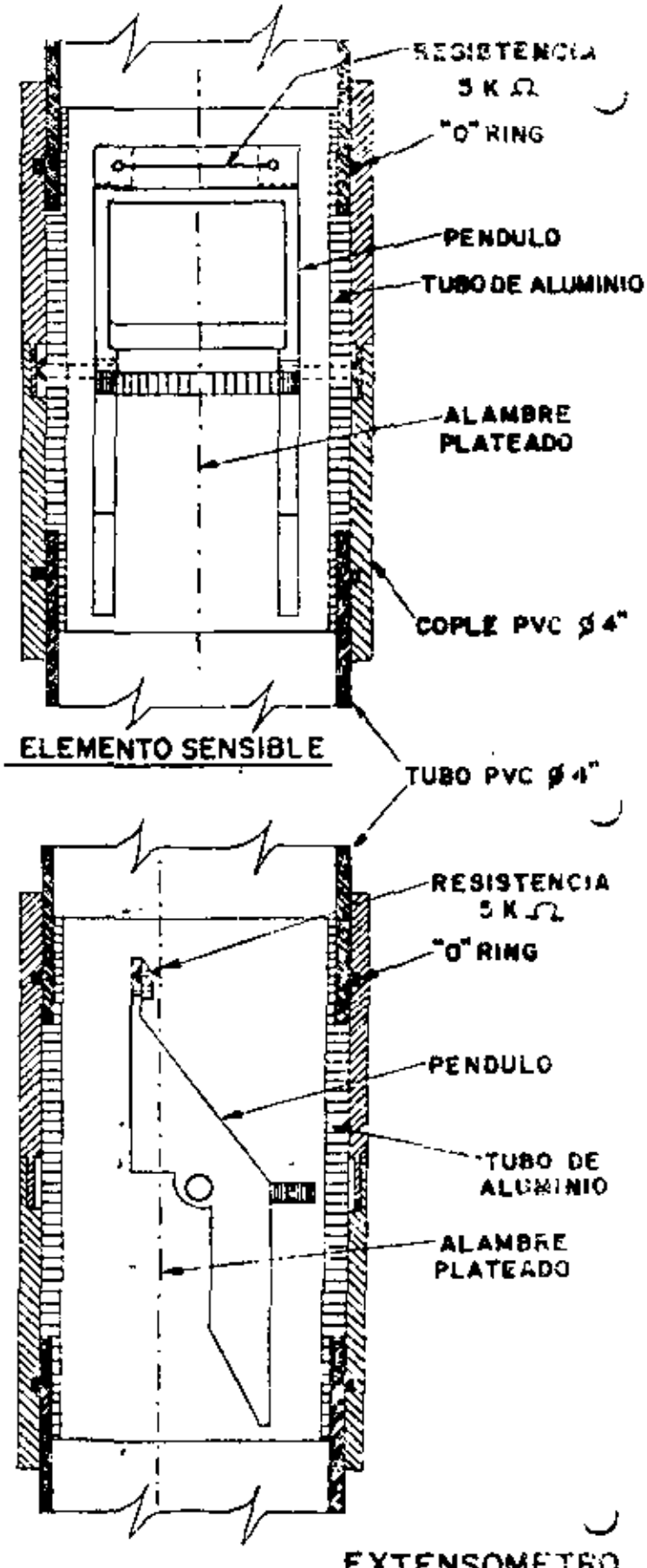

EXTENSOMETRO TRANSVERSAL

Fig 4a

Fig. 5

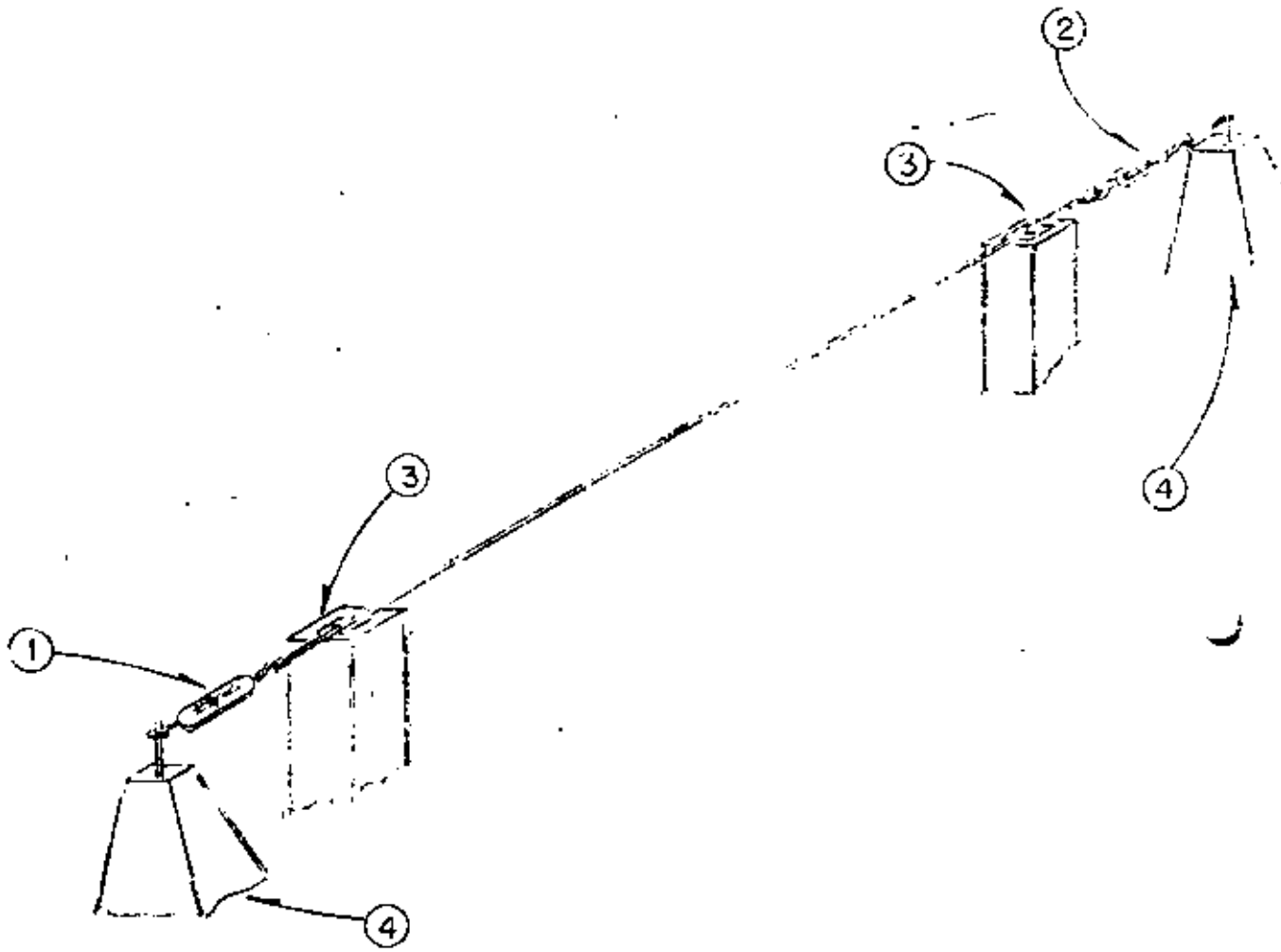

1.- Resorte de tensión variable, calibrado

2.- Tensor

3.- Indices de medición

4.- Bases de apoyo

EXTENSOMETRO DE CINTA CON RESORTE DE TENSION VARIABLE

Fig. 6

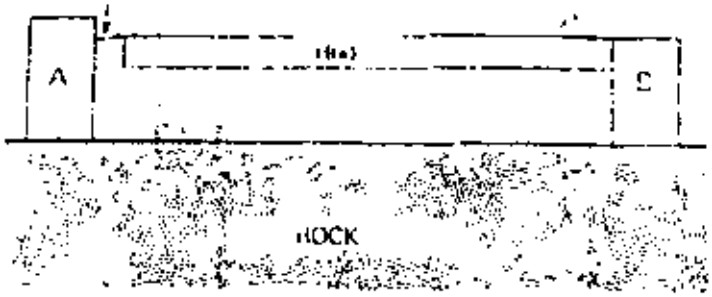

482

Fig. 2. The rod strain-meter, with [illegible] of steel or fused quartz.

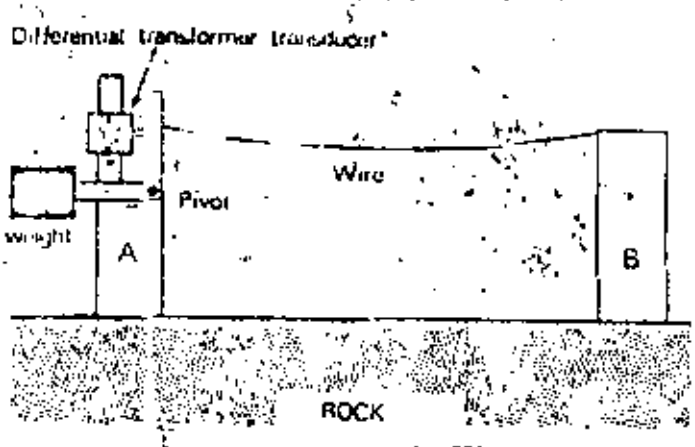

Fig. 7

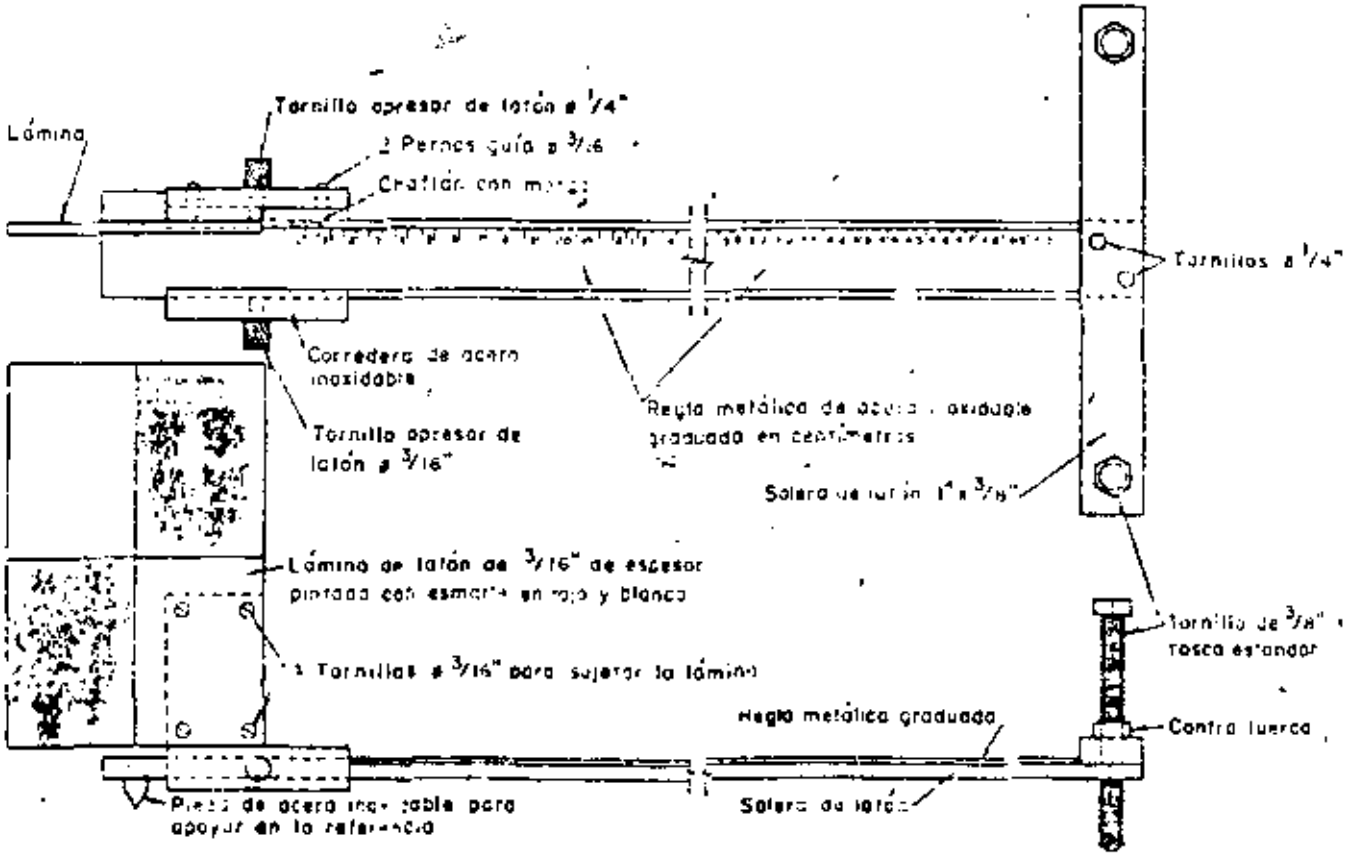

MIRA DESLIZANTE

Fig. 8

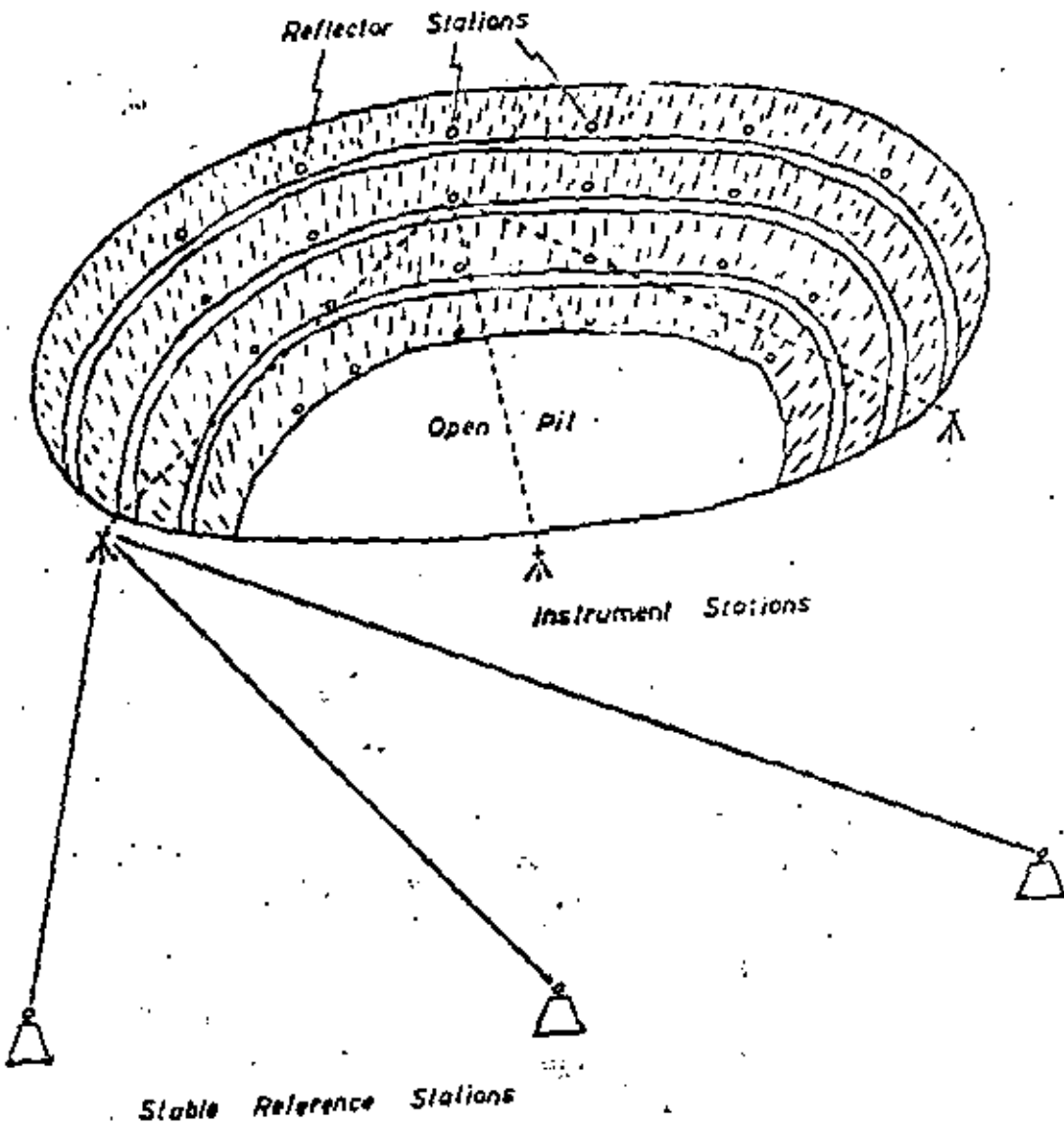
Reflector Stations
Open Pit
Instrument Stations
Stable Reference Stations

Fig. 8a

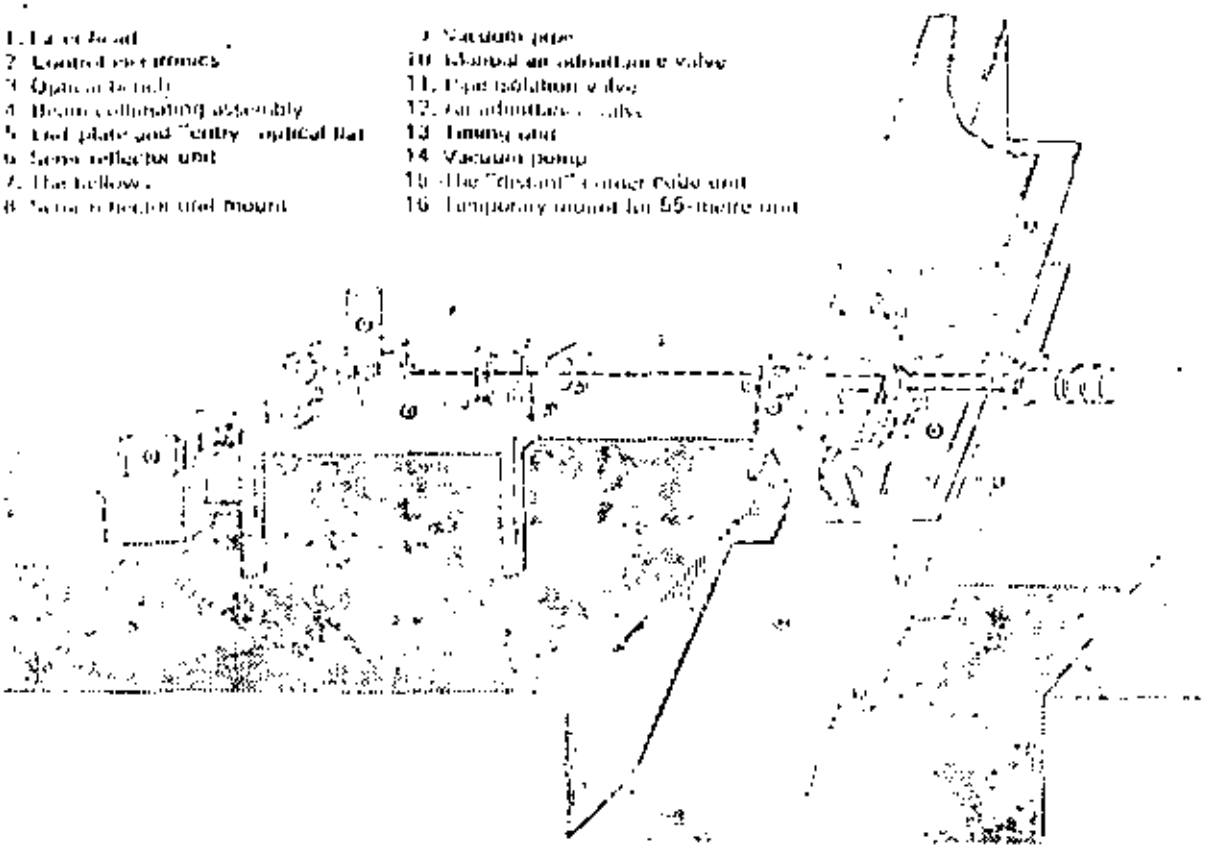
1. Laser head
2. Control electronics
3. Optical bench
4. Beam collimating assembly
5. End plate and "entry" optical flat
6. Servo reflector unit
7. Flat bellows
8. Servo reflector tilt mount
9. Vacuum pipe
10. Manual air admittance valve
11. Pipe isolation valve
12. Air admittance valve
13. Tuning unit
14. Vacuum pump
15. Flat "distant" corner cube unit
16. Temporary mount for 55-metre unit

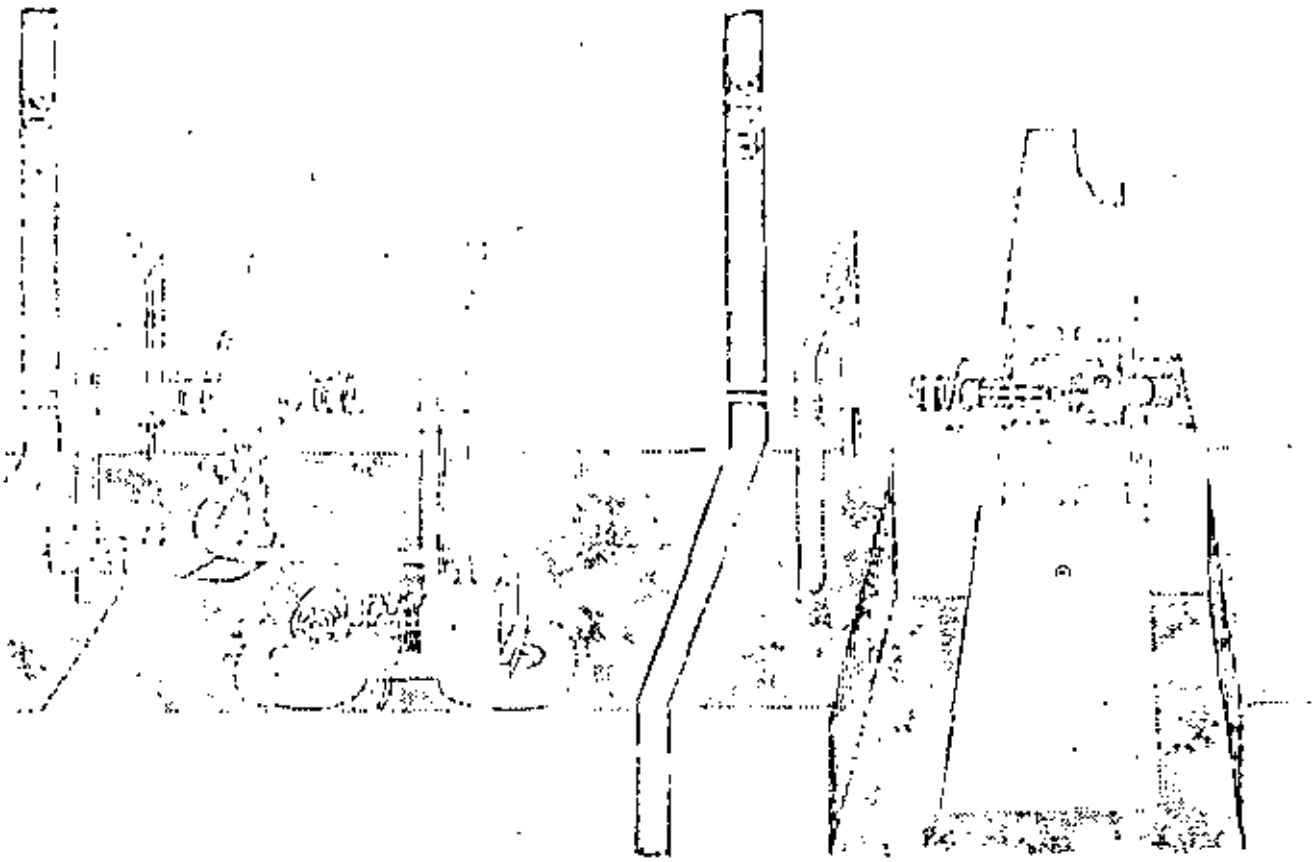

Fig. 9

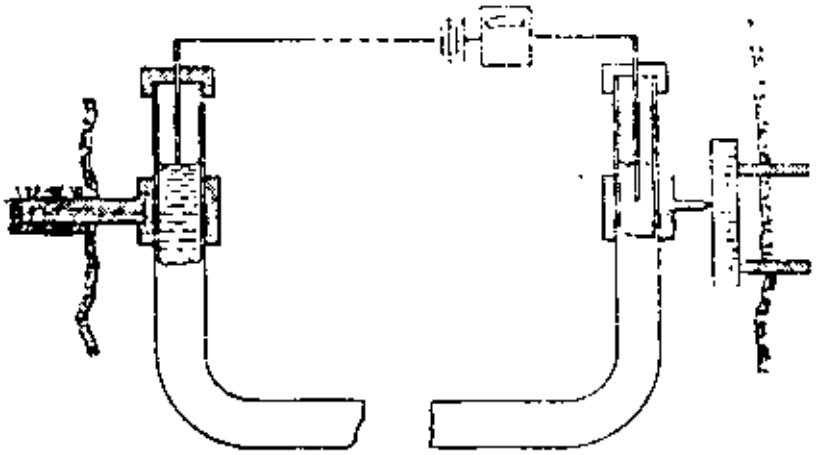

Fig. 10

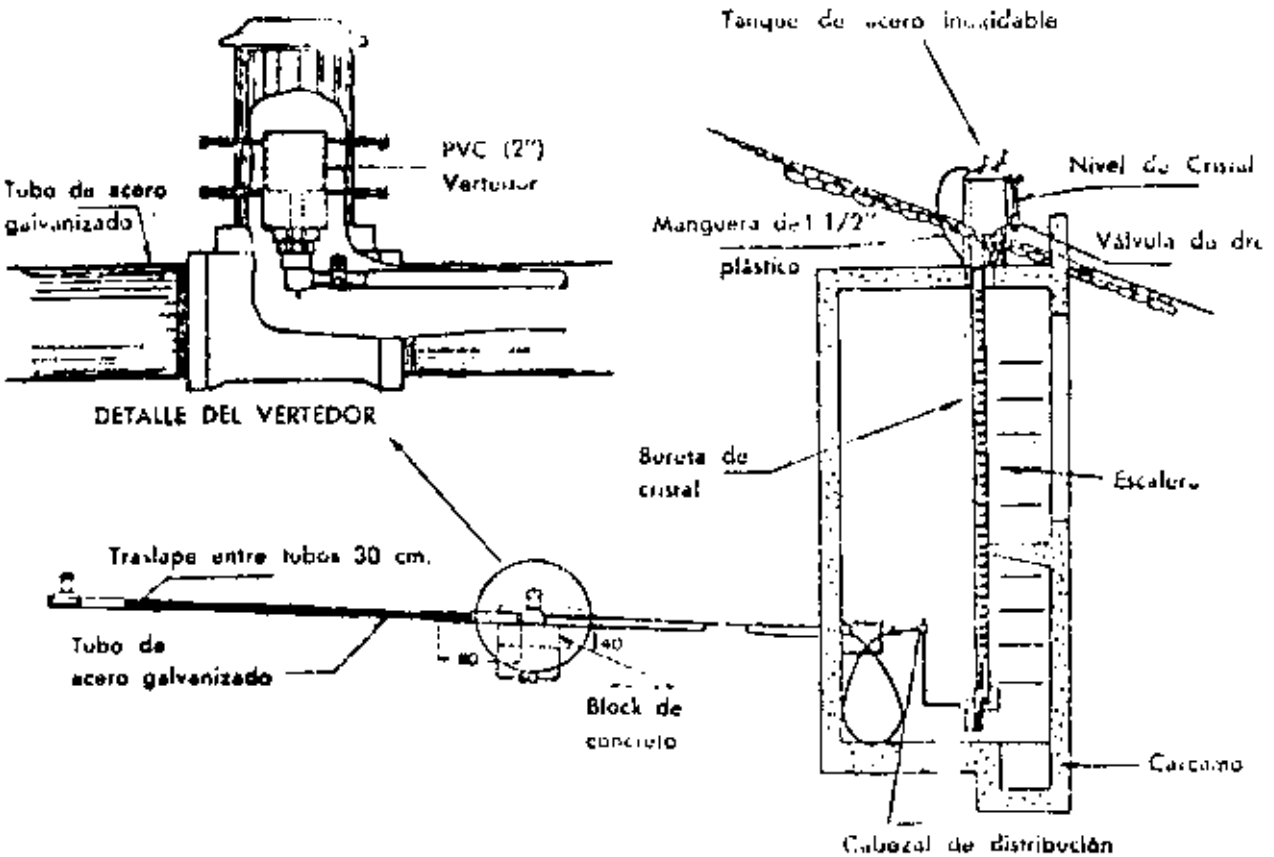

El Nivel Hidráulico, fue diseñado en el Instituto de Ingeniería de la Universidad Nacional Autónoma de Mexico para la C.F.E. y se fabrica bajo licencia por Co[illegible]temas, S. A.

Fig. 11

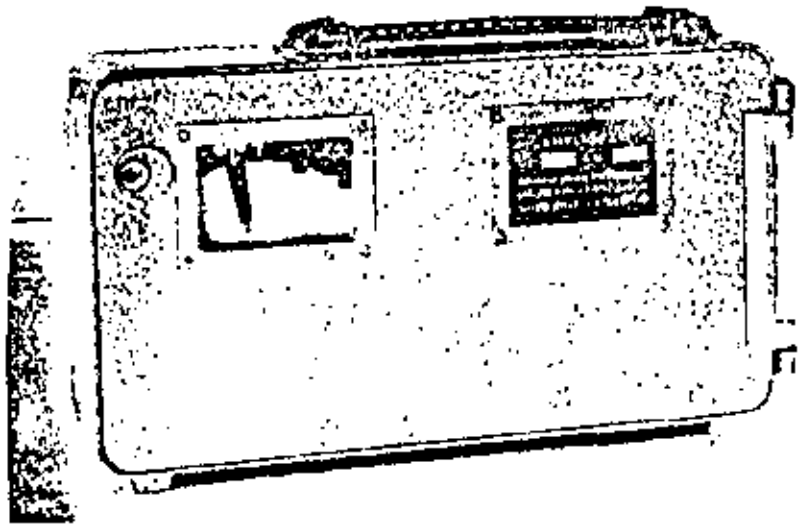

Fig. 12

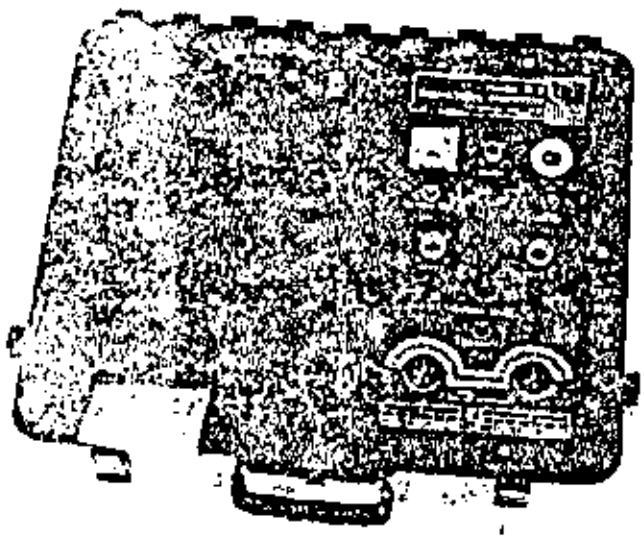

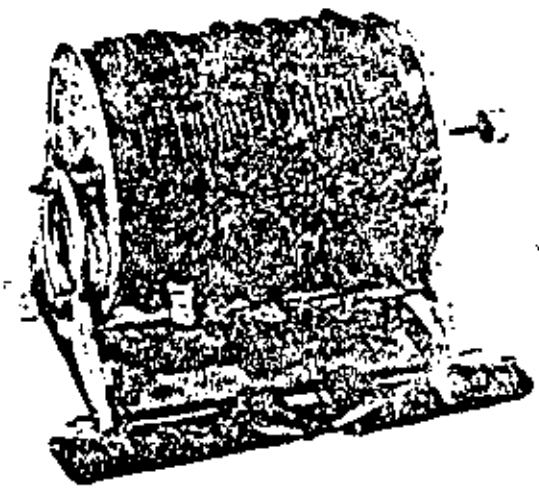

above: control unit for the S-3 System

above right: optional 1000-foot transducer cable with breast reel

right: two transducer packages

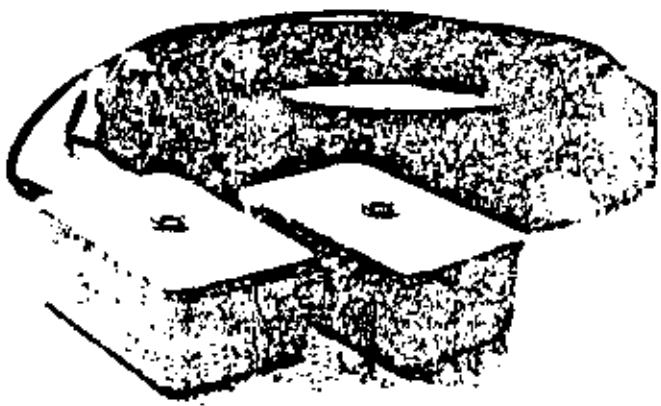

PANEL DE MEDICION PARA CELDAS DE PRESION MOD. GS - TNC

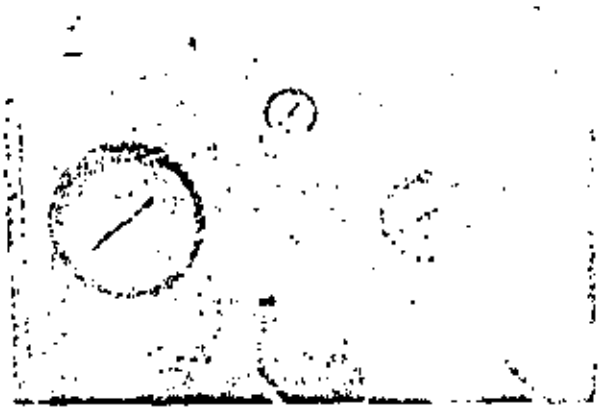

El Panel de medición Mod. GS - TNC, consiste un tanque neumático colocado en una caja portátil de madera o de metal. En esta caja son instalados un par de manometros con rangos de 0-4 Kg./cm² y 0-15 Kg./cm². Además de los manometros está provisto de llaves de control y conexiones para las tuberias de entrada y salida en las celdas.

Este panel puede ser usado para leer de una a 25 celdas, auxiliándose con un interruptor múltiple de paso.

GATO HIDRAULICO PLANO SERIE GS - GF

El gato plano serie GS-GF, se utiliza para medir esfuerzos de relajación en la roca o para medir presiones aplicadas durante las pruebas de carga en pilotes.

Modelo	Dimensiones	Presión Máxima
GS-GF40"	40x40cm (16"x16")	140 Kg/cm²(2000 psi)
GS-GF40	40 cm ø (16" ø)	140 Kg/cm²(2000 psi)
GS-GF20"	20x20cm (8"x 8")	140 Kg/cm²(2000 psi)
GS-GF20	20 cm ø (8" ø)	350 Kg/cm²(2000 psi)

Sobre pedidos especiales se pueden fabricar gatos planos con mayores rangos o dimensiones.

CELDAS DE CARGA HIDRAULICA PARA TUNELES SERIE CCH

Este tipo de celda está diseñado para uso en los adornos metálicos de túneles y puede resistir cambios de humedad y temperatura, así como posible daños ocasionados por explosiones o vibraciones normales de trabajo en la excavación de túneles, minas, galerías, etc.

Las lecturas de las celdas son tomadas directamente por medio de un manómetro. Este tipo de celdas se fabrican en los siguientes modelos:

Modelo	Rango	Aproximación
GS-CCH 25	0-25 Ton.	0.1%
GS-CCH 50	0-50 Ton.	0.5%
GS-CCH 100	0-100 Ton.	1.0%
GS-CCH 150	0-150 Ton.	2.0%

Fig. 14

Type BL-5.10 TA

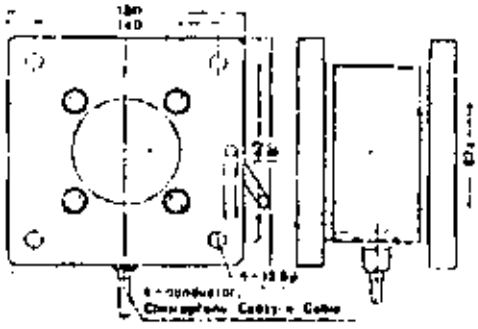

Type BL-20.50 TA

Fig. 15

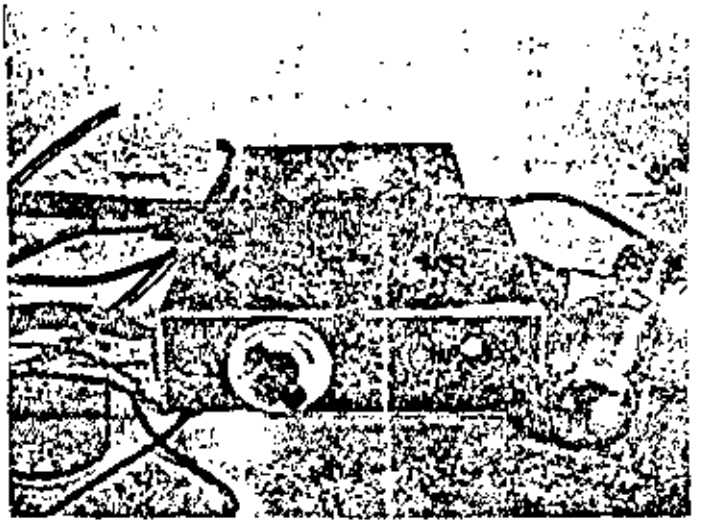


9 05 A M
MAY 3, 1952
APR 25
TEST
FAILURE


10 0h A M
MAY 3, 1952
FAILURE

Fig. 16

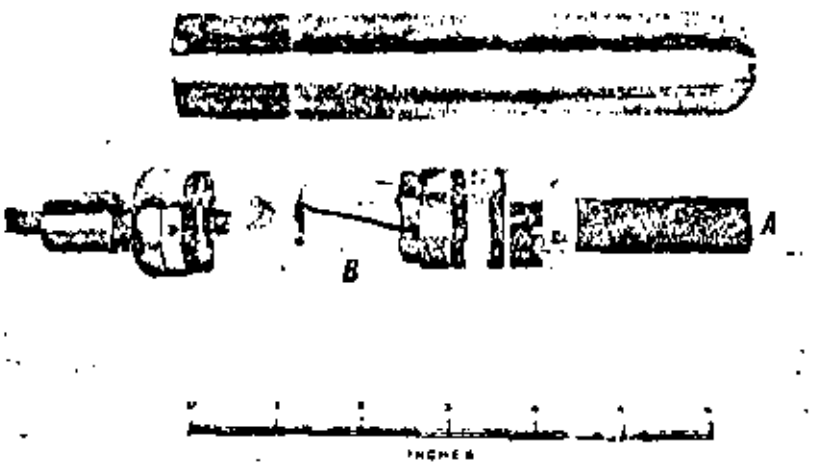
A
B
INCHES

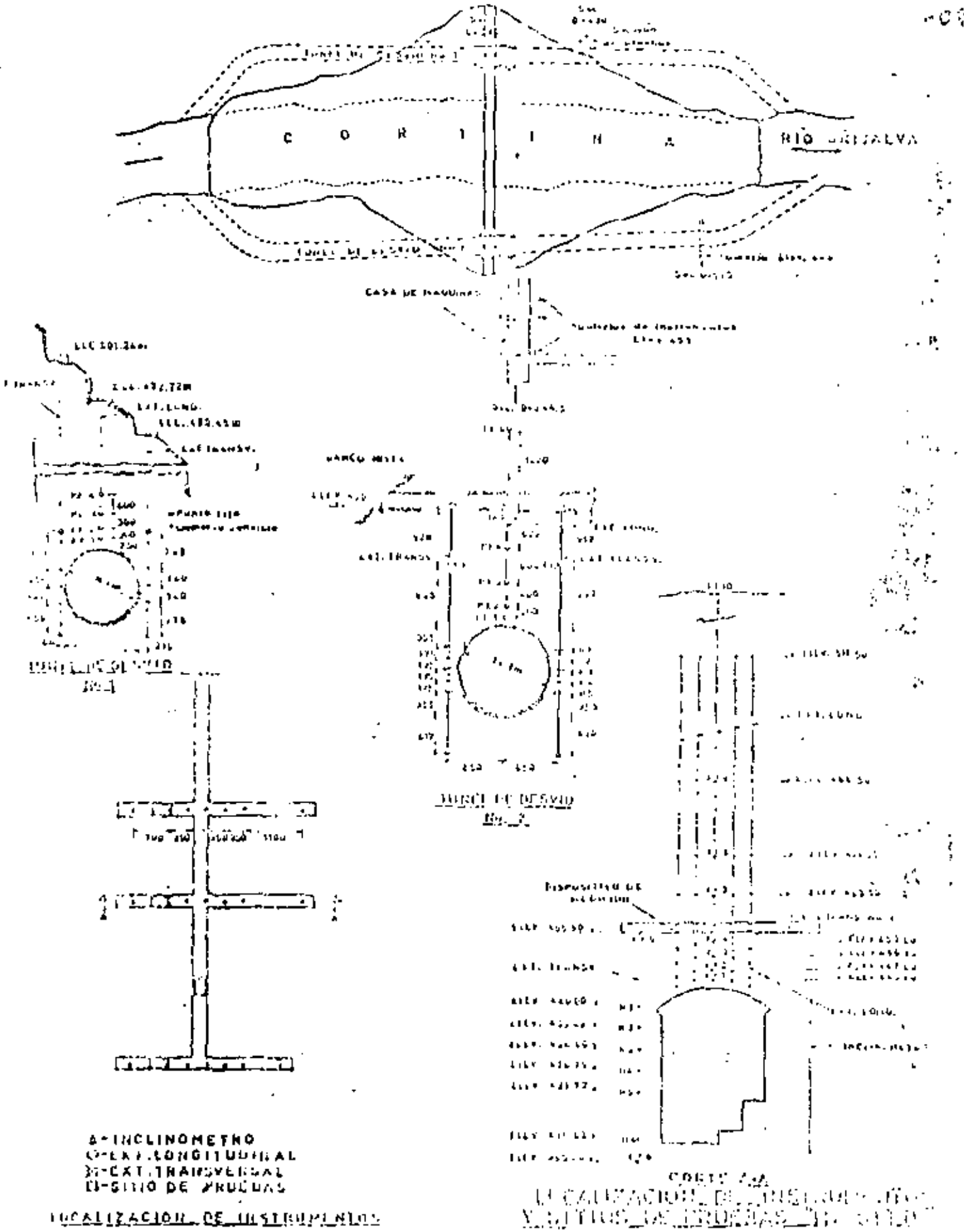

LOCALIZACION DE INSTRUMENTOS
CASA DE MAQUINAS

CORTE A-A
LOCALIZACION DE INSTRUMENTOS
Y SALIDAS DE CONDUCTOS

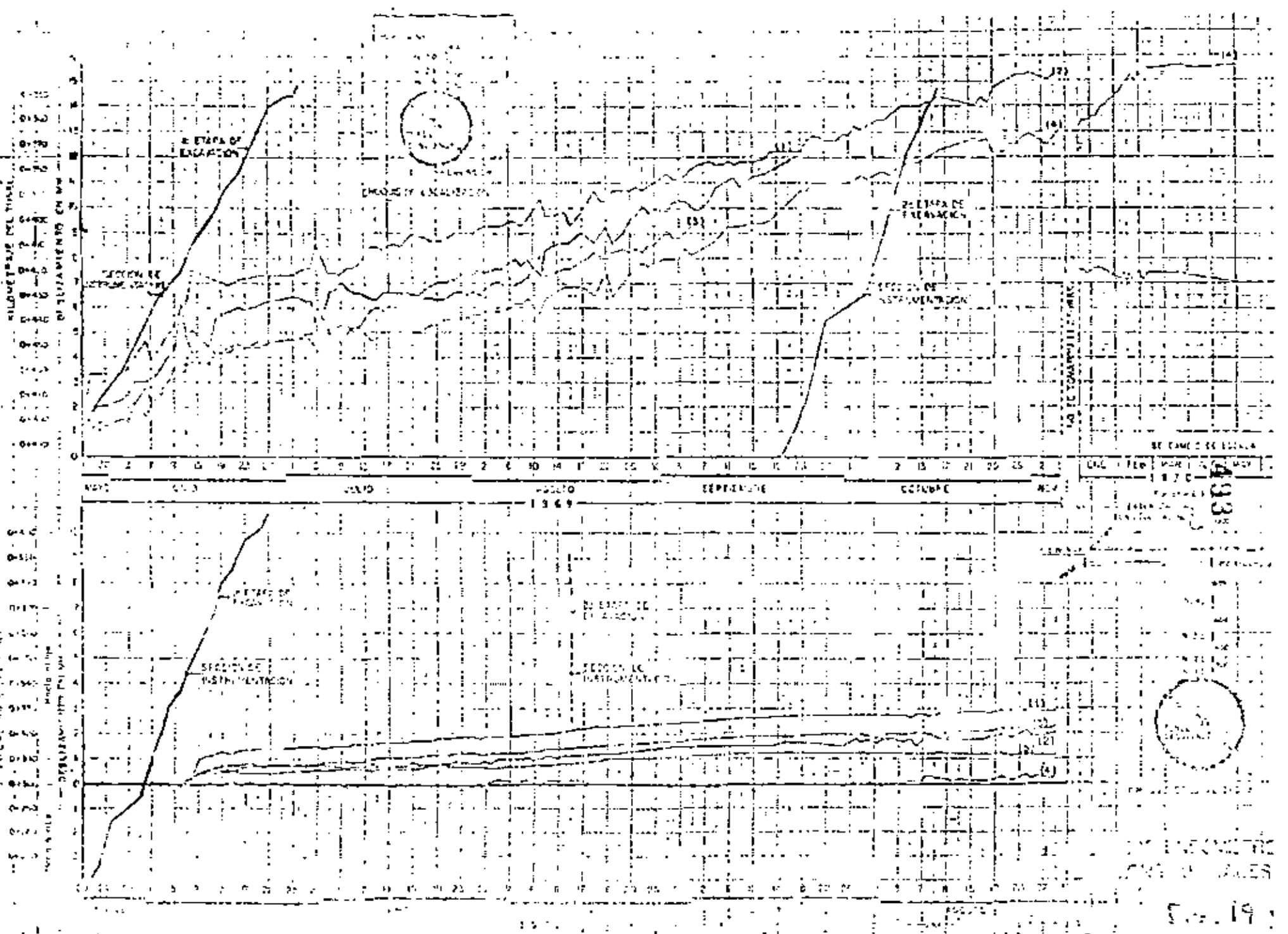

494

Fig. 20

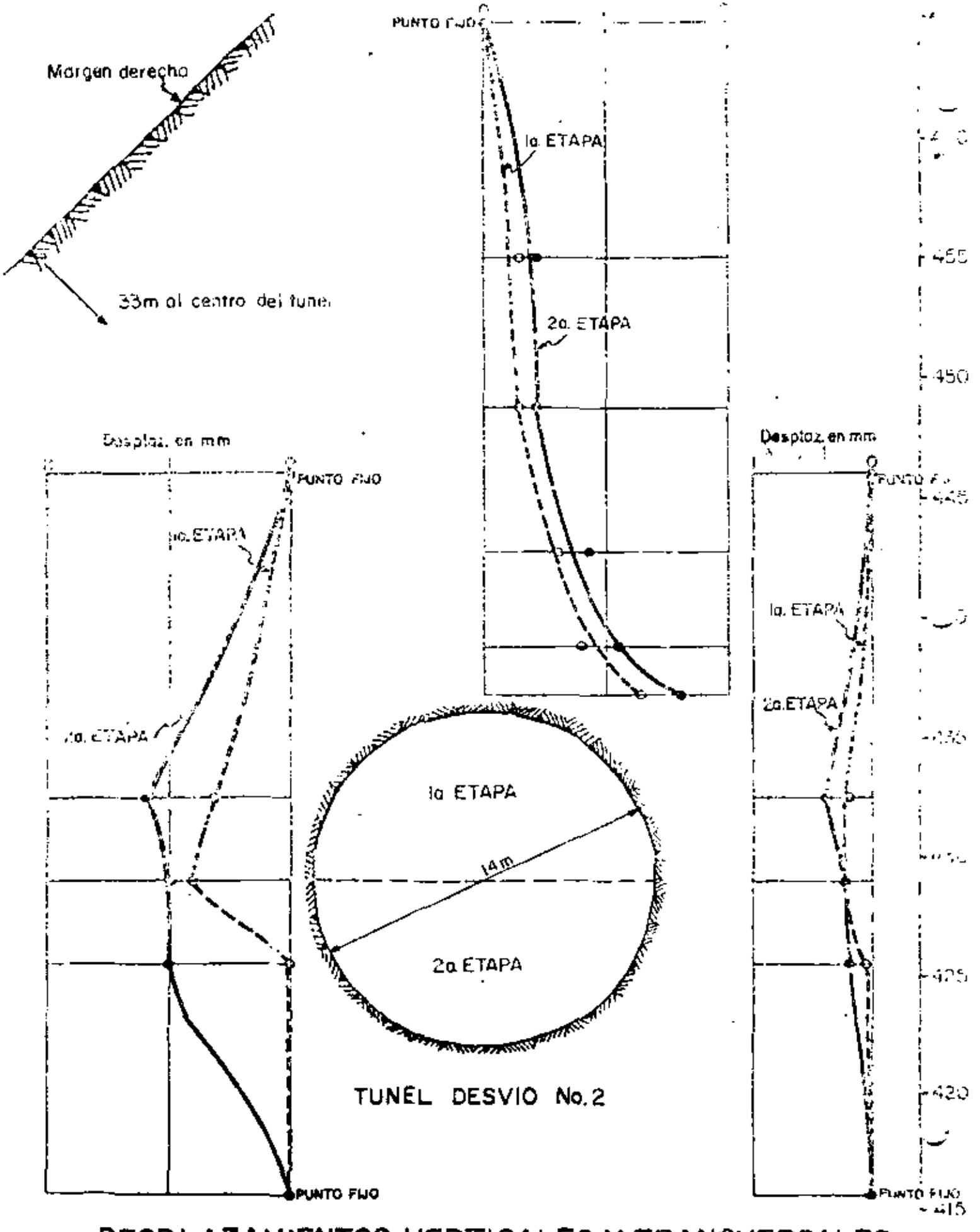

TUNEL DESVIO No. 2

DESPLAZAMIENTOS VERTICALES Y TRANSVERSALES Fig. 2

FECHA	8-FEB-71	8-FEB-71	11-MAR-71	6-ABR-71	6-MAY-71	12-JUN-71	6-JUL-71	3-AGO-71	18-SEP-71	15-OCT-71	16-NOV-71	11-DIC-71	5-ENE-72	18-FEB-72	R-72
	(-4)	(-3)	(-4)	(-4)	(-3)	(-5)	(-9)	(-9)	(-5)	(-12)	(-4)	(-23)	(-)	(-8)	(-)
	(-1)	(-9)	(-8)	(-5)	(-5)	(-5)	(+5)	(+2)	(+9)	(+2)	(-2)	(-5)	(-5)	+2	(-6)

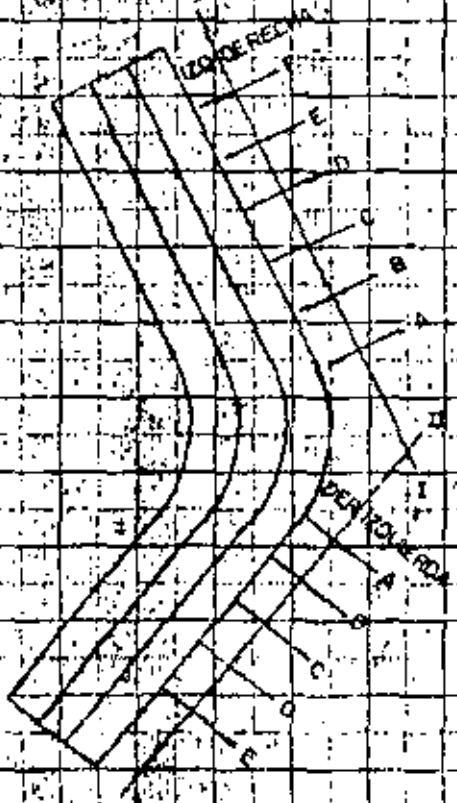

CROQUIS DE ORGANIZACION

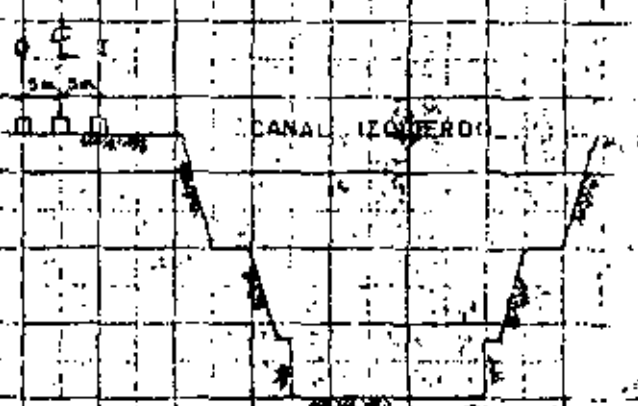

CORTE

NOTA VALORES DENTRO DE LOS CIRCULOS INDICAN DESPLAZAMIENTOS EN m/m

ACORTAMIENTOS (-)

ALARGAMIENTOS (+)

P.H. ANGOSTURA

VERTEDOR

DESPLAZAMIENTOS SUPERFICIALES

(Con estación total)

LINEA

SECCION

ESTACION

27-MAY-72	14-JUN-72	12-JUL-72	19-AUG-72	20-SEP-72	21-OCT-72	17-NOV-72	16-DEC-72	10-JAN-73	14-FEB-73	14-MAR-73	11-APR-73	3-MAY-73
(-7)	(-16)											
(-3)	(+6)	(+4)	(+12)	(+2)	(+5)	(±2)	(-3)	(-5)	(-7)	(-8)	(-10)	(-9)

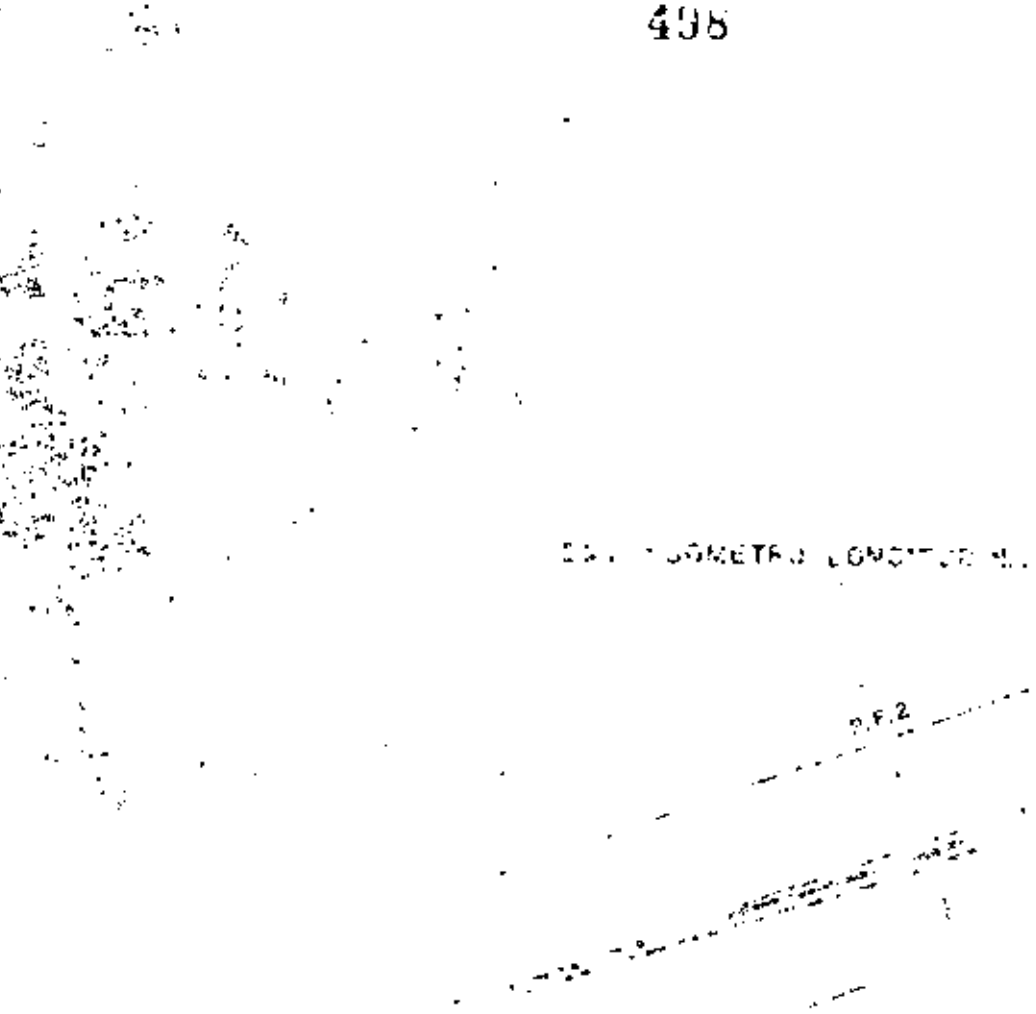
P.F.2

CANAL IZQUIERDO

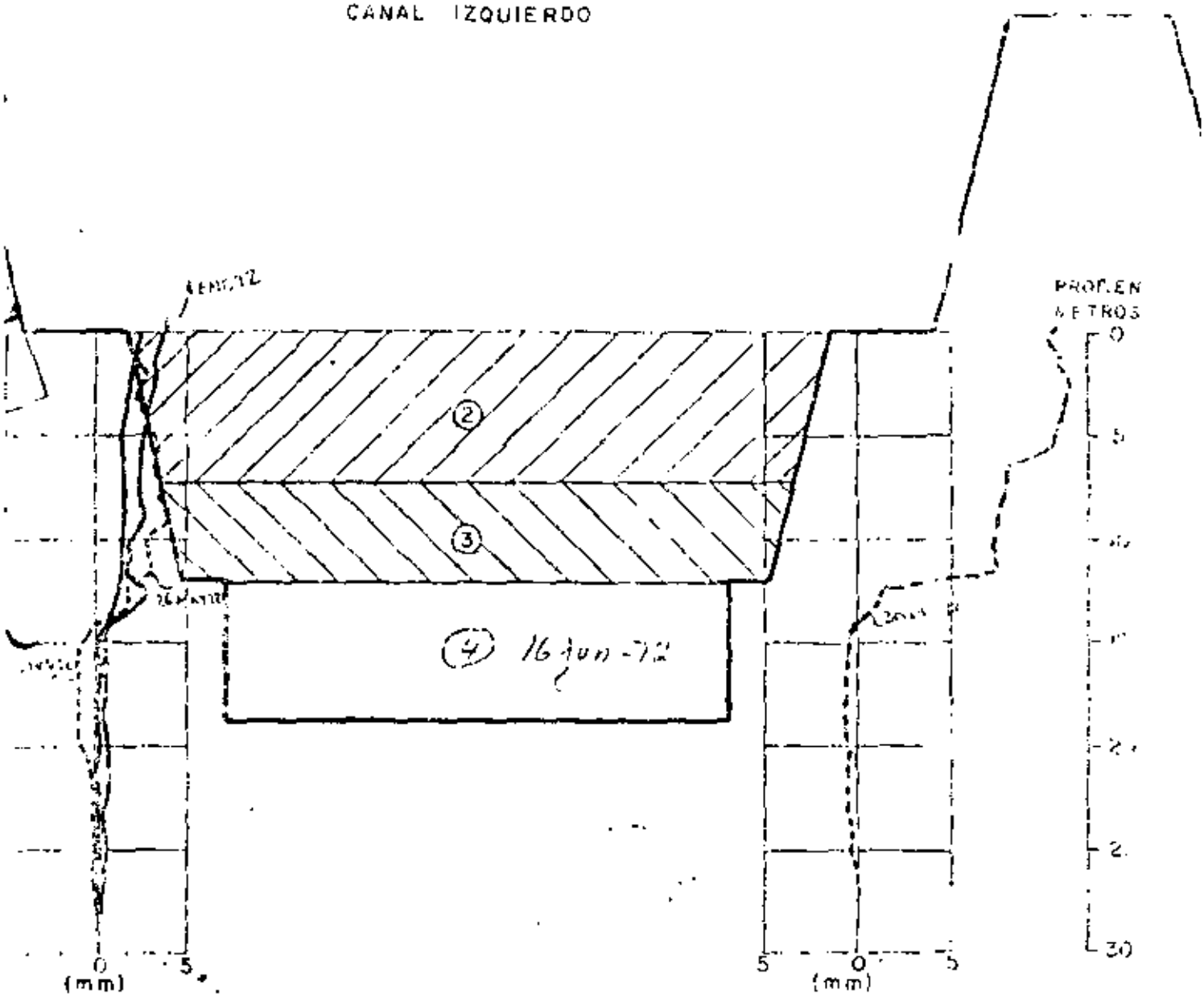

INCLINOMETRO 12

INCLINOMETRO 13

DESPUES DE PRECORTE
DESPUES DE BANQUEO ZONA ②
DESPUES DE BANQUEO ZONA ③

500

CANAL DERECHO

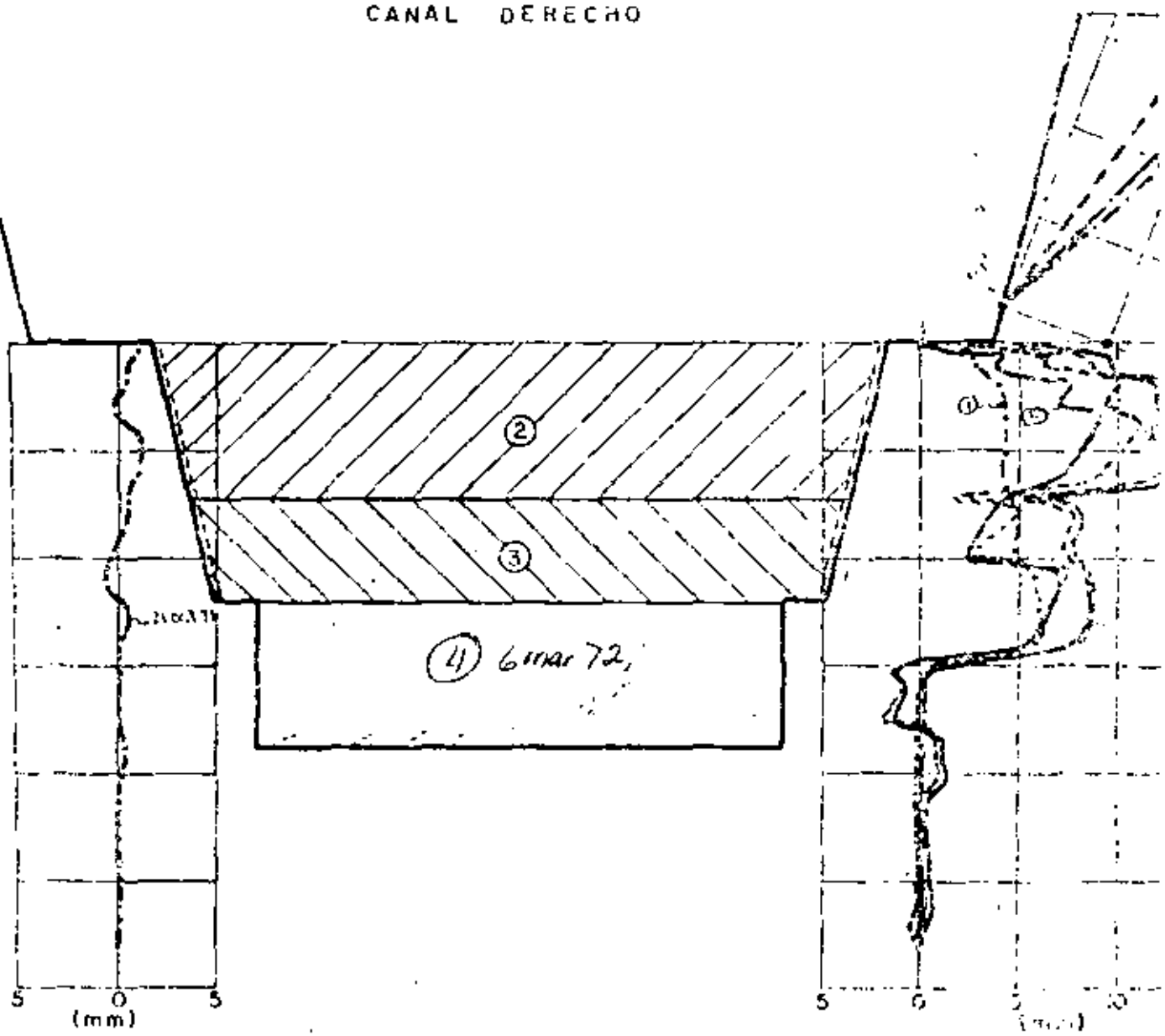

INCLINOMETRO 14

INCLINOMETRO

ANGOSTURA, CHIS.

DOR

ETRO 14 y 15

D:D

EXTENSOMETRO LONGITUDINAL 22

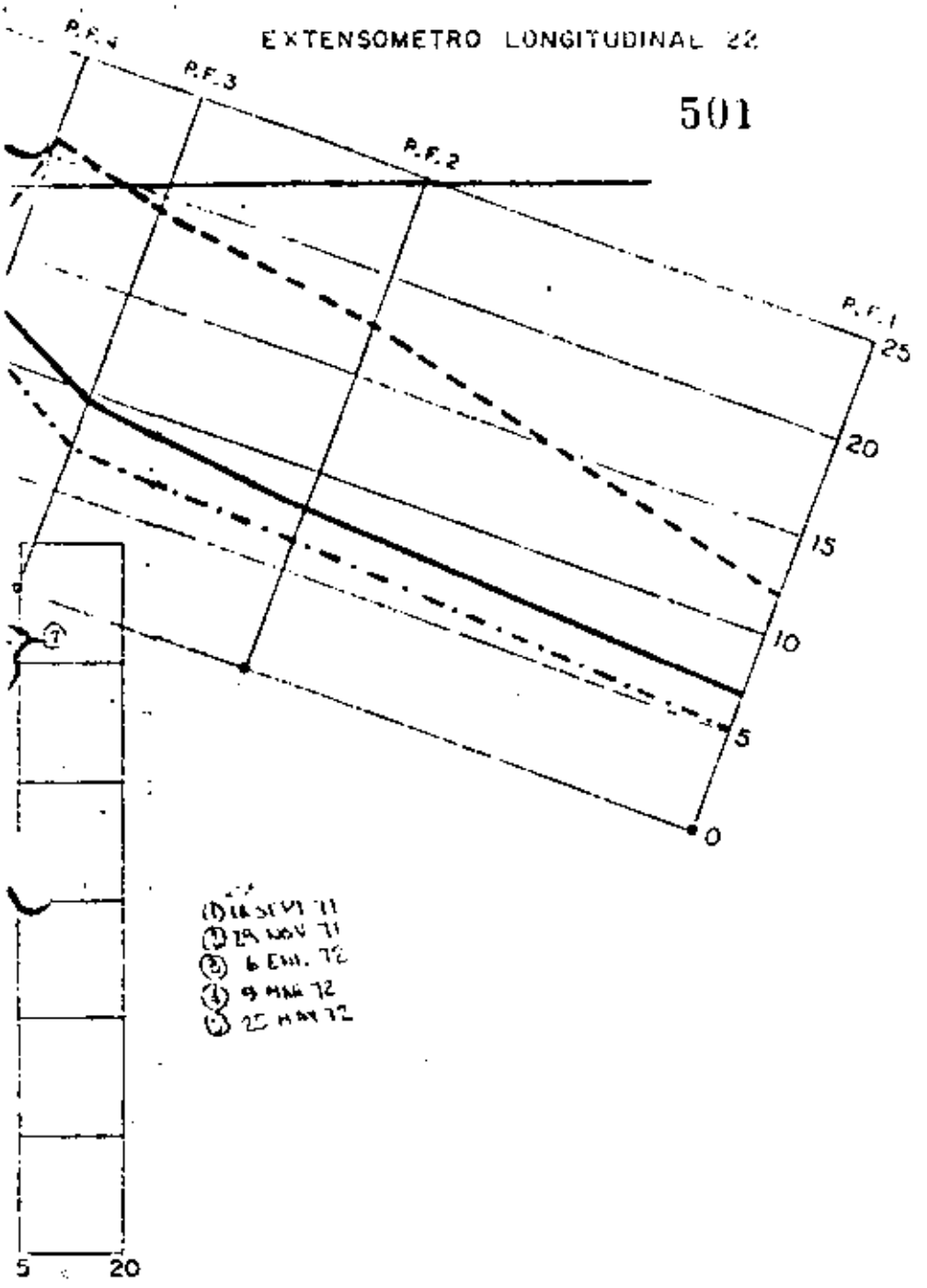

FECHA DE VOLADURAS

CANAL	ZONA	PRECORTE		BANQUEO
		PARED IZQ.	PARED DER.	PARED IZQ.
IZQUIERDO	②			25-NOV-71
	③			2-MAR-72
DERECHO	②	20-OCT-71	9-SEP-71	9-NOV-71
	③	20-OCT-71	9-SEP-71	

EXTENSOMETRO L

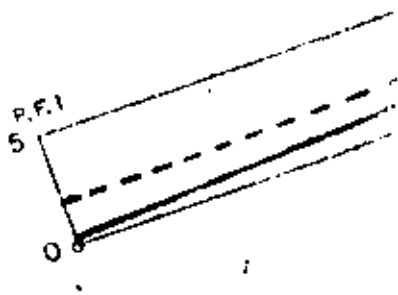

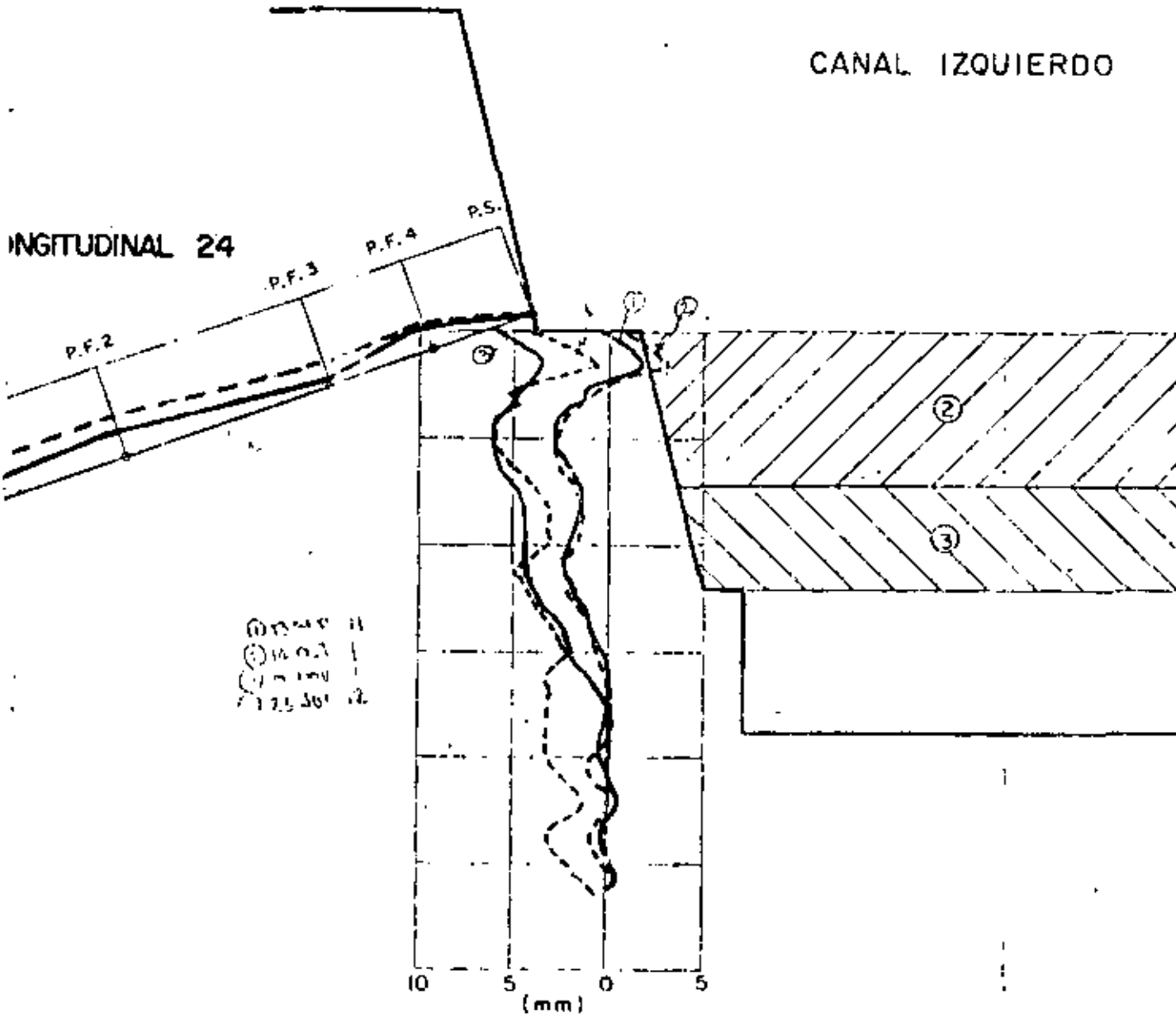

INCLINOMETRO 16

—·—·— DESPUES DEL CORTE
——— DESPUES DE BANQUEO ZONA 2
— — — DESPUES DE BANQUEO ZONA 3

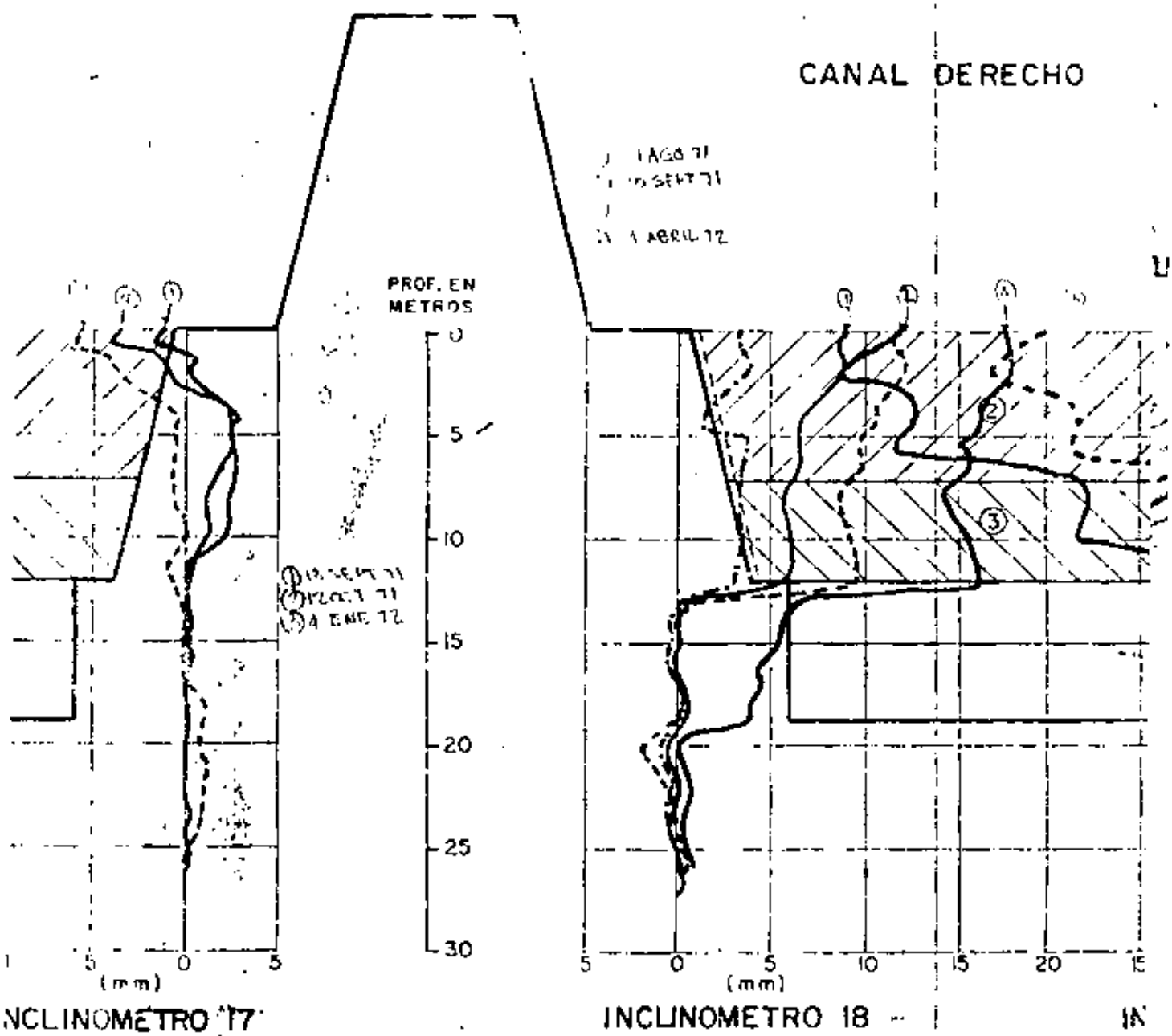

P. H. ANGOSTURA, CHIS.

VERTEDOR

EST. 0+400

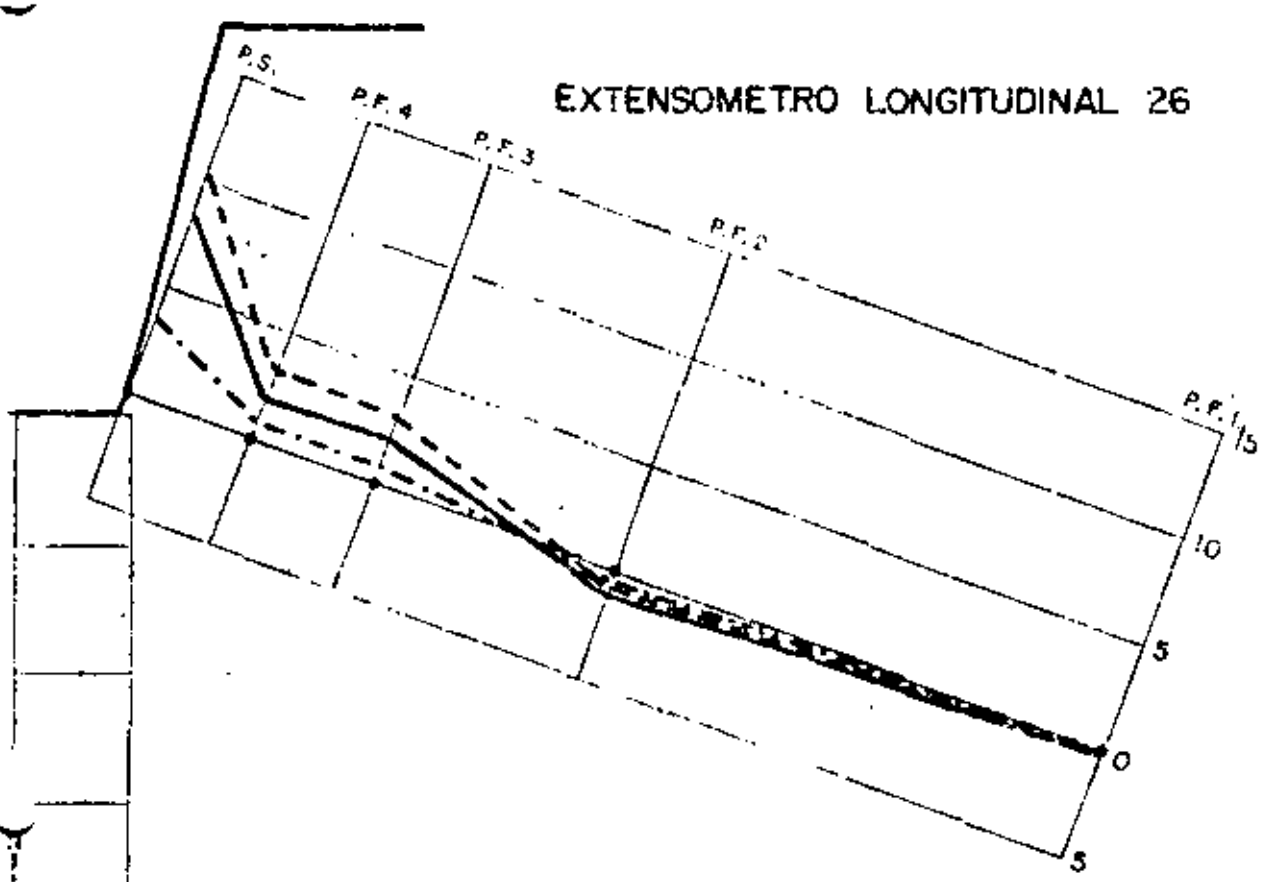

EXTENSOMETRO LONGITUDINAL 26

FECHA DE VOLADURAS

CANAL	ZONA	PRECORTE		BANQUEO	
		PARED IZQ.	PARED DER.	PARED IZQ.	PARED DER.
IZQUIERDO	②			10-SEP-71	10-SEP-71
	③			27-OCT-71	27-OCT-71
DERECHO	②	24-JUL-71	21-JUL-71	31-JUL-71	31-JUL-71
	③	24-JUL-71	21-JUL-71	20-SEP-71	20-SEP-71

Fig. 24

EXTENSOMETR

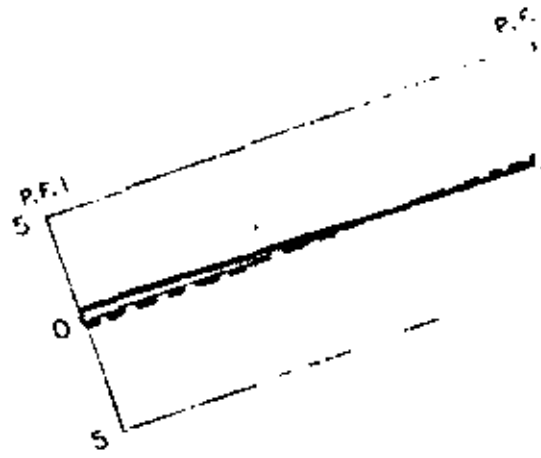

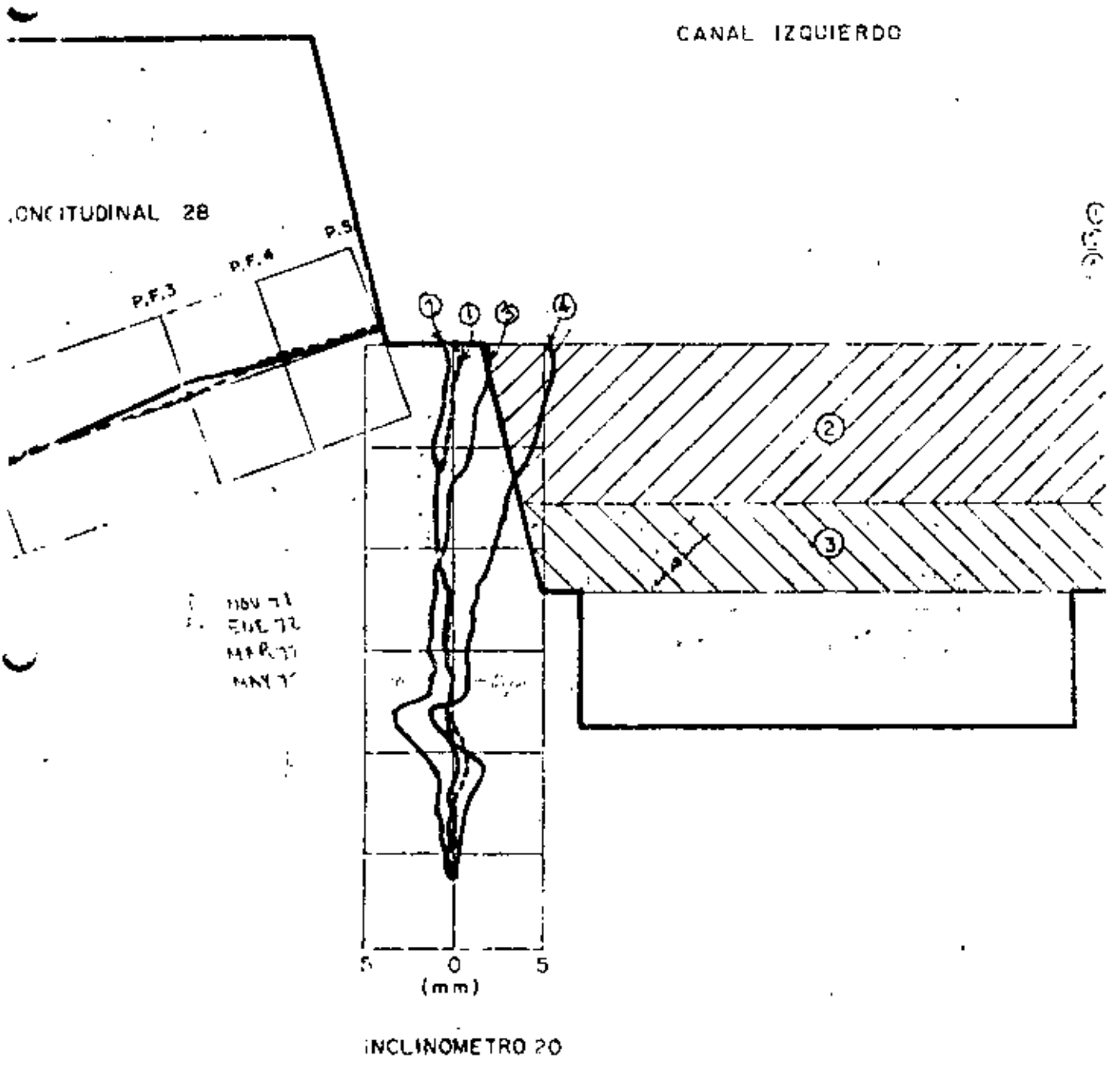

INCLINOMETRO 20

— · — DESPUES DE BANQUEO ZONA ②
— — · DESPUES DE BANQUEO ZONA ③

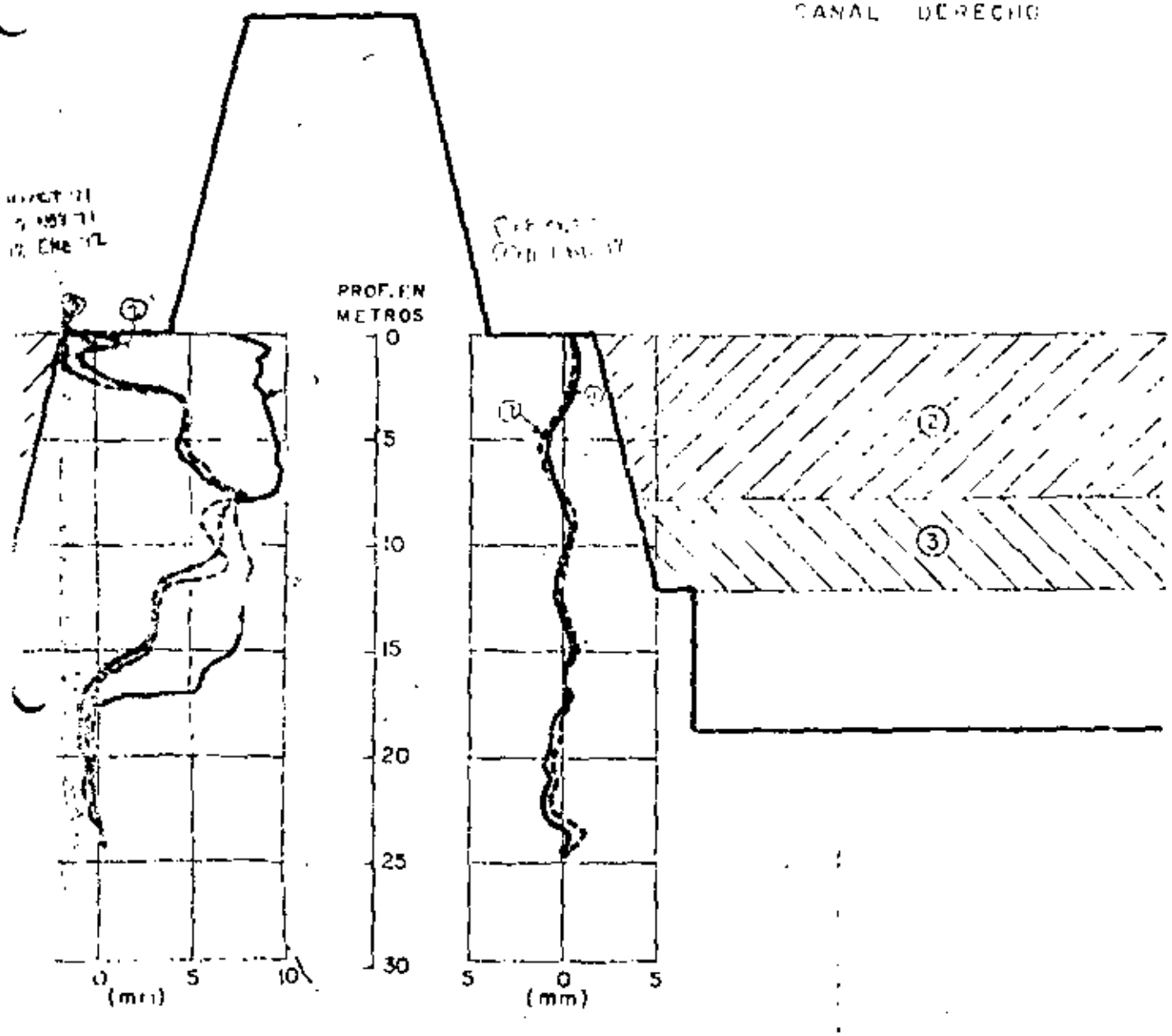

INCLINOMETRO 21 INCLINOMETRO 22

P. H. ANGOSTURA, CHIS.

VERTEDOR

DESPLAZAMIENTO HORIZONTAL EN DIRECCION NORMAL AL EJE DE LOS CANALES.

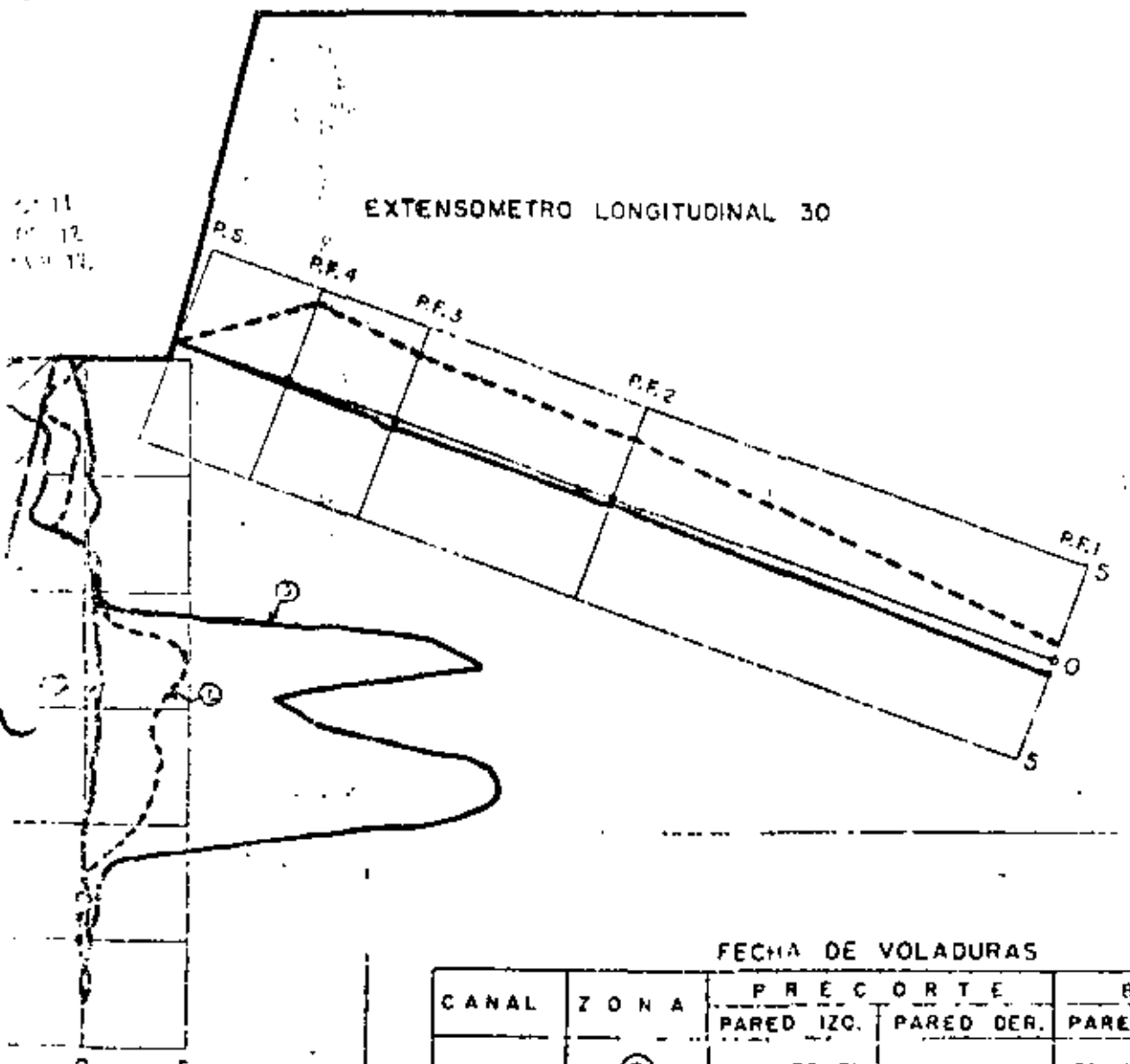

LINOMETRO 23

FECHA DE VOLADURAS

CANAL	ZONA	PRECORTE		BANQUEO	
		PARED IZQ.	PARED DER.	PARED IZQ.	PARED DE
IZQUIERDO	②	18-AGO-71		28-AGO-71	28-AGO-7
	③	18-AGO-71		9-OCT-71	9-OCT-7
DERECHO	②	2-JUN-71		24-AGO-71	24-AGO-7
	③	2-JUN-71		20-OCT-71	20-OCT-7

Fig. 25

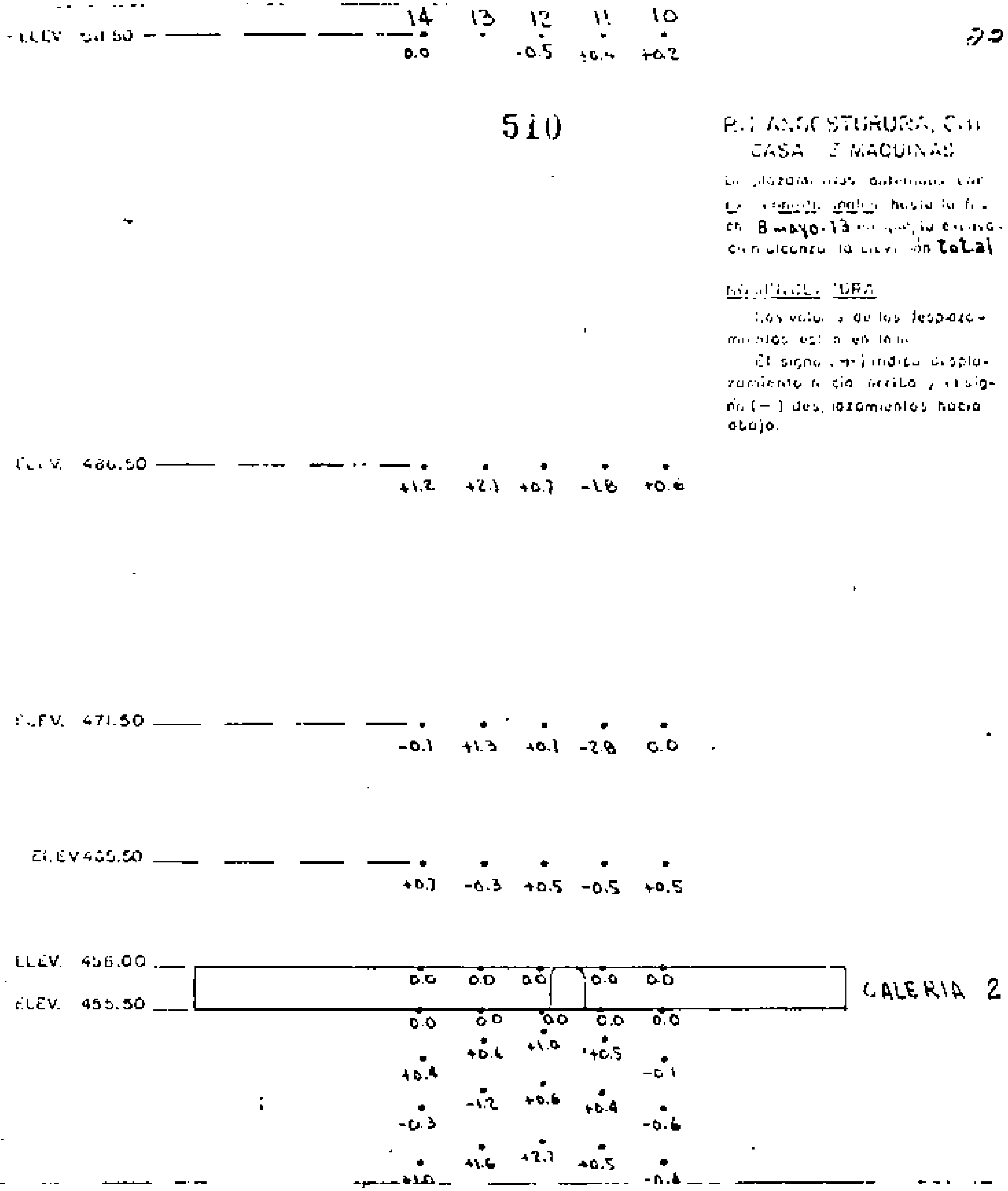

P.H. ANGOSTURA, Chis.
CASA DE MAQUINAS

Desplazamientos determinados con el péndulo inverso hasta la fecha en 8-mayo-73 en que la excavación alcanzó la elevación total

NOMENCLATURA

Los valores de los desplazamientos están en mm.

El signo (+) indica desplazamiento hacia arriba y el signo (−) desplazamientos hacia abajo.

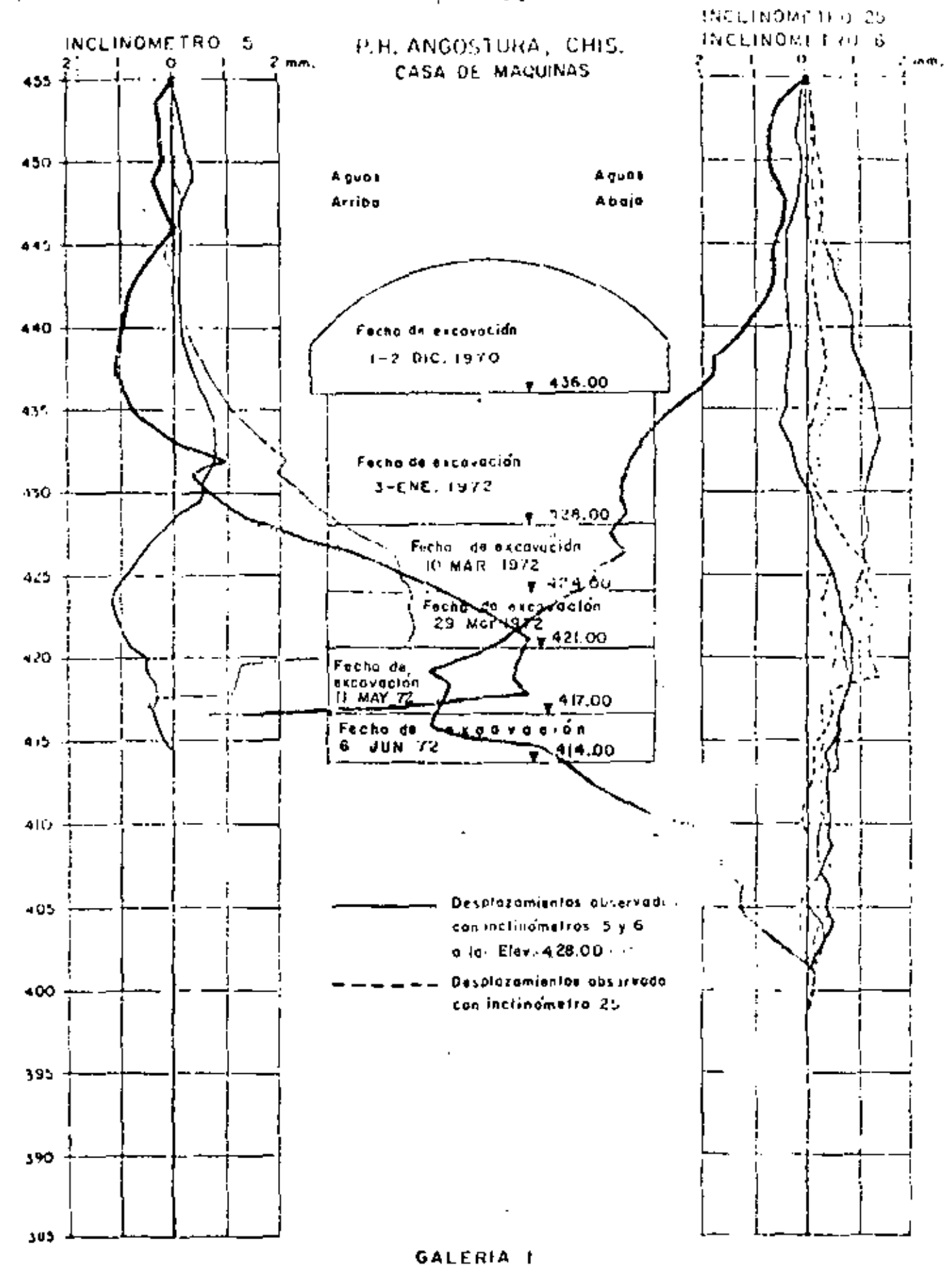

GALERIA 1

Desplazamientos observados después de excavación elevación 428.00

Fig. 27

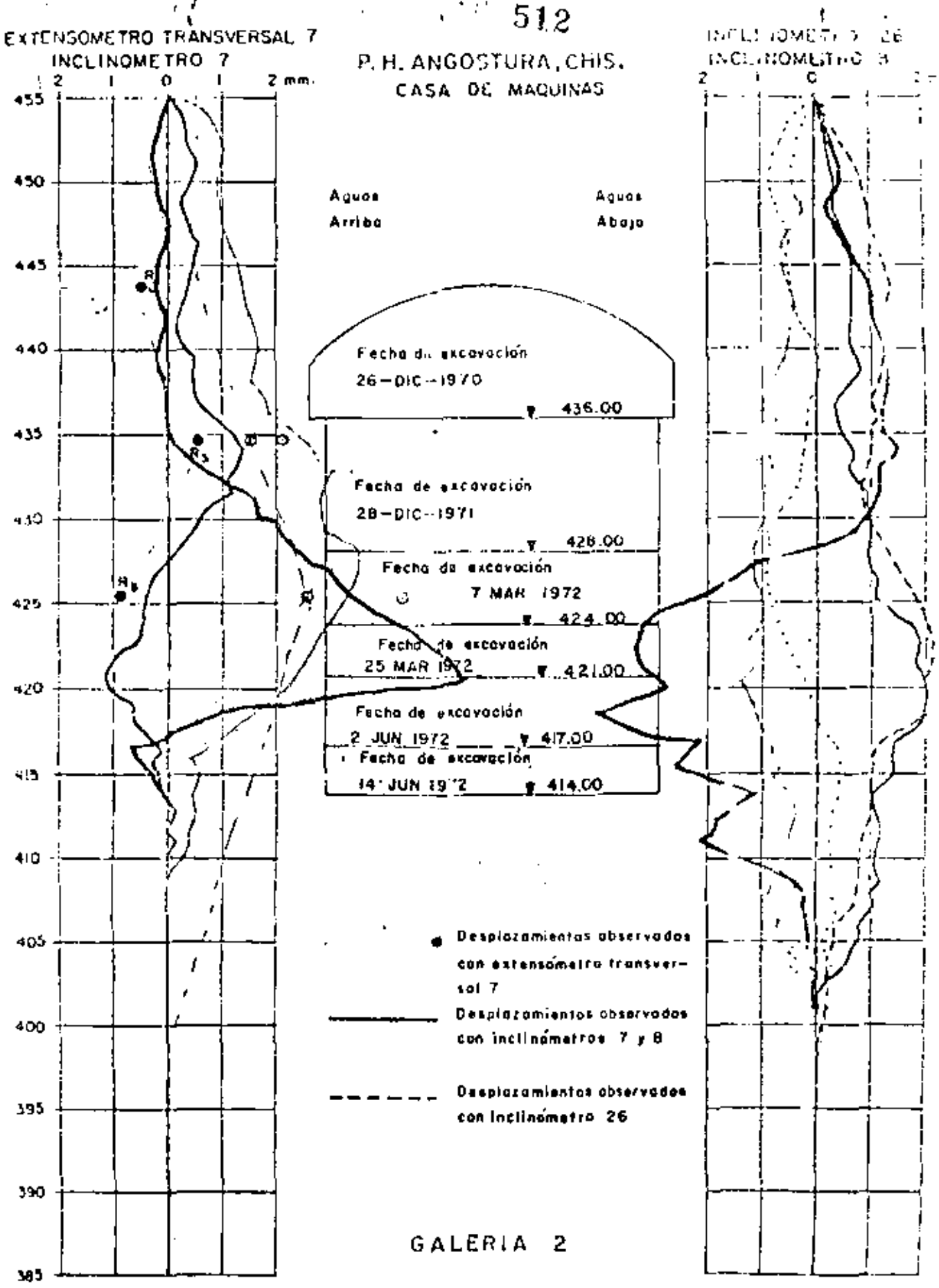

Desplazamientos observados después de excavar a la elevación 428.00

FIG. 28

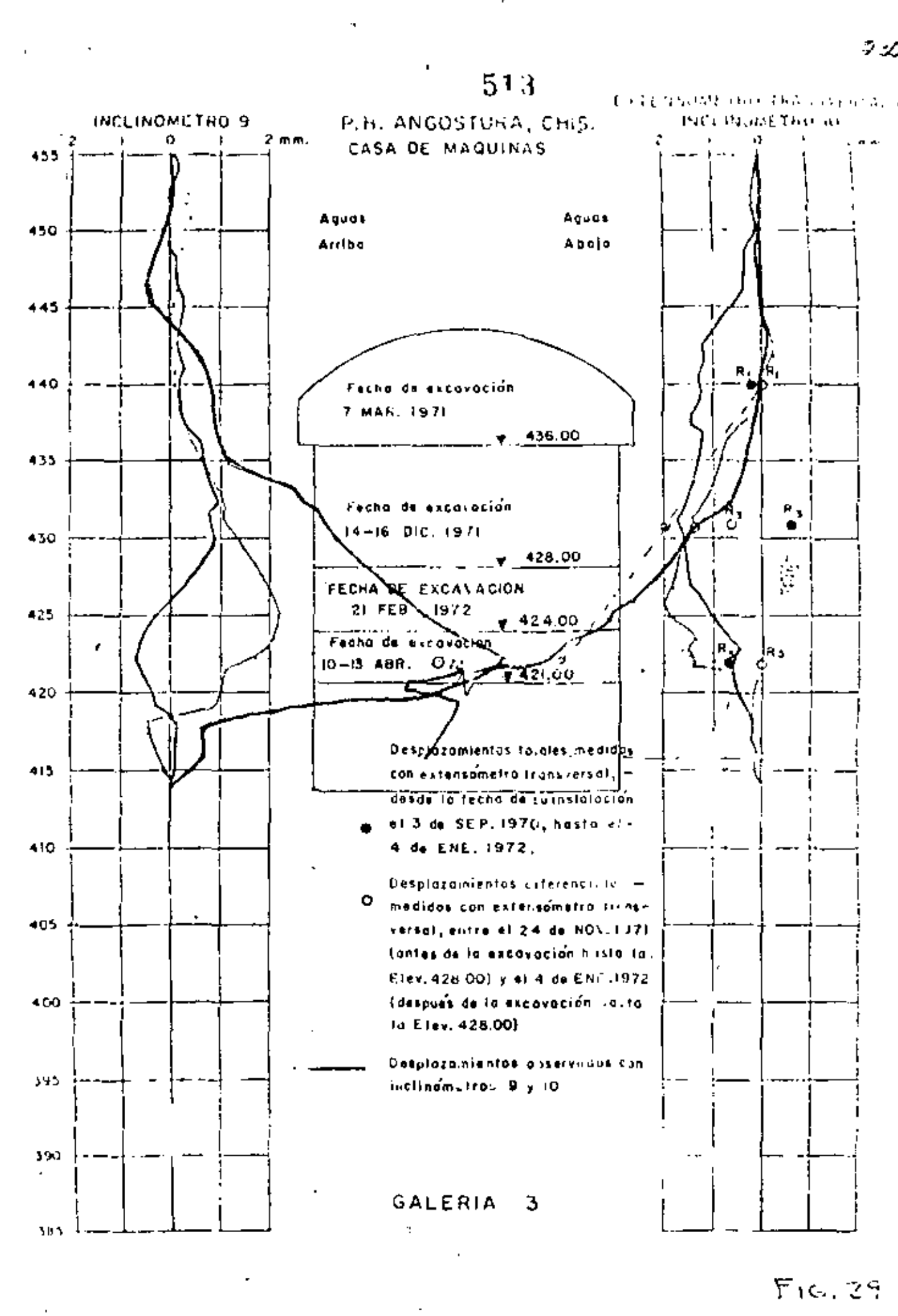
INCLINOMETRO 9
P.H. ANGOSTURA, CHIS.
CASA DE MAQUINAS
2 0 2 mm.
Aguas Arriba
Aguas Abajo
455
450
445
440
435
430
425
420
415
410
405
400
395
390
385
Fecha de excavación
7 MAR. 1971
436.00
Fecha de excavación
14-16 DIC. 1971
428.00
FECHA DE EXCAVACION
21 FEB. 1972
424.00
Fecha de excavación
10-13 ABR. 72
421.00
Desplazamientos totales medidos con extensómetro transversal, desde la fecha de instalación el 3 de SEP. 1970, hasta el 4 de ENE. 1972.
Desplazamientos diferenciales medidos con extensómetro transversal, entre el 24 de NOV. 1971 (antes de la excavación hasta la Elev. 428.00) y el 4 de ENE. 1972 (después de la excavación hasta la Elev. 428.00)
Desplazamientos observados con inclinómetros 9 y 10
GALERIA 3

FIG. 29

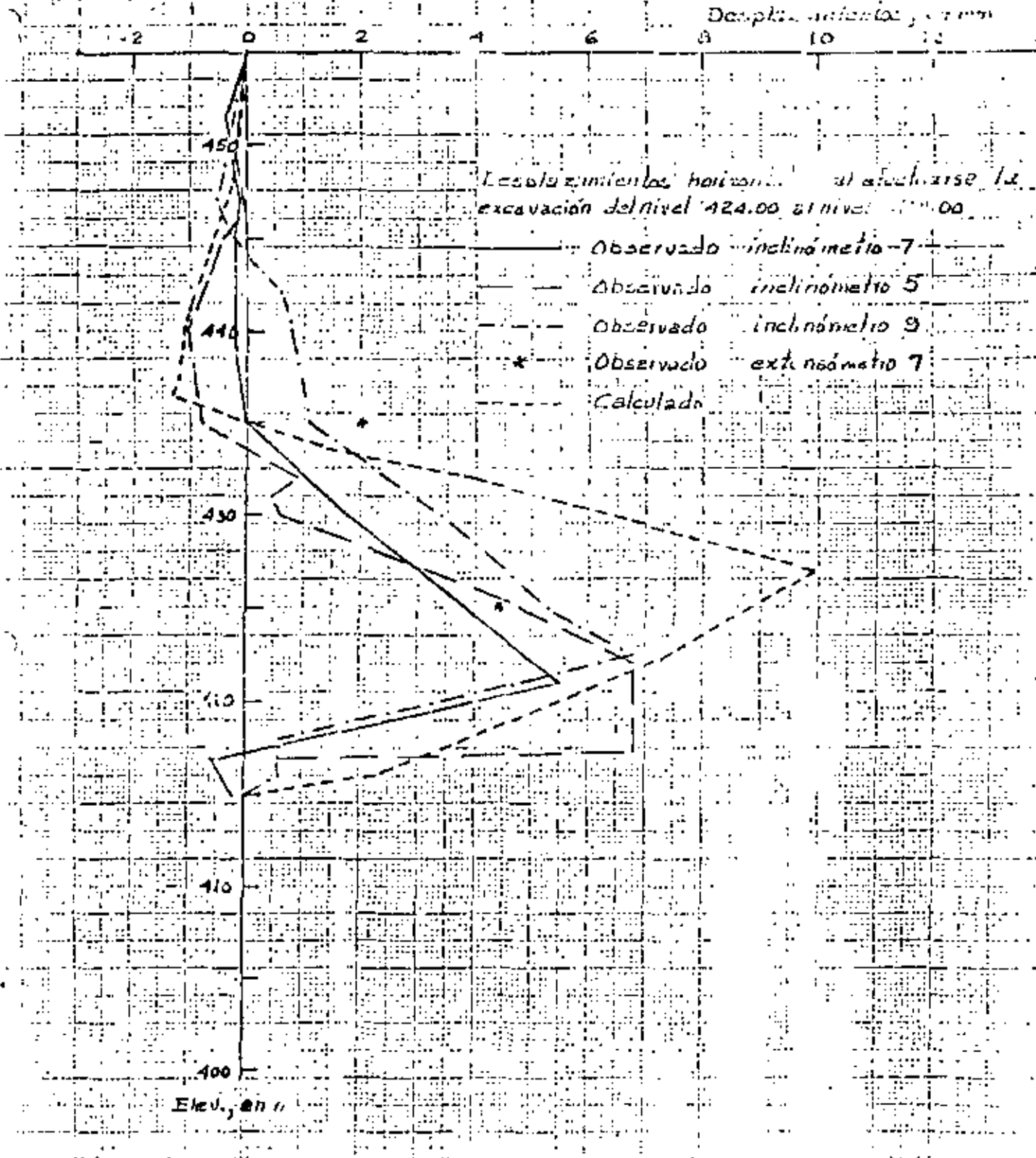

Desplazamientos horizontales observados y calculados con comportamiento elástico lineal en tercera etapa de excavación. Inclinómetros 5, 7 y 9; extensómetro 7